



**BHP  
Petroleum**

VIC/P31  
MINERVA-1  
WELL COMPLETION REPORT  
INTERPRETATIVE

**VIC/P31, MINERVA-1**

**WELL COMPLETION REPORT**

**INTERPRETATIVE VOLUME**

**PREPARED BY: A. Locke**

**70286\_1.WCR**

**DATE: March 1994**

**BHP PETROLEUM PTY. LTD.  
A.C.N. 006 918 832**



# TABLE OF CONTENTS

Page

1	WELL INDEX SHEET . . . . .	1
2	WELL SUMMARY . . . . .	3
3	HYDROCARBONS . . . . .	4
4	STRATIGRAPHY . . . . .	5
5	STRUCTURE . . . . .	7
6	GEOPHYSICAL DISCUSSION . . . . .	8
6.1	Seismic Coverage . . . . .	8
6.2	Post-Drill Mapping . . . . .	8
6.3	Velocities . . . . .	8
7	GEOLOGICAL DISCUSSION . . . . .	9
7.1	Previous Work . . . . .	9
7.2	Regional Geology . . . . .	9
7.3	Contribution to Geological Concepts and Conclusions . . . . .	10

## FIGURES

1. Location Map
2. Stratigraphic Section
3. Predicted vs Actual

## APPENDICES

1. Palynological Report
2. Petrology Report
3. Geochemistry Report
4. Petrophysics Report
5. RFT Report
6. DST Report
7. Special Core Analysis

## ENCLOSURES

1. Composite Log
2. Minerva-1, Top Main Reservoir, Depth Structure Map

1 WELL INDEX SHEET

COMPANY:	BHP Petroleum Pty Ltd	WELL:	Minerva-1	TYPE:	W/cat
SPUDDED:	1200 hrs 8th March 1993	BASIN:	Otway	TENEMENT:	VIC/P31
COMPLETED:	1600 hrs 17th April 1993	ELEV. W.D.:	57.0m	Lat:	38° 42' 12.23" South
TD:	2425 mRT	R.T.:	25.0 m	Long:	142° 57' 12.34" East
STATUS:	Cased & Suspended			1st FLANGE:	30" @ 156m

FORMATION/ MARKER	TOPS (m) DRILL	SEISMIC TVDS	TWT	LITHOLOGICAL SUMMARY/ REMARKS
				No Returns 82 - 560m
Heytesbury/ Nirranda Group	82	57		
Wangerrip Group Pember Mudstone	550	525		Silty claystone with minor (from casing shoe) interbedded sandstone and pebbly conglomerate
Pebble Point	657	632		Medium to coarse sandstone with minor clay and dolomite
Base Tertiary U/C Sherbrook Group	785 785	760 760	708 708	Claystone with trace sandstone and minor dolomite increasing towards the base
Upper Shipwreck Group	1474	1448	1178	Sandstone interbedded with silty claystone
Lower Shipwreck Group	2112	2080	1536	Interbedded sandstone, siltstone and claystone
Otway Group	2293	2257	1622	Argillaceous sandstone interbedded with claystone

LOGS:

SUITE 1

DLL-MSFL-AS-GR-AMS-SP  
 CST  
 CSI (VSP)

SUITE 2

DLL-MSFL-GR-AMS-SP  
 SDT-LDL-CNL-GR-AMS-FMS  
 CSI (VSP)  
 RFT-HP  
 CST

SUITE 3

DLL-MSFL-SDT-AMS

SUITE 4

DLL-MSFL-SDT-AMS  
 LDL-CNL-GR-FMS-AMS  
 CSI (VSP)  
 CST

VIC/P31  
Minerva-1  
Interpretative Well Completion Report

---

SWC: SHOT 127 REC 121  
STORED: KESTREL Management,  
Mt Waverley, VIC

DITCH SAMPLES: 560-2425m  
CORES: Core-1 1821.0-1828.0m  
43% Recovery  
Core-2 1828.0-1842.5m  
92% Recovery  
Core-3 1842.5-1847m  
100% Recovery

---

CASING/TUBING SIZE	30"	13.375"	9.625"	7"
LANDED AT (m)	115	550	1189.37	2107
CEMENT (sacks)	351	503	311	305

---

TEST RESULTS, FLUID ANALYSIS, LOST CIRCULATION, (INTERVAL, CAUSES) PLUGS , REMARKS

Suspension Plug was set 1650 - 1800m; 89 sacks cement  
Suspension Plug was set 1018 - 1068m; 60 sacks cement  
Suspension Plug was set 110 - 160m; 60 sacks cement

RFT:

Three RFT runs made, 33 pretests carried out and three segregated samples were taken

## 2 WELL SUMMARY

Minerva-1 was drilled as an exploration well designed to test the hydrocarbon potential of the Minerva structure. It was spudded on the 8th March 1993 in 57m of water, by the Semi Submersible 'Byford Dolphin'. The well is located in the northern area of permit VIC/P31 in the eastern offshore Otway Basin (Figure 1). Minerva-1 is 7km from the nearest landfall and 26.5km east of the Pecten-1A well.

The primary target was the sandstones of the Late Cretaceous Lower Shipwreck Group within a tilted fault block. The structure is sealed by the overlying claystones of the Upper Shipwreck Group. Secondary targets exist throughout the Late Cretaceous Sherbrook Group, Wangerrip Group and Nirranda Group, all of which show anticlinal closure with only minor fault dependence.

Gas bearing sands were encountered within both the Sherbrook Group and the Upper Shipwreck Sandstone. A total of 0.2m of net gas sand is interpreted in the Sherbrook Group over a 25m gross interval with an average porosity of 11% and an average water saturation of 65%. In the Upper Shipwreck Group two gas zones, with 2.9m and 118.5m of net gas sand are interpreted with average porosities of 14% and 18% and average water saturations of 57 and 19% respectively.

The well was production tested and flowed at approximately 29MMSCFD.

The well was cased and suspended as a future gas producer on the 17th April 1993.

### 3 HYDROCARBONS

There were no hydrocarbon shows recorded in the Tertiary section. Ditch gas readings were not recorded until part way through the Cretaceous at 956mRT, where background readings of up to 0.3%, consisting dominantly of C1 with minor amounts of C2 and C3, were recorded.

Minor gas only was recorded until 1170m RT where gas was recorded up to 1% in thin sands of the Sherbrook Group. No fluorescence was observed in these sands. Log interpretation (Appendix 4) indicates 0.2m of net gas sand over a 25m gross interval (1% N/G) with an average porosity of 11% and an average water saturation of 65%.

A further gas bearing interval was intersected over two sands, between 1645 - 1670mRT in the Upper Shipwreck Group, where gas readings peaked at 4%. Again no fluorescence was observed throughout these sands. Log interpretation indicates a total of 3.9m of net gas sand over a 25m gross interval (16% N/G), with an average porosity of 16% and an average water saturation of 57%.

On penetrating the lower sands in the Upper Shipwreck Group at 1815mRT the gas increased to between 0.1 - 2%. Log interpretation indicates a total of 118.5m of net gas sand over a 133m gross interval (89% N/G), with an average porosity of 18% and an average water saturation of 19%.

RFT pretests were only run over the gas bearing intervals in the Upper Shipwreck Group. Interpretation of the RFT pretest pressures does not conclusively indicate that the two gas bearing intervals in the Upper Shipwreck Group are in different pressure regimes (Appendix 5). The CO<sub>2</sub> content is significantly different in the two sands; 0.32 mole% by vol in the upper sand and 1.89 mole % by volume in the lower sand. This suggests the sands may be isolated but the difference may also be due to compositional changes with time. Gas/water contacts could not be determined from wireline logs due to the increase in shale content, however interpretation of the RFT pressure gradients, indicates gas/water contacts at 1912.8mTVDSS and 1920.0mTVDSS for the two upper sands and 1914.7mTVDSS for the lower sand.

Three fluid samples were taken from the gas bearing intervals in Minerva-1. The sample from 1942.5mRT recovered dry gas whereas the samples from 1649.8 and 1931.0mRT recovered gas and condensate.

#### 4 STRATIGRAPHY

The stratigraphic sequence penetrated at Minerva-1 was very similar to the anticipated section (Figure 3). Minerva-1 reached a total depth of 2425mRT, terminating in the Albian aged Otway Group. Delineation of age units is based primarily on log correlation with nearby wells, together with palynology (Appendix 1).

The stratigraphic section is shown in Figure 3 and Enclosure 1. Age, lithology, and drilling data are marked on the composite well log accompanying this report. No ditch cuttings were obtained above 560m.

##### Otway Group (2425 - 2293 mRT)

The top 132m of the Albian aged Otway Group was penetrated by the Minerva-1 well and consists of interbedded argillaceous lithic quartzose sandstone and medium to dark grey claystone, with minor coal. The sands are generally light grey, fine to medium grained, subangular to subrounded and moderately to well sorted. The sands contain rare feldspar, traces of carbonaceous flecks and coal fragments with poor visible porosity.

##### Lower Shipwreck Group (2293 - 2112mRT)

The Shipwreck group was deposited as a vast delta system and changes regionally from non-marine/fluvial facies onshore in the north to nearshore and offshore/deltaic in the southern permit areas. The base of the Lower Shipwreck Group is marked by an unconformity which was formed in response to reactivation of rift activity in the Cenomanian.

In the Minerva-1 well 181m of Lower Shipwreck Group sediments were intersected. The sequence consists of interbedded sandstone, argillaceous sandstone and silty claystone. The sands are generally clear to very light grey, fine to medium grained, friable with abundant loose grains, subangular and moderately sorted.

##### Upper Shipwreck Group (2112 - 1474mRT)

The base of the Upper Shipwreck Group is marked by a Turonian unconformity.

A 638m section of Upper Shipwreck sediments were intersected in the Minerva-1 well, which consist of argillaceous siltstones grading to silty claystones towards the top, and interbedded sandstones increasing in abundance towards the base. Three cores were cut over the intervals 1821.0 - 1828.0m (43% recovery); 1828.0 - 1842.5m (92% recovery); and 1842.5 - 1847.0m (100% recovery). The core consisted of interbedded sandstone, conglomeratic sandstone and claystone. The sands are medium grey, medium to coarse grained, subangular to subrounded, poorly sorted with common grey argillaceous matrix. The sands generally have good reservoir characteristics. A core study is currently being compiled and will be presented in the Minerva-2 report.

---

Sherbrook Group (1474 - 785mRT)

The base of the Sherbrook Group is marked by a regional, angular to occasionally parallel unconformity which formed in response to the breakup and onset of seafloor spreading, at around 85 Ma.

In Minerva-1 a 689m section of medium to dark grey claystones were intersected with minor interbedded sandstone. The sand content increases towards the top of the Sherbrook Group, consisting of light grey, medium to coarse grained, poorly sorted quartz grains. The claystones of the Sherbrook Group act as the seal for the underlying Shipwreck Group.

Wangerrip Group (785 - 560mRT first release)

Pebble Point Formation (785 - 657mRT)  
Pember Mudstone (657 - 560mRT first release)  
Dilwyn Formation (no returns)

The base of the Wangerrip Group is marked by a regional unconformity which may represent a starvation of sediment in combination with a relative fall in sea level. The Wangerrip Group sediments prograde over this unconformity, and are deposited as a regressive deltaic sequence.

In Minerva-1 Wangerrip Group sediments were intersected with only the basal 225m sampled from cuttings. The base of the section consists of 128m of medium to coarse grained sandstone of the Pebble Point Formation. This passes up into the silty claystones of the Pember Mudstone. The Dilwyn Formation was not sampled, however it is known to consist of sands and silts elsewhere in the permit.

Heytesbury/Nirranda Group (No returns)

The Nirranda Group was not sampled in this well, however is interpreted to consist of shoreface sands overlain by marls and limestones of the Narrawaturk Marl.

The Heytesbury Group was not sampled during the drilling of this well, however is interpreted to consist of a prograding bioclastic sequence.

## 5 STRUCTURE

The Minerva structure is an anticline that has been broken up into two rotated fault blocks by northwest-southeast trending normal faults. The Minerva-1 well tested the northern block. Both of the fault blocks have three-way dip closure in combination with fault closure to the southwest.

The Minerva structure began development at the end of the Early Cretaceous and continued forming during the Late Cretaceous. It experienced very little growth during the Early Tertiary until the Oligocene or more recent times where significant growth has occurred. Two distinct phases of normal faulting are evident. The Early Cretaceous - Late Cretaceous faults terminating within the Sherbrook Group claystones and the Late Cretaceous - Tertiary faults extending from the water bottom and soling out within the claystones of the Upper Shipwreck Group.



## 6 GEOPHYSICAL DISCUSSION

### 6.1 Seismic Coverage

The Minerva structure is defined by a 1 by 1 to 1.5 kilometre grid of 2D seismic data which was acquired in 1980, 1981 and 1991. The data acquired in 1980 and 1981 were reprocessed in 1991 together with the 1991 acquisition. The data are of good quality and are favourably located to give optimum imaging of the faults in the area. A closer seismic line spacing would be required to more accurately map horizons and correlate faults over the Minerva structure.

### 6.2 Post-Drill Mapping

Minerva-1 encountered a gas column two seismic events (approximately 260 metres) deeper than the prognosed primary target depth. A map of the top of the main reservoir was created subsequent to the drilling of Minerva-1 and is included in this report as Enclosure 2.

### 6.3 Velocities

A smoothed seismic velocity model was created to be used for pre-drill depth conversion. The velocity model was then intersected with seismic times for the five horizons interpreted. This enabled the calculation of smoothed average and interval velocities. The interval velocities were then used to convert time to depth.

Despite some differences in the prognosed versus actual formation tops the prognosed time-depth relationship was very close to the actual time-depth relationship in Minerva-1. This implies that the velocity model was reasonably accurate.

The following table compares the prognosed depth for four of the horizons with the actual depth taken from the VSP for the SAME TWO-WAY TIME.

HORIZON	TWT (ms)	PROGNOSSED (metres SS)	VSP DEPTH (meters SS)	DIFF (metres)	DIFF (%)
A	612	615 (3253 m/s Vint)	624 (2880 m/s)	9	1.4
B	944	1155 (2587 m/s Vint)	1102 (2993 m/s)	53	4.6
C	1230	1525 (3693 m/s Vint)	1530 (3698 m/s)	5	0.3
D	1628	2260	2266	6	0.3

## 7 GEOLOGICAL DISCUSSION

### 7.1 Previous Work

Two wells were drilled in permit Vic/P31 prior to Minerva-1, viz. Mussel-1 (ESSO, 1969) and Eric The Red-1 (BHPP, 1993).

Mussel-1 was drilled to a TD of 2450mRT where part of the drill string twisted off. Fishing operations were unsuccessful with electric logs being run to 2286mRT. The well was plugged and abandoned on the 18th September, 1969. The primary target was the Late Cretaceous Shipwreck Group on a structural high within a tilted fault block. Seismic remapping by BHPP has suggested the well was drilled off structure.

Eric The Red-1 was drilled to a TD of 1875mRT in the Otway Group sediments. The primary objective of the well was the Late Cretaceous Shipwreck Group, with the Otway and Sherbrook Groups as secondary objectives. The well was plugged and abandoned, without encountering hydrocarbon shows, on 6 March 1993

### 7.2 Regional Geology

The Otway Basin, situated on the southeastern margin of Australia, is one of a series of basins formed in association with the breakup of Gondwana and Australia's separation from Antarctica.

Rifting within Gondwana was initiated at Late Jurassic to very Early Cretaceous time. Early Cretaceous sediments have only been penetrated in Pecten-1A in the permit area, however are known directly onshore from the permit area and to the west. Rifting produced northwest-southeast oriented normal faulting which controlled the major structural style of the area. Sediments deposited within the Early Cretaceous rift and post-rift sequences thicken southwestwards across faults towards the basin centre.

From Valanginian to Barremian times, it is interpreted that the Pretty Hill Formation was deposited in the permit as alluvial fan sands, silts and clays in tilted half-graben settings. An ensuing sag phase due to thermal cooling and contraction of the crust led to a regional unconformity above the Pretty Hill Formation. The Eumeralla Formation was deposited from the Aptian to the latest Albian during the sag, comprising of both fluvial and lacustrine sands, silts and clays, with common coals deposited in a lake margin coal-swamp environment.

Reactivation of rift activity is interpreted at the earliest Cenomanian, which created a regional unconformity above the Eumeralla Formation. The rifting enhanced the structural style of the previous rifting episode, generating a series of northwest-southeast trending terraces, such as the Mussel Terrace, stepping down into the basin.

Rifting continued from the Cenomanian to the Santonian. During this time sediments of the Upper and Lower Shipwreck Groups were deposited, with the two separated by an unconformity dated approximately at 90 Ma. The sediments were deposited as a vast delta

---

system changing regionally from non-marine/fluviol facies onshore in the north to nearshore and offshore/deltaic in the south.

The end of the second rifting episode, and the inception of sea-floor spreading, is suggested to occur in the permit area at 85Ma, which resulted in a compressive episode which gently folded the Shipwreck Group sediments. This resulted in a regional to occasionally parallel unconformity.

The Sherbrook Group sediments onlap and downlap the breakup unconformity. The sediments consist predominantly of distal clays and silts which grade vertically to more proximal delta sand/silt facies. During the deposition of the Sherbrook Group the basin underwent continued northeast-southwest extension along pre-existing normal faults, coincident with periods of northwest-southeast compression. The compression overprinted the previous minor regional folding.

Overlying the regional unconformity above the Sherbrook Group are Maastrichtian to Middle Eocene Wangerrip Group sediments. After a rapid marine transgression, which is often represented by a basal sand of the Pebble Point Formation, the Wangerrip Group prograded basinward, being deposited as a regressive sequence in deltaic settings represented by sands and silts of the Pember Mudstone and Dilwyn Formation.

The Nirranda Group, comprising of the Mepunga Formation shoreface sands overlain by marls and limestones of the Narrawaturk Marl, unconformably overlies the Wangerrip Group. The Nirranda Group represents a large marine transgression at Late Eocene time.

Northwest-southeast compressional tectonism was reactivated at earliest Oligocene time, with partial inversion of some faults, folding of strata and formation of a regional unconformity.

Open marine conditions since the Oligocene have produced the prograding, bioclastic carbonate sequence of the Heytesbury Group. Minor extension and some compressional tectonism have continued until present day, particularly in the northeast of the permit area, resulting in the partial erosion of the Heytesbury and Nirranda Group sediments.

### **7.3 Contribution to Geological Concepts and Conclusions**

Minerva-1 was drilled as an exploration well in order to test the hydrocarbon potential of the Lower Shipwreck Group in the Minerva structure.

Gas was encountered over a 25m interval in the secondary objective, Sherbrook Group. A total of 0.2m of net gas sand is interpreted with an average porosity of 11% and an average water saturation of 65%. Although this sand is uneconomical at this location due to the thin nature of the sands and low reservoir quality, it is possible that it may thicken and become better quality elsewhere on the structure.

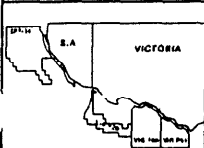
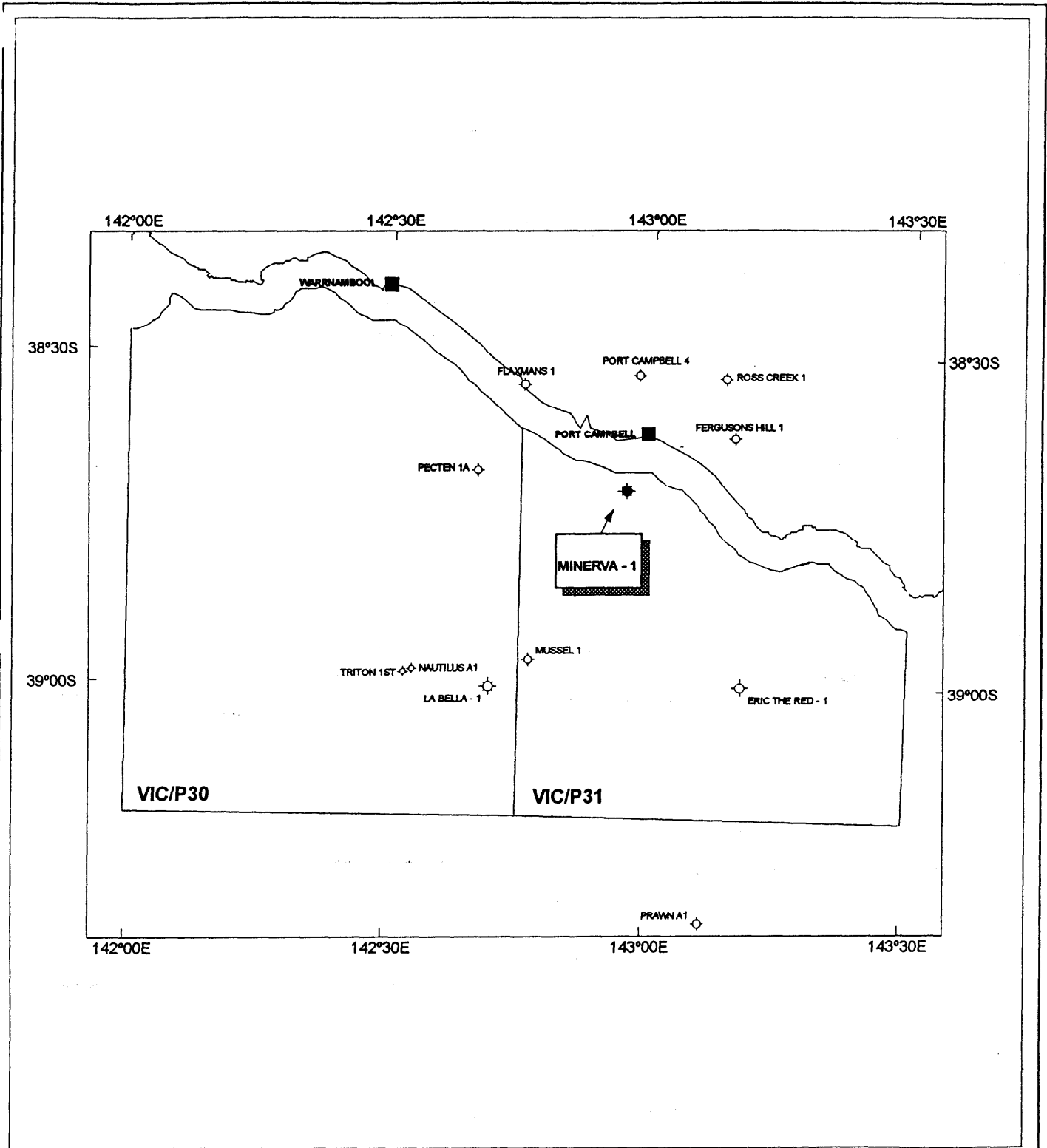
In the Upper Shipwreck Group two sands with 2.9m and 118.5m of net gas sand were encountered, with average porosities of 14% and 18% and average water saturations of 57% and 19% respectively. Interpretation of the results of the program does not conclusively prove that the two sands are in different pressure regimes.

The claystones of the Upper Shipwreck act as both a vertical and basal seal to the upper gas reservoir and as a vertical seal to the lower sand. Therefore these claystones exhibit excellent seal properties over the Minerva structure.

An investigation of the source rock character and thermal maturity of the drilled sequence has been carried out and is presented in Appendix 3. Four SWC samples from the Late Cret. Sherbrook and Shipwreck Groups were analysed which revealed a predominance of Type II/III to Type III, mainly gas-prone organic matter. HI values were generally less than 150, with the exception of a coal sample (1837.1mRT) which was characterised by more strongly liquids-prone organic matter. S1 and S2 yields suggest that expulsion from these samples would only be possible at relatively advanced levels of thermal maturity. As secondary cracking of liquids to gas is likely to occur at relatively advanced levels of maturity, the source rocks are likely to be more gas prone than is indicated by the source rock data.

A condensate and water-extract, acquired from the cold-trapping of the 1649.8mRT and 1942.5mRT RFT gases, were subjected to a range of geochemical analyses. GC data from the water-extract suggest that it was generated from higher land-plant-derived organic matter within the source sediments deposited under strongly oxic, terrestrial conditions. Biomarker data, though, point to aquatically derived organic matter in clastic sediments deposited under relatively oxic (possibly marine to marginal marine) conditions. This ambiguity probably arises from the use of condensate data in inferring source organic matter type, provenance and thermal maturity. Because condensates are maturity- or phase-affected or both, the relative abundances of their constituent compounds, and the values of parameters based on them, may not be a true reflection of their source characteristics.

However the data appear to be sufficiently similar to infer the co-genesis of the Minerva-1 gases and condensates which, from aromatic biomarker and stable carbon isotope data, appear to have been generated at depth, at thermal maturities in excess of 1.6% VR, rather than in association with liquids with the oil-generative window.



**MINERVA-1 LOCATION MAP**



**MINERVA-1  
LOCATION MAP**



# OTWAY BASIN STRATIGRAPHIC COLUMN

System Period	Epoch General	Group	Formation	Lithology	Depositional Env	Reservoir Source	Shows		
TERTIARY		Heytesbury	Port Campbell Limestone		Marine	SEAL	<ul style="list-style-type: none"> <li>☉ Fahley-1</li> <li>☉ Curdes-1</li> <li>☉ Linton-1</li>   <li>☉ Port Campbell-1,</li> <li>☉ North Paaratte-3,</li> <li>☉ Najaba-1A,</li> <li>☉ Minerva-1, La Bella-1</li> <li>☉ North Paaratte-1 &amp; 2,</li> <li>☉ Grumby-1, Iona-1,</li> <li>☉ Wallaby Creek-1,</li> <li>☉ Caroline-1</li>   <li>☉ Port Campbell-4</li> <li>☉ Windermere-1,</li> <li>☉ Crayfish-1A</li> <li>☉ Katnook-2</li>   <li>☉ Katnook-1, Katnook-2</li> <li>☉ Troes-1ST</li> <li>☉ Katnook-2, Katnook-3,</li> <li>☉ Ladbroke Grove-1,</li> <li>☉ Wallaby Creek-1</li> <li>☉ Laura-1</li>   <li>☉ Sawpit-1</li> <li>☉ Kalangadoo-1</li> </ul>		
			Gellibrand Marl						
		Nirranda	Narrawaturk		Marginal Marine	R			
			Mepunga						
		Wangerrip	Dilwyn		Marginal Marine	R			
			Pember						
			Pebble Point						
		CRETACEOUS	Maastrichtian	Sherbrook				Fluvio/Deltaic	SEAL
			Campanian					Marine	S
			Santonian	Shipwreck (Informal)	Upper Shipwreck			Fluvial and Marginal Marine	
Coniacian									
Turonian									
Cenomanian			Lower Shipwreck						
Albian	Otway		Eumeralla		Fluvial/Lucastrine	SEAL			
Aptian							S		
Barremian			Crayfish Subgroup			SEAL			
Hauterman						R			
Valanginian									
Berriasian									
JURASSIC		Casterton Beds		Fluvial/Lucastrine	SEAL				
Tithonian					R				
Kimmeridgian									
Oxfordian									
	Paleozoic	Undifferentiated Paleozoic Basement							



# MORGAN PALAEO ASSOCIATES

PALYNOLOGICAL/PETROLEUM GEOLOGICAL CONSULTANTS

POSTAL ADDRESS: Box 161, Maitland, South Australia 5573

DELIVERIES: 1 Shannon Tce, Maitland, South Australia 5573

Phone (088) 32 2795 Fax (088) 32 2798

## FINAL PALYNOLOGY OF BHPP MINERVA #1, OFFSHORE OTWAY BASIN, VICTORIA, AUSTRALIA

BY

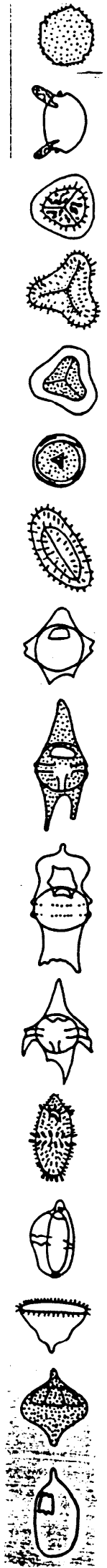
ROGER MORGAN AND NIGEL HOOKER

BHP PETROLEUM PTY. LTD.  
DO NOT RETAIN IN PERSONAL FILES  
**FILE COPY**  
PLEASE RETURN TO  
EXPLORATION INFORMATION  
CENTRE

for BHP PETROLEUM

September 1993

REF.OTW.RPMINRVA





FINAL PALYNOLOGY OF BHPP MINERVA #1  
OFFSHORE OTWAY BASIN, VICTORIA, AUSTRALIA

BY

ROGER MORGAN AND NIGEL HOOKER

<b>CONTENTS</b>		<b>PAGE</b>
I	SUMMARY	3
II	INTRODUCTION	5
III	PALYNOSTRATIGRAPHY	6
IV	CONCLUSIONS	18
V	REFERENCES	18

FIGURE 1 : CRETACEOUS REGIONAL FRAMEWORK, OTWAY BASIN

FIGURE 2 : ZONATION USED HEREIN

FIGURE 3 : MATURITY PROFILE : MINERVA #1

## I SUMMARY

- 563.0m(swc) 1% dinos, 594.0m(swc) 3% : middle *diversus* Zone : Early Eocene : marginally marine
- 617.0m(swc) 6% dinos : lower *diversus* Zone : Early Eocene : marginally marine
- 627.0m(swc) 10% dinos, 651.0m(swc) 4% : upper *balmei* Zone : late Paleocene : nearshore marine
- 760.0m(swc) 3% dinos : lower *balmei* Zone : early Paleocene : very nearshore marine
- 783.0m(swc) 42% dinos, 810.0m(swc) dinos absent, 838.5m(swc) 6% : *longus* Zone (783m *druggii* dino Zone ) : Maastrichtian : marginal, non-marine and nearshore upsection
- 897.0m(swc) 2% dinos, 954.0m(swc) 2%, 991.0m(swc) 14% : upper *senectus* Zone (897 upper *australis* dino Zone, 954m, 991m lower *australis* dino Zone) : Campanian : very nearshore marine
- 1054.0m(swc) 4% dinos, 1105.5m(swc) 6%, 1149.0m(swc) 8% : middle *senectus* Zone (all upper *aceras* Zone) : Campanian : very nearshore marine
- 1166.0m(swc) 13% dinos : lower *senectus* Zone (middle *aceras* dino Zone) : Campanian : nearshore marine
- 1179.0m(swc) 7% dinos, 1193.0m(swc) 17%, 1220.0m(swc) 12%, 1260.0m(swc) 16%, 1271m(cutts) (19%), 1298.0m(swc) 21% : upper *apoxyexinus* Zone (*aceras* dino Zone) : latest Santonian : nearshore marine
- 1325m(cutts) (15% dinos), 1351.0m(swc) 18%, 1398.0m(swc) 13%, 1410m(cutts) (24%), 1453.0m(swc) 8% : upper *apoxyexinus* Zone (1325m, 1351m upper *cretacea* dino Zone, 1398m, 1410m, 1453m lower *cretacea* dino Zone) : Santonian : nearshore marine
- 1502.0m(swc) 16%, 1510m(cutts) (31%), 1562.0m(swc) 8%, 1597.0m(swc) 8% : middle *apoxyexinus* Zone (1502m, 1510m upper *porifera* dino Zone : Santonian : nearshore marine
- 1616m(cutts) (26% dinos), 1629.0m(swc) 12%, 1647.0m(swc) 22%, 1660.0m(swc) 7%, 1690.0m(swc) 14%, 1699m(cutts) (24%), 1723.0m(swc) 12%, 1747.0m(swc) 14%, 1766.0m(swc) 14%, 1790m(cutts) (22%), 1805.0m(swc) 15% : lower *apoxyexinus* Zone : Santonian : nearshore marine
- 1820m(cutts) (17% dinos), 1837.3m(CORE) dinos absent, 1838.1m(CORE) 3%, 1839.7m(CORE) 16%, 1840.3m(CORE) 13% dinos, 1872.5m(swc) 2%, 1889m(cutts) (5%), 1916m(cutts) (13%), 1947.5m(swc), dinos absent, 1949m(cutts) (4%), 2003m(cutts) (11%), 2027m(cutts) (14%), 2035.0m(swc) 33%, 2061.0m(swc)

12%, 2084m(cutts) (5%) : *mawsonii* Zone (2084m *infusorioides* dino Zone :  
Coniacian-Turonian : mixed nearshore to non-marine

~~2098.0~~<sup>2099</sup>m(swc) 1% dinos, 2093m(cutts) (17%), 2101.0m(swc) 16%, 2102m(cutts) (15%),  
2105m(cutts) (15%), 2117m(cutts) (15%), 2123.0m(swc) 5%, 2142.0m(swc) 1% :  
*distocarinatus* Zone (2089m, 2093m, 2101m, 2102m, 2105m all *infusorioides* dino  
Zone) : Cenomanian : nearshore and marginal marine

2150m(cutts) dinos absent, 2157.5m(swc) absent, 2180m(cutts) (trace dinos) apparently  
*distocarinatus* Zone but markers could be caved in the cuttings and are absent from  
the swc : apparently Cenomanian : non-marine but possibly brackish at 2180m but  
marine indicators could be caved

2212.5m(swc) almost barren, 2222m(cutts) (4% dinos but most are clearly caved),  
2261m(cutts) (2% dinos possibly caved), 2270m(cutts) (trace dinos possibly caved) :  
zone indeterminate : swc almost barren, cuttings lack diagnostic markers : possibly  
brackish to very nearshore but saline markers may be caved

2294.0m(swc) trace spiny acritarchs, 2318m(cutts) (1% dinos clearly caved), 2321.0m(swc)  
trace spiny acritarchs, 2324m(cutts) (1% dinos mostly clearly caved), 2333m(cutts)  
(dinos absent), 2354m(cutts) (dinos absent), 2360.0m(swc) trace spiny acritarchs,  
2392.5m(swc) dinos absent, 2408m(cutts) (dinos absent), 2412.0m(swc) almost  
barren, 2425m(cutts) (dinos absent) : possibly *paradoxa* Zone but not typically so :  
possibly Albian : non-marine to slightly brackish : depends on richer assemblages at  
2294.5m, 2321.0m, 2324m, 2392.5m.

## II INTRODUCTION

During drilling three batches of cuttings (12 samples) were studied on an urgent basis at Maitland. Following this, a two person team was placed offshore on the Byford Dolphin and studied a further 16 cuttings over eight days. These samples were reported in 10 faxed reports. After well completion, a further fifty four samples (50 swcs, 4 from core) were submitted for detailed study. All results are summarised herein.

Palynomorph occurrence data are shown as Appendix I and include the urgent and followup samples and form the basis for the assignment of the samples to sixteen spore-pollen and dinoflagellate units of Early Eocene to Cenomanian age.

Specimen counts were made on all assemblages and expressed in the raw data as percentages. In the running text, percentages from cuttings are always bracketed (5%) to show that they may be inaccurate due to caving.

The Cretaceous spore-pollen zonation is essentially that of Dettmann and Playford (1969), but has been significantly modified and improved by various authors since, and most recently discussed in Helby et al (1987), as shown on Figure 1. The Late Cretaceous zonation has been modified by Morgan (1992) in project work for BHPP (Figure 2). Tertiary zones are essentially those of Partridge (1976).

Maturity data was generated in the form of Spore Colour Index, and is plotted on Figure 3 Maturity Profile of Minerva #1. The oil and gas windows on Figure 3 follow the general consensus of geochemical literature. The oil window corresponds to spore colours of light-mid brown (Staplin Spore Colour Index of 2.7) to dark brown (3.6). These correspond to vitrinite reflectance values of 0.6% to 1.3%. Geochemists argue variations on kerogen type, basin type and basin history. The maturity interpretation is thus open to reinterpretation using the basic colour observations as raw data. However, the range of interpretation philosophies is not great, and probably would not move the oil window by more than 200 metres.

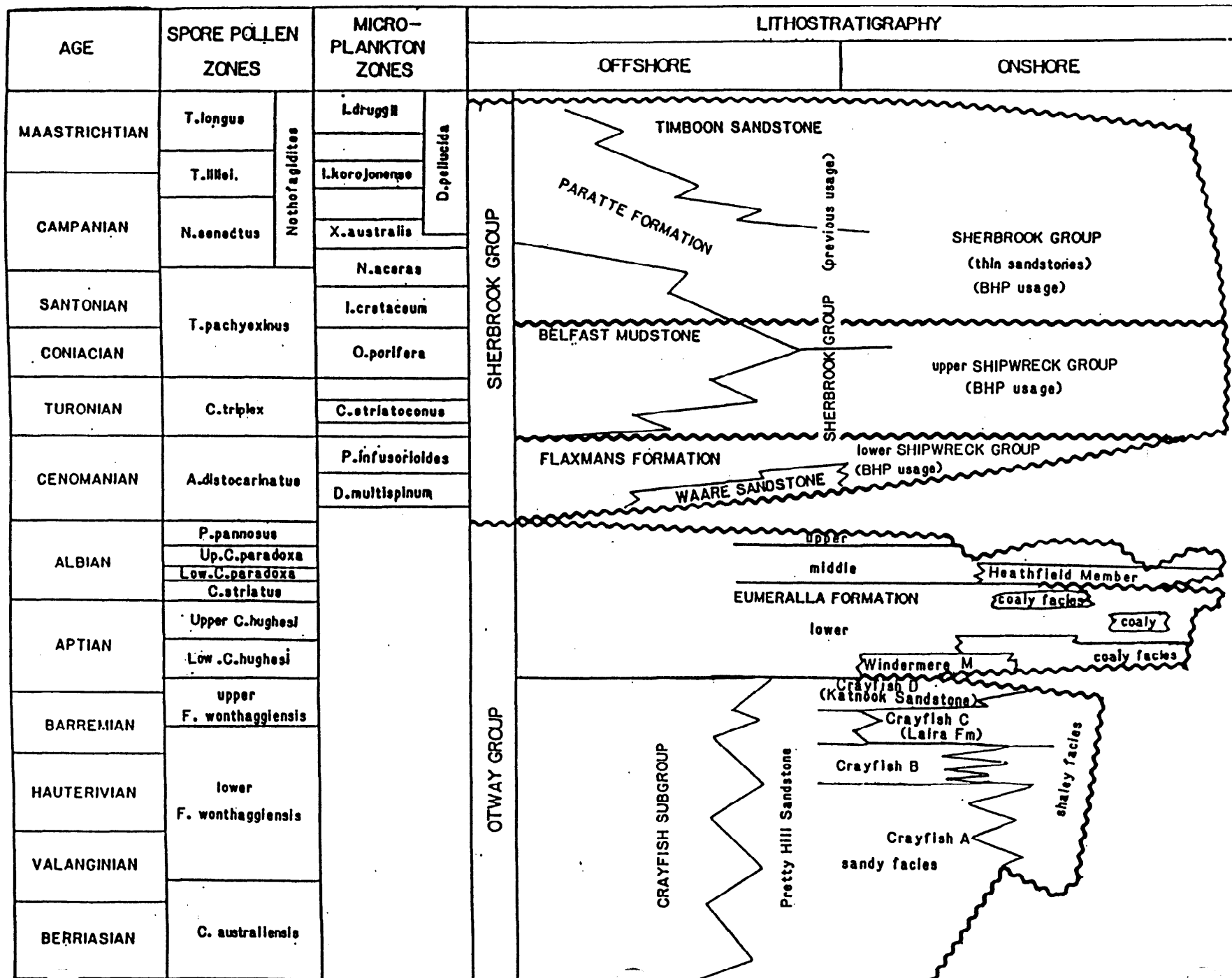


FIG. 1. CRETACEOUS REGIONAL FRAMEWORK, OTWAY BASIN

SPORE-POLLEN ZONES	SPORE-POLLEN HORIZONS	DINOFLAGELLATE ZONES	DINOFLAGELLATE HORIZONS
LONGUS	upper T. confessus 1 T. sectilis G. rudata • 1b N. senectus • 1d	DRUGGII	M. conorata 1a M. conorata 1c M. druggii 1e I. pellucida 2
	lower T. sabulosus 2a T. longus 2b		
LILLEI	upper T. sectilis 3a	KOROJONENSE	I. korojonense 3 I. cretacea
	lower T. lillei 3b		I. korojonense 3c I. pellucida
SENECTUS	upper G. rudata 7a	upper AUSTRALIS	X. australis 4 X. ceratoides A. wisemaniae A. suggestium 4a
	middle T. sabulosus 7e	lower ACERAS	N. aceras 5 N. semireticulata X. australis • 6
	lower N. senectus 9a	upper ACERAS	N. tuberculata 7 X. australis 7b N. tuberculata 7c N. semireticulata O. obesa 7d
APOXYEXINUS	upper A. cruciformis 1% A. cruciformis 1-4%	middle ACERAS	T. suspectum Heterosphaeridium 10%+ 8 Heterosphaeridium 20%+ 9
	middle 11	lower ACERAS	N. aceras 9b
	lower A. cruciformis 10%+ 12 A. cruciformis 10%+ 12a	upper CRETACEA	I. belfastense 10 A. denticulata Heterosphaeridium 20%+ 10a I. belfastense A. denticulata 11a
MAWSONII	A. distocarinatus 12c	lower CRETACEA	I. cretacea 11b
	consistent 13 A. distocarinatus P. mawsonii 15a	PORIFERA	O. porifera 12b
DISTOCARINATUS		STRIATOCONUS	C. edwardsii 14
	common saccates A. cruciformis	INFUSORIOIDES	C. edwardsii • 15 C. edwardsii • 15b
		-----	dinoflagellates

FIGURE 2 ZONATION USED HEREIN SHOWING THE NUMBERED HORIZONS AGAINST THE EXISTING FORMAL ZONATION.

• = frequent (4-10%) ● = common (11-30%)

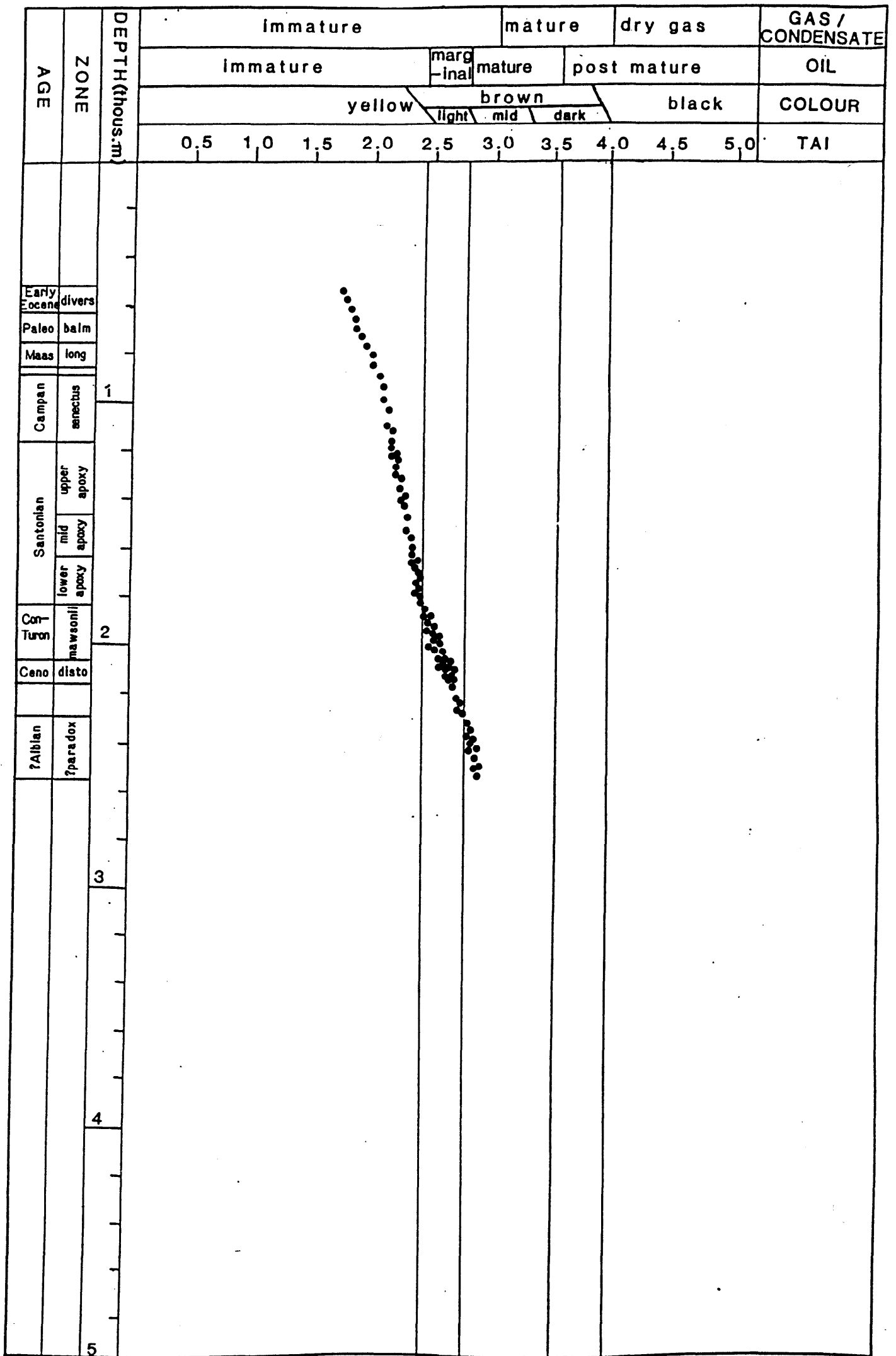


FIGURE 3 MATURITY PROFILE : MINERVA # 1

### III PALYNOSTRATIGRAPHY

#### A 563.0m(swc), 594.0m(swc) : middle *diversus* Zone

Assignment to the middle *Malvacipollis diversus* of Early Eocene age is indicated at the top by the absence of younger indicators and at the base on oldest *Banksieaeidites arcuatus*, *Proteacidites tuberculiformis* and *Triporopollenites ambiguus*. Common species are *Falcisporites similis* and *Dilwynites granulatus*, with frequent *Lygistepollenites florinii*, *Haloragacidites harrisii*, *Podosporites microsaccatus* and *Proteacidites* spp. Minor Permian and Cretaceous reworking was seen.

Amongst the rare dinoflagellates, *Deflandrea pachyceros* and *D. obliquipes* are consistent with the Early Eocene age.

Marginally marine environments are indicated by the dominant and diverse spore-pollen, abundant cuticle fragments, and rare (1% and 3% downhole) dinoflagellates and their low diversity. Freshwater algae (*Botryococcus* 6% and 3% downhole) indicate significant lacustrine influence.

Colourless palynomorphs indicate immaturity for hydrocarbons.

#### B 617.0(swc) : lower *diversus* Zone

Assignment to the lower *M. diversus* Zone of Early Eocene age is indicated at the top by the absence of younger indicators and at the base on oldest *Periporopollenites demarcatus* and *Malvacipollis diversus*. Minor downhole mud contamination is considered responsible for a single *Proteacidites pachypolus* specimen. Common taxa are *Proteacidites*, *Dilwynites* and *Falcisporites* while frequent taxa are *Cyathidites* and *P. microsaccatus*. Minor Permian reworking was seen.

Amongst the very scarce dinoflagellates, *D. obliquipes* is consistent with the Early Eocene age.

Marginally marine environments are indicated by the minor (6%) dinoflagellates and their low diversity, together with the dominant and diverse spore-pollen.

Colourless palynomorphs indicate immaturity for hydrocarbons.



**C 627.0m(swc), 651.0m(swc) : upper *balmei* Zone**

Assignment to the upper *Lygistepollenites balmei* Zone of late Paleocene age is indicated at the top by youngest *Gambierina rudata*, *G. edwardsii* and *L. balmei*, and at the base by oldest *Proteacidites grandis*. Common taxa are *Dilwynites* and *Falcisporites* while frequent taxa include *Proteacidites*, *Gleicheniidites* and *Cyathidites*. Minor Permian reworking was seen.

Amongst the dinoflagellates, *Deflandrea speciosus*, *D. truncata* and *D. dilwynensis* with *Alisocysta margarita* (627m only) and without *Apectodinium* spp, are consistent with the spore-pollen zone.

Nearshore marine environments are indicated by common and diverse spore-pollen and rare dinoflagellates (10% and 4% downhole) with frequent cuticle.

Colourless spores and pollen indicate immaturity for hydrocarbons.

**D 760.0m(swc) : lower *balmei* Zone**

Assignment to the lower *L. balmei* Zone of early Paleocene age is indicated at the top and base by the absence of younger and older indicators respectively. *Falcisporites* and *Dilwynites* are very common with *Proteacidites* frequent. *G. edwardsii*, *G. rudata* and *L. balmei* are consistent and indicate the zone. Very minor Eocene caving and mud contamination is evident by the presence of *Anacolosidites acutullus*.

Very rare dinoflagellates include *D. speciosa* and *D. dilwynensis*, consistent with the spore-pollen zone. *Thalassiphora delicata* and *Hafniasphaera septata* are rare distinctive elements.

Very nearshore marine environments are indicated by the dominant and diverse spore-pollen, abundant cuticle, and rare (3%) dinoflagellates of low to moderate diversity.

Colourless spore colours indicate immaturity for hydrocarbons.

**E 783.0m(swc), 810.0m(swc), 838.5m(swc) : *longus* Zone**

Assignment to the *Tricolpites longus* spore-pollen Zone of Maastrichtian age is indicated at the top by youngest *T. longus* supported by the dinoflagellates and at the base on oldest *T. longus* and *Tetracolporites verrucosus*. All three samples are lean of palynomorphs and dominated by inertinite. At 783m, oldest *Stereisporites punctatus* and the dominance of *G. rudata* over *Nothofagidites endurus* indicate the upper *longus* Zone while at 838.5m, *N. endurus* dominance over *G. rudata* indicates the lower *longus* Zone. Common are *Falcisporites*, *Dilwynites* and *Proteacidites*. *Tricolporites lillei* is very rare at 838.5m only. Very minor Permian and Triassic reworking were seen.

At 783m, abundant *Manumiella coronata* indicates the *druggii* dinoflagellate Zone of latest Maastrichtian age, correlative with the upper *longus* spore-pollen Zone. At 838.5m, the rare presence of *Isabelidinium korojonense* and *Isabelidinium cretacea* indicates the *I. korojonense* Zone of Campanian to early Maastrichtian age. This zone is usually seen up to the top of the *T. lillei* spore-pollen Zone but is here associated with the *T. longus* Zone. The difference is minor, and may represent minor caving or reworking, or fine tuning of the zonation.

Environments are different in all three samples. At 838.5m, marginal marine environments are indicated by dominant and diverse spore-pollen, minor low diversity dinoflagellates (6%) with significant freshwater algae (10%). At 810m, non-marine lacustrine environments are suggested by the dominant and diverse spore-pollen, absence of dinoflagellates, common freshwater algae (16%) and frequent cuticle. At 783m, nearshore marine environments are indicated by the very common dinoflagellates (42%) despite their low diversity, and frequent and diverse spore-pollen.

Yellow spore colours indicate immaturity for hydrocarbons.

**F 897.0m(swc), 954.0m(swc), 991.0m(swc) : upper *senectus* Zone**

Assignment to the upper *Nothofagidites senectus* Zone of lower Campanian age is indicated at the top by the absence of younger markers and confirmed by the dinoflagellates, and at the base by oldest *Gambierina rudata*, also confirmed by the dinoflagellates. The apparent absence of the *T. lillei* Zone of mid Campanian to early Maastrichtian age may be caused by unconformity or condensation, or it may

exist unsampled in the 58.5m sample gap. *Nothofagidites* are frequent to common (5-13%) in this subzone, but scarce (1% or less) beneath. Rare but consistent are *Tricolpites sabulosus*, *T. confessus* and *G. rudata* and *Tricolporites apoxyexinus* is present at 897m only. Overall, *Falcisporites* and *Proteacidites* are common, with *Dilwynites*, *Microcachryidites* and *Nothofagidites* frequent. At 991m, *T. sabulosus* is unusually frequent at 6% of the assemblage. Rare Permian reworking was seen.

Amongst the dinoflagellates, the upper *Xenikoon australis* dinoflagellate Zone is indicated at 897m by youngest *X. australis* above youngest *Nelsoniella aceras* and *N. semireticulata*. *X. australis* is rare but still the most consistent dinoflagellate species. At 954m and 991m lower *X. australis* Zone is indicated at the top by youngest *N. semireticulata* and at the base by the absence of older indicators and the continued presence of frequent *X. australis*, the only frequent dinoflagellate. Youngest *Areosphaeridium suggestium* at 954m is consistent with the assignment.

Environments are very nearshore marine as shown by the low dinoflagellate content (2%, 2% and 14% down section) and low dinoflagellate diversity. Clearly 991m is the most marine with highest dinoflagellate content and diversity.

Yellow spore colours indicate immaturity for hydrocarbons.

#### **G 1054.0m(swc), 1105.5m(swc), 1149.0m(swc) : middle *senectus* Zone**

Assignment to the middle *N. senectus* Zone of early Campanian age is indicated at the top by the absence of younger indicators and is confirmed by dinoflagellate data and at the base by oldest *T. sabulosus*, also confirmed by dinoflagellate data. Common are *Falcisporites* and *Proteacidites* with frequent *Cyathidites*, *Dilwynites*, *Microcachryidites* and *Phyllocladidites mawsonii*. Consistent are *Amosopollis cruciformis*, *N. endurus*, *N. senectus*, *T. confessus*, *Tricolpites gillii* and *T. sabulosus*. At 1149m, *T. apoxyexinus* occurs. Rare Triassic, Permian and Early Cretaceous reworking was seen.

Amongst the dinoflagellates, *Nelsoniella tuberculata* occurs in all samples, indicating the upper *Nelsoniella aceras* dinoflagellate Zone, correlative with the middle *senectus* spore-pollen Zone. Further, the presence of *X. australis* to the base indicates the upper part of this subzone. The most frequent taxa are *Spiniferites*, *Heterosphaeridium* and *X. australis* with *N. aceras* and *N. tuberculata* rare but consistent.

Very nearshore marine environments are indicated by the rare low diversity dinoflagellates (4%, 6% and 8% downhole), abundant and diverse spore-pollen, common cuticle and significant freshwater algae (1%, 5% and 2% downhole).

Yellow spore colours indicate immaturity for hydrocarbons.

#### **H 1166.0m(swc) : lower *senectus* Zone**

Assignment to the lower *N. senectus* Zone of earliest Campanian age is indicated at the top by the absence of younger indicators and at the base on oldest *N. endurus*. Very common is *Falcisporites* while *Cyathidites*, *Dilwynites*, *Gleicheniidites*, *Microcachrydites* and *Proteacidites* are frequent. *N. endurus* is rare. Minor Permian reworking was seen.

Amongst the dinoflagellates, the presence of *Nelsoniella aceras* without *N. tuberculata* and the presence of common *Heterosphaeridium* (10%) indicate the middle *aceras* dinoflagellate Zone. *Heterosphaeridium solida* and *H. heterocanthum* are the only frequent dinoflagellates.

Nearshore marine environments are indicated by the low dinoflagellate content (13%) and their low to moderate diversity, coupled with the dominant and diverse spores and pollen.

Yellow spore colours indicate immaturity for hydrocarbons.

#### **I 1179.0m(swc), 1193.0m(swc), 1220.0m(swc), 1260.0m(swc), 1271m(cutts), 1298.0m(swc) : upper *apoxyexinus* Zone (*aceras* dino Zone)**

Assignment to the upper *Tricolporites apoxyexinus* Zone is indicated at top and base by very rare *Amosopollis cruciformis* (1% or less) without younger or older markers, and is confirmed by dinoflagellate data. Large nondescript *Proteacidites* spp occur to the base of this interval, but not below it. A further interval of upper *apoxyexinus* Zone occurs below this point associated with the *cretacea* dino Zone. Overall, the assemblage is fairly bland with *Falcisporites* and *Dilwynites* common and *Cyathidites*, *Microcachrydites* and *Proteacidites* frequent. *Australopollis obscurus* is consistent at 1-2% of the assemblage to the interval base but very rare beneath. A single specimen of *N. senectus* at 1220.0m suggests extension of the *senectus* Zone

down to this point, but may also represent minor mud contamination. Minor Permian and Triassic reworking were seen.

Amongst the dinoflagellates, *N. aceras* occurs to the interval base without younger indicators and indicates the *N. aceras* dinoflagellate Zone. The subzone cannot be determined from these swc samples where *Heterosphaeridium* content is 3-7%. The major acme of *Heterosphaeridium* (20%+) may only be visible in cuttings. Of the dinoflagellates, only *Heterosphaeridium* and *Trithyrodinium* are frequent. Rare but consistent are *N. aceras* and *Odontochitina porifera* while rare but inconsistent are *Isabelidinium cretaceum* (1298m), *Odontochitina obesa* (1220 and 1260m) and *Areosphaeridium suggestium* (1193m).

Environments are nearshore marine with low dinoflagellate content (7%, 17%, 12%, 16%, (19%), 21% downhole) and low to moderate diversity, abundant and diverse spore-pollen and rare algal acritarchs (absent to 3%).

Yellow spore colours indicate immaturity for hydrocarbons.

**J 1325m(cutts), 1351.0m(swc), 1398.0m(swc), 1410m(cutts), 1453.0(swc) :  
upper *apoxyexinus* Zone (*cretacea* dino Zone)**

Assignment to the upper *T. apoxyexinus* Zone is indicated by rare *A. cruciformis* (1% or less) without younger or older markers and is confirmed by dinoflagellate data. Large *Proteacidites* spp are absent here, but consistent above. *A. obscurus* occurs rarely (1% or less) to the interval base but not below. Otherwise the assemblage is nondescript with very common *Falcisporites*, common *Dilwynites* and frequent *Cyathidites*, *Microcachrydites*, *Podosporites microsaccatus* and *Proteacidites*. Small *Proteacidites* comprise 2-7% of the assemblage but are extremely rare or absent in section beneath. *T. apoxyexinus* occurs at 1398m and 1453m.

Amongst the dinoflagellates, youngest *Amphidiadema denticulata* and *Isabelidinium belfastense* at 1325m(cutts) and oldest *A. denticulata* and *I. belfastense* at 1351.0m(swc) indicate the upper *Isabelidinium cretaceum* dinoflagellate Zone. Youngest *Chatangiella victoriensis* and *Trithyrodinium glabrum* at 1351m are consistent. Below this, the absence of younger indicators at the top and oldest *I. cretaceum* at the base indicates assignment of 1398-1453m to the lower *cretaceum* dinoflagellate Zone. *Heterosphaeridium* spp continue to be the most frequent dinoflagellate, but with consistent diverse *Trithyrodinium* spp.

Nearshore marine environments are indicated by low dinoflagellate content ((15%), 18%, 13% (24%), 8% downhole) and low to moderate diversity, coupled with dominant and diverse spore-pollen assemblages.

Yellow spore colours indicate immaturity for hydrocarbons.

**K 1502.0m(swc), 1510m(cutts), 1562.0m(swc), 1597.0m(swc) : middle *apoxyexinus* Zone**

Assignment to the middle *T. apoxyexinus* Zone is indicated at the top by youngest consistent to frequent *A. cruciformis* (2-4% compared with 1% or less above), and at the base by the absence of older markers. Within the interval, *Cyathidites*, *Dilwynites*, *Falcisporites* and *Microcachrydites* are all common to very frequent. *A. cruciformis* is frequent (4%) in all except the shallowest sample (2%). *Ornamentifera sentosa* occurs at 1502.0 and 1510m. *Proteacidites* are extremely rare to absent. Minor Permian reworking was seen.

Amongst the dinoflagellates, *Isabelidium rectangulare* occurs at 1502 and 1510m, indicating the upper *porifera* dinoflagellate Zone. Youngest *Circulodinium deflandrei* occurs at 1510m and confirms the spore-pollen subzone. Oldest *O. porifera* occurs in swc at 1453m. *Heterosphaeridium* and *Trithyrodinium* are the most common dinoflagellates.

Environments are nearshore marine as shown by the low dinoflagellate content (16%, 31%, 8%, 8% downhole) and their low to moderate diversity, with dominant and diverse spore-pollen.

Yellow spore colours indicate immaturity for hydrocarbons.

**L 1616m(cutts), 1629.0m(swc), 1647.0m(swc), 1660.0m(swc), 1690.0(swc), 1699m(cutts), 1723.0m(swc), 1747.0m(swc), 1766.0m(swc), 1790m(cutts), 1805.0m(swc) : lower *apoxyexinus* Zone**

Assignment to the lower *T. apoxyexinus* Zone of Santonian age is indicated at the top by the downhole influx of *A. cruciformis* ((11%), 4%, 9%, 8%, 9%, (15%), 3%, 1%, 9%, (12%), 8%) compared with 2-4% above, and at the base by the base of this acme and the absence of older indicators. Within the interval, saccate pollen are common

to very common, especially *Falcisporites* and *Microcachryidites*. *Dilwynites* are frequent to common towards the top (5-15% in the interval 1616-1723m) but are common to very common towards the base (24-40% in the interval 1747-1805m). *A. cruciformis* is very frequent to common in most samples although apparently more common in the cuttings than the swcs. *Cicatricosisporites australiensis* is rare but consistent. A single specimen of *Appendicisporites distocarinatus* occurs at 1805m but may be slightly reworked. *T. apoxyexinus* was not seen but is always extremely rare.

Amongst the dinoflagellates, *Heterosphaeridium* spp and *Circulodinium* spp are the most frequent with *Trithyrodinium* spp fairly consistent to the interval base. Single specimens of *Cribroperidinium edwardsii* at 1647m and 1747m are considered reworked. Youngest *Aptea* sp occurs at 1747m and youngest *Chlamydophorella ambigua* at 1790m and are consistent with the spore-pollen zone. *Conosphaeridium* spp occur rarely as single specimens (*C. striatoconus* at 1616m and 1790m both cuttings, *C. tubulosum* at 1647.0m swc) are presumably in place and consistent with the spore-pollen zone. The existing formal dinoflagellate zones cannot be crisply recognised on these criteria.

Environments are nearshore marine with low dinoflagellate content ((26%), 12%, 22%, 7%, 14%, (24%), 12%, 14%, 14%, (22%), 15%) and low to moderate diversity, coupled with abundant and diverse spores and pollen and mostly inertinite dominated kerogen, occasionally with frequent cuticle.

Yellow to light brown spore colours indicate immaturity for hydrocarbons.

**M 1820m(cutts), 1837.3m(CORE), 1838.1m(CORE), 1839.7m(CORE), 1840.3m(CORE), 1872.5m(sw), 1889m(cutts), 1916m(cutts), 1947.5m(sw), 1949m(cutts) 2003m(cutts), 2027m(cutts), 2035.0(sw), 2061.0m(sw), 2084m(cutts) : mawsonii Zone**

Assignment to the *Phyllocladidites mawsonii* spore-pollen Zone of Coniacian-Turonian age is indicated at the top by youngest consistent *Appendicisporites distocarinatus* (supported by the decline in *A. cruciformis*) and at the base on oldest *P. mawsonii*, supported by oldest *Clavifera triplex* in swcs at 2101.0m. Within the interval, saccate pollen often dominate with *Falcisporites*, *Microcachryidites* and *Podosporites* all common. *Cyathidites* and *Dilwynites* are also frequent to common, although many samples in this interval are of cuttings and may be contaminated. *A.*

*distocarinatus*, *C. triplex* and *P. mawsonii* are rare but consistent and *Cyatheacidites tectifera* and *Coptospora pileosa* are extremely rare. *A. cruciformis* is rare to frequent (2-5%) in cores and swcs above 1872.5m, and very rare to absent beneath. In cuttings, *A. cruciformis* can be common but is considered caved.

Dinoflagellates are generally scarce with *Heterosphaeridium* spp the most frequent but with age diagnostic taxa generally absent. Caving from younger zones is consistent in this largely cuttings sampled interval including *N. aceras*, *A. denticulata*, *O. porifera*, *I. rectangularis* and *Trithyrodinium* spp. At the base, youngest *C. edwardsii* at 2084m indicates the *Palaeohystrichophora infusorioides* dinoflagellate Zone for that sample only.

Environments appear to be mostly nearshore to very nearshore with occasional non-marine beds. Dinoflagellate content is generally low ((17%), absent, 3%, 16%, 13%, 2%, (5%), (13%), absent, (4%), (11%), (14%), 33%, 12%, (15%)) with low to moderate diversity, but this could be an overestimate caused by caving of richer overlying marine section. Environments may therefore be largely non-marine to marginal marine. Spores and pollen are common and diverse with common to abundant cuticle, and significant to common freshwater algae (often 3-10% *Botryococcus*).

Light brown spore colours indicate marginal maturity for oil generation, but immaturity for gas/condensate.

**N 2093m(cutts), 2098.0m(swc), 2101.0m(swc), 2102m(cutts), 2105m(cutts), 2117m(cutts), 2123.0m(swc), 2142.0m(swc) : *distocarinatus* Zone**

Assignment to the *A. distocarinatus* spore-pollen Zone of Cenomanian age is indicated by the presence of *A. distocarinatus* without younger or older indicators. Within the interval, swc yields are variable. In the swcs, *Falcisporites* are very common with *Cyathidites* and *Microcachrydites* common and *Dilwynites* frequent. In the cuttings, *Dilwynites* tend to be more common but are considered caved. Oldest *C. triplex* in swcs occurs at 2101m. *A. distocarinatus*, *A. tricornitatus* and *A. cruciformis* are consistent throughout. Minor Permian and Early Cretaceous reworking was seen.

Amongst the dinoflagellates, *C. edwardsii* occurs in the upper part of the section indicating that 2089, 2093, 2101, 2102 and 2105m all belong to the *P. infusorioides*



dinoflagellate Zone. *C. edwardsii* is most common in the cuttings at 2102m. Of the other taxa, *Heterosphaeridium* and *Spiniferites* are the most frequent.

Nearshore and marginal marine environments are indicated by the low to very low dinoflagellate content (1%, (17%), 16%, (15%), (15%), (15%), 5%, 1% downhole) and their low diversity. These dinoflagellate contents may be too high, as most of the higher values are from cuttings and may be caved. Other features include the dominant and diverse dinoflagellates, common cuticle and significant freshwater algal content (5%, 4%, 1%, 7%, 4%, 12%, 3%, absent downhole).

Light brown spore colours indicate marginal maturity for oil but immaturity for gas/condensate.

**O 2150m(cutts), 2157.5m(swc), 2180m(cutts) : apparently *distocarinatus* Zone.**

The swc is very lean and lacks zone markers and the two cuttings samples contain *A. distocarinatus* without younger or older markers, suggesting the *distocarinatus* spore-pollen Zone of Cenomanian age. This marker could however be caved into these cuttings. *Phyllocladidites eunuchus* also occurs to the interval base but not below. Overall, *Cyathidites*, *Falcisporites* and *Microcachryidites* are the common taxa with the simple fern spores *Gleicheniidites* and *Laevigatosporites* common in the swc only. Minor Permian reworking was seen.

Dinoflagellates only occur at 2180m in cuttings, consist of a single species (*C. edwardsii* suggesting the *infusorioides* dino Zone) but may well be caved.

Non-marine environments with strong lacustrine influence are suggested by the frequent to common freshwater algae (6%, 14% and 4% *Botryococcus* downhole), absence of dinoflagellates (except for 2 possibly caved specimens in cuttings at 2180m) and dominance of rich and diverse spore pollen.

Light brown spore colours indicate marginal maturity for oil and immaturity for gas/condensate.

**P 2212.5m(swc), 2222m(cutts), 2261m(cutts), 2270.0m(swc) : indeterminate**

The swc is extremely lean, almost barren, and cannot be assigned. The cuttings contain a fair assemblage lacking *A. distocarinatus* and the spore influx seen below

and so are very nondescript and not similar to the interval above or the one below. They are considered indeterminate here. *Falcisporites similis* is abundant with common *Cyathidites* spp and *Microcachryidites* and frequent Araucarian pollen and *Osmundacidites wellmanni*. Minor Permian reworking was seen.

Dinoflagellates occur in all three cuttings samples but include obviously caved taxa such as *O.porifera* and *Trithyrodinium* spp. Clearly the entire assemblage may be caved.

Environments appear to be brackish to very nearshore marine with dinoflagellate content of barren, (4%), (2%), (trace) downhole, but the presence of frequent freshwater algae (barren, (4%), (absent), (8%) *Botryococcus* downhole) suggests possible non-marine environments with the dinoflagellates all caved. Common cuticle and dominant and diverse spore-pollen are consistent.

Light brown spore colours indicate marginal maturity for oil, but immaturity for gas/condensate.

**Q 2294.0m(swc), 2318m(cutts), 2321.0m(swc), 2324m(cutts), 2333m(cutts), 2354m(cutts), 2360.0m(swc), 2392.5m(swc), 2408m(cutts), 2412.0m(swc), 2425m(cutts) : possibly *paradoxa* Zone**

Assignment of this interval is not straight forward. Several samples within the interval (2294.5m swc, 2321.0m swc, 2324m cutts, 2392.5m swc) contain richer spore assemblages than above, including youngest *Coptospora paradoxa* (in 3 swcs only), *Crybelosporites striatus*, *Foraminisporis asymmetricus*, *Trilobosporites tribotrys*, *T. trioreticulatus*, *Triporeletes reticulatus* as well as a downhole influx of *Cicatricosisporites australienesis* (5-10%). The swcs also lack *A. distocarinatus*. Usually this richer spore flora is associated with a change to spore dominated assemblages at the top of the Otway Group. Here, however, spores are still mostly minor with assemblages still dominated by saccate pollen (*Falcisporites* and *Microcachryidites*). Thus, although the assemblage is not typical, assignment to the Albian *Coptospora paradoxa* Zone is possible. The unusual assemblages may be related to the lean and unusual sandy lithologies.

Cuttings in this interval generally do contain *A. distocarinatus* and do not contain *C. paradoxa* or the spore influx, and so favour *distocarinatus* zonal assignment. These may however be largely caved into the lean sandy lithologies. The swc at 2412.0m is

extremely lean reflecting the unfavourable lithologies. If shale interbeds had occurred, the data may have been more definitive.

Dinoflagellates are extremely rare, present only in the cuttings samples and are probably all caved. Many are obviously caved, including *C. striatoconus* and *Isabelidium* spp.

Environments are non-marine to slightly brackish as shown by the total absence of dinoflagellates or spiny acritarchs from some samples, and the presence of only very rare spiny acritarchs in others. The rare dinoflagellates are almost certainly all caved. Spores and pollen are common and diverse in most microfloras.

Light to mid brown spore colours indicate early maturity for oil and early marginal maturity for gas/condensate.

#### IV CONCLUSIONS

At the top, the sampled section is Tertiary (Paleocene to Early Eocene) in very nearshore marine and marginally marine environments. Conformably beneath this, the entire Late Cretaceous appears to present although the mid Campanian to earliest Maastrichtian *lillei* Zone is either condensed or lost by unconformity. This section is mostly very nearshore marine to non-marine towards the base (Cenomanian to Coniacian *distocarinatus* to *mawsonii* Zones) and nearshore marine above (Santonian to Maastrichtian *apoxyxinus* to *longus* Zones). At the base, the Albian *paradoxa* Zone usually seen in the Otway Group may be present but unfavourable lithofacies preclude confident assignment.

#### V REFERENCES

- Dettmann ME and Playford G (1969) Palynology of the Australian Cretaceous : a review In Stratigraphy and Palaeontology. Essays in honour of Dorothy Hill, **KSW Campbell ED.** ANU Press, Canberra 174-210
- Helby RJ, Morgan RP and Partridge AD (1987) A palynological zonation of the Australian Mesozoic In Studies in Australian Mesozoic Palynology Assoc. **Australas. Palaeontols. Mem 4** 1-94
- Morgan RP (1992) Overview of new cuttings based Late Cretaceous correlations, Otway Basin, Australia **unpubl. rept. for BHPP**
- Partridge AD (1976) The geological expression of eustacy in the early Tertiary of the Gippsland Basin **APEA J 16(1)** 73-79.

26th May, 1994

NOTE TO: FILE  
FROM: SIMON HORAN  
OUR REF: sth.012:tt  
COPIES:

---

### PALYNOLOGICAL SAMPLES PROCESSING AND SAMPLE EXAMINATION METHODOLOGY

Following discussion with Roger Morgan, the sample processing techniques and sample examination methodology used in palynological studies of the Fergusons Hill-1, Ross Creek-1, Mussel-1, Pecten-1A, Triten-1ST, La Bella-1, Eric the Red-1, Minerva-1, Minerva-2A and Loch Ard-1 is listed below.

Sample processing usually involves the following steps. Extra techniques are only used if required:

- a) digest about 10gm of crushed rock in 50% HF overnight
- b) wash out several times over 10 micron polyester sieve. Acidify with conc HCl if fluorosilicate gel forms
- c) heavy liquid separation used concentrate  $ZnBr_2$  with SG of 2.0
- d) wash out float fraction over 10 micron polyester sieve. Acidify if  $Zn(OH)_2$  precipitate forms
- e) mount a sieved kerogen slide
- f) oxidise in Schutze Solution (conc 30%  $HNO_3$  with crystalline  $KClO_3$ )
- g) wash out over 10 micron polyester sieve
- h) add 5% KOH to dissolve humic acids
- i) wash out over 10 micron polyester sieve
- j) examine under microscope for satisfactory oxidation. Repeat steps (f) to (g) if required
- k) heavy liquid separation using  $ZnBr_2$  solution (SG of 2.0)
- l) wash out float fraction using polyester sieve. Acidify if  $Zn(OH)_2$  precipitate forms
- m) dehydrate onto coverslip
- n) mount microscope slides using Eukitt medium

Sample examination usually involved the following steps:

- a) scan two traverses at a x10 to log the bulk of the assemblage and get some idea of age
- b) scan at x40 and count the first 100 specimens to get percentage contents for each species. From this, saline "Microplankton Content" (%) can be developed to provide an index of marine influence. Where the sample is too lean to provide 100 specimens, frequency is estimated from the specimens

26th May, 1994

- seen with A = abundant, C = common, F = frequent, R = rare
- c) return to x10 to scan at least two large coverslips to log rare species, and finalise age conclusions. Log more slides if required
  - d) develop "Salines Microplankton Diversity" by counting up total species identified of dinoflagellates plus spiny acritarchs, as a second index of marine influence. This count includes species seen both inside and outside the court
  - e) develop "Freshwater Microplankton Content" by totally all freshwater algal elements (*Botryococcus*, *Schizosporis*, *Paralecaneella*, *Leiosphaeridia*, *Nummus*)
  - f) examine sieved kerogen slide for specimens of *Cyathidites* to establish spore colour for Spore colour Maturity Index

AGE	PALYNOLOGICAL ZONES	HIGHEST DATA				LOWEST DATA				
		Preferred Depth	Rtg	Alternate Depth	Rtg	Preferred Depth	Rtg	Alternate Depth	Rtg	
NEOGENE	Plei	T. pleistocenicus								
	Plio	M. lipsus								
	Mio	C. bifurcatus								
		T. bellus								
	Olig	P. tuberculatus								
PALEOGENE		upper N. asperus								
	L.Eb	mid N. asperus								
	Mid Eb	lower N. asperus								
		P. asperopolus								
		upper M. diversus								
		mid M. diversus $\phi/\ast$	563	2		594	0			
		lower M. diversus $\phi/\ast$	617	2		617	0			
		upper L. balmei $\phi$	627	0		651	0			
		lower L. balmei $\phi/\ast$	760	2		760	0			
		upper T. longus $\phi/\ast$	783	0						
LATE CRETACEOUS		lower T. longus $\phi$				839	0	870	?	
		T. lillei								
	Camp	N. senectus $\ast/\phi$	897	2		1166	0			
		up T. apoxyexinus $\phi$	1179	2		1453	2			
		mid T. apoxyexinus $\phi$	1502	1		1597	2			
		low T. apoxyexinus $\phi$	1616	3		1805	1			
		P. mawsonii $\phi/\phi$	1820	3		2089	0			
		A. distocarinatus $\ast/\phi$	2098	2		2142	0	2279	4	
	EARLY CRETACEOUS		P. pannosus							
			upper C. paradoxa $\ast$	?2294						
Alb		lower C. paradoxa $\ast$				?2425				
		C. striatus								
		upper C. hughesi								
	lower C. hughesi									
	F. wonthaggiensis									
	up C. australiensis									

Environments :

- o lacustrine (algal acritarchs).
- $\phi$  non-marine (no or very few 5% algal acritarchs).
- $\ast$  brackish (spiny acritarch, no or very few dinoflagellates 1%).
- $\ast/\phi$  marginal marine (1-5% very low diversity dinoflagellates).
- $\phi$  nearshore marine (6-30% low to medium diversity dinoflagellates).
- $\phi/\phi$  intermediate marine (31-60% medium diversity dinoflagellates).
- $\phi/\ast$  offshore marine (61%-80% medium to high diversity dinoflagellates).
- $\phi$  far offshore marine/oceanic (81%-100% high diversity dinoflagellates and/or planktonic forams).

Confidence Ratings :

- 0 : good to excellent with numerous zone fossils in core/svc.
- 1 : fair with rare zone fossils in core/svc.
- 2 : poor with non-diagnostic assemblage in core/svc. Often occurs next to a distinctive 0 to 1 rating, lacking the zone fossil seen adjacent.
- 3 : good with extinction event (top range) in cuttings.
- 4 : poor to fair with inception event (base range) in cuttings and therefore may be picked too low if caved or too high if swamped by cavings.
- 5 : poor with non-diagnostic assemblage in cuttings. Usually seen adjacent to a higher rating and picked on the absence of key zone fossil.
- 7 : no confidence. Picked as a best guess in very poor data.

Data recorded by : Roger Morgan and Nigel Hooker Sept 83

Data revised by : Roger Morgan April 94

PALYNOLOGICAL DATA SHEET

Basin: OTWAY DINOFLAGELLATE ZONES

ELEVATION: \_\_\_\_\_

KD \_\_\_\_\_

CU \_\_\_\_\_

WELL NAME: MINERVA-1

TOTAL DEPTH: \_\_\_\_\_

AGE	PALYNOLOGICAL ZONES	HIGHEST DATA				LOWEST DATA			
		Preferred Depth	Rtg	Alternate Depth	Rtg	Preferred Depth	Rtg	Alternate Depth	Rtg
LATE CRETACEOUS	M. druggii	783	0			783	0		
	I. korojonense								
	upper X. australis	897	0			897	2		
	lower X. australis	954	1			991	0		
	N. aceras	1054	1			1298	0		
	I. cretaceum	1325	3			1453	0		
	O. porifera	1502	2			1510	4		
	C. striatoconus								
	P. infusorioides	2084	0			2105	4	2101	0

Environments :

- 0 lacustrine (algal acritarchs).
- 1 non-marine (no or very few 5% algal acritarchs).
- \* brackish (spiny acritarch, no or very few dinoflagellates 1%).
- \*/\* marginal marine (1-5% very low diversity dinoflagellates).
- \* nearshore marine (6-30% low to medium diversity dinoflagellates).
- \*/\* intermediate marine (31-60% medium diversity dinoflagellates).
- \*/\* offshore marine (61%-80% medium to high diversity dinoflagellates).
- ⊙ far offshore marine/oceanic (81%-100% high diversity dinoflagellates and/or planktonic forams).

Confidence Ratings :

- 0 : good to excellent with numerous zone fossils in core/svc.
- 1 : fair with rare zone fossils in core/svc.
- 2 : poor with non-diagnostic assemblage in core/svc. Often occurs next to a distinctive 0 to 1 rating, lacking the zone fossil seen adjacent.
- 3 : good with extinction event (top range) in cuttings.
- 4 : poor to fair with inception event (base range) in cuttings and therefore may be picked too low if caved or too high if swamped by cavings.
- 5 : poor with non-diagnostic assemblage in cuttings. Usually seen adjacent to a higher rating and picked on the absence of key zone fossil.
- 7 : no confidence. Picked as a best guess in very poor data.

Data recorded by: Roger Morgan and Nigel Hooker - Sept 83

Data revised by: Roger Morgan April 94



MINERVA #1 - palynological data -

MORGAN PALAEO ASSOCIATES

BOX 171 MAITLAND S.A. AUSTRALIA 5573

PH.(088)322795 FAX.(088)322798

CLIENT: BHPP

WELL: MINERVA #1

FIELD / AREA: OTWAY

ANALYST: ROGER MORGAN

DATE: JULY '93

NOTES: ALL DEPTHS ARE IN METRES

FIGURES REPRESENT PERCENTAGES BASED ON 100 SPECIMEN COUNT

"X" INDICATES RARE PRESENCE OUTSIDE THE COUNT

IN UNCOUNTED SAMPLES "A"= ABUNDANT "C"= COMMON "F"= FEW

"R"= RARE

"X"= VERY RARE

RANGE CHART OF OCCURRENCES BY % & LOWEST APPEARANCE: grouped

	1	2	3	4	5	6	7	8	9	10	11	12	13	14	15	16	17	18	19	20	21	22	23	24	25	26	27	28	29	30	31	32	33	34	35	36	37	38		
	DIMYLLIACELLATE	REINHARDING : CRETAECUS	REINHARDING : PERITHIA	REINHARDING : TRINASSIC	SCHIZOSPORIS RETICULATUS	GOTRYOCOCCLUS	FROMER FRAGILIS	MINIUS HOMOICULATUS	SCHIZOSPORIS PARVIS	SCHIZOSPORIS	SCHIZOSPORIS PSILATA	PHARIBADES	PARALECCHIELLA	CRASSOSPIRERA GONCIANA	VERVANCHIUM	CAUCA SP	HETEROSPIRERIUM HETEROCANTHUM	HETEROSPIRERIUM SOLIDUM	ISABELIINIUM CRETAECUM	HICPHYSTRIDIUM	HETEROSPIRERIUM COMPLEX	CONUSPIRERIUM STRIATOCORNUS	CRIBROPERIDIUM SP	PALAEOPERIDIUM CRETAECUM	CIRCULODINIUM GEFLANDREI	ERODOSPIRERIUM PIRACHTES	ODONTOCHITINA OPERCULATA	ODONTOCHITINA PUKIFERA	ODONTOCHITINA DEKRIKOSUM	TRITHYKODINIUM GLABRUM	CILIMYDOPHORELLA NYEI	HETEROSPIRERIUM CONJUNCTUM	SPINIFERTES FURCATUS RHODUS	TRITHYKODINIUM MANSHELLII PSILATE	HYSPILOCHITINUM PULCHRUM	MONOCHITINA CRISTATA	HELETSOSPIRERIUM	FLUORINIUM DENNETI		
0563.0 SWC	1																																							
0594.0 SWC	3	X	X	X	X																																			
0617.0 SWC	6		X	X	X																																			
0627.0 SWC	10																																							
0651.0 SWC	4		X	X	X																																			
0760.0 SWC	3																																							
0783.0 SWC	42																																							
0810.0 SWC	1																																							
0838.5 SWC	6																																							
0897.0 SWC	2																																							
0954.0 SWC	2		X	X	X																																			
0991.0 SWC	14		X	X	X																																			
1054.0 SWC	4	X	X	X	X																																			
1105.5 SWC	6	X	X	X	X																																			
1149.0 SWC	8																																							
1166.0 SWC	14		2																																					
1179.0 SWC	7																																							
1193.0 SWC	20																																							
1220.0 SWC	12																																							
1260.0 SWC	16		X	X	X																																			
1271 CUTTS	19		X	X	X																																			
1298.0 SWC	21		X	X	X																																			
1325 CUTTS	15																																							
1351.0 SWC	18																																							
1398.0 SWC	12	X	X	X	X																																			
1410 CUTTS	24																																							
1453.0 SWC	8		2																																					
1502.0 SWC	16		X	X	X																																			
1510 CUTTS	31		X	X	X																																			
1562.0 SWC	8		X	X	X																																			
1597.0 SWC	9																																							
1616 CUTTS	1																																							
1629.0 SWC	12		X	X	X																																			
1647.0 SWC	22																																							
1660.0 SWC	7																																							
1690.0 SWC	14																																							
1699 CUTTS	24																																							
1723.0 SWC	12		X	X	X																																			
1747.0 SWC	14		X	X	X																																			
1766.0 SWC	14																																							
1790 CUTTS	22																																							
1805.0 SWC	15																																							
1820 CUTTS	17																																							
1837.3 CORE																																								
1838.1 CORE	3																																							
1839.7 CORE	16																																							
1840.3 CORE	13																																							
1872.5 SWC	2																																							
1886-89 CUTTS	5		X	X	X																																			
1910-16 CUTTS	13																																							
1943-49 CUTTS	4																																							
1947.5 SWC																																								
1997-03 CUTTS	11																																							
2021-27 CUTTS	14		X	X	X																																			
2035.0 SWC	33		X	X	X																																			
2061.0 SWC	12																																							
2084 CUTTS	5																																							
2093 CUTTS	17																																							
2098.0 SWC	1																																							
2101.0 SWC	16																																							
2102 CUTTS	15																																							
2105 CUTTS	15																																							
2117 CUTTS	15																																							
2123.0 SWC	5		2																																					











	191	192	193	194	195	196	197	198	199	200	201	202	203	204	205	206	207	208	209	210	211	212	213	214	215	216	217	218	219	220	221	222	223	224	225	226	227	228		
0563.0 SWC	5																																							
0594.0 SWC																																								
0617.0 SWC	1																																							
0627.0 SWC	2																																							
0651.0 SWC	2																																							
0760.0 SWC	1																																							
0783.0 SWC																																								
0810.0 SWC																																								
0838.5 SWC																																								
0897.0 SWC	1																																							
0954.0 SWC	1																																							
0991.0 SWC																																								
1054.0 SWC	1																																							
1105.5 SWC																																								
1149.0 SWC	1																																							
1166.0 SWC	X																																							
1179.0 SWC	2																																							
1193.0 SWC	1																																							
1220.0 SWC																																								
1260.0 SWC	1																																							
1271 CUTTS																																								
1298.0 SWC																																								
1325 CUTTS																																								
1351.0 SWC																																								
1398.0 SWC																																								
1410 CUTTS																																								
1453.0 SWC																																								
1502.0 SWC																																								
1510 CUTTS																																								
1562.0 SWC	1																																							
1597.0 SWC																																								
1616 CUTTS																																								
1629.0 SWC																																								
1647.0 SWC																																								
1660.0 SWC	1																																							
1690.0 SWC	1																																							
1699 CUTTS																																								
1723.0 SWC																																								
1747.0 SWC	2																																							
1766.0 SWC																																								
1790 CUTTS																																								
1805.0 SWC	X																																							
1820 CUTTS																																								
1837.3 CORE																																								
1838.1 CORE																																								
1839.7 CORE																																								
1840.3 CORE	1																																							
1872.5 SWC	X																																							
1886-89 CUTTS	X																																							
1910-16 CUTTS																																								
1943-49 CUTTS	2																																							
1947.5 SWC	4																																							
1997-03 CUTTS																																								
2021-27 CUTTS																																								
2035.0 SWC	1																																							





Index numbers are the columns in which species appear.

INDEX NUMBER	SPECIES
150	AEQUITRIRADITES SPINULOSUS
178	AEQUITRIRADITES TILCHAENESIS
131	AEQUITRIRADITES VERRUCOSUS
120	ALISOCYSTA MARGARITA
189	AMOSOPOLLIS CRUCIFORMIS
64	AMPHIDIADEMA DENTICULATA
255	ANACOLOADITES ACUTULLUS
124	APECTODINIUM HOMOMORPHUM
177	APPENDICISPORITES DISTOCARINATUS cf
193	APPENDICISPORITES TRICORNITATUS
62	APTEA SP
129	APTEODINIUM AUSTRALENSE
50	APTEODINIUM GRANULATUM
132	ARAUCARIACITES AUSTRALIS
105	AREOLIGERA SP
130	AREOSPHAERIDIUM CAPRICORNUM
100	AREOSPHAERIDIUM SUGGESTIUM
219	ASTEROPOLLIS ASTEROIDES
205	AUSTRALOPOLLIS OBSCURIS
151	BALMEISPORITES HOLODICTYUS
165	BALMEISPORITES TRIDICTYUS
275	BANKSIEAEIDITES ARCUATUS
280	BEAUPREADITES TRIGONALIS
152	BIRETRISPORITES
6	BOTRYOCOCCUS
51	CADDASPHAERA HALOSA
41	CALLAOISPHAERIDIUM ASYMMETRICUM
133	CALLIALASPORITES DAMPIERI
190	CALLIALASPORITES TRILOBATUS
134	CALLIALASPORITES TURBATUS
260	CAMEROZONOSPORITES BULLATUS
265	CAMEROZONOSPORITES LATROBENSIS
206	CAMEROZONOSPORITES OHAIENSIS
195	CAMEROZONOSPORITES ROBUSTA
200	CAMEROZONOSPORITES SP
72	CANNINGIA SPINOSA
58	CASSIDIUM SP
16	CAUCA SP
166	CERATOSPORITES EQUALIS
81	CHATANGIELLA SVERDRUPIANA
87	CHATANGIELLA TRIPARTITA
88	CHATANGIELLA VICTORIENSIS
65	CHLAMYDOPHORELLA AMBIGUA
31	CHLAMYDOPHORELLA NYEI
153	CICATRICOSISPORITES AUSTRALIENSIS
180	CICATRICOSISPORITES FOVEOAUSTRALIENSIS
135	CICATRICOSISPORITES LUDBROOKIAE
215	CICATRICOSISPORITES MEGA AUSTRALIENSIS
228	CICATRICOSISPORITES RADIATUS
183	CINGUTRILETES CLAVUS
25	CIRCULODINIUM DEFLANDREI
66	CIRCULODINIUM SOLIDA
204	CLAVIFERA TRIPLEX
37	CLEISTOSPHAERIDIUM
182	CONCAVISSIMISPORITES PENOLAENSIS
22	CONOSPHAERIDIUM STRIATOCONUS
83	CONOSPHAERIDIUM TUBULOSUM
154	CONTIGNISPORITES COOKSONIAE
213	CONTIGNISPORITES GLEBULENTUS
167	COPTOSPORA PARADOXA
207	COPTOSPORA PILEOSA
155	COPTOSPORA WRINKLY
111	CORDOSPHAERIDIUM INODES
156	COROLLINA TOROSUS
67	CORONIFERA
14	CRASSOSPHAERA CONCINNA
194	CRIBROPERIDINIUM EDWARDSII
23	CRIBROPERIDINIUM SP
136	CRYBELOSPORITES STRIATUS
276	CUPANEIDITES ORTHOTEICHUS
198	CYATHEACIDITES TECTIFERA
137	CYATHIDITES AUSTRALIS
256	CYATHIDITES GIGANTIS
138	CYATHIDITES MINOR
168	CYCADOPITES FOLLICULARIS
55	CYCLONEPHELIUM COMPACTUM
46	CYMATIOSPHAERA
112	DEFLANDREA DILWYNENSIS
125	DEFLANDREA OBLIQUIPES

53 NELSONIELLA ACERAS  
104 NELSONIELLA SEMIRETICULATA  
103 NELSONIELLA TUBERCULATA  
210 NEORAISTRICKIA  
208 NEVESISPORITES  
257 NOTHOFAGIDITES BRACHYSPINOLOSUS  
262 NOTHOFAGIDITES EMARCIDUS  
237 NOTHOFAGIDITES ENDURUS  
246 NOTHOFAGIDITES FLEMINGII  
234 NOTHOFAGIDITES PROTO ENDURUS  
224 NOTHOFAGIDITES PROTO SENECTUS  
214 NOTHOFAGIDITES SENECTUS  
8 NUMMUS MONOCULATUS  
59 OCCISUCYSTA SP  
73 ODOTCHITINA OBESA  
36 ODONTOCHITINA COSTATA  
57 ODONTOCHITINA CRIBROPODA  
54 ODONTOCHITINA NO HORNS  
96 ODONTOCHITINA OBESOPORIFERA  
27 ODONTOCHITINA OPERCULATA  
28 ODONTOCHITINA PORIFERA  
43 ODONTOCHITINA STUBBY  
60 ODONTOCHITINA VERY STUBBY  
21 OLIGOSPHAERIDIUM COMPLEX  
71 OLIGOSPHAERIDIUM DICTYOPHORUM  
40 OLIGOSPHAERIDIUM PULCHERRINUM  
116 OPERCULODINIUM  
225 ORNAMENTIFERA MINIMA  
220 ORNAMENTIFERA SENTOSA  
143 OSMUNDACIDITES WELLMANII  
29 OVOIDINIUM VERRUCOSUM  
44 PALAEOHYSTRICHOSPHORA INFUSORIOIDES  
24 PALAEOPERIDIUM CRETACEUM  
12 PALAMBAGES  
13 PARALECANIELLA  
199 PERINOPOLLENITES ELATOIDES  
271 PERIPOROPOLLENITES DEMARCATUS  
231 PERIPOROPOLLENITES POLYORATUS  
281 PERIPOROPOLLENITES VESICUS  
144 PEROTRILETES JUBATUS/MORGANII  
186 PEROTRILETES MAJUS  
161 PEROTRILETES WHITFORDENSIS  
211 PHIMOPOLLENITES PANNOSUS  
192 PHYLLOCLADIDITES EUNUCHUS  
197 PHYLLOCLADIDITES MAWSONII  
232 PHYLLOCLADIDITES VERRUCATUS  
181 PILOSPORITES NOTENSIS  
145 PODOSPORITES MICROSACCATUS  
203 PROTEACIDITES SP  
263 PROTEACIDITES ANNULARIS  
267 PROTEACIDITES BUN GRANDIS  
264 PROTEACIDITES GRANDIS  
251 PROTEACIDITES HAPUKUI  
272 PROTEACIDITES INCURVATIS  
277 PROTEACIDITES KOPIENSIS  
226 PROTEACIDITES LARGE  
273 PROTEACIDITES ORNATUS  
268 PROTEACIDITES OTWAYENSIS  
274 PROTEACIDITES PACHYPOLUS  
252 PROTEACIDITES RETICULOCONCAVUS  
282 PROTEACIDITES TUBERCULIFORMIS  
48 PTEROSPERMELLA AUSTRALIENSIS  
146 RETITRILETES AUSTRICLAVATIDITES  
217 RETITRILETES CIRCOLUMENUS  
187 RETITRILETES FACETUS  
2 REWORKING : CRETACEOUS  
3 REWORKING : PERMIAN  
4 REWORKING ; TRIASSIC  
10 SCHIZOSPORIS  
9 SCHIZOSPORIS PARVUS  
11 SCHIZOSPORIS PSILATA  
5 SCHIZOSPORIS RETICULATUS  
162 SENECTOTETRADITES VARIRETICULATUS  
238 SESTROSPORITES PSEUDOALVEOLATUS  
89 SPINIDIUM SP  
33 SPINIFERITES FURCATUS/RAMOSUS  
209 SPINOZONOCOLPITES PROMINATUS  
188 STERIESPORITES ANTIQUASPORITES  
253 STERIESPORITES PUNCTATUS  
110 TANYOSPHAERIDIUM "GRANULATUM"  
91 TANYOSPHAERIDIUM SALPINX  
269 TETRACOLPORITES OAMARUENSIS  
247 TETRACOLPORITES VERRUCOSUS  
117 THALASSIPHORA DELICATA

125 DEFLANDREA OBLIQUIPES  
128 DEFLANDREA PACHYCERAS  
113 DEFLANDREA SPECIOSA  
118 DEFLANDREA TRUNCATA  
201 DENSOISPORITES VELATUS  
97 DICONODINIUM PUSILLUM  
157 DICTYOPHYLLIDITES  
173 DICTYOTOSPORITES COMPLEX  
242 DICTYOTOSPORITES FILOSUS  
216 DICTYOTOSPORITES SPECIOSUS  
158 DILWYNITES GRANULATUS  
227 DILWYNITES TUBERULATUS  
1 DINOFLAGELLATE CONTENT  
98 DINOGYMNIIUM ACUMINATUM  
121 DIPHYES COLLIGERUM  
82 DISPHAERIA MACROPYLA  
114 EOCLADOPYXIS PENICULATA  
239 ERICIPITES SCABRATUS  
74 ESCHARISPHAERIDIUM SP  
102 EUCLADINIUM MADURENSE  
26 EXOCHOSPHAERIDIUM PHRAGMITES  
139 FALCISPORITES GRANDIS  
140 FALCISPORITES SIMILIS  
126 FIBROCYSTA BIPOLARIS  
122 FIBROCYSTA VECTENSE  
38 FLORENTINIA DEANEI  
159 FORAMINISPORIS ASYMMETRICUS  
184 FORAMINISPORIS DAILYI  
160 FORAMINISPORIS WONTHAGGIENSIS  
202 FOVEOGLEICHENIIDITES  
169 FOVEOTRILETES PARVIRETUS  
7 FROMEA FRAGILIS  
244 GAMBIERINA EDWARDSI  
243 GAMBIERINA RUDATA  
236 GAMBIERINA TWISTED  
92 GILLINIA HYMENOPHORA  
119 GLAPHYROCYSTA DIVARICATUM  
123 GLAPHYROCYSTA cf MEDUSETTIFORMIS  
174 GLEICHENIIDITES  
115 HAFNIACYSTA SEPTATA  
261 HALORAGACIDITES HARRISII  
241 HERKOSPORITES ELLIOTTI  
32 HETEROSPHAERIDIUM CONJUNCTUM  
17 HETEROSPHAERIDIUM HETEROCANTHUM  
93 HETEROSPHAERIDIUM LATEROBRACHIUS cf  
18 HETEROSPHAERIDIUM SOLIDA  
77 HYSTRICHODINIUM FURCATUM  
35 HYSTRICHODINIUM PULCHRUM  
127 HYSTRICHOSPHAERIDIUM TUBIFERUM  
223 INTERULOBITES INTRAVERRUCATUS  
78 ISABELIDINIUM BALMEI  
56 ISABELIDINIUM BELFASTENSE  
45 ISABELIDINIUM COOKSONAE  
19 ISABELIDINIUM CRETACEUM  
68 ISABELIDINIUM KOROJONENSE  
106 ISABELIDINIUM PELLUCIDUM  
63 ISABELIDINIUM RECTANGULARE  
90 ISABELIDINIUM RECTANGULARE CONTRACTUM  
75 ISABELIDINIUM SP  
94 ISABELIDINIUM THOMASII  
95 ISABELIDINIUM TRIPARITA  
175 ISCHYOSPORITES PUNCTATUS  
39 KIOKANSIUM POLYPES  
107 KIOKANSIUM SP  
141 KLUKISPORITES SCABERIS  
191 LAEVIGATOSPORITES OVATUS  
185 LEPTOLEPIDITES MAJOR  
170 LEPTOLEPIDITES VERRUCATUS  
233 LILIACIDITES  
196 LILIACIDITES KAITANGATAENSIS  
179 LYCOPODIACIDITES ASPERATUS  
245 LYGISTIPOLLENITES BALMEI  
229 LYGISTIPOLLENITES FLORINII  
101 MADURADINIUM PENTAGONUM  
270 MALVACIPOLLIS DIVERSUS  
266 MALVACIPOLLIS SUBTILIS  
108 MANUMIELLA CORONATA  
109 MANUMIELLA DRUGGII  
20 MICRHYSTRIDIUM  
142 MICROCACHRYIDITES ANTARCTICUS  
42 MICRODINIUM ORNATUM  
52 MICRODINIUM SP  
47 MILLIOUDIDIUM  
53 NELSONIELLA ACERAS

117 THALASSIPHORA DELICATA  
76 TRICHODINIUM  
240 TRICOLPITES "MINOR"  
230 TRICOLPITES CONFESSUS  
222 TRICOLPITES GILLII  
248 TRICOLPITES LONGUS  
235 TRICOLPITES SABULOSUS  
218 TRICOLPITES SP  
212 TRICOLPITES VARIVERRUCATUS  
258 TRICOLPITES WAIPAWAENSIS  
278 TRICOLPORITES  
221 TRICOLPORITES APOXYEXINUS  
249 TRICOLPORITES LILLIEI  
254 TRILETES TUBERCULIFORMIS  
163 TRILOBOSPORITES TRIBOTRYS  
147 TRILOBOSPORITES TRIORETICULOSUS  
171 TRIPOROLETES BIRETICULATUS  
172 TRIPOROLETES RADIATUS  
148 TRIPOROLETES RETICULATUS  
164 TRIPOROLETES SIMPLEX  
279 TRIPOROPOLLENITES AMGIBUUS  
250 TRIPOROPOLLENITES SECTILIS  
99 TRITHYRODINIUM  
79 TRITHYRODINIUM FINE GRANULATE  
30 TRITHYRODINIUM GLABRUM  
84 TRITHYRODINIUM MARSHALLII  
34 TRITHYRODINIUM MARSHALLII PSILATE  
85 TRITHYRODINIUM PUNCTATE  
61 TRITHYRODINIUM RETIC "THICK"  
69 TRITHYRODINIUM SUSPECTUM  
70 TRITHYRODINIUM THICK VERMIC  
149 VELOSPORITES TRIQUETRUS  
259 VERRUCOSISPORITES KOPUKUENSIS  
15 VERYHACHIUM  
176 VITREISPORITES PALLIDUS  
80 XENASCUS CERATOIDES  
86 XENIKOON AUSTRALIS  
49 XIPHOPHORIDIUM ALATUM

# MORGAN PALAEO ASSOCIATES

PALYNOLOGICAL/PETROLEUM GEOLOGICAL CONSULTANTS

POSTAL ADDRESS: Box 161, Maitland, South Australia 5573  
DELIVERIES: 1 Shannon Tce, Maitland, South Australia 5573  
Phone (088) 32 2795 Fax (088) 32 2798

EXPLORATION PETROLEUM PTY. LTD.

DO NOT RETAIN IN PERSONAL FILES

FILE COPY

PLEASE RETURN TO  
EXPLORATION INFORMATION  
CENTRE

## PALYNOLOGY OF 6 NEW SAMPLES FROM MINERVA-1

### OTWAY BASIN, AUSTRALIA

BY

ROGER MORGAN

APRIL 1994

#### I SUMMARY

860-70m(cutts) : apparently *longus* Zone but may be caved (*balmei* and *longus* elements caving to mask *lillei* Zone) : apparently Maastrichtian : very nearshore : immature.

2089.0m(swc) : *mawsonii* Zone (*infusorioides* dino Zone) : Coniacian-Turonian : very nearshore : marginally mature.

2215.0m(swc) : almost barren and indeterminate.

2273-79m(cutts) : *distocarinatus* Zone : Cenomanian : non-marine lacustrine : marginally mature.

2319.0m(swc), 2359.5m(swc) : possibly *paradoxa* Zone but not typically so (identical to earlier samples) : possibly Albian : slightly brackish : early mature for oil.

#### II INTRODUCTION

These samples were submitted by Simon Horan to clarify aspects of the palynology as reported at well completion. The zonation used is that for Minerva-1 (Morgan and Hooker 1994). Raw data is presented in Appendix I.



**D 2273-79m(cutts) : *distocarinatus* Zone**

Assignment to the *A. distocarinatus* Spore Pollen Zone is indicated by the presence of *A. distocarinatus* without younger or older markers. *Falcisporites* spp. are abundant with *Cyathidites* and *Microcachryidites* frequent. Minor Permian reworking was seen.

Non-marine environments are indicated by the total lack of dinoflagellates and the abundant and diverse spore pollen. Common freshwater algae (13% *Botryococcus*) suggest a lake environment.

Light brown spore colour indicates marginal maturity for oil and immaturity for gas/condensate.

**E 2319.0m(swc), 2359.5m(swc) : possibly *paradoxa* Zone**

Both assemblages are rather bland, dominated by common to abundant *Falcisporites* with common *Cyathidites* and *Microcachryidites*. *A. distocarinatus* was absent, *C. paradoxa* extremely rare at 2319m only, and *F. asymmetricus* very rare in both samples. *Cicatricosisporites australiensis* was consistent in both (4% and 2% downhole). Overall, the assemblage is identical to those already described from Minerva-1 but lacks the spore diversity and frequency of *C. paradoxa* normally seen in the Eumeralla Formation. As previously discussed this may be due to the sandy lithofacies. The samples are therefore considered "possibly *paradoxa* Zone, but not typically so."

Extremely rare spiny acritarchs (<1% and 2% downhole) and diverse and abundant spore pollen indicate brackish environments.

Mid to light brown spore colours indicate early maturity for oil but early marginal maturity for gas/condensate.

#### IV CONCLUSIONS

The 870m sample suggests that the *lillei* Zone is extremely or faulted out in the sample gap 870m to 897m. The logs also suggest some lost section at this point, relative to Minerva-2A.

The 2087m sample extends the base of the *mawsonii* Zone down the well by 3m and places it within the distinctive basal *mawsonii* claystone marker.

The 2215.0m swc was intended to document the *distocarinatus* Zone but was too lean to provide definitive data. The cuttings at 2279m extends the *distocarinatus* Zone down to close to the top of the "Eumeralla Sands."

The two basal swcs were intended to document the assemblage in the "Eumeralla Sands" and hopefully provide an undisputed *paradoxa* assignment. The assemblages were not significantly different from those described earlier.

#### V REFERENCES

Morgan R and Hooker N (1993) Final palynology of BHPP Minerva-1, offshore Otway Basin, Victoria, Australia unpubl. rept. for BHPP.

OTW.MINERV6



BASIN: OTWAY SPORE-POLEN ZONES ELEVATION: KP \_\_\_\_\_ GL: \_\_\_\_\_  
 WELL NAME: MINERVA-1 TOTAL DEPTH: \_\_\_\_\_

AGE	PALYNOLOGICAL ZONES	HIGHEST DATA				LOWEST DATA			
		Preferred Depth	Rtg	Alternate Depth	Rtg	Preferred Depth	Rtg	Alternate Depth	Rtg
NEOGENE	Plei	T. pleistocenicus							
	Plio	M. lipsus							
	Mio	C. bifurcatus							
		T. bellus							
	Olig	P. tuberculatus							
PALEOGENE	L.Eb	upper N. asperus							
	Mid Eb	mid N. asperus							
		lower N. asperus							
	Parl Eb	P. asperopolus							
		upper M. diversus							
	Eo	mid M. diversus	563	2		594	0		
		lower M. diversus	617	2		617	0		
		upper L. balmei	627	0		651	0		
	Fale	lower L. balmei	760	2		760	0		
		Bas	upper T. longus	783	0				
lower T. longus					839	0	870	?	
LATE CRETACEOUS	Camp	T. lillei							
		N. senectus	897	2		1166	0		
	Sant	up T. apoxyxinus	1179	2		1453	2		
		mid T. apoxyxinus	1502	1		1597	2		
	Con	low T. apoxyxinus	1616	3		1805	1		
	Ar	P. mawsonii	1820	3		2089	0		
	Per	A. distocarinatus	2098	2		2142	0	2279	4
EARLY CRETACEOUS	Alb	P. pannosus							
		upper C. paradoxa	2294						
		lower C. paradoxa				2425			
	Act	upper C. hughesi							
		lower C. hughesi							
	L.Ne	F. wonthaggiensis							
E.Ne	up C. australiensis								

Environments :

- 0 lacustrine (algal acritarchs).
- Ø non-marine (no or very few 5% algal acritarchs).
- \* brackish (spiny acritarch, no or very few dinoflagellates 1%).
- \*/Ø marginal marine (1-5% very low diversity dinoflagellates).
- Ø nearshore marine (6-30% low to medium diversity dinoflagellates).
- Ø/Ø intermediate marine (31-60% medium diversity dinoflagellates).
- Ø/Ø offshore marine (61%-80% medium to high diversity dinoflagellates).
- Ø far offshore marine/oceanic (81%-100% high diversity dinoflagellates and/or planktonic forams).

Confidence Ratings :

- 0 : good to excellent with numerous zone fossils in core/svc.
- 1 : fair with rare zone fossils in core/svc.
- 2 : poor with non-diagnostic assemblage in core/svc. Often occurs next to a distinctive 0 to 1 rating, lacking the zone fossil seen adjacent.
- 3 : good with extinction event (top range) in cuttings.
- 4 : poor to fair with inception event (base range) in cuttings and therefore may be picked too low if caved or too high if swamped by cavings.
- 5 : poor with non-diagnostic assemblage in cuttings. Usually seen adjacent to a higher rating and picked on the absence of key zone fossil.
- 7 : no confidence. Picked as a best guess in very poor data.

Data recorded by : Roger Morgan and Nigel Hooker Sept 83  
 Data revised by : Roger Morgan April 94



26th May, 1994

NOTE TO: FILE  
FROM: SIMON HORAN  
OUR REF: sth.012:tt  
COPIES:

---

### PALYNOLOGICAL SAMPLES PROCESSING AND SAMPLE EXAMINATION METHODOLOGY

Following discussion with Roger Morgan, the sample processing techniques and sample examination methodology used in palynological studies of the Fergusons Hill-1, Ross Creek-1, Mussel-1, Pecten-1A, Triten-1ST, La Bella-1, Eric the Red-1, Minerva-1, Minerva-2A and Loch Ard-1 is listed below.

Sample processing usually involves the following steps. Extra techniques are only used if required:

- a) digest about 10gm of crushed rock in 50% HF overnight
- b) wash out several times over 10 micron polyester sieve. Acidify with conc HCl if fluorosilicate gel forms
- c) heavy liquid separation used concentrate  $ZnBr_2$  with SG of 2.0
- d) wash out float fraction over 10 micron polyester sieve. Acidify if  $Zn(OH)_2$  precipitate forms
- e) mount a sieved kerogen slide
- f) oxidise in Schutze Solution (conc 30%  $HNO_3$  with crystalline  $KClO_3$ )
- g) wash out over 10 micron polyester sieve
- h) add 5% KOH to dissolve humic acids
- i) wash out over 10 micron polyester sieve
- j) examine under microscope for satisfactory oxidation. Repeat steps (f) to (g) if required
- k) heavy liquid separation using  $ZnBr_2$  solution (SG of 2.0)
- l) wash out float fraction using polyester sieve. Acidify if  $Zn(OH)_2$  precipitate forms
- m) dehydrate onto coverslip
- n) mount microscope slides using Eukitt medium

Sample examination usually involved the following steps:

- a) scan two traverses at a x10 to log the bulk of the assemblage and get some idea of age
- b) scan at x40 and count the first 100 specimens to get percentage contents for each species. From this, saline "Microplankton Content" (%) can be developed to provide an index of marine influence. Where the sample is too lean to provide 100 specimens, frequency is estimated from the specimens

26th May, 1994

- seen with A = abundant, C = common, F = frequent, R = rare
- c) return to x10 to scan at least two large coverslips to log rare species, and finalise age conclusions. Log more slides if required
  - d) develop "Salines Microplankton Diversity" by counting up total species identified of dinoflagellates plus spiny acritarchs, as a second index of marine influence. This count includes species seen both inside and outside the court
  - e) develop "Freshwater Microplankton Content" by totalling all freshwater algal elements (*Botryococcus*, *Schizosporis*, *Paralecaneella*, *Leiosphaeridia*, *Nummus*)
  - f) examine sieved kerogen slide for specimens of *Cyathidites* to establish spore colour for Spore colour Maturity Index

MINERVA #1 .. 6 infill samples ..

MORGAN PALAEO ASSOCIATES : Palynological Consultants  
 Box 161, Maitland, South Australia, 5573  
 Phone (088) 322795 ... Fax (088) 322798

C L I E N T: BHPP

W E L L: MINERVA #1: 6 INFILL SAMPLES

F I E L D / A R E A: OFFSHORE OTWAY BASIN

A N A L Y S T: Roger Morgan Ph.D.

D A T E: February '94

N O T E S: all sample depths are in metres

all figures are percentages in a 100 specimen count

"X" indicates rare presence outside the grain count

in uncounted samples "A" = Abundant "C" = Common

"F" = Frequent "R" = Rare

RANGE CHART OF OCCURRENCES BY HIGHEST APPEARANCE: by groups

	1	2	3	4	5	6	7	8	9	10	11	12	13	14	15	16	17	18	19	20	21	22	
BOTRYOCOCCUS																							
APTEA SP																							
DEFLANDREA SPECIOSUS																							
MANUIELLA CORONATA																							
MICHRYSIIDIUM SP																							
NUMMUS																							
OLIGOSPHAERIDIUM COMPLEX																							
SPINIFERITES FURCATUS/RAMOSUS																							
TRICOLPITES CONFESSUS																							
CRIBROPERIDIUM EDWARDSII																							
HETEROSPHAERIDIUM HETEROANTHUM																							
VERYACHIUM																							
AQUITRIRADITES VERRUCOSUS																							
ANOSOPOLLIS CRUCIFORMIS																							
CAMEROZONOSPORITES OHAIENSIS																							
CAMEROZONOSPORITES ROBUSTA																							
CERATOSPORITES EQUALIS																							
CICATRICOSPORITES AUSTRALIENSIS																							
CLAVIFERA TRIPLEX																							
CYATHIDITES AUSTRALIS																							
CYATHIDITES MINOR																							
DILUVINITES GRANULATUS																							
360-70 CUTTS	1	X	X	1	3	1	X	X	1	.	.	.	X	X	1	X	3	1	0	1	2	10	
389.0 SWC	.	.	.	.	.	2	1	1	.	X	2	.	.	.	.	.	1	1	.	7	18	10	
415.0 SWC	.	.	.	.	.	.	.	.	.	.	.	.	.	.	.	.	.	.	.	.	R	.	
473-79 CUTTS	13	.	.	.	.	.	.	.	.	.	.	.	.	.	.	.	1	.	.	.	6	.	
419.0 SWC	.	.	.	.	.	.	.	.	.	.	.	X	.	.	.	.	.	4	.	7	18	2	
459.5 SWC	.	.	.	.	2	.	.	.	.	.	.	.	.	.	.	.	2	2	.	6	17	.	





PEROTRILETES JUBATUS/MORGANII

TRIPOROLETES RADIATUS

CYCADOPITES FOLLICULARIS

REWORKING: TRIASSIC

67

68

69

70

0860-70 CUTTS	.	.	.	.	0860-70 CUTTS
2089.0 SWC	.	.	.	.	2089.0 SWC
2215.0 SWC	.	.	.	.	2215.0 SWC
2273-79 CUTTS	.	.	.	.	2273-79 CUTTS
2319.0 SWC	X	1	.	2	2319.0 SWC
2359.5 SWC	.	.	3	.	2359.5 SWC



SPECIES LOCATION INDEX

and numbers are the columns in which species appear.

INDEX NUMBER	SPECIES
13	AEQUITRIRADITES VERRUCOSUS
14	AMOSOPOLLIS CRUCIFORMIS
54	APPENDICISPORITES DISTOCARINATUS
2	APTEA SP
51	ARAUCARIACITES AUSTRALIS
52	BALMEISPORITES HOLODICTYUS
1	BOTRYOCOCCUS
55	CALLIALASPORITES DAMPIERI
56	CALLIALASPORITES TURBATUS
15	CAMEROZONOSPORITES OHAIENSIS
16	CAMEROZONOSPORITES ROBUSTA
17	CERATOSPORITES EQUALIS
18	CICATRICOSISPORITES AUSTRALIENSIS
61	CICATRICOSISPORITES LUDBROOKIAE
19	CLAVIFERA TRIPLEX
62	COPTOSPORA PARADOXA
57	COPTOSPORA PILEOSA
58	COROLLINA TOROSUS
10	CRIBROPERIDINIUM EDWARDSII
63	CRYBELOSPORITES STRIATUS
20	CYATHIDITES AUSTRALIS
5	CYATHIDITES GIGANTIS
21	CYATHIDITES MINOR
69	CYCADOPITES FOLLICULARIS
3	DEFLANDREA SPECIOSUS
22	DILWYNITES GRANULATUS
23	ERICIPITES SCABRATUS
24	FALCISPORITES GRANDIS
25	FALCISPORITES SIMILIS
64	FORAMINISPORIS ASYMMETRICUS

26 GAMBIERINA EDWARDSII  
27 GAMBIERINA RUDATA  
28 GLEICHENIIDITES  
29 HALORAGACIDITES HARRISII  
11 HETEROSPHAERIDIUM HETEROCANTHUM  
30 ISABELIDINIUM PELLUCIDA  
60 ISCHYOSPORITES PUNCTATUS  
31 LAEVIGATOSPORITES OVATUS  
66 LEPTOLEPIDITES VERRUCATUS  
32 LYGISTIPOLLENITES BALMEI  
33 LYGISTIPOLLENITES FLORINII  
4 MANUMIELLA CORONATA  
5 MICHRYSTIIDIDIUM SP  
34 MICROCACHRYIDITES ANTARCTICUS  
35 NOTHOFAGUS ENDURUS  
6 NUMMUS  
7 OLIGOSPHAERIDIUM COMPLEX  
36 OSMUNDACIDITES WELLMANII  
67 PEROTRILETES JUBATUS/MORGANII  
37 PHYLLOCLADIDITES MAWSONII  
38 PODOSPORITES MICROSACCATUS  
39 POLYPOROPOLLENITES POLYORATUS  
40 PROTEACIDITES  
41 RETITRILETES AUSTRICLAVATIDITES  
70 REWORKING: TRIASSIC  
8 SPINIFERITES FURCATUS/RAMOSUS  
42 STEREISPORITES ANTIQUISPORITES  
9 TRICOLPITES CONFESSUS  
43 TRICOLPITES GILLII  
44 TRICOLPITES LONGUS  
45 TRICOLPITES SABULOSUS  
46 TRICOLPITES WAIPAWAENSIS  
47 TRICOLPORITES APOXYEXINUS  
48 TRICOLPORITES LILLIEI  
68 TRIPOROLETES RADIATUS  
49 TRIPOROLETES RETICULATUS  
50 TRIPOROPOLLENITES SECTILIS  
12 VERYHACHIUM  
53 VITREISPORITES PALLIDUS



**PETROLOGY REPORT**  
**MINERVA #1**



**PETROLOGY REPORT**

**MINERVA #1**

**OTWAY BASIN**

Report prepared for BHP Petroleum Pty Ltd

by

**Dr S E PHILLIPS**

ACS LABORATORIES PTY LTD  
31 Flemington St  
Frewville SA 5063

December 1993

ACS Laboratories Pty Ltd shall not be liable or responsible for any loss, cost, damages or expenses incurred by the client, or any other person or company, resulting from any information or interpretation given in this report. In no case shall ACS Laboratories Pty Ltd be responsible for consequential damages including, but not limited to, lost profits, damages for failure to meet deadlines and lost production arising from this report.

## CONTENTS

	PAGE
1. SUMMARY	3
2. INTRODUCTION	7
3. METHODS	8
4. PETROLOGY	
4.1 Minerva #1, Core plug 9, depth 1823.47m	9
4.2 Minerva #1, Core plug 11, depth 1824.00m	11
4.3 Minerva #1, Core plug 12, depth 1828.15m	16
4.4 Minerva #1, Core plug 17, depth 1829.57m	18
4.5 Minerva #1, Core plug 18, depth 1829.87m	23
4.6 Minerva #1, Core plug 30, depth 1833.50m	28
4.7 Minerva #1, Core plug 34, depth 1834.70m	35
4.8 Minerva #1, Core plug 37, depth 1835.60m	38
4.9 Minerva #1, Core plug 49, depth 1840.60m	41
4.10 Minerva #1, Core plug 52, depth 1842.80m	43
4.11 Minerva #1, Core plug 53, depth 1843.10m	46
4.12 Minerva #1, Core plug 56, depth 1844.05m	48
4.13 Minerva #1, Core plug 58, depth 1844.60m	50
4.14 Minerva #1, Core plug 61, depth 1845.52m	53
4.15 Minerva #1, Core plug 64A, depth 1846.42m	55
4.16 Minerva #1, Core plug 65, depth 1846.72m	58
5. XRD TABLES	64
6. DISCUSSION	65
7. CONCLUSIONS	69
8. GLOSSARY	70

## 1. SUMMARY

BHP Petroleum submitted 16 core plugs from Minerva #1 in the Otway Basin, for detailed petrological analysis. The study was designed to ascertain the factors controlling reservoir quality (clay mineralogy, fracturing and diagenetic alteration) and to identify any changes in sediment provenance between the upper and lower sand units. Selected samples were studied in thin section, by X-ray diffraction and Scanning Electron Microscopy.

All the samples from Minerva #1 have been classified as fine to very coarse grained, poor to well sorted sandstones. For the purposes of this discussion the upper and lower sand units were considered to be separated by a micaceous sandstone at 1840.60m (core plug 49). Quartzarenites tend to be coarser grained and concentrate in the lower sand unit. The lithology, texture and mineralogy of each sample studied is summarised in Table 1. This data is based on thin section, SEM and XRD results.

TABLE 1. SUMMARY OF LITHOLOGY, TEXTURE AND MINERALOGY - MINERVA #1

Core plug	9	11	12	17	18	30	34	37
Depth (m)	1823.47	1824.0	1828.15	1829.57	1829.87	1833.50	1834.70	1835.6
Lithology	Sst	Sublith-arenite	Sst	Quartz-arenite	Sub-arkose	Sublith-arenite	Sst	Sst
Grain size	m-crs	medium	coarse	v crs	vc-gran	fine-m	m-crs	medium
Sorting	poor	p-mod	mod	poor	v poor	mod	mod	mod
Structures	?bedding	-	-	-	-	stylolites	-	-
Framework grains								
Quartz	*	68	*	79	81	62	*	*
Feldspar	*	1	*	tr	5	2	*	*
Lithics	-	4	-	tr	1	9	-	-
Mica	-	2	*	-	*	tr	*	*
Coal	-	-	-	-	tr	-	-	-
Accessory	-	tr	-	tr	tr	tr	-	-
Matrix								
Clay	-	-	*	-	-	4	-	-
Opaque material	-	tr	?	-	-	tr	-	-
Authigenic minerals								
Glaucony	-	2	-	-	-	tr	-	-
Pyrite	-	tr	-	2	2	4	*	*
Kaolin	*	6	*	3	1	10	*	*
Quartz	*	2	*	2	tr	tr	*	*
Illite	-	3	-	-	-	*	-	-
Fe oxide	-	tr	-	-	-	1	-	-
Carbonate	-	-	-	-	-	tr	-	*
Porosity								
Intergranular	*	4	*	10	5	2	*	*
Dissolution	*	7	*	2	2	4	*	*
Intragranular	-	-	-	tr	-	-	-	-
Fractures	-	-	-	-	1	-	-	-
Micropores	*	*	*	*	-	1	-	*
Drilling mud	-	*	-	1	1	-	*	*
Routine core analysis								
Porosity %	15.8	19.6	19.5	12.3	10.3	9.4	13.5	18.6
Permeability mD	1660	229	2076	1874	681	0.72	188	318

Sst = sandstone

m = medium, crs = coarse, v = very, gran = granule, vc = very coarse

mod = moderate, tr = trace, p = poor

Note: all figures are based on visual estimates not point counts. Where the presence of a mineral has been noted in the SEM or XRD it is marked with an \*.

TABLE 1 continued

Core plug	49	52	53	56	58	61	64A	65
Depth (m)	1840.6	1842.8	1843.1	1844.05	1844.6	1845.52	1846.42	1846.72
Lithology	mic Sst	Sst	Sst	Sst	Quartz-arenite	Sst	Quartz-arenite	Quartz-arenite
Grain size	fine	m-crs	v crs	crs	medium	crs	m-v crs	crs
Sorting	mod-well	mod	poor-mod	v poor	well	mod	mod-poor	mod
Structures	-	-	-	-	laminae	-	graded bedding	graded bedding
Framework grains								
Quartz	*	*	*	*	64	*	68	73
Feldspar	*	-	-	*	1	-	tr	tr
Lithics	?	?	?	-	1	-	3	3
Mica	*	*	-	*	tr	*	tr	tr
Coal	-	-	-	-	-	-	tr	tr
Accessory	-	-	-	-	tr	-	tr	tr
Matrix								
Clay	-	-	-	-	-	-	-	-
Opaque material	-	-	-	-	-	-	-	-
Authigenic minerals								
Glaucony	-	-	-	-	-	-	tr	-
Pyrite	*	-	-	-	2	*	tr	tr
Kaolin	*	*	*	*	tr	*	1	1
Quartz	*	*	*	*	16	*	12	10
Illite	*	*	*	-	-	-	-	-
Fe oxide	-	-	-	-	-	-	-	-
Carbonate	-	-	-	-	-	-	-	tr
Porosity								
Intergranular	*	*	*	*	10	*	10	8
Dissolution	*	-	*	*	3	?	5	4
Intragranular	-	-	-	-	-	-	-	-
Fractures	-	-	-	-	-	-	-	-
Micropores	*	*	-	-	tr	-	-	-
Drilling mud	-	*	-	-	2	-	tr	tr
Routine core analysis								
Porosity %	16.4	12.9	15.7	15.2	15.8	15.7	17.7	14.4
Permeability mD	17.2	709	5854	402	647	5641	3022	1371

Sst = sandstone, mic = micaceous

m = medium, crs = coarse, v = very, gran = granule

mod = moderate, tr = trace, p = poor

Note: all figures are based on visual estimates not point counts. Where the presence of a mineral has been noted in the SEM or XRD it is marked with an \*.

Reservoir quality is highly variable and there are a number of different controls. In the lower sand unit relatively high permeability's of 5854 mD (core plug 53, depth 1843.10m), 5641 mD (core plug 61, depth 1845.52m) and 3022 mD (core plug 64A, depth 1846.42m) have been reported from routine core analysis. In this zone permeability has probably been enhanced by fracturing. There are remnants of porosity in the fractures which would further enhance reservoir quality. Primary intergranular pores are dominant in the lower sand unit and in the SEM these appear to be elongate, but this may be an artefact of fracturing.

Reservoir quality has also been influenced by kaolinisation and silicification. Where kaolin is abundant in the upper sand unit, microporosity probably contributes to total porosity. The micropores range in diameter from 5 to 10 microns and occur between single kaolin platelets and between booklets. Permeability is low in those samples that have high percentages of kaolin and/or are dominated by secondary porosity (core plug 11, depth 1824.00m and core plug 30, depth 1833.50m). The secondary pores lack interconnection and where present the pore throats are probably blocked by kaolin. It is possible that the pore filling kaolin in the upper sand could migrate during production but this is unlikely to be a major problem since less than approximately 4% would be pore filling kaolin. Silicification is pronounced in the lower sand



unit where it has reduced pore size and provided a rigid framework to resist mechanical compaction and hence preserve porosity.

Grain size, sorting and bedding have also influenced reservoir quality in some sandstones. Typically where sorting is very poor then porosity and permeability are limited. Where coarse sands have moderate sorting then porosity and permeability are better preserved (eg core plug 12, depth 1828.15m). Bedding would limit vertical permeability in core plug 30 (depth 1833.50m) and possibly core plug 58 (depth 1844.60m).

Mineralogically the samples are mature to submature with a dominance of monocrystalline quartz (62-81%) and minor to trace amounts of alkali feldspars, lithics, mica, coal fragments and accessory minerals (zircon, tourmaline, sphene, epidote, ?monazite and ?amphibole). Detrital clay matrix is rare and only evident in the sublitharenite of core plug 30 (depth 1833.50m) where it represents 4% of the sample and concentrates in stylolites. Authigenic minerals are dominated by quartz and kaolinite with minor to trace amounts of pyrite, glaucony, illite, iron oxide, clinochlore and carbonate. Silicification is concentrated in the lower sand (10-16%) and kaolinite is more abundant (1-10%) in the upper sand. Based on XRD traces the kaolinite is typically well ordered and highly crystalline in the upper sand and slightly less crystalline in the lower sand unit. Kaolinite has replaced grains and filled pores. Grains of glaucony are commonly altered and probably reworked. Pyrite occurs dominantly as framboids (20 to 40 microns diameter) and there is a suggestion of bladed marcasite in the upper sand unit (core plug 30, 1833.50m). Illite, clinochlore and iron oxides are typically present as alteration products probably forming from feldspars, lithics and micas. These alteration products appear to concentrate in the upper sand. Traces of carbonate spar were noted in 3 samples (core plug 30, depth 1833.50m; core plug 37, depth 1835.6m and core plug 65, depth 1846.72m).

Contamination from drilling mud is apparent in thin section, XRD and SEM studies. In thin section the mud is present rimming pores and blocking pore throats. The XRD traces record the presence of barite, halite, sylvite and montmorillonite. In the SEM traces of barium, sylvite and gypsum were noted.

Sediment provenance does not appear to show any dramatic changes between the upper and lower sand units. It would appear to have been derived from granitic and metamorphic terranes with minor ?volcanic and sedimentary input. Subtle changes in provenance at selected times within each sand unit are evident. Highly altered lithics are thought to represent chloritised volcanics but these do not occur in all samples. The occurrence of granule size grains of labile feldspars and polycrystalline quartz in the subarkose of core plug 18 (depth 1829.87m) may suggest a phase of uplift or perhaps close proximity to a granitic sediment source at this time. The apparent concentration of lithics in the upper sand could be attributed to hydraulic sorting rather than a change in sediment provenance.

In terms of depositional environments it is clear that the very coarse sediments of the lower sand unit reflect a high energy regime and where graded bedding is evident there was a waning of energy. Fragments of coal indicate that the depositional environment was probably close to a terrestrial setting. The upper sand unit contains evidence of a shallow marine environment and perhaps phases of exposure and oxidation. Grains of glaucony and glaucony rims on detrital grains in core plug 11 (depth

1824.00m) suggest that there has been minimal reworking of the glaucony. In contrast the glaucony in core plug 30 (depth 1833.50m) shows evidence of oxidation, and ?marcasite was recognised in this sample. Marcasite forms under low temperatures, when conditions are acidic in a near surface environment. Therefore, it is possible that core plug 30 represents a phase of exposure during sedimentation. Core plugs 18 (depth 1829.87m) and 17 (depth 1829.57m) both lack glaucony. This characteristic has probably resulted from the fact that glaucony formation is inhibited by high rates of sedimentation and these are both very coarse sands that would be deposited in a high energy environment. Alternatively these coarse sands may represent a more terrestrial depositional environment.

The most pronounced phases of diagenesis have been the alteration and dissolution of labile grains, precipitation of kaolinite and quartz, mechanical compaction and fracturing. Minor authigenic glaucony, pyrite, illite, carbonate spar, clinochlore and iron oxide are also apparent. The concentration of kaolinite in the upper sand unit and silica in the lower sand unit may indicate that there was no interconnection in the circulation of ground waters between these intervals. Alternatively if the elements for kaolinisation are locally derived this distribution could reflect the lower mineralogical maturity of the upper sand unit. The only other event which is apparent is the development of hydrocarbon envelopes on zircons. These rims could have resulted when either hydrocarbons migrated through this zone, or as a reaction with organic matter in situ. Hydrocarbon envelopes are apparent in clean sands from the lower unit which tends to favour the hypothesis that hydrocarbons have migrated through the sequence. Fractures are partially cemented by crushed grains of quartz and rare quartz overgrowths. There is a slight decrease in silicification away from the fractures. Fractures could have acted as conduits for acidic waters which resulted in the dissolution of labile grains and creation of secondary porosity.

Although there are differences in diagenetic alteration between individual samples and the upper and lower sand units, the overall pattern of diagenetic alteration is similar and has been summarised in Table 2.

TABLE 2. DIAGENETIC ALTERATION

Event	Early	Middle Diagenetic Stage	Late
glauconite	----		
pyrite/marcasite	----		
weathering	----	-----	
compaction		-----	
kaolin	----	-----	
silicification	----		----
dissolution			-----
fractures		?-----	
hydrocarbons			-----

## 2. INTRODUCTION

BHP Petroleum Pty Ltd submitted 16 core plugs from Minerva #1 in the Otway Basin, for detailed petrological analysis. The same samples formed part of a SCAL study undertaken by ACS Laboratories Pty Ltd. The petrology was designed to ascertain the factors controlling reservoir quality (clay mineralogy, fracturing and diagenetic alteration) and to identify any changes in sediment provenance between the upper and lower sand units.

Table 3 below records the services provided and routine core analysis results for each sample:

TABLE 3 SAMPLES AND SERVICES PROVIDED

Core Plug	Depth (m)	Thin Section	XRD	SEM	Porosity (%)	Permeability (mD)
9	1823.47	-	-	*	15.8	1660
11	1824.00	*	*	*	19.6	229
12	1828.15	-	-	*	19.5	2076
17	1829.57	*	*	*	12.3	1874
18	1829.87	*	*	*	10.3	681
30	1833.50	*	*	*	9.4	0.72
34	1834.70	-	*	*	13.5	188
37	1835.60	-	*	*	18.6	318
49	1840.60	-	-	*	16.4	17.2
52	1842.80	-	*	*	12.9	709
53	1843.10	-	-	*	15.7	5854
56	1844.05	-	-	*	15.2	402
58	1844.60	*	-	-	15.8	647
61	1845.52	-	-	*	15.7	5641
64A	1846.42	*	-	-	17.7	3022
65	1846.72	*	*	*	14.4	1371

### 3. METHODS

Core plugs were impregnated with araldite prior to thin section preparation. Blue dye was used in the araldite to facilitate description of porosity and permeability. Thin sections were systematically scanned to determine lithology, composition, porosity and textural relationships. All percentages given in thin section descriptions are based on visual estimates, not point counts. Rock classifications are based on the work of Folk (1974) for clastics and Dunham (1962) for carbonates.

To determine bulk mineralogy by X-ray diffraction, samples were ground in a Siebtechnik mill and back mounted into aluminium holders. Continuous scans were run of these powder pressings from  $3^{\circ}$  to  $75^{\circ}$   $2\theta$ , at  $1^{\circ}$ /minute, using Co K alpha radiation, 50kV and 35mA, on a Philips PW1050 diffractometer. For detailed clay mineralogy a less than 5 micron size fraction was separated. This was done by hand crushing, addition of dispersion solution, mechanical shaking for 10 minutes and settling of the dispersed material in a water column according to Stokes' Law. The less than 5 micron fraction was pipetted off and prepared as an oriented sample on ceramic plates held under vacuum. Samples were saturated with Mg solution and treated with glycerol. Continuous scans of oriented clay samples were run from  $3^{\circ}$  to  $35^{\circ}$   $2\theta$  at  $1^{\circ}$ /minute. Peaks were identified by comparison with JCPDS files stored in a computer program called XPLOt.

Scanning electron microscope (SEM) studies were undertaken on broken segments of samples mounted with araldite on aluminium pin-type stubs. The samples were evaporatively coated with carbon (15nm) and gold/palladium (20nm) prior to viewing in a Philips 505 Scanning Electron Microscope at 20kV. The elemental composition of each mineral photographed was identified using a Tracor Northern (TN 5500) energy dispersive spectrometer.

## 4. PETROLOGY

### 4.1 Minerva #1, Core plug 9, depth 1823.47m

#### Scanning electron microscopy

The sample is a medium to coarse grained, poorly sorted, mineralogically mature sandstone (Fig. 1a). Grains are typically subangular with low sphericity and there is a weak alignment of elongate grains that may indicate bedding. Porosity is a combination of primary intergranular pores and secondary dissolution pores. The latter have resulted from the partial dissolution of feldspars to produce honeycomb pores and other labile grains have been completely removed resulting in grain size pores. Permeability could be restricted by the orientation of grains and the presence of abundant kaolin. However, there would be minor microporosity associated with the kaolin. There is the possibility that some of the kaolin could migrate during production.

Framework grains were identified of quartz and K-feldspars. Authigenic minerals are comprised of quartz and kaolin. Quartz overgrowths are not extensively developed and can be recognised due to euhedral rhombohedra and druse. There appear to be two phases of kaolin which line and partially fill pores, and block pore throats. Subhedral kaolin booklets that are approximately 10 microns in diameter (Fig. 1b) are intermixed with anhedral booklets that are 1 to 2 microns in diameter (Fig. 1c). These booklets are rarely intergrown with the quartz overgrowths.

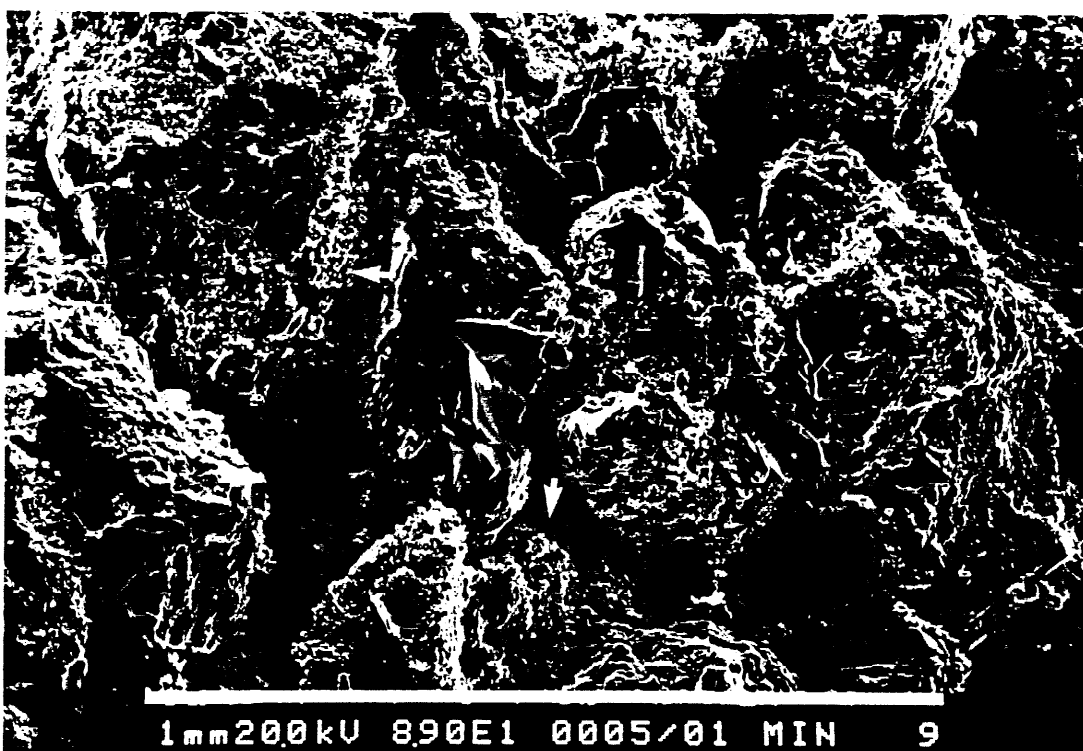


Figure 1a

General view illustrating the subangular nature of grains and poor sorting. Intergranular pores are lined and partially filled by a coating of kaolin (arrows). It is possible that some of the pore filling kaolin was lost during sample preparation. Minerva #1, core plug 9, depth 1823.47m. Scale bar 1mm.



**Figure 1b**

This pore throat is blocked by subhedral kaolin booklets (arrow) that are approximately 10 microns in diameter. Adjacent quartz overgrowths appear to have been inhibited by the kaolin. Minerva #1, core plug 9, depth 1823.47m. Scale bar 0.1mm.



**Figure 1c**

Anhedral kaolin partially filling a pore. The kaolin is intergrown with a quartz overgrowth (arrow). Coarser kaolin is apparent along the margins of the pore. Minerva #1, core plug 9, depth 1823.47m. Scale bar 0.1mm.

#### 4.2 Minerva #1, Core plug 11, depth 1824.00m

##### Thin section description

Rock classification: Sublitharenite

Texture:

The sample is a medium grained, poor to moderately sorted, mineralogically and texturally submature sublitharenite (Fig. 2). Grains range in diameter from 0.07mm (very fine sand) to 2.2mm (granules) and are typically subangular with low sphericity. Granules are rare and a minor percentage is comprised of polycrystalline quartz. Texturally the sample is grain supported with dominantly tangential and concavo-convex grain contacts. There are no sedimentary structures apparent. Deformation of lithics, rare sutured grain contacts and bent micas indicate that there has been moderate mechanical compaction.

Porosity:

Porosity is a combination of primary and secondary pores. The primary pores are intergranular in nature but interconnection has been limited by compaction. Secondary pores are grain sized and due to the removal of labile grains. Feldspars have been partially corroded to produce honeycomb porosity. The relatively high percentage of secondary pores would slightly limit permeability due to the lack of interconnection between these pores.

Visual Estimate of Composition		%
Framework grains	Quartz	68
	Feldspars	1
	Lithics	4
	Mica	2
	Accessory minerals	tr
Matrix	Opaque material	tr
Authigenic minerals and cements	Glaucony/glauconite	2
	Pyrite	tr
	Kaolin	6
	Quartz	2
	Illite	3
Porosity	Iron oxide	tr
	Intergranular	4
	Dissolution	7

Framework grains:

Monocrystalline quartz has straight to slightly undulose extinction, vacuoles scattered throughout the crystal and rare mineral inclusions of apatite, mica, rutile needles and tourmaline. Polycrystalline quartz has undulose extinction and straight crystal boundaries. K-feldspars have been either corroded to leave a skeleton of the former grain or extensively sericitised. Rare examples are relatively fresh and show carlsbad and tartan twins typical of orthoclase and microcline respectively. Lithics of micaceous schist are dominant, there are lesser amounts of quartzite, chert and highly altered grains that are difficult to identify. In some instances these altered lithics could have been volcanic in origin. Mica flakes are in various phases of alteration to illite especially where flakes are crenulated between sutured contacts. Angular zircon is very fine sand in size and green tourmaline is fine sand in size.

Matrix:

Discontinuous opaque stringers indicate the presence of trace amounts of organic matter.

Authigenic minerals and cements:

Grains of glaucony vary in colour from pale yellow to green and all have a wormy texture typical of glauconite. Where glauconite is squeezed between grains it has altered to illite. Remnants of detrital quartz are evident within the glauconite. Rarely glauconite forms partial rims on grains. It is possible that the glauconite replaced a detrital matrix. Kaolin which has formed due to the alteration of micas and feldspars has resulted in coarse crystal size (up to 60 microns) and subhedral booklets. There is minor illite associated with this kaolin. A second phase of pore filling kaolin has a very fine crystal size and anhedral habit. Straight grain contacts and rare quartz druse indicate the presence of syntaxial quartz overgrowths. Minute fluid inclusions are scarce within the overgrowths. Rare pyrite framboids that are up to 20 microns in diameter are clustered along grain margins. Pyrite also forms isolated patches of cement. Minor oxidation of micas and possibly other grains is apparent.

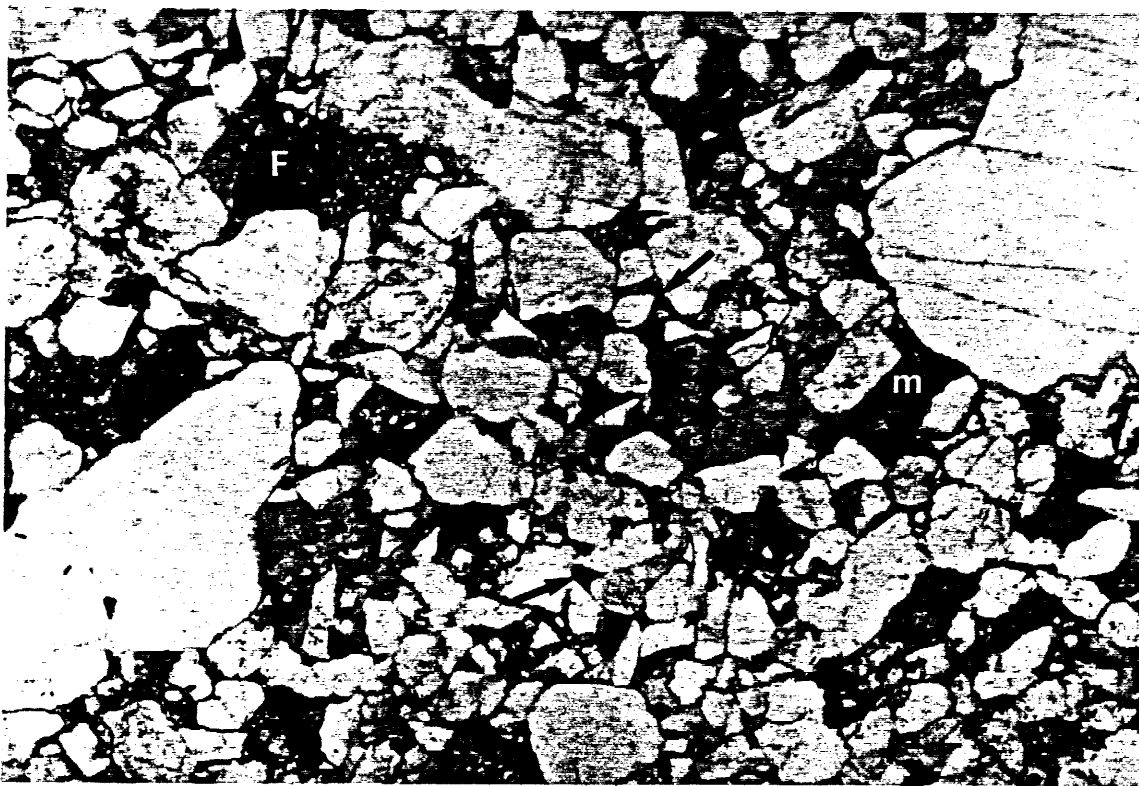


**Figure 2**

Poorly sorted, medium grained sublitharenite with grain size dissolution pores (P) and minor intergranular porosity (arrows). Note the corroded feldspar (F) and adjacent deformed lithic. Other dusty brown grains are composed of lithics, micas (M) and feldspars replaced by kaolin and illite. Minerva #1, core plug 11, 1824.0m. Plane light. Field of view 2.72mm.



### X-ray diffraction

The bulk XRD trace (Fig. 3a) indicates that quartz is the dominant mineral with minor kaolinite and trace amounts of feldspar (possibly microcline) and illite/muscovite. Detection of sylvite indicates that there was some contamination from drilling mud. The illite peaks in the clay fraction (Fig. 3b) are broad and this could be attributed to the poorly crystalline nature of glauconite which overlaps with these peaks. Glauconite was only identified in thin section. The clay fraction is dominated by kaolinite which is very well ordered and highly crystalline. In addition there is minor quartz and feldspar.

### Scanning electron microscopy

The sample is a medium grained, poor to moderately sorted, mineralogically submature sandstone. Grains are typically subangular to subrounded and there does not appear to be any preferred alignment of grains. Porosity is moderate and there is a higher percentage of secondary pores than core plug 9 (depth 1823.47m). These secondary pores are commonly grain size (Fig. 4a) and attributed to the dissolution of labile grains. Primary intergranular pores are rarely interconnected thus permeability is probably limited. Deformed and altered lithics have further reduced reservoir quality by filling pores and blocking pore throats. There would be minor microporosity associated with the authigenic kaolin. Traces of drilling mud were identified in the pores from the presence of barite.

Framework grains of quartz, K-feldspar and muscovite are evident. Authigenic minerals are dominated by kaolin with minor quartz and pyrite. Typically the kaolin is anhedral and less than 2 microns in diameter, but there are coarser more euhedral booklets that are up to 20 microns in diameter (Fig. 4b). The finer kaolin is intergrown with quartz overgrowths and tends to block pore throats. The quartz overgrowths occur as rhombohedral crystals and druse. Rare pyrite framboids were concentrated along the cleavage planes of micas.

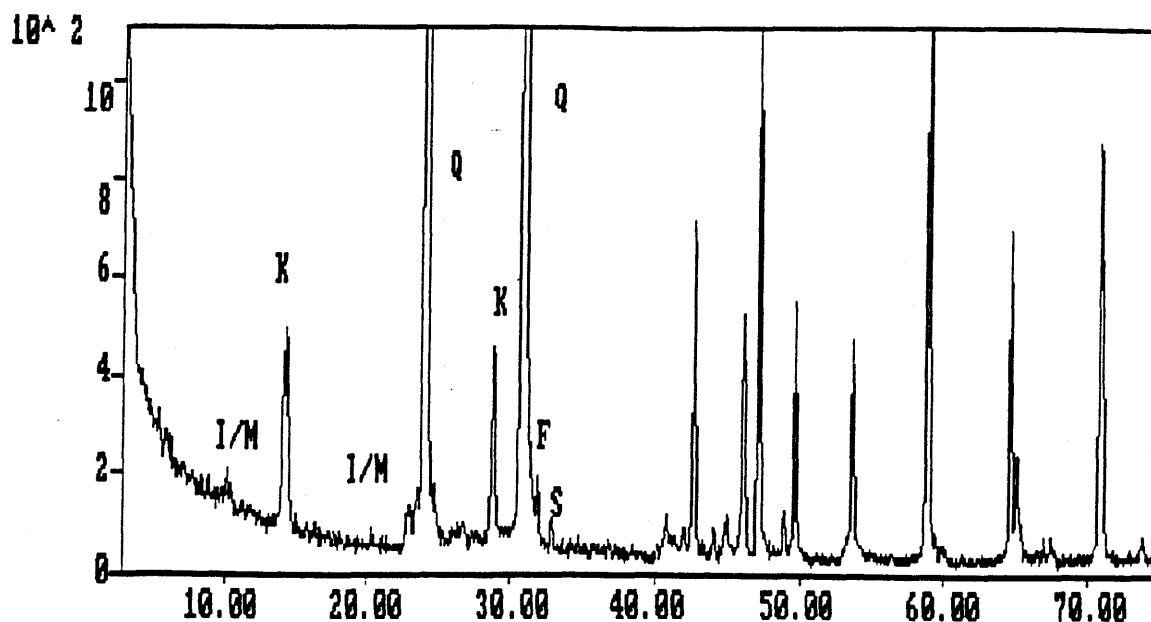


Figure 3a

Bulk XRD trace of Minerva #1, core plug 11, depth 1824.0m. The horizontal axis is in degrees two theta and the vertical axis is in counts of peak intensity. Only the strongest peaks for each mineral identified have been labelled. I/M = illite/muscovite, K = kaolinite, Q = quartz, F = feldspar, S = sylvite.

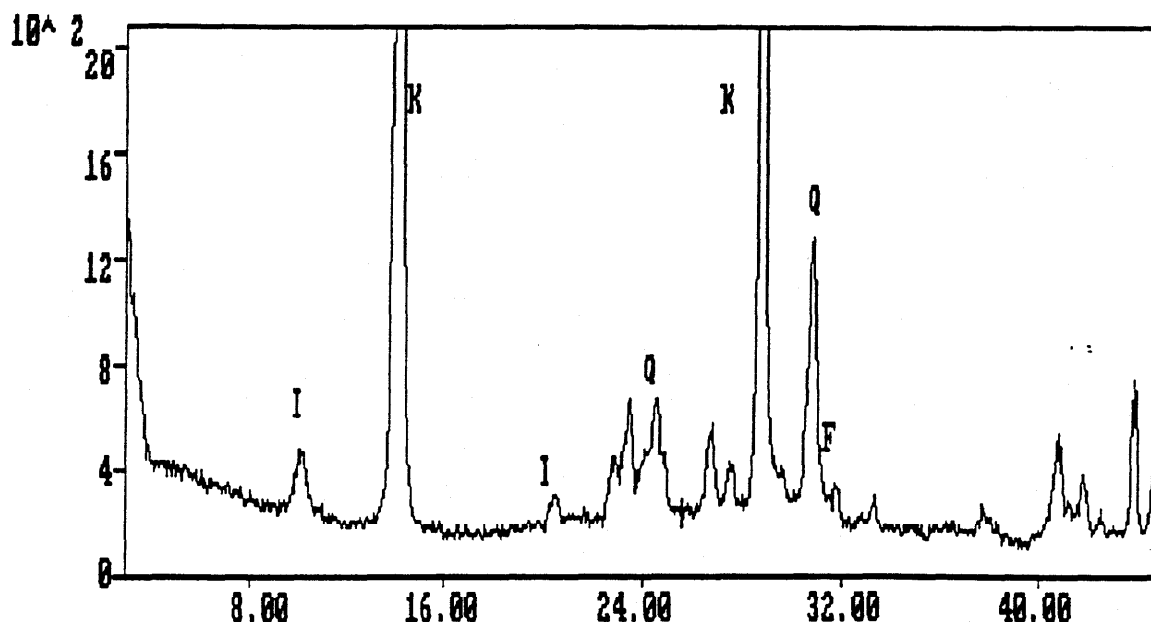


Figure 3b

XRD trace of the clay fraction from Minerva #1, core plug 11, depth 1824.0m. The horizontal axis is in degrees two theta and the vertical axis is in counts of peak intensity. Only the strongest peaks for each mineral identified have been labelled. I = illite, K = kaolinite, Q = quartz, F = feldspar.

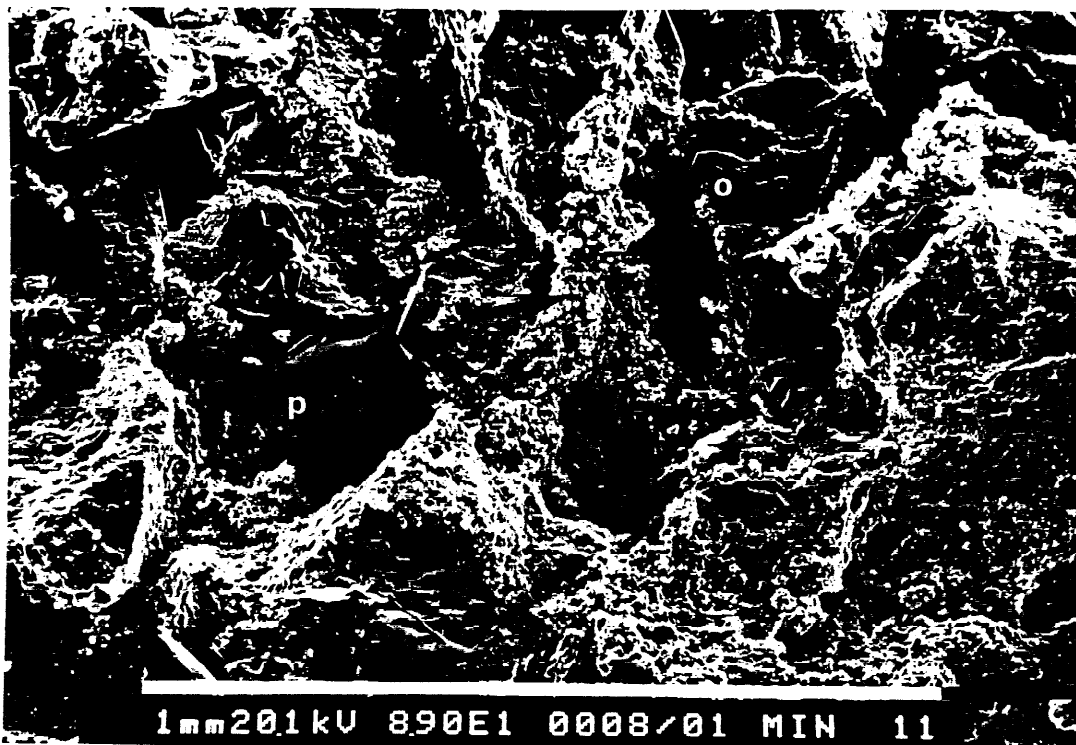


Figure 4a

Secondary pores (P) in this medium grained sandstone are grain size. It is possible that some are due to grain plucking during sample preparation. Pores are lined and partially filled with kaolin (arrow). Quartz overgrowths (o) are evident from the presence of euhedral terminations on grains. Minerva #1, core plug 11, depth 1824.0m. Scale bar 1mm.



Figure 4b

Mixture of fine and coarse kaolin booklets adjacent to a quartz overgrowth (o). The coarse booklets tend to have ragged edges (arrow) which should improve microporosity. Minerva #1, core plug 11, depth 1824.0m. Scale bar 0.1mm.

#### 4.3 Minerva #1, Core plug 12, depth 1828.15m

##### Scanning electron microscopy

The sample is a coarse grained, moderately sorted, mineralogically mature sandstone. Grains are commonly subangular to subrounded with low to moderate sphericity. Porosity is dominated by primary intergranular pores with minor secondary pores (Fig. 5a). The latter have been produced by the partial dissolution of K-feldspars. Porosity would also include some micropores associated with the authigenic kaolin (Fig. 5b). There are minor amounts of kaolin blocking pore throats that could have migrated during testing.

Framework grains are dominated by quartz with minor K-feldspar and biotite. The feldspar has been corroded and the biotite is bent and altered. Problems with charging during SEM examination may indicate the presence of organic matter. Authigenic minerals of quartz and kaolin are apparent. The quartz overgrowths have euhedral rhombohedral terminations and there are rare druse which have slightly reduced pore sizes. Kaolin booklets (Fig. 5b) are subhedral to euhedral and approximately 10 to 20 microns in diameter. There are examples of vermiform kaolin. The finer kaolin noted in previous samples appears to be absent. One pore was noted which has been bridged by a platy material that could represent an authigenic clay (Fig. 5c). It was not possible to get the beam onto this part of the sample to use the EDS system for chemical assessment. The adjacent quartz overgrowth has remnants of a fibrous material which probably reflects detrital illite trapped in an overgrowth. Given that only one pore was noted with the pore bridging material it is unlikely to cause significant problems. In other samples where similar features were observed the pore bridging material was identified as sylvite.

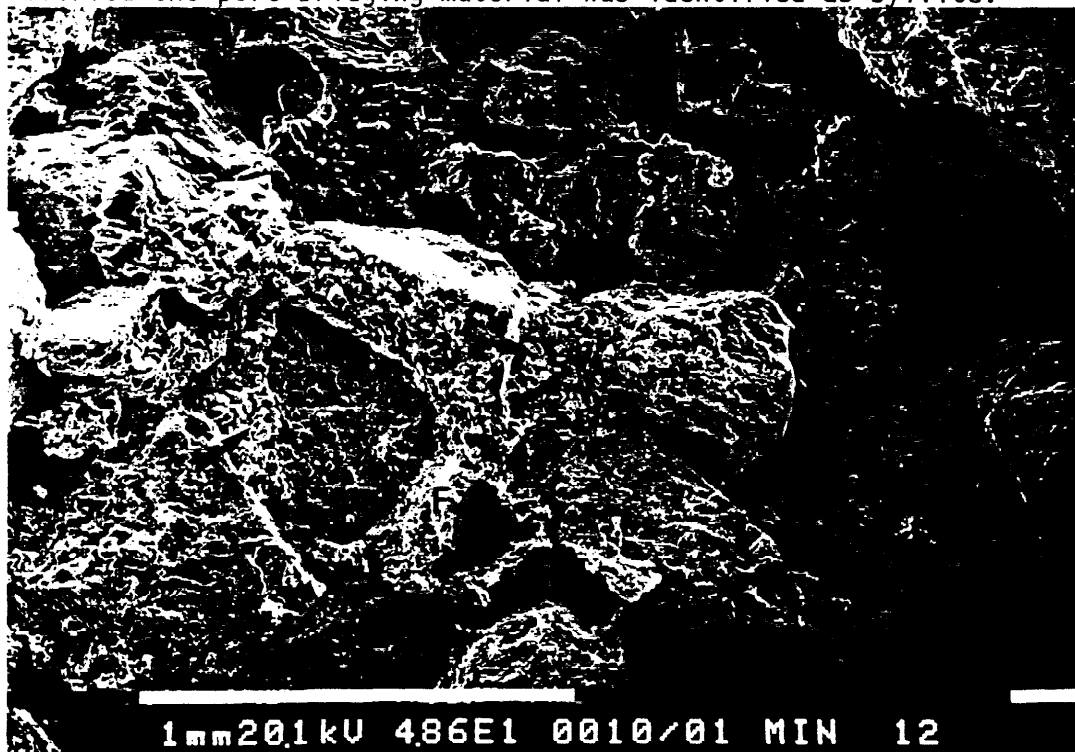


Figure 5a

General view of coarse grained sandstone with good intergranular pores and an example of a secondary dissolution pore due to partial dissolution of a K-feldspar (F). Authigenic kaolin (arrows) has partially filled pores. Minerva #1, core plug 12, depth 1828.15m. Scale bar 1mm.



Figure 5b

There are 2 locations for micropores associated with this kaolin. Micropores occur between subhedral to euhedral kaolin booklets (A) and between individual platelets within the booklets (B). The latter are most abundant where the kaolin has a ragged edge. The micropores from these 2 locations are interconnected. Minerva #1, core plug 12, depth 1828.15m. Scale bar 0.1mm

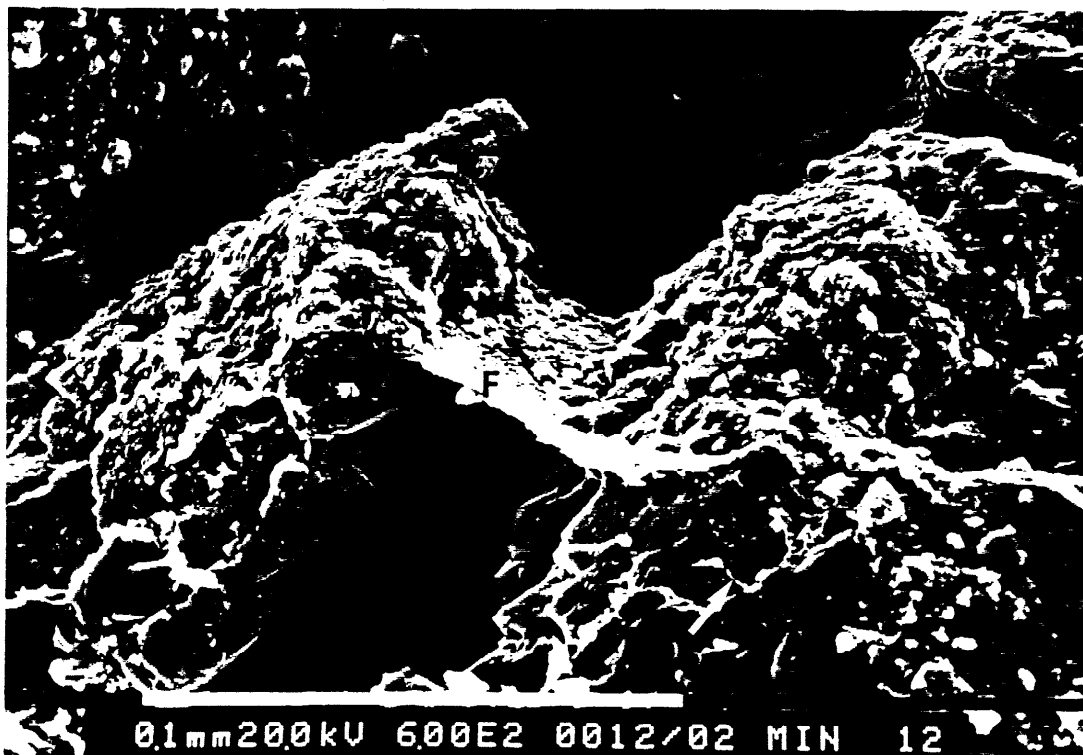


Figure 5c

In this one pore there is fibrous material (F) bridging the pore. The surface appears to be covered by anhedral lumps that could represent drilling mud. Quartz overgrowths (o) on the surrounding grains have a druse habit and there are traces of fibrous material (arrow). The latter could be detrital illite trapped during precipitation of the overgrowth. Minerva #1, core plug 12, depth 1828.15m. Scale bar 0.1mm

#### 4.4 Minerva #1, Core plug 17, depth 1829.57m

##### Thin section description

Rock classification: Quartzarenite

##### Texture:

The sample is a very coarse grained, poorly sorted, texturally submature and mineralogically mature quartzarenite (Fig. 6a). Grains range in diameter from approximately 0.1mm (very fine sand) to 6.0mm (pebbles) and commonly are subangular to subrounded with low to moderate sphericity. There has been minor grain fracturing of the coarser grains which tend to be better rounded. A high percentage of the coarse grains consist of polycrystalline quartz. Texturally the quartzarenite is grain supported with tangential and concavo-convex grain contacts. Fracturing of grains and minor sutured contacts indicate that there has been significant mechanical compaction.

##### Porosity:

Porosity is dominated by primary intergranular pores which tend to be elongate due to interconnection. The latter would have been enhanced by grain fracturing. Corrosion of feldspars has resulted in minor secondary honeycomb porosity and there are rare intragranular pores (Fig. 6b). Porosity has been restricted by poor sorting. In addition there is evidence of contamination by drilling mud. Rarely pores are rimmed and partially filled by quartz silt, mud and barite.

Visual Estimate of Composition		%
Framework grains	Quartz	79
	Feldspar	tr
	Lithics	tr
	Accessory minerals	tr
Matrix		nd
Authigenic minerals and cements	Pyrite	2
	Kaolin	3
	Quartz	2
Porosity	Intergranular	10
	Dissolution	2
	Intragranular	tr
Drilling mud		1

##### Framework grains:

Quartz is both monocrystalline and polycrystalline. Monocrystalline quartz has straight to slightly undulose extinction, scattered vacuoles and rare mineral inclusions of apatite, mica and rutile needles. Polycrystalline quartz has undulose extinction and straight crystal boundaries. K-feldspars have been extensively corroded. Grains which have been replaced by extremely fine kaolin and pyrite, and contain remnants of quartz were probably volcanic lithics. Angular very fine sand size zircon is the only accessory mineral.

##### Authigenic minerals and cements:

Pyrite framboids and octahedra, and anhedral patches of cement concentrate along grain margins and have partially replaced grains. Individual framboids and octahedra range from 3 to 25 microns in diameter. Pore filling and grain replacing kaolin consists of subhedral booklets that are up to 20 microns in diameter. Euhedral terminations on quartz druse indicate the presence of rare syntaxial quartz overgrowths.

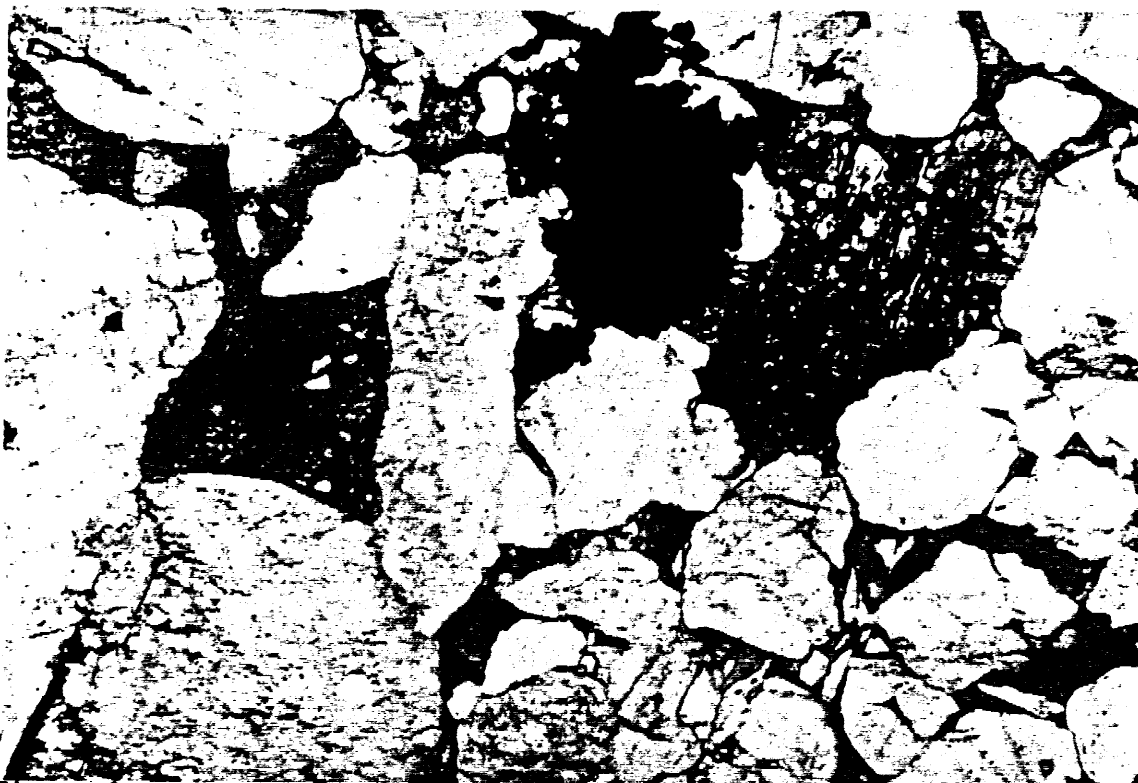


Figure 6a

Poorly sorted quartzarenite with a dusty corroded K-feldspar and patch of pyrite cement (opaque). The fine silt in one pore is contaminant from the drilling mud. Minerva #1, core plug 17, depth 1829.57m. Plane light. Field of view 2.72mm.



Figure 6b

Intragranular pores (arrows) have formed in the coarser quartz grains and there is evidence of minor grain fracturing (F). The latter would have enhanced permeability. Traces of drilling mud can be seen in some pores. Minerva #1, core plug 17, depth 1829.57m. Plane light. Field of view 2.72mm.

### X-ray diffraction

The mineralogy of this sample is dominated by quartz. In addition there were trace amounts of kaolinite, sylvite, halite and pyrite detected in the bulk XRD trace (Fig. 7a). The presence of sylvite and halite indicate that there has been contamination by drilling mud. In the clay fraction (Fig. 7b) this is confirmed by the presence of montmorillonite. Kaolin peaks are sharp and relatively high in the clay trace but this is a reflection of the well ordered nature of the kaolin and its crystallinity rather than the relative amount of kaolin. Trace amounts of clinocllore and illite were the only other clays identified. These clays are probably present as alteration products of the feldspars and lithics.

### Scanning electron microscopy

The sample is a coarse grained, poorly sorted, mineralogically mature sandstone. Grains are commonly subangular with low to moderate sphericity. Primary intergranular pores are well preserved (Fig. 8a) and the elongate nature of these pores indicates that there is good interconnection and hence permeability. Rare secondary dissolution pores have resulted from the partial corrosion of K-feldspars. There would be traces of microporosity associated with the authigenic kaolin.

Framework grains of quartz are dominant and there is minor K-feldspar. Kaolin, quartz and pyrite represent the authigenic phases in this sandstone. Kaolin booklets are various sizes (Fig. 8b) and the coarser booklets tend to be more euhedral. Fine subhedral kaolin which is approximately 2 to 5 microns in diameter is intergrown with quartz overgrowths. This may indicate that the fine kaolin precipitated before the coarser crystals. Coarser kaolin is up to 20 microns in diameter and is rarely vermiform. It tends to block pore throats and is associated with drilling mud in one pore (Fig. 8b). Quartz overgrowths typically occur as druse which may indicate that silicification was not extensive. Rare octahedral pyrite crystals were observed.



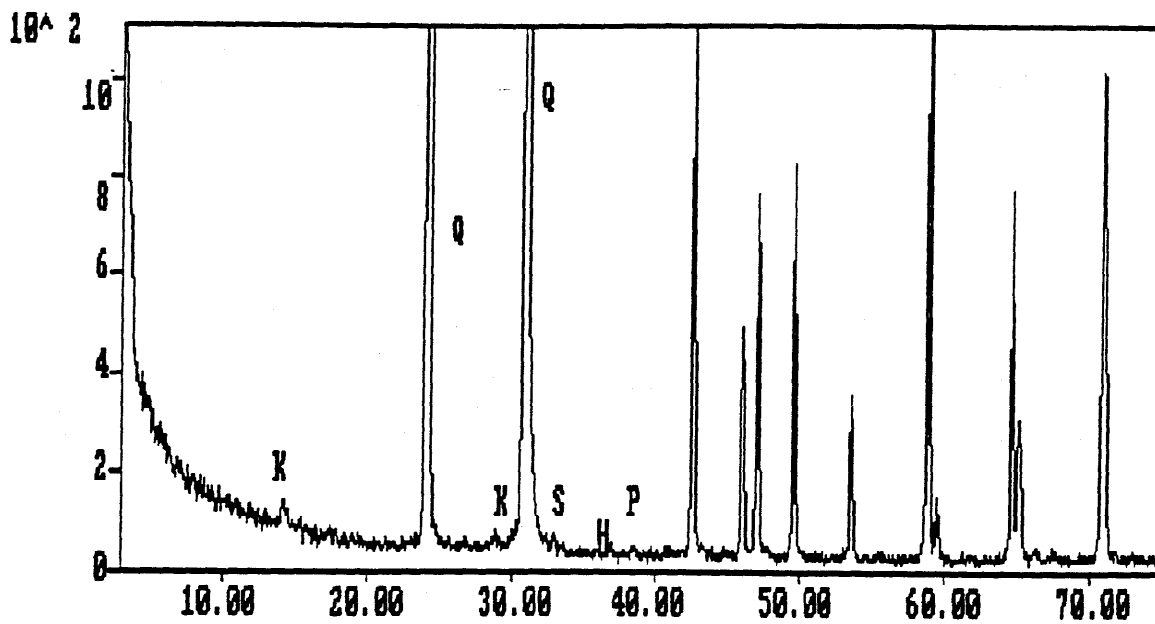


Figure 7a  
Bulk XRD trace of Minerva #1, core plug 17, depth 1829.57m. The horizontal axis is in degrees two theta and the vertical axis is in counts of peak intensity. Only the strongest peaks for each mineral identified have been labelled. K = kaolinite, Q = quartz, S = sylvite, H = halite, P = pyrite.

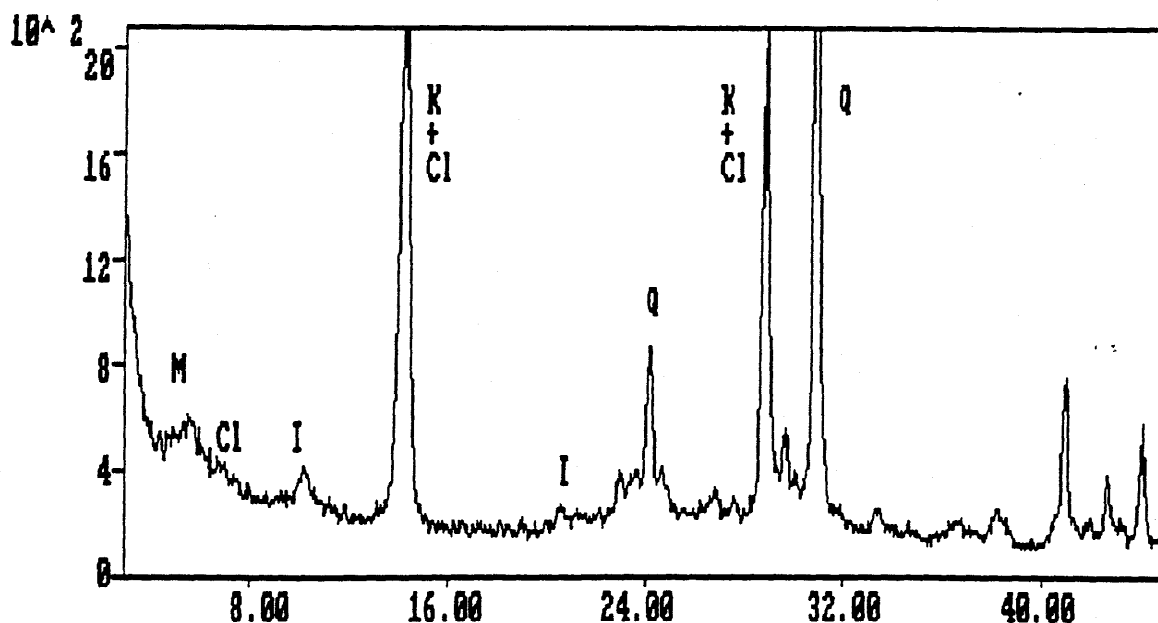


Figure 7b  
XRD trace of the clay fraction from Minerva #1, core plug 17, depth 1829.57m. The horizontal axis is in degrees two theta and the vertical axis is in counts of peak intensity. Only the strongest peaks for each mineral identified have been labelled. M = montmorillonite, Cl = clinochlore, I = illite, K = kaolinite, Q = quartz.



Figure 8a

Coarse grained, poorly sorted sandstone with elongate primary intergranular pores (P). Dissolution pores have resulted from the corrosion of K-feldspars (F). Note the relative lack of quartz overgrowths and pore filling kaolin. Minerva #1, core plug 17, depth 1829.57m. Bar scale 1mm.

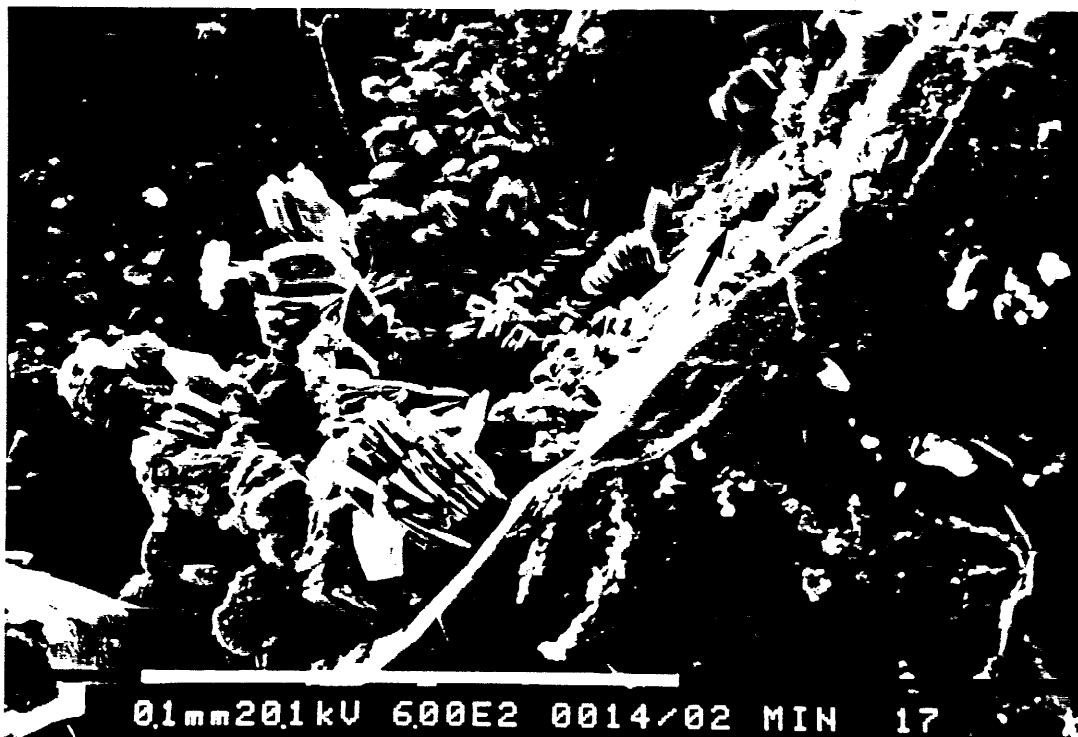


Figure 8b

At least two phases of kaolin are apparent in this photomicrograph. The finer crystals are intergrown (arrow) with quartz overgrowths. At least some of the coarser euhedral crystals are coated by drilling mud (D). Micropores are evident between the platelets of the coarser kaolin. Minerva #1, core plug 17, depth 1829.57m. Bar scale 1mm.

#### 4.5 Minerva #1, Core plug 18, depth 1829.87m

##### Thin section description

Rock classification: Subarkose

Texture:

The sample is very coarse to granular, very poorly sorted, mineralogically and texturally submature subarkose. Grains range in diameter from approximately 0.14mm (fine sand) to 1cm (cobbles) and are typically subrounded with low to moderate sphericity. The coarse fraction is dominated by polycrystalline quartz and feldspars. Texturally the sample is grain supported with tangential and sutured grain contacts. There are no sedimentary structures apparent.

Porosity:

Porosity is a combination of primary intergranular pores and secondary dissolution pores. Secondary pores have resulted from the corrosion of feldspars. A high percentage of these corroded feldspars have fractured due to their weakened state (Fig. 9). In addition there has been fracturing of polycrystalline quartz grains. Porosity has been limited by the infiltration of drilling mud which partially rims pores. Angular silt size quartz and minor opaques are associated with the mud. Rare interconnections are apparent between primary pores and these have been enhanced by grain fracturing. Typically pore throats are blocked by the finer grains and sutured contacts.

Visual Estimate of Composition		%
Framework grains	Quartz	81
	Feldspars	5
	Lithics	1
	Coal	tr
	Accessory minerals	tr
Matrix		nd
Authigenic minerals and cements	Pyrite	2
	Kaolin	1
	Quartz	tr
Porosity	Intergranular	5
	Dissolution	2
	Fracture	1
Drilling mud		1

Framework grains:

Polycrystalline quartz is common, it has undulose extinction and straight crystal boundaries typical of a granitic source. Rare mineral inclusions of rutile, muscovite and apatite are evident in the polycrystalline quartz. Monocrystalline quartz has straight to slightly undulose extinction and scarce inclusions of zircon and apatite. Feldspars are composed of alkali varieties (possibly orthoclase) which lack twinning and show minor evidence of alteration. Lithics of granite and fine micaceous schist are evident. The granite lithics are coarse grained in size and more abundant than the schist. Granite lithics have both fine and medium crystal sizes. A segment of angular carbonaceous material 8mm in length and 1mm wide is probably a coalified plant fragment. Rounded fine sand size zircon is the only accessory mineral.

Authigenic minerals and cements:

Patches of opaques and single crystals concentrate along crystal and

grain boundaries. Where these opaques form octahedra and framboids it suggests the presence of pyrite. Rare grains have been completely replaced by ?pyrite. Kaolin booklets up to 40 microns in diameter and rare kaolin with a vermiform habit is scattered throughout one coarse K feldspar. Finer grains of feldspar have been completely replaced by kaolin booklets. Rare quartz overgrowths are suggested by the presence of euhedral terminations on detrital grains and there are isolated fluid inclusions in the overgrowths.

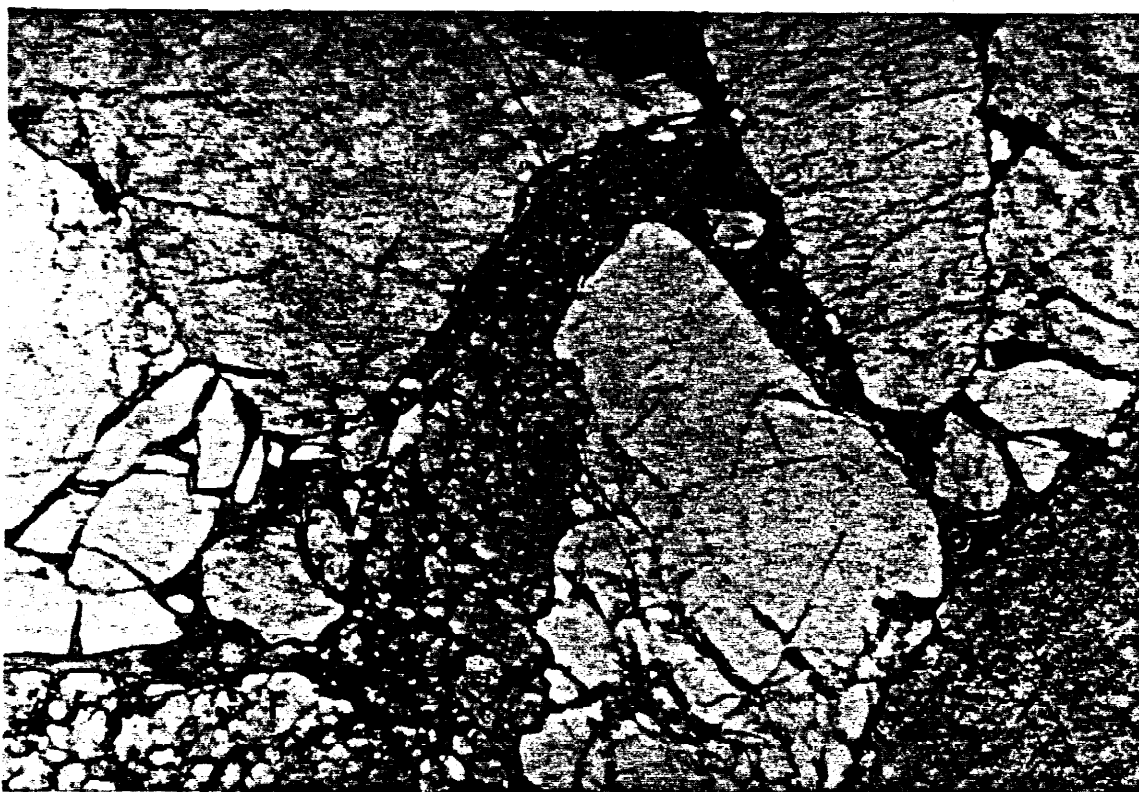


**Figure 9**

Feldspars (F) have been partially dissolved and fractured in this poorly sorted subarkose. Intergranular pores (blue) could have been enlarged during this disruption and there is minor drilling mud (arrow) blocking pore throats. Traces of pyrite (opaque) are also apparent. Minerva #1, core plug 18, depth 1829.87m. Plane light. Field of view 2.72mm.

### X-ray diffraction

Although the rock is described as a subarkose there was no feldspar detected in the bulk XRD trace (Fig. 10a). This is attributed to the fact that XRD does not detect minerals which represent less than 5% of the rock unless the mineral is highly crystalline or has a preferred orientation. Quartz is the dominant mineral in the bulk trace and there are trace amounts of kaolinite, barite, sylvite, halite and pyrite. The barite, sylvite and halite indicate that there has been contamination from drilling mud. This contamination is confirmed by the presence of montmorillonite in the clay fraction (Fig. 10b). Kaolinite is the dominant clay mineral but it is not as well ordered and crystalline as the kaolinite in core plug 17 (depth 1829.57m). There is a trace amount of illite in the clay fraction which is probably an alteration product of the feldspars or the result of disaggregation of micaceous lithics. Quartz was also detected in the clay fraction.

### Scanning electron microscopy

The sample is a very coarse grained, very poorly sorted quartz rich sandstone. Grains are subangular to subrounded with low sphericity. The very poor sorting has limited porosity but there are primary intergranular pores evident. Pore spaces and throats are commonly blocked by drilling mud contaminants in this sample (Figs 11a & b). Euhedral bladed gypsum crystals have precipitated in pore throats and there are coatings of sylvite rimming pores. These contaminants have probably caused an artificial reduction in porosity and permeability.

Framework grains are dominated by quartz and there are trace amounts of mica. Authigenic minerals of quartz, kaolin and pyrite are evident. Rare euhedral druse have precipitated on some detrital quartz grains (Fig. 11b). Kaolin booklets are subhedral and approximately 10 to 15 microns in diameter. Pyrite framboids are apparent on pore margins and these have diameters up to 15 microns.

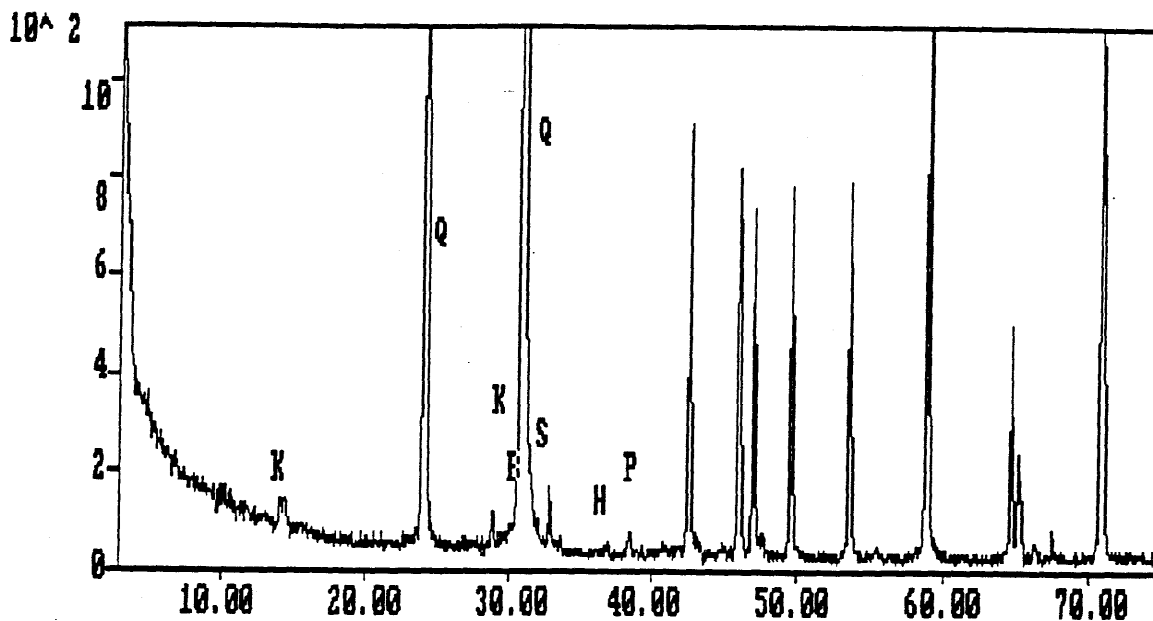


Figure 10a

Bulk XRD trace of Minerva #1, core plug 18, depth 1829.87m. The horizontal axis is in degrees two theta and the vertical axis is in counts of peak intensity. Only the strongest peaks for each mineral identified have been labelled. K = kaolinite, Q = quartz, B = barite, S = sylvite, H = halite, P = pyrite.

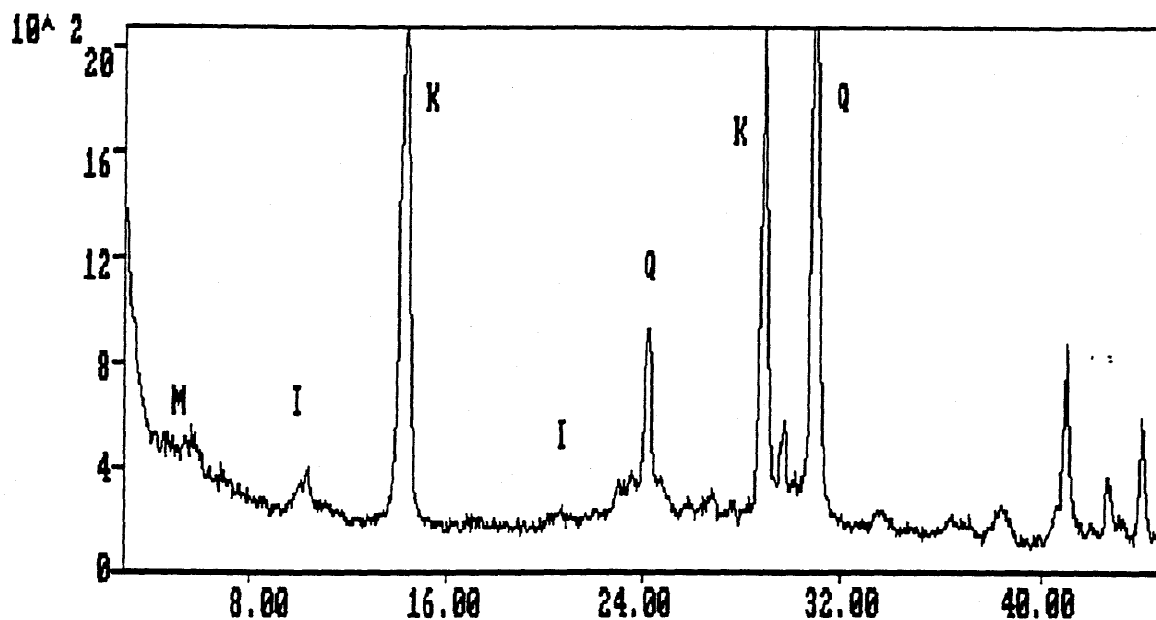


Figure 10b

XRD trace of the clay fraction from Minerva #1, core plug 18, depth 1829.87m. The horizontal axis is in degrees two theta and the vertical axis is in counts of peak intensity. Only the strongest peaks for each mineral identified have been labelled. M = montmorillonite, I = illite, K = kaolinite, Q = quartz.



Figure 11a

General view of very poorly sorted, very coarse grained sandstone. Primary intergranular pores are evident between grains and drilling mud forms a coating on grains. Euhedral bladed gypsum crystals (arrow) have blocked a pore throat. Minerva #1, core plug 18, depth 1829.87m. Bar Scale 1mm.



Figure 11b

Quartz overgrowths (o) have a thick coating (A) of KCl (sylvite) which has precipitated out of the drilling mud. The cluster of crystals on the left hand side is also a mixture of contaminants including rare kaolin platelets (arrow) which have migrated with the drilling mud. Minerva #1, core plug 18, depth 1829.87m. Bar Scale 10 microns.

4.6 Minerva #1, Core plug 30, depth 1833.50m

## Thin section description

Rock classification: Sublitharenite

Texture:

The sample is a fine to medium grained, moderately sorted, mineralogically and texturally submature sublitharenite. Low amplitude stylolites (Fig. 12a) indicate that there has been significant compaction. Stylolites are filled with opaque material and anhedral dark brown clay. Framework grains range in diameter from approximately 0.07mm (very fine sand) to 0.52mm (coarse sand) and typically are subangular to subrounded with low to moderate sphericity. Texturally the sample is grain supported with tangential and sutured contacts. The latter are dominant adjacent to the stylolites and where ductile lithics have been deformed.

Porosity:

Porosity is limited by the sutured nature of grain contacts and the abundance of authigenic clay. Pores are typically secondary in nature due to the complete and partial dissolution of labile grains. There are minor intergranular pores but there does not appear to be any interconnection between pores. Microporosity would be associated with the kaolin but this would not improve permeability.

Visual Estimate of Composition		%
Framework grains	Quartz	62
	Feldspar	2
	Lithics	9
	Mica	tr
	Accessory minerals	tr
Matrix	Clay	4
	Opaque material	tr
Authigenic minerals and cements	Glaucony	tr
	Pyrite	4
	Kaolin	10
	Quartz	tr
	Iron oxide	1
	Carbonate	tr
Porosity	Intergranular	2
	Dissolution	4
	Micropores	1

Framework grains:

Quartz is both monocrystalline and polycrystalline. The monocrystalline quartz has straight to slightly undulose extinction, scattered vacuoles and rare mineral inclusions of muscovite, rutile needles, apatite and zircon. Polycrystalline quartz has undulose extinction and straight crystal boundaries. K-feldspars are in various stages of alteration to illite and kaolin, and there are examples which have been extensively corroded. The lack of twinning suggests that orthoclase could be the dominant feldspar. One feldspar with tartan twinning typical of microcline is apparent. Lithics include examples of micaceous schist, granite, metasediments and highly altered grains which could not be identified. Commonly these ductile lithics have been deformed during compaction and have filled adjacent pores. Mica flakes are highly deformed and altered, partially to iron oxide and pyrite. Micas tend to



be associated with the stylolites. Rounded fine sand size zircon, brown tourmaline, sphene, ?monazite and ?amphibole represent the accessory minerals.

Matrix:

Dark brown anhedral clays concentrate in those areas where stylolites have formed. These were probably detrital clay stringers that were more susceptible to compaction.

Authigenic minerals and cements:

Grain size patches of opaque material with bladed crystals protruding from the edges could indicate the presence of marcasite. Elsewhere there are framboids and cubes that are probably composed of pyrite. Massive opaque material concentrates in the stylolites. Kaolin has replaced grains and filled pores throughout the sample (Fig. 12b). Booklets are typically subhedral and range in diameter from approximately 2 to 30 microns. Where kaolin has a very fine crystal size it is commonly anhedral. Mica flakes replaced by kaolin booklets are up to 50 microns in diameter. There are isolated examples of vermiform kaolin filling pores. Rarely adjacent to quartz overgrowths the contact between kaolin booklets and quartz is jagged. Syntaxial quartz overgrowths are rare and outlined by dust rims and euhedral terminations. Scarce fluid inclusions can be located in the overgrowths. Grains of grey to pale yellow glaucony include minor illite and iron oxide and have been highly deformed during compaction. There are other grains which lack deformation that have been completely replaced by or altered to iron oxide. Traces of clear subhedral to euhedral rhombic carbonate spar have partially replaced isolated grains.



**Figure 12a**  
 General view illustrating sutured contacts along stylolites (arrow) outlined by opaque material and anhedral clays. Secondary dissolution pores (blue) are evident. Minerva #1, core plug 30, depth 1833.50m. Plane light. Field of view 0.88mm.

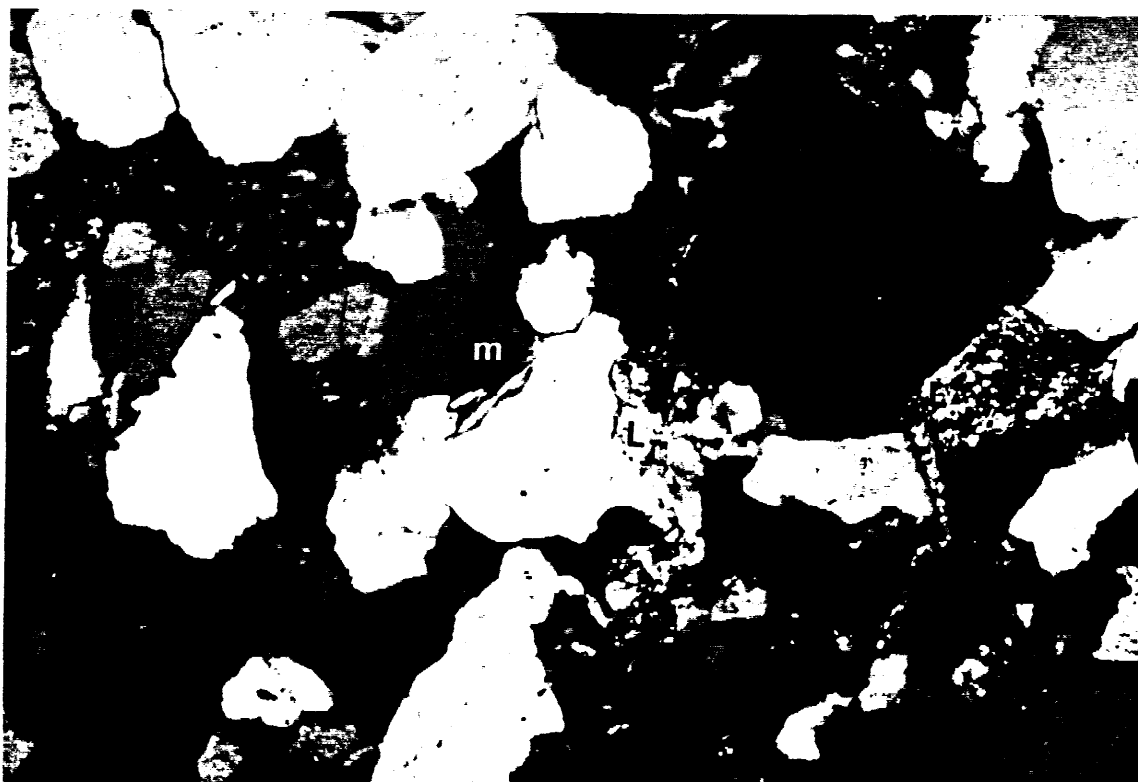


**Figure 12b**  
 Same field of view as Figure 12a, but in crossed nicols. Deformed micaceous lithics (L) are evident. Examples of pore filling kaolin and kaolin that has replaced a mica (M) are apparent.

### X-ray diffraction

The bulk XRD trace (Fig. 13a) is dominated by quartz with subdominant highly crystalline kaolinite. The well ordered nature of the kaolinite has resulted in high peaks which do not necessarily reflect the abundance of this mineral. Other minerals identified from the bulk XRD were illite/muscovite, feldspar (possibly microcline) and pyrite. Based on the thin section description there is both illite and muscovite present. Although feldspars are thought to represent less than 5% of the total rock composition they were detected in the XRD. This is probably the result of preferred orientation during sample preparation but might also be explained by the presence of minor feldspars in some of the lithics. In the clay fraction (Fig. 13b) kaolinite is the dominant clay mineral with minor illite. Quartz and feldspar were also identified in the clay fraction. Again the trace indicates that the kaolin is very well ordered and highly crystalline. The illite is probably the major component of the detrital clay matrix.

### Scanning electron microscopy

The sample is a fine grained, moderately well sorted, mineralogically mature sandstone. Grains appear to be subangular with low to moderate sphericity. Porosity is poorly preserved, there are rare secondary dissolution pores that are grain sized and isolated intergranular pores (Fig. 14a). The latter have been preserved where quartz overgrowths are apparent. Typically pores are filled with authigenic kaolin that indicates there should be some microporosity. Secondary pores have probably resulted from the dissolution of labile grains. Permeability is probably poor in this sample due to the dominance of secondary pores which lack interconnection. The abundance of pore filling kaolin may cause problems with migration during production if there is room for the kaolin to move.

Framework grains are dominated by quartz with minor corroded K-feldspar and mica. Authigenic minerals of quartz, kaolin and illite are apparent. Quartz overgrowths have euhedral rhombohedral terminations (Fig. 14b) which were precipitated prior to the pore filling kaolin. Silicification is not extensively developed in this sample. Kaolin is the most abundant authigenic mineral, it forms subhedral to euhedral booklets and rare verms that are approximately 10 microns in diameter (Fig. 14b). Micropores are better developed between booklets rather than between platelets within the booklets. Traces of authigenic illite (Fig. 14c & d) form patches associated with blocky subhedral kaolin. This illite has probably precipitated due to the alteration of a lithic. The illite is composed of Si, Al and K (Fig. 14d) and is lettuce-like rather than fibrous in habit. It is unlikely that the illite has contributed to low permeability in this sample.

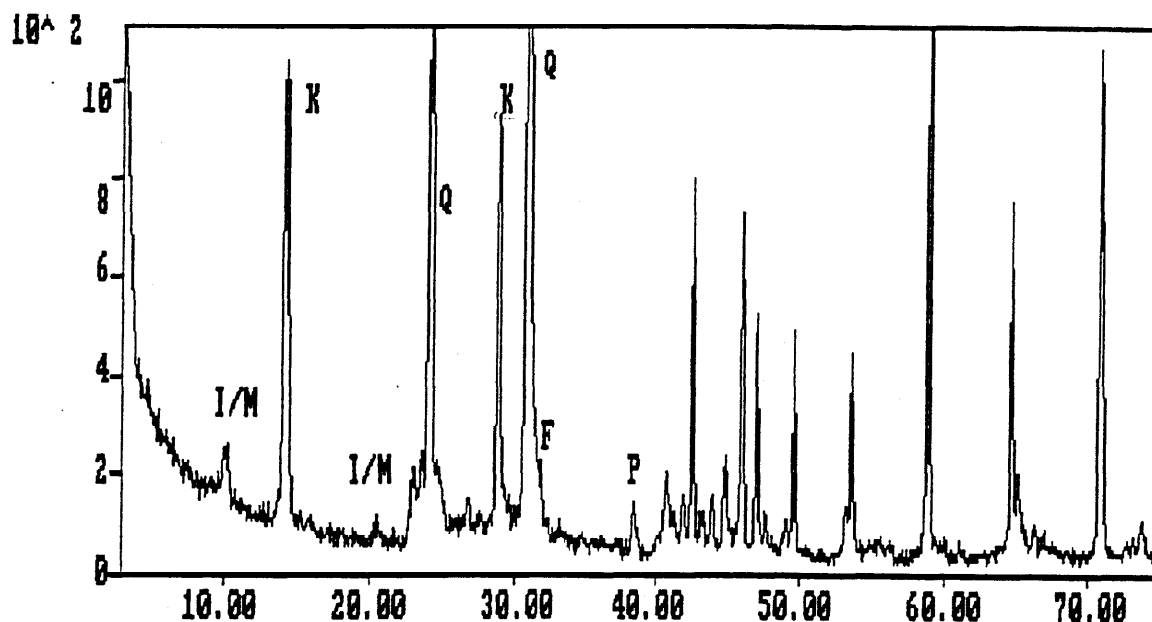


Figure 13a  
Bulk XRD trace of Minerva #1, core plug 30, depth 1833.50m. The horizontal axis is in degrees two theta and the vertical axis is in counts of peak intensity. Only the strongest peaks for each mineral identified have been labelled. I/M = illite/muscovite, K = kaolinite, Q = quartz, F = feldspar, P = pyrite.

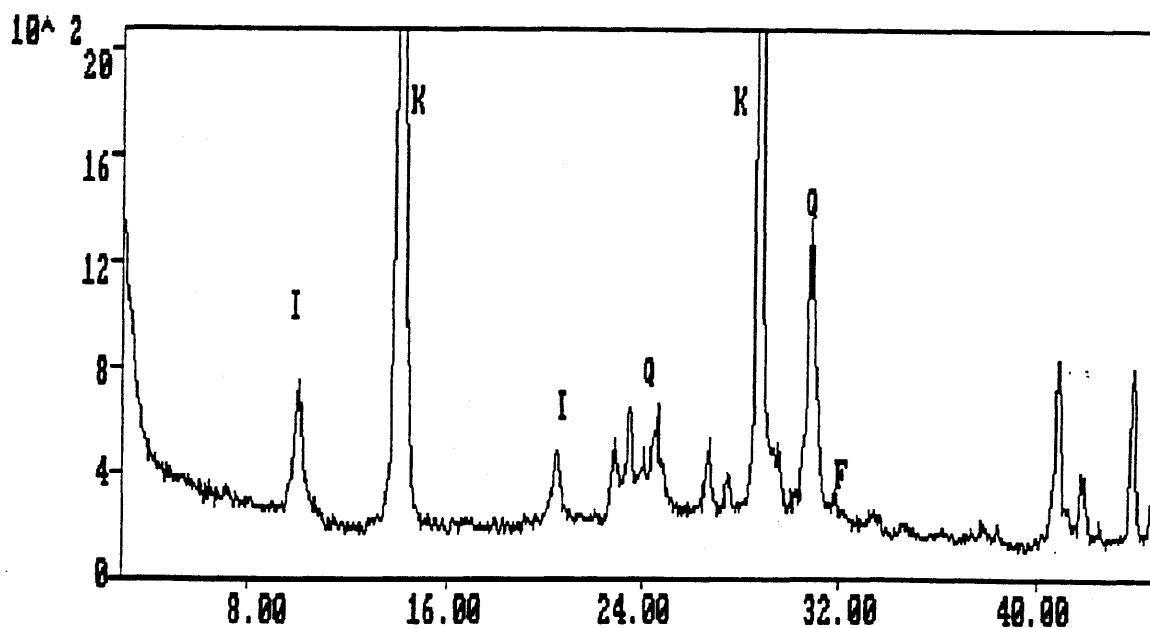


Figure 13b  
XRD trace of the clay fraction from Minerva #1, core plug 30, depth 1833.50m. The horizontal axis is in degrees two theta and the vertical axis is in counts of peak intensity. Only the strongest peaks for each mineral identified have been labelled. I = illite, K = kaolinite, Q = quartz, F = feldspar.

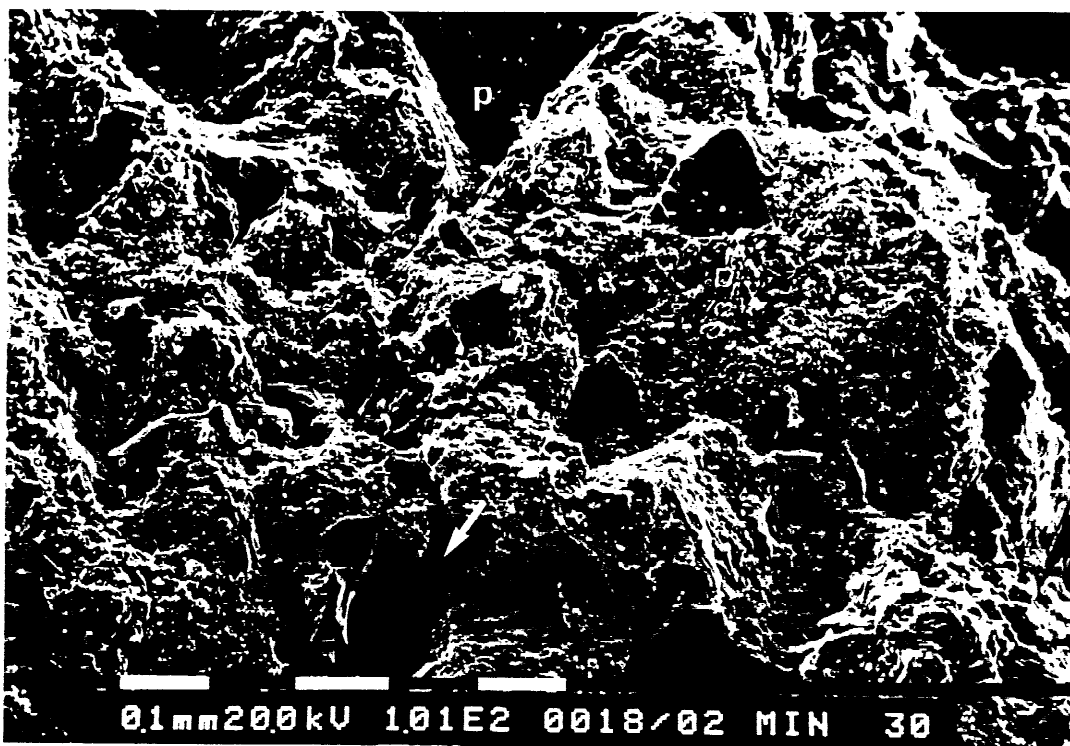


Figure 14a

Reservoir quality is poor in this fine grained, moderately well sorted sandstone. Rare primary intergranular pores (P) have been preserved but the majority are secondary dissolution pores (arrow). Grains are coated and pores filled by kaolin. Minerva #1, core plug 30, depth 1833.50m. Bar scale 0.1mm.



Figure 14b

Euhedral quartz overgrowths (o) precipitated prior to pore filling kaolin. Micropores between the kaolin booklets are up to 5 microns in size. Minerva #1, core plug 30, depth 1833.50m. Bar scale 0.1mm.



Figure 14c

Patches of authigenic illite (arrow) that are associated with blocky kaolin probably formed due to the alteration of a lithic. Minerva #1, core plug 30, depth 1833.50m. Bar scale 10 microns.

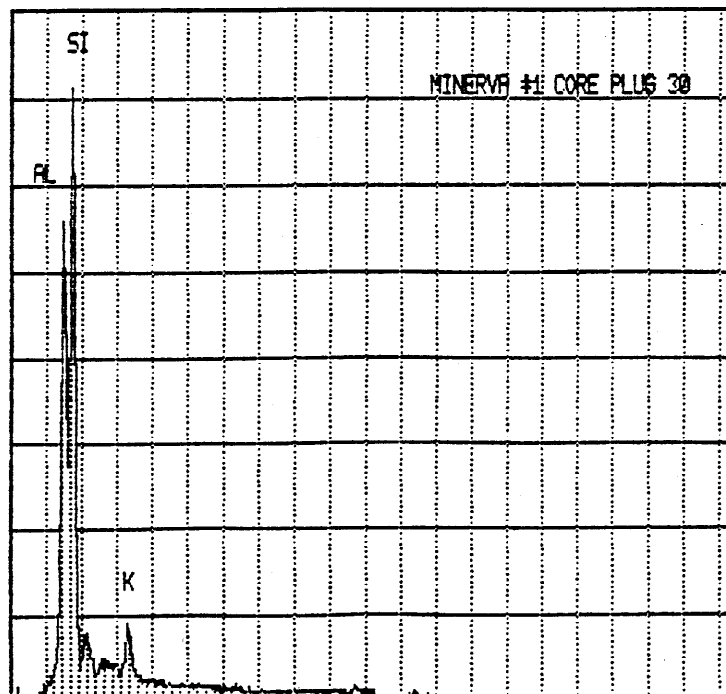


Figure 14d

EDS trace of the illite shown in Figure 14c. Only Al, Si and K were detected.

#### 4.7 Minerva #1, Core plug 34, depth 1834.70m

##### X-ray diffraction

The bulk XRD trace (Fig. 15a) is dominated by quartz with minor kaolinite and feldspar. The feldspar could be either orthoclase or microcline. Trace amounts of pyrite were also detected in the bulk fraction. Identification of montmorillonite in the clay trace (Fig. 15b) indicates that there is probably contamination from the drilling mud. Highly crystalline and well ordered kaolinite is the dominant clay mineral. There is minor illite present which is poorly crystalline. Quartz and feldspar were also identified in the clay fraction.

##### Scanning electron microscopy

The sample is a medium to coarse grained, moderately sorted sandstone. Grains are typically subrounded to subangular with low sphericity. Porosity is moderate and dominated by intergranular pores. These pores do not appear to be well interconnected which could be due to mechanical compaction. Corroded feldspars have formed minor honeycomb porosity (Fig. 16a). Permeability is unlikely to be good in this sample.

Framework grains of quartz and K-feldspar were identified. Authigenic minerals include quartz, kaolin and pyrite. Quartz overgrowths commonly have rhombohedral terminations but there are examples of druse. Trapped within the overgrowths there are dust rims of detrital illite (Fig. 16b). Silicification has reduced pore size and partially blocked pore throats. Kaolin is typically anhedral and less than 5 microns in diameter. Rare euhedral booklets and verms are up to 10 microns in diameter. Kaolin is typically located within pores (Fig. 16b). Pyrite framboids tend to concentrate along grain margins and range in diameter from 10 to 40 microns.

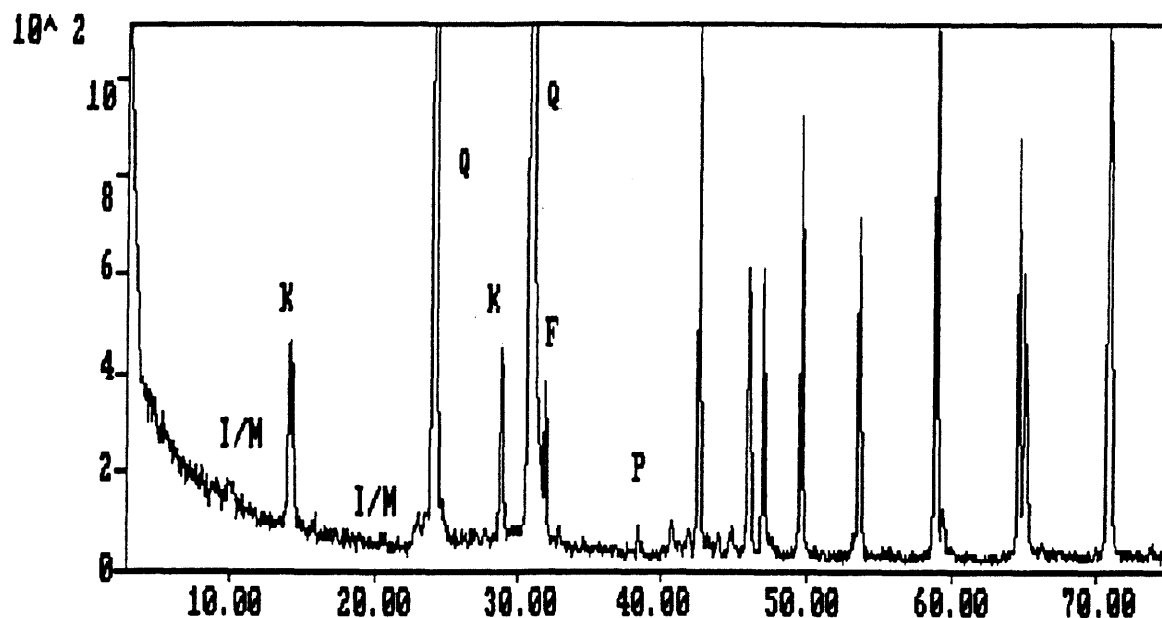


Figure 15a

Bulk XRD trace of Minerva #1, core plug 34, depth 1834.70m. The horizontal axis is in degrees two theta and the vertical axis is in counts of peak intensity. Only the strongest peaks for each mineral identified have been labelled. I/M = illite/muscovite, K = kaolinite, Q = quartz, F = feldspar, P = pyrite.

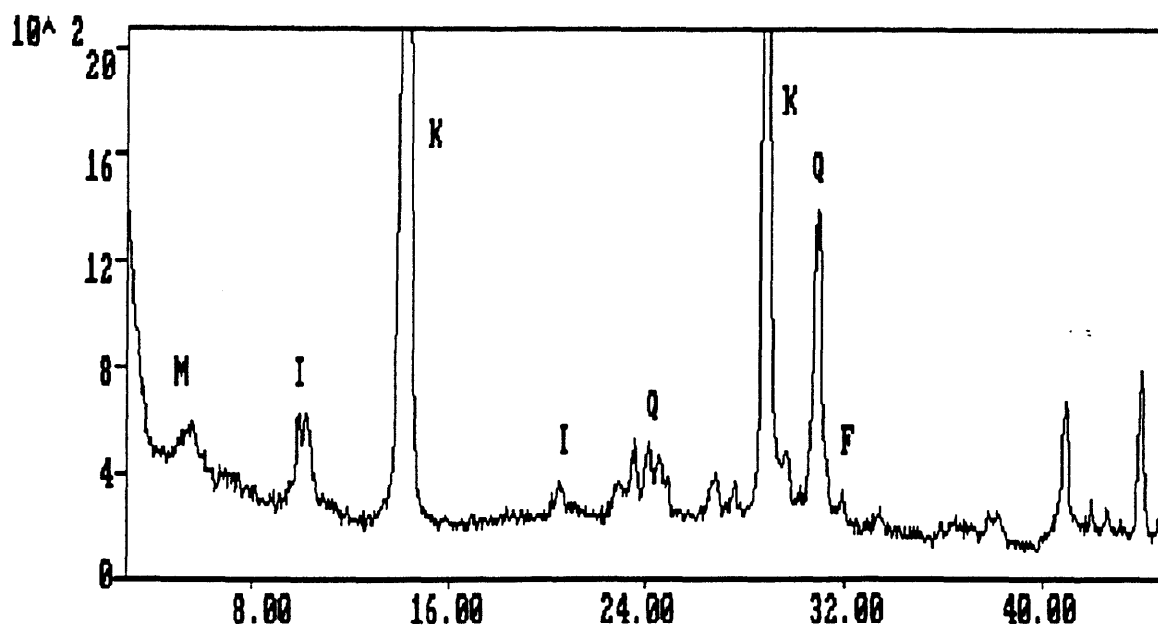


Figure 15b

XRD trace of the clay fraction from Minerva #1, core plug 34, depth 1834.70m. The horizontal axis is in degrees two theta and the vertical axis is in counts of peak intensity. Only the strongest peaks for each mineral identified have been labelled. M = montmorillonite, I = illite, K = kaolinite, Q = quartz, F = feldspar.





Figure 16a

General view of medium to coarse grained, moderately sorted sandstone. The central grain is a highly corroded K-feldspar (F). Elsewhere there are intergranular pores which tend to be triangular in shape when surrounded by quartz overgrowths (arrows). Minerva #1, core plug 34, depth 1834.70. Scale bar 0.1mm.

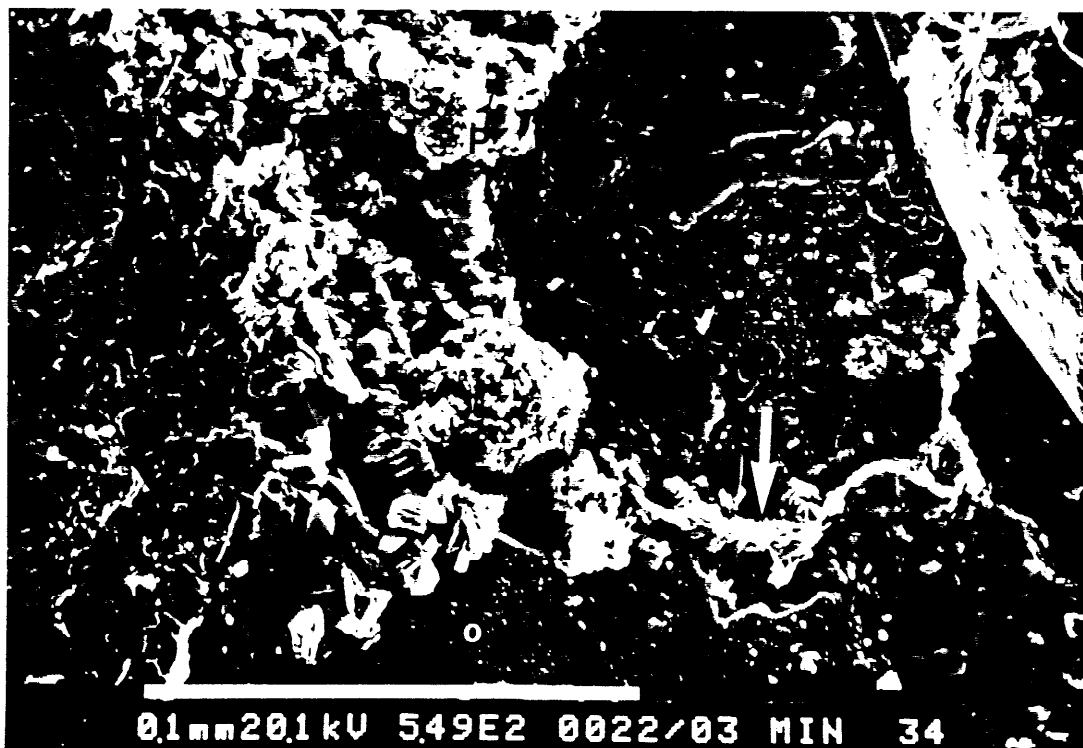


Figure 16b

Closer view of the area immediately above a quartz overgrowth illustrated in Figure 16a. Detrital illite (arrow) with a platy habit is aligned tangentially to a grain surface that was later overgrown by quartz (o). The illite represents a dust rim trapped in the overgrowth. The adjacent pore is filled with anhedral to subhedral kaolin and rare pyrite (P) framboids. Minerva #1, core plug 34, depth 1834.70. Scale bar 0.1mm.

#### 4.8 Minerva #1, Core plug 37, depth 1835.60m

##### X-ray diffraction

The mineralogy is dominated by quartz in the bulk XRD trace (Fig. 17a). There is minor kaolinite and dolomite/ankerite, and trace amounts of illite/muscovite and pyrite. The carbonate is relatively crystalline but the species can not be differentiated due to the lack of secondary peaks. In the clay fraction (Fig. 17b) kaolinite is the major clay, it is well ordered and highly crystalline. Minor to trace amounts of poorly crystalline illite and possibly clinocllore are also evident. The presence of montmorillonite could indicate contamination from the drilling mud. Quartz and feldspar (possibly microcline) were also identified in the clay fraction.

##### Scanning electron microscopy

The sample is a medium grained, moderately sorted sandstone (Fig. 18a). Commonly grains are subangular with low to moderate sphericity. Grain contacts are typically tangential but there are examples of concavo-convex contacts that indicate there has been moderate mechanical compaction. Porosity is a combination of primary intergranular pores and secondary dissolution pores. The intergranular pores are not well interconnected and this would have limited permeability. Minor numbers of pores are filled with kaolin that has micropores between individual booklets.

Framework grains of quartz and corroded K-feldspar are evident. Quartz grains have overgrowths with a druse habit (Fig. 18a) suggesting only minor or incomplete silicification. The next most abundant authigenic mineral is kaolin which fills pores and has at least two different crystal sizes (Fig. 18b). Fine kaolin is anhedral and blocky with an average diameter of 2 microns. Coarser kaolin occurs as subhedral, pseudo-hexagonal booklets that are approximately 10 microns in diameter. Rare examples of pyrite framboids are located along grain margins and in pore throats.

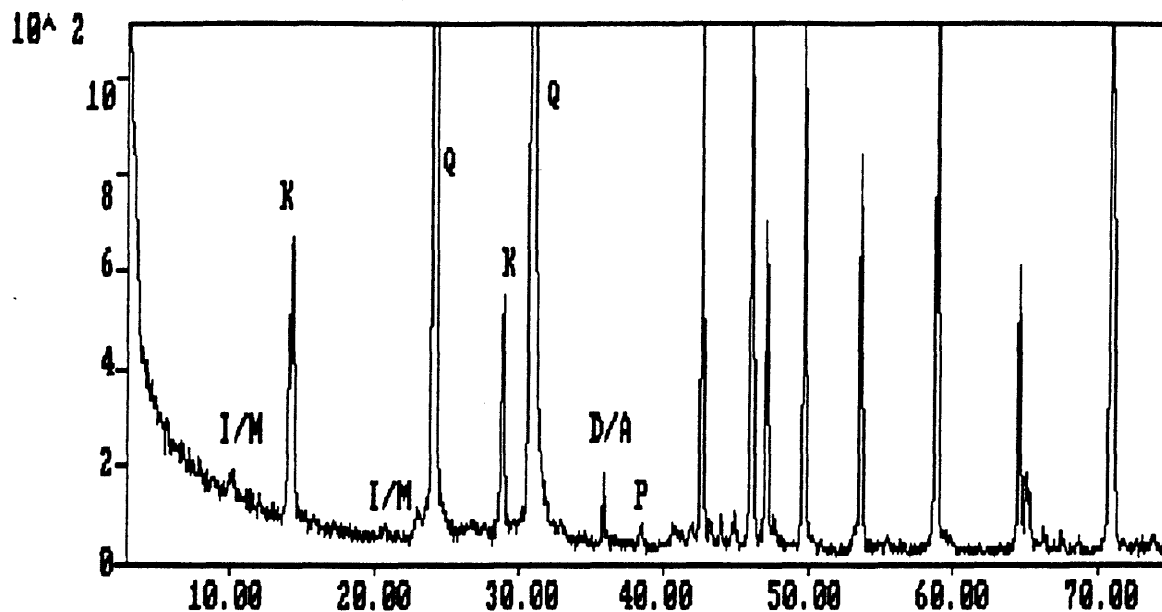


Figure 17a  
Bulk XRD trace of Minerva #1, core plug 37, depth 1835.60m. The horizontal axis is in degrees two theta and the vertical axis is in counts of peak intensity. Only the strongest peaks for each mineral identified have been labelled. I/M = illite/muscovite, K = kaolinite, Q = quartz, D/A = dolomite/ankerite, P = pyrite.

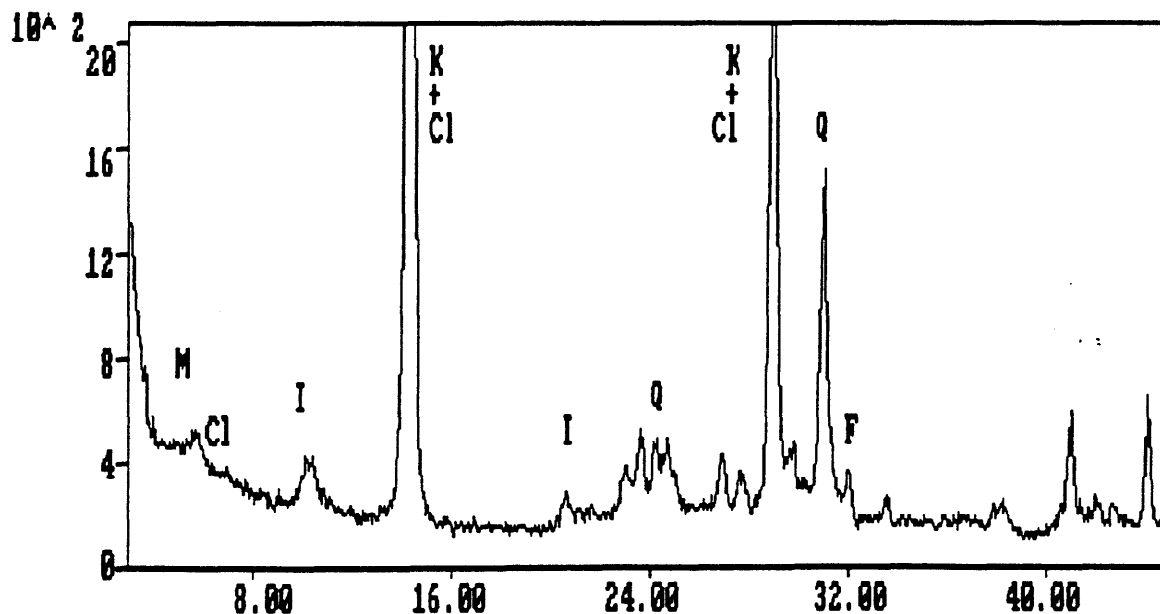


Figure 17b  
XRD trace of the clay fraction from Minerva #1, core plug 37, depth 1835.60m. The horizontal axis is in degrees two theta and the vertical axis is in counts of peak intensity. Only the strongest peaks for each mineral identified have been labelled. M = montmorillonite, Cl = clinochlore, I = illite, K = kaolinite, Q = quartz, F = feldspar.

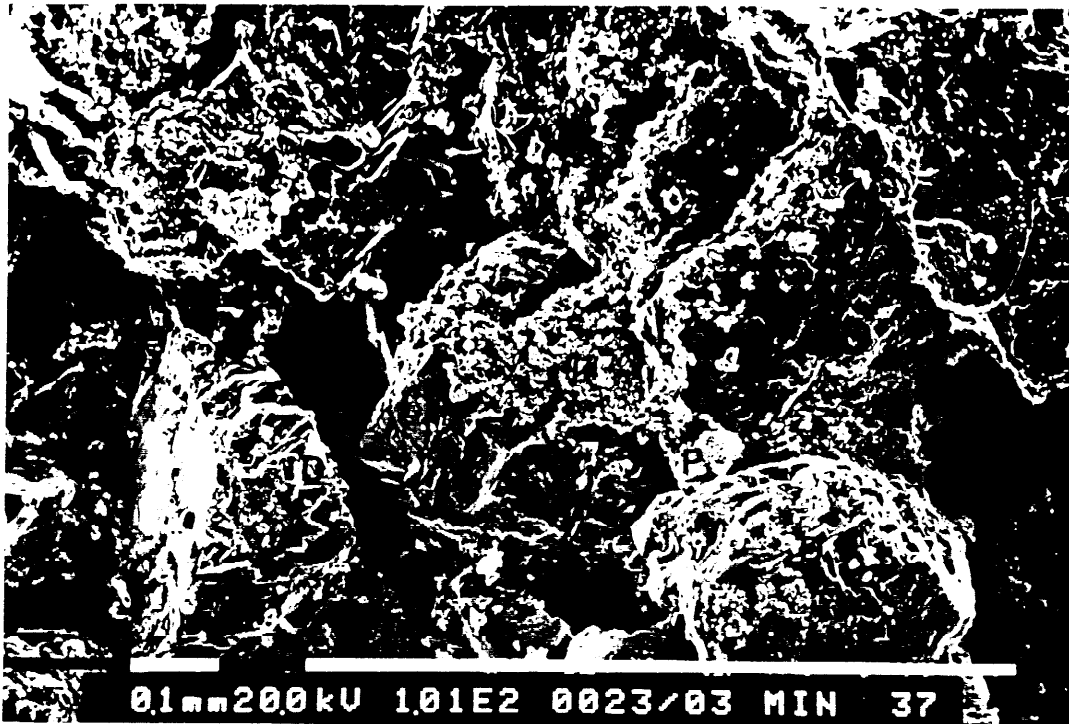


Figure 18a

General view illustrating a medium grained, moderately sorted sandstone. Pores are reduced in size by quartz druse (D) and blocked by kaolin (K). Rare pyrite (P) framboids are evident blocking pore throats. Minerva #1, core plug 37, depth 1835.60m. Bar scale 0.1mm.



Figure 18b

Pore filling kaolin with at least two different crystal sizes. Blocky anhedral kaolin is approximately 2 microns in diameter (A) and the coarser kaolin (B) is 10 microns. Bar scale 0.1mm.

#### 4.9 Minerva #1, Core plug 49, depth 1840.60m

##### Scanning electron microscopy

The sample is a fine grained, moderately well sorted, micaceous sandstone (Fig. 19a). Grains tend to be subangular with moderate sphericity. Porosity is dominated by secondary dissolution pores that are unlikely to be well interconnected. These pores are typically grain size and can be attributed to dissolution of labile grains such as feldspars. Commonly intergranular pores have been filled with kaolin. This suggests that a relatively high percentage of the porosity is microporosity. Permeability is unlikely to be good given the secondary nature of pores.

Framework grains of quartz, corroded K-feldspars, micas and ?altered lithics are evident. Silicification has been restricted to isolated quartz druse. Kaolin represents the dominant authigenic mineral. It has a variety of habits that differ according to the mechanism of formation. Euhedral pseudo-hexagonal platelets that form booklets and rare verms are up to 15 microns in diameter. These kaolin booklets have precipitated from solution in pore spaces (Fig. 19b). Elsewhere the kaolin is anhedral to subhedral, blocky or platy and ranges in diameter from 2 to 5 microns. This phase of kaolin is associated with lettuce-like illite. The combined mineralogy may indicate that both minerals have formed as alteration products of a lithic (Fig. 19c). Pyrite framboids that are approximately 10 microns in diameter have clustered in one pore.

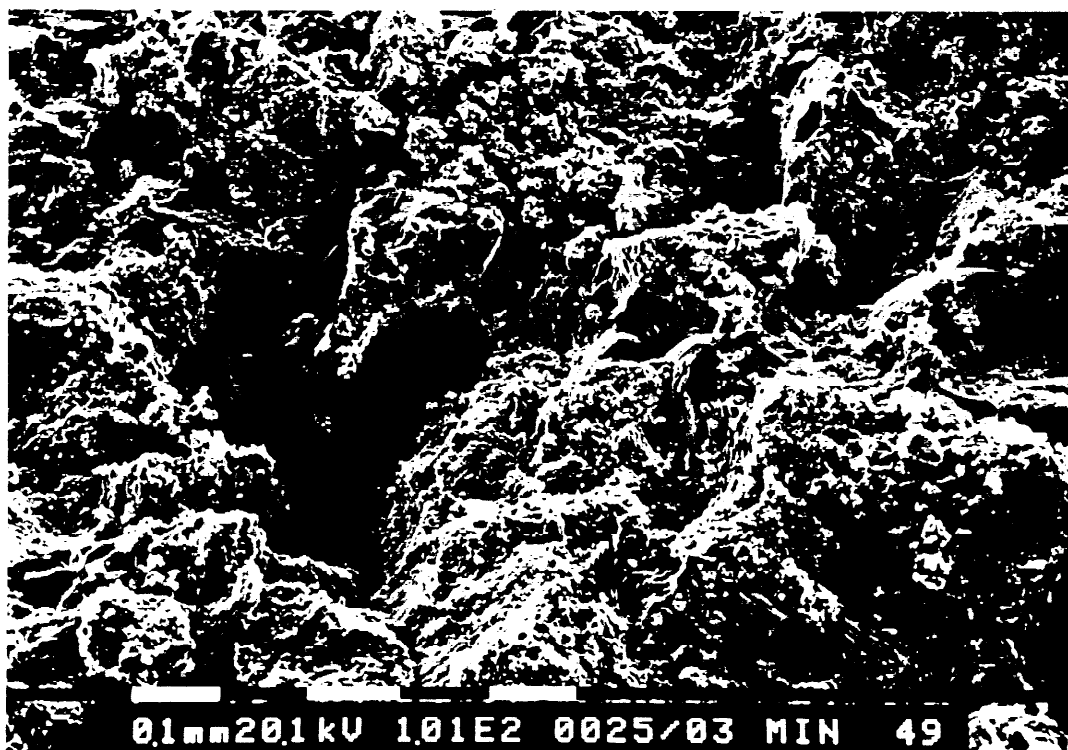


Figure 19a

This field of view illustrates the limited development of porosity in this fine grained moderately well sorted sandstone. Those pores which are apparent, are dominantly secondary in nature. Minerva #1, core plug 49, depth 1840.60m. Bar scale 0.1mm.



Figure 19b

Euohedral pore filling kaolin. Crystal size is finer on the margins of the pore (arrow) and there are traces of illite associated with this phase. Micropores are well developed between the euohedral kaolin booklets. Minerva #1, core plug 49, depth 1840.60m. Bar scale 0.1mm.

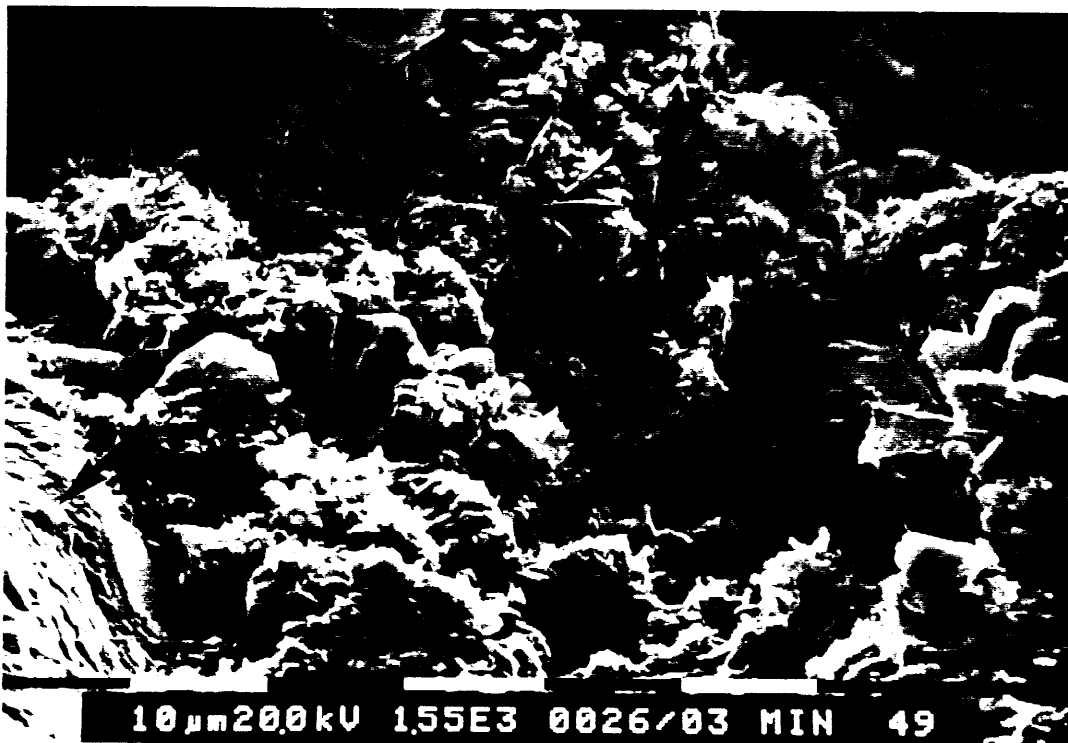


Figure 19c

This intergrowth of anhedral to subhedral kaolin and lettuce-like illite probably represents an altered lithic. The surface of an adjacent quartz grain (arrow) is pitted suggesting the influence of corrosion. Minerva #1, core plug 49, depth 1840.60m. Bar scale 10 microns.

#### 4.10 Minerva #1, Core plug 52, depth 1842.80m

##### X-ray diffraction

Quartz is the major component of the bulk fraction (Fig. 20a). Trace amounts of illite/muscovite, kaolinite and sylvite were also detected. The sylvite probably was introduced into the sample as a contaminant during drilling. Minor amounts of montmorillonite identified in the clay fraction (Fig. 20b) may also represent drilling mud contaminant. Kaolinite is the dominant clay mineral, it is not as well ordered as previous samples. Illite also has broad peaks indicating that it is probably poorly crystalline. Traces of clinocllore could be associated with the montmorillonite or represent alteration of micas or lithics in the sample. Quartz was the only other mineral identified in the clay fraction.

##### Scanning electron microscopy

The sample is a medium to coarse grained, moderately sorted mineralogically mature sandstone. Grains appear angular due to the abundance of quartz overgrowths (Fig. 21a). Porosity is dominantly primary and intergranular but interconnections between pores have been limited by silicification. Porosity is also reduced by pore filling kaolin. Micropores associated with the kaolin are limited to pores between booklets.

Framework grains are dominated by quartz with rare flakes of mica and ?altered lithics. Quartz overgrowths have precipitated throughout the sample thus prior to silicification this was probably a clean sand. Quartz overgrowths are typically euhedral rhombohedra and there are numerous examples of druse. Euhedral to subhedral kaolin booklets and verms were precipitated after the quartz overgrowths. These pseudo-hexagonal platelets are 15 to 20 microns in diameter. A phase of kaolin with a finer crystal size (approximately 5 microns) is associated with illite and thought to represent altered lithics. Rarely this fine kaolin has a ragged edged vermiform habit.

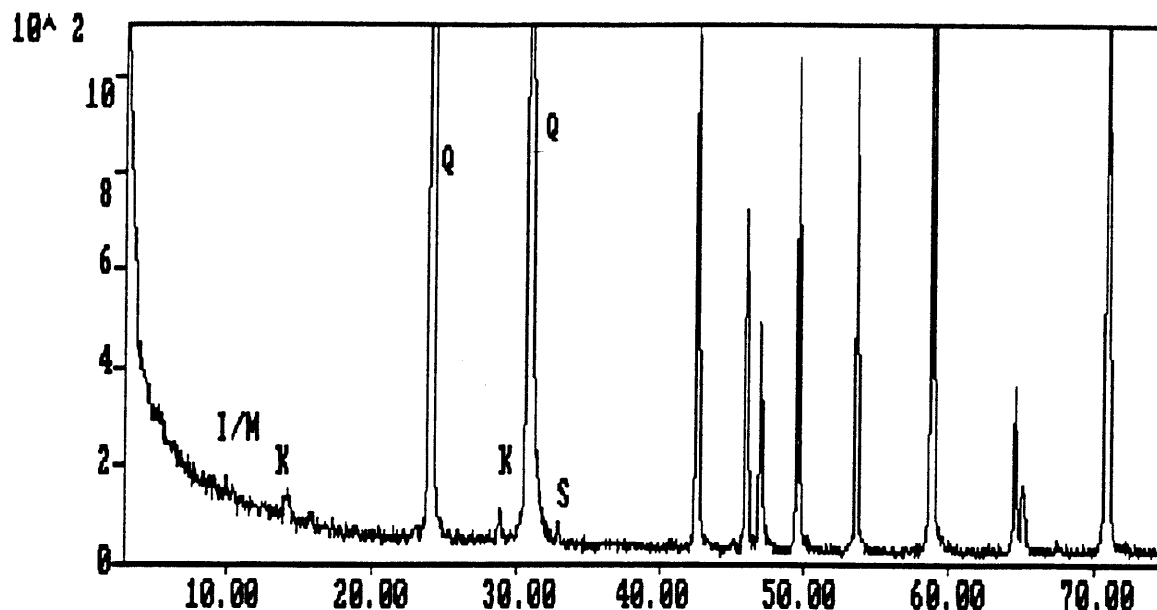


Figure 20a  
Bulk XRD trace of Minerva #1, core plug 52, depth 1842.80m. The horizontal axis is in degrees two theta and the vertical axis is in counts of peak intensity. Only the strongest peaks for each mineral identified have been labelled. I/M = illite/muscovite, K = kaolinite, Q = quartz, S = sylvite.

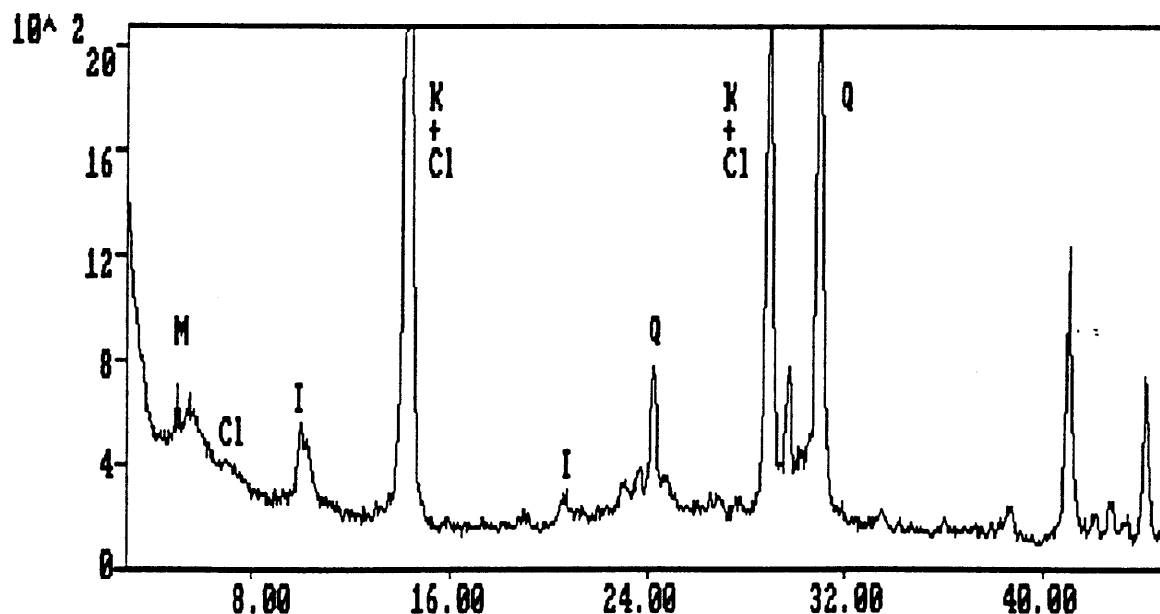


Figure 20b  
XRD trace of the clay fraction from Minerva #1, core plug 52, depth 1842.80m. The horizontal axis is in degrees two theta and the vertical axis is in counts of peak intensity. Only the strongest peaks for each mineral identified have been labelled. M = montmorillonite, Cl = clinochlore, I = illite, K = kaolinite, Q = quartz.





Figure 21a

Euhedral terminations on the quartz in this medium to coarse grained sandstone indicate the extent of silicification. Angular, primary intergranular pores are preserved between the overgrowths. Minerva #1, core plug 52, depth 1842.80m. Bar scale 0.1mm.

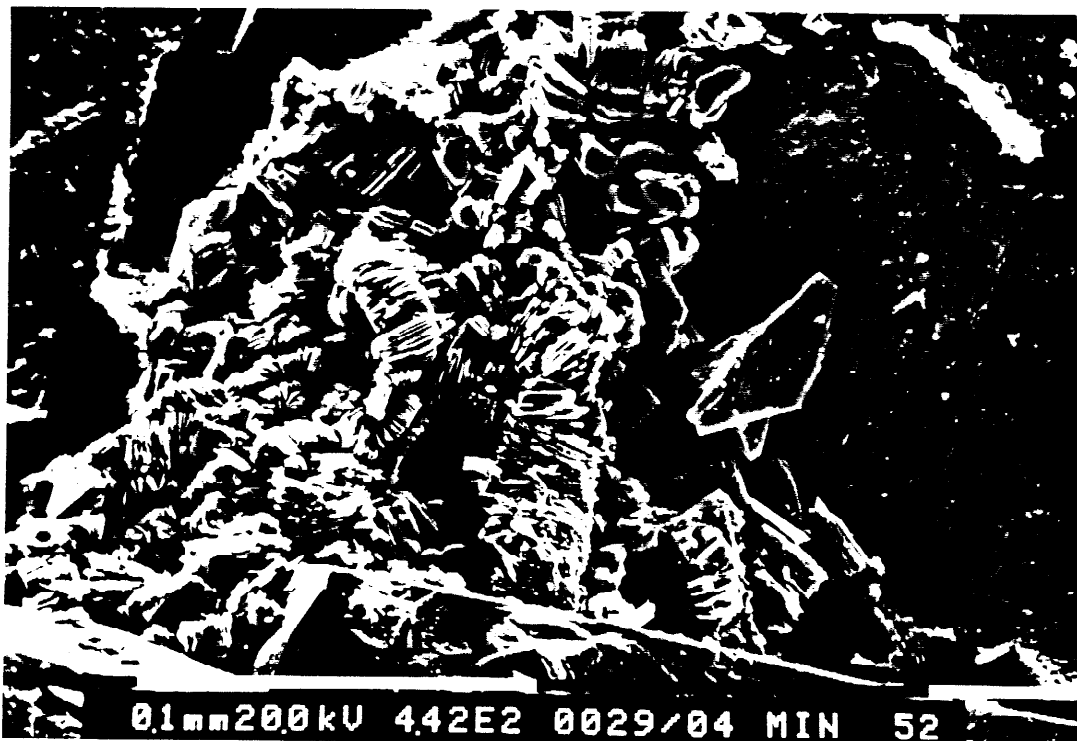


Figure 21b

Kaolin booklets typically have straight edges and thus micropores are restricted to those areas between booklets. These micropores are up to 10 microns in diameter. This pore filling kaolin is enclosed by euhedral quartz overgrowths. Minerva #1, core plug 52, depth 1842.80m. Bar scale 0.1mm.

#### 4.11 Minerva #1, Core plug 53, depth 1843.10m

##### Scanning electron microscopy

The sample is a very coarse grained, poor to moderately sorted, mineralogically mature sandstone. Typically grains are subangular with low to moderate sphericity. Texturally the sample is grain supported with point and tangential grain contacts. Porosity is dominated by elongate intergranular pores (Fig. 22a) and there are rare secondary grain size pores. The elongate nature of intergranular pores indicates that the pores are interconnected and therefore permeability should be good.

Quartz was the only framework grain identified which indicates this is probably a quartzarenite. Authigenic minerals are restricted to quartz, kaolin and illite. Quartz forms overgrowths that have euhedral rhombohedral terminations and occur as druse. The latter appear to be dominant which suggests that silicification was not extensive. Very fine anhedral kaolin that has a diameter of less than 2 microns has replaced grains. This kaolin is associated with rare subhedral kaolin booklets that are approximately 5 microns in diameter and traces of platy illite. This mixture of kaolin and illite suggests that a lithic has been replaced. Where the very fine kaolin is adjacent to quartz overgrowths (Fig. 22b) the overgrowths appear to have been inhibited. This suggests that silicification occurred after the alteration of the lithic.



Figure 22a

General view of poorly sorted, very coarse grained sandstone with elongate intergranular pores. Quartz druse (arrows) are apparent on selected grains. Minerva #1, core plug 53, depth 1843.10m. Bar scale 1mm.



Figure 22b

Quartz druse have been inhibited by very fine anhedral kaolin (arrows). In places silicification enclosed the kaolin. Minerva #1, core plug 53, depth 1843.10m. Bar scale 1mm.

#### 4.12 Minerva #1, Core plug 56, depth 1844.05m

##### Scanning electron microscopy

The sample is a coarse grained, very poorly sorted sandstone (Fig. 23a). Grains are subangular with low to moderate sphericity. Texturally the sandstone is grain supported with dominantly tangential grain contacts. Porosity is a mixture of primary intergranular pores and secondary dissolution pores. Secondary pores are more abundant than core plug 53 and hence permeability is probably less than the previous sample.

Quartz is the dominant framework grain and there was minor corroded K-feldspars and mica flakes. The latter indicate that this sample is not as mineralogically mature as core plug 53. Authigenic minerals of quartz and kaolin are apparent. Silicification has resulted in the presence of quartz druse and euhedral rhombohedral terminations that partially reduce pore size. Anhedral very fine kaolin has replaced grains and there are traces of coarser subhedral kaolin booklets that are up to 10 microns in diameter (Fig. 23b).

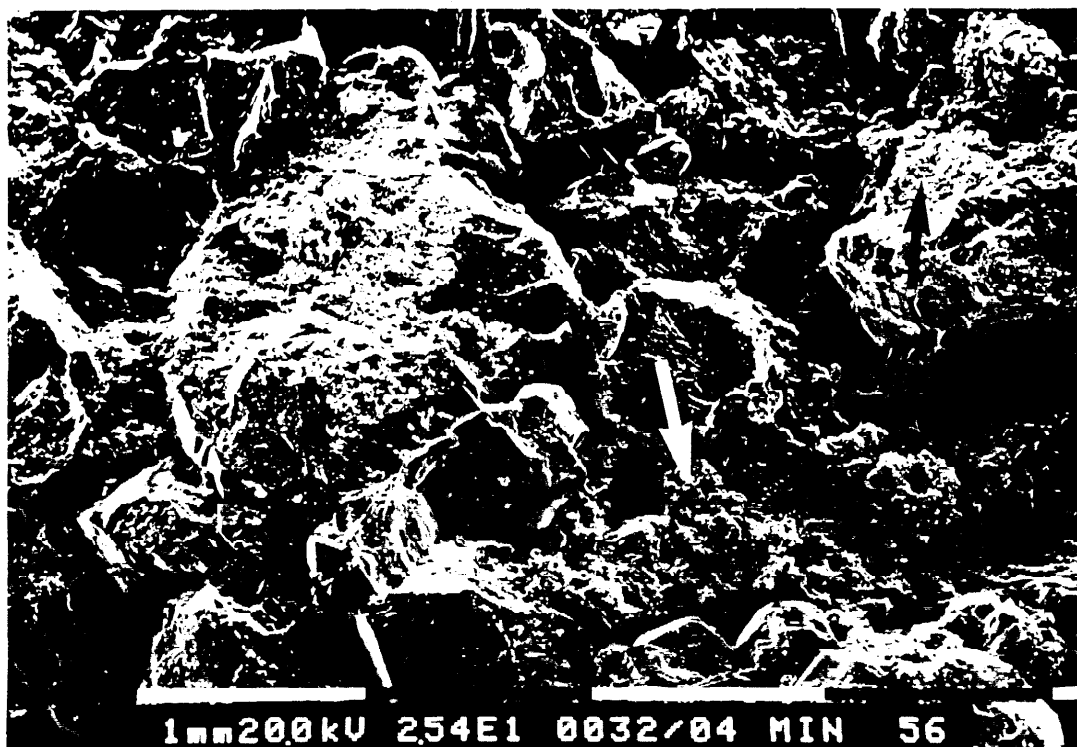


Figure 23a

Primary intergranular pores are not well interconnected in this sandstone. In part this is attributed to silicification, mechanical compaction and the presence of kaolin (arrows). Minerva #1, core plug 56, depth 1844.05m. Bar scale 1mm.

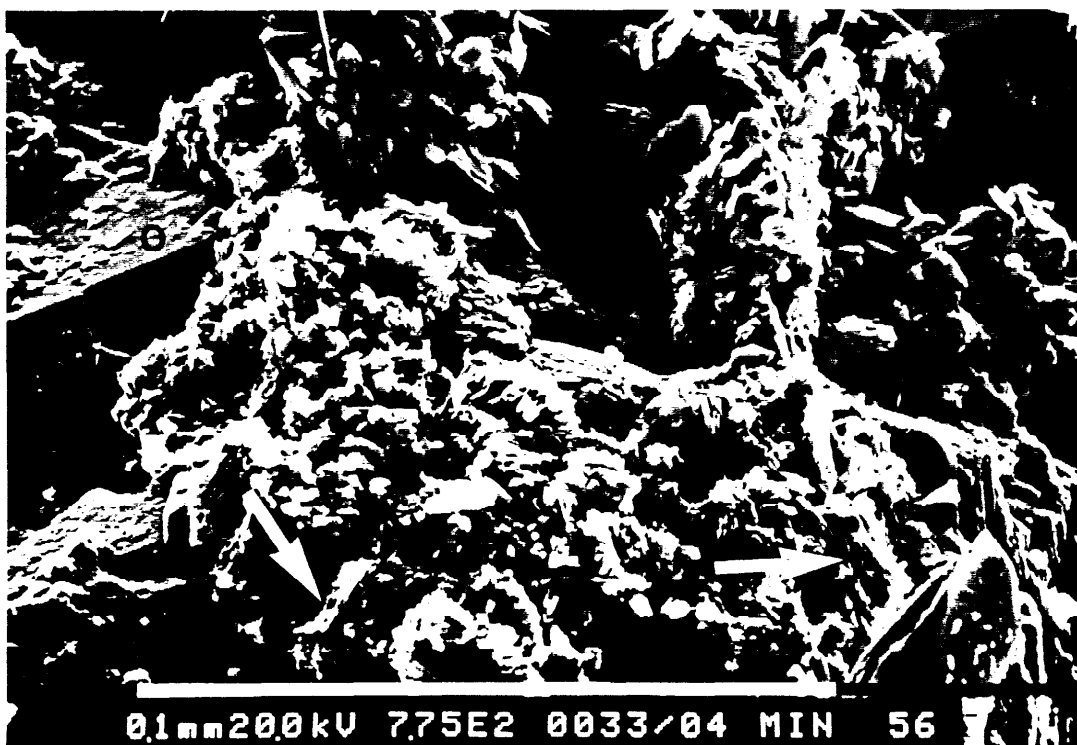


Figure 23b

Anhedra kaolin intermixed with coarser platelets (arrows) that could represent altered micas. Euhedral quartz overgrowths (o) are also apparent. Minerva #1, core plug 56, depth 1844.05m. Bar scale 0.1mm.

4.13 Minerva #1, Core plug 58, depth 1844.60m

## Thin section description

Rock classification: Quartzarenite

Texture:

The sample is a well sorted, medium grained, mineralogically and texturally mature quartzarenite. Framework grains range in diameter from approximately 0.10mm (very fine sand) to 3.0mm (granules) and were commonly subrounded with moderate sphericity prior to silicification. Texturally the quartzarenite is grain supported with dominantly tangential grain contacts. Rare contorted lithics indicate that there has been moderate mechanical compaction. Bedding is illustrated by changes in grain size from medium to very coarse sand. Typically beds are up to 3mm in width which indicates that they should be described as laminae. Contacts between laminae are gradational and planar. A fracture zone cross cuts the laminae at approximately right angles. The fracture zone varies in width from 2 to 4 mm and is filled with angular quartz and silt (Fig. 24a). Fine quartz silt has an average diameter of 15 microns and rare quartz sand has evidence of minor quartz overgrowths. There is no obvious increase in silicification immediately adjacent to the fracture (Fig. 24b) nor when compared with a zone one centimetre from the fracture (Fig. 24c).

Porosity:

Porosity is apparent throughout the sample, including the fracture zone. Pores are typically primary and intergranular in nature. The angular outline of pores is controlled by the presence of quartz overgrowths and pore size is controlled by grain size. Thus in the fracture zone intergranular pores are much smaller than those in the surrounding quartzarenite. Rare secondary pores have resulted from the corrosion of feldspars (honeycomb porosity) and elsewhere there are oversize pores that have resulted from the dissolution of adjacent labile grains. Micropores can be recognised between kaolin booklets. Contamination from drilling mud has reduced porosity and permeability.

Visual Estimate of Composition		%
Framework grains	Quartz	64
	Feldspar	1
	Lithics	1
	Mica	tr
	Accessory minerals	tr
Matrix		nd
Authigenic minerals and cements	Pyrite	2
	Kaolin	tr
	Quartz	16
Porosity	Intergranular	10
	Dissolution	3
	Micropores	tr
Drilling mud		2

Framework grains:

Monocrystalline quartz is dominant, it has straight to slightly undulose extinction, scattered vacuoles and rare mineral inclusions of apatite, muscovite, zircon and rutile needles. Where vacuoles are aligned in trails this could indicate an earlier phase of healed fractures. Isolated grains of polycrystalline quartz have undulose extinction and

either straight or sutured crystal boundaries. Feldspars are either highly altered or corroded and probably alkali in composition. Lithics of micaceous metasediments have been deformed during compaction and are difficult to identify due to extensive alteration and corrosion. Other lithics can be recognised as siltstone and dusty chert. Bent and altered muscovite flakes are up to 0.5mm in length. The only accessory minerals identified were rounded medium sand size grains of epidote and silt size zircon with a hydrocarbon envelope.

Authigenic minerals and cements:

Pyrite octahedra of various sizes have partially replaced rare quartz grains especially along the dust rims of quartz overgrowths. Opaques have accumulated along the cleavage planes of micas and there are massive opaques replacing other grains. Clusters of pyrite framboids are rare in pore throats and along pore margins. Subhedral to anhedral booklets of kaolin that are up to 10 microns in diameter have replaced grains and rarely fill intergranular pores. Kaolin appears to be restricted to one small patch in the section. Syntaxial quartz overgrowths are pervasive throughout the section. Euhedral terminations, straight grain contacts, triple point junctions and dust rims all outline the overgrowths. Rarely illitic clay is recognised in the dust rims. Euhedral terminations are either rhombohedral or drusy in habit. Fluid inclusions are evident in the overgrowths.

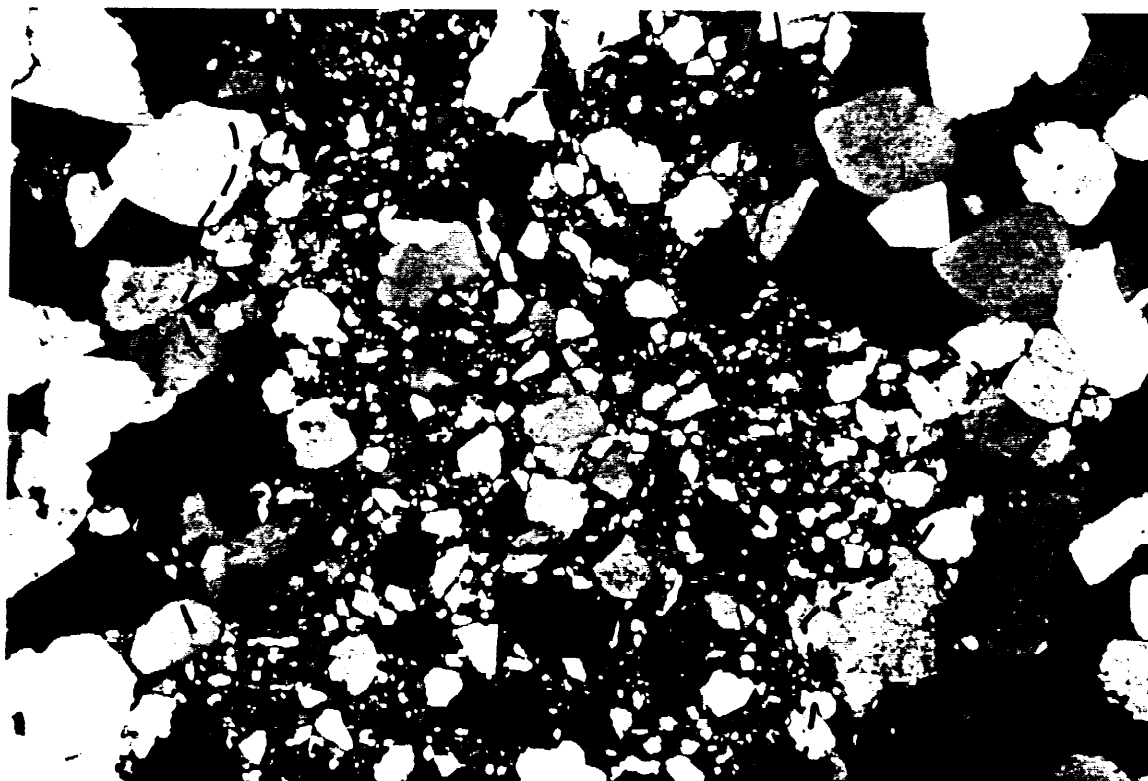


**Figure 24a**

The fracture (dashed lines) is filled with angular quartz and fine silt. Adjacent framework grains of monocrystalline quartz have an average grain size of medium sand. Minerva #1, core plug 58, depth 1844.60m. Crossed nicols. Field of view 2.72mm.

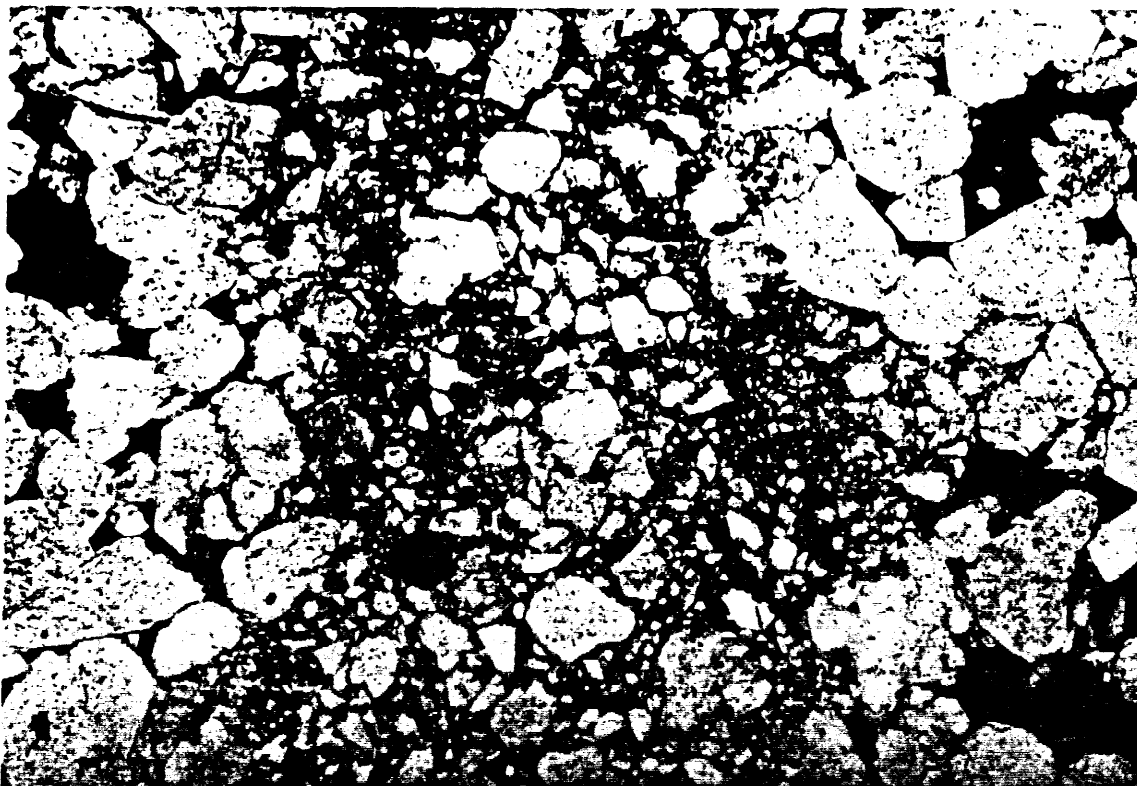


Figure 24b

Same field of view as Figure 24a in plane light. Note the preservation of porosity (blue) in the fracture zone and immediately either side of this zone. Pores are a combination of primary intergranular and secondary pores. Traces of drilling mud (brown) are evident partially filling pores.

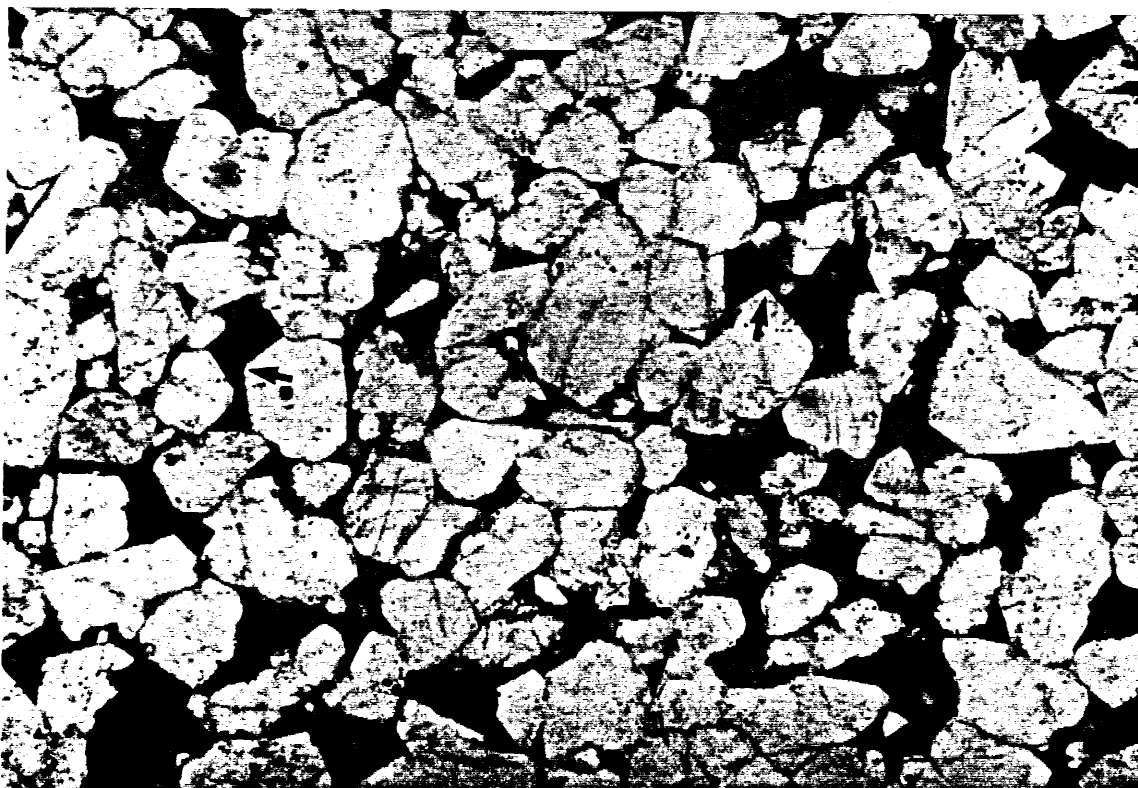


Figure 24c

General field of view 1 centimetre from the fracture zone. It does not show any increase or decrease in silicification when compared to the area juxtaposed to the fracture. Quartz overgrowths are apparent from the euhedral terminations (arrows) on quartz grains. Minerva #1, core plug 58, depth 1844.60m. Plane light. Field of view 2.72mm.



#### 4.14 Minerva #1, Core plug 61, depth 1845.52m

##### Scanning electron microscopy

The sample is a coarse grained, moderately sorted, mineralogically mature sandstone (Fig. 25a). Grains are commonly subangular with moderate sphericity. Angularity has probably been introduced by silicification. Texturally the sandstone is grain supported with tangential and lesser numbers of point contacts. Porosity is dominated by primary intergranular pores with examples that are interconnected. There may be secondary dissolution pores but these features could also have been produced by grain plucking during sample preparation.

Framework grains are dominated by quartz with rare micas (biotite). Quartz, kaolin and pyrite represent the authigenic minerals. Euhedral rhombohedral terminations are dominant on the quartz overgrowths. Silicification has been extensive throughout the sample. Kaolin is less abundant than quartz, it is represented by two different crystal sizes and habits. Anhedral fine kaolin is 1 to 2 microns in diameter and appears to have replaced grains. Pseudo-hexagonal platelets of kaolin that are 10 to 15 microns in diameter form booklets and rare verms. This coarser kaolin appears to have precipitated in pores. Pyrite framboids also have a variety of crystal sizes. Framboids which are approximately 8 microns in diameter are associated with anhedral kaolin. Coarser framboids which are up to 20 microns in diameter concentrate along grain margins (Fig. 25b)



Figure 25a

Moderately sorted, coarse grained sandstone in which the grains appear to be angular due to silicification. Primary intergranular pores are well preserved but reduced in size by the quartz overgrowths. Overgrowths are evident from the euhedral terminations on detrital grains. Minerva #1, core plug 61, depth 1845.52m. Bar scale 1mm.

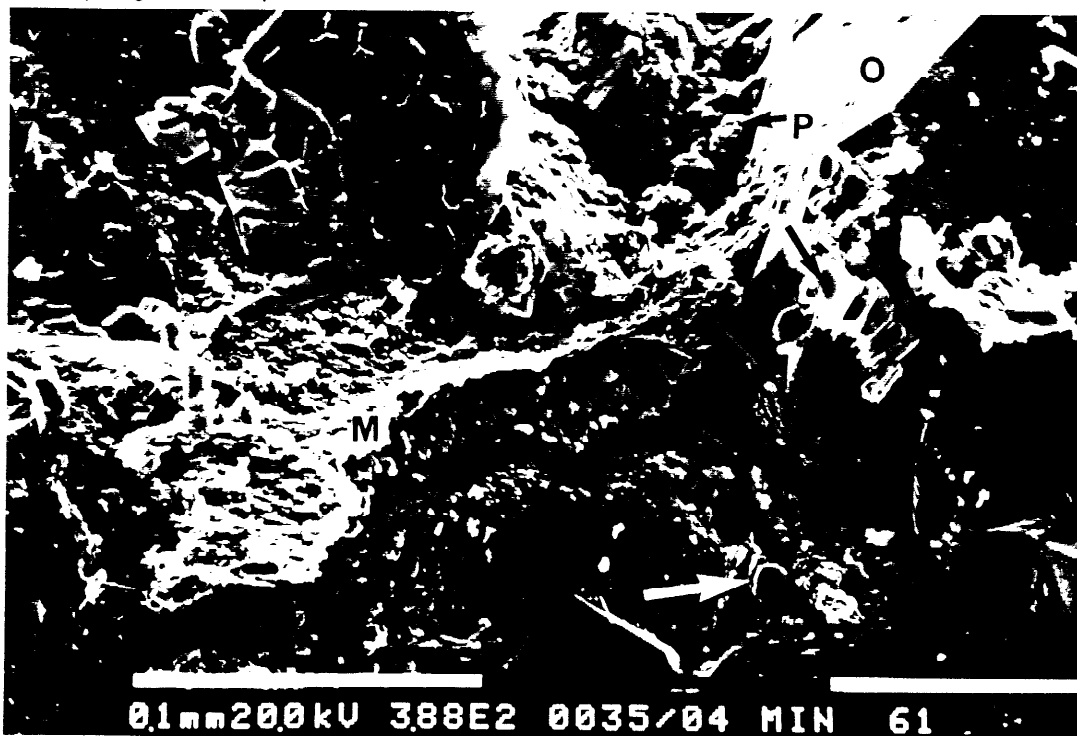


Figure 25b

This field of view shows a pore throat that is blocked by quartz overgrowths (o), a mica flake (M) and pyrite framboids (P). Subhedral booklets of kaolin (arrows) and pyrite framboids concentrate along the pore margins. Minerva #1, core plug 61, depth 1845.52m. Bar scale 0.1mm.

#### 4.15 Minerva #1, Core plug 64A, depth 1846.42m

##### Thin section description

Rock classification: Quartzarenite

Texture:

The sample is a medium to very coarse grained, moderate to poorly sorted, mineralogically and texturally mature quartzarenite. Graded beds with relatively sharp planar contacts show a gradation in grain size from very coarse sand to medium sand. It is unknown whether the beds are fining or coarsening upwards because the section is not oriented. Sorting in the medium grained sands is better than the coarse sand that is poorly sorted. Grains range in diameter from approximately 0.06mm (coarse silt) to 2.5mm (granules) and were typically subrounded with moderate sphericity prior to silicification. Texturally the sample is grain supported with tangential and concavo-convex grain contacts. Deformation of ductile lithics and micas indicates that there has been moderate mechanical compaction.

Porosity:

Porosity is a mixture of primary intergranular pores (Figs 26a & b) and secondary dissolution pores. Intergranular pores are elongate and angular. This shape is attributed to silicification which was not extensive enough to block pore throats. Permeability should be good for this sample. Secondary pores are typically grain size but there are examples of oversize pores. Other secondary pores are honeycomb in nature and occur where labile grains (lithics and feldspars) have been partially corroded. Minor contamination from drilling mud is apparent on pore margins and very fine angular quartz silt has blocked pore throats.

Visual Estimate of Composition		%
Framework grains	Quartz	68
	Feldspar	tr
	Lithics	3
	Mica	tr
	Coal	tr
	Accessory minerals	tr
Matrix		nd
Authigenic minerals and cements	Glaucony	tr
	Pyrite	tr
	Kaolin	1
	Quartz	12
Porosity	Intergranular	10
	Dissolution	5
Drilling mud		tr

Framework grains:

Monocrystalline and polycrystalline quartz is apparent. Monocrystalline quartz has straight to slightly undulose extinction, scattered vacuoles and rare mineral inclusions of apatite, zircon, rutile needles, tourmaline, biotite and muscovite. Where vacuoles are aligned in trails this could represent either a healed fracture or has been inherited from a metamorphic terrane. Polycrystalline quartz concentrates in the coarser sand fraction. Typically this variety of quartz has undulose extinction and either straight or sutured crystal boundaries. Rare alkali feldspars that lack twinning have been either corroded or partially replaced by kaolin. Lithics are dominated by chloritised

volcanics. In addition there are minor micaceous metasediments and rare examples of quartzite. One flake of muscovite that is 1.1mm in length occurs in a very coarse sand size bed. Other bent micas have been replaced by chlorite. Angular chips of fragmented carbonaceous material probably represent coal. Rounded silt size zircon has a hydrocarbon envelope and there are rare examples of silt size ?monazite and epidote.

Authigenic minerals and cements:

Traces of pyrite are scattered through out the sample as minute cubes, framboids and octahedra that either partially replace grains or cluster along pore margins. Subhedral booklets and verms of kaolin that are up to 20 microns in diameter have partially replaced K-feldspars. Elsewhere grains have been completely replaced by kaolin booklets that are less than 5 microns in diameter. Subhedral to anhedral kaolin booklets and verms that fill pores are typically 10 microns in diameter. Quartz overgrowths are dominated by druse rather than euhedral rhombohedral terminations. Fluid inclusions are evident in the overgrowths. Rare dust rims of iron oxide are pronounced. Silicification has been inhibited adjacent to chloritised lithics. Rare pale green grains of glaucony could be composed of chlorite or glauconite. The grain texture is vaguely wormy which suggests at least some glauconite is present.

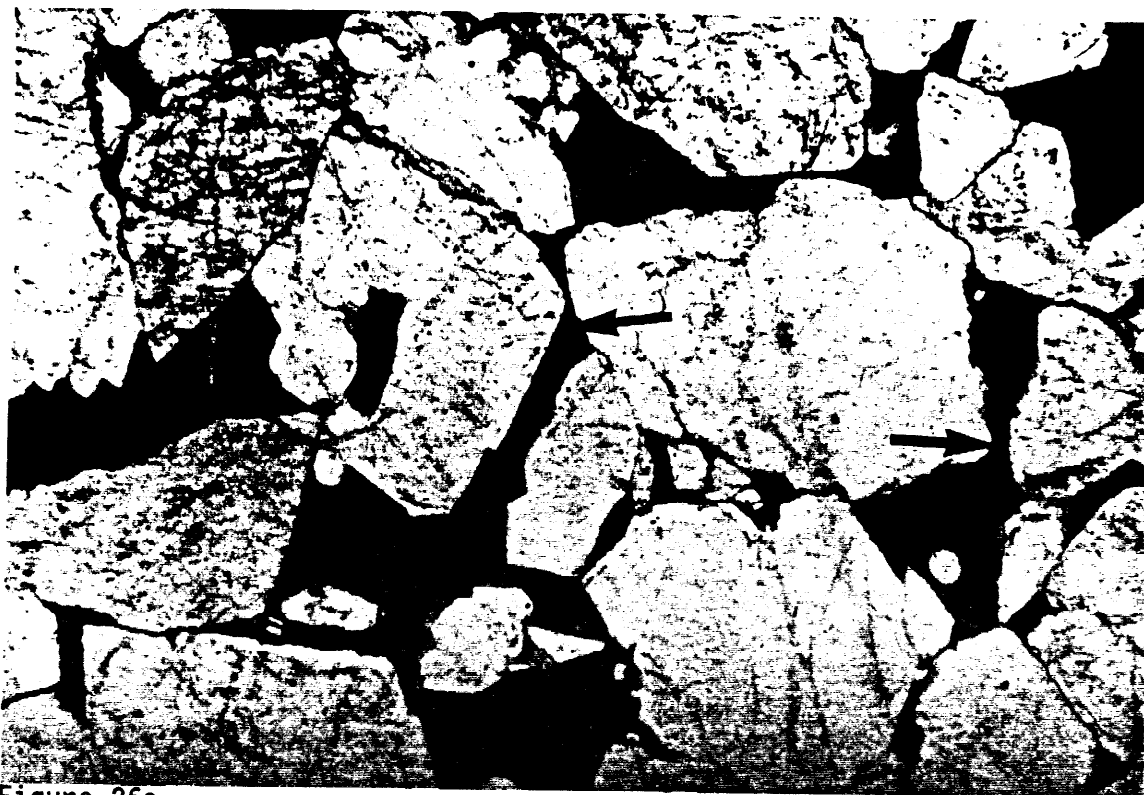


Figure 26a

Excellent preservation of intergranular pores (blue) is apparent in this coarse to very coarse grained bed. Interconnections (arrows) between pores indicate that permeability is also good. Euhedral terminations on quartz grains outline the presence of syntaxial overgrowths. Minerva #1, core plug 64A, depth 1846.42m. Plane light. Field of view 2.72mm.

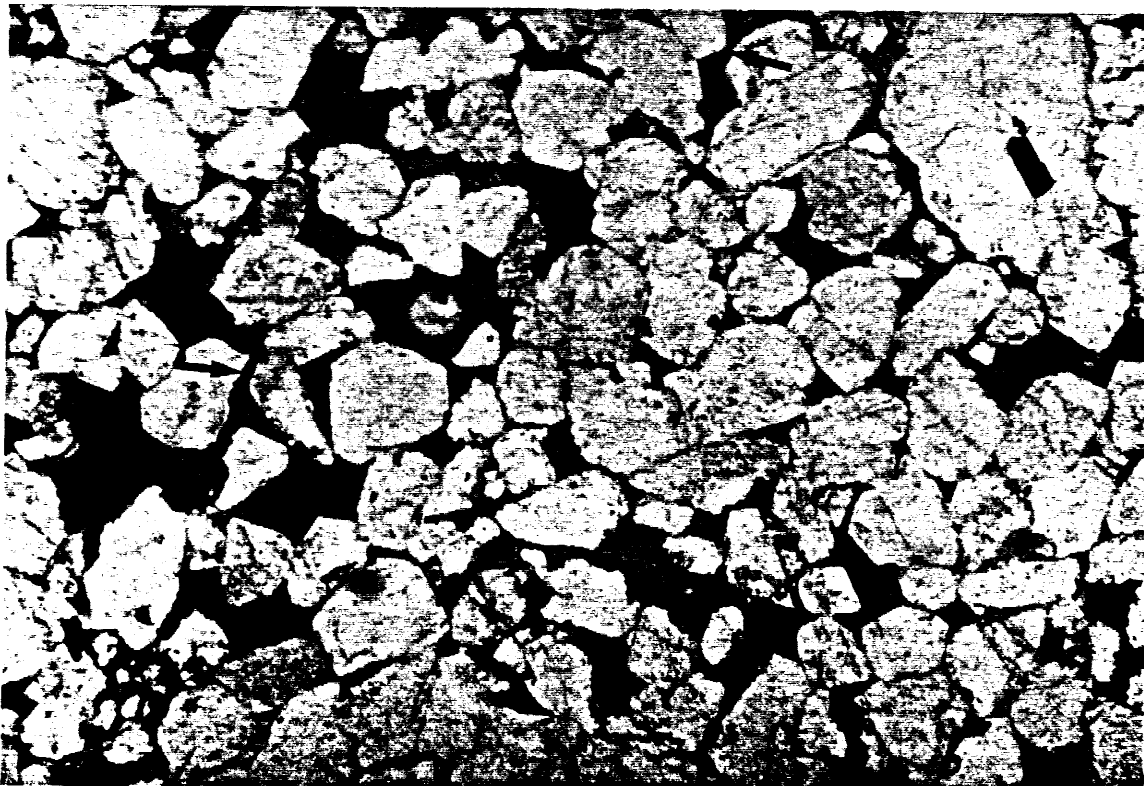


Figure 26b

In this bed of medium grained sand, intergranular pores (blue) still show evidence of interconnection (arrows). Silicification is indicated by the angular outline of detrital grains. Minerva #1, core plug 64A, depth 1846.42m. Plane light. Field of view 2.72mm.

4.16 Minerva #1, Core plug 65, depth 1846.72m

## Thin section description

Rock classification: Quartzarenite

Texture:

The sample is a coarse grained, moderately sorted, texturally and mineralogically mature quartzarenite. There is evidence of graded bedding with possibly some disruption of the beds. Contacts between beds are relatively sharp where sorting is good. Grains range in diameter from approximately 0.08mm (very fine sand) to 2.0mm (granules) and typically grains were subrounded with moderate sphericity prior to silicification. Texturally the quartzarenite is grain supported with dominantly point and tangential grain contacts. Rare sutured contacts indicate that there has been minor mechanical compaction.

Porosity:

Porosity is a combination of primary and secondary pores (Fig. 27). Pore size varies according to grain size in the bed. Primary pores are intergranular in nature and typically have an elongate angular shape. Angularity has been caused by the presence of euhedral quartz overgrowths. Secondary pores are grain size and can be attributed to the dissolution of labile grains. Skeletons of feldspars indicate that these grains have been corroded to produce honeycomb pores. Rare pores and pore throats are blocked by drilling mud.

Visual Estimate of Composition		%
Framework grains	Quartz	73
	Feldspars	tr
	Lithics	3
	Micas	tr
	Coal	tr
	Accessory minerals	tr
Matrix		nd
Authigenic minerals and cements	Pyrite	tr
	Kaolin	1
	Quartz	10
	Carbonate	tr
Porosity	Intergranular	8
	Dissolution	4
Drilling mud		tr

Framework grains:

Monocrystalline quartz has straight to slightly undulose extinction, scattered vacuoles and rare mineral inclusions of apatite, biotite, tourmaline, rutile and zircon. Polycrystalline quartz is a minor component of the quartz fraction, it has undulose extinction and straight crystal boundaries. Feldspars are commonly highly altered either due to corrosion or replacement by kaolin. Lithics consist of micaceous schist, other metasediments, chert and granite. Metamorphic fragments represent a high percentage of these lithics. Rare flakes of muscovite that up to 0.45mm in length, have ragged terminations and are partially altered. One biotite flake has been replaced by iron oxide. An angular fragmented segment of opaque material is possibly a coal fragment. The only accessory mineral is a single rounded medium size grain of brown ?amphibole. Cleavage is not apparent in the grain and this makes identification difficult.

Authigenic minerals and cements:

Syntaxial quartz overgrowths are the dominant cement and are uniformly distributed throughout the sample. Overgrowths are outlined by straight grain contacts, euhedral rhombohedral terminations and rare druse. Where dust rims are trapped in the overgrowths there is evidence of multiple stages of silicification. Fluid inclusions are evident in the quartz overgrowths. Minor opaques that form anhedral masses have partially replaced isolated grains. Elsewhere there are pyrite framboids located along grain margins. Grains have been replaced by kaolin and there are subhedral kaolin booklets with an average diameter of 10 microns filling isolated pores. There is one pore in which the kaolin is associated with drilling mud which could suggest there has been some migration of fines. Where micas have been replaced by kaolin the booklets are up to 40 microns in diameter. Rare anhedral crystals of clear carbonate spar have precipitated after the quartz overgrowths. The spar occurs on pore margins.

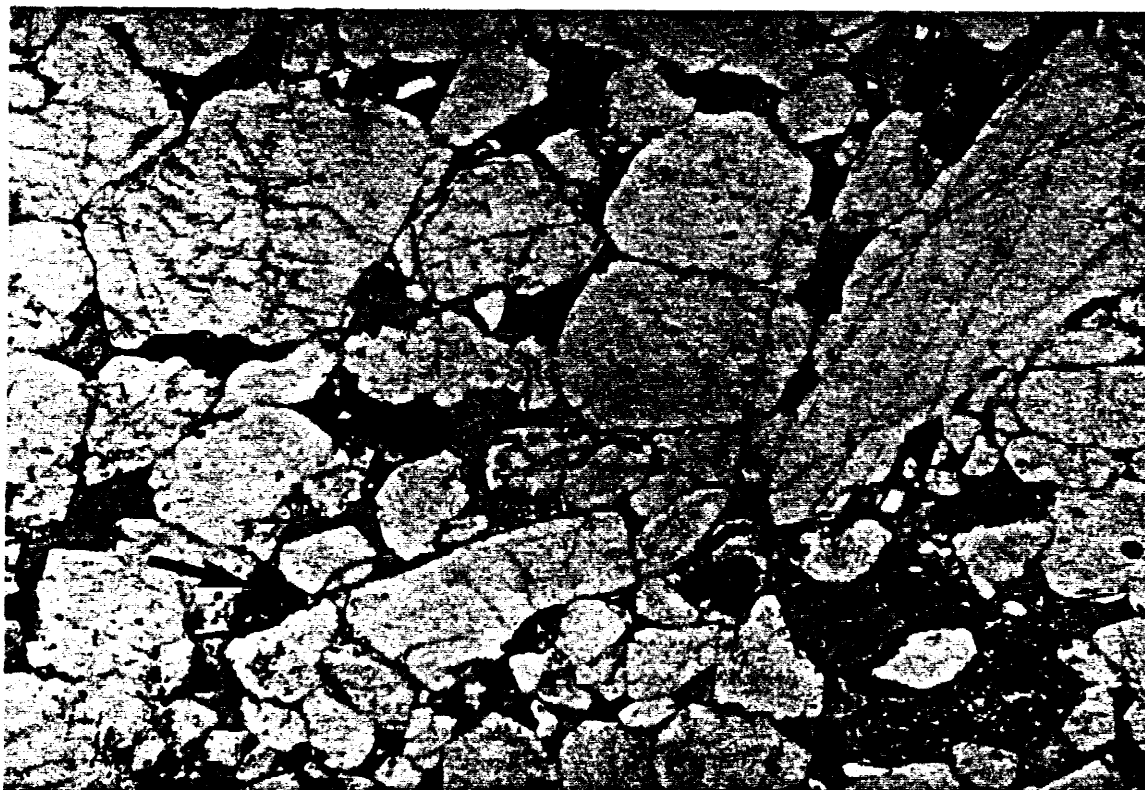


**Figure 27.**

Porosity is a combination of angular primary intergranular pores and grain size dissolution pores in this moderately sorted, coarse grained quartzarenite. Euhedral terminations on grains and the angularity of pores indicates the presence of quartz overgrowths. Dusty altered lithics (L) and traces of drilling mud (arrows) rimming pores are also apparent. Minerva #1, core plug 65, depth 1846.72m. Plane light. Field of view 2.72mm.

### X-ray diffraction

Bulk XRD (Fig. 28a) illustrates the dominance of quartz in this sample. There are trace amounts of kaolinite and pyrite and various contaminants associated with the drilling mud. The latter are comprised of barite, sylvite and possibly halite. Again kaolinite is the dominant clay in the clay fraction (Fig. 28b), it is not as highly crystalline and well ordered as previous samples. Traces of poorly crystalline illite and randomly interstratified clays were also detected. The interstratified clays could be associated with the drilling mud contaminant. Quartz was also detected in the clay fraction.

### Scanning electron microscopy

The sample is a coarse grained, moderately sorted, mineralogically mature sandstone (Fig. 29a). Grains are subangular to subrounded with moderate sphericity. Texturally the sandstone is grain supported with tangential grain contacts dominant. Porosity is moderate and controlled by the degree of silicification and sorting. Primary intergranular pores are well preserved but there are limited interconnections between pores.

Quartz was the only framework grain recognised which indicates that the sandstone is mineralogically mature. Quartz and kaolin are present as authigenic minerals and cements. Quartz overgrowths with euhedral rhombohedral terminations have a uniform distribution throughout the sample. Kaolin has two different crystal sizes and habits. Anhedral fine crystals of kaolin concentrate in patches that appear to have replaced grains. Subhedral booklets and platelets are 10 to 15 microns in diameter. The latter are found on grain margins and associated with the finer kaolin. Rare patches of lettuce-like illite/smectite (Fig. 29b) contains traces of barium (Fig. 29c) which indicates this is a contaminant from the drilling mud.



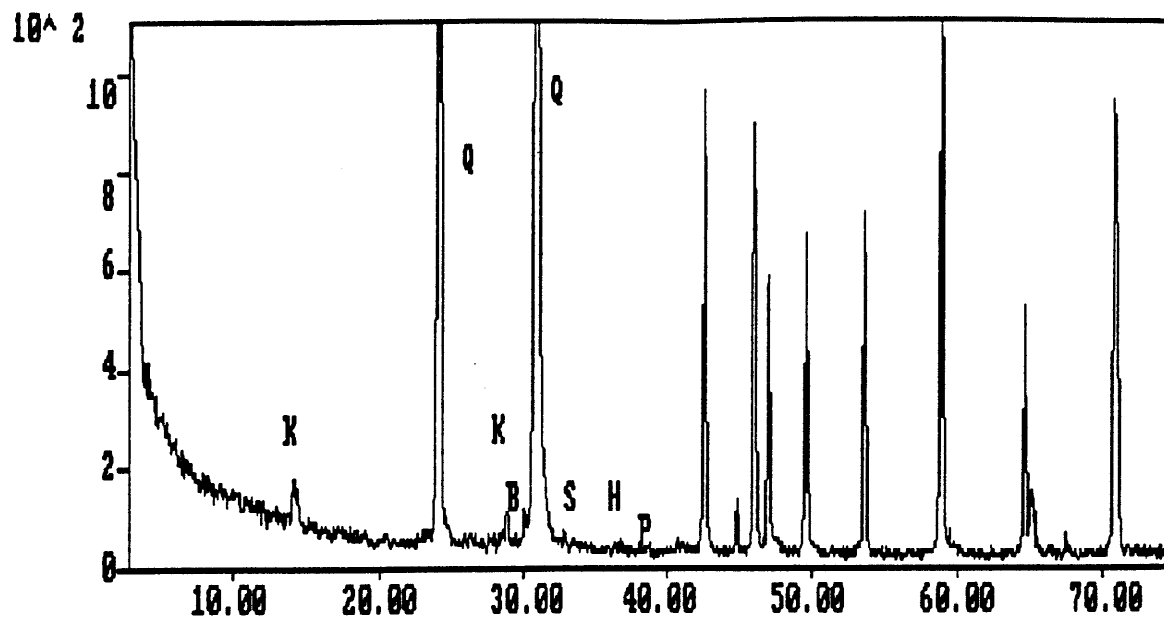


Figure 28a

Bulk XRD trace of Minerva #1, core plug 65, depth 1846.72m. The horizontal axis is in degrees two theta and the vertical axis is in counts of peak intensity. Only the strongest peaks for each mineral identified have been labelled. K = kaolinite, Q = quartz, B = barite, S = sylvite, H = halite, P = pyrite.

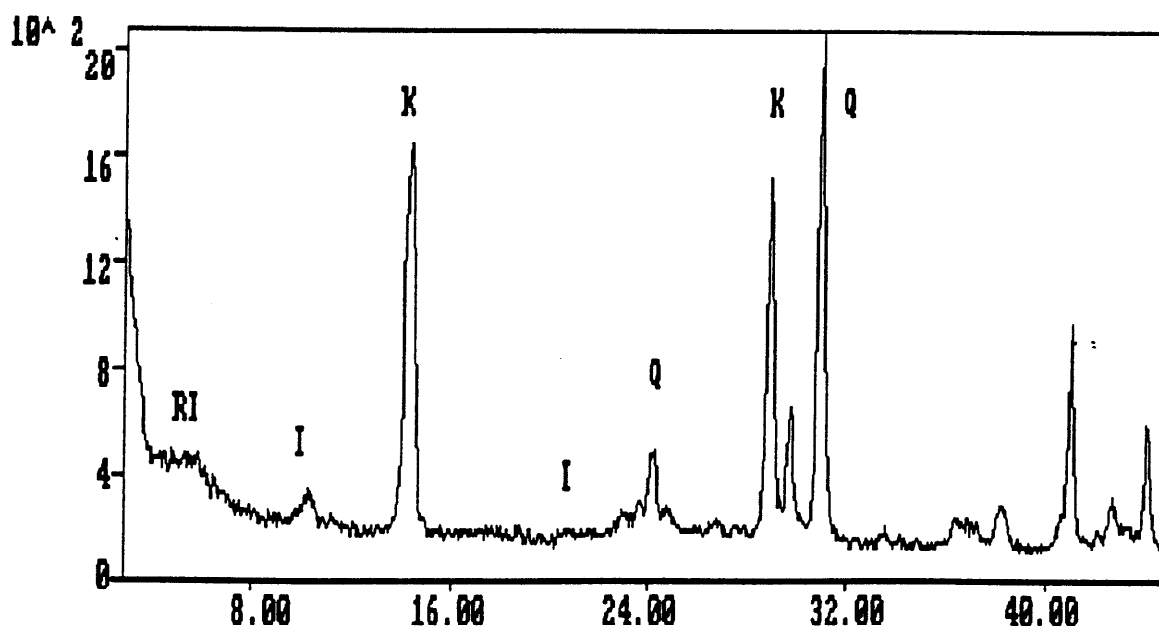


Figure 28b

XRD trace of the clay fraction from Minerva #1, core plug 65, depth 1846.72m. The horizontal axis is in degrees two theta and the vertical axis is in counts of peak intensity. Only the strongest peaks for each mineral identified have been labelled. RI = randomly interstratified clay, I = illite, K = kaolinite, Q = quartz.



Figure 29a

General view of coarse grained, moderately sorted sandstone. Primary intergranular pores are dominant with rare examples of elongate pores (arrows). Grains appear to be angular due to precipitation of quartz overgrowths. Minerva #1, core plug 65, depth 1846.72m. Bar scale 1mm.

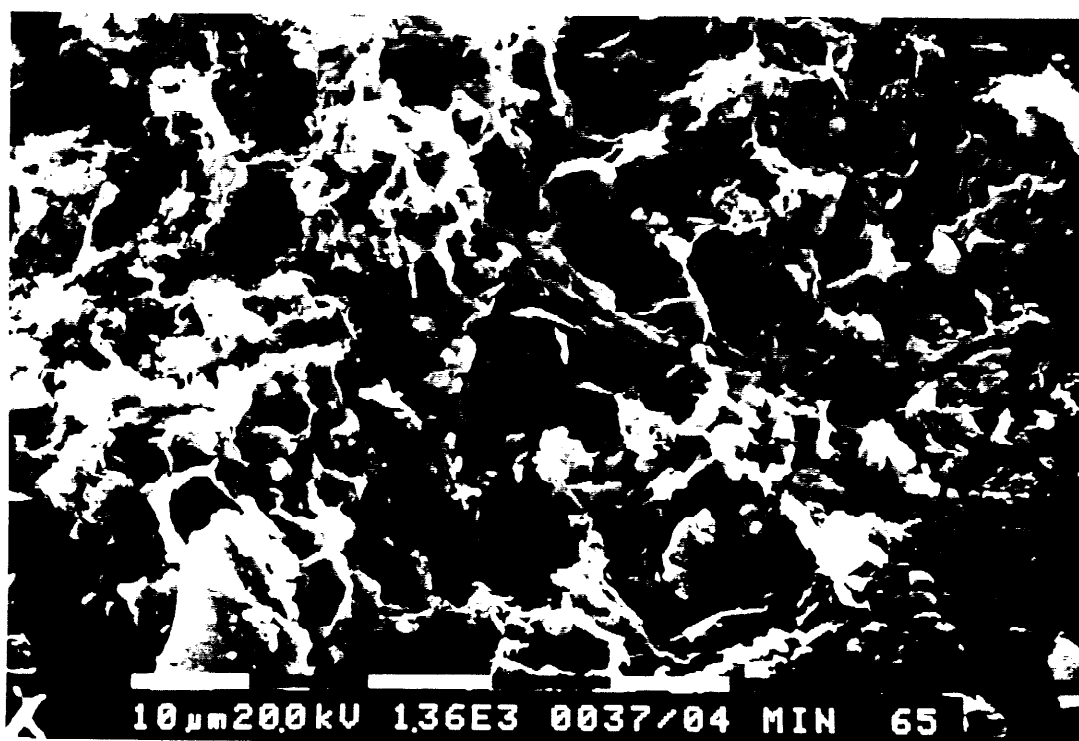


Figure 29b

Lettuce-like illite/smectite occurs as patches on grain surfaces. It is thought to represent a contaminant from the drilling mud rather than an authigenic mineral. Minerva #1, core plug 65, depth 1846.72m. Bar scale 10 microns.

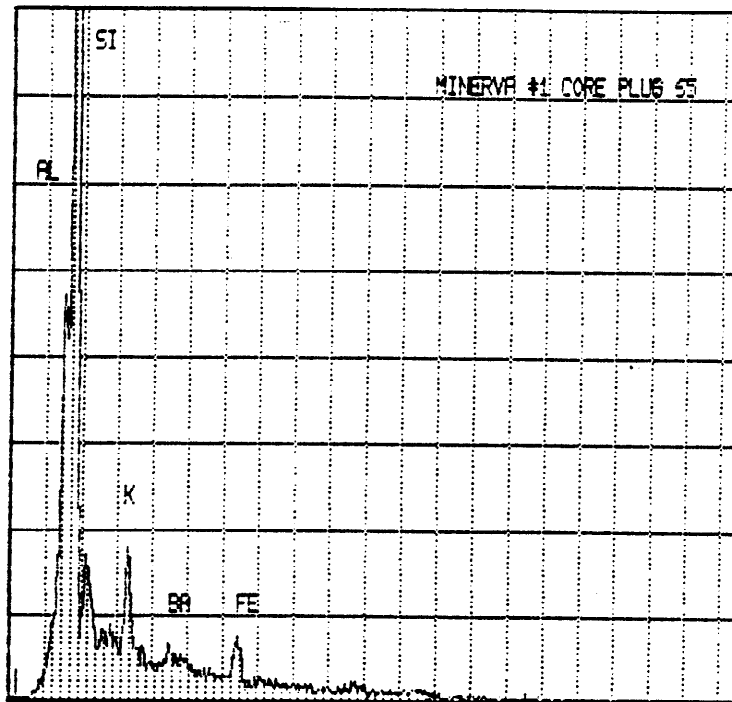


Figure 29c

EDS trace of illite/smectite illustrated in Figure 29b. A trace of barium indicates that it is probably a contaminant. Minerva #1, core plug 65, depth 1846.72m.

## 5. XRD TABLES

TABLE 4. BULK XRD MINERALOGY MINERVA #1

Core Plug	Depth (m)	I/M	Kaol	Qtz	Fel	D/A	Pyr	Others
<i>Strongest peak height in counts</i>								
11	1824.0	207	502	16044	121	-	-	Sy
17	1829.57	-	137	14562	-	-	49	Sy, Ha
18	1829.87	-	146	19054	-	-	74	Sy, Ha, Ba
30	1833.50	257	1039	19048	184	-	139	-
34	1834.70	173	468	20630	370	-	88	-
37	1835.60	180	653	21243	-	185	82	-
52	1842.80	142	152	14200	-	-	-	Sy
65	1846.72	-	174	15210	-	-	32	Sy, Ha, Ba

I/M = illite/muscovite, Kaol = kaolinite, Qtz = quartz, Fel = feldspar, D/A = dolomite/ankerite, Pyr = pyrite, Sy = sylvite, Ha = halite, Ba = barite.

TABLE 5 CLAY XRD MINERALOGY MINERVA #1

Core Plug	Depth (m)	Mont	Clin	Kaol	Illite	Qtz	Fel
<i>Strongest peak height in counts</i>							
11	1824.0	-	-	4814	473	1273	356
17	1829.57	602	417	2169	410	3371	-
18	1829.87	559	-	2088	384	3575	-
30	1833.50	-	-	5492	742	1377	344
34	1834.70	575	-	5082	622	1394	318
37	1835.60	498	377	4054	420	1517	362
52	1842.80	640	tr	2864	554	2859	-
65	1846.72	462*	-	1642	298	2142	-

\* randomly interstratified clay

Mont = montmorillonite, Clin = clinchlore, Kaol = kaolinite, Qtz = quartz, Fel = feldspar.

All the XRD results are summarised in the tables above. To facilitate between-sample comparisons of relative abundance for the same mineral, the results in each table are given in counts of peak height. These figures are based on the strongest line for each mineral detected. Caution should be used in assessing relative abundance from these figures since peak height is also significantly affected by factors such as crystal size and crystallinity. For these reasons the figures are even more unreliable when comparing different minerals in the same sample. For example, based on peak height alone carbonate minerals will always appear less abundant than similar proportions of quartz because of differences in crystallinity. Clay minerals will also appear to be less abundant than quartz in a bulk XRD trace because of differences in crystal size.

Furthermore, comparison should not be made between peak heights given for bulk samples and those for the clay fractions because results have been influenced by the sampling and preparation methods. XRD will not detect minerals that represent less than approximately 5% of the total rock composition.

## 6. DISCUSSION

### a. Lithology and mineralogy

All the samples studied from Minerva #1 have been classified as fine to very coarse grained, poor to well sorted sandstones. For the purposes of this discussion the sandstones have been subdivided into an upper and lower sand unit separated by a fine grained micaceous sandstone at 1840.60m (core plug 49). Only those core plugs described from thin section can be accurately described lithologically as subarkose (core plug 18, depth 1829.87m), sublitharenites (core plug 11, depth 1824.00m and core plug 30 depth 1833.50m), and quartzarenites (core plug 17, depth 1829.57m; core plug 58, depth 1844.60m; core plug 64A, depth 1846.42m and core plug 65, depth 1846.72m). The quartzarenites tend to be coarser grained and concentrate in the lower sand unit.

Mineralogically the samples are mature to submature with a dominance of monocrystalline quartz (62-81%) in all samples. Feldspar contents range from a trace amount to 5% and are consistently composed of altered and corroded alkali varieties (orthoclase and microcline). Lithics are slightly more abundant in the upper sand (trace to 9%) than the lower sand (trace to 3%). The only other framework grains are micas (trace to 2%), fragments of coal and trace amounts of accessory minerals (zircon, tourmaline, sphene, epidote, ?monazite and ?amphibole). Detrital clay matrix is rare and only evident in the sublitharenite of core plug 30 (depth 1833.50m) where it represents 4% of the sample and concentrates in stylolites. Authigenic minerals are dominated by quartz and kaolinite with minor to trace amounts of pyrite, glaucony, illite, iron oxide, clinocllore and carbonate. Silicification is concentrated in the lower sand (10-16%) and kaolinite is more abundant (1-10%) in the upper sand. Based on XRD traces the kaolinite is typically well ordered and highly crystalline in the upper sand and slightly less crystalline in the lower sand unit. Kaolinite has replaced grains and filled pores. Grains of glaucony are commonly altered and probably reworked. Pyrite occurs dominantly as framboids (20 to 40 microns diameter) and there is a suggestion of bladed marcasite in the upper sand unit (core plug 30, 1833.50m). Illite, iron oxides and possibly clinocllore are typically present as alteration products probably forming from feldspars, lithics and micas. These alteration products appear to concentrate in the upper sand. Traces of carbonate spar were noted in 3 samples (core plug 30, depth 1833.50m; core plug 37, depth 1835.60m and core plug 65, depth 1846.72m).

Contamination from drilling mud is apparent in thin section, XRD and SEM studies. In thin section the mud is present rimming pores and blocking pore throats. The XRD traces record the presence of barite, halite, sylvite and montmorillonite. In the SEM traces of barium, sylvite and gypsum were noted. It is possible that the traces of randomly interstratified clays in core plug 65 (depth 1846.72m) are also contaminants.

### b. Sediment provenance and depositional environments

Sediment provenance does not appear to show any dramatic changes between the upper and lower sand units. It would appear to have been derived from granitic and metamorphic terranes with minor ?volcanic and sedimentary input. However, this hypothesis does not negate the possibility that the majority of the sand has been reworked from an earlier deposit and the more labile components removed. Siltstone and

chert lithics indicate the reworking of older sediments.

Both sand units are characterised by monocrystalline quartz with straight to slightly undulose extinction and minor polycrystalline quartz with straight crystal boundaries. These characteristics are typical of sediments derived from a granitic terrane. This provenance is further confirmed by the concentration of K-feldspars, rare granitic lithics and accessory minerals of zircon and tourmaline. A metamorphic source for some of the sediment is indicated by the nature of lithics which are typically dominated by metasediments and micaceous schist, and the presence of epidote in the accessory minerals.

Subtle changes in provenance at selected times within each sand unit are evident. Highly altered lithics are thought to represent chloritised volcanics but these do not occur in all samples. The occurrence of granule size grains of labile feldspars and polycrystalline quartz in the subarkose of core plug 18 (depth 1829.87m) may suggest a phase of uplift or perhaps close proximity to a granitic sediment source at this time.

The apparent concentration of lithics in the upper sand could be attributed to hydraulic sorting rather than a change in sediment provenance. The highest proportion of lithics occur in the fine to medium grained sublitharenites (core plugs 11 and 30), whereas the coarser sands have only minor to trace numbers of lithics.

In terms of depositional environments it is clear that the very coarse sediments of the lower sand unit must have been transported by either traction and bed load, or turbidity currents, thus a high energy regime is indicated. Graded bedding in these sands reflect the progressive waning of energy perhaps in response to friction with the lower part of sediment load. Fragments of coal indicate that the depositional environment was probably close to a terrestrial setting.

The overlying shales are reported to contain <sup>dinoflagellates</sup>~~graptolites~~ and there are beds of coal. Although these samples did not form part of this study it does indicate a marked change in sea level between the upper and lower sand units. Perhaps there was an oscillating shoreline.

The upper sand unit contains evidence of a shallow marine environment and perhaps phases of exposure and oxidation. Grains of glaucony and glaucony rims on detrital grains in core plug 11 (depth 1824.00m) suggest that there has been minimal reworking of the glaucony. The glaucony is interpreted as glauconite which forms at the sediment-water interface in shallow marine environments when pH is near 8 and Eh is at the oxidation-reduction boundary. In contrast the glaucony in core plug 30 (depth 1833.50m) shows evidence of oxidation, and ?marcasite was recognised in this sample. Marcasite forms under low temperatures, when conditions are acidic in a near surface environment. Therefore, it is possible that core plug 30 represents a phase of exposure during sedimentation. Core plugs 18 (depth 1829.87m) and 17 (depth 1829.57m) both lack glaucony. This characteristic has probably resulted from the fact that glaucony formation is inhibited by high rates of sedimentation and these are both very coarse sands that would be deposited in a high energy environment. Alternatively these coarse sands may represent a more terrestrial depositional environment.

### c. Diagenetic alteration

The most pronounced phases of diagenesis have been the alteration and dissolution of labile grains, precipitation of kaolinite and quartz, mechanical compaction and fracturing. Minor authigenic glaucony, pyrite, illite, carbonate spar and iron oxide are also apparent. The concentration of kaolinite in the upper sand unit and silica in the lower sand unit may indicate that there was no interconnection in the circulation of ground waters between these intervals. Alternatively if the elements for kaolinisation are locally derived this distribution could reflect the lower mineralogical maturity of the upper sand unit.

Although there are differences in diagenetic alteration between individual samples and the upper and lower sand units, the overall pattern of diagenetic alteration is similar. The earliest phases of diagenesis would have been the precipitation of glauconite, pyrite and possibly marcasite. Alteration of organic matter and clays could have supplied the iron for these minerals and the sulphur probably became available due to the activity of sulphate reducing bacteria. Later reworking and exposure of glaucony grains would have resulted in the oxidation.

Alteration of lithics and feldspars could also represent early phases of diagenesis since weathering may have begun in the source area and continued during transport. It is clear that replacement and corrosion occurred after the sediment was deposited. Probably the chloritisation of volcanic lithics occurred at this time with the Fe and Mg being derived from the breakdown of ferromagnesian minerals. Alteration of lithics and feldspars to illite and kaolin was probably favoured by acidic pore waters. Kaolin also formed due to the replacement of micas. These different mechanisms by which kaolin formed would help to explain the various crystal habits and sizes recognised in the SEM study. Replacement of feldspars resulted in the fine crystal sizes (2-5 microns) which tend to be anhedral booklets, whilst kaolin formed from micas is typically very coarse in crystal size (up to 50 microns), euhedral and vermiform. Kaolin booklets that fill pores (10 - 20 microns) are thought to have precipitated from solution and probably developed later in the sequence when feldspars were dissolved to form secondary pores. This phase of leaching occurred after the initial silicification and possibly due to either the upwards migration of fluids expelled during compaction, or flushing by meteoric waters that could have entered along the fractures.

Mechanical compaction has resulted in the gradual loss of primary porosity due to grain rotation. In the sublitharenite of core plug 30 (depth 1833.50m) compaction has progressed further due to the ductile nature of detrital clays and stylolites have developed. The exact timing and nature of fracturing can not be obtained from thin section. The fracture in core plug 58 (depth 1844.60m) is filled with the debris that resulted from movement and there are suggestions of minor silicification. The latter may indicate that fractures developed prior to silicification. There is a slight decrease in silicification from 12 to 10% in sands a few centimetres away from the fracture. This fact does not provide strong evidence to support the possibility that the fracture acted as a conduit for silica rich fluids. However, it is possible that acidic fluids moving along the fracture have resulted in the extensive feldspar dissolution.

Silicification is restricted in the upper sand unit and typically druse

have precipitated rather than the rhombohedral terminations that characterise the lower sand unit. Silica was probably derived from solution in the pore waters initially when conditions were alkaline and later could represent an end product of feldspar dissolution. The latter is most likely where there are jagged contacts between quartz overgrowths and kaolin.

Traces of carbonate in core plugs 30 (depth 1833.50m) and 65 (depth 1846.72m) probably precipitated late in the diagenetic sequence when conditions were slightly alkaline. The only other event which is apparent is the development of hydrocarbon envelopes on zircons. These rims form from the polymerisation of organic matter and could have developed either when hydrocarbons migrated through this zone, or as a reaction with organic matter in situ. Hydrocarbon envelopes are apparent in clean sands from the lower unit which tends to favour the hypothesis that hydrocarbons have migrated through the sequence since organic matter is unlikely to be in situ in these high energy sands.

#### d. Reservoir quality

Reservoir quality is highly variable and there are a number of different controls which are interrelated. In the lower sand unit high permeability's of 5854 mD (core plug 53, depth 1843.10m), 5641 mD (core plug 61, depth 1845.52m) and 3022 mD (core plug 64A, depth 1846.42m) have been reported from routine core analysis. In this zone permeability has probably been enhanced by fracturing. There are remnants of porosity in the fractures which would further enhance reservoir quality. Primary intergranular pores are dominant in the lower sand unit and in the SEM these appear to be elongate, but this may be an artefact of fracturing.

Diagenetic alteration especially kaolinisation and silicification have influenced reservoir quality. Where kaolin is abundant in the upper sand unit, microporosity probably contributes to total porosity. The micropores range in diameter from 5 to 10 microns and occur between single kaolin platelets and between booklets. Permeability is low in those samples that have high percentages of kaolin and/or are dominated by secondary porosity (core plug 11, depth 1824.00m and core plug 30, depth 1833.50m). The secondary pores lack interconnection and where present the pore throats are probably blocked by kaolin. It is possible that the pore filling kaolin in the upper sand could migrate during production but this is unlikely to be a major problem since less than approximately 4% would be pore filling kaolin. Silicification in the lower sand unit has reduced pore size and blocked some pore throats but also provides a rigid framework to resist mechanical compaction and hence preserve porosity.

Grain size, sorting and bedding have also influenced reservoir quality in some sandstones. Typically where sorting is very poor then porosity and permeability are limited. Where coarse sands have moderate sorting then porosity and permeability are better preserved (eg core plug 12, depth 1828.15m). Bedding would limit vertical permeability in core plug 30 (depth 1833.50m) and possibly core plug 58 (depth 1844.60m).



## 7. CONCLUSIONS

1. Sediment provenance does not vary significantly between the upper and lower sand units. Sediments were dominantly derived from granitic, metamorphic and ?volcanic terranes.
2. Kaolinite is the dominant clay mineral, it concentrates in the upper sand unit where it is highly crystalline and well ordered. There are micropores associated with the kaolin and it is possible that pore filling kaolin could migrate during production.
3. Diagenetic alteration included phases of alteration and dissolution of labile grains, precipitation of kaolinite and quartz, mechanical compaction and fracturing. Minor authigenic glaucony, pyrite, illite, carbonate spar, clinocllore and iron oxide are also apparent. Silicification is most pronounced in the lower sand unit.
4. Reservoir quality has been controlled by the interaction of a number of factors including grain size, sorting, precipitation of authigenic minerals (kaolinite and quartz) and fracturing.

## 8. GLOSSARY OF TERMS

Boehm lamellae

Parallel trails of vacuoles in quartz that are thought to form during deformation (metamorphism) of grains.

Framboid

A cluster of pyrite crystals with a spheroidal outline.

Glaucony

A term used to describe green minerals without any genetic connotations. If the green minerals can be identified, a specific mineral name is given.

Honeycomb Porosity

Secondary porosity produced by the corrosion (etching) of detrital grains.

Hydrocarbon envelope

Solid bitumen surrounding a mineral containing radioactive elements. Radiation causes polymerisation of hydrocarbon chains within oil that rims grains.

nd

Abbreviation meaning not detected.

Vacuole

Gas or liquid filled inclusion.

3

5



**BHP PETROLEUM PTY. LTD.**  
A.C.N. 006 918 832

**GEOCHEMICAL EVALUATION OF MINERVA-1**

**OTWAY BASIN**

**OFFSHORE VICTORIA AUSTRALIA**

**PREPARED BY: J. PRESTON**  
**SENIOR GEOCHEMIST**

**0538.rep**

**DATE: April, 1994**

## TABLE OF CONTENTS

		Page
1	INTRODUCTION . . . . .	1
2	SOURCE ROCK CHARACTERISATION . . . . .	2
2.1	Screening Analyses . . . . .	2
2.1.1	Total Organic Carbon (TOC) . . . . .	2
2.1.2	Rock-Eval Pyrolysis . . . . .	2
2.2	Thermal Maturity . . . . .	3
3	FLUIDS CHARACTERISATION . . . . .	4
3.1	Whole-Oil GC Analysis . . . . .	4
3.2	Saturate Fraction GC Analyses . . . . .	4
3.3	GC-MS (Branched/Cyclics) Analysis . . . . .	4
3.3.1	Terpane Parameters . . . . .	5
3.3.2	Sterane Parameters . . . . .	6
3.4	GC-MS(Aromatics) Analysis . . . . .	8
3.5	Gas Analysis . . . . .	9
3.5.1	Chemical Composition . . . . .	9
3.5.2	Stable Carbon Isotopic Composition . . . . .	9
4	CONCLUSIONS . . . . .	10
 APPENDIX		
1	SIR GC-MS (B/C) Mass Fragmentograms: 1942.5m Condensate	
2	SIR GC-MS (AROMS) Mass Fragmentograms: 1942.5m Condensate	
3	SIR GC-MS (B/C) Mass Fragmentograms: 1649.8m Water Extract	
4	SIR GC-MS (AROMS) Mass Fragmentograms: 1649.8m Water Extract	

## LIST OF FIGURES

- Figure 1 TOC versus Depth  
Figure 2 TOC versus HI  
Figure 3 TOC versus S1 + S2  
Figure 4 HI versus OI  
Figure 5 HI versus Tmax  
Figure 6 Maceral Composition Data  
Figure 7 Tmax versus Depth  
Figure 8 PI versus Depth  
Figure 9 VR and Coal Maceral Identification: histograms  
Figure 10 Vitrinite Reflectance versus Depth  
Figure 11 Whole-Oil GC trace (C<sub>1</sub>-C<sub>33</sub>): 1942.5m condensate  
Figure 12 Whole-Oil GC trace (C<sub>1</sub>-C<sub>8</sub>): 1942.5m condensate  
Figure 13 Whole-Oil GC data (normalised): 1942.5m condensate  
Figure 14 Whole-Oil GC data: Paraffin Indices (cross-plot)  
Figure 15 Saturates-GC trace: 1649.8m water-extract  
Figure 16 Saturates-GC trace : 1942.5m condensate  
Figure 17 Saturates-GC Data: normalised relative abundances  
- 1649.8m water-extract and 1942.5m condensate (comparative)  
Figure 18 Saturates-GC Data: normalised relative abundances  
- 1649.8m water-extract and 1942.5m condensate (comparative)  
Figure 19 Pristane/nC<sub>17</sub> versus Phytane/nC<sub>18</sub>  
Figure 20 m/z 191 and m/z 217 biomarker traces: 1649.8m water-extract  
Figure 21 m/z 191 and m/z 217 biomarker traces: 1942.5m condensate  
Figure 22a Normalised Abundances: Terpanes (m/z 191)  
Figure 22b Calculated Parameters: Terpanes (m/z 191)  
Figure 23a Normalised Abundances: Steranes (m/z 217)  
Figure 23b Calculated Parameters: Steranes (m/z 217)  
Figure 24a Normalised Abundances/Calculated Parameters: Terpanes (m/z 191)  
Figure 24b Normalised Abundances/Calculated Parameters: Steranes (m/z 217)  
Figure 25 Pristane/Phytane versus Hopane/Sterane (Ratio C)  
Figure 26 Facies Interpretation based on Sterane Abundances - (R Isomers only)  
Figure 27 Pristane/Phytane versus C<sub>29</sub>R/C<sub>27</sub>R  
Figure 28 C<sub>29</sub> 20S/(20S + 20R) versus C<sub>29</sub> ββ/(ββ + αα)  
Figure 29 MPI-1-derived Rc(a) versus Depth  
Figure 30 Log (Retene/9-MP) versus Log (1,7-DMP/X)  
Figure 31 Log (1-MP/9-MP) versus Log (1,2,5-TMN/1,3,6-TMN)  
Figure 32 Gas Analysis Data - Normalised Abundances  
Figure 33 Gas Isotope Maturation Plot - 1  
Figure 34 Gas Isotope Maturation Plot - 2  
Figure 35 Gas Characterisation Plot

## LIST OF TABLES

Table 1-1	Geologic and General Data - Sediments
Table 1-2	Geologic and General Data - Fluids
Table 2	TOC/Rock-Eval Pyrolysis Data
Table 3	Vitrinite Reflectance and Coal Maceral Data
Table 4	Summary of Whole-Oil Analysis : 1942.5m Condensate
Table 5	Summary of GC Data - Alkane Distributions
Table 6	Summary of GC Data - Alkane Compositional Data
Table 7-1	Saturate Fraction SIR GC-MS Data : 1649.8m Water-Extract - Detailed Compound Analysis
Table 7-2	Saturate Fraction SIR GC-MS Data : 1649.8m Water-Extract - Calculated Parameters
Table 8-1	Saturate Fraction SIR GC-MS Data : 1942.5m Condensate - Detailed Compound Analysis
Table 8-2	Saturate Fraction SIR GC-MS Data : 1942.5m Condensate - Calculated Parameters
Table 9-1	Saturate Fraction SIR GC-MS Data : 1942.5m Condensate (topped) - Detailed Compound Analysis
Table 9-2	Saturate Fraction SIR GC-MS Data : 1942.5m Condensate (topped) - Calculated Parameters
Table 10	Aromatic GC-MS Data : 1649.8 Water-Extract
Table 11	Aromatic GC-MS Data : 1942.5m Condensate
Table 12	Gas Analysis Data : 1649.8m Sample
Table 13	Gas Analysis Data : 1931.0m Sample
Table 14	Stable Carbon Isotope Data : 1649.8m and 1931.0m Gases

## LIST OF ENCLOSURES

Enclosure 1	Geochemical Log
-------------	-----------------

---

**1 INTRODUCTION**

Following completion of the Minerva-1 well, a programme was undertaken to evaluate the source rock character and thermal maturity of the drilled sequence, and the fluids recovered from it.

The evaluation of source rock character firstly involved analysis of four sidewall cores for total organic carbon (TOC) content by Geotech, Perth. Three of the samples (including one coal) yielded a TOC greater than 1.0%, and were accordingly pyrolysed by the Rock-Eval method.

In an attempt to evaluate the thermal maturity of the Minerva-1 section, vitrinite reflectance measurements were made on eight SWCs from the well.

Two gas samples, recovered by RFT from 1649.8m and 1942.5m, were analysed by CSIRO, North Ryde, for their chemical and stable carbon isotopic compositions. In an attempt to gain more information relating to the source of the gases and their associated fluids, the RFT gas samples were subjected to cold-trapping by Petrolab, Adelaide. A condensate sample was obtained from the 1942.5m RFT gas sample; however, water was recovered from the 1649.8m RFT gas sample and was solvent-extracted for its dissolved hydrocarbons. The condensate and extract were then analysed by whole-oil and whole-extract GC, separated, and analysed by the saturate fraction GC, GC-MS (branched/cyclics) and GC-MS (aromatics) techniques.

This report provides a compilation of the petroleum geochemistry data obtained from the Minerva-1 well, together with an interpretation of these data.



---

## 2 SOURCE ROCK CHARACTERISATION

### 2.1 Screening Analyses

#### 2.1.1 Total Organic Carbon (TOC)

Four samples analysed for total organic content (TOC) originated in the Late Cretaceous Sherbrook and Shipwreck Groups (Table 1-1, Table 2). Although 0.5% TOC is commonly used as the minimum requirement for a petroleum source rock, it is uncommon for sediments from the southern margin of Australia with less than 1.0% TOC to be significant petroleum sources. On the basis of four samples, it is clear that the Late Cretaceous section in Minerva-1 contains some potential petroleum source rocks, the TOC values of two samples ranging from 1.34-1.68% (Table 2, Figure 1 and Enclosure 1). Note that one sample, from 1837.1m, consisted of coal (TOC=40.50%).

#### 2.1.2 Rock-Eval Pyrolysis

The three samples in which the TOC was found to exceed 1.0% were pyrolysed using the Rock-Eval method. Two of these samples from 1342-1747m, gave HI values of 94-102 and S1+S2 yields of 1.31-1.75 mg/g (Figures 2 and 3), indicating poor generative potential, chiefly for gas, with perhaps minor amounts of condensate. The data from the 1837.1m sample (HI=449) suggest that there is much greater potential for liquids generation in the coals.

It is clear from the S1+S2 yields of the Minerva-1 samples that expulsion, if any, would be possible only at relatively high levels of thermal maturity. At such levels of thermal maturity, considerable secondary cracking of liquids to gas would occur, such that these source rocks would perhaps be even more gas-prone than indicated by the source character data.

The Rock-Eval pyrolysis data listed in Table 2 are summarised in the form of crossplots in Figures 4 and 5. Figure 4 reflects the overall quality of the kerogen in the samples analysed, in terms of their oil-prone or gas-prone character: two samples plot in the gas/condensate-prone Type II/III and Type III areas of the diagram (HI < 150). The more liquids-prone character of the coal sample is reflected in its more obvious Type II affinity.

Figure 5 reflects the generative capacity of the samples, in terms of their overall quantitative potential; only the coal sample exceeds the threshold of significant hydrocarbon generation and expulsion, despite its thermal immaturity.

Maceral petrography associated with the vitrinite reflectance determinations shows that the organic matter in most of the samples is dominated by inertinite, followed by vitrinite (Figure 6). However, liptinitic/exinitic (Type II) macerals are identified in all samples except 2215m (described as 100% inertinite), confirming the presence of some liquids-prone components. In some samples, the Type II macerals appear to be supplemented by oil-prone alginitic (Type I) macerals.

## 2.2 Thermal Maturity

Rock-Eval parameters which are often used for maturity assessment are Tmax and Production Index (PI). A Tmax value of 435°C, and a PI value of 0.10, are regarded as marking the entrance to the oil-generative window.

As Table 2 and Figure 7 show, values of Tmax are 432°C in the case of two samples, with an anomalously low value of 424°C from the coal. Values of PI (Figure 8) are less than 0.10 in the 1342-1523m interval, but PI reaches 0.10 in the coal.

There is therefore broad agreement between the maturity estimates based on the PI and Tmax data, namely that the 1342-1523m section is thermally immature, and the coal-bearing section around 1837.1m marginally mature.

Vitrinite reflectance measurements on nine samples from the 1130-2392.5m interval range up to 0.75% (See Table 3/ 3A and Figures 9 and 10). Values for four samples in the 1130-1747m interval occupy the immature 0.42-0.53% range. Values of 0.62-0.63% at 1947.5-2215m indicate marginal maturity, though a value of 0.75% at 2392.5m suggests early oil-generative maturity at this depth. These data concur with the Tmax and PI values from the Rock-Eval data.

Because kerogens will generate products with markedly different compositions as thermal maturity progresses, it follows that certain analyses and the interpretation of their results will be fundamentally affected by maturity, in particular Rock-Eval pyrolysis data. The observation that the drilled interval has not attained thermal maturity means that this need not be a consideration in the interpretation of geochemical data from the Minerva-1 well. The poor source quality of parts of the drilled sequence cannot be attributed to advanced thermal maturity, but more to organic matter type and/or its preservation state.

---

### 3 FLUIDS CHARACTERISATION

#### 3.1 Whole-Oil GC Analysis

One condensate sample, obtained by the cold-trapping of a gas sample from 1942.5m (Table 1-2), was analysed by the whole-oil GC method. The whole-oil GC data for this sample are presented in Table 4; the corresponding whole-oil GC trace is shown in Figure 11 (C<sub>1</sub>-C<sub>33</sub> range), Figure 12 (C<sub>1</sub>-C<sub>8</sub> gasoline range), and Figure 13 (normalised plot).

Paraffin Index data from the condensate are plotted in Figure 14, and suggest (if taken at face value) that the condensate was expelled from its source rock at about 135°C.

#### 3.2 Saturate Fraction GC Analyses

Water was recovered from the cold-trapping of the 1649.8m RFT gas sample, and was solvent-extracted for its dissolved hydrocarbons.

Both the 1942.5m condensate sample, and the 1649.8m water-extract, were separated into their constituent fractions by liquid chromatography. The 1649.8m water-extract consisted of 96% saturates; however, no separation data were reported by the laboratory for the 1942.5m condensate.

The saturate fractions of the condensate and water-extract were analysed by the saturate fraction GC method. The resulting saturate GC traces are shown in Figures 15 and 16; the n-alkane distribution data are reported in Table 5, normalised in Figure 17, and compared in Figure 18; the n-alkane compositional data for the condensate and water-extract are listed in Table 6, and summarised in Figure 19. Note that the value of Pr/Ph (9.03) and the ratio of Pr/nC<sub>17</sub> to Ph/n C<sub>18</sub> (4.36) in the 1649.8m fluid are typical of hydrocarbons generated from terrestrial (non-marine) sediments containing higher land plant-derived organic matter. No value for Pr/Ph was reported for the 1942.5m condensate.

#### 3.3 GC-MS (Branched/Cyclics) Analysis

The branched and cyclic compounds were isolated from the saturate fractions of the condensate and water-extract and analysed by the SIR GC-MS technique. Selected m/z 191 (triterpane) and m/z 217 (sterane) biomarker distributions are given in Figures 20-21; full suites of mass fragmentograms are provided in this report as Appendices 1 and 3.

Detailed compound abundances and calculated parameters are listed in Tables 7 to 9; normalised compound abundances and values for calculated parameters for the m/z 191 ions (terpanes) are summarised in Figures 22a-23a, and for the m/z 217 ions (steranes) in Figures 22b-23b. Figures 24a-24b compare normalised compound abundances and values of calculated parameters for the condensate and water-extract. Note that these plots are based on compound abundances from the topped fluid in the case of 1942.5m condensate.

### 3.3.1 Terpane Parameters

The relative abundance of  $C_{27}$  triterpanes,  $18\alpha(H)$ -hopane (Ts) and  $17\alpha(H)$ -hopane (Tm), is theoretically useful for the maturity assessment of medium to high maturity oils. With increasing maturity, more of the maturable  $C_{27}$  triterpane (Tm) is converted to the stable  $C_{27}$  triterpane (Ts). The relative amounts of Ts and Tm in the condensate and water-extract show a predominance of stable (Ts) over maturable (Tm) ( $Ts/Ts+Tm = 58-61\%$ ), suggesting that they are thermally mature. Note that the  $Ts/Ts+Tm$  parameter is lithofacies-dependent, and should be used with some caution as an absolute indicator of thermal maturity (it is best used as a maturity indicator of oils from a common source of consistent organic facies).

Moretanes are diastereomers of the hopanes, and, being less stable than the latter, are destroyed more rapidly with increasing maturity. The moretane/hopane ratio decreases from about 0.80 in immature bitumens to values of 0.15-0.05 in mature source rocks and oils. The relative abundances of the  $C_{29}$  and  $C_{30}$  moretanes and hopanes in the condensate and water-extract reveal a predominance of hopanes (moretane/hopane = 0.08-0.10), implying that they are mature. (Note that, like  $Ts/Ts+Tm$ , the moretane/hopane parameter is to some extent lithofacies-dependent, its value, for example, being higher in Tertiary source rocks.)

The  $C_{31}22S$ -hopane/ $C_{31}22R$ -hopane ratio can be used to assess thermal maturity. As maturity increases, the proportion of the 22S isomer increases at the expense of the biologically produced 22R isomer, until equilibrium is reached, at which point the 22S isomer accounts for about 60% of the mixture. This is achieved soon after the onset of oil generation (at about 0.60% VR, before significant oil generation has occurred), limiting the use of this parameter at higher levels of maturity. In the water-extract and condensate, the 22S isomer accounts for 60-61% of the mixture, implying that isomeric equilibrium has been reached, and that the source rocks in both cases were thermally matured at least to the point of initial oil-generation. Note that the 22S isomer of the  $C_{32}$  hopanes forms 60% of the isomeric mixture, concurring with the  $C_{31}$  hopane data.

Note that the distributions of terpane compounds in the water-extract and condensate are very similar (figures 22a, 22b and 24a), minor differences being reported values for C<sub>28</sub> 28,30-bisnorhopane and C<sub>29</sub>-moretanes. The C<sub>28</sub> 28,30-bisnorhopane (BNH) present in the 1649.8m water-extract is probably derived from the original (post-diagenetic) free bitumen (S<sub>0</sub>) in thermally immature claystones around 1649.8m, and was present in the water recovered by the RFT at this depth. Hence the 1649.8m water-extract appears to consist of both gas-associated condensate (migrated) with minor amounts of free bitumen (indigenous).

### 3.3.2 Sterane Parameters

The relative proportion of the geological 20S and biological 20R isomers of the C<sub>28</sub> and C<sub>29</sub>ααα (normal) steranes, expressed as the 20S/20S+20R ratios, is perhaps the most reliable biomarker maturity parameter (it is not greatly influenced by lithofacies variations). Equilibrium, when the 20S isomer forms about 52-55% of the mixture, is reached at, or around, 0.80% vitrinite reflectance. In the Minerva-1 condensate and water-extract, the 20S isomer forms 51% of the C<sub>29</sub> mixture, suggesting expulsion of these fluids from its source sediment at, or beyond, 0.80% vitrinite reflectance.

The relative proportions of C<sub>29</sub> normal (ααα) and iso-(ββα) steranes can be effective in assessing the thermal maturity of source rocks and oils. The normal (ααα) steranes, produced biologically, become less dominant relative to the iso-steranes (ββα) with increasing maturity, until equilibrium is reached at a value of ββα/(ββα+ααα) of about 67-71% (VR=0.90%). In the Minerva-1 condensate and water-extract, the iso-steranes dominate the normal steranes (ββα/ααα+ββα = 57-60%), suggesting that the source rock was matured to 0.8-0.9% VR at the time they were expelled. This maturity estimate is inconsistent with that based on stable carbon isotope data derived from the gas with which the 1649.8m water-extract was intimately associated (see section 3.5.2).

Diasterane/sterane ratios are affected by both thermal maturity and inorganic (lithological) characteristics of the source rock. Conversion of steranes to diasteranes is catalysed by clay minerals, so that diasterane/sterane ratios are typically low (less than 0.30) in carbonate source rocks and derived oils. A high-Eh (oxidising) depositional environment and increasing thermal maturity can each result in a high diasterane/sterane ratio. C<sub>29</sub> diasteranes constitute 44% of the C<sub>29</sub> normal/iso-/diasterane mixture in the Minerva-1 condensate and water-extract, implying that these hydrocarbons were expelled from thermally mature clastic source rocks. It is difficult to make a better estimate of the absolute level of thermal maturity at which the condensate and water-extract were expelled from their sources (the proportion of diasteranes being partly dependent on lithofacies).

Note that the distributions of sterane compounds in the water-extract and condensate are, like the terpene distributions, very similar (Figure 23a, 23b and 24b). Perhaps the only conspicuous difference is the value of Ratio C (ratio of  $C_{30}$  hopanes and moretanes to  $C_{29}$  total steranes). The general assumption about triterpane/sterane ratios is that steranes are derived mainly from algae and higher plants, whereas triterpanes come mainly from bacteria. However, the relationship between organic facies and triterpane/sterane ratio is complex, and cannot always be used with confidence. When absolute concentrations of biomarkers are high, high triterpane/sterane ratios are taken to indicate a high degree of microbial input; where concentrations are low, high ratios are taken to indicate greater contribution from land-plants than from algae. Low triterpane/sterane ratios together with high absolute biomarker concentrations, are associated with coals, shales and oils (eg. South East Asia and New Zealand); low ratios in conjunction with low absolute abundances may indicate a dominance of higher-plant and fungal material (Waples et al., 1991). Triterpane/sterane ratios as expressed by Ratio C are low in the water-extract (0.36), and higher in the condensate (1.09), but each suggests generation from source sediments deposited in a relatively oxic, aquatic environment. (Note that Figure 25 shows data from the 1649.8m water-extract only, since a Pr/Ph value was not reported for the 1942.5m condensate - see also Figure 27).

Figure 26, a triangular plot of  $C_{27}$ ,  $C_{28}$  and  $C_{29}$  normal steranes, shows a dominance of  $C_{27}$  compounds, the data plotting within the marginal marine field. Note that S isomers of the normal steranes were not reported for either the water-extract or the condensate, and Figure 26 is constructed accordingly (R isomers only).

Figure 27 shows a crossplot of Pr/Ph ratio versus  $C_{29}R/C_{27}R$  for the 1942.5m condensate, further suggesting a relatively oxic, aquatic environment for deposition of the source sediments, based on the dominance of the  $C_{27}R$  steranes relative to  $C_{29}R$ .

Plots of  $\beta\beta/(\beta\beta + \alpha\alpha)$  versus  $20S/(20S + 20R)$  for the  $C_{29}$  steranes are effective in describing and comparing the thermal maturity of source rocks or oils; data for any oils which plot away from the maturity trend-line in such plots should be re-examined in the light of the disagreement between the two parameters (Peters and Moldowan, 1993). As Figure 28 shows, data for the condensate and water-extract plot together, suggesting that the two data sets are comparable and correlable.

A note of caution should be made regarding the use of biomarker data from condensates. Condensates are formed either from source rocks under high thermal stress or by phase-separation from an oil, and exist in the subsurface in the gas phase. These processes usually result in a significant variation in the values of important biomarker ratios and parameters in condensates

compared with co-genetic oils (Woodhouse, 1991). This means that the absolute values of such ratios and parameters may not be a true reflection of the nature of the source organic matter and its maturity. In addition, many of the maturity indicators based on biomarker abundances are only of value at lower levels of maturity because they reach isomeric equilibrium so early, rendering them less useful at the levels of maturity appropriate to the generation of gases and condensates. However, the biomarker data for the water-extract and condensate, notwithstanding these effects, can be used for comparative purposes; they are sufficiently similar to leave little doubt that the Minerva-1 fluids are co-genetic, and may be of further value in the correlation of the Minerva-1 hydrocarbons with those recovered from nearby wells.

### 3.4 GC-MS(Aromatics) Analysis

The aromatics fractions from the 1649.8m water-extract and 1942.5m condensate were analysed by the SIR GC-MS technique. Full suites of mass fragmentograms are provided in this report as Appendices 2 and 4. Detailed compound abundances, and parameters calculated from them, are listed in Tables 10 and 11.

The primary application of these data is for maturity assessment. Perhaps the most widely used parameter is the Methylphenanthrene Index (MPI-1), due to its better calibration against the vitrinite reflectance scale, equivalent values of which can be calculated (Radke et al, 1982). Figure 29 shows a plot of MPI-derived vitrinite reflectance values versus depth for the Minerva-1 condensate and water-extract. These fluids give values of  $R_c(a)\%$  (1.07 and 0.84%) which are disparate, and appropriate to moderate levels of thermal maturity in the oil-generative window (implying oil-associated gas). However, if the MPI-1 values are converted to  $R_c(b)\%$ , using an algorithm appropriate to thermal maturities greater than 1.35% VR, then values of 1.63% and 1.86% VR are obtained, consistent with the thermogenic gas indicated by the gas isotope data (see section 3.5.2).

The relative abundances of certain aromatic compounds can be applied to source input assessment, particularly the degraded diterpanes, such as 1,2,5-TMN, 1,7-DMP, 1-MP and retene, which are thought to be derived from resin precursors in conifers (such as Araucariaceae, Cupressaceae and Podocarpaceae in the Jurassic to Lower Cretaceous of Australia). Source sediments which pre-date the appearance of such conifers in the Late Triassic will display different distributions of degraded aromatic compounds, so that the data provide a useful correlation tool. Figures 30 and 31 show crossplots of ratios involving these compounds; while the latter shows a grouping of the condensate and water-extract data, implying a similar source, Figure 30 does not (the reason for this is not clear, but may relate to low concentrations of aromatic compounds in the analysed fluids).

---

### 3.5 Gas Analysis

Two gas samples, recovered by RFT from 1649.8m and 1931.0m in Minerva-1 were analysed by CSIRO, North Ryde for their chemical and stable carbon isotopic compositions. (The water-extract isolated by cold-trapping of the 1649.8m sample has already been discussed.)

#### 3.5.1 Chemical Composition

The chemical compositions of the RFT gases are summarised in Tables 12 and 13, normalised in Figure 32. The gases are chemically very similar, containing 94% methane, though the 1931.0m gas contains slightly more carbon-dioxide than the 1649.8m gas.

#### 3.5.2 Stable Carbon Isotopic Composition

The stable carbon isotope data for the two gases are listed in Table 14, and values for individual hydrocarbon species cross-plotted in Figures 33 and 34. As these figures show, the carbon isotope compositions of the gases are very similar, leaving their co-genetic origin in little doubt. Figure 33 indicates that the gases were expelled from their source rocks at thermal maturities equivalent to over 2.0% VR, early in the dry-gas-generative window, whereas Figure 34 suggests 1.5-1.6% VR, within the wet-gas window.

Figure 35 is an attempt to characterise the gases in terms of the isotopic compositions of their methane components and the relative amounts of their C<sub>2</sub>+ components. This plot suggests that the gases are non-associated (ie. they were not generated along with oil, but produced by the thermal cracking of oils) and that they were migrated from depth.



## CONCLUSIONS

Four SWC samples, from the Late Cretaceous Sherbrook and Shipwreck Groups, were analysed for their TOC content. Three samples (including one coal) yielded values greater than 1.0%, and were accordingly analysed by Rock-Eval pyrolysis. The resulting data revealed a predominance of Type II/III to Type III, mainly gas-prone organic matter with HI values less than 150, with the exception of the coal sample (1837.1m) characterised by more strongly liquids-prone organic matter. While liptinitic/exinitic (Type II) macerals were identified in most samples (supplemented by a sparse alginitic component), suggesting some liquids potential, it is clear from the S1+S2 yields that expulsion from these samples would be possible only at relatively advanced levels of thermal maturity; at such levels, secondary cracking of liquids to gas would occur, such that these source rocks would, in the event, become even more gas-prone than indicated by the source character data.

Thermal maturity data, namely Tmax, PI and vitrinite reflectance measurements, suggest that the 1130-1747m interval is thermally immature, the 1947.5-2215m interval marginally mature, and the interval down to 2392.5m early oil-generative mature. The generative potential of the sediments has therefore not been realised at the Minerva-1 location.

A further inference is that the quality of these source rocks can not be linked to advanced maturity, their relative leanness being more a function of the type and preservation state of their contained organic matter.

A condensate and a water-extract, acquired from the cold-trapping of the 1942.5m and 1649.8m RFT gases, were subjected to whole-oil GC and whole-extract GC (as appropriate), saturates-GC, GC-MS (branched/cyclics) and GC-MS (aromatics) analysis. Paraffin Index data from the condensate suggest that it was expelled from its source rock at about 135°C (close to peak-oil generation). Saturate fraction GC data from the water-extract suggest that it was generated from higher land-plant-derived organic matter within source sediments deposited under strongly oxic conditions. Biomarker data, from SIR GC-MS analysis of the saturates and aromatics fractions, suggest that the fluids were generated from aquatically derived organic matter incorporated into clastic source sediments deposited under relatively oxic conditions, possibly in a marine to marginally marine environment. Isomeric equilibria were found to be exceeded in the case of those biomarker indicators appropriate to lower levels of thermal maturity, others (such as the relative abundances of Ts/Tm, and moretanes/hopanes) indicating advanced maturities. Values of  $R_c(b)\%$ , calculated from MPI-1 using an algorithm appropriate to maturities greater than 1.35% VR, fall in

---

the 1.63-1.86% range, consistent with the 1.5-1.6% (or greater) values obtained from stable carbon isotope data from the 1649.8m and 1931.0m gases. These data further confirm that the gases were generated by the thermal cracking of liquids at depth rather than in association with liquids within the oil-generative window.

Caution should be exercised when biomarker data from condensates are used to make inferences regarding source organic matter type, provenance, and thermal maturity. The absolute values of compound abundances, and ratios based on them, may not be a true reflection of these source characteristics, in that they are either maturity- or phase-affected, or both. However, such data may still be useful for comparative purposes, being sufficiently similar to infer the co-genesis of the Minerva-1 gas/condensates, and being of potential value for correlation with hydrocarbons recovered from nearby wells.

---

**REFERENCES**

**BOREHAM, C.J., CRICK, I.H., and POWELL, T.G., 1988, "Alternative Calibration of the Methylphenanthrene Index Against Vitrinite Reflectance: Application to Maturity Measurements on Oils and Sediments" Org. Geochem., 12, 289-294.**

**PETERS, K.E., and MOLDOWAN, J.M., 1993, "The Biomarker Guide" (Prentice Hall, 363pp).**

**RADKE, M., WELTE, D.H., and WILLSCH, H., 1982, "Geochemical Study on a Well in the Western Canada Basin: Relation of the Aromatic Distribution Pattern to Maturity of Organic Matter" Geoch. Cosmochim. Acta, 46, 1-10.**

**WAPLES, D.W., and MACHIHARA, T., 1991, "Biomarkers for Geologists : A Practical Guide to the Application of Steranes and Triterpanes in Petroleum Geology" (AAPG Methods in Exploration, No. 9, 91pp).**

TABLE 1-1

GEOLOGIC & GENERAL DATA - SEDIMENTS

WELL NAME = MINERVA-1  
 COUNTRY = Australia  
 BASIN = Otway

DEPTH UNIT = Metres  
 DATE OF JOB = Apr 93

DEPTH 1	DEPTH 2	GEOLOGIC PERIOD/EPOCH	GEOLOGIC AGE	FORMATION	PRIMARY LITHOLOGY	PERCENT PRIMARY	SECONDARY LITHOLOGY	PERCENT SECONDARY	SAMPLE TYPE	SAMPLE QUALITY	CONTRACTOR	SAMPLE PICKED	TEMPERATURE (deg. C)
1130.00	1130.00	L. CRET	-	SHERGP	-	-	-	-	SWC	-	GTS	NO	-
1342.00	1342.00	L. CRET	-	SHERGP	-	-	-	-	SWC	-	GTS	NO	-
1523.00	1523.00	L. CRET	-	SHIPGP	-	-	-	-	SWC	-	GTS	NO	-
1747.00	1747.00	L. CRET	-	SHIPGP	-	-	-	-	SWC	-	GTS	NO	-
1837.10	1837.10	L. CRET	-	SHIPGP	-	-	-	-	SWC	-	GTS	NO	-
1947.50	1947.50	L. CRET	-	SHIPGP	-	-	-	-	SWC	-	GTS	NO	-
2157.50	2157.50	L. CRET	-	SHIPGP	-	-	-	-	SWC	-	GTS	NO	-
2215.00	2215.00	L. CRET	-	SHIPGP	-	-	-	-	SWC	-	GTS	NO	-
2392.50	2392.50	E. CRET	-	OTWAGP	-	-	-	-	SWC	-	GTS	NO	-

N.B. Code definitions at end of table  
 - = No data

MINV 1 / PE 900058 / P158

CODE DEFINITIONS FOR TABLE 1

-----  
 GEOLOGICAL PERIOD CODES  
 -----

E.CRET = Early Cretaceous  
 L.CRET = Late Cretaceous

-----  
 GEOLOGICAL AGE CODES  
 -----

-----  
 FORMATION CODES  
 -----

OTWAGP = Otway Group  
 SHERGP = Sherbrook Group  
 SHIFGP = Shipwreck Group

-----  
 PRIMARY/SECONDARY LITHOLOGY CODES  
 -----

-----  
 SAMPLE TYPE CODES  
 -----

SWC = Sidewall Core

-----  
 SAMPLE QUALITY CODES  
 -----

-----  
 CONTRACTOR CODES  
 -----

GTS = Geotechnical Services

TABLE 1-2

GEOLOGIC & GENERAL DATA - FLUIDS

DEPTH 1	DEPTH 2	SAMPLE DESCRIPTION	GEOLOGIC PERIOD/EPOCH	GEOLOGIC AGE	FORMATION	SAMPLE TYPE	SAMPLE QUALITY	CONTRACTOR	TEMPERATURE (deg. C)
1649.80	1649.80	GAS	L. CRET	-	SHIPGP	RFT	-	CSI	-
1649.80	1649.80	COLD-TRAPPED COND	L. CRET	-	SHIPGP	RFT	-	GTS	-
1649.80	1649.80	COLD-TRAPPED COND	L. CRET	-	SHIPGP	RFT	-	GTS	-
1931.00	1931.00	GAS	L. CRET	-	SHIPGP	RFT	-	CSI	-
1942.50	1942.50	COLD-TRAPPED COND	L. CRET	-	SHIPGP	RFT	-	GTS	-
1942.50	1942.50	TOPPED	L. CRET	-	SHIPGP	RFT	-	GTS	-

WELL NAME = MINERVA-1  
 COUNTRY = Australia  
 BASIN = Otway

DEPTH UNIT = Metres  
 DATE OF JOB = Aug 93-Mar 94

N.B. Code definitions at end of table  
 - = No data

CODE DEFINITIONS FOR TABLE 1

-----  
GEOLOGICAL PERIOD CODES  
-----

L.CHET = Late Cretaceous

-----  
GEOLOGICAL AGE CODES  
-----

FORMATION CODES

-----  
SHIPGP = Shipwreck Group  
-----

-----  
SAMPLE TYPE CODES  
-----

RFT = Repeat Fm Test

-----  
SAMPLE QUALITY CODES  
-----

CONTRACTOR CODES

-----  
CSI = C.S.I.R.O  
GTS = Geotechnical Services  
-----

TABLE 2

TOC AND ROCK-EVAL PYROLYSIS DATA - SEDIMENTS

WELL NAME = MINERVA-1  
 COUNTRY = Australia  
 BASIN = Otway

DEPTH UNIT = Metres  
 DATE OF JOB = Apr 93

DEPTH 1	DEPTH 2	TOC	TMAX	S0	S1	S2	S3	S1+S2	S2/S3	PI	PC	HI	OI	INSTRUMENT	SAMPLE TYPE	CONTRACTOR PICKED
1342.00	1342.00	1.68	432	-	.04	1.71	.37	1.75	4.62	.02	.15	102	22	RE2	SWC	GTS NO
1523.00	1523.00	1.34	432	-	.05	1.26	.81	1.31	1.56	.04	.11	94	60	RE2	SWC	GTS NO
1747.00	1747.00	.37	-	-	-	-	-	-	-	-	-	-	-	RE2	SWC	GTS NO
1837.10	1837.10	40.50	424	-	19.70	181.98	1.28	201.68	142.17	.10	16.74	449	3	RE2	SWC	GTS NO

TOC = Total organic carbon  
 S2 = HC generating potential  
 HI = Hydrogen index

TMAX = Max. temperature  
 S3 = Organic carbon dioxide  
 OI = Oxygen index

S0 = Volatile gaseous HC's  
 PI = Production index  
 = no data

S1 = Volatile hydrocarbons (HC's)  
 PC = Pyrolysable carbon  
 N.B. Code defn's at end of table.



CODE DEFINITIONS FOR TABLE 2

INSTRUMENT CODES

RE2 = Rock-Eval II

SAMPLE TYPE CODES

SMC = Sidewall Core

CONTRACTOR CODES

GTS = Geotechnical Services

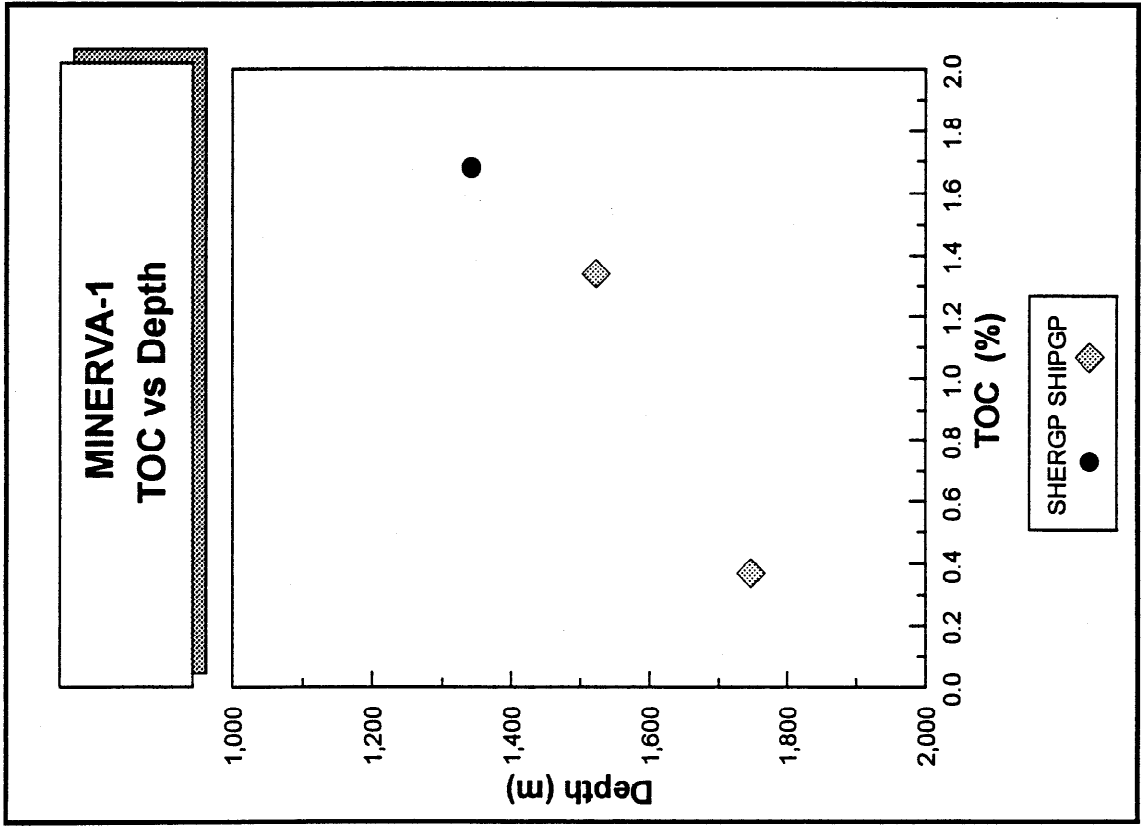
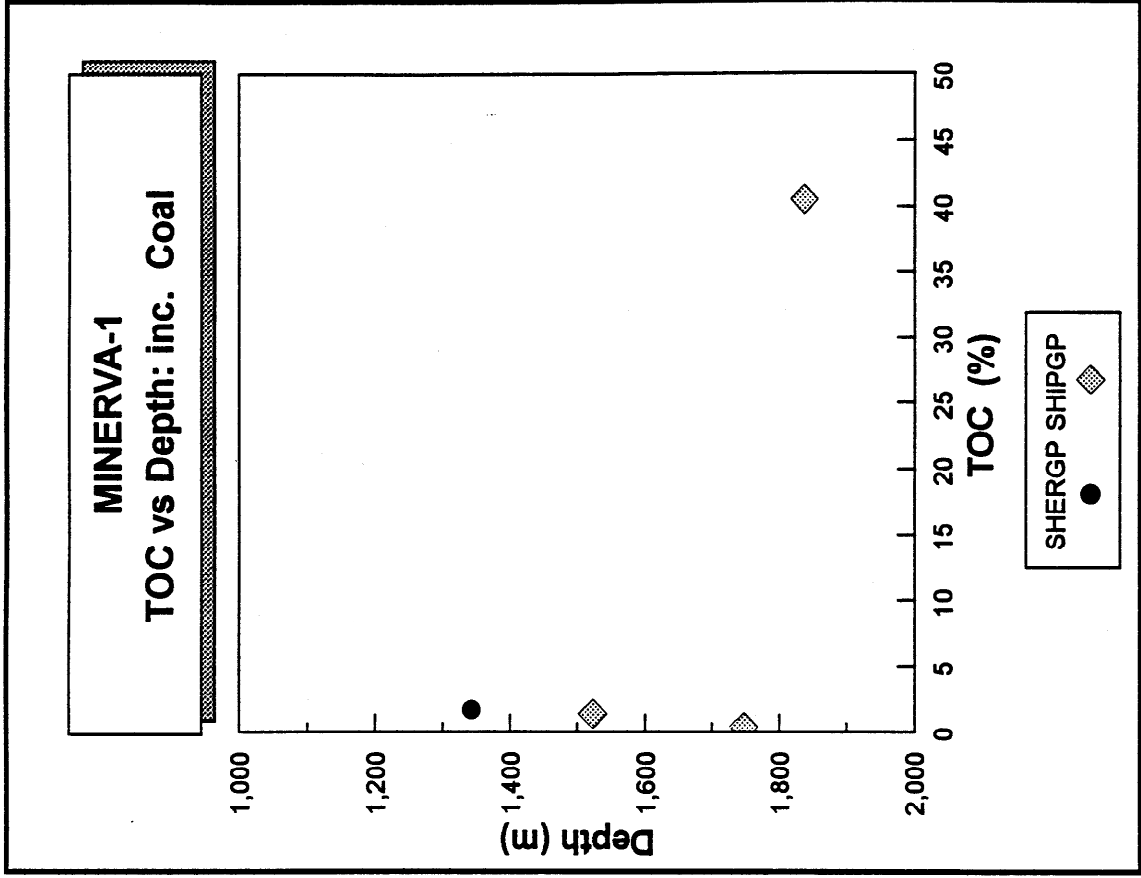


Figure 1

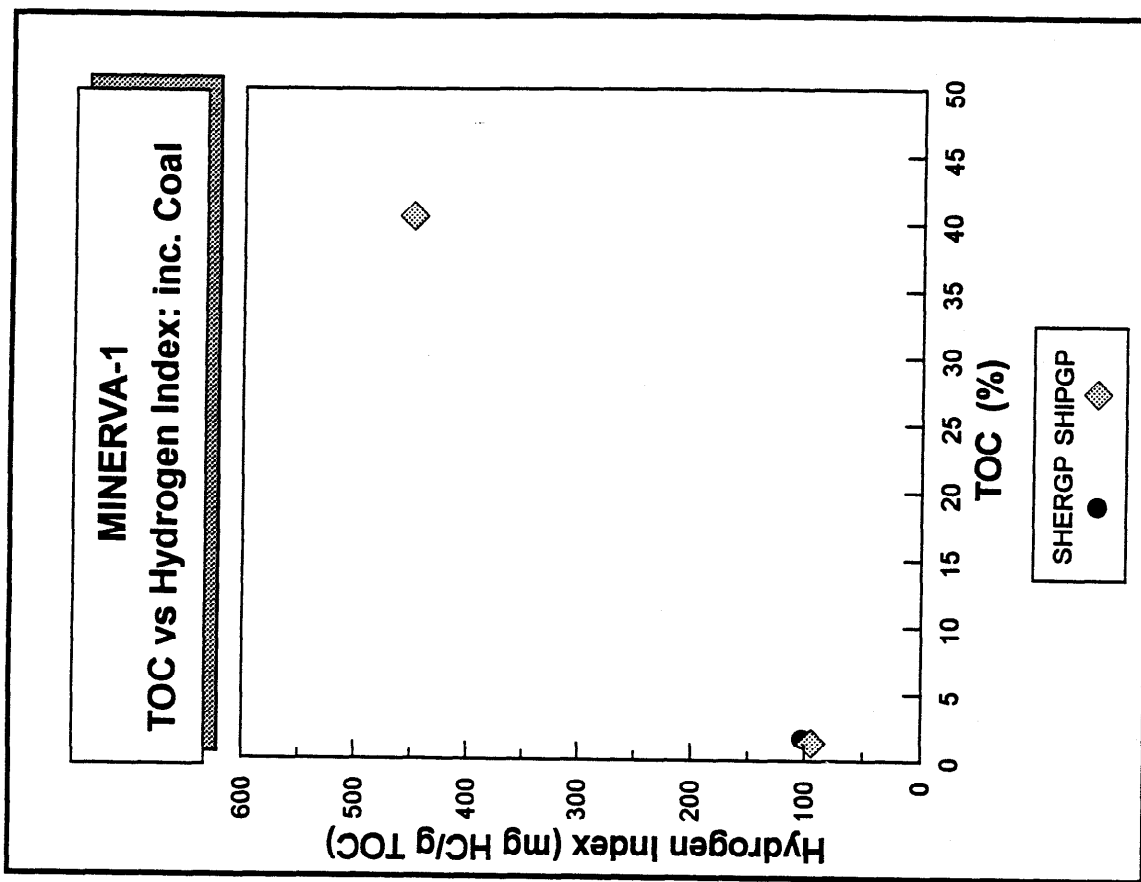
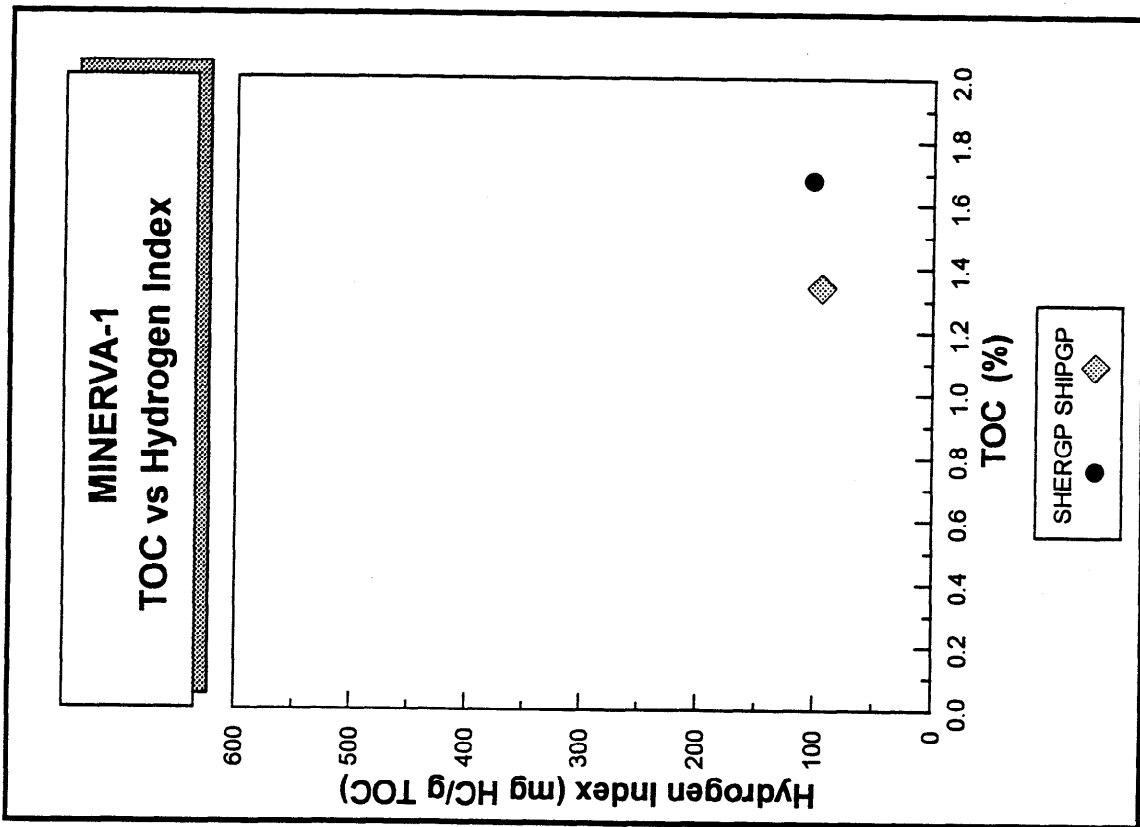


Figure 2

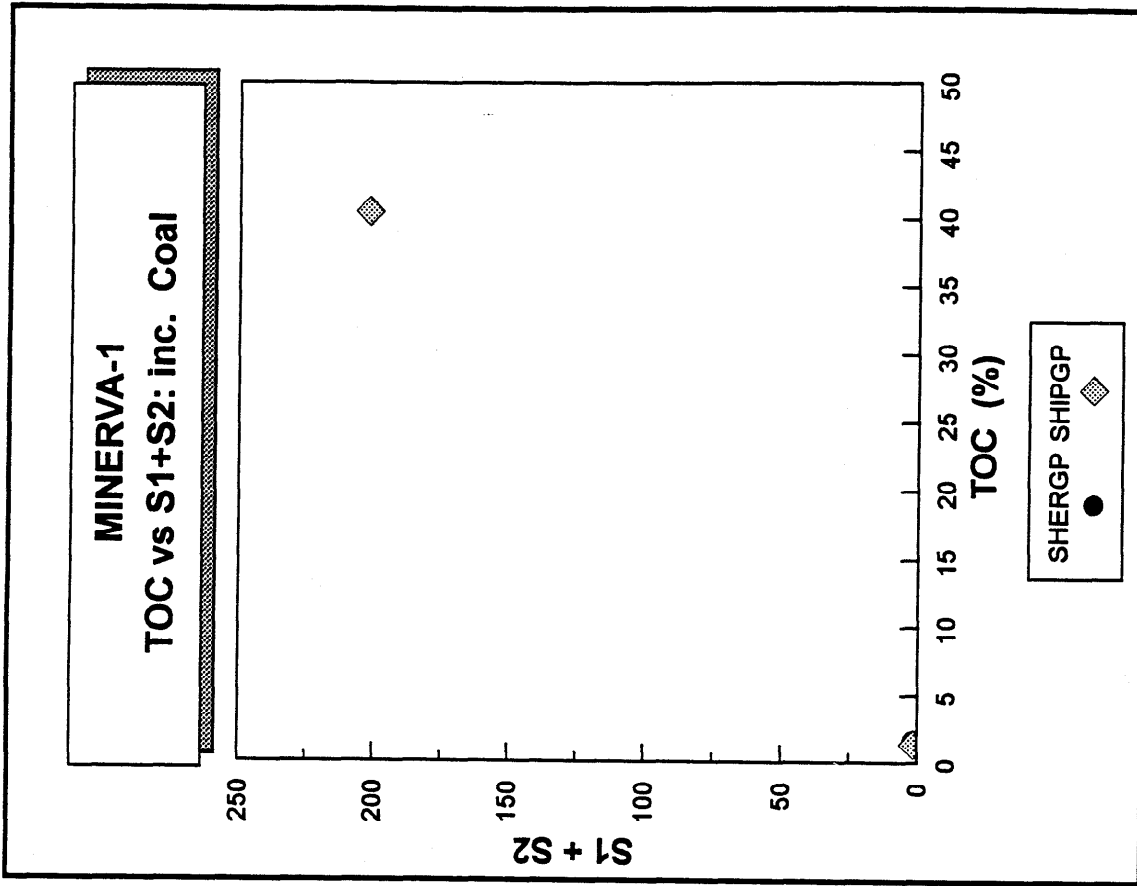
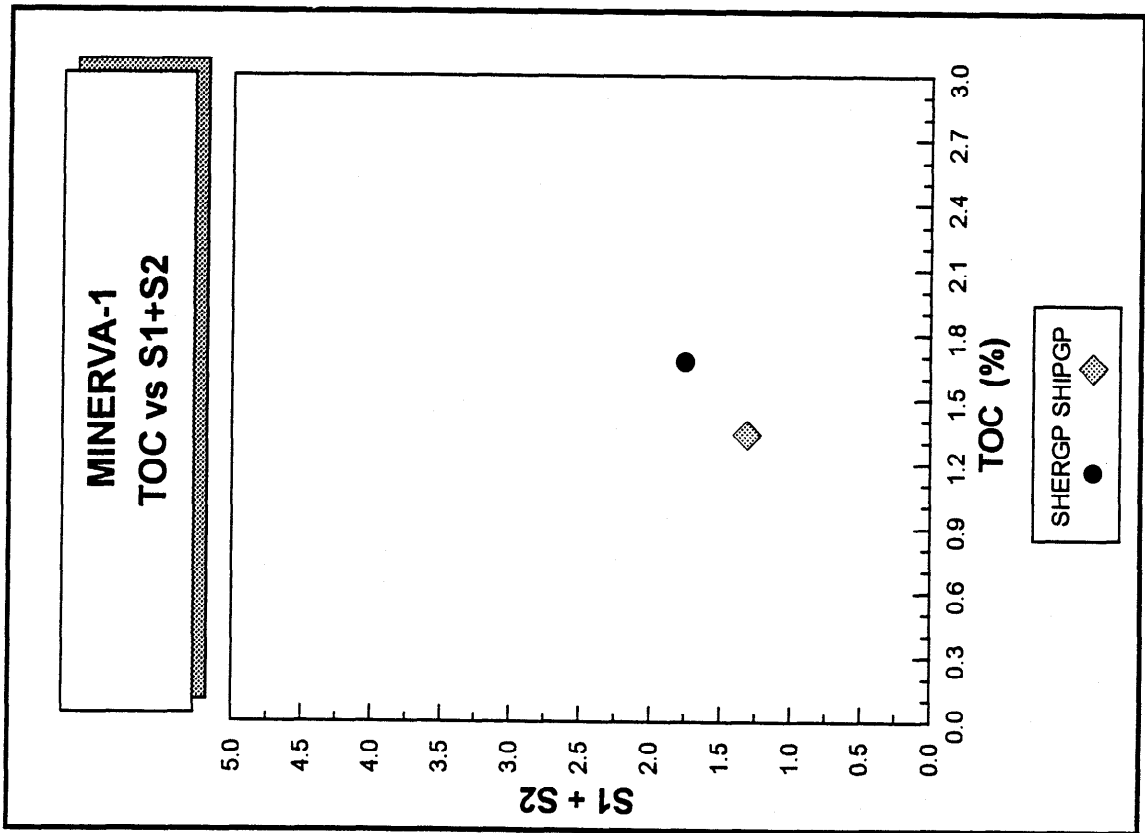
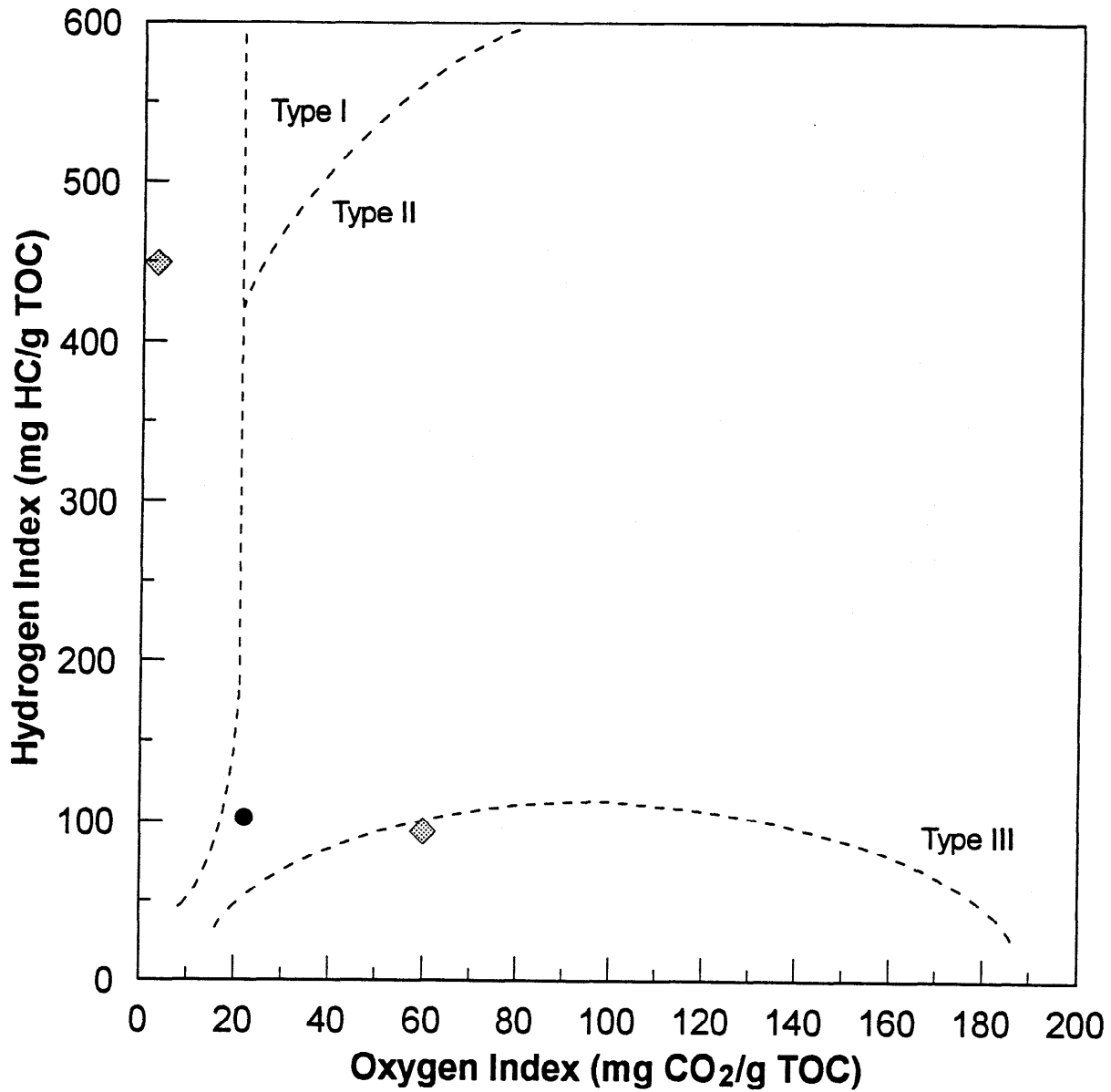


Figure 3

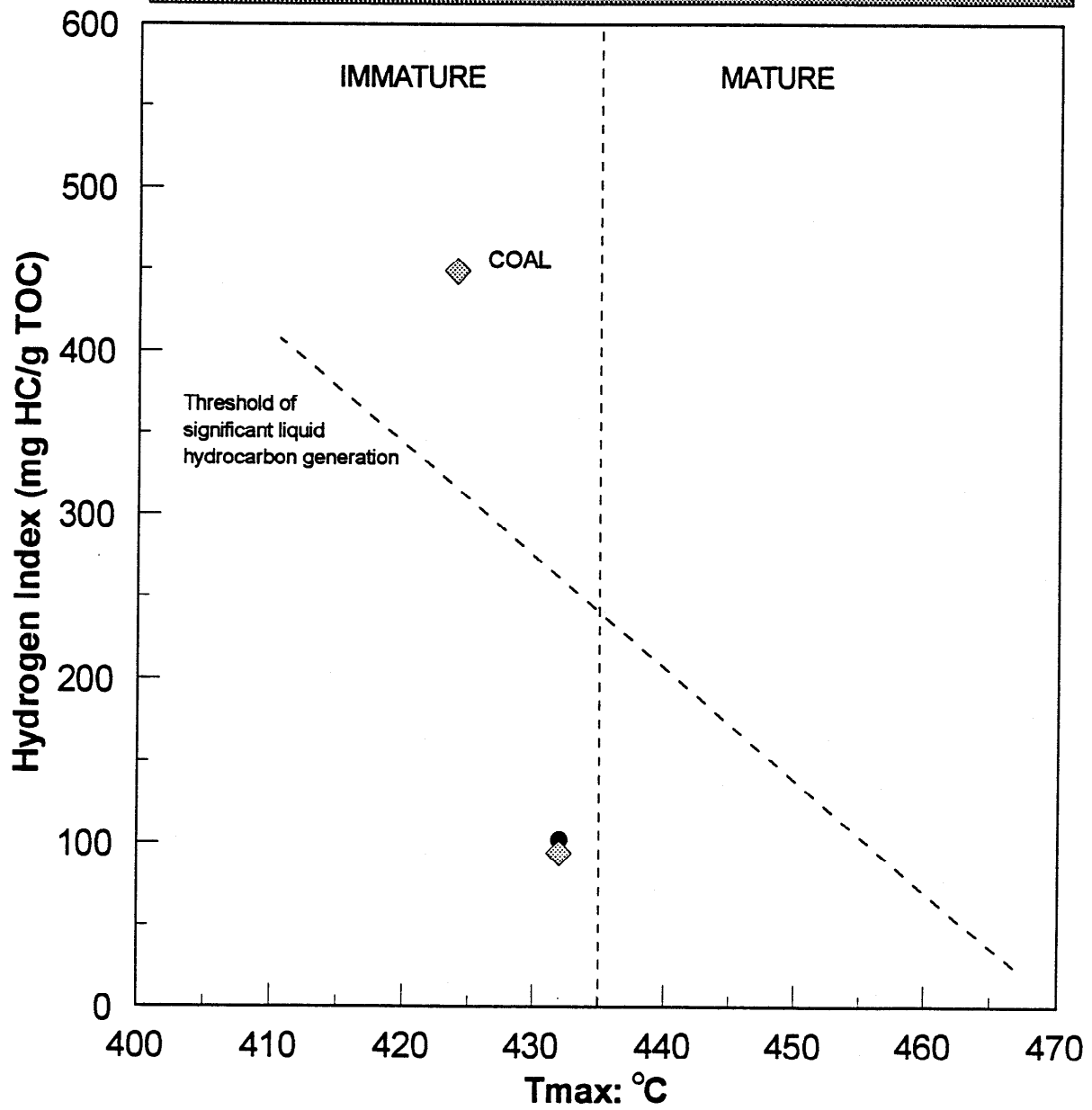
# MINERVA-1 Hydrogen Index vs Oxygen Index



SHERGP SHIPGP  
● ◆

Figure 4

# MINERVA-1 Hydrogen Index vs Tmax



SHERGP SHIPGP  
● ◆

Figure 5

# MINERVA-1 Maceral Composition Data

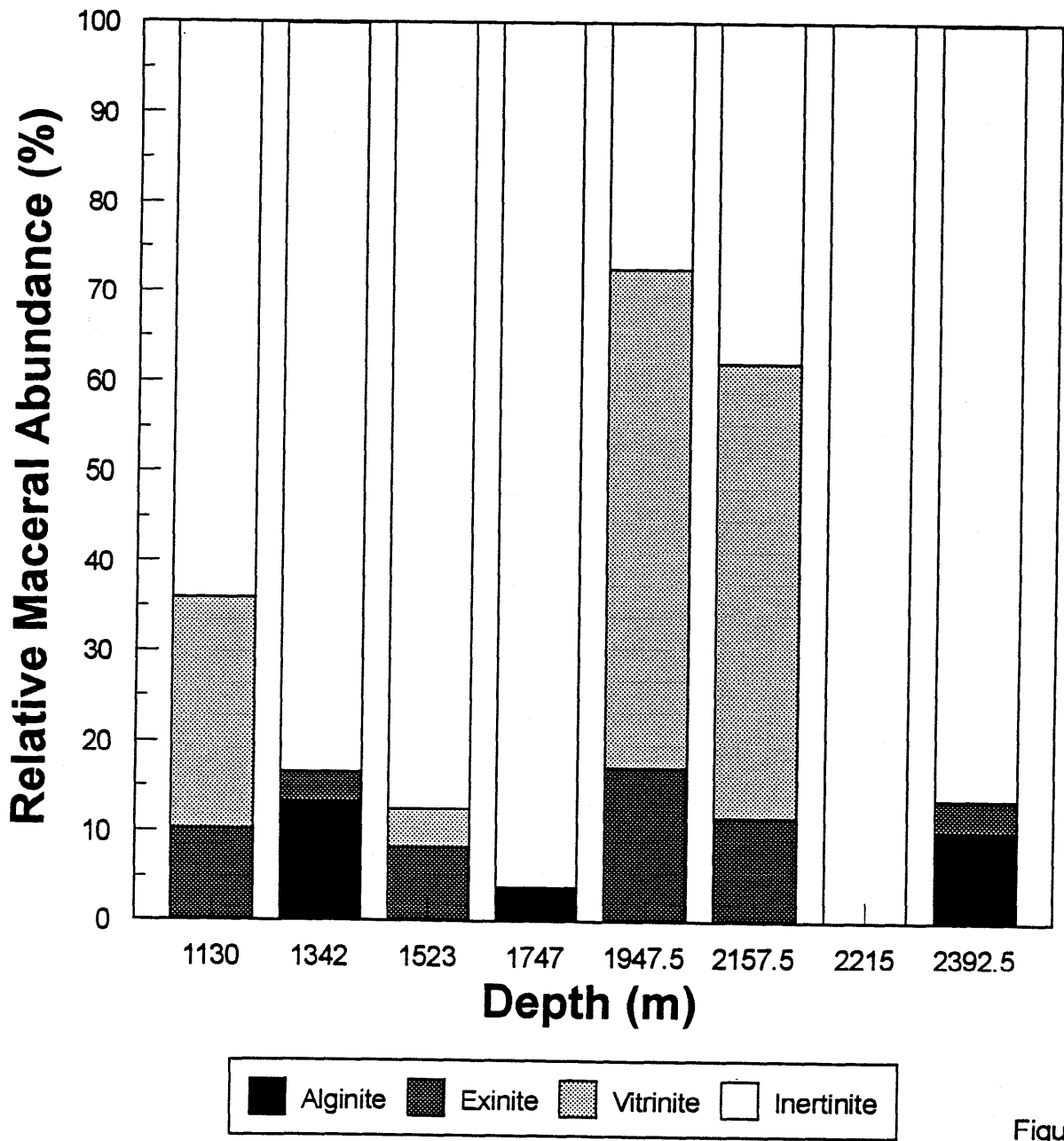
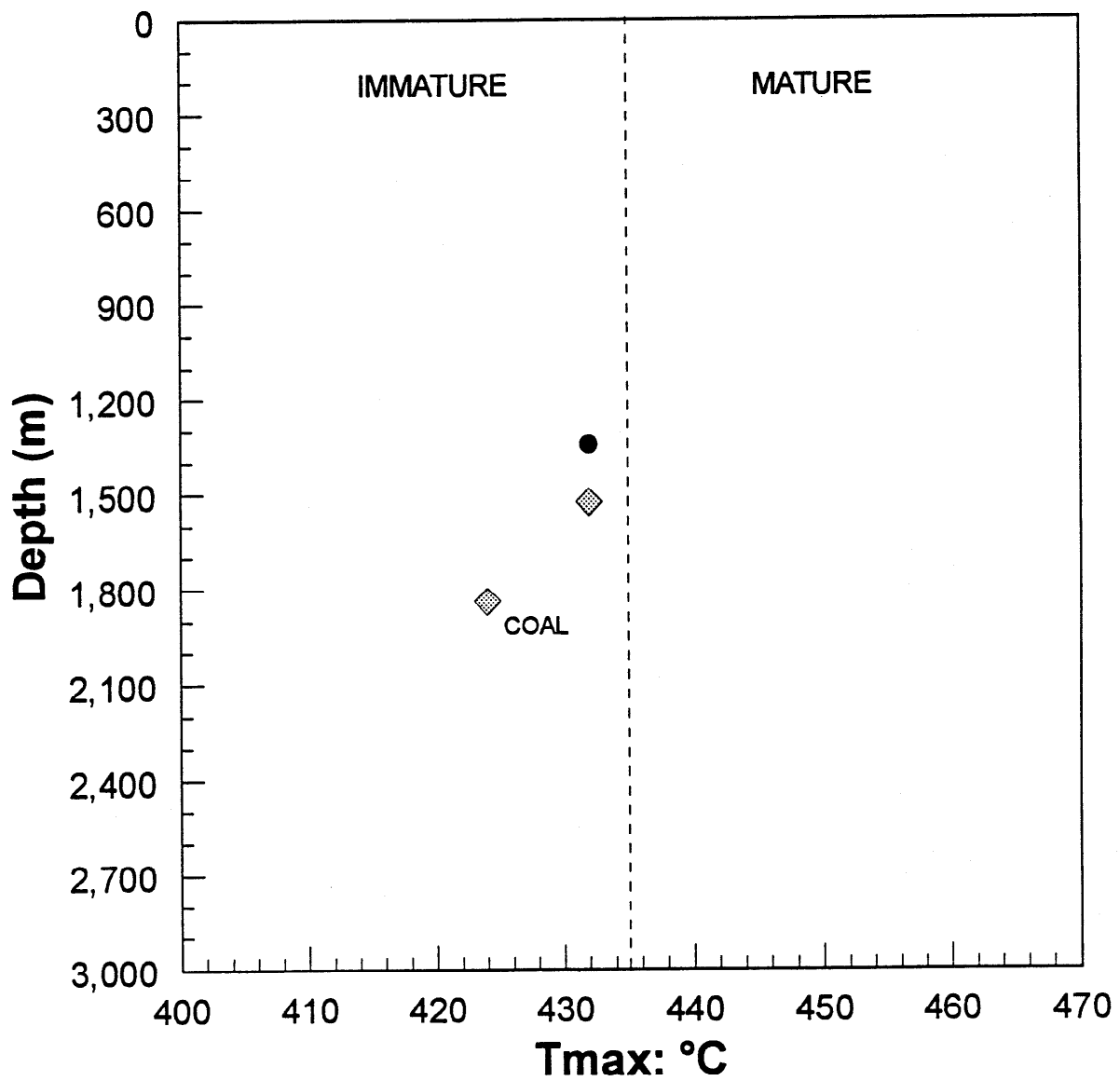


Figure 6

# MINERVA-1 Tmax vs Depth



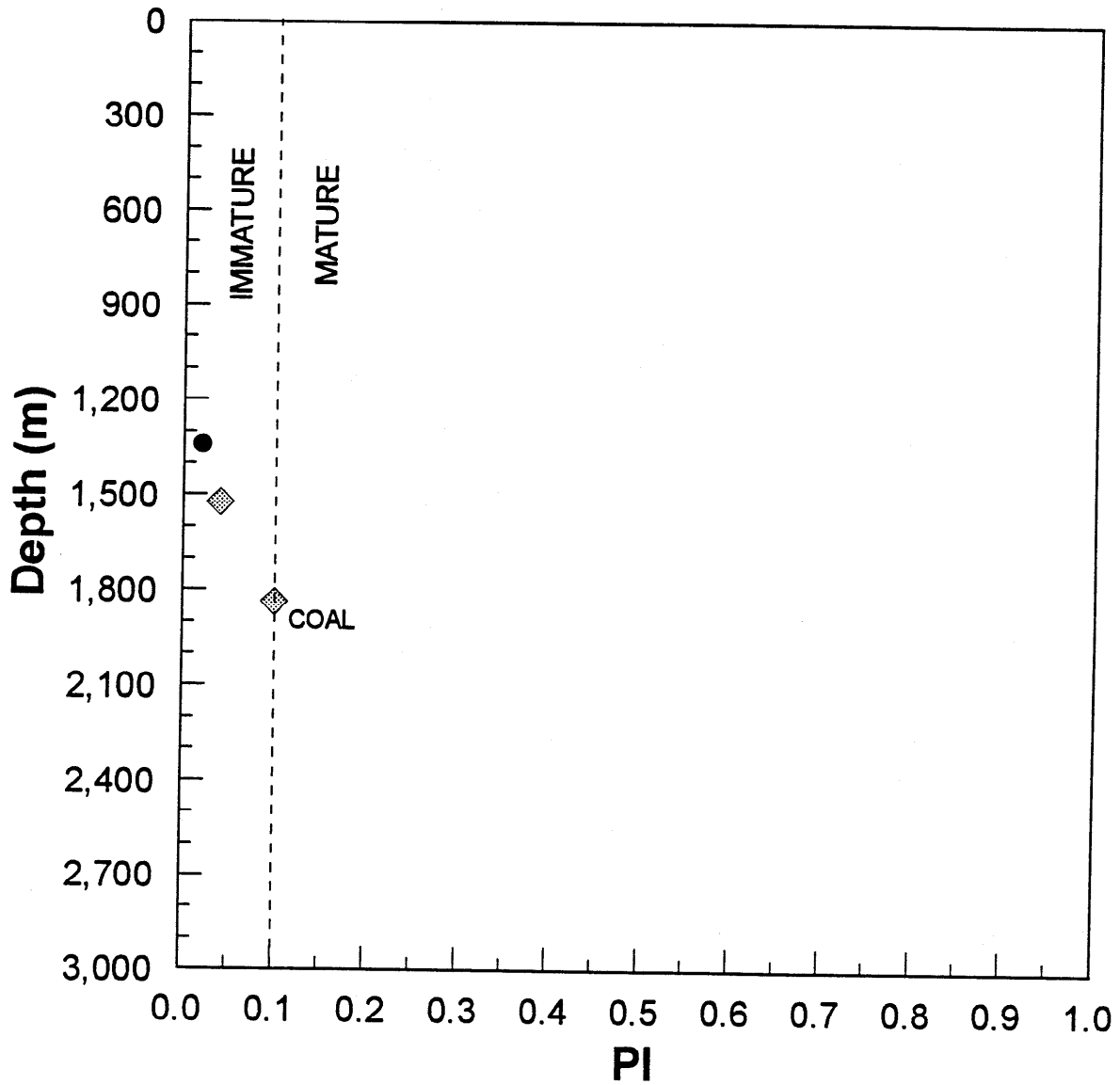
SHERGP SHIPGP

● ◆

Figure 7



# MINERVA-1 PI vs Depth



SHERGP SHIPGP  
● ◆

Figure 8

TABLE 3

VITRINITE REFLECTANCE AND COAL MACERAL DATA - SEDIMENTS  
ALL MACERAL POPULATIONSWELL NAME = MINERVA-1  
COUNTRY = Australia  
BASIN = OtwayDEPTH UNIT = Metres  
DATE OF JOB = June 93

DEPTH 1	DEPTH 2	POPULATION TYPE	MEAN % REFL.	MINIMUM % REFL.	MAXIMUM % REFL.	NUMBER READINGS	STANDARD DEVIATION	-----MACERAL COMPOSITION-----				SOURCE OF DATA
								% ALGINITE	% EXINITE	% VITRINITE	% INERTINITE	
1130.00	1130.00	V	.42	.29	.57	29	.09	0.00	10.30	25.60	64.10	GTS
1342.00	1342.00	V	.50	.42	.57	12	.04	13.30	3.30	0.00	83.30	GTS
1523.00	1523.00	V	.53	.41	.64	28	.06	0.00	8.30	4.20	87.50	GTS
1747.00	1747.00	V	.53	.40	.74	15	.09	3.80	0.00	0.00	96.20	GTS
1947.50	1947.50	V	.63	.53	.71	26	.05	0.00	17.20	55.40	27.40	GTS
2157.50	2157.50	V	.62	.57	.71	27	.03	0.00	11.60	50.50	37.90	GTS
2215.00	2215.00	V	.62	.57	.67	2	.07	0.00	0.00	0.00	100.00	GTS
		I	1.70	1.38	1.90	8	.19					
2392.50	2392.50	V	.75	.60	.94	9	.12	10.30	3.40	0.00	86.20	GTS

-----  
 N.B. Code definitions at end of table  
 - = no data

MINV 1 / PE900058 / P172

CODE DEFINITIONS FOR TABLE 3

POPULATION TYPE CODES

I = INERTINITE  
V = VITRINITE

CONTRACTOR CODES

GTS = Geotechnical Services

## JOB NO. 1933A, MINERVA-1, OTWAY BASIN

Sample No(s)	Depth(m)/ Sample type	R <sub>max</sub> V (%)	Range (%)	N	Description Including Liptinite Fluorescence Characteristics
v7853	1130 SWC10	0.42	0.29-0.57	29	Sparse sporinite, bright yellow to orange, sparse cutinite, yellow to orange, rare resinite, greenish yellow, rare lamalginite and liptodetrinite, yellow to orange. (Siltstone>> coal. Coal rare, V only. Vitrite. Dom abundant, I>V>L. Inertinite abundant, vitrinite common, liptinite sparse. Oil drops rare, greenish yellow. Mineral fluorescence pervasive, faint green. Iron oxides common. Pyrite sparse.)
v7854	1342.0 SWC99	0.50	0.42-0.57	12	Sparse lamalginite and cutinite, yellow to orange, rare sporinite and liptodetrinite, yellow to orange. Rare tasmanitid-derived telalginite, bright yellow. (Silty claystone. Dom abundant, I>L>V. Inertinite abundant, liptinite sparse, vitrinite rare. Mineral fluorescence pervasive, weak yellow to orange. Iron oxides sparse. Pyrite abundant.)
v7855	1523 SWC89	0.53	0.41-0.64	28	Sparse sporinite, yellow to orange, rare cutinite, yellow to orange, rare lamalginite, bright greenish yellow to yellow, rare liptodetrinite, greenish yellow to orange. (Clayey siltstone. Dom abundant, I>L>V. Inertinite abundant, liptinite and vitrinite sparse. Oil drops rare, greenish yellow. Mineral fluorescence pervasive, weak green. Glauconite rare. Fossil fragments rare. Iron oxides sparse. Pyrite abundant.)
v7856	1747.0 SWC75	0.53	0.40-0.74	15	Sparse lamalginite, yellow to dull orange, rare liptodetrinite, yellow to dull orange. (Sandstone. Dom abundant, I>L>V. Inertinite abundant, liptinite sparse, vitrinite rare. Bitumen rare, dull orange to brown. Oil drops rare, yellow. Mineral fluorescence pervasive, weak yellow to orange. Iron oxides sparse. Glauconite sparse. Pyrite abundant.)
v7857	1947.5 SWC65	0.63	0.53-0.71	26	Major sporinite, greenish yellow to orange, abundant cutinite, yellow to orange, sparse resinite, bright greenish yellow, sparse liptodetrinite, greenish yellow to orange. (Coal>>shaly coal. Coal dominant, V>I>L. Vitrite>duroclarite>clarite> inertite. Mineral-free maceral group composition of the coal: vitrinite - 55%, inertinite - 28%, liptinite - 17%. Shaly coal abundant, V>L>I. Duroclarite>clarite. Mineral-free maceral group composition of the shaly coal: vitrinite - 50%, inertinite - 17%, liptinite - 33%. Iron oxides rare. Pyrite sparse.)
v7858	2157.5 SWC123	0.62	0.57-0.71	27	Abundant sporinite, yellow to dull orange, common resinite, yellow to orange, sparse cutinite, orange to dull orange, rare liptodetrinite, yellow to dull orange. (Coal dominant. Duroclarite>clarodurite>vitrinite>inertite>clarite. Mineral-free maceral group composition of the coal: vitrinite - 50%, inertinite - 38%, liptinite - 12%. Vitrinite fluorescence common. Pyrite abundant.)

TABLE 3A

## \*JOB NO. 1933A, MINERVA-1, OTWAY BASIN

Sample No(s)	Depth(m)/ Sample type	R <sub>v</sub> max (%)	Range (%)	N	Description Including Liptinite Fluorescence Characteristics
v7859	2215 SWC121 R <sub>1</sub>	0.62 1.70	0.57-0.67 1.38-1.90	2 8	Rare lamalginite and liptodetrinite yellow to orange. (Silty claystone>>coal. Coal rare, V only. Vitrite. Dom sparse, I>L. Inertinite sparse, liptinite rare, vitrinite absent. Mineral fluorescence pervasive, moderate orange. Iron oxides sparse. Pyrite rare.)
v7860	2392.5 SWC109	0.75	0.60-0.94	9	Sparse lamalginite, orange to dull orange, sparse liptodetrinite, yellow to dull orange, rare cutinite and sporinite, orange to dull orange. (Calcareous siltstone>>coal. Coal rare, inertinite only. Inertite only. Dom abundant, I>L>V. Inertinite abundant, liptinite sparse, vitrinite rare. Bitumen sparse, dull orange to brown. Oil drops sparse, yellow. Mineral fluorescence pervasive, weak yellow to orange. Rare glauconite. Iron oxides sparse. Pyrite sparse.)

### FIGURE 9

#### VITRINITE REFLECTANCE AND COAL MACERAL IDENTIFICATION

WELL: MINERVA-1

CLIENT: BHP PETROLEUM

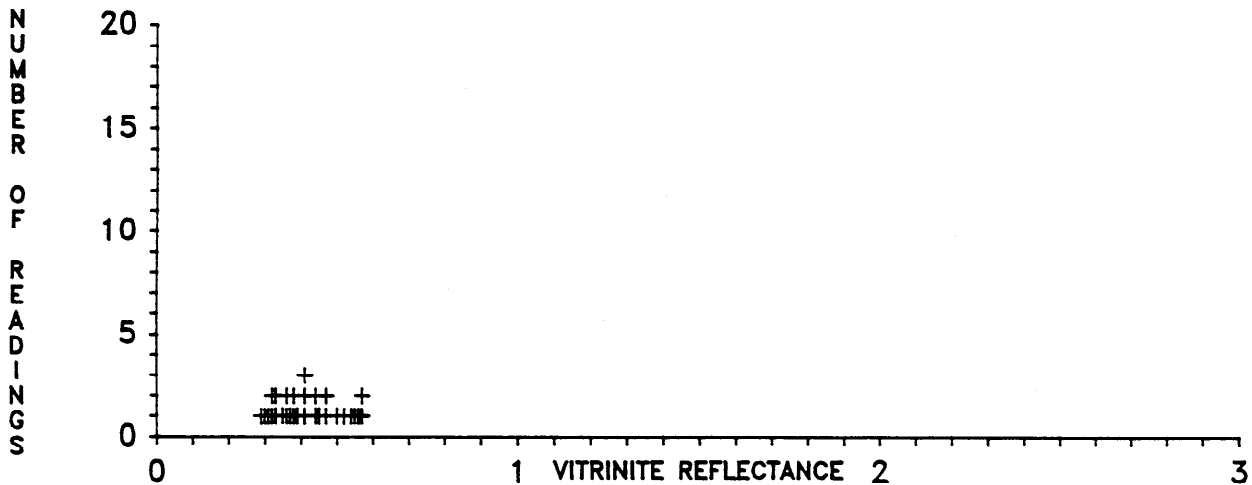
SAMPLE TYPE: SWC

SAMPLE ID: 1130.0 METRES

DATE: JUNE 1993

(Total No. of Readings=29) 0.29 0.30 0.31 0.32 0.32 0.33 0.33 0.35 0.36 0.36 0.37 0.38 0.38 0.39 0.41 0.41 0.41  
0.44 0.44 0.45 0.47 0.47 0.50 0.52 0.54 0.55 0.56 0.57 0.57

VITRINITE REFLECTANCE							MACERAL IDENTIFICATION				
POPULATION Number	%	No. of Readings	Mean Ro (%)	Min Ro (%)	Max Ro (%)	STD Dev (%)	Comments	% Vitrinite	% Inertinite	% Liptinite	% Bitumen
1	100.0	29	0.42	0.29	0.57	0.09	INDIGENOUS(+)	25.60	64.10	10.30	0.00



SAMPLE ID: 1342.0 METRES

SAMPLE TYPE: SWC

(Total No. of Readings=12) 0.42 0.45 0.47 0.47 0.49 0.50 0.51 0.51 0.53 0.53 0.55 0.57

VITRINITE REFLECTANCE							MACERAL IDENTIFICATION				
POPULATION Number	%	No. of Readings	Mean Ro (%)	Min Ro (%)	Max Ro (%)	STD Dev (%)	Comments	% Vitrinite	% Inertinite	% Liptinite	% Bitumen
1	100.0	12	0.50	0.42	0.57	0.04	INDIGENOUS(+)	3.20	80.60	16.20	0.00

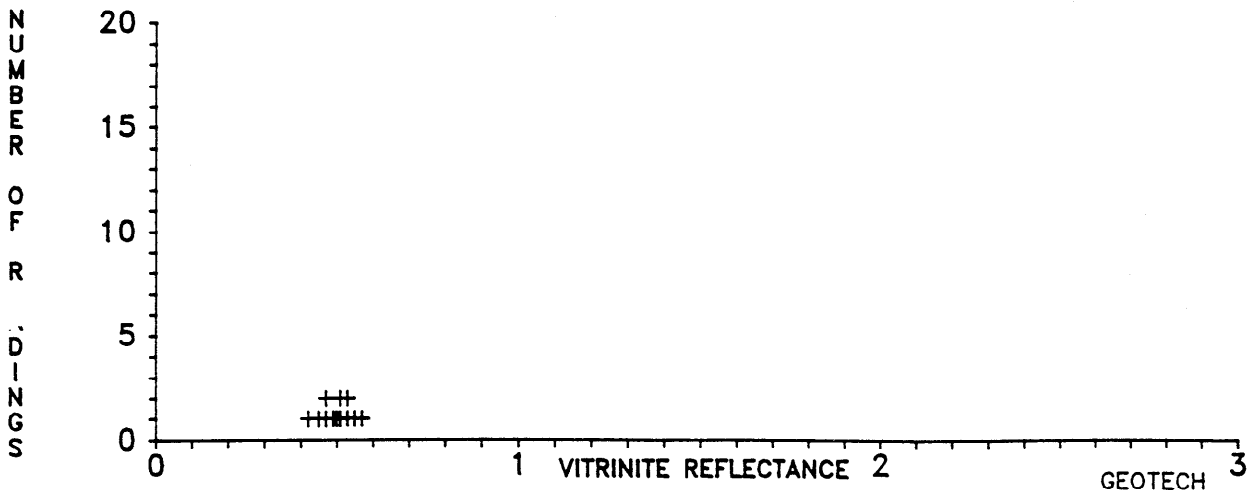


FIGURE 9 (cont'd)

VITRINITE REFLECTANCE AND COAL MACERAL IDENTIFICATION

WELL: MINERVA-1

CLIENT: BHP PETROLEUM

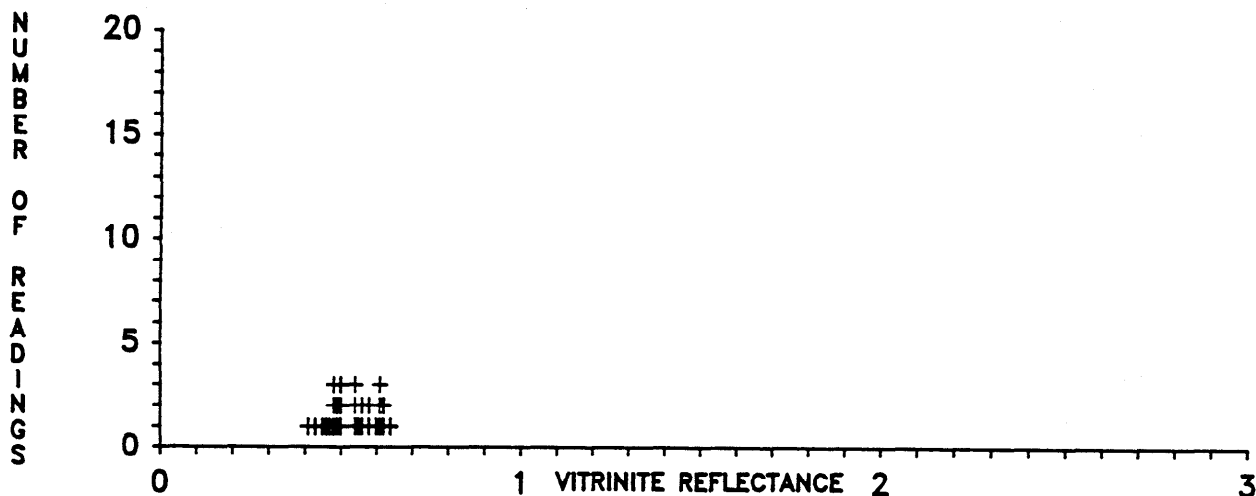
SAMPLE TYPE: SWC

SAMPLE ID: 1523.0 METRES

DATE: JUNE 1993

(Total No. of Readings=28) 0.41 0.43 0.45 0.46 0.47 0.48 0.48 0.48 0.49 0.49 0.50 0.50 0.50 0.54 0.54 0.54 0.55  
0.56 0.56 0.58 0.58 0.60 0.61 0.61 0.61 0.62 0.62 0.64

VITRINITE REFLECTANCE							MACERAL IDENTIFICATION				
POPULATION Number	%	No. of Readings	Mean Ro (%)	Min Ro (%)	Max Ro (%)	STD Dev (%)	Comments	% Vitrinite	% Inertinite	% Liptinite	% Bitumen
1	100.0	28	0.53	0.41	0.64	0.06	INDIGENOUS(+)	4.20	87.50	8.30	0.00



SAMPLE ID: 1747.0 METRES

SAMPLE TYPE: SWC

(Total No. of Readings=15) 0.40 0.47 0.47 0.48 0.48 0.49 0.49 0.50 0.51 0.51 0.56 0.57 0.60 0.69 0.74

VITRINITE REFLECTANCE							MACERAL IDENTIFICATION				
POPULATION Number	%	No. of Readings	Mean Ro (%)	Min Ro (%)	Max Ro (%)	STD Dev (%)	Comments	% Vitrinite	% Inertinite	% Liptinite	% Bitumen
1	100.0	15	0.53	0.40	0.74	0.09	INDIGENOUS(+)	3.60	89.30	3.60	0.00

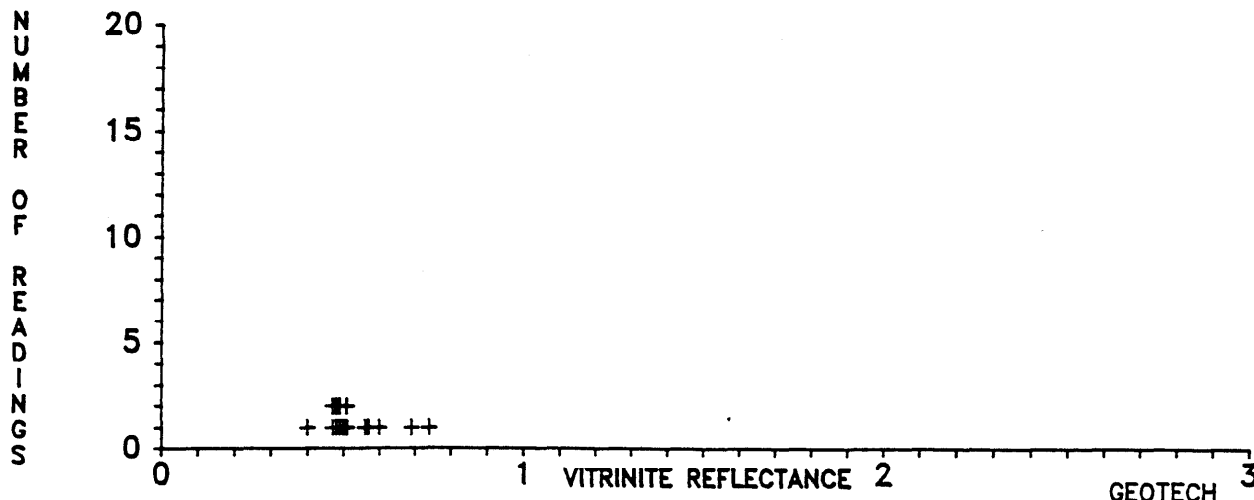


FIGURE 9 (cont'd)

VITRINITE REFLECTANCE AND COAL MACERAL IDENTIFICATION

WELL: MINERVA-1

CLIENT: BHP PETROLEUM

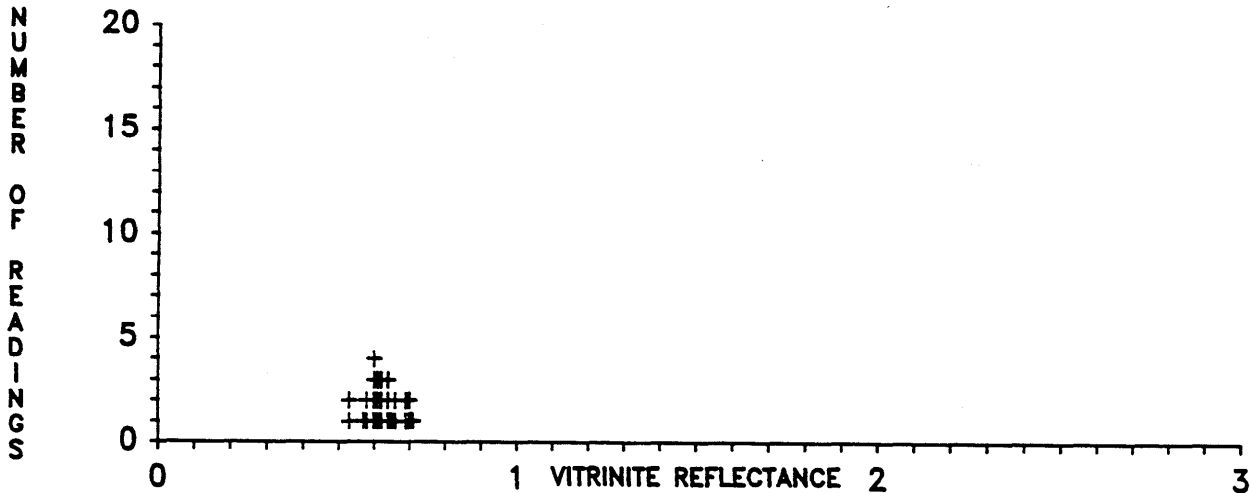
SAMPLE TYPE: SWC

SAMPLE ID: 1947.5 METRES

DATE: JUNE 1993

(Total No. of Readings=26) 0.53 0.53 0.57 0.58 0.58 0.60 0.60 0.60 0.60 0.61 0.61 0.61 0.62 0.62 0.62 0.64 0.64  
0.64 0.65 0.66 0.66 0.69 0.69 0.70 0.71

VITRINITE REFLECTANCE							MACERAL IDENTIFICATION				
POPULATION Number	%	No. of Readings	Mean Ro (%)	Min Ro (%)	Max Ro (%)	STD Dev (%)	Comments	% Vitrinite	% Inertinite	% Liptinite	% Bitumen
1	100.0	26	0.63	0.53	0.71	0.05	INDIGENOUS(+)	55.40	27.40	17.20	0.00



SAMPLE ID: 2157.5 METRES

SAMPLE TYPE: SWC

(Total No. of Readings=27) 0.57 0.58 0.58 0.59 0.59 0.59 0.60 0.61 0.61 0.61 0.61 0.62 0.62 0.63 0.63 0.63 0.63 0.63  
0.63 0.63 0.64 0.64 0.64 0.64 0.65 0.65 0.65 0.66 0.71

VITRINITE REFLECTANCE							MACERAL IDENTIFICATION				
POPULATION Number	%	No. of Readings	Mean Ro (%)	Min Ro (%)	Max Ro (%)	STD Dev (%)	Comments	% Vitrinite	% Inertinite	% Liptinite	% Bitumen
1	100.0	27	0.62	0.57	0.71	0.03	INDIGENOUS(+)	50.50	37.90	11.60	0.00

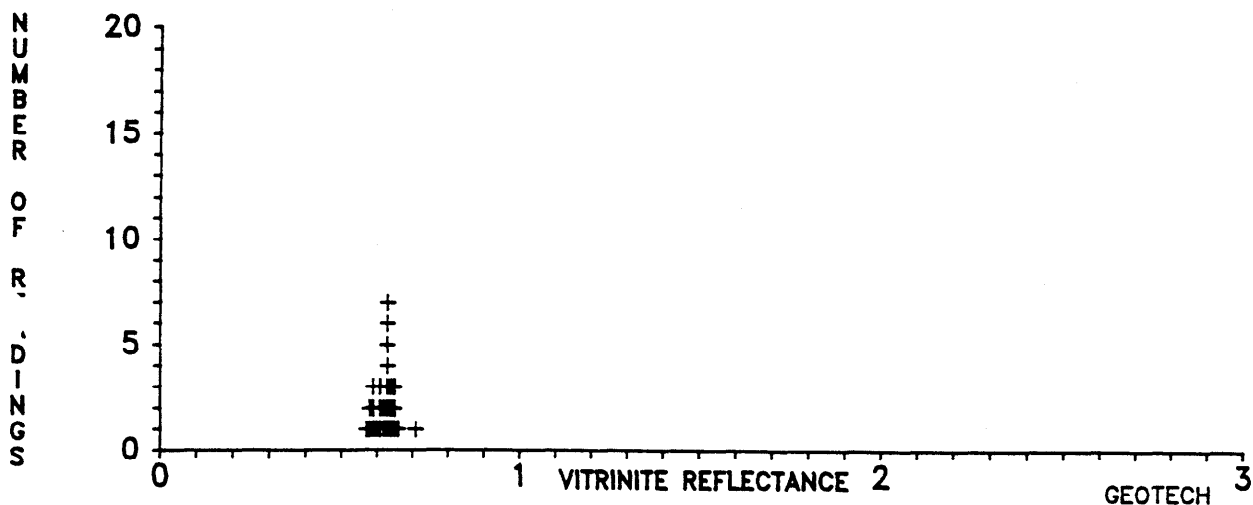




FIGURE 9 (cont'd)

VITRINITE REFLECTANCE AND COAL MACERAL INDENTIFICATION

WELL: MINERVA-1

CLIENT: BHP PETROLEUM

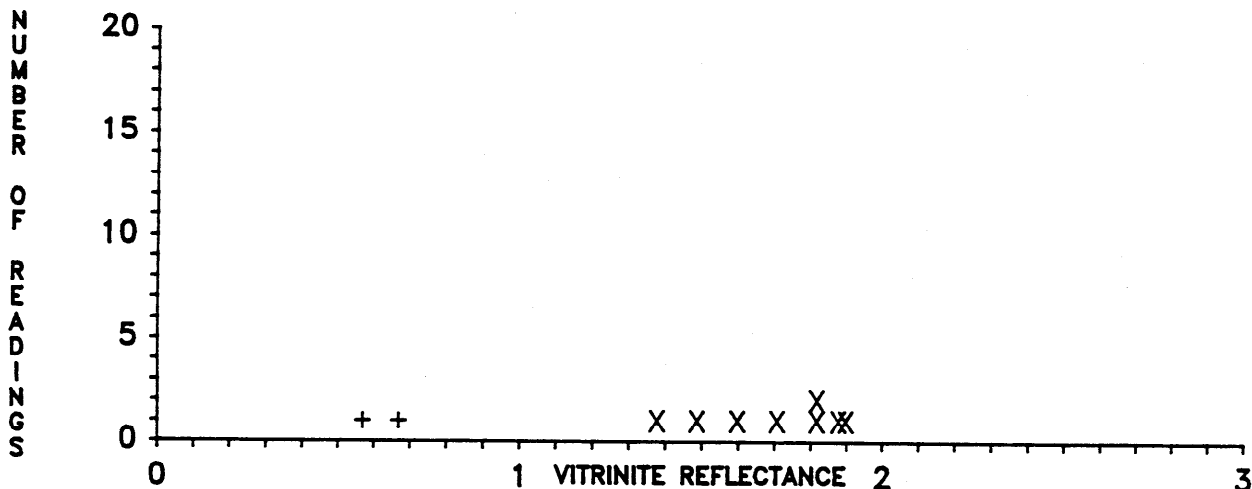
SAMPLE TYPE: SWC

SAMPLE ID: 2215.0 METRES

DATE: JUNE 1993

(Total No. of Readings=10) 0.57 0.67 1.38 1.49 1.60 1.71 1.82 1.82 1.88 1.90

VITRINITE REFLECTANCE							MACERAL IDENTIFICATION				
POPULATION Number	%	No. of Readings	Mean Ro (%)	Min Ro (%)	Max Ro (%)	STD Dev (%)	Comments	% Vitrinite	% Inertinite	% Liptinite	% Bitumen
1	20.0	2	0.62	0.57	0.67	0.08	INDIGENOUS(+)	33.30	33.40	33.30	0.00
2	80.0	8	1.70	1.38	1.90	0.19	INERTINITE(X)				

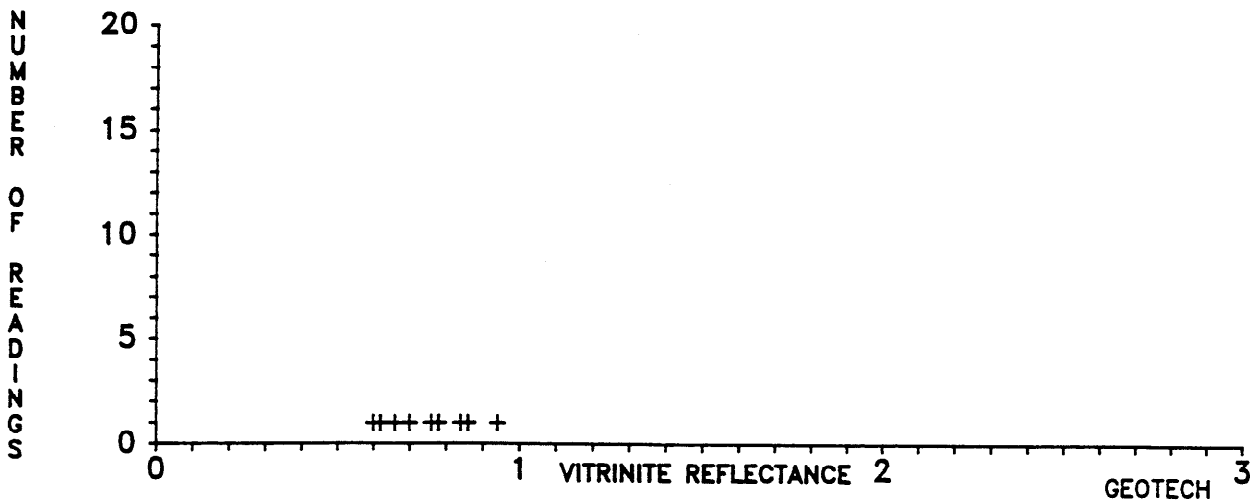


SAMPLE ID: 2392.5 METRES

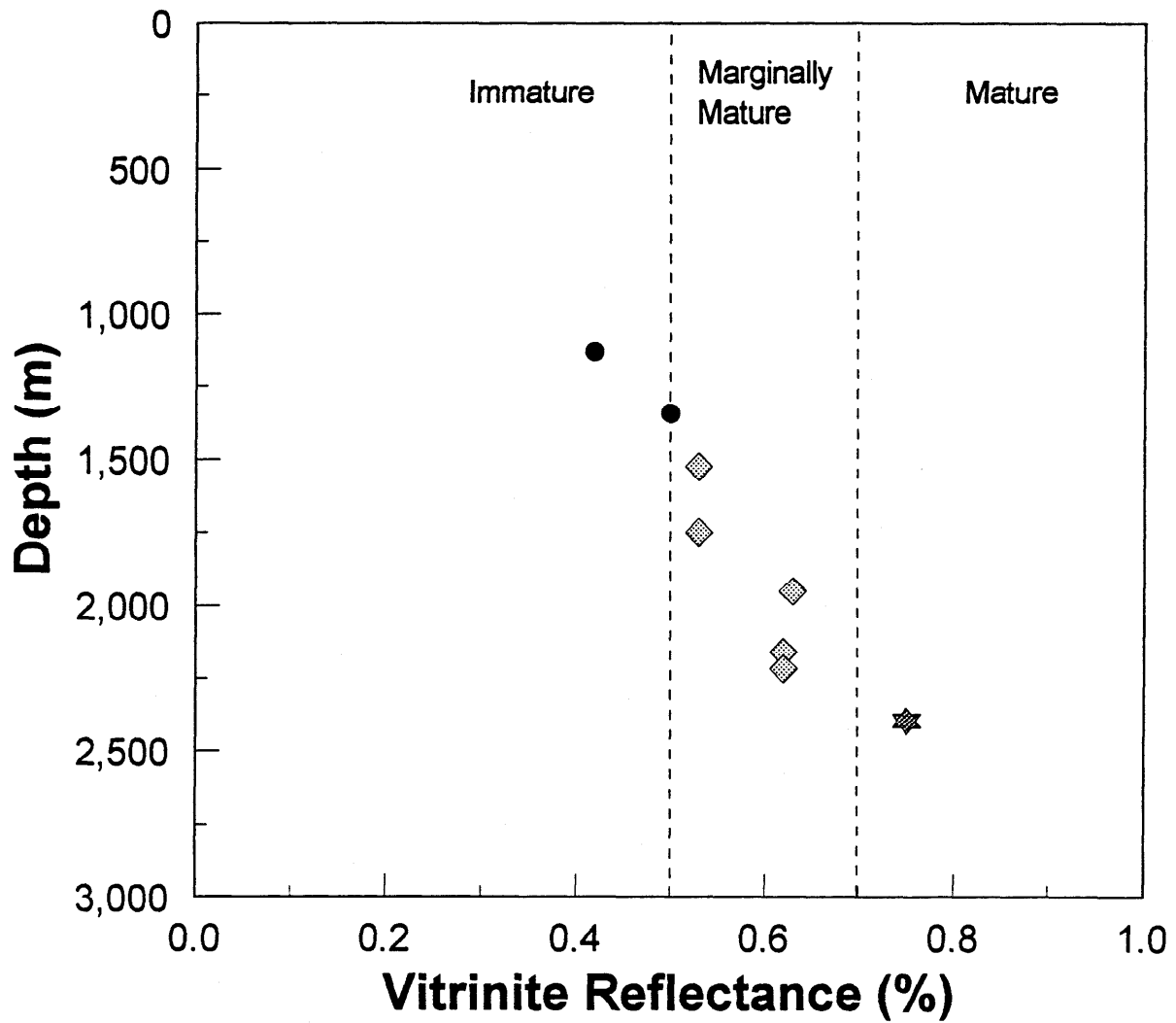
SAMPLE TYPE: SWC

(Total No. of Readings=9) 0.60 0.62 0.66 0.70 0.76 0.78 0.84 0.86 0.94

VITRINITE REFLECTANCE							MACERAL IDENTIFICATION				
POPULATION Number	%	No. of Readings	Mean Ro (%)	Min Ro (%)	Max Ro (%)	STD Dev (%)	Comments	% Vitrinite	% Inertinite	% Liptinite	% Bitumen
1	100.0	9	0.75	0.60	0.94	0.11	INDIGENOUS(+)	3.20	80.60	12.90	3.30



# MINERVA-1 Vitrinite Reflectance vs Depth



SHERGP SHIPGP OTWAYGP

● ◆ ★

Figure 10

TABLE 4

## SUMMARY OF WHOLE OIL ANALYSIS

WELL = MINERVA-1                      DEPTH 1 = 1942.50                      DEPTH UNIT = Metres  
 COUNTRY = Australia                      DEPTH 2 = 1942.50                      DATE OF JOB = Jan 94  
 BASIN = Otway

DESCRIPTION : COLD-TRAPPED COND

## COMPOSITION BY CARBON NUMBER

## COMPOSITION OF C4-C8 FRACTION

Data Type = ALL CMPDS

Carbon Number	Rel. Wt %	Compound	Rel. Wt %
1 - 3	-	isobutane (A)	0.02
4	0.28	n-butane (B)	0.26
5	3.12	isopentane (C)	0.99
6	20.06	n-pentane (D)	1.65
7	32.44	2,2-dimethylbutane (E)	0.18
8	18.26	cyclopentane (F)	0.47
9	8.47	2,3-dimethylbutane (G)	0.34
10	7.34	2-methylpentane (H)	1.89
11	3.50	3-methylpentane (I)	1.24
12	2.42	n-hexane (J)	3.29
13	1.73	methylcyclopentane (K)	3.63
14	0.81	2,4-dimethylpentane (L)	0.35
15	0.29	benzene (M)	2.26
16	0.29	cyclohexane (N)	7.24
17	0.14	1,1-dimethylcyclopentane (O)	0.58
18	0.12	2-methylhexane (P)	1.56
19	0.13	3-methylhexane (Q)	2.37
20	0.10	1 cis-3-dimethylcyclopentane (R)	0.69
21	0.04	1 trans-3-dimethylcyclopentane (S)	1.33
22	0.05	1 trans-2-dimethylcyclopentane (T)	0.14
23	-	n-heptane (U)	4.87
24	0.03	methylcyclohexane (V)	13.77
25	0.33	1 cis-2-dimethylcyclopentane (W)	0.30
26	0.01	n-toluene (X)	6.48
27	-	n-octane (Y)	5.03
28	0.01	ethylbenzene (Z)	1.13
29	0.01	M+P-xylene (AA)	3.08
30	-	O_xylene (BB)	0.84
31	-		
32	-		
33	-		

## CALCULATED DATA - C12+ FRACTION

## CALCULATED DATA - C4-C8 FRACTION

Pristane/Phytane -  
 Pristane/n-C17 -  
 Phytane/n-C18 -  
 TMTD/Pristane -  
 (C21+C22)/(C28+C29) 4.32

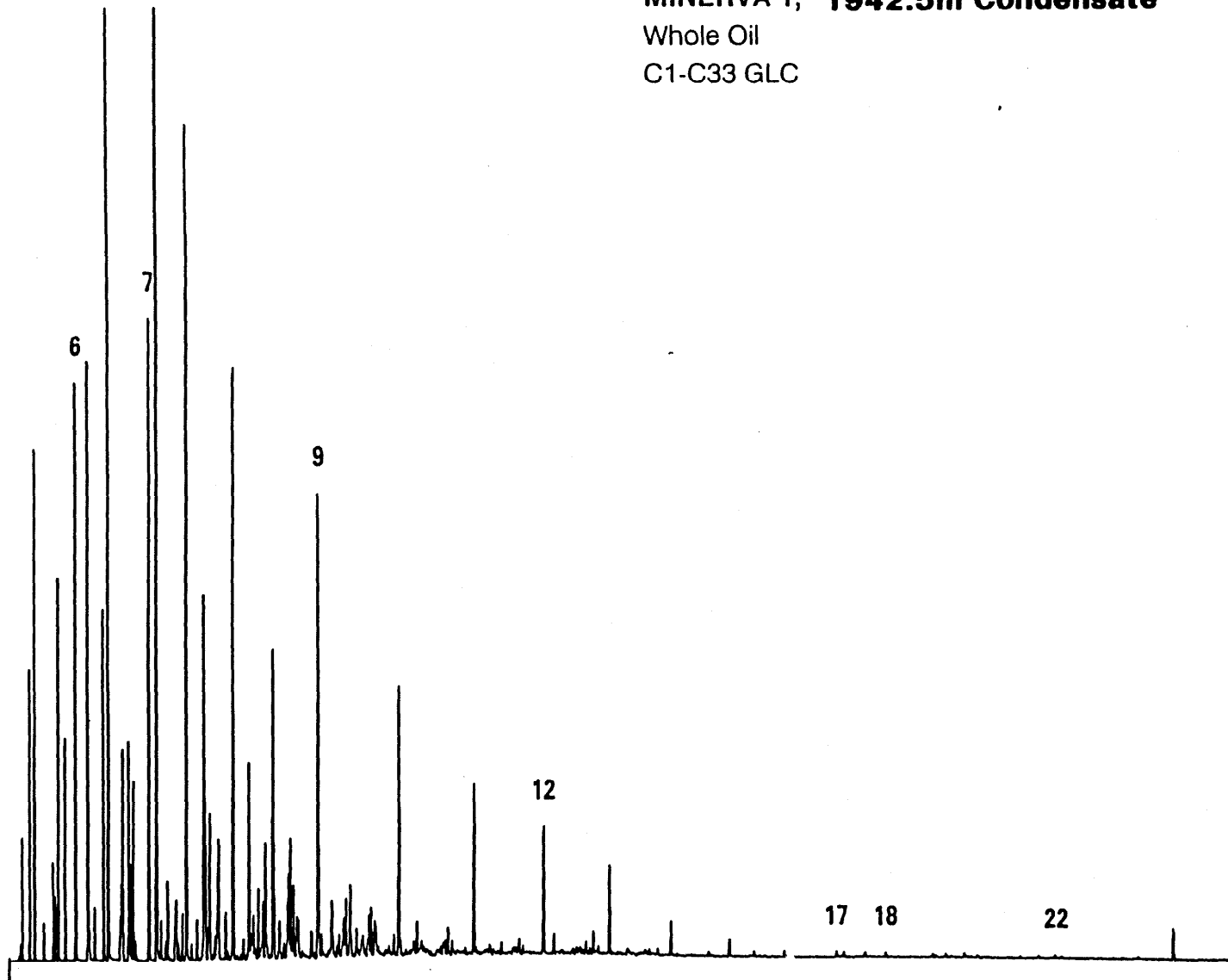
Paraffin Index I 1.82  
 Paraffin Index II 14.96  
 N/K (Maturity) 2.00  
 C/D (Maturity) 0.60  
 J/K (Maturity) 0.91  
 I/M (Water Washing) 0.55  
 I/J (Biodegradation) 0.38

TMTD = Trimethyltridecane  
 - = Below detection limit  
 or not measured

Paraffin Index I = (P+Q) / (R+S+T)  
 Paraffin Index II = %U in all compounds  
 N to V and including  
 2,2-DiMeC6 and 2,3-DiMeC5

**FIGURE 11**

**MINERVA 1, 1942.5m Condensate**  
Whole Oil  
C1-C33 GLC



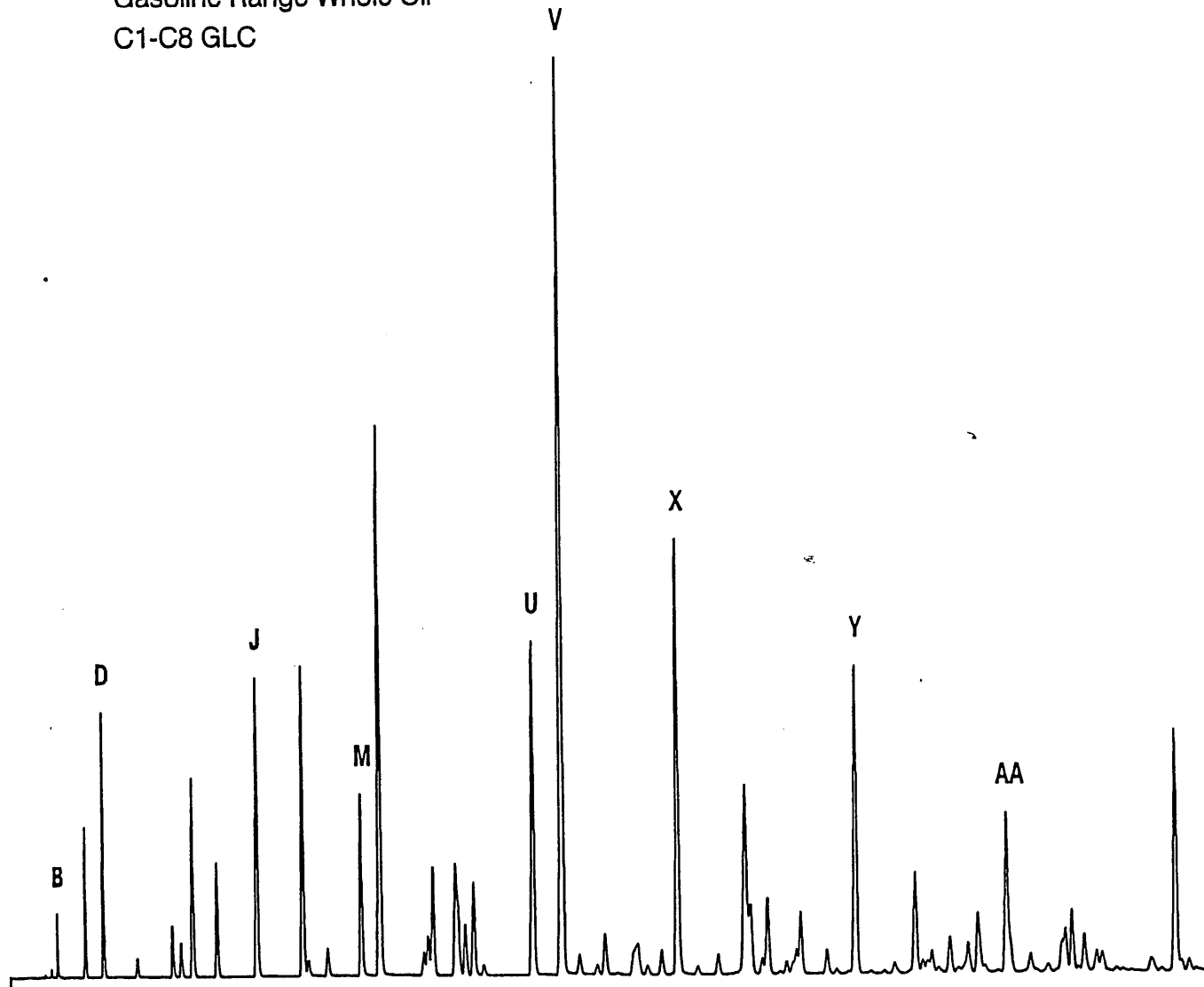
2030W01

**FIGUR 11**

FIGURE 12

**MINERVA 1, 1942.5m Condensate**  
Gasoline Range Whole Oil  
C1-C8 GLC

C4-C8 Compounds



- A isobutane
- B n-butane
- C isopentane
- D n-pentane
- E 2,2-dimethylbutane
- F cyclopentane
- G 2,3-dimethylbutane
- H 2-methylpentane
- I 3-methylpentane
- J n-hexane
- K methylcyclopentane
- L 2,4-dimethylpentane
- M benzene
- N cyclohexane
- O 1,1-dimethylcyclopentane
- P 2-methylhexane
- Q 3-methylhexane
- R 1 cis-3-dimethylcyclopentane
- S 1 trans-3-dimethylcyclopentane
- T 1 trans-2-dimethylcyclopentane
- U n-heptane
- V methylcyclohexane
- W 1 cis-2-dimethylcyclopentane
- X toluene
- Y n-octane
- Z ethylbenzene
- AA M + P-xylene
- BB O-xylene

FIGURE 12

# MINERVA-1

Whole Oil GC Data: 1942.5m Condensate  
Normalised Compound Abundances

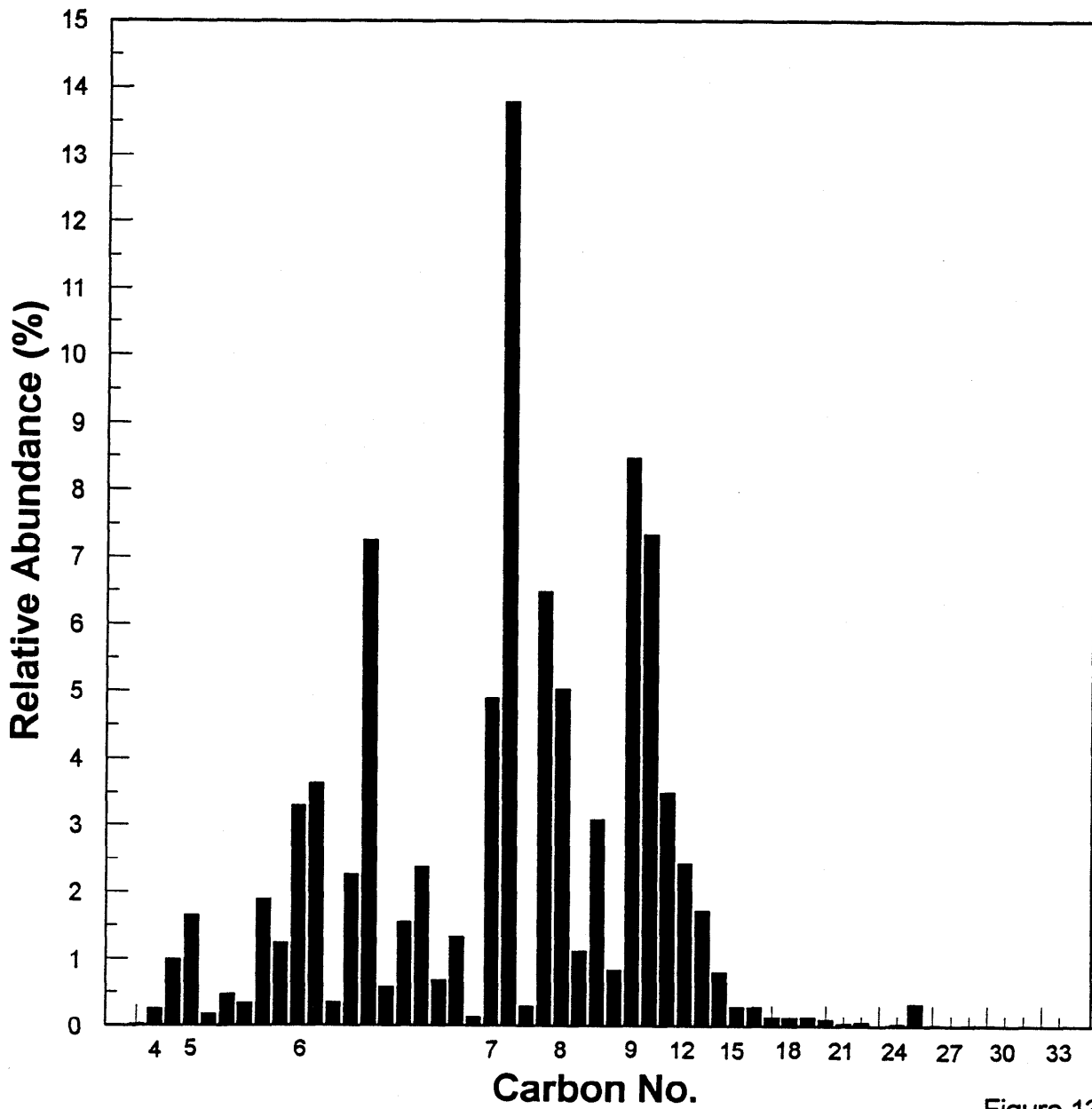


Figure 13

**MINERVA-1**  
**Whole Oil GC Data: 1942.5m Condensate**  
**Paraffin Index I vs Paraffin Index II**

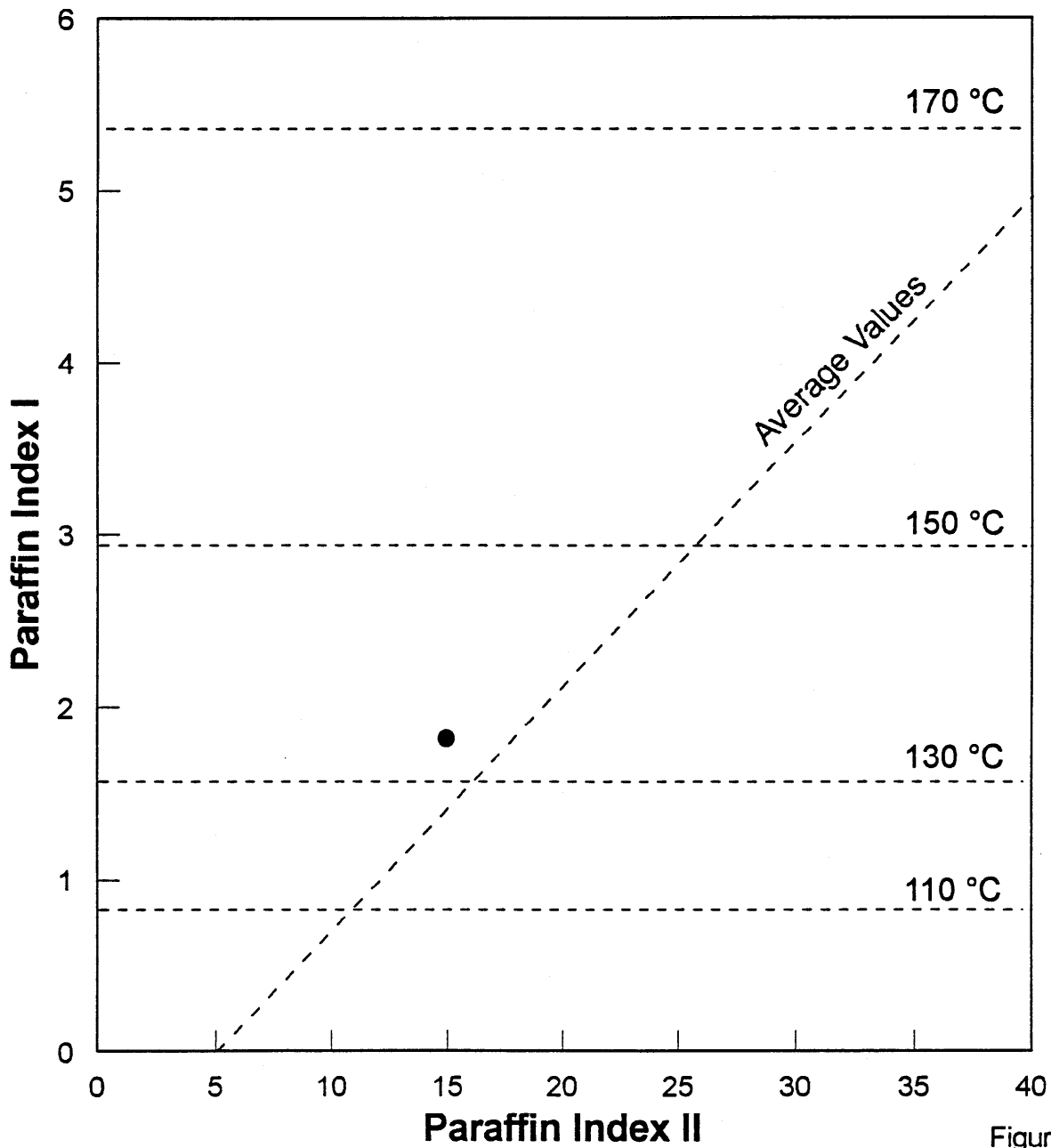
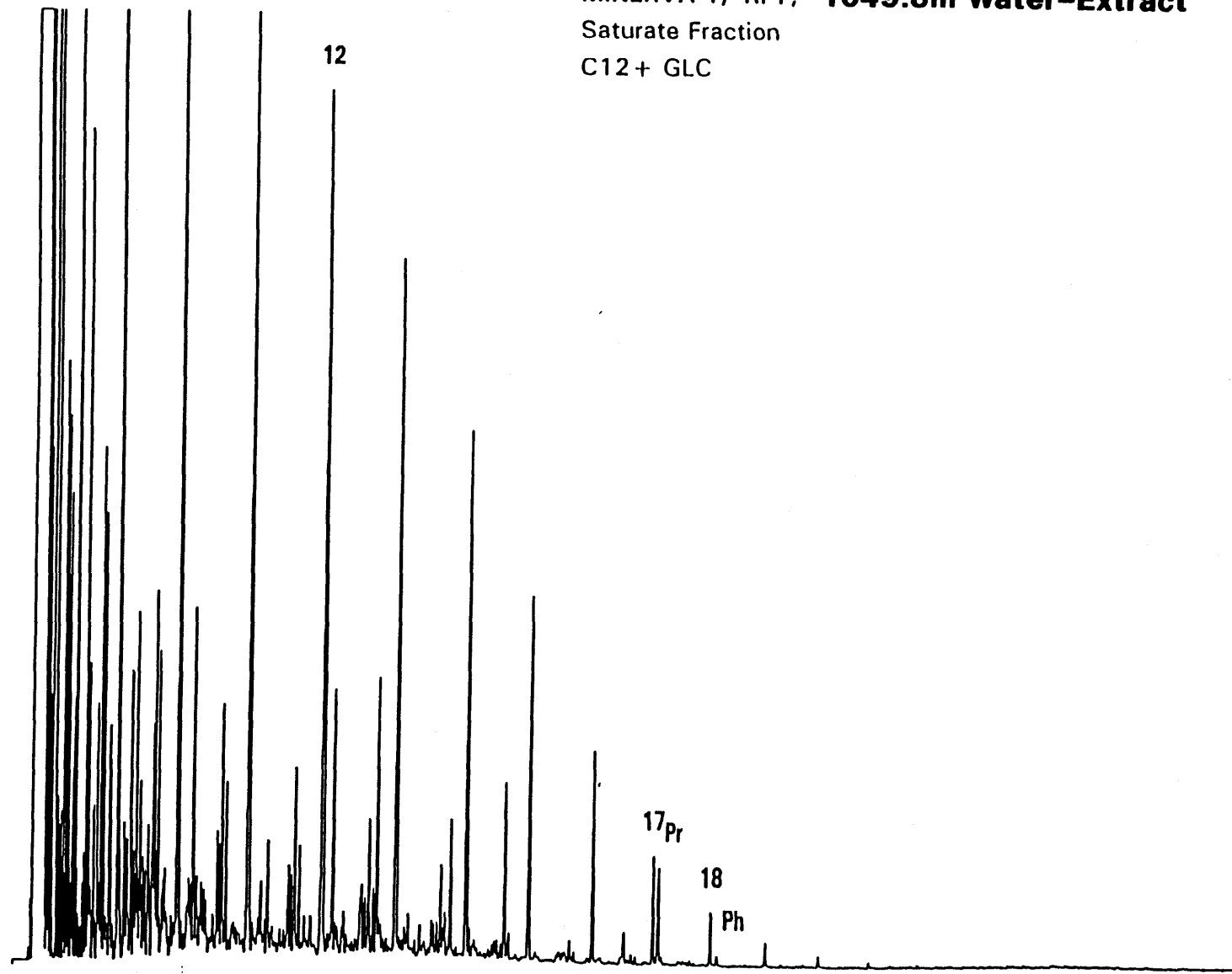


Figure 14

MINERVA 1, RFT, 1649.8m Water-Extract  
Saturate Fraction  
C12+ GLC



2030004

FIG. 15



**MINERVA 1, 1942.5m Condensate**  
Saturate Fraction  
C12+ GLC

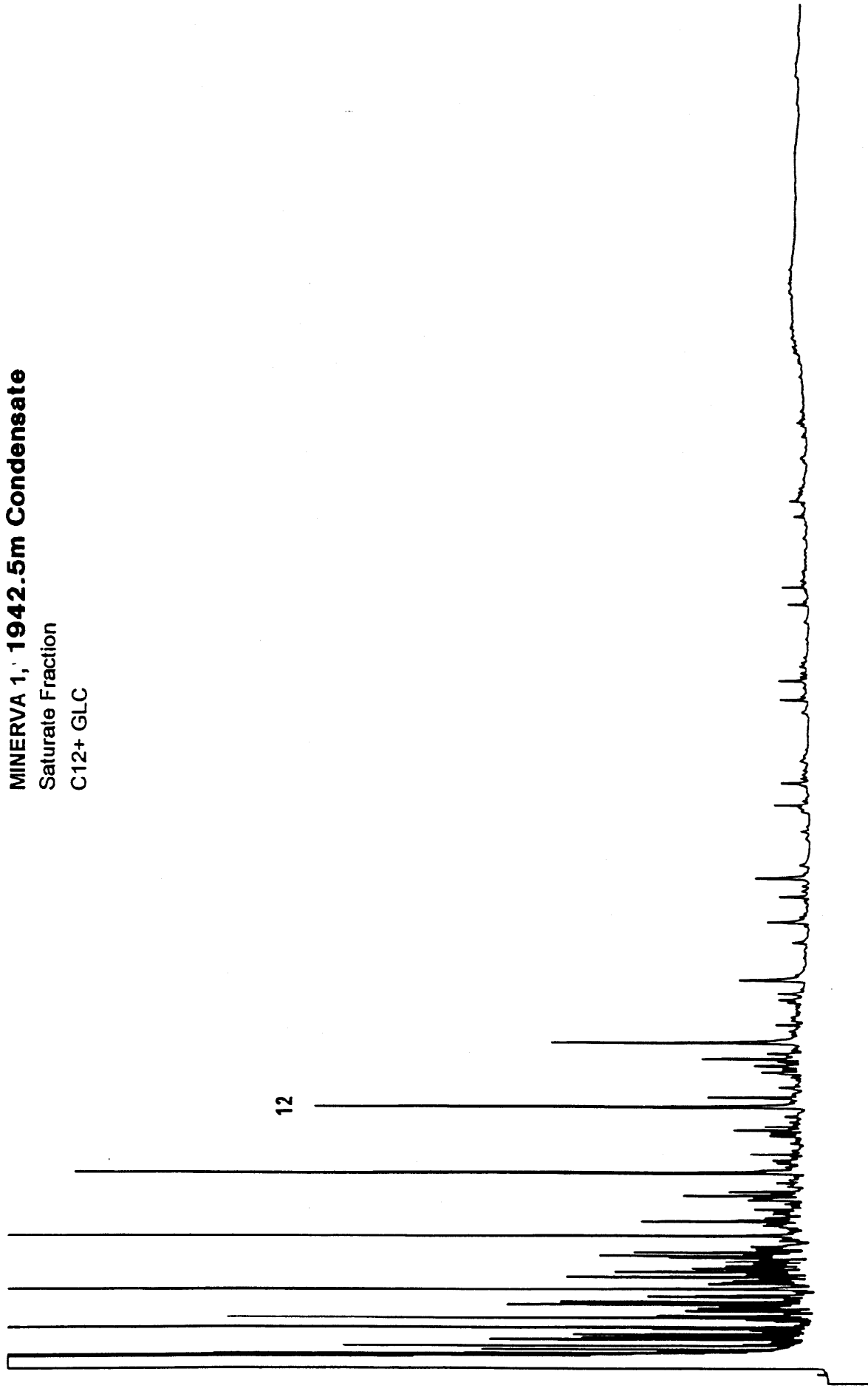


**FIGURE 16**

TABLE 5

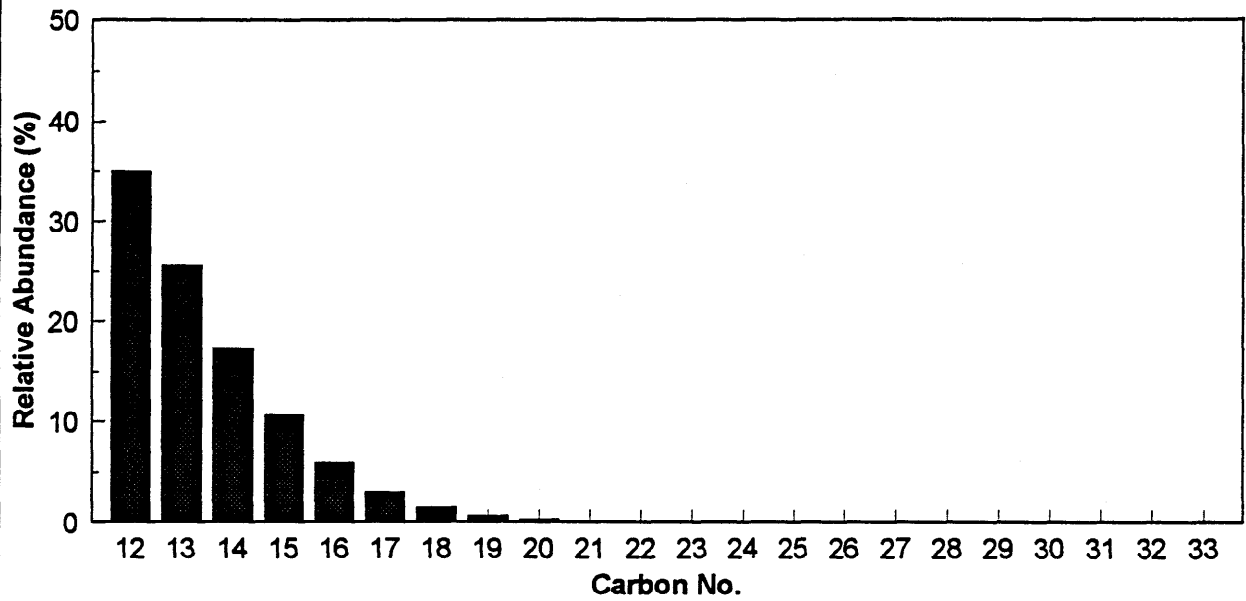
SUMMARY OF GAS CHROMATOGRAPHY DATA - CONDENSATES  
ALKANE DISTRIBUTIONS

WELL NAME = MINERVA-1															DEPTH UNIT = Metres														
COUNTRY = Australia															DATE OF JOB = Jan-Mar 94														
BASIN = Otway																													
DEPTH 1	DEPTH 2	nC12	nC13	nC14	TMTD	nC15	nC16	IC18	nC17	IC19	nC18	IC20	nC19	nC20	nC21	nC22	nC23	nC24	nC25	nC26	nC27	nC28	nC29	nC30	nC31	nC32	nC33		
1649.80	1649.80	33.5	24.5	16.5	.6	10.2	5.7	.2	2.9	3.1	1.4	.3	.7	.3	.1	0.0	0.0	0.0	0.0	0.0	0.0	0.0	0.0	0.0	0.0	0.0	0.0	0.0	0.0
1942.50	1942.50	48.8	30.4	11.8	-	6.7	2.3	-	2.9	3.1	1.4	.3	.7	.3	.1	0.0	0.0	0.0	0.0	0.0	0.0	0.0	0.0	0.0	0.0	0.0	0.0	0.0	0.0

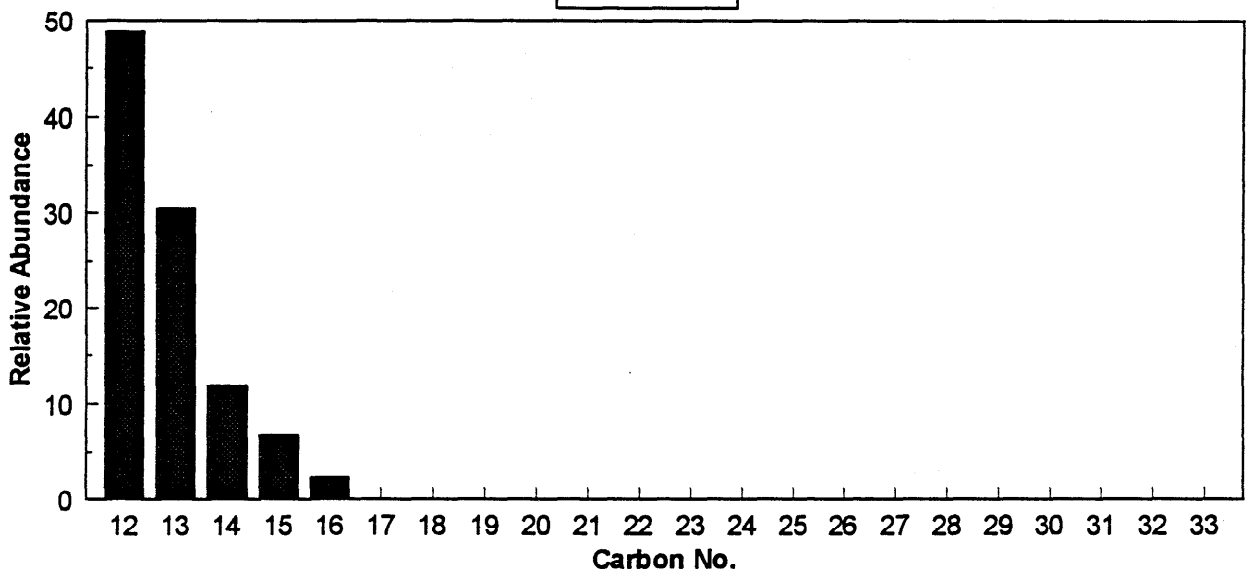
-----  
 i = iso                    n = normal                    N.B. Values are relative %  
 - = no data                TMTD = Trimethyltridecane

# MINERVA-1: Condensates

## GC (Sats): Normalised Compound Abundances



■ 1649.8m

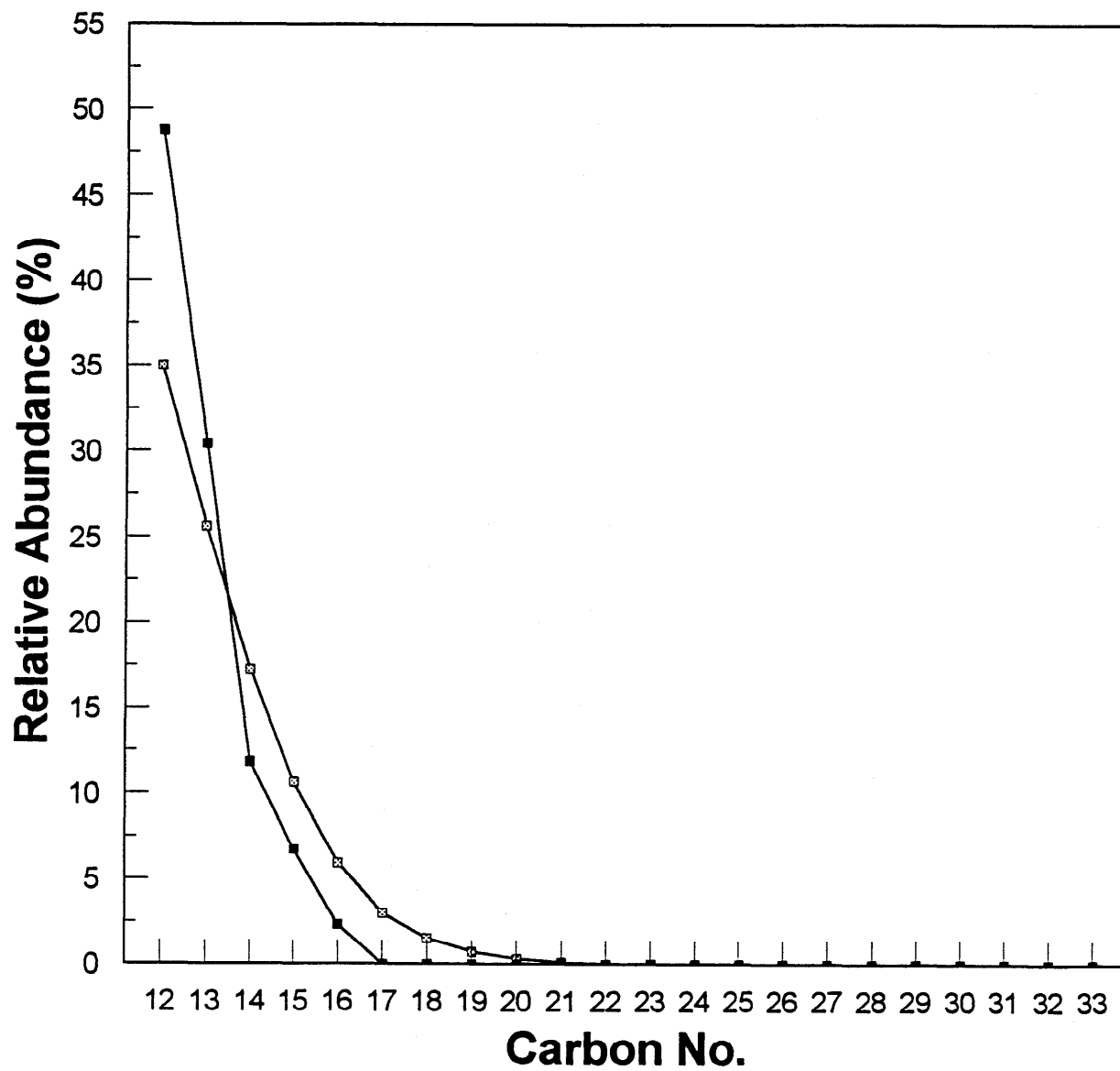


■ 1942.5m

Figure 17

# MINERVA-1: Condensates

## GC (Sats) Normalised Relative Abundances



1649.8m 1942.5m

Figure 18

TABLE 6

SUMMARY OF GAS CHROMATOGRAPHY DATA - CONDENSATES  
ALKANE COMPOSITIONAL DATA

WELL NAME	DEPTH 1	DEPTH 2	ANALYSIS TYPE	PRISTANE/PHYTANE	PRISTANE/n-C17	PHYTANE/n-C18	TMTD/PRISTANE	CPI(I)	CPI(II)	(C21+C22)/(C28+C29)
MINERVA-1										
Australia			SF	9.03	1.09	0.25	0.19	-	-	-
Otway	1649.80	1649.80	SF							
	1942.50	1942.50	SF							

DEPTH UNIT = Metres  
DATE OF JOB = Jan-Mar 94

WELL NAME = MINERVA-1  
COUNTRY = Australia  
BASIN = Otway

CPI = Carbon preference index  
SF = Saturate fraction  
TMTD = Trimethyltridecane  
WE = Whole extract

**MINERVA-1: 1649.8m Water-Extract  
Pristane/n-C17 vs Phytane/n-C18**

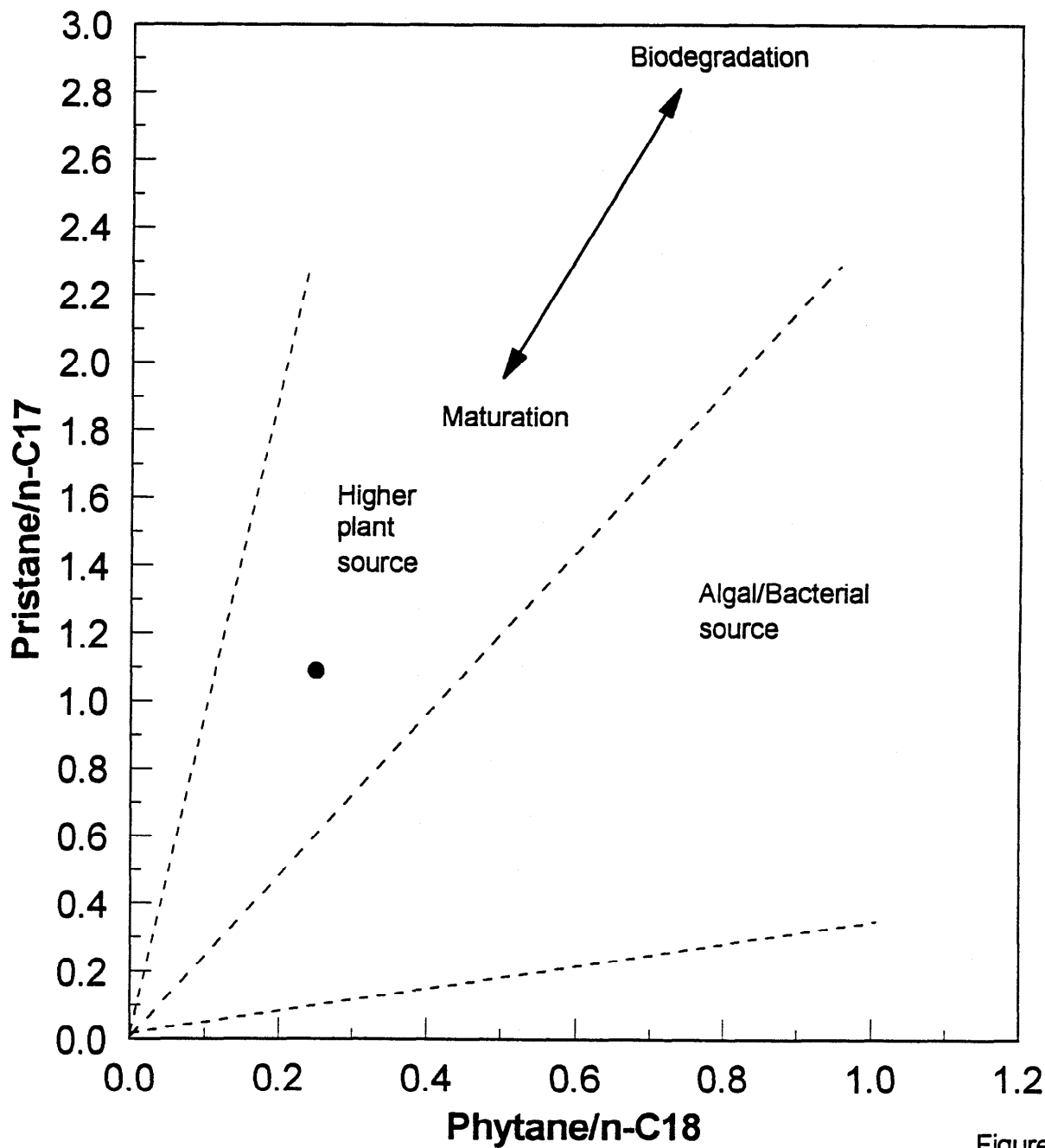
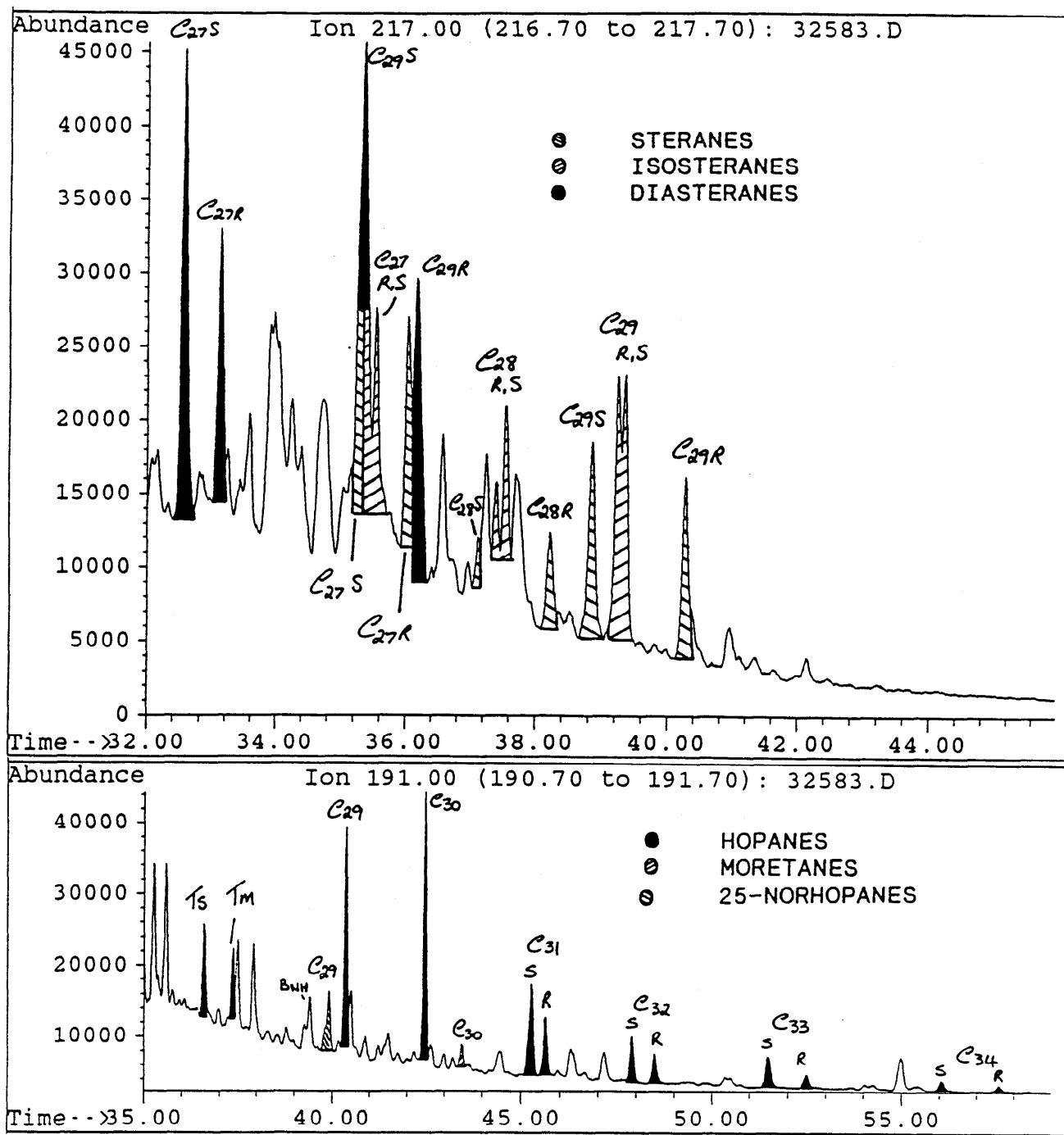


Figure 19

**m/z 217 and m/z 191 BIOMARKER TRACES: 1649.8m Water-Extract**



**FIGURE 20**

**m/z 217 and m/z 191 BIOMARKER TRACES: 1942.5m Condensate**

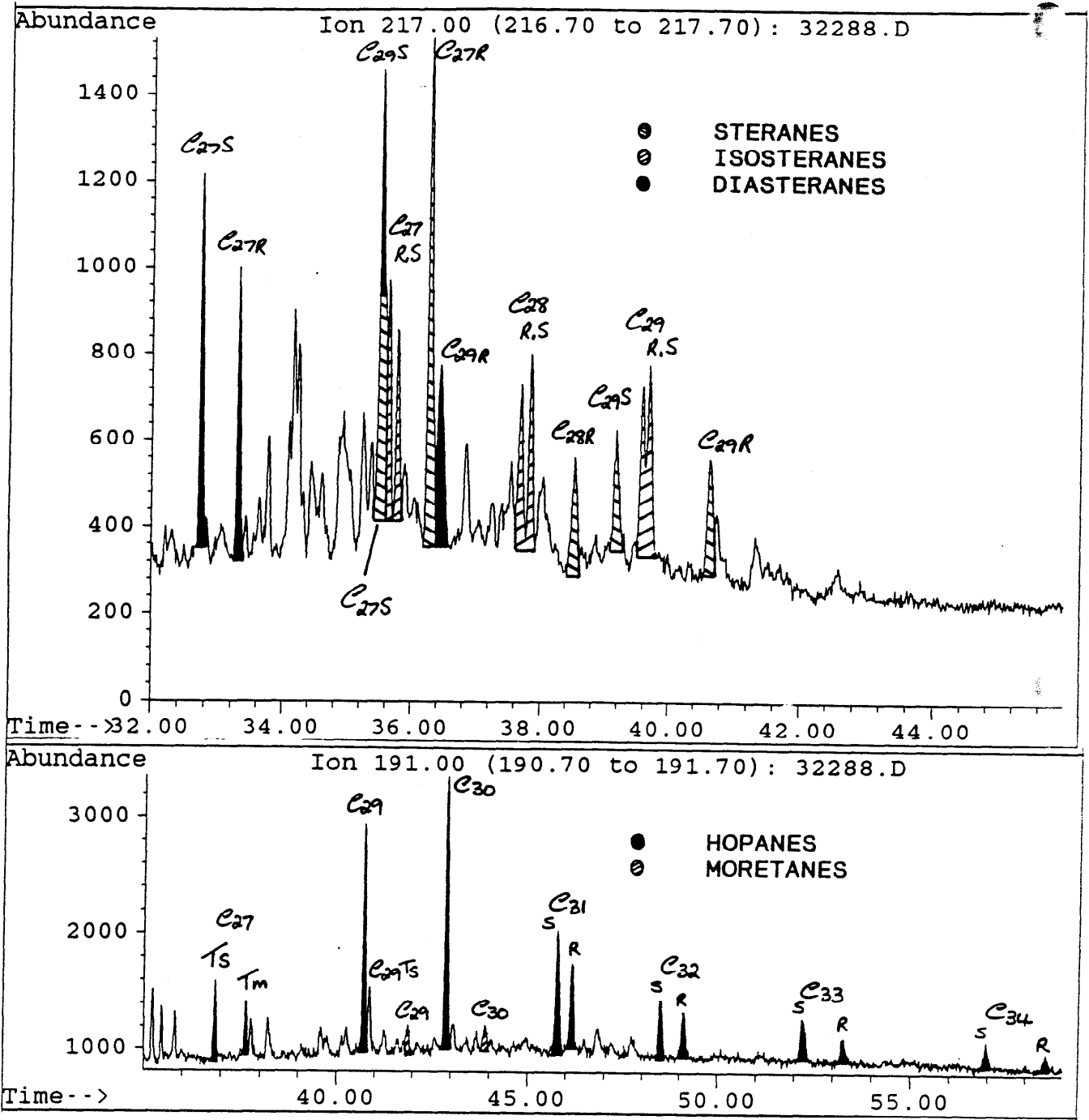


**FIGURE 21**



TABLE 7-1

SATURATE FRACTION SIR GC/MS DATA - WATER-EXTRACT			DETAILED COMPOUND ANALYSIS		
WELL = MINERVA-1	DESCRIPTION : COLD-TRAPPED COND			DEPTH UNIT = Metres	DATE OF JOB = Jan-Mar 94
COUNTRY = Australia	DEPTH 1 = 1649.80	DEPTH 2 = 1649.80			
BASIN = Otway					
COMPOUND	ION	RELATIVE AMOUNT	COMPOUND	ION	RELATIVE AMOUNT
C23 Tricyclic	191	1800.0	C24 Tricyclic	191	1224.0
C25 Tricyclic	191	753.0	C26 Tricyclic	191	900.0
C28 Tricyclic	191	1001.0	C29 Tricyclic	191	851.0
C24 Tetracyclic	191	883.0			
C27 Hopane (Ts)	191	12796.0	C27 Hopane (Tm)	191	8083.0
C27 Hopane (17B)	191	-			
C28 Hopane (25,30)	191	-	C28 Hopane (28,30)	191	7312.0
C29 Hopane	191	30252.0	C29 Moretane	191	-
C29 Demeth. Hopane	191	8666.0	C29 Hopane (BB)	191	-
C30 Hopane	191	37026.0	C30 Moretane	191	3111.0
C30 Hopane (BB)	191	-			
C31S Hopane	191	13074.0	C31R Hopane	191	8435.0
C31S+R Hopane (BB)	191	-	C31S+R Moretane	191	-
C32S Hopane	191	6639.0	C32R Hopane	191	4388.0
C32S+R Hopane (BB)	191	-	C32S+R Moretane	191	-
C33S Hopane	191	-	C33R Hopane	191	-
Gammacerane	191	-	Oleanane (18a)	191	-
Unknown 1	191	-	Unknown 2	191	-
Unknown 3	191	9266.0	Unknown 4	191	-
C27 Demeth. Hopane	177	-	C28 Demeth. Hopane	177	-
C29 Hopane	177	-	C29 Demeth. Hopane	177	-
C29 Moretane	177	-	C29 Hopane (BB)	177	-
Unknown 3	177	-			
C30 2-Methylhopane	205	-	C31 2-Methylhopane	205	-
C31S Hopane	205	-	C31R Hopane	205	-
C31S+R Moretane	205	-	C31S+R Hopane (BB)	205	-
C21 Sterane	217	-	C22 Sterane	217	-
C27S Normal Sterane	217	-	C27R Normal Sterane	217	15990.0
C27S Isosterane	217	-	C27R Isosterane	217	-
C27S Diasterane	217	-	C27R Diasterane	217	-
C28S Normal Sterane	217	3414.0	C28R Normal Sterane	217	6040.0
C28S Isosterane	217	-	C28R Isosterane	217	-
C28S Diasterane	217	-	C28R Diasterane	217	-
C29S Normal Sterane	217	13448.0	C29R Normal Sterane	217	12871.0
C29S Isosterane	217	18468.0	C29R Isosterane	217	16934.0
C29S Diasterane	217	28947.0	C29R Diasterane	217	20737.0
C27S+R Isosterane	218	51483.0	C28S+R Isosterane	218	23661.0
C29S+R Isosterane	218	57201.0			
C27S Diasterane	259	14133.0	C27R Diasterane	259	9629.0
C28S Diasterane	259	13072.0	C28R Diasterane	259	9524.0
C29S Diasterane	259	13907.0	C29R Diasterane	259	10382.0
16a Phyllocladane	123	-	16B Phyllocladane	123	-
Beyerene	123	-	Labdane	123	-
Fichtelite	123	-	Rimuanene	123	-
Nortetracyclane	123	-	Pimerane	123	-
Isopimerane	123	-	Kaurane	123	-
Norisopimerane	123	-	Unknown 1	123	-
Drimane	123	7588.0	Homodrimane	123	4500.0
Rearranged Drimane 1	123	12882.0	Rearranged Drimane 2	123	5880.0
Eudesmane	123	-			
C15 Alkylcyclohexane	83	-	C17 Alkylcyclohexane	83	-
C21 Alkylcyclohexane	83	-	C22 Alkylcyclohexane	83	-
C25 Alkylcyclohexane	83	-	C29 Alkylcyclohexane	83	-

- = no data IUPAC names corresponding to common names used here are shown at the end of the tables

## SATURATE FRACTION SIR GC/MS DATA - WATER EXTRACT

## CALCULATED DATA

DESCRIPTION : COLD-TRAPPED COND

WELL = MINERVA-1                      DEPTH 1(m) = 1649.80                      DEPTH UNIT = Metres  
 COUNTRY = Australia                      DEPTH 2(m) = 1649.80                      DATE OF JOB = Jan-Mar 94  
 BASIN = Otway

## ----- TERPANE PARAMETERS -----

PARAMETER	ION(s)	VALUE
% Ts / (Ts + Tm)	191	61.29
% C29 M / (C29 H + C29 M)	191	-
% C30 M / (C30 H + C30 M)	191	7.75
% C31S H / (C31S H + C31R H)	191	60.78
% C31S H / (C31S H + C31R H)	205	-
% C32S H / (C32S H + C32R H)	191	60.21
% U1-U4 / (U1-U4 + C30 H)	191	-
% U1 / (U1 + C30 H)	191	-
% U2 / (U2 + C30 H)	191	-
% U3 / (U3 + C30 H)	191	20.02
% U4 / (U4 + C30 H)	191	-
% C29 H / (C29 H + C30 H)	191	44.97
% C31 2-MeH / (C31 2-MeH + C30 H)	191, 205	-
% C29 BB / (C29 BB + C 29H + C29 M)	191	-
% C29 DeMe / (C29 DeMe + C29H)	177	-
% C28 H's / (C28 H's + C30 H)	191	-
% (Ts + Tm + C28 H's) / C29(H + M) + C30(H + M)	191	-
% Oleanane (18a) / (Oleanane + C30H)	191	-
% Drimane / Homodrimane	123	168.62
% Rea. Drimanes / (Drimane + Homodrimane)	123	155.21
% C22 Alkycyclohex. / C30 H	83, 191	-
% C29 Alkycyclohex. / C30 H	83, 191	-
% C23-C29 Tricyclics / C30 H	191	17.63
% (C30 H + C30 M) / (C29(NS's + IS's + DS's)	191, 217	36.03

## ----- STERANE PARAMETERS -----

PARAMETER	ION(s)	VALUE
% C27 ST's / (C27 + C28 + C29) ST's	217	-
% C28 ST's / (C27 + C28 + C29) ST's	217	-
% C29 ST's / (C27 + C28 + C29) ST's	217	-
% C27S NS / (C27S NS + C27R NS)	217	-
% C28S NS / (C28S NS + C28R NS)	217	36.11
% C29S NS / (C29S NS + C29R NS)	217	51.10
% C27 NS's / C29 NS's	217	-
% C27 IS's / C29 IS's	217	-
% C27 DS's / C29 DS's	217	-
% C27 DS's / C27 ST's	217	-
% C28 DS's / C28 ST's	217	-
% C29 DS's / C29 ST's	217	44.60
% C27 IS's / (C27 IS's + C27 NS's)	217	-
% C28 IS's / (C28 IS's + C28 NS's)	217	-
% C29 IS's / (C29 IS's + C29 NS's)	217	57.36

NOTES : H = Hopane                      M = Moretane                      Me = Methyl                      NS = Normal Sterane  
 IS = Iso Sterane                      DS = Dia Sterane                      ST = NS + IS + DS                      U = Unknown  
 - = no data available

TABLE 8-1

WELL = MINERVA-1		SATURATE FRACTION SIR GC/MS DATA - CONDENSATE			DEPTH UNIT = Metres	
COUNTRY = Australia		DETAILED COMPOUND ANALYSIS			DATE OF JOB = Jan-Mar 94	
BASIN = Otway		DEPTH 1 = 1942.50		DEPTH 2 = 1942.50		
COMPOUND	ION	RELATIVE AMOUNT	COMPOUND	ION	RELATIVE AMOUNT	
C23 Tricyclic	191	-	C24 Tricyclic	191	-	
C25 Tricyclic	191	-	C26 Tricyclic	191	-	
C28 Tricyclic	191	-	C29 Tricyclic	191	-	
C24 Tetracyclic	191	-				
C27 Hopane (Ts)	191	-	C27 Hopane (Tm)	191	-	
C27 Hopane (17B)	191	-				
C28 Hopane (25.30)	191	-	C28 Hopane (28.30)	191	-	
C29 Hopane	191	-	C29 Moretane	191	-	
C29 Demeth. Hopane	191	-	C29 Hopane (BB)	191	-	
C30 Hopane	191	-	C30 Moretane	191	-	
C30 Hopane (BB)	191	-				
C31S Hopane	191	-	C31R Hopane	191	-	
C31S+R Hopane (BB)	191	-	C31S+R Moretane	191	-	
C32S Hopane	191	-	C32R Hopane	191	-	
C32S+R Hopane (BB)	191	-	C32S+R Moretane	191	-	
C33S Hopane	191	-	C33R Hopane	191	-	
Gammacerane	191	-	Oleanane (18a)	191	-	
Unknown 1	191	-	Unknown 2	191	-	
Unknown 3	191	-	Unknown 4	191	-	
C27 Demeth. Hopane	177	-	C28 Demeth. Hopane	177	-	
C29 Hopane	177	-	C29 Demeth. Hopane	177	-	
C29 Moretane	177	-	C29 Hopane (BB)	177	-	
Unknown 3	177	-				
C30 2-Methylhopane	205	-	C31 2-Methylhopane	205	-	
C31S Hopane	205	-	C31R Hopane	205	-	
C31S+R Moretane	205	-	C31S+R Hopane (BB)	205	-	
C21 Sterane	217	-	C22 Sterane	217	-	
C27S Normal Sterane	217	-	C27R Normal Sterane	217	-	
C27S Isosterane	217	-	C27R Isosterane	217	-	
C27S Diasterane	217	-	C27R Diasterane	217	-	
C28S Normal Sterane	217	-	C28R Normal Sterane	217	-	
C28S Isosterane	217	-	C28R Isosterane	217	-	
C28S Diasterane	217	-	C28R Diasterane	217	-	
C29S Normal Sterane	217	-	C29R Normal Sterane	217	-	
C29S Isosterane	217	-	C29R Isosterane	217	-	
C29S Diasterane	217	-	C29R Diasterane	217	-	
C27S+R Isosterane	218	-	C28S+R Isosterane	218	-	
C29S+R Isosterane	218	-				
C27S Diasterane	259	-	C27R Diasterane	259	-	
C28S Diasterane	259	-	C28R Diasterane	259	-	
C29S Diasterane	259	-	C29R Diasterane	259	-	
16a Phyllocladane	123	-	16B Phyllocladane	123	-	
Beyerene	123	-	Labdane	123	-	
Fichtelite	123	-	Rimuanane	123	-	
Nortetracyclane	123	-	Pimerane	123	-	
Isopimerane	123	-	Kaurane	123	-	
Norisopimerane	123	-	Unknown 1	123	-	
Drimane	123	7537.0	Homodrimane	123	3614.6	
Rearranged Drimane 1	123	14403.0	Rearranged Drimane 2	123	6942.0	
Eudesmane	123	-				
C15 Alkylcyclohexane	83	-	C17 Alkylcyclohexane	83	-	
C21 Alkylcyclohexane	83	-	C22 Alkylcyclohexane	83	-	
C25 Alkylcyclohexane	83	-	C29 Alkylcyclohexane	83	-	

- = no data IUPAC names corresponding to common names used here are shown at the end of the tables

## SATURATE FRACTION SIR GC/MS DATA - CONDENSATE

## CALCULATED DATA

DESCRIPTION : COLD-TRAPPED COND

WELL - MINERVA-1                      DEPTH 1(m) - 1942.50                      DEPTH UNIT - Metres  
 COUNTRY - Australia                      DEPTH 2(m) - 1942.50                      DATE OF JOB - Jan-Mar 94  
 BASIN - Otway

## ----- TERPANE PARAMETERS -----

PARAMETER	ION(s)	VALUE
* Ts / (Ts + Tm)	191	-
* C29 M / (C29 H + C29 M)	191	-
* C30 M / (C30 H + C30 M)	191	-
* C31S H / (C31S H + C31R H)	191	-
* C31S H / (C31S H + C31R H)	205	-
* C32S H / (C32S H + C32R H)	191	-
* U1-U4 / (U1-U4 + C30 H)	191	-
* U1 / (U1 + C30 H)	191	-
* U2 / (U2 + C30 H)	191	-
* U3 / (U3 + C30 H)	191	-
* U4 / (U4 + C30 H)	191	-
* C29 H / (C29 H + C30 H)	191	-
* C31 2-MeH / (C31 2-MeH + C30 H)	191, 205	-
* C29 BB / (C29 BB + C 29H + C29 M)	191	-
* C29 DeMe / (C29 DeMe + C29H)	177	-
* C28 H's / (C28 H's + C30 H)	191	-
* (Ts + Tm + C28 H's) / C29(H + M) + C30(H + M)	191	-
* Oleanane (18a) / (Oleanane + C30H)	191	-
* Drimane / Homodrimane	123	208.51
* Rea. Drimanes / (Drimane + Homodrimane)	123	191.41
* C22 Alkycyclohex. / C30 H	83, 191	-
* C29 Alkycyclohex. / C30 H	83, 191	-
* C23-C29 Tricyclics / C30 H	191	-
* (C30 H + C30 M) / (C29(NS's + IS's + DS's))	191, 217	-

## ----- STERANE PARAMETERS -----

PARAMETER	ION(s)	VALUE
* C27 ST's / (C27 + C28 + C29) ST's	217	-
* C28 ST's / (C27 + C28 + C29) ST's	217	-
* C29 ST's / (C27 + C28 + C29) ST's	217	-
* C27S NS / (C27S NS + C27R NS)	217	-
* C28S NS / (C28S NS + C28R NS)	217	-
* C29S NS / (C29S NS + C29R NS)	217	-
* C27 NS's / C29 NS's	217	-
* C27 IS's / C29 IS's	217	-
* C27 DS's / C29 DS's	217	-
* C27 DS's / C27 ST's	217	-
* C28 DS's / C28 ST's	217	-
* C29 DS's / C29 ST's	217	-
* C27 IS's / (C27 IS's + C27 NS's)	217	-
* C28 IS's / (C28 IS's + C28 NS's)	217	-
* C29 IS's / (C29 IS's + C29 NS's)	217	-

NOTES : H = Hopane                      M = Moretane                      Me = Methyl                      NS = Normal Sterane  
 IS = Iso Sterane                      DS = Dia Sterane                      ST = NS + IS + DS                      U = Unknown  
 - = no data available

TABLE 9-1

SATURATE FRACTION SIR GC/MS DATA - CONDENSATE			DETAILED COMPOUND ANALYSIS		
WELL = MINERVA-1					
COUNTRY = Australia					DEPTH UNIT = Metres
BASIN = Otway					DATE OF JOB = Jan-Mar 94
	DEPTH 1 = 1942.50		DEPTH 2 = 1942.50		
COMPOUND	ION	RELATIVE AMOUNT	COMPOUND	ION	RELATIVE AMOUNT
C23 Tricyclic	191	-	C24 Tricyclic	191	-
C25 Tricyclic	191	-	C26 Tricyclic	191	-
C28 Tricyclic	191	-	C29 Tricyclic	191	-
C24 Tetracyclic	191	-			
C27 Hopane (Ts)	191	709.0	C27 Hopane (Tm)	191	511.0
C27 Hopane (17B)	191	-			
C28 Hopane (25,30)	191	-	C28 Hopane (28,30)	191	-
C29 Hopane	191	1979.0	C29 Moretane	191	267.3
C29 Demeth. Hopane	191	-	C29 Hopane (BB)	191	-
C30 Hopane	191	2299.0	C30 Moretane	191	229.1
C30 Hopane (BB)	191	-			
C31S Hopane	191	1078.0	C31R Hopane	191	711.0
C31S+R Hopane (BB)	191	-	C31S+R Moretane	191	-
C32S Hopane	191	537.0	C32R Hopane	191	350.0
C32S+R Hopane (BB)	191	-	C32S+R Moretane	191	-
C33S Hopane	191	-	C33R Hopane	191	-
Gammacerane	191	-	Oleanane (18a)	191	-
Unknown 1	191	-	Unknown 2	191	-
Unknown 3	191	559.0	Unknown 4	191	-
C27 Demeth. Hopane	177	-	C28 Demeth. Hopane	177	-
C29 Hopane	177	-	C29 Demeth. Hopane	177	-
C29 Moretane	177	-	C29 Hopane (BB)	177	-
Unknown 3	177	-			
C30 2-Methylhopane	205	-	C31 2-Methylhopane	205	-
C31S Hopane	205	-	C31R Hopane	205	-
C31S+R Moretane	205	-	C31S+R Hopane (BB)	205	-
C21 Sterane	217	-	C22 Sterane	217	-
C27S Normal Sterane	217	-	C27R Normal Sterane	217	1173.0
C27S Isosterane	217	-	C27R Isosterane	217	-
C27S Diasterane	217	-	C27R Diasterane	217	-
C28S Normal Sterane	217	-	C28R Normal Sterane	217	279.0
C28S Isosterane	217	-	C28R Isosterane	217	-
C28S Diasterane	217	-	C28R Diasterane	217	-
C29S Normal Sterane	217	283.0	C29R Normal Sterane	217	270.0
C29S Isosterane	217	447.0	C29R Isosterane	217	396.0
C29S Diasterane	217	1039.0	C29R Diasterane	217	422.0
C27S+R Isosterane	218	1754.0	C28S+R Isosterane	218	1182.0
C29S+R Isosterane	218	1424.0			
C27S Diasterane	259	514.0	C27R Diasterane	259	339.0
C28S Diasterane	259	584.0	C28R Diasterane	259	315.7
C29S Diasterane	259	257.0	C29R Diasterane	259	219.2
16a Phyllocladane	123	-	16B Phyllocladane	123	-
Beyerene	123	-	Labdane	123	-
Fichtelite	123	-	Rimuane	123	-
Nortetracyclane	123	-	Pimerane	123	-
Isopimerane	123	-	Kaurane	123	-
Norisopimerane	123	-	Unknown 1	123	-
Drimane	123	-	Homodrimane	123	-
Rearranged Drimane 1	123	-	Rearranged Drimane 2	123	-
Eudesmane	123	-			
C15 Alkylcyclohexane	83	-	C17 Alkylcyclohexane	83	-
C21 Alkylcyclohexane	83	-	C22 Alkylcyclohexane	83	-
C25 Alkylcyclohexane	83	-	C29 Alkylcyclohexane	83	-

- - no data IUPAC names corresponding to common names used here are shown at the end of the tables

## SATURATE FRACTION SIR GC/MS DATA - CONDENSATE

## CALCULATED DATA

DESCRIPTION : TOPPED

WELL = MINERVA-1      DEPTH 1(m) = 1942.50      DEPTH UNIT = Metres  
 COUNTRY = Australia      DEPTH 2(m) = 1942.50      DATE OF JOB = Jan-Mar 94  
 BASIN = Otway

## ----- TERPANE PARAMETERS -----

PARAMETER	ION(s)	VALUE
* Ts / (Ts + Tm)	191	58.11
* C29 M / (C29 H + C29 M)	191	11.90
* C30 M / (C30 H + C30 M)	191	9.06
* C31S H / (C31S H + C31R H)	191	60.26
* C31S H / (C31S H + C31R H)	205	-
* C32S H / (C32S H + C32R H)	191	60.54
* U1-U4 / (U1-U4 + C30 H)	191	-
* U1 / (U1 + C30 H)	191	-
* U2 / (U2 + C30 H)	191	-
* U3 / (U3 + C30 H)	191	19.56
* U4 / (U4 + C30 H)	191	-
* C29 H / (C29 H + C30 H)	191	46.26
* C31 2-MeH / (C31 2-MeH + C30 H)	191, 205	-
* C29 BB / (C29 BB + C 29H + C29 M)	191	-
* C29 DeMe / (C29 DeMe + C29H)	177	-
* C28 H's / (C28 H's + C30 H)	191	-
* (Ts + Tm + C28 H's) / C29(H + M) + C30(H + M)	191	-
* Oleanane (18a) / (Oleanane + C30H)	191	-
* Drimane / Homodrimane	123	-
* Rea. Drimanes / (Drimane + Homodrimane)	123	-
* C22 Alkycyclohex. / C30 H	83, 191	-
* C29 Alkycyclohex. / C30 H	83, 191	-
* C23-C29 Tricyclics / C30 H	191	-
* (C30 H + C30 M) / (C29(NS's + IS's + DS's))	191, 217	88.49

## ----- STERANE PARAMETERS -----

PARAMETER	ION(s)	VALUE
* C27 ST's / (C27 + C28 + C29) ST's	217	-
* C28 ST's / (C27 + C28 + C29) ST's	217	-
* C29 ST's / (C27 + C28 + C29) ST's	217	-
* C27S NS / (C27S NS + C27R NS)	217	-
* C28S NS / (C28S NS + C28R NS)	217	-
* C29S NS / (C29S NS + C29R NS)	217	51.18
* C27 NS's / C29 NS's	217	-
* C27 IS's / C29 IS's	217	-
* C27 DS's / C29 DS's	217	-
* C27 DS's / C27 ST's	217	-
* C28 DS's / C28 ST's	217	-
* C29 DS's / C29 ST's	217	51.14
* C27 IS's / (C27 IS's + C27 NS's)	217	-
* C28 IS's / (C28 IS's + C28 NS's)	217	-
* C29 IS's / (C29 IS's + C29 NS's)	217	60.39

NOTES : H = Hopane      M = Moretane      Me = Methyl      NS = Normal Sterane  
 IS = Iso Sterane      DS = Dia Sterane      ST = NS + IS + DS      U = Unknown  
 - = no data available

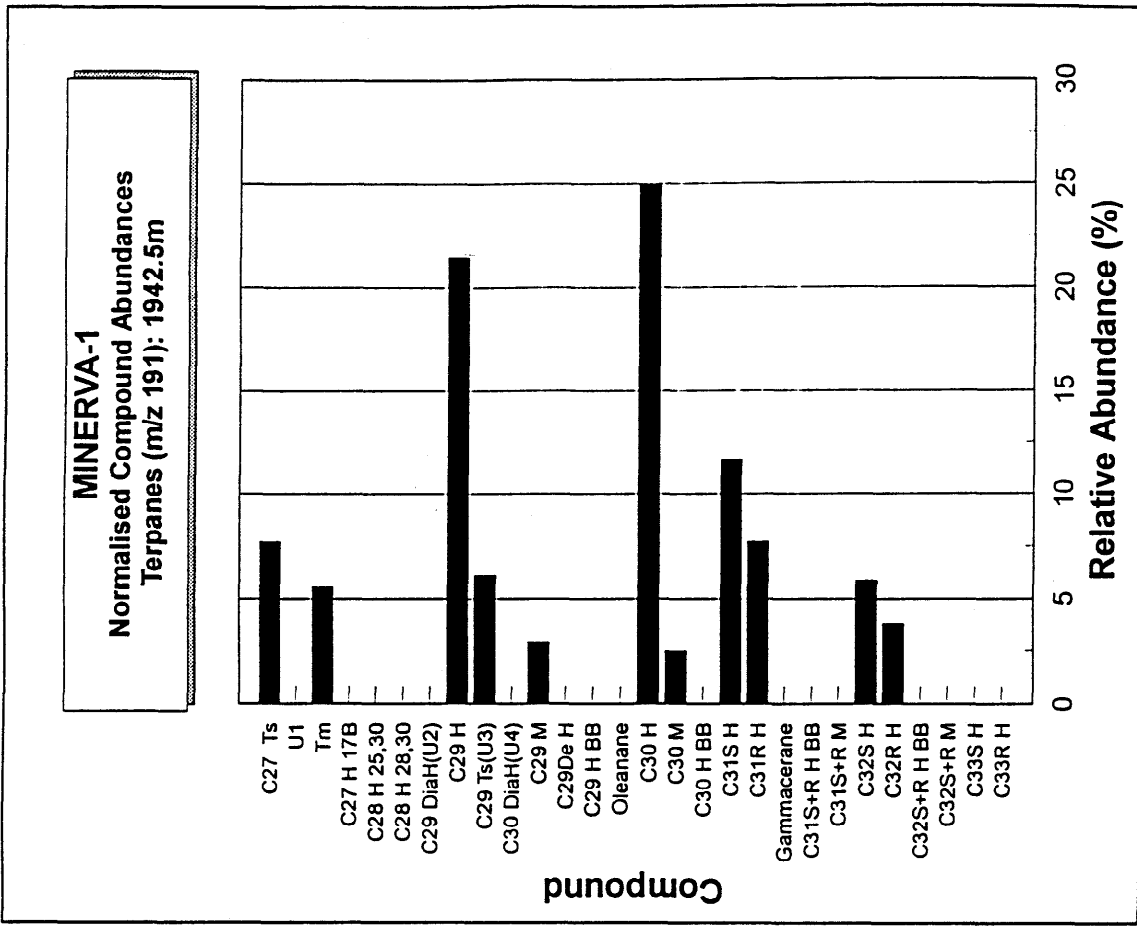
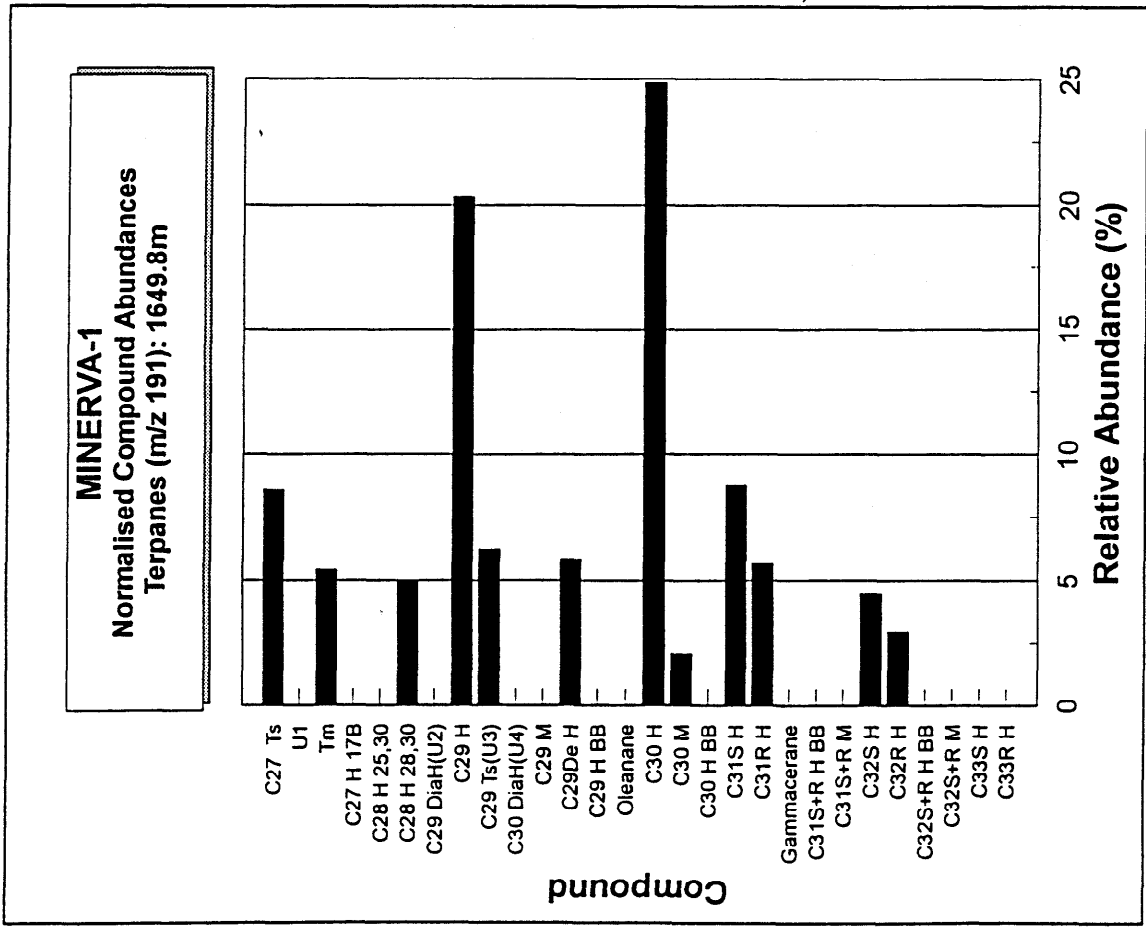


Figure 22a

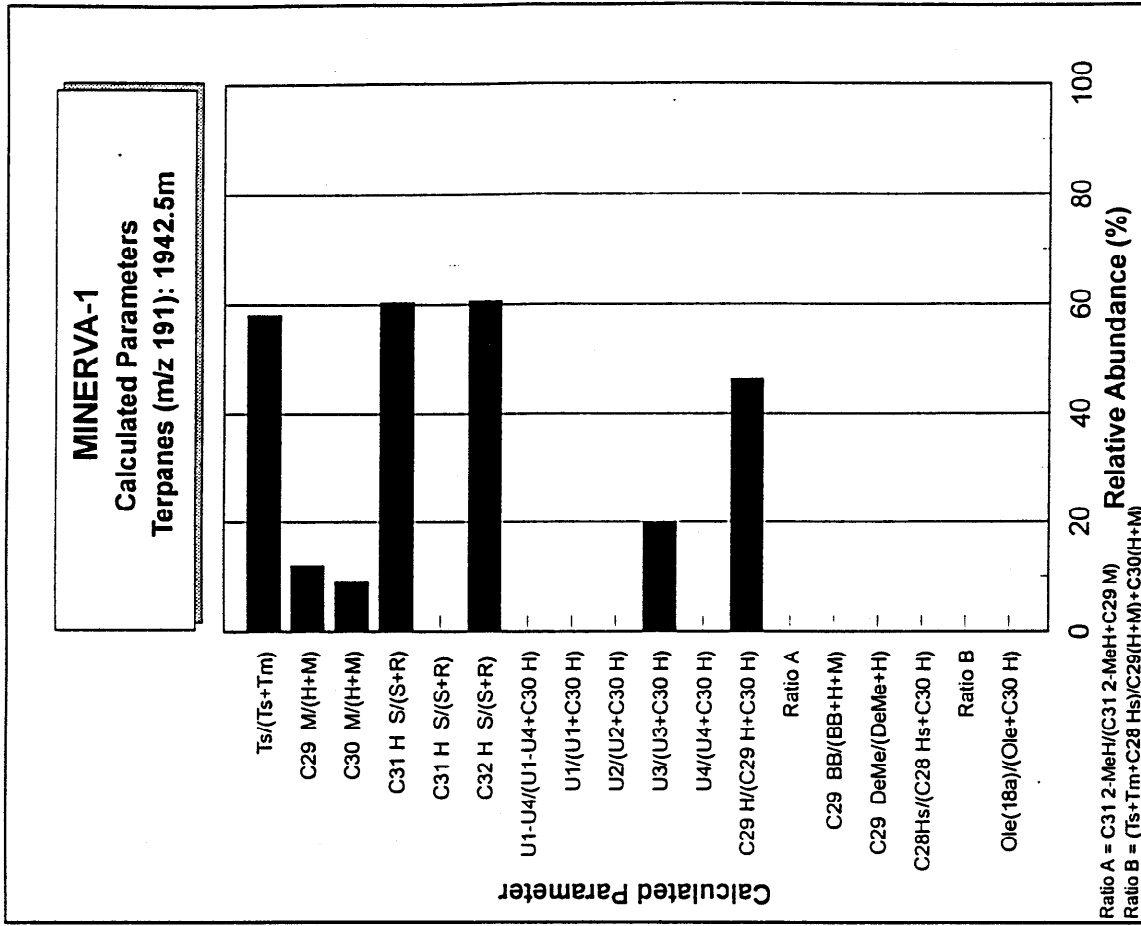
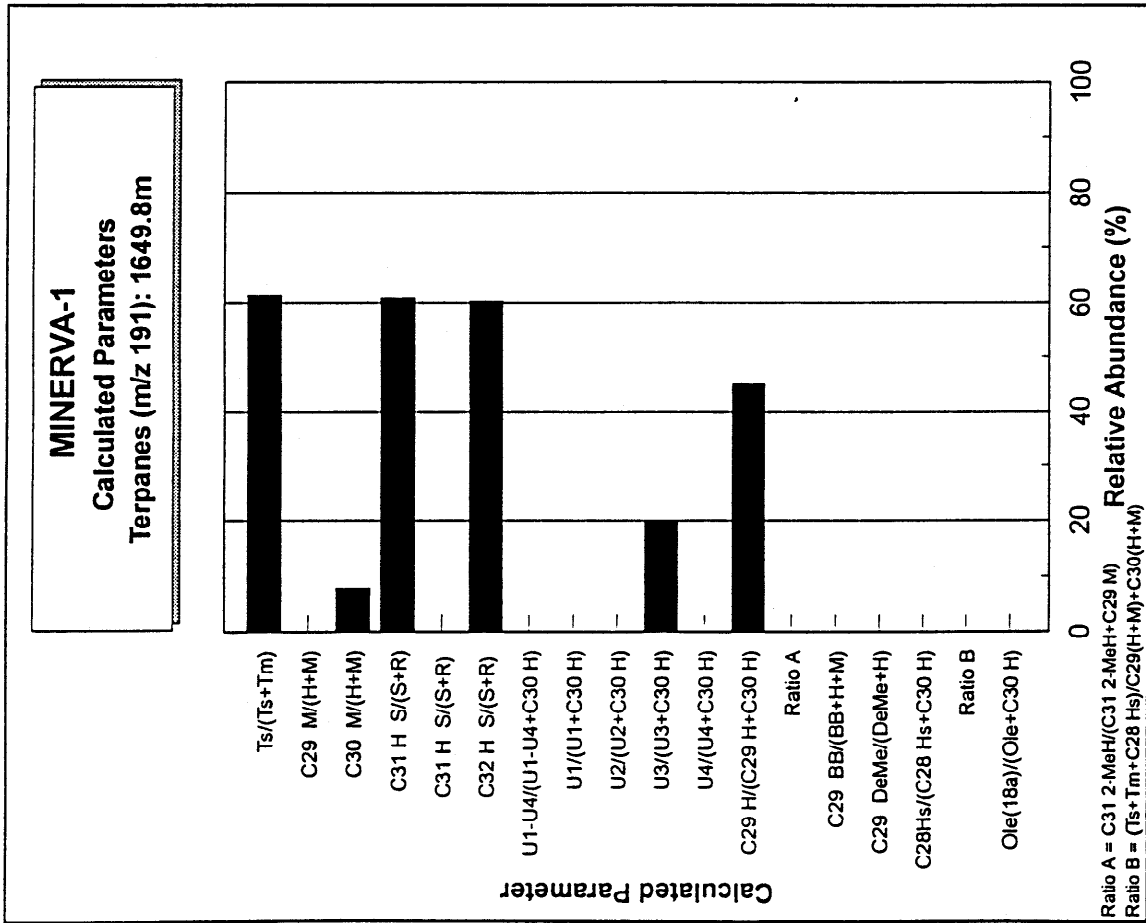


Figure 22b



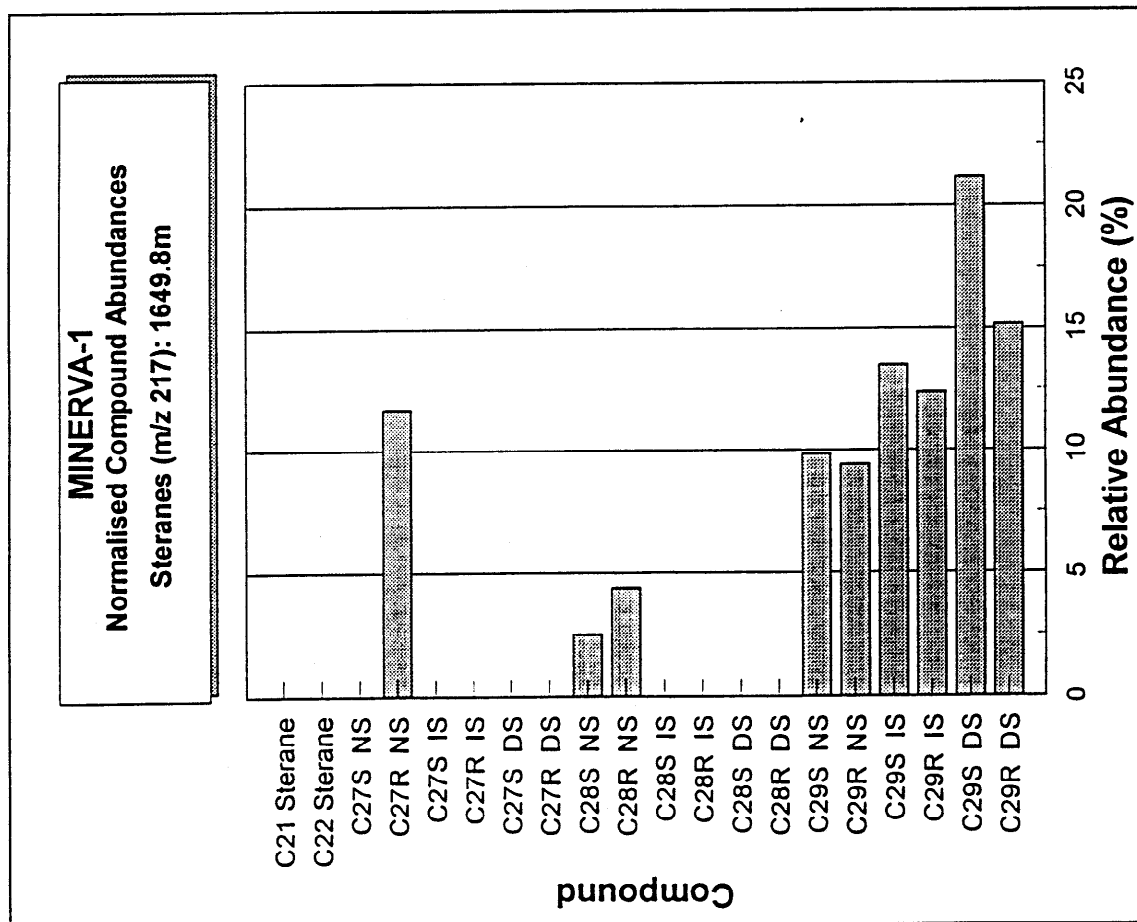
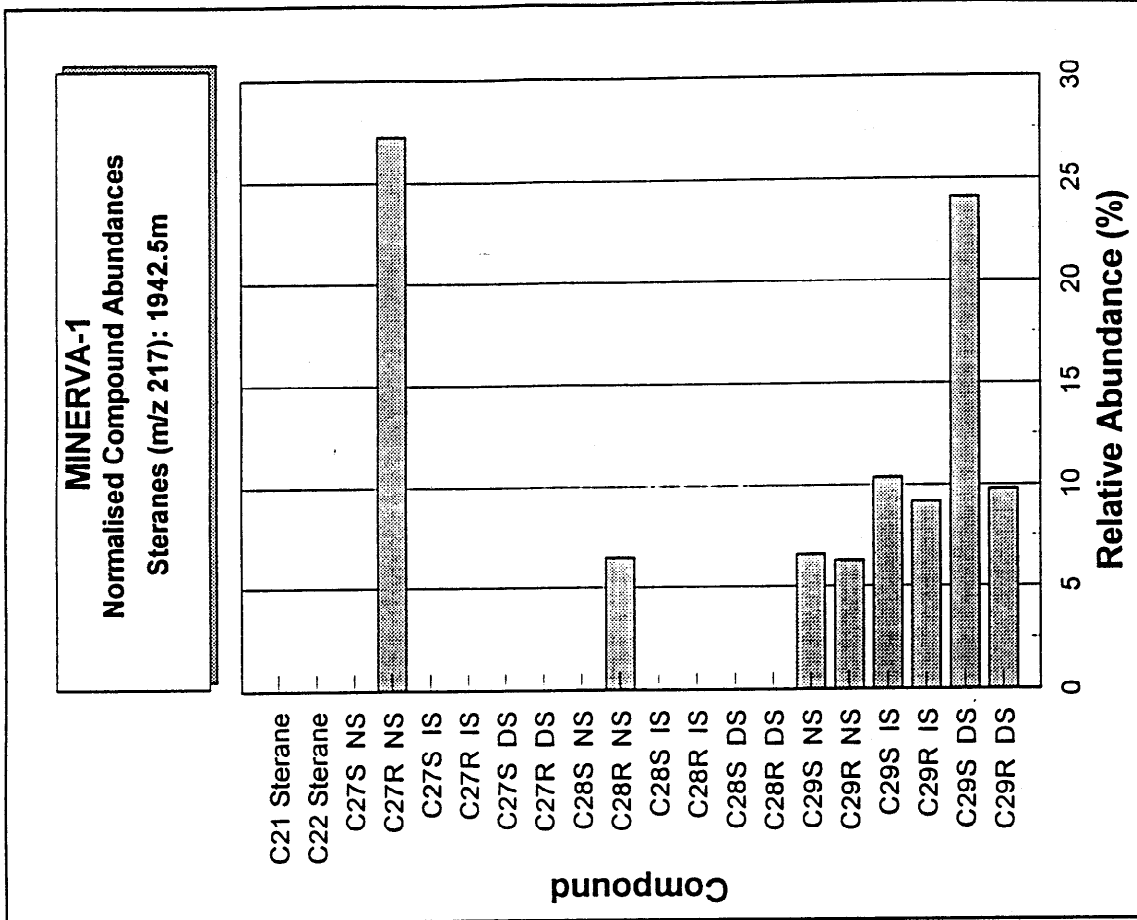


Figure 23a

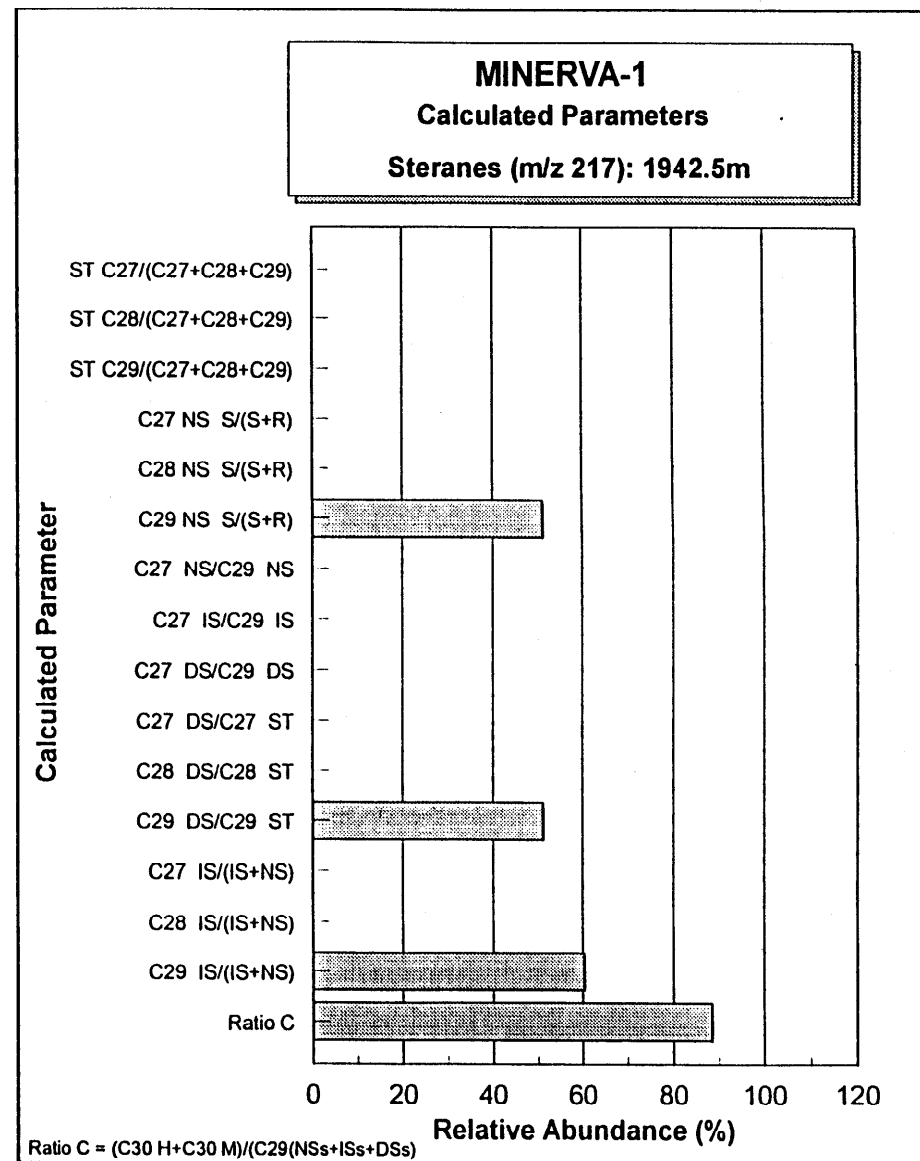
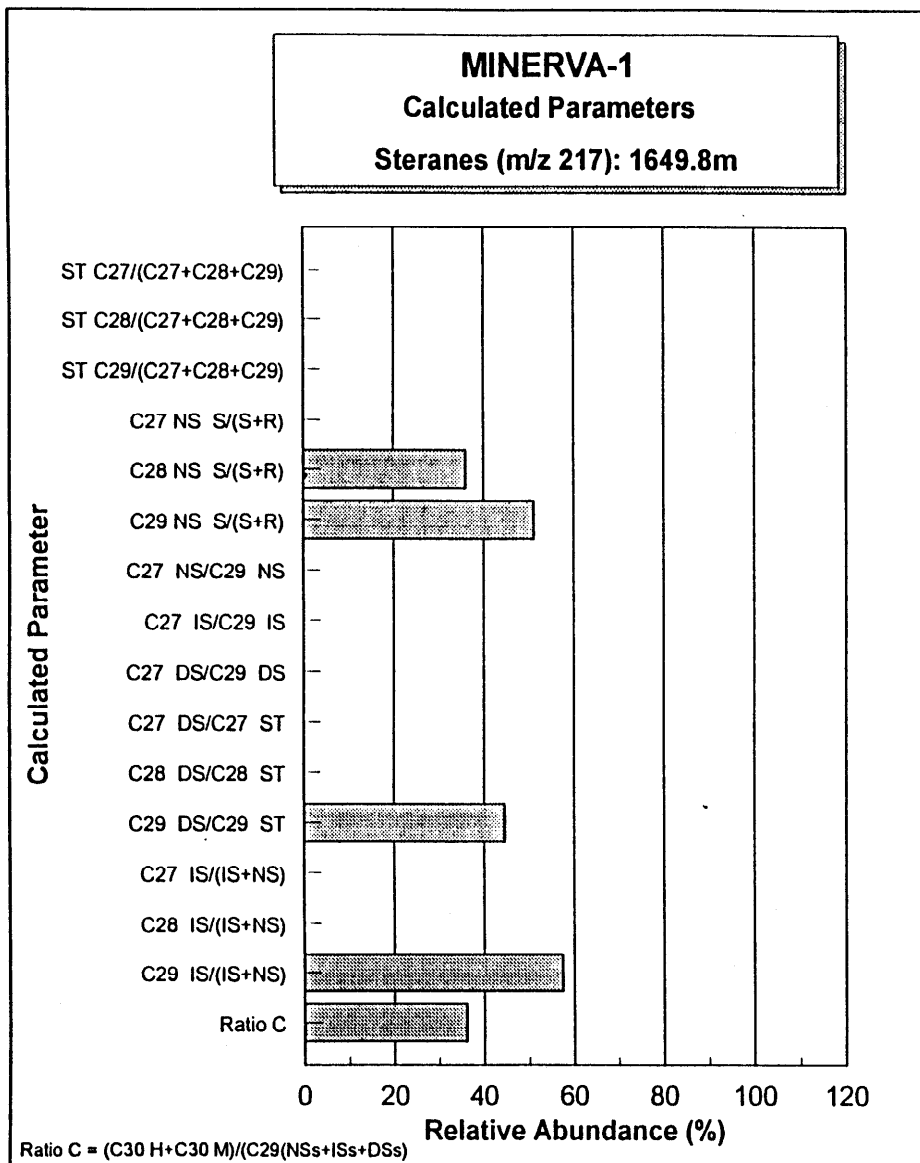


Figure 23b

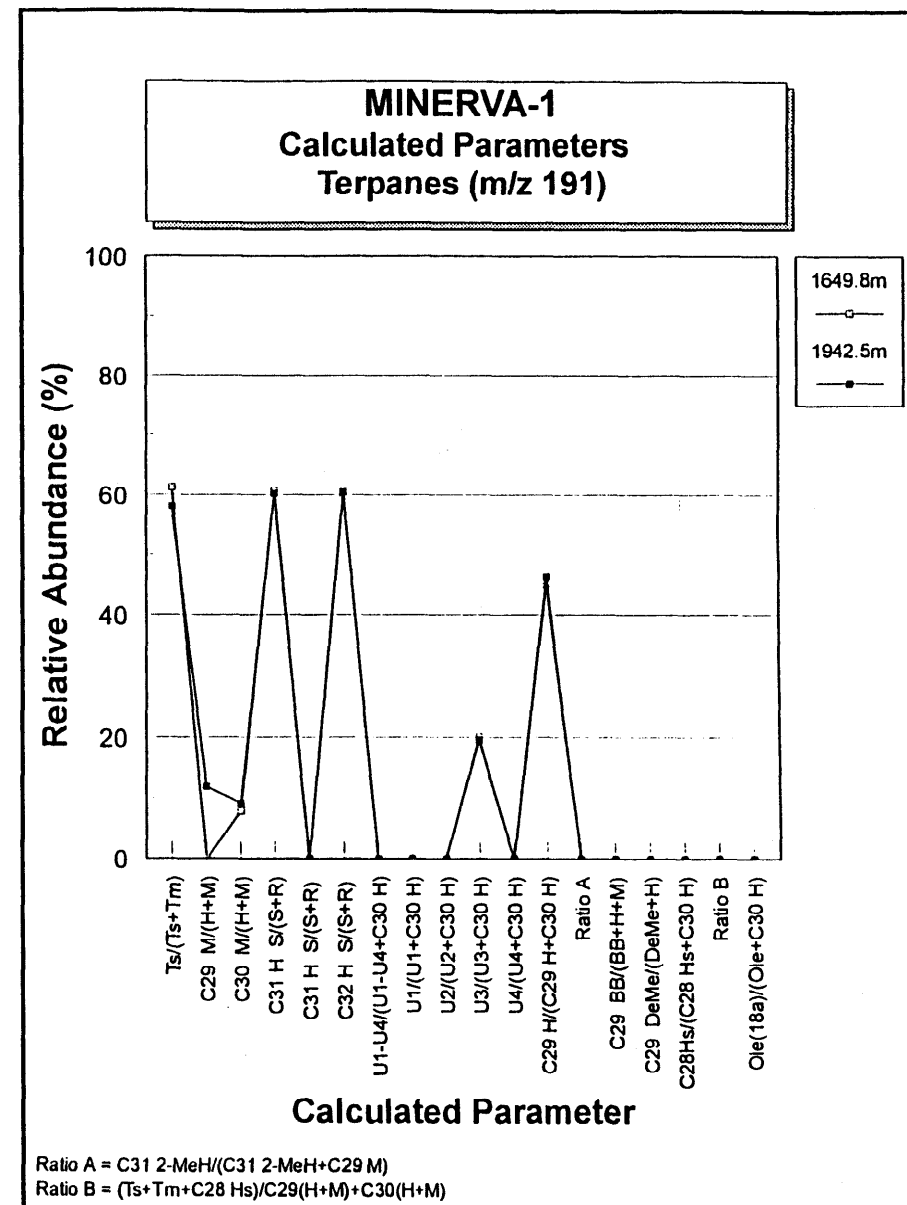
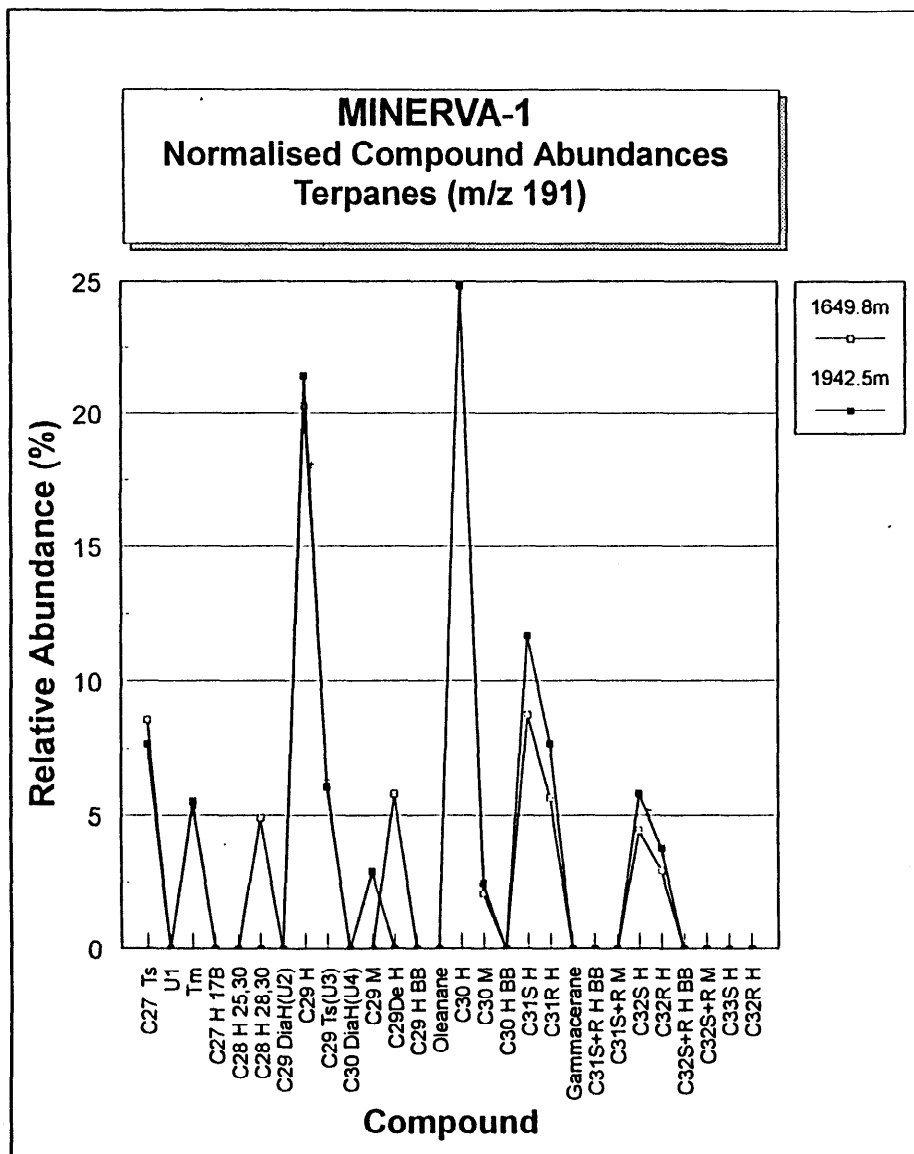


Figure 24a

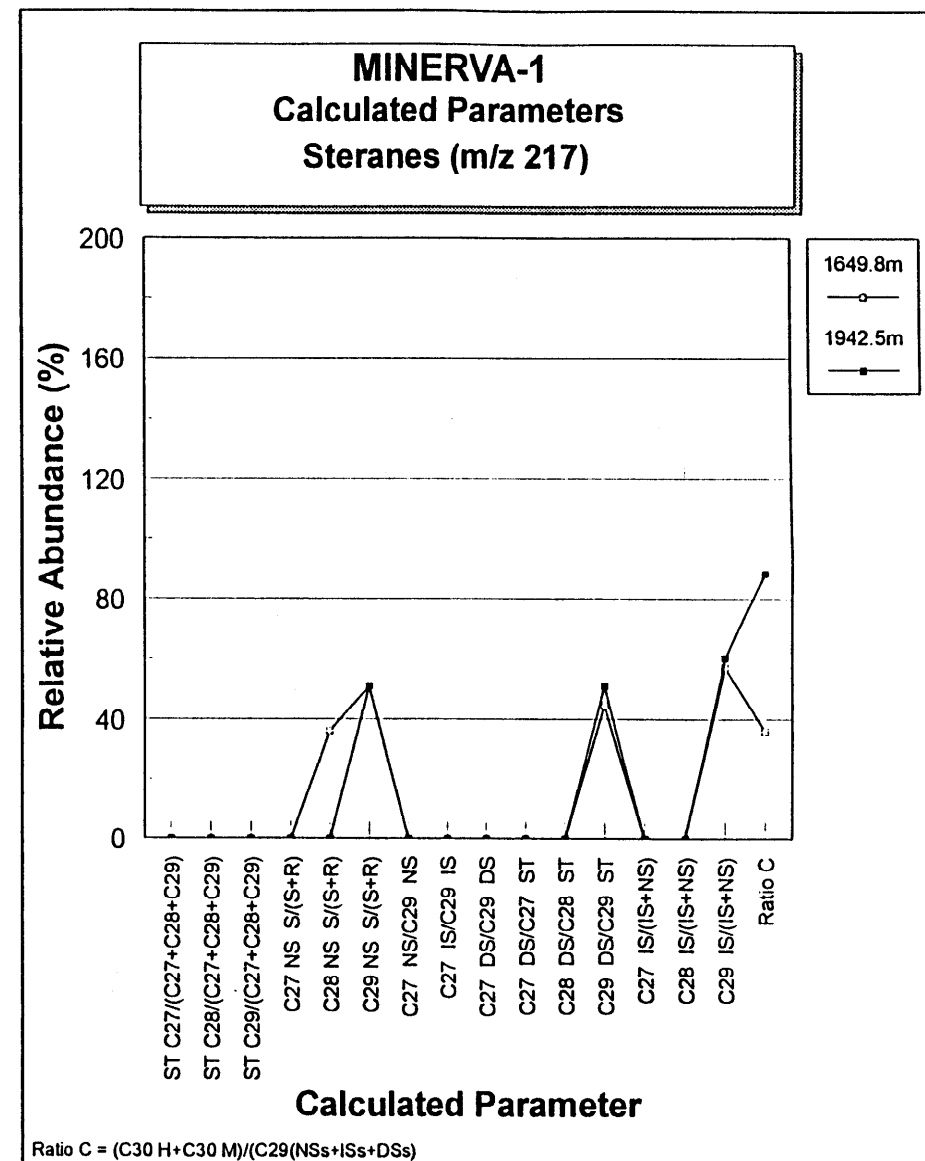
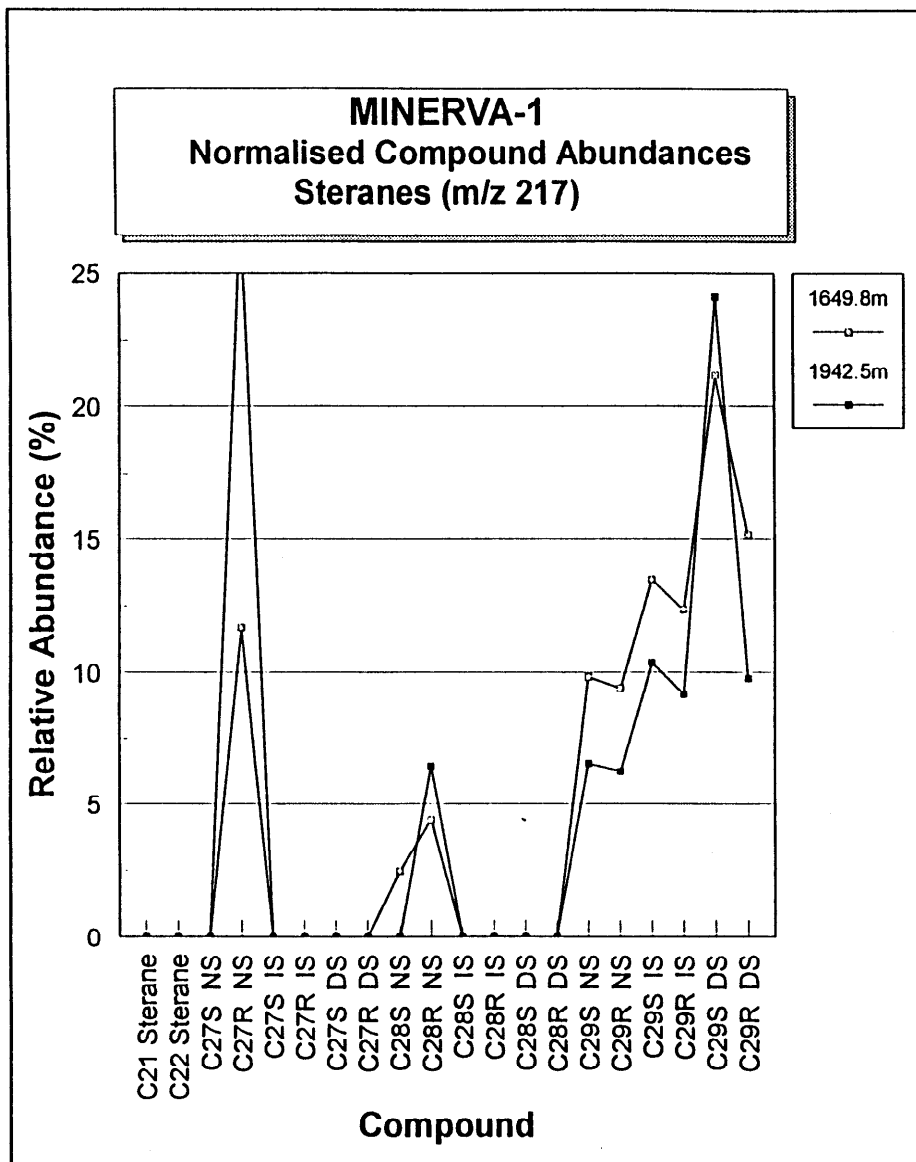


Figure 24b

**MINERVA-1: 1649.8m Water Extract  
Pristane/Phytane vs Hopane/Sterane Ratio**

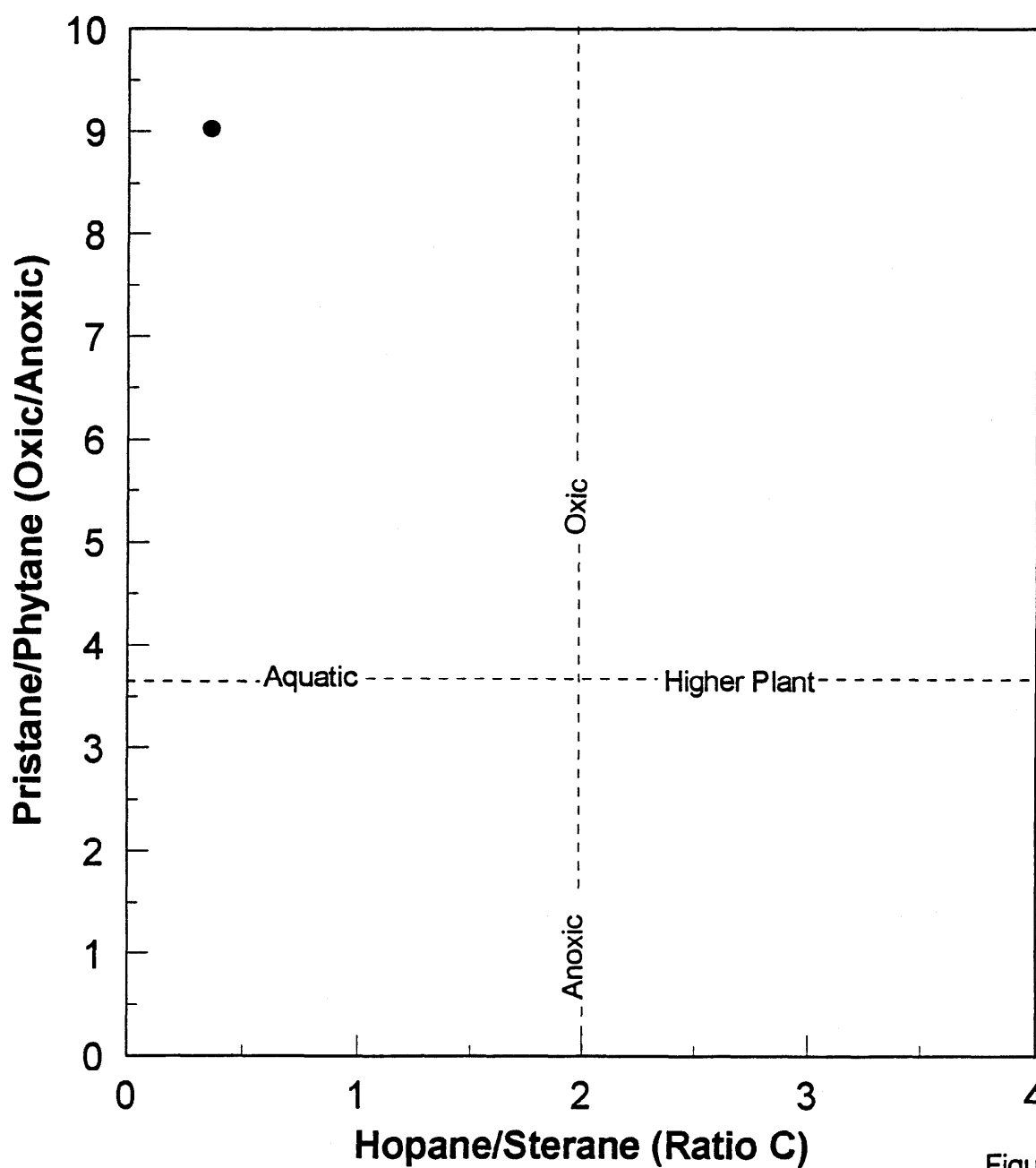
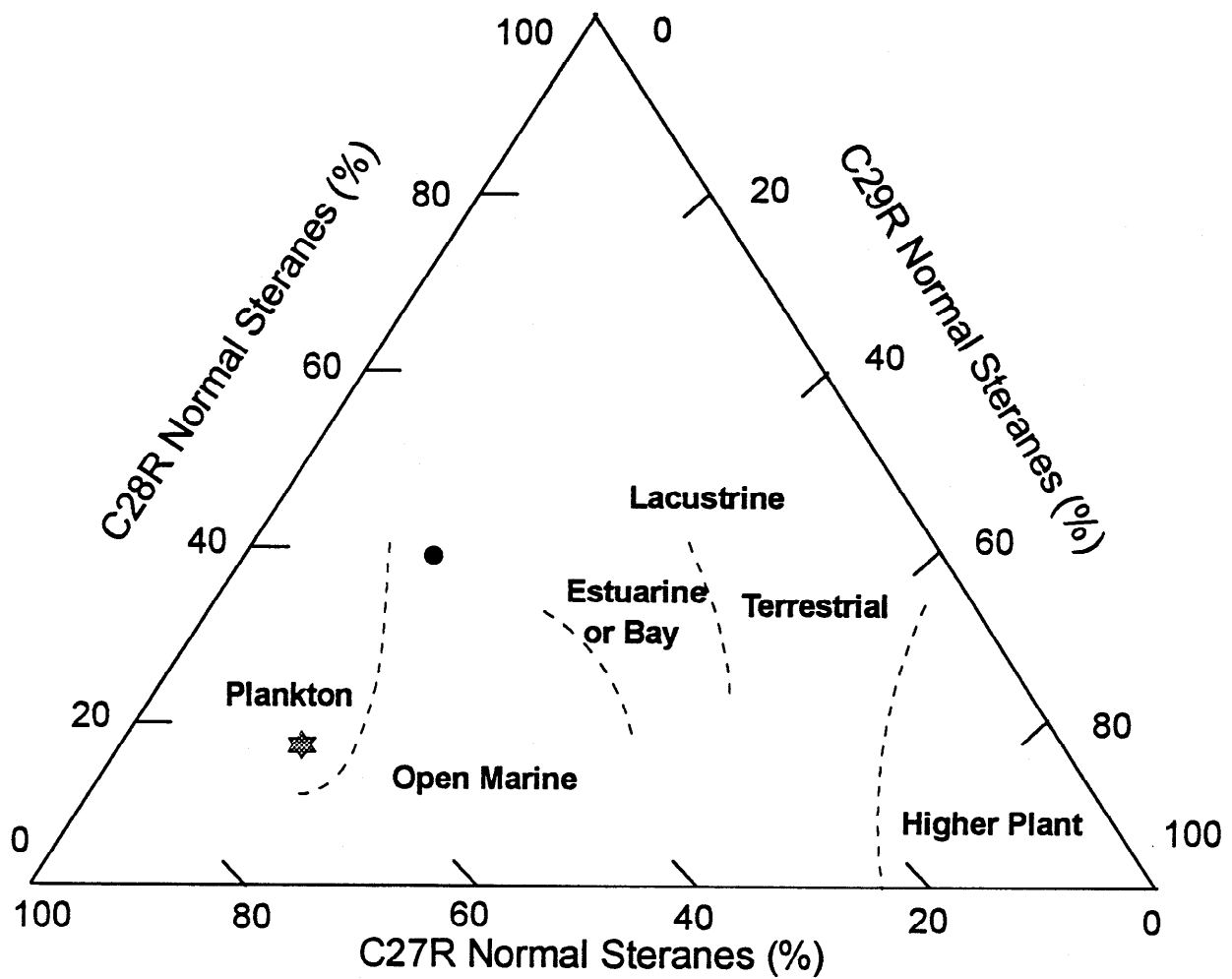


Figure 25

# MINERVA-1: Condensates

## Facies Interpretation based on Sterane Abundances (R Isomers Only)



1649.8m	1942.5m
●	★

Figure 26

**MINERVA-1: 1649.8m Water Extract  
Pristane/Phytane vs C29R/C27R**

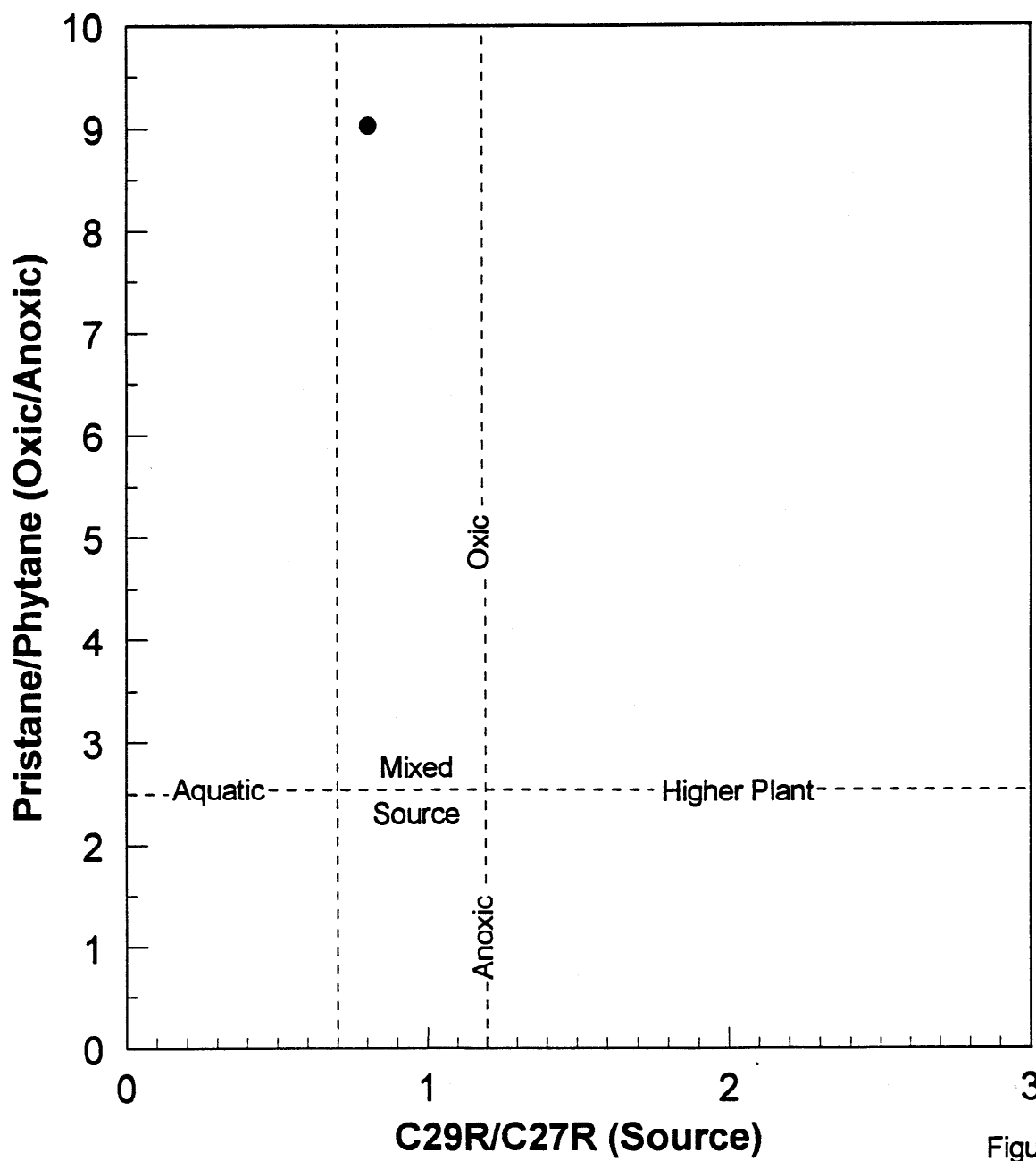
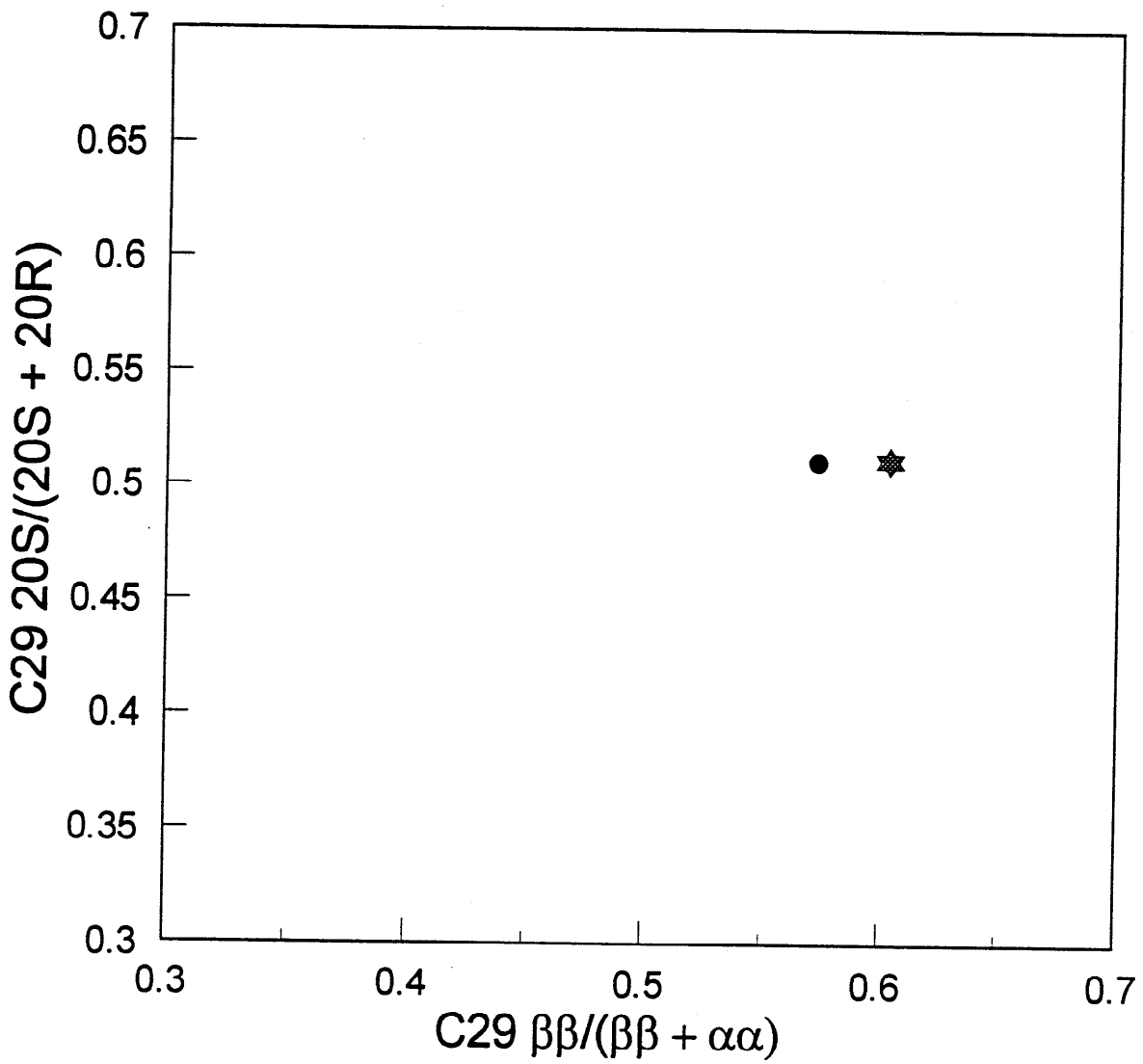


Figure 27

# MINERVA-1

C29  $20S/(20S + 20R)$  vs C29  $\beta\beta/(\beta\beta + \alpha\alpha)$



1649.8m    1942.5m  
●            ★

Figure 28



TABLE 10

## DI &amp; TRI NUCLEAR AROMATIC GC/MS DATA - WATER EXTRACT

DESCRIPTION : COLD-TRAPPED COND

WELL = MINERVA-1  
 COUNTRY = Australia  
 BASIN = Otway

DEPTH UNIT = Metres  
 DATE OF JOB = Jan-Mar 94

DEPTH 1 = 1649.80

DEPTH 2 = 1649.80

## A. DETAILED COMPOUND ANALYSIS

COMPOUND	ION	RELATIVE AMOUNT
-----	---	-----
1,5-Dimethylnaphthalene	156	48038.0
1,6-Dimethylnaphthalene	156	205160.0
1,8-Dimethylnaphthalene	156	-
2,6-Dimethylnaphthalene	156	256121.0
2,7-Dimethylnaphthalene	156	-
1,4+2,3-Dimethylnaphthalene	156	101189.0
1,2,5-Trimethylnaphthalene	170	109144.0
1,2,7-Trimethylnaphthalene	170	-
1,3,6-Trimethylnaphthalene	170	67221.0
1,3,7-Trimethylnaphthalene	170	46790.0
2,3,6-Trimethylnaphthalene	170	32154.0
1,3,5+1,4,6-Trimethylnaphthalene	170	53799.0
Phenanthrene	178	38619.0
1-Methylphenanthrene	192	12728.0
2-Methylphenanthrene	192	13937.0
3-Methylphenanthrene	192	11978.0
9-Methylphenanthrene	192	14777.0
1,7-Dimethylphenanthrene	206	8802.0
Compound X (1,3 + 3,9 + 2,10 + 3,10-DMP)	206	13492.0
Retene	219	7024.0
Cadalene	198	-
Eudalene	184	-

## B. CALCULATED DATA

PARAMETER	ION	VALUE
-----	---	-----
DNR-1 = (2,6-DMN + 2,7-DMN) / 1,5-DMN	156	-
DNR-2 = 2,7-DMN / 1,8-DMN	156	-
DNR-5 = 1,6-DMN / 1,8-DMN	156	-
DNR-6 = ((2,6-DMN + 2,7-DMN) / 1,4+2,3-DMN)*0.91	156	-
TNR-1 = (2,3,6-TMN / 1,3,5+1,4,6-TMN)*0.82	170	0.49
TNR-5 = (1,2,5-TMN / 1,3,6-TMN)*0.75	170	1.22
TNR-6 = 1,2,7-TMN / 1,3,7-TMN	170	-
MPR-1 = (2-MP + 3-MP) / 1-MP	192	2.04
MPI-1 = (1.5 x (2-MP + 3-MP)) / (0.667*Ph + 1-MP + 9-MP)	178,192	0.73
MPI-2 = (3 x 2-MP) / (0.667*Ph + 1-MP + 9-MP)	178,192	0.78
Rc(a) = (0.6 x MPI-1) + 0.4	na	0.84
Rc(b) = (-0.6 x MPI-1) + 2.3	na	1.86
1,7-Dimethylphenanthrene / Compound X	206	0.65
Retene / 9-Methylphenanthrene	192,219	0.48
1-Methylphenanthrene / 9-Methylphenanthrene	192	0.86

Notes : DMN = Dimethylnaphthalene TMN = Trimethylnaphthalene - = no data  
 MP = Methylphenanthrene Ph = Phenanthrene na = not applicable

TABLE 11

## DI &amp; TRI NUCLEAR AROMATIC GC/MS DATA - CONDENSATE

DESCRIPTION : COLD-TRAPPED COND

WELL = MINERVA-1  
 COUNTRY = Australia  
 BASIN = Otway

DEPTH UNIT = Metres  
 DATE OF JOB = Jan-Mar 94

DEPTH 1 = 1942.50

DEPTH 2 = 1942.50

## A. DETAILED COMPOUND ANALYSIS

COMPOUND -----	ION ---	RELATIVE AMOUNT -----
1,5-Dimethylnaphthalene	156	184080.0
1,6-Dimethylnaphthalene	156	889276.0
1,8-Dimethylnaphthalene	156	0.0
2,6-Dimethylnaphthalene	156	902411.0
2,7-Dimethylnaphthalene	156	0.0
1,4+2,3-Dimethylnaphthalene	156	350861.0
1,2,5-Trimethylnaphthalene	170	290906.0
1,2,7-Trimethylnaphthalene	170	0.0
1,3,6-Trimethylnaphthalene	170	200361.0
1,3,7-Trimethylnaphthalene	170	159937.0
2,3,6-Trimethylnaphthalene	170	148514.0
1,3,5+1,4,6-Trimethylnaphthalene	170	141342.0
Phenanthrene	178	183774.0
1-Methylphenanthrene	192	54218.0
2-Methylphenanthrene	192	94126.0
3-Methylphenanthrene	192	90043.0
9-Methylphenanthrene	192	69641.0
1,7-Dimethylphenanthrene	206	24706.0
Compound X (1,3 + 3,9 + 2,10 + 3,10-DMP)	206	73721.0
Retene	219	3810.0
Cadalene	198	-
Eudalene	184	-

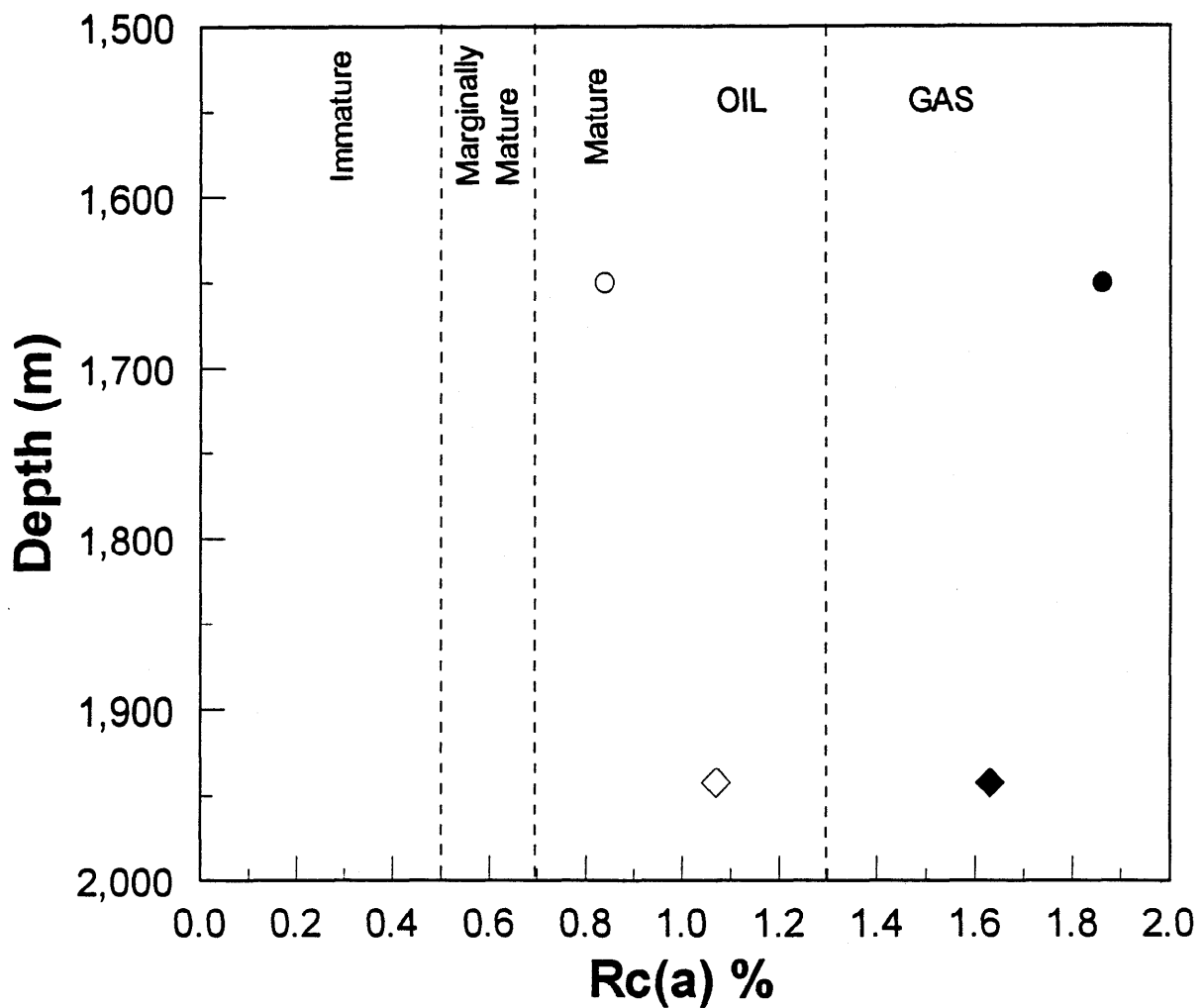
## B. CALCULATED DATA

PARAMETER -----	ION ---	VALUE -----
DNR-1 = (2,6-DMN + 2,7-DMN) / 1,5-DMN	156	4.90
DNR-2 = 2,7-DMN / 1,8-DMN	156	0.00
DNR-5 = 1,6-DMN / 1,8-DMN	156	0.00
DNR-6 = ((2,6-DMN + 2,7-DMN) / 1,4+2,3-DMN)*0.91	156	2.34
TNR-1 = (2,3,6-TMN / 1,3,5+1,4,6-TMN)*0.82	170	0.86
TNR-5 = (1,2,5-TMN / 1,3,6-TMN)*0.75	170	1.09
TNR-6 = 1,2,7-TMN / 1,3,7-TMN	170	0.00
MPR-1 = (2-MP + 3-MP) / 1-MP	192	3.40
MPI-1 = (1.5 x (2-MP + 3-MP)) / (0.667*Ph + 1-MP + 9-MP)	178,192	1.12
MPI-2 = (3 x 2-MP) / (0.667*Ph + 1-MP + 9-MP)	178,192	1.15
Rc(a) = (0.6 x MPI-1) + 0.4	na	1.07
Rc(b) = (-0.6 x MPI-1) + 2.3	na	1.63
1,7-Dimethylphenanthrene / Compound X	206	0.34
Retene / 9-Methylphenanthrene	192,219	0.05
1-Methylphenanthrene / 9-Methylphenanthrene	192	0.78

Notes : DMN = Dimethylnaphthalene TMN = Trimethylnaphthalene - = no data  
 MP = Methylphenanthrene Ph = Phenanthrene na = not applicable

# MINERVA-1

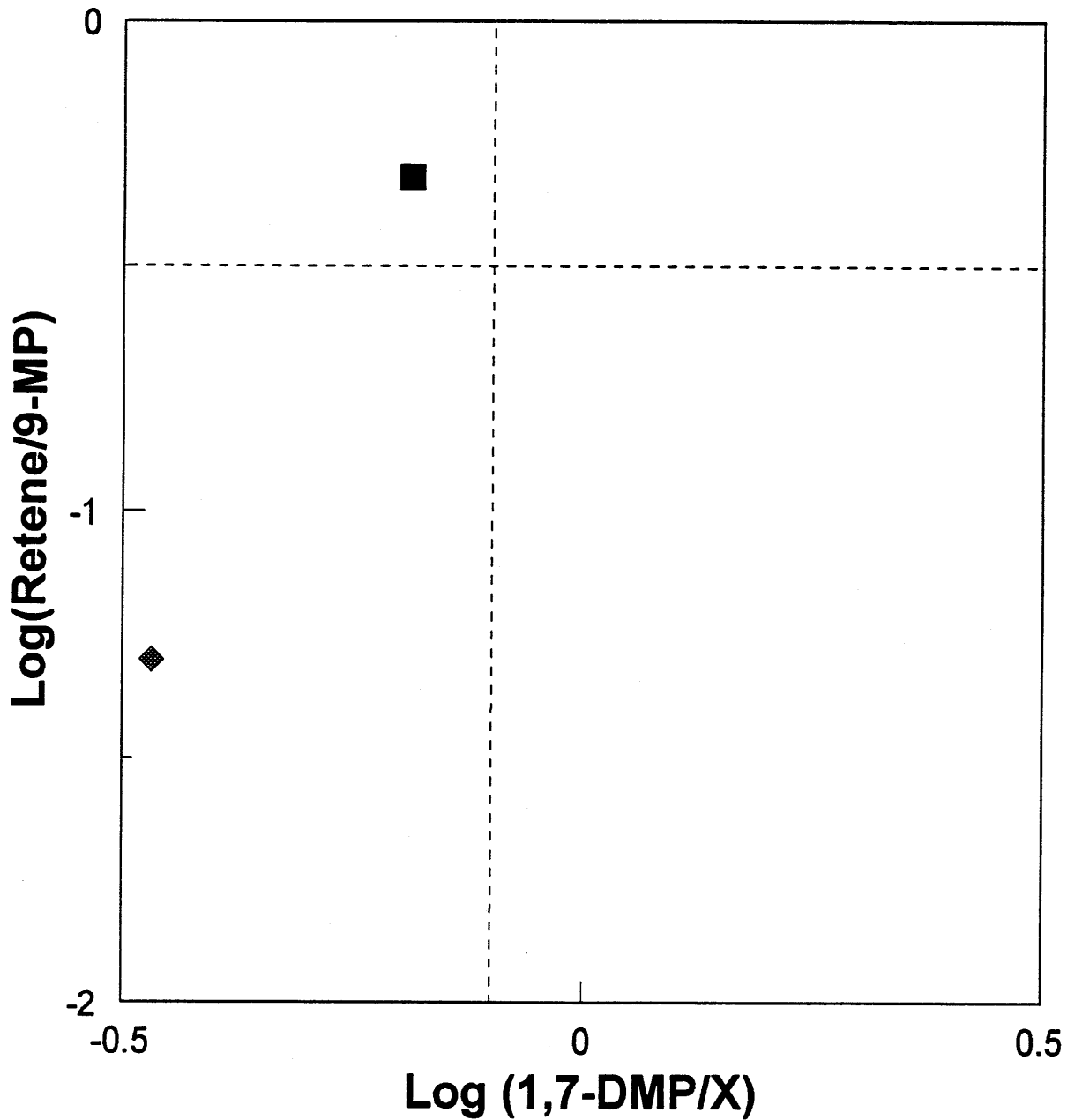
## MPI-1-derived Rc(a) and Rc(b) vs Depth



1649.8m	1942.5m	1649.8m	1942.5m
Rc(a)	Rc(a)	Rc(b)	Rc(b)
○	◇	●	◆

Figure 29

**MINERVA-1**  
**Log(Retene/9-MP) vs Log(1,7-DMP/X)**

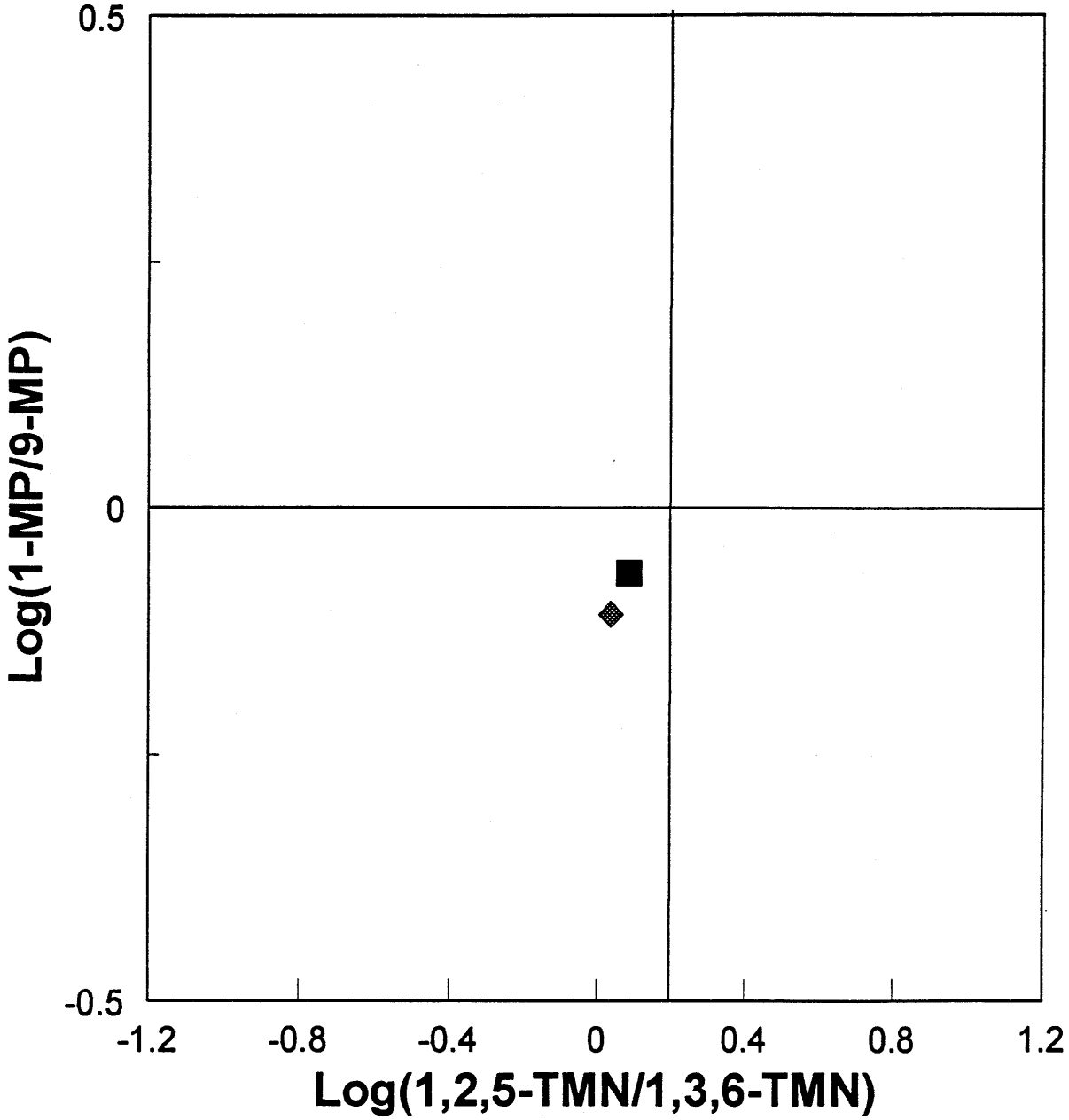


1649.8m 1942.5m



Figure 30

**MINERVA-1**  
**Log(1-MP/9-MP) vs Log(1,2,5-TMN/1,3,6-TMN)**



1649.8m 1942.5m  
■ ◆

Figure 31

TABLE 12

## GAS ANALYSIS DATA

=====

WELL = MINERVA-1  
 COUNTRY = Australia  
 BASIN = Otway

DEPTH UNIT = Metres  
 DATE OF JOB = Aug 93

DESCRIPTION : RFT

DEPTH 1(m) = 1649.80

DEPTH 2(m) = 1649.80

COMPOUND	% by VOLUME
-----	-----
Methane	94.35
Ethane	2.48
Propane	.98
IsoButane	.16
n-Butane	.19
IsoPentane	.06
n-Pentane	.05
C6+	.01
Carbon Dioxide	.23
Nitrogen	1.44
Hydrogen Sulphide	-
Oxygen	.05
Hydrogen	-
Helium	-
Argon	-

-----  
 NOTES : - = not reported

## TABLE 13

## GAS ANALYSIS DATA

=====

WELL = MINERVA-1  
 COUNTRY = Australia  
 BASIN = Otway

DEPTH UNIT = Metres  
 DATE OF JOB = Aug 93

DESCRIPTION : RFT

DEPTH 1(m) = 1931.00

DEPTH 2(m) = 1931.00

COMPOUND	% by VOLUME
-----	-----
Methane	93.71
Ethane	2.16
Propane	.81
IsoButane	.10
n-Butane	.17
IsoPentane	.03
n-Pentane	.06
C6+	.12
Carbon Dioxide	1.71
Nitrogen	1.08
Hydrogen Sulphide	-
Oxygen	.05
Hydrogen	-
Helium	-
Argon	-

-----  
 NOTES : - = not reported

# MINERVA-1

## Gas Analysis Data

### Normalised Relative Abundances

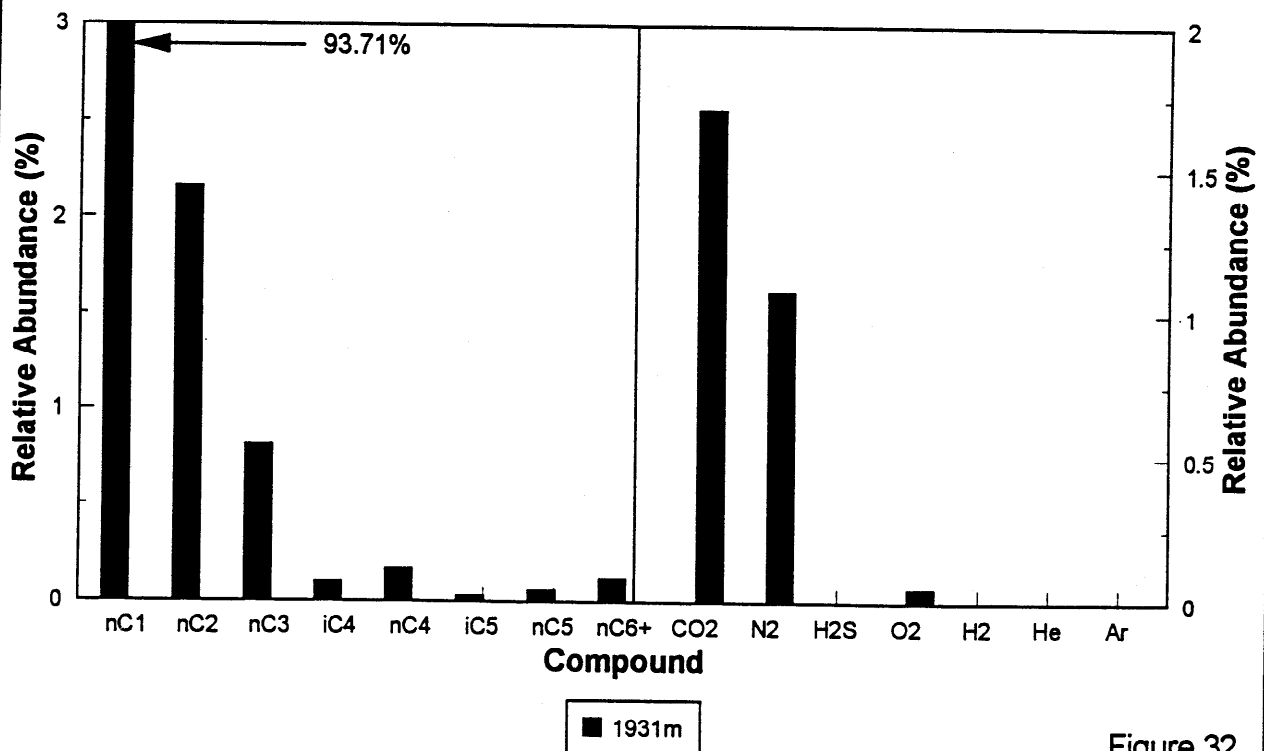
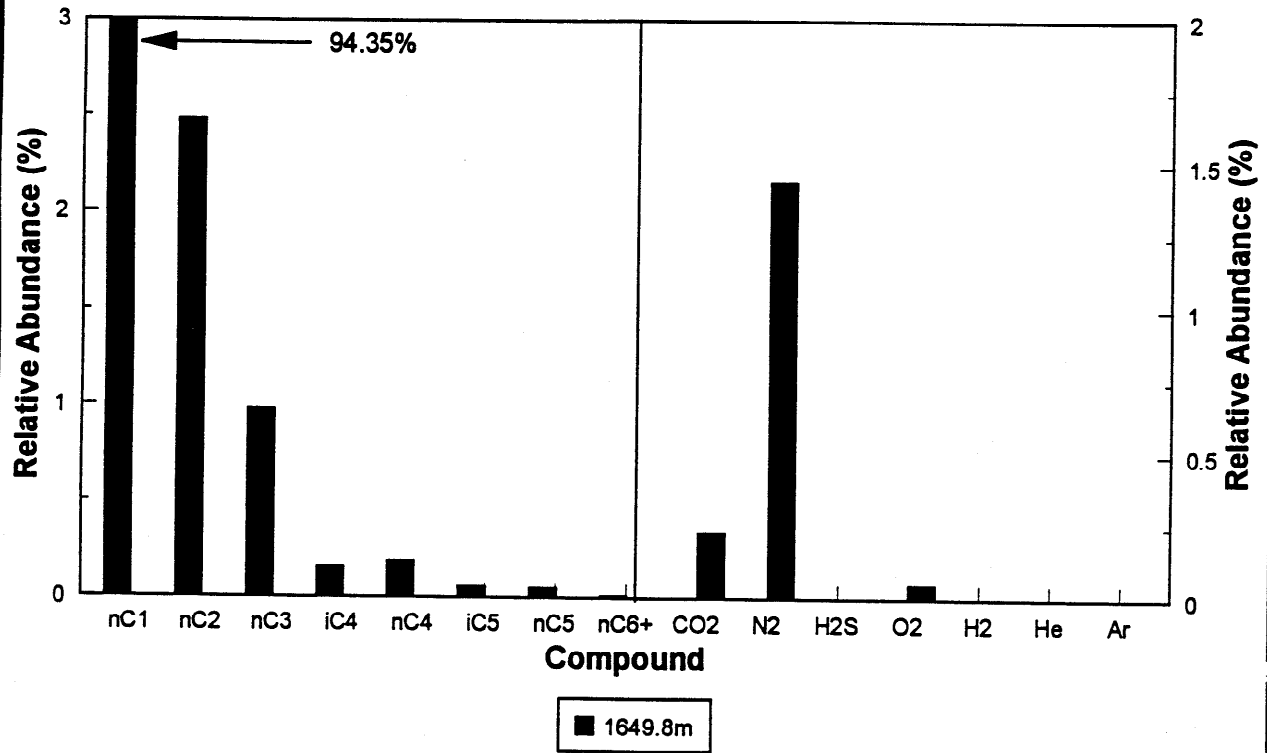


Figure 32



TABLE 14

CARBON ISOTOPE ANALYSIS DATA - GAS

WELL NAME = MINERVA-1  
 COUNTRY = Australia  
 BASIN = Otway

DEPTH UNIT = Metres  
 DATE OF JOB = Aug 93

DEPTH 1	DEPTH 2	delta C VALUES							
		METHANE	ETHANE	PROPANE	ISO-BUTANE	n-BUTANE	ISO-PENTANE	n-PENTANE	CARBON DIOXIDE
1649.80	1649.80	-34.30	-24.80	-25.50	-	-25.50	-	-25.90	-26.10
1931.00	1931.00	-34.10	-24.10	-25.40	-	-25.60	-	-26.20	-13.10

All values permil relative to PDB  
 - = no data

# GAS ISOTOPE MATURATION PLOT 1 MINERVA-1

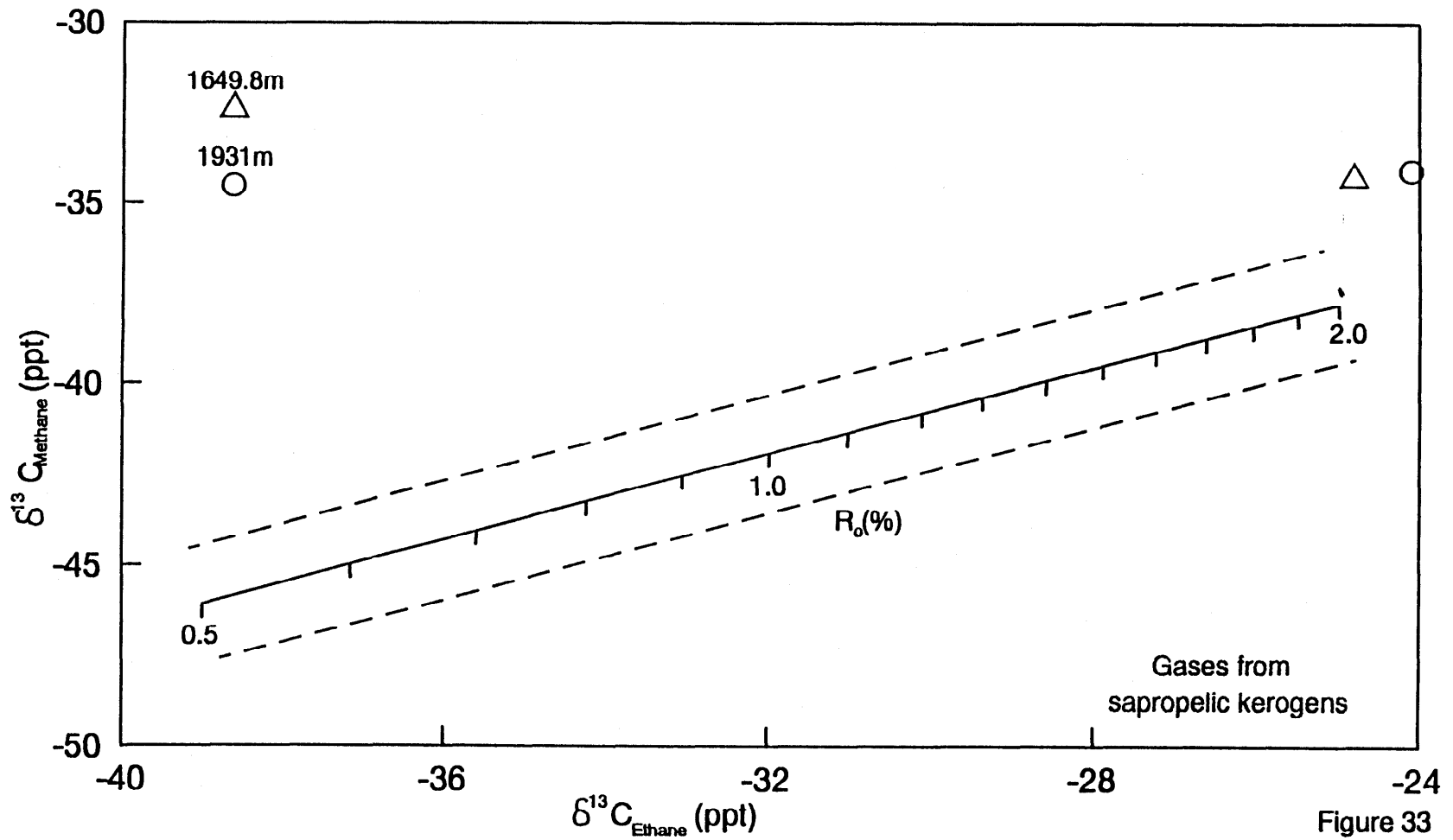


Figure 33

# GAS ISOTOPE MATURATION PLOT 2

MINERVA-1

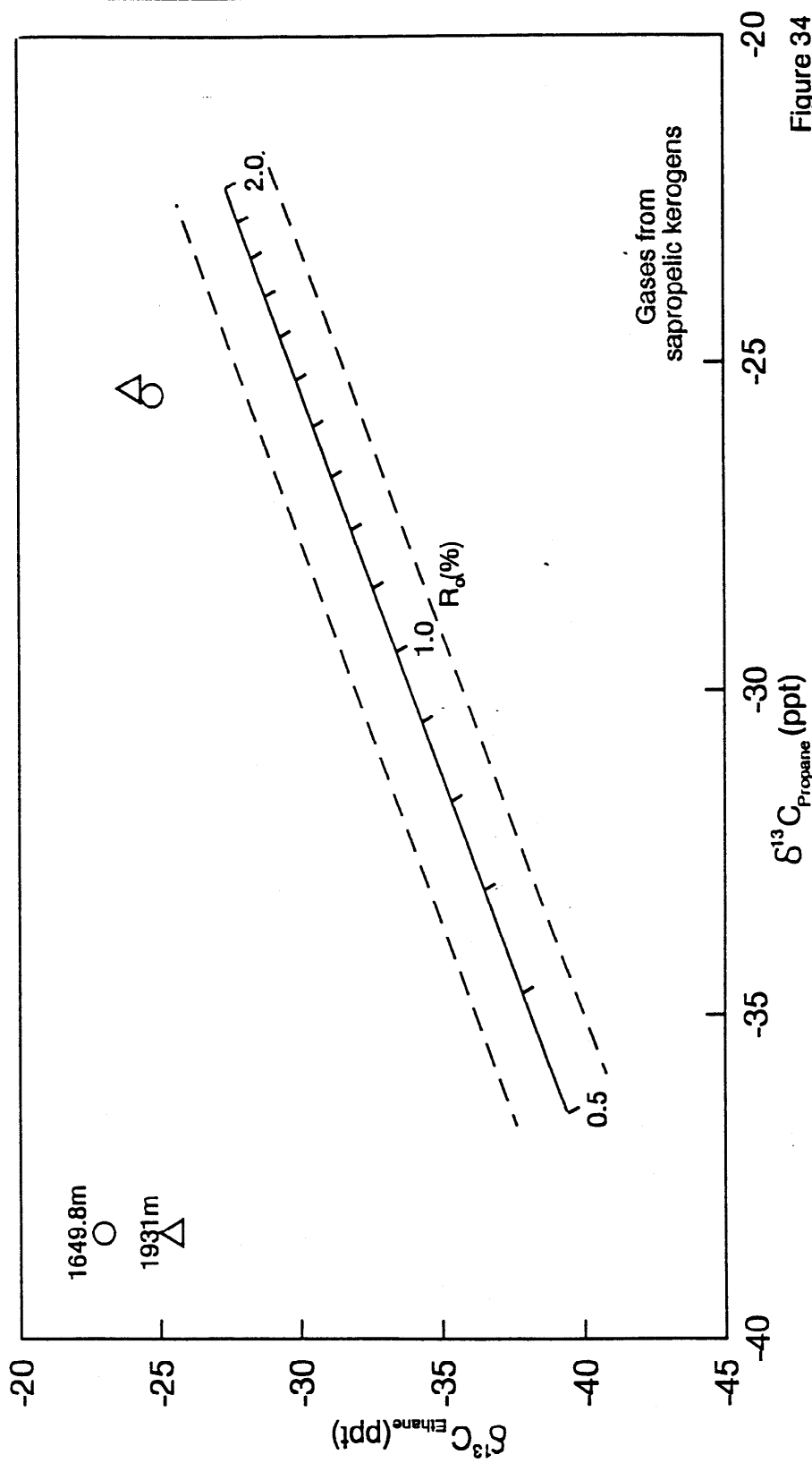


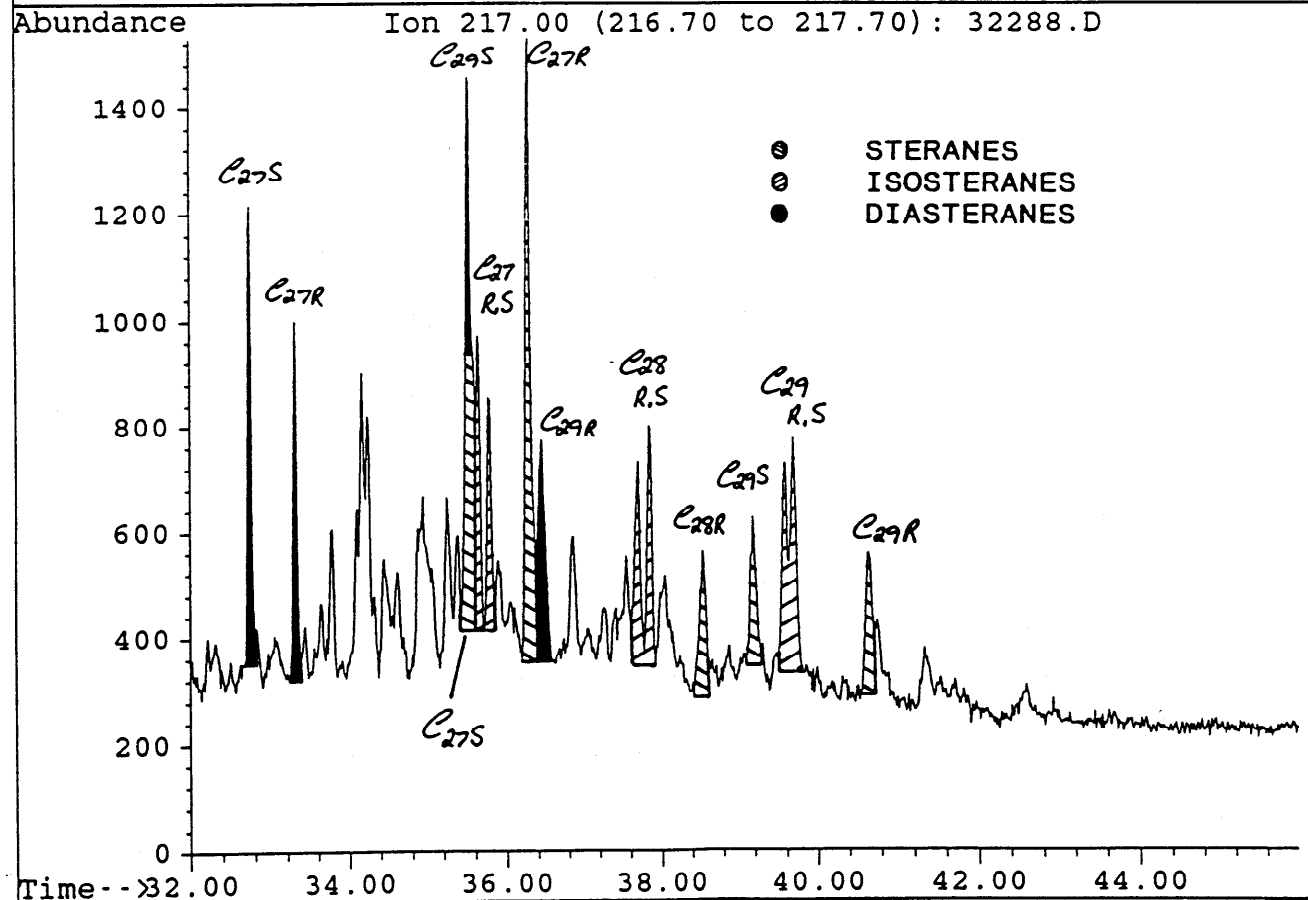
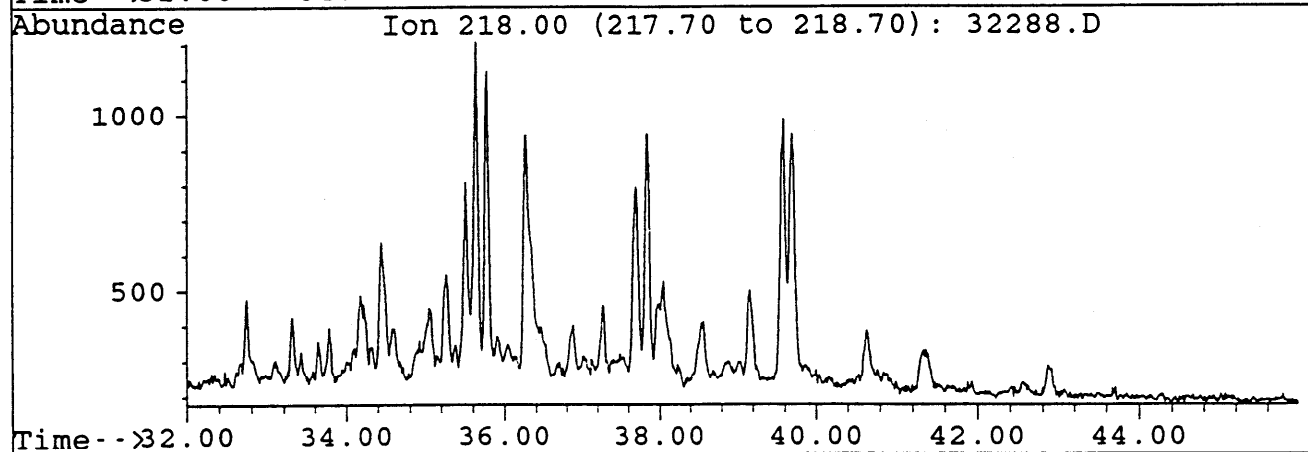
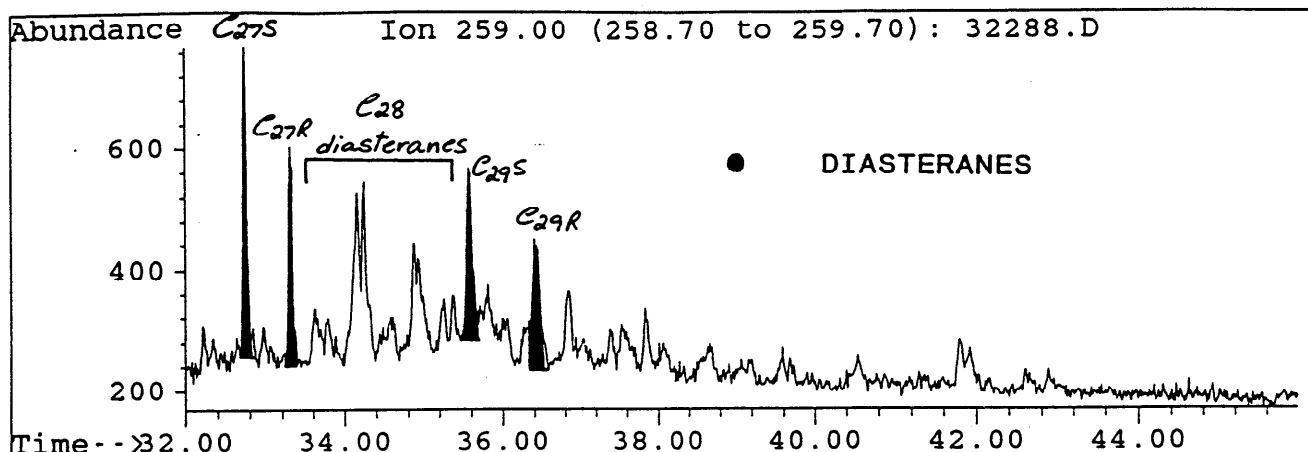
Figure 34



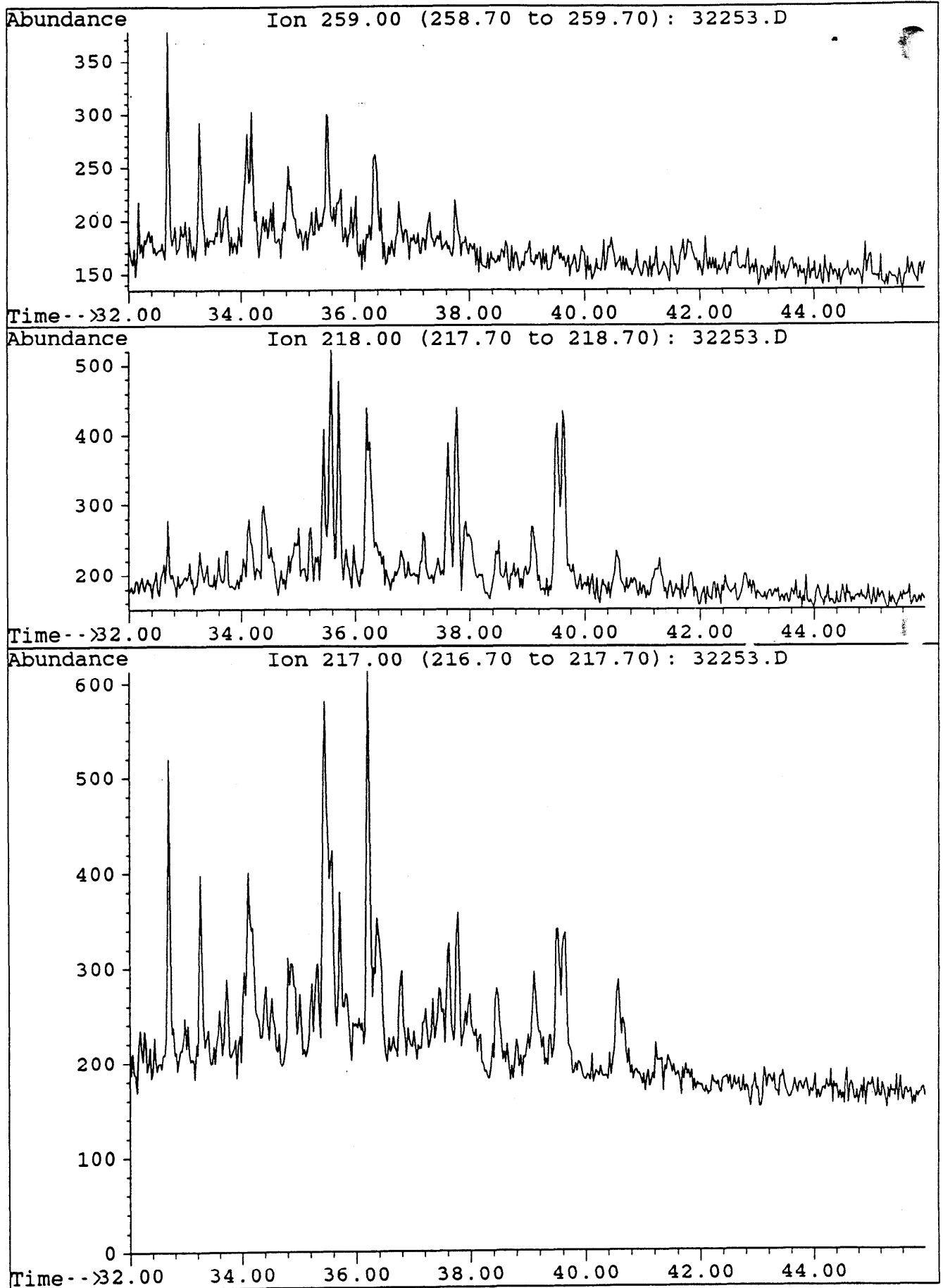
**APPENDIX 1**

**SIR GC-MS (B/C) MASS FRAGMENTOGRAMS : 1942.5m CONDENSATE**

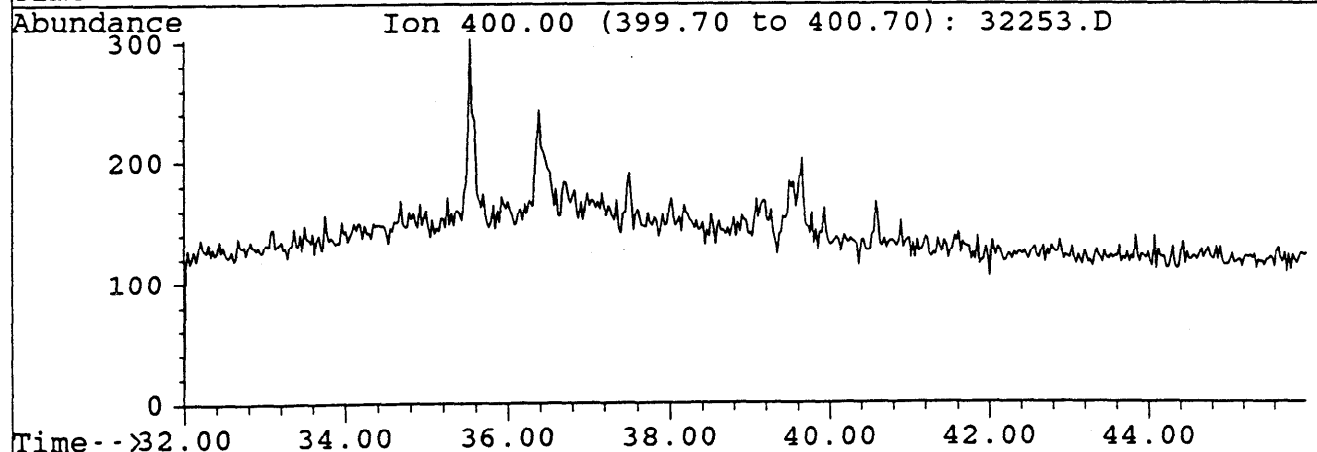
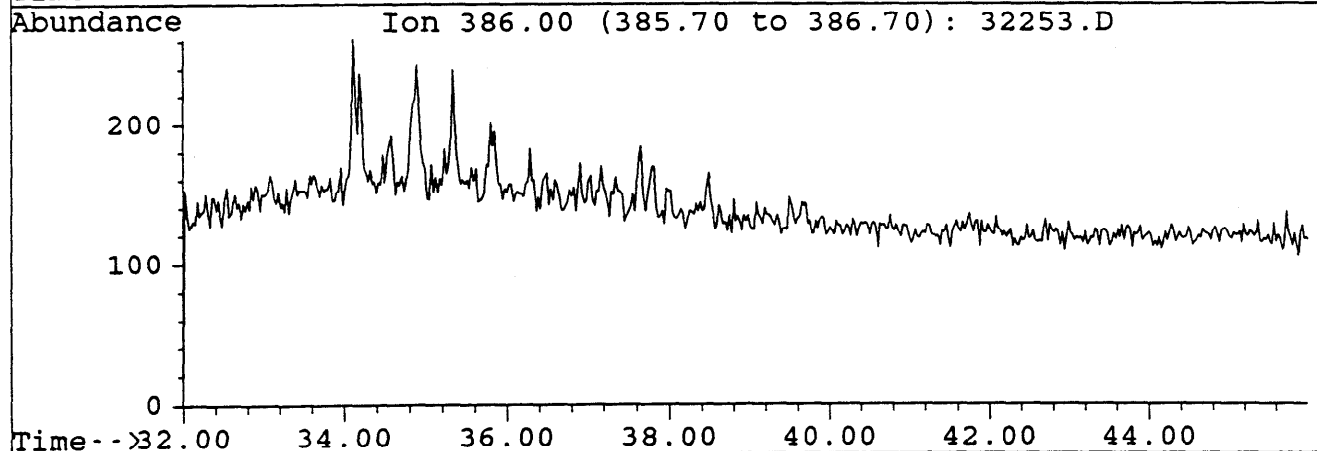
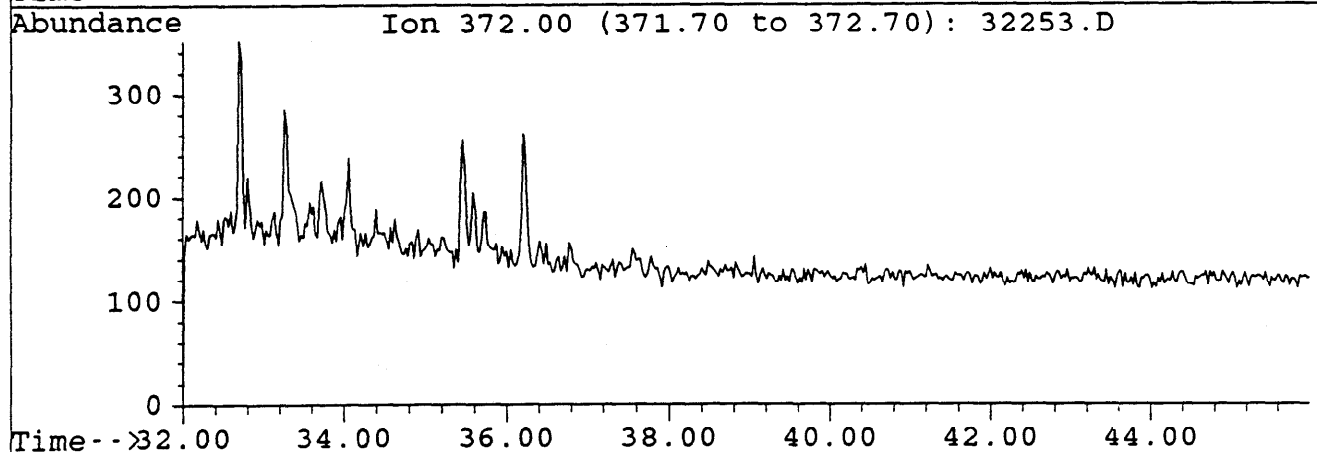
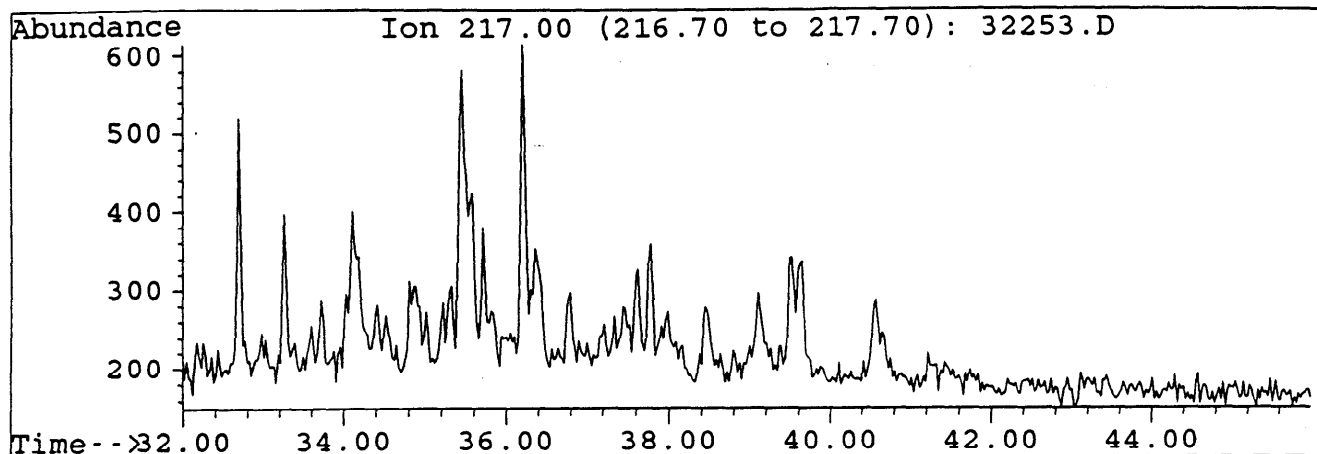
File : 32288.D  
 Sample : MINERVA#1, RFS-AD-1157. L-008. TOPPED. B/C  
 Misc. Info : COL#143. GEC. 25-1-94.



File : 32253.D  
Sample : MINERVA#1, RFS-AD-1157, L-008. COLD TRAP LIQ  
Misc. Info : COL#143. 17-1-94. GEC. B/C.

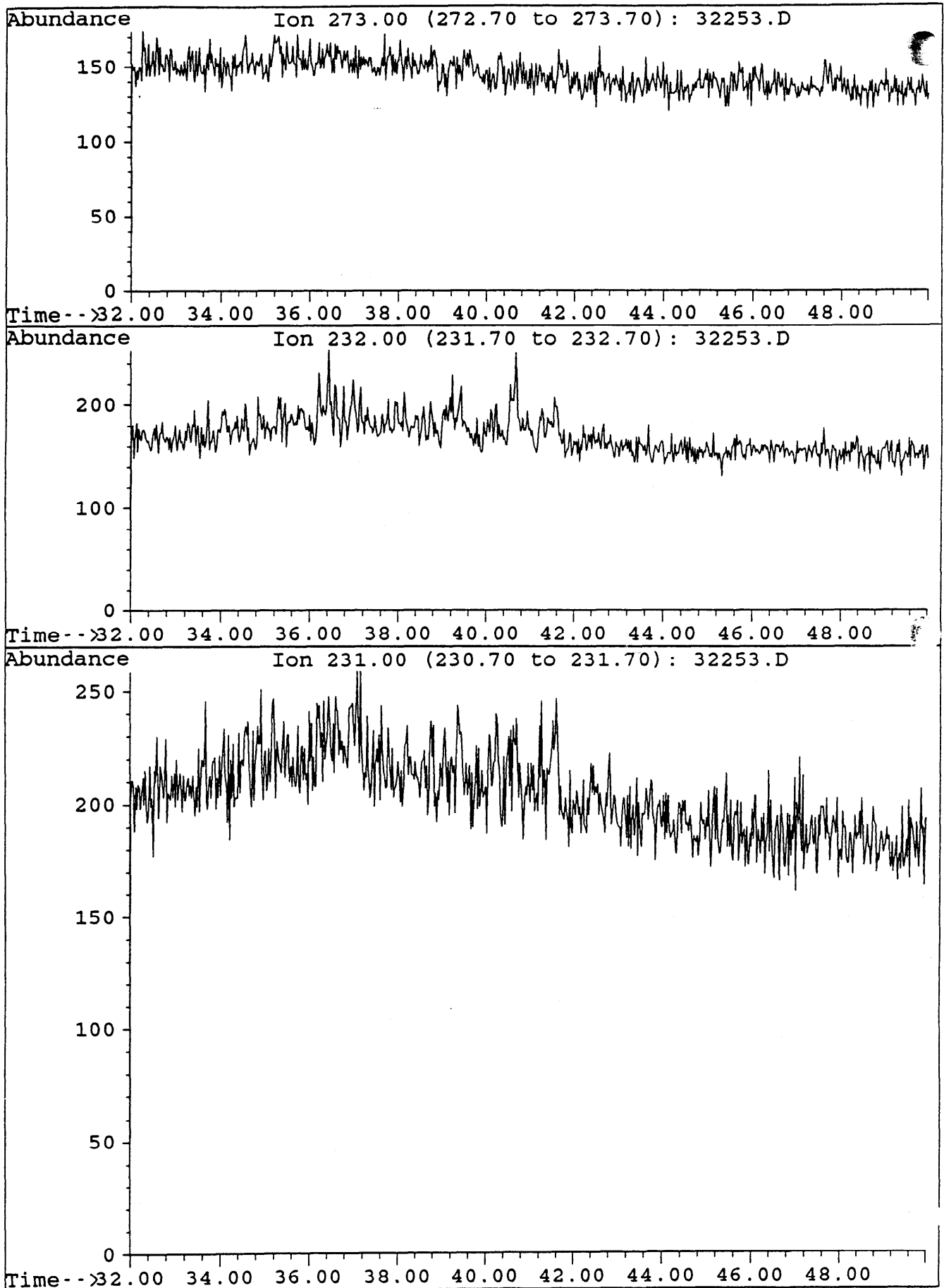


File : 32253.D  
Sample : MINERVA#1, RFS-AD-1157, L-008. COLD TRAP LIQ  
Misc. Info : COL#143. 17-1-94. GEC. B/C.

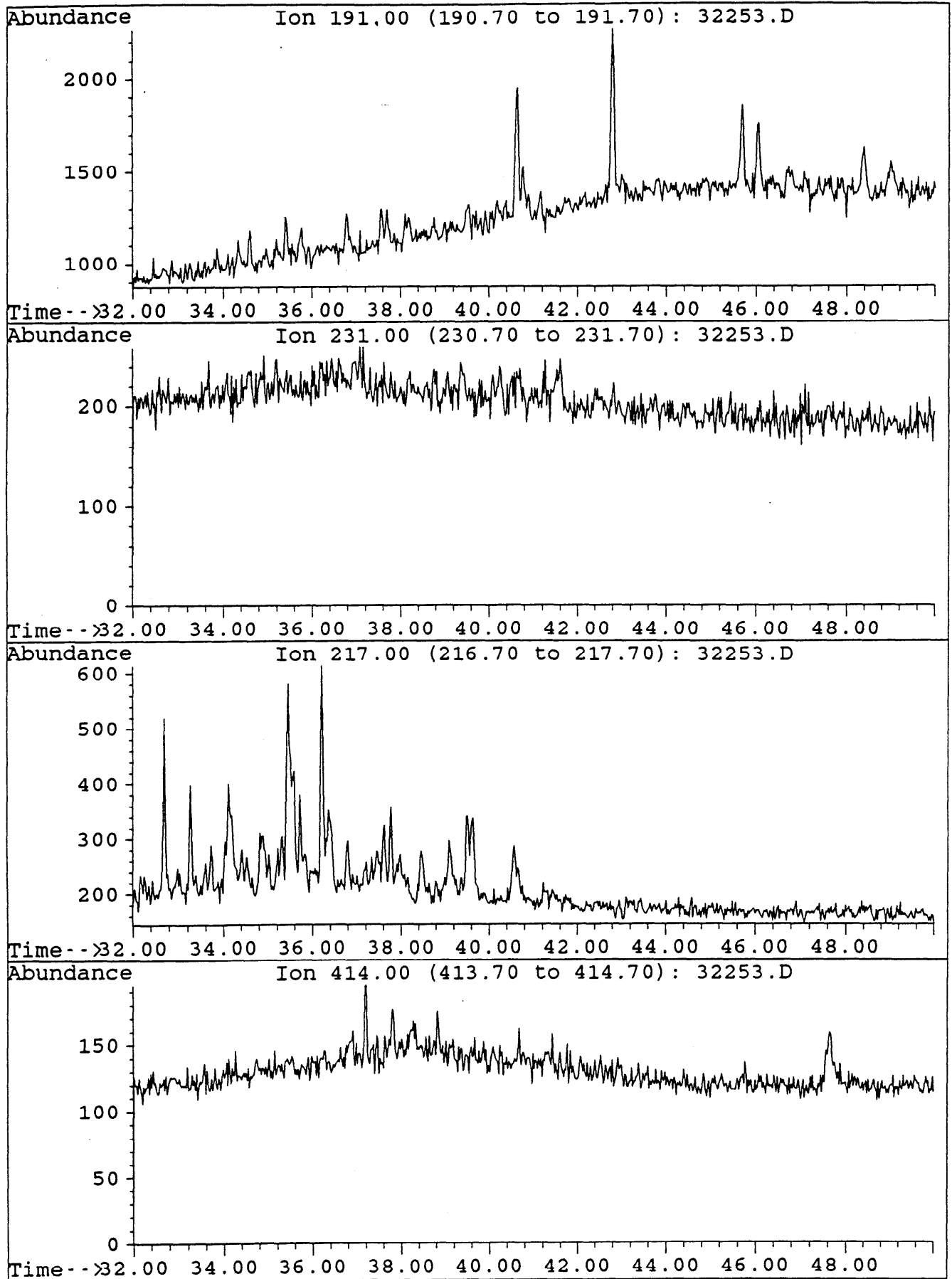




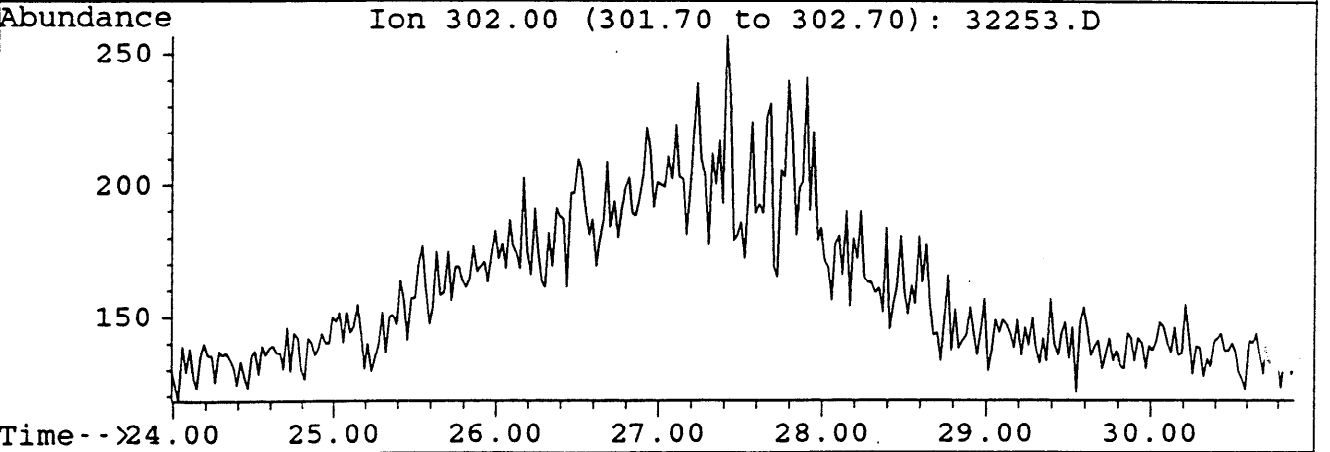
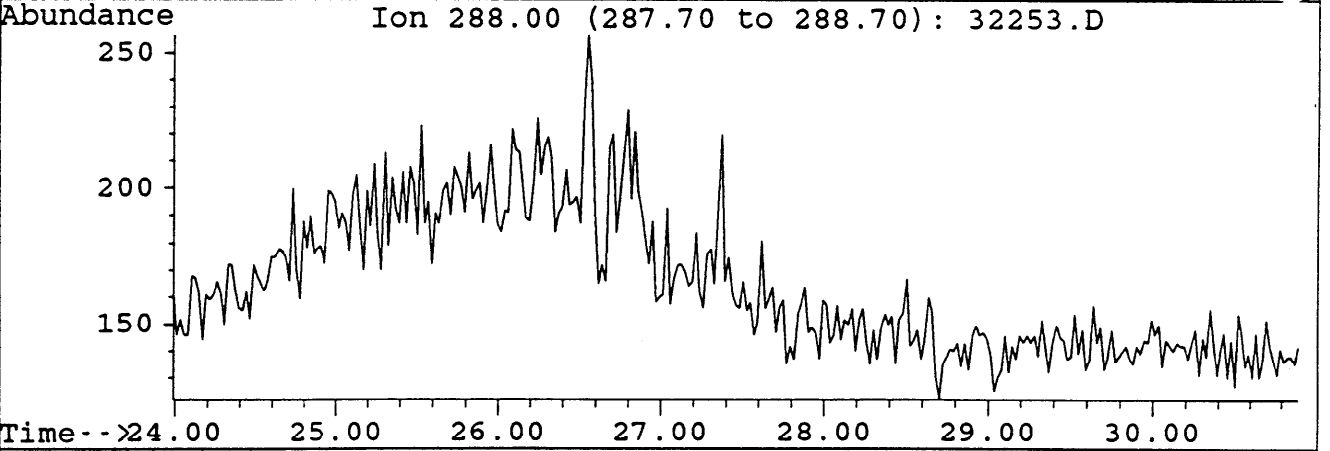
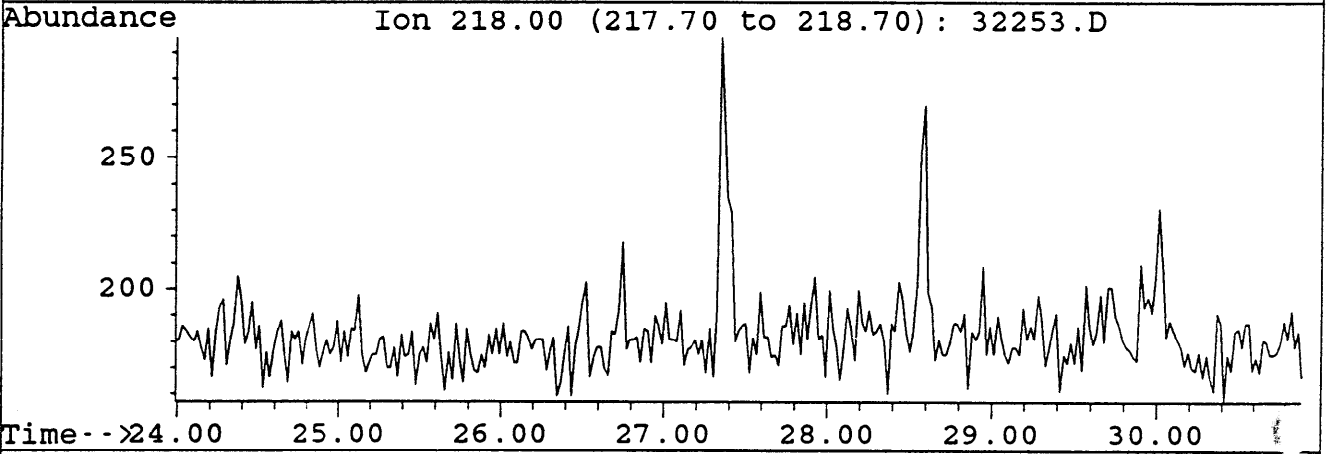
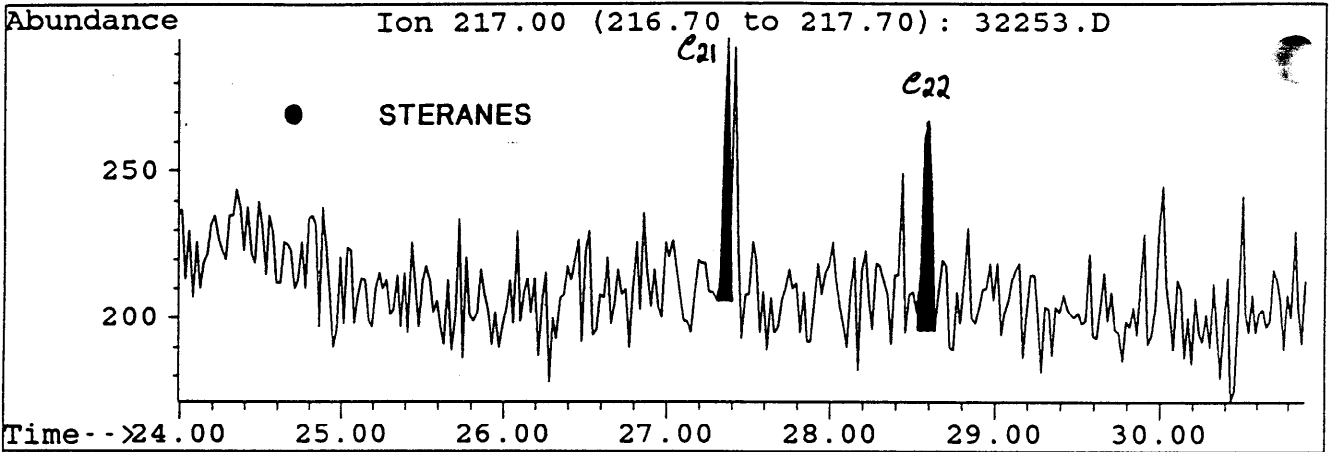
File : 32253.D  
Sample : MINERVA#1, RFS-AD-1157, L-008. COLD TRAP LIQ  
Misc. Info : COL#143. 17-1-94. GEC. B/C.



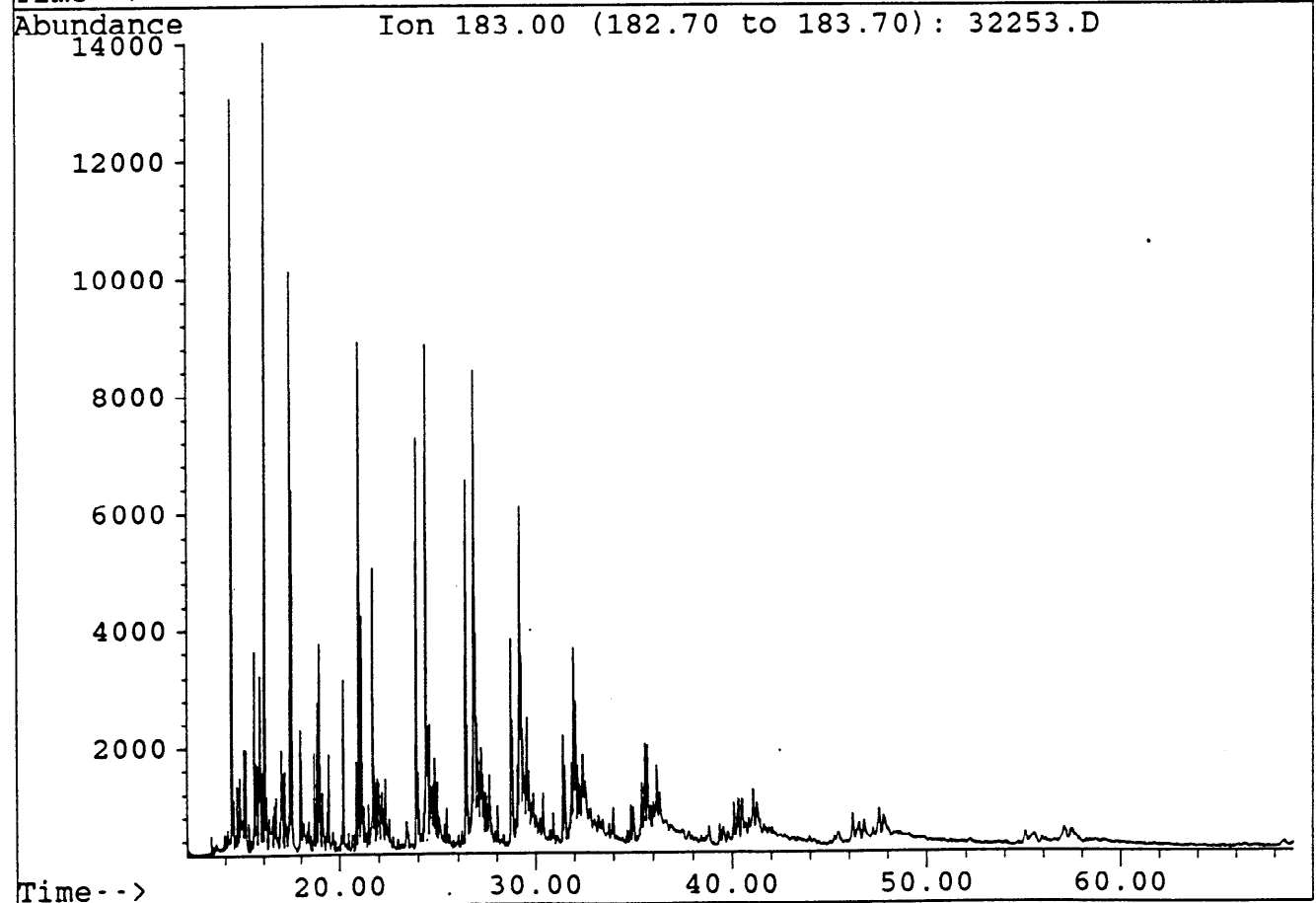
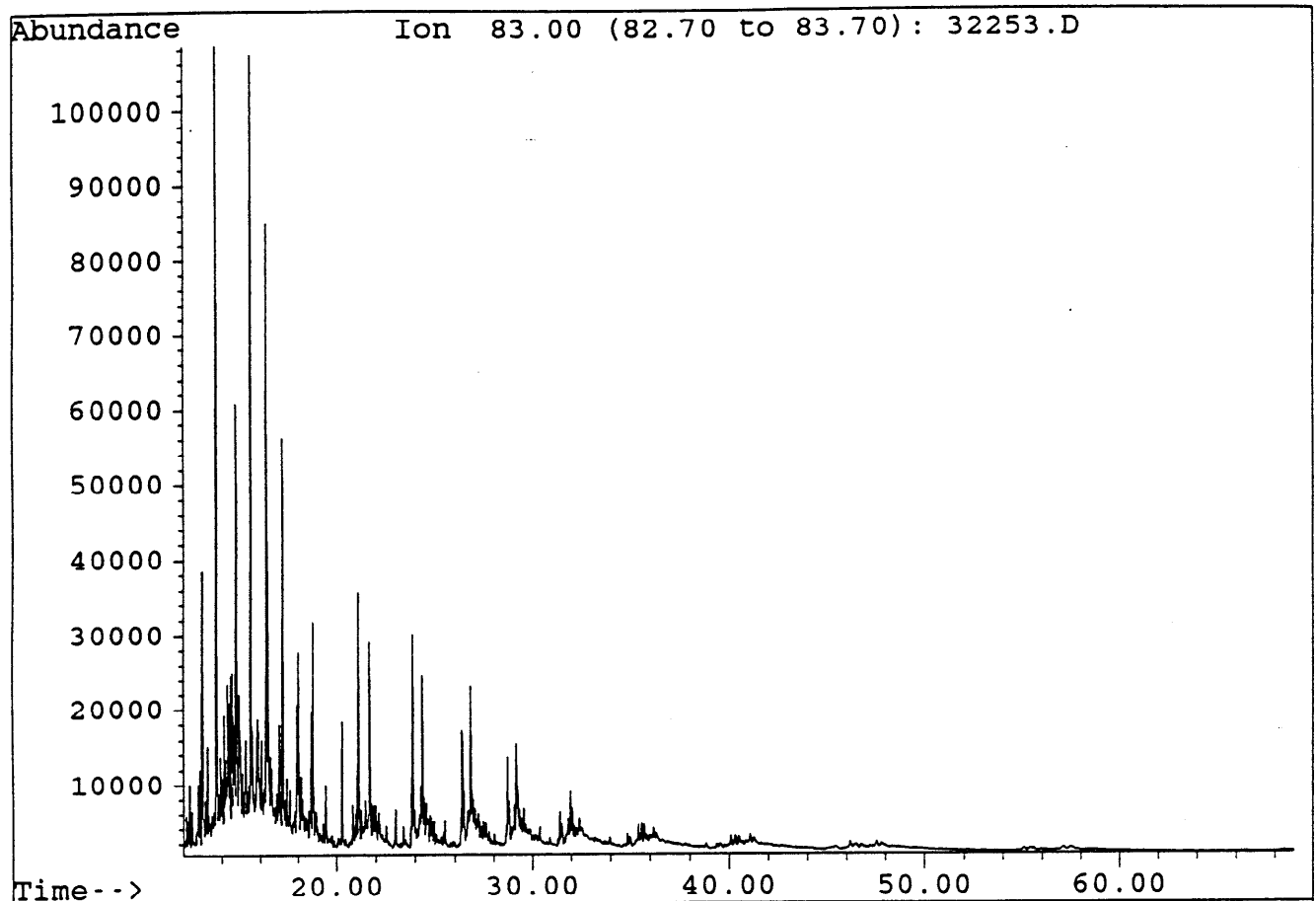
File : 32253.D  
Sample : MINERVA#1, RFS-AD-1157, L-008. COLD TRAP LIQ  
Misc. Info : COL#143. 17-1-94. GEC. B/C.



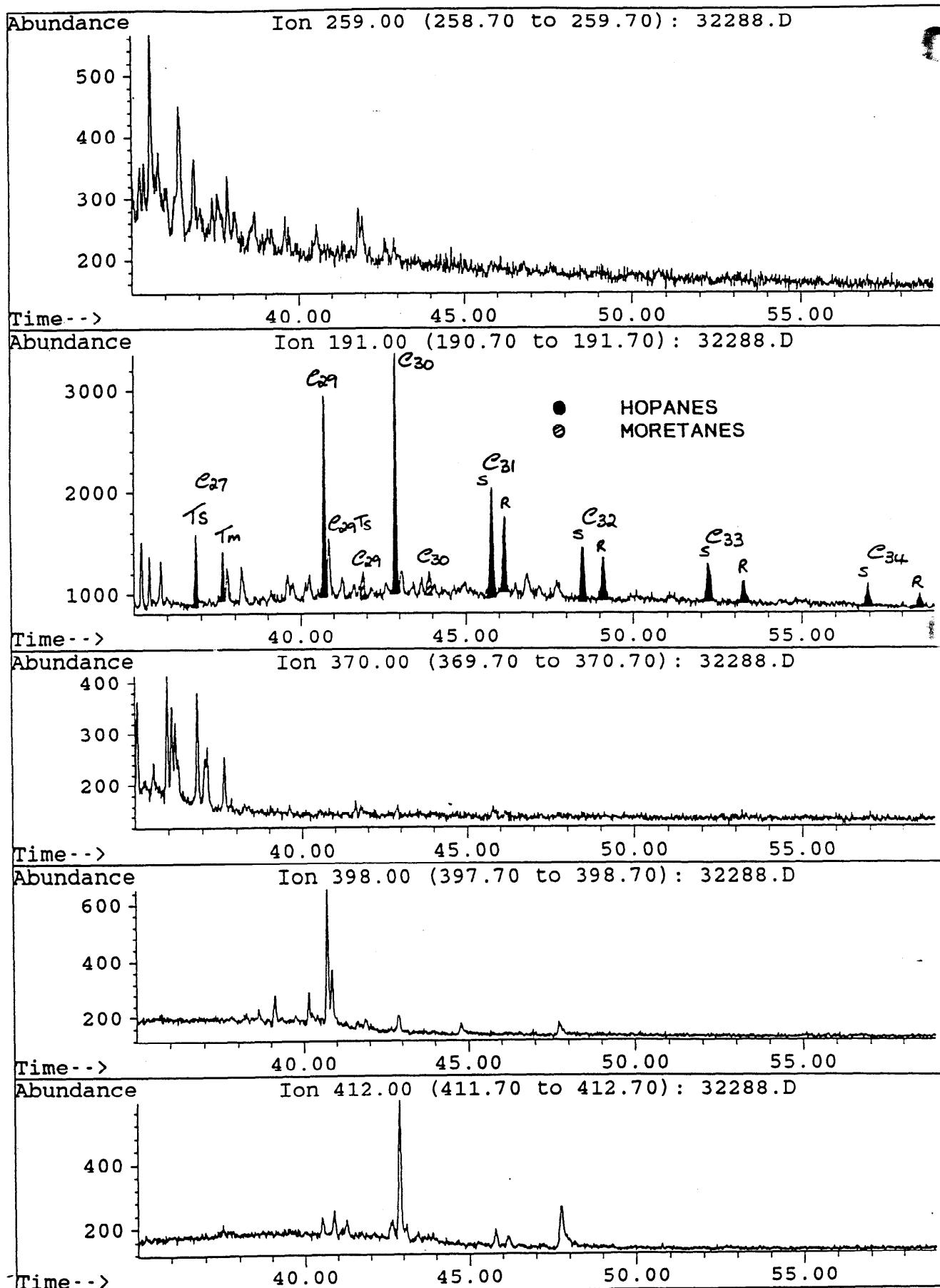
File : 32253.D  
Sample : MINERVA#1, RFS-AD-1157, L-008. COLD TRAP LIQ  
Misc. Info : COL#143. 17-1-94. GEC. B/C.



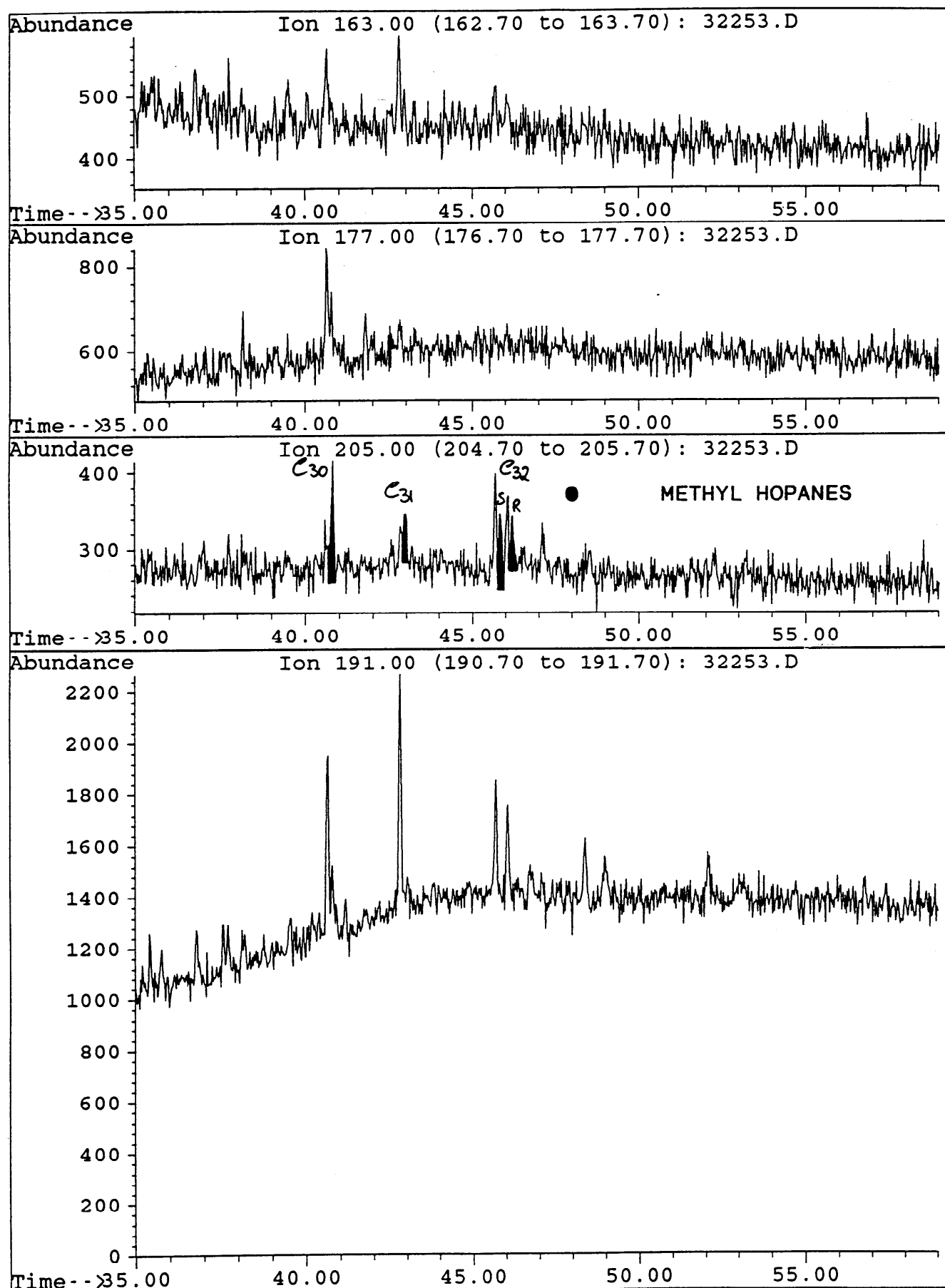
File : 32253.D  
Sample : MINERVA#1, RFS-AD-1157, L-008. COLD TRAP LIQ  
Misc. Info : COL#143. 17-1-94. GEC. B/C.



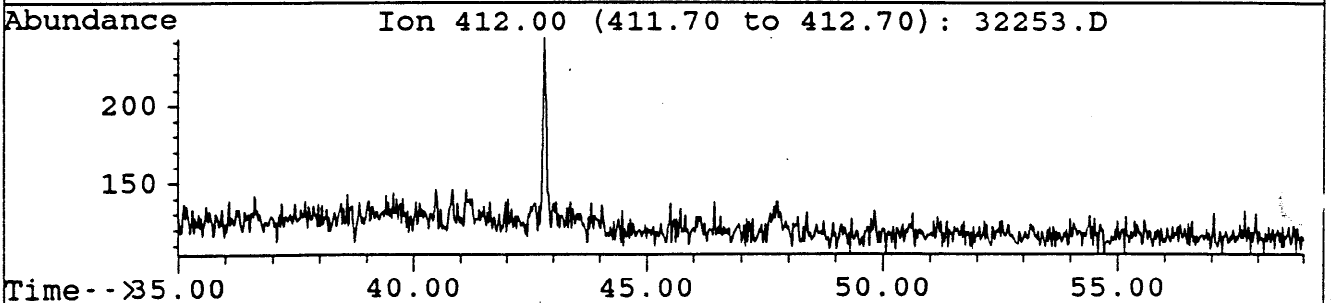
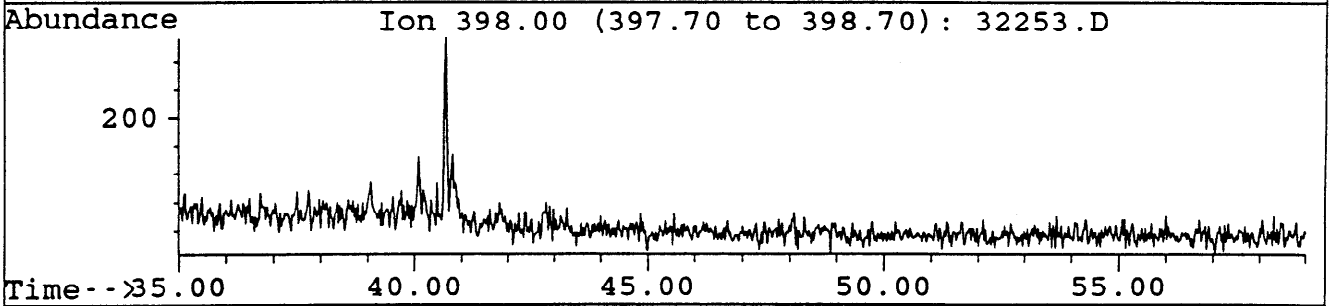
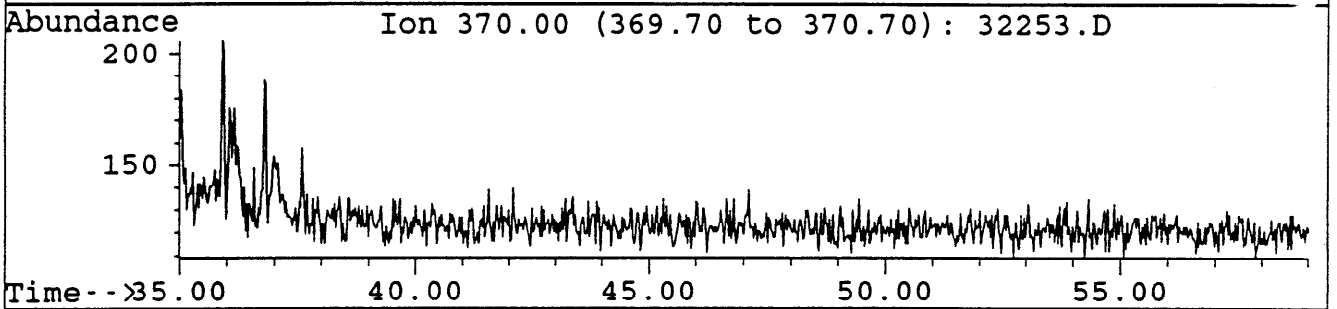
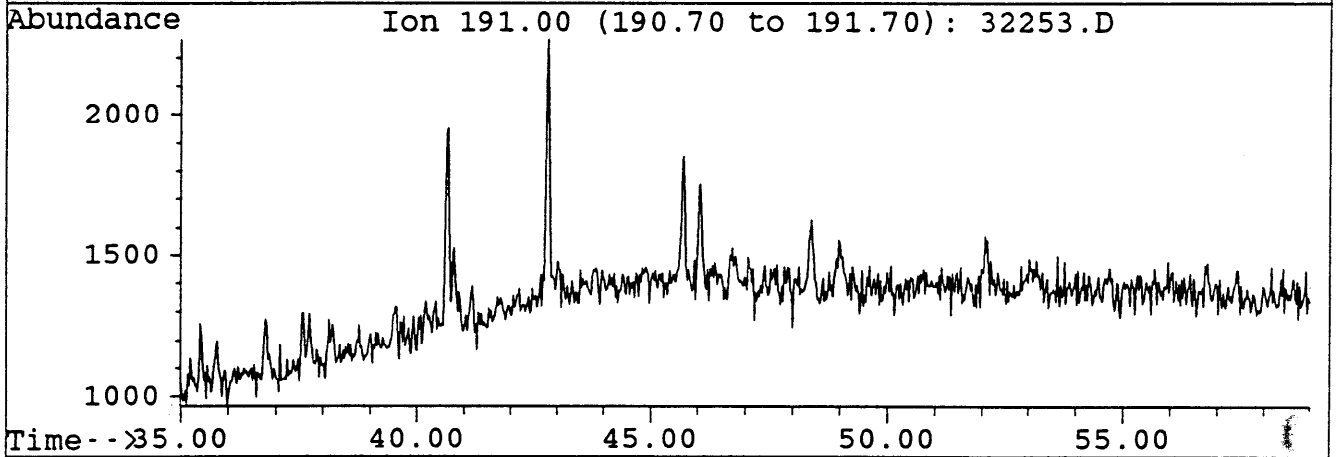
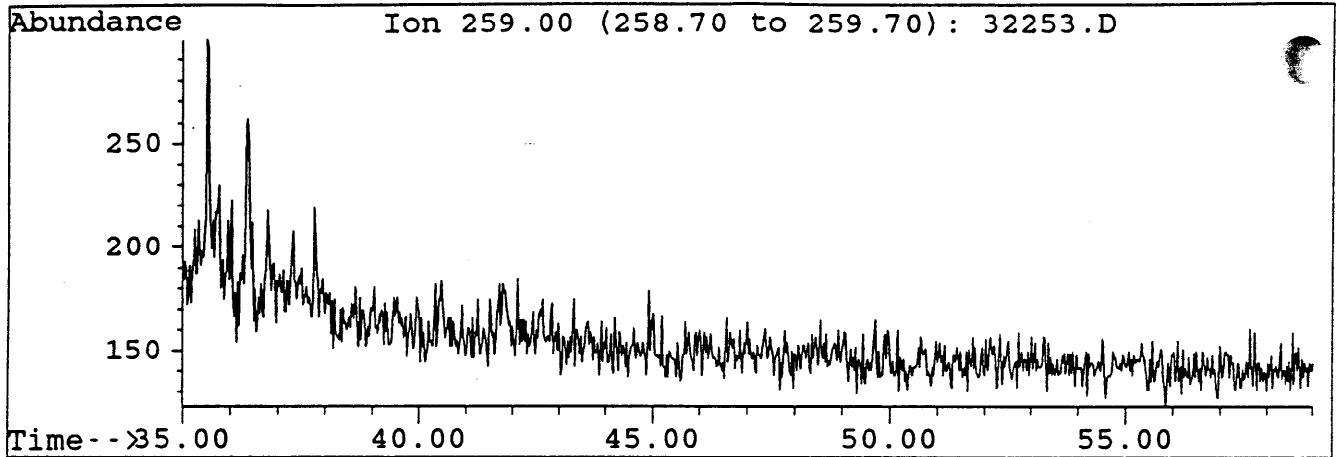
File : 32288.D  
Sample : MINERVA#1, RFS-AD-1157. L-008. TOPPED. B/C  
Misc. Info : COL#143. GEC. 25-1-94.



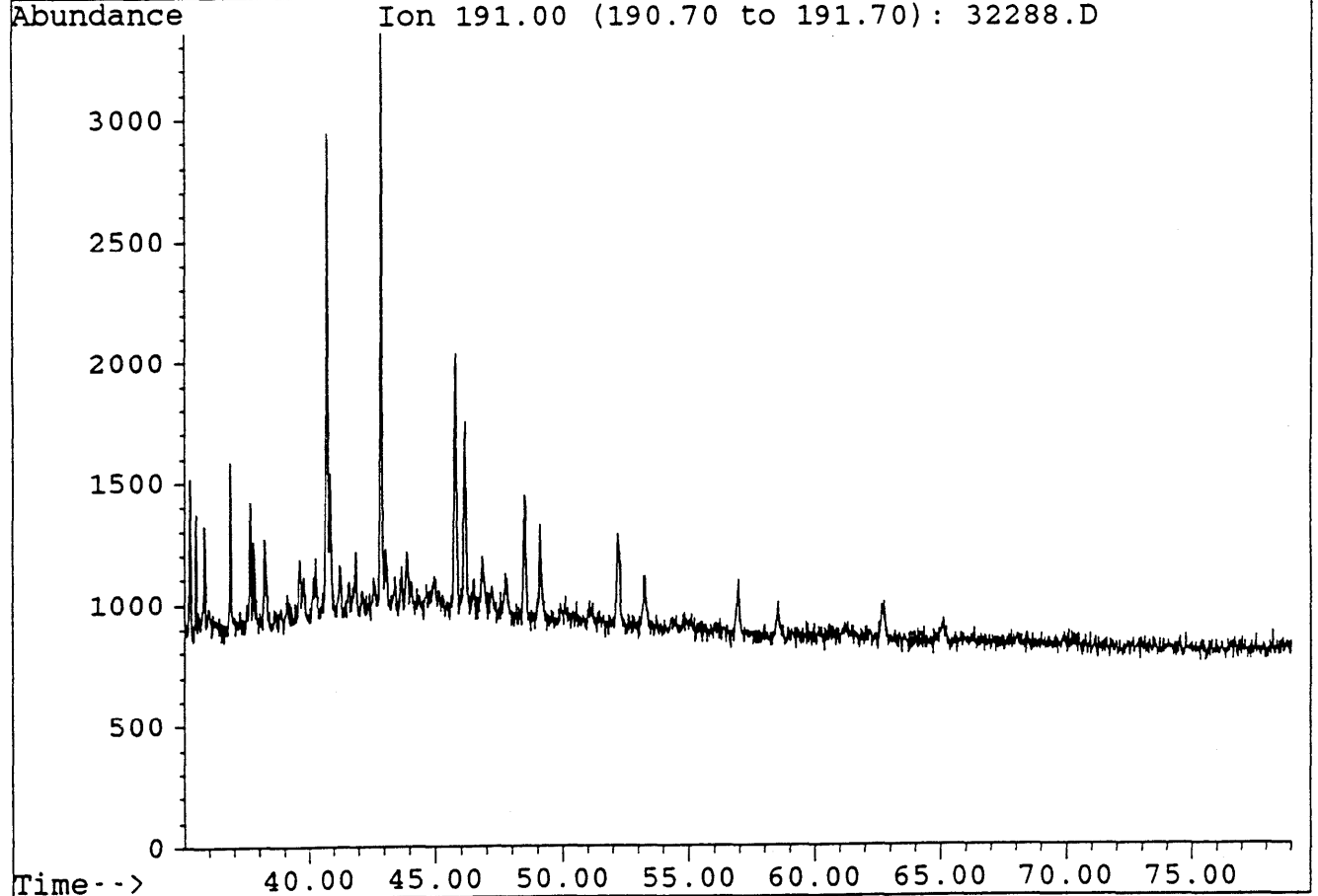
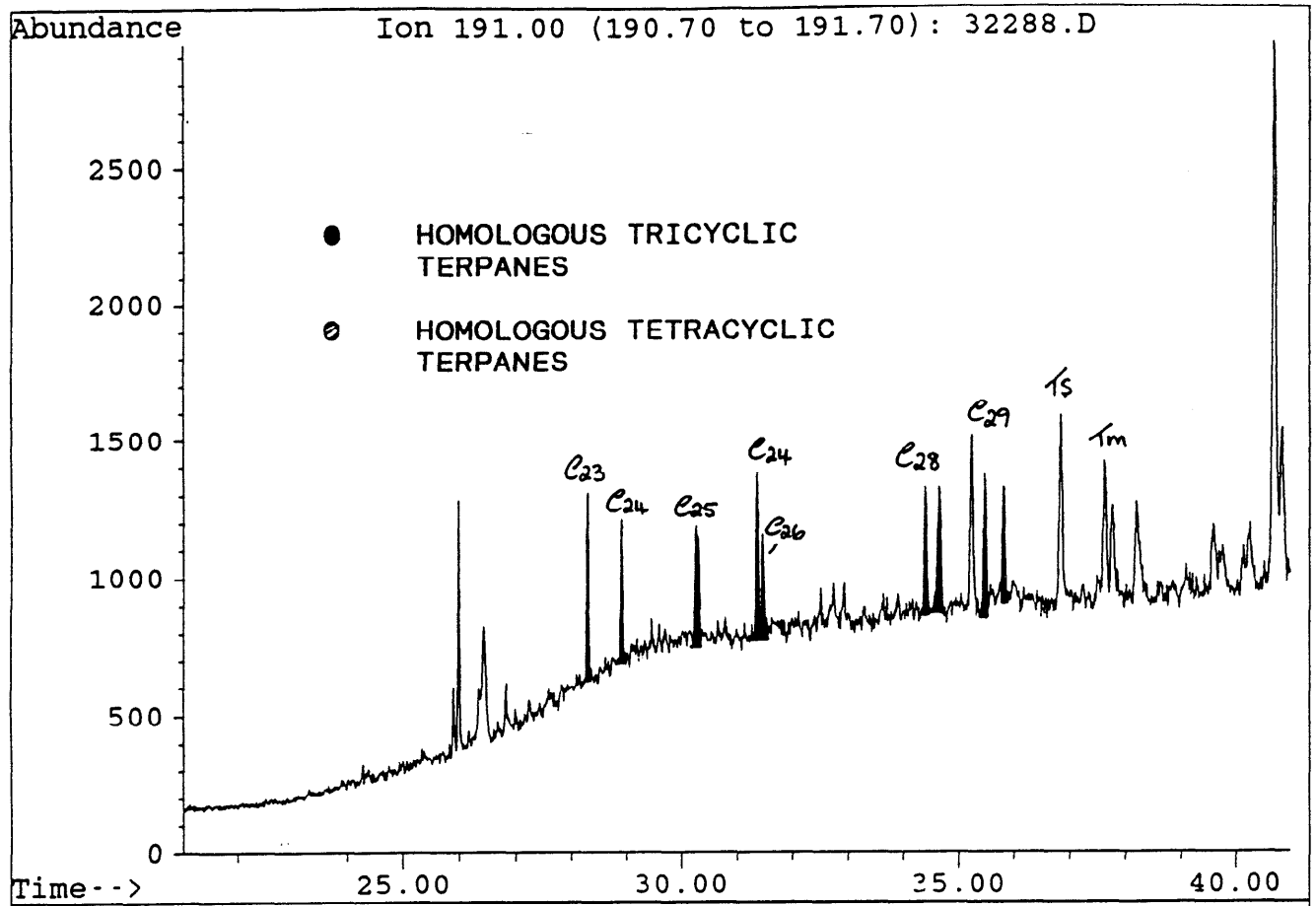
File : 32253.D  
Sample : MINERVA#1, RFS-AD-1157, L-008. COLD TRAP LIQ  
Misc. Info : COL#143. 17-1-94. GEC. B/C.



File : 32253.D  
Sample : MINERVA#1, RFS-AD-1157, L-008. COLD TRAP LIQ  
Misc. Info : COL#143. 17-1-94. GEC. B/C.

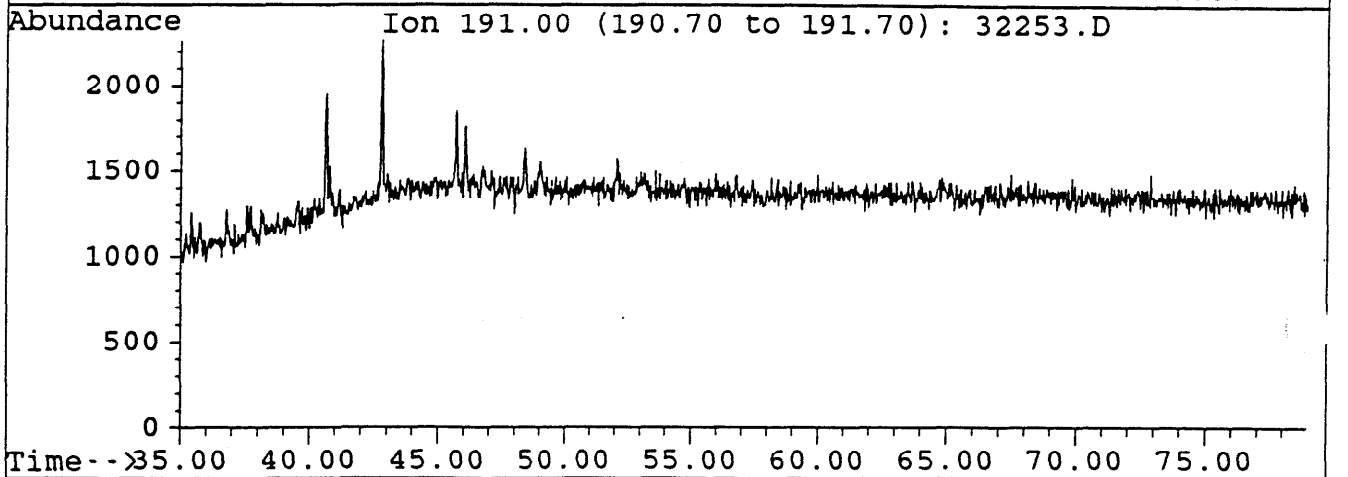
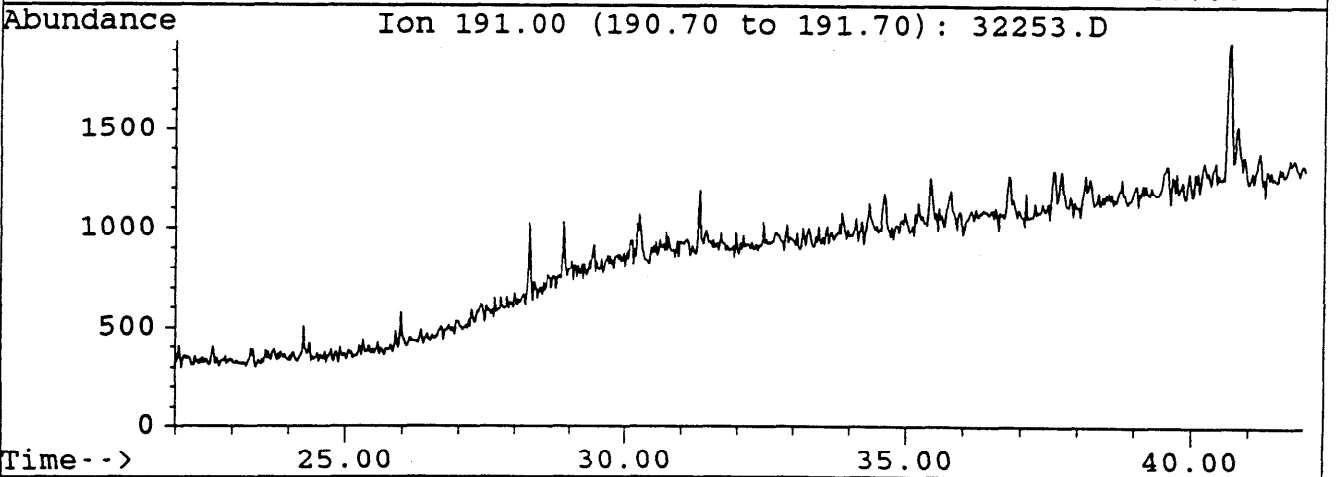
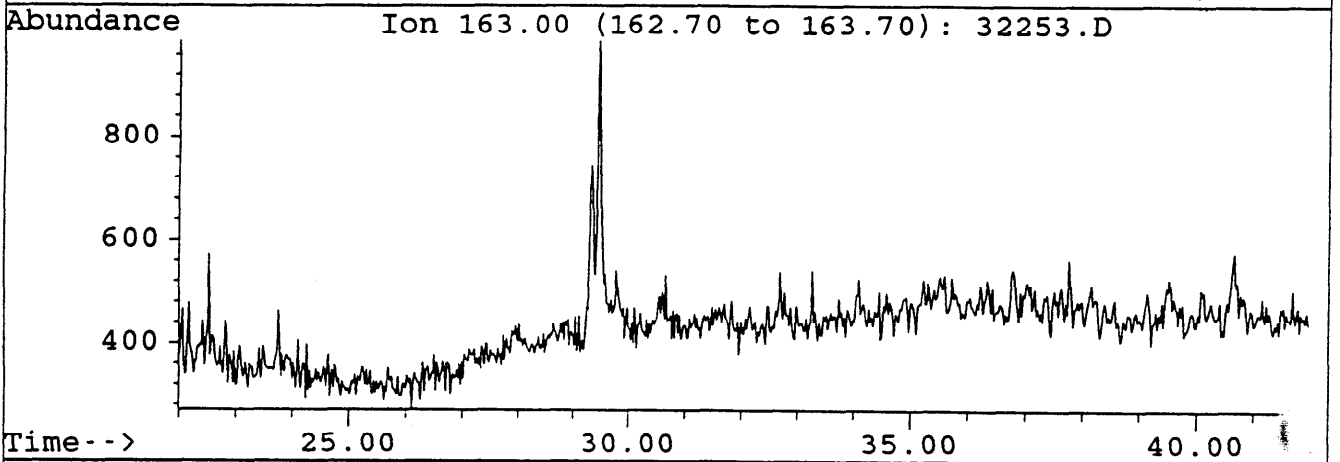
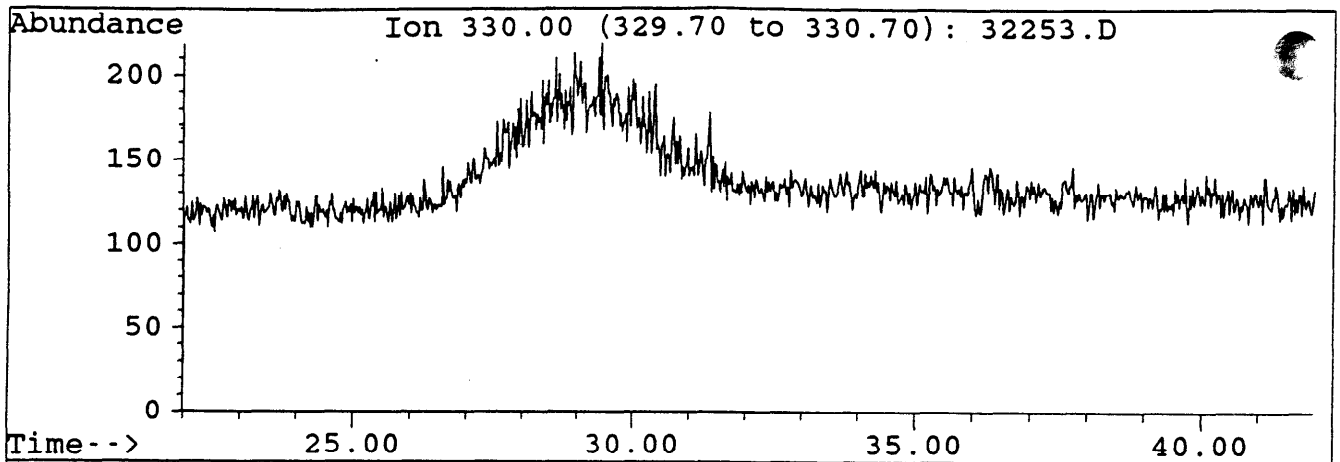


File : 32288.D  
Sample : MINERVA#1, RFS-AD-1157. L-008. TOPPED. B/C  
Misc. Info : COL#143. GEC. 25-1-94.

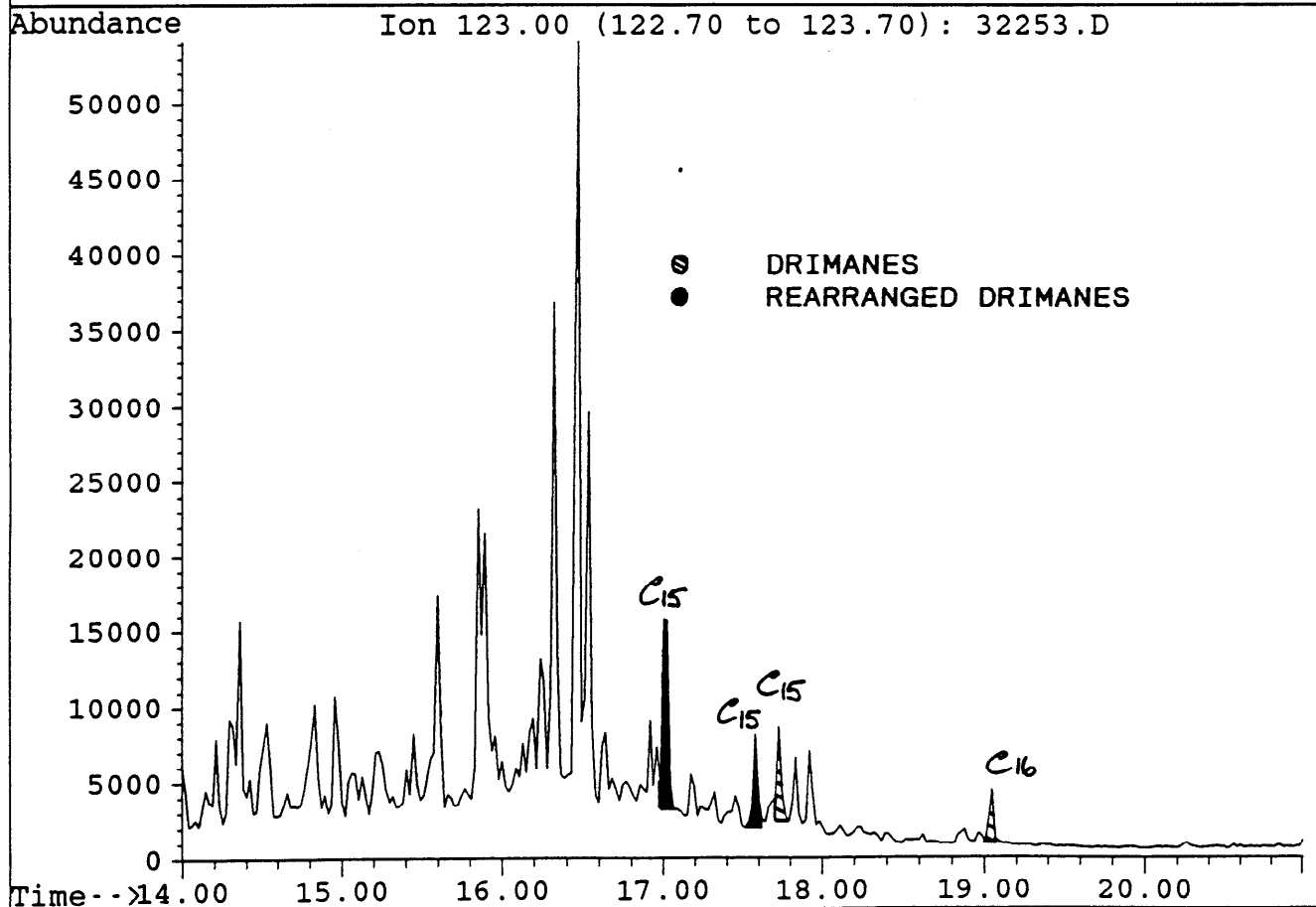
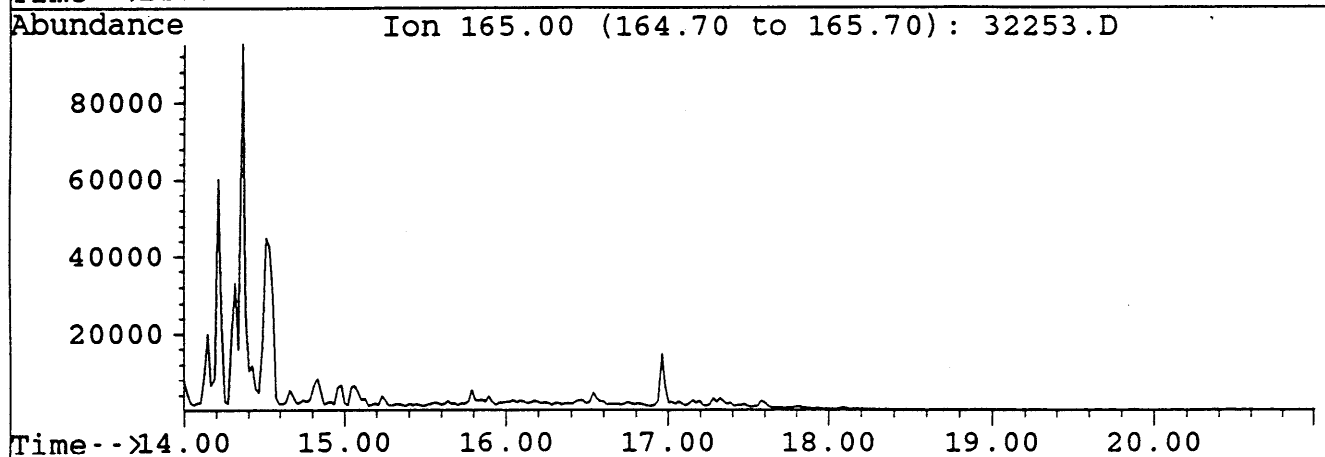
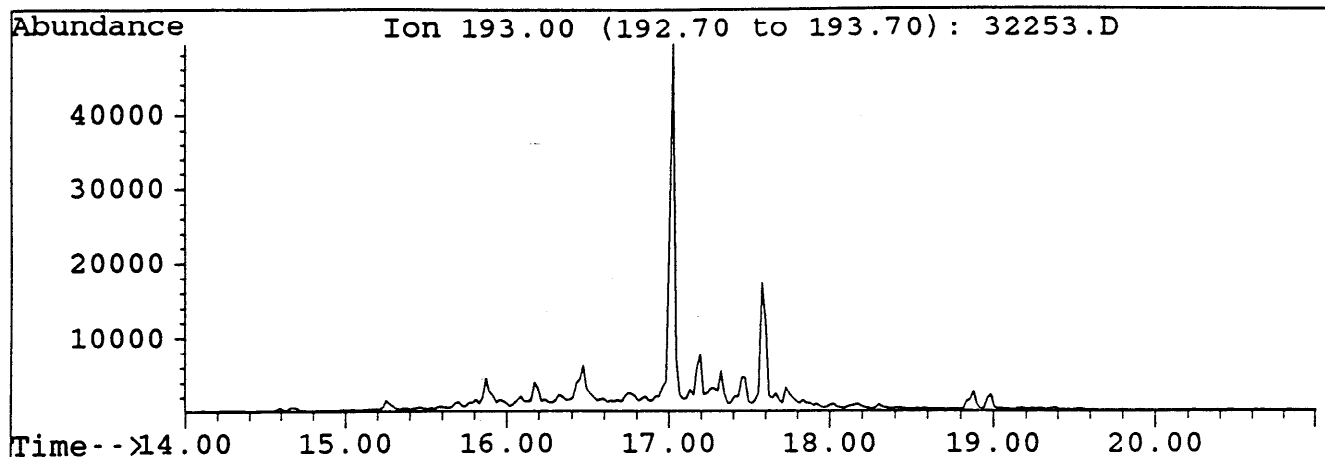




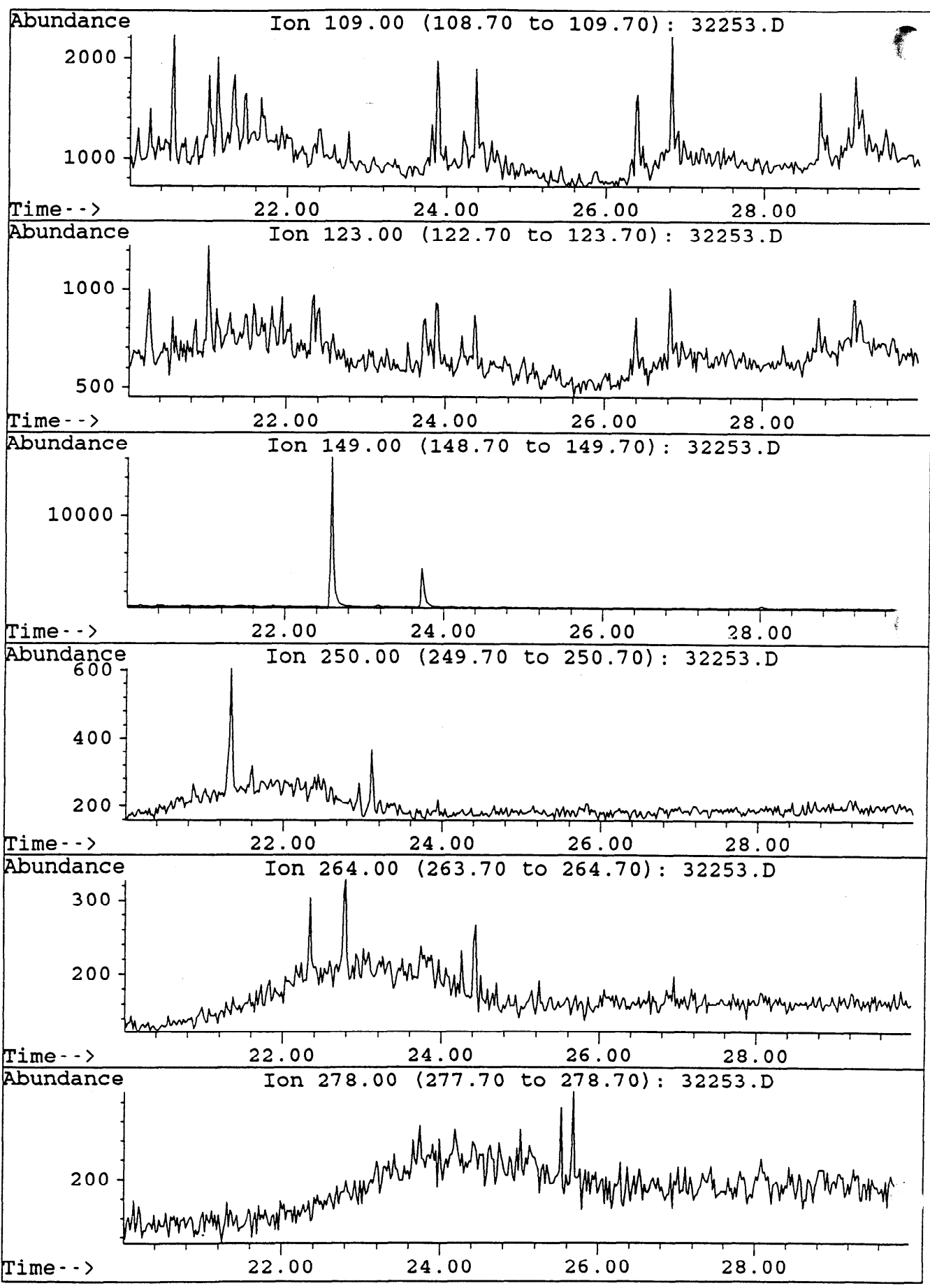
File : 32253.D  
Sample : MINERVA#1, RFS-AD-1157, L-008. COLD TRAP LIQ  
Misc. Info : COL#143. 17-1-94. GEC. B/C.



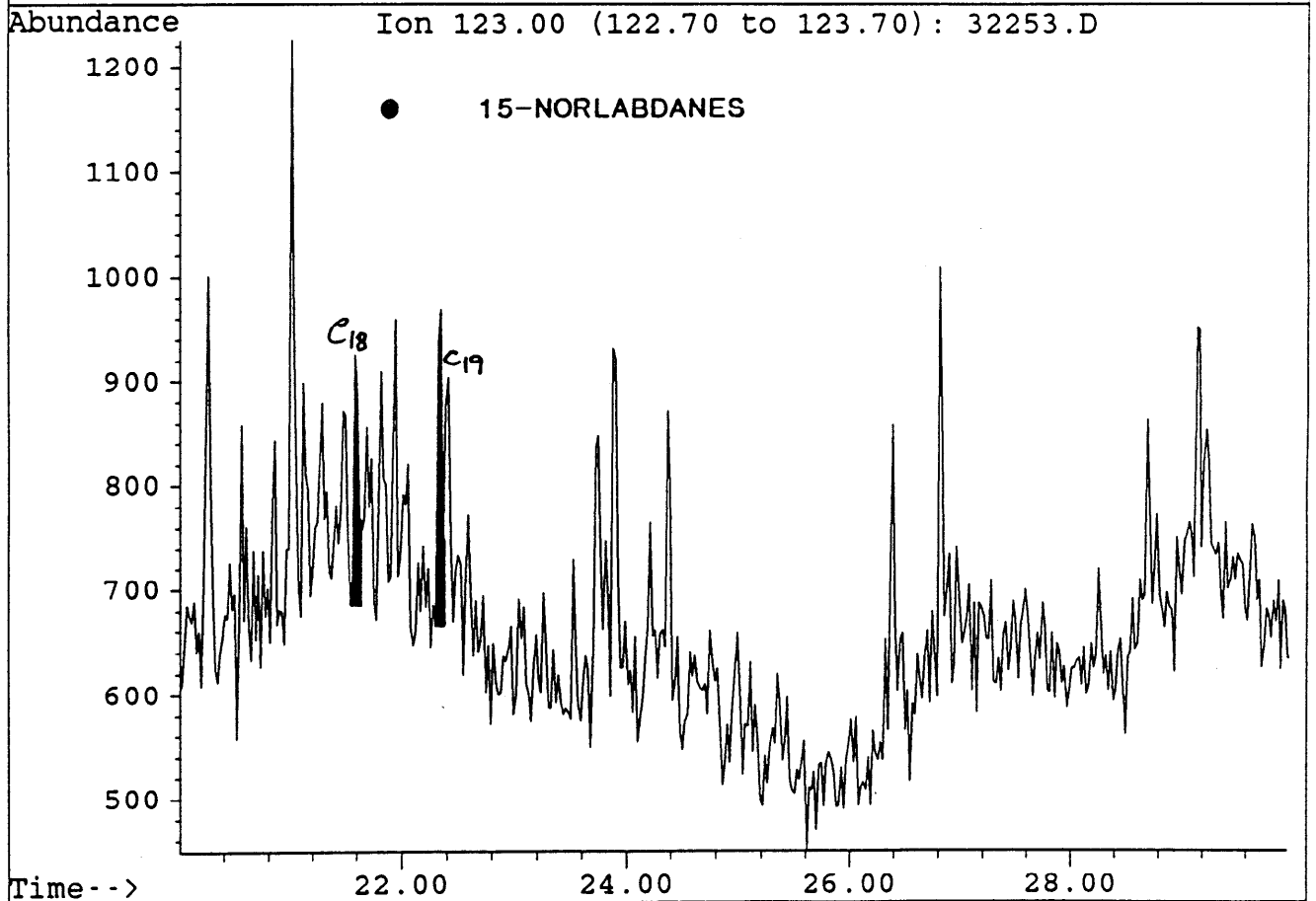
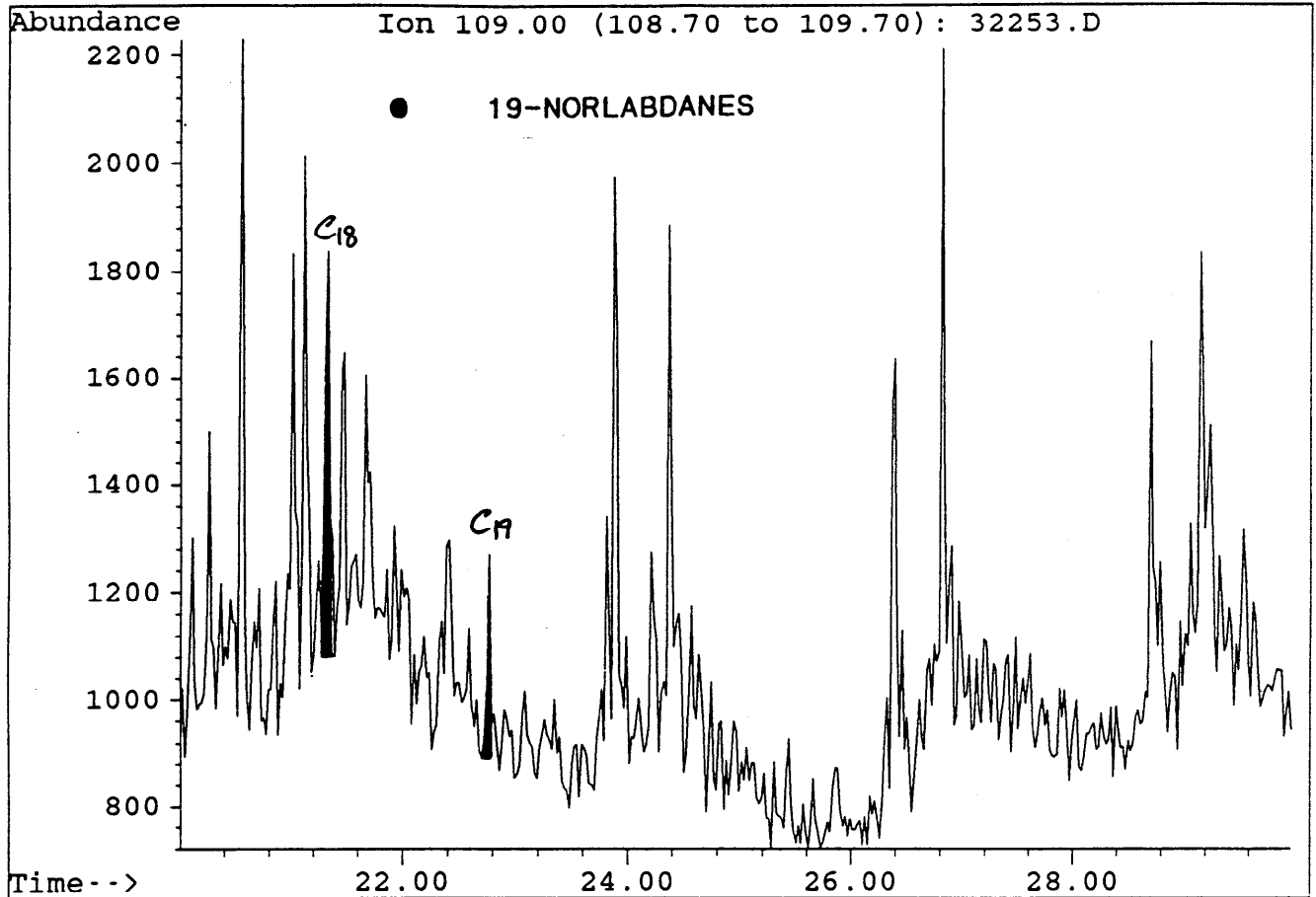
File : 32253.D  
Sample : MINERVA#1, RFS-AD-1157, L-008. COLD TRAP LIQ  
Misc. Info : COL#143. 17-1-94. GEC. B/C.



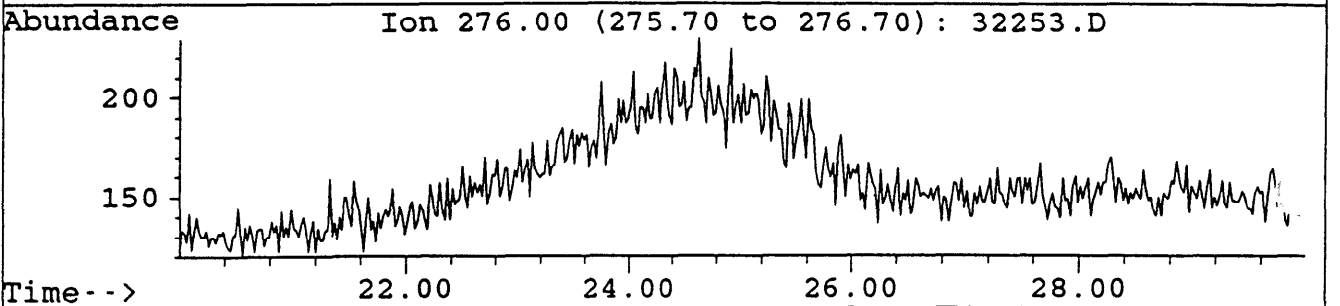
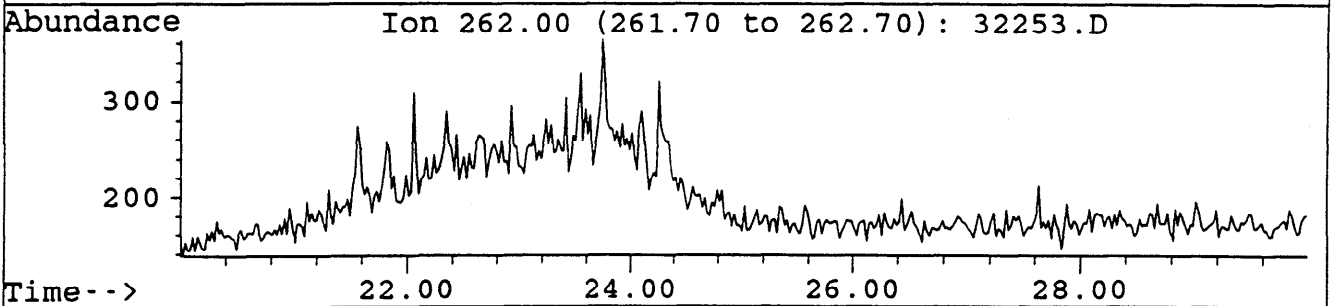
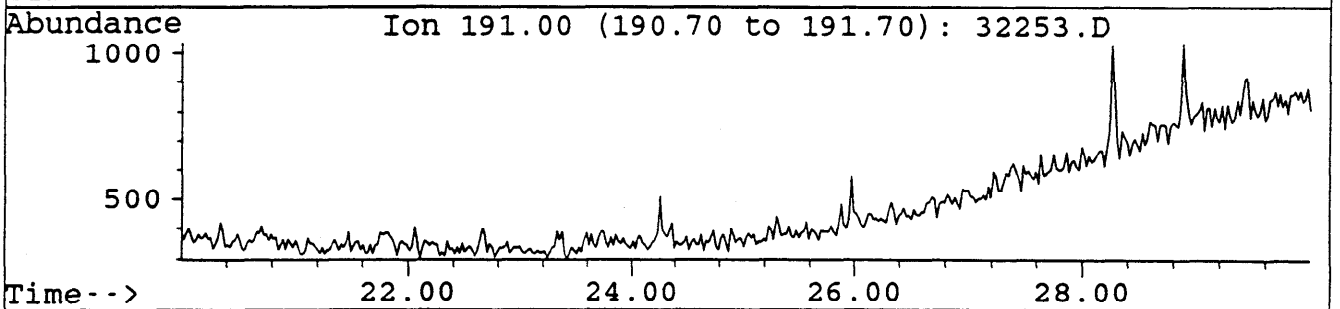
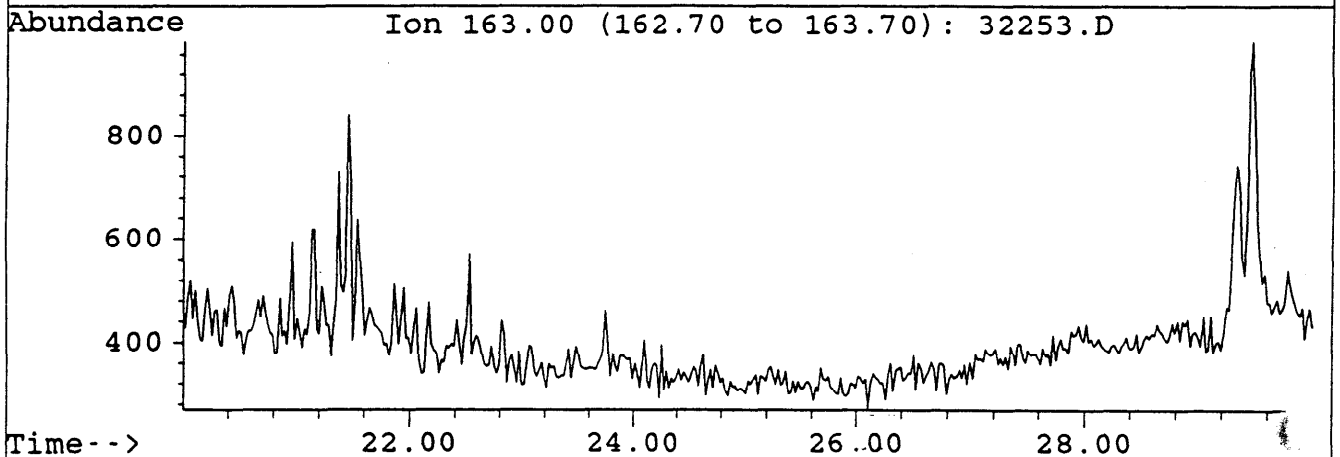
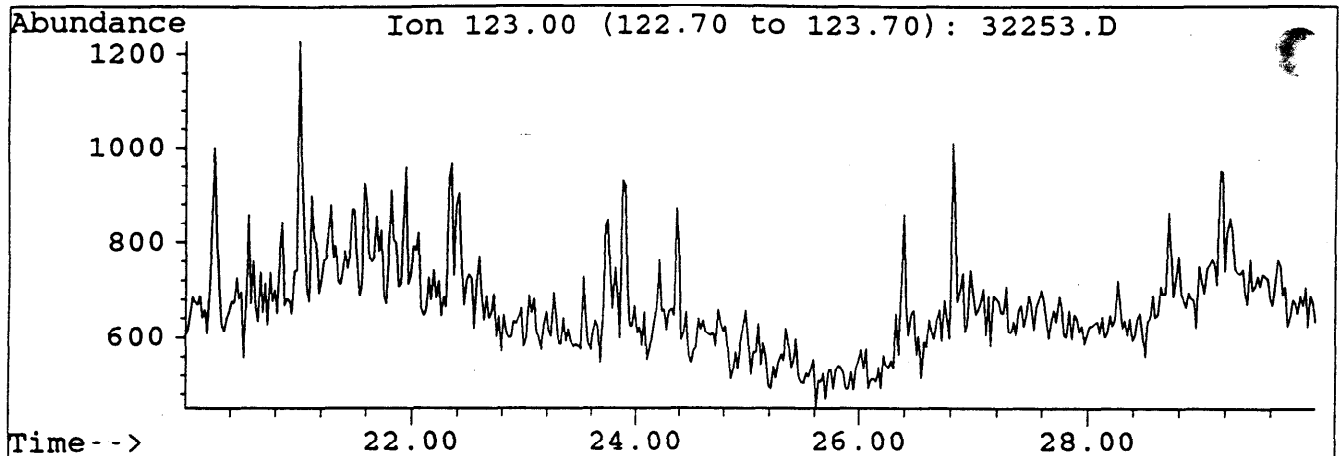
File : 32253.D  
Sample : MINERVA#1, RFS-AD-1157, L-008. COLD TRAP LIQ  
Misc. Info : COL#143. 17-1-94. GEC. B/C.



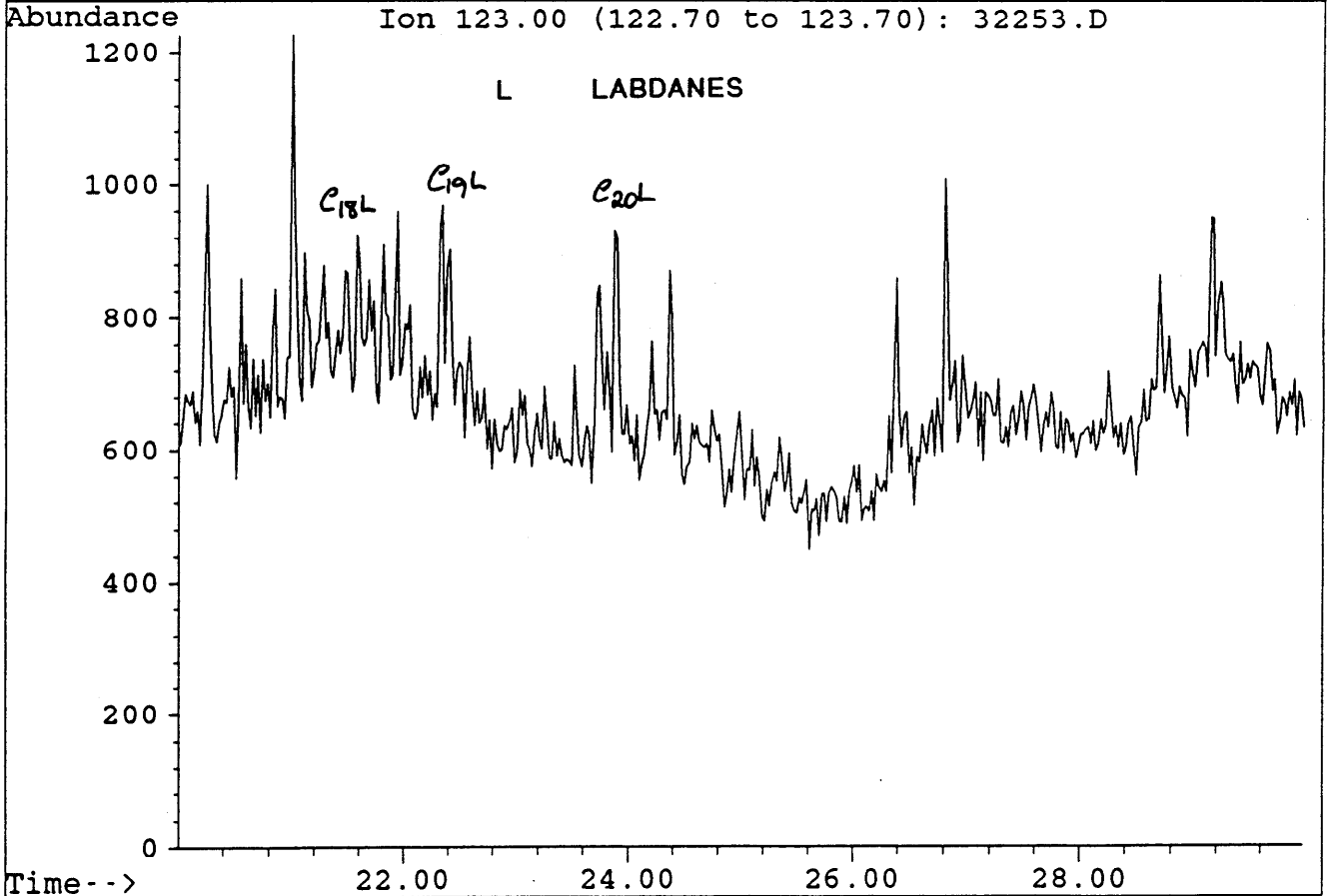
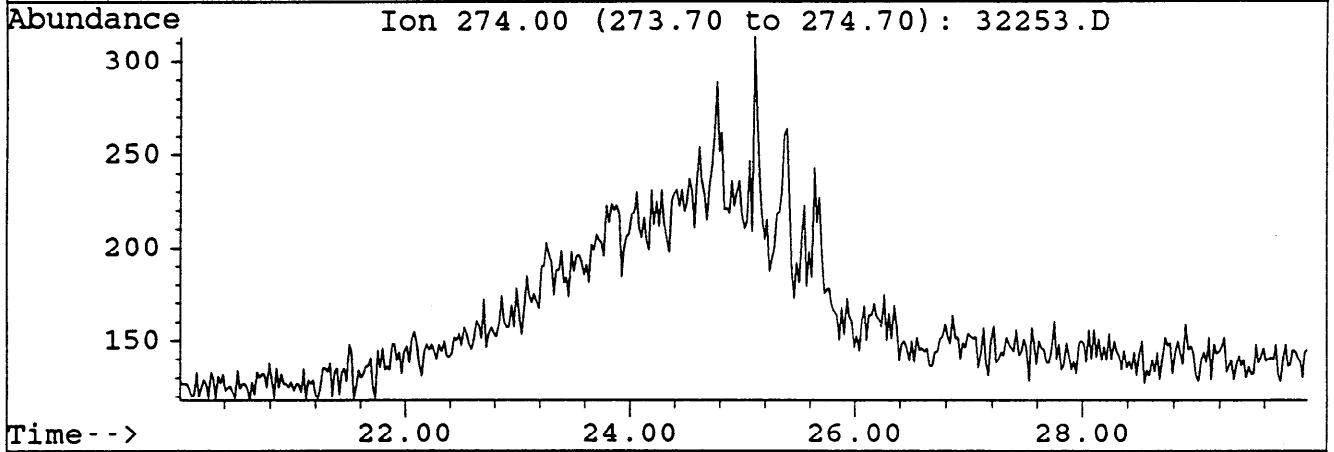
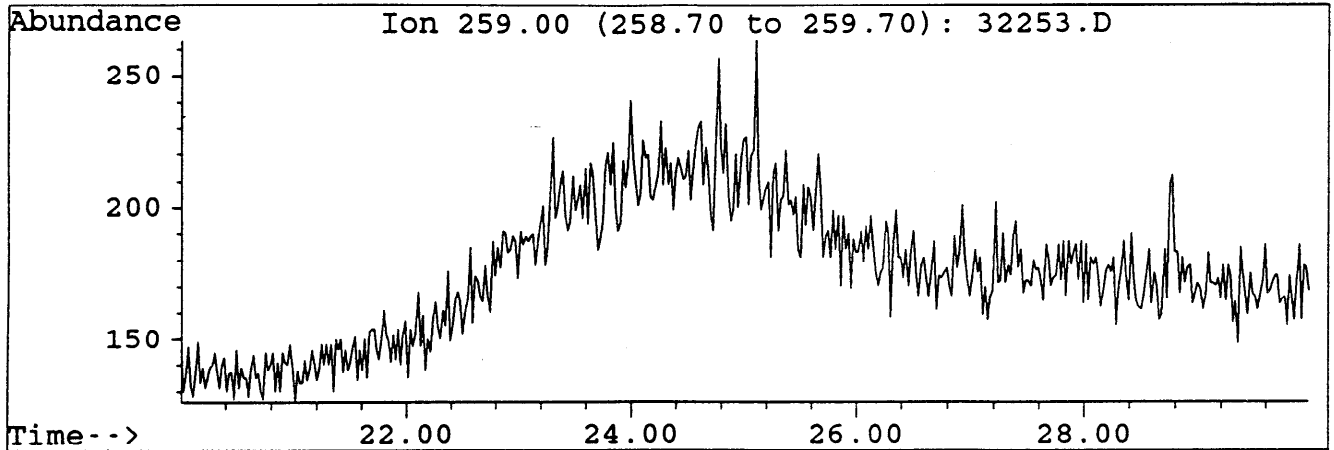
File : 32253.D  
Sample : MINERVA#1, RFS-AD-1157, L-008. COLD TRAP LIQ  
Misc. Info : COL#143. 17-1-94. GEC. B/C.



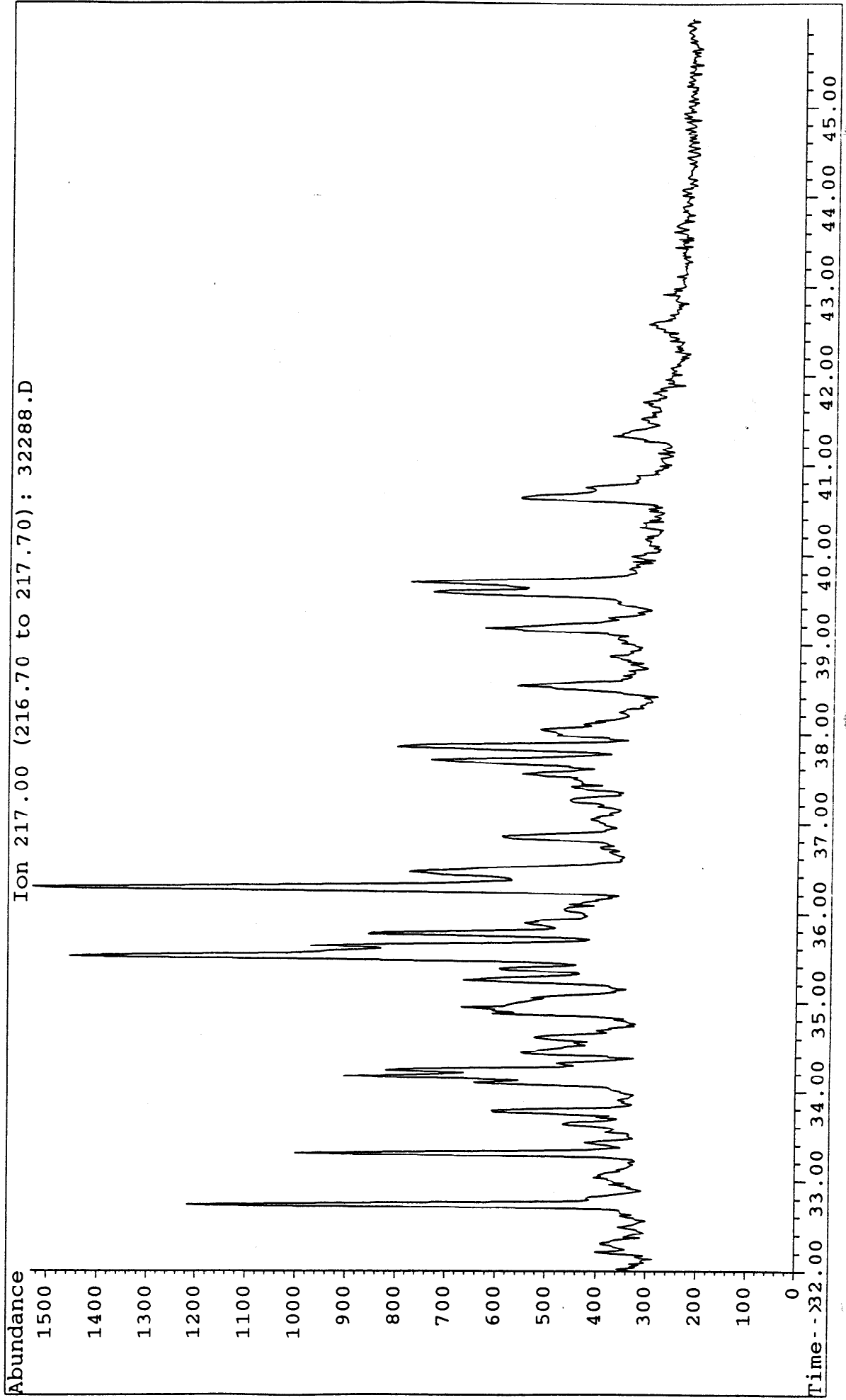
File : 32253.D  
Sample : MINERVA#1, RFS-AD-1157, L-008. COLD TRAP LIQ  
Misc. Info : COL#143. 17-1-94. GEC. B/C.



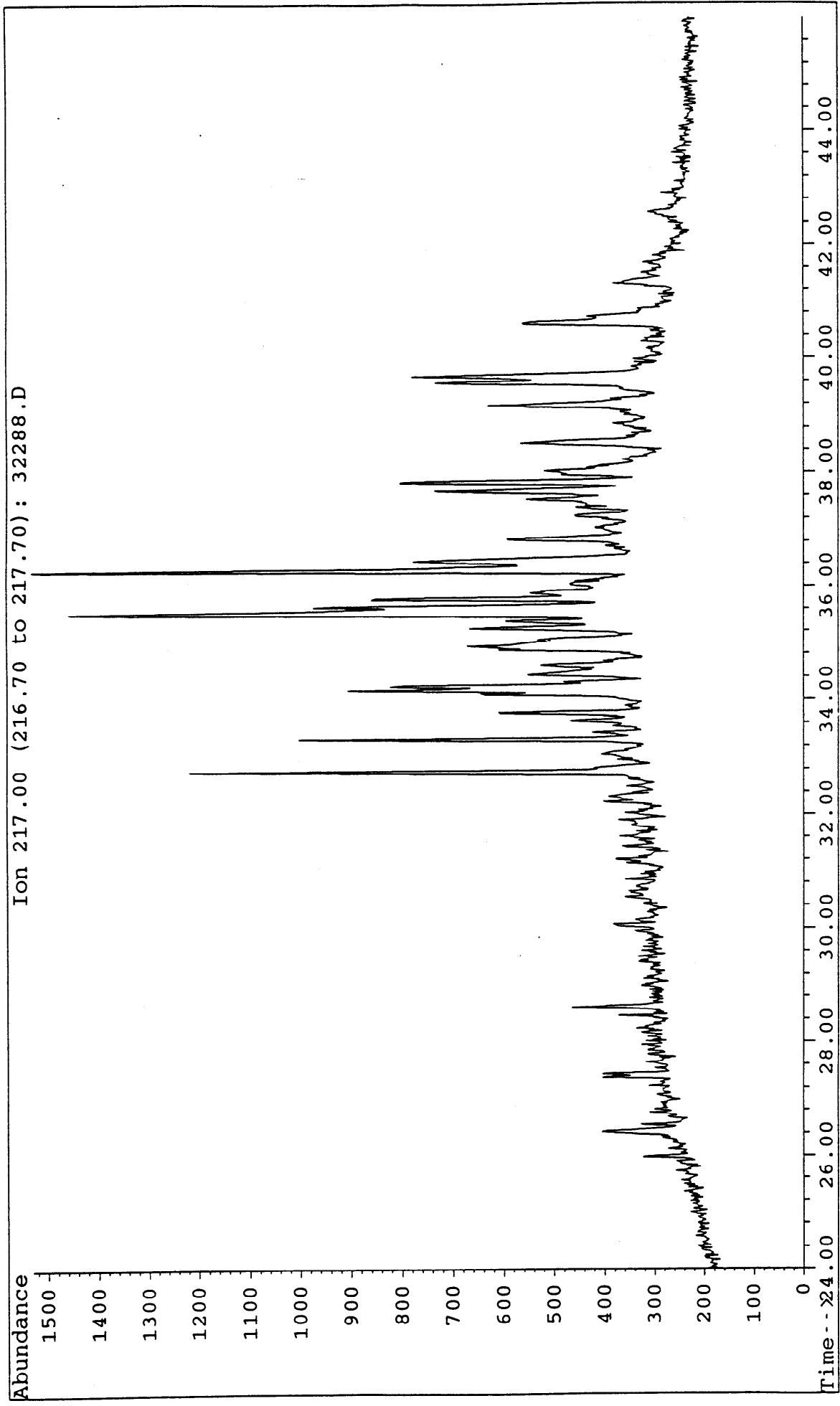
File : 32253.D  
Sample : MINERVA#1, RFS-AD-1157, L-008. COLD TRAP LIQ  
Misc. Info : COL#143. 17-1-94. GEC. B/C.



File : 32288.D  
Sample : MINERVA#1, RFS-AD-1157. L-008. TOPPED. B/C  
Misc. Info : COL#143. GEC. 25-1-94.

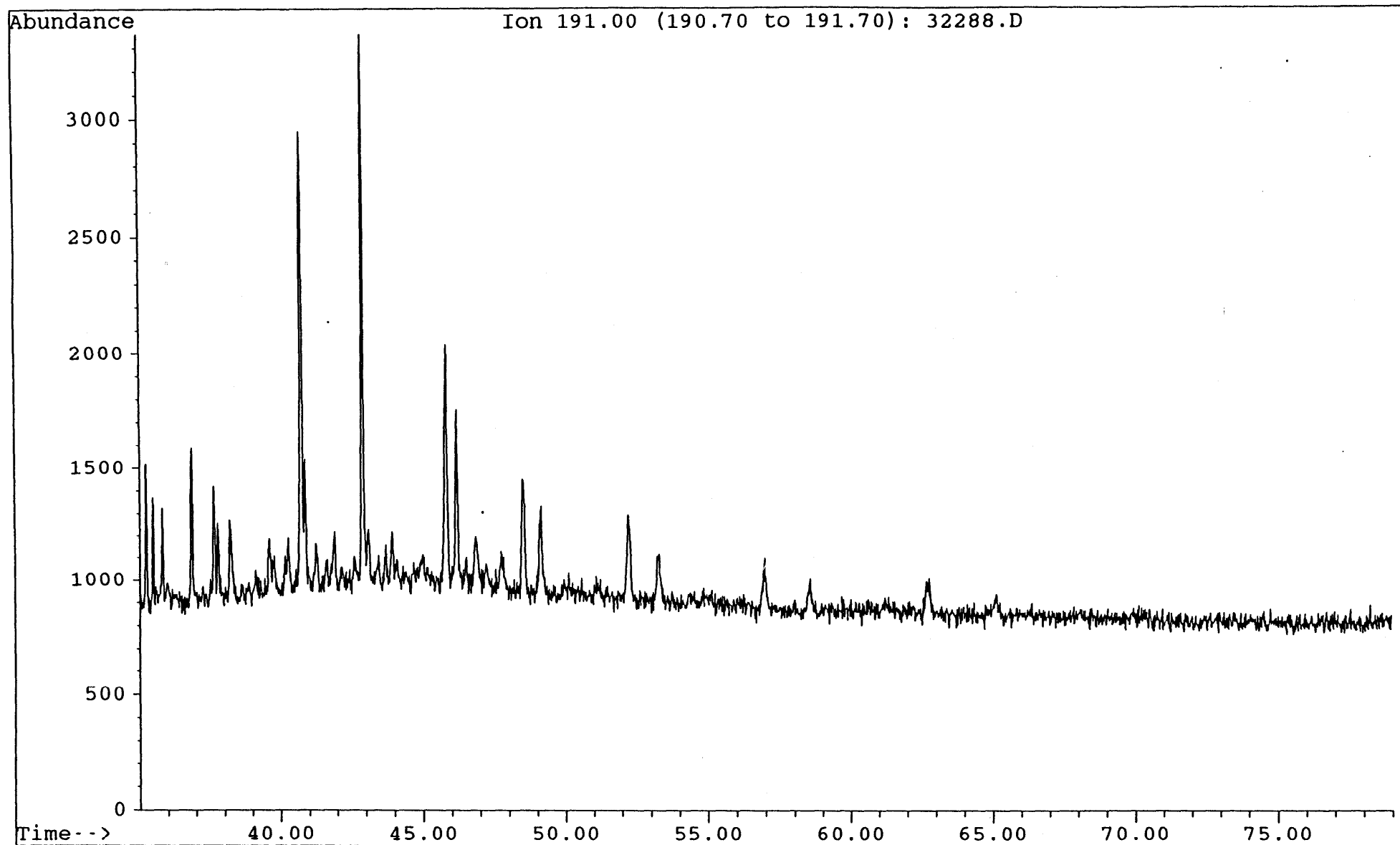


File : 32288.D  
Sample : MINERVA#1, RFS-AD-1157. L-008. TOPPED. B/C  
Misc. Info : COL#143. GEC. 25-1-94.

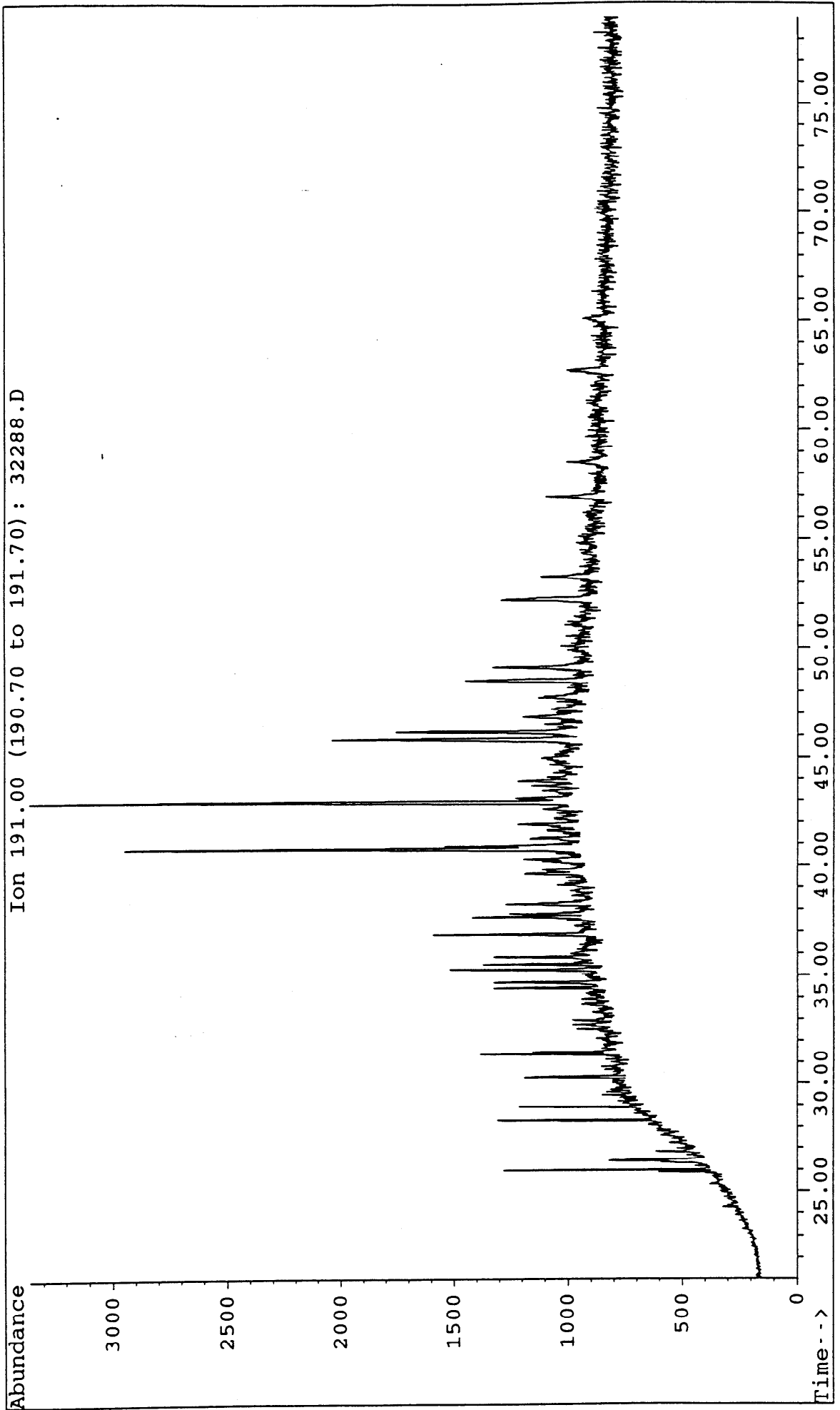


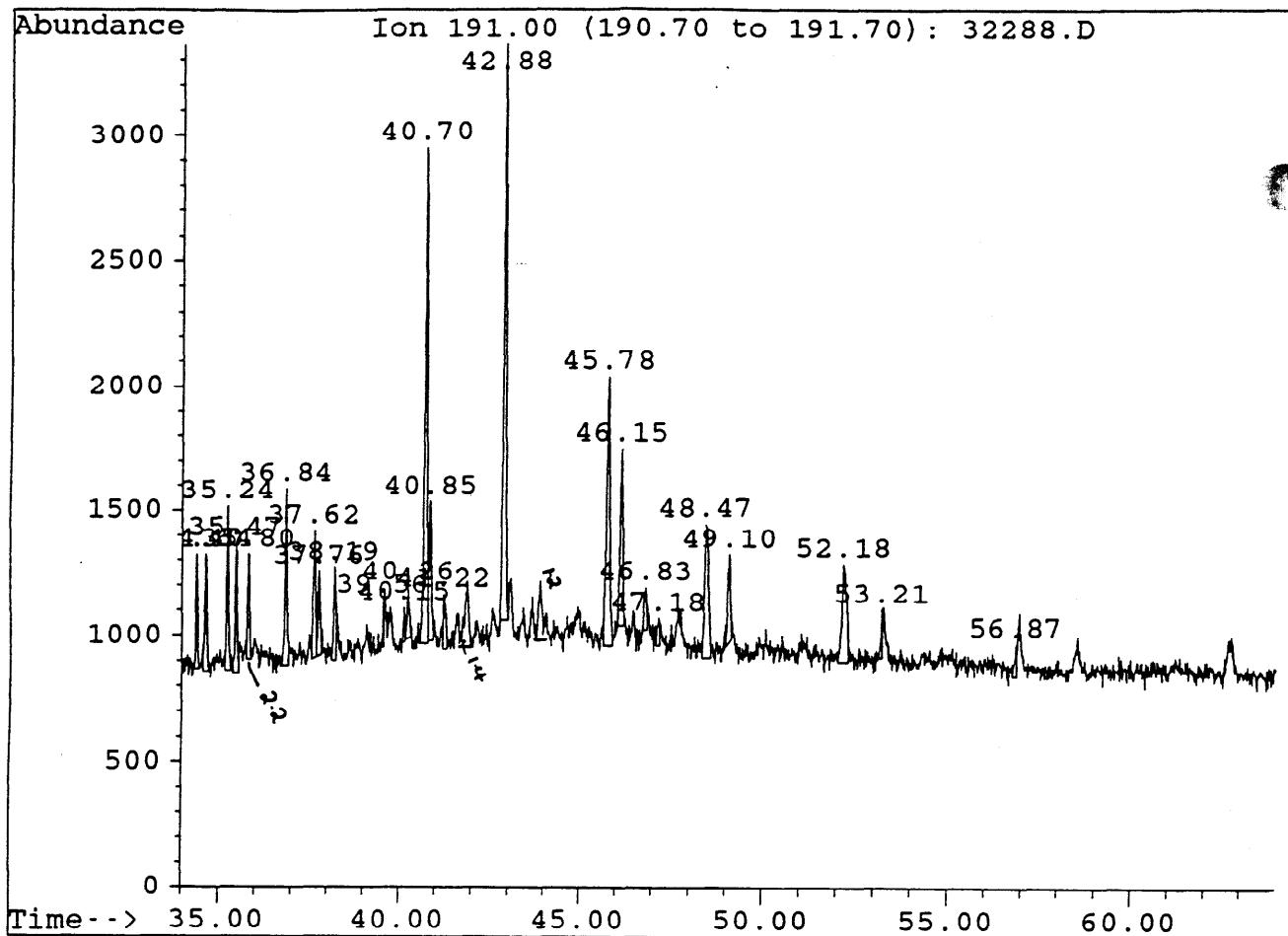


File : 32288.D  
Sample : MINERVA#1, RFS-AD-1157. L-008. TOPPED. B/C  
Misc. Info : COL#143. GEC. 25-1-94.



File : 32288.D  
Sample : MINERVA#1, RFS-AD-1157. L-008. TOPPED. B/C  
Misc. Info : COL#143. GEC. 25-1-94.

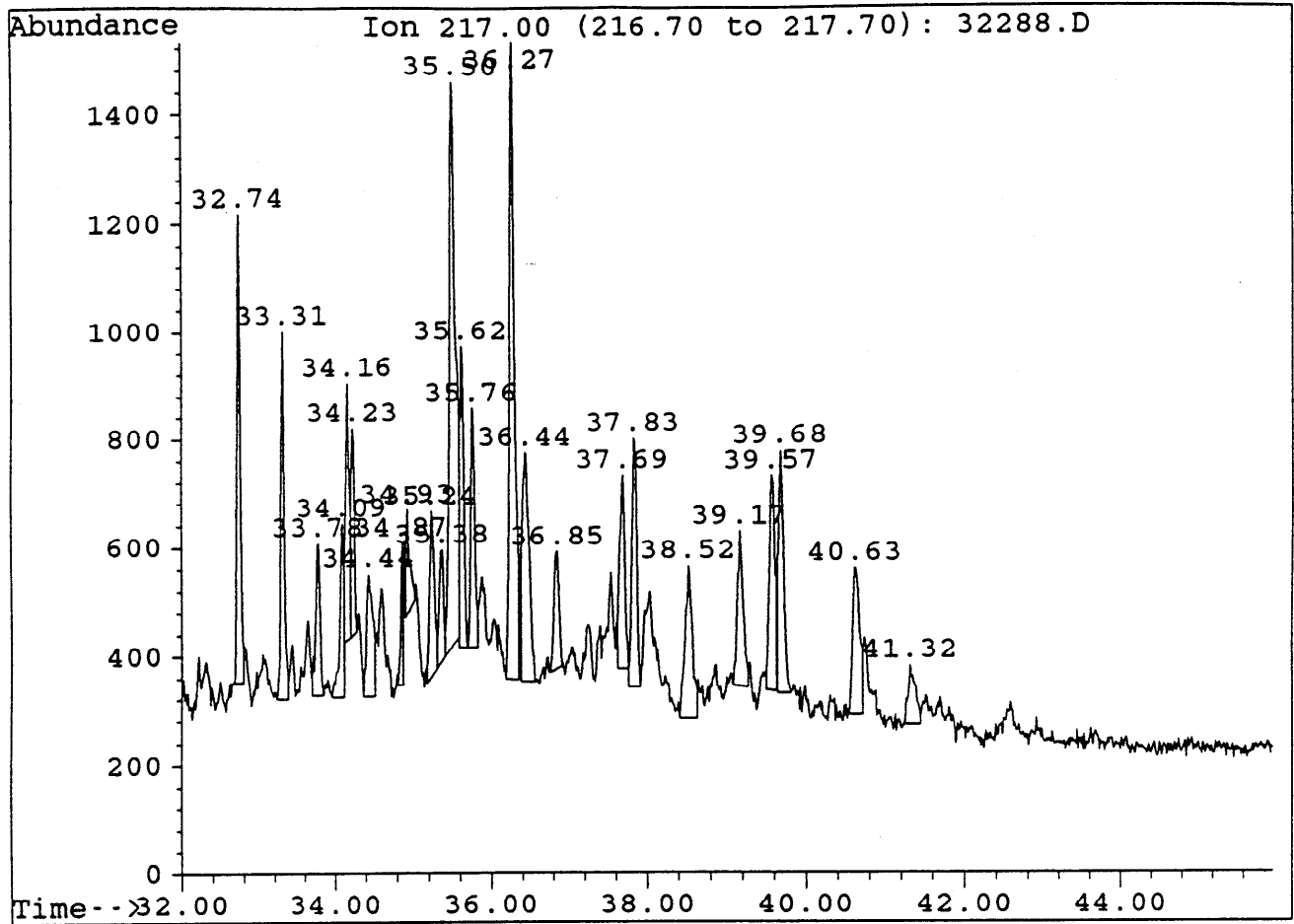




Sample : MINERVA#1, RFS-AD-1157. L-008. TOPPED. B/C

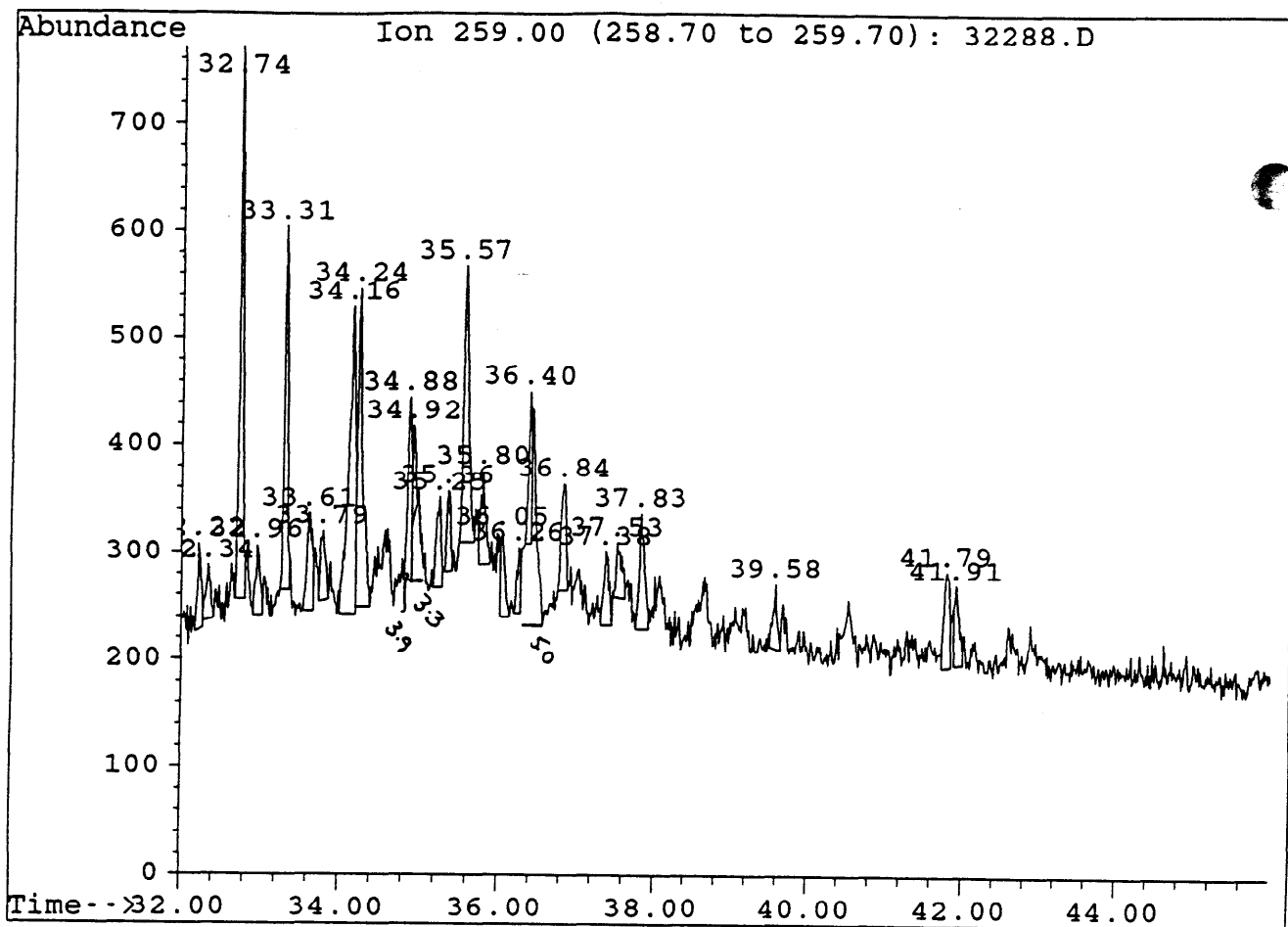
Peak	Ret.Time	Area	Height	Area %	Ratio %
1	34.40	1518	457	2.27	13.11
2	34.64	1978	467	2.95	17.08
3	35.24	2646	658	3.95	22.85
4	35.47	1930	522	2.88	16.67
5	35.80	1451	420	2.17	12.53
6	36.84	2987	709 <i>TS</i>	4.46	25.80
7	37.62	2116	511 <i>TM</i>	3.16	18.28
8	37.76	1439	335	2.15	12.43
9	38.19	1694	372	2.53	14.63
10	39.56	385	191	0.57	3.33
11	40.15	412	139	0.62	3.56
12	40.26	865	201	1.29	7.47
13	40.70	9898	1979 <i>29M</i>	14.78	85.49
14	40.85	2519	559 <i>29TS</i>	3.76	21.76
15	41.22	1063	218	1.59	9.18
16	42.88	11578	2299 <i>30M</i>	17.29	100.00
17	45.78	6895	1078 <i>31S</i>	10.30	59.55
18	46.15	3760	711 <i>32M</i>	5.61	32.48
19	46.83	841	170	1.26	7.26
20	47.18	493	112	0.74	4.26
21	48.47	4078	537 <i>32S</i>	6.09	35.22
22	49.10	1960	350 <i>32R</i>	2.93	16.11
23	52.18	3466	394	5.18	29.94
24	53.21	504	192	0.75	4.35
25	56.87	493	131	0.74	4.26

$29M = \frac{1.4}{2.2} * 420$   
 $30M = \frac{1.2}{2.2} * 420$



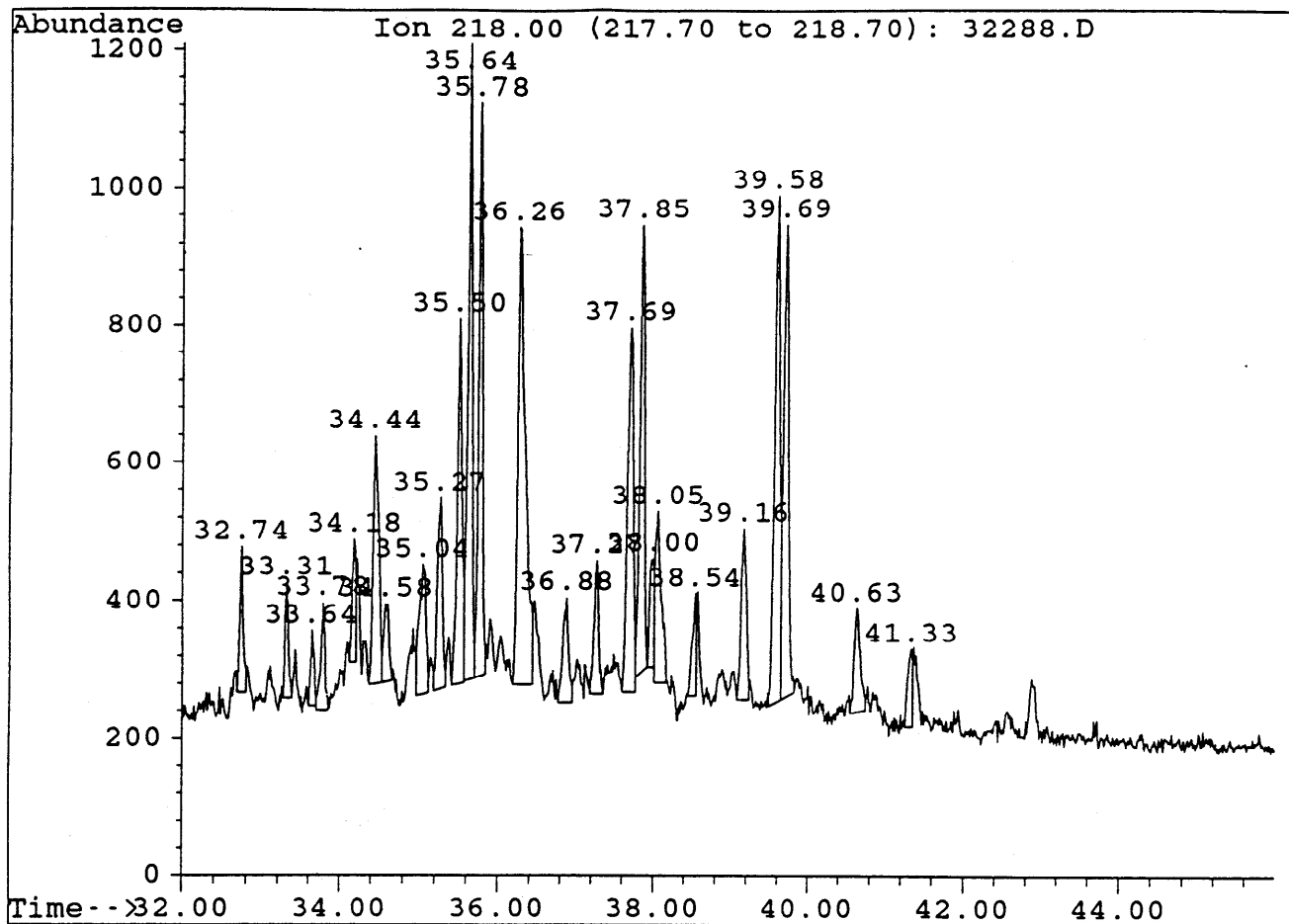
Sample : MINERVA#1, RFS-AD-1157. L-008. TOPPED. B/C

Peak	Ret.Time	Area	Height	Area %	Ratio %
1	32.74	2665	864	5.74	43.87
2	33.31	2145	679	4.62	35.31
3	33.78	1145	279	2.47	18.85
4	34.09	1340	319	2.89	22.06
5	34.16	1642	470	3.54	27.03
6	34.23	1063	377	2.29	17.50
7	34.44	1337	225	2.88	22.01
8	34.87	646	261	1.39	10.63
9	34.93	634	170	1.37	10.44
10	35.24	1311	312	2.83	21.58
11	35.38	846	211 <del>27</del>	1.82	13.93
12	35.50	6075	<u>1039</u> <i>dia S</i>	13.09	100.00
13	35.62	1760	556	3.79	28.97
14	35.76	1613	441	3.48	26.55
15	36.27	5454	<u>1173</u> <i>27R</i>	11.75	89.78
16	36.44	2565	<u>422</u> <i>29 dia R</i>	5.53	42.22
17	36.85	1004	213	2.16	16.53
18	37.69	1576	357	3.40	25.94
19	37.83	2034	458	4.38	33.48
20	38.52	1810	<u>279</u> <i>28R</i>	3.90	29.79
21	39.17	1413	<u>283</u> <i>29S</i>	3.04	23.26
22	39.57	1920	<u>396</u> <i>isoR</i>	4.14	31.60
23	39.68	1976	<u>447</u> <i>isoS</i>	4.26	32.53
24	40.63	1714	<u>270</u> <i>29R</i>	3.69	28.21
25	41.32	717	110	1.55	11.80



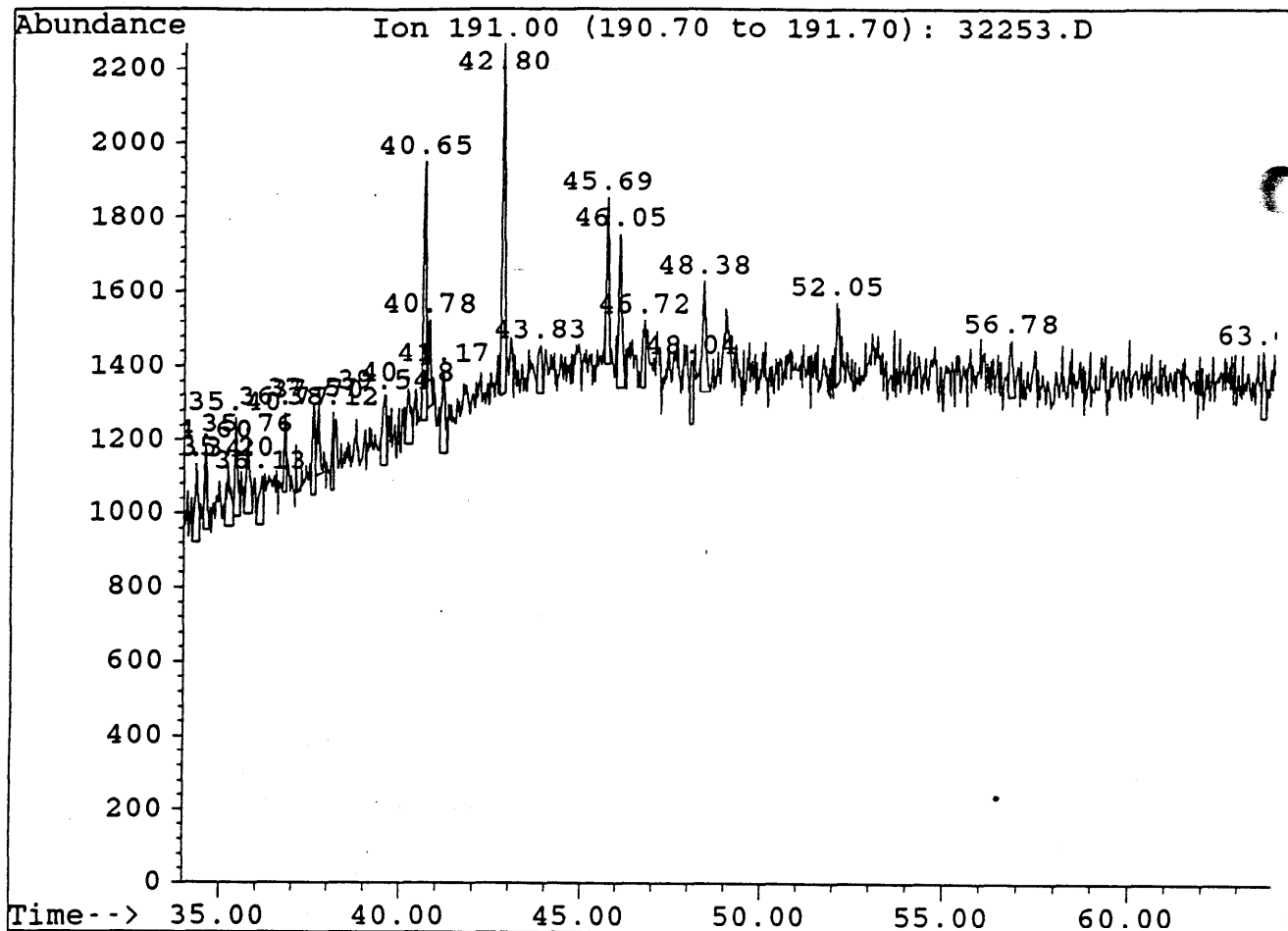
Sample : MINERVA#1, RFS-AD-1157. L-008. TOPPED. B/C

Peak	Ret.Time	Area	Height	Area %	Ratio %
1	32.22	268	82	1.98	15.54
2	32.34	204	52	1.51	11.83
3	32.74	1643	<u>514</u> 275	12.15	95.25
4	32.96	261	66	1.93	15.13
5	33.31	1013	<u>339</u> 27R	7.49	58.72
6	33.61	432	91	3.20	25.04
7	33.79	282	65	2.09	16.35
8	34.16	1725	<u>287</u> 285	12.76	100.00
9	34.24	1265	<u>297</u> 285	9.36	73.33
10	34.88	628	$\frac{3.3}{3.9} * 171 + 171$ 28R	4.64	36.41
11	34.92	212	76	1.57	12.29
12	35.25	355	85	2.63	20.58
13	35.36	254	75	1.88	14.72
14	35.57	1181	<u>257</u> 295	8.73	68.46
15	35.80	350	87	2.59	20.29
16	36.05	278	$\frac{5.0}{3.9} * 171$ 79	2.06	16.12
17	36.26	208	62	1.54	12.06
18	36.40	466	142	3.45	27.01
19	36.84	458	100	3.39	26.55
20	37.38	314	70	2.32	18.20
21	37.53	256	52	1.89	14.81
22	37.83	512	108	3.79	29.1
23	39.58	221	60	1.63	12.81
24	41.79	437	89	3.23	25.33
25	41.91	298	74	2.20	17.28



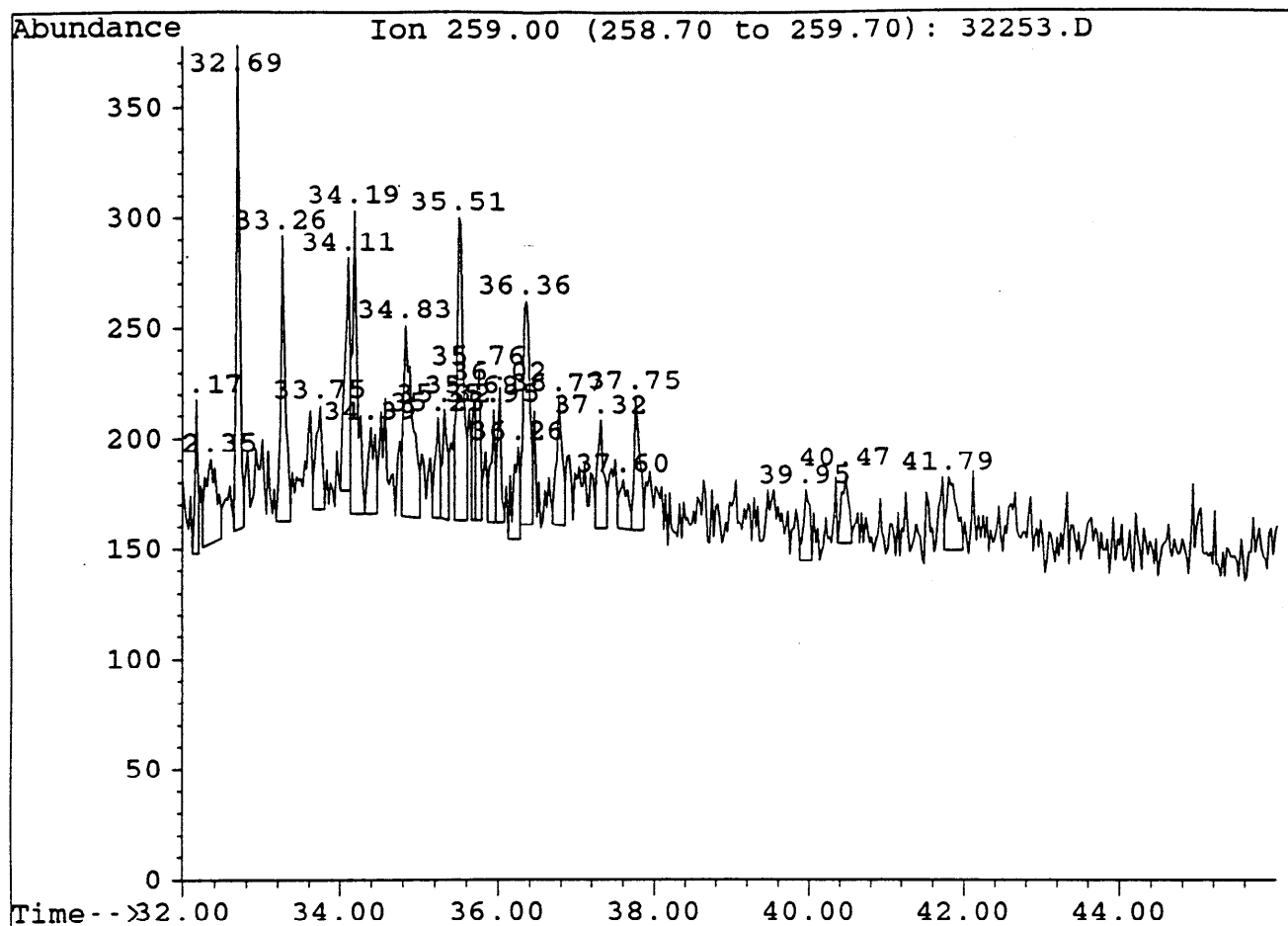
Sample : MINERVA#1, RFS-AD-1157. L-008. TOPPED. B/C

Peak	Ret.Time	Area	Height	Area %	Ratio %
1	32.74	658	211	1.67	14.60
2	33.31	511	167	1.30	11.34
3	33.64	333	110	0.85	7.39
4	33.78	592	157	1.51	13.13
5	34.18	598	178	1.52	13.27
6	34.44	1845	357	4.69	40.93
7	34.58	510	111	1.30	11.31
8	35.04	1096	190	2.79	24.31
9	35.27	1270	277	3.23	28.17
10	35.50	2256	530	5.74	50.04
11	35.64	3406	922	8.67	75.55
12	35.78	2946	832	7.50	65.35
13	36.26	4508	665	11.47	100.00
14	36.88	801	153	2.04	17.77
15	37.27	802	194	2.04	17.79
16	37.69	2735	529	6.96	60.67
17	37.85	2768	653	7.04	61.40
18	38.00	683	158	1.74	15.15
19	38.05	1212	248	3.08	26.89
20	38.54	580	149	1.48	12.87
21	39.16	1145	248	2.91	25.40
22	39.58	3542	740	9.01	78.57
23	39.69	3199	684	8.14	70.96
24	40.63	817	151	2.08	18.12
25	41.33	486	113	1.24	10.78



Sample : MINERVA#1, RFS-AD-1157, L-008. COLD TRAP LIQ

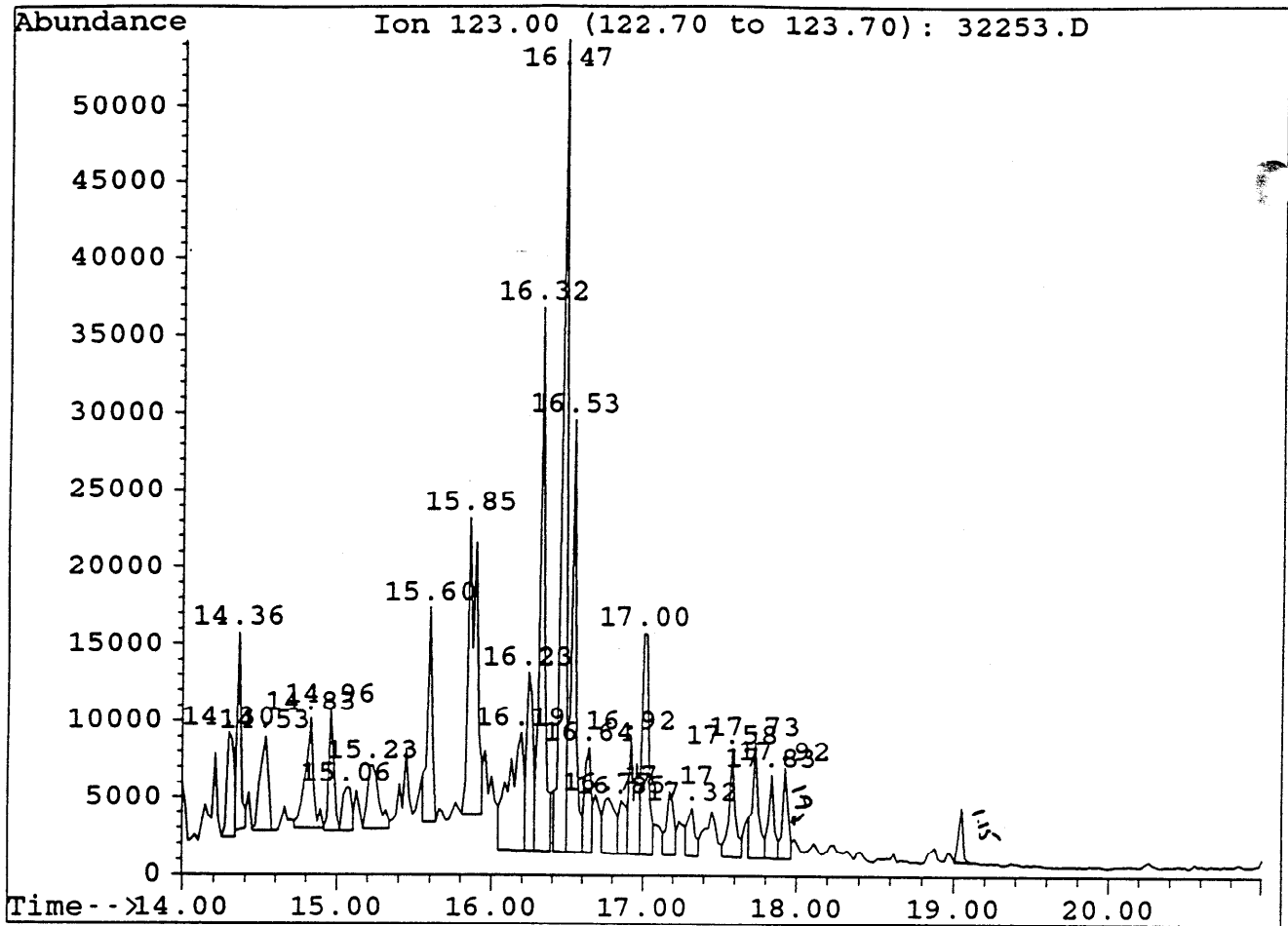
Peak	Ret.Time	Area	Height	Area %	Ratio %
1	34.34	1436	213	3.69	28.26
2	34.60	1028	228	2.64	20.23
3	35.20	1318	171	3.38	25.94
4	35.40	1377	268	3.53	27.10
5	35.76	1391	201	3.57	27.38
6	36.13	1051	132	2.70	20.68
7	36.77	1035	219	2.66	20.37
8	37.57	1349	247	3.46	26.55
9	37.70	921	188	2.36	18.13
10	38.12	865	213	2.22	17.02
11	39.54	1332	190	3.42	26.22
12	40.18	1119	152	2.87	22.02
13	40.65	3899	700	10.01	76.74
14	40.78	1085	229	2.79	21.35
15	41.17	1569	227	4.03	30.88
16	42.80	5081	946	13.04	100.00
17	43.83	938	129	2.41	18.46
18	45.69	2155	448	5.53	42.41
19	46.05	2752	413	7.06	54.16
20	46.72	1012	182	2.60	19.92
21	48.04	1001	171	2.57	19.70
22	48.38	2214	299	5.68	43.5
23	52.05	1059	214	2.72	20.84
24	56.78	994	154	2.55	19.56
25	63.65	974	182	2.50	19.17



Sample : MINERVA#1, RFS-AD-1157, L-008. COLD TRAP LIQ

Peak	Ret.Time	Area	Height	Area %	Ratio %
1	32.17	173	70	2.02	23.60
2	32.35	375	40	4.38	51.16
3	32.69	681	220	7.96	92.91
4	33.26	550	129	6.43	75.03
5	33.75	249	47	2.91	33.97
6	34.11	511	106	5.97	69.71
7	34.19	594	137	6.94	81.04
8	34.39	252	39	2.95	34.38
9	34.83	682	86	7.97	93.04
10	35.25	189	45	2.21	25.78
11	35.32	214	49	2.50	29.20
12	35.51	733	137	8.57	100.00
13	35.69	165	54	1.93	22.51
14	35.76	220	67	2.57	30.01
15	35.95	193	51	2.26	26.33
16	36.02	175	61	2.05	23.87
17	36.26	265	42	3.10	36.15
18	36.36	632	101	7.39	86.22
19	36.77	314	57	3.67	42.84
20	37.32	283	49	3.31	38.61
21	37.60	167	22	1.95	22.78
22	37.75	294	61	3.44	40.11
23	39.95	170	32	1.99	23.19
24	40.47	192	32	2.24	26.19
25	41.79	283	33	3.31	38.61

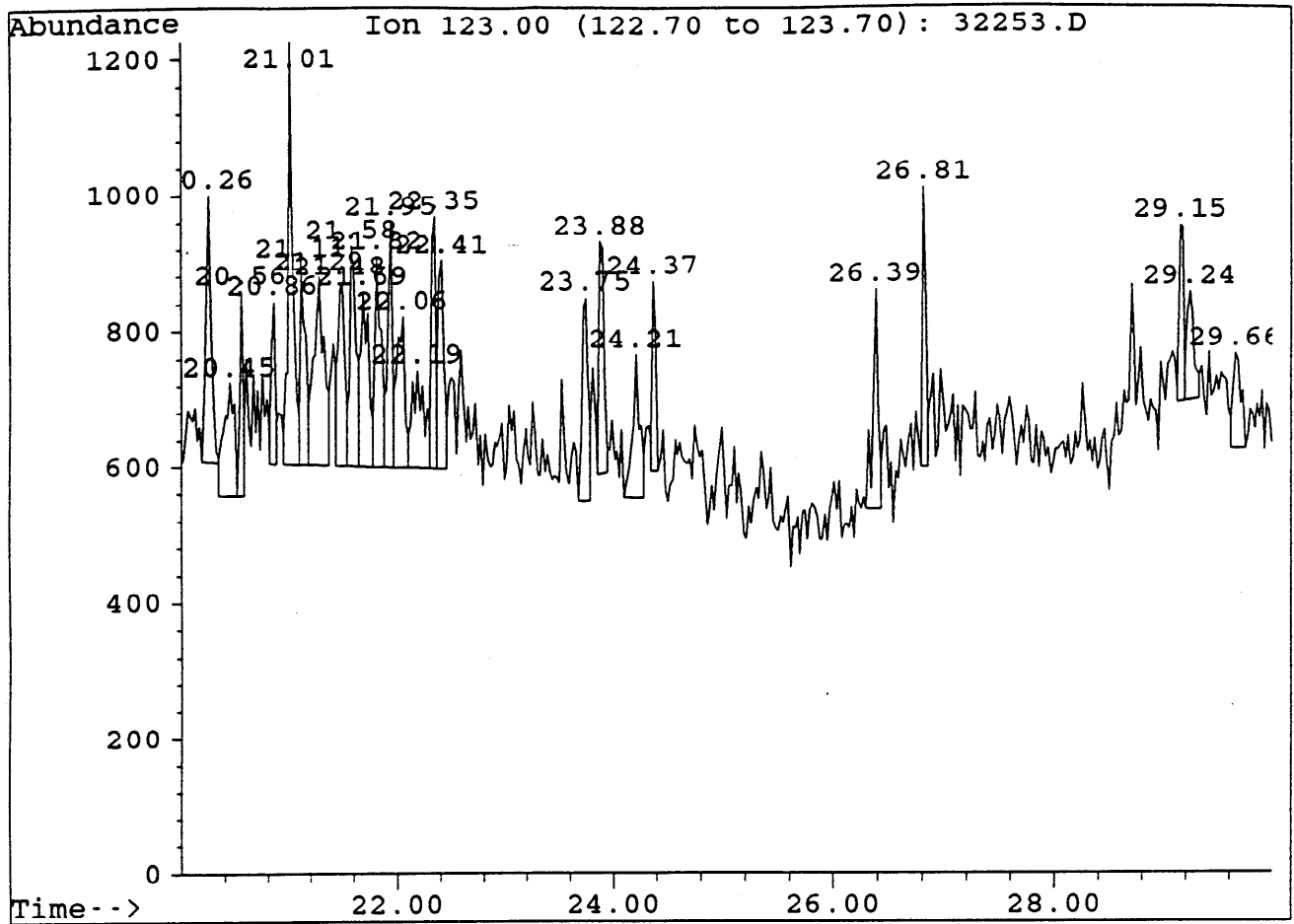




Sample : MINERVA#1, RFS-AD-1157, L-008. COLD TRAP LIQ

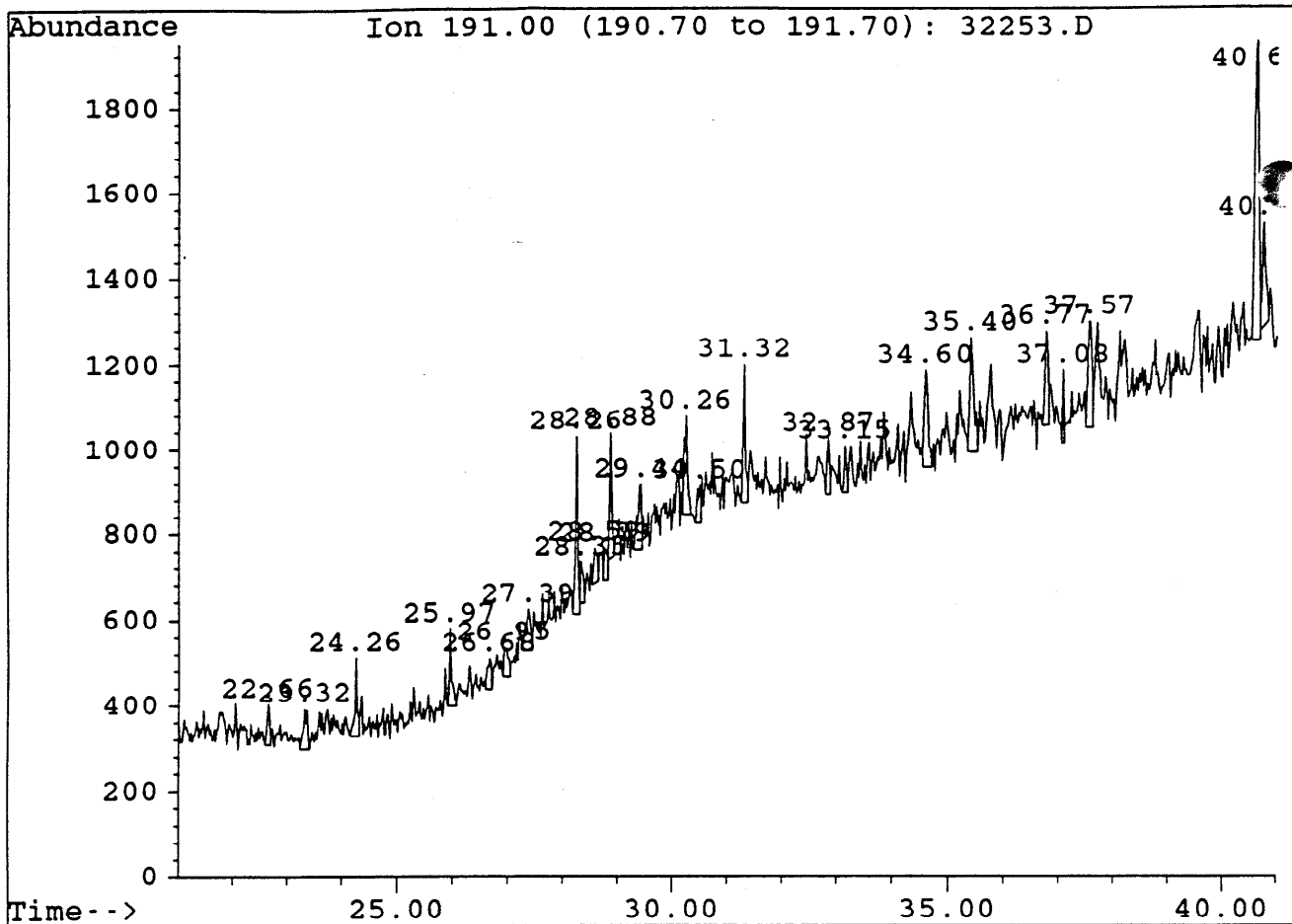
Peak	Ret.Time	Area	Height	Area %	Ratio %
1	14.30	22974	6907	2.83	19.27
2	14.36	20431	12948	2.51	17.13
3	14.53	22721	6239	2.80	19.06
4	14.83	27212	7262	3.35	22.82
5	14.96	18578	7964	2.29	15.58
6	15.06	11668	2841	1.44	9.79
7	15.23	22218	4183	2.73	18.63
8	15.60	28992	14043	3.57	24.31
9	15.85	75064	19363	9.24	62.95
10	16.19	51205	7649	6.30	42.94
11	16.23	33317	11627	4.10	27.94
12	16.32	82652	35352	10.17	69.32
13	16.47	119238	52729	14.68	100.00
14	16.53	63044	28204	7.76	52.87
15	16.64	20135	6829	2.48	16.89
16	16.77	19475	3608	2.40	16.33
17	16.85	12175	3440	1.50	10.21
18	16.92	26081	7676	3.21	21.87
19	17.00	43583	<u>14403</u> R <sub>1</sub>	5.36	36.55
20	17.17	13349	4151	1.64	11.20
21	17.32	9793	3087	1.21	8.21
22	17.58	19763	<u>6942</u> R <sub>2</sub>	2.43	16.5
23	17.73	20383	<u>7537</u> D	2.51	17.09
24	17.83	13644	5497	1.68	11.44
25	17.92	14753	5972	1.82	12.37

HO =  $\frac{1.15}{1.9} *$



Sample : MINERVA#1, RFS-AD-1157, L-008. COLD TRAP LIQ

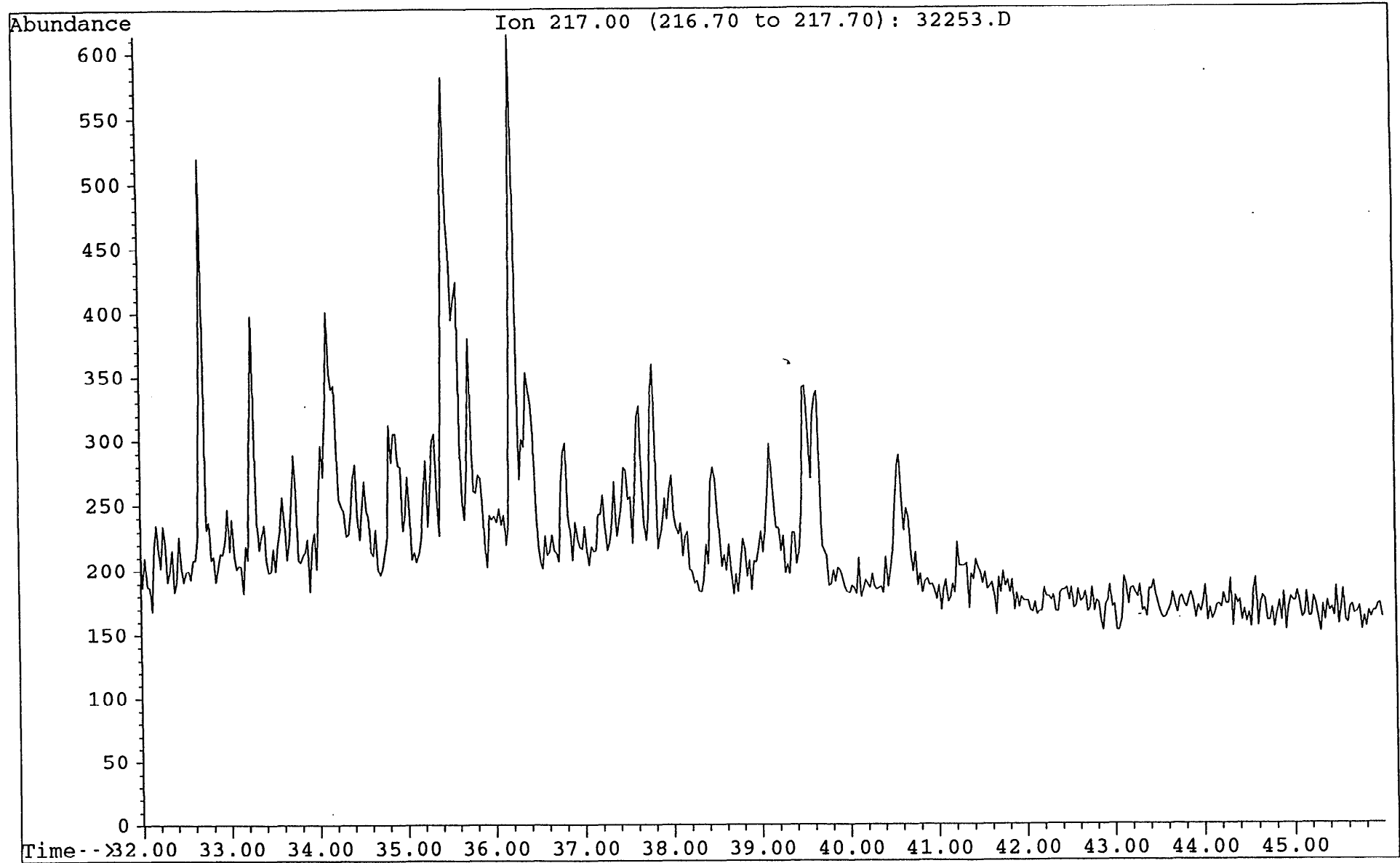
Peak	Ret.Time	Area	Height	Area %	Ratio %
1	20.26	1325	393	4.78	63.86
2	20.45	1083	169	3.91	52.19
3	20.56	675	302	2.44	32.53
4	20.86	615	239	2.22	29.64
5	21.01	2075	623	7.49	100.00
6	21.11	1007	296	3.63	48.53
7	21.29	1943	277	7.01	93.64
8	21.48	1215	271	4.39	58.55
9	21.58	1346	325	4.86	64.87
10	21.69	1270	257	4.58	61.20
11	21.82	1295	311	4.67	62.41
12	21.95	1065	362	3.84	51.33
13	22.06	1137	223	4.10	54.80
14	22.19	1101	145	3.97	53.06
15	22.35	1130	373	4.08	54.46
16	22.41	1082	308	3.91	52.14
17	23.75	1313	301	4.74	63.28
18	23.88	1106	344	3.99	53.30
19	24.21	981	212	3.54	47.28
20	24.37	646	279	2.33	31.13
21	26.39	1136	323	4.10	54.75
22	26.81	1020	413	3.68	49.16
23	29.15	749	258	2.70	36.10
24	29.24	718	157	2.59	34.60
25	29.66	673	139	2.43	32.43



Sample : MINERVA#1, RFS-AD-1157, L-008. COLD TRAP LIQ

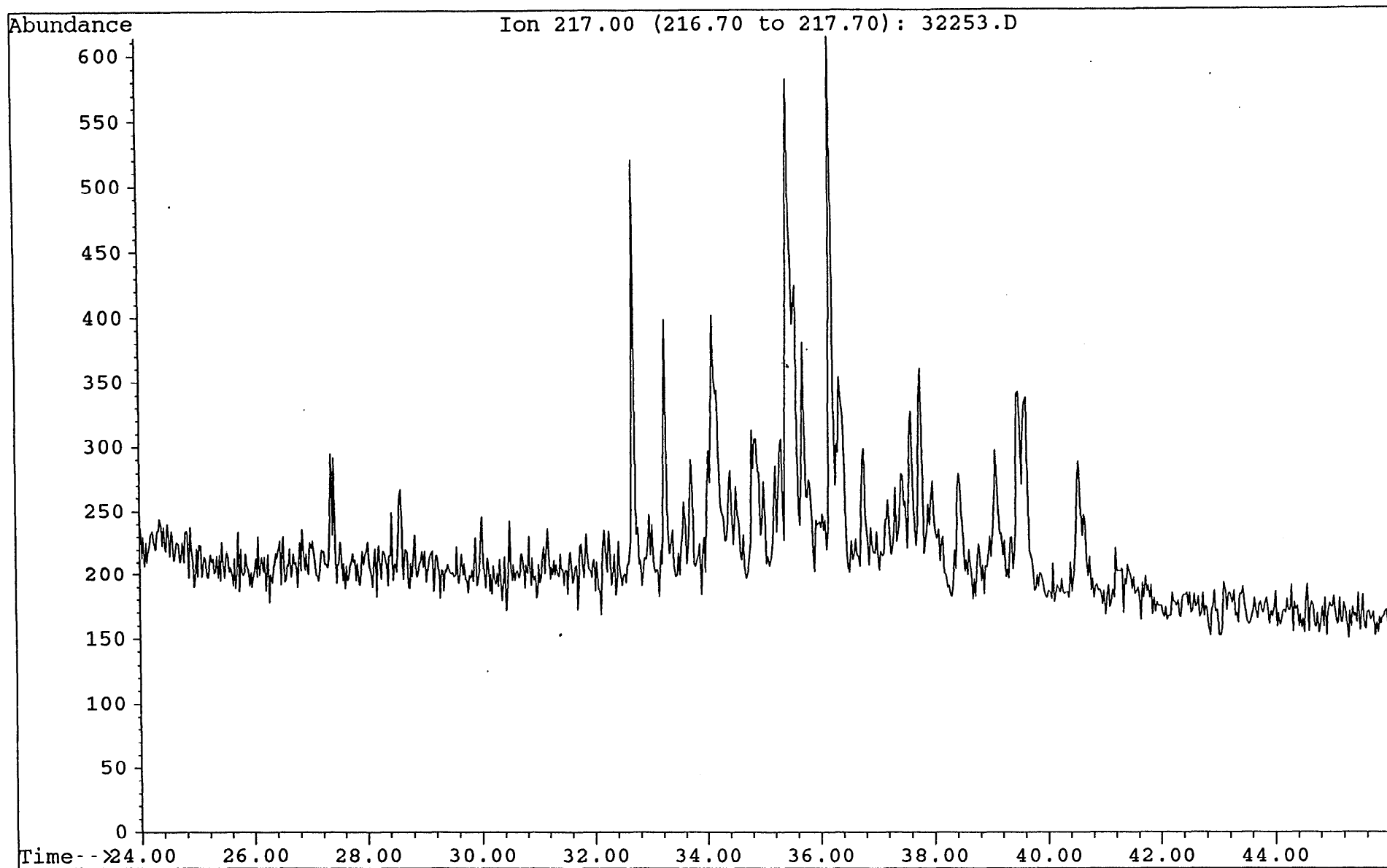
Peak	Ret.Time	Area	Height	Area %	Ratio %
1	22.66	332	96	1.62	8.52
2	23.32	492	95	2.41	12.62
3	24.26	640	185	3.13	16.41
4	25.97	521	182	2.55	13.36
5	26.68	320	73	1.56	8.21
6	26.95	406	70	1.98	10.41
7	27.39	578	95	2.83	14.82
8	28.26	1298	419	6.35	33.29
9	28.35	325	97	1.59	8.34
10	28.59	352	83	1.72	9.03
11	28.79	345	74	1.69	8.85
12	28.88	773	290	3.78	19.83
13	29.44	717	155	3.51	18.39
14	30.26	1049	234	5.13	26.90
15	30.50	382	92	1.87	9.80
16	31.32	1039	327	5.08	26.65
17	32.87	414	134	2.02	10.62
18	33.15	325	111	1.59	8.34
19	34.60	1028	228	5.03	26.37
20	35.40	1377	268	6.73	35.32
21	36.77	1035	219	5.06	26.55
22	37.08	328	172	1.60	8.
23	37.57	1349	247	6.59	34.60
24	40.65	3899	700	19.06	100.00
25	40.78	1132	235	5.53	29.03

File 32253.D  
Sample : MINERVA#1, RFS-AD-1157, L-008. COLD TRAP LIQ  
Misc. Info : COL#143. 17-1-94. GEC. B/C.



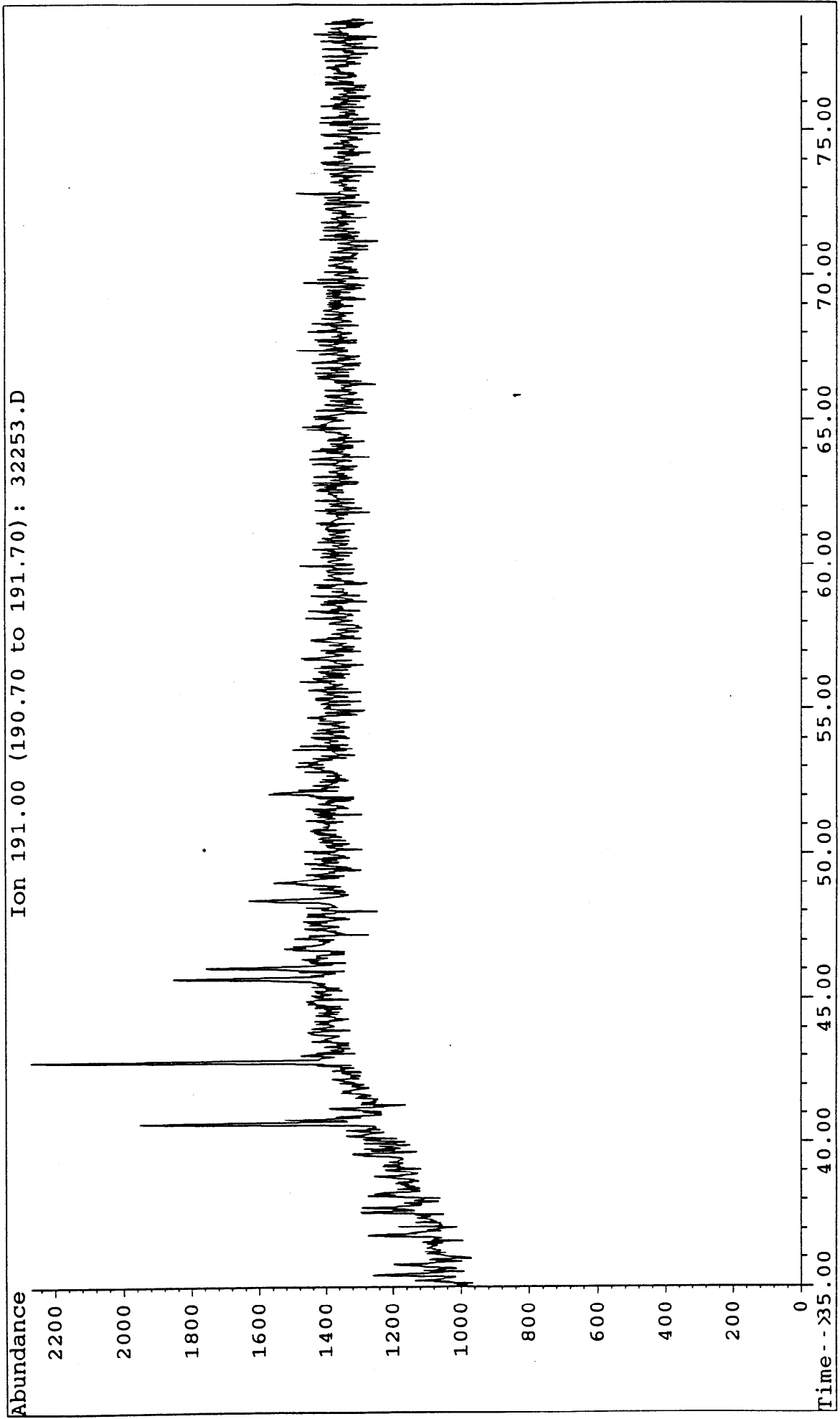
MINV1/PE900058/P254

File : 32253.D  
Sample : MINERVA#1, RFS-AD-1157, L-008. COLD TRAP LIQ  
Misc. Info : COL#143. 17-1-94. GEC. B/C.

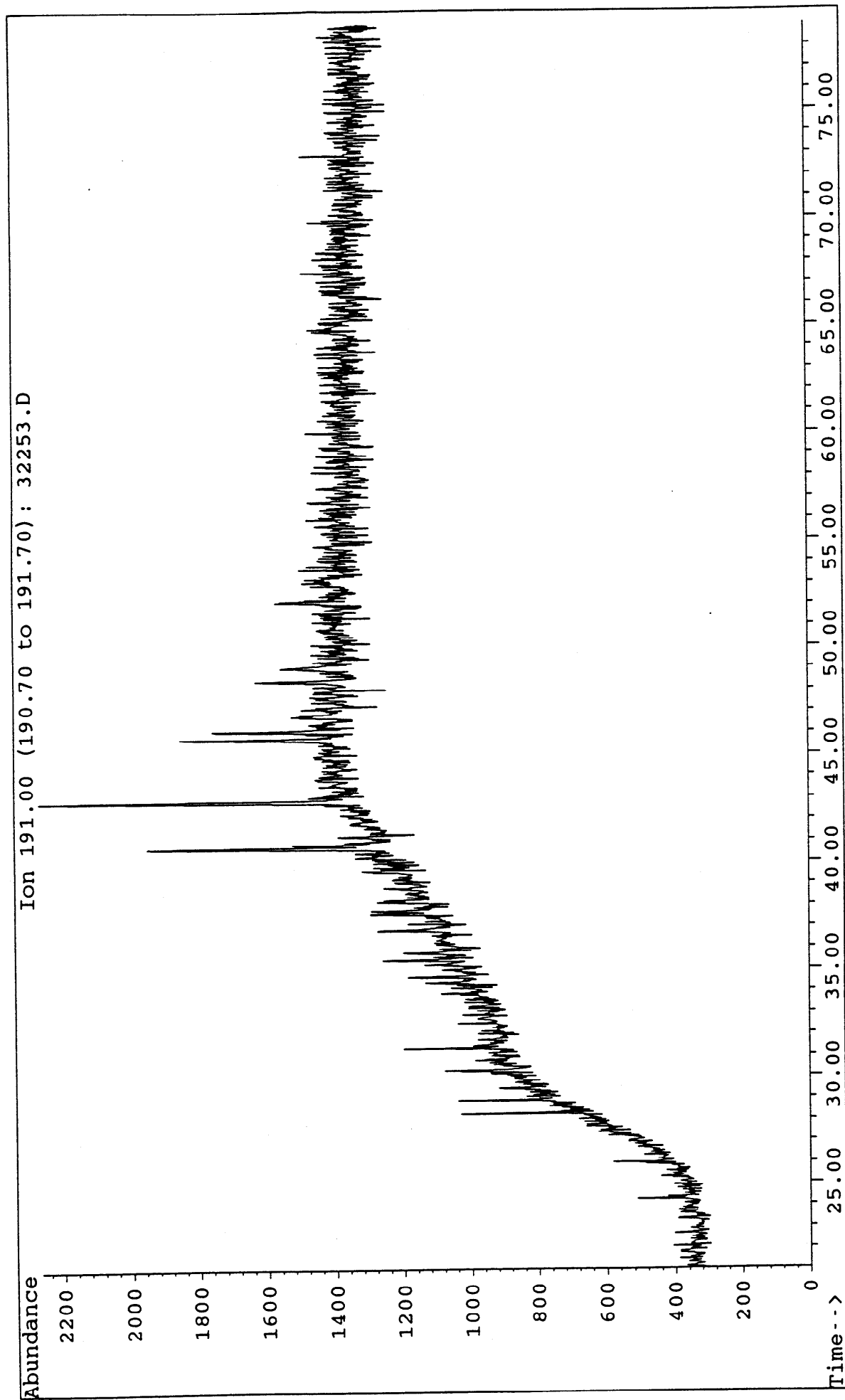


MINV 1/PE900058/P255

File . 32253.D  
Sample : MINERVA#1, RFS-AD-1157, L-008. COLD TRAP LIQ  
Misc. Info : COL#143. 17-1-94. GEC. B/C.



File : 32253.D  
Sample : MINERVA#1, RFS-AD-1157, L-008. COLD TRAP LIQ  
Misc. Info : COL#143. 17-1-94. GEC. B/C.

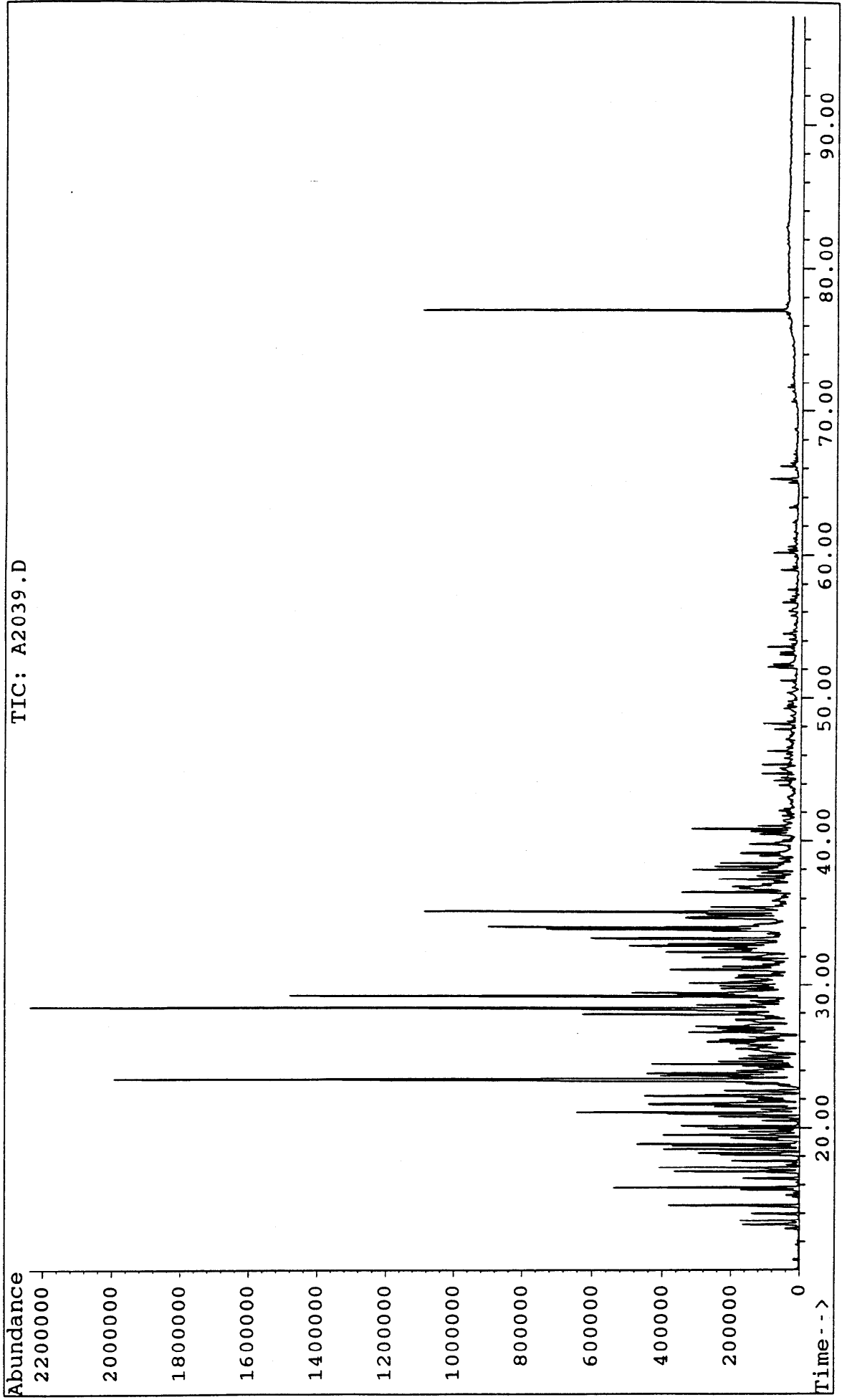


**APPENDIX 2**

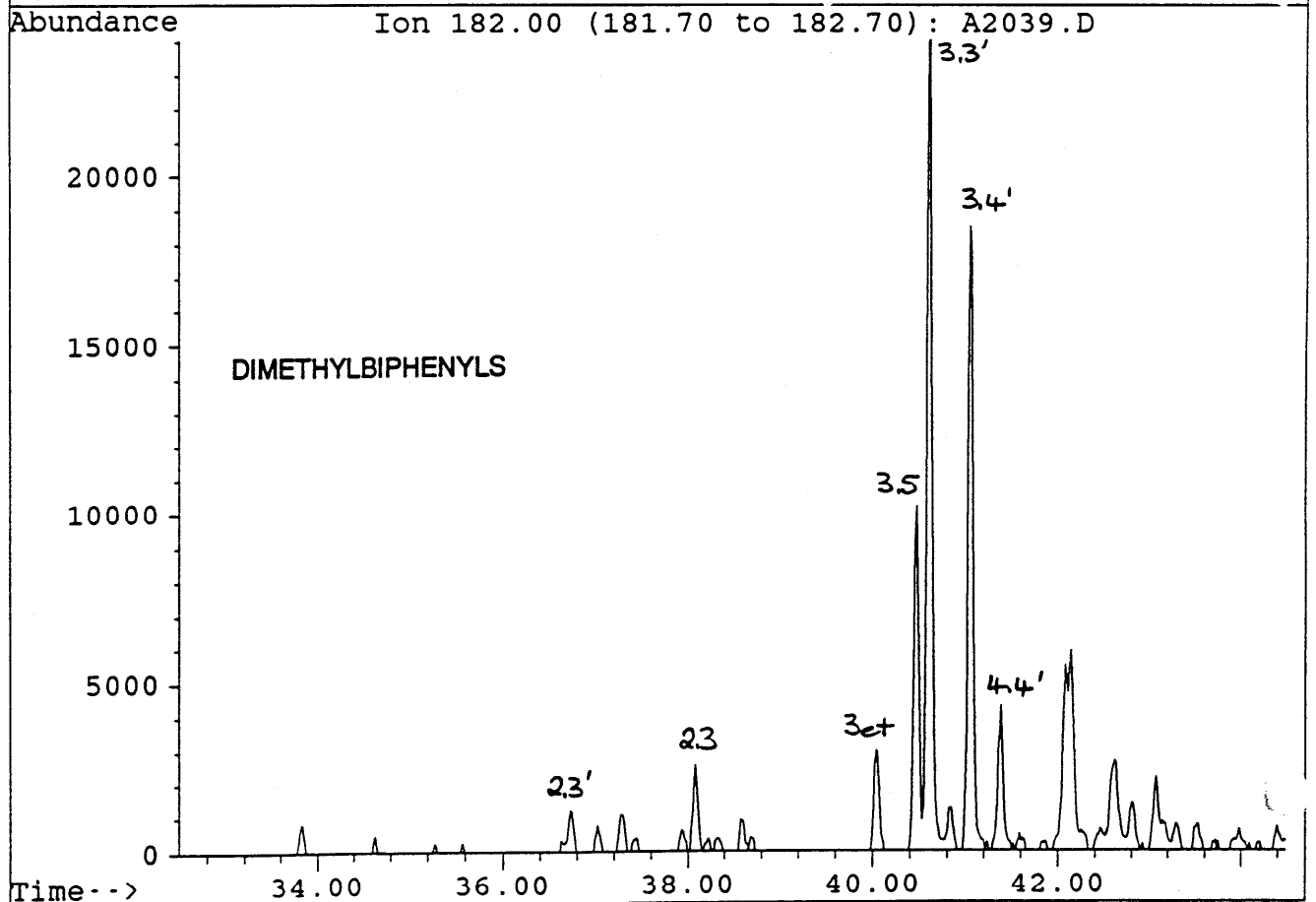
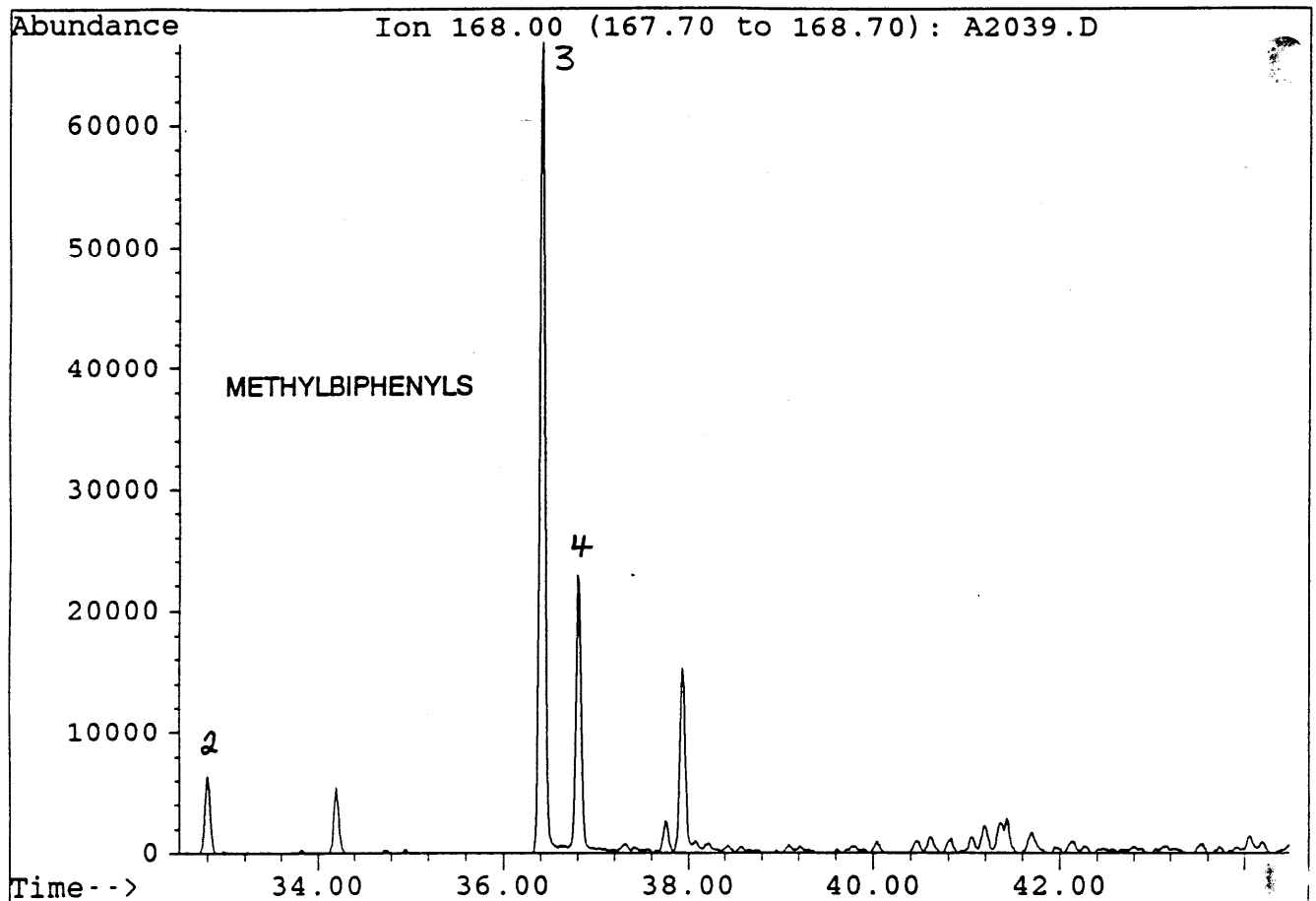
**SIR GC-MS (AROMS) MASS FRAGMENTOGRAMS : 1942.5m CONDENSATE**



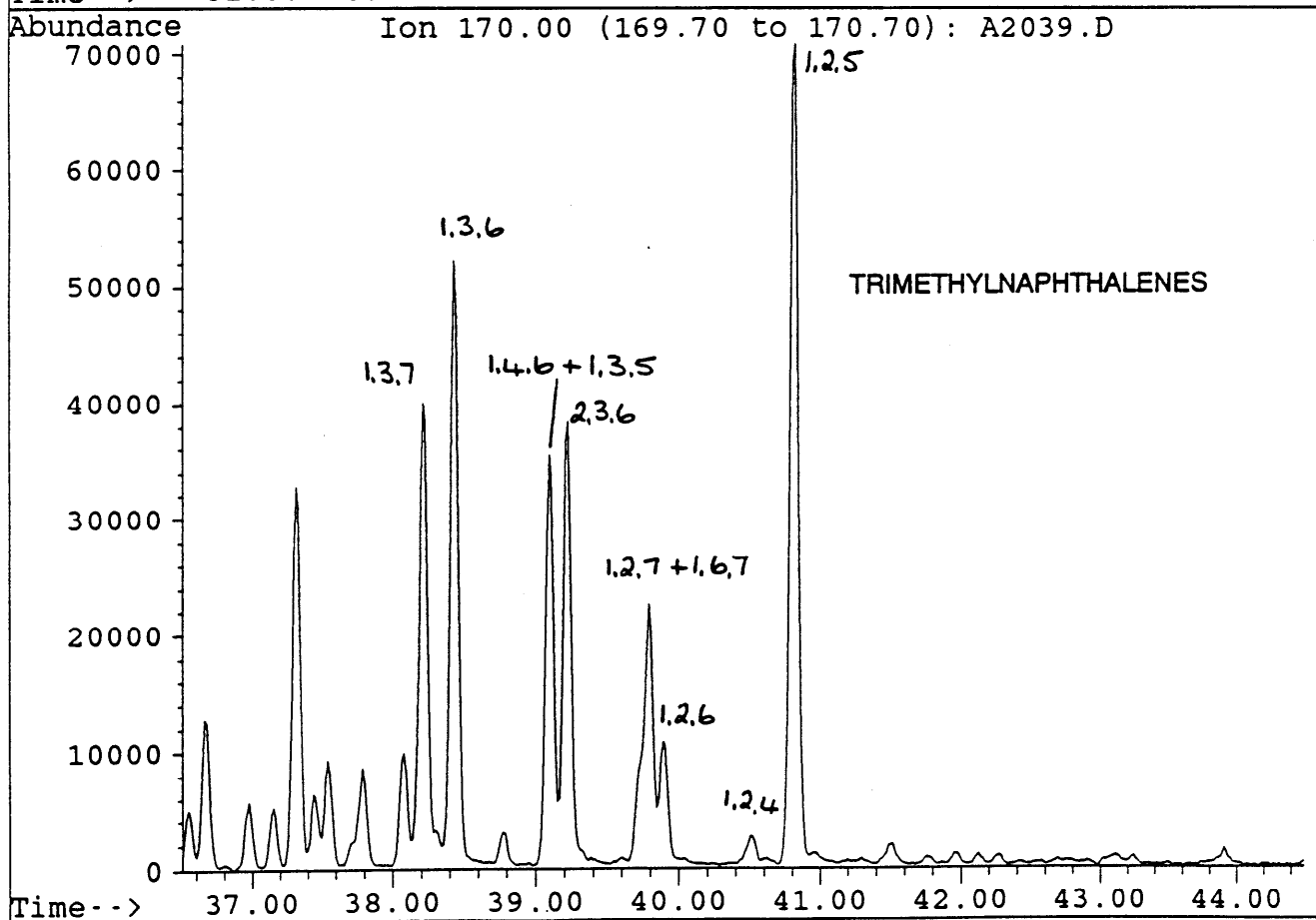
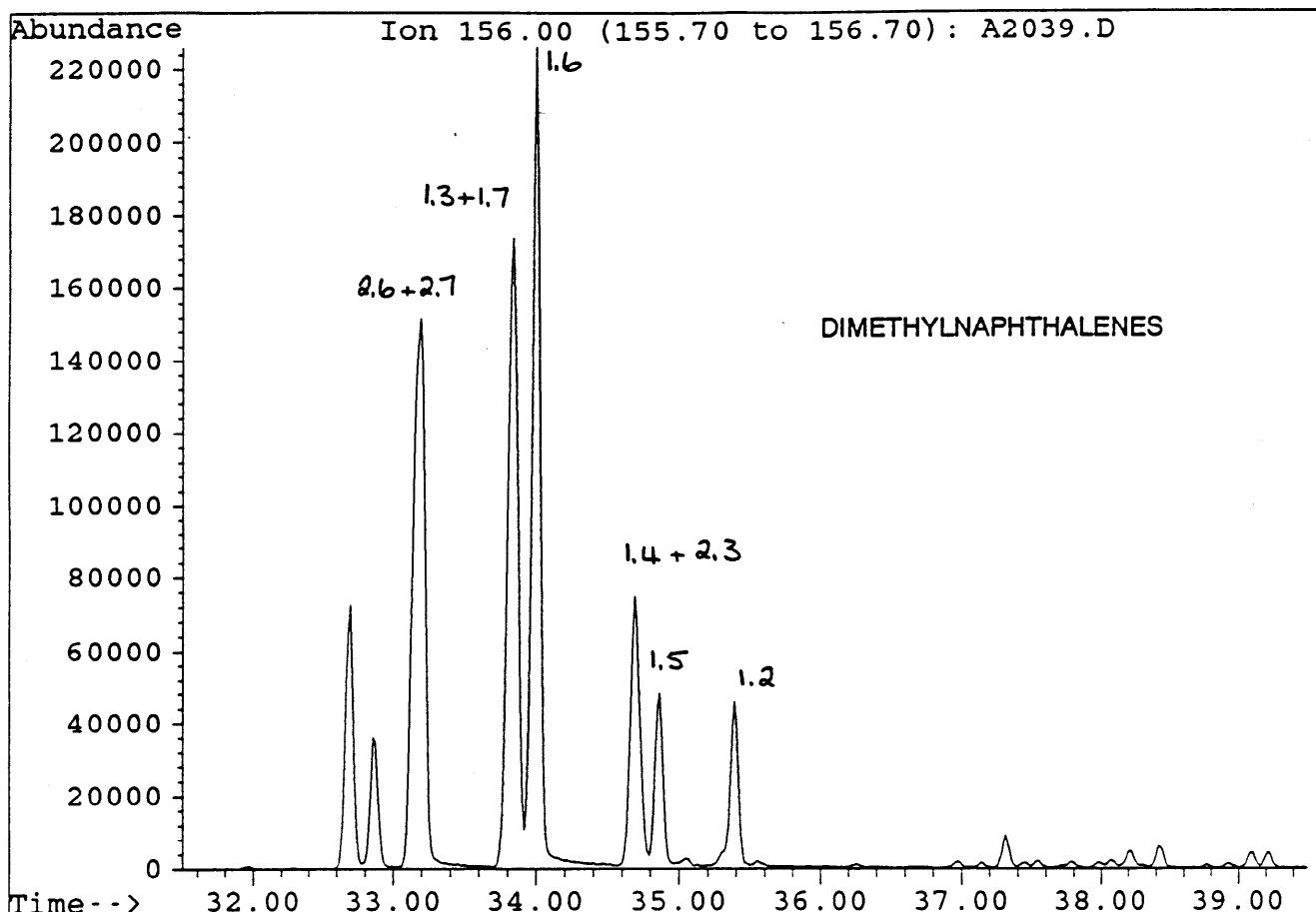
File A2039.D  
Sample : MINERVA#1, RFS-AD-1157. L-008. AKOS.  
Misc. Info : COL#155. 17-1-94. GEC.



File : A2039.D  
Sample : MINERVA#1, RFS-AD-1157. L-008. AROS.  
Misc. Info : COL#155. 17-1-94. GEC.

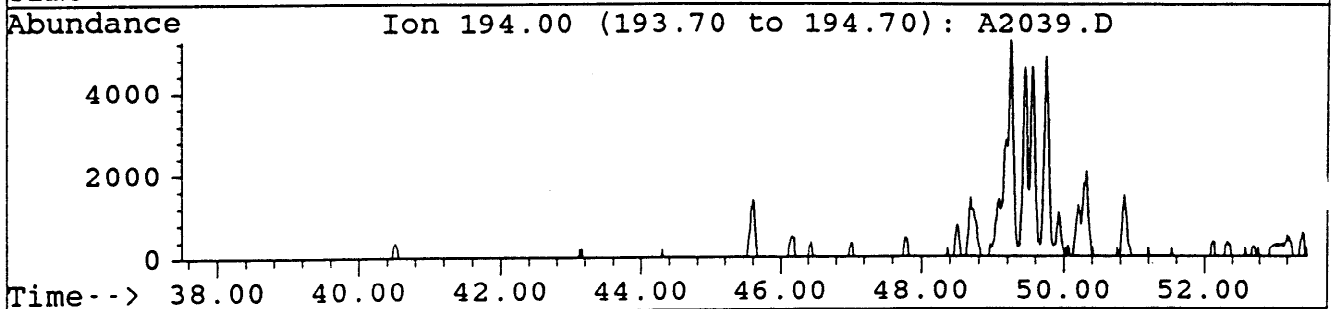
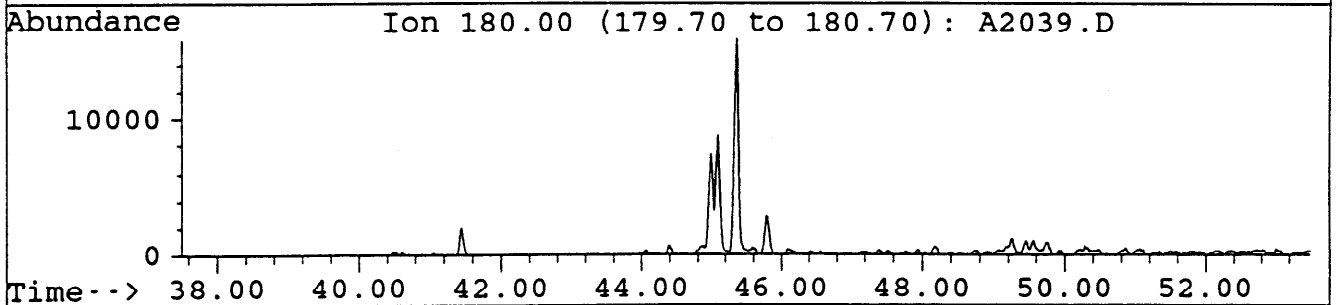
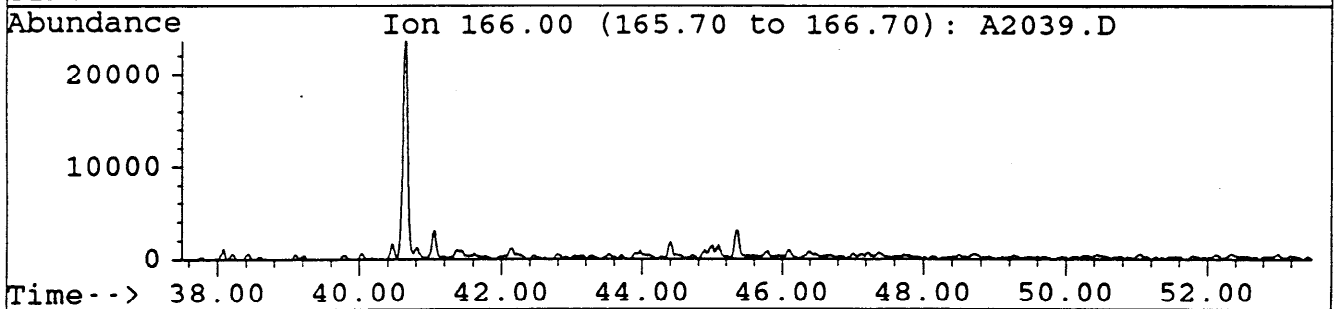
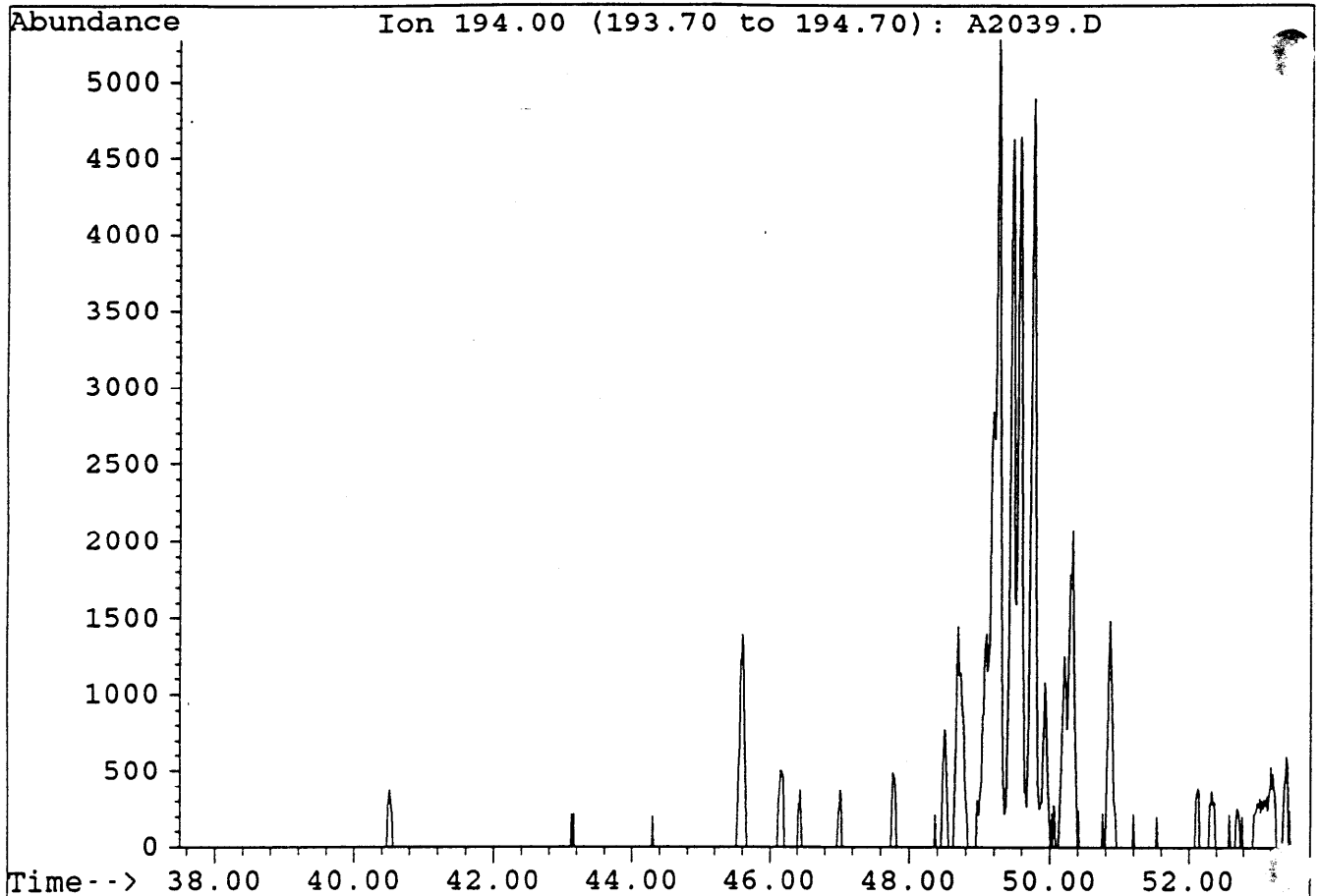


File : A2039.D  
Sample : MINERVA#1, RFS-AD-1157. L-008. AROS.  
Misc. Info : COL#155. 17-1-94. GEC.

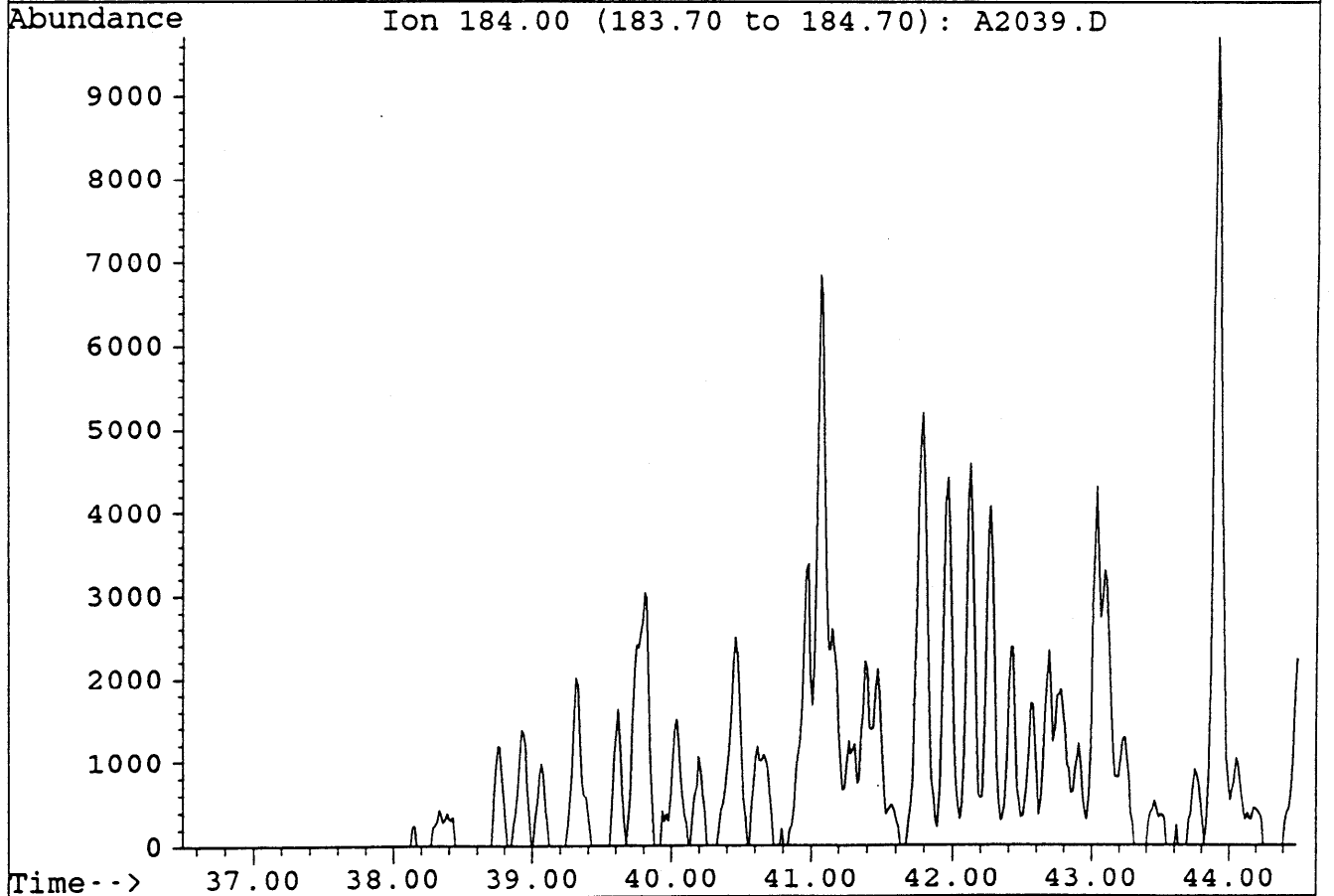
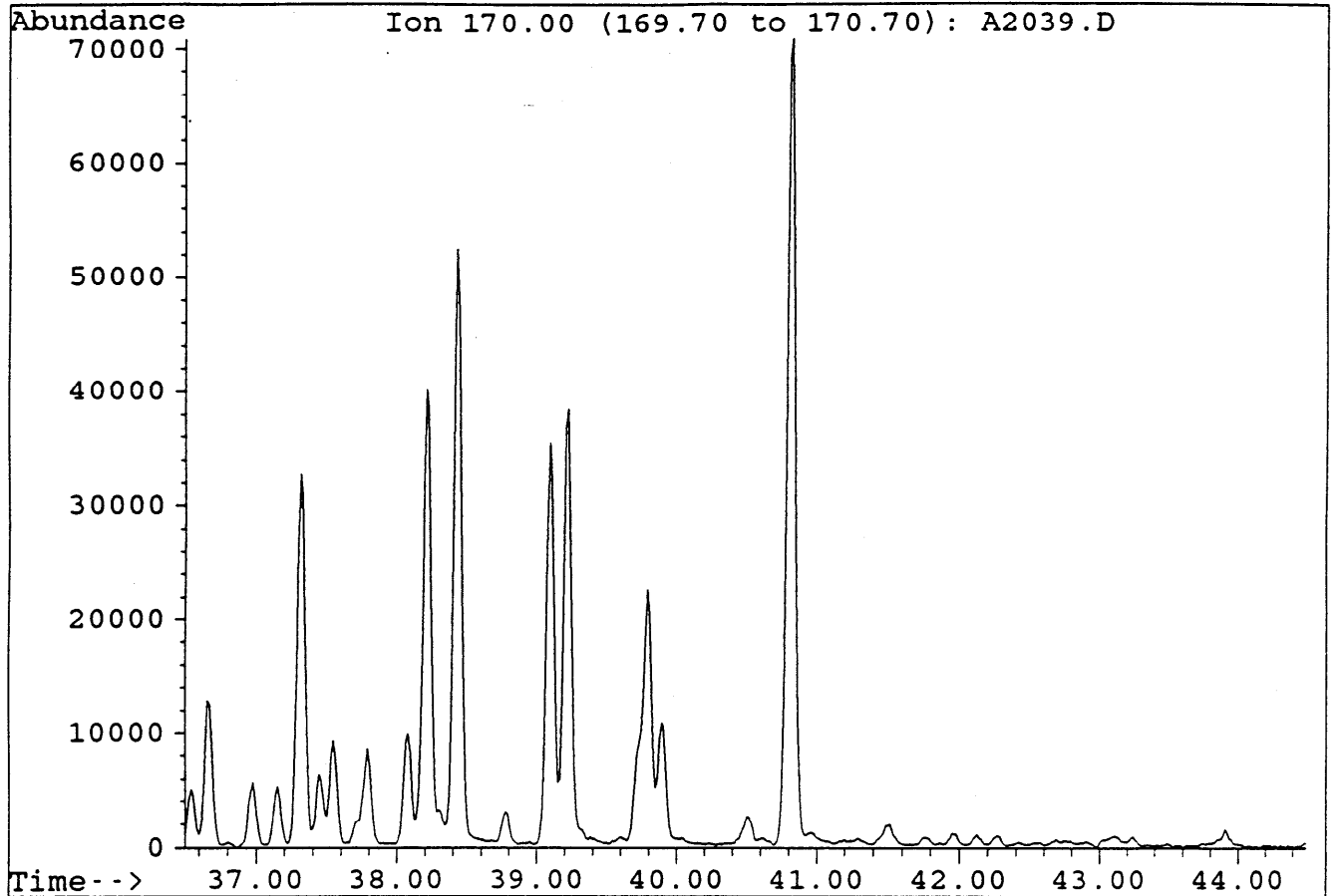


File : A2039.D  
Sample : MINERVA#1, RFS-AD-1157. L-008. AROS.  
Misc. Info : COL#155. 17-1-94. GEC.

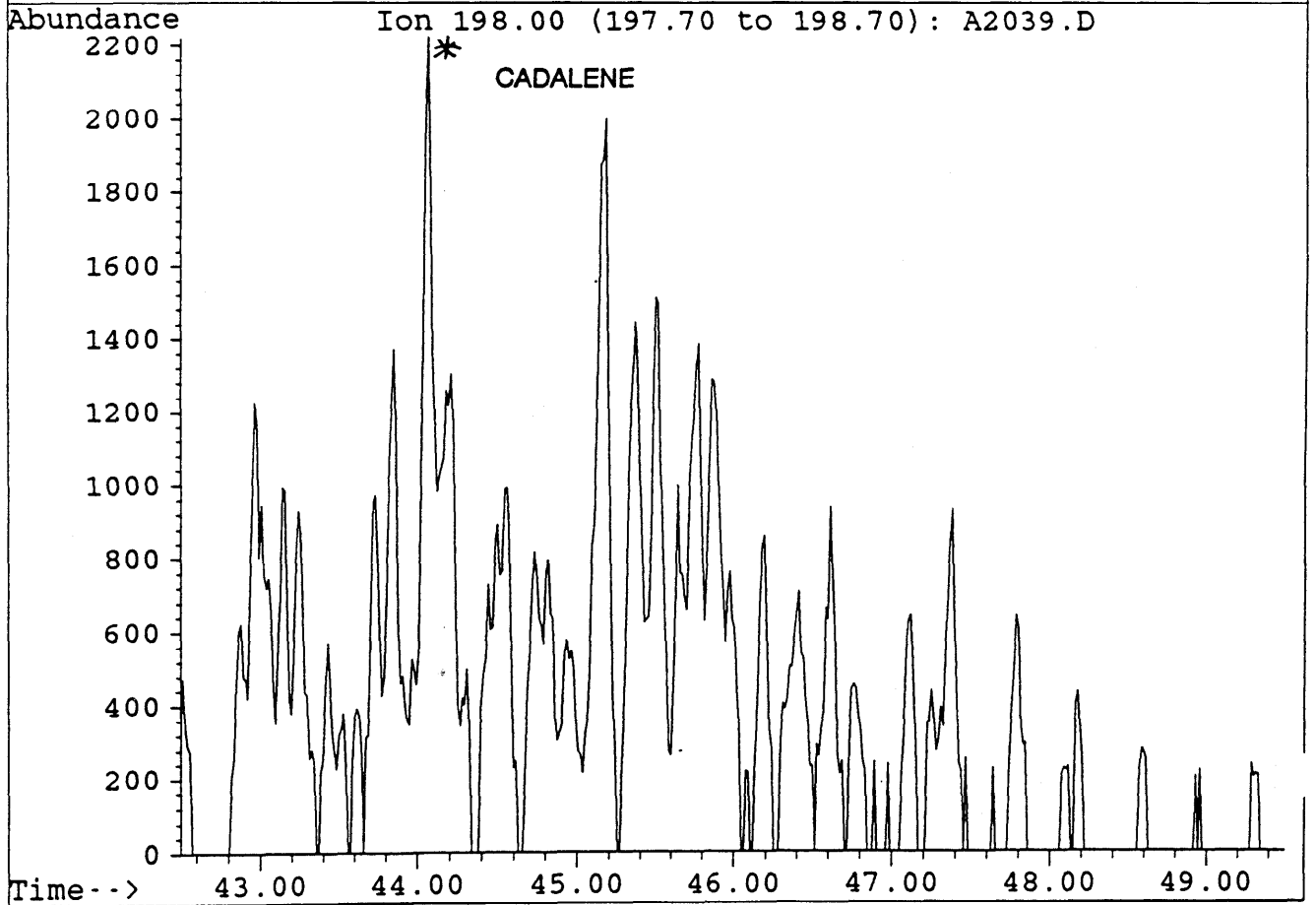
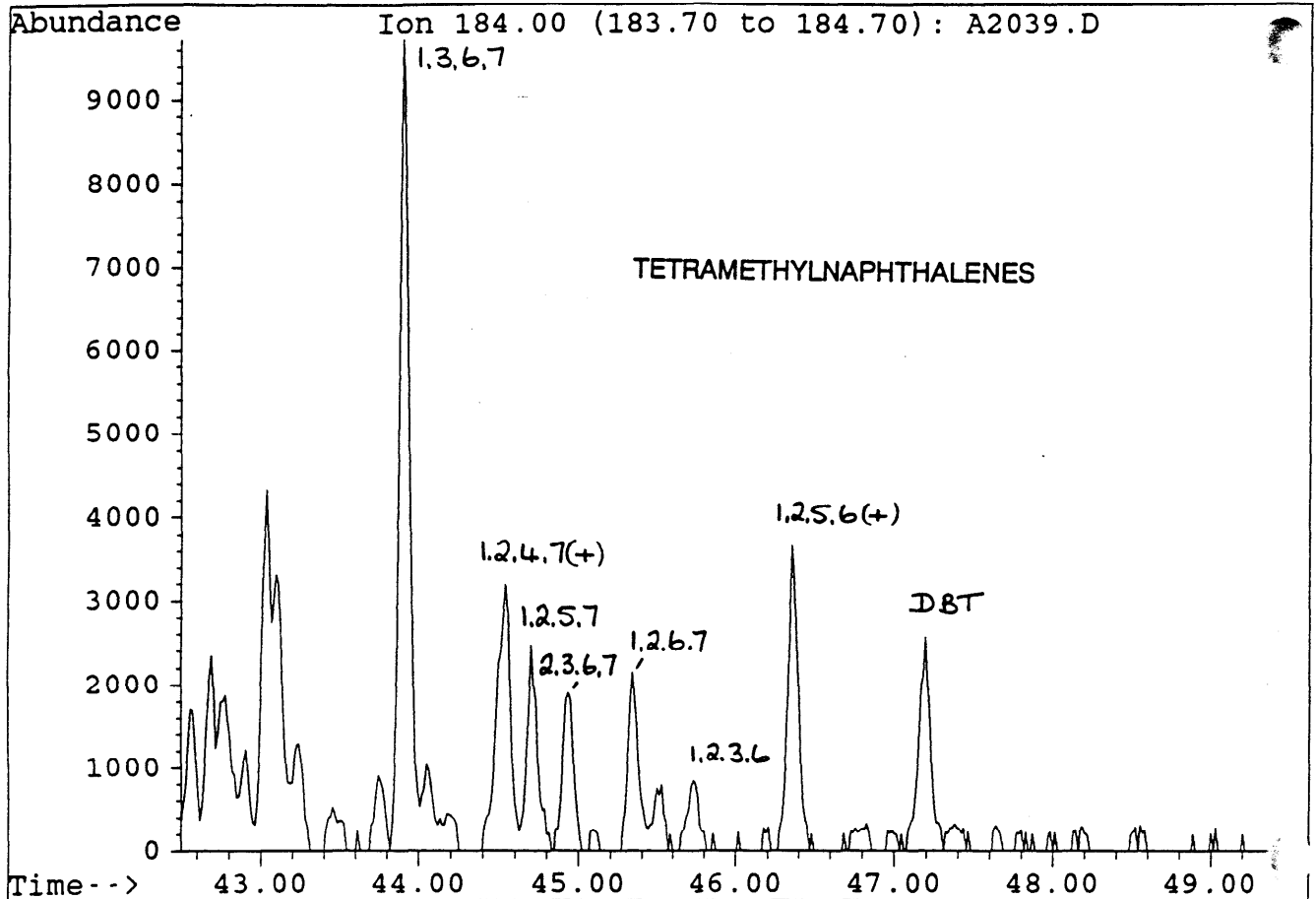
FLUORENES



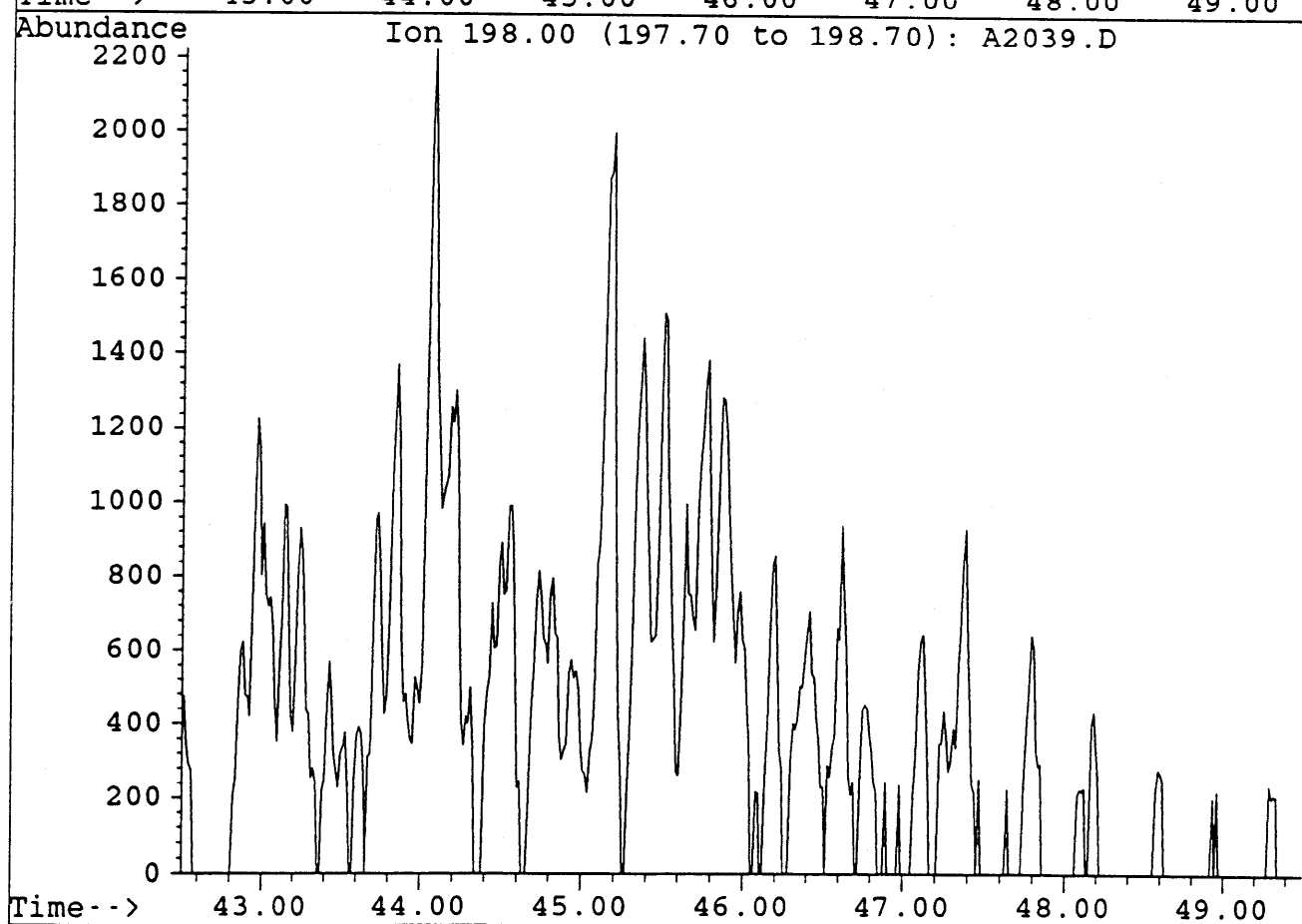
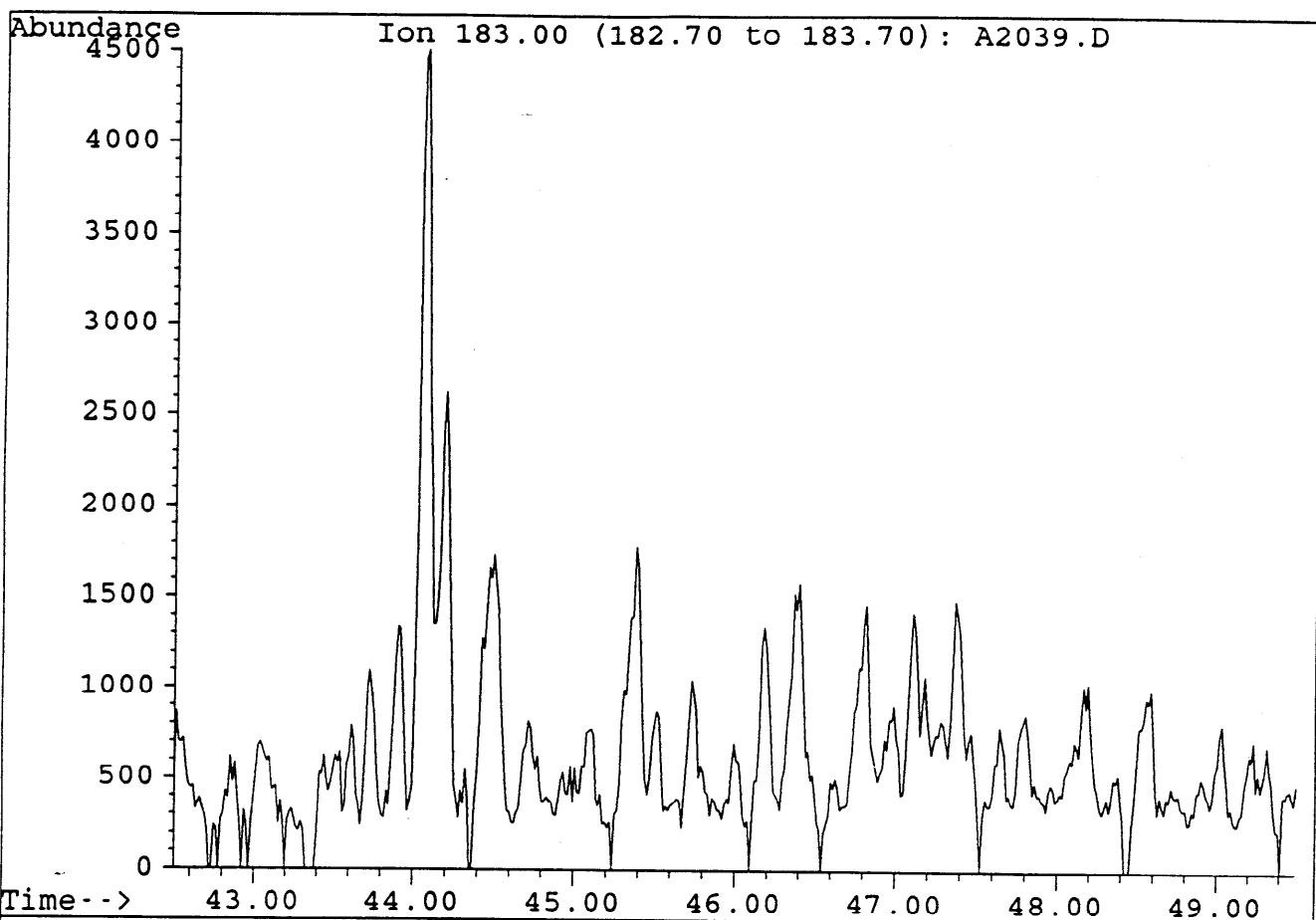
File : A2039.D  
Sample : MINERVA#1, RFS-AD-1157. L-008. AROS.  
Misc. Info : COL#155. 17-1-94. GEC.



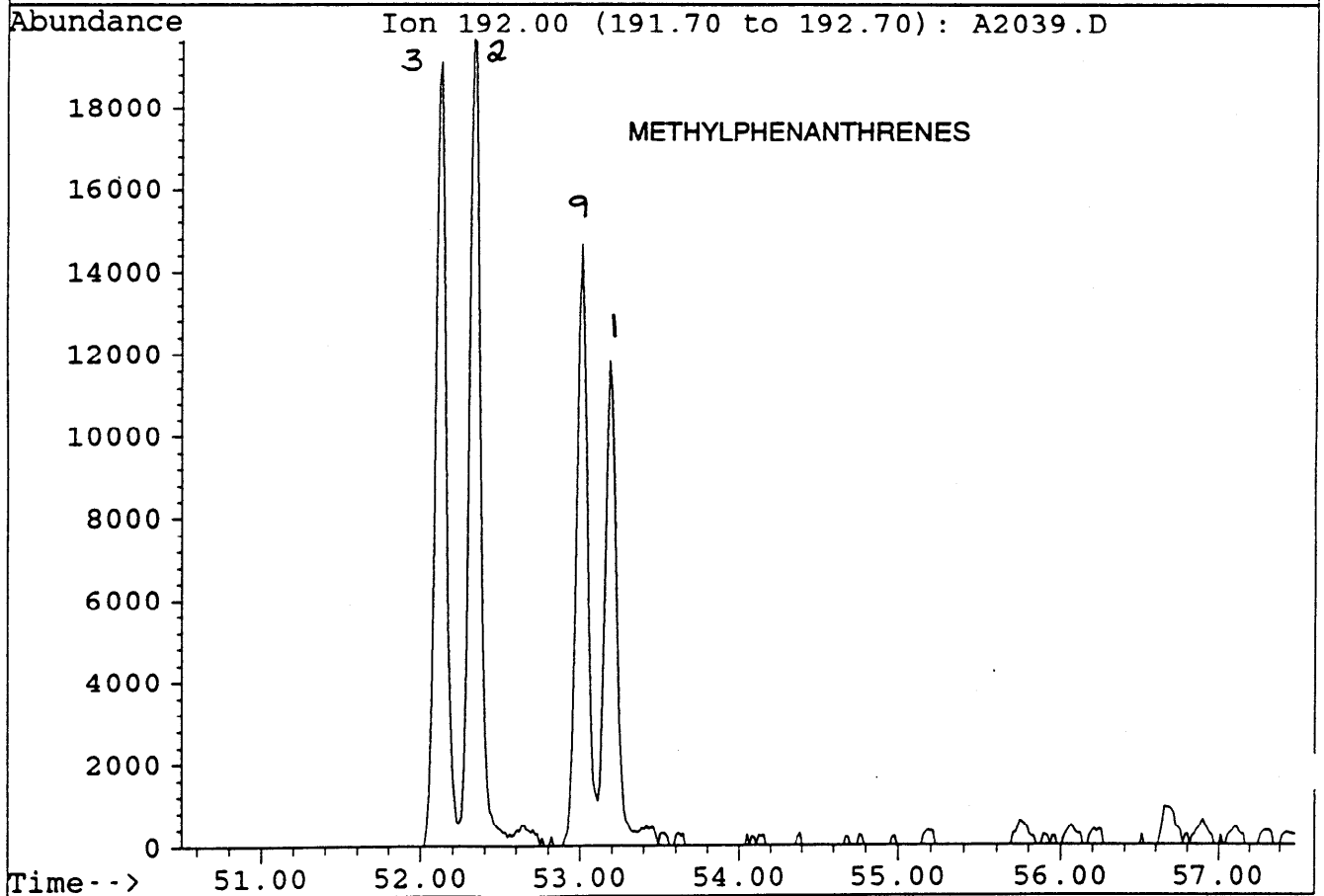
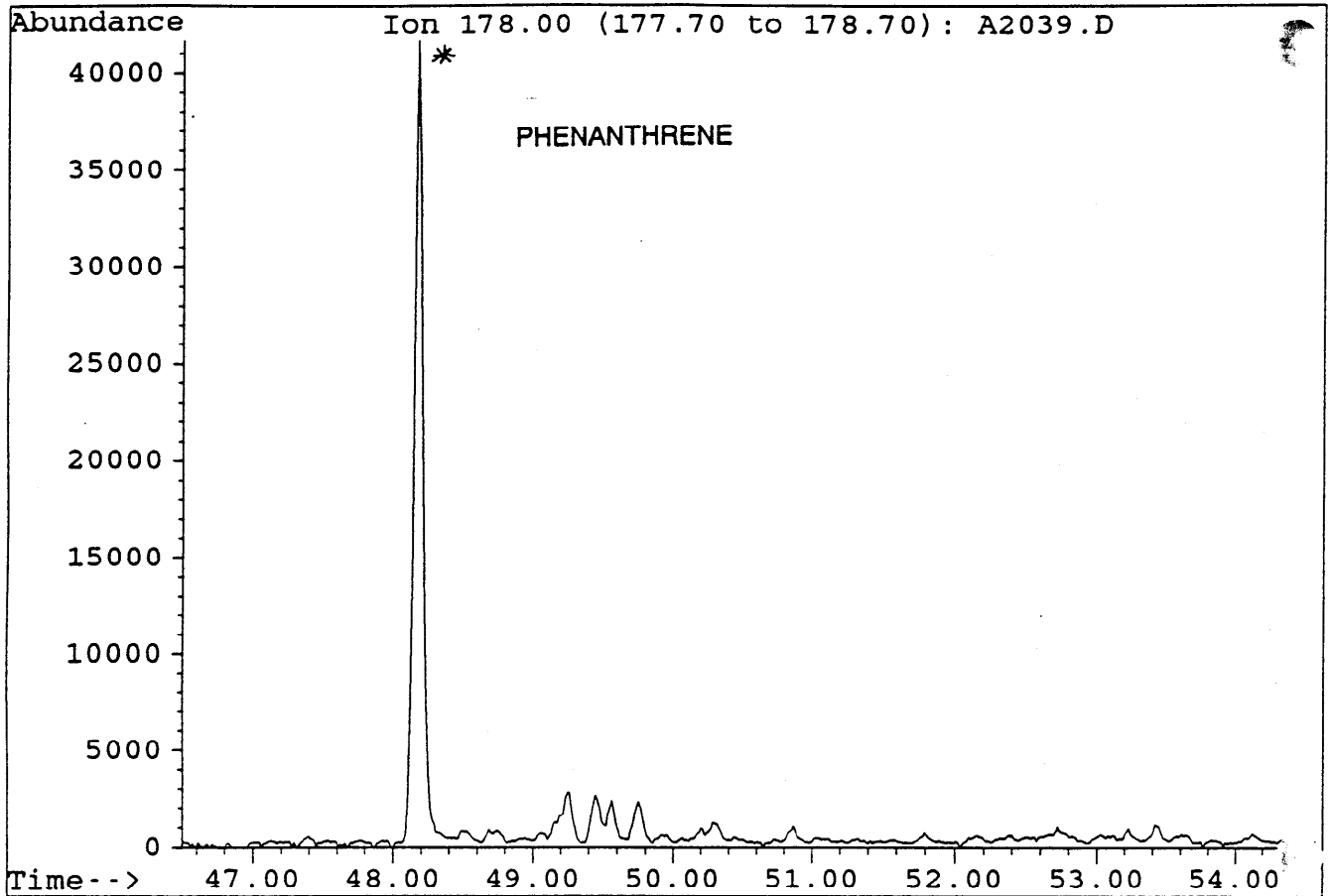
File : A2039.D  
Sample : MINERVA#1, RFS-AD-1157. L-008. AROS.  
Misc. Info : COL#155. 17-1-94. GEC.



File : A2039.D  
Sample : MINERVA#1, RFS-AD-1157. L-008. AROS.  
Misc. Info : COL#155. 17-1-94. GEC.

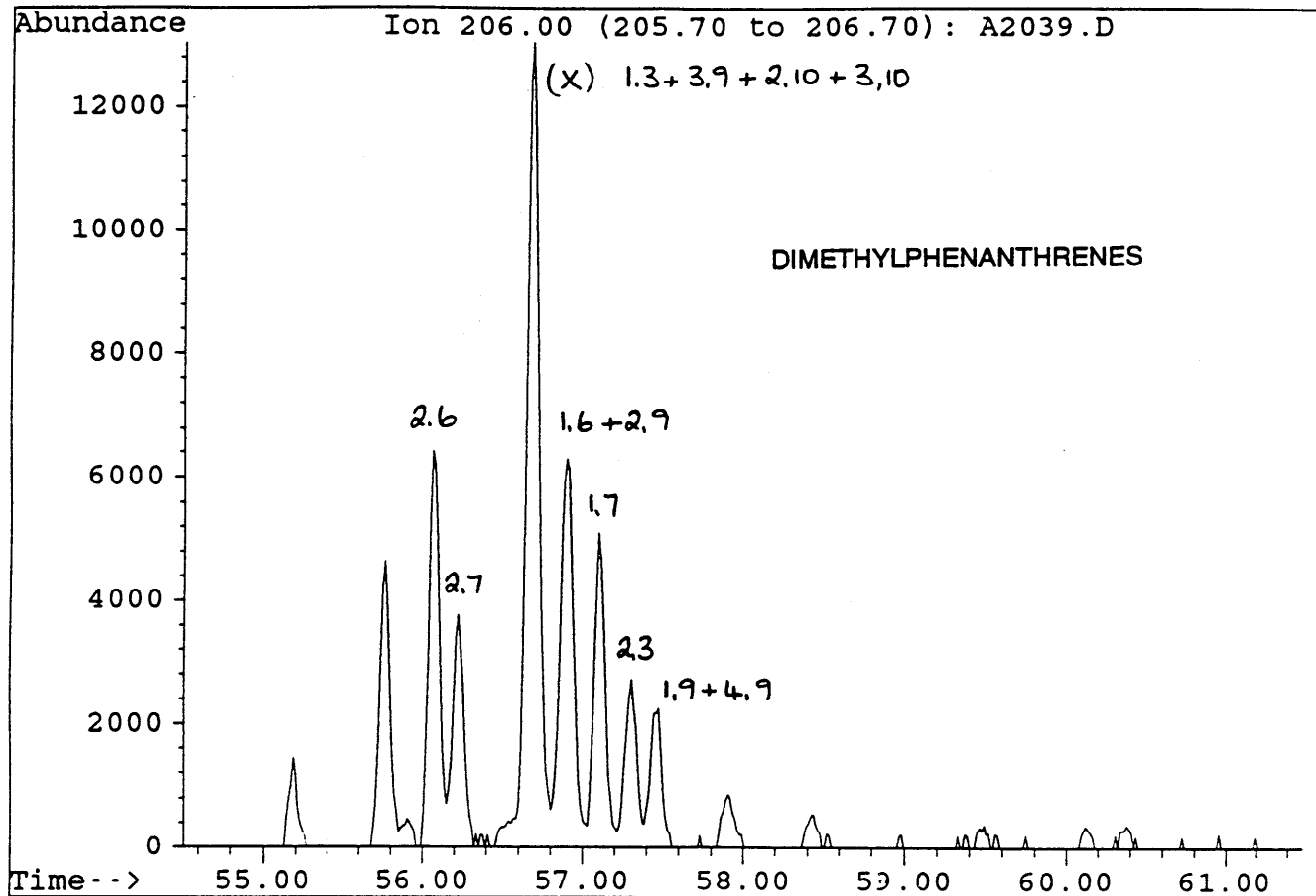


File : A2039.D  
Sample : MINERVA#1, RFS-AD-1157. L-008. AROS.  
Misc. Info : COL#155. 17-1-94. GEC.

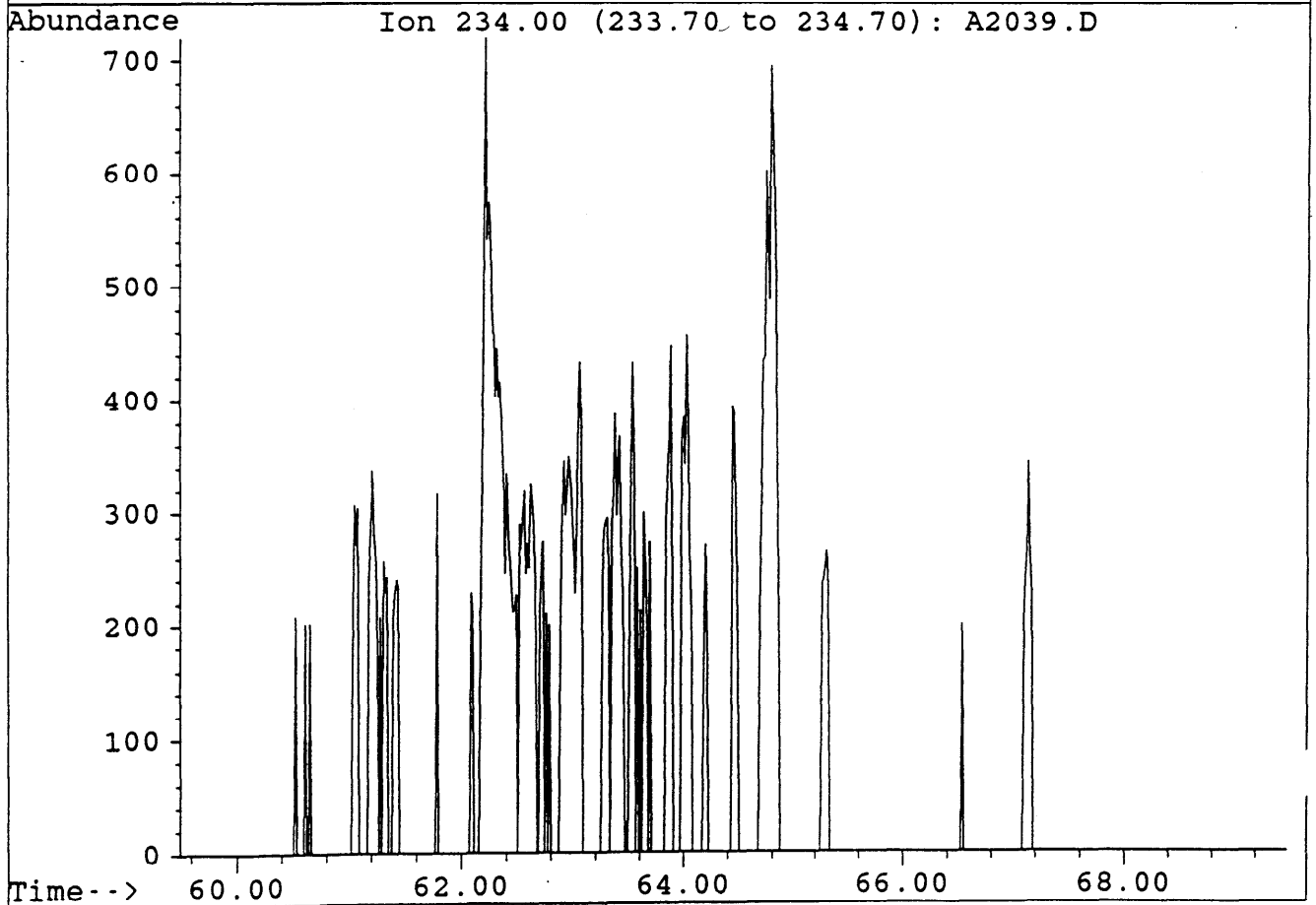
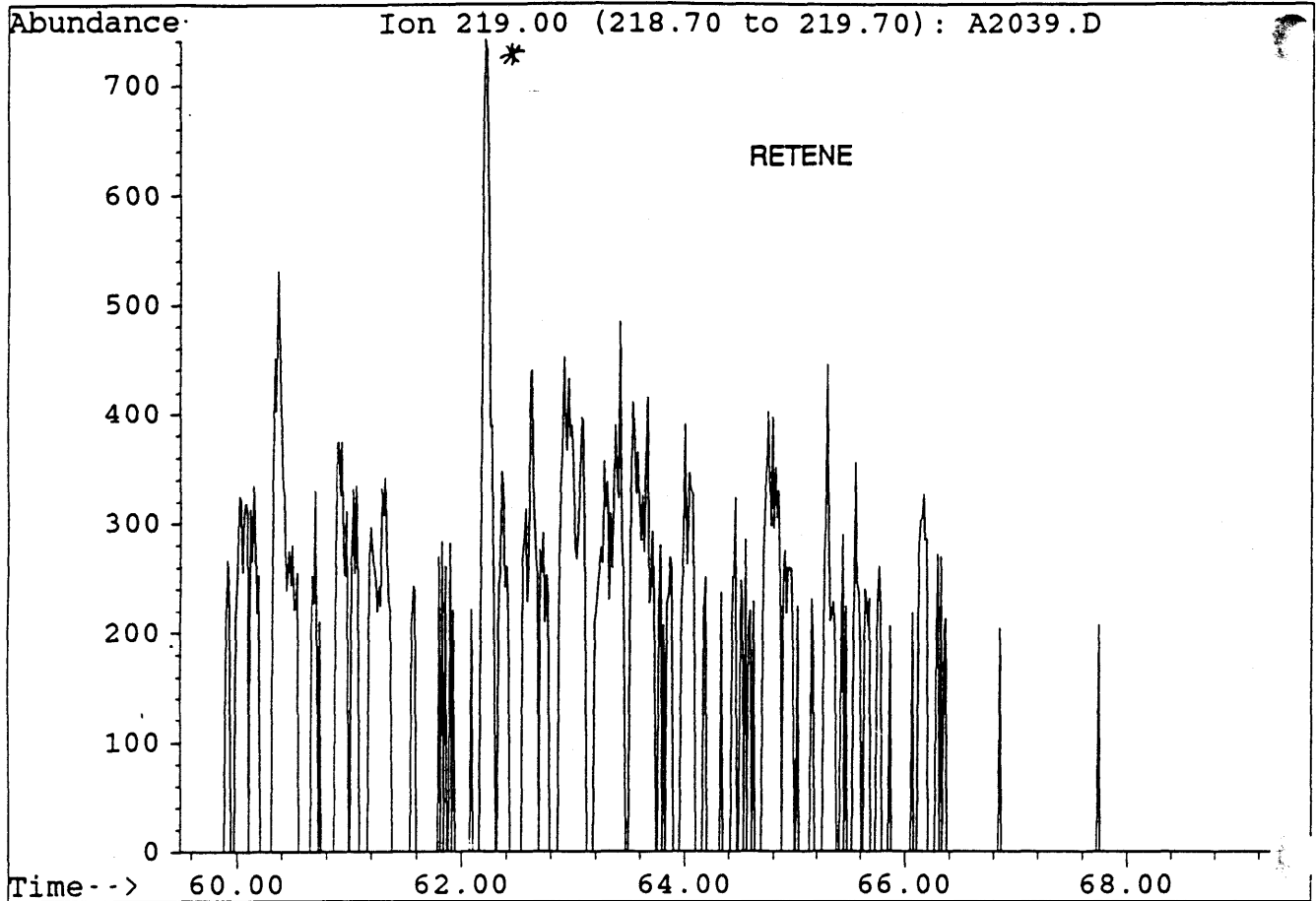


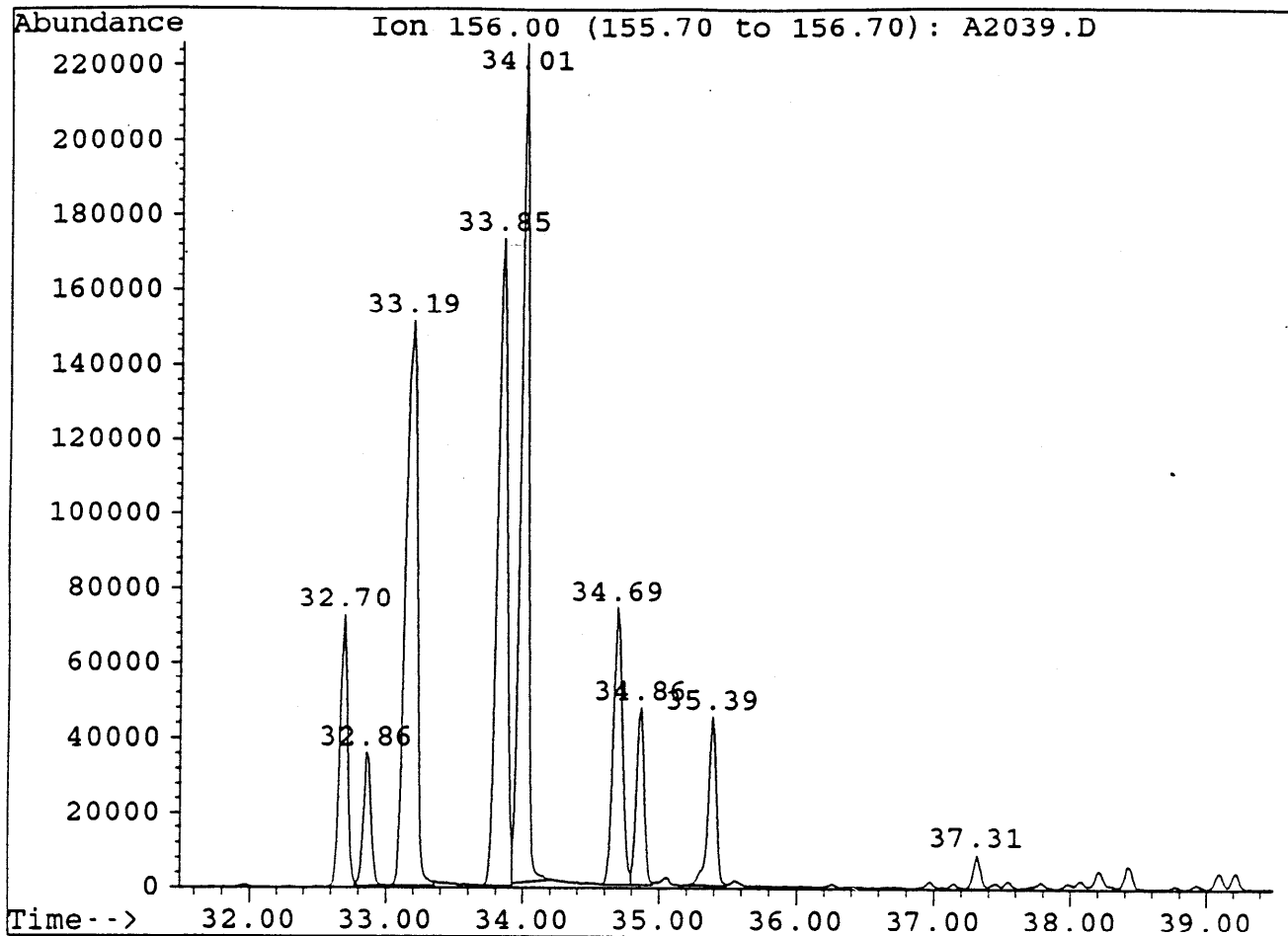


File : A2039.D  
Sample : MINERVA#1, RFS-AD-1157. L-008. AROS.  
Misc. Info : COL#155. 17-1-94. GEC.



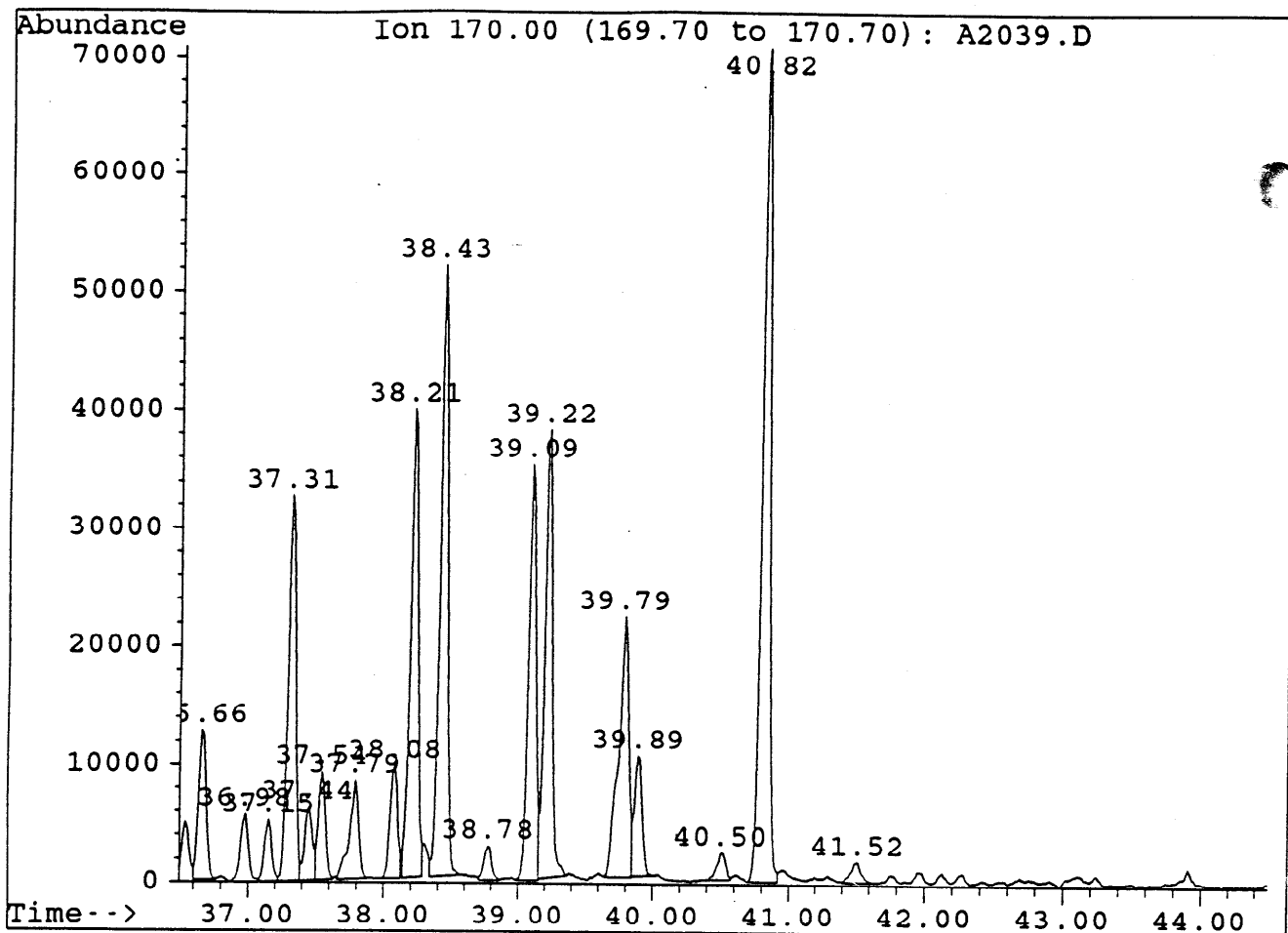
File : A2039.D  
Sample : MINERVA#1, RFS-AD-1157. L-008. AROS.  
Misc. Info : COL#155. 17-1-94. GEC.





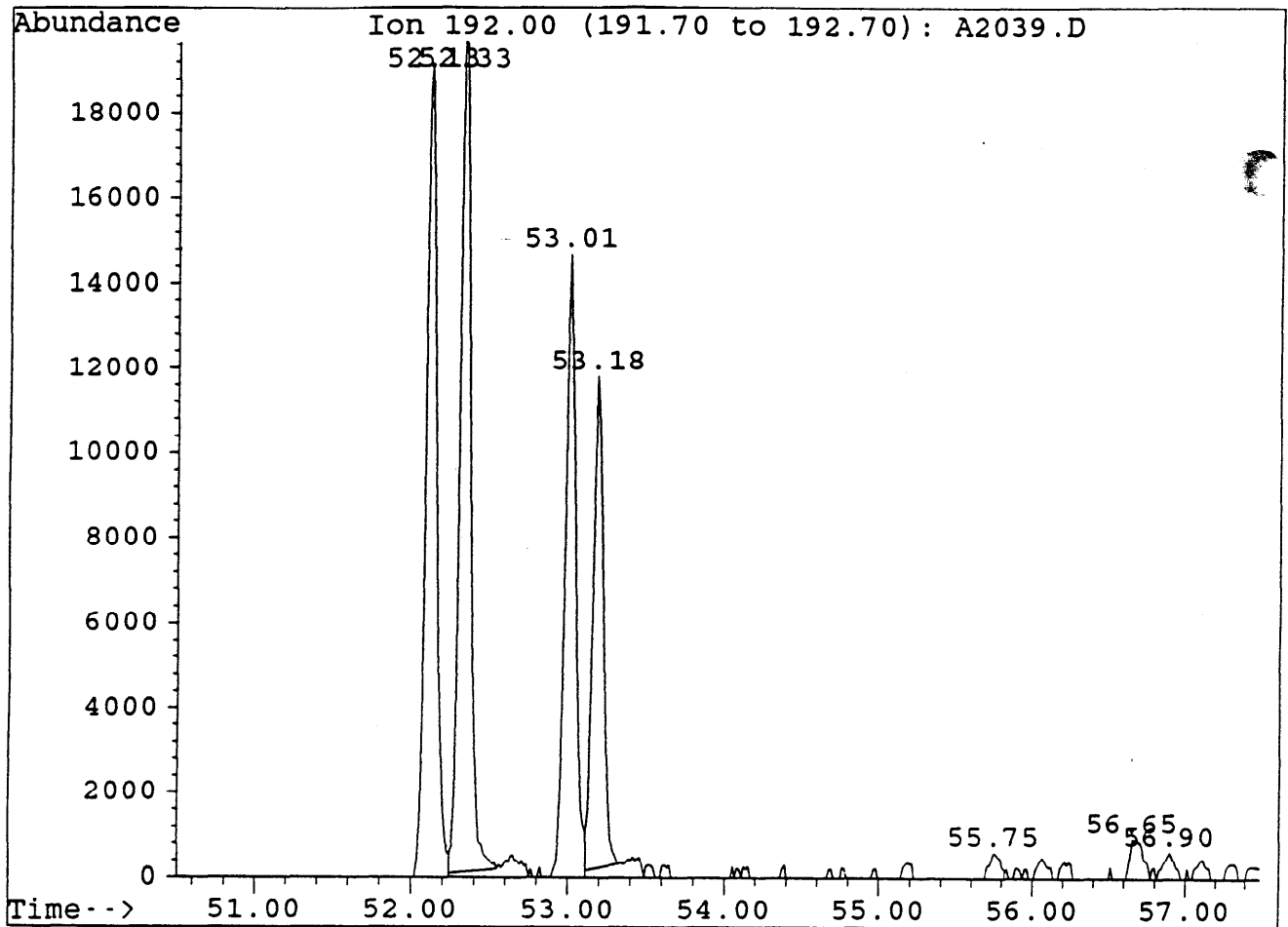
Sample : MINERVA#1, RFS-AD-1157. L-008. AROS.

Peak	Ret.Time	Area	Height	Area %	Ratio %
1	32.70	289424	73024	7.54	32.07
2	32.86	135629	35733	3.53	15.03
3	33.19	902411 <sup>26+</sup>	151391	23.50	100.00
4	33.85	869914 -	173360	22.65	96.40
5	34.01	889276 <sup>16</sup>	224377	23.15	98.54
6	34.69	350861 <sup>14+</sup>	74077	9.14	38.88
7	34.86	184080 <sup>15</sup>	47392	4.79	20.40
8	35.39	186952 -	45108	4.87	20.72
9	37.31	32060	9174	0.83	3.55



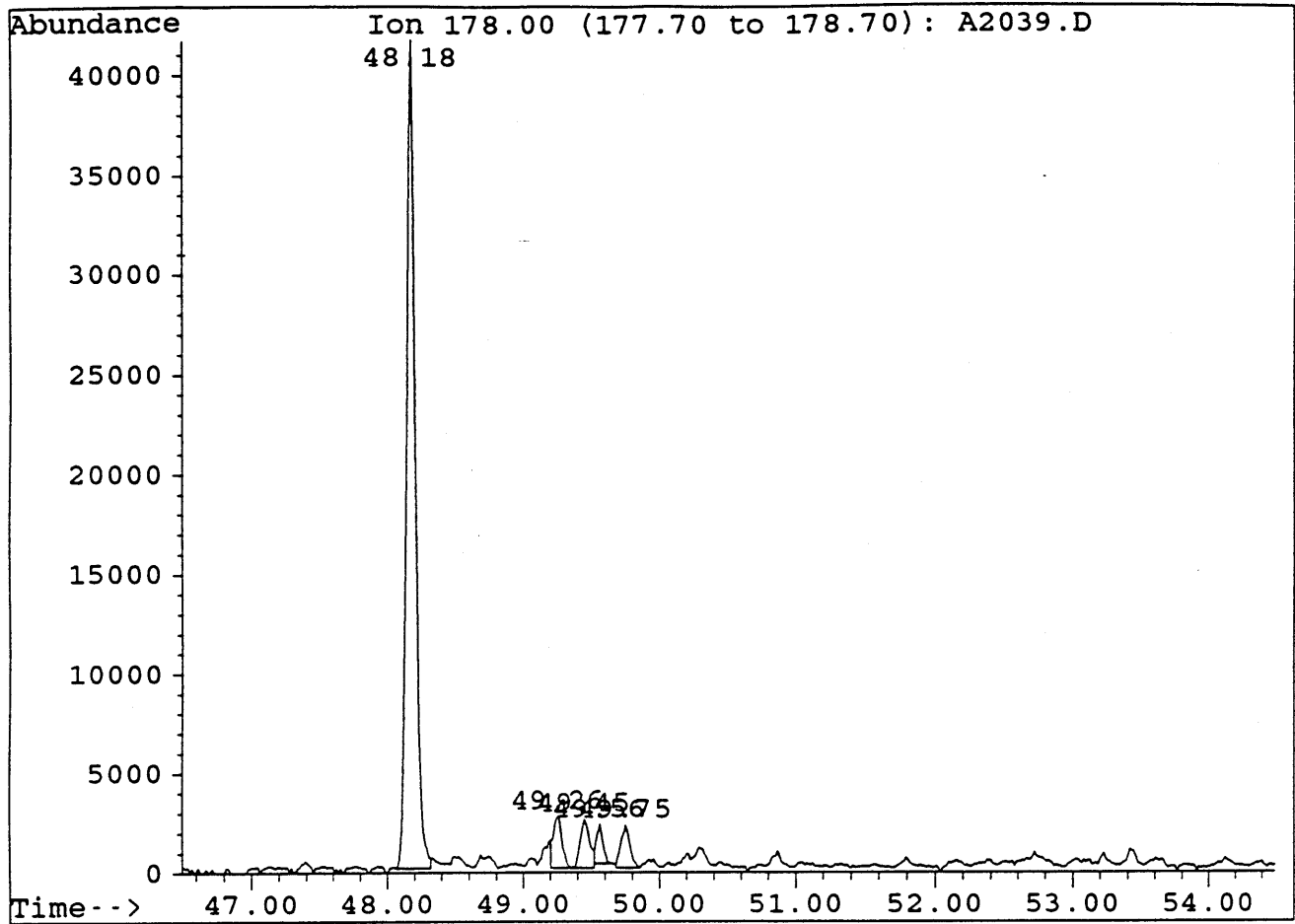
Sample : MINERVA#1, RFS-AD-1157. L-008. AROS.

Peak	Ret.Time	Area	Height	Area %	Ratio %
1	36.66	48309	12676	3.25	16.61
2	36.98	23333	5782	1.57	8.02
3	37.15	19833	5218	1.34	6.82
4	37.31	131202	32701	8.83	45.10
5	37.44	25904	6224	1.74	8.90
6	37.54	32948	9138	2.22	11.33
7	37.79	38562	8369	2.60	13.26
8	38.08	37731	9617	2.54	12.97
9	38.21	<u>159937</u> 137	39690	10.77	54.98
10	38.43	<u>200361</u> 136	51756	13.49	68.87
11	38.78	11181	2825	0.75	3.84
12	39.09	<u>141342</u> 146	35265	9.52	48.59
13	39.22	<u>148514</u> 236	37856	10.00	51.05
14	39.79	115337	22087	7.77	39.65
15	39.89	39423 -	10158	2.65	13.55
16	40.50	10514	2286	0.71	3.61
17	40.82	<u>290906</u> 125	70576	19.59	100.00
18	41.52	9885	1756	0.67	3.40



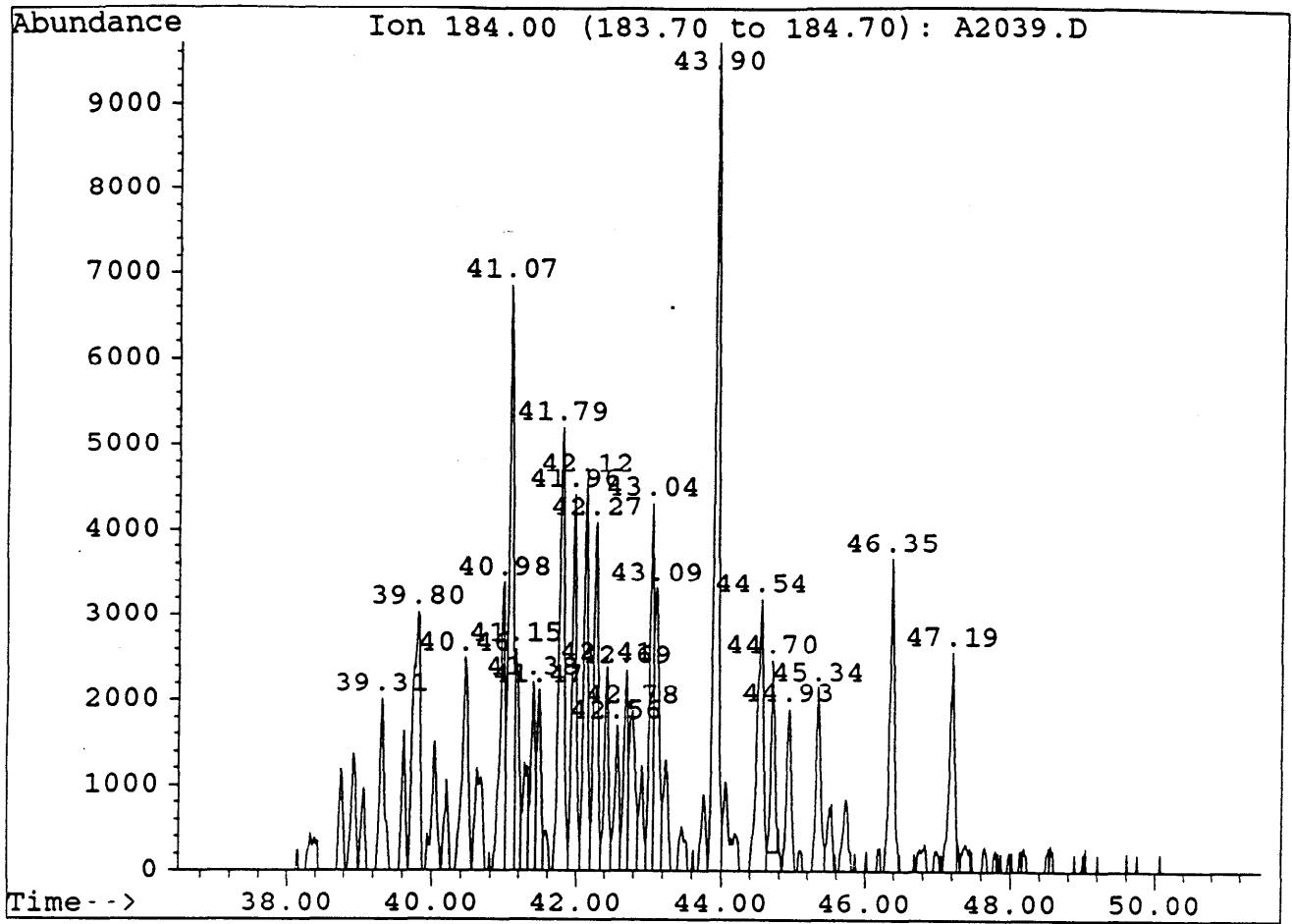
Sample : MINERVA#1, RFS-AD-1157. L-008. AROS.

Peak	Ret.Time	Area	Height	Area %	Ratio %
1	52.13	90043 3	19144	28.14	95.66
2	52.33	94126 2	19532	29.41	100.00
3	53.01	69641 9	14688	21.76	73.99
4	53.18	54218 1	11559	16.94	57.60
5	55.75	3143	614	0.98	3.34
6	56.65	5607	931	1.75	5.96
7	56.90	3232	629	1.01	3.43



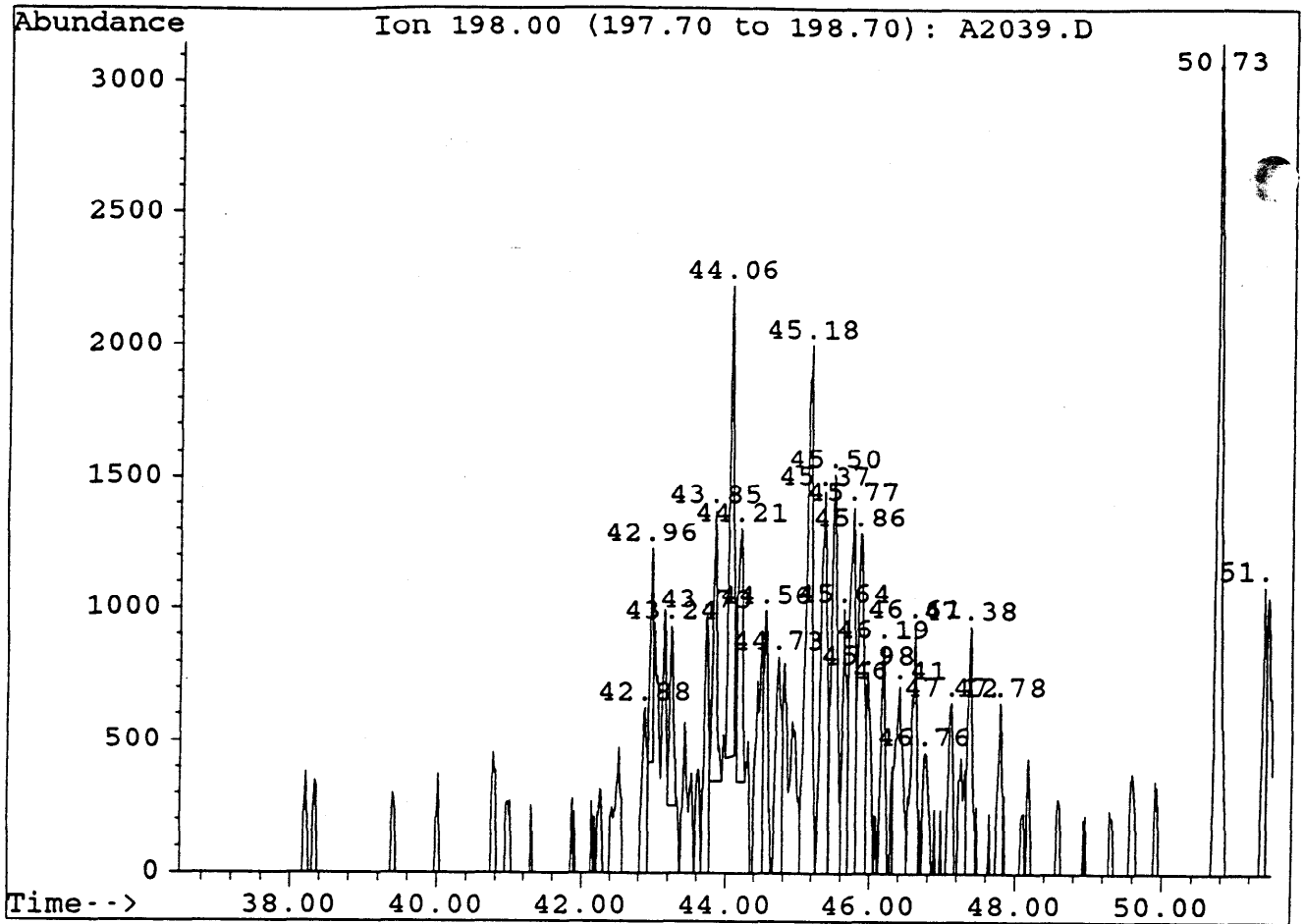
Sample : MINERVA#1, RFS-AD-1157. L-008. AROS.

Peak	Ret.Time	Area	Height	Area %	Ratio %
1	48.18	183774 <i>P</i>	41504	82.41	100.00
2	49.26	11124	2600	4.99	6.05
3	49.45	11984	2457	5.37	6.52
4	49.56	6211	1967	2.79	3.38
5	49.75	9911	2146	4.44	5.39



Sample : MINERVA#1, RFS-AD-1157. L-008. AROS.

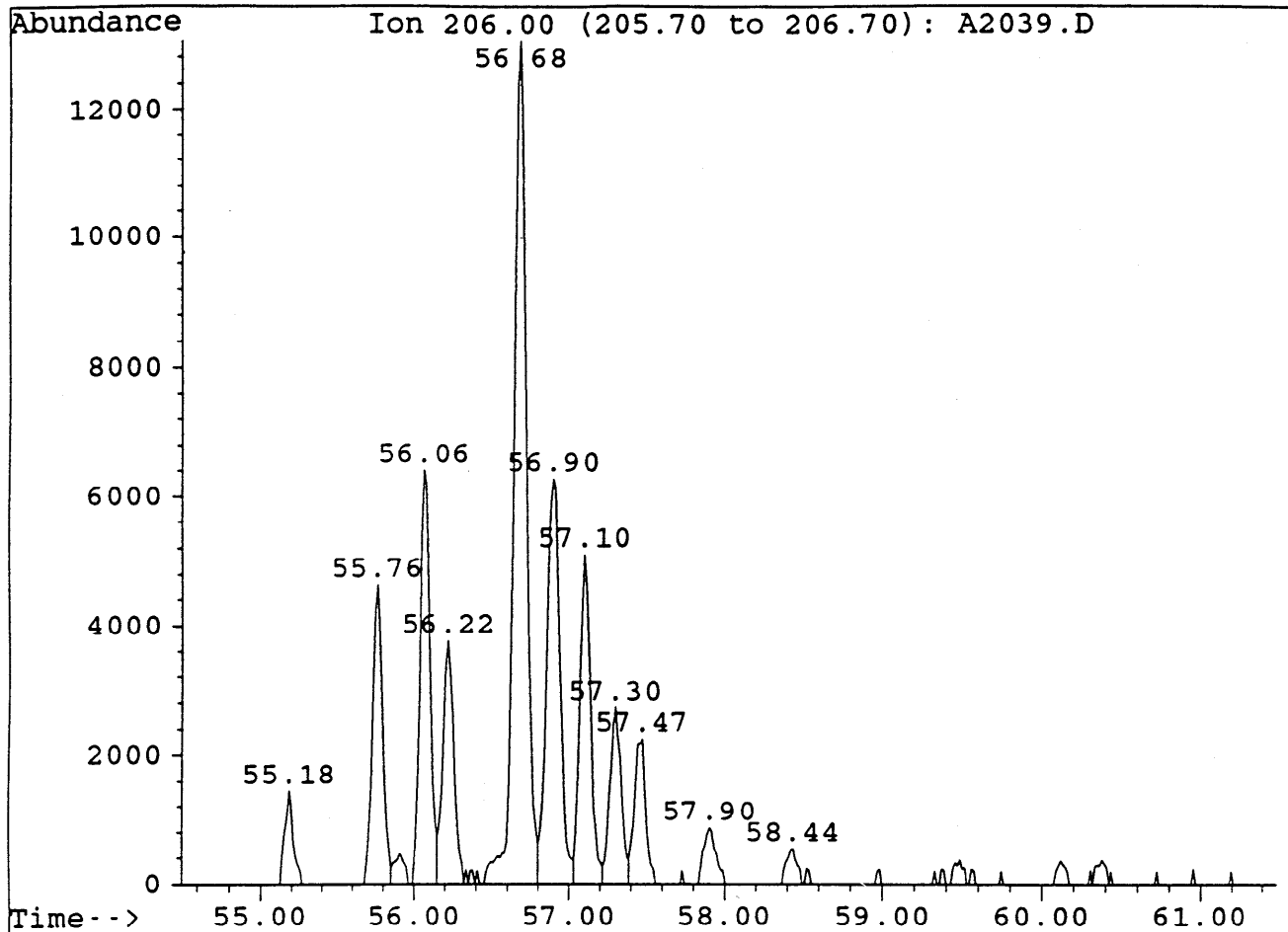
Peak	Ret.Time	Area	Height	Area %	Ratio %
1	39.31	9344	2012	2.38	21.67
2	39.80	20634	3042	5.26	47.86
3	40.46	14244	2502	3.63	33.04
4	40.98	16452	3389	4.19	38.16
5	41.07	32238	6869	8.22	74.77
6	41.15	8745	2605	2.23	20.28
7	41.38	9442	2215	2.41	21.90
8	41.47	8313	2120	2.12	19.28
9	41.79	27503	5215	7.01	63.79
10	41.96	19719	4433	5.03	45.73
11	42.12	19300	4610	4.92	44.76
12	42.27	17511	4097	4.46	40.61
13	42.41	10109	2389	2.58	23.45
14	42.56	7486	1705	1.91	17.36
15	42.69	9217	2355	2.35	21.38
16	42.78	10749	1880	2.74	24.93
17	43.04	16516	4334	4.21	38.31
18	43.09	14380	3323	3.67	33.35
19	43.90	43116	9730	10.99	100.00
20	44.54	19424	3193	4.95	45.05
21	44.70	8414	2244	2.15	19.51
22	44.93	9296	1908	2.37	21.56
23	45.34	10358	2152	2.64	24.02
24	46.35	16859	3669	4.30	39.10
25	47.19	12878	2568	3.28	29.87



Sample : MINERVA#1, RFS-AD-1157. L-008. AROS.

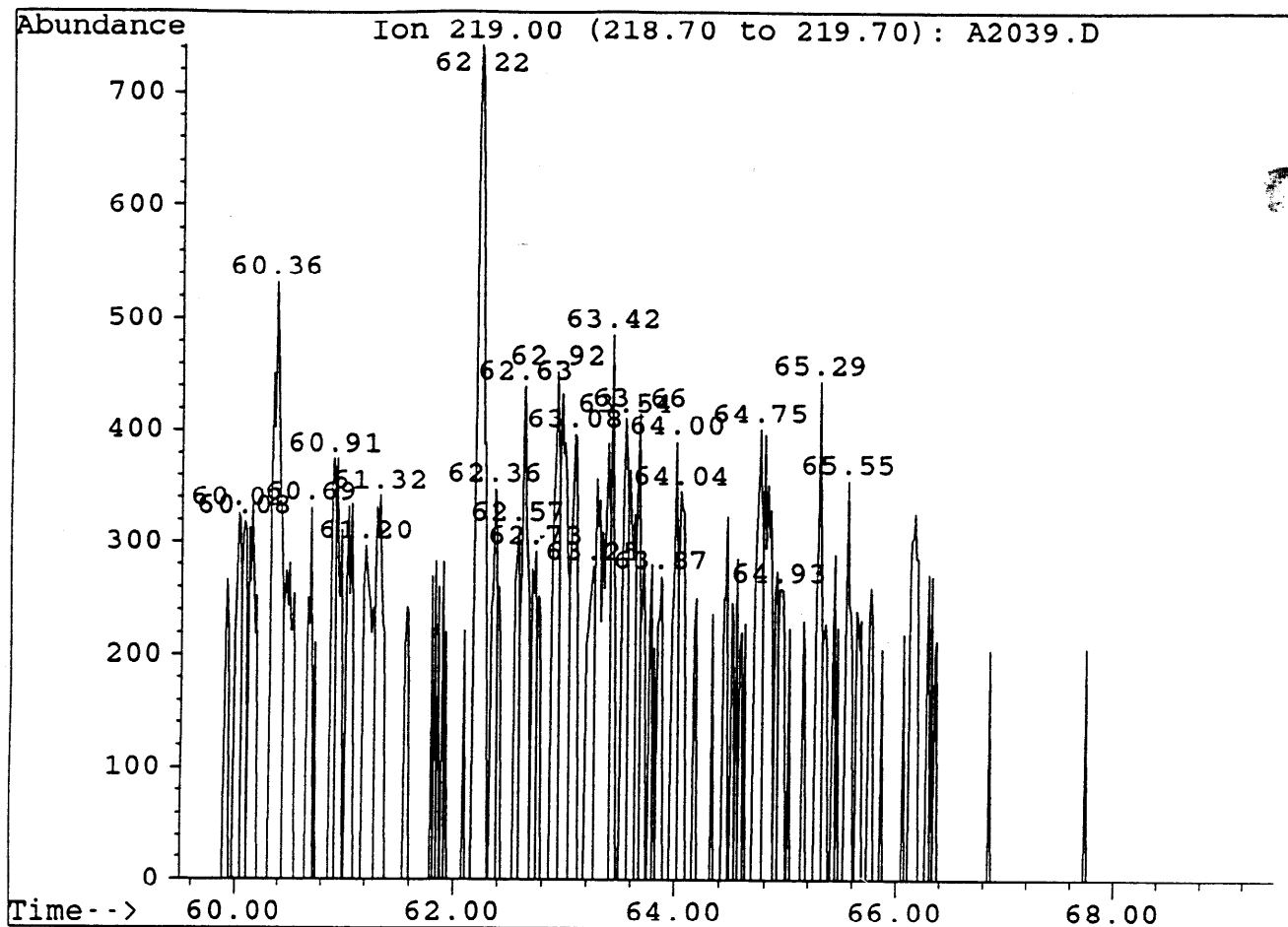
Peak	Ret.Time	Area	Height	Area %	Ratio %
1	42.88	3054	624	2.31	20.19
2	42.96	2444	808	1.85	16.15
3	43.24	2526	677	1.91	16.70
4	43.73	4388	974	3.32	29.00
5	43.85	3963	1027	2.99	26.19
6	44.06	7561	1782	5.71	49.97
7	44.21	4103	962	3.10	27.12
8	44.56	4053	992	3.06	26.79
9	44.73	4610	818	3.48	30.47
10	45.18	12376	2000	9.35	81.80
11	45.37	8731	1446	6.60	57.71
12	45.50	8253	1513	6.24	54.55
13	45.64	4326	999	3.27	28.59
14	45.77	7344	1386	5.55	48.54
15	45.86	7552	1288	5.71	49.91
16	45.98	3041	764	2.30	20.10
17	46.19	3667	862	2.77	24.24
18	46.41	4938	710	3.73	32.64
19	46.61	4642	940	3.51	30.68
20	46.76	2431	458	1.84	16.07
21	47.12	2702	646	2.04	17.86
22	47.38	3908	934	2.95	25.8
23	47.78	2624	646	1.98	17.34
24	50.73	15130	3148	11.43	100.00
25	51.39	3975	1087	3.00	26.27





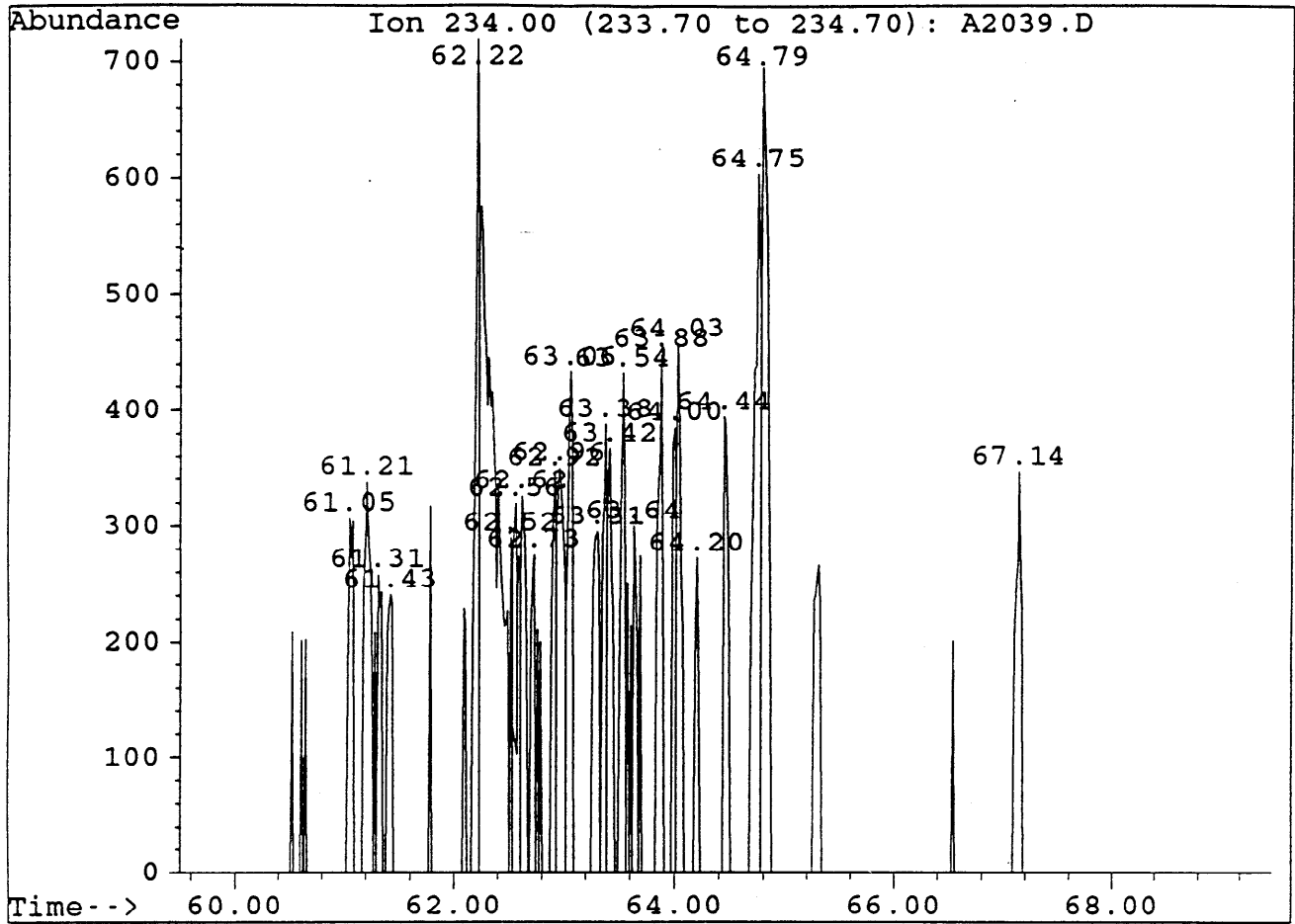
Sample : MINERVA#1, RFS-AD-1157. L-008. AROS.

Peak	Ret.Time	Area	Height	Area %	Ratio %
1	55.18	5597	1459	2.29	7.59
2	55.76	21433	4649	8.76	29.07
3	56.06	29908	6426	12.23	40.57
4	56.22	18272	3775	7.47	24.79
5	56.68	73721 x	13056	30.14	100.00
6	56.90	38266	6285	15.65	51.91
7	57.10	24706 /7	5099	10.10	33.51
8	57.30	14035	2720	5.74	19.04
9	57.47	11241	2248	4.60	15.25
10	57.90	4834	873	1.98	6.56
11	58.44	2555	545	1.04	3.47



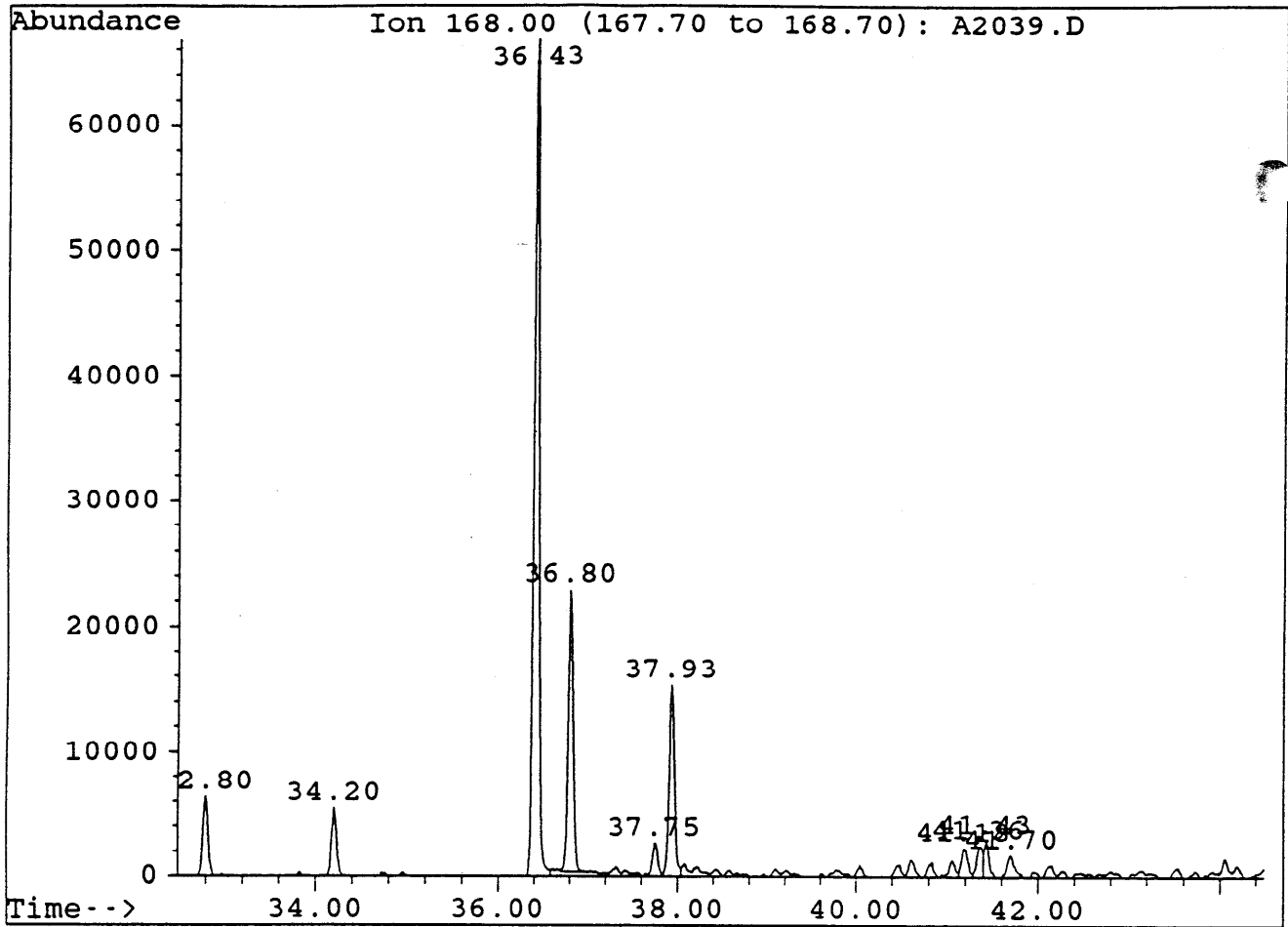
Sample : MINERVA#1, RFS-AD-1157. L-008. AROS.

Peak	Ret.Time	Area	Height	Area %	Ratio %
1	60.02	1190	326	3.42	31.23
2	60.08	806	319	2.32	21.15
3	60.36	3042	532	8.74	79.84
4	60.69	881	331	2.53	23.12
5	60.91	1164	375	3.34	30.55
6	61.20	1748	297	5.02	45.88
7	61.32	1455	342	4.18	38.19
8	62.22	<u>3810</u> <i>R</i>	742	10.94	100.00
9	62.36	1230	348	3.53	32.28
10	62.57	946	313	2.72	24.83
11	62.63	1719	440	4.94	45.12
12	62.73	890	292	2.56	23.36
13	62.92	1847	453	5.31	48.48
14	63.08	1480	397	4.25	38.85
15	63.25	1277	278	3.67	33.52
16	63.42	880	486	2.53	23.10
17	63.54	1469	411	4.22	38.56
18	63.66	864	416	2.48	22.68
19	63.87	863	270	2.48	22.65
20	64.00	1256	391	3.61	32.97
21	64.04	1060	346	3.04	27.82
22	64.75	1682	402	4.83	44.
23	64.93	849	259	2.44	22.28
24	65.29	1299	445	3.73	34.09
25	65.55	1106	356	3.18	29.03



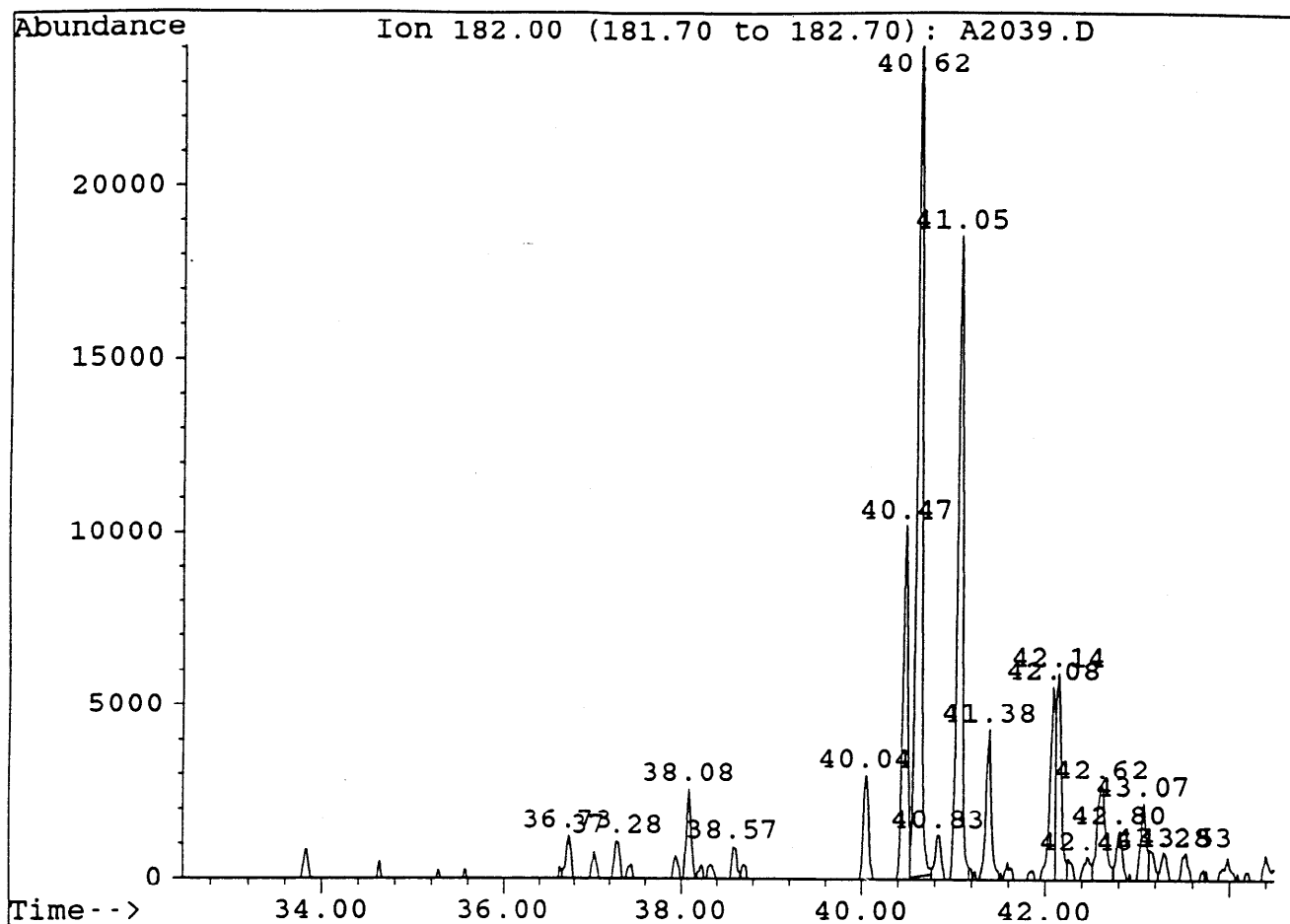
Sample : MINERVA#1, RFS-AD-1157. L-008. AROS.

Peak	Ret.Time	Area	Height	Area %	Ratio %
1	61.05	949	307	3.25	36.03
2	61.21	1413	338	4.84	53.64
3	61.31	628	258	2.15	23.84
4	61.43	779	241	2.67	29.57
5	62.22	1995	720	6.83	75.74
6	62.52	476	290	1.63	18.07
7	62.56	446	205	1.53	16.93
8	62.62	999	326	3.42	37.93
9	62.73	646	275	2.21	24.53
10	62.92	1012	346	3.46	38.42
11	62.96	1559	350	5.34	59.19
12	63.06	1289	433	4.41	48.94
13	63.31	1173	295	4.01	44.53
14	63.38	1114	388	3.81	42.29
15	63.42	1022	367	3.50	38.80
16	63.54	1149	432	3.93	43.62
17	63.64	658	300	2.25	24.98
18	63.88	1466	448	5.02	55.66
19	64.00	954	385	3.26	36.22
20	64.03	1145	457	3.92	43.47
21	64.20	598	272	2.05	22.70
22	64.44	1154	394	3.95	43.81
23	64.75	2632	603	9.01	99.92
24	64.79	2634	696	9.01	100.00
25	67.14	1330	346	4.55	50.49



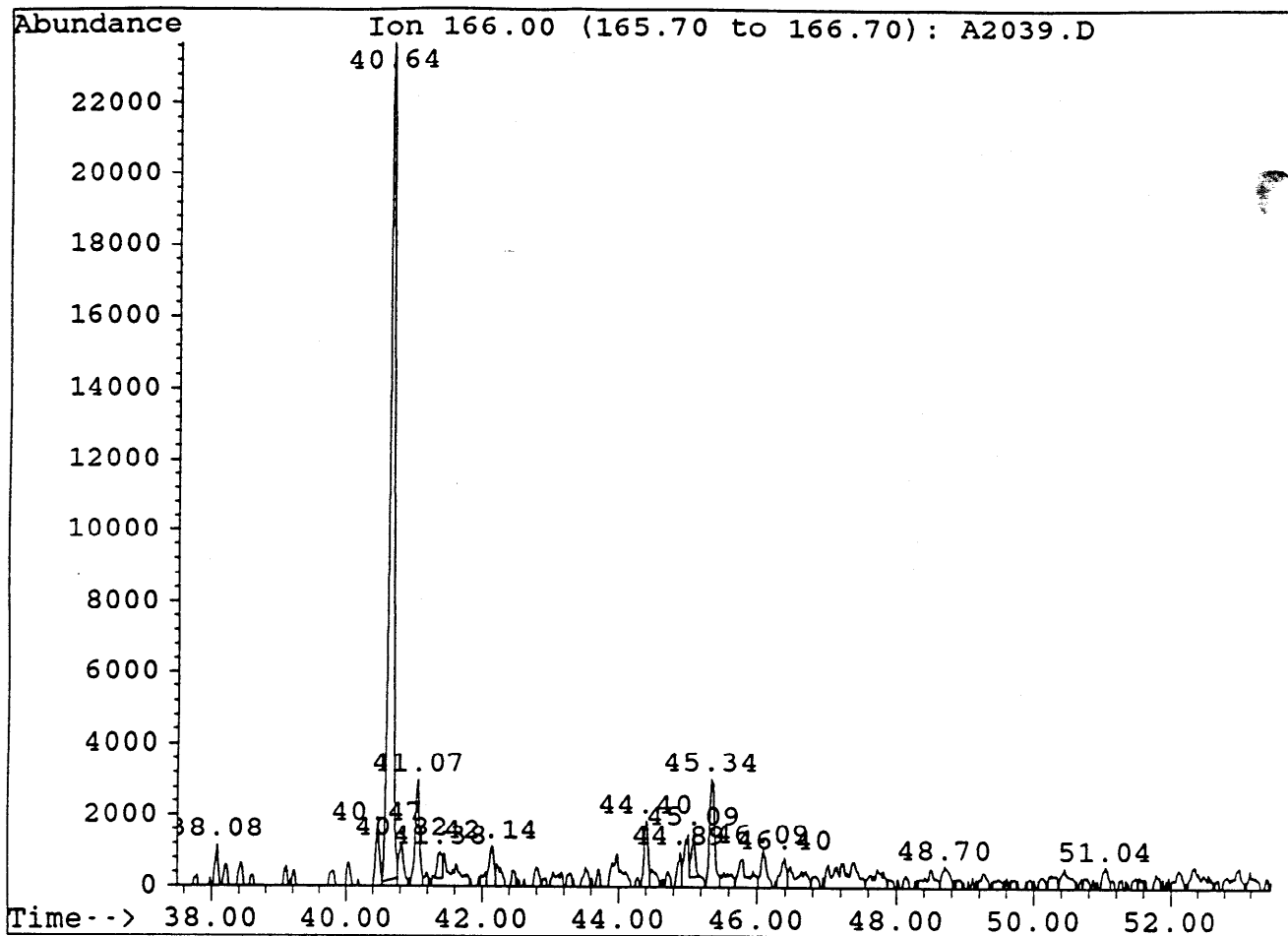
Sample : MINERVA#1, RFS-AD-1157. L-008. AROS.

Peak	Ret.Time	Area	Height	Area %	Ratio %
1	32.80	25614	6444	4.90	9.62
2	34.20	21230	5545	4.07	7.97
3	36.43	266344	66768	51.00	100.00
4	36.80	88948	22561	17.03	33.40
5	37.75	11067	2658	2.12	4.16
6	37.93	64908	15346	12.43	24.37
7	41.18	11737	2274	2.25	4.41
8	41.36	12276	2509	2.35	4.61
9	41.43	10018	2914	1.92	3.76
10	41.70	10108	1746	1.94	3.80



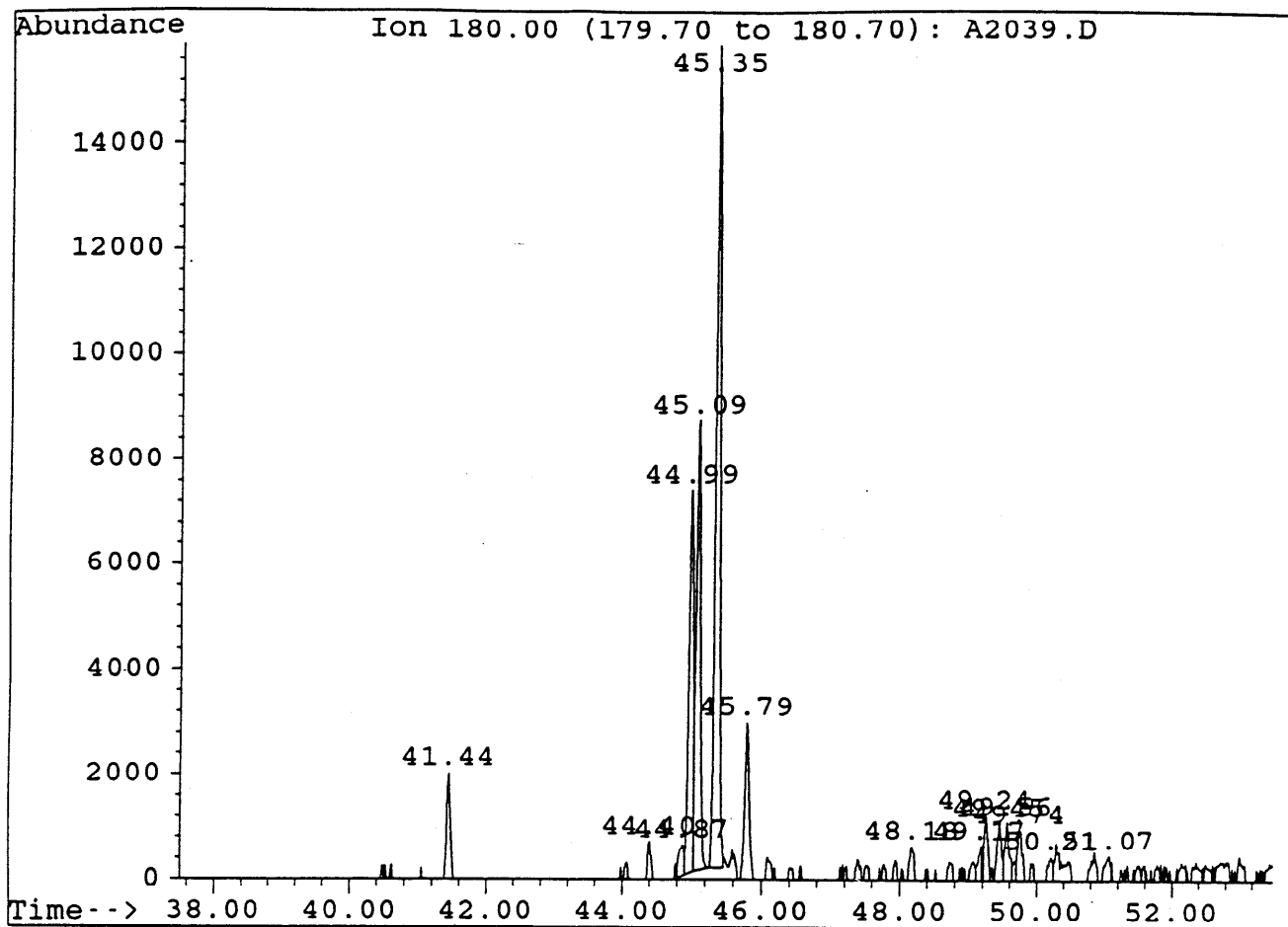
Sample : MINERVA#1, RFS-AD-1157. L-008. AROS.

Peak	Ret.Time	Area	Height	Area %	Ratio %
1	36.73	4897	1234	1.36	5.01
2	37.28	4519	1084	1.25	4.62
3	38.08	9384	2575	2.60	9.60
4	38.57	3561	943	0.99	3.64
5	40.04	12341	2999	3.42	12.63
6	40.47	39589	10224	10.97	40.51
7	40.62	97728	23994	27.08	100.00
8	40.83	5833	1277	1.62	5.97
9	41.05	74423	18576	20.62	76.15
10	41.38	17931	4334	4.97	18.35
11	42.08	23906	5561	6.62	24.46
12	42.14	22141	5962	6.13	22.66
13	42.46	3568	651	0.99	3.65
14	42.62	18010	2705	4.99	18.43
15	42.80	6428	1420	1.78	6.58
16	43.07	9597	2222	2.66	9.82
17	43.28	3505	777	0.97	3.59
18	43.53	3543	774	0.98	3.63



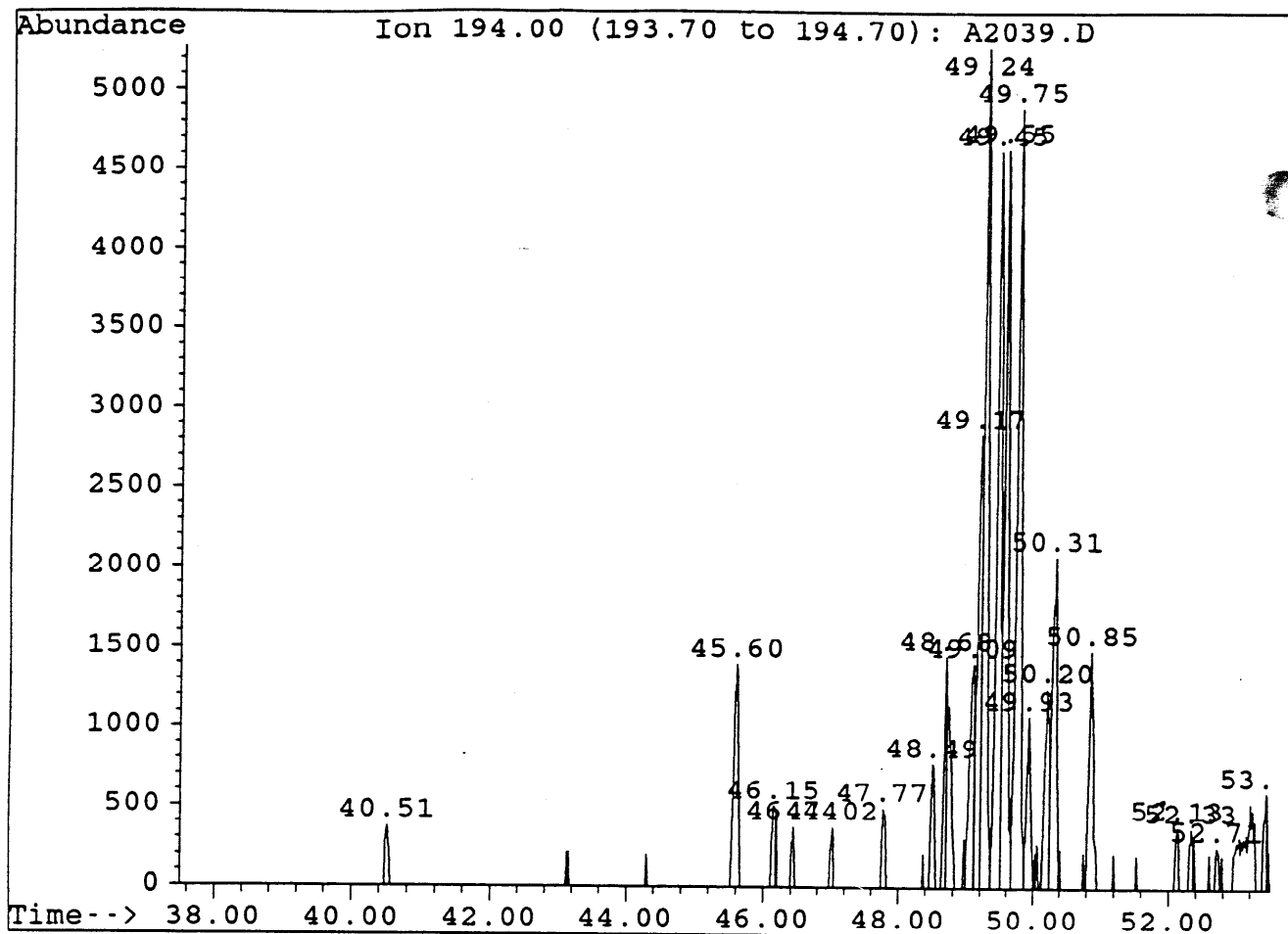
Sample : MINERVA#1, RFS-AD-1157. L-008. AROS.

Peak	Ret.Time	Area	Height	Area %	Ratio %
1	38.08	3762	1171	1.80	3.24
2	40.47	6855	1645	3.28	5.90
3	40.64	116242	23549	55.60	100.00
4	40.82	6138	1204	2.94	5.28
5	41.07	14133	3024	6.76	12.16
6	41.38	4054	771	1.94	3.49
7	42.14	5966	1146	2.85	5.13
8	44.40	7930	1875	3.79	6.82
9	44.89	3961	1005	1.89	3.41
10	45.09	4572	1261	2.19	3.93
11	45.34	16096	3077	7.70	13.85
12	46.09	6089	1053	2.91	5.24
13	46.40	5003	882	2.39	4.30
14	48.70	4642	624	2.22	3.99
15	51.04	3623	597	1.73	3.12



Sample : MINERVA#1, RFS-AD-1157. L-008. AROS.

Peak	Ret.Time	Area	Height	Area %	Ratio %
1	41.44	7360	2023	3.83	10.92
2	44.40	2425	722	1.26	3.60
3	44.87	3012	619	1.57	4.47
4	44.99	32517	7316	16.93	48.26
5	45.09	36526	8582	19.02	54.21
6	45.35	67382	15690	35.09	100.00
7	45.79	13537	2999	7.05	20.09
8	48.18	2866	640	1.49	4.25
9	49.17	2367	644	1.23	3.51
10	49.24	4490	1249	2.34	6.66
11	49.45	5141	1094	2.68	7.63
12	49.56	5074	1114	2.64	7.53
13	49.74	4644	967	2.42	6.89
14	50.21	2113	450	1.10	3.14
15	51.07	2583	470	1.35	3.83

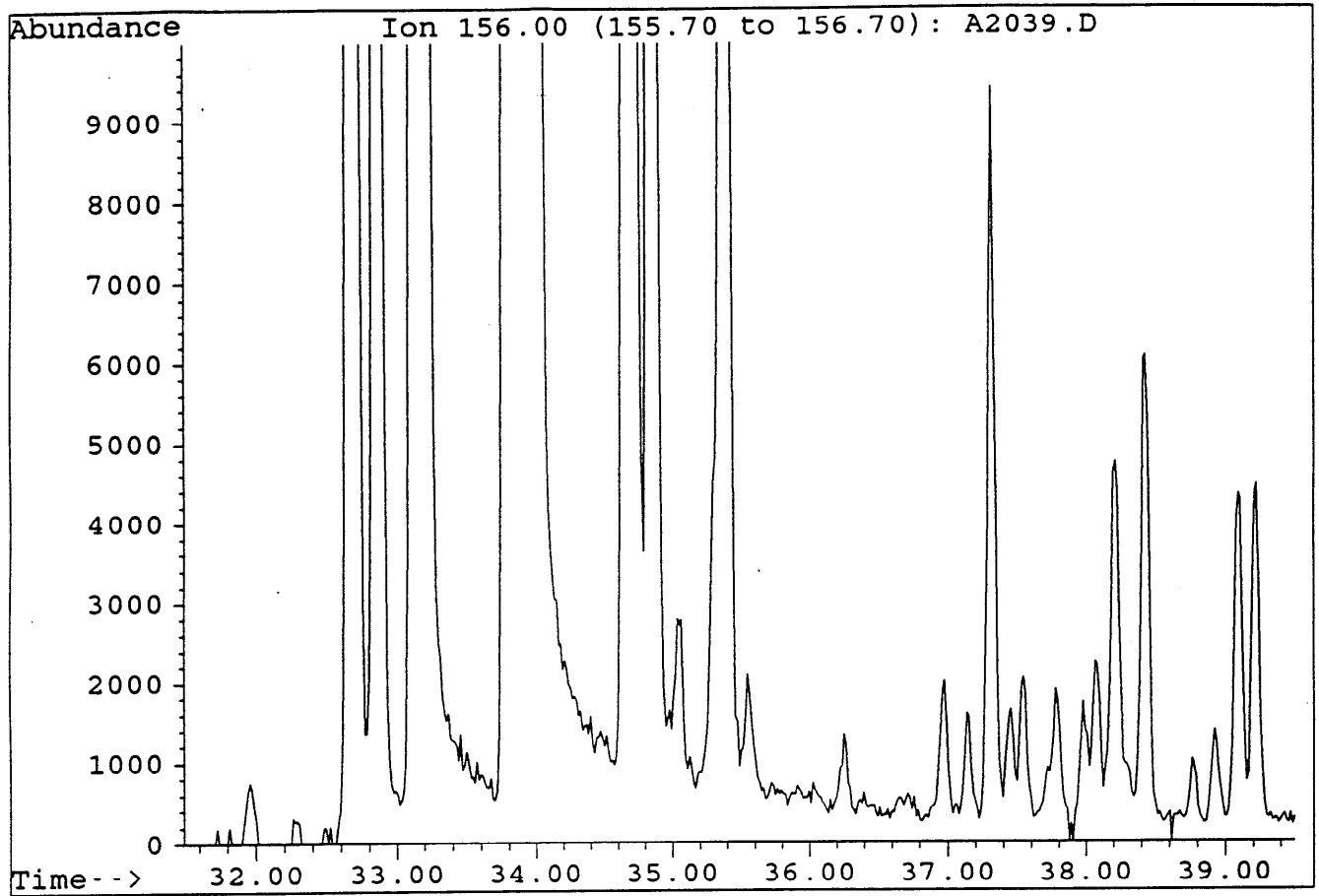


Sample : MINERVA#1, RFS-AD-1157. L-008. AROS.

Peak	Ret.Time	Area	Height	Area %	Ratio %
1	40.51	1291	373	0.80	5.52
2	45.60	6784	1399	4.21	29.00
3	46.15	1846	506	1.15	7.89
4	46.44	971	372	0.60	4.15
5	47.02	1031	373	0.64	4.41
6	47.77	1728	493	1.07	7.39
7	48.49	2883	777	1.79	12.32
8	48.68	4097	1450	2.55	17.51
9	49.09	6660	1407	4.14	28.47
10	49.17	12209	2840	7.59	52.19
11	49.24	22782	5273	14.15	97.39
12	49.45	21754	4623	13.52	92.99
13	49.55	20839	4636	12.95	89.08
14	49.75	23393	4890	14.53	100.00
15	49.93	4485	1077	2.79	19.17
16	50.20	5877	1253	3.65	25.12
17	50.31	10355	2077	6.43	44.27
18	50.85	6706	1490	4.17	28.67
19	52.13	1208	385	0.75	5.16
20	52.33	1310	370	0.81	5.60
21	52.71	794	258	0.49	3.39
22	53.43	1953	597	1.21	8.3



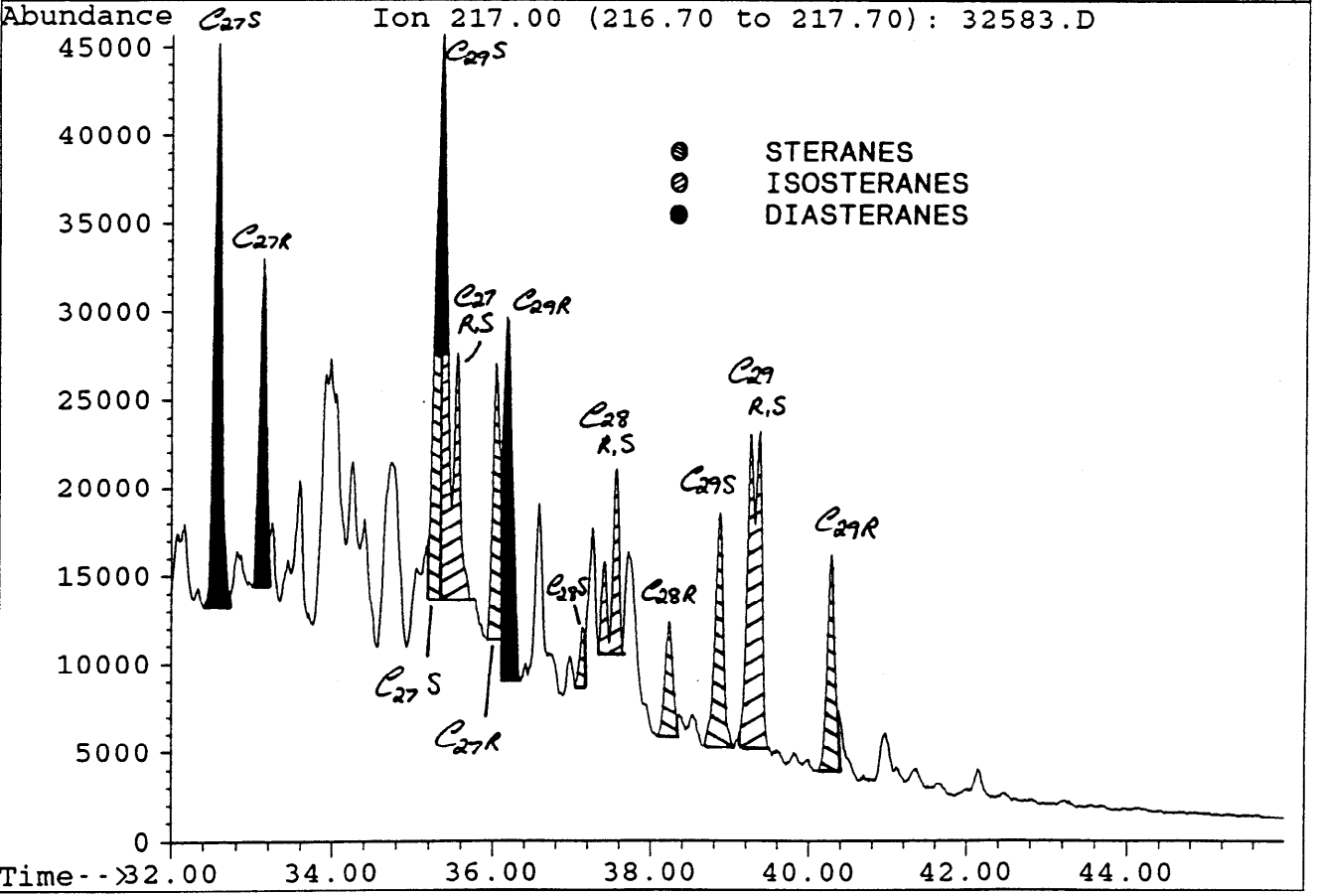
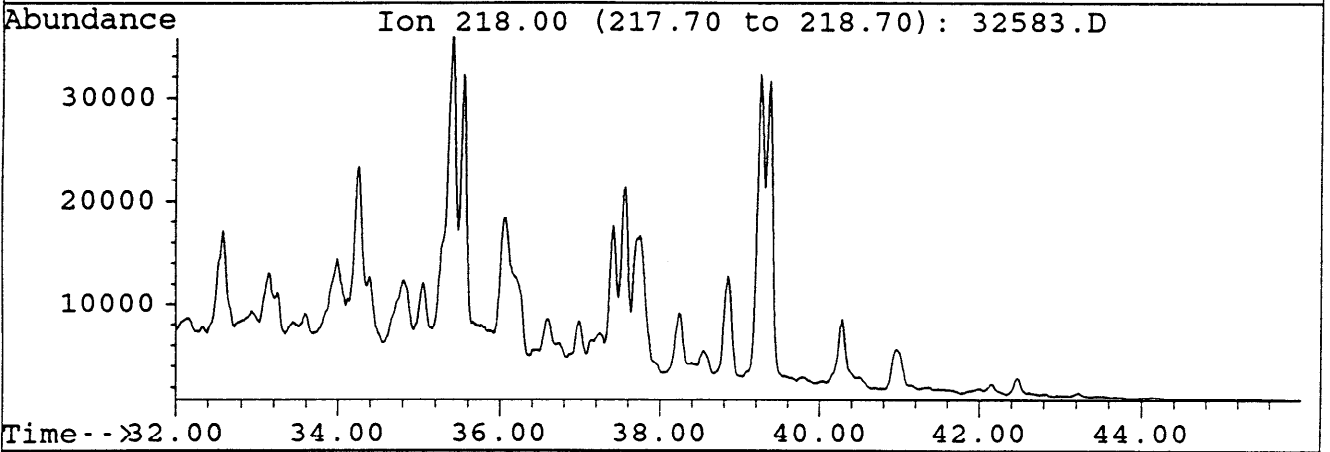
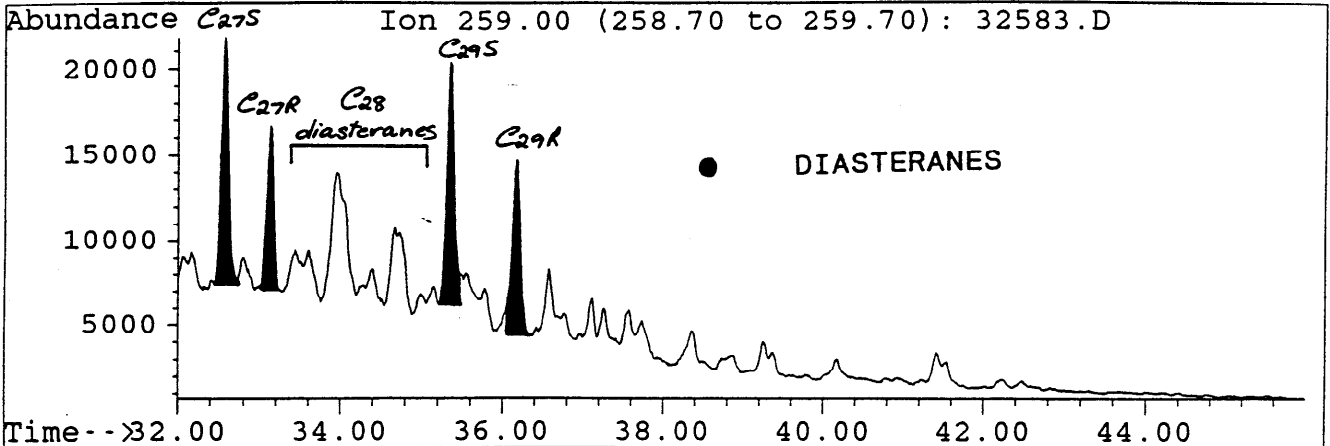
File : A2039.D  
Sample : MINERVA#1, RFS-AD-1157. L-008. AROS.  
Misc. Info : COL#155. 17-1-94. GEC.



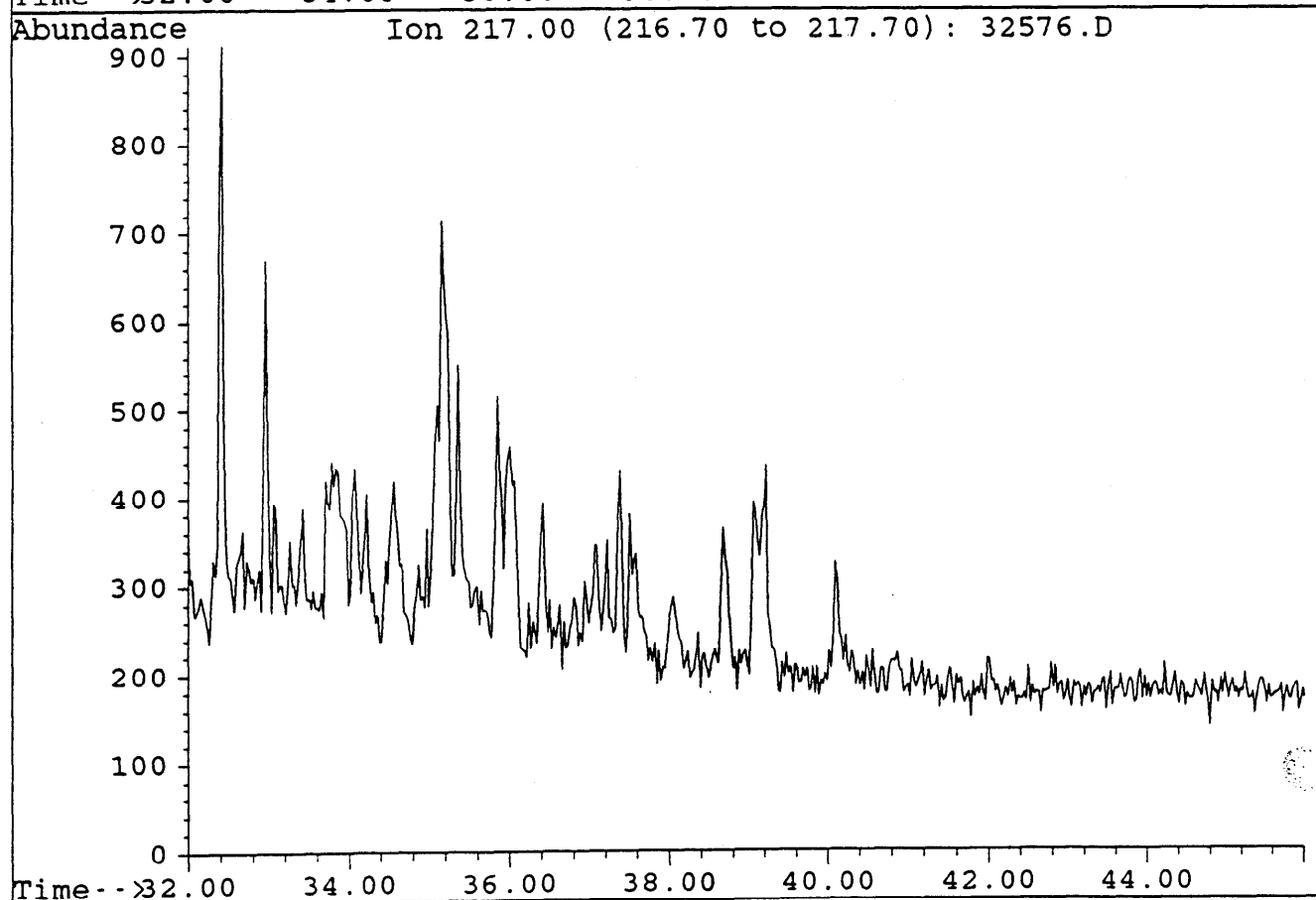
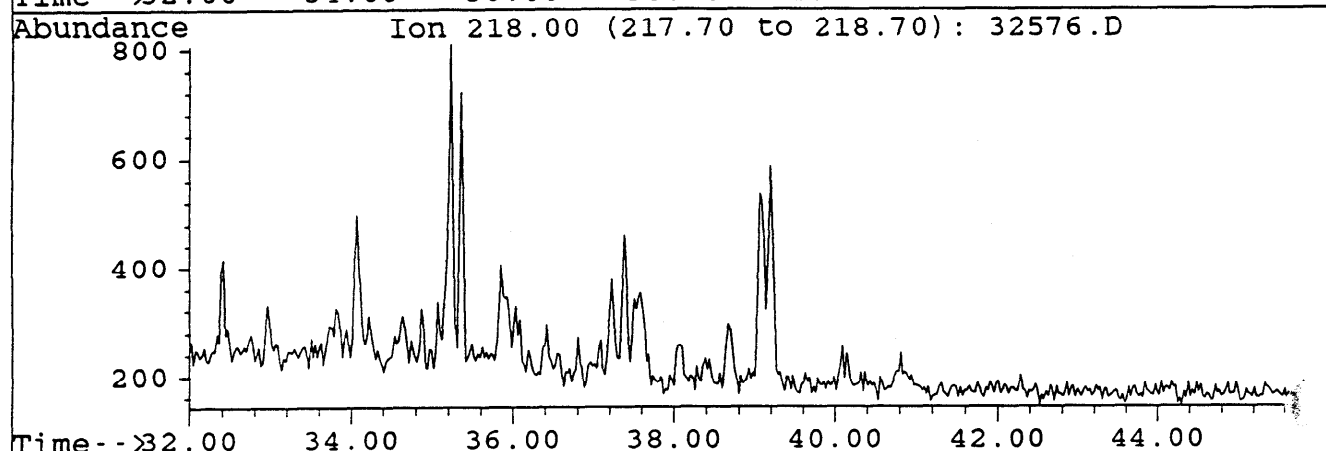
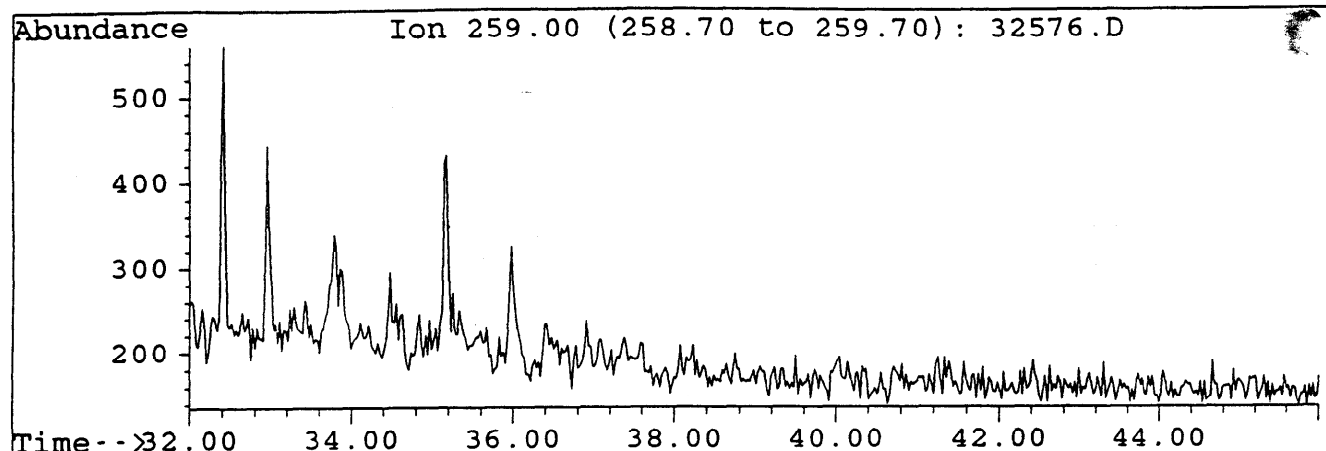
**APPENDIX 3**

**SIR GC-MS (B/C) MASS FRAGMENTOGRAMS : 1649.8m WATER-EXTRACT**

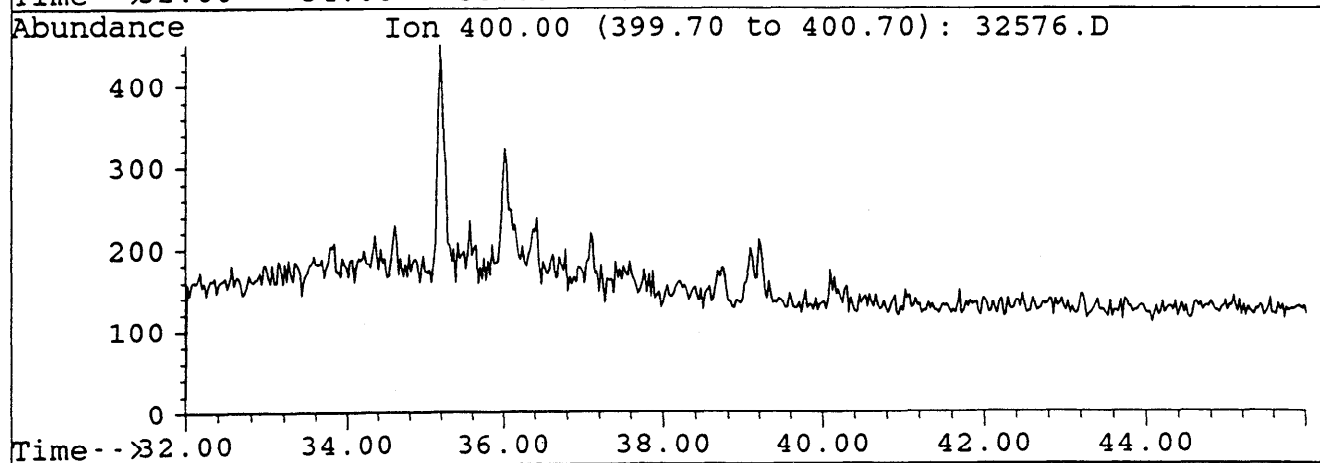
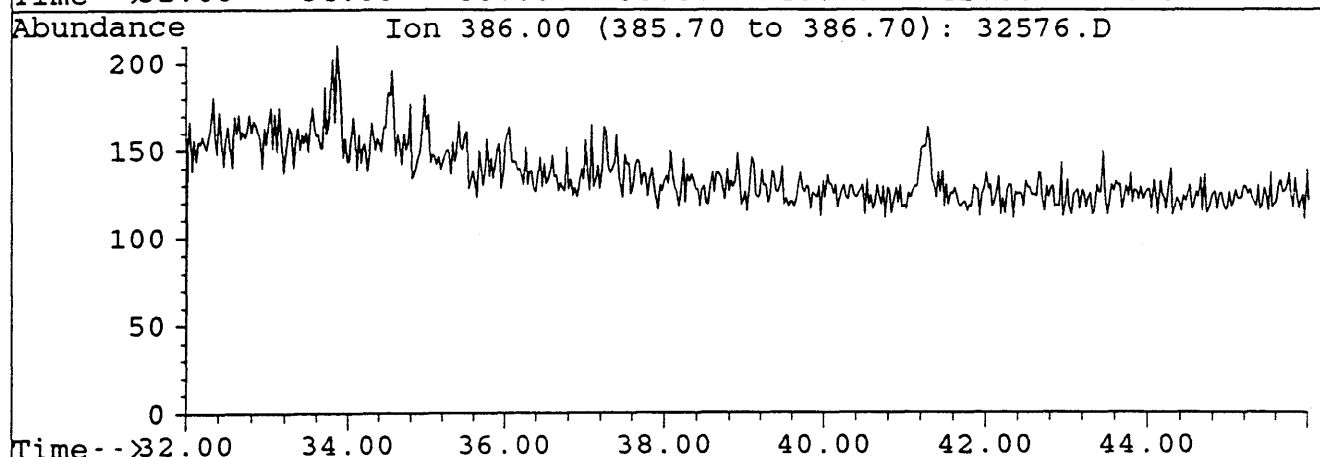
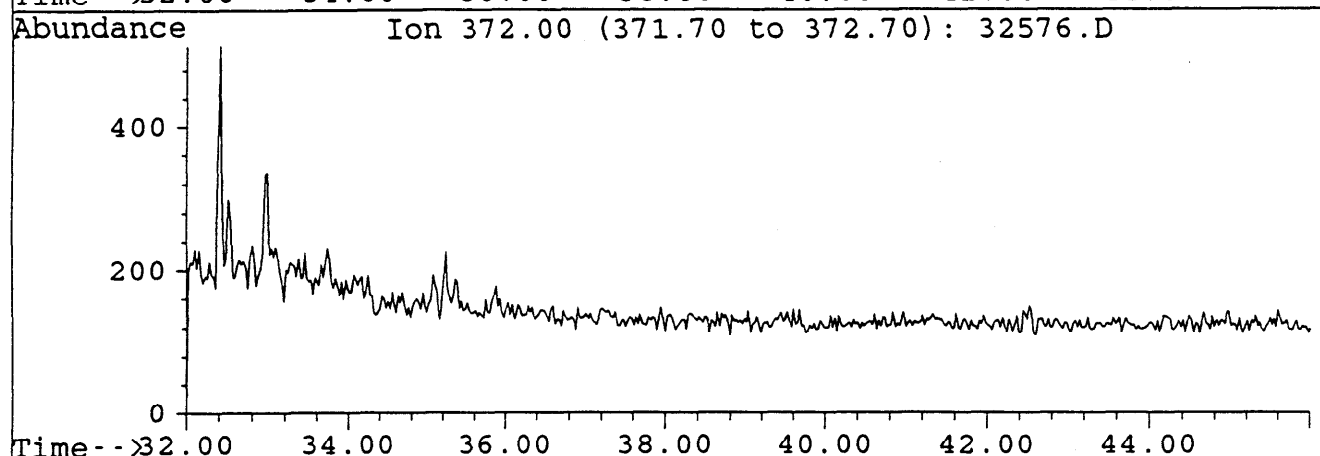
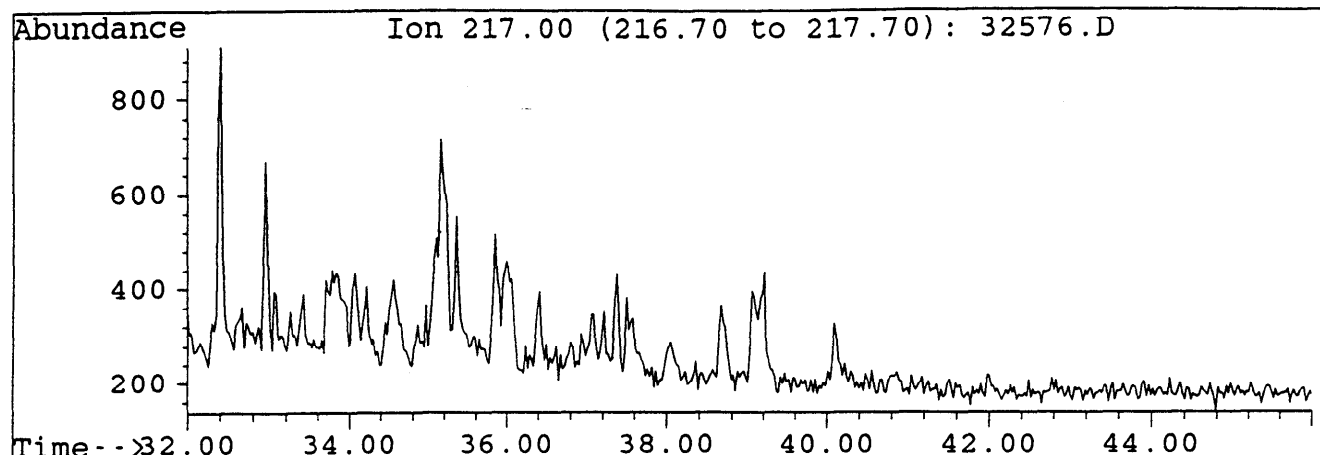
File : 32583.D  
 Sample : MINERUA-1 RFT TOPPED B/C  
 Misc. Info : col#143, 18/3/94 SB



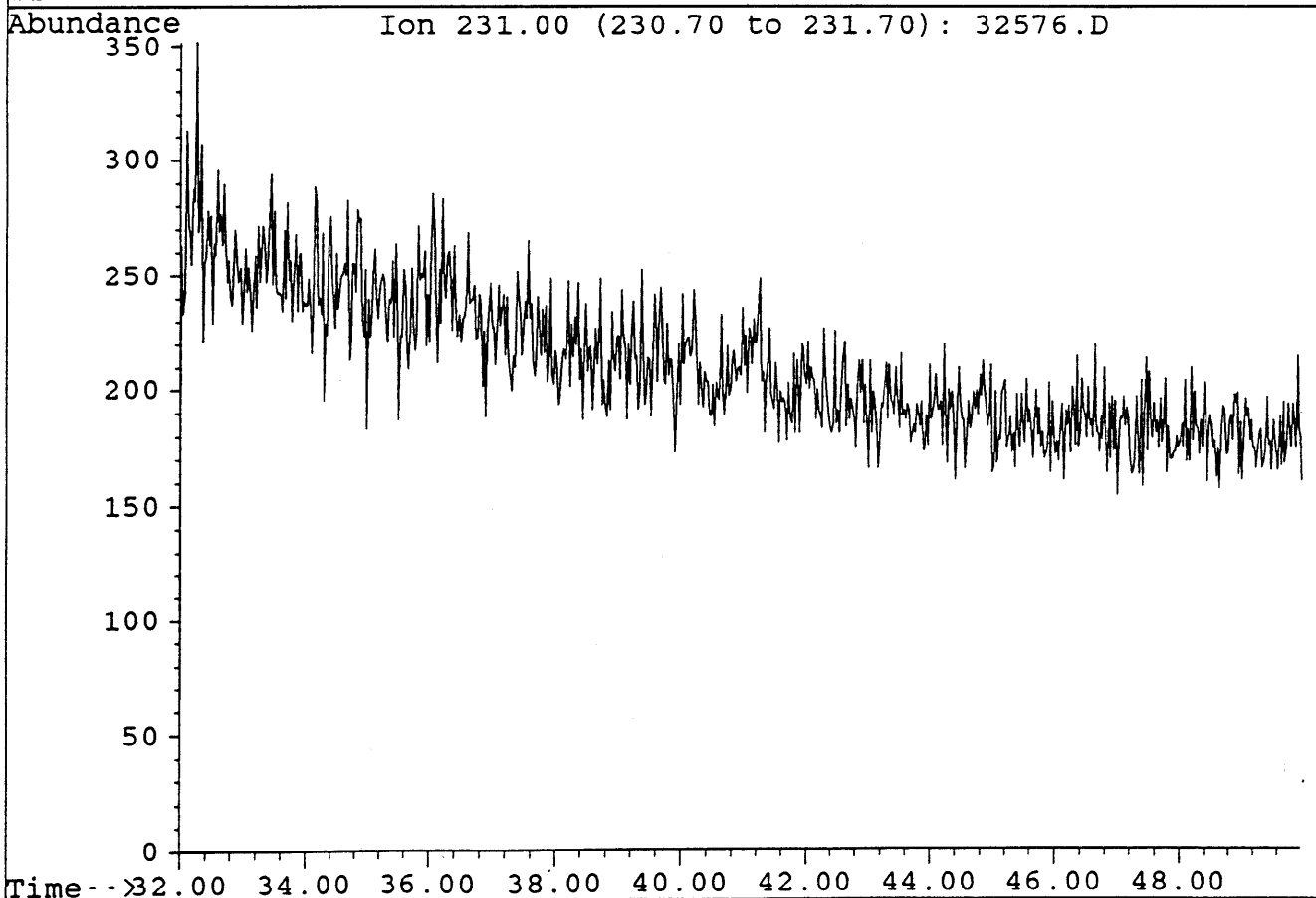
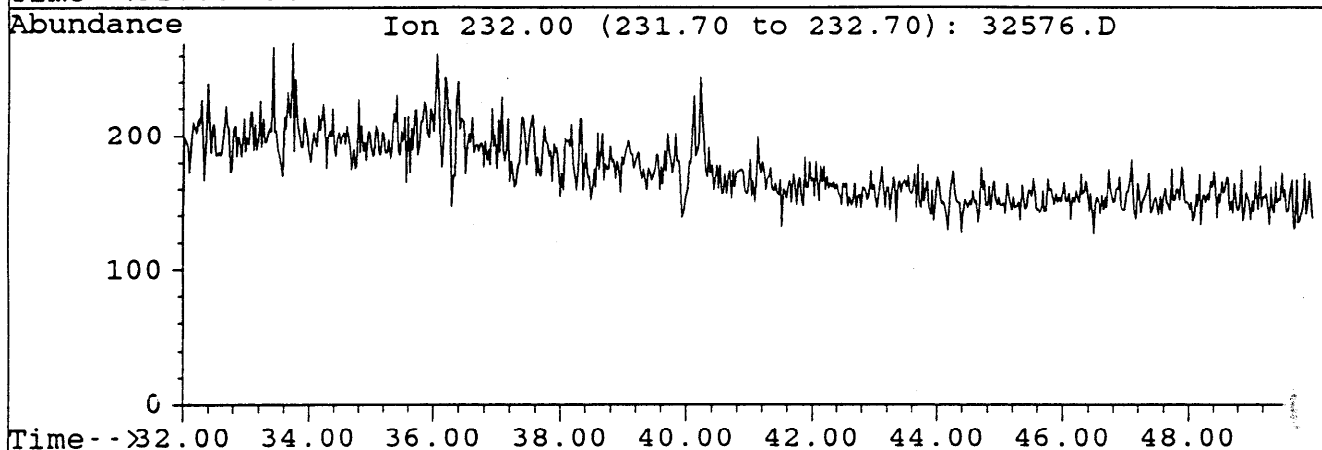
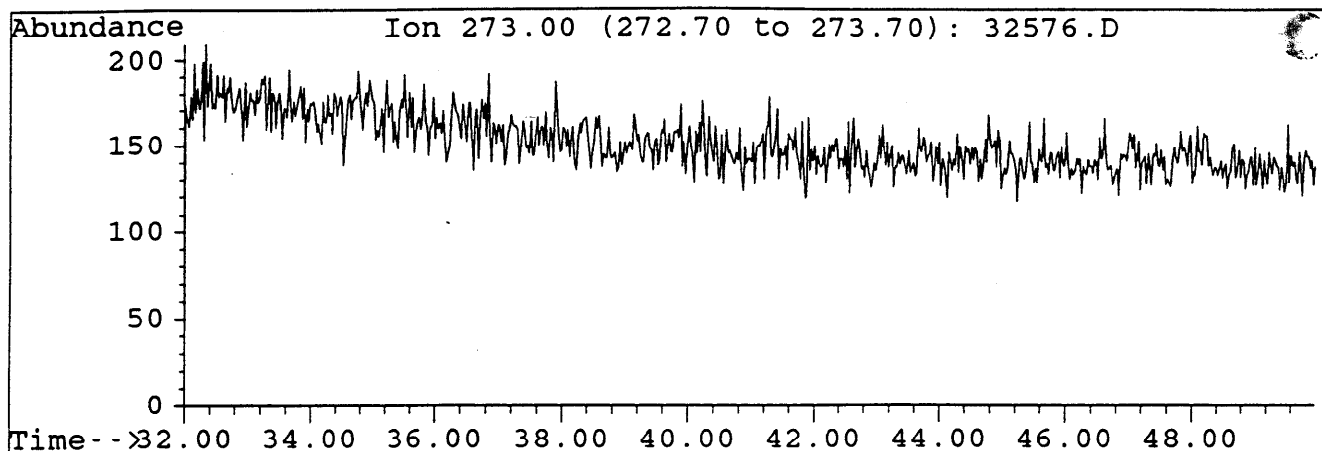
File : 32576.D  
Sample : MINERVA-1 RFT  
Misc. Info : COL#143, 1/1800, 17/3/94, DJ



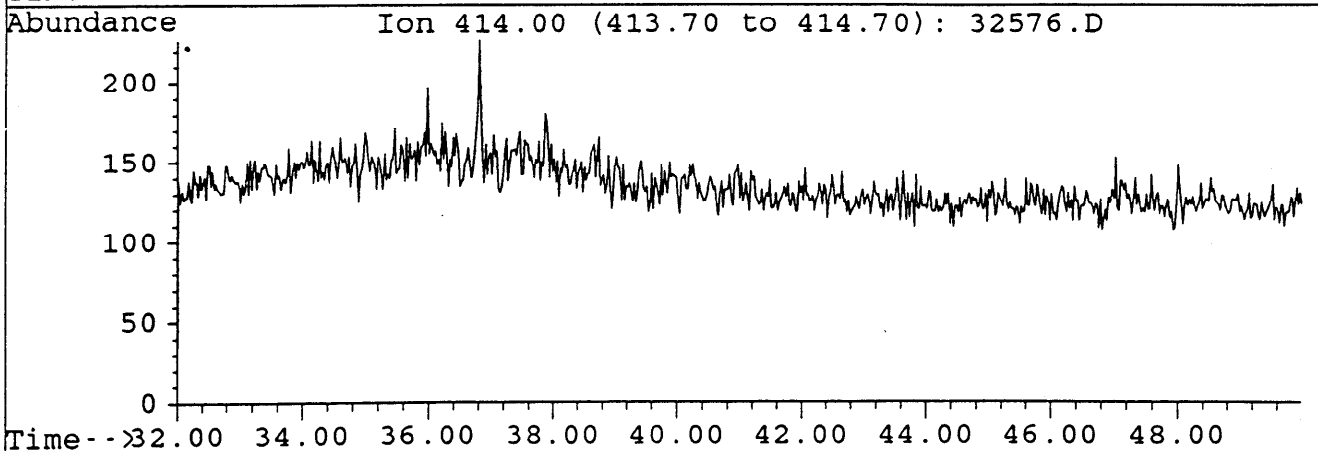
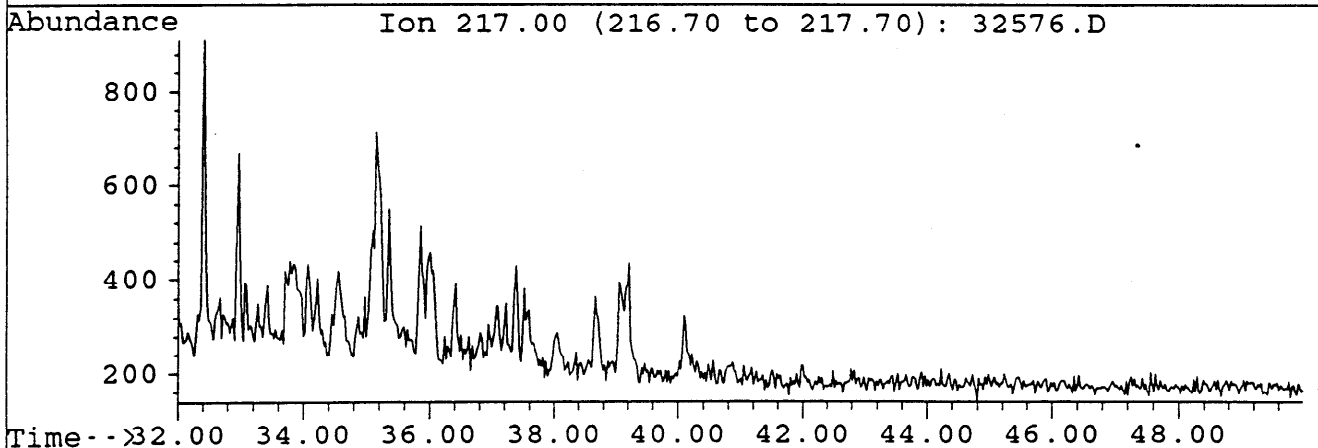
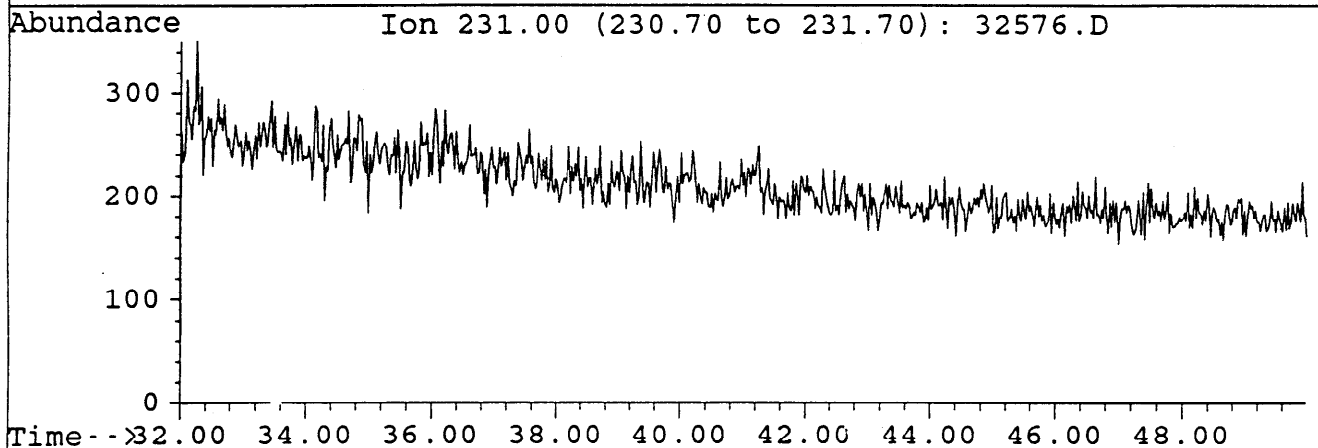
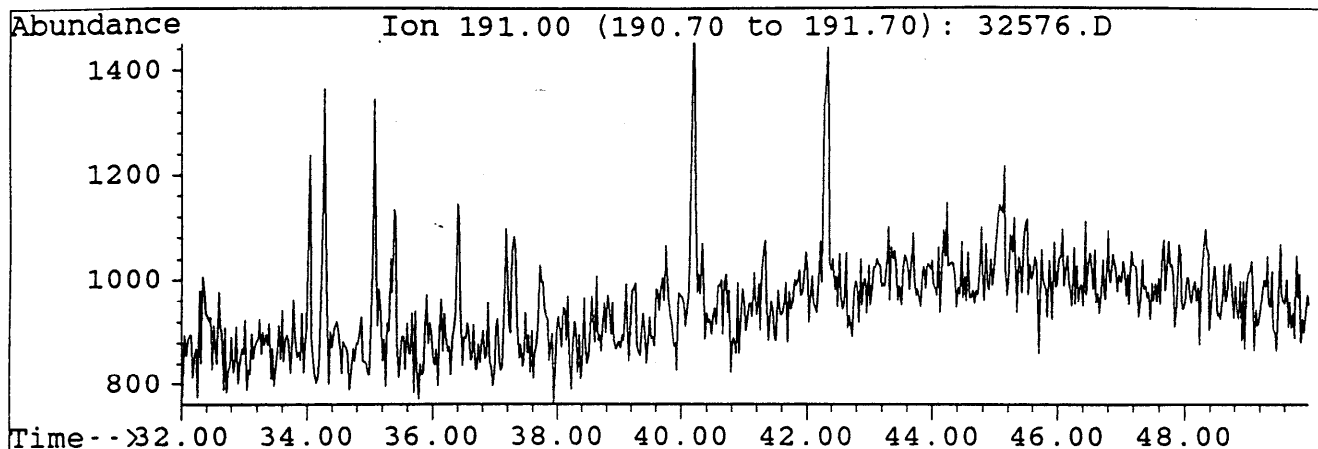
File : 32576.D  
Sample : MINERVA-1 RFT  
Misc. Info : COL#143, 1/1800, 17/3/94, DJ



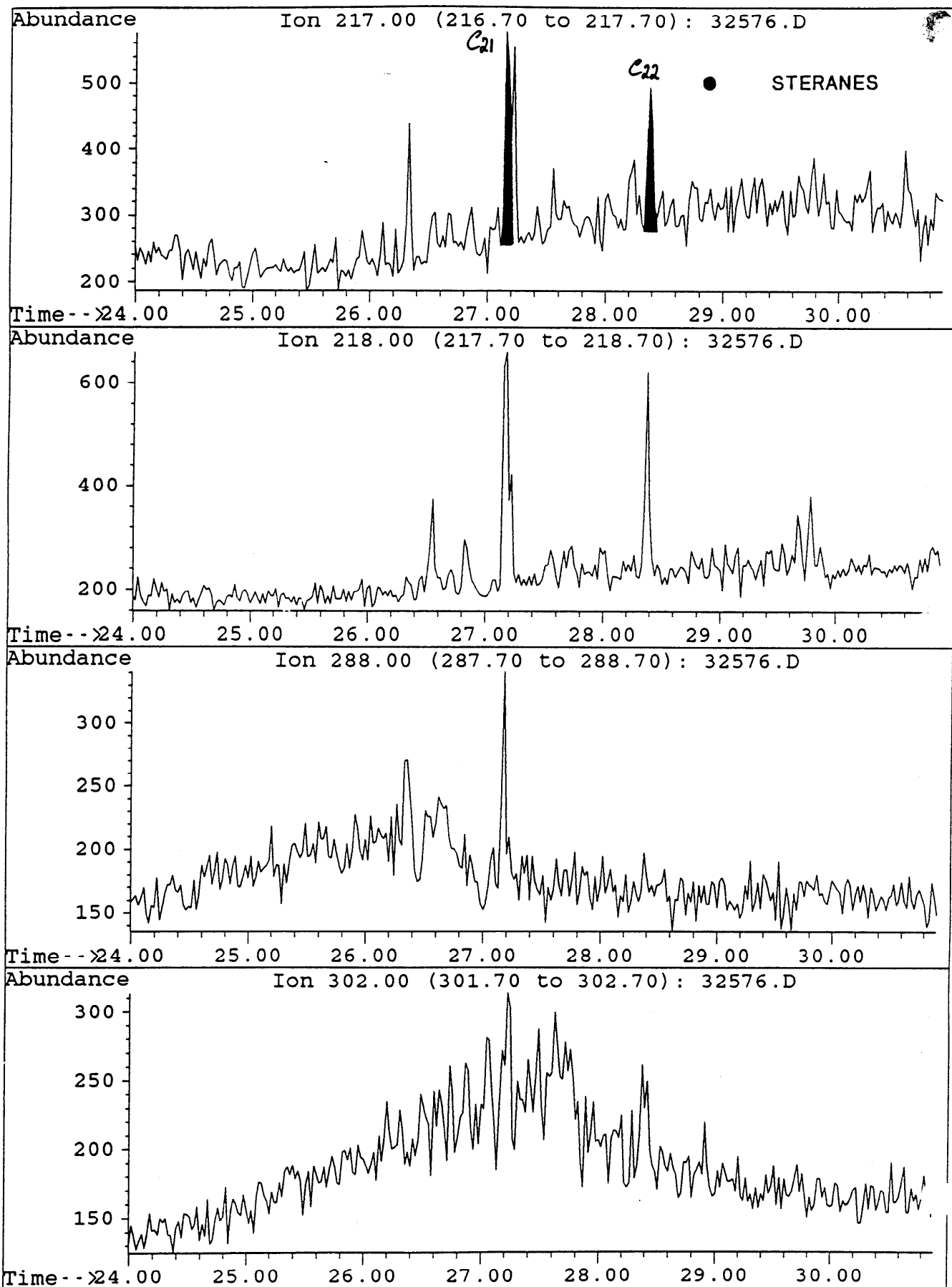
File : 32576.D  
Sample : MINERVA-1 RFT  
Misc. Info : COL#143, 1/1800, 17/3/94, DJ



File : 32576.D  
Sample : MINERVA-1 RFT  
Misc. Info : COL#143, 1/1800, 17/3/94, DJ

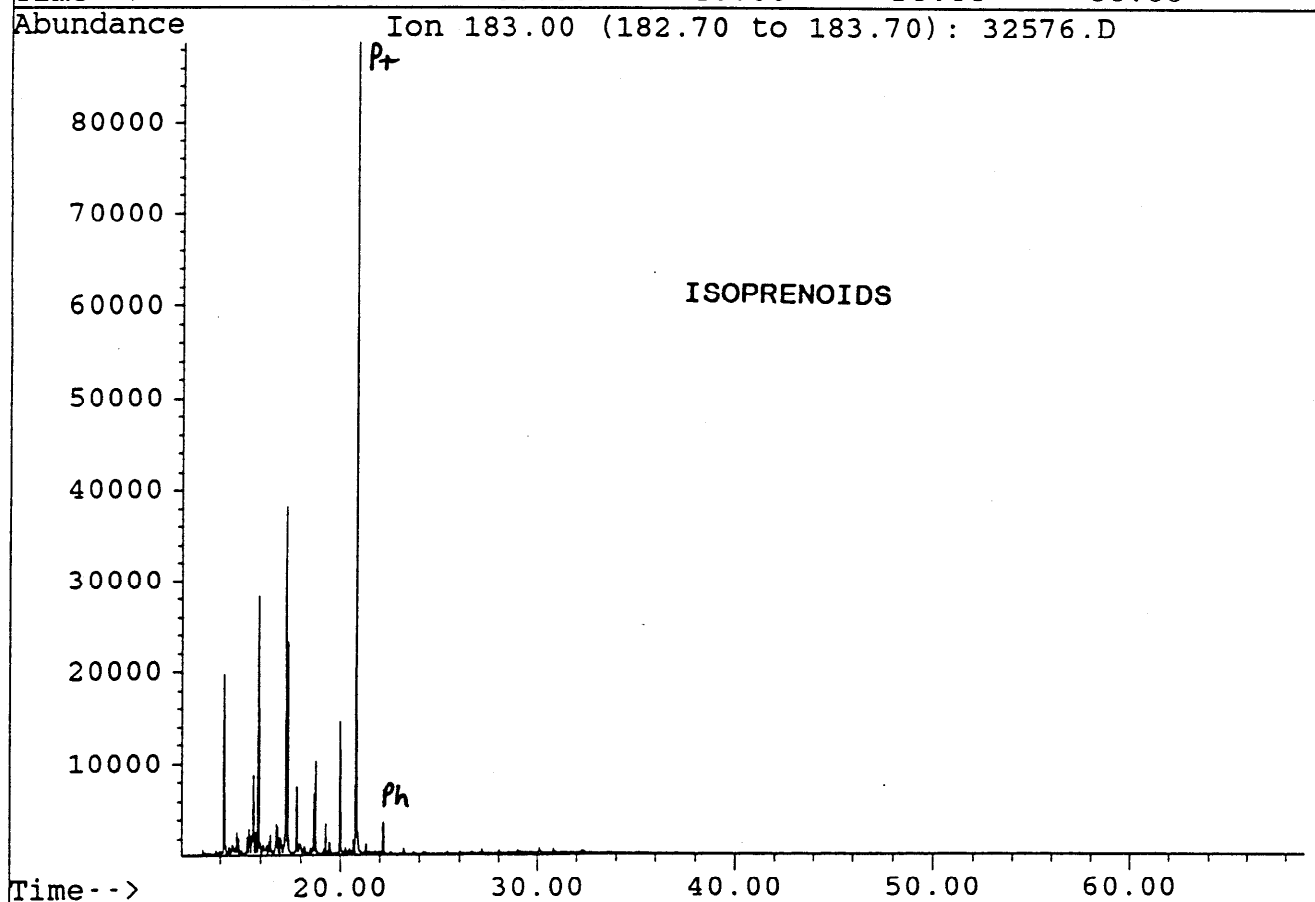
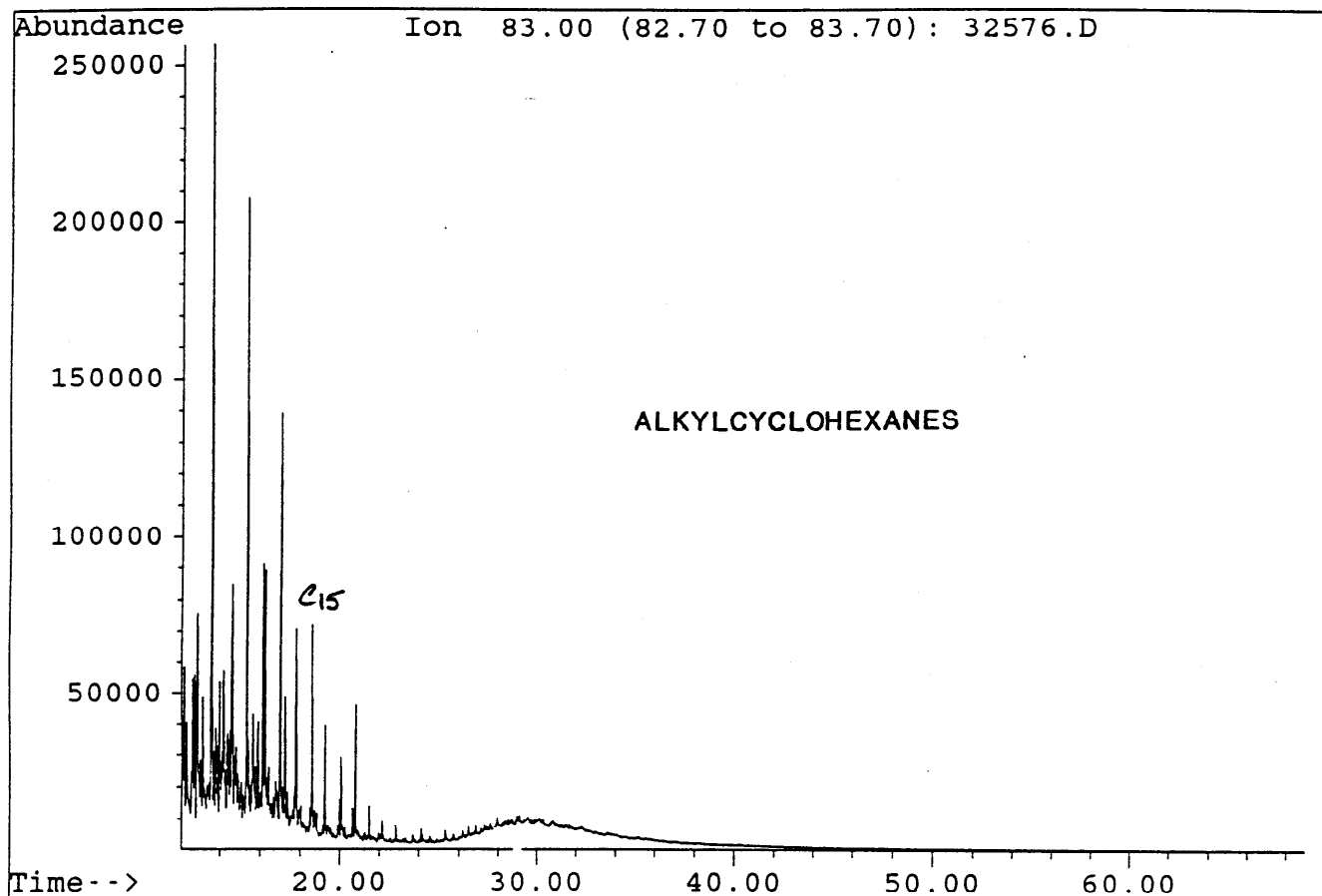


File : 32576.D  
Sample : MINERVA-1 RFT  
Misc. Info : COL#143, 1/1800, 17/3/94, DJ

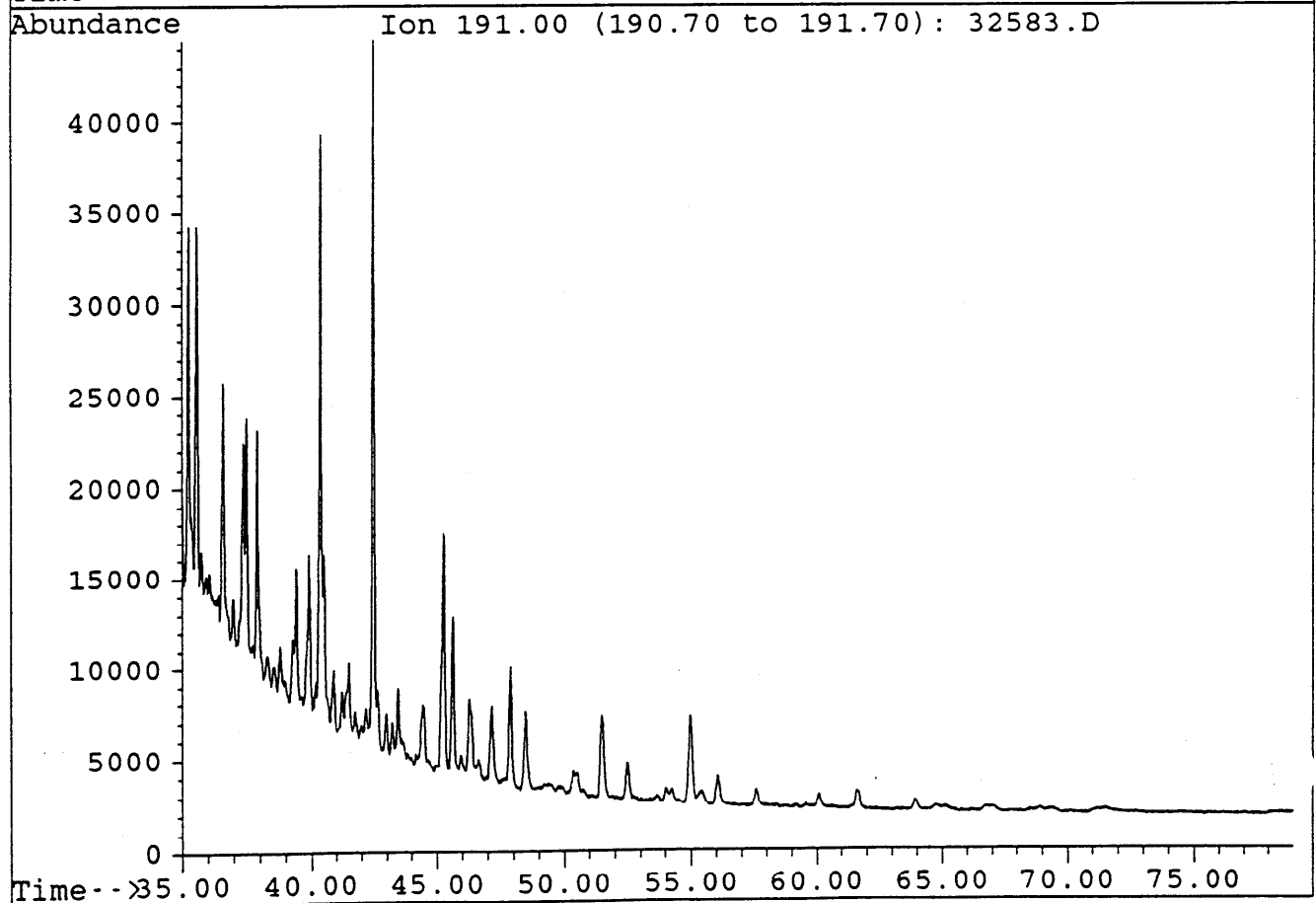
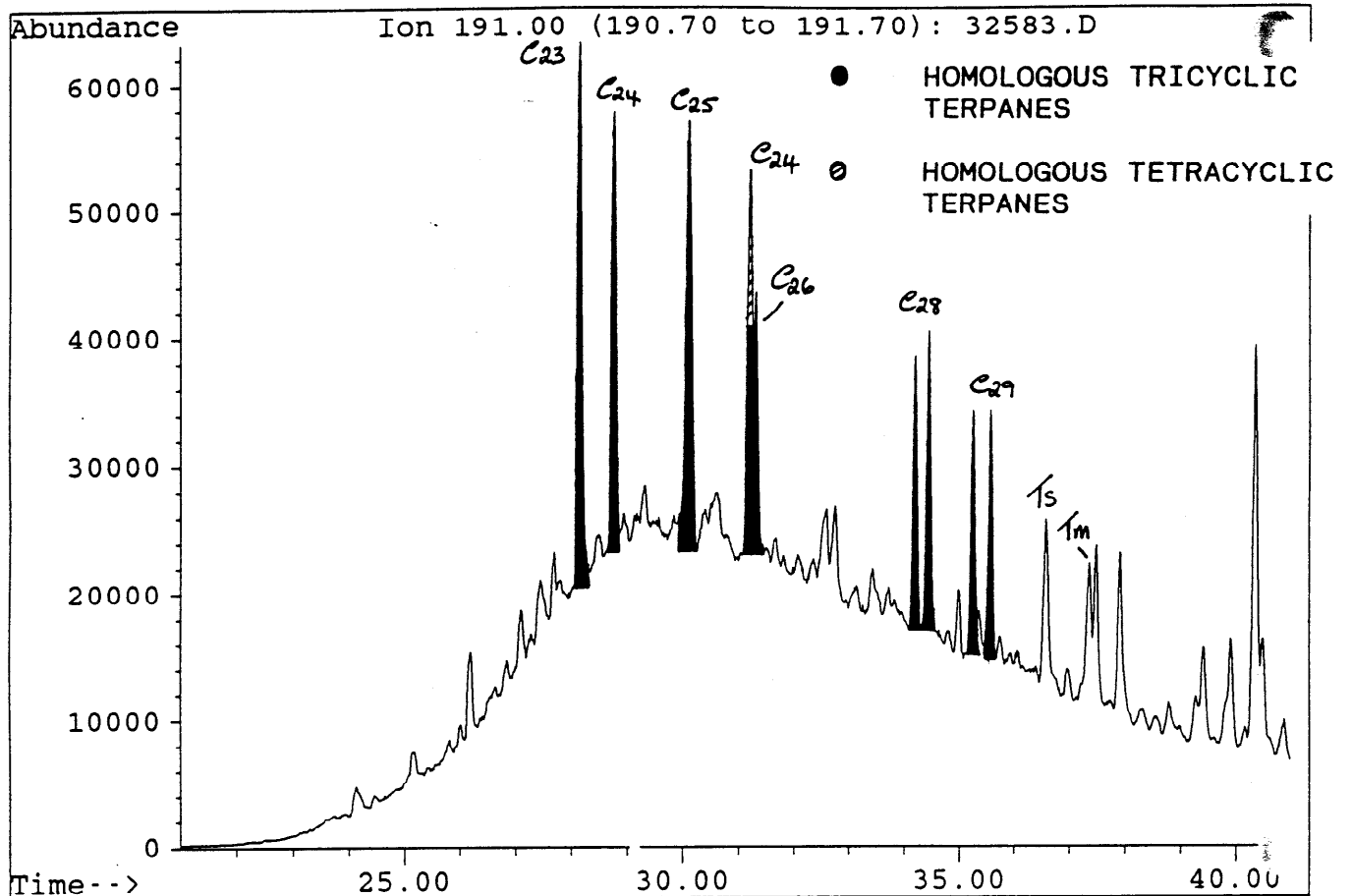




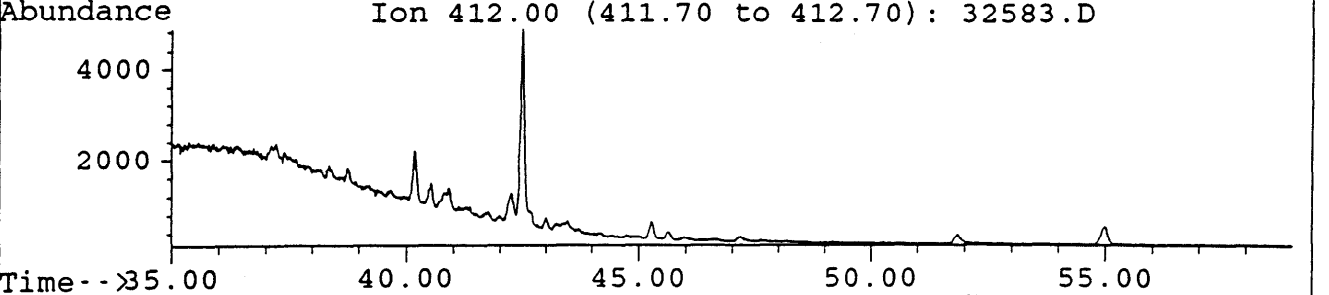
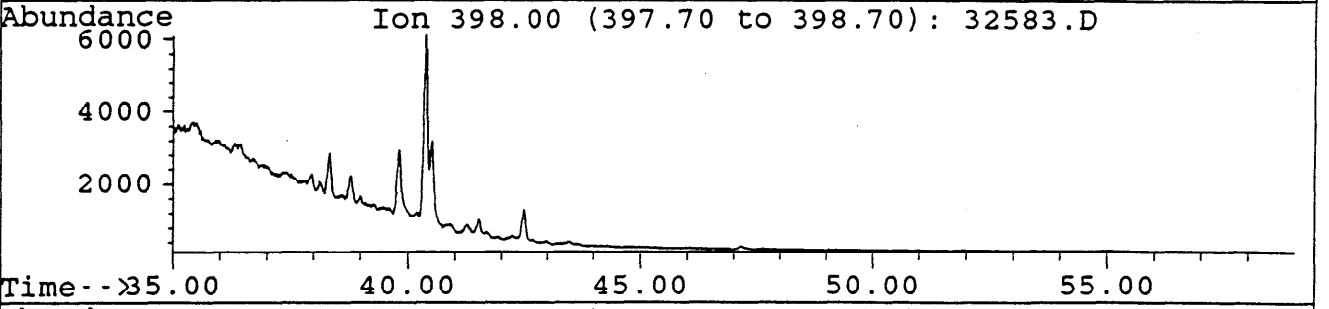
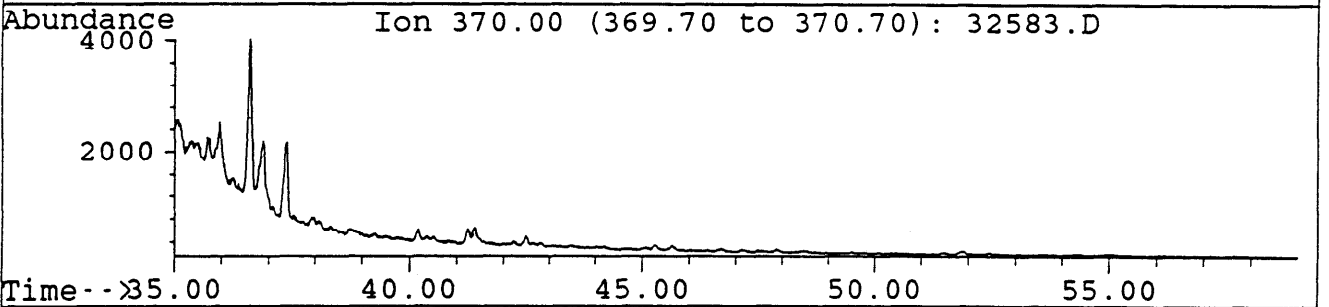
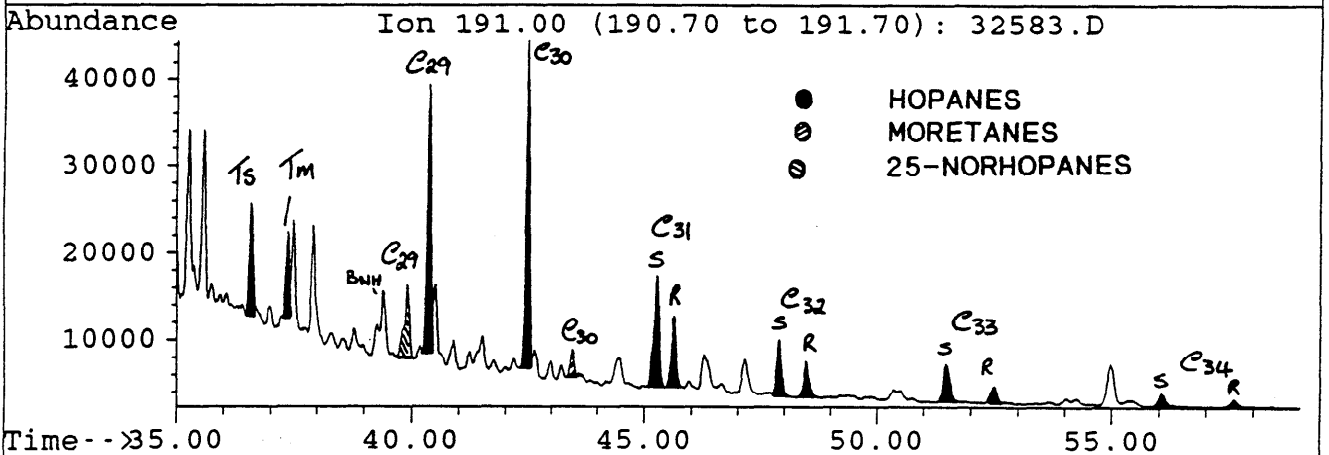
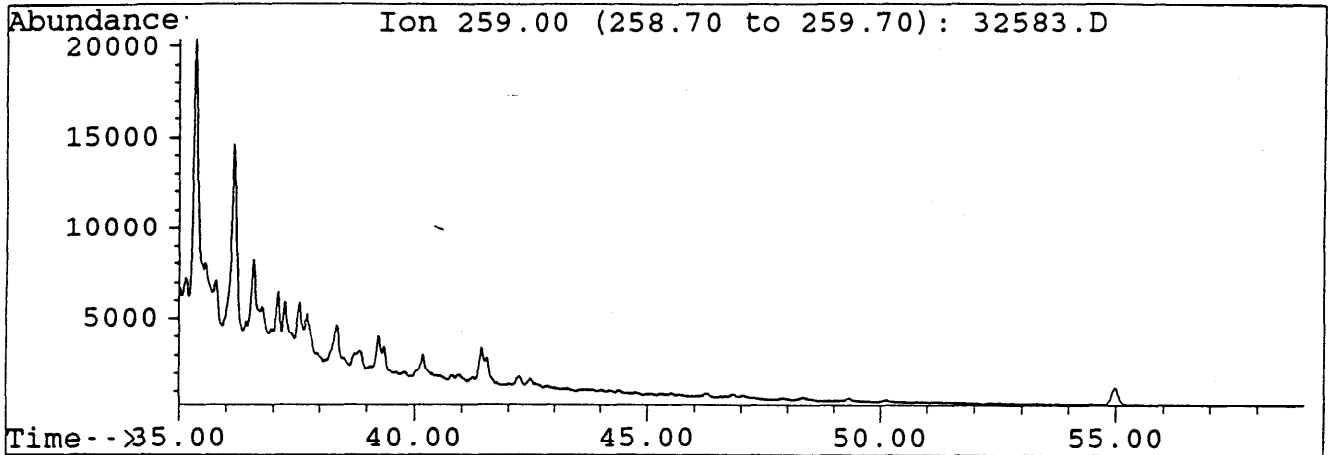
File : 32576.D  
Sample : MINERVA-1 RFT  
Misc. Info : COL#143, 1/1800, 17/3/94, DJ



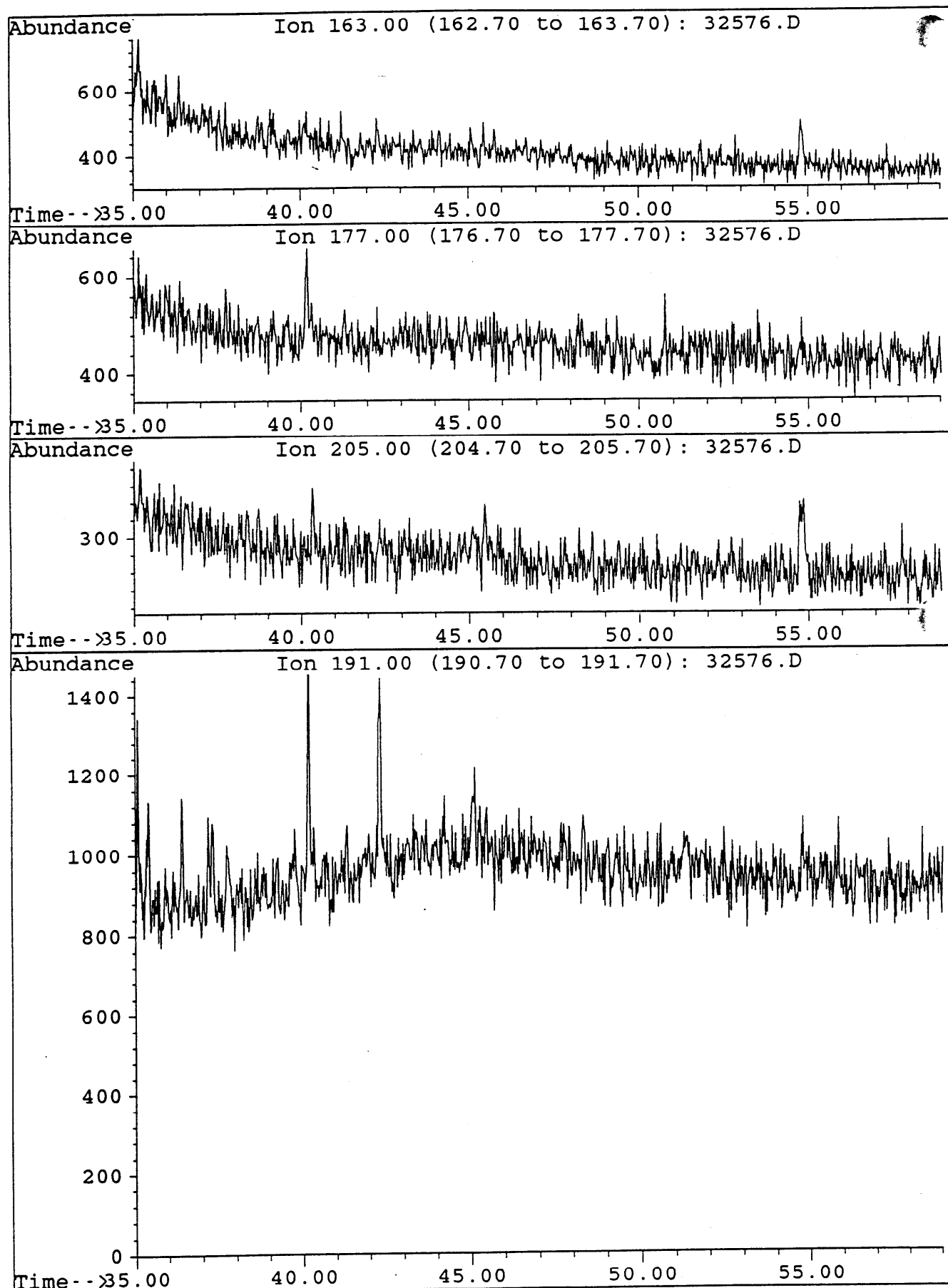
File : 32583.D  
Sample : MINERUA-1 RFT TOPPED B/C  
Misc. Info : col#143, 18/3/94 SB



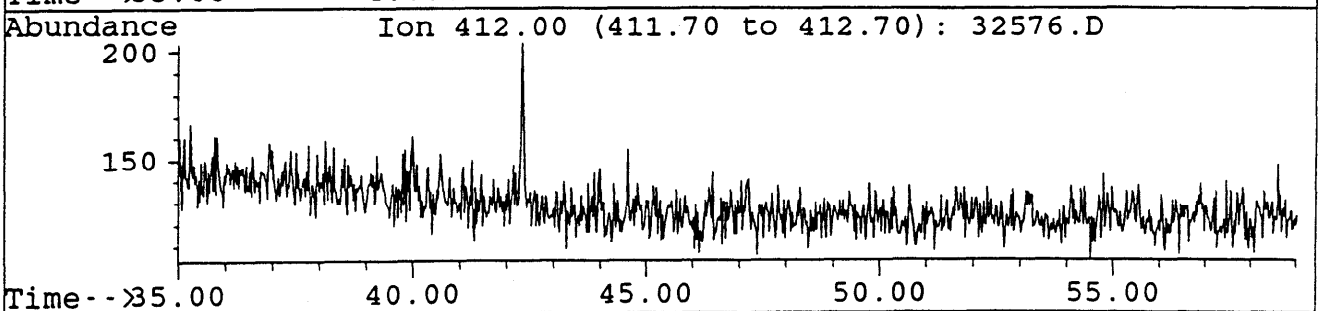
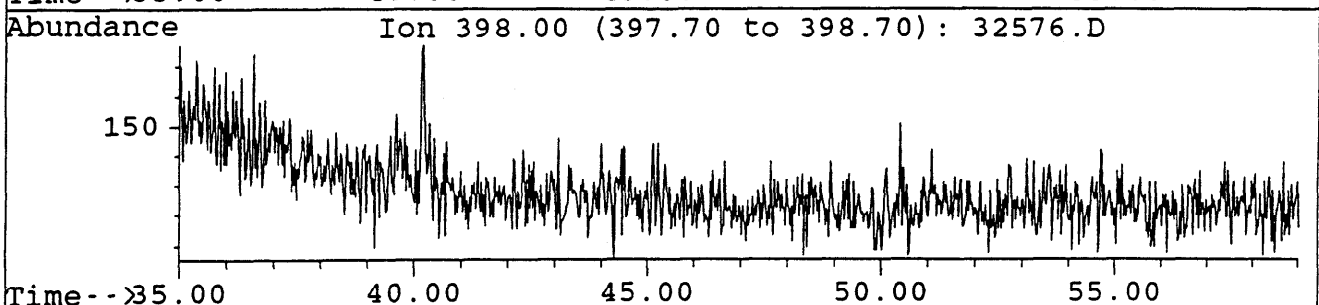
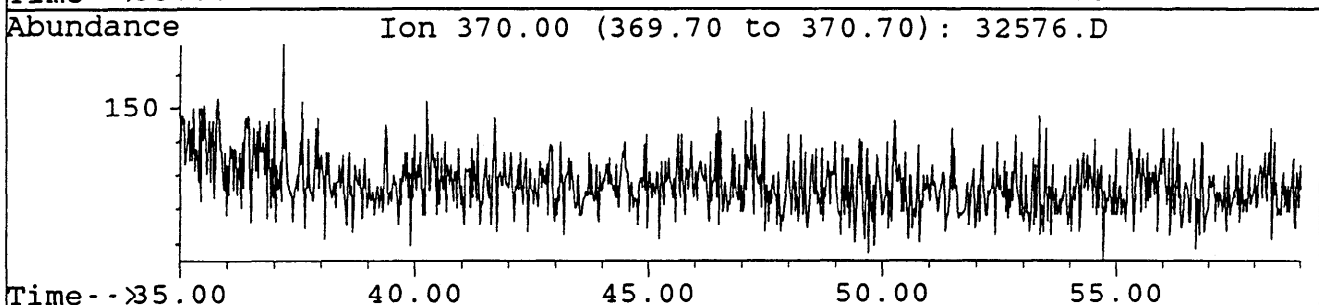
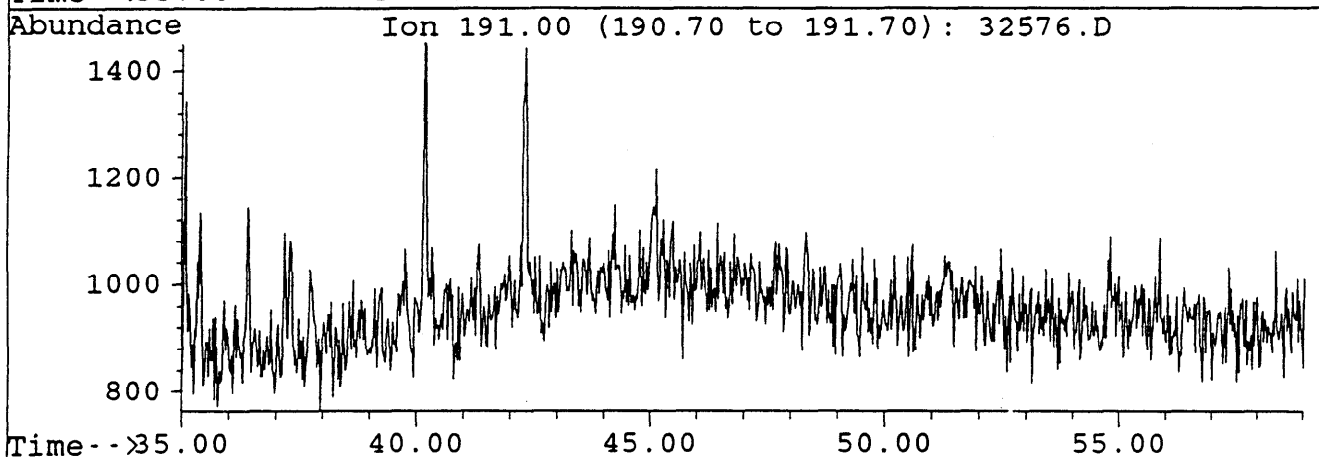
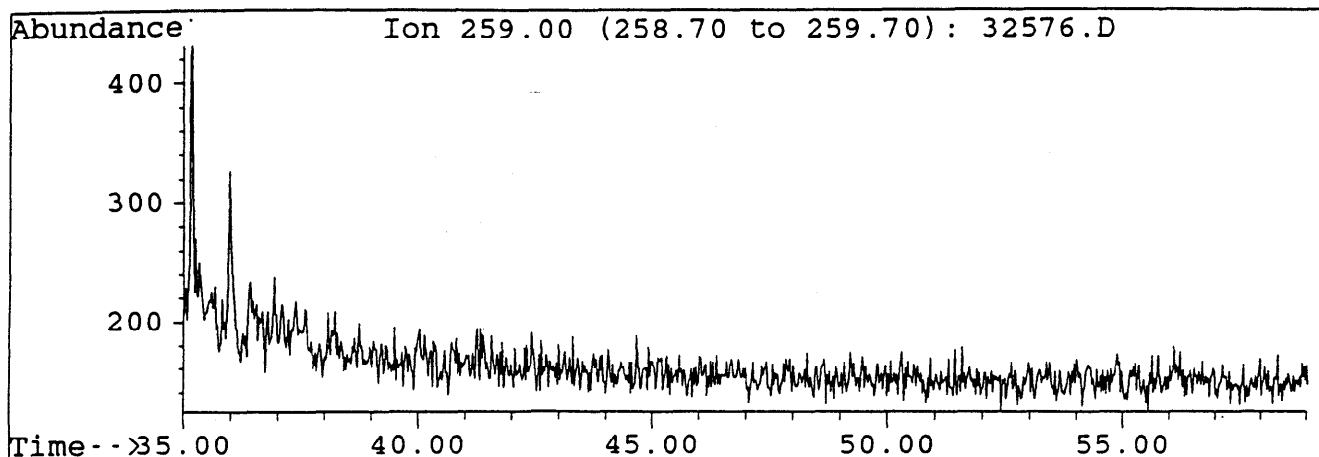
File : 32583.D  
Sample : MINERUA-1 RFT TOPPED B/C  
Misc. Info : col#143, 18/3/94 SB



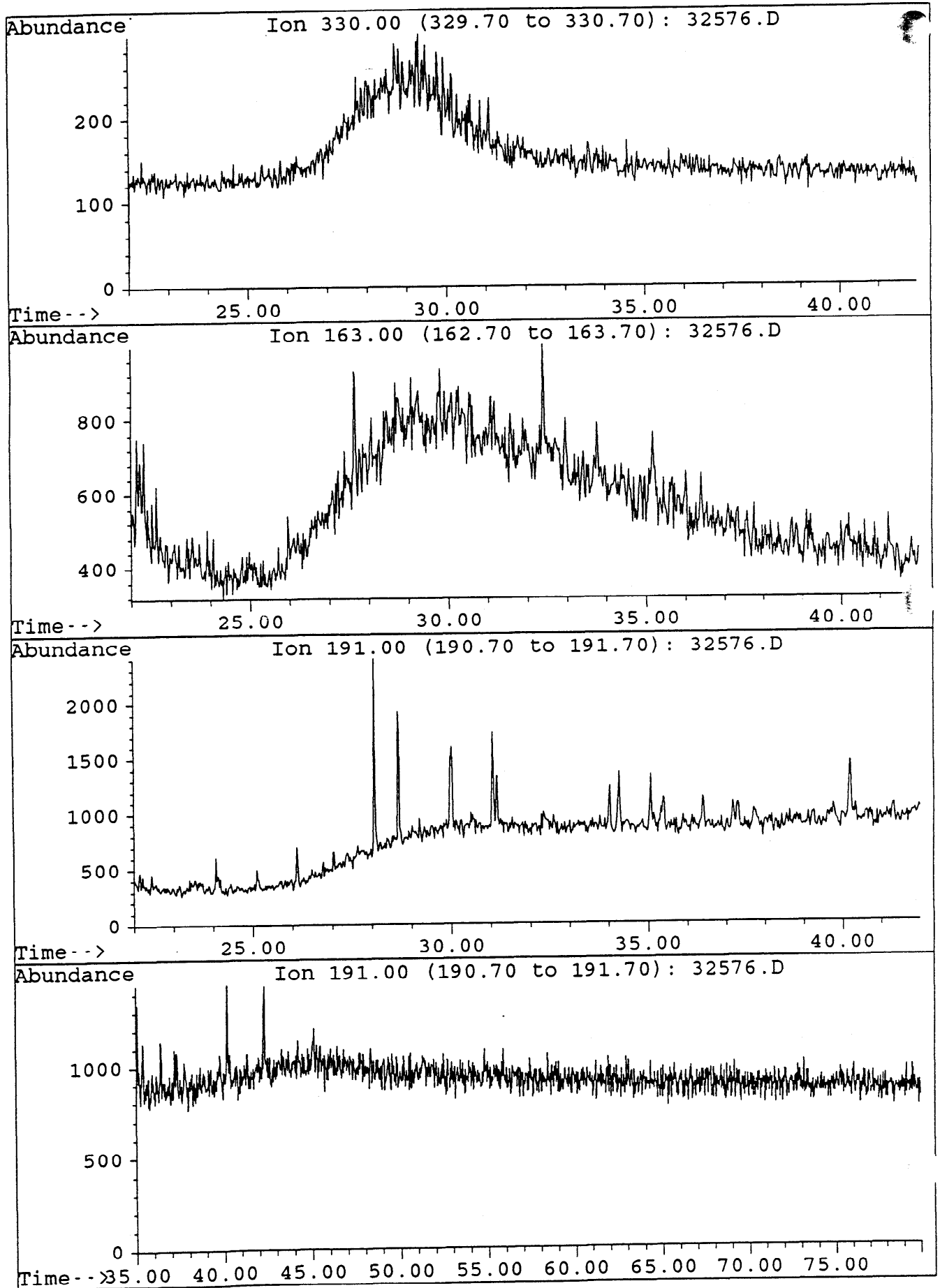
File : 32576.D  
Sample : MINERVA-1 RFT  
Misc. Info : COL#143, 1/1800, 17/3/94, DJ



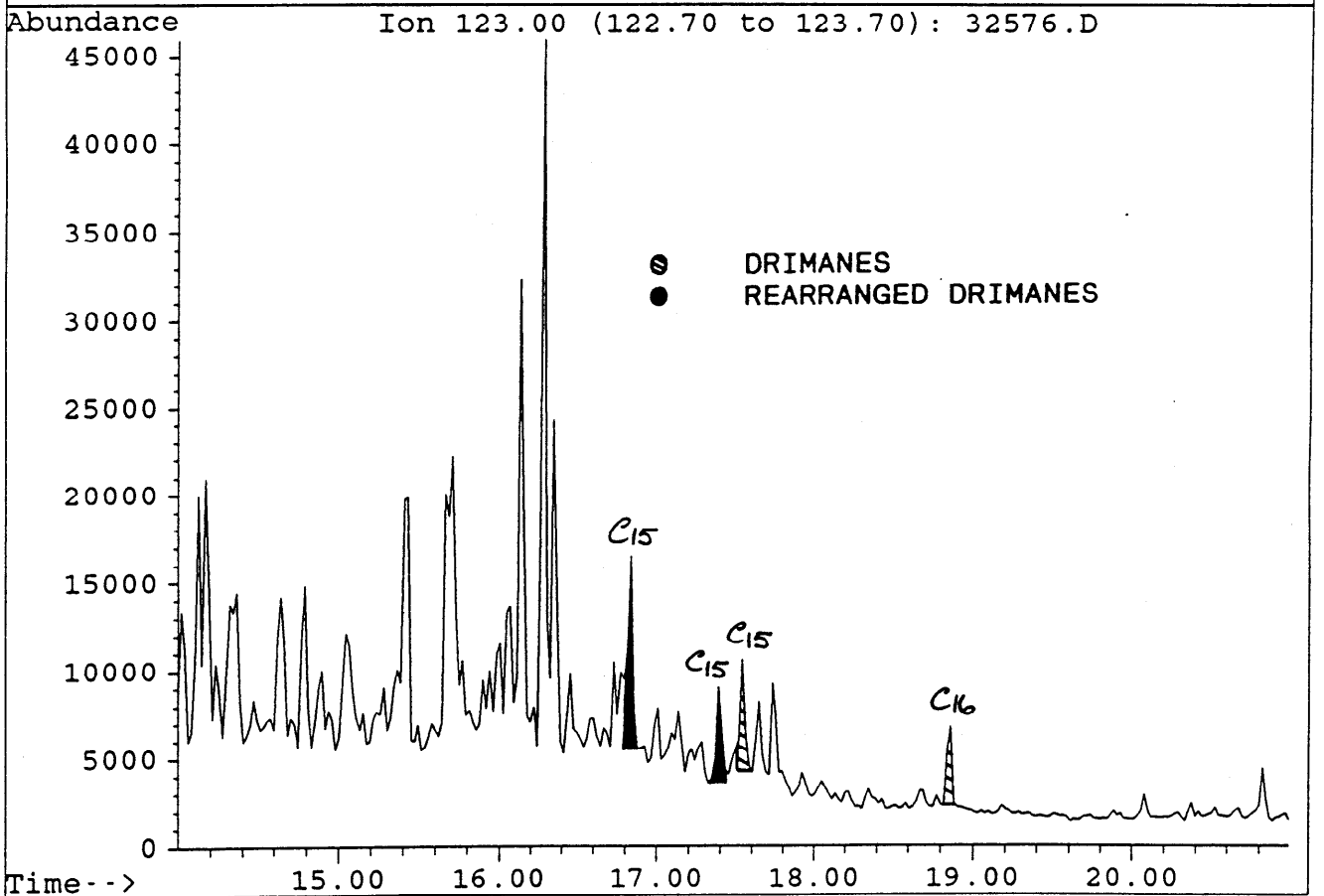
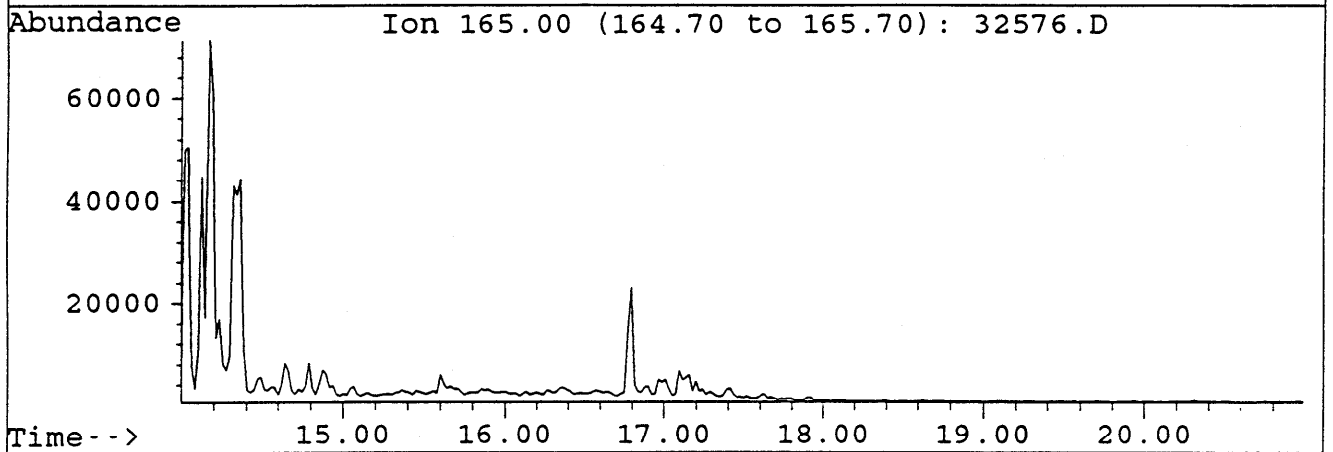
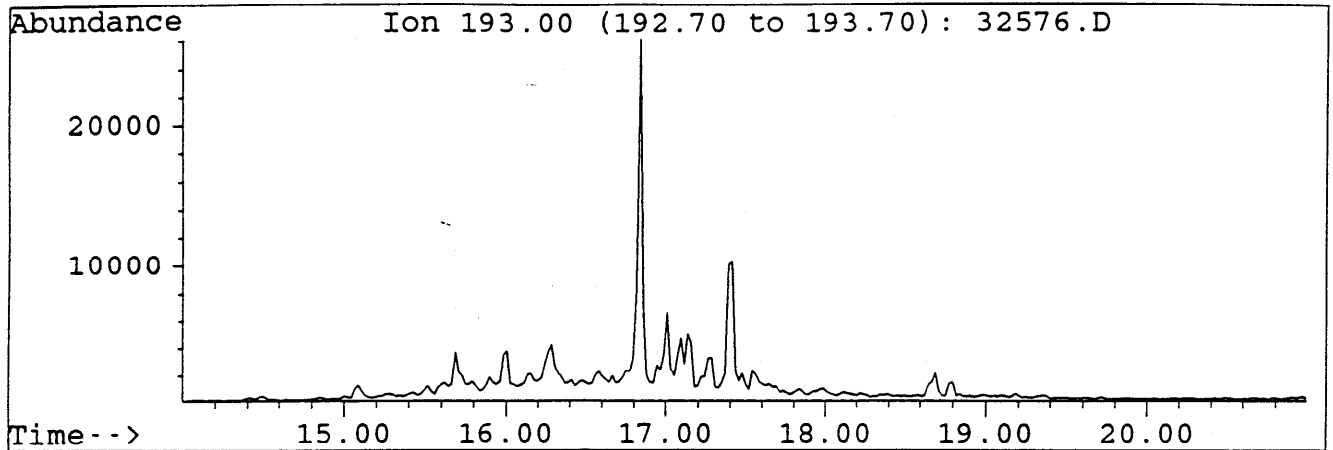
File : 32576.D  
Sample : MINERVA-1 RFT  
Misc. Info : COL#143, 1/1800, 17/3/94, DJ



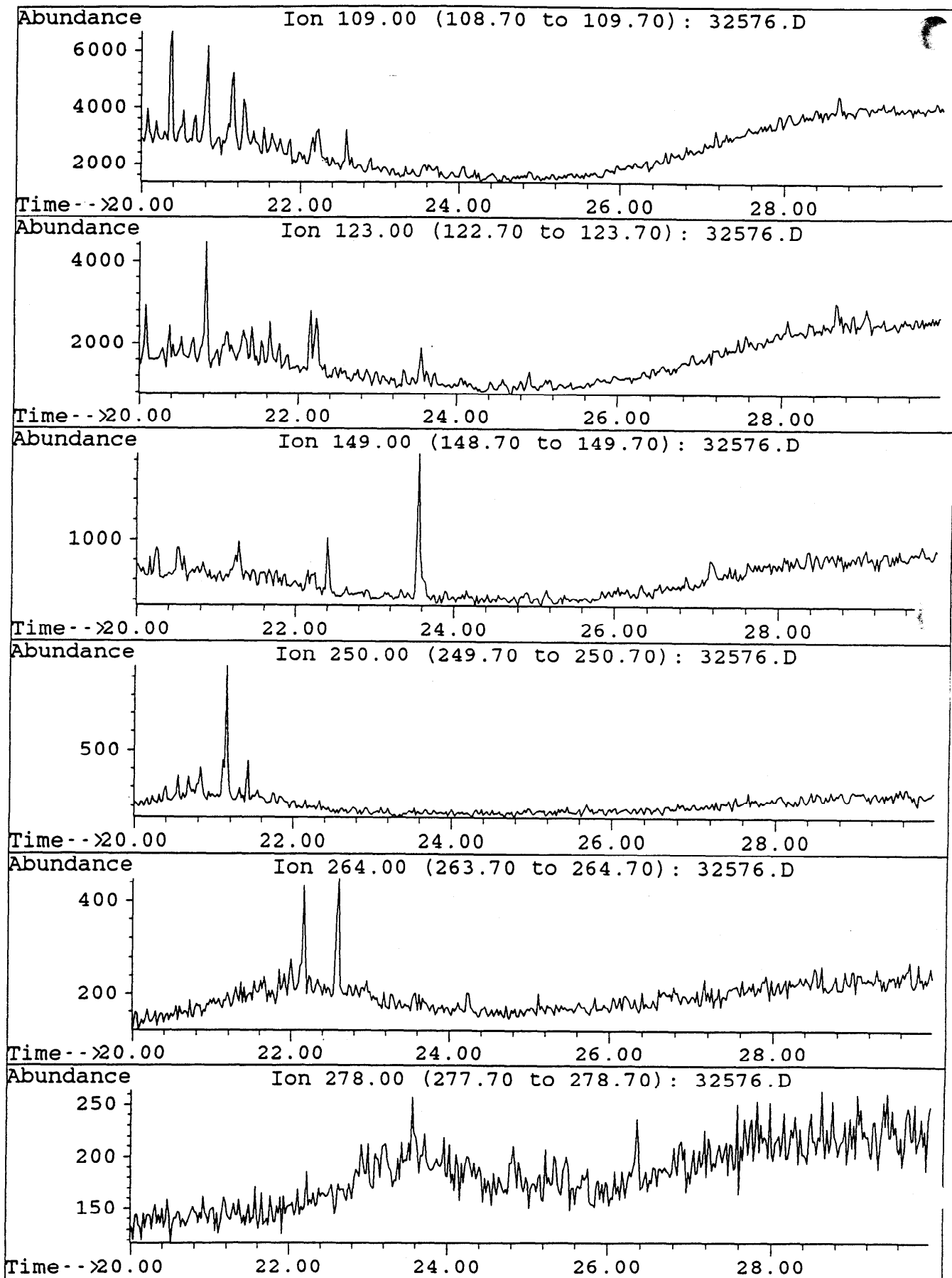
File : 32576.D  
Sample : MINERVA-1 RFT  
Misc. Info : COL#143, 1/1800, 17/3/94, DJ



File : 32576.D  
Sample : MINERVA-1 RFT  
Misc. Info : COL#143, 1/1800, 17/3/94, DJ

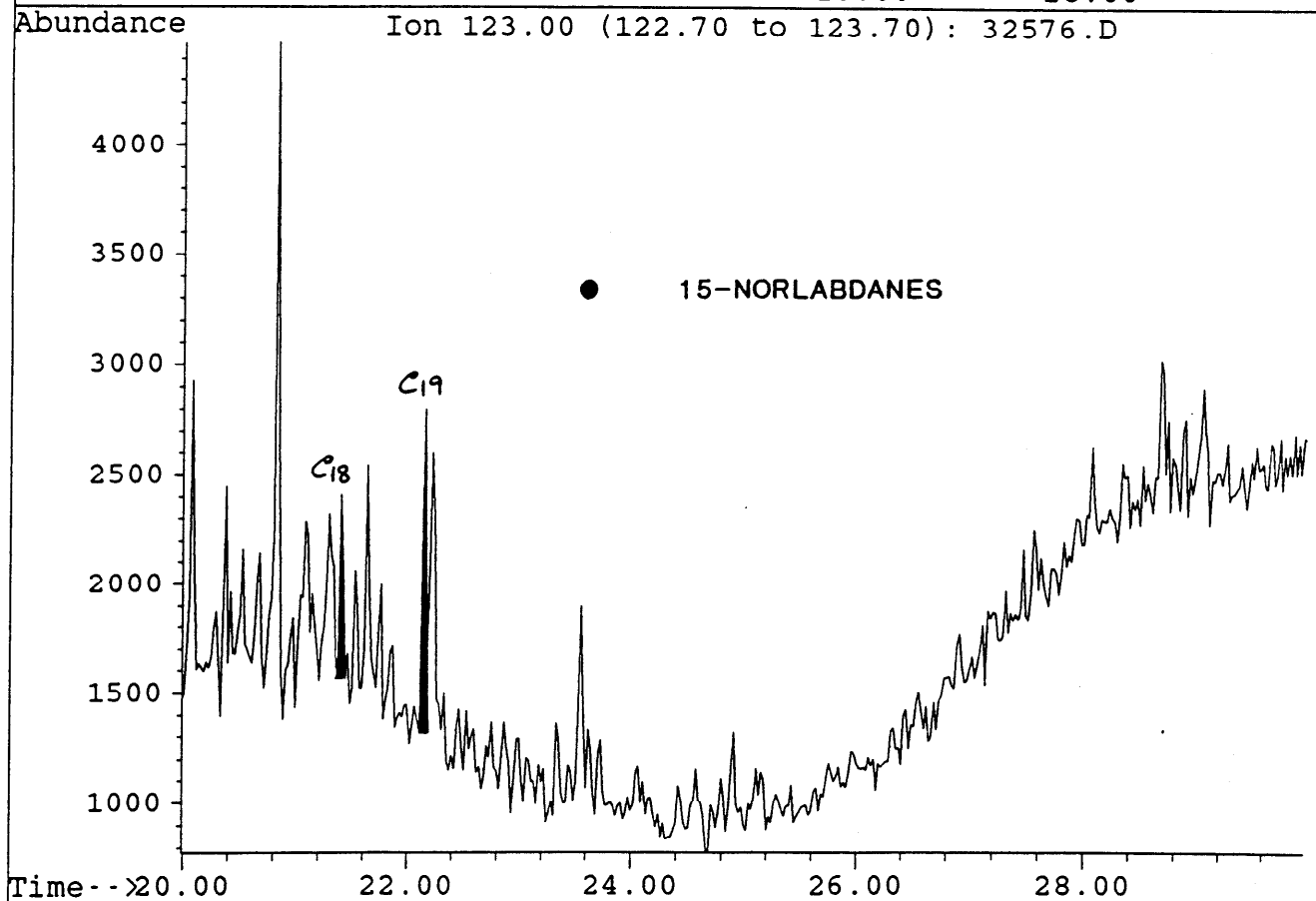
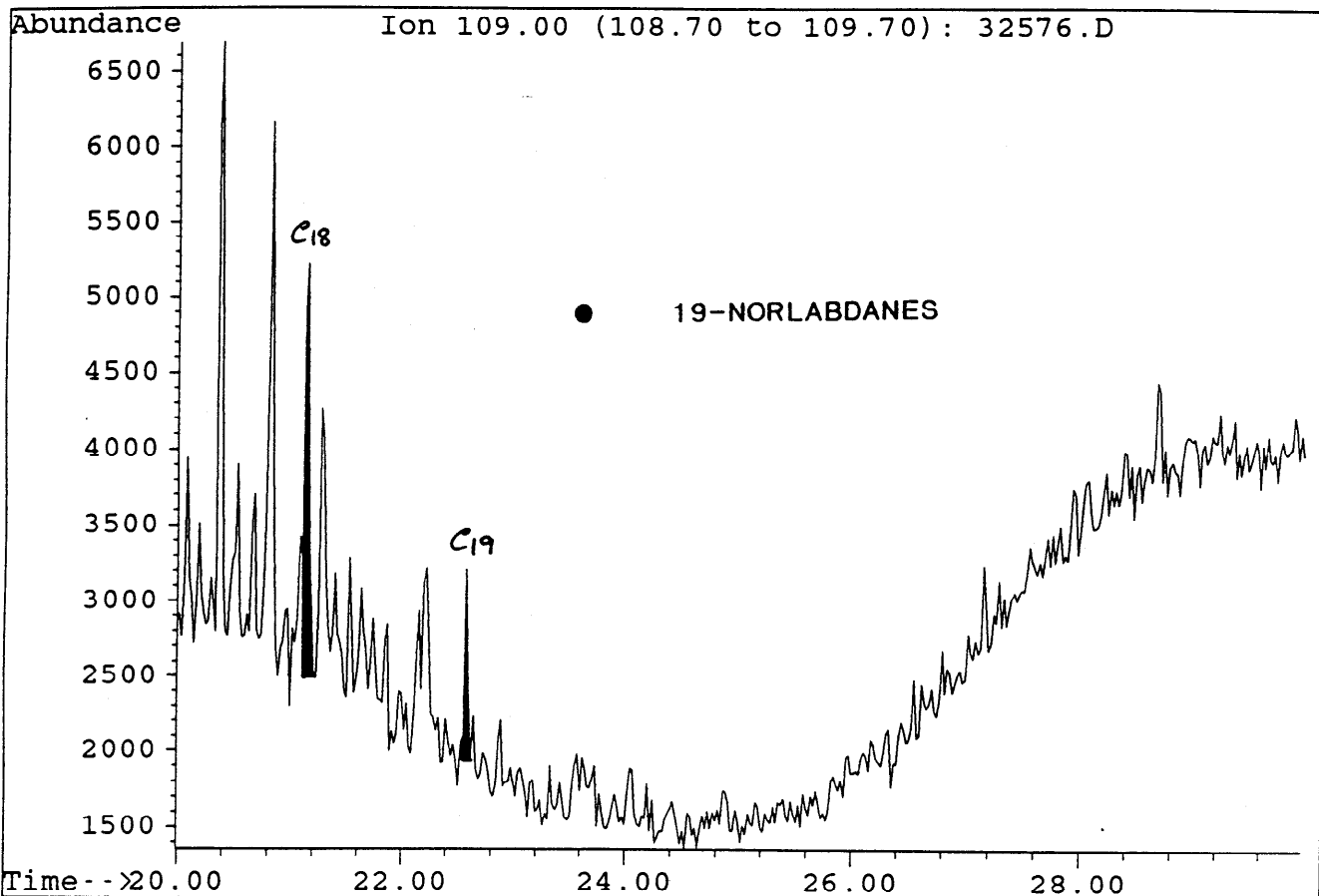


File : 32576.D  
Sample : MINERVA-1 RFT  
Misc. Info : COL#143, 1/1800, 17/3/94, DJ

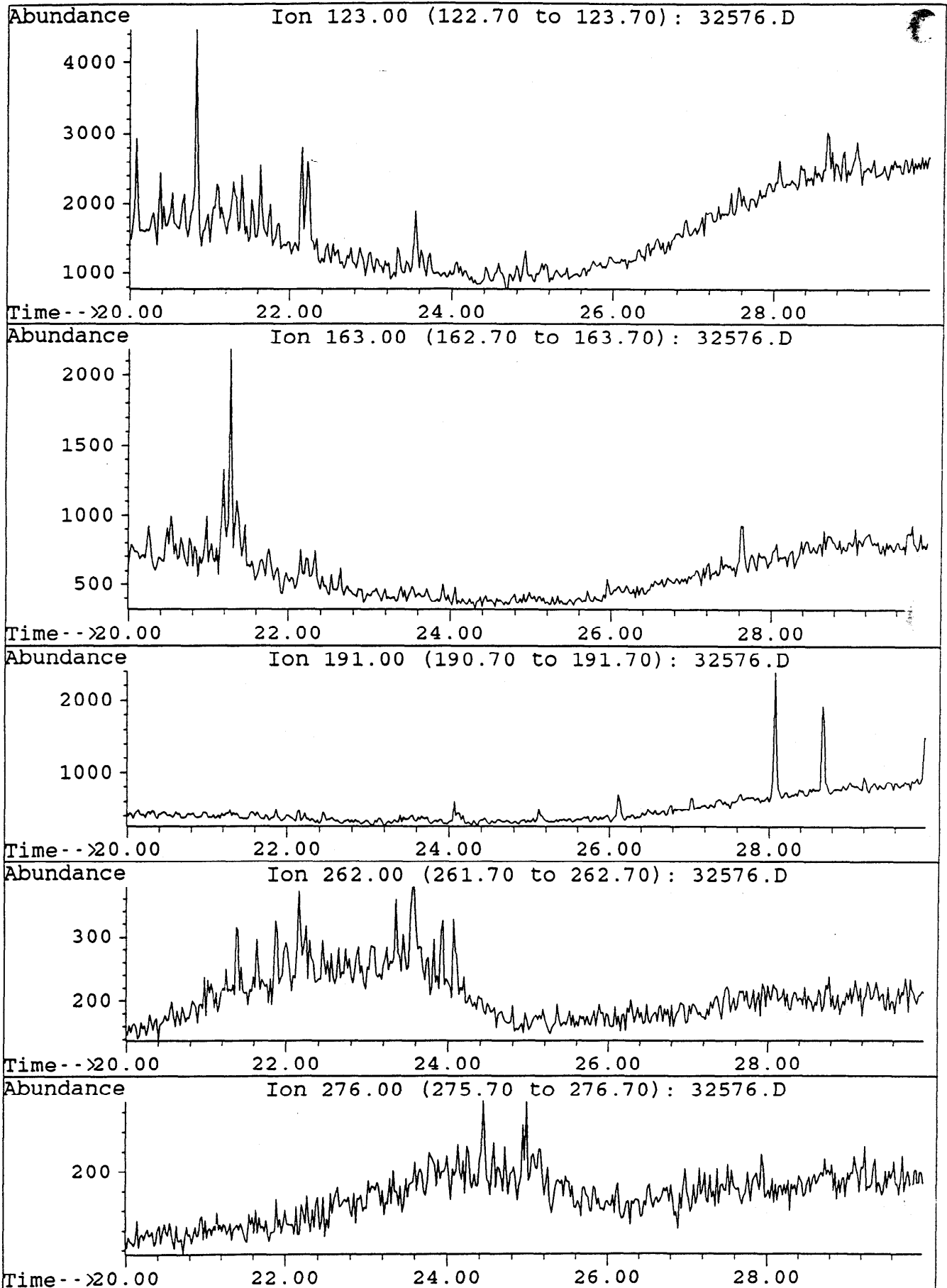




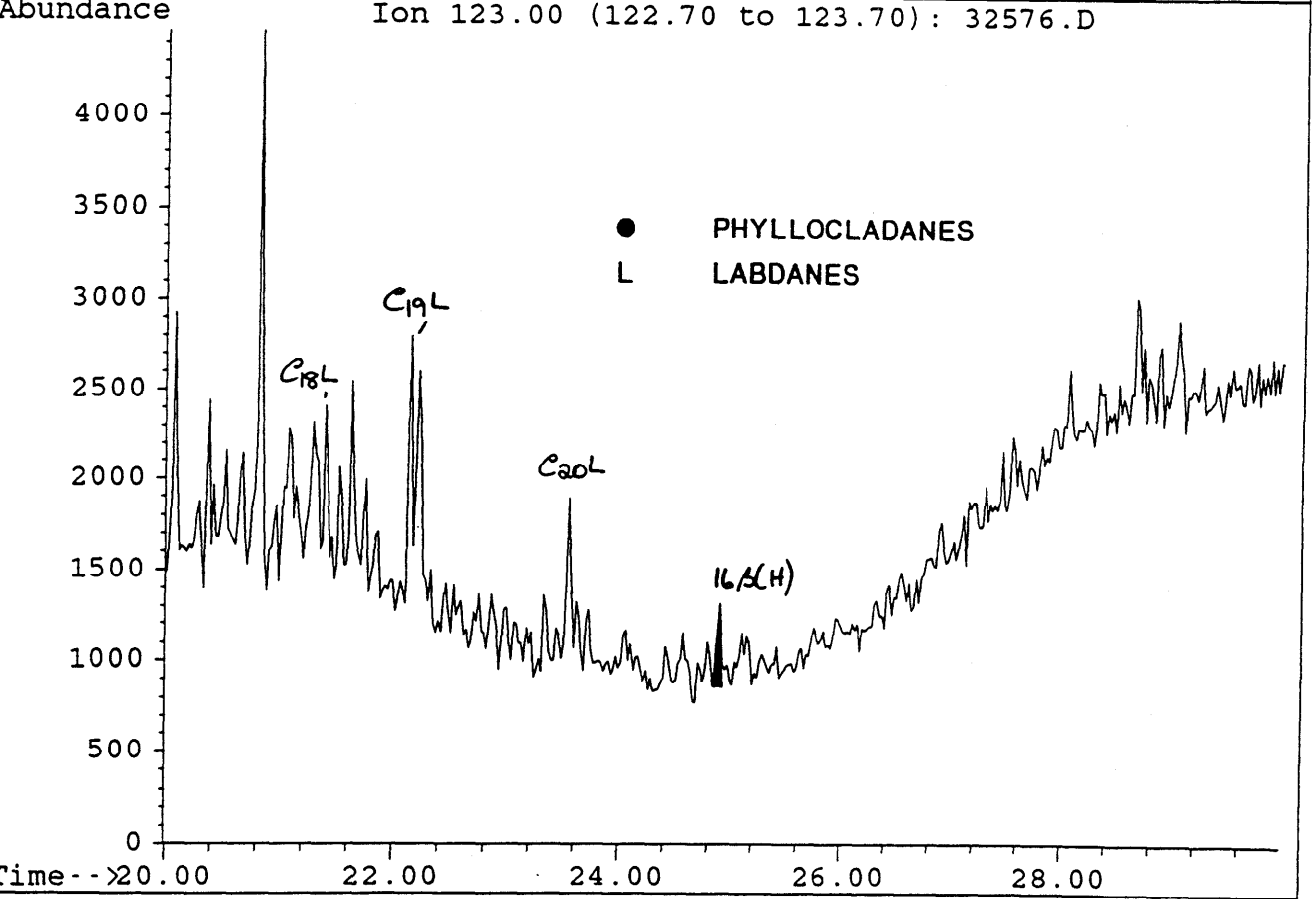
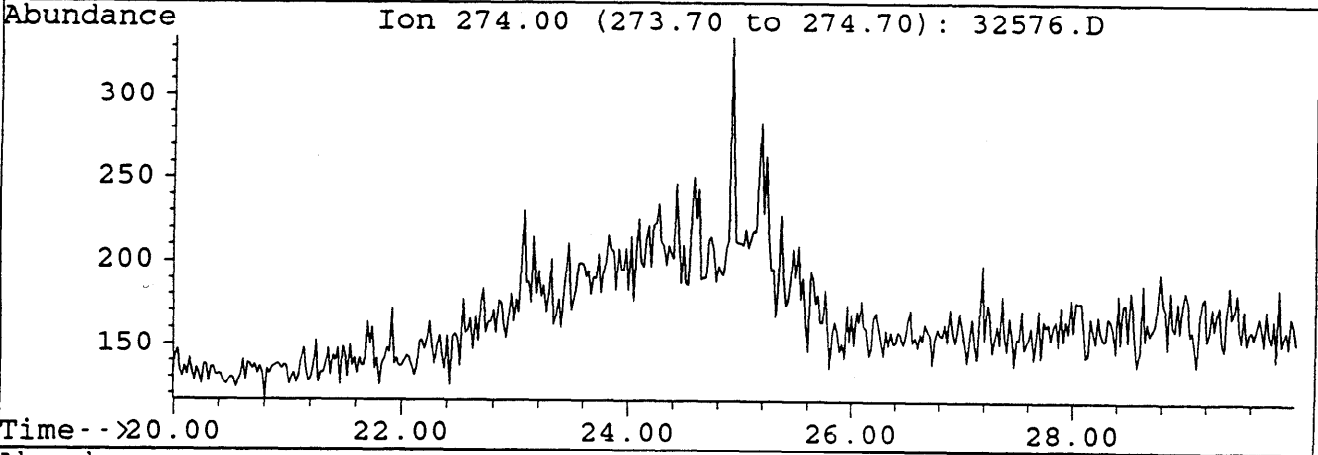
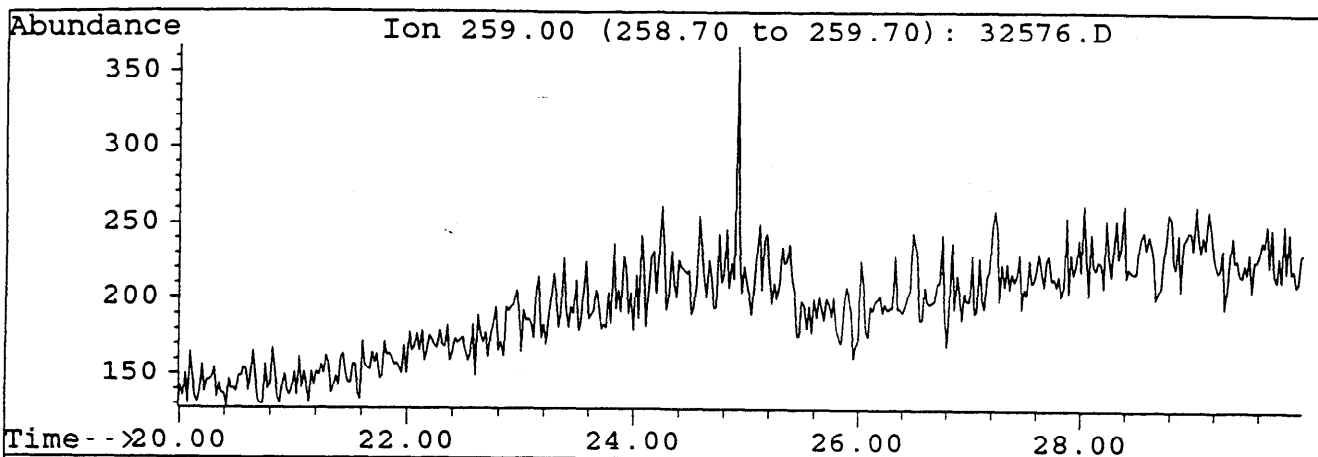
File : 32576.D  
Sample : MINERVA-1 RFT  
Misc. Info : COL#143, 1/1800, 17/3/94, DJ



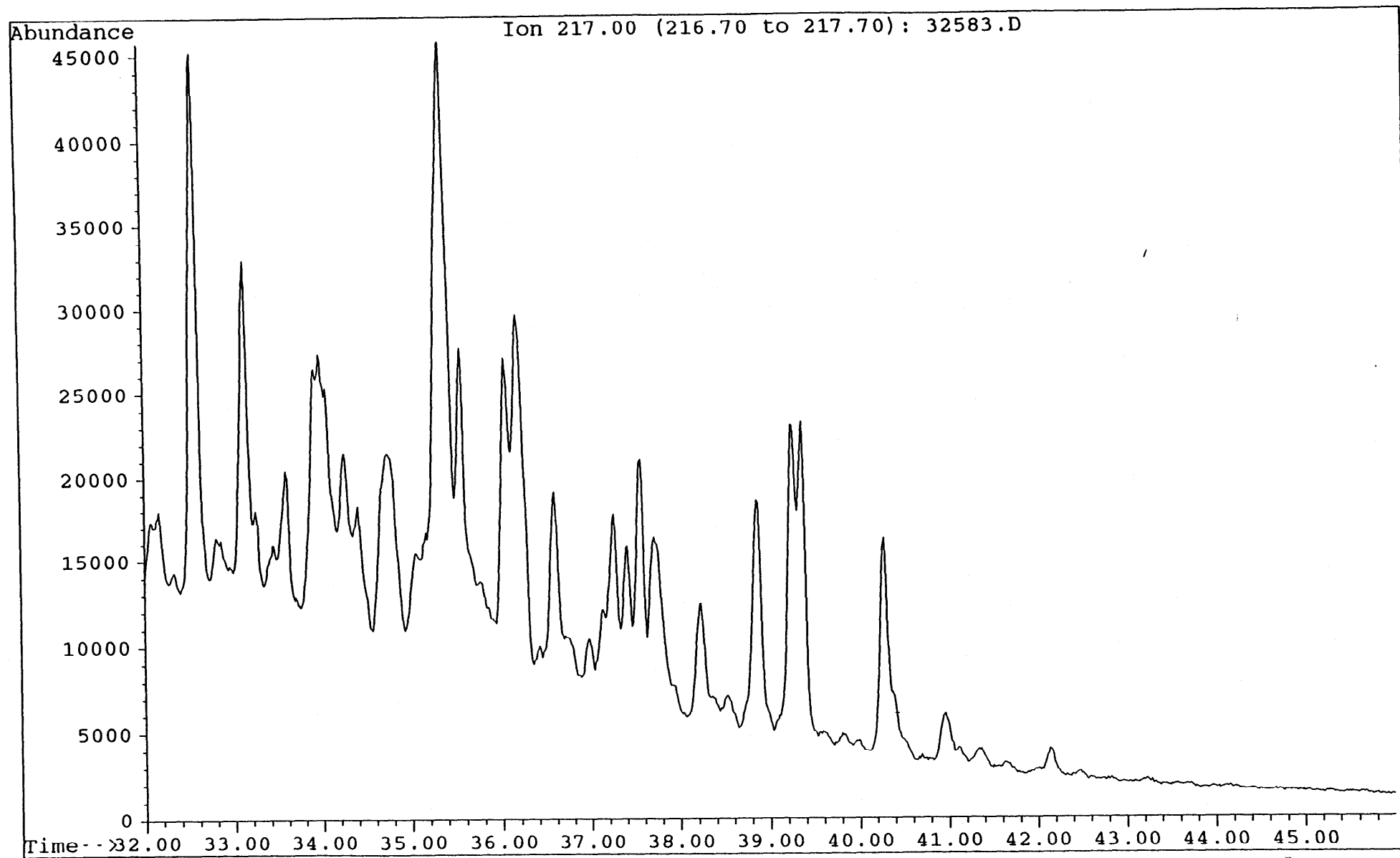
File : 32576.D  
Sample : MINERVA-1 RFT  
Misc. Info : COL#143, 1/1800, 17/3/94, DJ



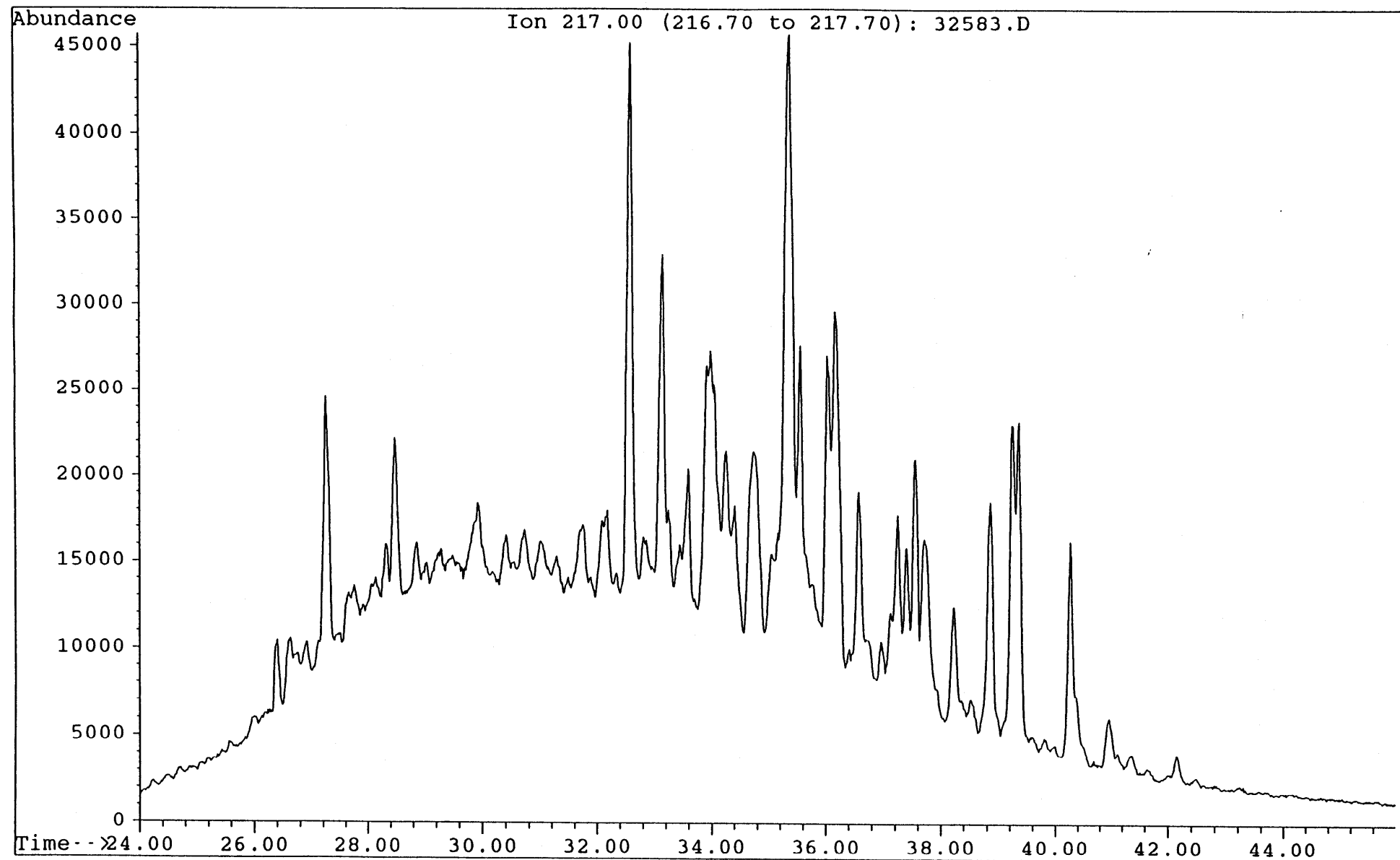
File : 32576.D  
Sample : MINERVA-1 RFT  
Misc. Info : COL#143, 1/1800, 17/3/94, DJ



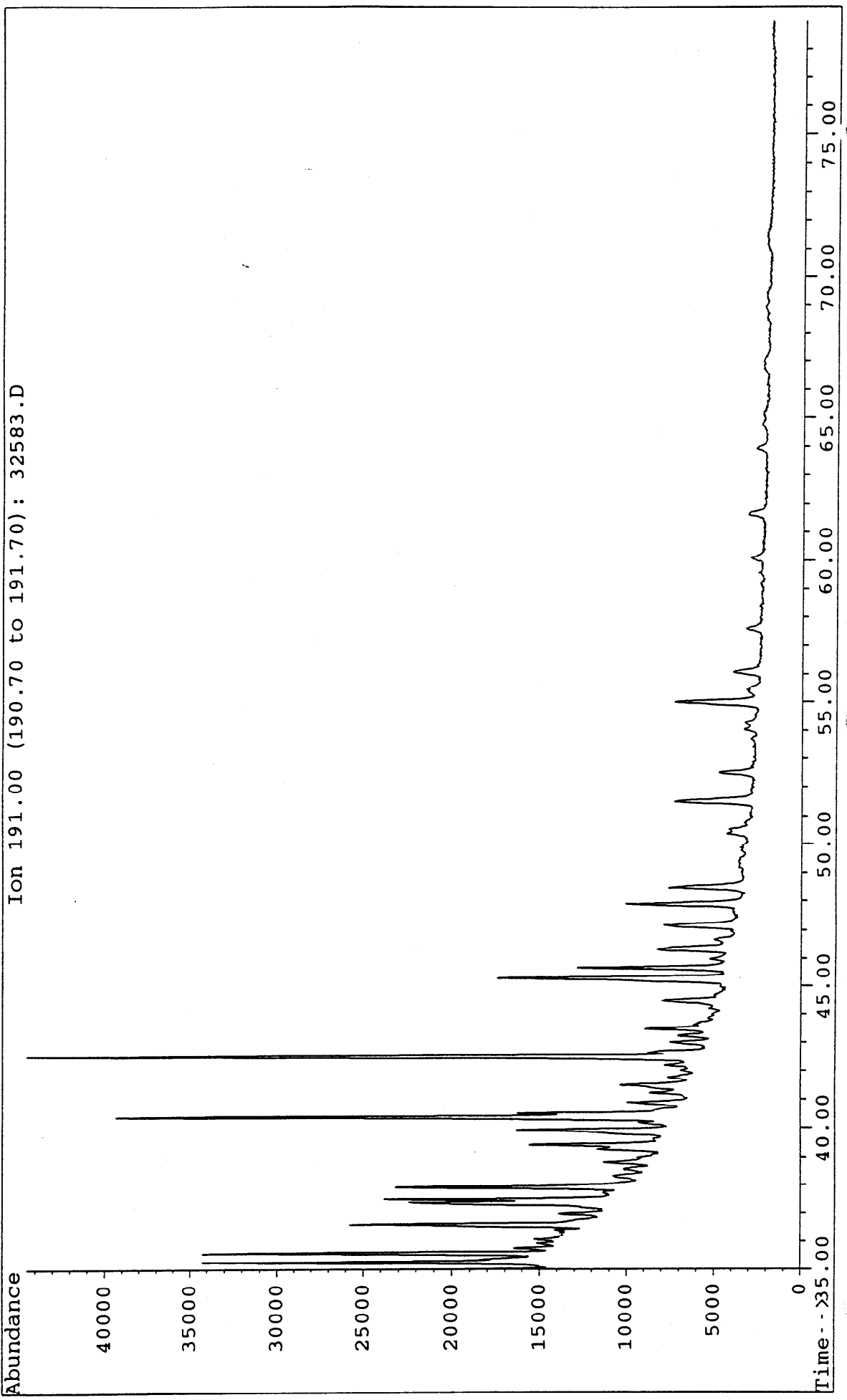
File : 32583.D  
Sample : MINERUA-1 RFT TOPPED B/C  
Misc. Info : col#143, 18/3/94 SB



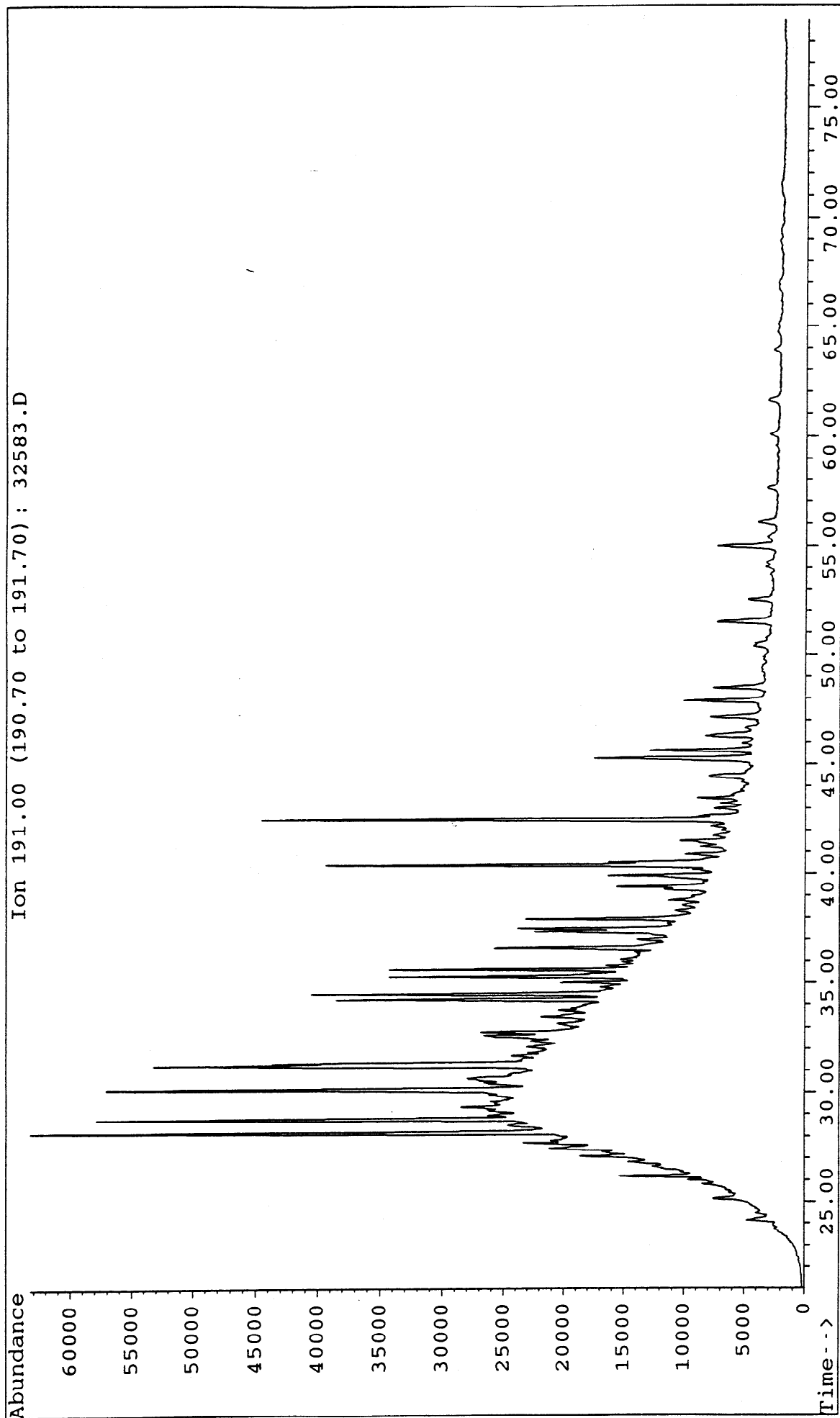
File : 32583.D  
Sample : MINERUA-1 RFT TOPPED B/C  
Misc. Info : col#143, 18/3/94 SB

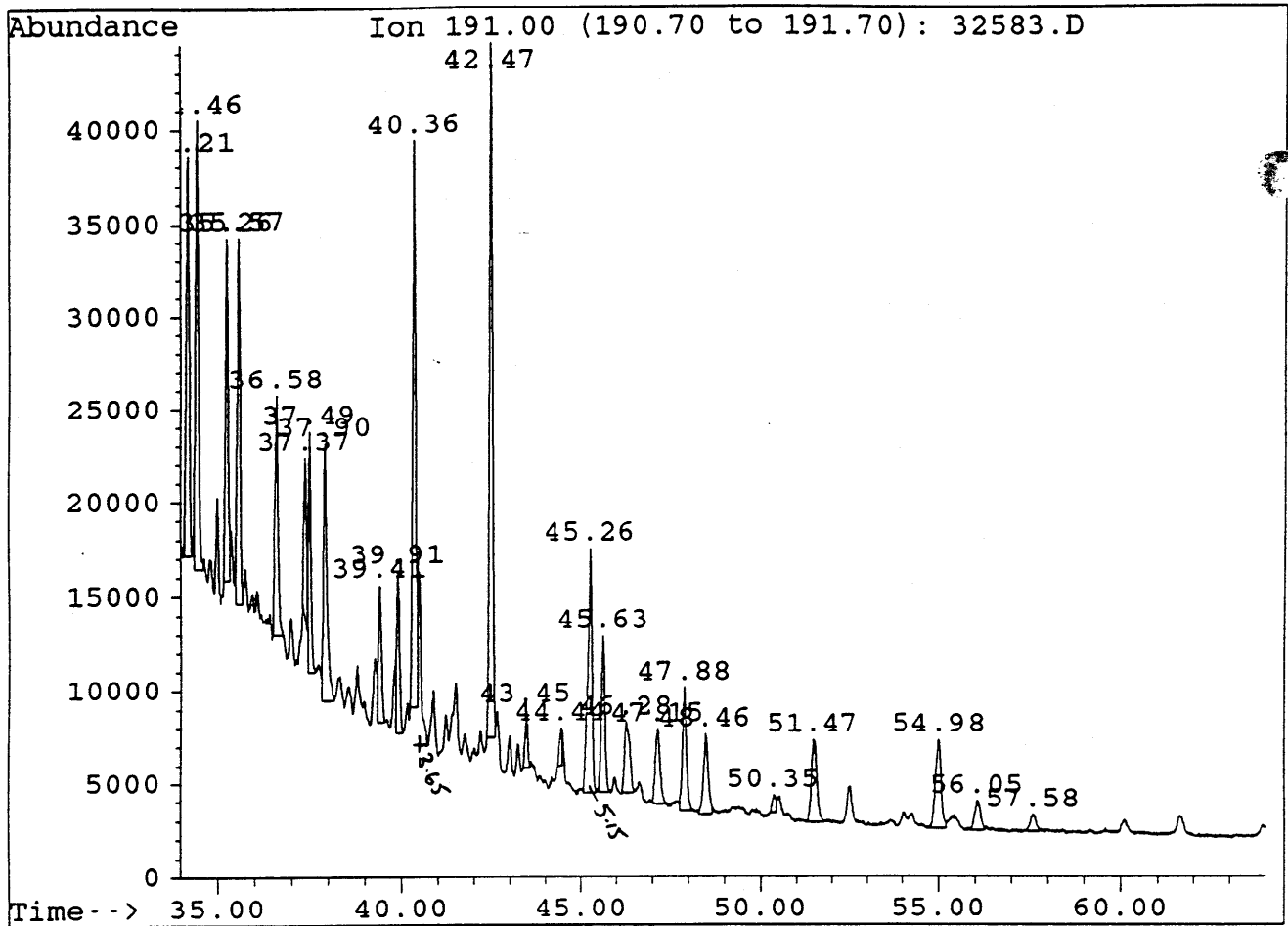


File : 32583.D  
Sample : MINERUA-1 RFT TOPPED B/C  
Misc. Info : col#143, 18/3/94 SB



File : 32583.D  
Sample : MINERUA-1 RFT TOPPED B/C  
Misc. Info : col#143, 18/3/94 SB



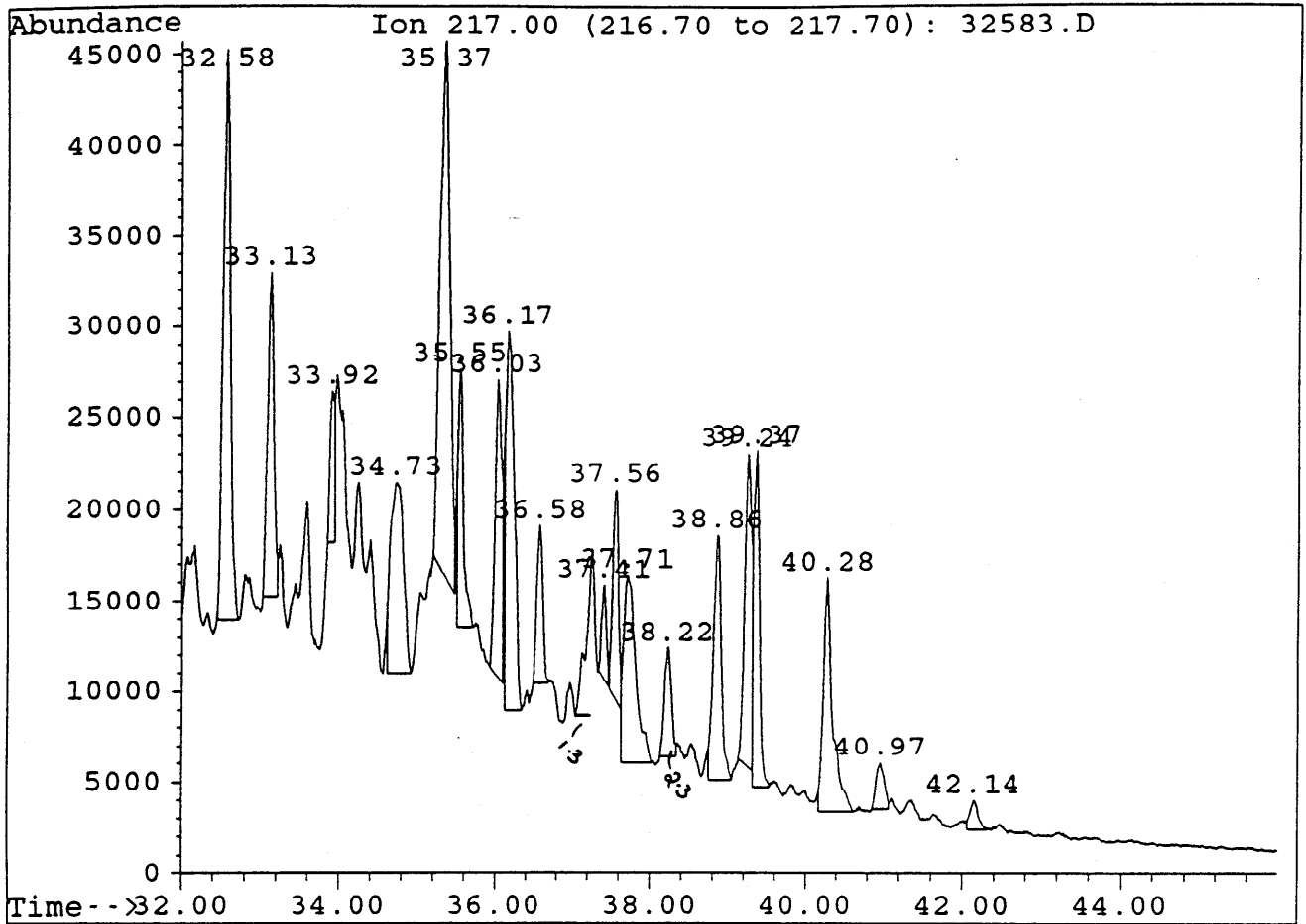


Sample : MINERUA-1 RFT TOPPED B/C

Peak	Ret.Time	Area	Height	Area %	Ratio %
1	34.21	114489	21392	6.72	53.64
2	34.46	134686	24120	7.91	63.11
3	35.26	96673	18406	5.67	45.30
4	35.57	101158	19653	5.94	47.40
5	36.58	76811	<u>12796</u> Ts	4.51	35.99
6	37.37	43754	<u>8083</u> Tm	2.57	20.50
7	37.49	61155	12835	3.59	28.65
8	37.90	91664	13729	5.38	42.95
9	39.41	43341	<u>7312</u> BWH	2.54	20.31
10	39.91	45244	<u>8666</u> 29 25-NOR	2.66	21.20
11	40.36	179443	<u>30252</u> 29H	10.53	84.08
12	42.47	213424	<u>37026</u> 30H	12.53	100.00
13	43.45	16871	<u>3111</u> 30M	0.99	7.90
14	44.44	11188	2037	0.66	5.24
15	45.26	111784	<u>13074</u> 31S	6.56	52.38
16	45.63	59365	<u>8435</u> 31R	3.48	27.82
17	46.28	40602	3875	2.38	19.02
18	47.15	37480	4092	2.20	17.56
19	47.88	51323	<u>6639</u> 32S	3.01	24.05
20	48.46	40261	<u>4388</u> 32R	2.36	18.86
21	50.35	7154	992	0.42	3.35
22	51.47	48111	4490	2.82	22.5
23	54.98	51354	4779	3.01	24.06
24	56.05	17241	1560	1.01	8.08
25	57.58	9202	863	0.54	4.31

Handwritten notes:  $\frac{3.65}{5.15} * \rightarrow$  pointing to peak 15.



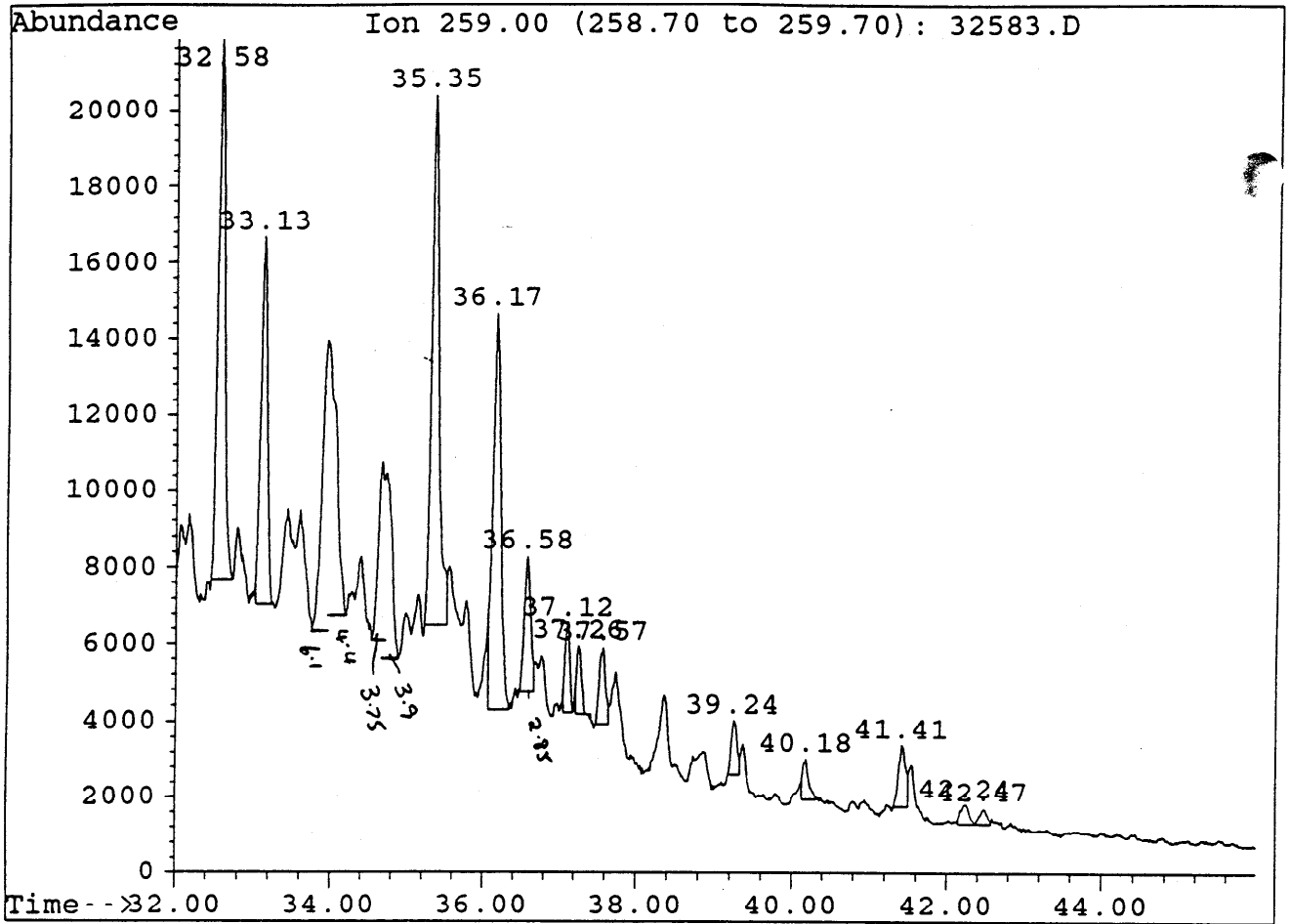


Sample : MINERUA-1 RFT TOPPED B/C

Peak	Ret.Time	Area	Height	Area %	Ratio %
1	32.58	194796	31252	11.14	73.61
2	33.13	102319	17762	5.85	38.67
3	33.92	36830	8344	2.11	13.92
4	34.73	118867	10465	6.80	44.92
5	35.37	264620	28947	15.14	100.00
6	35.55	67497	14142	3.86	25.51
7	36.03	102349	15990	5.85	38.68
8	36.17	145099	20737	8.30	54.83
9	36.58	46521	8708	2.66	17.58
10	37.41	22468	4818	1.29	8.49
11	37.56	61128	11280	3.50	23.10
12	37.71	111708	10336	6.39	42.21
13	38.22	39038	6040	2.23	14.75
14	38.86	95420	13448	5.46	36.06
15	39.24	111047	16934	6.35	41.96
16	39.37	93032	18468	5.32	35.16
17	40.28	105602	12871	6.04	39.91
18	40.97	18487	2528	1.06	6.99
19	42.14	11458	1659	0.66	4.33

28S  
= 1.3  
2.3\*

28R  
28S  
isoR  
isoS

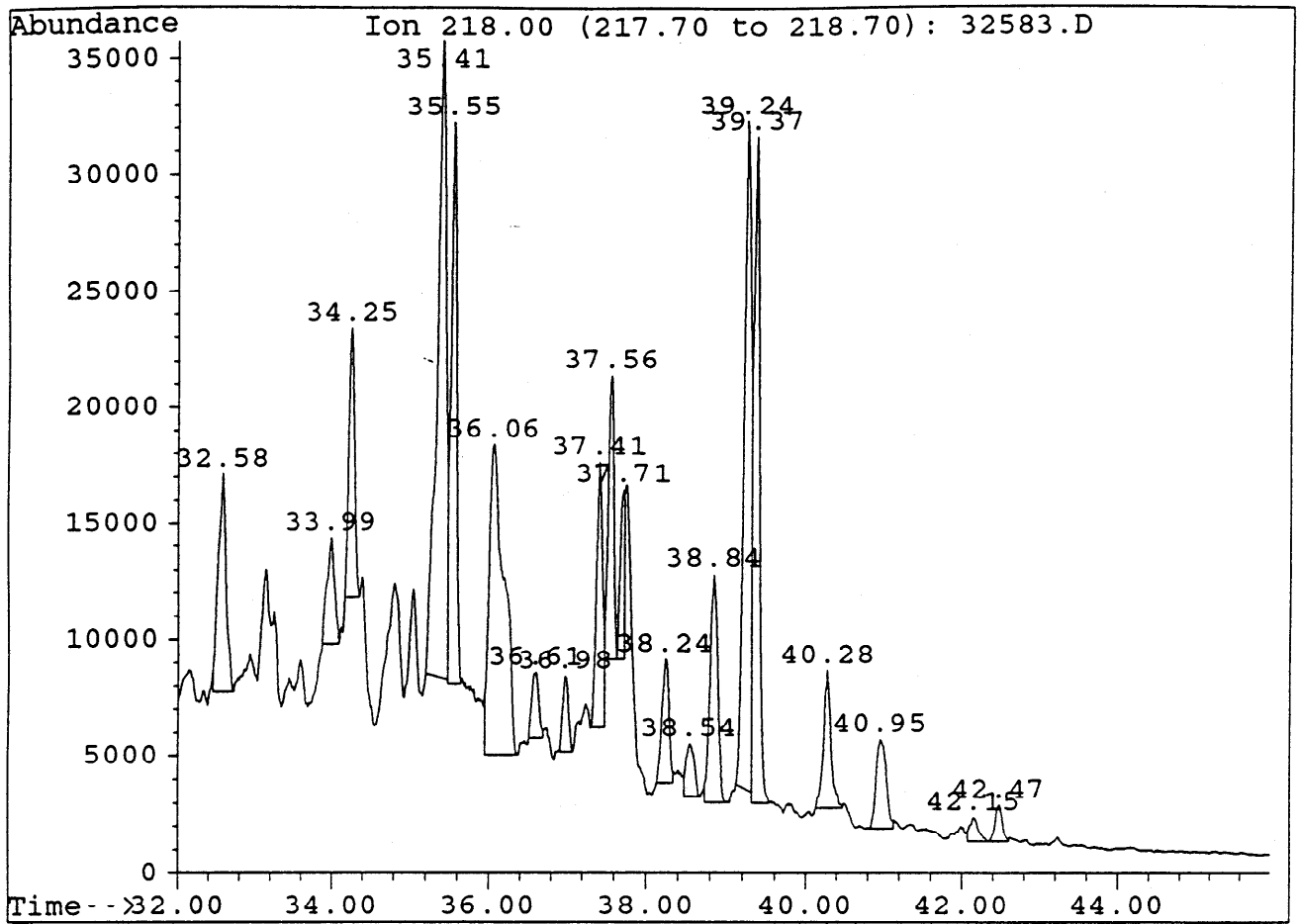


Sample : MINERUA-1 RFT TOPPED B/C

Peak	Ret.Time	Area	Height	Area %	Ratio %
1	32.58	85856	<u>14133</u> 27S	21.76	88.92
2	33.13	57720	<u>9629</u> 27R	14.63	59.78
3	35.35	96556	<u>13907</u> 29S	24.47	100.00
4	36.17	73638	<u>10382</u> 29R	18.67	76.26
5	36.58	20517	3548	5.20	21.25
6	37.12	10153	2331	2.57	10.52
7	37.26	7446	1776	1.89	7.71
8	37.57	11275	1986	2.86	11.68
9	39.24	7680	1422	1.95	7.95
10	40.18	5941	1101	1.51	6.15
11	41.41	10671	1642	2.70	11.05
12	42.24	4102	558	1.04	4.25
13	42.47	2962	445	0.75	3.07

$$28S = \frac{6.1 + 4.4}{2.85} * 3548$$

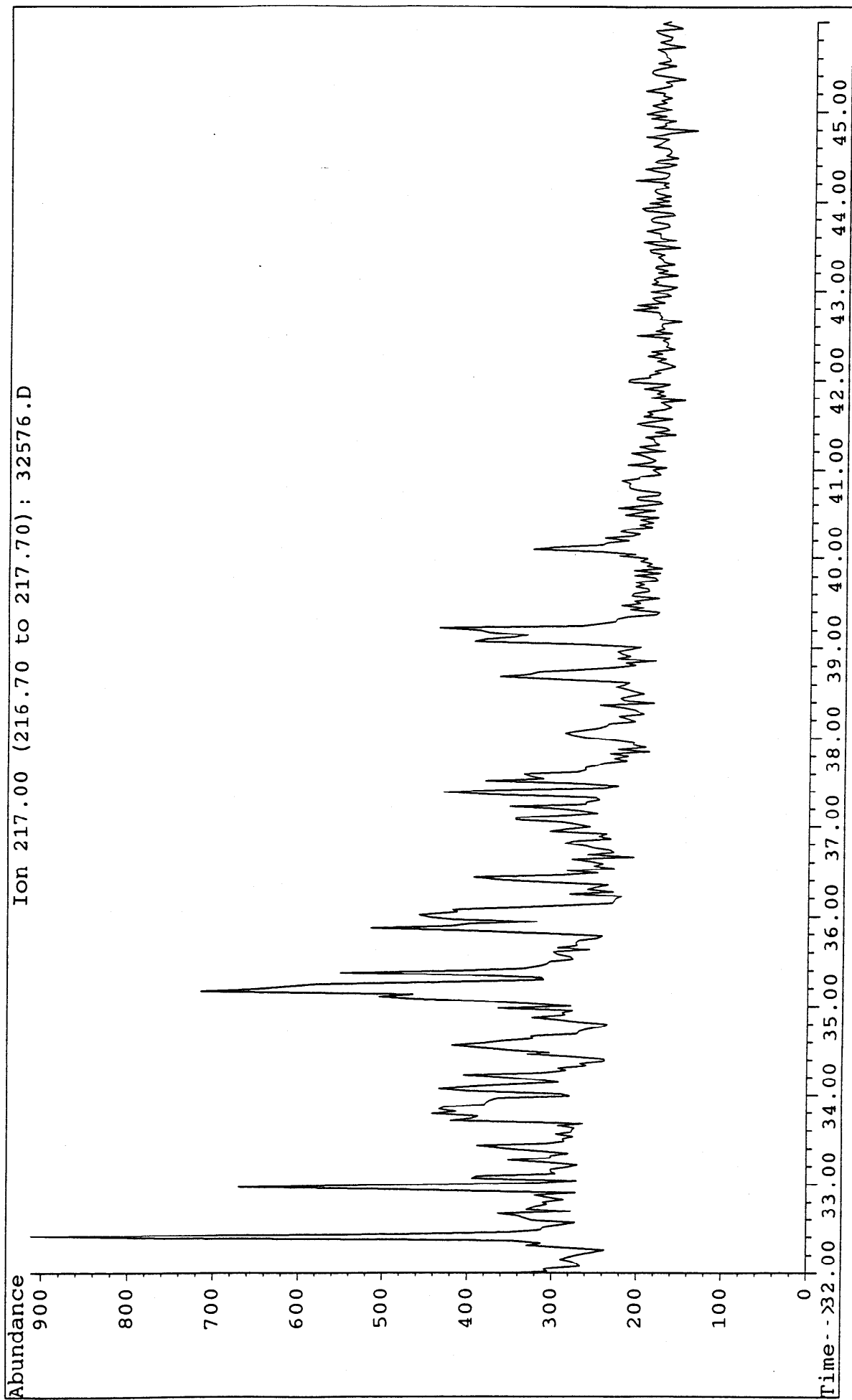
$$28R = \frac{3.75 + 3.9}{2.85} * 3548$$



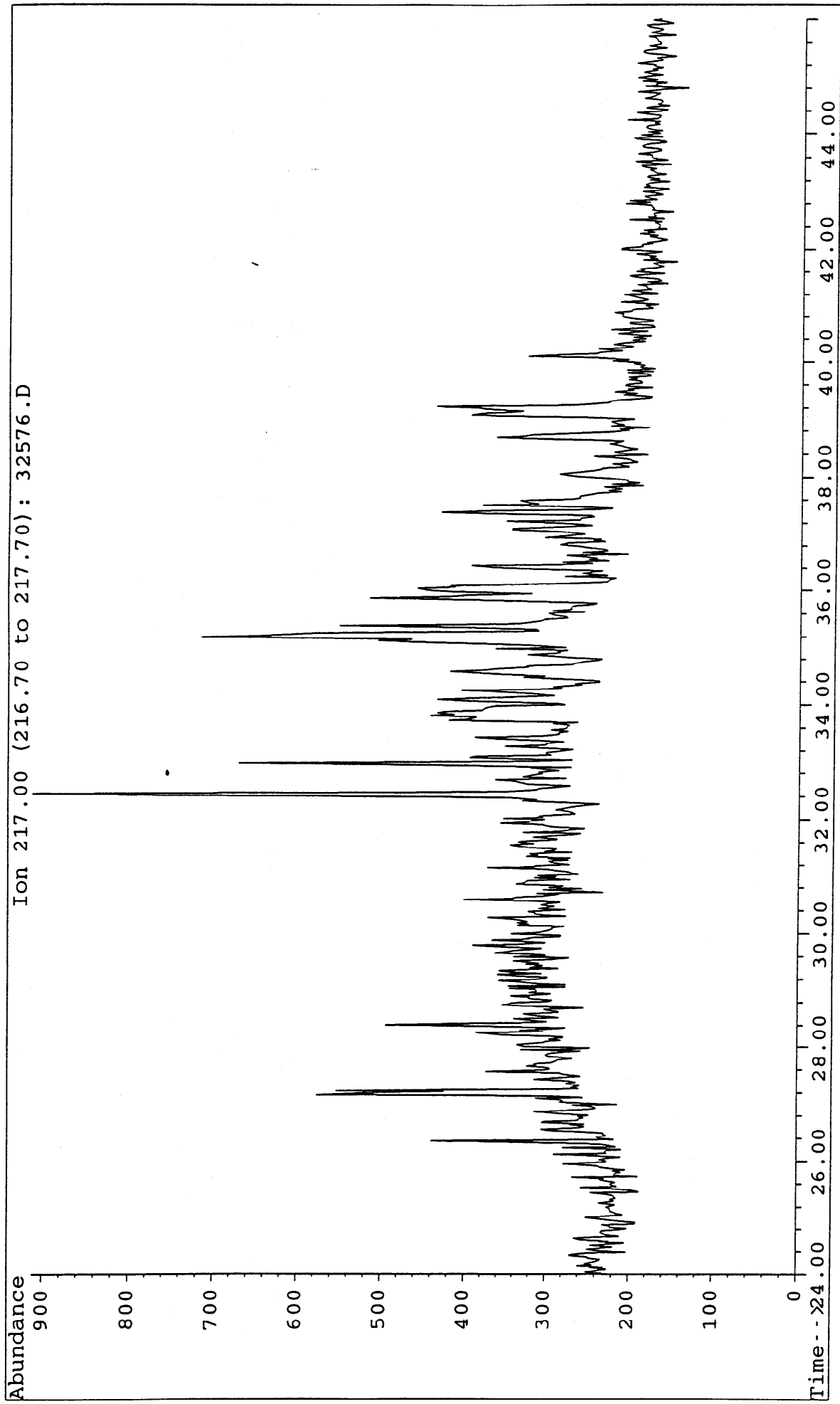
Sample : MINERUA-1 RFT TOPPED B/C

Peak	Ret.Time	Area	Height	Area %	Ratio %
1	32.58	66392	9395	4.79	30.59
2	33.99	30948	4601	2.23	14.26
3	34.25	61719	11570	4.45	28.44
4	35.41	217046	27341	15.67	100.00
5	35.55	120114	24142	8.67	55.34
6	36.06	175550	13380	12.67	80.88
7	36.61	17170	2822	1.24	7.91
8	36.98	16242	3239	1.17	7.48
9	37.41	63541	11442	4.59	29.28
10	37.56	59140	12219	4.27	27.25
11	37.71	29089	7299	2.10	13.40
12	38.24	33754	5297	2.44	15.55
13	38.54	15928	2251	1.15	7.34
14	38.84	64378	9773	4.65	29.66
15	39.24	182074	28624	13.14	83.89
16	39.37	143058	28577	10.33	65.91
17	40.28	37621	5867	2.72	17.33
18	40.95	34250	3803	2.47	15.78
19	42.15	7721	1041	0.56	3.56
20	42.47	9779	1544	0.71	4.51

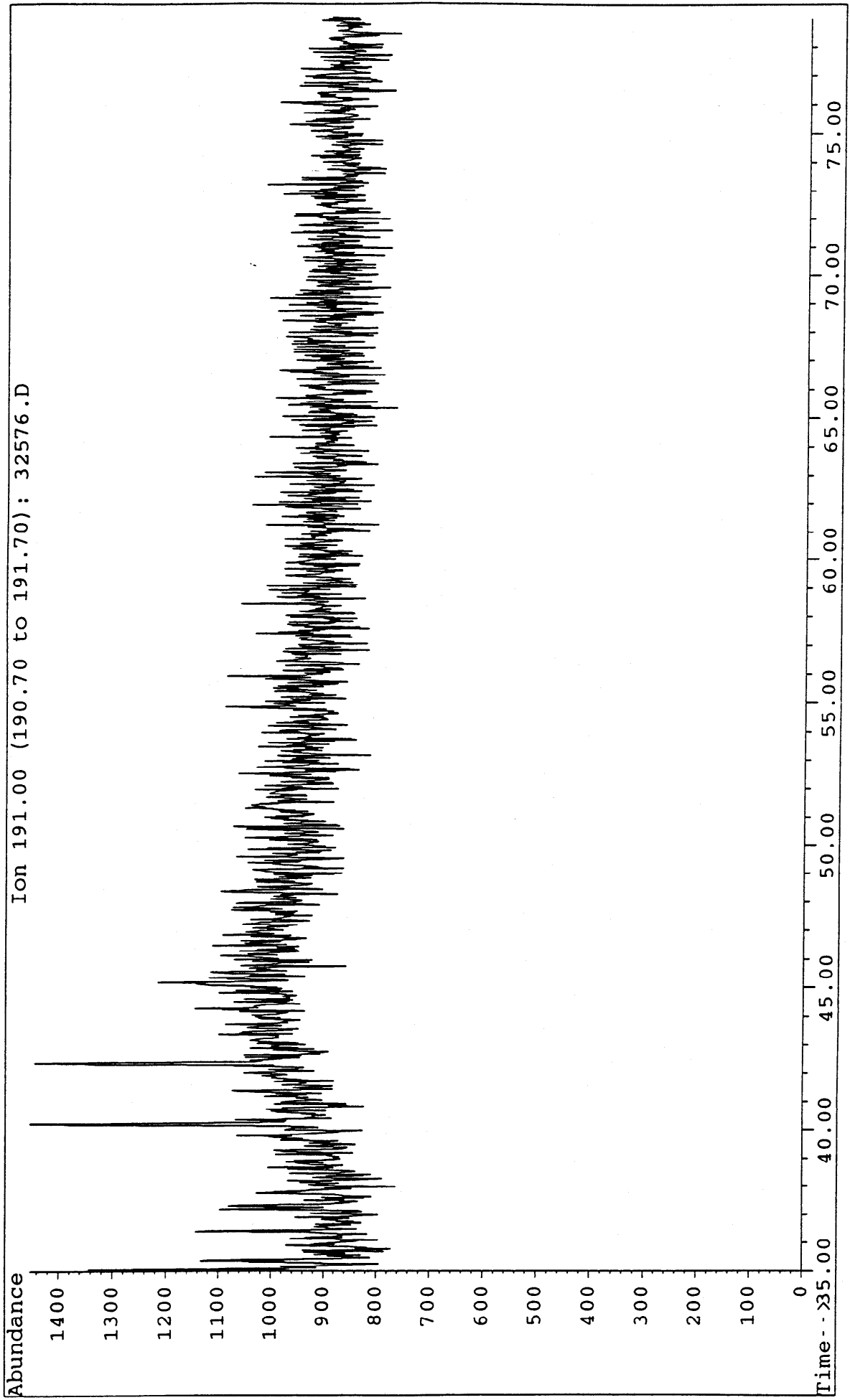
File : 32576.D  
Sample : MINERVA-1 RFT  
Misc. Info : COL#143, 1/1800, 17/3/94, DJ



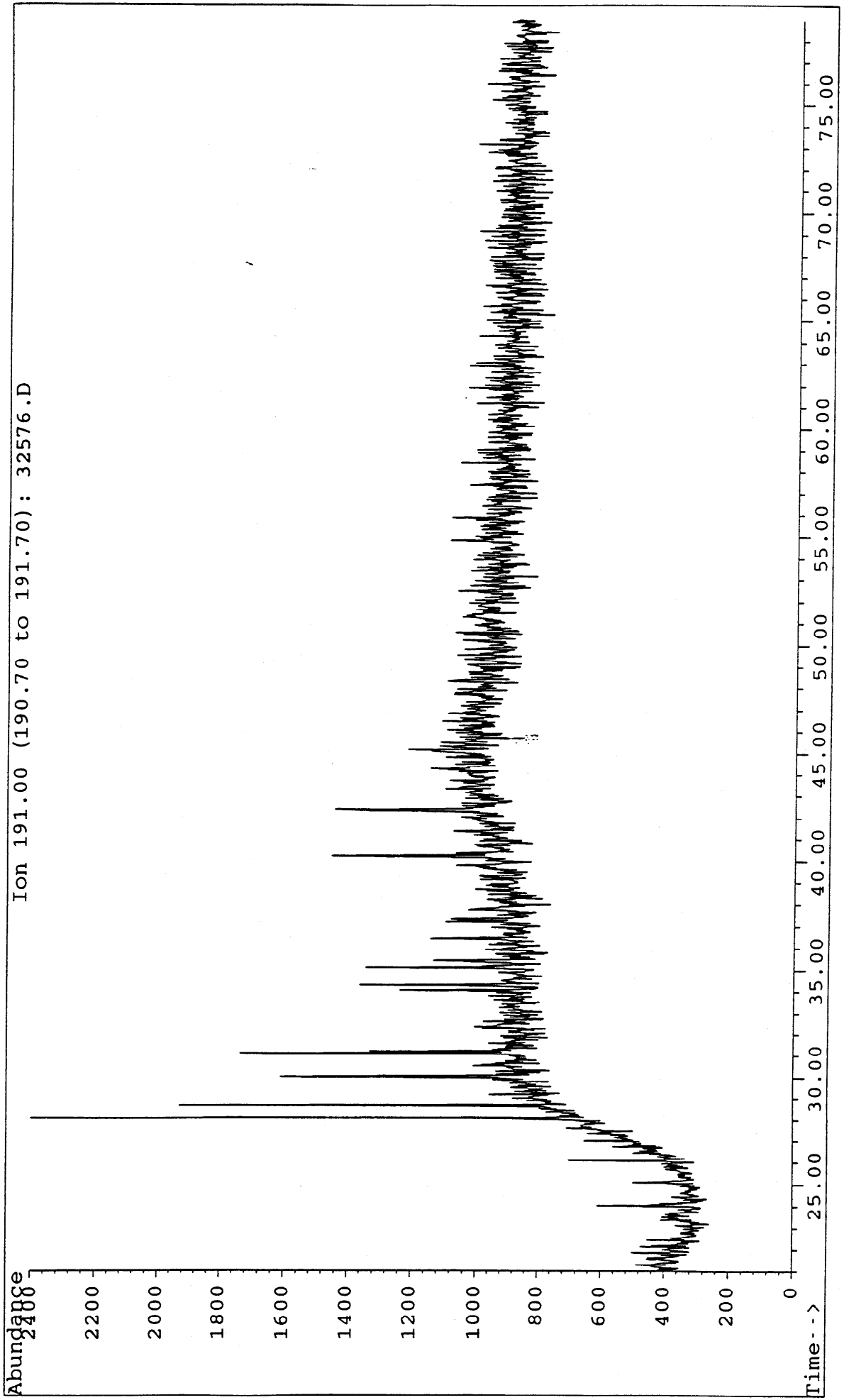
File : 32576.D  
Sample : MINERVA-1 RFT  
Misc. Info : COL#143, 1/1800, 17/3/94, DJ

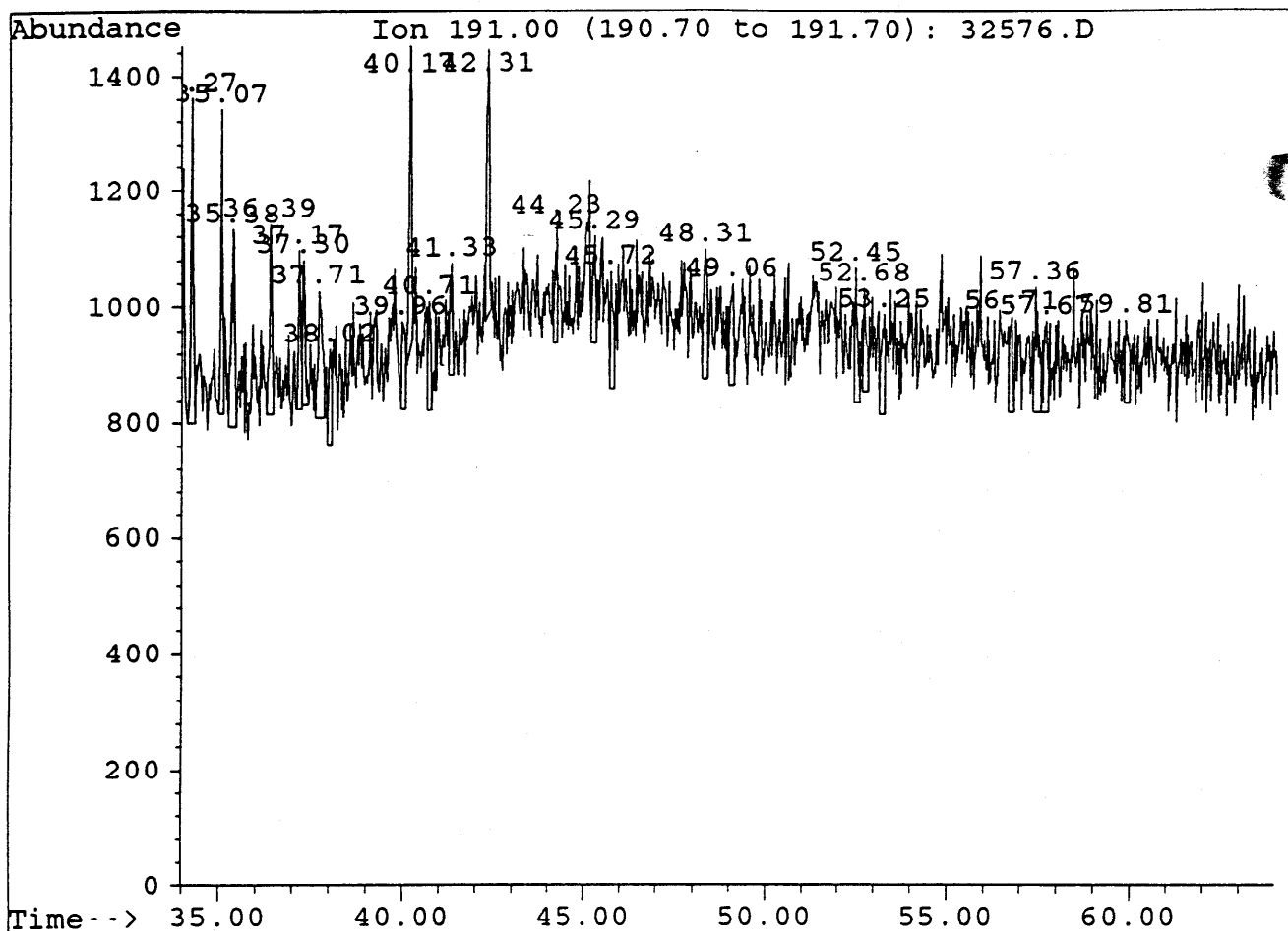


File : 32576.D  
Sample : MINERVA-1 RFT  
Misc. Info : COL#143, 1/1800, 17/3/94, DJ



File : 32576.D  
Sample : MINERVA-1 RFT  
Misc. Info : COL#143, 1/1800, 17/3/94, DJ

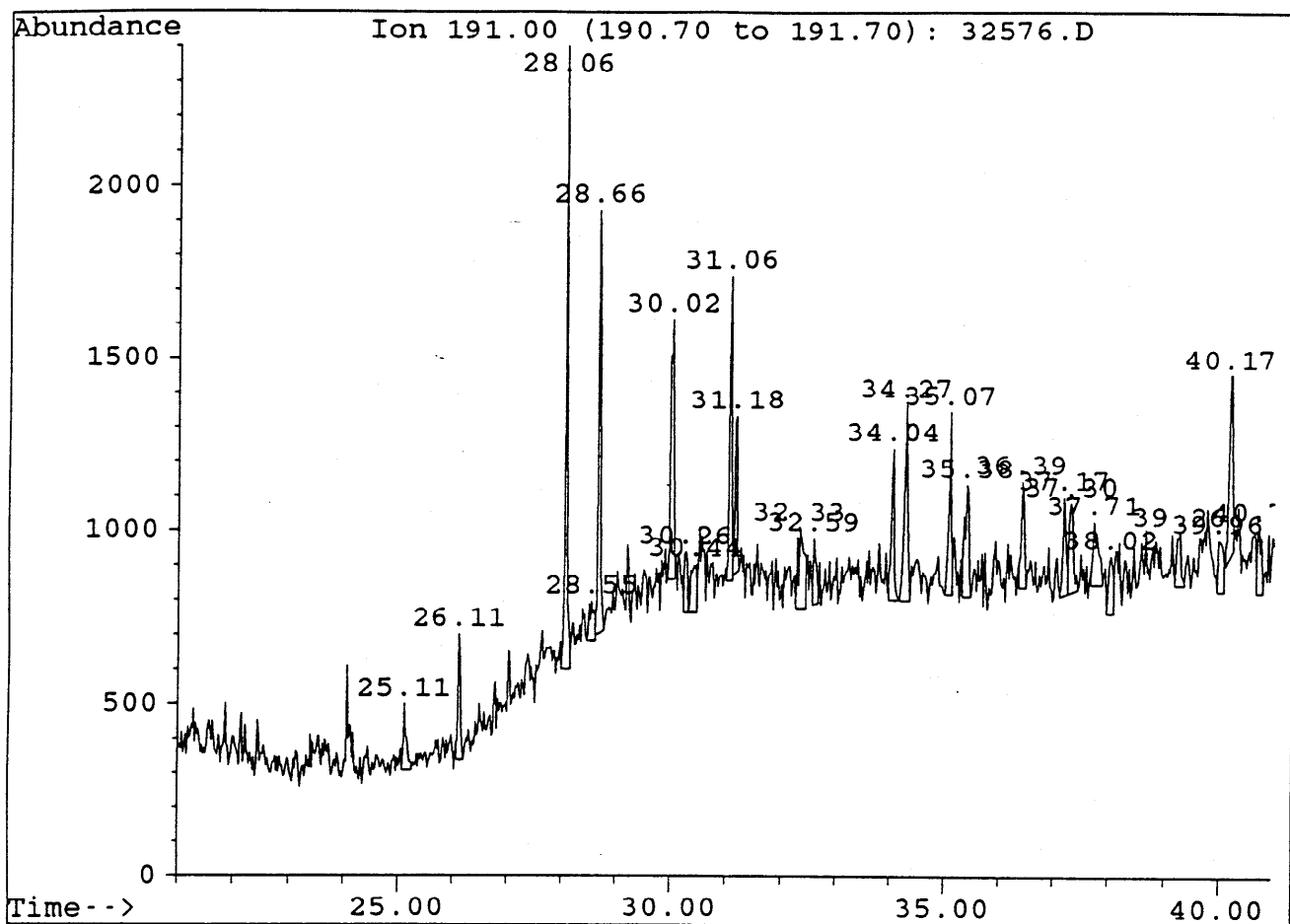




Sample : MINERVA-1 RFT

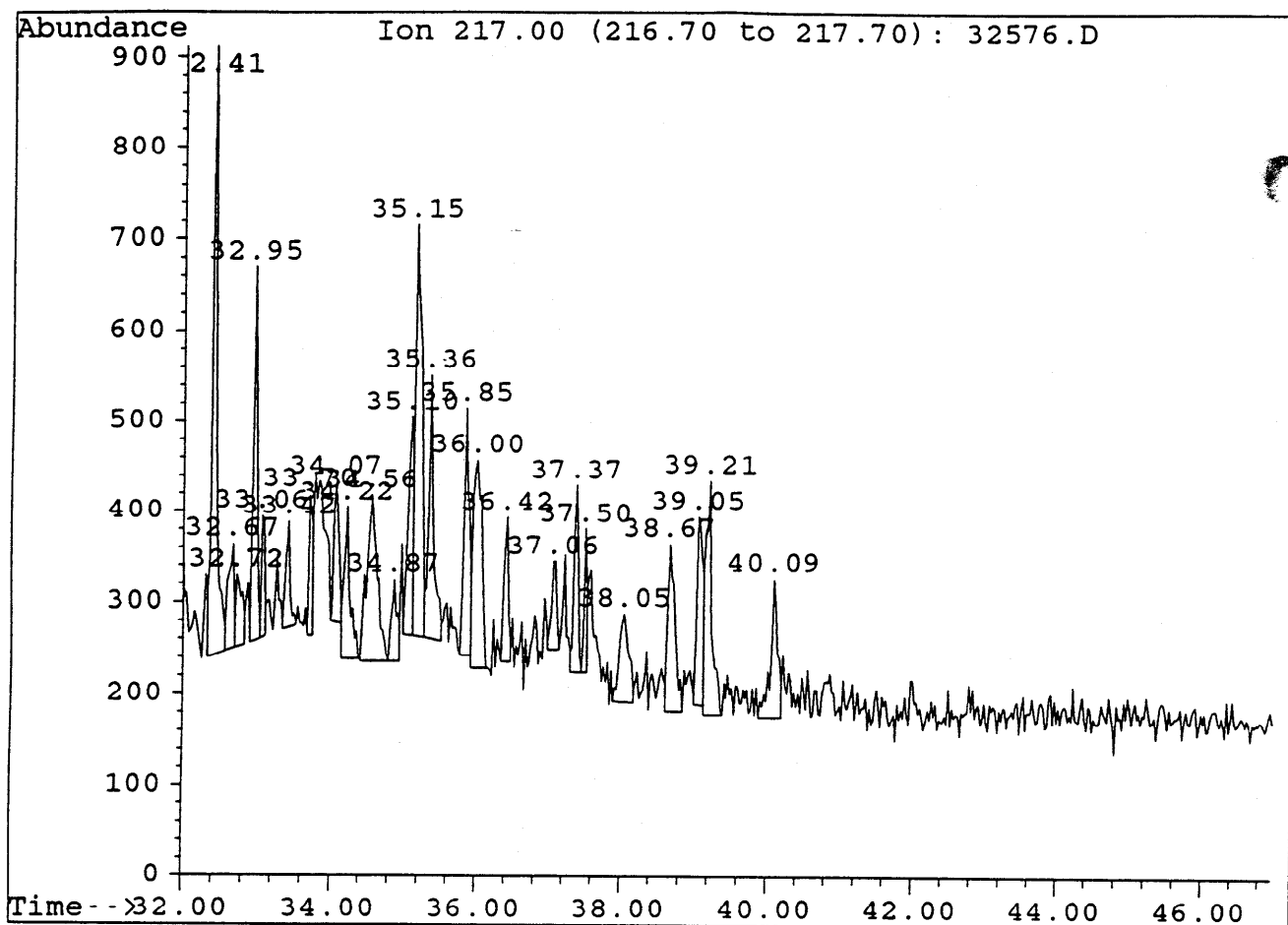
Peak	Ret.Time	Area	Height	Area %	Ratio %
1	34.27	2377	564	6.88	92.20
2	35.07	1845	528	5.34	71.57
3	35.38	2211	340	6.40	85.76
4	36.39	1662	328	4.81	64.47
5	37.17	1189	272	3.44	46.12
6	37.30	1287	247	3.72	49.92
7	37.71	1917	219	5.55	74.36
8	38.02	990	166	2.86	38.40
9	39.96	995	149	2.88	38.60
10	40.17	2578	519	7.46	100.00
11	40.71	977	187	2.83	37.90
12	41.33	910	192	2.63	35.30
13	42.31	2458	455	7.11	95.35
14	44.23	985	210	2.85	38.21
15	45.29	929	183	2.69	36.04
16	45.72	1042	200	3.01	40.42
17	48.31	1448	223	4.19	56.17
18	49.06	1112	174	3.22	43.13
19	52.45	1020	230	2.95	39.57
20	52.68	891	177	2.58	34.56
21	53.25	1169	172	3.38	45.35
22	56.71	901	165	2.61	34.55
23	57.36	1588	216	4.59	61.60
24	57.67	1132	157	3.27	43.91
25	59.81	957	142	2.77	37.12





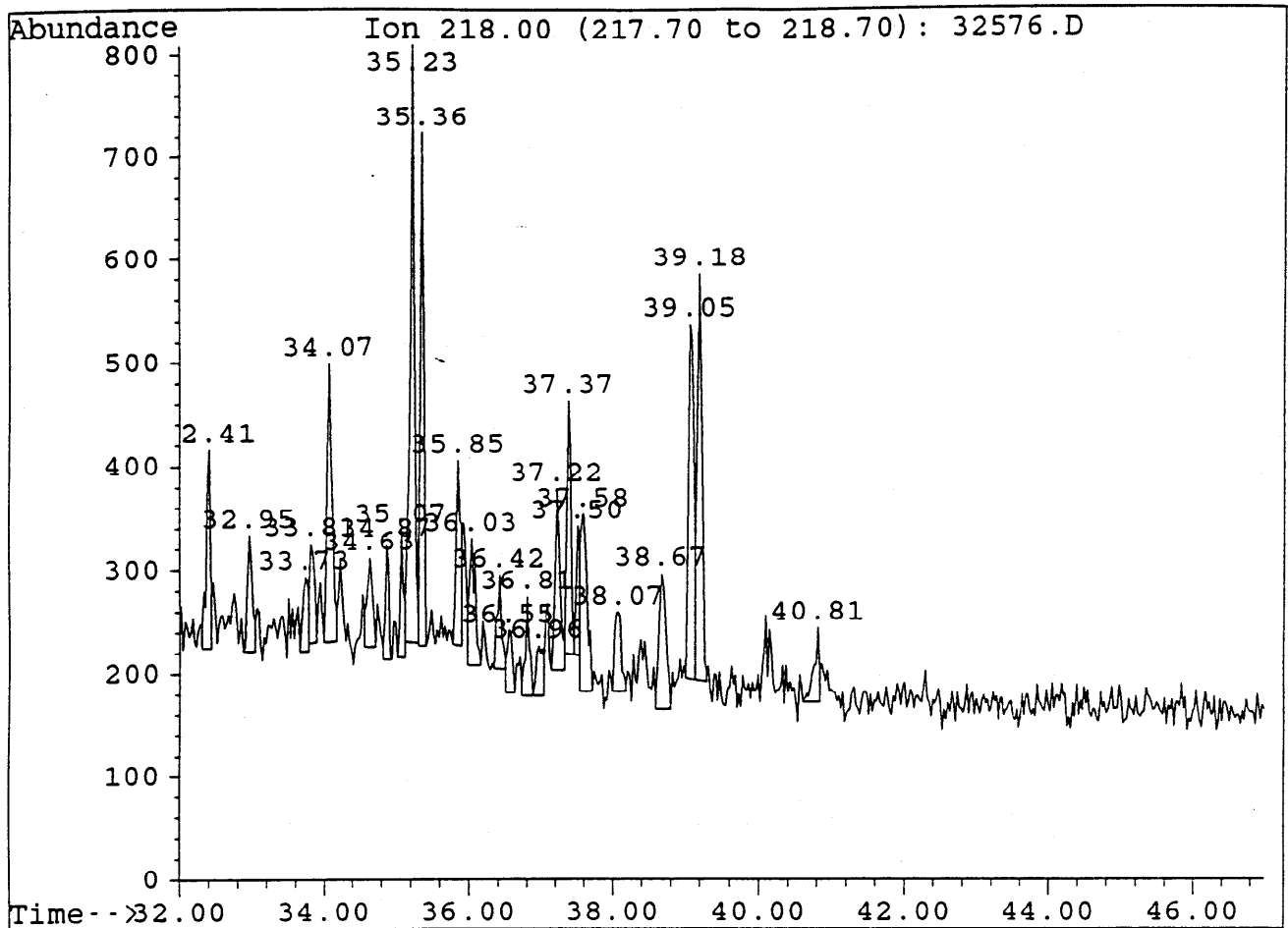
Sample : MINERVA-1 RFT

Peak	Ret.Time	Area	Height	Area %	Ratio %
1	25.11	720	193 <sup>20</sup>	1.76	16.66
2	26.11	1135	367 <sup>21</sup>	2.77	26.27
3	28.06	4321	1800 <sup>23</sup>	10.55	100.00
4	28.55	709	113	1.73	16.41
5	28.66	3559	1224 <sup>24</sup>	8.69	82.37
6	30.02	3268	753 <sup>25</sup>	7.98	75.63
7	30.26	645	174	1.57	14.93
8	30.44	1001	139	2.44	23.17
9	31.06	2653	883 <sup>24+27</sup>	6.48	61.40
10	31.18	1368	2 x 450 <sup>26</sup>	3.34	31.66
11	32.33	1813	232	4.43	41.96
12	32.59	668	190	1.63	15.46
13	34.04	1611	437	3.93	37.28
14	34.27	2354	564 <sup>28</sup>	5.75	54.48
15	35.07	1845	528	4.50	42.70
16	35.38	1693	323 <sup>29</sup>	4.13	39.18
17	36.39	1246	308	3.04	28.84
18	37.17	1282	284	3.13	29.67
19	37.30	1374	256	3.35	31.80
20	37.71	1276	182	3.12	29.53
21	38.02	990	166	2.42	22.91
22	39.26	876	151	2.14	20.27
23	39.96	995	149	2.43	23.03
24	40.17	2578	518	6.29	59.66
25	40.71	977	187	2.39	22.61



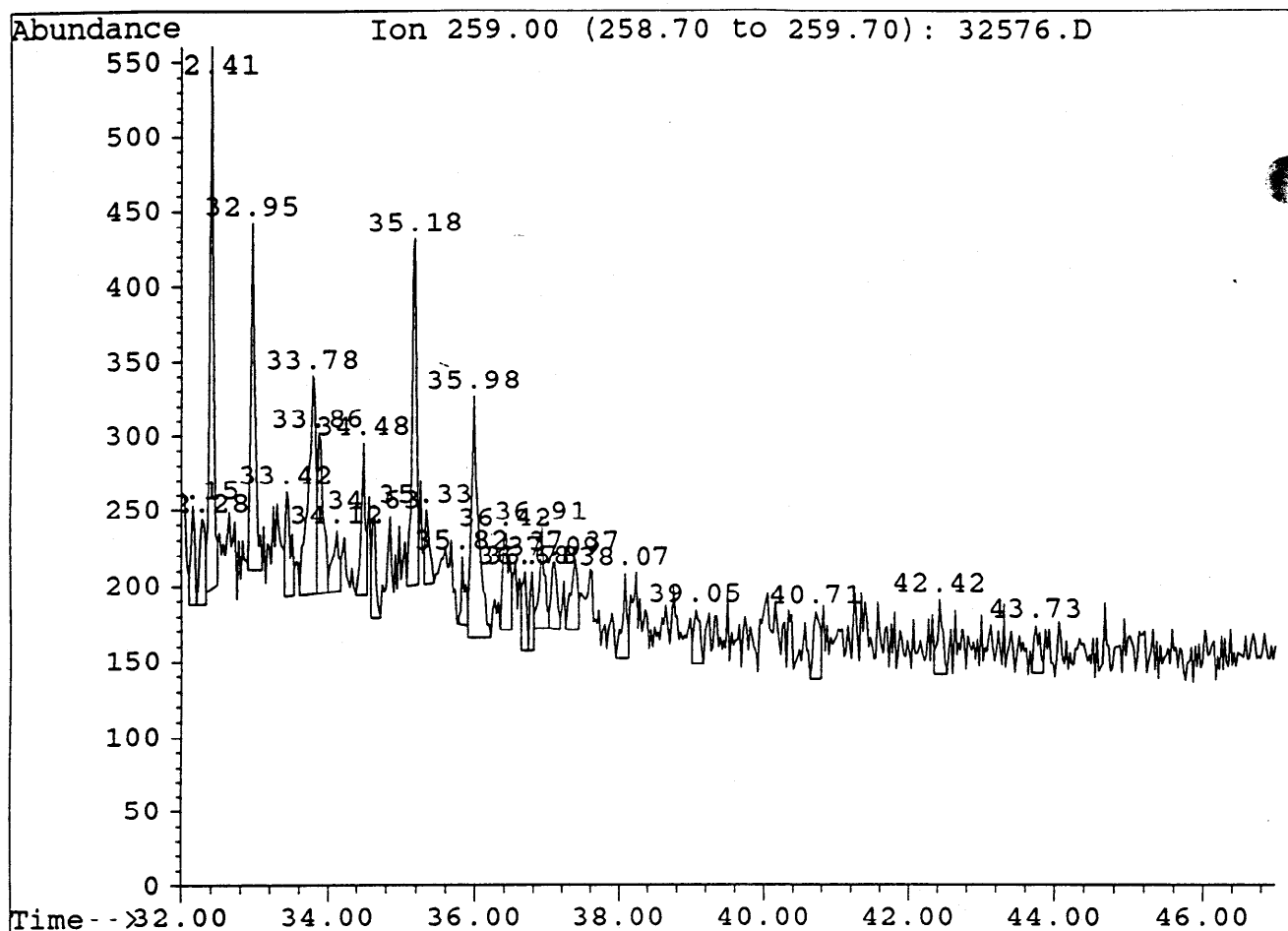
Sample : MINERVA-1 RFT

Peak	Ret.Time	Area	Height	Area %	Ratio %
1	32.41	2862	672	10.31	100.00
2	32.67	614	117	2.21	21.45
3	32.72	454	79	1.64	15.86
4	32.95	1368	412	4.93	47.80
5	33.06	457	133	1.65	15.97
6	33.42	482	114	1.74	16.84
7	33.70	640	157	2.30	22.36
8	34.07	752	155	2.71	26.28
9	34.22	924	167	3.33	32.29
10	34.56	1867	184	6.72	65.23
11	34.87	519	90	1.87	18.13
12	35.10	1267	241	4.56	44.27
13	35.15	2659	453	9.58	92.91
14	35.36	1383	293	4.98	48.32
15	35.85	1410	273	5.08	49.27
16	36.00	1837	230	6.62	64.19
17	36.42	674	159	2.43	23.55
18	37.06	466	97	1.68	16.28
19	37.37	836	206	3.01	29.21
20	37.50	446	157	1.61	15.58
21	38.05	877	96	3.16	30.64
22	38.67	1203	184	4.33	42.00
23	39.05	1214	206	4.37	42.42
24	39.21	1501	258	5.41	52.45
25	40.09	1054	152	3.80	36.83



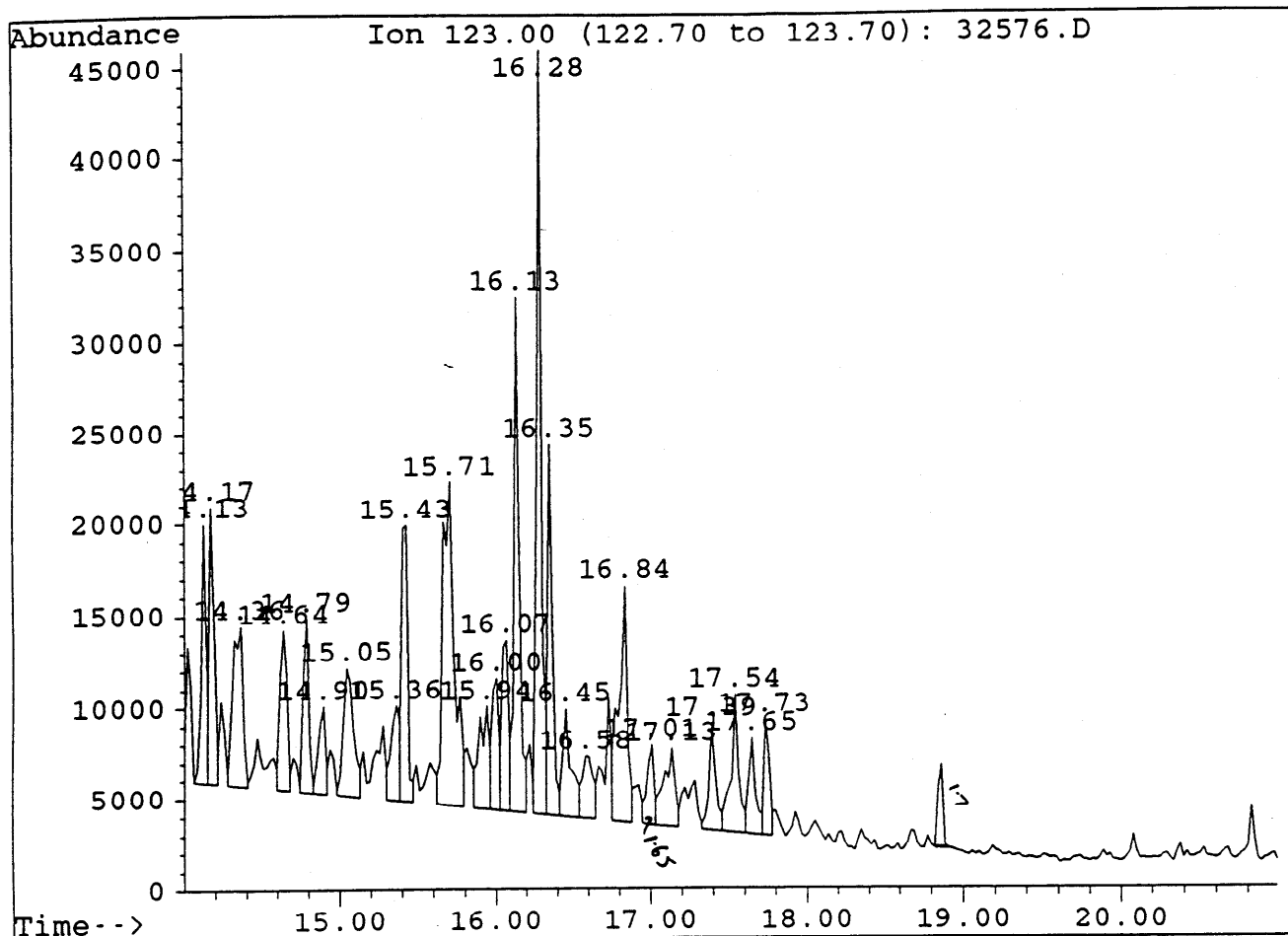
Sample : MINERVA-1 RFT

Peak	Ret.Time	Area	Height	Area %	Ratio %
1	32.41	781	192	3.86	32.47
2	32.95	505	112	2.49	21.00
3	33.73	431	72	2.13	17.92
4	33.81	384	95	1.90	15.97
5	34.07	1332	268	6.58	55.38
6	34.63	460	86	2.27	19.13
7	34.87	376	111	1.86	15.63
8	35.07	418	123	2.06	17.38
9	35.23	2405	579	11.87	100.00
10	35.36	1614	497	7.97	67.11
11	35.85	856	178	4.23	35.59
12	36.03	626	122	3.09	26.03
13	36.42	398	91	1.97	16.55
14	36.55	294	61	1.45	12.22
15	36.81	381	96	1.88	15.84
16	36.96	355	49	1.75	14.76
17	37.22	856	175	4.23	35.59
18	37.37	956	245	4.72	39.75
19	37.50	446	125	2.20	18.54
20	37.58	1073	172	5.30	44.62
21	38.07	504	77	2.49	20.96
22	38.67	843	131	4.16	35.05
23	39.05	1841	343	9.09	76.55
24	39.18	1755	393	8.67	72.97
25	40.81	363	72	1.79	15.09



Sample : MINERVA-1 RFT

Peak	Ret.Time	Area	Height	Area %	Ratio %
1	32.15	229	65	2.11	17.92
2	32.28	313	56	2.88	24.49
3	32.41	1278	363	11.75	100.00
4	32.95	860	232	7.91	67.29
5	33.42	335	70	3.08	26.21
6	33.78	1071	146	9.85	83.80
7	33.86	544	105	5.00	42.57
8	34.12	260	39	2.39	20.34
9	34.48	414	102	3.81	32.39
10	34.63	252	67	2.32	19.72
11	35.18	1040	231	9.56	81.38
12	35.33	186	48	1.71	14.55
13	35.82	173	44	1.59	13.54
14	35.98	1046	161	9.62	81.85
15	36.42	428	63	3.94	33.49
16	36.68	190	52	1.75	14.87
17	36.78	176	52	1.62	13.77
18	36.91	328	66	3.02	25.67
19	37.09	243	43	2.23	19.01
20	37.37	310	47	2.85	24.26
21	38.07	268	56	2.46	20.97
22	39.05	200	36	1.84	15.6
23	40.71	300	45	2.76	23.47
24	42.42	251	50	2.31	19.64
25	43.73	181	32	1.66	14.16

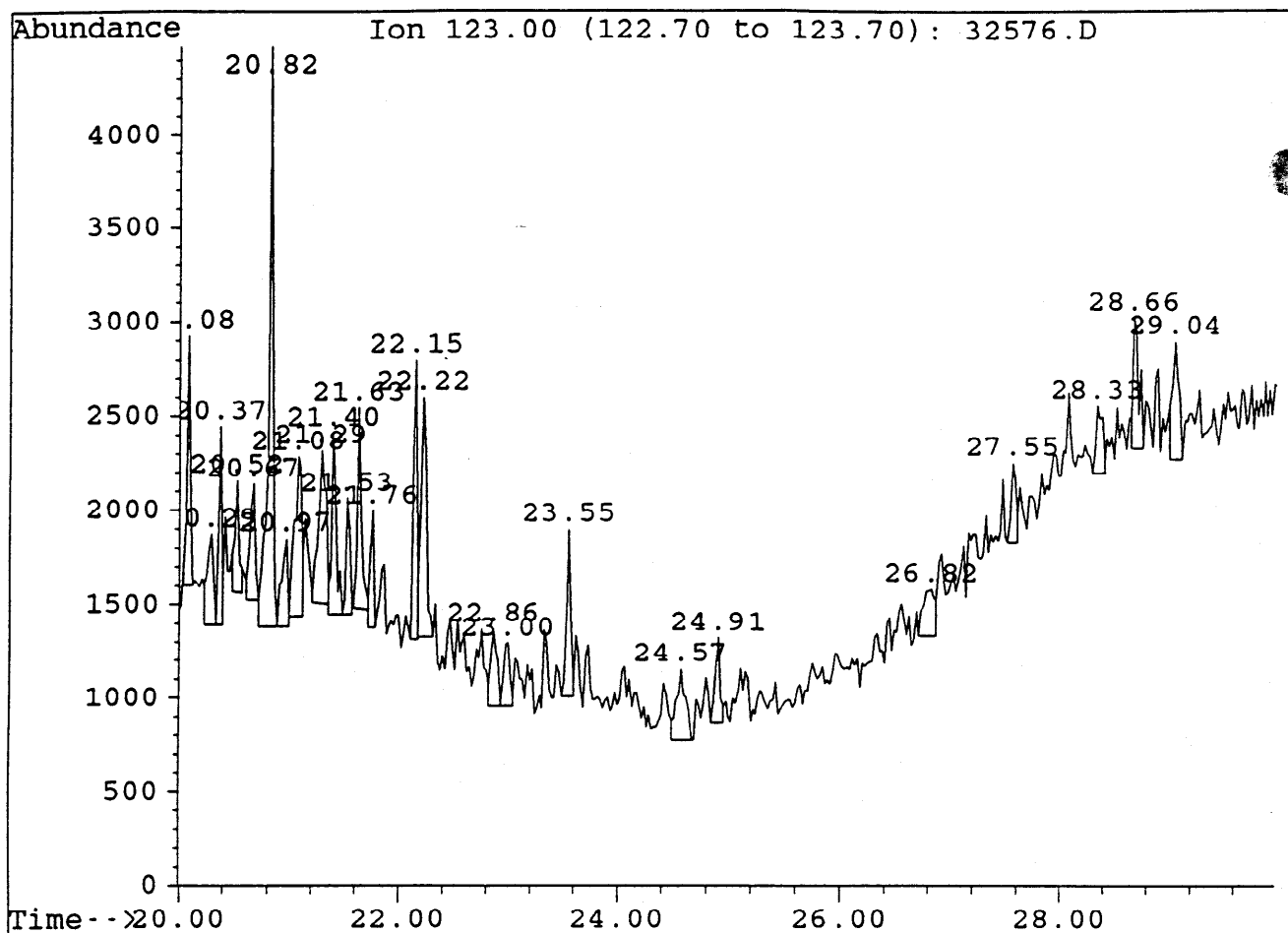


Sample : MINERVA-1 RFT

Peak	Ret.Time	Area	Height	Area %	Ratio %
1	14.13	30142	14054	3.61	32.73
2	14.17	31929	15069	3.83	34.67
3	14.36	39618	8697	4.75	43.02
4	14.64	28437	8731	3.41	30.88
5	14.79	24115	9493	2.89	26.18
6	14.90	15294	4785	1.83	16.61
7	15.05	33453	7018	4.01	36.32
8	15.36	20759	5182	2.49	22.54
9	15.43	41393	15062	4.96	44.94
10	15.71	91870	17640	11.01	99.75
11	15.94	25439	5605	3.05	27.62
12	16.00	21737	7212	2.60	23.60
13	16.07	28333	9325	3.40	30.76
14	16.13	68250	28146	8.18	74.11
15	16.28	92099	41848	11.04	100.00
16	16.35	41779	20296	5.01	45.36
17	16.45	23555	5923	2.82	25.58
18	16.58	17002	3432	2.04	18.46
19	16.84	49068	<u>12882 R<sub>1</sub></u>	5.88	53.28
20	17.01	13469	4368	1.61	14.62
21	17.13	21788	4308	2.61	23.66
22	17.39	17135	<u>5880 R<sub>2</sub></u>	2.05	18.60
23	17.54	26070	<u>7588 D</u>	3.12	28.31
24	17.65	16265	5296	1.95	17.66
25	17.73	15449	6387	1.85	16.77

HO  

$$= \frac{1.7}{1.65} \times 4368$$



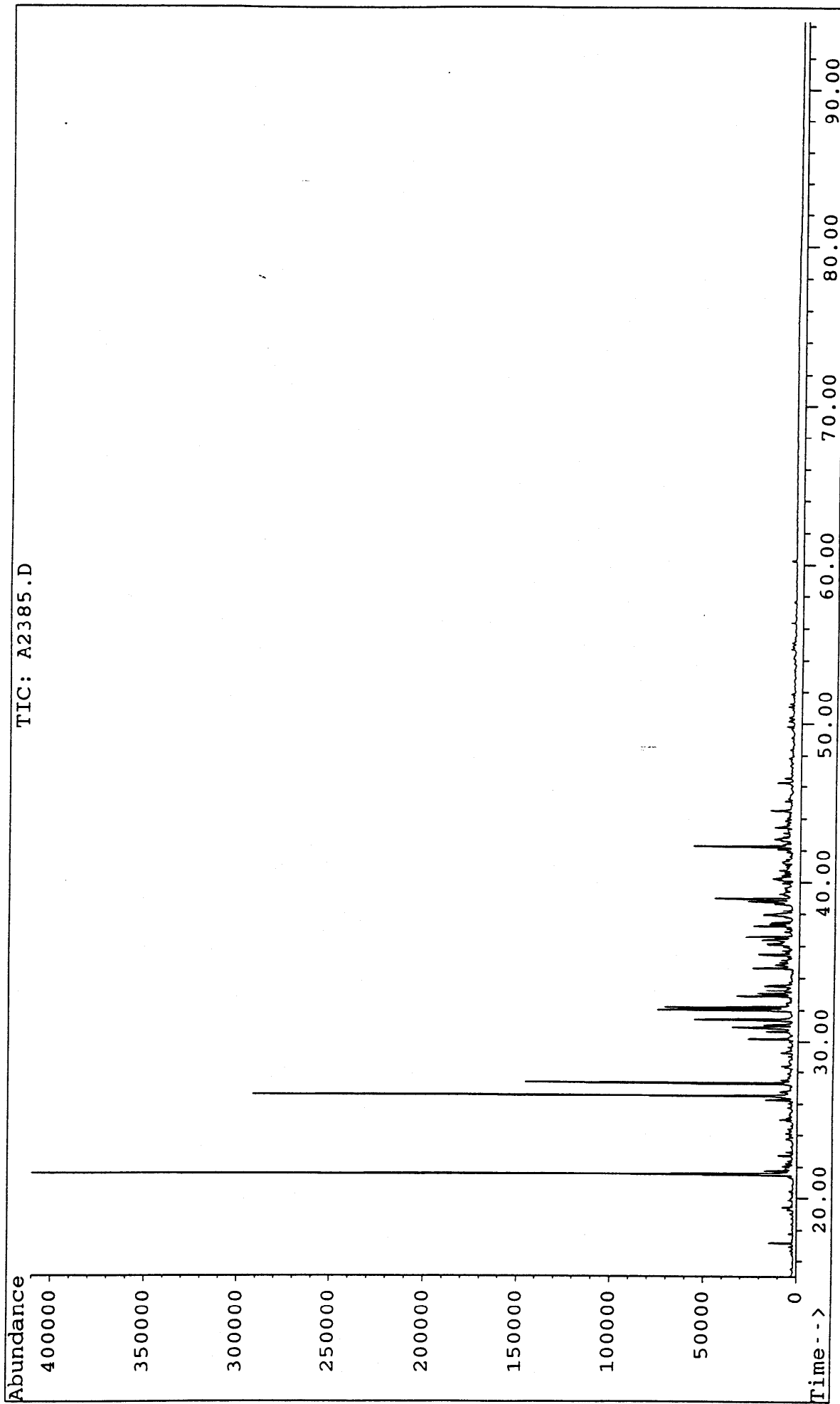
Sample : MINERVA-1 RFT

Peak	Ret.Time	Area	Height	Area %	Ratio %
1	20.08	2708	1328	4.21	31.18
2	20.29	1788	481	2.78	20.58
3	20.37	2346	1054	3.65	27.01
4	20.52	1520	596	2.37	17.50
5	20.67	1939	618	3.02	22.32
6	20.82	8686	3092	13.52	100.00
7	20.97	1753	467	2.73	20.18
8	21.08	4225	853	6.58	48.64
9	21.29	4047	811	6.30	46.59
10	21.40	2759	966	4.29	31.76
11	21.53	1561	618	2.43	17.97
12	21.63	2699	1068	4.20	31.07
13	21.76	1334	619	2.08	15.36
14	22.15	3721	1490	5.79	42.84
15	22.22	4259	1281	6.63	49.03
16	22.86	1632	419	2.54	18.79
17	23.00	1389	342	2.16	15.99
18	23.55	2552	896	3.97	29.38
19	24.57	2077	377	3.23	23.91
20	24.91	1466	454	2.28	16.88
21	26.82	1914	252	2.98	22.04
22	27.55	1380	423	2.15	15.8
23	28.33	1505	362	2.34	17.33
24	28.66	2582	697	4.02	29.73
25	29.04	2408	631	3.75	27.72

**APPENDIX 4**

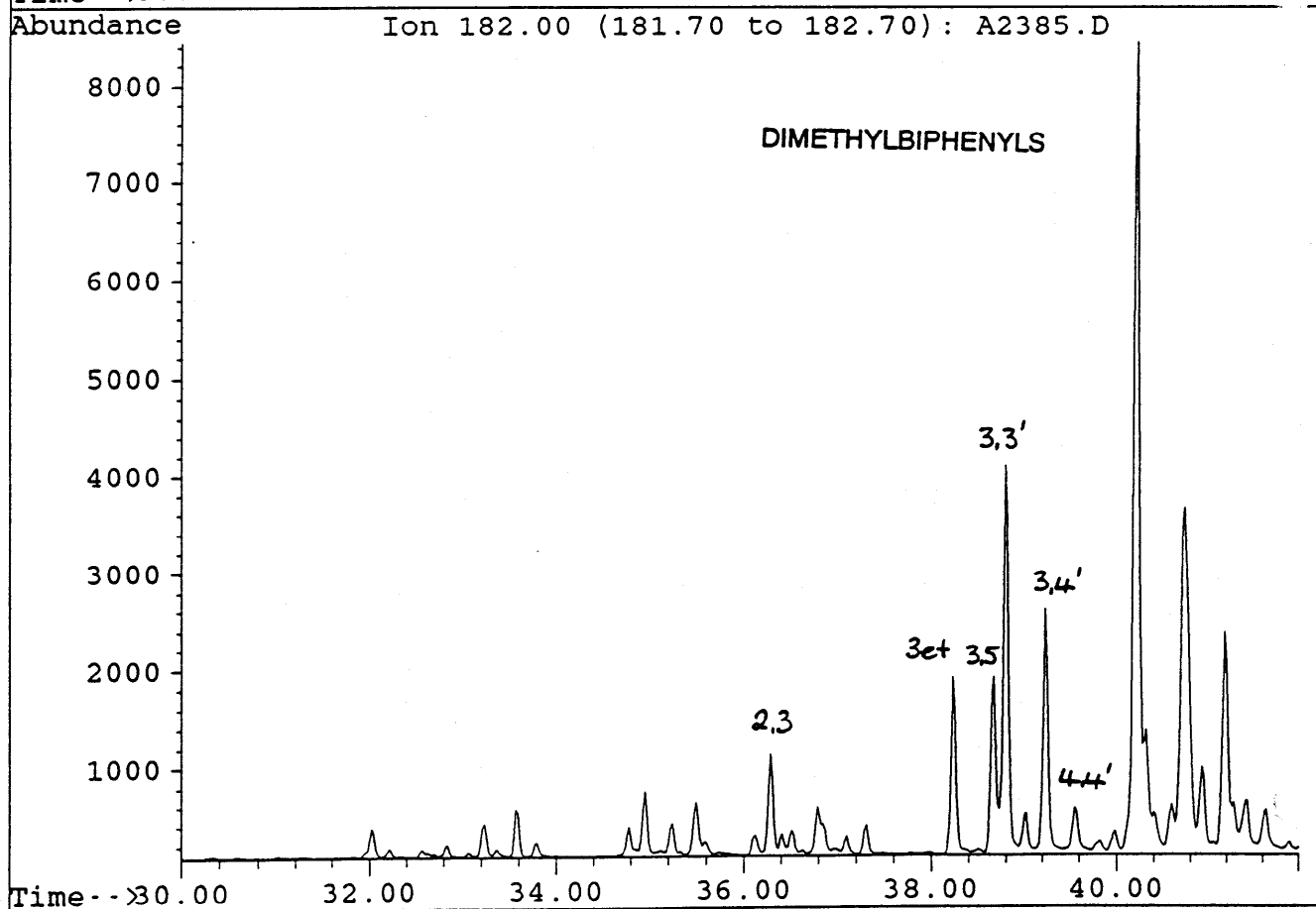
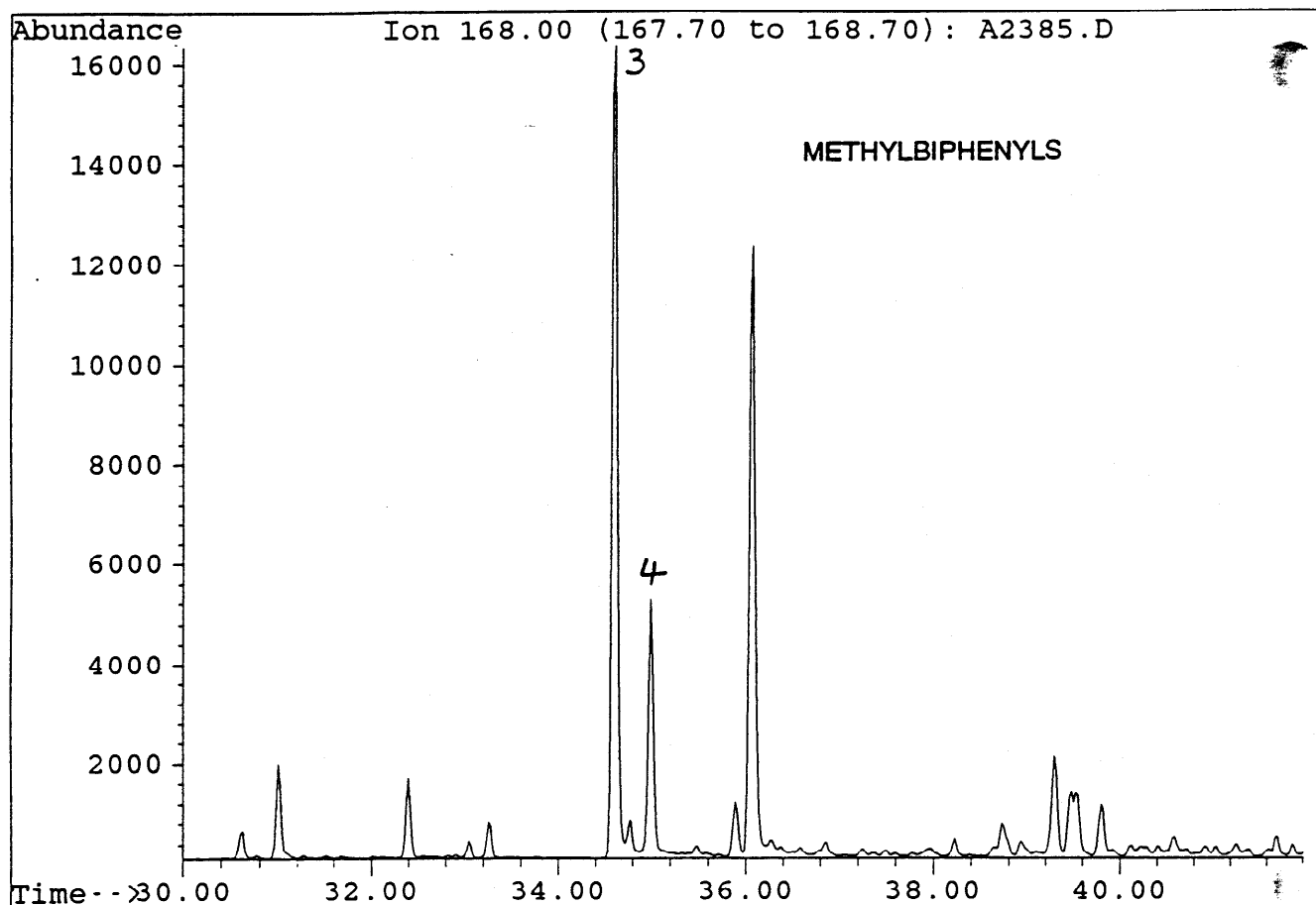
**SIR GC-MS (AROMS) MASS FRAGMENTOGRAMS : 1649.8m WATER-EXTRACT**

File A2385.D  
Sample : MINERVA-1, RFT 14/3/94. AROS  
Misc. Info : COL#155. 16-3-94. SB

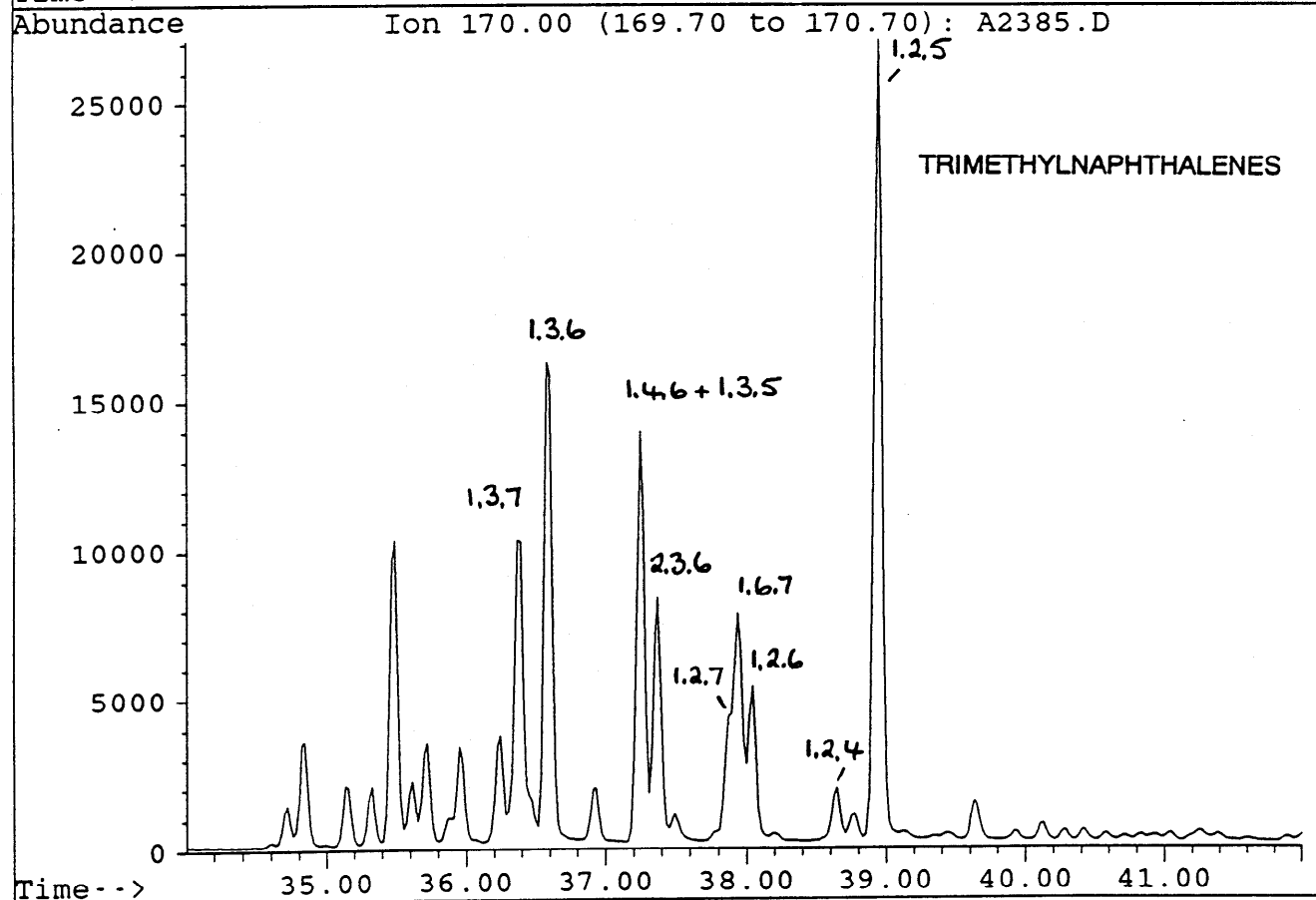
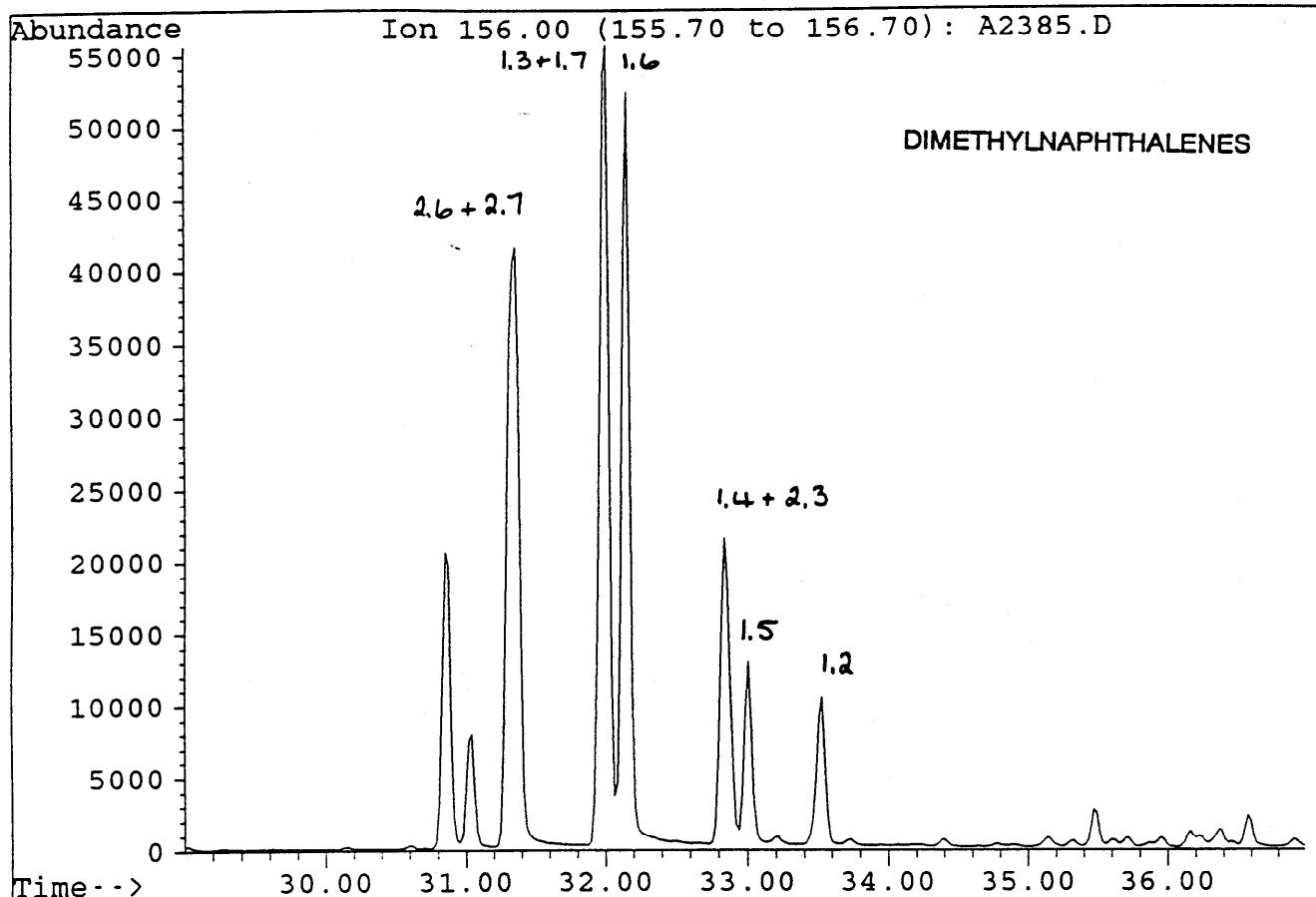




File : A2385.D  
Sample : MINERVA-1, RFT 14/3/94. AROS  
Misc. Info : COL#155. 16-3-94. SB

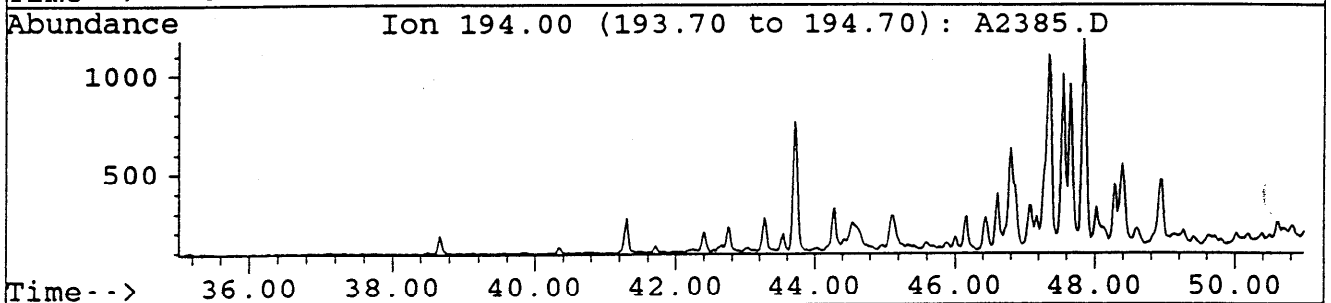
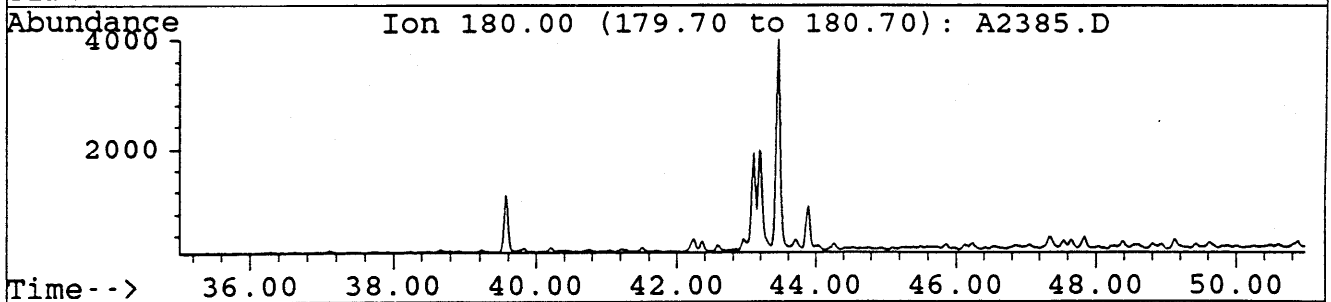
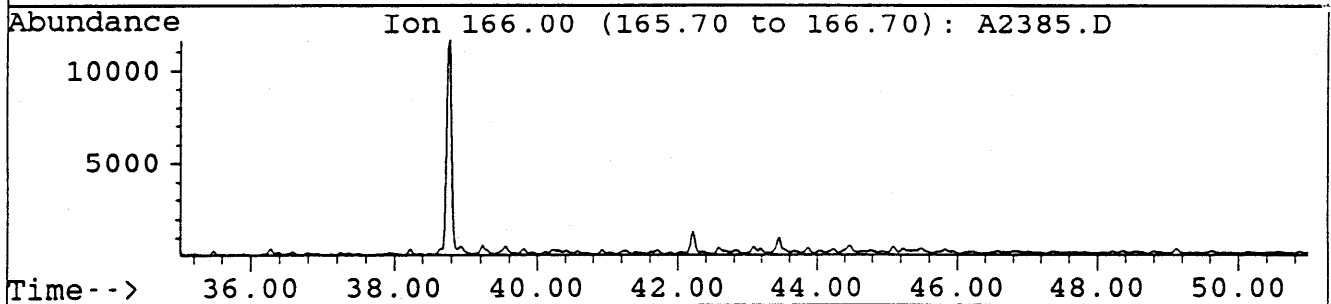
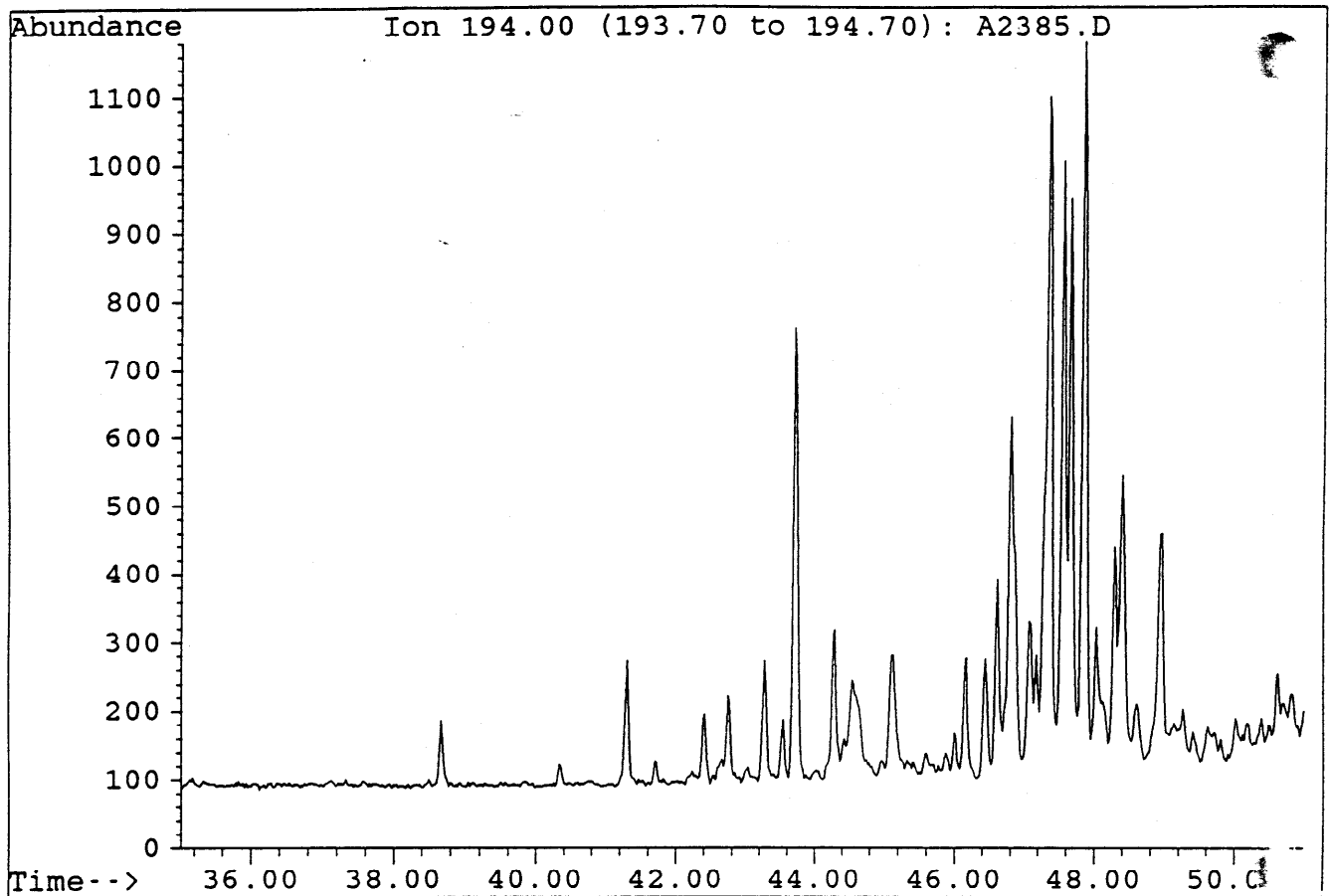


File : A2385.D  
Sample : MINERVA-1, RFT 14/3/94. AROS  
Misc. Info : COL#155. 16-3-94. SB

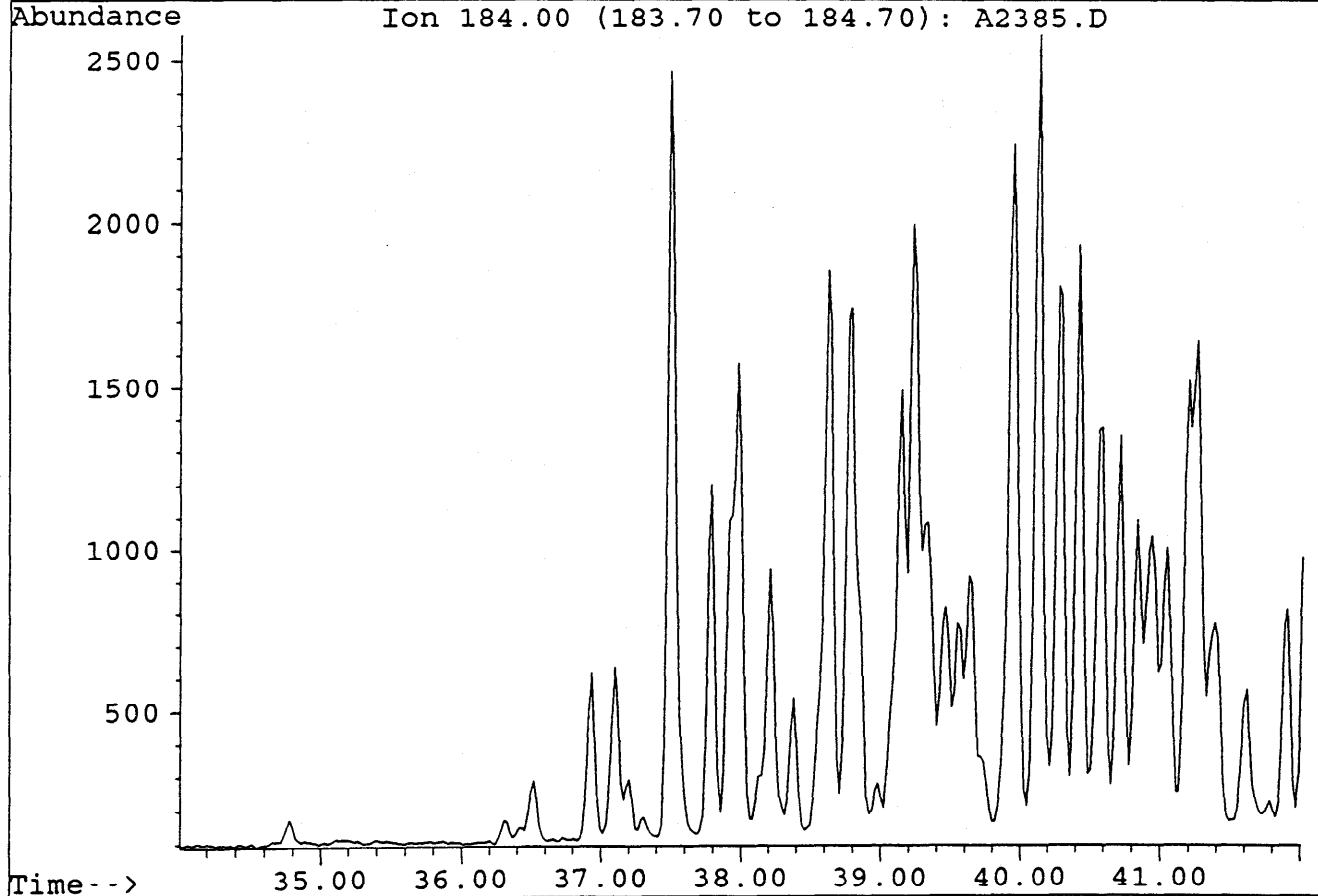
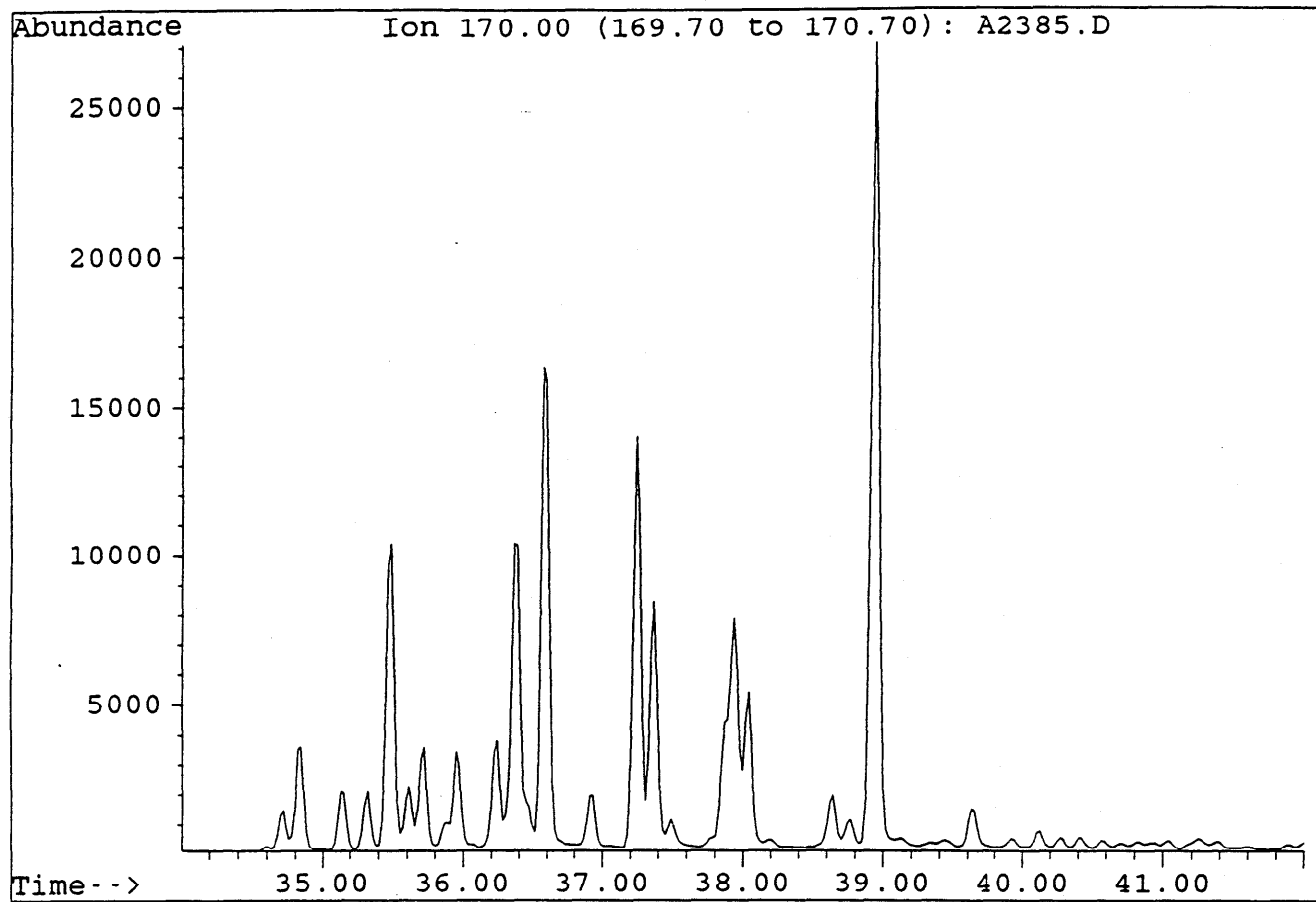


File : A2385.D  
Sample : MINERVA-1, RFT 14/3/94. AROS  
Misc. Info : COL#155. 16-3-94. SB

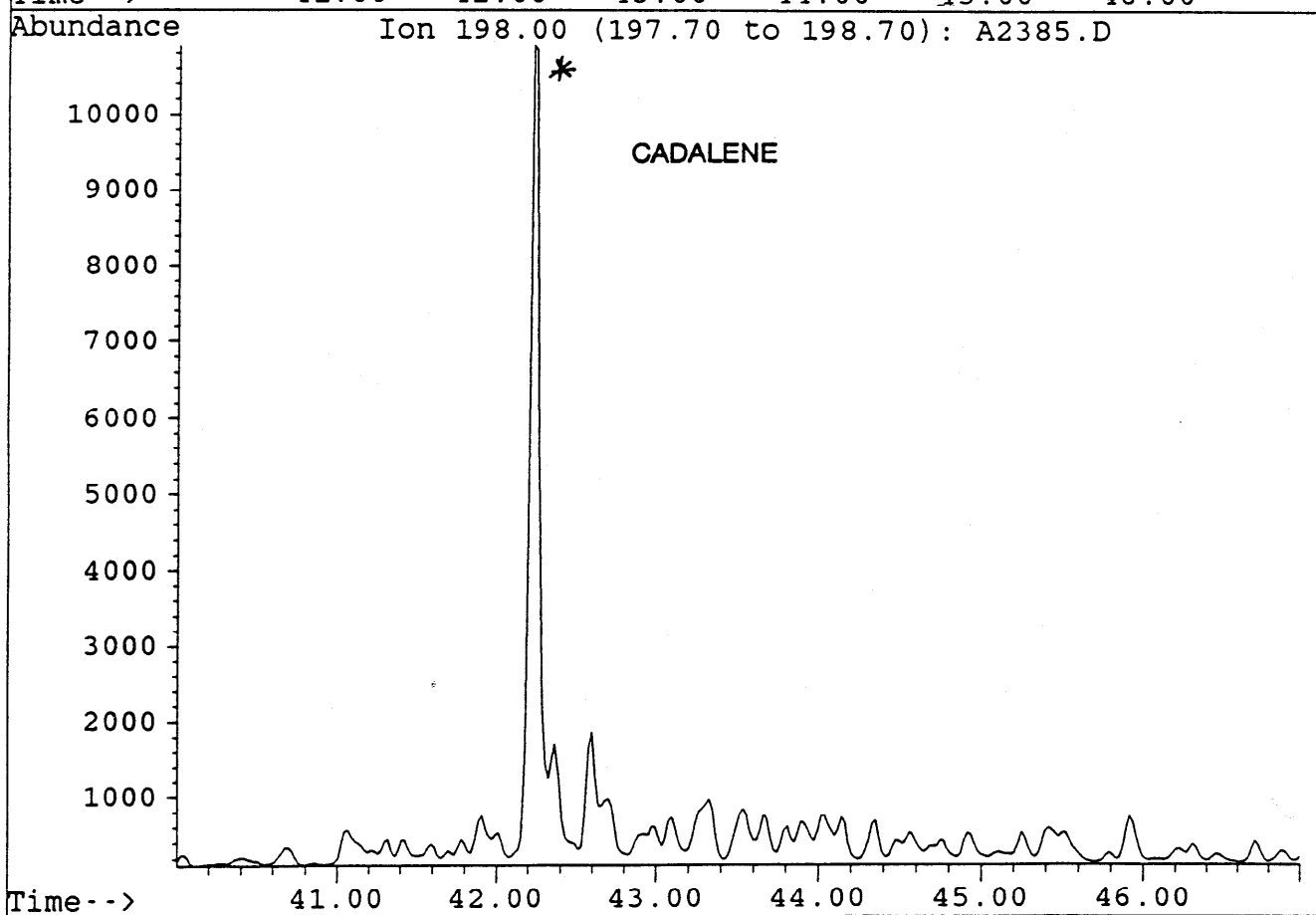
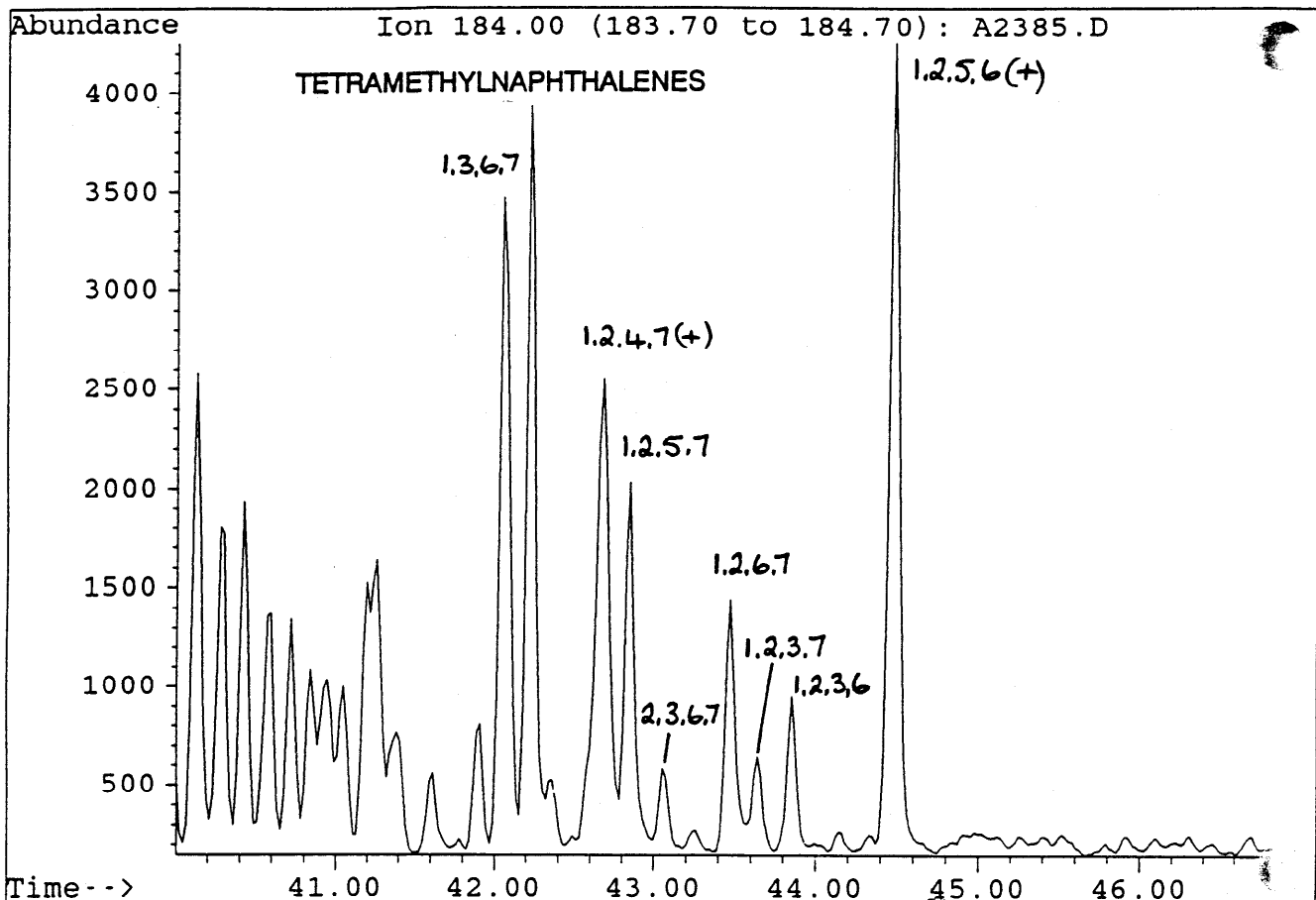
FLUORENES



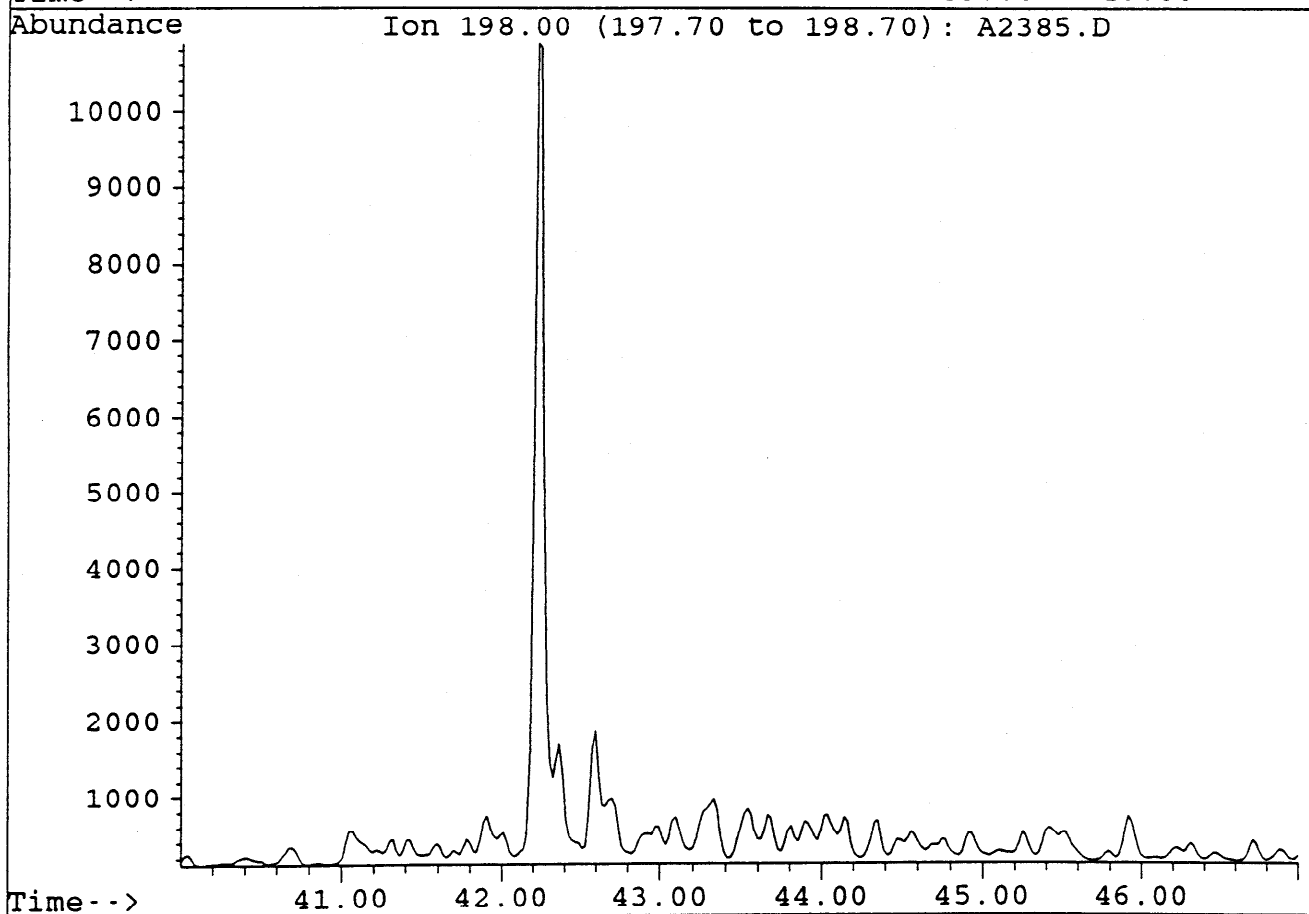
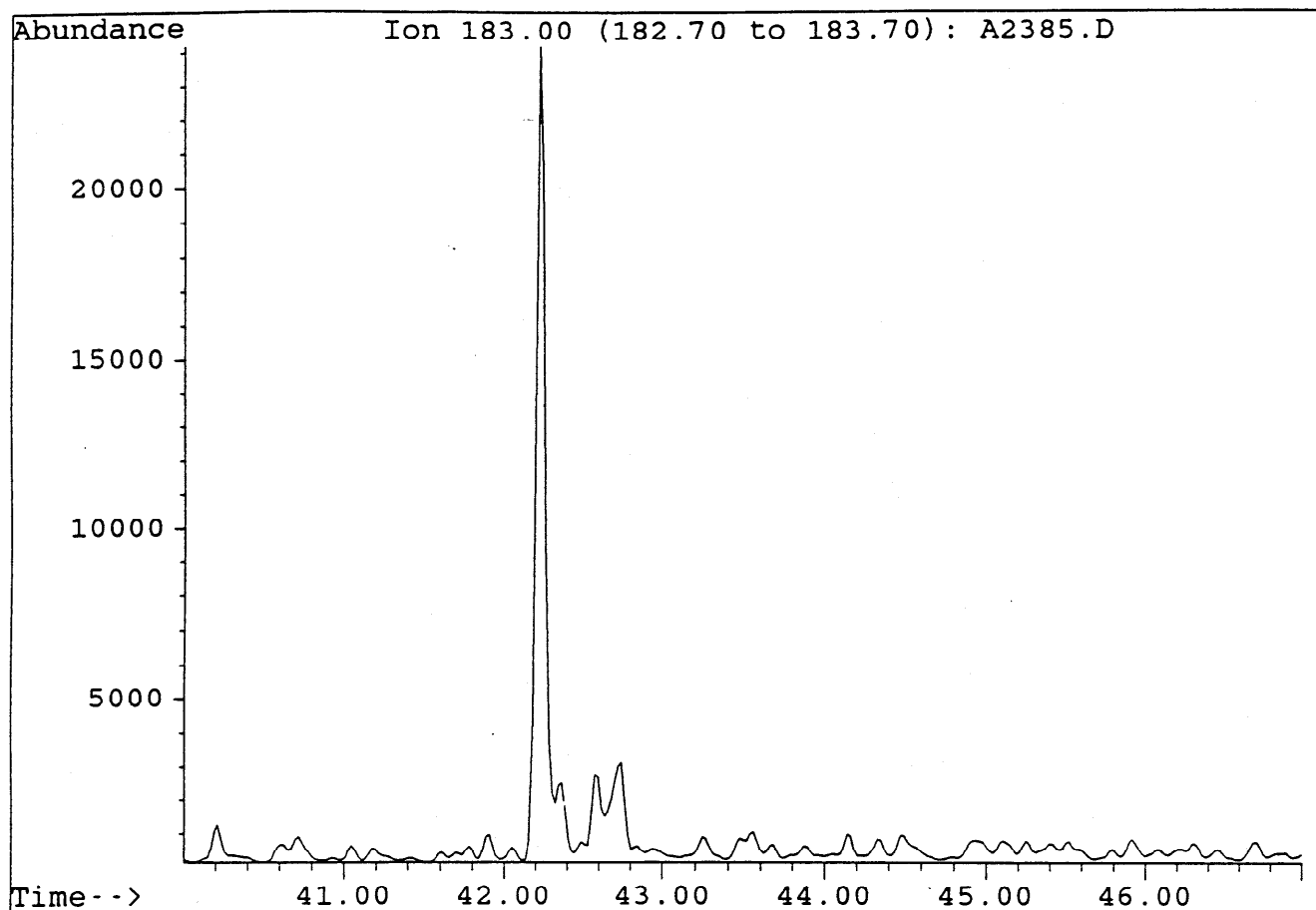
File : A2385.D  
Sample : MINERVA-1, RFT 14/3/94. AROS  
Misc. Info : COL#155. 16-3-94. SB



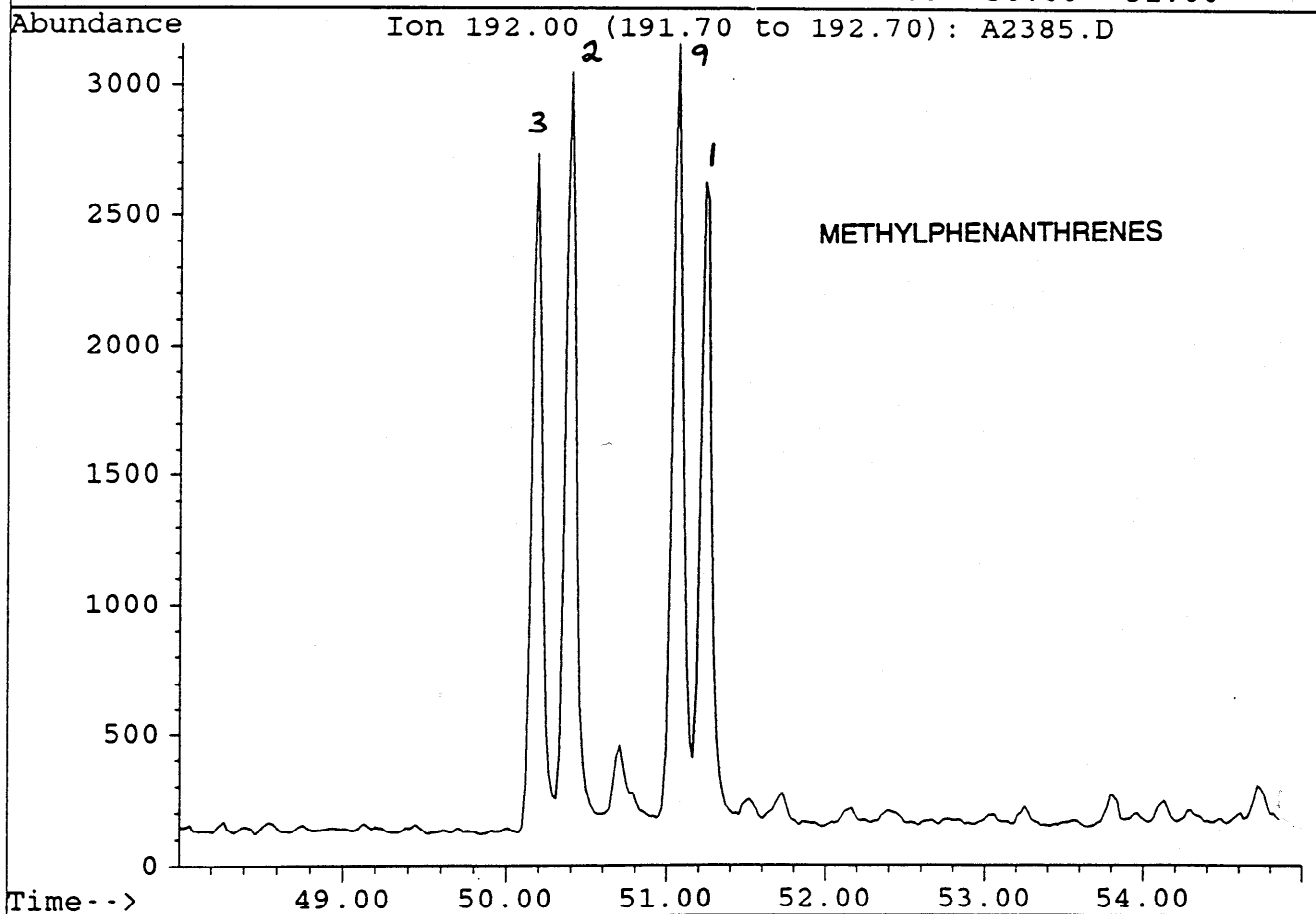
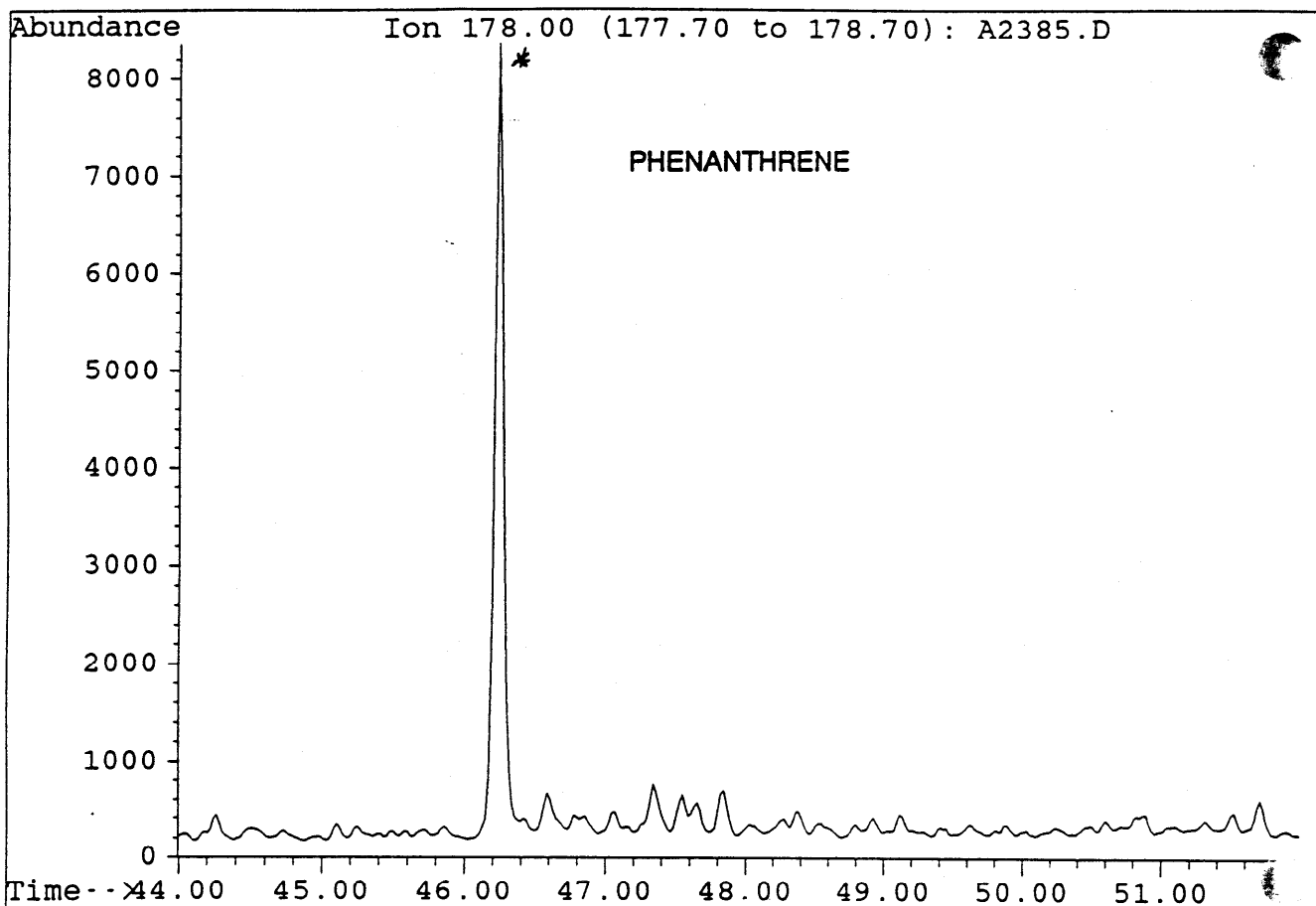
File : A2385.D  
Sample : MINERVA-1, RFT 14/3/94. AROS  
Misc. Info : COL#155. 16-3-94. SB



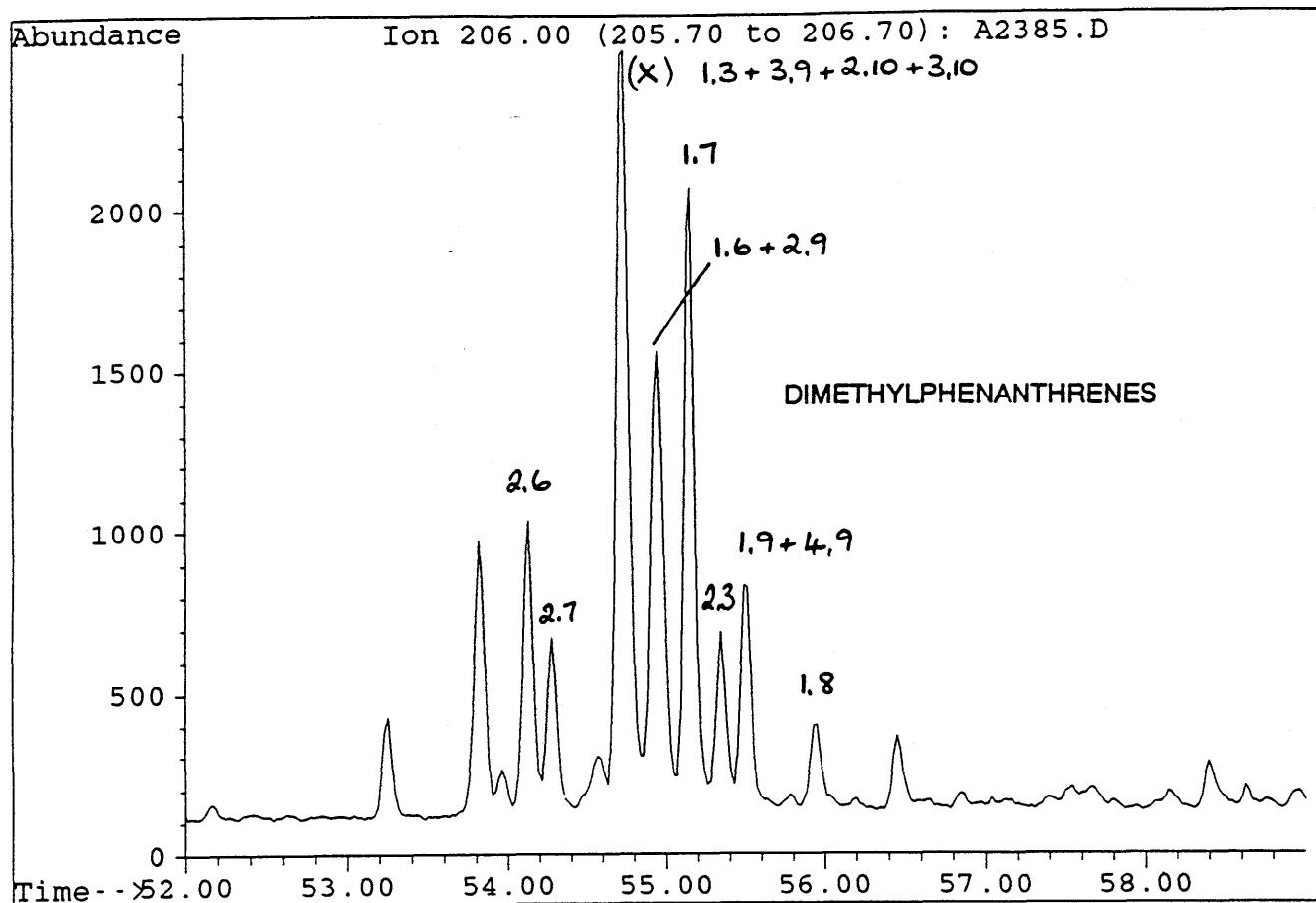
File : A2385.D  
Sample : MINERVA-1, RFT 14/3/94. AROS  
Misc. Info : COL#155. 16-3-94. SB



File : A2385.D  
Sample : MINERVA-1, RFT 14/3/94. AROS  
Misc. Info : COL#155. 16-3-94. SB

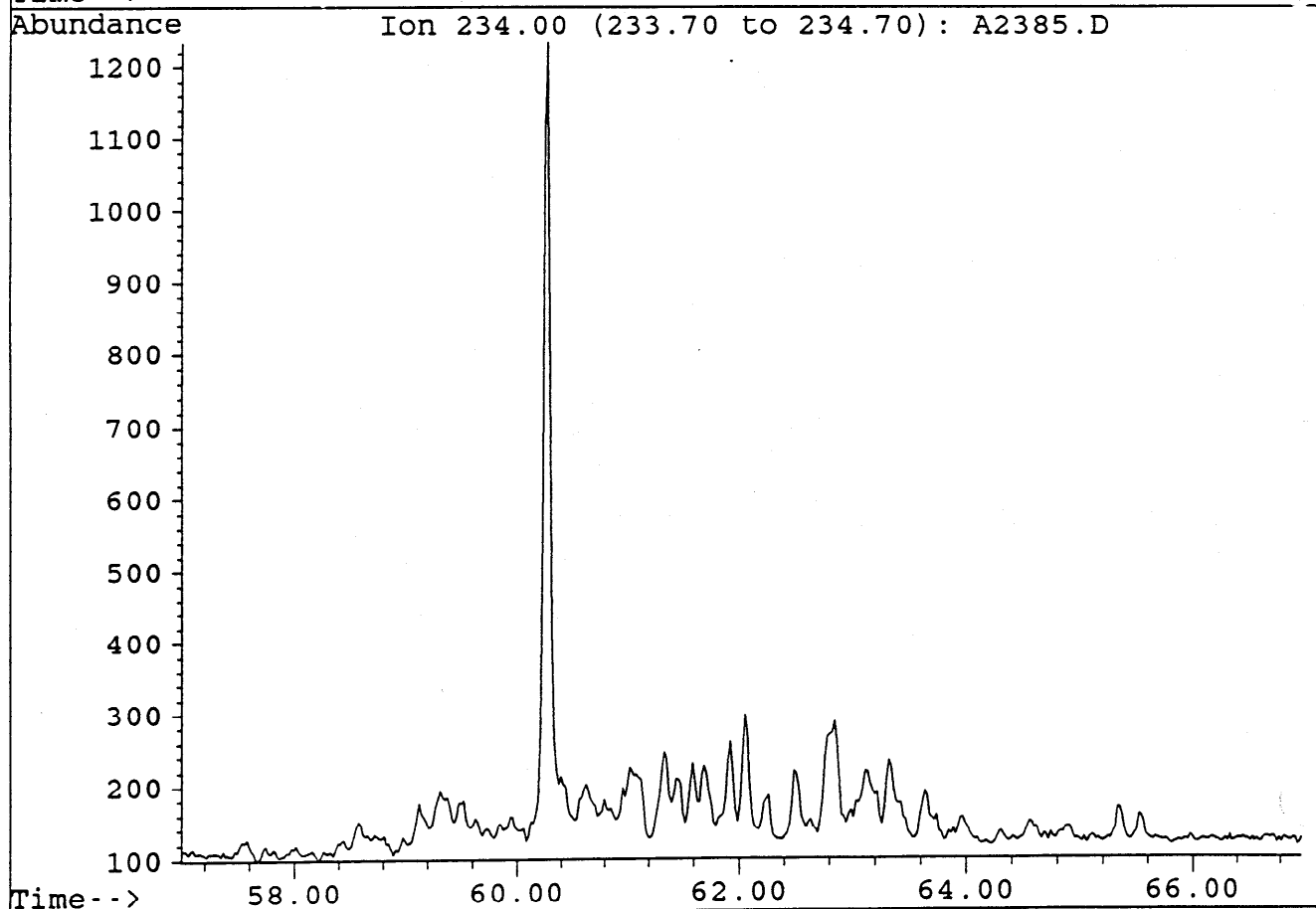
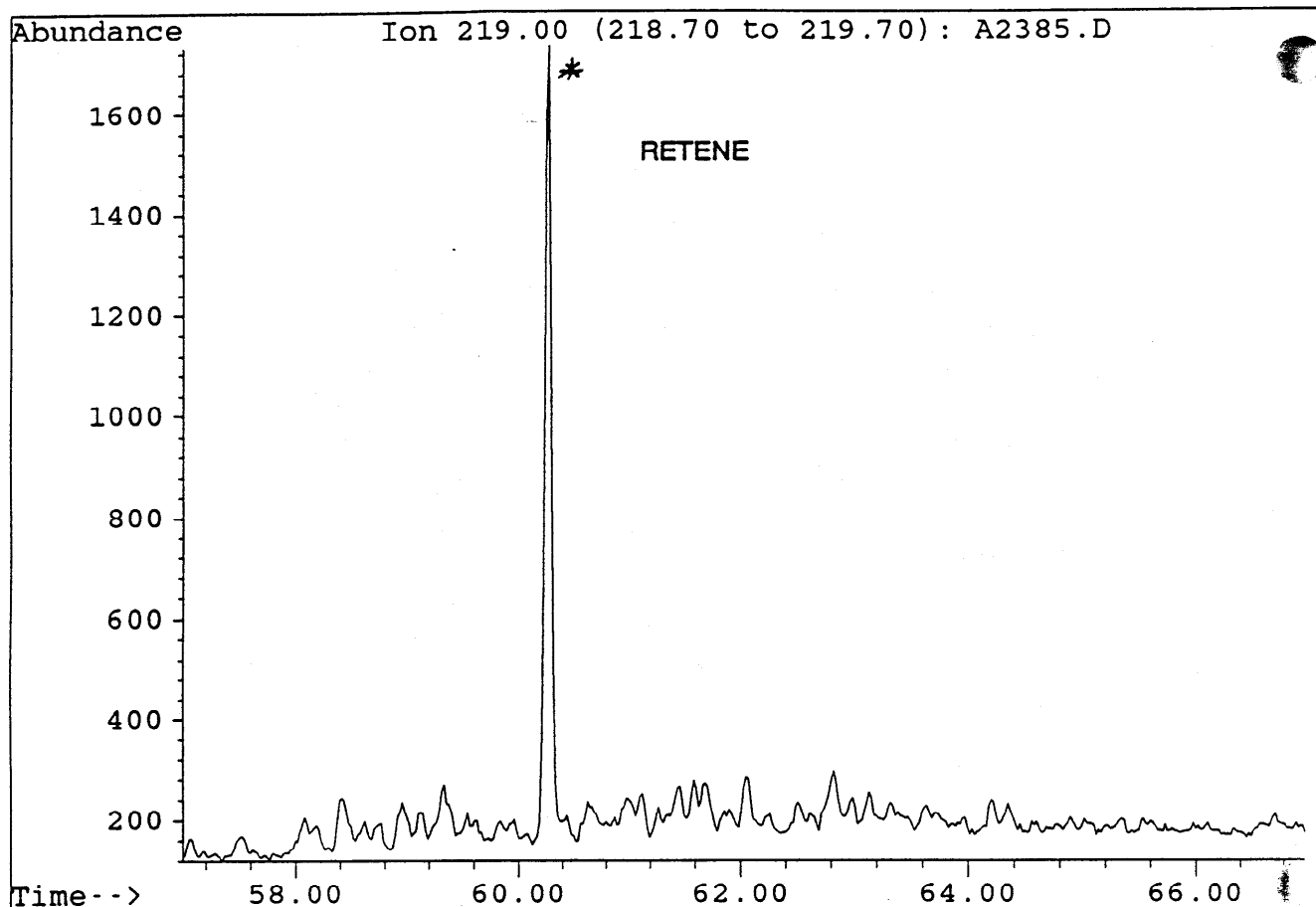


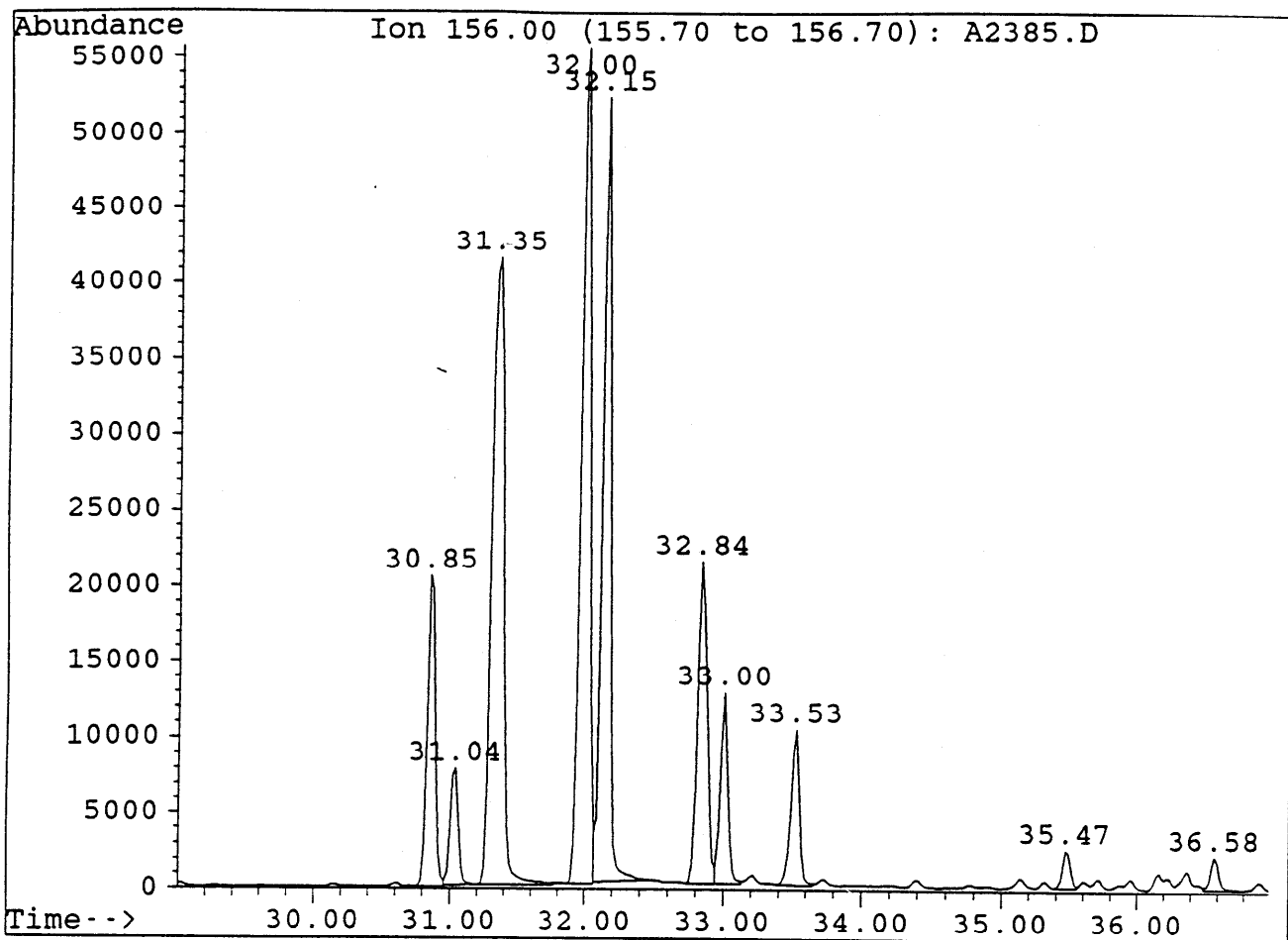
File : A2385.D  
Sample : MINERVA-1, RFT 14/3/94. AROS  
Misc. Info : COL#155. 16-3-94. SB





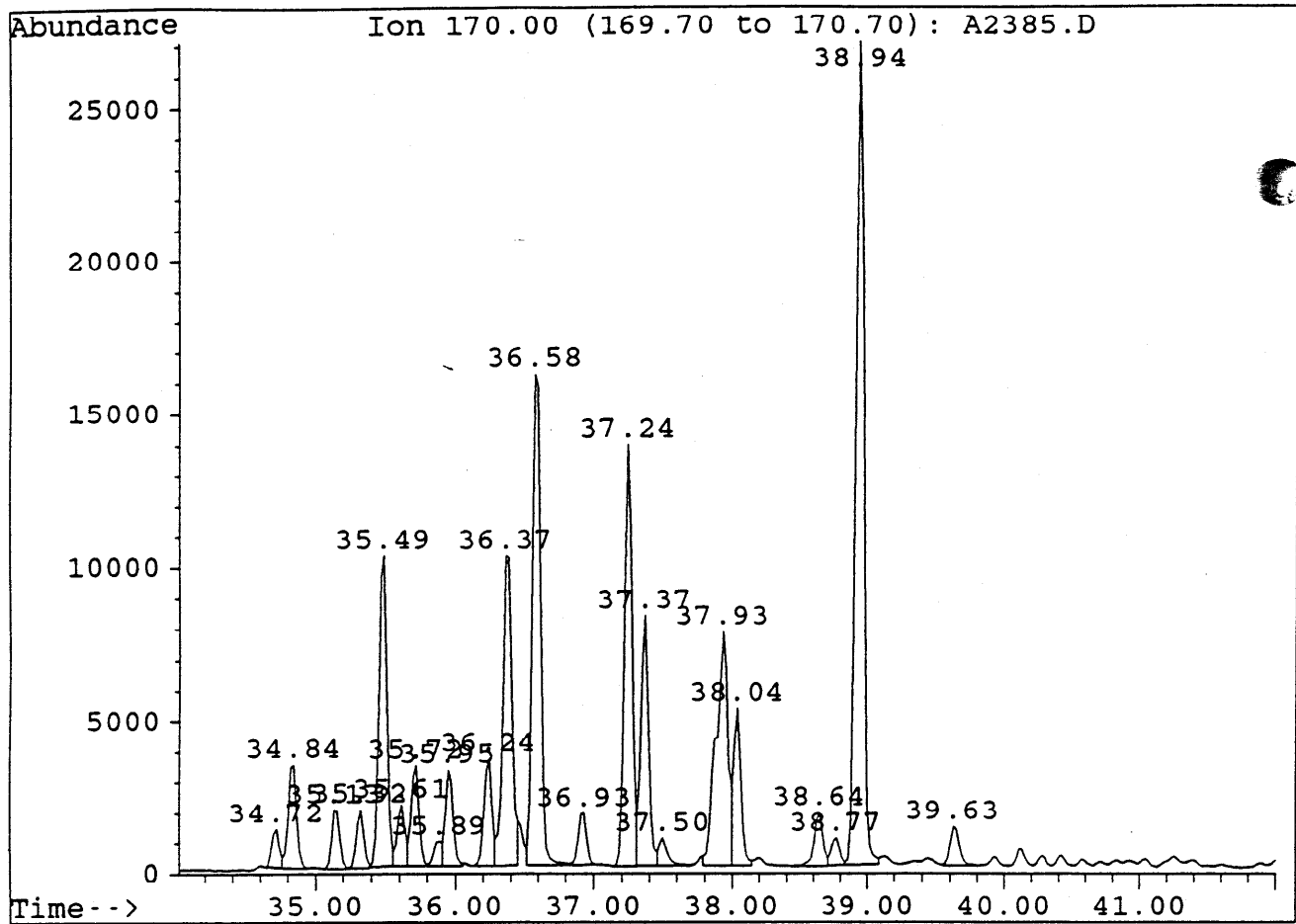
File : A2385.D  
Sample : MINERVA-1, RFT 14/3/94. AROS  
Misc. Info : COL#155. 16-3-94. SB





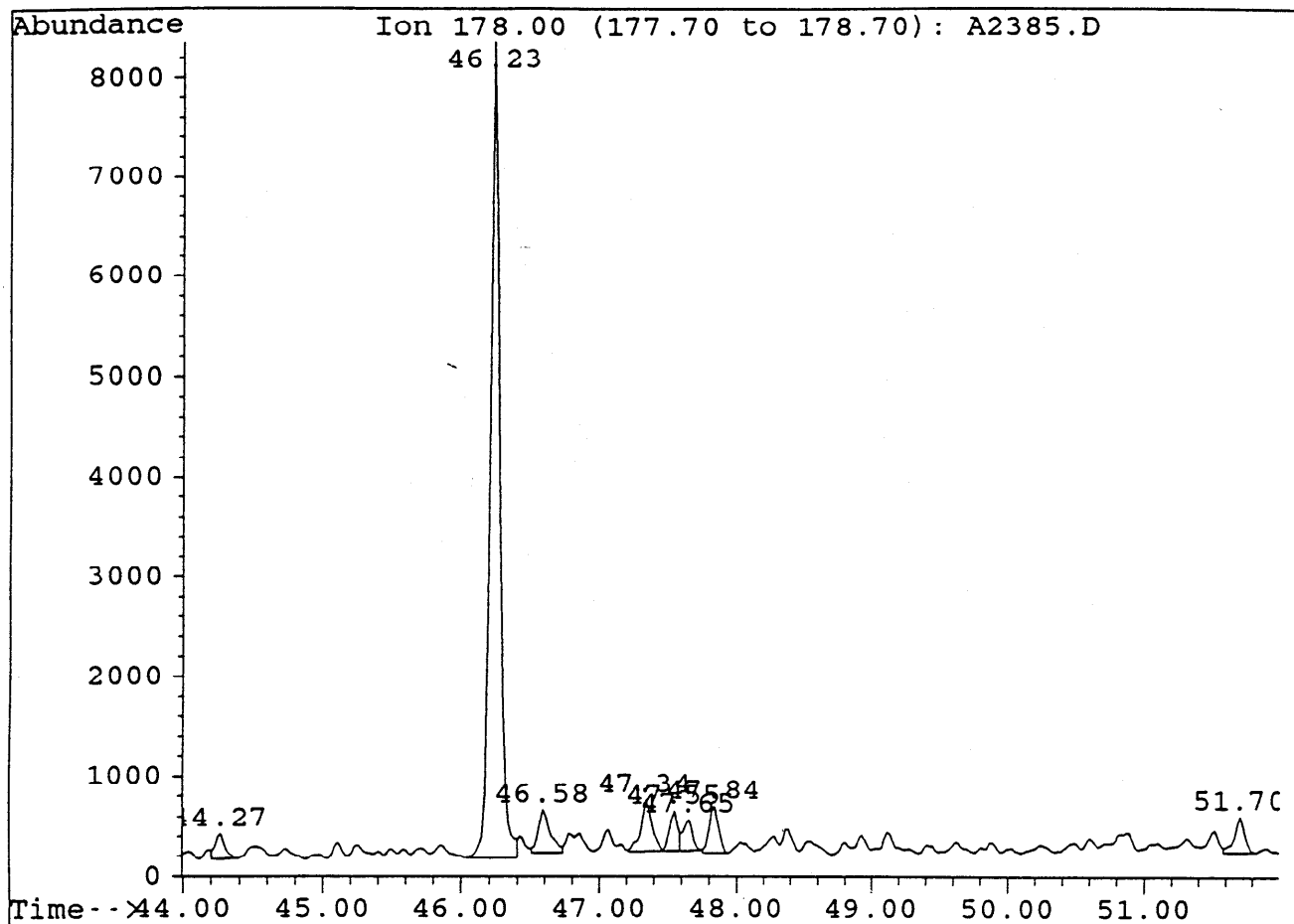
Sample : MINERVA-1, RFT 14/3/94. AROS

Peak	Ret.Time	Area	Height	Area %	Ratio %
1	30.85	83417	20525	7.94	31.92
2	31.04	31630	7786	3.01	12.10
3	31.35	<u>256121</u> 26+	41431	24.38	98.00
4	32.00	261356 -	55371	24.88	100.00
5	32.15	<u>205160</u> 16	51944	19.53	78.50
6	32.84	<u>101189</u> 14+	21253	9.63	38.72
7	33.00	<u>48038</u> 15	12599	4.57	18.38
8	33.53	44756	10250	4.26	17.12
9	35.47	9858	2485	0.94	3.77
10	36.58	8999	2143	0.86	3.44



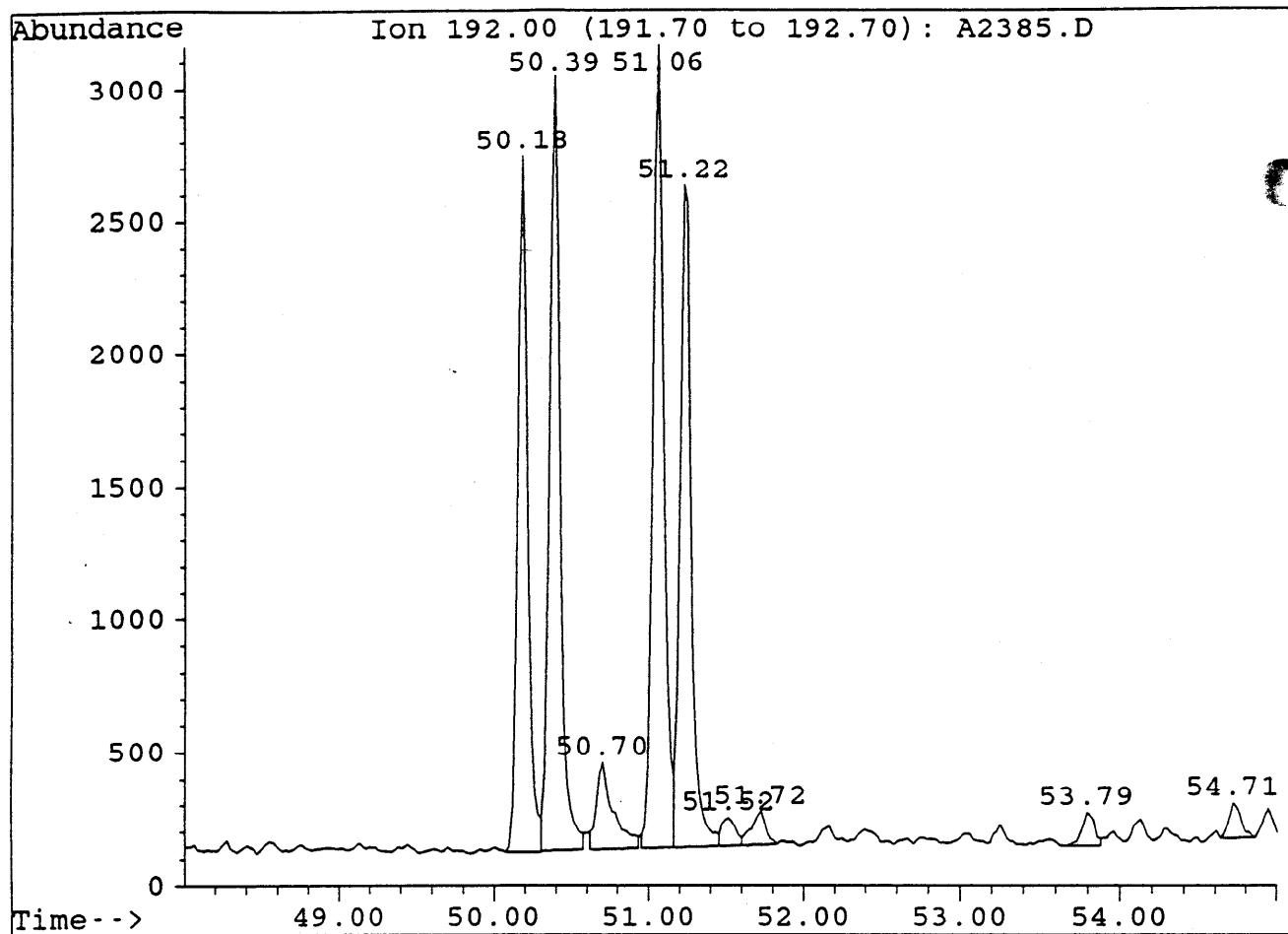
Sample : MINERVA-1, RFT 14/3/94. AROS

Peak	Ret.Time	Area	Height	Area %	Ratio %
1	34.72	4794	1274	0.91	4.39
2	34.84	13932	3408	2.63	12.76
3	35.13	7851	1942	1.48	7.19
4	35.32	7095	1942	1.34	6.50
5	35.49	40537	10165	7.66	37.14
6	35.61	7897	2033	1.49	7.24
7	35.72	12744	3327	2.41	11.68
8	35.89	3654	806	0.69	3.35
9	35.95	11695	3165	2.21	10.72
10	36.24	14598	3557	2.76	13.37
11	36.37	<u>46790</u> 137	10112	8.84	42.87
12	36.58	<u>67221</u> 136	16048	12.70	61.59
13	36.93	7166	1706	1.35	6.57
14	37.24	<u>53799</u> 146*	13779	10.17	49.29
15	37.37	<u>32154</u> 236	8173	6.08	29.46
16	37.50	3679	907	0.70	3.37
17	37.93	48506	7629	9.17	44.44
18	38.04	18053	5137	3.41	16.54
19	38.64	8036	1764	1.52	7.36
20	38.77	3812	903	0.72	3.49
21	38.94	<u>109144</u> 125	26865	20.63	100.00
22	39.63	6022	1300	1.14	5



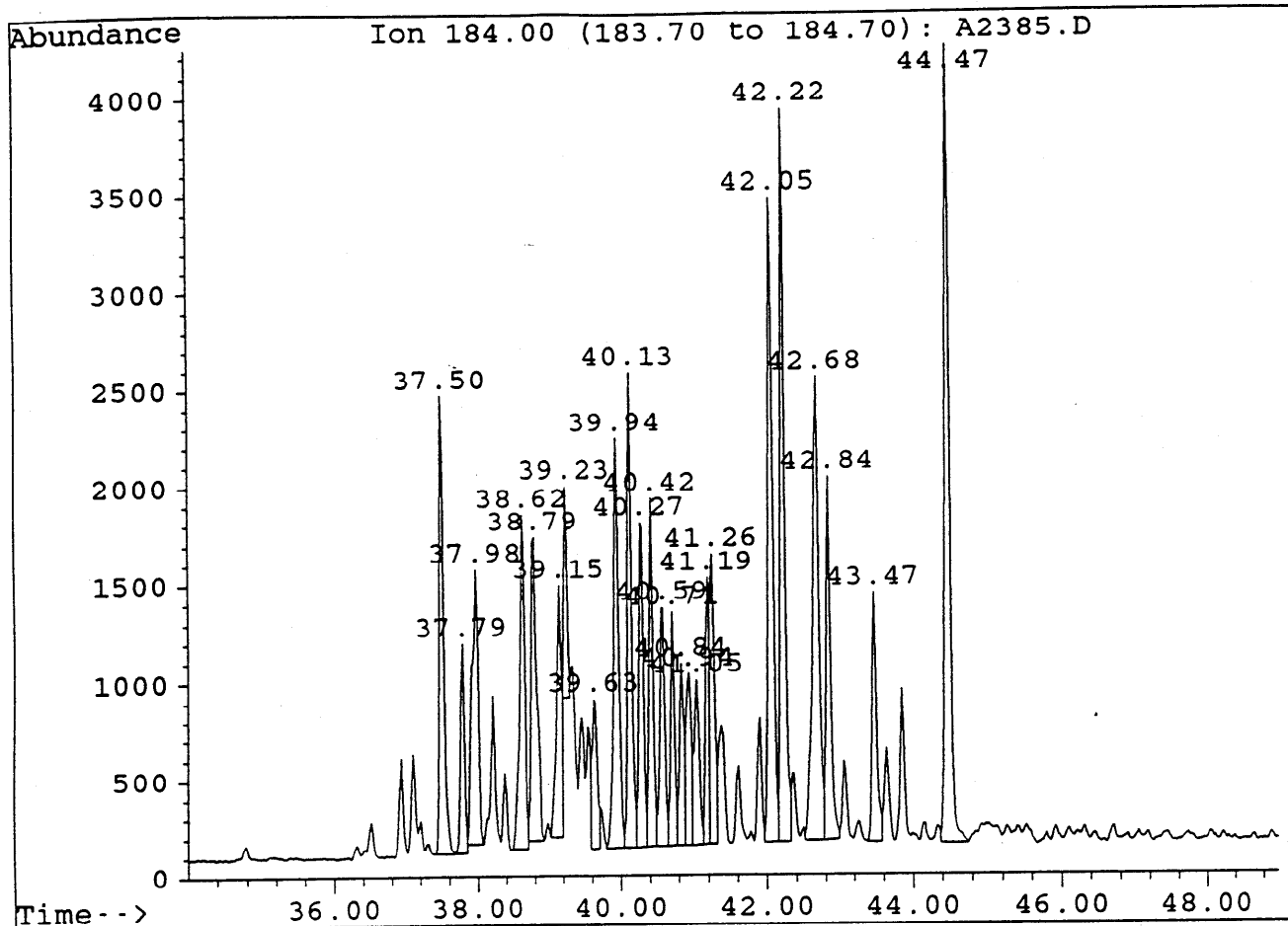
Sample : MINERVA-1, RFT 14/3/94. AROS

Peak	Ret.Time	Area	Height	Area %	Ratio %
1	44.27	1169	258	2.21	3.03
2	46.23	<u>38619</u> <i>p</i>	8175	73.17	100.00
3	46.58	2652	434	5.02	6.87
4	47.34	2907	520	5.51	7.53
5	47.55	1757	402	3.33	4.55
6	47.65	1466	318	2.78	3.80
7	47.84	2262	473	4.29	5.86
8	51.70	1947	369	3.69	5.04



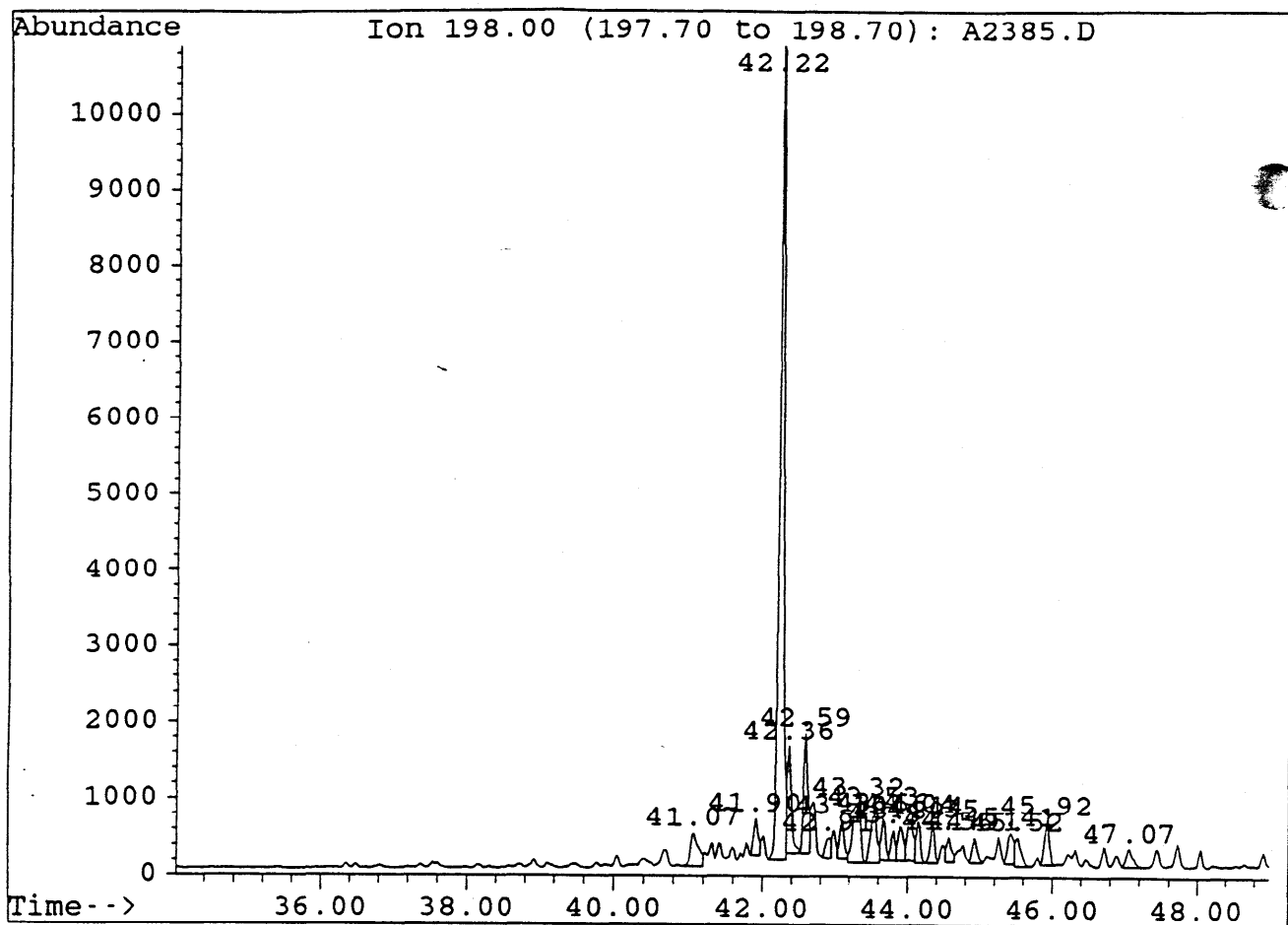
Sample : MINERVA-1, RFT 14/3/94. AROS

Peak	Ret.Time	Area	Height	Area %	Ratio %
1	50.18	<u>11978</u> 3	2616	20.41	81.06
2	50.39	<u>13937</u> 2	2918	23.74	94.32
3	50.70	2469	325	4.21	16.71
4	51.06	<u>14777</u> 9	3020	25.17	100.00
5	51.22	<u>12728</u> 1	2483	21.68	86.13
6	51.52	628	103	1.07	4.25
7	51.72	793	124	1.35	5.37
8	53.79	671	124	1.14	4.54
9	54.71	720	132	1.23	4.87



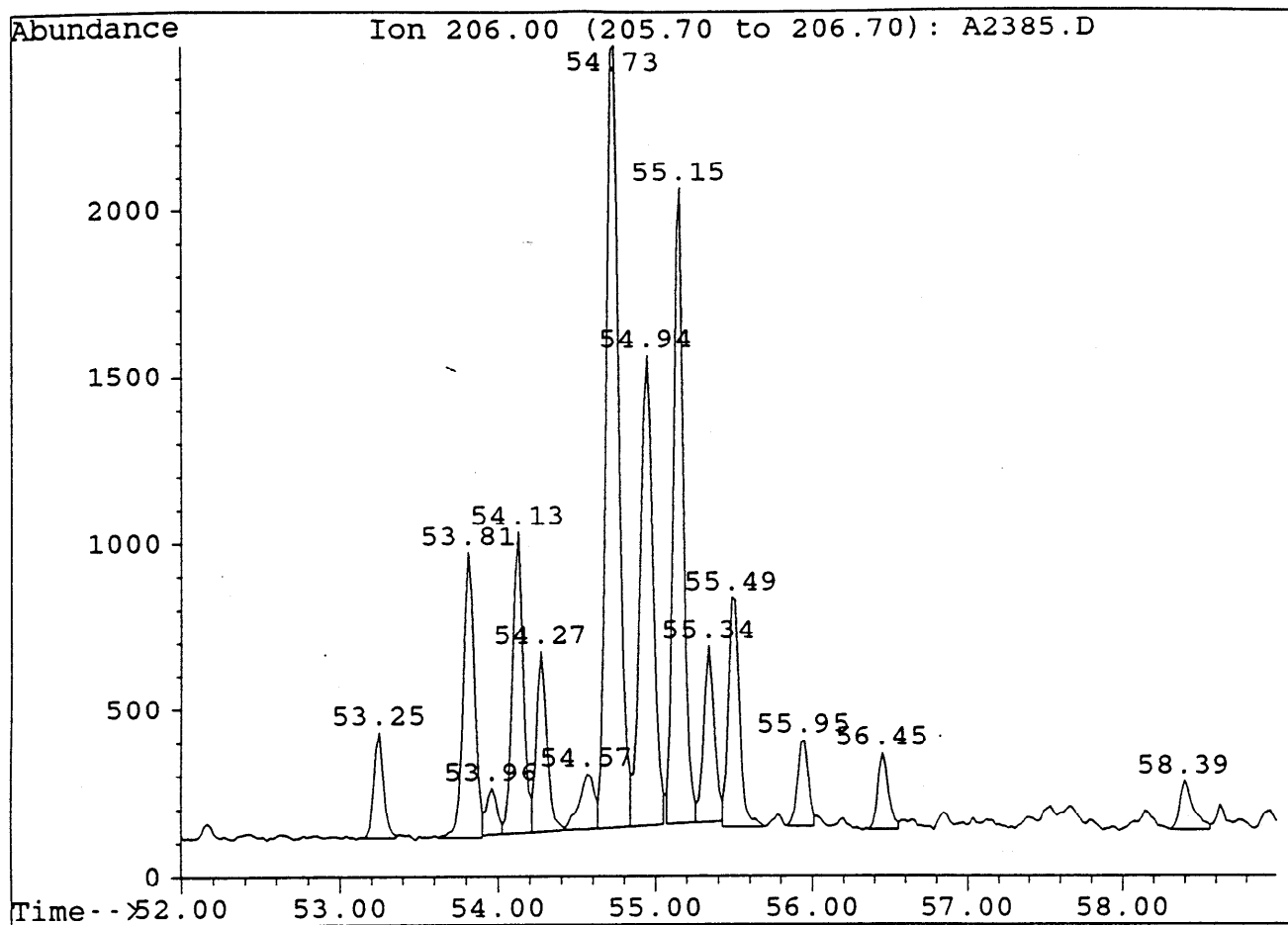
Sample : MINERVA-1, RFT 14/3/94. AROS

Peak	Ret.Time	Area	Height	Area %	Ratio %
1	37.50	9617	2352	4.81	51.74
2	37.79	4031	1076	2.02	21.69
3	37.98	8225	1408	4.12	44.25
4	38.62	8601	1712	4.31	46.28
5	38.79	8561	1555	4.29	46.06
6	39.15	6684	1292	3.35	35.96
7	39.23	3583	1077	1.79	19.28
8	39.63	3668	772	1.84	19.74
9	39.94	10730	2101	5.37	57.73
10	40.13	9927	2438	4.97	53.41
11	40.27	7224	1660	3.62	38.87
12	40.42	6750	1786	3.38	36.32
13	40.59	5856	1223	2.93	31.51
14	40.71	4719	1197	2.36	25.39
15	40.84	4059	936	2.03	21.84
16	40.94	4504	882	2.25	24.23
17	41.05	3892	846	1.95	20.94
18	41.19	5062	1366	2.53	27.24
19	41.26	6079	1484	3.04	32.71
20	42.05	15402	3306	7.71	82.87
21	42.22	15465	3766	7.74	83.21
22	42.68	14967	2377	7.49	80.53
23	42.84	7884	1856	3.95	42.42
24	43.47	5667	1279	2.84	30.49
25	44.47	18586	4094	9.30	100.00



Sample : MINERVA-1, RFT 14/3/94. AROS

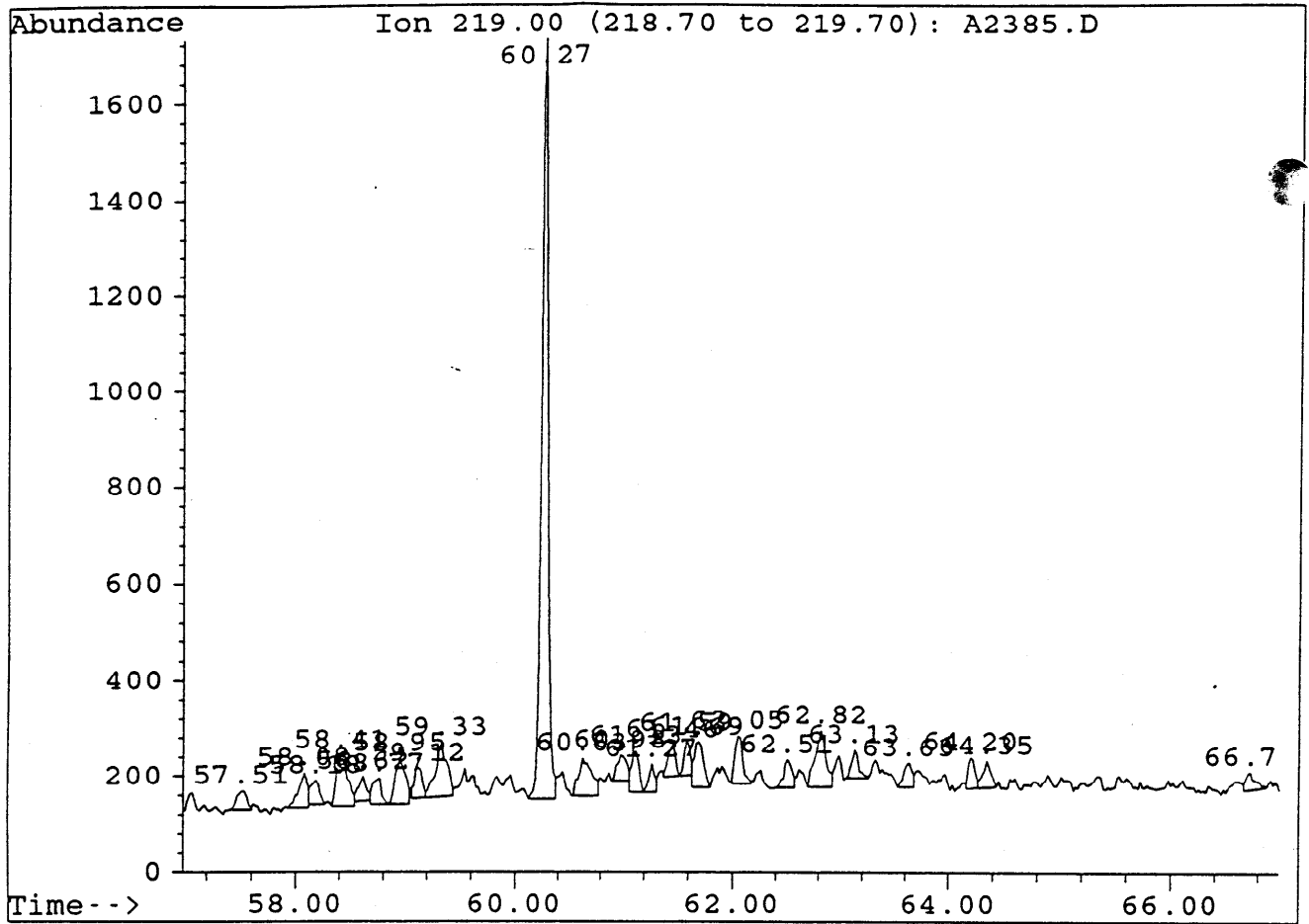
Peak	Ret.Time	Area	Height	Area %	Ratio %
1	41.07	3417	432	3.25	7.08
2	41.90	2208	482	2.10	4.58
3	42.22	48234	10685	45.89	100.00
4	42.36	5464	1396	5.20	11.33
5	42.59	6871	1569	6.54	14.25
6	42.91	1530	262	1.46	3.17
7	43.10	2189	489	2.08	4.54
8	43.32	5813	781	5.53	12.05
9	43.53	4242	654	4.04	8.79
10	43.66	2123	535	2.02	4.40
11	43.81	1561	390	1.49	3.24
12	43.89	2423	444	2.31	5.02
13	44.04	3046	540	2.90	6.32
14	44.14	2085	538	1.98	4.32
15	44.35	2101	493	2.00	4.36
16	44.56	1530	329	1.46	3.17
17	44.91	1598	331	1.52	3.31
18	45.41	2470	401	2.35	5.12
19	45.52	1962	378	1.87	4.07
20	45.92	2643	565	2.51	5.48
21	47.07	1590	241	1.51	3.30



Sample : MINERVA-1, RFT 14/3/94. AROS

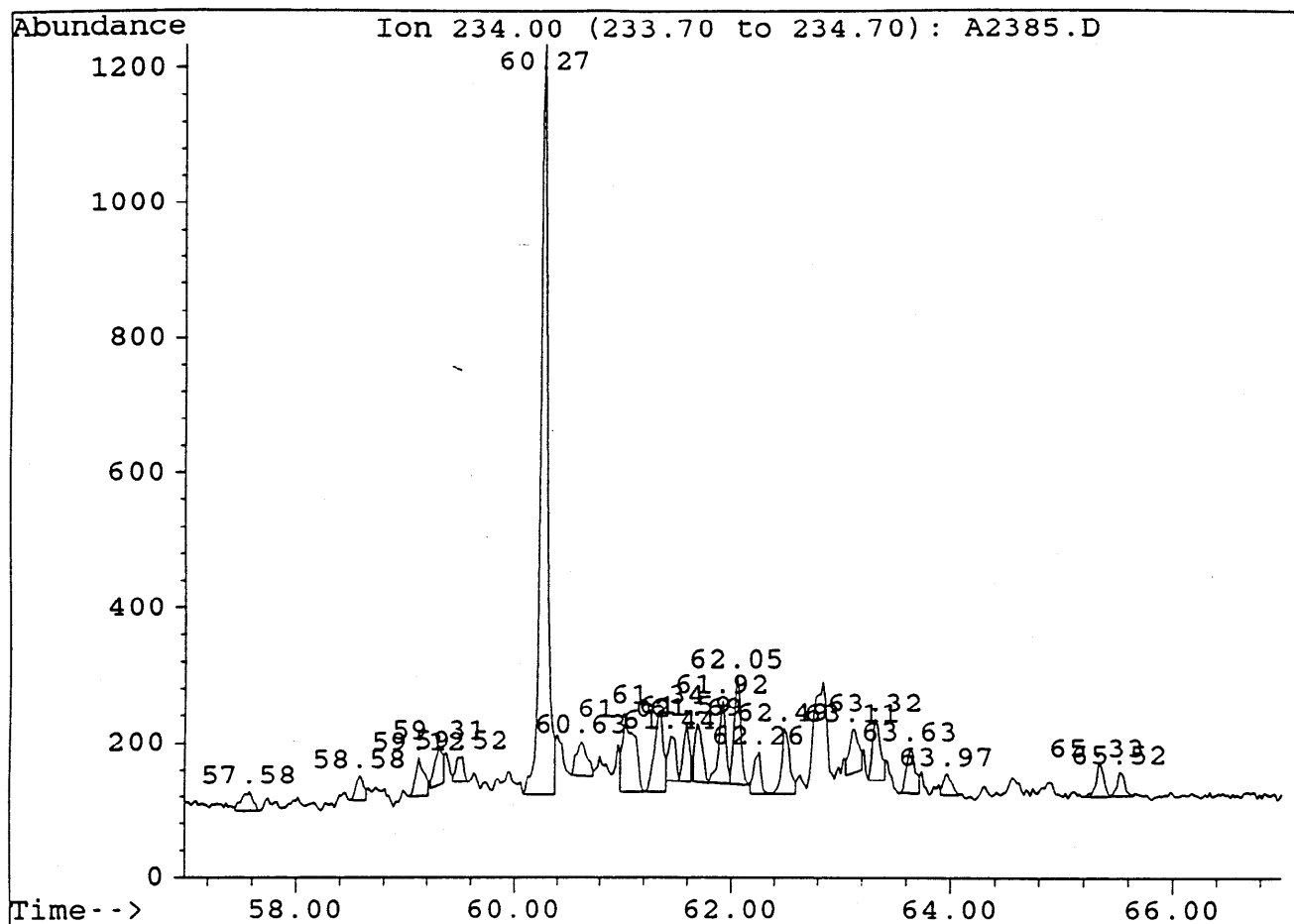
Peak	Ret.Time	Area	Height	Area %	Ratio %
1	53.25	1365	316	2.55	10.12
2	53.81	4210	856	7.86	31.20
3	53.96	646	139	1.21	4.79
4	54.13	4300	907	8.02	31.87
5	54.27	2433	541	4.54	18.03
6	54.57	1124	165	2.10	8.33
7	54.73	<u>13492</u> x	2353	25.18	100.00
8	54.94	8139	1411	15.19	60.32
9	55.15	<u>8802</u> 17	1910	16.43	65.24
10	55.34	2432	527	4.54	18.03
11	55.49	3383	689	6.31	25.07
12	55.95	1262	258	2.36	9.35
13	56.45	1105	229	2.06	8.19
14	58.39	890	145	1.66	6.60





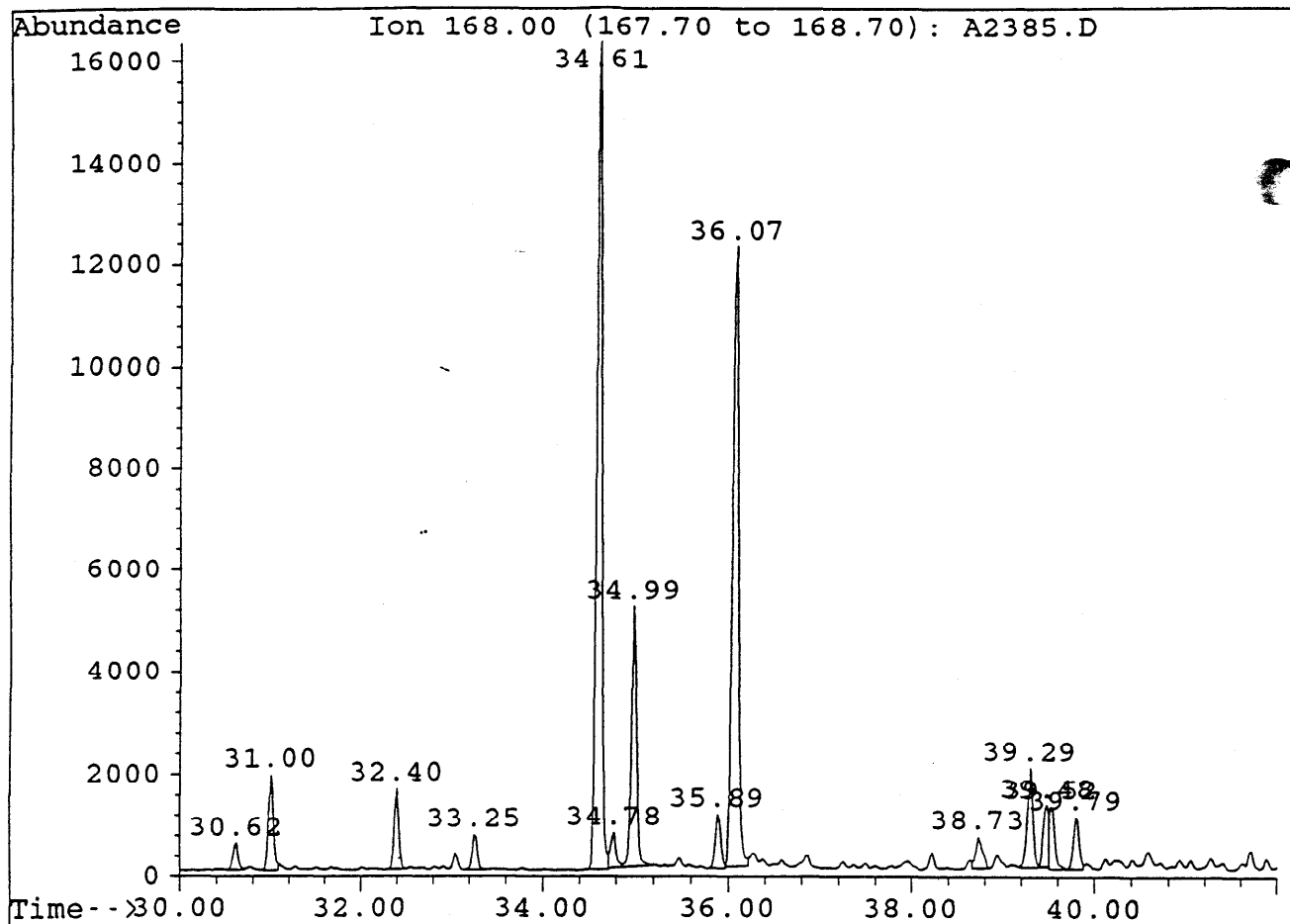
Sample : MINERVA-1, RFT 14/3/94. AROS

Peak	Ret.Time	Area	Height	Area %	Ratio %
1	57.51	231	38	1.38	3.29
2	58.08	418	72	2.49	5.95
3	58.18	260	50	1.55	3.70
4	58.41	778	106	4.63	11.08
5	58.62	267	52	1.59	3.80
6	58.77	273	53	1.63	3.89
7	58.95	601	95	3.58	8.56
8	59.12	303	63	1.80	4.31
9	59.33	831	113	4.95	11.83
10	60.27	<u>7024</u> R	1580	41.82	100.00
11	60.63	688	80	4.10	9.79
12	60.98	346	54	2.06	4.93
13	61.13	386	87	2.30	5.50
14	61.27	249	60	1.48	3.54
15	61.46	318	68	1.89	4.53
16	61.59	278	78	1.66	3.96
17	61.69	540	95	3.22	7.69
18	62.05	514	100	3.06	7.32
19	62.51	319	58	1.90	4.54
20	62.82	848	119	5.05	12.07
21	63.13	268	60	1.60	3.82
22	63.63	278	51	1.66	3.9
23	64.20	283	66	1.69	4.05
24	64.35	274	56	1.63	3.90
25	66.73	220	34	1.31	3.13



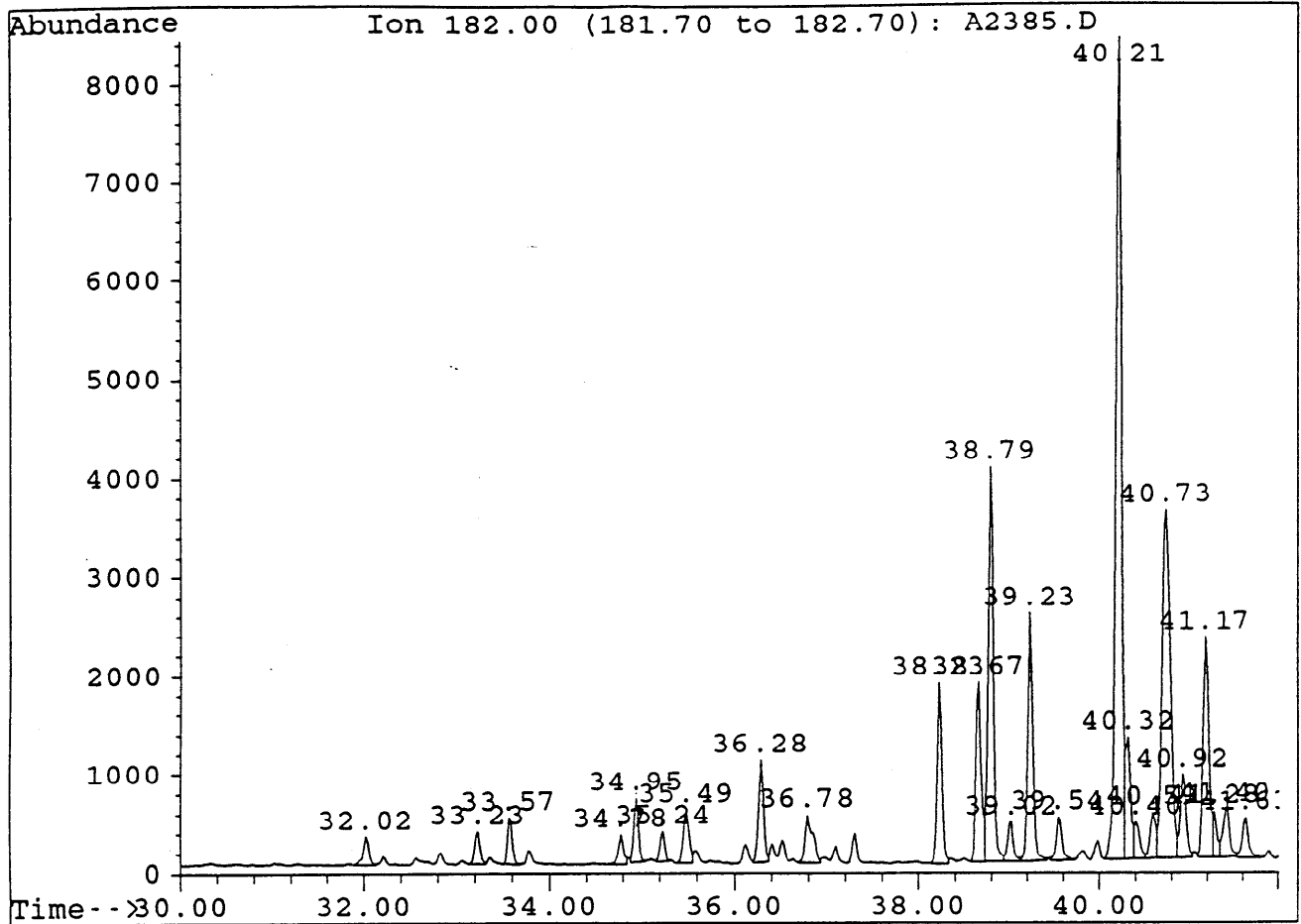
Sample : MINERVA-1, RFT 14/3/94. AROS

Peak	Ret.Time	Area	Height	Area %	Ratio %
1	57.58	196	28	1.47	3.66
2	58.58	191	37	1.43	3.57
3	59.12	307	58	2.30	5.74
4	59.31	312	60	2.34	5.83
5	59.52	174	38	1.31	3.25
6	60.27	5349	1112	40.14	100.00
7	60.63	356	51	2.67	6.66
8	61.02	838	99	6.29	15.67
9	61.34	694	120	5.21	12.97
10	61.44	319	66	2.39	5.96
11	61.59	334	88	2.51	6.24
12	61.69	406	87	3.05	7.59
13	61.92	539	123	4.04	10.08
14	62.05	673	162	5.05	12.58
15	62.26	299	63	2.24	5.59
16	62.49	535	97	4.01	10.00
17	63.11	383	65	2.87	7.16
18	63.32	460	90	3.45	8.60
19	63.63	373	67	2.80	6.97
20	63.97	168	32	1.26	3.14
21	65.33	248	48	1.86	4.64
22	65.52	173	37	1.30	3.23



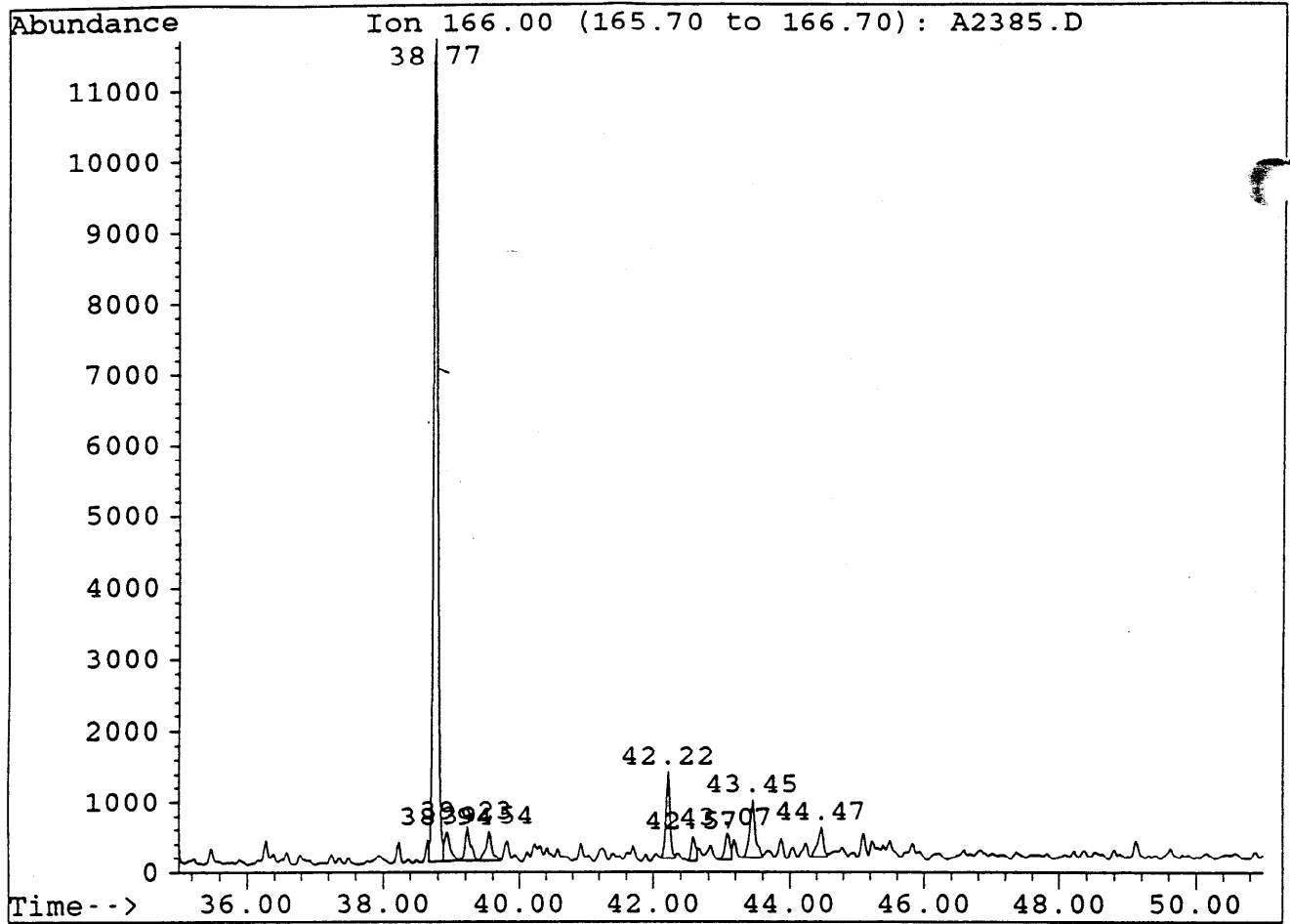
Sample : MINERVA-1, RFT 14/3/94. AROS

Peak	Ret.Time	Area	Height	Area %	Ratio %
1	30.62	2075	540	1.10	3.17
2	31.00	6999	1876	3.72	10.69
3	32.40	5673	1594	3.02	8.66
4	33.25	2640	711	1.40	4.03
5	34.61	65495	16231	34.81	100.00
6	34.78	2904	701	1.54	4.43
7	34.99	20025	5070	10.64	30.57
8	35.89	4316	1079	2.29	6.59
9	36.07	52163	12151	27.73	79.64
10	38.73	3233	631	1.72	4.94
11	39.29	8250	1951	4.39	12.60
12	39.48	5271	1218	2.80	8.05
13	39.52	4538	1236	2.41	6.93
14	39.79	4544	1021	2.42	6.94



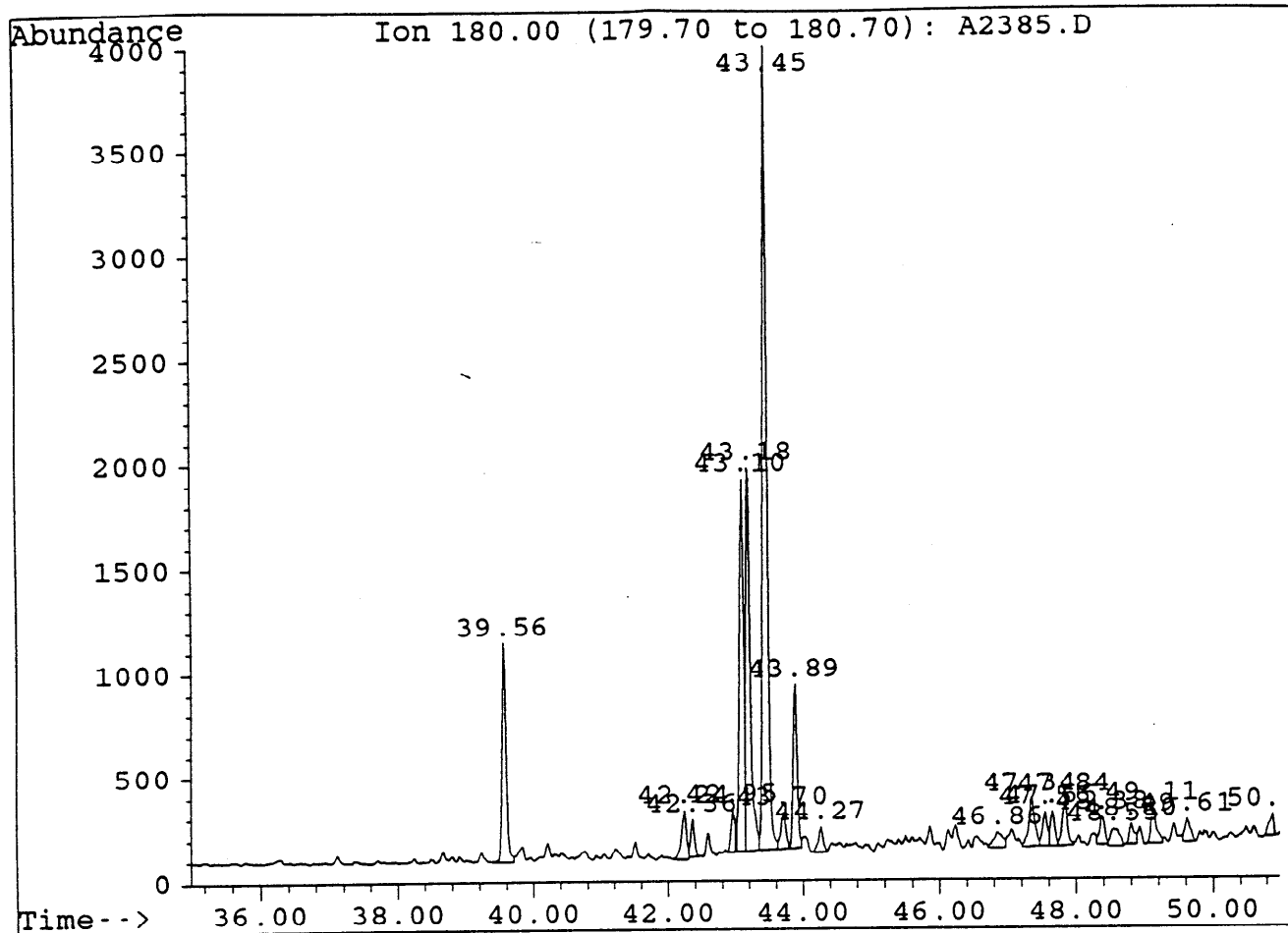
Sample : MINERVA-1, RFT 14/3/94. AROS

Peak	Ret.Time	Area	Height	Area %	Ratio %
1	32.02	1321	292	0.88	3.65
2	33.23	1289	331	0.86	3.56
3	33.57	1700	476	1.14	4.69
4	34.78	1240	306	0.83	3.42
5	34.95	2308	646	1.54	6.37
6	35.24	1132	310	0.76	3.12
7	35.49	2238	541	1.50	6.18
8	36.28	3876	1036	2.59	10.70
9	36.78	2860	482	1.91	7.89
10	38.23	7095	1831	4.74	19.58
11	38.67	7862	1821	5.26	21.70
12	38.79	16150	3994	10.80	44.57
13	39.02	1810	401	1.21	5.00
14	39.23	9970	2508	6.67	27.51
15	39.54	1983	445	1.33	5.47
16	40.21	36236	8317	24.23	100.00
17	40.32	4840	1227	3.24	13.36
18	40.40	1351	377	0.90	3.73
19	40.59	2023	464	1.35	5.58
20	40.73	22511	3516	15.05	62.12
21	40.92	3708	838	2.48	10.23
22	41.17	10047	2226	6.72	27.73
23	41.28	1344	462	0.90	3.71
24	41.40	2556	485	1.71	7.05
25	41.63	2111	414	1.41	5.83



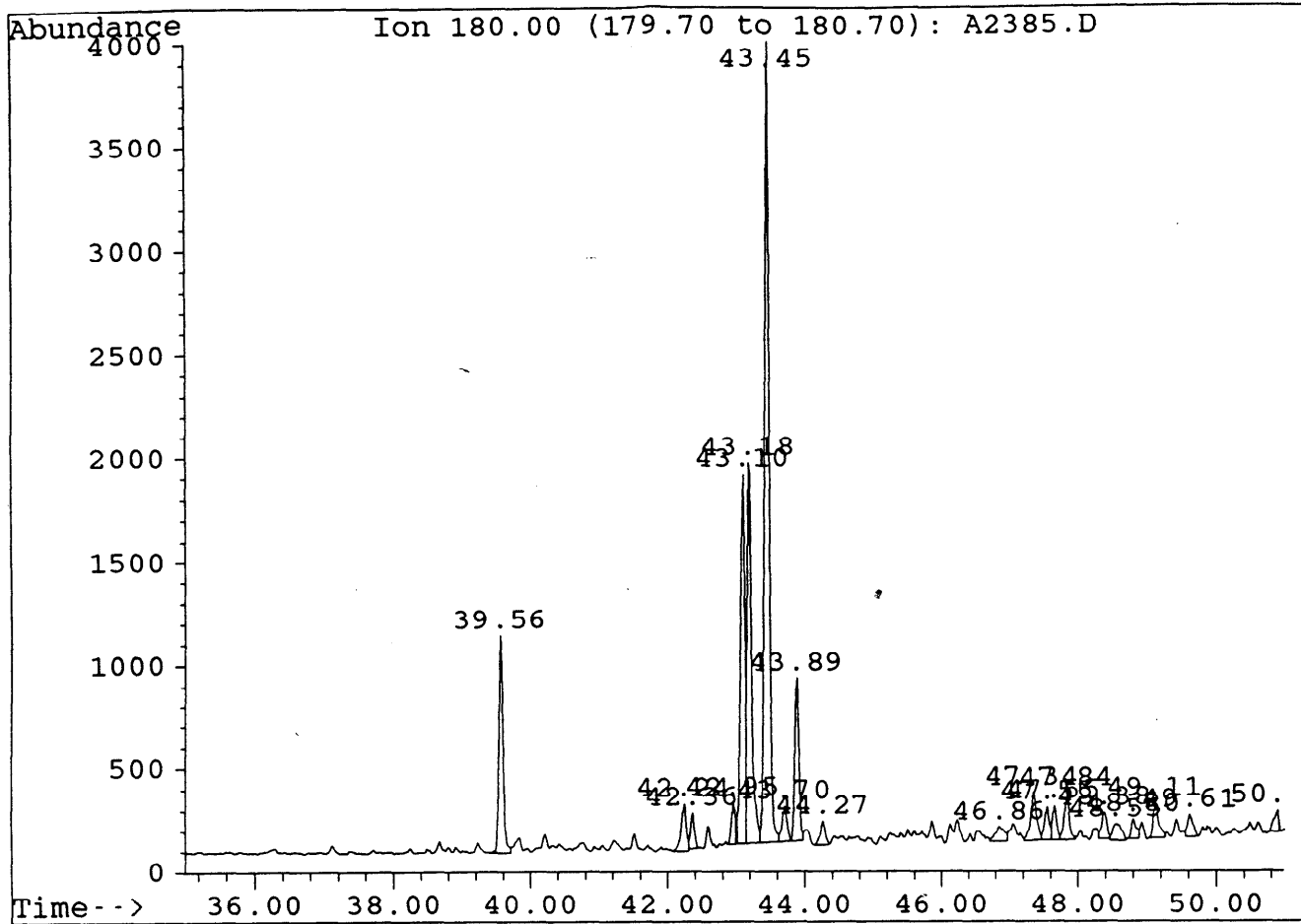
Sample : MINERVA-1, RFT 14/3/94. AROS

Peak	Ret.Time	Area	Height	Area %	Ratio %
1	38.77	52172	11558	68.53	100.00
2	38.94	2484	417	3.26	4.76
3	39.23	2707	489	3.56	5.19
4	39.54	2747	414	3.61	5.27
5	42.22	5186	1234	6.81	9.94
6	42.57	1594	350	2.09	3.06
7	43.07	1941	383	2.55	3.72
8	43.45	4645	825	6.10	8.90
9	44.47	2651	427	3.48	5.08



Sample : MINERVA-1, RFT 14/3/94. AROS

Peak	Ret.Time	Area	Height	Area %	Ratio %
1	39.56	4426	1050	8.28	26.51
2	42.24	1225	229	2.29	7.34
3	42.36	662	175	1.24	3.96
4	42.95	848	201	1.59	5.08
5	43.10	7541	1785	14.11	45.16
6	43.18	8390	1837	15.70	50.25
7	43.45	16697	3862	31.25	100.00
8	43.70	891	172	1.67	5.34
9	43.89	3372	784	6.31	20.20
10	44.27	581	117	1.09	3.48
11	46.86	678	72	1.27	4.06
12	47.34	1466	232	2.74	8.78
13	47.55	827	164	1.55	4.95
14	47.65	680	167	1.27	4.07
15	47.84	1151	224	2.15	6.89
16	48.38	664	128	1.24	3.98
17	48.55	725	82	1.36	4.34
18	48.80	520	97	0.97	3.11
19	49.11	971	168	1.82	5.82
20	49.61	606	108	1.13	3.63
21	50.89	505	104	0.95	3.02



Sample : MINERVA-1, RFT 14/3/94. AROS

Peak	Ret.Time	Area	Height	Area %	Ratio %
1	39.56	4426	1050	8.28	26.51
2	42.24	1225	229	2.29	7.34
3	42.36	662	175	1.24	3.96
4	42.95	848	201	1.59	5.08
5	43.10	7541	1785	14.11	45.16
6	43.18	8390	1837	15.70	50.25
7	43.45	16697	3862	31.25	100.00
8	43.70	891	172	1.67	5.34
9	43.89	3372	784	6.31	20.20
10	44.27	581	117	1.09	3.48
11	46.86	678	72	1.27	4.06
12	47.34	1466	232	2.74	8.78
13	47.55	827	164	1.55	4.95
14	47.65	680	167	1.27	4.07
15	47.84	1151	224	2.15	6.89
16	48.38	664	128	1.24	3.98
17	48.55	725	82	1.36	4.34
18	48.80	520	97	0.97	3.11
19	49.11	971	168	1.82	5.82
20	49.61	606	108	1.13	3.63
21	50.89	505	104	0.95	3.02

PE602764

This is an enclosure indicator page.  
The enclosure PE602764 is enclosed within the  
container PE900058 at this location in this  
document.

The enclosure PE602764 has the following characteristics:

ITEM-BARCODE = PE602764  
CONTAINER\_BARCODE = PE900058  
    NAME = Minerva 1 Geochemical log  
    BASIN = Otway  
    PERMIT = VIC/P31  
    TYPE = WELL  
    SUBTYPE = WELL-LOG  
    DESCRIPTION = Minerva 1 Geochemical log, Appendix 3  
    REMARKS = old barcode PE900062 replaced with  
              PE602764  
DATE-CREATED = \*  
DATE-RECEIVED = \*  
    W\_NO = W1079  
    WELL-NAME = MINERVA 1  
CONTRACTOR =  
CLIENT\_OP\_CO =

(Inserted by DNRE - Vic Govt Mines Dept)



4

**BHP PETROLEUM PTY LTD.**

**VIC P31 MINERVA-1**

**LOG INTERPRETATION REPORT**

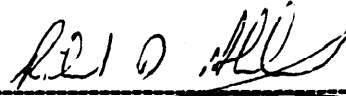
**Prepared By:**



---

**ANDY CALCRAFT**  
**Consultant Petrophysicist**

**Authorised By:**



---

**RICK ALDRED**  
**Senior Petrophysicist**

**May 1993**

**Ref: ac0656.aga**

**File: Min-1/PP/SO1/r**

## Summary

Minerva-1 was drilled as an exploration well on the Minerva structure in VIC P31, approximately 145 kilometres South-East of Portland, Victoria, Australia. The well was designed to test the reservoir and hydrocarbon potential of sandstones within the Shipwreck Group and was spudded on the 8th March 1993 and reached a total depth of 2425m within Otway Group sediments.

Gas bearing sandstones were encountered within the Sherbrook group and the Upper Shipwreck Sandstone.

The well was production tested and flowed at approximately 29 MMSCFD.

Zone	Depth mRT	Gross m	Net m	N/G %	Porosity %	Sw %
Sherbrook	1170	25	.2	1	11	65
Up Shipwreck	1645 - 1655	10	1.4	14	12	54
Up Shipwreck	1655 - 1670	15	2.5	17	15	59
Up Shipwreck	1815-1948	133	118.5	89	18	19
Up Shipwreck	1815 - 2149	219 *	179.5	82 **	14	-
Lr Shipwreck	2149-2293	144	50.1	35 **	12	-
Otway	2293-2410	117	32.7	28 **	12	-

Notes: \* Section of 115 m not logged with LDL-CNL, not included  
\*\* Net reservoir, not net pay.

## TABLE OF CONTENTS

		Page
1.	INTRODUCTION .....	1
2.	AVAILABLE DATA .....	2
	2.1 MWD data .....	2
	2.2 Conventional Cores .....	2
	2.3 Sidewall Cores .....	2
	2.4 Wireline Formation Tests .....	2
	2.5 Production and Drillstem Tests .....	3
	2.6 Logs Run .....	3
3.	HOLE CONDITIONS .....	4
	3.1 Caliper .....	4
	3.2 Borehole Fluids .....	4
	3.3 Temperature .....	5
4.	DATA PREPARATION .....	6
	4.1 Log Data .....	6
	4.2 Interpretation Model .....	6
	4.2.1 CRA .....	6
	4.2.2 Optimal .....	6
	4.2.3 Pef .....	6
	4.3 Core Data .....	6
5	SHERBROOK GAS SHOW (1170 mRT) .....	7
	5.1 Mineralogy .....	7
	5.2 Interpretation Model .....	7
	5.3 Input Parameters .....	7
	5.4 Water Saturation .....	7
	5.5 Results .....	7
6	UPPER SHIPWRECK GAS SANDS (1649 - 1618 mRT) .....	9
	6.1 Mineralogy .....	9
	6.2 Interpretation Model .....	9
	6.3 Input Parameters .....	9
	6.4 Water Saturation .....	9
	6.5 Results .....	9
7	UPPER SHIPWRECK GAS SAND (1815.5 - 2149 mRT) .....	10
	7.1 Mineralogy .....	10
	7.2 Interpretation Model .....	10
	7.3 Input Parameters .....	10
	7.4 Water Saturation .....	10
	7.5 Results .....	11
8	LOWER SHIPWRECK SAND (2149 - 2293 mRT) .....	12
	8.1 Mineralogy .....	12
	8.2 Interpretation Model .....	12
	8.3 Input Parameters .....	12
	8.4 Water Saturation .....	12
	8.5 Results .....	12
9	OTWAY GROUP ?Eumerella Formation (2293 mRT - TD) .....	13
	9.1 Mineralogy .....	13
	9.2 Interpretation Model .....	13

	9.3	Input Parameters .....	13
	9.4	Water Saturation .....	13
	9.5	Results .....	13
10		REFERENCES .....	14

## TABLES

1	Minerva-1 Log Evaluation Parameters
2	Summary of Results

## FIGURES

1	Stabilised Bottom Hole Temperature
2	Gamma vs RT, Sherbrook gas show, 1130 - 1185 mRT
3	Sonic vs Gamma Ray, Sherbrook gas show, 1130-1185 mRT
4	Neutron-Density Crossplot, Upper Shipwreck shale, 1640-1700 mRT
5	Neutron-Density Crossplot, Upper Shipwreck gas sand, 1816 - 2149 mRT
6	Neutron-Density Crossplot, Upper Shipwreck water sand, 1947-2149 mRT
7	Rxo vs RT, Upper Shipwreck sand, 1815.5 - 2020 mRT
8	Density-Neutron Crossplot, Lower Shipwreck
9	Density-Neutron Crossplot, Otway group
10	Pickett Plot, Upper Shipwreck sand, 1815 - 2000 mRT, $m = 1.9$
11	Pickett Plot, Upper Shipwreck sand, 1815 - 2000 mRT, $m = 1.2$
12	Pickett Plot, Lower Shipwreck and Otway intervals

## ENCLOSURES

1	Composite Log Plot 1130 - TD
2	MWD and Wireline Comparison Plot, 1600 - 2000 mRT
3	Final Interpretation Plot

---

## 1. INTRODUCTION

Minerva-1 was drilled as an exploration well on the Minerva structure in VIC P31, approximately 145 kilometres South-East of Portland, Victoria, Australia. The well was designed to test the reservoir and hydrocarbon potential of sandstones within the Shipwreck Group.

Minerva-1 spudded on 8th March 1993 and reached a total depth of 2425m. The Shipwreck Group was encountered at 1448 m RT.

The abbreviations used for depth measurements in this report are:

RT	Rotary table height (25 m) above Mean Seal Level (MSL).
m	Metres measured by driller below RT
m RT	Metres measured by logger below RT
m ss	Metres true vertical depth below MSL

## 2. AVAILABLE DATA

### 2.1 MWD data

Teleco Sonat MWD equipment recorded a gamma ray log and a short normal resistivity from 560m to TD.

### 2.2 Conventional Cores

The interval 1821 to 1847m was cored after encountering good gas shows in good quality sandstone within the Upper Shipwreck Group. Three coring attempts were made:

Core No	Interval mRT	Cut m	Recovered m	Recovery %
1	1821 - 1828	7	3.04	43
2	1828 - 1842.5	14.5	13.3	92
3	1842.5 - 1847	4.5	4.5	100

### 2.3 Sidewall Cores

Run	Shot	Recovered	Misfire	Lost	Empty
1	46	46	-	-	-
2	60	57	-	3	-
3	30	30	-	-	-
4	21	21	-	-	3

### 2.4 Wireline Formation Tests

An RFT, repeat formation tester, was run in Minerva-1 in suite 2 and three RFT runs were made. Thirty-three pre-tests were attempted, twenty-eight were successful, three tight and two possibly seal failures. Three segregated samples were recovered from 1649.8, 1942.5 and 1931.0 mRT within the Upper Shipwreck Group. All samples recovered gas but those from 1649.8 and 1931.0 mRT recovered condensate as well. For more detail refer to the Minerva-1 RFT Report.

## 2.5 Production and Drillstem Tests

The intervals 1838 - 1825 and 1821 - 1816 mRT within the Upper Shipwreck was production tested. The maximum stabilised flow rate was 28.8 MMSCFD. Three sets of gas samples were collected for further analysis.

For more information refer to the Minerva-1 Production Test Report. (In preparation)

## 2.6 Logs Run

Logs Run	Top m RT	Bottom m RT
<b>Suite 1, 14 March 1993</b>		
DLL/MSFL/AS/GR/AMS/SP	549	1,199
CSI (VSP)	150	1189
CST	563	1193
<b>Suite 2, 21 March 1993</b>		
DLL/MSFL/GR/AMS/SP	1,189	2,019
SDT/LDL/CNL/GR/AMS/FMS	1,189	2,014
CSI (VSP)	920	2,017
RFT-HP	1,649	1,992
CST		
<b>Suite 3, 25 March 1993</b>		
DLL/MSFL/SDT/AMS	1,800	2,098
<b>Suite 4, 4 April 1993</b>		
DLL/MSFL/SDT/AMS	2,109.5	2,419.5
LDL/CNL/GR/FMS/AMS	2,109.5	2,414
CSI	1,992	2,420
CST	2,120	2,420



### 3. HOLE CONDITIONS

#### 3.1 Caliper

The objective section was drilled with an 8.5" bit. Hole conditions were good with occasional minor caliper excursions. Caliper excursions were not sufficient to cause interpretation problems with the density-neutron logs.

A 7" liner was set at 2107 mRT and the section to 2425m (TD) was drilled with a 6" bit. The borehole was generally in gauge except for a short interval associated with claystone between 2195 and 2205m.

#### 3.2 Borehole Fluids

The objective section was drilled with a KCl polymer mud with the following properties:

Suite Number	1	2	3	4
Type	KCl PHPA	KCL PHPA	KCl PHPA	KCl PHPA
Weight g/cc	1.12	1.15	1.15	1.15
Viscosity	50	45	45	46
Rm	0.169 @ 22°C	0.100 @ 21°C	0.099 @ 18°C	0.091 @ 24°C
Rmf	0.144 @ 22°C	0.084 @ 22°C	0.089 @ 18°C	0.080 @ 24°C
Rmc	0.210 @ 22°C	0.120 @ 22°C	0.128 @ 18°C	0.105 @ 20°C
Rm (Arps)	0.093 @ 58°C	0.045 @ 57.5°C	0.038 @ 80.8°C	0.037 @ 89.7°C
Rm (AMS)	0.082 @ 58°C	0.018 @ 72.5°C	0.037 @ 80.8°C	0.028 @ 89.7°C

### 3.3 Temperature

The following maximum temperatures were recorded:

Tool	Depth (m)	Circ Time (hours)	Time since Circulation (hours)	(Dt+T)/Dt	BHT °C
<b>Suite 1</b>					
DLL	1,189	0.75	5.55	0.144	58
VSP	1,189	0.75	12.00	0.092	63
<b>Suite 2</b>					
DLL	2,019	0.25	8.5	0.111	83
SDT-CNL	2,014	0.25	14.00	0.082	89
VSP	1,992	0.25	20.50	0.064	93
RFT/HP	2,017	0.25	40.50	0.040	-
<b>Suite 3</b>					
DLL	2,098	1.25	6.00	0.143	81
<b>Suite 4</b>					
DLL	2,419.5	1.08	7.33	0.126	90
LDL	2,109.5	1.08	11.75	0.094	96
CSI	2,420	1.08	16.75	0.075	-
CST	2,420	1.08	-	-	-

Extrapolated bottom hole temperatures were 72, 99 and 108 °C for Suites 1, 2 and 4 respectively as illustrated by Figure 1.

---

## 4. DATA PREPARATION

### 4.1 Log Data

Wireline data was imported into WDS (Well Data System, Atlas Wireline) and Geolog (Mincom) for storage, display, manipulation and interpretation. All Suite 2 and 4 logs were depth matched to the Gamma Ray log recorded with the resistivity logs. Suites 1 and 3 logs consisted of DLL-SDT logs run in one run.

Environmental corrections were carried out using algorithms that emulate the appropriate correction charts (Schlumberger, 1989).

### 4.2 Interpretation Model

#### 4.2.1 CRA

CRA, a deterministic complex lithology shaly sand model, was selected for this analysis because CRA is fast, handles gas corrections well and robust. It was not possible to make it work with the sonic log as the only porosity log. For the short interval in the Sherbrook Formation Optima was used instead.

#### 4.2.2 Optima

Optima is a probabilistic petrophysical model that accommodates up to six different minerals if sufficient input curves are present. The model works by minimising an error function when actual log measurements and associated uncertainties are compared with reconstructed log values. This type of model is often used for analysis of complex mineralogy with many different log measurements. It does not rely on any a particular logging measurement and is useful for handling either odd log combinations or reduced logging suites. In the top hole section in Minerva-1 density and neutron logs are unavailable but a gas show needed evaluation.

#### 4.2.3 Pef

The Pef was affected by Baryte in the drilling mud and was considered unreliable and was not used for the analysis.

### 4.3 Core Data

Conventional core plugs were cut at 30 cm intervals along the core. Routine core measurements were made at atmospheric conditions.

---

## 5 SHERBROOK GAS SHOW (1170 mRT)

### 5.1 Mineralogy

This unit consists of sandy claystone grading to very fine to fine grained clayey sandstone. There are thin sandstone bands at 1170 and 1173 mRT. Minor components include glauconite, mica, pyrite and carbonaceous matter.

### 5.2 Interpretation Model

The obvious petrophysical model for this interval is a simple shaly sand since the only porosity log available is the sonic. After experimentation with several interpretation models Optima was chosen. Though it is a probabilistic model designed for complex lithology, it is not dependent on any particular logging measurement and can be used with a simple lithological model when few logs are available.

The mineral model was simplified to a shale or clay and sandstone combination since the gamma ray and sonic are only two non resistivity logs available. The Raymer-Hunt-Gardiner sonic to porosity transform was selected for the analysis because experience suggests that in the 10-20% porosity range it is more reliable than the Wyllie time average relationship.

### 5.3 Input Parameters

Refer to Table 1

### 5.4 Water Saturation

Water resistivity for this interval is not known. A water sand was not encountered.

The SSP is 11mV which equates to an  $R_w$  of 0.108 ohmm at 25°C. The  $R_w$  adopted was 0.252 ohmm at 25°C or a salinity of 23,300 ppm, the same as that used for the Upper Shipwreck Sands below 1816 mRT. This water resistivity permits computation of reasonable, but not necessarily correct, water saturations.

### 5.5 Results

The log analysis suggests that average porosity is 11% with an average water saturation of 65% in 1 metre of net pay (Refer to Table 2, Summary of Results). The uncertainty of the analysis is relatively high because of the lack of data available for this interval. The two thin sandstones are regarded as a minor gas show.

Should the sands remain gas bearing and become thicker and better quality at other locations on the Minerva structure, then they may be worthwhile as secondary completion

---

opportunities. If so then, consideration should be given to logging a density-neutron suite over these sands.

Discussion with the explorationists suggests that the borehole may intersect a major fault somewhere between 1000-1200 mRT. The gas may have migrated up the a fault.

---

## 6 UPPER SHIPWRECK GAS SANDS (1649 - 1618 mRT)

### 6.1 Mineralogy

This section mostly consists of a silty shaly claystone that grades to a clayey siltstone. Kaolin, from altered feldspars is commonly described from sidewall core. Other minor components described are rare to traces of glauconite, microcrystalline mica, mica flakes and carbonaceous detritus. The sandstone at 1650 m is described as fine grained, with good to very good visual porosity and is calcareous, clayey, with carbonaceous flecks and traces of microcrystalline pyrite from one sidewall core. The lower sandstone, at 1663 m is described as very fine grained, clayey, with poor to fair visual porosity from one sidewall core from 1670 m: slightly below the best porosity development.

### 6.2 Interpretation Model

The quick look interpretation carried out immediately after logging used CRA, a complex lithology and satisfactory results obtained. This model has been used for the final analysis.

A three mineral, quartz, shale and dolomite model was selected. As an experiment pyrite and kaolin were added but the results did not change significantly and were removed.

### 6.3 Input Parameters

Refer to Table 1

### 6.4 Water Saturation

A water resistivity of 0.252 ohmm at 25 °C (salinity 23,300 ppm) was selected since this was used for the Upper Shipwreck gas sands below 1815m. RFT interpretation suggests that these gas sands are on a the same gas gradient implying a common free water level. The use of this value computes reasonable water saturations but they are not necessarily correct.

Rw from the SSP is estimated at 0.129 ohmm at 25°C equivalent to a salinity of 33,600 ppm chloride. This is not considered reliable since the sands are thin, surrounding shales may be gas bearing and are not true shales or clays but clayey siltstones grading to silty claystones.

### 6.5 Results

Refer to table 2.

---

## 7 UPPER SHIPWRECK GAS SAND (1815.5-2149 mRT)

### 7.1 Mineralogy

This a quartz sandstone, conglomerate and shale sequence. Grain size is medium to coarse, in part pebbly. A light grey to off white cement clayey kaolinitic matrix was described with rare to common siliceous and occasionally pyritic cement. Traces of mica, lithic fragments, structural kaolinitic grains, coaly fragments were also described. Amber was common in some sidewall cores.

Conventional core data is available for the upper portion of the reservoir between 1821 and 1847 mRT and is consistent with sidewall descriptions.

### 7.2 Interpretation Model

The model adopted for this interval was a complex lithology model using dolomite as a generic dense mineral and pyrite as a heavy mineral. Kaolin was described from core but adding it made very little difference to the analysis and it was removed.

There are variations in resistivity character through the gas sand (Enclosure 1). The effect can be seen on an  $R_{xo}$  vs  $R_t$  crossplot (figure 7) which suggests that there are two groups of points that may relate to different rock types. The most likely explanation is mineralogical; pyrite and conglomerate were observed from the core at the top of the reservoir. Pyrite in particular is conductive and may suppress the resistivity response. A special core analysis program has been instituted to help define variations in rock type and petrophysical properties.

### 7.3 Input Parameters

Refer to Table 1.

### 7.4 Water Saturations

The SSP over a shaly band between 1945-1950m suggests an  $R_w$  of 0.132 ohmm at 25°C or 33,500 ppm. This, and other, shales are thin and the SSP deflection is depressed. Pickett Plots (figures 8 and 9) suggests that the  $R_w$  is about 0.11 ohmm at reservoir temperature or 0.252 ohmm at 25 °C if  $m$  is set to 1.9.

As figure 10 illustrates an alternative interpretation is possible. This interpretation is improbable because it requires an unrealistically low value of 1.2 for  $m$  in a consolidated sandstone and very fresh formation water (13,000 ppm). This latter interpretation also ignores the fact that shaly points tend to plot below the water line.

Low gas saturations are computed in the gas sand and water saturations average 100% below the gas-water contact, interpreted to be an water-down-to at 1944 mRT. This gas-

---

water contact is consistent with RFT measurements because there is considerable scatter on the pressure-depth plot.

Figure 6 shows that as at Le Bella-1 there is an apparent gas effect on the neutron-density logs immediately below the gas-water contact. The effect is not as extensive as at La Bella-1 and is similarly not fully understood. However, the possibility of gas within the mud filtrate invaded zone or some residual gas saturations was suggested by Schlumberger and is considered a reasonable explanation for Minerva-1. Study of the laterolog curves does suggest that there might be an incipient ramp starting at 1951.5 mRT consistent with residual hydrocarbons. The resistivity ramp at 1951.5 mRT could also be interpreted to suggest that the gas-water contact is deeper than the currently interpreted 1944 mRT or that the shale band at 1947 is acting as a local seal.

### 7.5 Results

There are computed hydrocarbon spikes associated with high shale content in the water sand but these are considered spurious.

At the base of the Upper Shipwreck coals are interpreted. These coals are usually thin, about 2 metres thick, and radioactive.



---

## 8 LOWER SHIPWRECK (2149 - 2293 mRT)

### 8.1 Mineralogy

This interval consists of shaly lithic sandstones and claystone. There is one sidewall core over this interval and this is a shaly lithic sandstone. Grain size ranges from fine to medium, occasionally coarse quartz and lithic grains. Feldspathic grains are common and the dominant cement is clay though there are traces of calcite and pyrite. Visual porosity was poor.

### 8.2 Interpretation Model

The model adopted for this interval was a shaly sand model with dolomite and pyrite as dense minerals.

Water resistivity is derived from the Upper Shipwreck and Pickett Plots.

There are washouts present between 2185 and 2205 mRT and the density log is reading mud so the analysis model uses the neutron-sonic combination.

### 8.3 Input Parameters

Refer to table 2.

### 8.4 Water Saturation

Water saturations average 100% except for a short interval 2190-2195 m RT where calculated water saturations are 55-50%. These are spurious and the rock may be a radioactive calcite cemented sandstone. Support for this possibility is provided by the Pef which increases from 3.0 to 4.5 barns/electron. Similarly the washouts between 2190-2205 mRT may be due to brittle calcareous rock since they have a high resistivity and no invasion profile. Such an interpretation may be consistent with a faulted and fracture zone. The current geophysical interpretation neither supports nor opposes this possibility.

## 5 Results

This interval is interpreted to be water bearing.

---

## 9 OTWAY GROUP ?Eumerella Formation (2293 - TD)

### 9.1 Mineralogy

This formation has not been penetrated before in this area but it consists of clayey lithic sandstones and sandy claystone. Sandstones are grey green to light grey, very fine to medium grained, with both quartz and lithic grains. There is common calcite or siliceous cement and rare pyrite. Weathered feldspar is common in some samples as is a clayey matrix. Carbonaceous flecks and lenses are common. Geological opinion suggests that some lithic material and argillaceous matter is probably chlorite. Claystone is described as hard, blocky, siliceous, with very fine mica flakes and carbonaceous flecks and laminae.

### 9.2 Interpretation Model

A CRA model with quartz, clay, chlorite and pyrite was used for this interval.

### 9.3 Input Parameters

Refer to table 2.

### 9.4 Water Saturation

Water saturations averaged 100% for this interval using the same water salinity as the Upper Shipwreck. The SP is not reliable because clean sands are absent.

### 9.5 Results

This interval is interpreted to be water bearing.

---

**REFERENCES**

BHPP, 1993 La Bella-1 Log Interpretation report, 1993

BHPP, 1993, Minerva-1 RFT Report, March 1993, (Min-1/RE/F05/R)

Schlumberger 1992, Log Interpretation Charts, Schlumberger Educational Services.

**Table**  
**Minerva-1 Log Evaluation Parameters**

Name	Sherbrook Fm	Upper Shipwreck	Upper Shipwreck	Upper Shipwreck	Upper Shipwreck	Lower Shipwreck	Lower Shipwreck	Lower Shipwreck	Lower Shipwreck	Lower Shipwreck	Otway grp Eumeralla
Top	1130	1600	1816	1980	2115	2149	2185	2217	2275	2293	2293
Bottom	1185	1816	1980	2020	2149	2185	2217	2275	2293	2425	2425
Logging Suite	1	2	2	2	4	4	4	4	4	4	4
Bit Size	12.25	8.5	8.5	8.5	6	6	6	6	6	6	6
Rhof	1.03	1.03	1.03	1.03	1.03	1.03	1.03	1.03	1.03	1.03	1.03
Gr Clean	50	20	20	20	20	15	15	15	15	60	60
Gr Shale	140	130	130	130	130	130	130	130	130	130	130
Rhob Shale		2.65	2.63	2.63	2.65	2.65	2.65	2.65	2.65	2.65	2.65
Nphi Shale		35	35	35	33	34	34	34	34	35	35
IX Shale	95	290	290	290	290	240	240	240	240	300	300
Rsh	15	25	25	25	25	25	25	25	25	20	20
Rmf	0.144	0.075	0.075	0.075	0.09	0.09	0.09	0.09	0.09	0.09	0.09
Rmf temperature deg C	23	86	86	86	86	86	86	86	86	86	86
Rm25 degrees C	0.139	0.173	0.173	0.173	0.208	0.208	0.208	0.208	0.208	0.208	0.208
Rmf salinity	45,485	35,344	35,344	35,344	28,827	28,827	28,827	28,827	28,827	28,827	28,827
Rw	0.11	0.11	0.11	0.11	0.15	0.15	0.15	0.15	0.15	0.15	0.15
Rw temperature	85	85	85	22	22	22	22	22	22	22	22
Rw25 degrees C	0.252	0.252	0.252	0.103	0.140	0.140	0.140	0.140	0.140	0.140	0.140
Salinity	23,333	23,333	23,333	64,472	44,935	44,935	44,935	44,935	44,935	44,935	44,935
HC Density SG	0.15	0.15	0.16	0.16	0.8	0.8	0.8	0.8	0.8	0.8	0.8
HC density API	Gas	Gas	Gas	Gas	45.4	45.4	45.4	45.4	45.4	45.4	45.4
a	1	1	1	1	1	1	1	1	1	1	1
m	2	1.9	1.9	1.9	1.9	2	2	2	2	2	2
n	2	2	2	2	2	2	2	2	2	2	2
Model	Optima	CRA	CRA	CRA	CRA	CRA	CRA	CRA	CRA	CRA	CRA
Neutron transform	TNPH	TNPH	TNPH	TNPH	TNPH	TNPH	TNPH	TNPH	TNPH	TNPH	TNPH
Acoustic transform	RIIG	AFF	AFF	AFF	AFF	AFF	AFF	AFF	AFF	AFF	AFF
Por Model	Sonic	Neutron-Sonic	Neutron-Density	Neutron-Density	Neutron-Density	Neutron-Density	Neutron - Sonic	Neutron-Density	Neutron-Density	Neutron-Density	Neutron-Density
<b>Minerals</b>											
Shale	y	Y	Y	Y	Y	Y	Y	Y	Y	Y	Y
Quartz	y	Y	Y	Y	Y	Y	Y	Y	Y	Y	Y
Lime											
Dolomite		Y	Y	Y	Y	Y	Y	Y	Y	Y	Y
Pyrite					Y	Y	Y	Y	Y	Y	Y
Chlorite					Y	Y	Y	Y	Y	Y	Y
<b>Logs Used</b>											0
MSFL/LLS/LLD	y y y	y y y	y y y	y y y	y y y	y y y	y y y	y y y	y y y	y y y	y y y
DTLN/DILF	n y	n y	n y	n y	n y	n y	n y	n y	n y	n y	n y
PEF/RHOB/TNPH	n n n	n n y	n y y	n y y	n y y	n y y	n y y	n y y	n y y	n y y	n y y
Remarks	Run 1, Res-Sonic only, gas show	Bad Hole, Minor gas	Main Gas Zone	Water	Water	Coals	Bad hole 2195-2205mRT		Otway Like character	Section not previously penetrated	

Table 2

WELL : Minerva-1

SUMMARY OF RESULTS  
=====

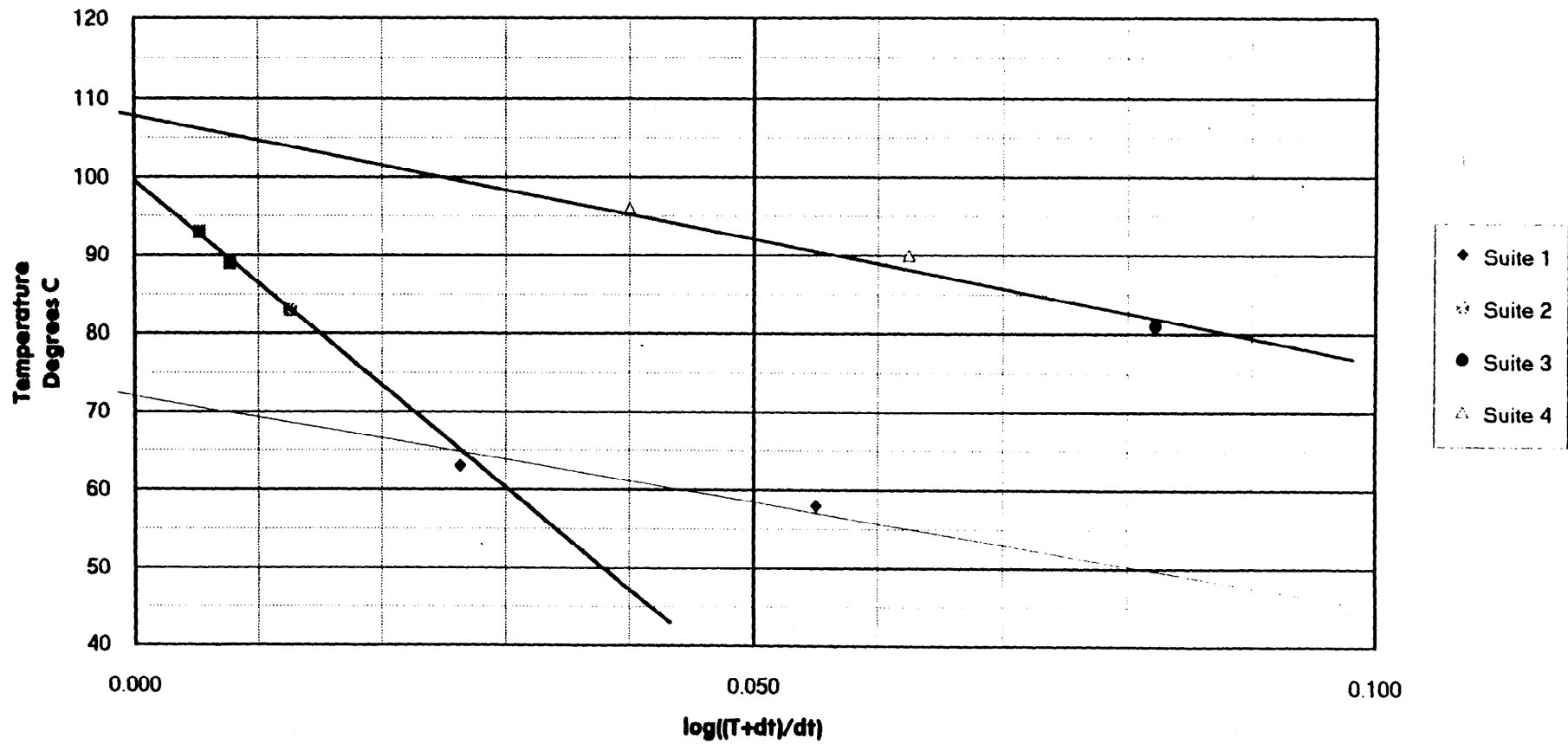
## CUT OFFS USED

Porosity >= 0.100  
Vshale <= 0.500

ZONE	DEPTH MD	GROSS	NET	N/G	POR	SW	E.P.C. (m)	E.H.C. (m)
NET PAY Water Saturation <= 0.700								
Sherbrook	1150.000 - 1175.000	25.0	0.2	1.	11.	65.	0.03	0.01
Up 1	1645.000 - 1655.000	10.0	1.4	14.	12.	54.	0.16	0.08
Upper 2	1655.000 - 1670.000	15.0	2.5	17.	15.	59.	0.39	0.18
Main Gas	1815.000 - 1948.000	133.0	118.5	89.	18.	19.	21.35	17.39
NET RESERVOIR Water Saturation <= 1.00								
Sherbrook	1150.000 - 1175.000	25.0	0.2	1.	11.	65.	0.03	0.01
Up 1	1645.000 - 1655.000	10.0	2.6	26.	12.	66.	0.30	0.10
Upper 2	1655.000 - 1670.000	15.0	4.6	31.	14.	65.	0.64	0.23
Main Gas	1815.000 - 1948.000	133.0	119.6	90.	18.	19.	21.48	17.41
Up Ship Wat	1948.000 - 2000.000	52.0	50.7	97.	17.	95.	8.48	0.45
Up Ship Tot	1815.000 - 2000.000	185.0	170.3	92.	18.	40.	29.96	17.86
Up Ship Wat	2115.000 - 2149.000	34.0	9.2	27.	14.	90.	1.26	0.12
Lr Ship	2149.000 - 2293.000	144.0	50.1	35.	12.	97.	6.00	0.18
Otway	2293.000 - 2410.000	117.0	32.7	28.	12.	93.	3.92	0.26

N.B. \*\*\* All thicknesses are calculated using data recorded along hole. \*\*\*  
\*\*\* File: c:\bhp\minerva\ressum.sum

# Minerva-1 Stabilized Bottom Hole Temperature

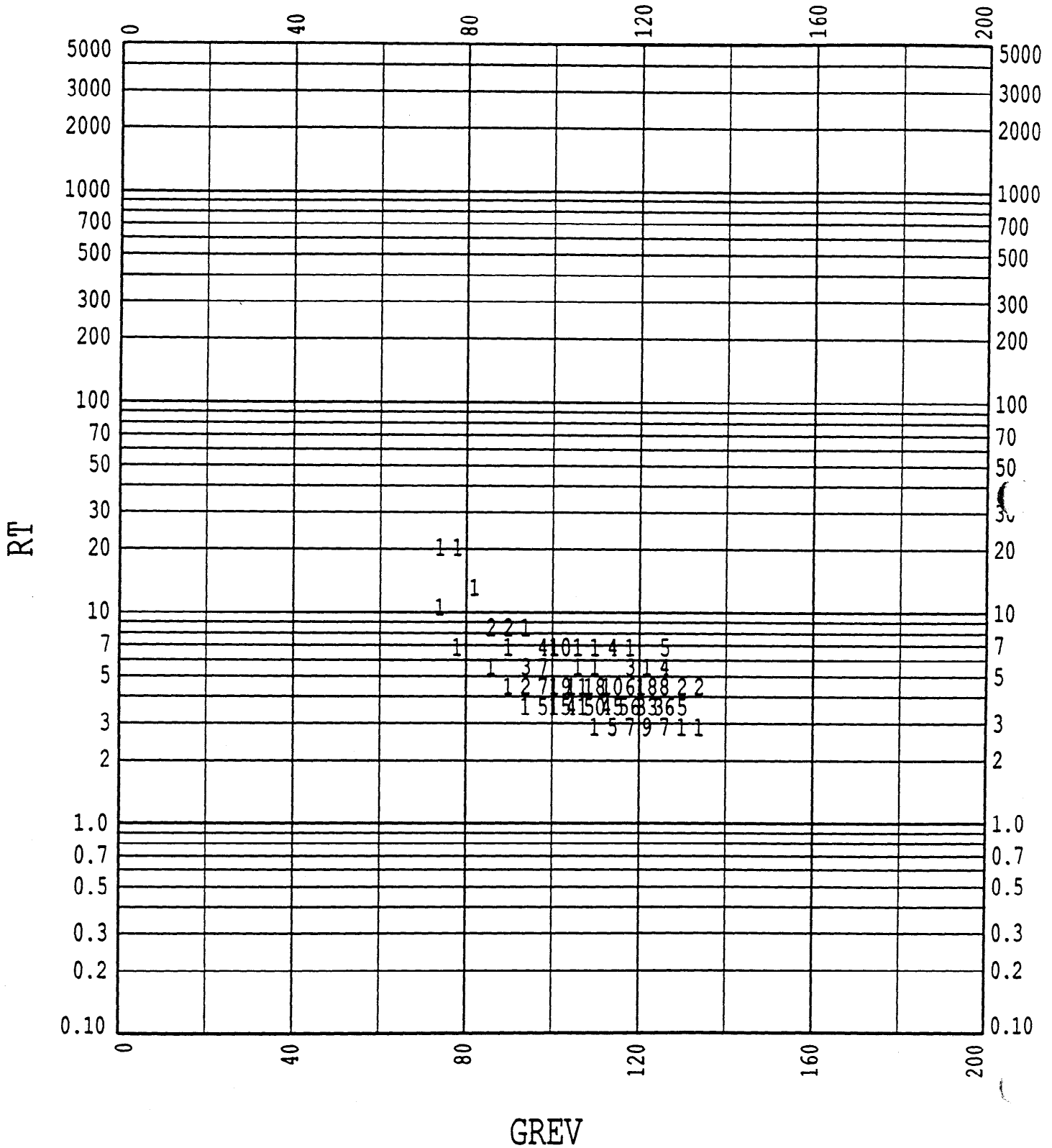


CROSSPLOT OF GREV AGAINST RT

Minerva-1

Sherbrook gas sand

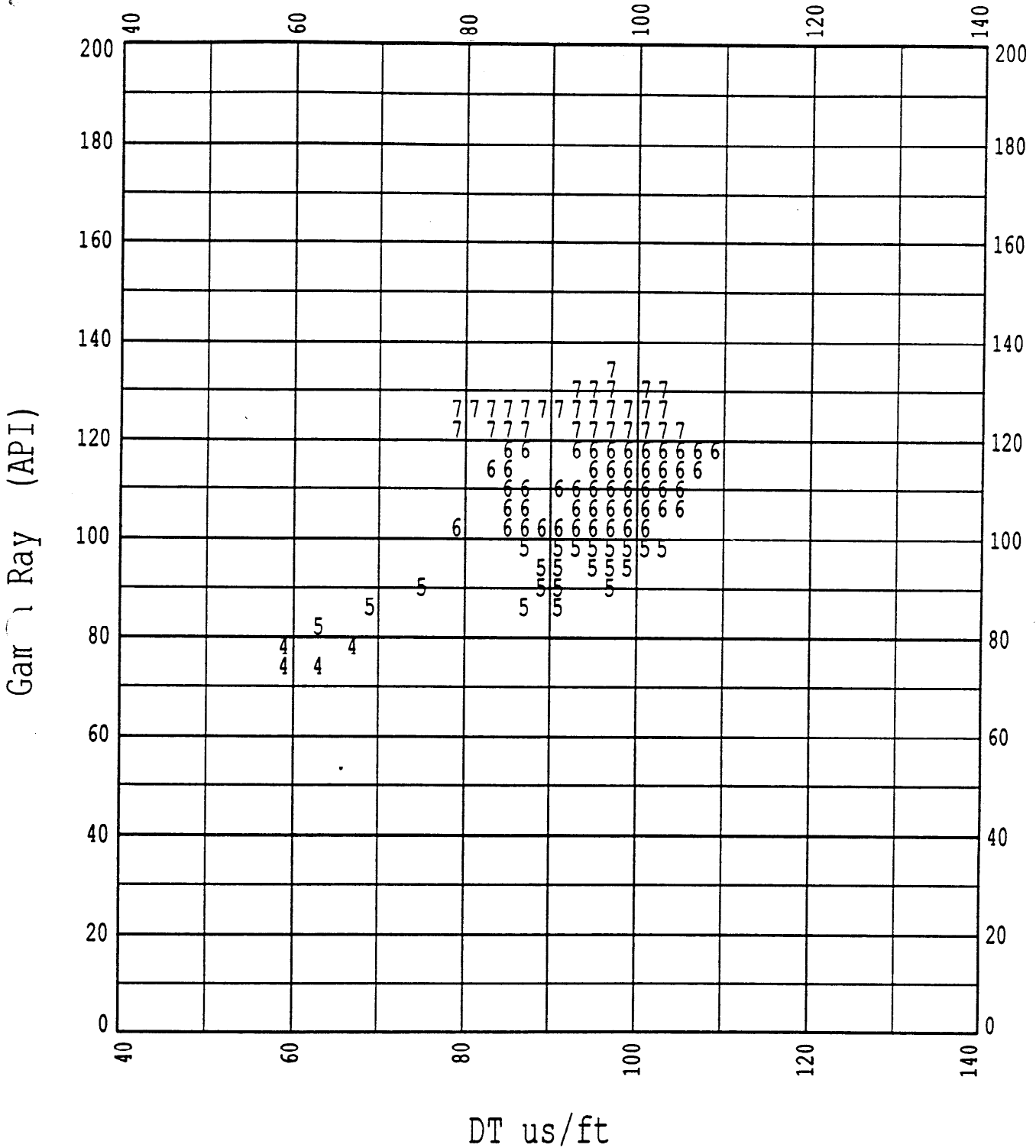
1170 mRT



Intervals:  
SHERBROOK

Figure 2

DT vs Gamma Ray  
Minerva-1  
Sherbrook gas show  
1170m



GREV

GREV

4      73.444 - 77.85  
5      81.563 - 99.381  
6      100.72 - 118.55  
7      120.77 - 133.54

————— 73.444 - 77.85  
————— 81.563 - 99.381  
————— 100.72 - 118.55  
————— 120.77 - 133.54

Intervals:  
SHERBROOK

Figure 3

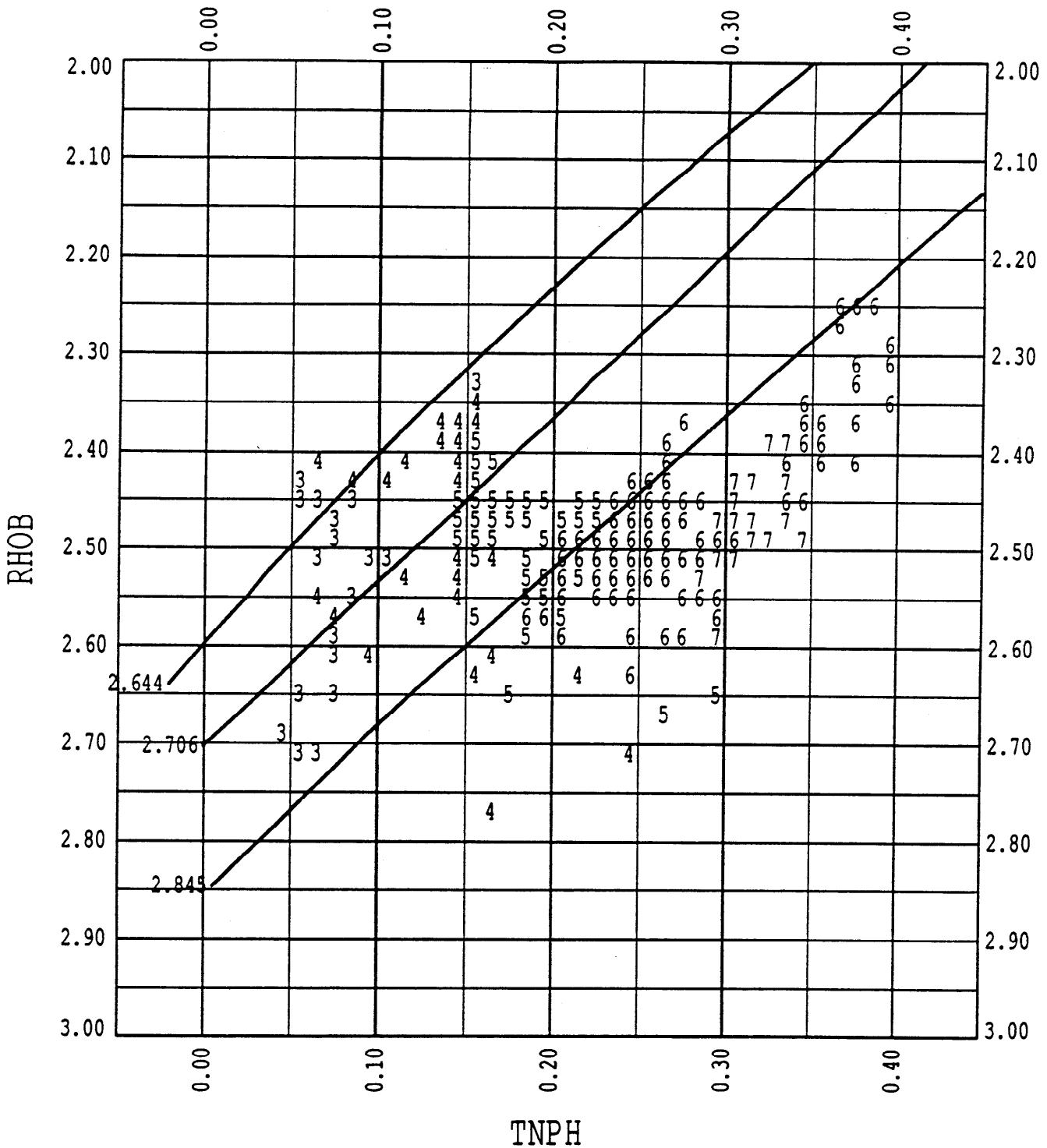


CROSSPLOT OF TNPH AGAINST RHOB

Minerva-1

Upper Shipwreck shale

1640-1700 mRT



GREV

3	42.742 - 59.039
4	60.432 - 79.856
5	80.722 - 99.765
6	100.35 - 119.87
7	121.41 - 131.54

GREV

—————	42.742 - 59.039
—————	60.432 - 79.856
—————	80.722 - 99.765
—————	100.35 - 119.87
—————	121.41 - 131.54

Acceptance expression:  
 RANGE (DEPTH,1640,1700) & CALI <= 9.5

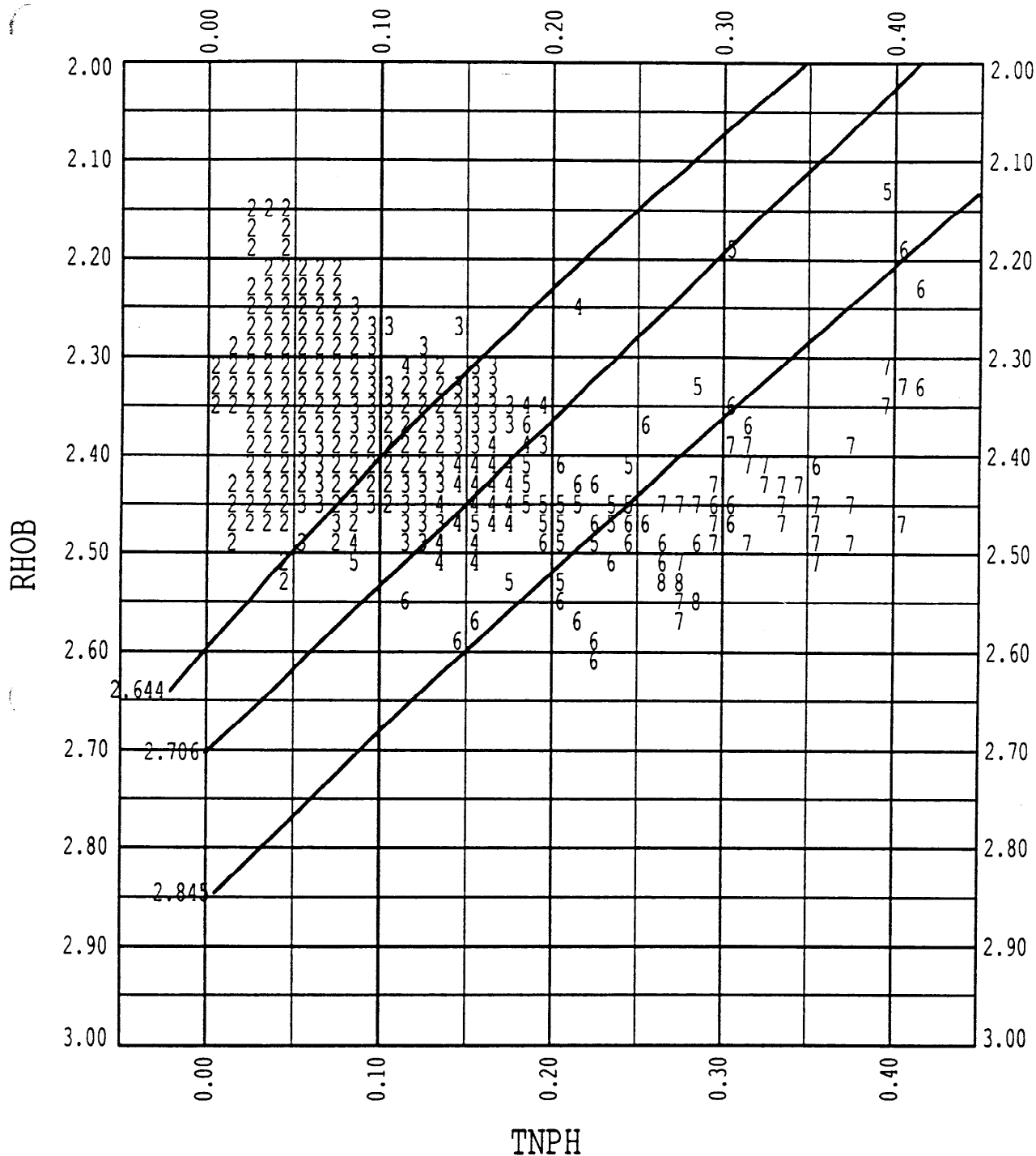
Figure 4

# CROSSPLOT OF TNPH AGAINST RHOB

Minerva-1

Upper Shipwreck Sand

1816-2149 mRT



GREV

GREV

2	25.917 - 39.886	—————	25.917 - 39.886
3	40.145 - 59.906	—————	40.145 - 59.906
4	60.216 - 78.709	—————	60.216 - 78.709
5	80.184 - 98.431	—————	80.184 - 98.431
6	100.93 - 119.36	—————	100.93 - 119.36
7	120.04 - 148.13	—————	120.04 - 148.13
8	151.52 - 153.06	—————	151.52 - 153.06

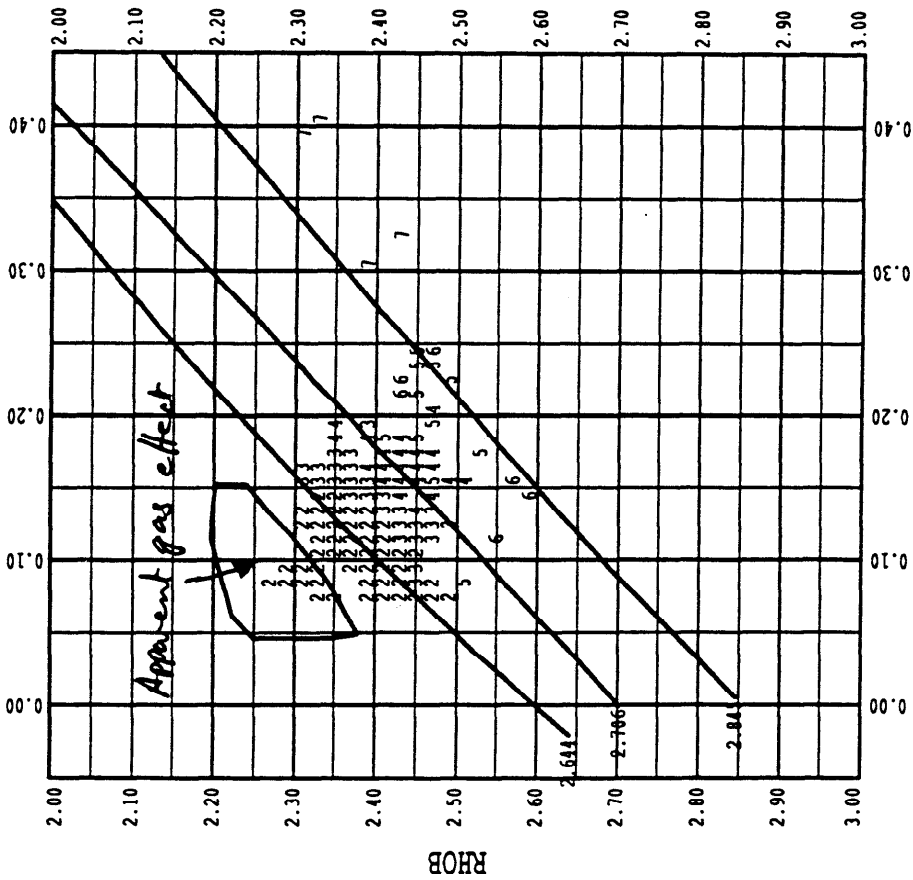
Intervals:

USMG1, USMG2, USMG3, USMG4, USW1, USW2

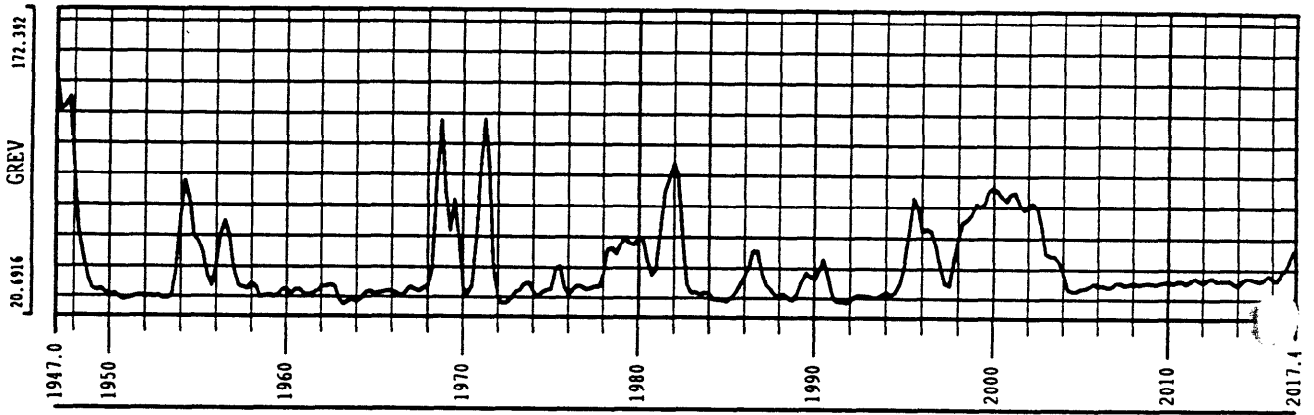
CROSSPLOT OF TNPH AGAINST RHOB

Minerva-1

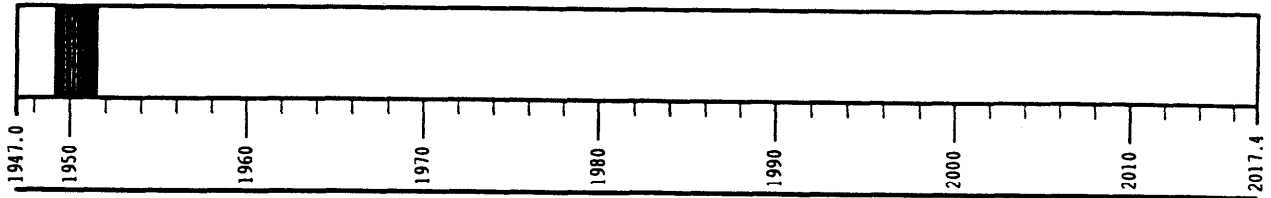
Upper Shipwreck water sand  
1947 - 2149 mRT



MINERVA-1

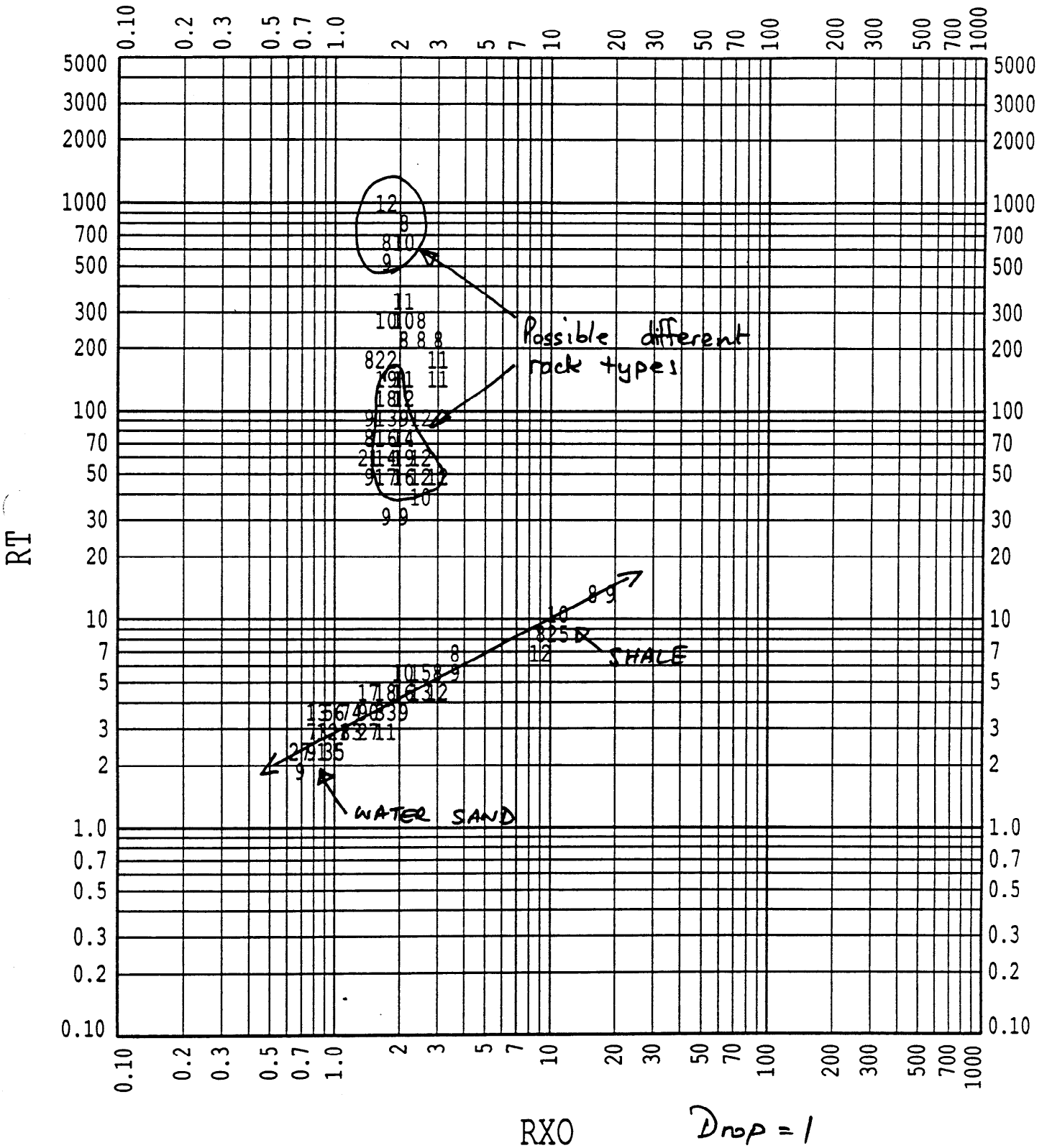


MINERVA-1



Apparent gas effect  
in water sand.

MINERVA-1  
 UPPER SHIPWRECK  
 CROSSPLOT OF RXO AGAINST RT



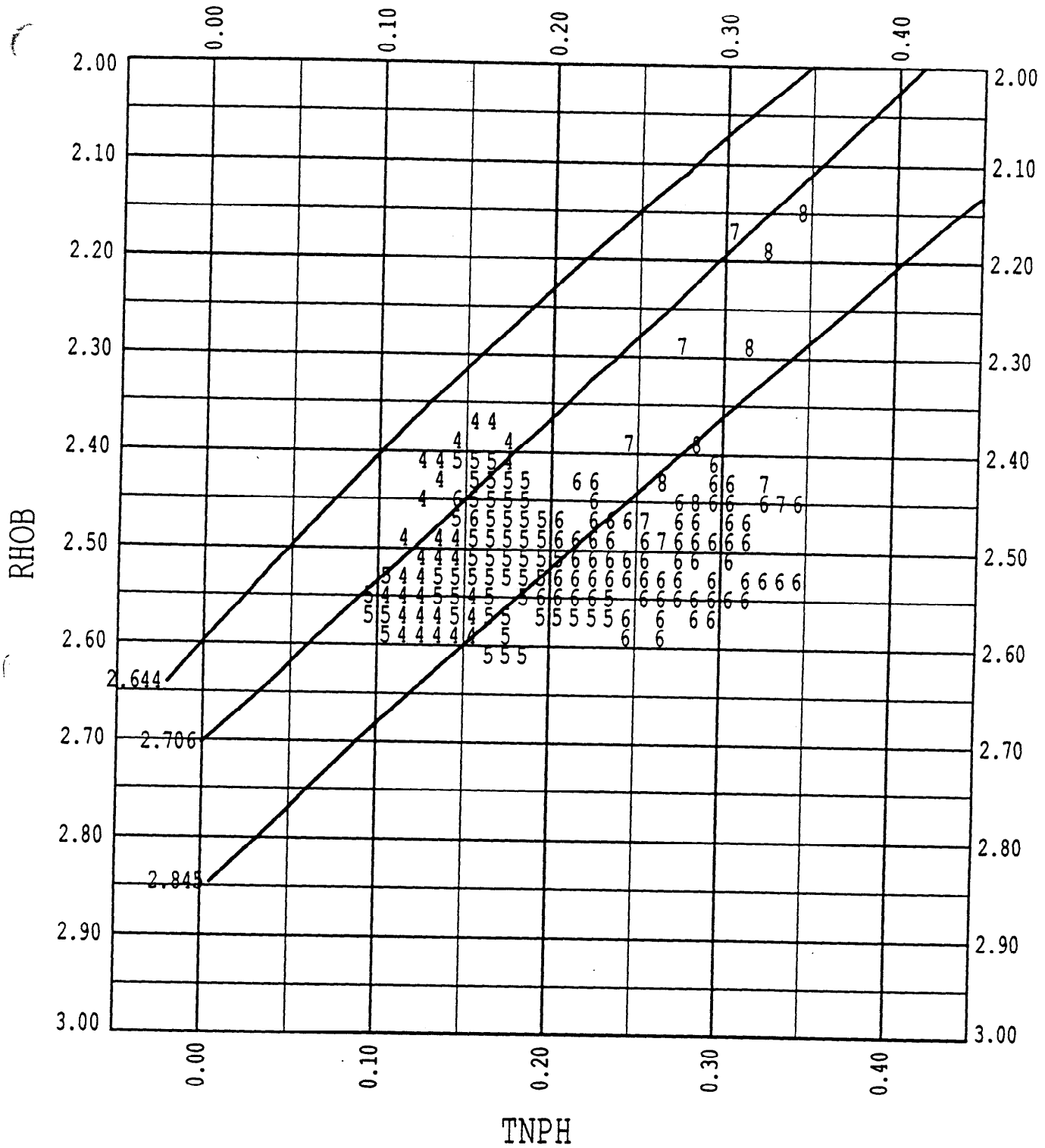
Intervals:  
 USG, USW1

Figure 7

# CROSSPLOT OF TNPH AGAINST RHOB

Minerva-1

Otway



GREV

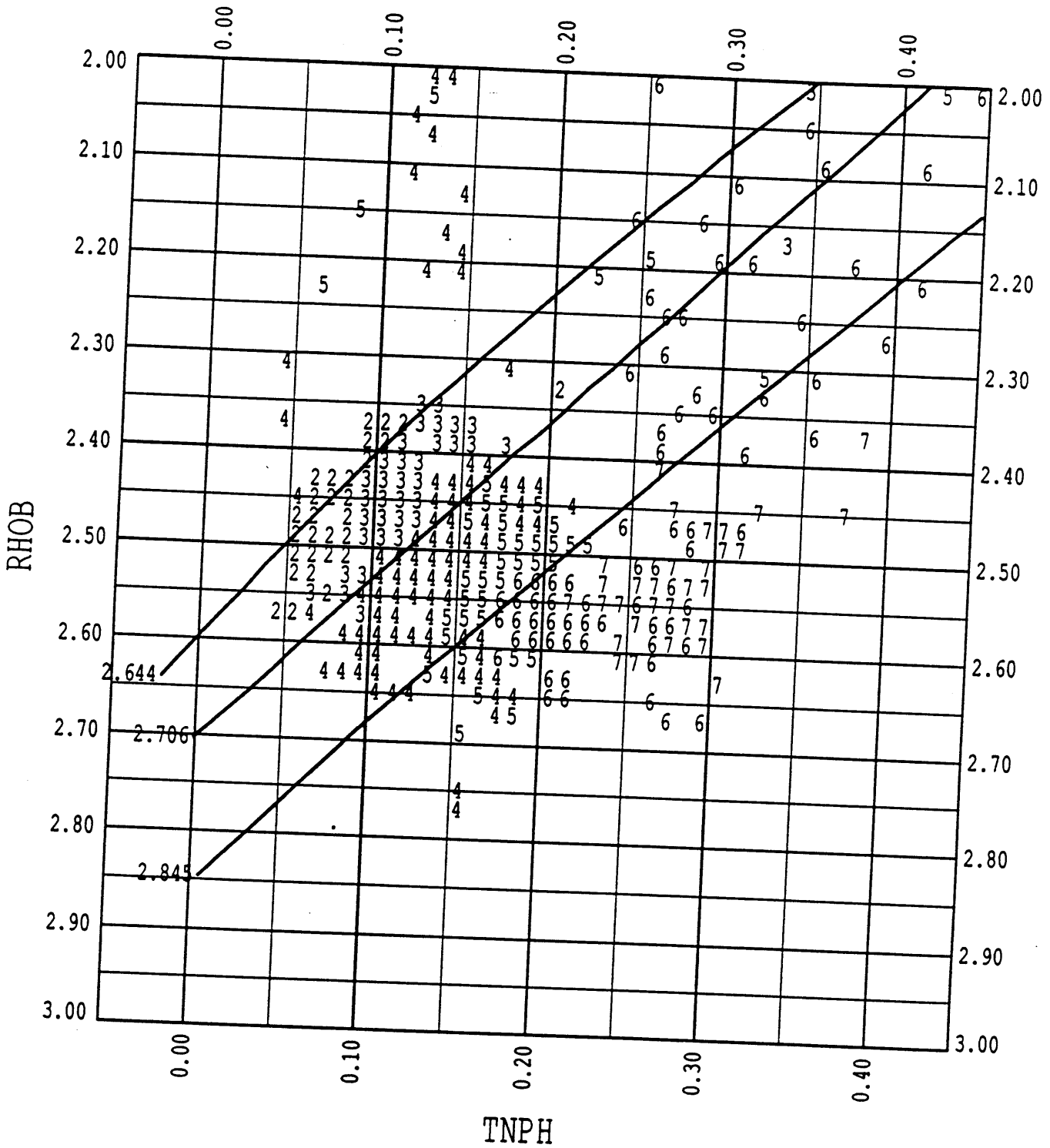
4	64.715 - 79.996
5	80.002 - 99.53
6	100.06 - 119.47
7	121.62 - 149.11
8	159.22 - 172.39

GREV

—————	64.715 - 79.996
—————	80.002 - 99.53
—————	100.06 - 119.47
—————	121.62 - 149.11
—————	159.22 - 172.39

Intervals:  
OTWAY

CROSSPLOT OF TNPH AGAINST RHOB  
 Minerva-1  
 Lower Shipwreck



GR\_COR

- 2 21.686 - 39.183
- 3 41.219 - 59.91
- 4 60.646 - 79.627
- 5 80.017 - 99.549
- 6 100.5 - 119.94
- 7 120.13 - 132.55

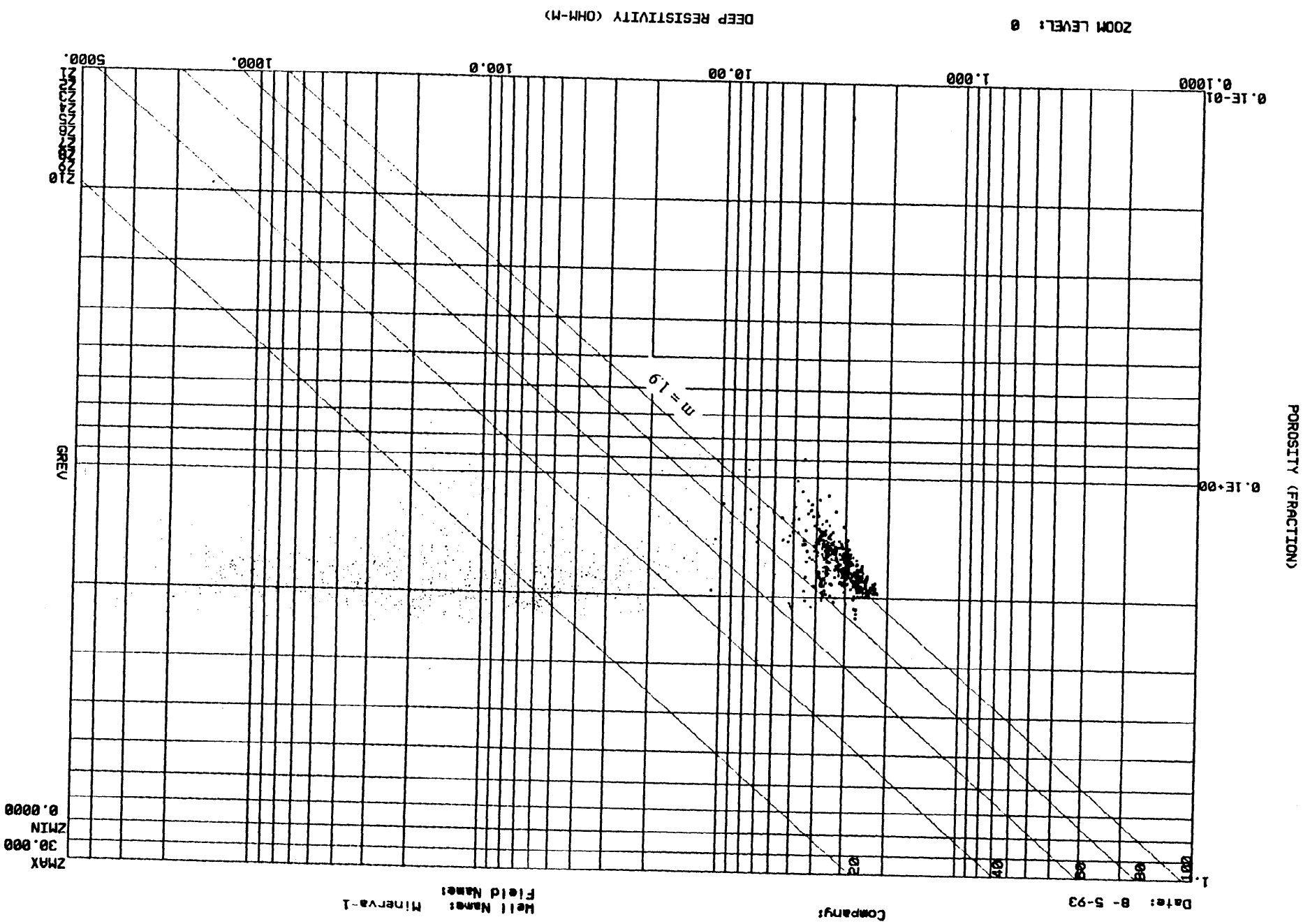
GR\_COR

- \_\_\_\_\_ 21.686 - 39.183
- \_\_\_\_\_ 41.219 - 59.91
- \_\_\_\_\_ 60.646 - 79.627
- \_\_\_\_\_ 80.017 - 99.549
- \_\_\_\_\_ 100.5 - 119.94
- \_\_\_\_\_ 120.13 - 132.55

Intervals:  
 LS

Figure 8

Pickett Plot  
Upper Shipwreck Sand



Date: 8-5-93

Company:

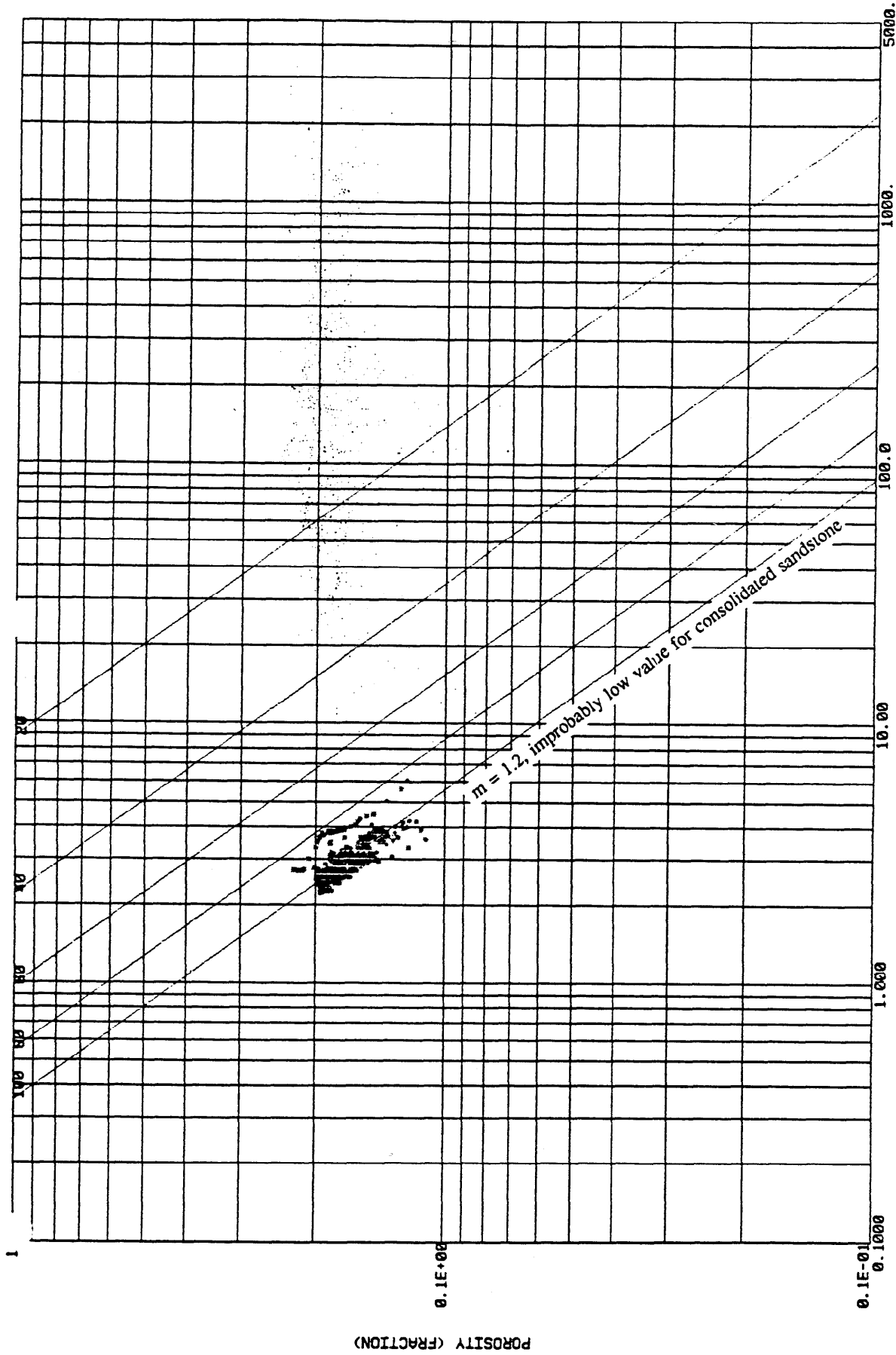
Well Name: Minerva-1

2000.0, 1945.0, 1945.0, 1815.0

Well Name: Minerva-1  
Field Name:

Company:

Date: 8-5-93



ZOOM LEVEL: 0 DEEP RESISTIVITY (OHM-M)

Pickett Plot  
Upper Shipwreck water sand

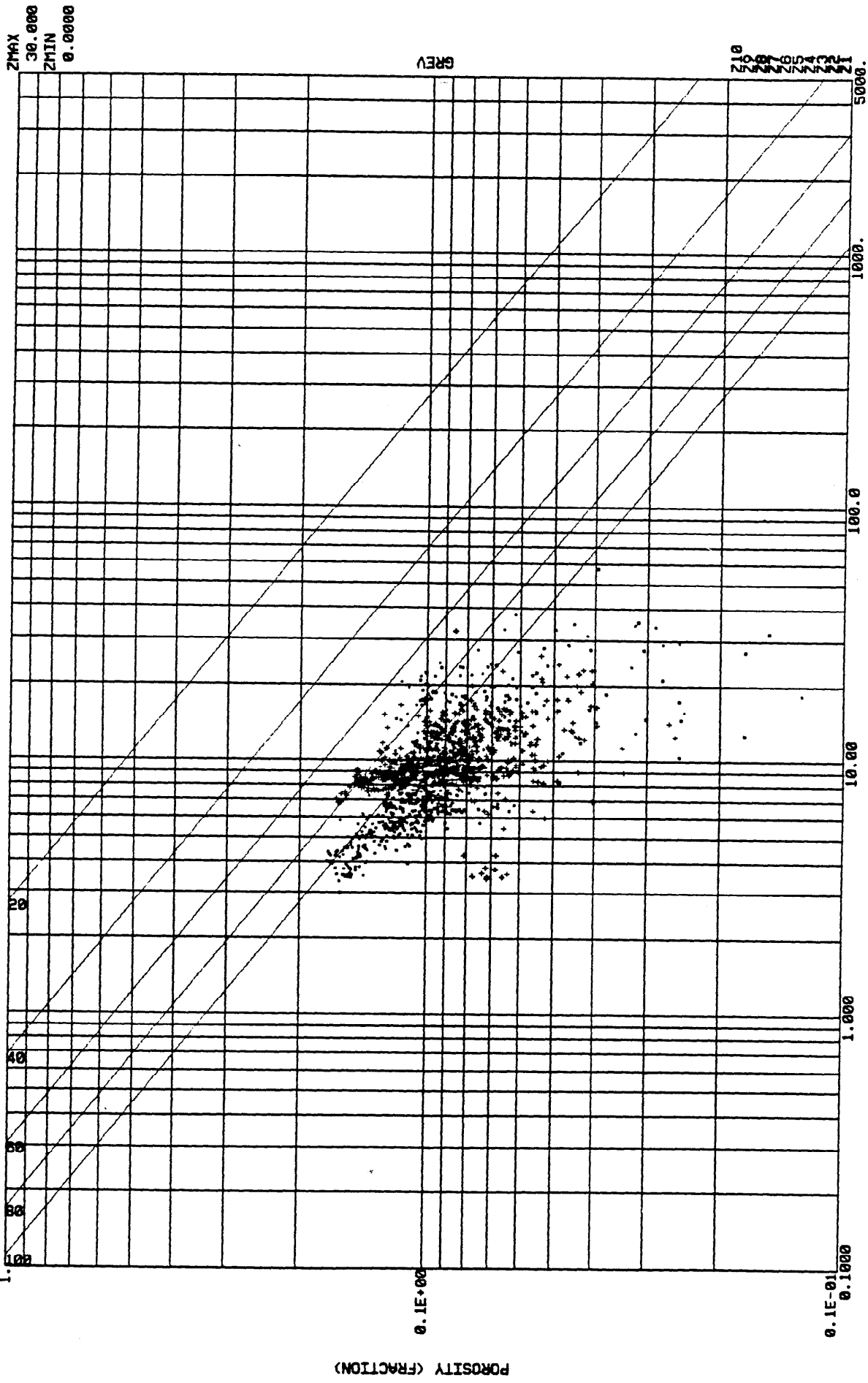
2000.0 1945.0 1815.0



Well Name: Minerva-1  
Field Name:

Company:

Date: 8-5-93



DEEP RESISTIVITY (OHM-M)

ZOOM LEVEL: 0

2415.0. 2293.0 2293.0. 2149.0

### Pickett Plot Lower Shipwreck Sandstone and Otway Group

Figure 12

PE602765

This is an enclosure indicator page.  
The enclosure PE602765 is enclosed within the  
container PE900058 at this location in this  
document.

The enclosure PE602765 has the following characteristics:

ITEM-BARCODE = PE602765  
CONTAINER\_BARCODE = PE900058  
    NAME = Minerva 1 Composite Plot  
    BASIN = Otway  
    PERMIT = VIC/P31  
    TYPE = WELL  
    SUBTYPE = WELL-LOG  
DESCRIPTION = Minerva 1 Composite Plot, Appendix 4  
REMARKS = old barcode PE900060 replaced with  
          PE602765  
DATE-CREATED = \*  
DATE-RECEIVED = \*  
    W\_NO = W1079  
    WELL-NAME = MINERVA 1  
CONTRACTOR =  
CLIENT\_OP\_CO =

(Inserted by DNRE - Vic Govt Mines Dept)

PE602766

This is an enclosure indicator page.  
The enclosure PE602766 is enclosed within the  
container PE900058 at this location in this  
document.

The enclosure PE602766 has the following characteristics:

ITEM-BARCODE = PE602766  
CONTAINER\_BARCODE = PE900058  
    NAME = Minerva 1 MWD & Wireline Comparison  
    BASIN = Otway  
    PERMIT = VIC/P31  
    TYPE = WELL  
    SUBTYPE = WELL-LOG  
    DESCRIPTION = Minerva 1 MWD & Wireline Comparison,  
                  Appendix 4  
    REMARKS = old barcode PE900061 replaced with  
              PE602766  
DATE-CREATED' = \*  
DATE-RECEIVED = \*  
    W\_NO = W1079  
    WELL-NAME = MINERVA 1  
    CONTRACTOR =  
    CLIENT\_OP\_CO =

(Inserted by DNRE ~ Vic Govt Mines Dept)

PE602767

This is an enclosure indicator page.  
The enclosure PE602767 is enclosed within the  
container PE900058 at this location in this  
document.

The enclosure PE602767 has the following characteristics:

ITEM-BARCODE = PE602767  
CONTAINER\_BARCODE = PE900058  
    NAME = Minerva 1 Final Interpretation  
    BASIN = Otway  
    PERMIT = VIC/P31  
    TYPE = WELL  
    SUBTYPE = WELL-LOG  
    DESCRIPTION = Minerva 1 Final Interpretation,  
    Appendix 4  
    REMARKS = old barcode PE900059 replaced with  
    PE602767  
DATE-CREATED = \*  
DATE-RECEIVED = \*  
    W\_NO = W1079  
    WELL-NAME = MINERVA 1  
CONTRACTOR =  
CLIENT\_OP\_CO =

(Inserted by DNRE - Vic Govt Mines Dept)

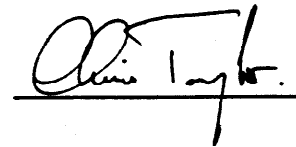


**Minerva-1**

**RFT REPORT**

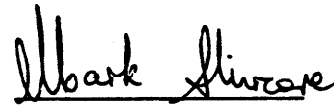
9<sup>th</sup> February 1993

Prepared by



**Chris Taylor**  
Reservoir Operations Engineer

Approved by



**Mark Shircore**  
Manager New Developments

## MEMORANDUM



TO: SEE DISTRIBUTION LIST  
FROM: NEW DEVELOPMENTS MANAGER  
DATE: 11th June, 1993  
OUR REF: MS:CT:1349:MEM  
FILE: MIN-1/WL/G02/R

### MINERVA-1 RFT REPORT

Please find attached the Minerva-1 RFT report.

#### Summary/Conclusions

The results of the Minerva-1 open hole RFT surveys indicated that the well intersected three gas and water bearing sands in the Upper Shipwreck Group. Two shallower gas bearing sands were interpreted in what was called the Top Upper Shipwreck Group 1 and 2 sands, with gas-water contacts at 1912.8 and 1920.0 mSS respectively. No gradients were determined in these sands due to the sparse number of pressure readings taken. The contacts were calculated assuming a common aquifer and gas gradient with the main reservoir section. The main reservoir sand contained a 98.7 m gas column with a GOC at 1914.7 mSS.

Three fluid samples were recovered from the Upper Shipwreck Group. Analysis of the samples recovered from 1623 and 1901.6 mSS indicated the presence of gas and condensate, both with a condensate-gas ratio (pentanes plus) of 5 stb/MMscf. The sample from 1913.0 mSS recovered dry gas and contained 1.8% carbon dioxide, 0.9% nitrogen, and 93.5% methane.

A handwritten signature in cursive script that reads "Mark Shircore".

MARK SHIRCORE  
NEW DEVELOPMENTS MANAGER

**Distribution List:**

General Manager Exploration - J. Mitchell

Production Geoscience Manager - R. Hogarth

Area Exploration Manager (Otway Basin) - R. Marlow

Senior Petroleum Geologist (Otway Basin) - M. Durham

Senior Petroleum Engineer - Darwin - P. Moore



## TABLE OF CONTENTS

1. OPERATIONS SUMMARY
2. CONCLUSIONS
3. GEOLOGY
4. RFT PROGRAM
  - 4.1 Objectives
  - 4.2 RFT Tool Configuration
  - 4.3 Open-hole Log Reference
  - 4.4 Tool Performance
5. RFT PRE-TEST INTERPRETATION
  - 5.1 Pressures
  - 5.2 Temperature
  - 5.3 Quality Control
  - 5.4 Reservoir Fluid Gradients
  - 5.5 Fluid Contacts
  - 5.6 Permeabilities
  - 5.7 Comparison to Other Wells
6. RFT SAMPLES
  - 6.1 Sampling Summary
  - 6.2 Hydrocarbon Properties
  - 6.3 Water Properties
7. REFERENCES

## LIST OF TABLES

Table 1	Minerva-1 Well Data
Table 2	Minerva-1 Pretest Data
Table 3a	Minerva-1 General Sample Data: Sample 1.
Table 3b	Minerva-1 General Sample Data: Sample 2.

## LIST OF FIGURES

Figure 1	Location Map
Figure 2	Pressure vs Depth: Raw Data
Figure 3	Temperature vs Depth
Figure 4	Temperature vs Time
Figure 5	Final - Initial Hydrostatic Pressures
Figure 6	Hydrostatic Pressure vs Depth: HP Gauge
Figure 7	HP - Strain Gauge Data
Figure 8	RFT Formation Pressure vs Depth: HP and Strain Gauge (psia)
Figure 9a	Interpreted RFT Data: Formation Pressure vs Depth (HP Gauge)
Figure 9b	Interpreted RFT Data: Formation Pressure vs Depth (Strain Gauge)
Figure 10a-1	Interpreted RFT Data: Formation Pressure vs Depth Expanded Scale (HP)
Figure 10b-1	Interpreted RFT Data: Formation Pressure vs Depth Expanded Scale (Str)
Figure 10a-2	Interpreted RFT Data: Formation Pressure vs Depth Expanded Scale (HP)
Figure 10b-2	Interpreted RFT Data: Formation Pressure vs Depth Expanded Scale (Str)
Figure 10a-3	Interpreted RFT Data: Formation Pressure vs Depth Expanded Scale (HP)
Figure 10b-3	Interpreted RFT Data: Formation Pressure vs Depth Expanded Scale (Str)
Figure 11	Interpreted RFT Data: Formation Pressure vs Depth Expanded Scale (HP & Strain Gauge)
Figure 12	Well Comparison: Pecten-1A, La Bella-1, Eric The Red-1, Minerva-1.
Figure 13	Gas Analysis Data: Petrolab vs Wellsite Results

## APPENDIX A: Petrolab PVT Analysis Results

## ENCLOSURES

Enclosure 1	Minerva-1 DDL-MSFL-GR Log, 21st March 1993.
-------------	---

1. OPERATIONS SUMMARY

Minerva-1 was spudded on the 8<sup>th</sup> March 1993 and reached TD on the 20<sup>th</sup> March 1993 at a depth of 2024 mRT. Suite 2 open hole logging commenced on the 21<sup>st</sup> March 1993, with RFT procedures lasting 24.5 hours between 13:30 hrs, 22<sup>nd</sup> March and 14:00 hours, 23<sup>rd</sup> March. Three RFT runs were made, during which 33 pretests were attempted. Of those, 28 were successful, 3 tight, and 2 possibly lost seals. Three segregated samples (1 gallon and 6 gallon chambers) were taken.

Following the RFT survey, CST's were taken and 7" casing set to 2108.0 mRT. The well was then deepened using a 6" bit to 2425.0 mRT and logged. The well was plugged back to 2074.0 mRT and production tested over the intervals 1816.0 to 1821.0 and 1825.0 to 1827.5 mRT, flowing at up to 28.4 MMscf/d with a CGR of 2 stb/MMscf, ( $T_{sep} = -1$  °C,  $P_{sep} = 220$  psig). Following the production test the well was suspended.

1821 m 28.4 MMscf/d

## 2. CONCLUSIONS

Based upon the data and interpretations contained in this report, the following conclusions can be made:

- 1/. Three gas bearing sands were intersected in the Upper Shipwreck Group.
- 2/. The two shallower gas sands (Top Upper Shipwreck 1 and 2 sands) have probable GWC's at 1912.8 and 1920.0 mSS respectively, (assuming a 0.171 psi/m gas gradient and common aquifer with the main reservoir). The deeper gas sand (Upper Shipwreck main reservoir sand) has a GWC at 1914.7 mSS.
- 3/. The Top Upper Shipwreck 1 sand unit is 2.2 psi underpressured, while the Top Upper Shipwreck 2 sand is 6.4 overpressured with respect to the main Upper Shipwreck reservoir sand (assuming a common 0.171 psi/m gas gradient).
- 4/. A water bearing sand was intersected below the gas in the Upper Shipwreck main reservoir sand. The aquifer had a pressure gradient of 1.40 psi/m, and is close to, or at, the expected hydrostatic pressure.
- 5/. Three fluid samples were recovered from the Upper Shipwreck Group. The sample from 1942.5 mRT recovered dry gas whereas the samples from 1649.8 and 1931.0 mRT both recovered gas and condensate. The table below details the gas compositions;

<u>Component</u>		<u>Mole %</u>		
		<u>1931.0</u>	<u>1942.5</u>	<u>1649.8</u> mRT
Carbon Dioxide	CO <sub>2</sub>	1.80	1.83	0.32
Nitrogen	N <sub>2</sub>	0.90	0.89	1.26
Methane	C <sub>1</sub>	93.45	93.47	94.05
Ethane	C <sub>2</sub>	2.22	2.24	2.53
Propane	C <sub>3</sub>	0.84	0.83	1.05
n-Butane	n-C <sub>4</sub>	0.12	0.11	0.18
i-Butane	i-C <sub>4</sub>	0.20	0.19	0.23
Pentane*	C <sub>5</sub> *	0.47	0.44	0.38

### 3. GEOLOGY

Minerva-1 was proposed in Vic/P31 in Offshore Otway Basin to test a tilted fault block at the Lower Shipwreck Group primary target level, plus coincident anticlinal closure at levels within the Tertiary section, (Figure 1). At the primary target depth the structure is formed by three way dip closure plus fault closure, with the major northwest-southeast trending bounding normal fault being downthrown to the southwest. The Primary Target reservoir was predicted at a depth of 1525 mRT at the top Lower Shipwreck Group, with porosities expected to be in the order of 24%. Claystones of the Upper Shipwreck Group were proposed to seal the primary target. Mature coals and lacustrine sediments of the Eumeralla Formation were predicted to charge the prospect via vertical migration up fault planes from kitchen areas surrounding the prospect.

Minerva-1 spudded at 1200 hours 8<sup>th</sup> March 1993. The well drilled to 1812 mRT (driller) at which depth gas shows were recorded from good quality sandstone. Three cores were subsequently cut from 1821 to 1847 mRT (driller). The well then drilled ahead to a total depth of 2425 mRT (RT=25 mASL) on 29<sup>th</sup> March 1993 in Otway Group sediments.

A total hydrocarbon column of 135 m is interpreted from wireline logs over the interval 1816 to 1951 mRT within sandstones and minor claystones of the basal section of the Upper Shipwreck Group. Reservoir sandstones are calculated to average 19% porosity and range from 1 to 10 D permeability over a calculated net to gross of 84% (net reservoir of 112 m). The accumulation is sealed by claystones within the upper section of the Upper Shipwreck Group. Secondary targets within the Tertiary section did not intersect any hydrocarbon bearing sand.

Table 1 contains the well data sheet which summarises well information.

### 4. RFT PROGRAM

#### 4.1. Objectives

The three main objectives of the Minerva-1 RFT program were as follows:

- a. Determine the fluid gradients and contacts within the reservoir sections of the Minerva-1 well.
- b. Recover representative hydrocarbon samples from the reservoir in order to determine PVT properties.
- c. Determine fluid types within the reservoir sections of the Minerva-1 well.

#### 4.2 RFT Tool Configuration

The formation sampling tool used on Minerva-1 was the Schlumberger RFT tool, incorporating a long nose probe with a standard packer and a HP quartz crystal gauge. The tool was run with an AMS and Gamma Ray sonde and three 1" stand-offs. A 1 gallon upper and a 6 gallon lower sample chamber were used, both with water cushions. Four x 20/1000" chokes were used in both the 1 and 6 gallon chambers.

#### 4.3 Open-Hole Log Reference

All Minerva-1 RFT depths were correlated to the 8½" open hole DLL-MSFL-GR hole log recorded on 21" March 1993, (see Enclosure 1).

The hole was in good condition over the intervals programmed for the RFT survey. The hole diameter was between 8½" and 8" over the entire RFT survey section.

#### 4.4 Tool Performance

##### RFT-B

Stabilisation times were relatively short for the HP pressure gauge. There were no operational problems with the tool.

## 5. RFT PRETEST INTERPRETATION

### 5.1 Pressures

All pretest and sample pressures are given in Table 2 and are shown plotted in Figure 2. Of the 33 pretests attempted; 28 pretests recorded good formation pressures, 3 were tight, and two pretests had suspected lost seals as they stabilised to near hydrostatic pressure with what appeared to be abnormal pressure buildup profiles.

All pretest pressures were obtained when both the HP and strain gauge pressures and temperatures had stabilised. As can be seen from the pressure vs depth plots, the HP formation pressures seem to have considerable scatter towards the base of the gas column. The cause of this scatter cannot be determined. All QC plots and analysis indicate good tool performance and repeatability.

### 5.2 Temperature

Figure 3 shows the temperatures measured in the Minerva-1 well versus depth, and Figure 4 shows the temperature versus time from the start of the RFT survey. The maximum temperature recorded during the RFT survey was 97.4 °C at 1992.0 mRT. This temperature was recorded 38.5 hours after circulation was stopped.

### 5.3 Quality Control

Initial and final HP gauge hydrostatic mud pressures recorded before and after each pretest were in reasonable agreement (see Table 2 and Figure 5). Figure 6 shows a plot of the hydrostatic pressure gradient measured with the HP gauge. The hydrostatic gradient indicates a mud specific gravity (SG) of 1.14. This is in good agreement with the mud gravity measured on the rig (1.15 S.G).

Figure 7 shows the pressure difference between the HP and strain gauges for all of the pretests. As can be seen from the figure, the average difference is  $14.9 \pm 1.0$  psi. As the HP gauge reads absolute pressure and the strain gauge reads gauge pressure, it would be expected that the pressure difference between the two gauges would be 14.7 psi. But, since the strain gauge is only absolutely accurate to within 0.1 % of full scale, ( $\pm 10$  psi), the difference of 14.9 psi between the strain and HP gauges is an extremely good result.

### 5.4 Reservoir Fluid Gradients

Figures 8 to 11 show the interpreted Minerva-1 RFT results. Three separate gas sand units were intercepted by the well; the Top Upper Shipwreck 1<sup>\*</sup> sand unit, (1648.8 to 1652.0 mRT), the Top Upper Shipwreck 2<sup>\*</sup> sand unit, (1661.0 to 1668.0 mRT), and the main reservoir section in the Upper Shipwreck Group (1816.0 to 1995.0<sup>\*</sup> mRT).

One valid pretest was obtained in the Top Upper Shipwreck 1 sand unit. The pressure point lies 2.2 psi below the extrapolated pressure gradient from the main reservoir, (Figure 9a). The validity of this pretest is confirmed as a gas sample was also recovered from the Top Upper Shipwreck 1 sand during run 3. The pretest performed prior to opening the lower chamber confirmed the formation pressure at this depth.

One pretest was performed in the Top Upper Shipwreck 2 sand. The pressure in this sand was 6.4 psi above the extrapolated pressure from the main reservoir, (Figure 9a). The validity of the test in the Top Upper Shipwreck 2 sand is less conclusive as there is only one data point and no sample data.

\*Informal naming used.



There were also two pretests performed in the lower section of the Top Upper Shipwreck 2 sand. Gamma ray logs indicate that this sand is a little shalier than the upper section. The two pretests performed in this shalier section of the Top Upper Shipwreck 2 sand had abnormal pretest buildups and stabilised to within a few psi of the hydrostatic pressure. This could indicate that the pressure in this lower part of the second sand was indeed within a few psi of hydrostatic, or that there was some kind of communication between the mud column and the formation. It seems that the latter conclusion is more likely.

As mentioned previously in section 5.1, the scatter in pretest data is considerable. Figure 8 shows both HP and strain gauge pretest data superimposed upon each other, (the strain gauge data has been converted to psia by adding 14.97 psi). Such that:

$$\sum (HP - (Strain+x))^2 \text{ is a minimum, } (x=14.97).$$

As can be seen in this figure, the strain gauge data seems to contain less scatter than does the HP data. It was decided to use the strain gauge data in the interpretation of the Minerva-1 RFT data.

Figures 10a-1 to 10b-3 show expanded scale HP(a) and strain gauge(b) pretest data. Figure 11 shows both HP and strain gauge data from the region around the GWC. This figure shows the considerable scatter observed in pretest data in the lower 10m of the gas column.

One possible explanation for the scatter in the recorded data is that the pretests which are overpressured were taken in locally supercharged sands. As the sand in which these pretests were taken appears on the logs to be of good quality and high porosity and permeability, supercharging seems unlikely.

The repeatability of these pressures was established with pretests 22 and 26, (Figure 10a-3) which were taken at the same depth but at different times, and both indicated an overpressuring at 1939.5 mRT, (1910.1 mSS). This effect is also apparent in the strain gauge data, (Figure 10b-3). The scatter however does not impact greatly on the overall interpretation of the data from the RFT survey.

A gas gradient of 0.171 psi/m (strain gauge) was interpreted over the main reservoir section from 1792.0 mSS to the GWC at 1914.7 mSS

A water gradient of 1.40 psi/m (both HP and strain gauge) was interpreted below 1914.7 mSS. Seven valid pretests were obtained over this section of the Lower Shipwreck Group defining this gradient well. It should be noted that there was no significant scatter in the aquifer pressure data which was taken immediately after the gas zone pretests.

Another interpretation of the data is shown in figure 9c. This is based upon the assumptions that the pretest data from the Top Upper Shipwreck 2 sand is supercharged, and that the Top Upper Shipwreck sand and the main Upper Shipwreck sand are in hydraulic communication. This interpretation results in a gas column gradient of 1.72 and a GWC at 1914.7 mSS. Either interpretation may be valid and the effect upon reserves etc. is insignificant regardless of which interpretation is used.

## 5.5 Fluid Contacts

Figures 10a-1 to 10b-3 show the interpreted Minerva-1 RFT results over the Upper Shipwreck sands. Shown in figures 9a and 9b are three gas water contacts (GWC) at 1912.8, 1914.7, and 1920.0 mSS. The upper contact is associated with the gas sand in the Top Upper Shipwreck 1 sand, the second contact is associated with the main reservoir sand unit in the Upper Shipwreck Group, and the third with the Top Upper Shipwreck 2 sand. Note; the position of the GWC in the Top Upper Shipwreck sands assumes a gas gradient of 0.171 psi/m and connection with the main gas sand's aquifer.

From pretest data it has been determined that the Top Upper Shipwreck 1 gas sand is underpressured by 2.2 psi with respect to the main reservoir sand unit, and the Top Upper Shipwreck 2 sand unit is over pressured by 6.4 psi. This assumes a common aquifer with the main reservoir unit. This assumption results in a GWC 1.9m shallower, and 5.3m deeper in the two Top Upper Shipwreck sands with respect to the main Upper Shipwreck reservoir sand.

The assumption of a common aquifer cannot be proven. However, the composition of the samples indicate that there are small compositional differences between the gas in the main reservoir and that present in the Top Upper Shipwreck 1 sand, indicating hydrostatic isolation of the gas zones.

## 5.6 Permeabilities

Spherical mobility estimates from the pretests are given in Table 2. The assumptions made to correct the calculated spherical mobility to horizontal permeability are:

1. Mud filtrate viscosity<sup>2</sup> = 0.34 cP  
(Temp = 90°C, Pressure = 2700 psia,  
Equivalent NaCl salinity = 25,000 ppm)
2.  $K_h/K_v = 1$

The correction used was:

$$K_h = [K_D \times (K_h/K_D)]/K_{rw}$$

Where,	$K_D$	=	Drawdown permeability = (Mobility) x (Filtrate Viscosity)
	$K_h/K_D$	=	1.0 ratio of horizontal to drawdown permeability. This is a function of $K_h/K_v$ and flow geometry; which is spherical, (Table A1, Ref [1]).
	$K_{rw}$	=	relative permeability to filtrate.

Reference [1] suggests the use of  $k_{rw} = 0.3$  for formations with a hydrocarbon saturation and a permeability greater than one Darcy, and  $k_{rw} = 0.15$  for permeabilities less than 1 Darcy. A  $k_{rw}$  of 1.0 is used for water saturated sands.

From the calculation results shown in Table 2, the main reservoir sand has permeabilities between 10 and 1800 mD, averaging about 600 mD. The Top Upper Shipwreck 1 and 2 sands have permeabilities in the order of 20 to 30 mD.

Initial welltest interpretation indicate that the permeability of the zones tested was in the order of 1000-2000 mD. Pretests performed in the sand where the testing was performed had permeabilities in the order of 1500 mD according to the pretest data interpretation. This illustrates the qualitative nature of the pretest spherical mobility calculation, especially in high permeability formations.

## 5.7 Comparison to other wells

The following discussion uses data obtained from Pecten-1A, Eric The Red-1 and La Bella-1.

Pecten-1A was drilled in 1967 by Shell in what is now VIC/P30. The well drillstem tested a small gas sand in the Lower Shipwreck Group. The well completion report states the SIBHP measured during the DST to be 2420 psig at 1688 mSS, (strain gauge).

La Bella-1 was drilled in 1993 by BHPP in the southeastern part of VIC/P30. The well was designed to test the fault dependant closure mapped at the Upper Shipwreck group. The well intersected a 68 m gross gas column in the Upper Shipwreck group. RFT data indicated an overpressured zone in the Lower Shipwreck Group with respect to the Upper Shipwreck Group .

Eric The Red-1 was also drilled in 1993 by BHPP in the southeastern part of VIC/P31. The well was a dry hole but intersected a large hydraulically continuous water bearing sand in the Upper Shipwreck Group. RFT data from the well indicated the sands in Eric the Red-1 were normally pressured with a gradient of 1.41 psi/m.

Figure 9 shows all of the available pressure data from VIC/P30 and VIC/P31. As can be seen in this figure, the single pressure point obtained in Pecten-1A lies along the observed pressure gradient of Eric The Red-1. This would indicate that Eric The Red-1 and Pecten-1A are, or have at one stage, been in hydraulic communication.

La Bella-1, on the other hand, has an overpressured Upper and Lower Shipwreck Group, (with respect to the other wells). This indicates that both the Upper and Lower Shipwreck Groups are not in pressure communication with the Shipwreck Groups as seen in Pecten-1A, Eric The Red-1, and Minerva-1.

The pretest data obtained from Minerva-1 in the aquifer lie on the line extrapolated through the data obtained from Eric The Red-1 and Pecten-1A. This would indicate that Eric The Red-1, Pecten-1, and Minerva-1 are now or were at one stage in hydraulic communication. The pressures in these wells are all close to, or at, normal hydrostatic pressure.

Another interpretation of the data is shown in figure 9c. This is based upon the assumptions that the pretest data from the Top Upper Shipwreck 2 sand is supercharged, and that the Top Upper Shipwreck sand and the main Upper Shipwreck sand are in hydraulic communication. This interpretation results in a gas column gradient of 1.72 and a GWC at 1914.7 mSS. Either interpretation may be valid and the effect upon reserves etc. is insignificant regardless of which interpretation is used.

## 5.5 Fluid Contacts

Figures 10a-1 to 10b-3 show the interpreted Minerva-1 RFT results over the Upper Shipwreck sands. Shown in figures 9a and 9b are three gas water contacts (GWC) at 1912.8, 1914.7, and 1920.0 mSS. The upper contact is associated with the gas sand in the Top Upper Shipwreck 1 sand, the second contact is associated with the main reservoir sand unit in the Upper Shipwreck Group, and the third with the Top Upper Shipwreck 2 sand. Note; the position of the GWC in the Top Upper Shipwreck sands assumes a gas gradient of 0.171 psi/m and connection with the main gas sand's aquifer.

From pretest data it has been determined that the Top Upper Shipwreck 1 gas sand is underpressured by 2.2 psi with respect to the main reservoir sand unit, and the Top Upper Shipwreck 2 sand unit is over pressured by 6.4 psi. This assumes a common aquifer with the main reservoir unit. This assumption results in a GWC 1.9m shallower, and 5.3m deeper in the two Top Upper Shipwreck sands with respect to the main Upper Shipwreck reservoir sand.

The assumption of a common aquifer cannot be proven. However, the composition of the samples indicate that there are small compositional differences between the gas in the main reservoir and that present in the Top Upper Shipwreck 1 sand, indicating hydrostatic isolation of the gas zones.

## 6. RFT SAMPLES

### 6.1 Sampling Summary

Fluid properties as determined at the wellsite are given in Tables 3 to 5. Two reservoir fluid samples were obtained from the main reservoir sand at 1931.0 and 1942.5 mRT. One sample was obtained from the Top Upper Shipwreck 1 sand at 1649.8 mRT.

The main reservoir sand contained a very dry gas with a specific gravity of 0.70, (Air=1.0, based upon a reservoir fluid gradient of 0.171 psi/m, @ 2500 psia, 95 °C). Wellsite analysis of the samples indicated low CO<sub>2</sub> (< 2.0%) and no H<sub>2</sub>S.

### 6.2 Hydrocarbon Properties

Tables 3a to 3b detail the data gathered on the wellsite regarding the recovered samples. The gas recovered from the 6 gallon chambers was passed through the mud-loggers gas chromatograph and the following gas compositions determined:

#### Minerva-1 Open Hole and RFT Data: Lower Chamber Gas Composition (%)

<u>Component</u>	<u>1931.0</u>	<u>1942.5</u>	<u>1649.8</u>	mRT
CO <sub>2</sub>	1.70	1.70	0.60	
C <sub>1</sub>	90.55	90.35	89.14	
C <sub>2</sub>	3.72	3.70	4.47	
C <sub>3</sub>	3.27	3.11	4.24	
i-C <sub>4</sub>	0.35	0.37	0.65	
n-C <sub>4</sub>	0.36	0.61	0.71	
C <sub>5</sub> <sup>+</sup>	0.05	0.16	0.19	
<b>Total</b>	<b>100</b>	<b>100</b>	<b>100</b>	

During the analysis of the gas samples using the mud logger's gas chromatograph, it was noted that the saturation indicator illuminated when the gas sample was injected for analysis. It was thought that the high concentrations of gas from the RFT sample were saturating the GC and causing possible erroneous readings. Analysis of diluted samples from the third sample (1649.8 mRT) indicated that GC seemed to be working properly while using undiluted samples.

Analysis of the data from the diluted samples, and comparing them with the undiluted samples, resulted in the conclusion that dilution of gas samples will NOT provide consistent compositional data from the wellsite GC. It is therefore recommended that during the GC analysis dilution of the sample should not take place.

Listed below is a summary of the fluid properties, as determined by Petrolab, of the reservoir samples taken at 1931.0, 1942.5, and 1649.5 mRT. Appendix A contains a copy of the Petrolab report.

**Summary of Results:**

		<u>1931.0</u>	<u>1942.5</u>	<u>1649.8</u>	mRT
Reservoir Temperature	T	237	257		°F
Reservoir Pressure	P	3820	4205		psig
Gas Expansion Factor	E	203.52	216.24		stb/rb
Gas Viscosity		0.0212	0.0223		cP
Density		0.1758	0.1926		gm/cc
Molecular Weight		20.47	21.11		
Gas Gravity		0.61	0.731		Air=1.0
Critical Pressure		683.6	718.2		psia
Critical Temperature		380.7	384.7		°R

**Reservoir Fluid Compositional Analysis:**

<u>Component</u>		<u>1931.0</u>	<u>Mole %</u> <u>1942.5</u>	<u>1649.8</u>	mRT
Carbon Dioxide	CO <sub>2</sub>	1.80	1.83	0.32	
Nitrogen	N <sub>2</sub>	0.90	0.89	1.26	
Methane	C <sub>1</sub>	93.45	93.47	94.05	
Ethane	C <sub>2</sub>	2.22	2.24	2.53	
Propane	C <sub>3</sub>	0.84	0.83	1.05	
n-Butane	n-C <sub>4</sub>	0.12	0.11	0.18	
i-Butane	i-C <sub>4</sub>	0.20	0.19	0.23	
Pentane*	C <sub>5</sub> *	0.47	0.44	0.38	
<b>Total</b>		<b>100.0</b>	<b>100.0</b>	<b>100.0</b>	

Figure 13 shows the ratio of the Petrolab determined compositions to the mudlogger's GC compositions. This graph indicates that the wellsite analysis of the samples is only really accurate for methane. All of the heavier components were analysed by Petrolab as having a smaller mole percent than the rig site analysis. This result indicates that the rig analysis of the gas samples should be treated only as qualitative and can be significantly different to the laboratory results.

### 6.3 Formation Water Properties

The liquid obtained from the 6 gallon RFT chambers recovered from 1931.0 and 1948.5 mAHDf was verified as mud filtrate by measurement of its resistivity, (See Tables 3a, and 3b).

## 7. REFERENCES

- [1] BHP Petroleum RFT Manual.  
December 1988.



# Well Data Sheet

Table 1.

<b>Well:</b>	<b>Minerva-1</b>	
<b>Permit:</b>	VIC/P31	
<b>Location:</b>	Lat:	38 ° 42 ' 12.23 " South
	Long:	142 ° 57 ' 12.34 " East
<b>Rig:</b>	Semi-Submersible Byford Dolphin	
<b>Seismic Reference Line:</b>	OE81A-2028	
<b>DF Elevation:</b>	25.0 m above MSL	
<b>Water Depth</b>	57.0 m	
<b>Well TD (8 1/2" Hole) :</b>	2025.0 mDF	
<b>Spud Date:</b>		
<b>Date Reached TD:</b>	21st March 1993	
<b>Well Status:</b>	Plugged & Abandoned	
<b>Casing Points:</b>	9 5/8 @ 1189.0 mDF	
<b>Reservoir Tops:</b>	Top Upper Shipwreck 1	mRT
	Top Upper Shipwreck 2	mRT
	Main Upper Shipwreck	mRT
<b>Datum Depth (GWC):</b>	1915.6	mSS
<b>Pressure at Datum:</b>	2746.4	psia
<b>Reservoir Temperature:</b>	97.0	° C @ 1992.0 mKB
<b>Trittium Used:</b>	No	
<b>Fluids In Well:</b>	Gas:	Yes
	Oil:	No
	Water:	Yes
<b>Contacts:</b>	GOC:	N/A
	OWC:	N/A
	GWC:	1915.6 mTVDSS

# MINERVA-1 OPEN HOLE RFT RESULTS

Test No.	Depth		Time hh:mm	Initial Hydrostatic Pressure		Formation Pressure		Temperature DegC	Final Hydrostatic Pressure		Mobility mD/cp	Permeability* mD	Comments
	mTVDDF	mTVDSS		Strain Gauge psig	HP Gauge psia	Strain Gauge psig	HP Gauge psia		Strain Gauge psig	HP Gauge psia			
0	1161.7	1139.2	15:00	1933.2	1944.2	0		58.8	1931.0	1944.7			Good test on casing
1	1651.5	1624.8	15:37	2721.5	2736.4	0	13.0		2719.7	2736.8			Tight
2	1650.8	1623.9	15:43	2718.8	2733.8	--	--	79.8	2717.8	2734.0			Tight
3	1649.8	1623.0	15:55	2716.1	2731.8	2678.9	2694.59	80.2	2715.8	2731.6	12.3	30	Good Test
4	1662.8	1635.8	16:05	2736.5	2752.4	2689.8	2705.43	80.7	2736.2	2752.1	7.8	20	Good Test
5	1662.2	1635.2	16:23	2741.6	2757.5	2739.9	2755.80	81.0	2741.5	2757.3	1.3	5	Possible lost seal
6	1666.5	1639.5	16:37	2742.1	2758.1	2740.5	2756.55	81.3	2741.8	2757.8	1.1	5	Possible lost seal
7	1666.8	1639.8	16:52	2742.5	2758.6	--	--	81.4	2742.3	2759.2			Tight
8	1817.0	1788.7	17:17	2983.4	2998.9	2709.5	2725.09	87.1	2982.5	2999.0	9.2	20	Good Test
9	1829.5	1801.0	17:30	3002.2	3017.7	2711.5	2726.08	87.2	3002.0	3017.8	1565	1800	Good Test
10	1838.0	1809.5	17:43	3015.3	3031.7	2713.1	2728.28	87.5	3015.3	3031.3	66	150	Good Test
11	1845.0	1816.4	17:55	3026.4	3043.7	2714.3	2729.17	88.3	3026.2	3042.4	1040	1200	Good Test
12	1867.0	1838.2	18:20	3061.8	3079.5	2718.3	2733.38	89.6	3061.5	3077.9	876	1000	Good Test
13	1875.5	1846.6	18:44	3075.5	3093.0	2719.3	2733.96	90.4	3075.4	3091.2	815	900	Good Test
14	1884.5	1855.5	19:00	3089.7	3106.9	2721.2	2736.13	91.1	3089.5	3105.8	105	240	Good Test
15	1890.6	1861.6	19:30	3099.8	3116.1	2722.3	2737.20	91.9	3099.7	3115.8	91	210	Good Test
16	1906.5	1877.3	19:45	3125.4	3143.4	2724.5	2739.36	92.6	3125.2	3141.5	426	970	Good Test
17	1919.0	1889.7	20:05	3145.5	3162.5	2726.7	2741.91	93.3	3145.5	3161.9	21	50	Good Test
18	1923.8	1894.5	20:35	3154.0	3169.4	2727.7	2742.19	94.1	3153.7	3169.7	114	260	Good Test
19	1931.0	1901.6	20:50	3165.1	3181.5	2728.6	2743.36	94.0	3165.2	3181.7	116	260	Good Test
20	1935.7	1906.3	21:00	3172.9	3189.6	2729.9	2744.70	94.5	3172.7	3189.5	266	600	Good Test
21	1937.6	1908.2	21:17	3176.3	3193.2	2730.0	2744.80	94.4	3175.9	3192.5	460	1000	Good Test
22	1939.5	1910.1	21:30	3179.3	3196.0	2730.6	2745.70	94.7	3179.2	3195.7			Good Test
23	1942.8	1913.3	21:40	3184.9	3202.2	2730.3	2746.01	95.0	3184.7	3201.2	3.4	10	Good Test
24	1949.2	1919.7	22:01	3195.8	3211.8	2738.2	2752.48	95.6	3195.6	3211.5	557	1300	Good Test
25	1941.9	1912.4	22:20	3184.2	3200.0	2731.2	2745.86	95.6	3183.0	3200.2	268	610	Good Test
26	1939.5	1910.1	22:40	3180.2	3196.3	2730.9	2745.92	95.2	3180.2	3196.9	20	45	Good Test
27	1941.0	1911.5	23:00	3182.6	3199.0	2730.4	2745.22	95.4	3182.5	3199.0	39.7	90	Good Test
28	1951.5	1921.9	23:14	3199.4	3216.7	2741.0	2755.98	95.4	3199.3	3216.1			Good Test
29	1953.2	1923.6	23:33	3202.4	3219.1	2743.5	2758.30	95.6	3202.3	3218.8	270	610	Good Test
30	1959.2	1929.8	23:45	3212.0	3229.4	2751.9	2766.66	96.0	3212.0	3228.8		0	Good Test
31	1966.2	1936.5	00:15	3223.7	3239.9	2761.7	2775.91	96.4	3223.6	3239.6	580	1100	Good Test
32	1972.2	1942.5	00:33	3233.3	3249.9	2769.9	2784.55	96.6	3233.4	3249.7	220	500	Good Test
33	1992.0	1962.1	00:55	3265.5	3282.3	2797.2	2811.95	97.4	3265.5	3281.9			Good Test
34	1931.0	1901.6	01:25	3167.5	3182.2	2729.0	2743.36		3167.1	3183.9			Sample Taken
35	1942.5	1913.0	05:46	3187.6	3203.2	2731.9	2746.28		3185.4	3201.6			Sample Taken
36	1649.8	1623.0	10:37	2718.3	2733.9	2679.2	2694.70		2716.8	2732.6			Sample Taken

Filtrate: Temp 194 Deg F  
 % NaCl 25000  
 Pressure 2700 psia  
 Viscosity 0.34

\*N.B. Permeabilities rounded.  
 K(h)/k(v)=1  
 Filtrate Viscosity = 0.34 cP  
 k(rw)=0.15 for k<1000 mD  
 k(rw)=0.30 for k>1000 mD

Table 2.

# RFT Sample Data Sheet

Table 3.

**Well: Minerva-1**

Date: 22nd March 1993

KB: 25.0 m

Sample No: 1 Depth: 1931.0 mAHKB

Formation Pressure: 2743.36 psia

	<u>Lower</u>	<u>Upper</u>	
Chamber No:		RFS-1227	
Chamber Size:	6	1	gal
Flowing Pressure:	Approx 2500	Approx 2450	psig
Time To Fill:	25	6	minutes
Opening Pressure:	1850	1800	psig
Gas Volume:	113	Preserved for	ft <sup>3</sup>
Total Liquids:	570	PVT Analysis	cc
Oil/Condensate Volume:	15		cc
Filtrate/Water Volume:	555		cc
Gas Oil Ratio:	--		Scf/Stb
Condensate Gas Ratio:	0.8		Stb/MMscf

**Oil/Condensate Analysis**

Specific Gravity:	Too small to measure	Air=1, Temp
Colour:	Too small to measure	
Fluorescence:	Bright Blue	

**Gas Analysis:**

C1:	90.55	%
C2:	3.72	%
C3:	3.27	%
iC4:	0.36	%
nC4:	0.37	%
C5+:	0.62	%
CO2:	1.70	%
H2S:	0	ppm
Specific Gravity	0.65	Air=1.0

**Water/Filtrate Analysis:**

	Filtrate		
	Lower	Upper	
Rw:	0.134		0.084
pH:			9.5
Cl-:			mg/l
Total Hardness (Ca/Mg):			
KCl:	24000		25000

**Tritium Analysis:**

Average Activity:	N/A	N/A	N/A	N/A	Bq/cc
Returns:					Bq/cc
% Filtrate:					

# RFT Sample Data Sheet

Table 4.

**Well: Minerva-1**

Date: 22nd March 1993

KB: 25.0 m

Sample No: 2 Depth: 1942.5

mAHKB

Formation Pressure: 2746.3 psia

	<u>Lower</u>	<u>Upper</u>
Chamber No:		RFS-1157
Chamber Size:	6	1 gal
Flowing Pressure:	Aprox 2200	Aprox 2500 psig
Time To Fill:	50	10 minutes
Opening Pressure:	2050	2000 psig
Gas Volume:	78	Preserved for ft <sup>3</sup>
Total Liquids:	830	PVT Analysis cc
Oil/Condensate Volume:	20	cc
Filtrate/Water Volume:	810	cc
Gas Oil Ratio:	--	Scf/Stb
Condensate Gas Ratio:	1.6	Stb/MMscf

## Oil/Condensate Analysis

Specific Gravity:	Too small to measure	Air=1, Temp
Colour:	Too small to measure	
Fluorescence:	Bright Blue	

## Gas Analysis:

C1:	90.35	%
C2:	3.70	%
C3:	3.11	%
iC4:	0.38	%
nC4:	0.62	%
C5+:	0.16	%
CO2:	1.7	%
H2S:	0	ppm
Specific Gravity	0.64	Air=1.0

## Water/Filtrate Analysis:

	Filtrate	
	Lower	Upper
Rw:		0.084
pH:	6.8	9.5
Cl-:	42000	
Total Hardness (Ca/Mg):		
KCl:	38000	25000

## Tritium Analysis:

Average Activity:	N/A	N/A	N/A	N/A	Bq/cc
Returns:					Bq/cc
% Filtrate:					

# RFT Sample Data Sheet

Table 5.

**Well: Minerva-1**

Date: 23rd March 1993

KB: 25.0 m  
 Sample No: 3 Depth: 1649.8

Formation Pressure: 2694.59 psia

	<u>Lower</u>	<u>Upper</u>	
Chamber No:	6	RFS-AD-1123	
Chamber Size:	Approx 2100	1	gal
Flowing Pressure:	25	Approx 2500	psig
Time To Fill:		6	minutes
Opening Pressure:	2100	2100	psig
Gas Volume:	77.7	Preserved for	ft^3
Total Liquids:	7500	PVT Analysis	cc
Oil/Condensate Volume:	film		cc
Filtrate/Water Volume:	--		cc
Gas Oil Ratio:	--		Scf/Stb
Condensate Gas Ratio:	--		Stb/MMscf

**Oil/Condensate Analysis**

Specific Gravity:	Too small to measure	Air=1, Temp
Colour:	Too small to measure	
Fluorescence:	Blue/White	

**Gas Analysis:**

C1:	89.14	%
C2:	4.47	%
C3:	4.24	%
iC4:	0.65	%
nC4:	0.72	%
C5+:	0.19	%
CO2:	0.6	%
H2S:	0	ppm
Specific Gravity	0.65	Air=1.0

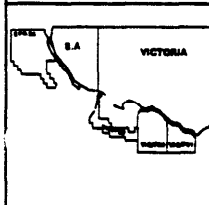
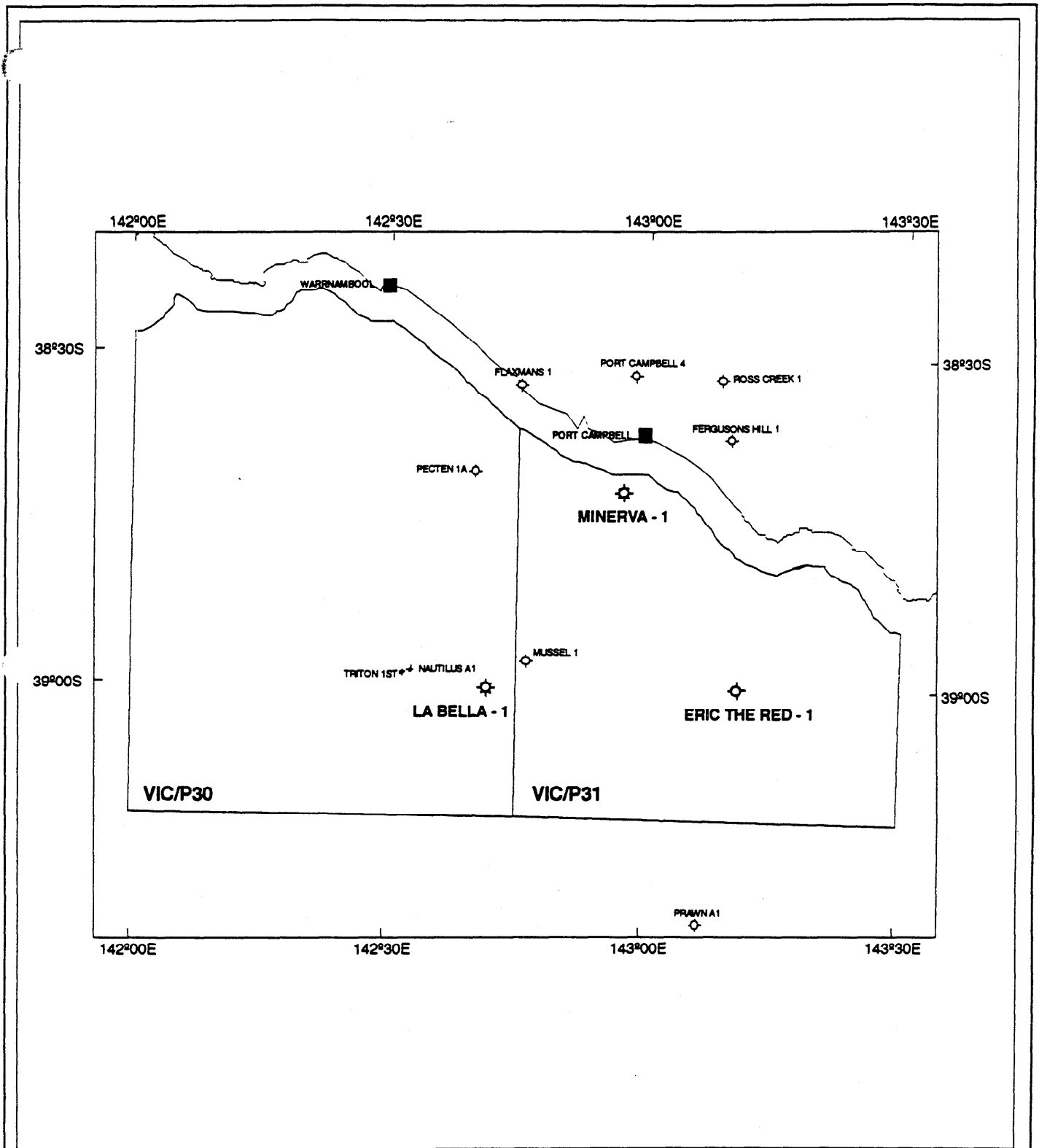
**Water/Filtrate Analysis:**

	<u>Filtrate</u>			
	<u>Lower</u>	<u>Upper</u>		<u>Drilled</u>
Rw:	0.089		0.084	
pH:	6.4		9.5	
Cl-:	45000			mg/l
Total Hardness (Ca/Mg):				
KCl:	42000		25000	

**Tritium Analysis:**

Average Activity:	N/A	N/A	N/A	N/A	Bq/cc
Returns:					Bq/cc
% Filtrate:					

Figure 1



VICP30/31  
 WELL LOCATIONS  
 LABELLA-1, ERIC THE RED-1 & MINERVA - 1



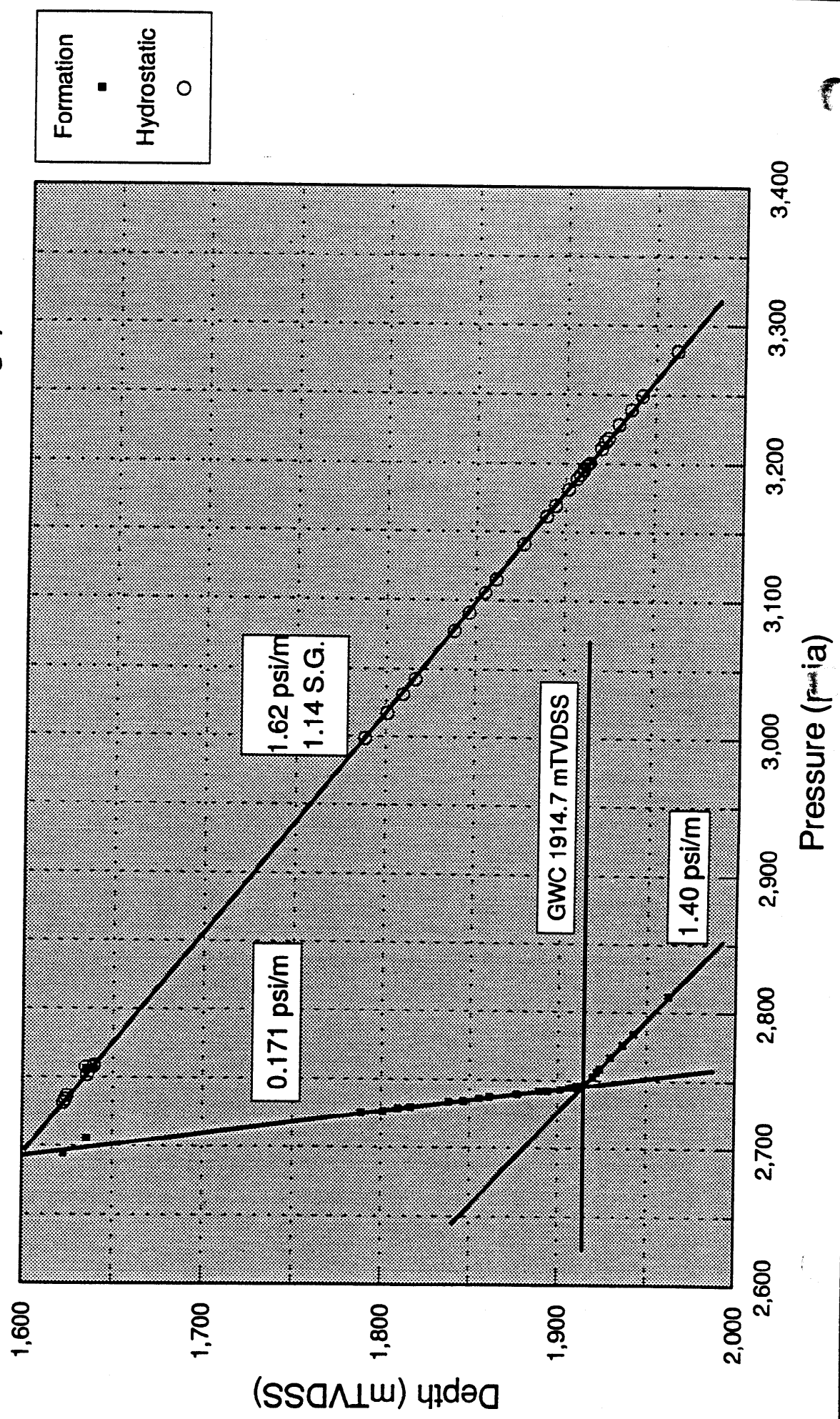
VICP30/P31  
 LOCATION MAP

AUTHOR:	DATE: 05/04/93
DRAWN BY: TDELPHN	DATE: 05/93

Figure 2.

# Minerva-1

## Hydrostatic & Formation Pressures (Strain Gauge)



# Minerva-1

## Formation Temperature vs Depth

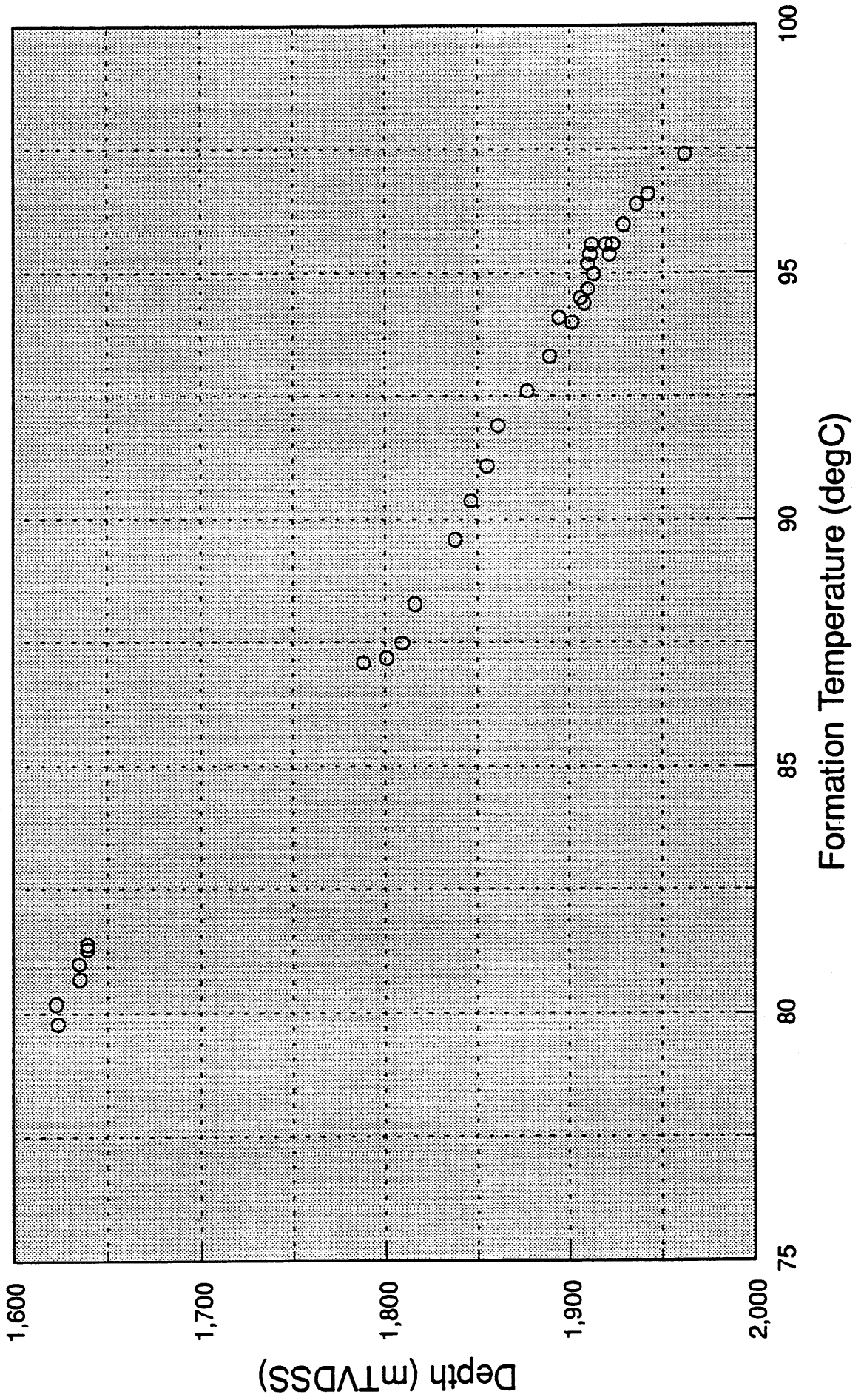


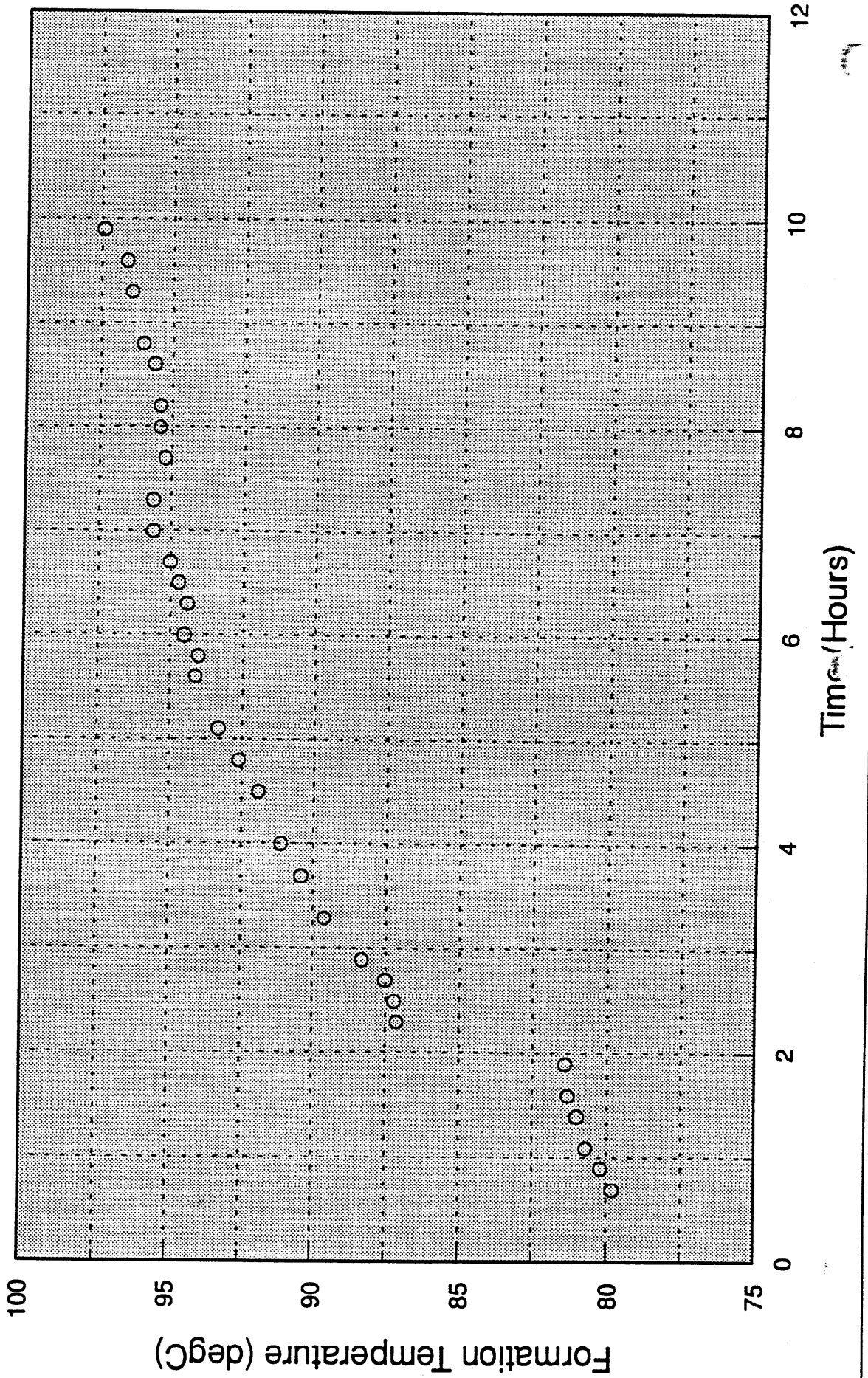
Figure 3.



Figure 4.

# Minerva-1

## Formation Temperature vs Time



# Minerva-1

## Final - Initial HP Gauge Pressures

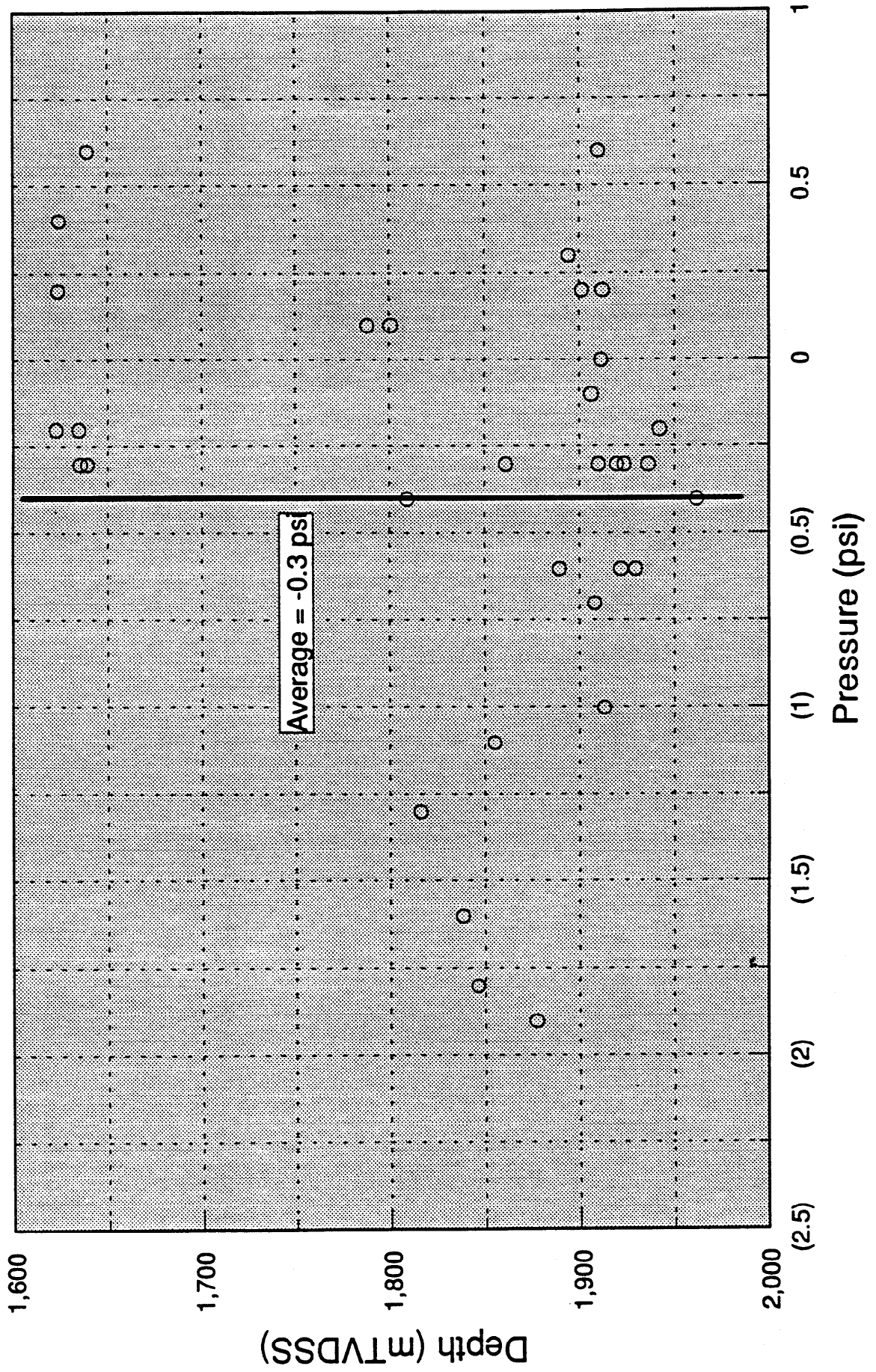


Figure 6.

# Minerva-1

## Hydrostatic Pressure (HP Gauge)

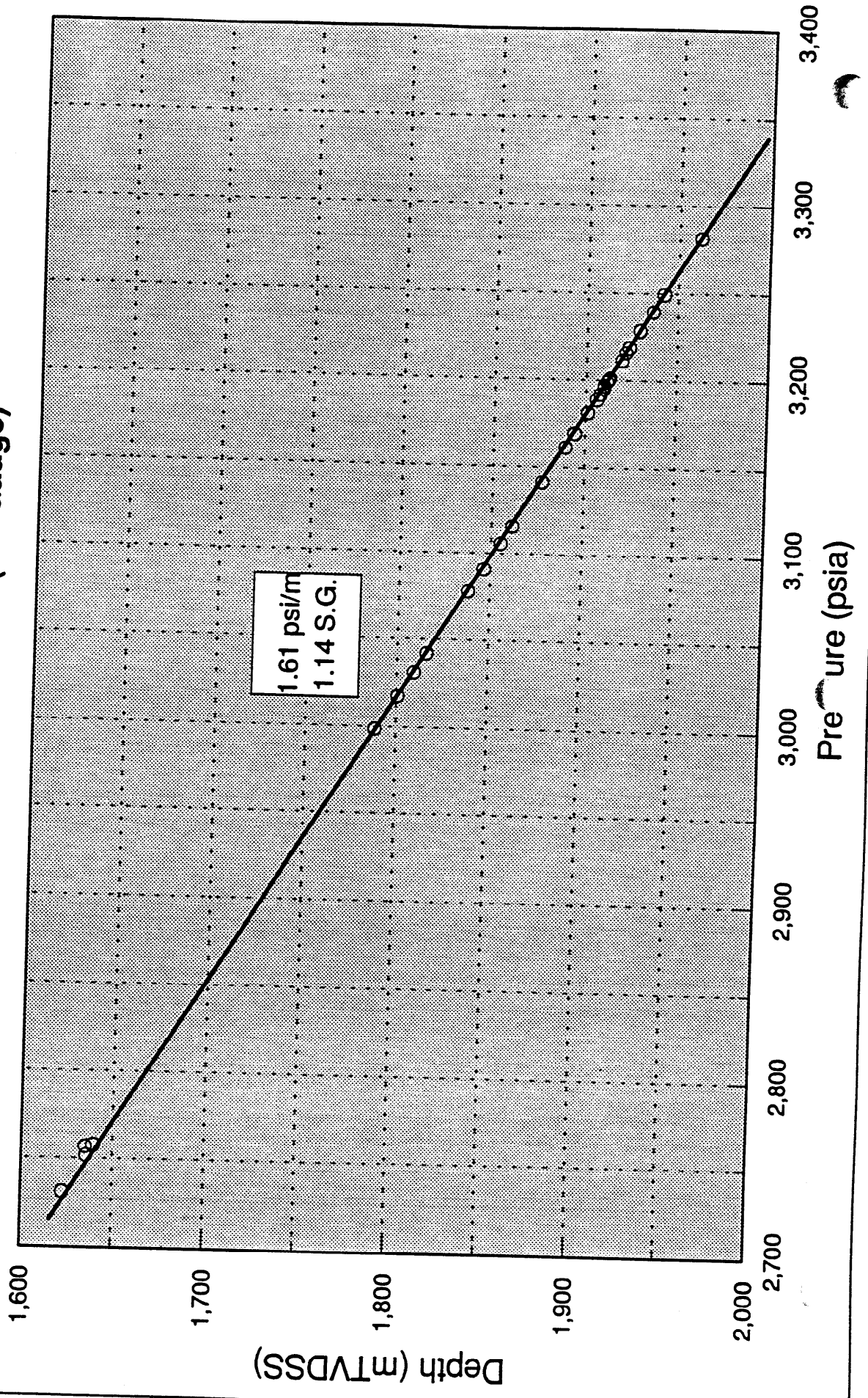
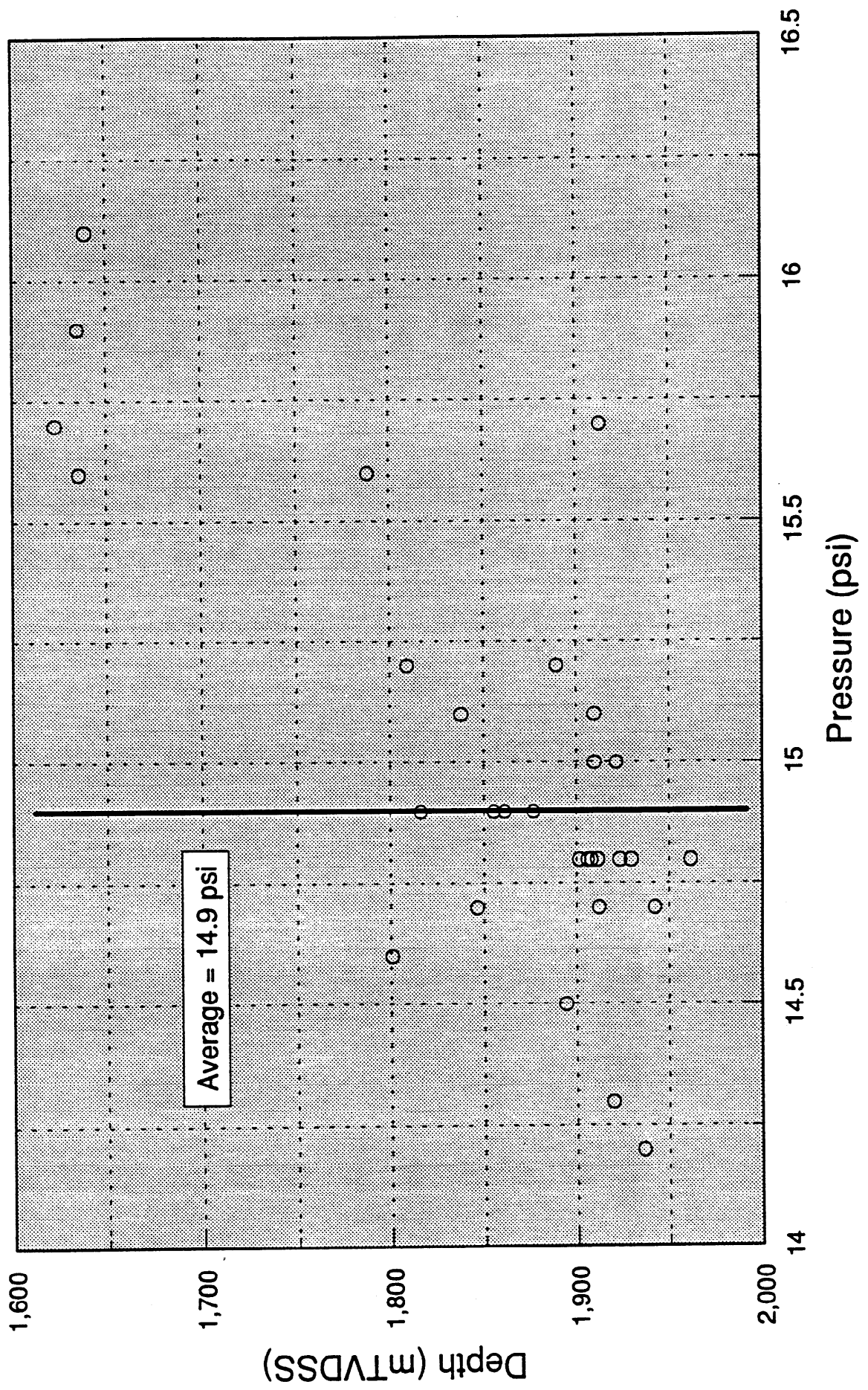


Figure 7.

# Minerva-1

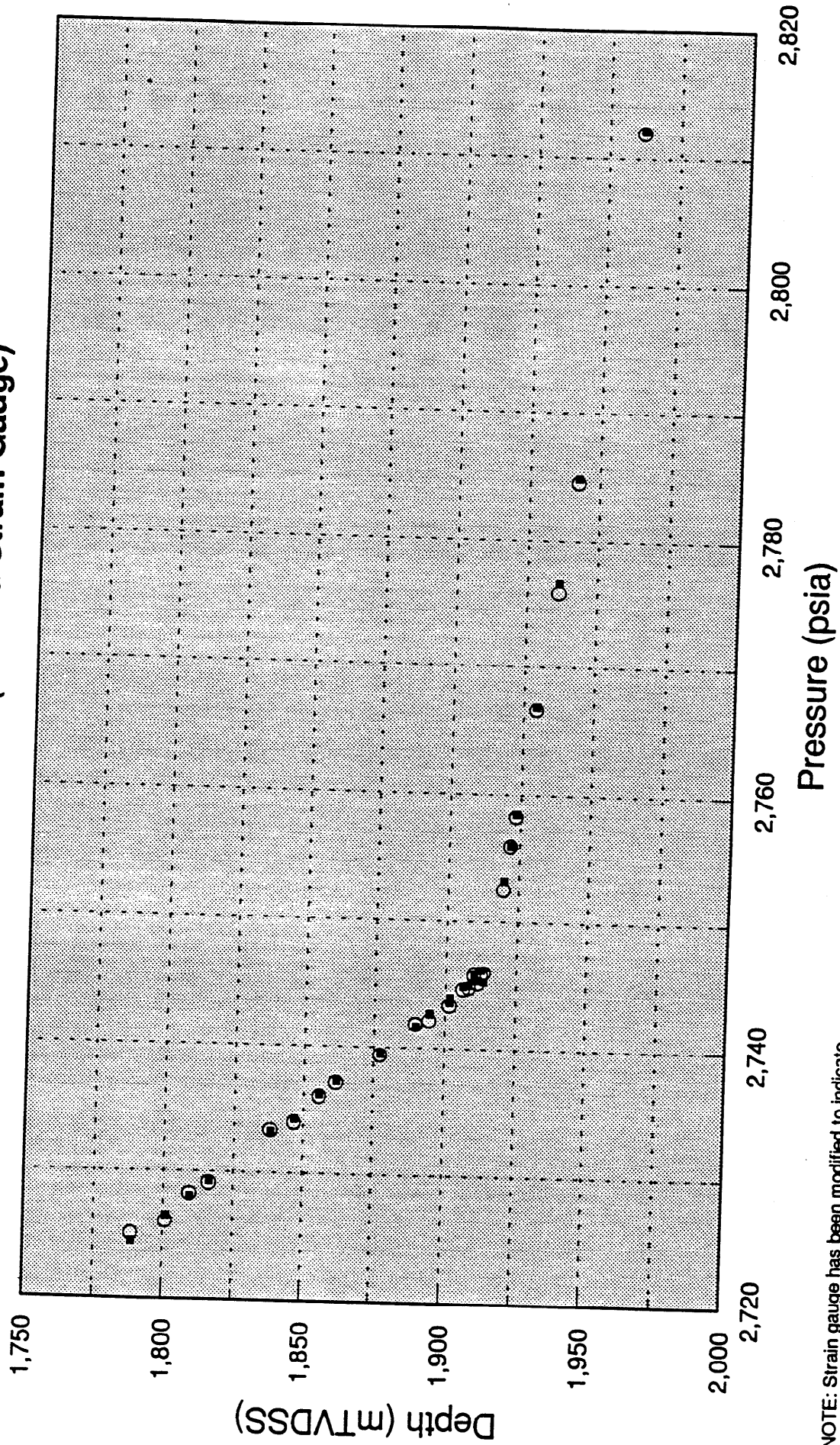
## HP - Strain Gauge Pressures





# Minerva-1

## Formation Pressure (HP and Strain Gauge)



NOTE: Strain gauge has been modified to indicate psia by adding 14.97 psi.

Figure 8.

# Minerva-1

## Formation Pressure (HP Gauge)

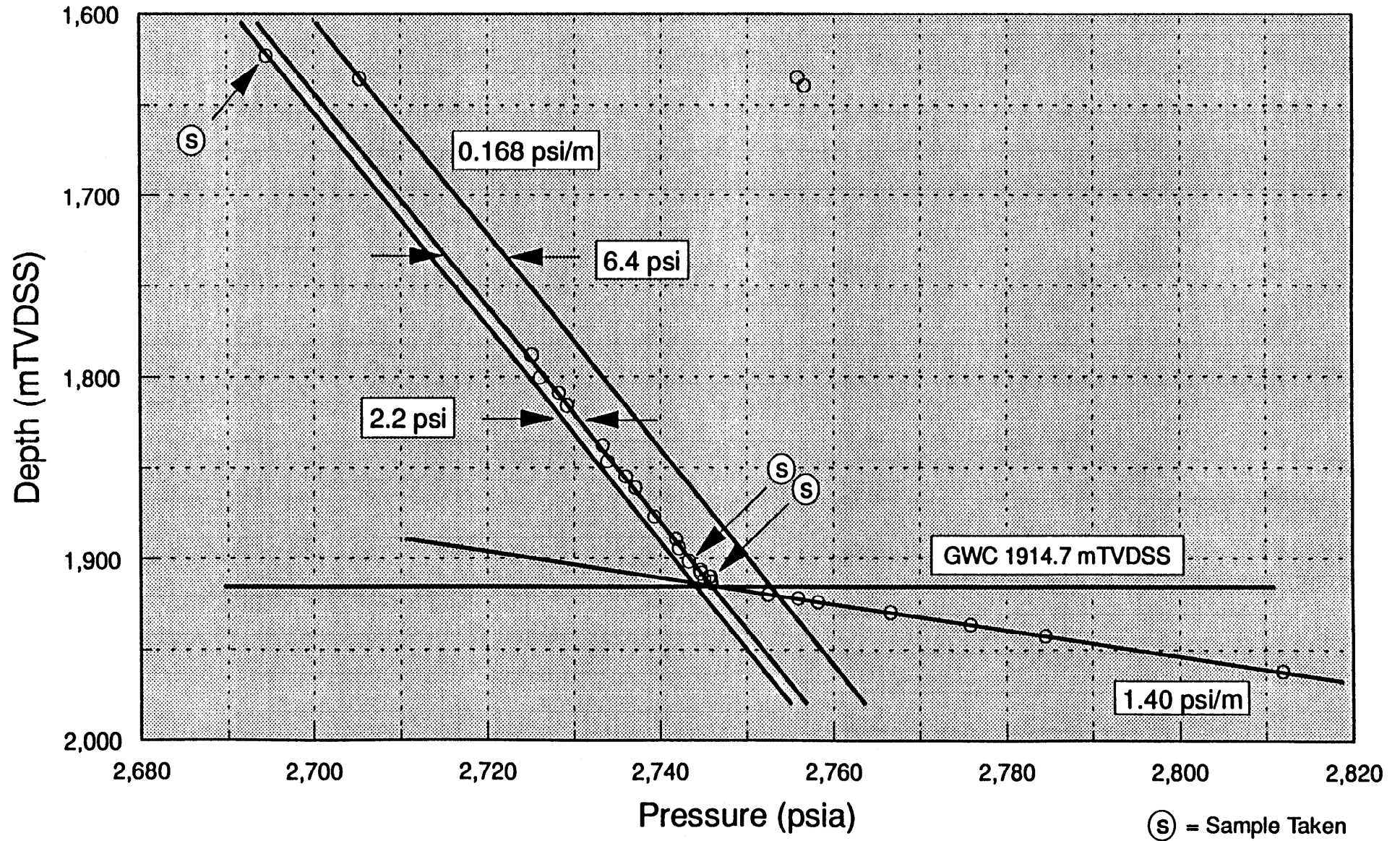
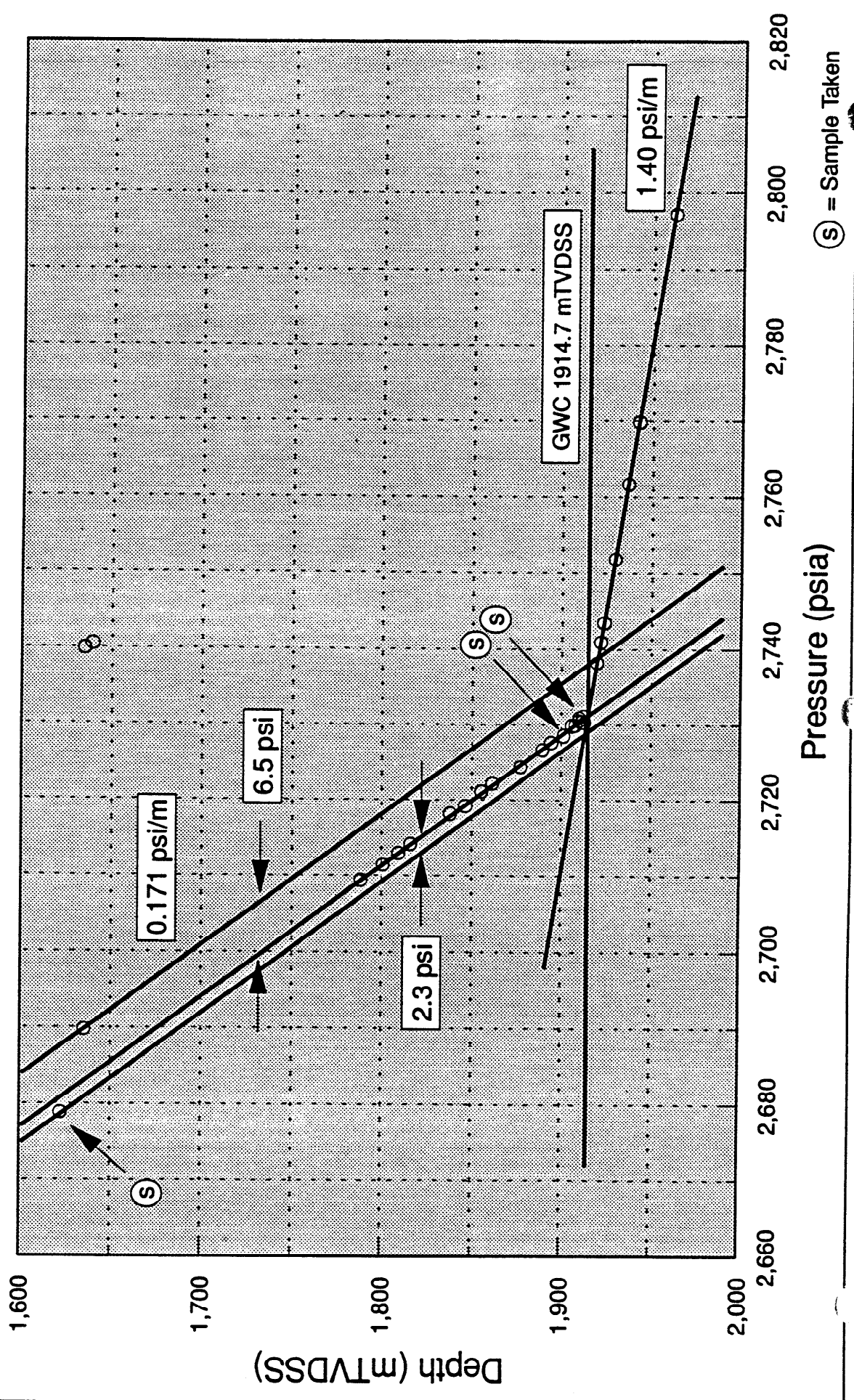


Figure 9a.

Figure 9b.

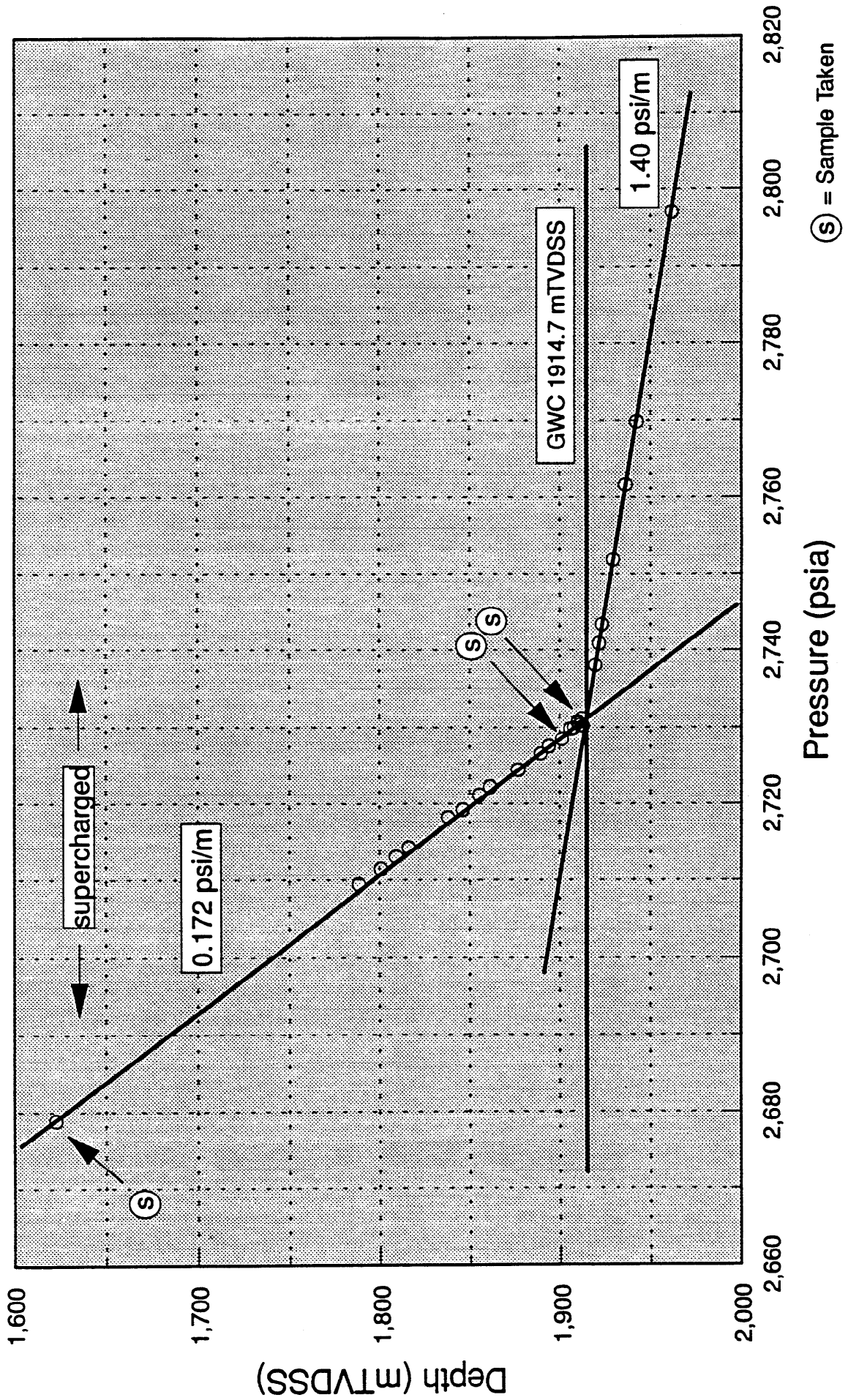
# Minerva-1

## Formation Pressure (Strain Gauge)



# Minerva-1

Formation Pressure (Strain Gauge)

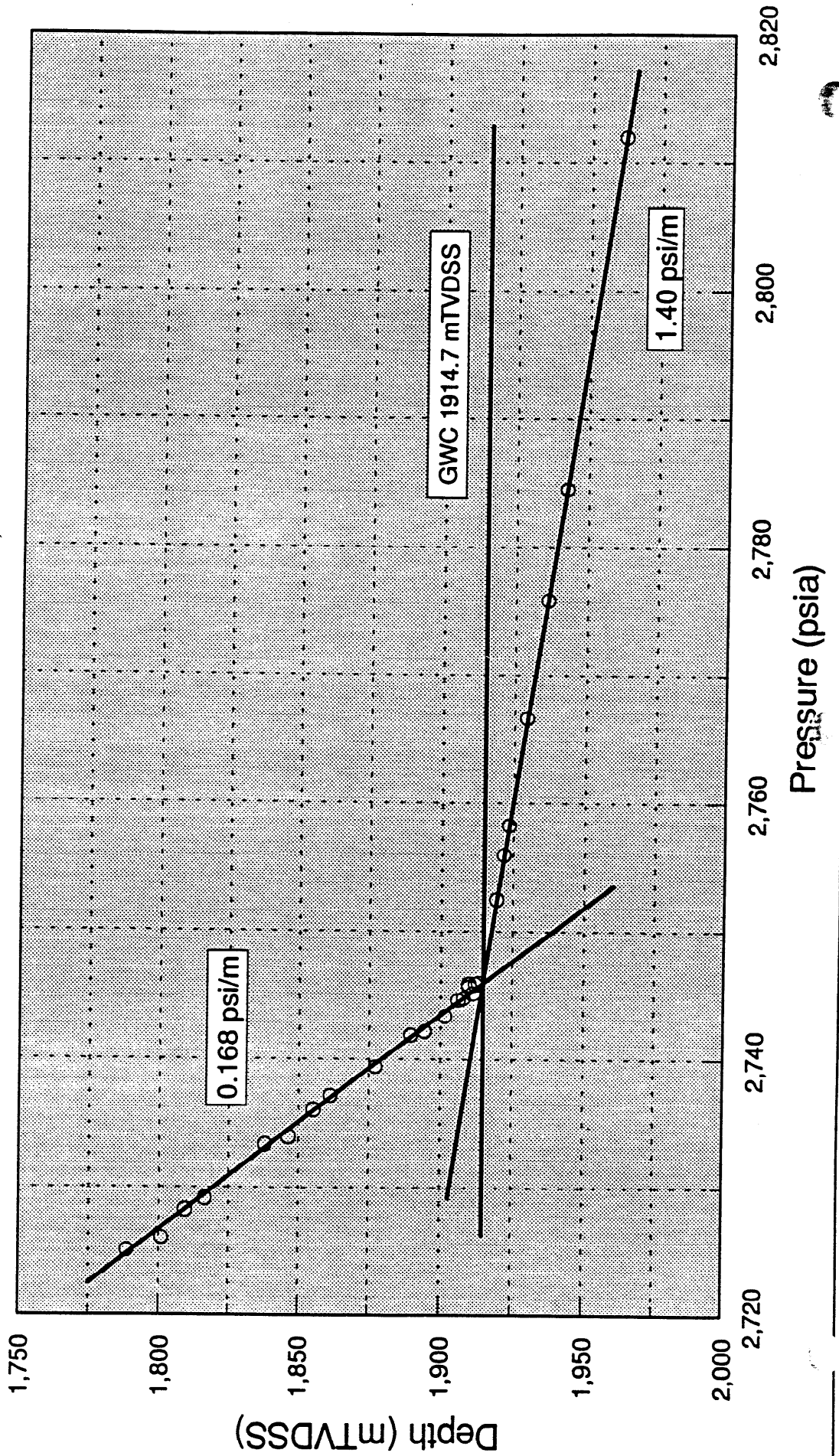




# Minerva-1

## Formation Pressure (HP Gauge)

### Expanded Scale



# Minerva-1

## Formation Pressure (Strain Gauge)

### Expanded Scale

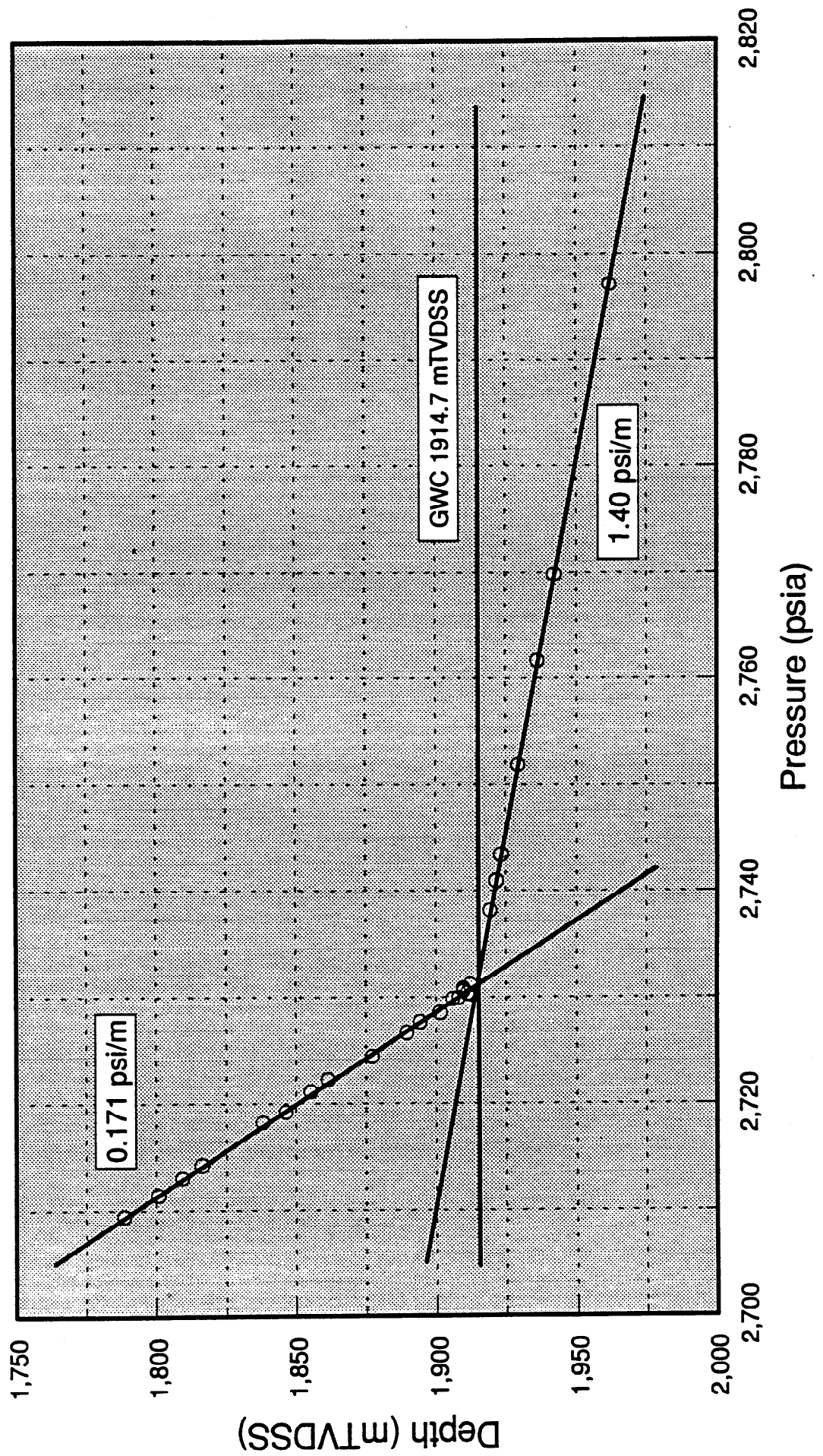
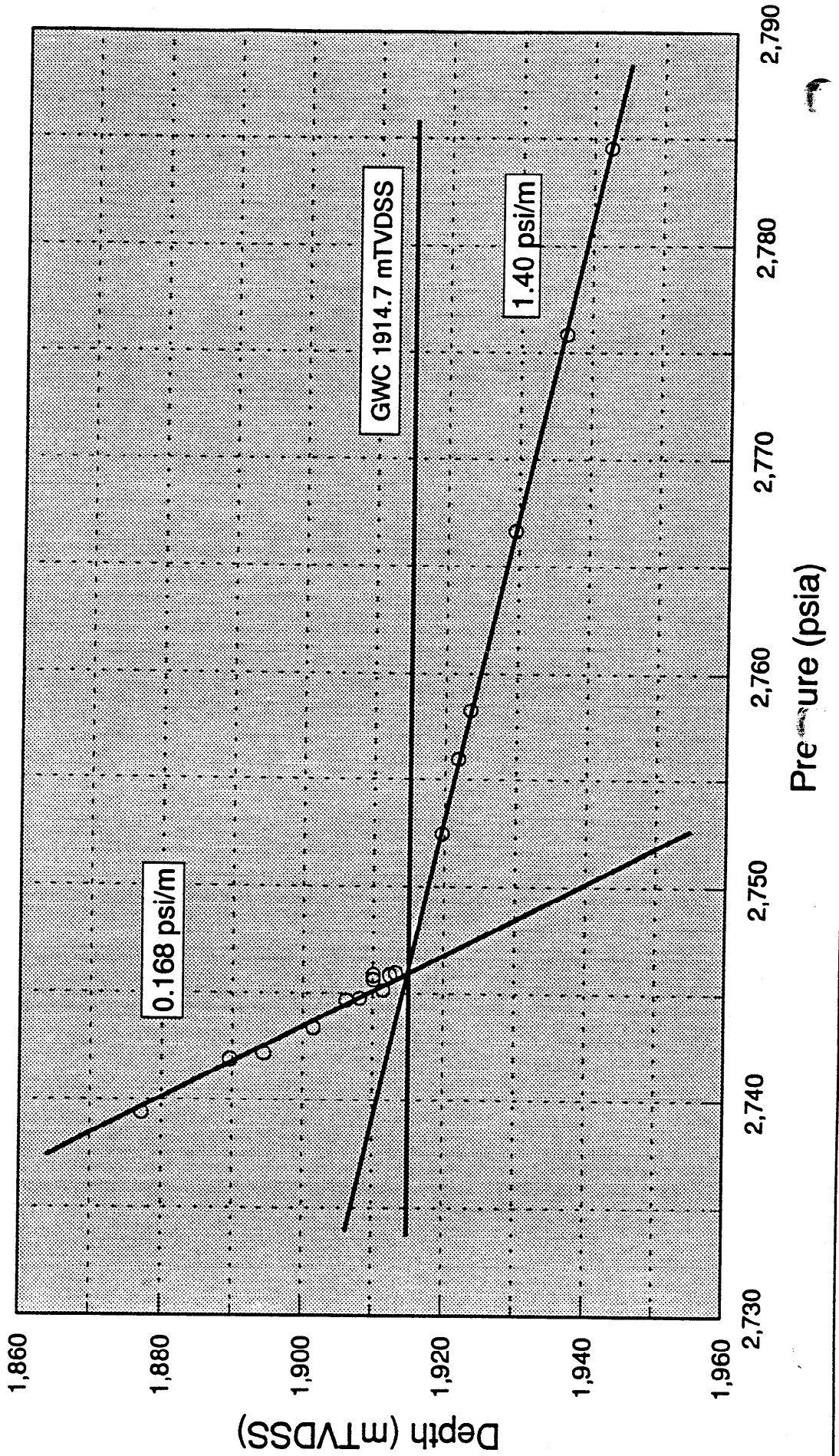


Figure 10a-2.

# Minerva-1

Formation Pressure (HP Gauge)

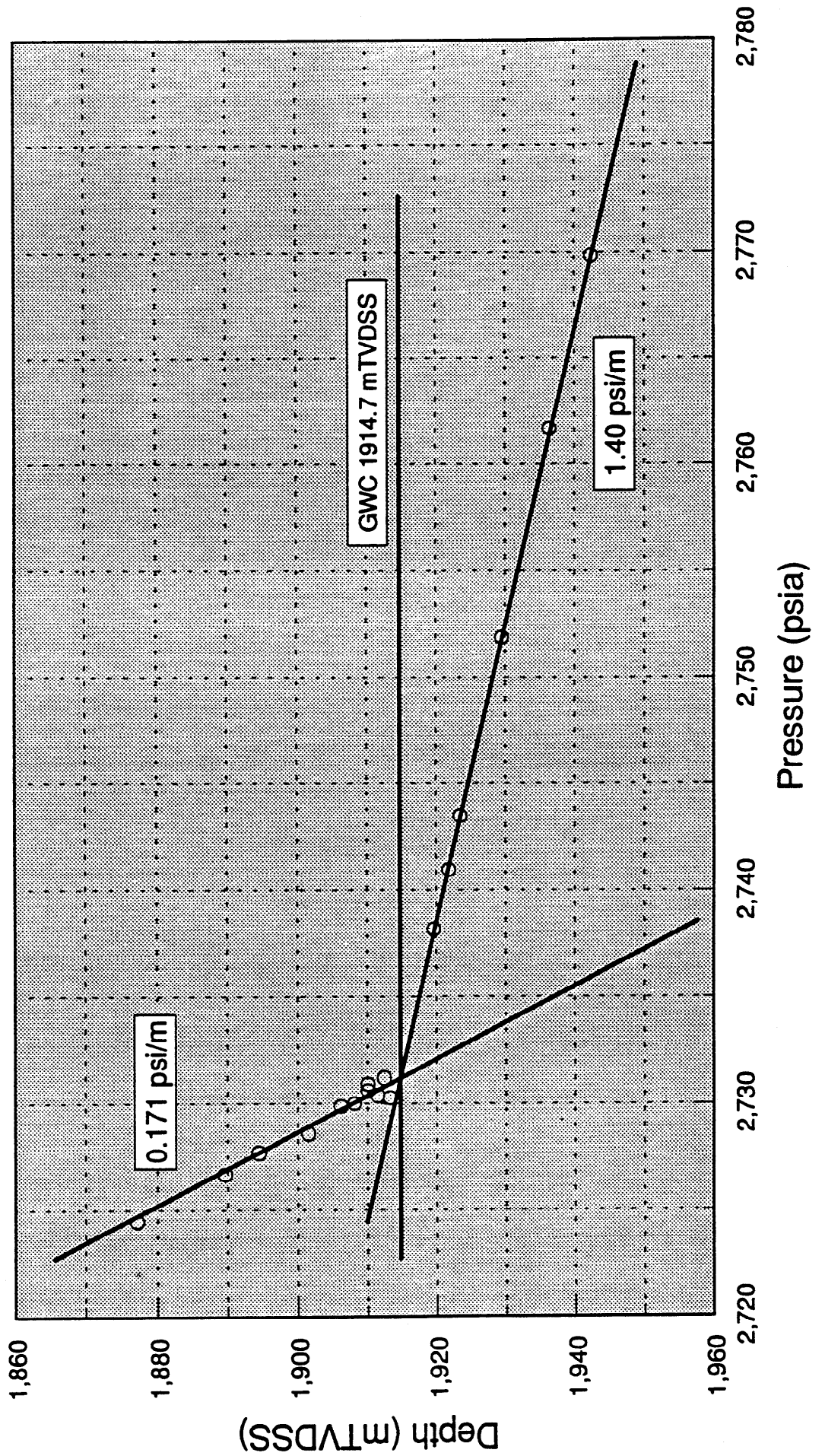
Expanded Scale



# Minerva-1

## Formation Pressure (Strain Gauge)

### Expanded Scale





# Minerva-1

## Formation Pressure (HP Gauge)

### Expanded Scale

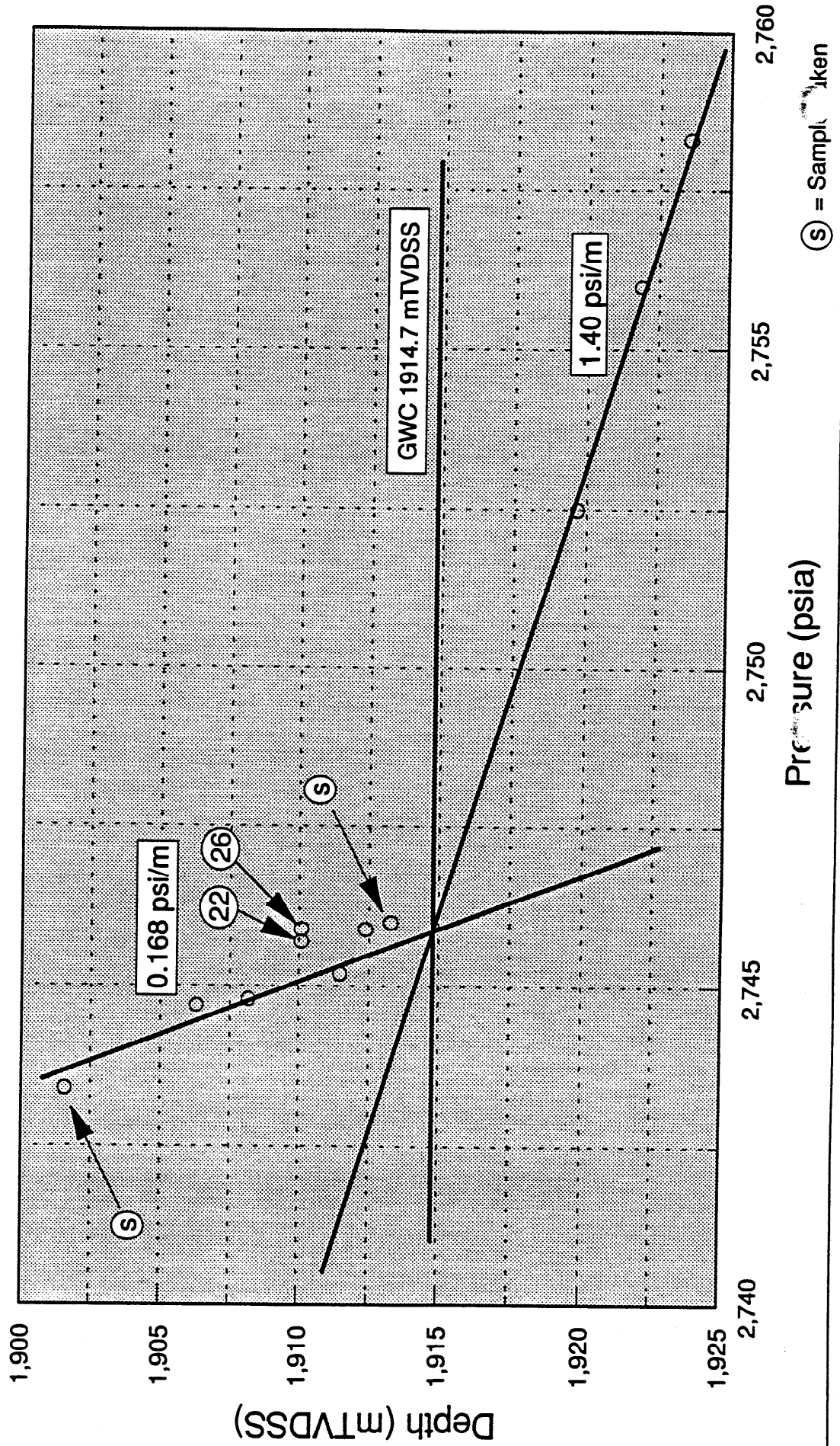


Figure 10a-3.

Figure 10b-3.

# Minerva-1

## Formation Pressure (Strain Gauge)

### Expanded Scale

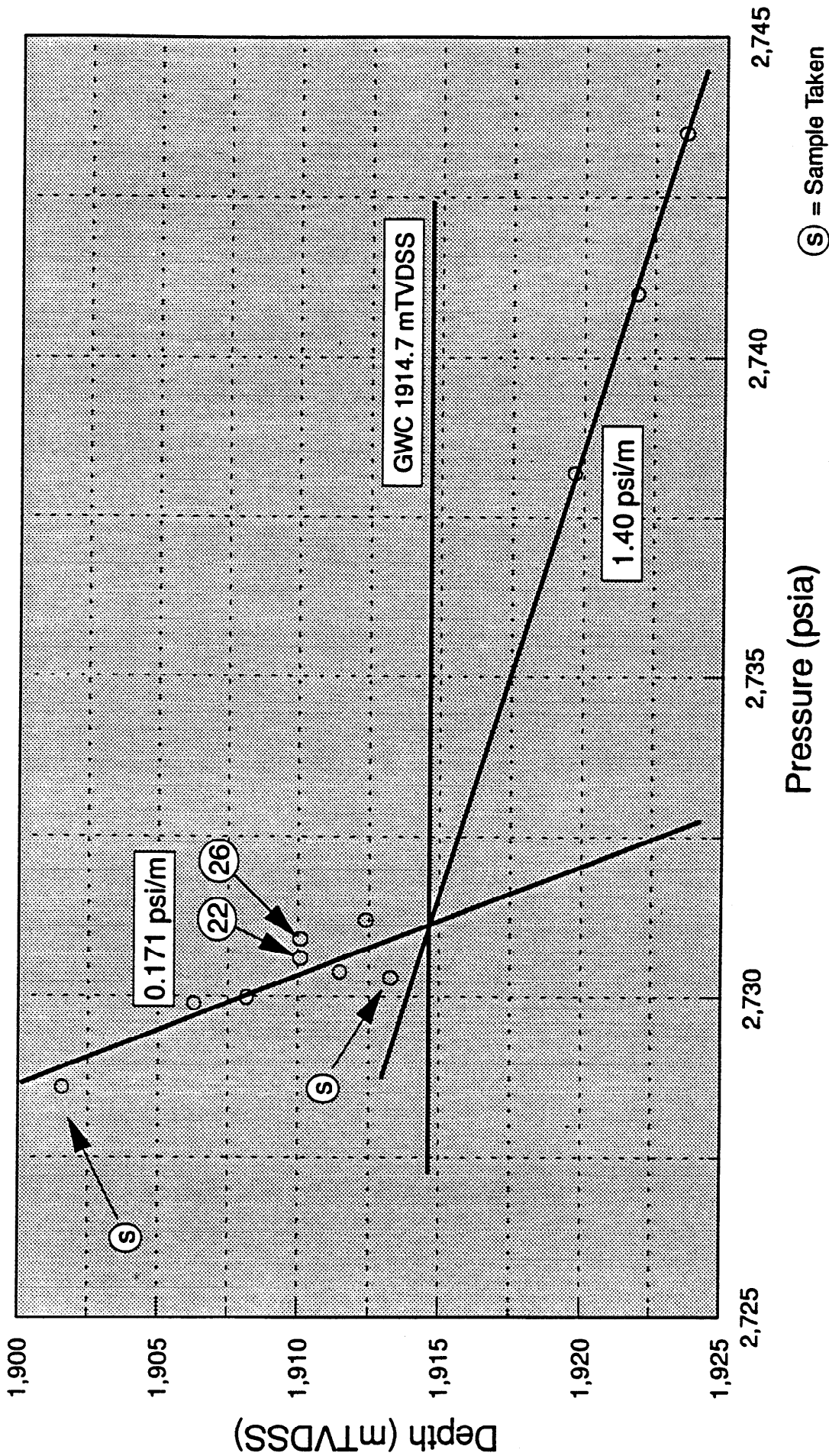
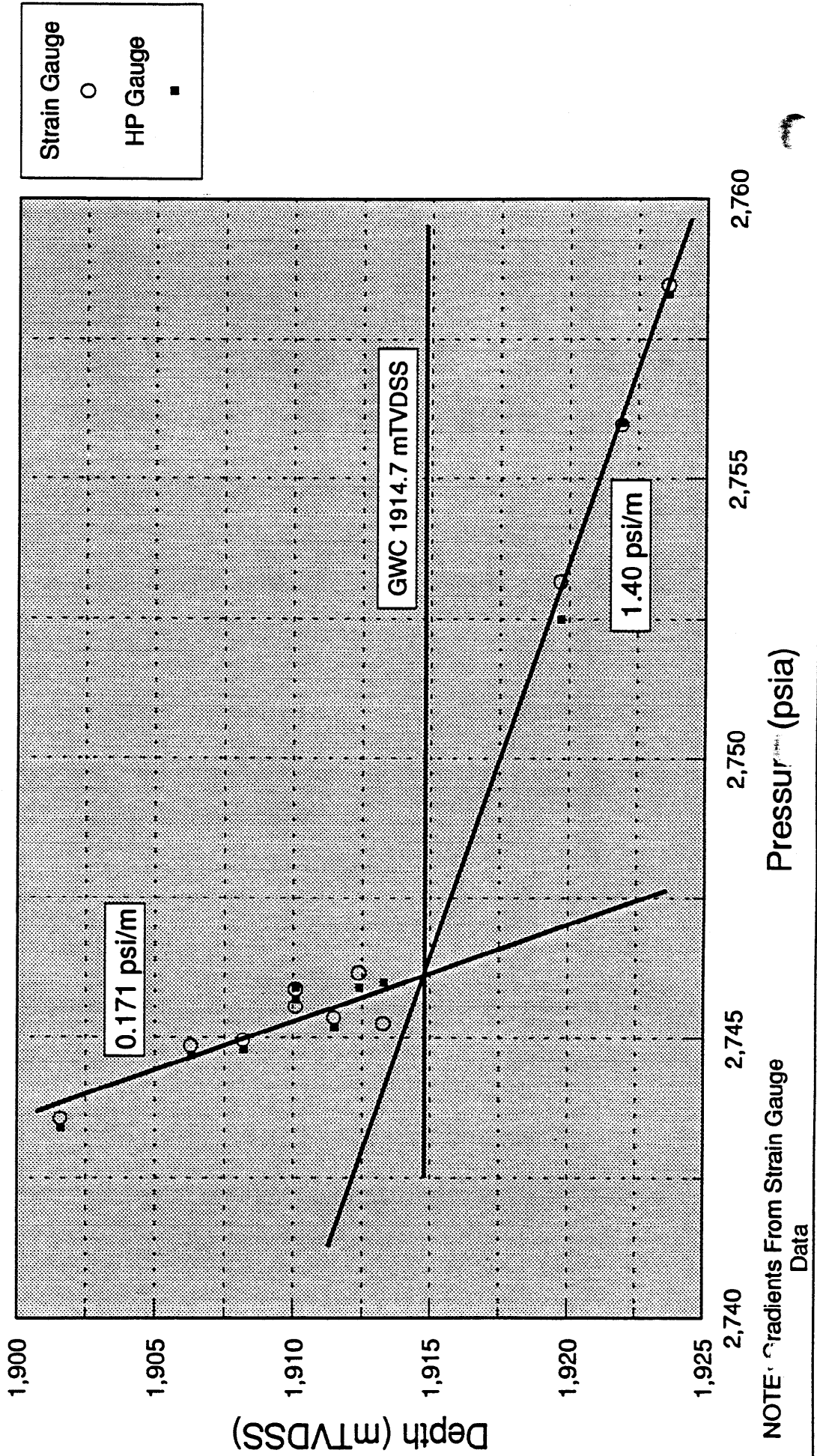


Figure 11.

# Minerva-1

## Formation Pressure (Strain & HP Gauge)

Expanded Scale



# VIC/P30 and VIC/P31 Formation Pressure Data

## Formation Pressure vs Depth (Strain Gauge)

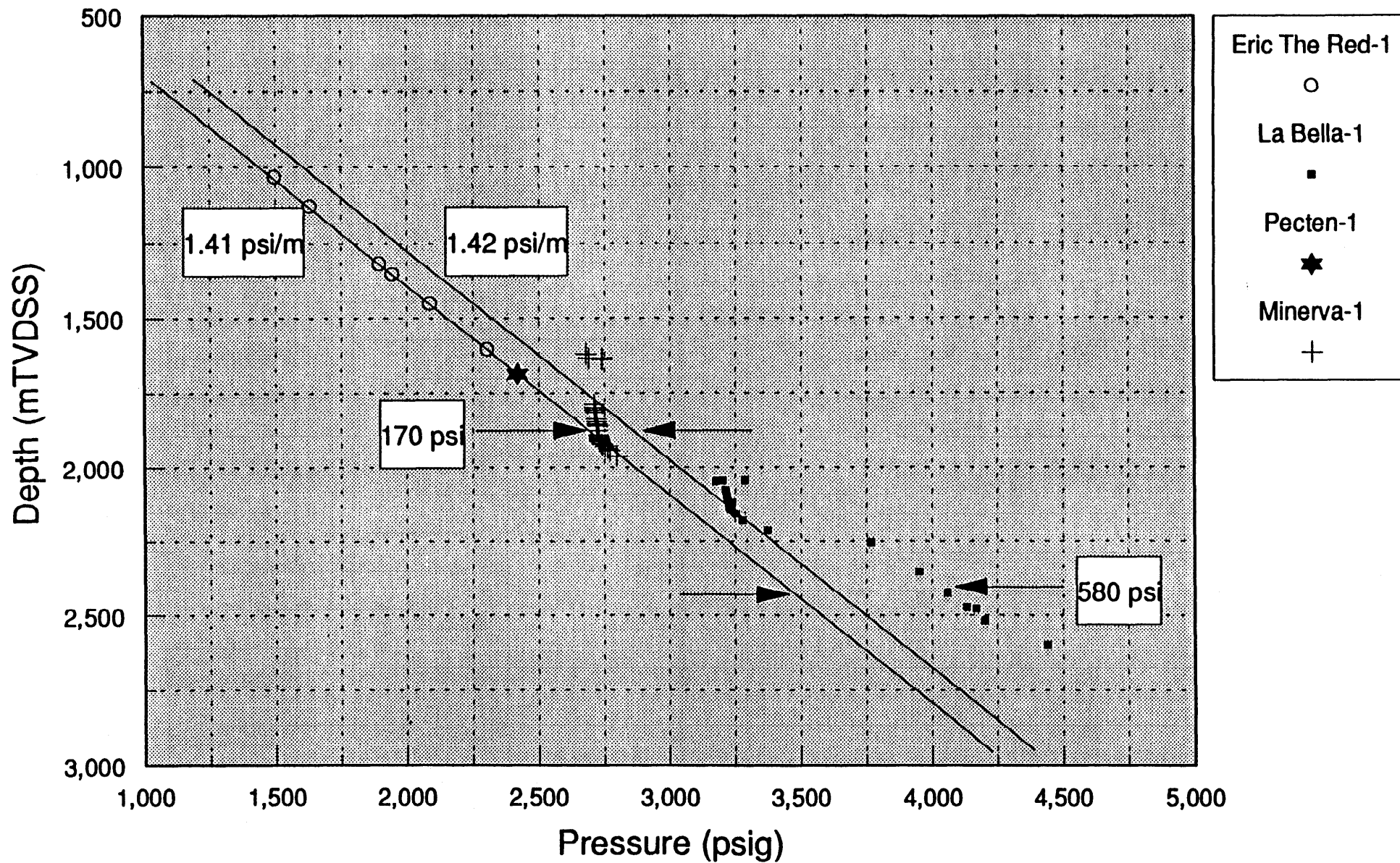
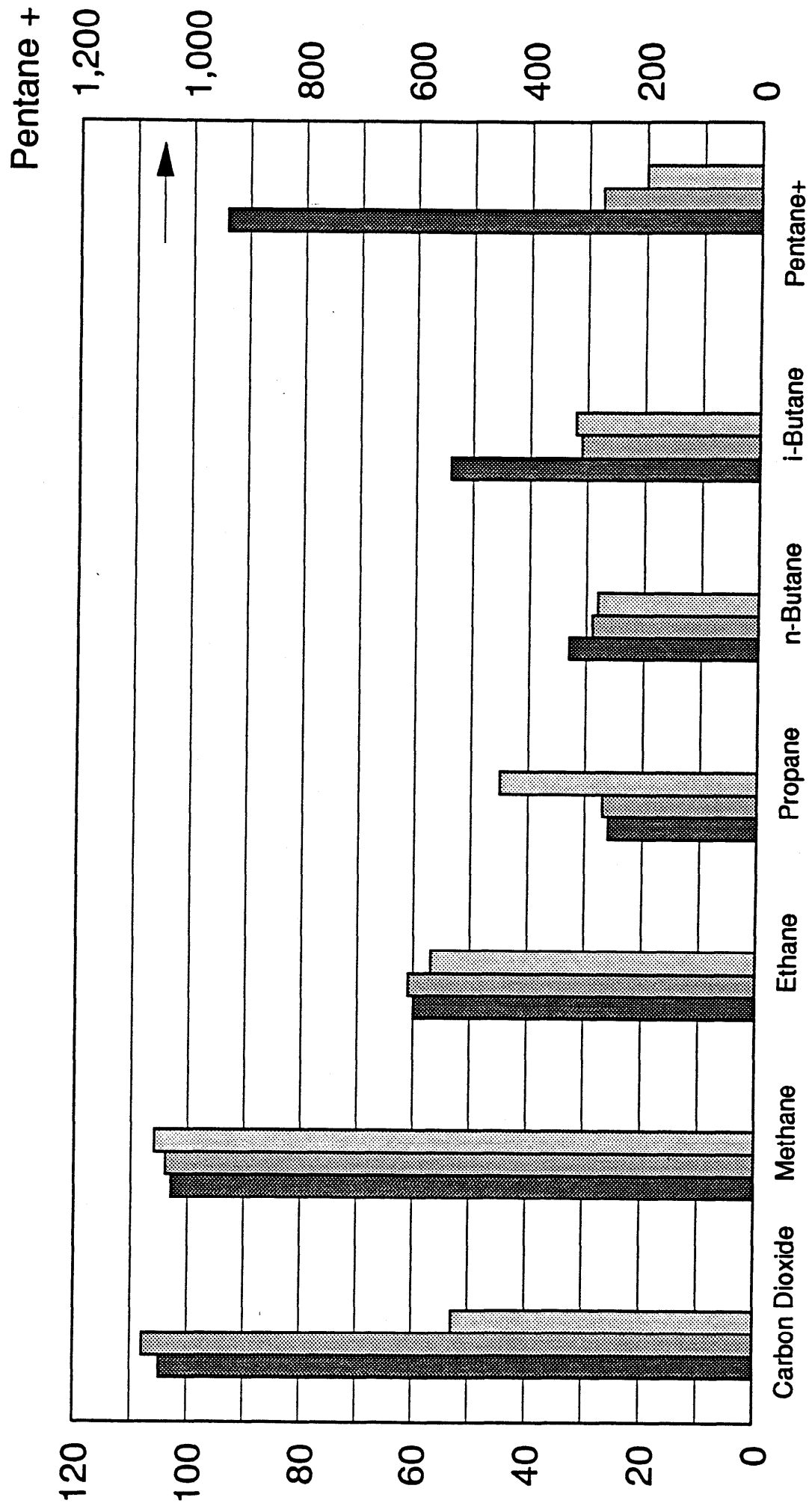




Figure 13.

# Minerva-1 Gas Analysis Data

Petrolab Results / Wellsite Analysis (%)



Legend:  
 1931.0 (darkest bar)  
 1948.5 (medium bar)  
 1649.8 mDF (lightest bar)

**APPENDIX A:**

**PETROLAB PVT ANALYSIS REPORT**

47 Woodforde Road, Magill,  
South Australia, 5072  
P.O. Box 410,  
Magill, South Australia, 5072



Fax: 364 1500  
Telex: AA88214  
Tel: (08) 364 1500  
(08) 333 0787

Reservoir Fluid and Core Services, Laboratory Consulting and Analysis

A. C. N. 008 130 667  
**Adelaide, April 30, 1993**  
**P. O. Box 410**  
**Magill**  
**S. A. 5072**

**B H P Petroleum Pty. Ltd.**  
**G. P. O. Box 1911-R**  
**Melbourne**  
**Vic. 3001**

**Subject: Reservoir Fluid Study**  
**Well : Minerva # 1**  
**File : B - 93013**

**Attention: Mr. Chris Taylor**  
**Mr. Keith Edwards**

**Dear Sirs,**

Please find enclosed our results of compositional analyses and constant mass studies performed on bottom hole samples transferred from RFT chambers # RFS AD-1123, # RFS AD-1227 and # RFS AD-1157 containing samples from subject well.

Representative low pressure samples from all RFT chambers were also transferred into gas cylinders for isotope and other geochemical analyses and forwarded to BHP in Melbourne.

During these constant composition expansions at the reservoir temperature, no dew point pressure was observed for the sample from RFT chamber # RFS AD-1157, but the sample from RFS AD-1123 exhibited a dew point at 2745 psig and sample from RFS AD-1227 a dew point at 1802 psig.

We thank BHP Petroleum Pty. Ltd. for the opportunity given to be of service. Please do not hesitate in contacting us should you require any further information or if we can assist you in any other way.

Yours Sincerely,

Jan G. Bon  
Manager

# PETROLAB

Company : BHP Petroleum Pty. Ltd.

Well : Minerva # 1

File : B 93013

## REPORT INDEX

Page

### RFS - AD - 1123

Summary of Results and Transfer Details	1
Field Characteristics	2
Compositional Analyses	3
Constant Mass Study	4-5
PLOTS:	
Relative Volume	6
Gas Formation Volume Factor	7
Gas Expansion Factor	8
Gas Deviation Factor	9
Specific Volume of Reservoir Fluid	10
Viscosity of Reservoir Fluid	11
Retrograde Liquid Deposit	12

### RFS - AD # 1227

Summary of Results and Transfer Details	13
Field Characteristics	14
Compositional Analyses	15
Constant Mass Study	16-17
PLOTS:	
Relative Volume	18
Gas Formation Volume Factor	19
Gas Expansion Factor	20
Gas Deviation Factor	21
Specific Volume of Reservoir Fluid	22
Viscosity of Reservoir Fluid	23
Retrograde Liquid Deposit	24

# PETROLAB

Company : BHP Petroleum Pty. Ltd.  
Well : Minerva # 1

File : B 93013

## REPORT INDEX

Page

RFS - AD - 1157

Summary of Results and Transfer Details	25
Field Characteristics	26
Compositional Analyses	27
Constant Mass Study	28
PLOTS:	
Relative Volume	29
Gas Formation Volume Factor	30
Gas Expansion Factor	31
Gas Deviation Factor	32
Specific Volume of Reservoir Fluid	33
Viscosity of Reservoir Fluid	34

## TRANSFER DETAILS

RFT Chamber	:	RFS - AD # 1123
Depth	:	1649.8 M KB
Capacity	:	1 Gallon
Run Type	:	Open Hole RFT
Received	:	April 01, 1993
Opening Pressure	:	1750 Psig @ 24 oC

Injected 100 cc's of mercury in chamber to stir up sample. Chamber compressed to 5000 psig with approximately 1810 cc's of water behind piston. Transferred 1800 cc's into Petrolab cylinders # L-010, L-044 and # L-011 @ 5000 psig. Last cylinder contains part of gas and water. Flashed rest of sample to atmosphere. Recovered another 212 cc's of water.

## SUMMARY OF RESULTS

### RESERVOIR FLUID IS GAS CONDENSATE

#### SATURATED VAPOUR :

Reservoir Temperature (°F)	:	176
Dew Point Pressure (psig)	:	2745
Gas Formation Volume Factor (Bg)	:	0.00576
Gas Expansion Factor (E)	:	173.68
Gas Deviation Factor (Z)	:	0.884
Specific Volume (CFT/LB)	:	0.12484
Density (gm/cc)	:	0.1283
Viscosity (centipoise)	:	0.0188
Molecular Weight	:	17.51
Gas Gravity (Air = 1.000)	:	0.606
Gross Heating Value (BTU/ft3)	:	1065

#### Total Plant Products in Reservoir Fluid (GPMM):

Ethane	:	1310
Propane	:	633
Butanes	:	343
Pentanes Plus	:	211

# P E T R O L A B

Company: BHP Petroleum Pty. Ltd.  
Well: Minerva # 1

Page: 2 of 34  
File : B 93013

## FIELD CHARACTERISTICS:

Formation Name	:	--
Date first well completed	:	--
Original reservoir pressure (psia)	:	--
@ datum (ft KBMD)	:	--
Original Gas-Liquid Ratio SCF/STB	:	--
Separator pressure (psig)	:	--
Separator temperature (°F)	:	--
Liquid gravity (°API @ 60 °F)	:	--

## WELL CHARACTERISTICS:

Depth datum (m)	:	KB
Elevation above MSL (m)	:	--
Total depth (m MD)	:	--
Producing interval (m)	:	--
Perforated intervals (m)	:	--
Casing Shoe (m KB)	:	--
Casing Size (inch)	:	--
Reservoir temperature (°F)	:	176
Last reservoir pressure (psia)	:	2694.6
@ datum (m TVD ss)	:	--
date	:	--
Status of well	:	--

## BOTTOM HOLE SAMPLING CONDITIONS:

Chamber #	:	RFS - AD # 1123
Run Type	:	Open hole RFT
Capacity	:	1 Gallon
Depth sampled (m KB)	:	1649.8
Sample type	:	Gas
Sampled by	:	Schlumberger

# P E T R O L A B

Company : BHP Petroleum Pty. Ltd.  
Well : Minerva # 1

Page : 3 of 34  
File : B 93013

## COMPOSITIONAL ANALYSIS OF Reservoir Fluid

RFS AD # 1123

Component	Mol %	GPM	
Oxygen	O2 0.00		Pressure Base : 14.696
Carbon Dioxide	CO2 0.32		Zsc : 0.998
Nitrogen	N2 1.26		Mol Weight : 17.51
Methane	C1 93.98		Gas Gravity : 0.606
Ethane	C2 2.53	0.677	Pc : 664.3
Propane	C3 1.05	0.290	Tc : 355.7
Iso-Butane	iC4 0.18	0.059	Mol Weight C6+ : 117.8
N-Butane	nC4 0.23	0.073	Density C6+ : 0.7107
Iso-Pentane	iC5 0.07	0.026	Mol Weight C7+ : 128.6
N-Pentane	nC5 0.05	0.018	Density C7+ : 0.7223
Hexanes	C6 0.08	0.031	Mol Weight C8+ : 146.9
Heptanes	C7 0.09	0.038	Density C8+ : 0.7399
Octanes	C8 0.03	0.014	Mol Weight C11+ : 168.8
Nonanes	C9 0.02	0.010	Density C11+ : 0.7583
Decanes	C10 0.02	0.011	Mol Weight C12+ : 175.0
Undecanes	C11 0.02	0.012	Density C12+ : 0.7631
Dodecanes Plus	C12+ 0.07	0.051	Heating Value (BTU/ft3)
TOTAL	100.00	1.310	Gross : 1065
			Nett : 961
			Wobbe Index : 1369
			Zpt * : 0.895

(P)ressure : 2745 psig (T)emperature: 176 °F



# P E T R O L A B

Company: BHP Petroleum Pty. Ltd.  
Well: Minerva # 1

Page: 4 of 34  
File: B 93013

## CONSTANT MASS STUDY @ 176 °F

Pressure (psig)	Relative Volume (V/Vsat) (1)	Formation Volume Factor (Bg) (2)	Gas Expansion Factor (E) (3)	Deviation Factor (Z)	Specific Volume (CFT/LB)	Gas Viscosity (Centipoise) (4)
5000	0.6256	0.00360	277.63	1.005	0.07810	0.0255
4500	0.6715	0.00387	258.65	0.971	0.08383	0.0241
4015	0.7295	0.00420	238.10	0.942	0.09107	0.0226
3604	0.7934	0.00457	218.90	0.920	0.09905	0.0214
3203	0.8747	0.00504	198.55	0.902	0.10920	0.0202
3007	0.9235	0.00532	188.07	0.894	0.11529	0.0196
2890	0.9543	0.00549	182.01	0.888	0.11913	0.0193
2745 *	1.0000	0.00576	173.68	0.884	0.12484	0.0188

\* Dew Point Pressure

- (1) Cubic feet of gas at indicated pressure and temperature per cubic foot at reservoir pressure
- (2) Cubic feet of gas at indicated pressure and temperature per cubic foot at 14.696 psia and 60 °F
- (3) Cubic feet of gas at 14.696 psia and 60 °F per cubic foot at indicated pressure and temperature
- (4) Calculated from correlation of Lee, Gonzales and Eakin

# P E T R O L A B

Company: Santos Limited  
Well: Minerva # 1

Page: 5 of 34  
File: B 93013

## CONSTANT MASS STUDY @ 176 °F

Pressure (psig)	Relative Volume (V/V <sub>sat</sub> ) (1)	Retrograde Liquid Deposit	
		(Bbl/MMSCF) (2)	(Volume%) (3)
2745 *	1.0000	0.00	0.00
2680 **	1.0232	1.18	0.12
2514	1.0889	2.31	0.23
2300	1.1871	4.29	0.42
2006	1.3623	8.32	0.81
1805	1.5183	13.87	1.35
1669	1.6469	16.51	1.61
1402	1.9700	18.96	1.85
1206	2.3042	19.98	1.95
955	2.9361	20.92	2.04

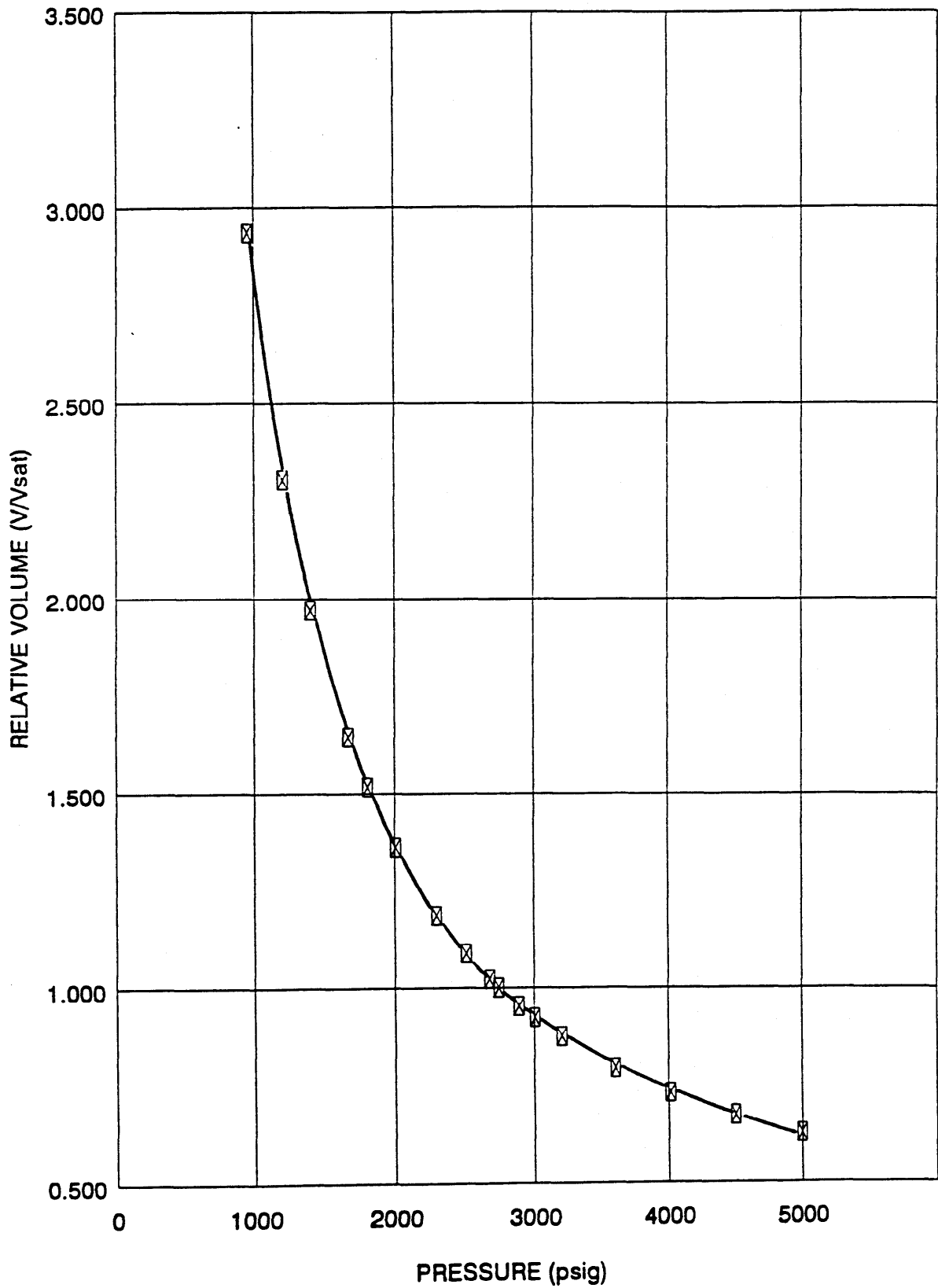
\* Dew Point Pressure

\*\* Reservoir Pressure

- (1) Cubic feet of gas at indicated pressure and temperature per cubic foot at saturation pressure
- (2) Barrels of liquid at indicated pressure and temperature per MMSCF of original reservoir fluid
- (3) Percent of reservoir hydrocarbon pore space at dew point

# PETROLAB

## RELATIVE VOLUME

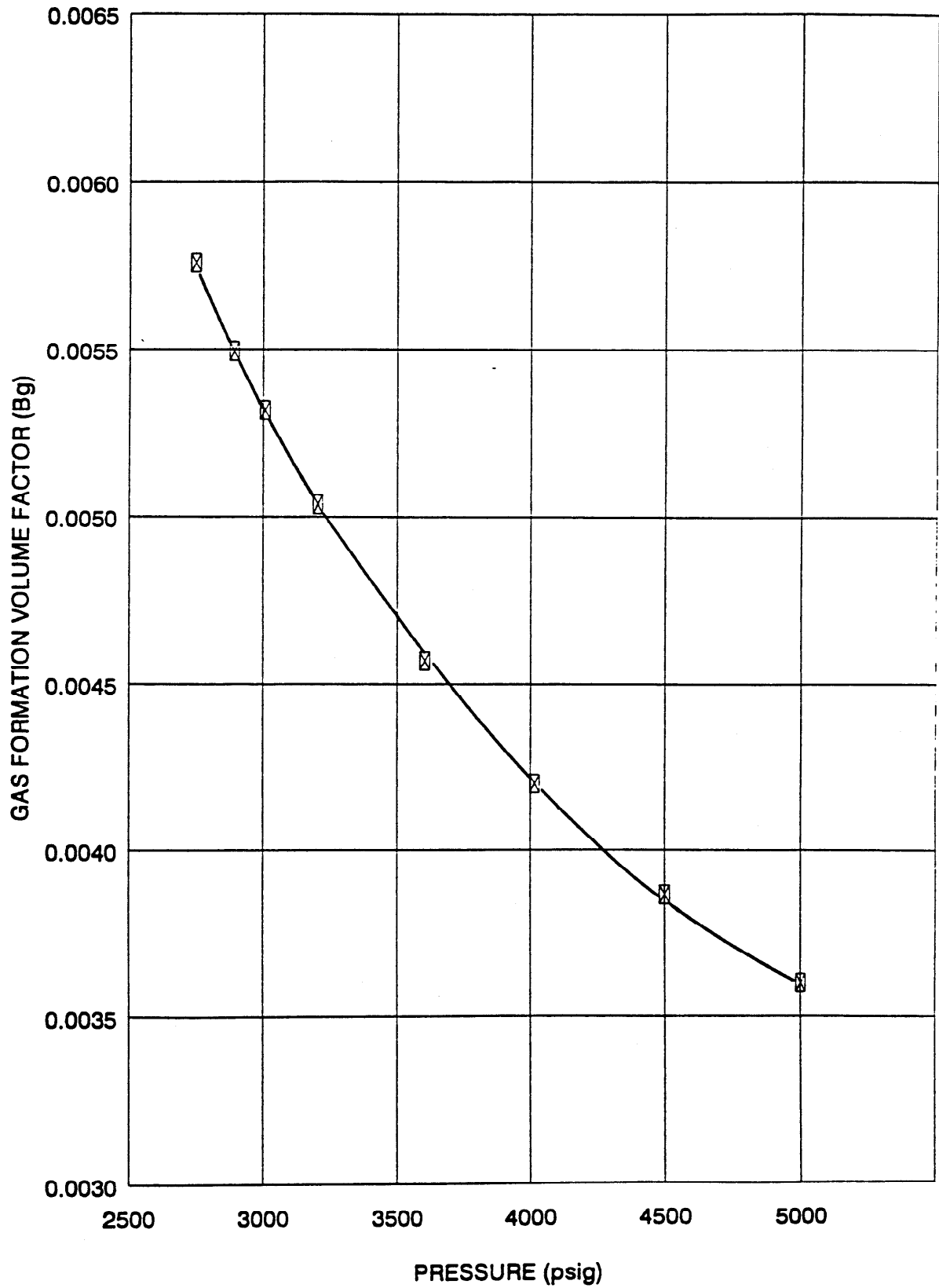


# PETROLAB

Company: BHP Petroleum Pty. Ltd.  
Well: Minerva # 1

Page: 7 of 34  
File : B 93013

## GAS FORMATION VOLUME FACTOR

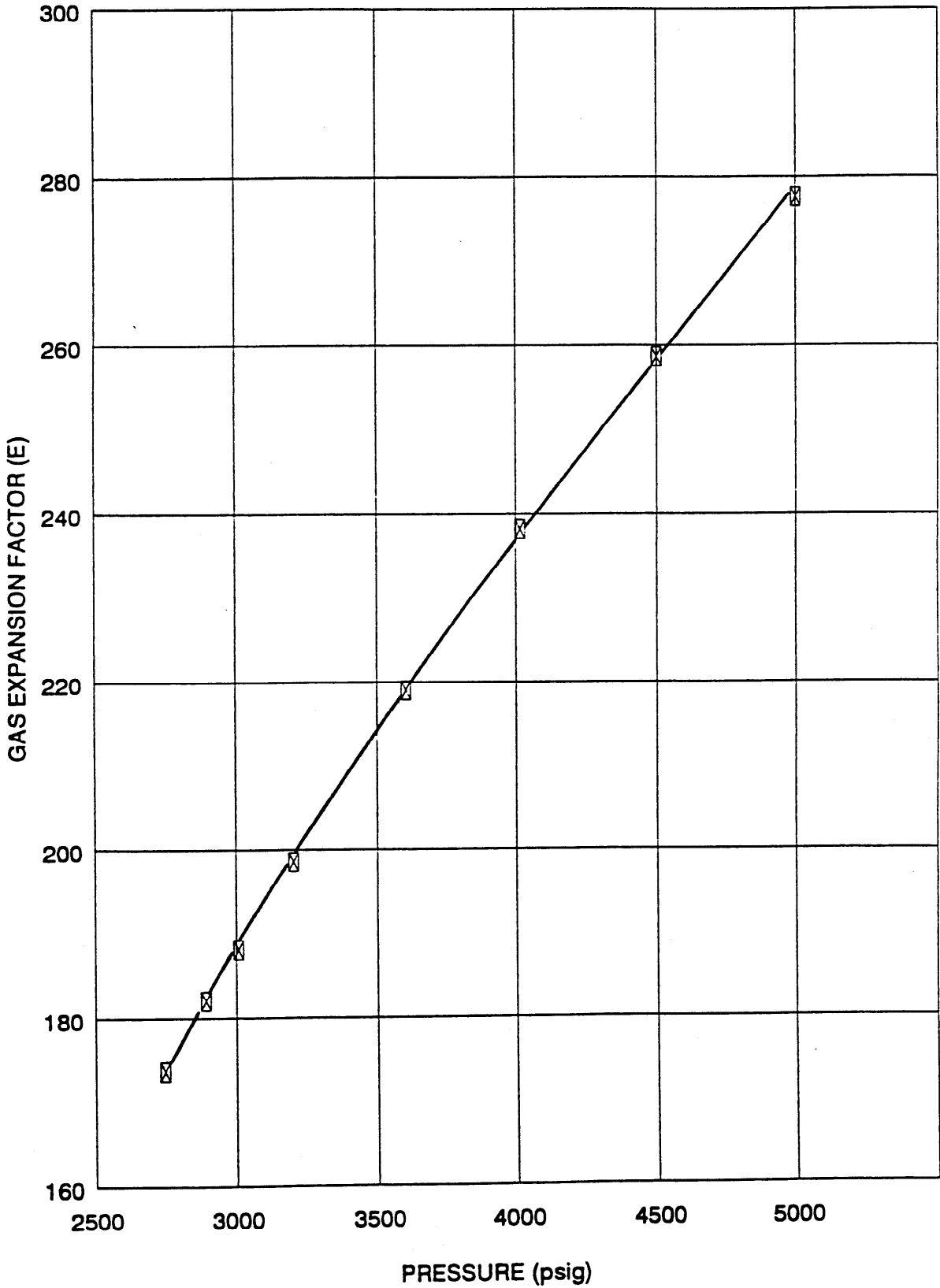


# PETROLAB

Company: BHP Petroleum Pty. Ltd.  
Well: Minerva # 1

Page: 8 of 34  
File : B 93013

## GAS EXPANSION FACTOR

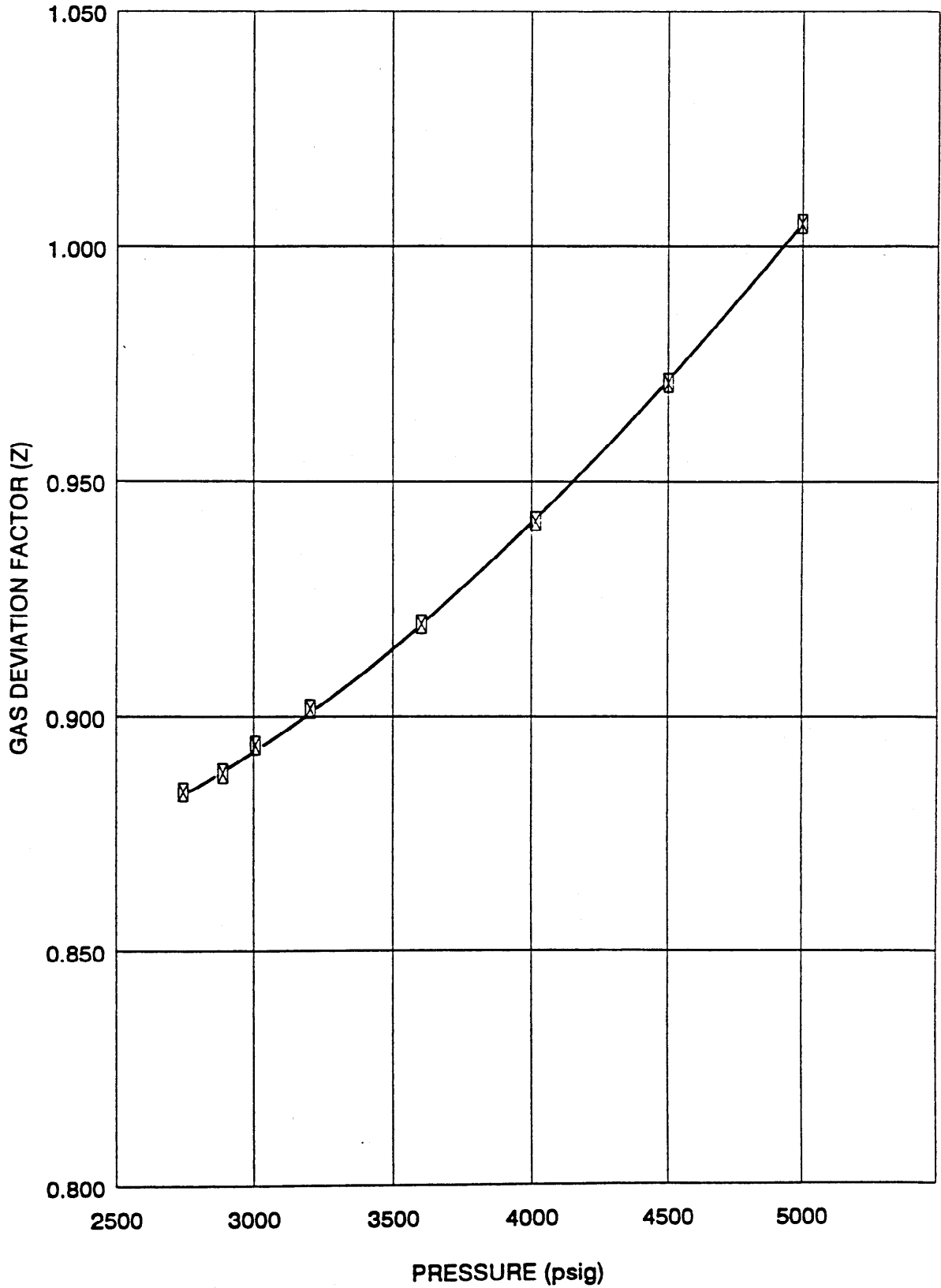


# PETROLAB

Company: BHP Petroleum Pty. Ltd.  
Well: Minerva # 1

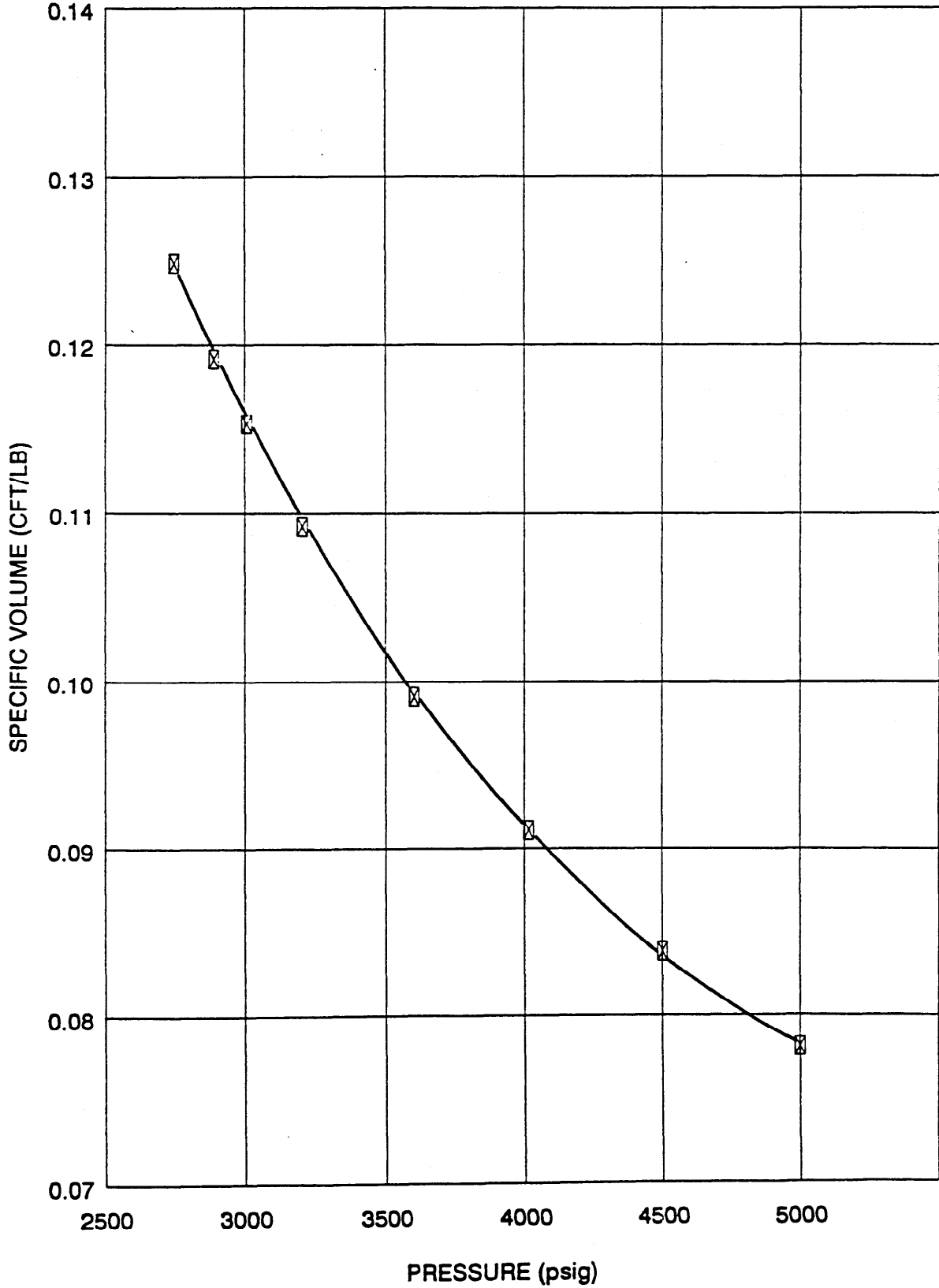
Page: 9 of 34  
File: B 93013

## GAS DEVIATION FACTOR



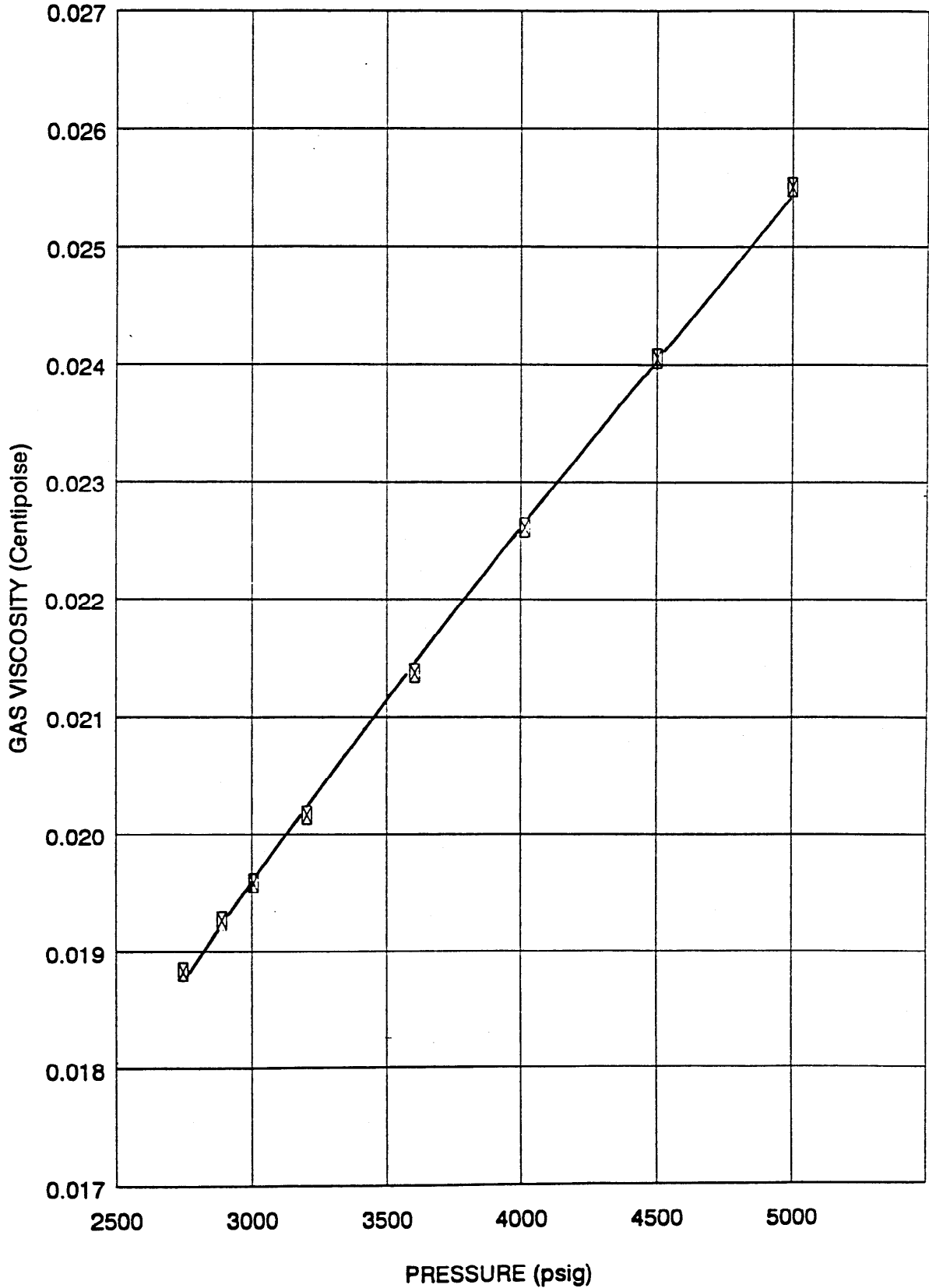
# PETROLAB

## RESERVOIR FLUID SPECIFIC VOLUME



# PETROLAB

## VISCOSITY OF RESERVOIR FLUID



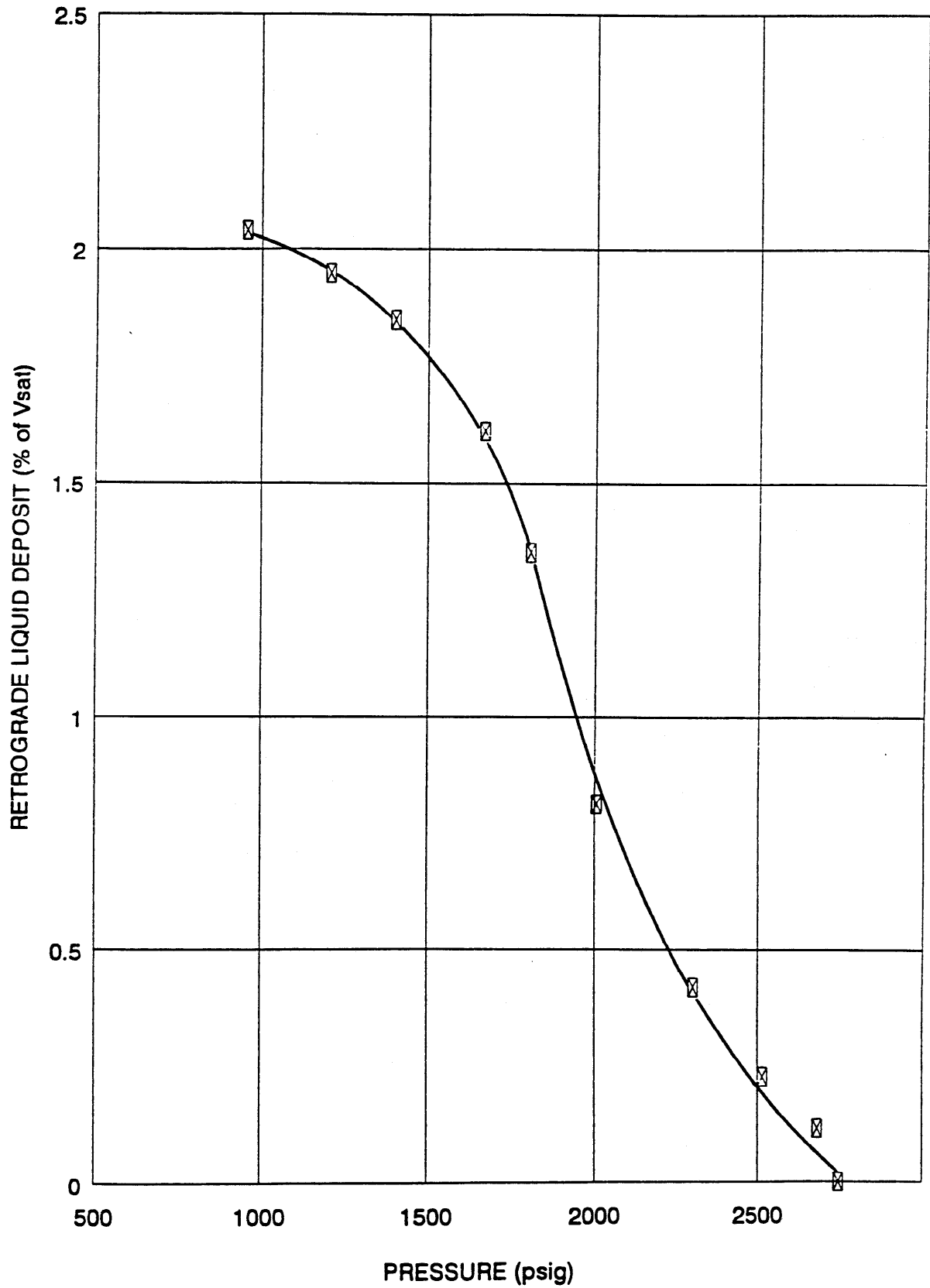


# PETROLAB

Company: BHP Petroleum Pty. Ltd.  
Well: Minerva # 1

Page: 12 of 34  
File : B 93013

## RETROGRADE CONDENSATION



# PETROLAB

Company: BHP Petroleum Pty. Ltd.  
Well: Minerva # 1

Page: 13 of 34  
File: B 93013

## TRANSFER DETAILS

RFT Chamber	:	RFS - AD # 1227
Depth	:	1931.0 M KB
Capacity	:	1 Gallon
Run Type	:	Open Hole RFT
Received	:	April 01, 1993
Opening Pressure	:	1750 Psig @ 21 oC

Injected 150 cc's of mercury in chamber to stir up sample. Chamber compressed to 5000 psig with approximately 1760 cc's of water behind piston. Transferred 1825 cc's into Petrolab cylinders # L-129, L-048 and # L-119 @ 5000 psig. Last cylinder contains part of gas and water. Flashed rest of sample to atmosphere. Recovered another 30 cc's of water.

## SUMMARY OF RESULTS

### RESERVOIR FLUID IS GAS CONDENSATE

#### SATURATED VAPOUR:

Reservoir Temperature (°F)	:	203
Dew Point Pressure (psig)	:	1802
Gas Formation Volume Factor (Bg)	:	0.00922
Gas Expansion Factor (E)	:	108.44
Gas Deviation Factor (Z)	:	0.8941
Specific Volume (CFT/LB)	:	0.19758
Density (gm/cc)	:	0.0811
Viscosity (centipoise)	:	0.0164
Molecular Weight	:	17.72
Gas Gravity (Air = 1.000)	:	0.613
Gross Heating Value (BTU/ft <sup>3</sup> )	:	1045

#### Total Plant Products in Reservoir Fluid (GPM):

Ethane	:	1130
Propane	:	536
Butanes	:	304
Pentanes Plus	:	202

# P E T R O L A B

Company: BHP Petroleum Pty. Ltd.  
Well: Minerva # 1

Page: 14 of 34  
File : B 93013

## FIELD CHARACTERISTICS:

Formation Name	:	--
Date first well completed	:	--
Original reservoir pressure (psia)	:	--
@ datum (ft KBMD)	:	--
Original Gas--Liquid Ratio SCF/STB)	:	--
Separator pressure (psig)	:	--
Separator temperature (°F)	:	--
Liquid gravity (°API @ 60 °F)	:	--

## WELL CHARACTERISTICS:

Depth datum (m)	:	KB
Elevation above MSL (m)	:	--
Total depth (m MD)	:	--
Producing interval (m)	:	--
Perforated intervals (m)	:	--
Casing Shoe (m KB)	:	--
Casing Size (inch)	:	--
Reservoir temperature (°F)	:	203
Last reservoir pressure (psia)	:	2743.4
@ datum (m TVD ss)	:	--
date	:	--
Status of well	:	--

## BOTTOM HOLE SAMPLING CONDITIONS:

Chamber #	:	RFS -- AD # 1227
Run Type	:	Open hole RFT
Capacity	:	1 Gallon
Depth sampled (m KB)	:	1931
Sample type	:	Gas
Sampled by	:	Schlumberger

# P E T R O L A B

Company : BHP Petroleum Pty. Ltd.  
Well : Minerva # 1

Page : 15 of 34  
File : B 93013

## COMPOSITIONAL ANALYSIS OF Reservoir Fluid

RFS AD # 1227

Component	Mol %	GPM	
Oxygen	O2 0.00		Pressure Base : 14.696
Carbon Dioxide	CO2 1.80		Zsc : 0.998
Nitrogen	N2 0.90		Mol Weight : 17.72
Methane	C1 93.45		Gas Gravity : 0.613
Ethane	C2 2.22	0.594	Pc : 671.0
Propane	C3 0.84	0.232	Tc : 357.4
Iso-Butane	iC4 0.12	0.039	Mol Weight C6+ : 104.1
N-Butane	nC4 0.20	0.063	Density C6+ : 0.6944
Iso-Pentane	iC5 0.05	0.018	Mol Weight C7+ : 109.7
N-Pentane	nC5 0.05	0.018	Density C7+ : 0.7013
Hexanes	C6 0.08	0.031	Mol Weight C8+ : 122.4
Heptanes	C7 0.14	0.059	Density C8+ : 0.7158
Octanes	C8 0.05	0.023	Mol Weight C11+ : 147.0
Nonanes	C9 0.05	0.025	Density C11+ : 0.7400
Decanes	C10 0.03	0.016	Mol Weight C12+ : --
Undecanes	C11 0.02	0.012	Density C12+ : --
Dodecanes Plus	C12+ 0.00	0.000	Heating Value (BTU/ft3)
TOTAL	100.00	1.130	Gross : 1045
			Nett : 943
			Wobbe Index : 1335
			Zpt * : 0.915

(P)ressure : 1802 psig (T)emperature: 203 °F

# P E T R O L A B

Company: BHP Petroleum Pty. Ltd.  
Well: Minerva # 1

Page: 16 of 34  
File: B 93013

## CONSTANT MASS STUDY @ 203 °F

Pressure (psig)	Relative Volume (V/Vsat) (1)	Formation Volume Factor (Bg) (2)	Gas Expansion Factor (E) (3)	Deviation Factor (Z)	Specific Volume (CFT/LB)	Gas Viscosity (Centipoise) (4)
5000	0.4077	0.00376	265.98	1.006	0.08055	0.0252
4008	0.4771	0.00440	227.28	0.945	0.09427	0.0225
3005	0.6089	0.00562	178.08	0.905	0.12032	0.0196
2729 **	0.6644	0.00613	163.21	0.897	0.13128	0.0188
2312	0.7798	0.00719	139.05	0.893	0.15409	0.0177
2110	0.8542	0.00788	126.95	0.893	0.16877	0.0172
2017	0.8938	0.00824	121.33	0.894	0.17660	0.0170
1802 *	1.0000	0.00922	108.44	0.894	0.19758	0.0164

\* Dew Point Pressure

\*\* Reservoir Pressure

(1) Cubic feet of gas at indicated pressure and temperature  
per cubic foot at reservoir pressure

(2) Cubic feet of gas at indicated pressure and temperature  
per cubic foot at 14.696 psia and 60 °F

(3) Cubic feet of gas at 14.696 psia and 60 °F  
per cubic foot at indicated pressure and temperature

(4) Calculated from correlation of Lee, Gonzales and Eakin

# P E T R O L A B

Company: Santos Limited  
Well: Minerva # 1

Page: 17 of 34  
File: B 93013

## CONSTANT MASS STUDY @ 203 °F

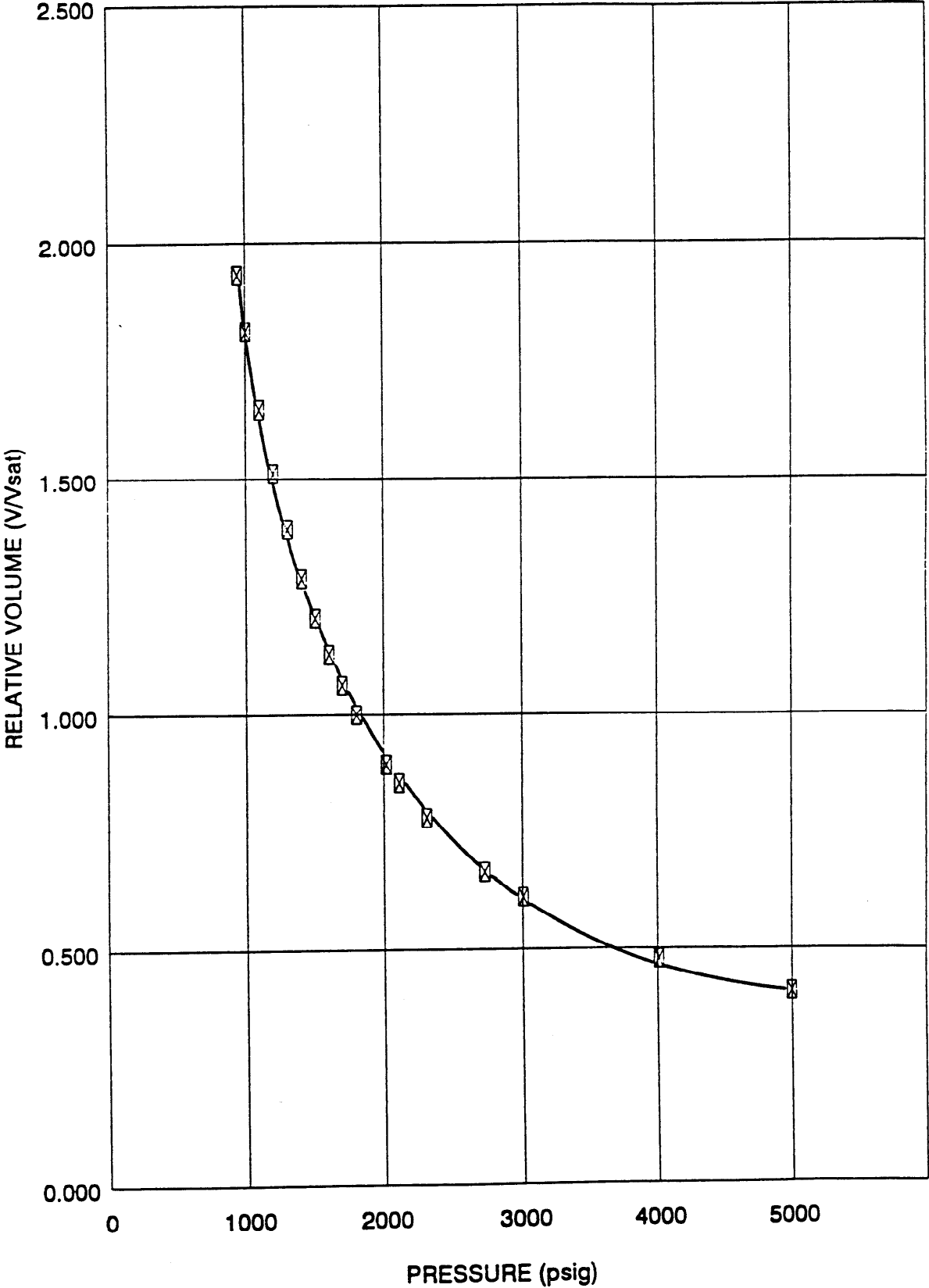
Pressure (psig)	Relative Volume (V/Vsat) (1)	Retrograde Liquid Deposit	
		(Bbl/MMSCF) (2)	(Volume%) (3)
1802 *	1.0000	0.00	0.00
1698	1.0624	1.21	0.07
1602	1.1267	2.45	0.15
1500	1.2046	3.67	0.22
1403	1.2899	5.42	0.33
1301	1.3928	7.52	0.46
1201	1.5109	8.92	0.54
1103	1.6472	9.27	0.56
1004	1.8131	9.45	0.58
850	2.1642	9.36	0.57

**\* Dew Point Pressure**

- (1) Cubic feet of gas at indicated pressure and temperature per cubic foot at saturation pressure
- (2) Barrels of liquid at indicated pressure and temperature per MMSCF of original reservoir fluid
- (3) Percent of reservoir hydrocarbon pore space at dew point

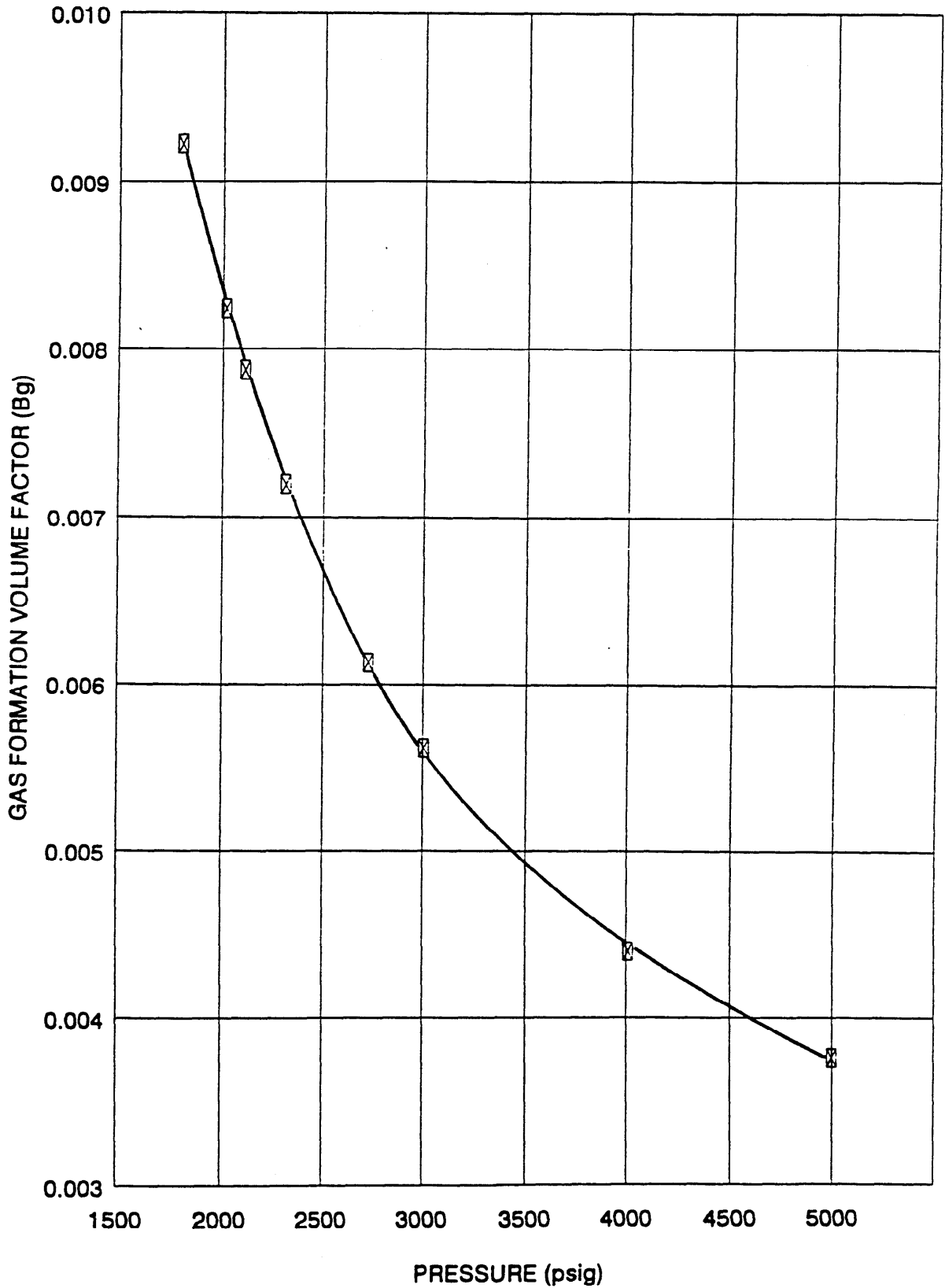
# PETROLAB

## RELATIVE VOLUME



# PETROLAB

## GAS FORMATION VOLUME FACTOR



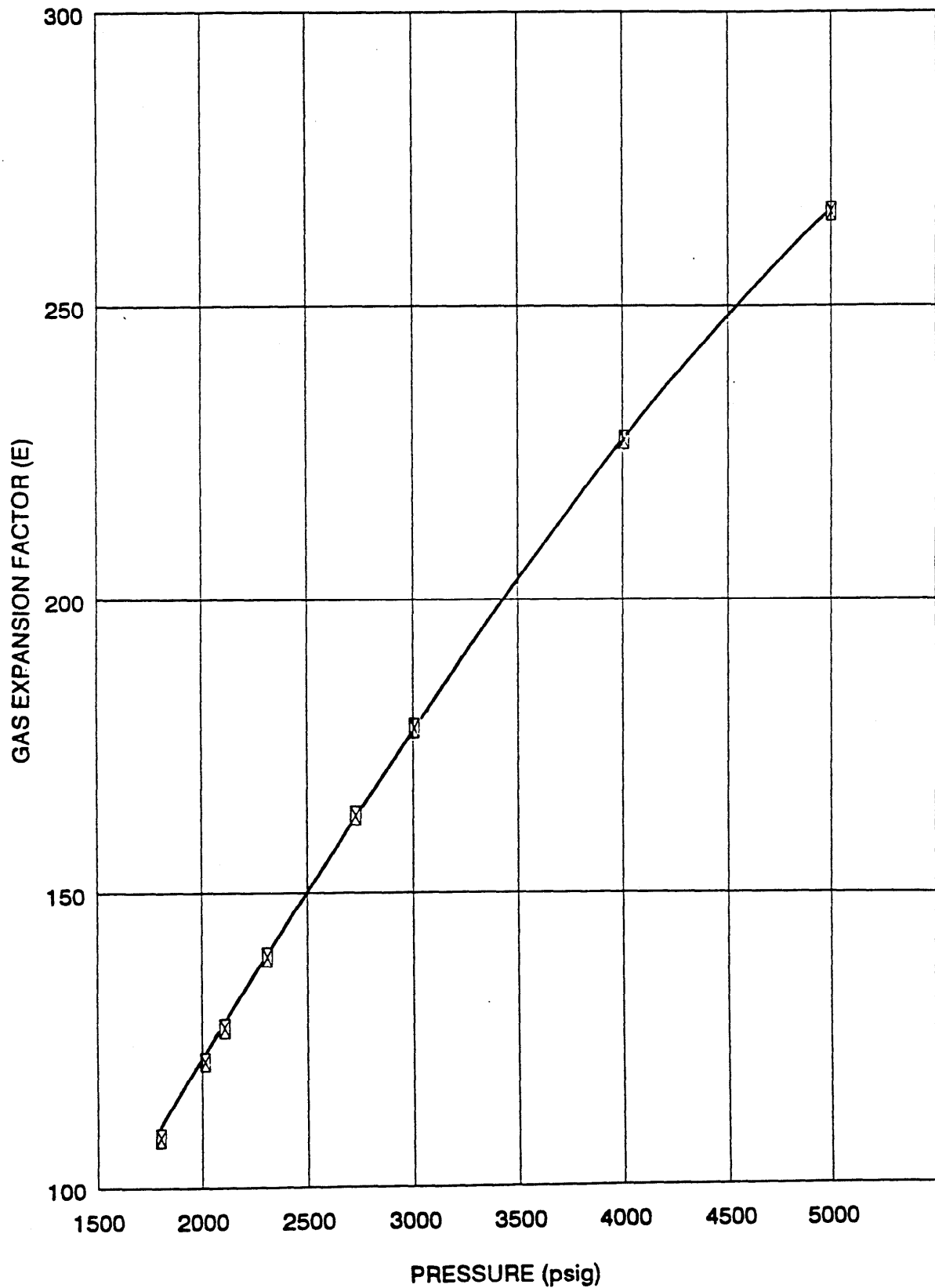


# PETROLAB

Company: BHP Petroleum Pty. Ltd.  
Well: Minerva # 1

Page: 20 of 34  
File : B 93013

## GAS EXPANSION FACTOR

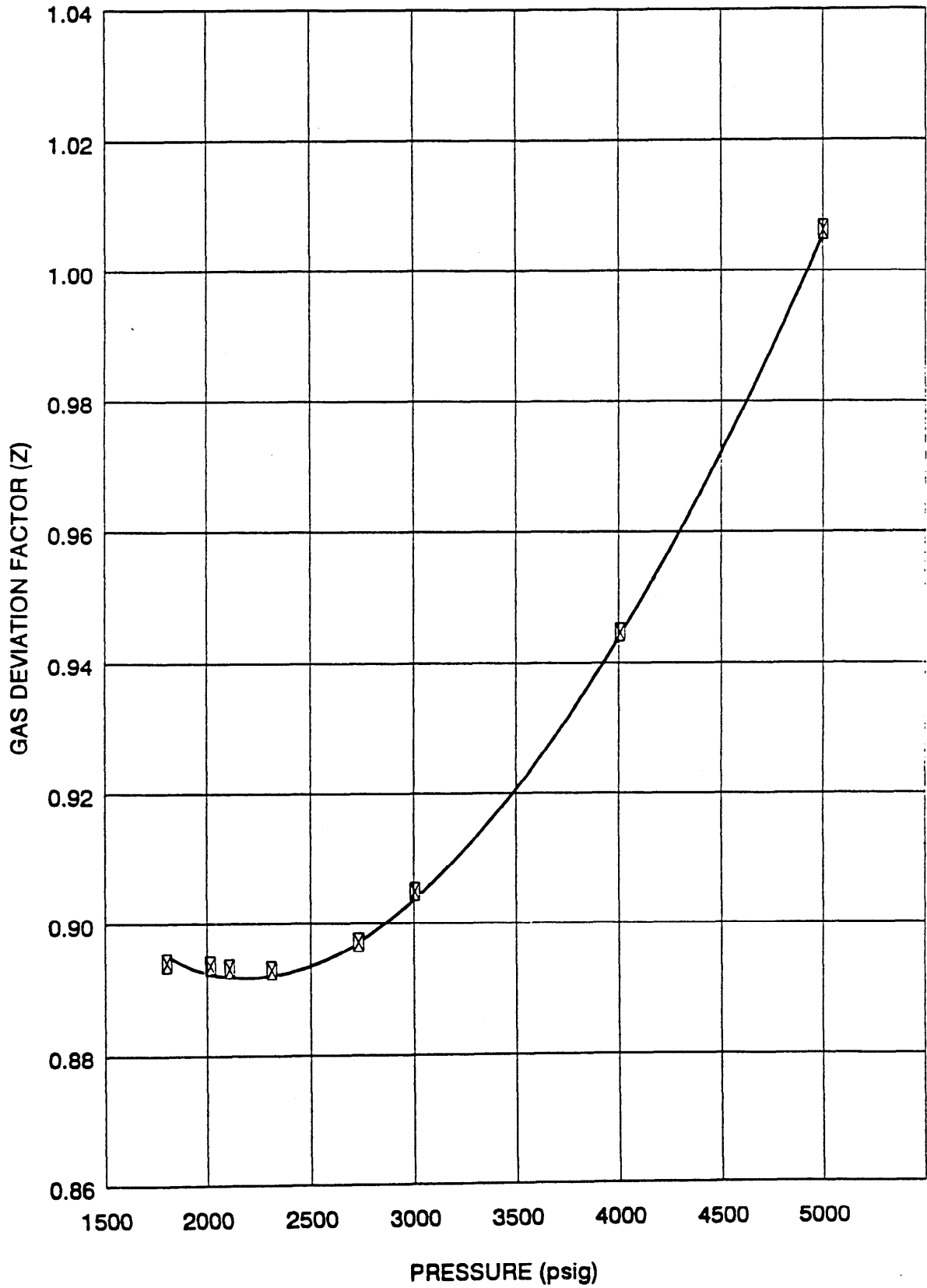


# PETROLAB

Company: BHP Petroleum Pty. Ltd.  
Well: Minerva # 1

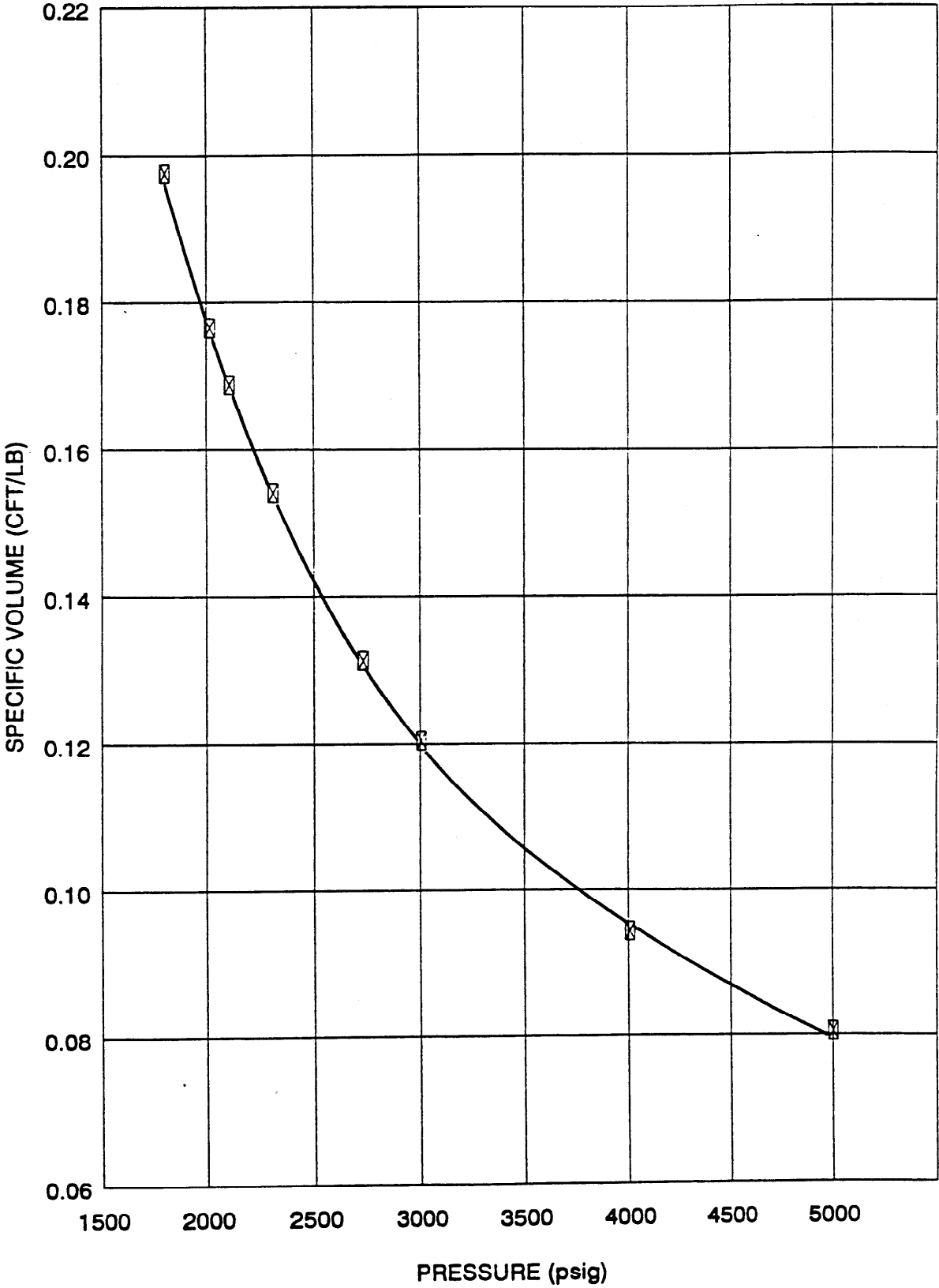
Page: 21 of 34  
File: B 93013

## GAS DEVIATION FACTOR



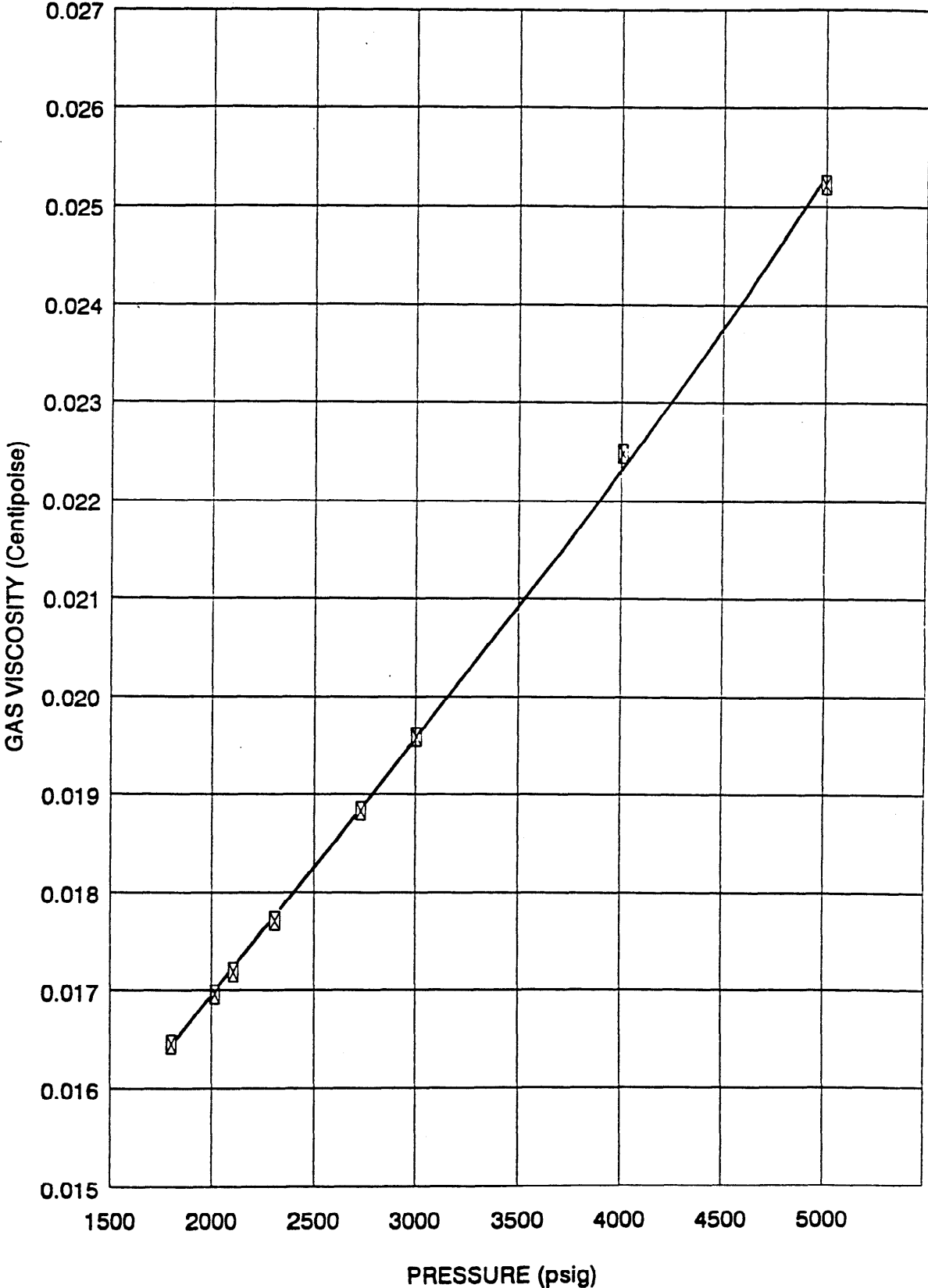
# PETROLAB

## RESERVOIR FLUID SPECIFIC VOLUME



# PETROLAB

## VISCOSITY OF RESERVOIR FLUID

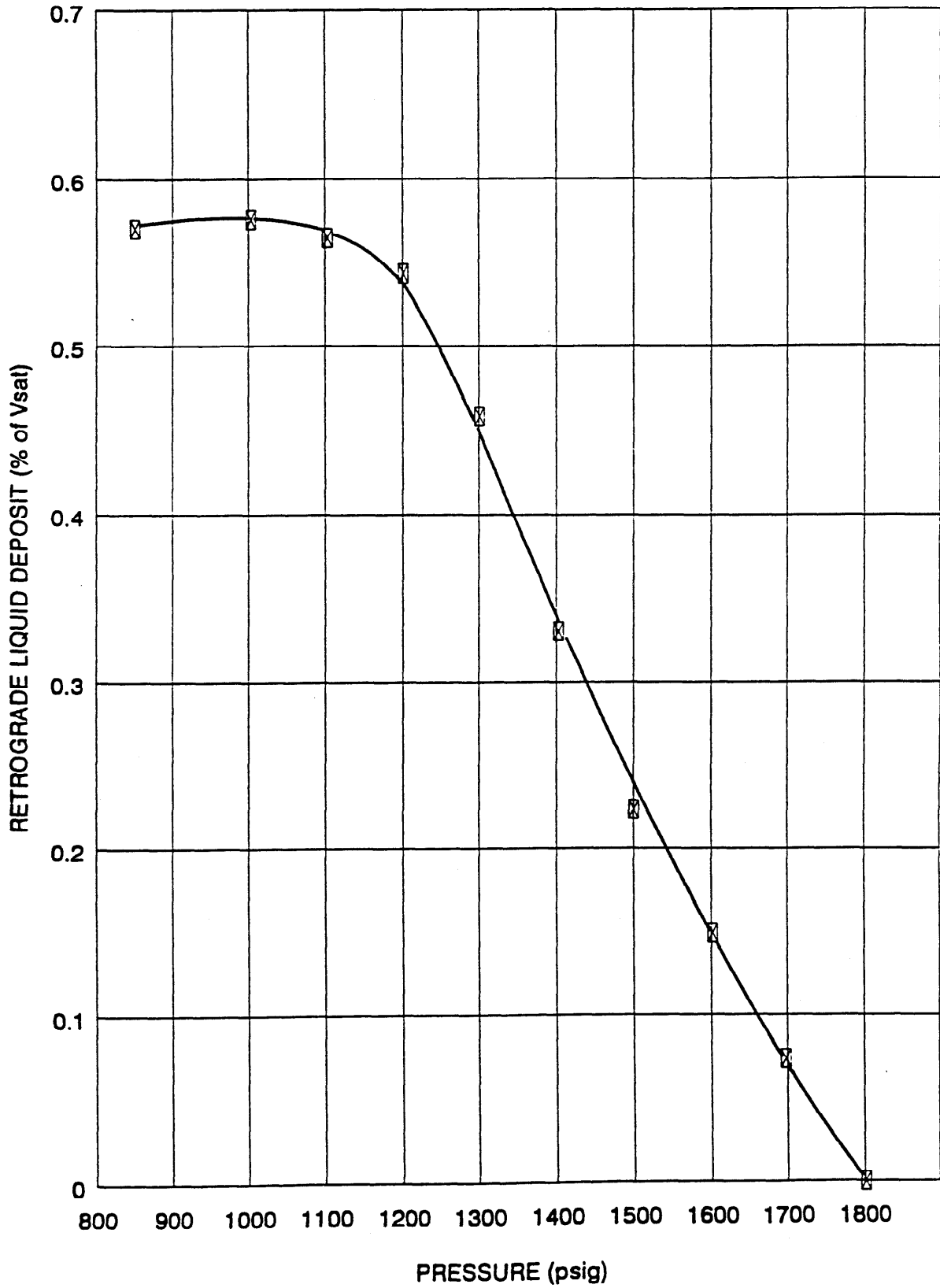


# PETROLAB

Company: BHP Petroleum Pty. Ltd.  
Well: Minerva # 1

Page: 24 of 34  
File: B 93013

## RETROGRADE CONDENSATION



# PETROLAB

Company: BHP Petroleum Pty. Ltd.

Well: Minerva # 1

Page: 25 of 34

File: B 93013

## TRANSFER DETAILS

RFT Chamber	:	RFS - AD # 1157
Depth	:	1942.5 M KB
Capacity	:	1 Gallon
Run Type	:	Open Hole RFT
Received	:	April 01, 1993
Opening Pressure	:	1690 Psig @ 18 oC

Injected 150 cc's of mercury in chamber to stir up sample. Chamber compressed to 5000 psig with approximately 2010 cc's of water behind piston. Transferred 1800 cc's into Petrolab cylinders # L-007, L-008 and # L-105 @ 5000 psig. Last cylinder contains part of gas and water. Flashed rest of sample to atmosphere. Recovered another 12 cc's of water.

## SUMMARY OF RESULTS

**RESERVOIR FLUID IS DRY GAS !! NO DEW POINT MEASURED**

**VAPOUR AT RESERVOIR CONDITIONS:**

Reservoir Temperature (°F)	:	203
Dew Point Pressure (psig)	:	-----
Gas Formation Volume Factor (Bg)	:	0.00621
Gas Expansion Factor (E)	:	161.07
Gas Deviation Factor (Z)	:	0.910
Specific Volume (CFT/LB)	:	0.13332
Density (gm/cc)	:	0.1202
Viscosity (centipoise)	:	0.0187
Molecular Weight	:	17.68
Gas Gravity (Air = 1.000)	:	0.612
Gross Heating Value (BTU/ft3)	:	1042

**Total Plant Products in Reservoir Fluid (GPMM):**

Ethane	:	1107
Propane	:	507
Butanes	:	278
Pentanes Plus	:	182

# P E T R O L A B

Company: BHP Petroleum Pty. Ltd.  
Well: Minerva # 1

Page: 26 of 34  
File : B 93013

## FIELD CHARACTERISTICS:

Formation Name	:	---
Date first well completed	:	---
Original reservoir pressure (psia)	:	---
@ datum (ft KBMD)	:	---
Original Gas-Liquid Ratio SCF/STB)	:	---
Separator pressure (psig)	:	---
Separator temperature (°F)	:	---
Liquid gravity (°API @ 60 °F)	:	---

## WELL CHARACTERISTICS:

Depth datum (m)	:	KB
Elevation above MSL (m)	:	---
Total depth (m MD)	:	---
Producing interval (m)	:	---
Perforated intervals (m)	:	---
Casing Shoe (m KB)	:	---
Casing Size (inch)	:	---
Reservoir temperature (°F)	:	203
Last reservoir pressure (psia)	:	2746.3
@ datum (m TVD ss)	:	---
date	:	---
Status of well	:	---

## BOTTOM HOLE SAMPLING CONDITIONS:

Chamber #	:	RFS - AD # 1157
Run Type	:	Open hole RFT
Capacity	:	1 Gallon
Depth sampled (m KB)	:	1942.5
Sample type	:	Gas
Sampled by	:	Schlumberger

# P E T R O L A B

Company : BHP Petroleum Pty. Ltd.  
Well : Minerva # 1

Page : 27 of 34  
File : B 93013

## COMPOSITIONAL ANALYSIS OF Reservoir Fluid

RFS AD # 1157

Component	Mol %	GPM	
Oxygen	O2 0.00		Pressure Base : 14.696
Carbon Dioxide	CO2 1.83		Zsc : 0.998
Nitrogen	N2 0.89		Mol Weight : 17.68
Methane	C1 93.48		Gas Gravity : 0.612
Ethane	C2 2.24	0.600	Pc : 671.3
Propane	C3 0.83	0.229	Tc : 357.2
Iso-Butane	iC4 0.11	0.036	Mol Weight C6+ : 102.3
N-Butane	nC4 0.19	0.060	Density C6+ : 0.6922
Iso-Pentane	iC5 0.05	0.018	Mol Weight C7+ : 107.3
N-Pentane	nC5 0.05	0.018	Density C7+ : 0.6984
Hexanes	C6 0.07	0.027	Mol Weight C8+ : 118.5
Heptanes	C7 0.13	0.055	Density C8+ : 0.7116
Octanes	C8 0.06	0.027	Mol Weight C11+ : 147.0
Nonanes	C9 0.04	0.020	Density C11+ : 0.7400
Decanes	C10 0.02	0.011	Mol Weight C12+ : --
Undecanes	C11 0.01	0.006	Density C12+ : --
Dodecanes Plus	C12+ 0.00	0.000	Heating Value (BTU/ft3)
TOTAL	100.00	1.107	Gross : 1042
			Nett : 940
			Wobbe Index : 1333
			Zpt * : 0.917

(P)ressure : 2732 psig (T)emperature: 203 °F



# P E T R O L A B

Company: BHP Petroleum Pty. Ltd.  
Well: Minerva # 1

Page: 28 of 34  
File: B 93013

## CONSTANT MASS STUDY @ 203 °F

Pressure (psig)	Relative Volume (V/Vsat) (1)	Formation Volume Factor (Bg) (2)	Gas Expansion Factor (E) (3)	Deviation Factor (Z)	Specific Volume (CFT/LB)	Gas Viscosity (Centipoise) (4)
5000	0.6119	0.00380	263.21	1.017	0.08159	0.0250
4517	0.6576	0.00408	244.94	0.987	0.08767	0.0237
4017	0.7177	0.00446	224.41	0.959	0.09569	0.0223
3495	0.8031	0.00499	200.57	0.934	0.10707	0.0208
2999	0.9186	0.00570	175.34	0.917	0.12247	0.0194
2732 *	1.0000	0.00621	161.07	0.910	0.13332	0.0187
2499	1.0893	0.00676	147.86	0.907	0.14523	0.0181
2205	1.2324	0.00765	130.70	0.906	0.16431	0.0173
2007	1.3540	0.00841	118.96	0.907	0.18052	0.0169
1801	1.5094	0.00937	106.71	0.908	0.20124	0.0164
1597	1.7040	0.01058	94.52	0.910	0.22719	0.0159
1300	2.1005	0.01304	76.68	0.915	0.28004	0.0153
1108	2.4731	0.01535	65.13	0.920	0.32973	0.0150

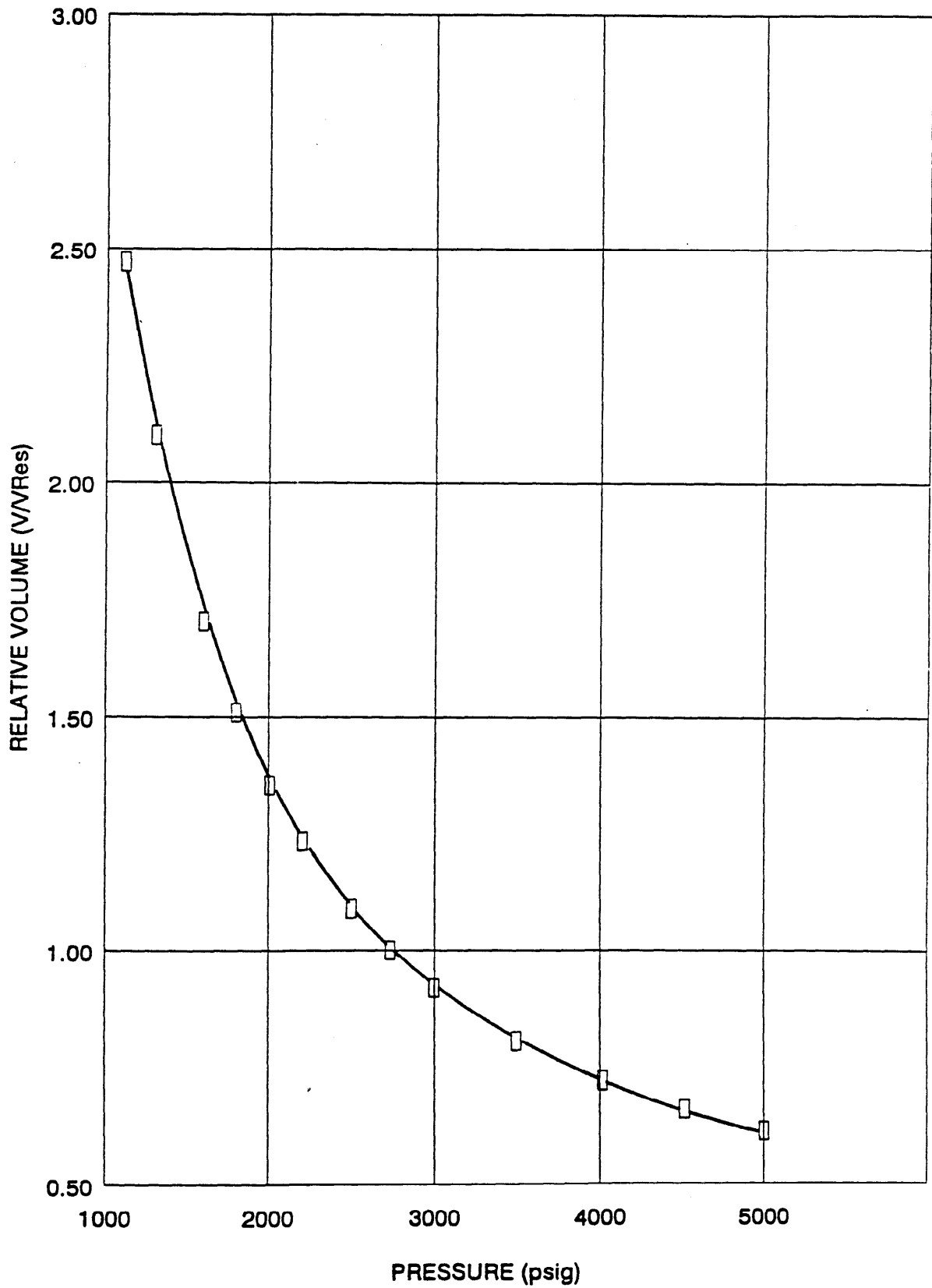
\* Reservoir Pressure

**!! NO DEW POINT FOUND RESERVOIR FLUID IS <sup>DRY</sup> ~~WET~~ GAS !!**

- (1) Cubic feet of gas at indicated pressure and temperature per cubic foot at reservoir pressure
- (2) Cubic feet of gas at indicated pressure and temperature per cubic foot at 14.696 psia and 60 °F
- (3) Cubic feet of gas at 14.696 psia and 60 °F per cubic foot at indicated pressure and temperature
- (4) Calculated from correlation of Lee, Gonzales and Eakin

# PETROLAB

## RELATIVE VOLUME

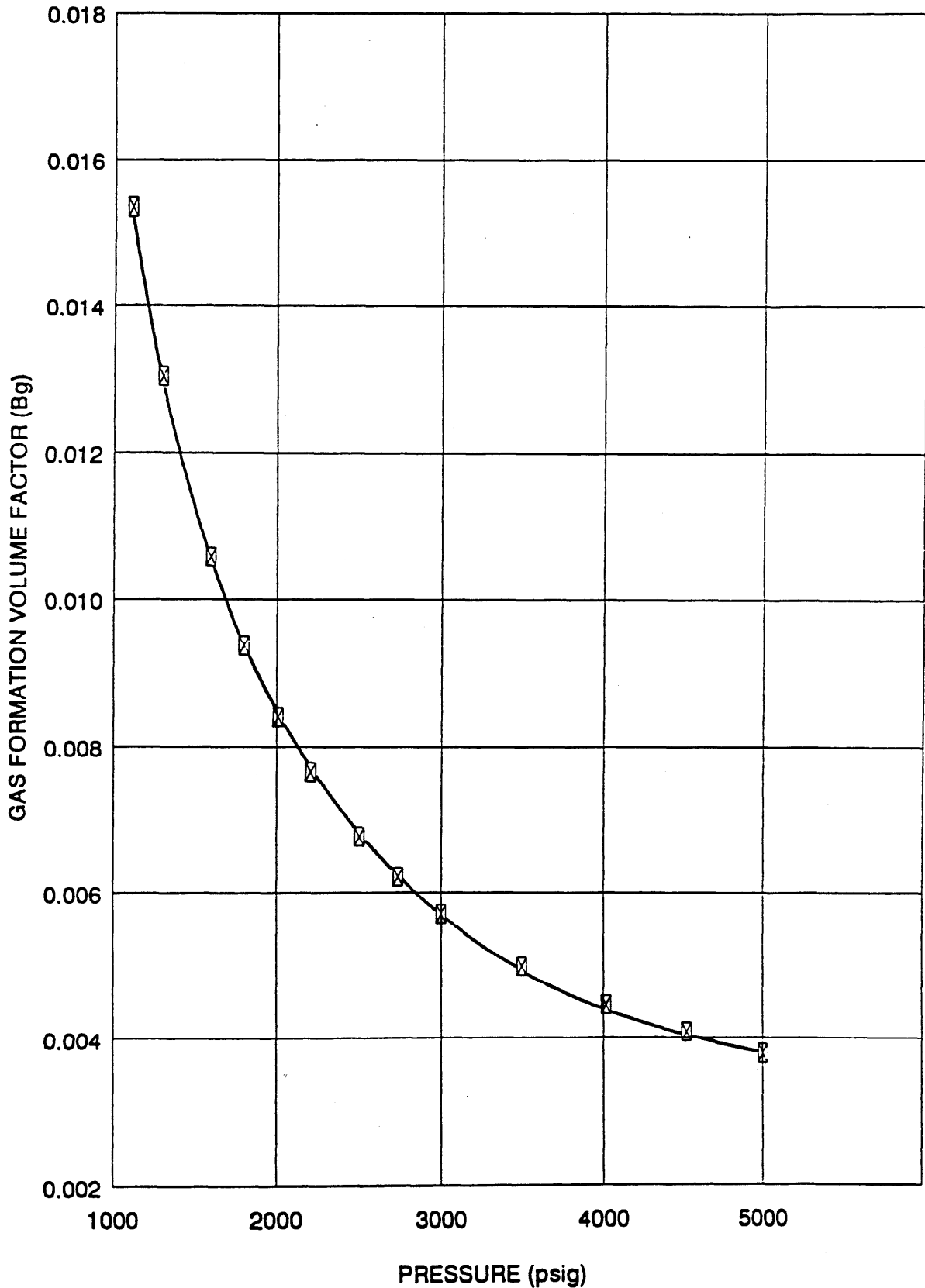


# PETROLAB

Company: BHP Petroleum Pty. Ltd.  
Well: Minerva # 1

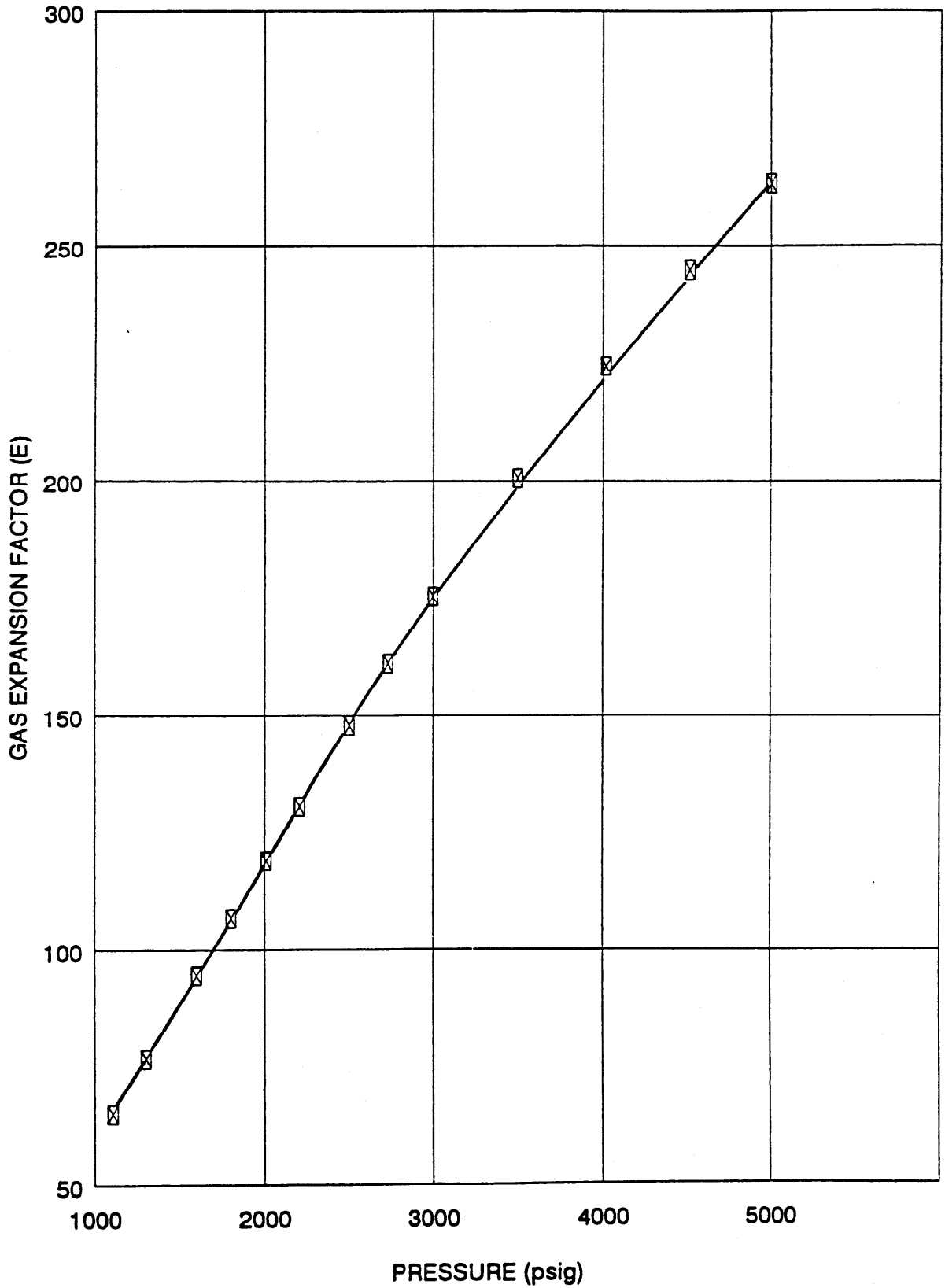
Page: 30 of 34  
File: B 93013

## GAS FORMATION VOLUME FACTOR



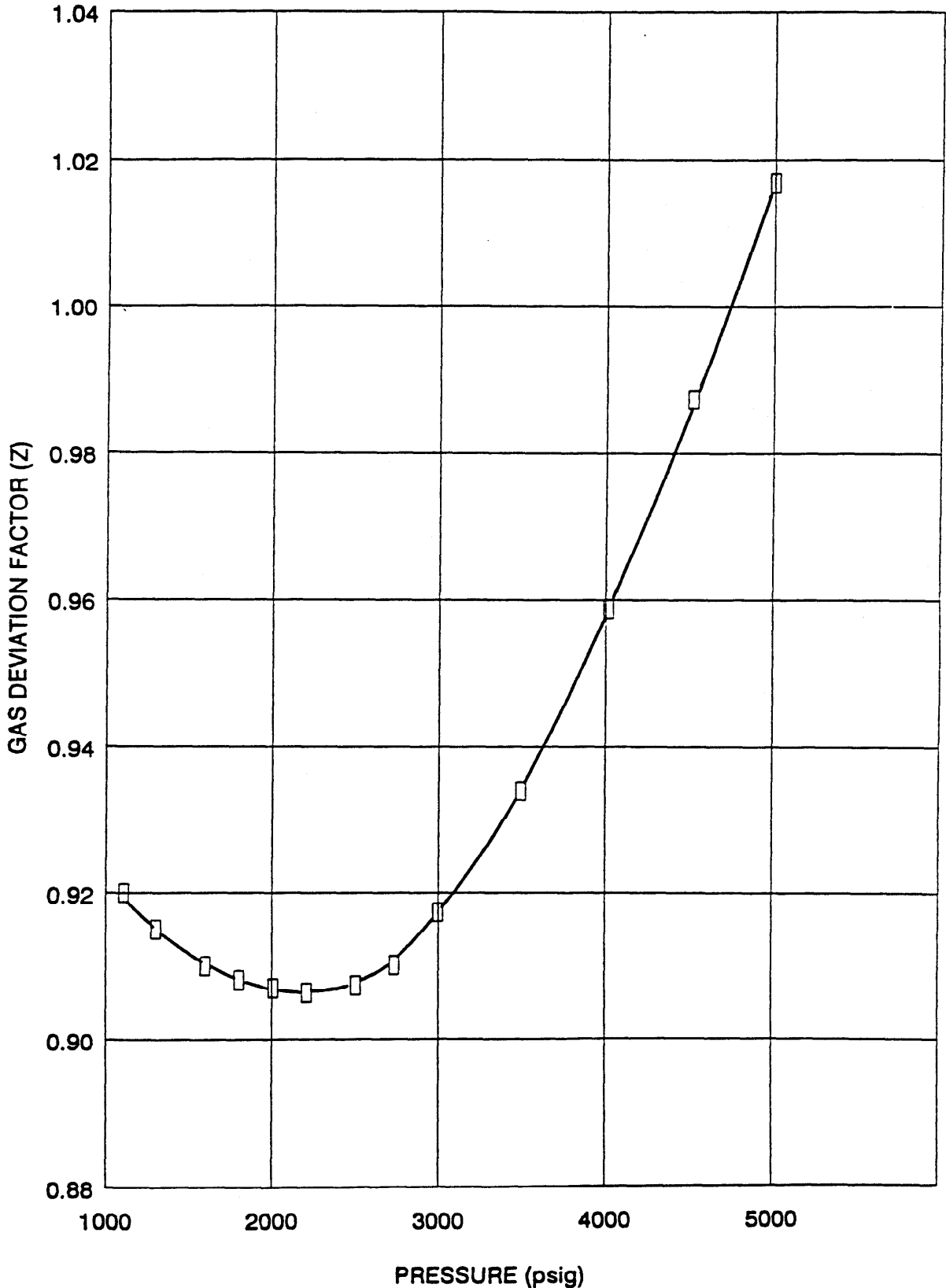
# PETROLAB

## GAS EXPANSION FACTOR



# PETROLAB

## GAS DEVIATION FACTOR

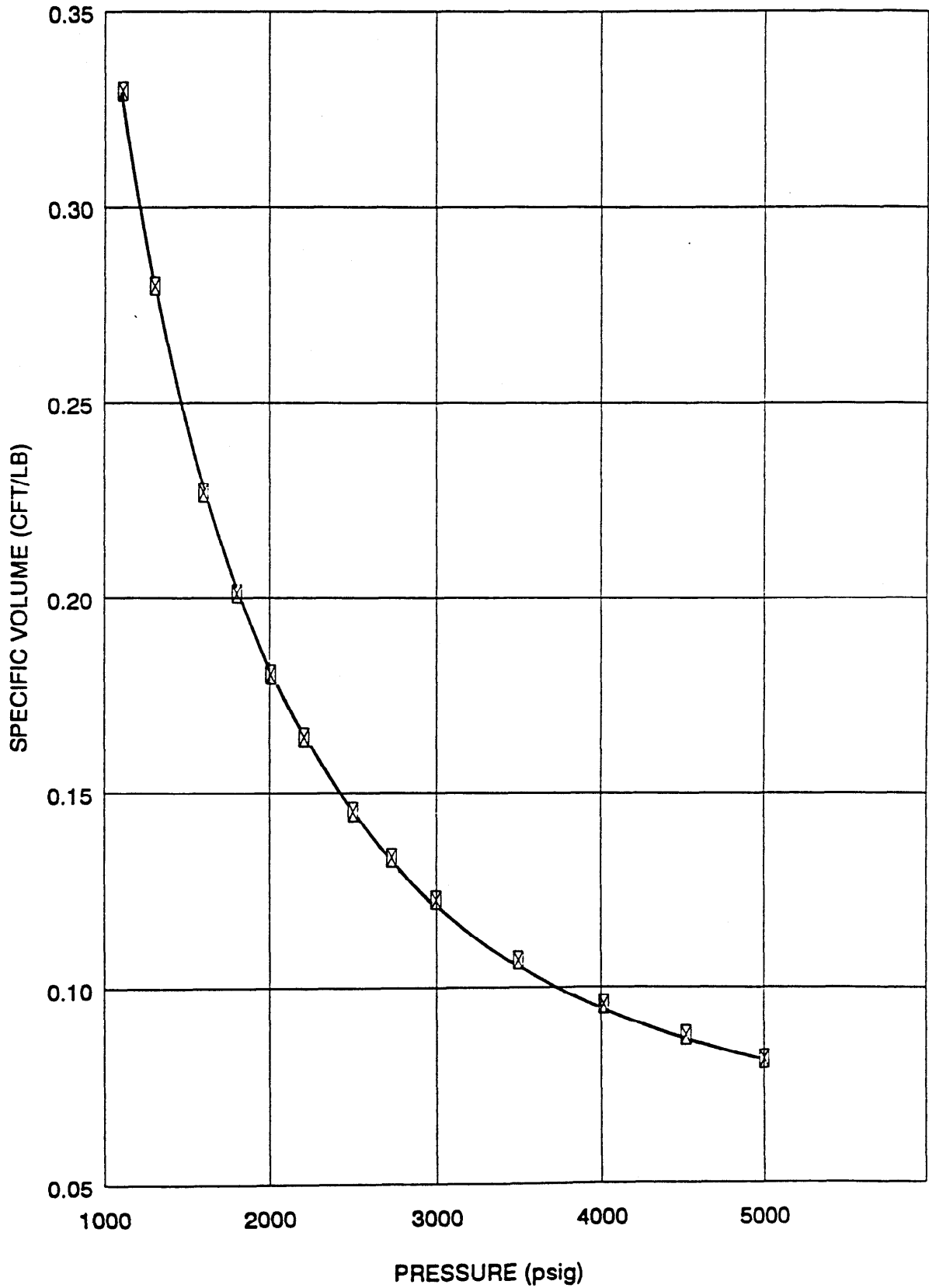


# PETROLAB

Company: BHP Petroleum Pty. Ltd.  
Well: Minerva # 1

Page: 33 of 34  
File: B 93013

## RESERVOIR FLUID SPECIFIC VOLUME

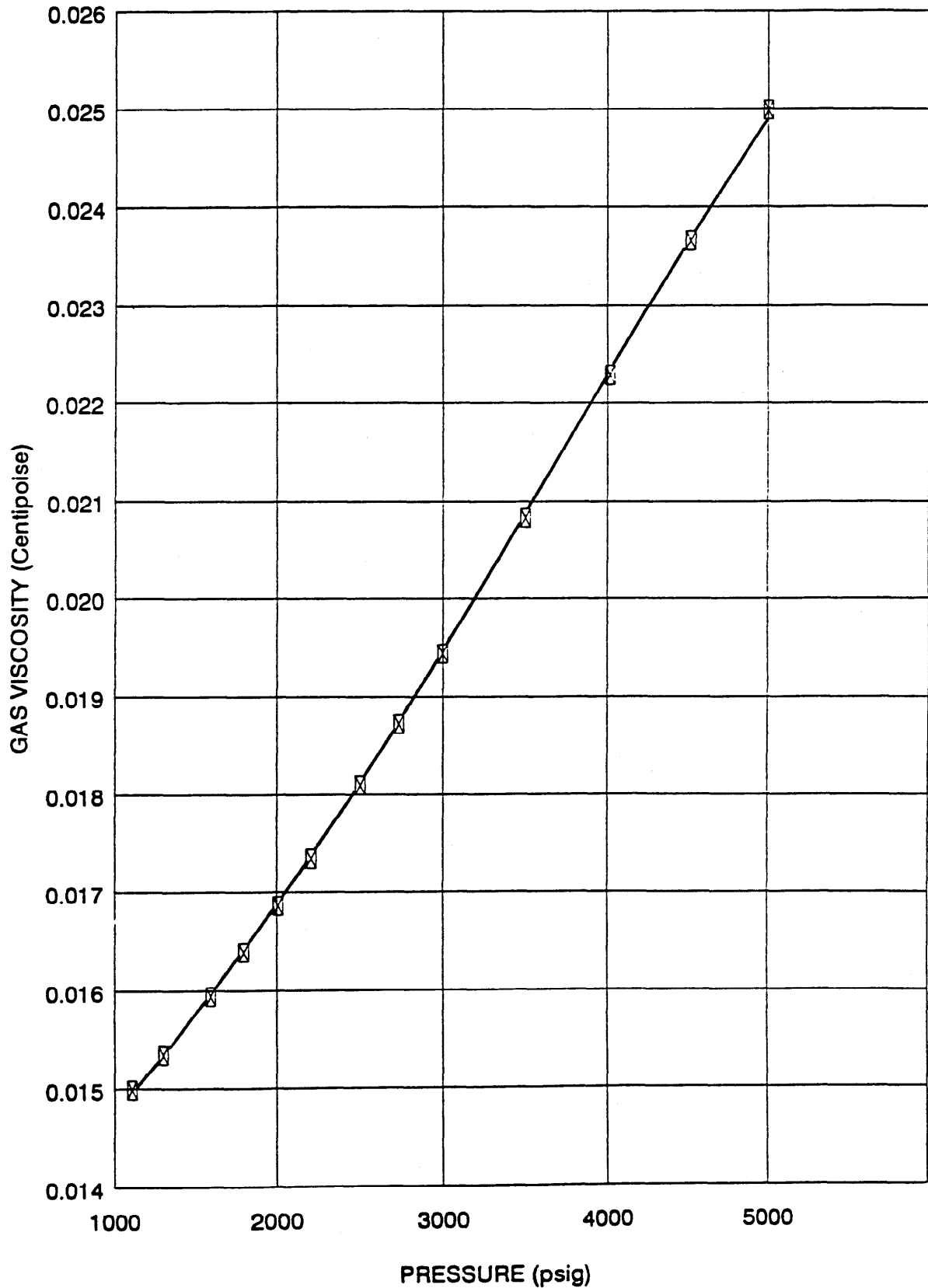


# PETROLAB

Company: BHP Petroleum Pty. Ltd.  
Well: Minerva # 1

Page: 34 of 34  
File : B 93013

## VISCOSITY OF RESERVOIR FLUID



**ENCLOSURE 1:**

**MINERVA-1 DLL-MSFL-SDT-GR-AMS LOG**



PE602768

This is an enclosure indicator page.  
The enclosure PE602768 is enclosed within the  
container PE900058 at this location in this  
document.

The enclosure PE602768 has the following characteristics:  
ITEM-BARCODE = PE602768  
CONTAINER\_BARCODE = PE900058  
NAME = Minerva 1 DLL-MSFL-AS-GR-AMS-SP 1:200  
BASIN = Otway  
PERMIT = VIC/P31  
TYPE = WELL  
SUBTYPE = WELL-LOG  
DESCRIPTION = Minerva 1 DLL-MSFL-AS-GR-AMS-SP 1:200,  
Appendix 5  
REMARKS = new barcode PE900148 replaced with  
PE602768  
DATE-CREATED = \*  
DATE-RECEIVED = \*  
W\_NO = W1079  
WELL-NAME = MINERVA 1  
CONTRACTOR =  
CLIENT\_OP\_CO =

(Inserted by DNRE - Vic Govt Mines Dept)

PE600589

This is an enclosure indicator page.  
The enclosure PE600589 is enclosed within the  
container PE900058 at this location in this  
document.

The enclosure PE600589 has the following characteristics:

ITEM-BARCODE = PE600589  
CONTAINER\_BARCODE = PE900058  
NAME = MINERVA 1 DLL-MSFL-AS-GR-AMS-SP  
(2024-1189 M)  
BASIN = OTWAY  
PERMIT = VIC/P31  
TYPE = WELL  
SUBTYPE = WELL-LOG  
DESCRIPTION = MINERVA 1 SUITE 2- RUN-2, 1/500,  
DLL-MSFL-AS-GR-AMS-SP (2024-1189 M)  
REMARKS =  
DATE-CREATED = 21/03/93  
DATE-RECEIVED = 20/05/93  
W\_NO = W1079  
WELL-NAME = MINERVA-1  
CONTRACTOR = SCHLUMBERGER  
CLIENT\_OP\_CO = BHP PETROLEUM PTY LTD

(Inserted by DNRE - Vic Govt Mines Dept)

6

**BHP Petroleum Pty. Ltd**

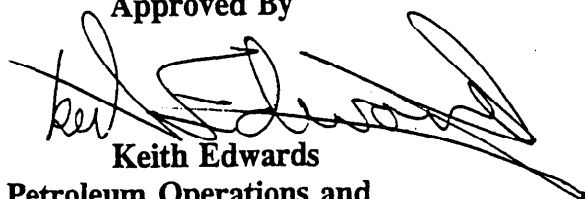
**Minerva-1**

**Drillstem Test Interpretation**

**Prepared By**

**DAVID PRICE**

**Approved By**

A handwritten signature in black ink, appearing to read 'Keith Edwards', is written over the printed name. The signature is stylized and somewhat cursive.

**Keith Edwards  
Petroleum Operations and  
Quality Systems Superintendent**

**OCTOBER 1993**

---

## TABLE OF CONTENTS

	Page
<b>1. SUMMARY AND CONCLUSIONS</b>	<b>1</b>
1.1 Summary	1
1.2 Conclusions	1
<b>2. OVERVIEW</b>	<b>3</b>
2.1 Well Summary	3
2.2 Summary Of The Geological Environment	3
2.3 Summary Of The Rft Survey	3
2.4 Tide Data Correction	4
2.5 Open Hole Log Reference	4
<b>3. DST PROGRAMME</b>	<b>5</b>
3.1 Objectives	5
3.2 Summary	5
3.3 Well Description	5
<b>4. FLOW PERIOD</b>	<b>7</b>
4.1 Production Rates	7
4.2 Pressures	7
<b>5. EQUIPMENT PERFORMANCE</b>	<b>10</b>
5.1 Downhole Equipment	10
5.2 Surface Equipment	10
5.3 Gauge Data	10
<b>6. INTERPRETATION</b>	<b>12</b>
6.1 Interpretation	12
6.2 Reservoir Description	21
6.3 Skin Calculations	23
6.4 Gas-In-Place Investigated	25
6.5 Reservoir Pressure	25
6.6 Pseudo-Pressure	26

---

## TABLE OF CONTENTS CONT'D

	Page
<b>7. SAMPLES</b>	<b>27</b>
7.1 Separator Samples	27
7.2 Bottomhole Samples	27
<b>REFERENCES</b>	<b>28</b>
<b>NOMENCLATURE</b>	<b>29</b>
<b>DATA SHEETS</b>	<b>30</b>
<b>APPENDIX 1 - TIDAL DATA</b>	<b>33</b>
<b>APPENDIX 2 - LOG SECTION</b>	<b>38</b>
<b>APPENDIX 3 - CORE DATA</b>	<b>40</b>
<b>APPENDIX 4 - FLOW PERIODS</b>	<b>42</b>
<b>APPENDIX 5 - GAUGE SELECTION</b>	<b>52</b>
<b>APPENDIX 6 - STRUCTURE MAP</b>	<b>59</b>
<b>APPENDIX 7 - WELL TEST PLOTS</b>	<b>60</b>
<b>APPENDIX 8 - BOUNDARIES</b>	<b>77</b>
<b>APPENDIX 9 - SKIN FACTOR</b>	<b>90</b>
<b>APPENDIX 10 - PRESSURE DATA</b>	<b>93</b>

---

**LIST OF FIGURES**

	Page
FIGURE 1 : TIDAL DATA - CHART AND MEASURED	33
FIGURE 2 : MINERVA-1 DDL-MSFL-AS-GR-AMS-DP LOG	39
FIGURE 3 : CORE PERMEABILITY PROFILE	41
FIGURE 4 : POROSITY - PERMEABILITY RELATIONSHIP	41
FIGURE 5 : TEST SEQUENCE CARTESIAN PLOT	43
FIGURE 6 : CLEAN-UP FLOW CARTESIAN PLOT	44
FIGURE 7 : FLOW PERIOD 1 CARTESIAN PLOT	45
FIGURE 8 : FLOW PERIOD 2 CARTESIAN PLOT	46
FIGURE 9 : FLOW PERIOD 3 CARTESIAN PLOT	47
FIGURE 10 : FLOW PERIOD 4 CARTESIAN PLOT	48
FIGURE 11 : FLOW PERIOD 4 - SURFACE DATA	50
FIGURE 12 : CLEAN-UP FLOW AND FLOW PERIOD 4 COMPARISON	51
FIGURE 13 : GAUGE 10883 PRESSURE RESPONSE	53
FIGURE 14 : GAUGE 10882 PRESSURE RESPONSE	54
FIGURE 15 : GAUGE 011 PRESSURE RESPONSE	55
FIGURE 16 : GAUGE 10065 PRESSURE RESPONSE	56
FIGURE 17 : GAUGE 10065 LOG-LOG PLOT	57
FIGURE 18 : GAUGE 011 AND 10065 COMPARISON	58
FIGURE 19 : TOP STRUCTURE - TOP LOWER SHIPWRECK	59
FIGURE 20 : DUAL POROSITY - ENTIRE INTERVAL DIAGNOSTIC PLOT	61
FIGURE 21 : DUAL POROSITY - ENTIRE INTERVAL HORNER PLOT	62
FIGURE 22 : DUAL POROSITY - PERFORATED INTERVAL DIAGNOSTIC PLOT	63
FIGURE 23 : DUAL POROSITY - PERFORATED INTERVAL HORNER PLOT	64
FIGURE 24 : DUAL PERMEABILITY - PERFORATED INTERVAL DIAGNOSTIC PLOT	65
FIGURE 25 : DUAL PERMEABILITY - PERFORATED INTERVAL HORNER PLOT	66
FIGURE 26 : DUAL PERMEABILITY - PERFORATED INTERVAL DIAGNOSTIC PLOT	67
FIGURE 27 : DUAL PERMEABILITY - PERFORATED INTERVAL HORNER PLOT	68
FIGURE 28 : DUAL PERMEABILITY - PERFORATED INTERVAL DIAGNOSTIC PLOT	69

<b>FIGURE 29 : DUAL PERMEABILITY - PERFORATED INTERVAL HORNER PLOT</b>	<b>70</b>
<b>FIGURE 30 : DUAL PERMEABILITY - PERFORATED INTERVAL DIAGNOSTIC PLOT</b>	<b>71</b>
<b>FIGURE 31 : DUAL PERMEABILITY - PERFORATED INTERVAL HORNER PLOT</b>	<b>72</b>
<b>FIGURE 32 : DUAL PERMEABILITY - 80% L DIAGNOSTIC PLOT</b>	<b>73</b>
<b>FIGURE 33 : DUAL PERMEABILITY - 80% L HORNER PLOT</b>	<b>74</b>
<b>FIGURE 34 : DUAL PERMEABILITY - 120% L DIAGNOSTIC PLOT</b>	<b>75</b>
<b>FIGURE 35 : DUAL PERMEABILITY - 120% L HORNER PLOT</b>	<b>76</b>
<b>FIGURE 36 : DUAL PERMEABILITY - NO BOUNDARY DIAGNOSTIC PLOT</b>	<b>78</b>
<b>FIGURE 37 : DUAL PERMEABILITY - NO BOUNDARY SEMI-LOG PLOT</b>	<b>79</b>
<b>FIGURE 38 : DUAL POROSITY - NO BOUNDARY DIAGNOSTIC PLOT</b>	<b>80</b>
<b>FIGURE 39 : DUAL POROSITY - NO BOUNDARY SEMI-LOG PLOT</b>	<b>81</b>
<b>FIGURE 40 : BOUNDARIES SCHEMATIC</b>	<b>82</b>
<b>FIGURE 41 : FINAL TRANSIENT FLOW REGIME</b>	<b>83</b>
<b>FIGURE 42 : DUAL PERMEABILITY - PARALLEL FAULTS L:L DIAGNOSTIC PLOT</b>	<b>84</b>
<b>FIGURE 43 : DUAL PERMEABILITY - PARALLEL FAULTS L:L HORNER PLOT</b>	<b>85</b>
<b>FIGURE 44 : DUAL PERMEABILITY - PARALLEL FAULTS L:3L DIAGNOSTIC PLOT</b>	<b>86</b>
<b>FIGURE 45 : DUAL PERMEABILITY - PARALLEL FAULTS L:3L HORNER PLOT</b>	<b>87</b>
<b>FIGURE 46 : DUAL PERMEABILITY - 90° FAULTS L:2L DIAGNOSTIC PLOT</b>	<b>88</b>
<b>FIGURE 47 : DUAL PERMEABILITY - 90° FAULTS L:2L HORNER PLOT</b>	<b>89</b>
<b>FIGURE 48 : TRANSIENT FLOW ASSUMPTION - SEMI-LOG PLOT</b>	<b>91</b>
<b>FIGURE 49 : TRANSIENT FLOW ASSUMPTION - SKIN PLOT</b>	<b>92</b>



# 1 SUMMARY AND CONCLUSIONS

10m standard

## 1.1 Summary

### DST : Top Lower Shipwreck Group

The interval 1816 to 1838 mRT in the Top Lower Shipwreck was tested on Minerva-1 to : 1827

- determine the near wellbore parameters
- determine whether the shale at the base of the perforations was sealing
- investigate the existence of a fault South-West of the well
- obtain valid PVT and trace element analysis

The well was flowed at 4 rates, 5.8, 17.0, 21.3 and 28.8 MMscf/d (164, 481, 603, 816  $\text{sm}^3 \times 10^3/\text{d}$ ), for approximately 6 hours per flow rate. The rates were stable and the gas produced had a specific gravity of 0.61. At the final, highest rate, the final bottomhole flowing pressure was 2675.6 psia (18448 kPa), a drawdown of 40.7 psi (281 kPa). The well head pressure was 1258 psia (8674 kPa).

## 1.2 Conclusions

### Flowing Conditions

The well continued to clean-up throughout the test. For periods 3 and 4 the flowing pressure increased throughout the period.

It was not possible to interpret the flowing period data.

### Productivity

The absolute open flow potential (AOF) was calculated to be 211.29 MMscf/d ( $6146 \text{ sm}^3 \times 10^3/\text{d}$ ).

### Datum Pressure

The datum has been assumed to be the GWC (1914.7 mTVDSS) and the pressure at the datum is 2746.0 psia (18933 kPa). The assumed gas gradient is 0.171 psi/m (see REFERENCE 6).

### Permeability Thickness

The kh measured from the analysis of the final buildup was 152.6 D-ft (46.5 D-m).

### Reservoir Model

The analysis of the buildup was based on a dual permeability system with flow from the perforated sand only.

The data did not provide a unique solution for the description of the two layers. However, for most likely case, the kh was distributed between two layers of high and low permeability, of 35.1 and 117.5 D-ft (9.3 and 37.2 D-m), respectively.

### Permeability

The average permeability for the perforated interval was 2.11 D. The high permeability layer was 8.45 D, and the low permeability layer was 1.78 D.

The upper perforated interval was not cored. The average core permeability of the cored section of the perforated interval (the bottom 13 metres) was 1.28 D. The high permeability layer is, most likely, in the upper perforated interval.

### Communication

The shale at the base of the perforations (1838 to 1843 mRT) was shown to be sealing.

### Skin

The total skin was determined, from the final build-up, to be 65.7.

Skin was factorised into Darcy and Non-Darcy components by assuming transient conditions. The mechanical component of this skin was 15.9. The Non-Darcy skin was calculated as  $0.0017 \text{ 1/(Mscf/d)}$  ( $6.0 \times 10^{-5} \text{ 1/(sm}^3\text{/d)}$ ).

The mechanical skin component is very high. If partial penetration is assumed to be responsible for this, calculations suggest that the high permeability layer contributed most of the flow.

### Boundary Analysis

A single noflow boundary was interpreted at 340 metres from the well. This is in good agreement with the mapped fault at 400 metres. No other boundaries were observed during the test.

The radius of investigation for the high and low permeability sands is 3800 and 1780 metres, respectively.

### Connected Volume

Structural maps suggest that areas within the radius of investigation are water filled. The DST was unable to detect the GWC, hence no gas volume was calculated using the radius of investigation.

### Test Design

All the test objectives were met, however the feasibility of underbalanced perforating in such wells should be reviewed as the high mechanical skin (probably due to formation damage from the overbalanced perforating) leaves some doubt as to the PI which would be achieved from the completion of a development well.

---

## **2 OVERVIEW**

### **2.1 Well Summary**

Minerva-1 was drilled in March-April 1993 by the semi-submersible drilling rig "Byford Dolphin" in the Victorian permit VIC/P31, approximately 145 kilometres South-East of Portland, in the Otway Basin. Open hole logs indicated the well had intersected a gross hydrocarbon column of 129 metres over the interval 1816 to 1945 mRT. The RFT was run and confirmed the presence of gas and established the gas water contact at 1944.5 mRT.

The well is in the Victorian permit VIC/P31, approximately 145 kilometres South-East of Portland, in the Otway Basin.

Three cores were cut over the interval 1821.8 to 1848 mRT. After drilling to 2108 mRT a 7" liner was run. The well was then drilled to a total depth of 2425 mRT. After final logging, the hole was cemented back to 2074 mRT.

Following a DST the well was suspended as a future gas producer.

### **2.2 Summary Of The Geological Environment**

#### **Description**

Cores reveal the sandstone to comprise moderately hard to friable, coarse to pebble grade, subrounded to subangular poorly sorted quartz grains, with rare light grey argillaceous matrix, common quartz cement, rare coally detritus and thin claystone laminae. Sedimentary structures consist of high angle cross bedding defined by distinct very coarse to granule size centimetre scale bedding with occasional 10 to 20 cm pebble conglomerate lags at the base of channel scours.

#### **Depositional Environment**

The depositional environment is interpreted to be fluvial channel (possibly braided to inter-distributary river channel) within a marginal to very nearshore marine setting. Sand bodies are probably oriented perpendicular to the shoreline (estimated to run approximately northwest to southeast) and are likely to have prograded laterally across a broad coastal delta plain. Due to the coarse grained nature and high energy environment it is unlikely that significant lateral barriers exist between individual sand bodies.

A coastal plain setting is strongly suggested by the shale interval encountered below the test zone. The shale is terminated at the top by a distinct erosional contact and a 10 to 15cm coal unit sits just below the top of the shale. The implied depositional setting for the shale unit is that of an interdistributary bay or mudflat which is in close proximity to a mangrove/marsh environment which would account for the coal fragments and thin coal seam. This shale should have good lateral extent but may have been incised by the overlying channel sands, and will be breached by minor faults within the Minerva Field.

### **2.3 Summary Of RFT Survey**

An RFT survey was run over 22-23 March 1993 to determine,

1. fluid gradients over the hydrocarbon interval and the aquifer,

2. the fluid contact(s), and
3. pressure continuity through the interval.

The RFT established the presence of both gas and water intervals. The pressures recorded enabled the calculation of fluid gradients and the depth of the gaswater contact (GWC). The results are as follows:

**Table 1 : RFT Survey Results Summary**

<b>gradient - gas</b>	0.171 <b>psi/m</b>
<b>gradient - water</b>	1.40 <b>psi/m</b>
<b>gas water contact (GWC)</b>	1914.7 <b>mTVDSS</b>
<b>GWC pressure</b>	2746.0 <b>psia</b>

The pretest pressures recorded were of reasonable quality and gave no indication of pressure anomalies over the gas and water intervals of the test sequence.

See REFERENCE 6, for further details.

#### **2.4 Tide Data Correction**

Although tidal data was gathered (see APPENDIX 1 - TIDAL DATA Figure 1), it was not used to adjust the pressure response. There were two reasons for this;

1. The reservoir fluid is gas and its compressibility tends to eliminate the effect of tidal variation.
2. The actual tidal variation over the test duration was small (less than 1 metre).

#### **2.5 Open Hole Log Reference**

All depths quoted in this report are as recorded by the petrophysical log "Suite-2, Run-2 DDL-MSFL-AS-GR-AMS-SP", run on 21 March 1993. Depths are measured from the rotary table in metres (mRT), which is 25 metres above mean sea level (MSL).

Core depths have been corrected to logged depths by adding 1 metre. The correction is based on a memorandum from the exploration geologist (see REFERENCE 1).

---

### 3 DST PROGRAMME

#### 3.1 Objectives

Minerva-1 was tested with the following reservoir objectives :

1. To determine the permeability of the formation and the Darcy and Non-darcy skin factors.
2. To determine whether the shale (1838-1843 mRT), at the base of the upper sand, was sealing. If not sealing, to assess the effective vertical permeability.
3. To investigate the existence of a major South-West sealing fault mapped approximately 400 metres from the well.
4. To obtain gas samples for detailed compositional analysis.

#### 3.2 Summary

Full details can be found in the well test programme (see REFERENCE 2).

The well was to be brought on production by flowing the well at a low choke until all the diesel used to provide an underbalance was produced and gas reached the surface. At that point the well was to be beaned up slowly to the maximum achievable rate for 3 hours of clean-up flow (flow rate was restricted by surface pipework to the burner). At the conclusion of this clean-up flow the well was to be shut-in for twice the flowing time (6 hours).

A 24 hour flow period, consisting of four 6 hour periods, was programmed. The well was to be opened at a suitable choke size, based on the clean-up flow, to obtain the desired rate.

Table 2 : Programmed Flow Rate Schedule

Flow Rate (Mscf/d)	Flowing Time (hours)	Cumulative Time (hours)
6000	6	6
15000	6	12
23000	6	18
28000	6	24

Separator samples were to be taken at the end of the initial and final flow periods. Three pairs of samples were required from each period.

At the completion of the flow period the well was to be shut-in for 24 hours.

Bottomhole samples were to be taken only after consultation with Melbourne, following analysis of the RFT sample from the well.

#### 3.3 Well Description

##### 3.3.1 Perforation Data

Two perforation runs were made due to weight limitations of the cable. Both runs were made over-balanced, using Schlumberger 5" O.D. casing guns with 22 gram RDX charges at 8 shots per foot.

On the first run the interval 1827.5 to 1838 mRT was perforated on 8 April 1993, with the guns fired at 07:35 hours. On the second run two intervals, 1825 to 1827.5 mRT and 1816 to 1821 mRT, were perforated. The guns for this run were fired on 9 April 1993 at 0400 hours. This meant that at the end, the following intervals were available for flow into the wellbore,

1816 to 1821 mRT  
1825 to 1838 mRT.

The interval 1821 to 1825 was not perforated to limit potential sand production. Core description over the unperforated interval indicated it may be less consolidated than the rest of the cored section. The unperforated interval would not restrict access of the sand to the wellbore.

After the first perforation run, the well started to flow due to the swabbing action of the guns being retrieved from the well. As a result, the bottom set of perforations (1827.5 to 1838 mRT) were bull headed with HEC to control the flow.

### 3.3.2 Assumptions On Tested Interval

There were two distinct scenarios for the interpretation of this interval. They depend on whether or not the shale at the base of the perforations isolates the perforated interval from the gas column below it (see APPENDIX 2 - LOG SECTION Figure 2).

Should the shale be isolating, the thickness would be assumed to be 22 metres. The perforation interval was designed to eliminate partial penetration effects in this scenario.

If the shale allowed communication, the reservoir extends down to the gas water contact (a thickness of 128.5 metres). Under this scenario, partial penetration effects would be substantial.

### 3.3.3 Tested Interval Permeability From Core Data

Three cores were cut in the Upper Shipwreck,

Core#1	1821.0 to 1828.0 mRT	43% recovery
Core#2	1828.0 to 1842.5 mRT	92% recovery
Core#3	1842.5 to 1847.0 mRT	100% recovery.

All but the top 5 metres of the perforated interval was cored (see APPENDIX 3 - CORE DATA Figure 3). The lower recovery of Core#1 is attributed to the interval 1824 to 1828 mRT.

The arithmetic average core permeability for the cored section of the perforated interval is 1.28 Darcies (see APPENDIX 3 - CORE DATA). Assuming, that the net sand thickness is 22 metres, the core measured permeability thickness for the interval would be 28.16 Darcy-m (92.38 Darcy-ft).

A plot of porosity versus log permeability (see APPENDIX 3 - CORE DATA Figure 4) showed that there was no obvious linear relationship. This does not rule out any relationship subject to grouping of data by facies.

## 4 FLOW PERIOD

### 4.1 Production Rates

The well was opened for clean-up flow on 10 April 1993 at 15:45 hours. The flow soon stabilised at a maximum safe rate of 28.25 MMscf/d on a 64/64 fixed choke. The well was shut-in at the LPRN at 19:35 hours.

The main flow sequence began on 11 April 1993 at 03:20 hours. The well was flowed at four rates for 6 hours for each rate. The details are summarised in the following table, (also, see APPENDIX 4 - FLOW PERIODS Figure 5),

**Table 3 : DST Production Rate Summary**

Flow Period	Start Time	Choke (inches)	Average Gas Rate (MMscf/d)	Separator Pressure (psig)	WHP (psig)	Gas Specific Gravity
10 April (clean-up)	15:45	64/64	28.25	630	1190	0.63 0.61
11 April - 1	03:20	20/64	5.76	210	2319	0.61
11 April - 2	09:59	38/64	16.96	443	2013	0.61
11 April - 3	15:20	48/64	23.14	608	1726	0.61
11 April - 4	21:20	64/64	28.80	699	1243	0.61

Note that the gas specific gravity changed over the clean-up period.

### 4.2 Pressures

#### 4.2.1 Bottomhole Flowing Pressures

##### Clean-up Flow Period (see APPENDIX 4 - FLOW PERIODS Figure 6)

The well took about one hour to produce all of the diesel cushion and get gas to surface. Once the choke was beaned up to 64/64, the bottomhole flowing pressure dropped to 2650 psia (measured at the gauge depth of 1792.47 mRT). The well continued to clean-up for the remainder of the period, with pressure increasing to 2665 psia. The trend was flattening out at the end of the clean-up period.

##### Flow Period 1 (see APPENDIX 4 - FLOW PERIODS Figure 7)

On opening the well, after the initial shut-in, bottomhole flowing pressure dropped to about 2650 psia, but, recovered immediately to around 2713 psia. At 1 hour into the flow period pressure was at 2713.1 psia and it steadily declined to 2713.0 psia at the end of the flow period. This is a very small pressure drop, but, there is a well defined trend. However, this flow period was not analysed due to evidence from subsequent flow periods that the well had not cleaned up.

Flow rates for the period were steady and were within  $\pm 0.4$  MMscf/d of the average rate.

##### Flow Period 2 (see APPENDIX 4 - FLOW PERIODS Figure 8)

Once the choke was established and flow stabilised, the bottomhole flowing pressure settled at 2698.07 psia by 2.3 hours. At the end of the flow period the pressure had risen to 2698.17 psia, an increase of 0.1 psi. Furthermore, the

flow rates recorded over the last 2.5 hours of the period were above the average rate. The well was still slowly cleaning up.

### **Flow Period 3 (see APPENDIX 4 - FLOW PERIODS Figure 9)**

By 0.5 hours pressure had settled to 2688.2 psia. Over the next hour it increased by 0.1 psi. By 2 hours the pressure had dropped back slightly (about 0.05 psi). From this point pressure increased for the remainder of the flow period. At 5.5 hours pressure was at 2688.4 psia. Flow rate was consistent for most of the flow period (most measured rates were within  $\pm 0.2$  MMscf/d).

Some minor pressure fluctuations occurred with the choke change. They relate to the transfer of flow from the fixed choke to the variable choke and back again, after the new fixed choke had been installed.

### **Flow Period 4 (see APPENDIX 4 - FLOW PERIODS Figure 10)**

At this maximum rate the well was still cleaning up. By 0.5 hours pressure bottomed and had begun to increase. After 1.5 hours the pressure had increased 1.2 psi. From 1.5 to 4 hours pressure continued to increase, but, less rapidly (0.4 psi). At this point, pressure decreased 1.4 psi in the next ten minutes. It settled at 2675.4 psi and began to increase once again, with a similar trend to that prior to the pressure drop.

Inspection of the well head pressures shows that, prior to 4 hours, well head pressure was declining (see APPENDIX 4 - FLOW PERIODS Figure 11). After the 4 hour reading, well head pressure firstly dropped and then increased to 1236 psig, an increase of 11 psi from the 4 hour reading. Furthermore, the well head pressure increased for the remainder of the flow period.

Gas rate averaged about 28.7 MMscf/d prior to the 4 hour reading. At four hours the gas rate firstly dropped then increased to average about 0.3 MMscf/d higher than that before the drop.

There is no obvious explanation for this event was but it was not a function of surface equipment or operations.

### **Discussion**

The well continued to clean-up throughout the test. This made the flow periods unsuitable for pressure transient analysis as pressure actually increased throughout some of the flow periods.

It is interesting to compare the clean-up flow period bottomhole flowing pressures to those of flow period 4, as they were on the same choke setting (see APPENDIX 4 - FLOW PERIODS Figure 12). Flow period 4 is flowing at a higher rate at a bottomhole flowing pressure,  $p_{wf}$ , about 12 psi higher than the final pressure for the clean-up flow period. Also, the final flowing wellhead pressure,  $p_{wh}$ , is 39 psi higher.



**Table 4 : Flow Period Comparison**

	<b>Clean-up Flow Period</b>	<b>Flow Period 4</b>	
<b>Choke</b>	64/64	64/64	<b>inches</b>
<b>Rate</b>	28.25	28.80	<b>MMscf/d</b>
<b>p<sub>wf</sub></b>	2664.11	2675.59	<b>psia</b>
<b>p<sub>wh</sub></b>	1190	1229	<b>psia</b>

In the context of this test, the change in flowing conditions is considerable and represents significant cleanup.

#### **4.2.2 Reservoir Pressure**

Reservoir pressure was 2716.4 psia psi (at the gauge depth of 1792.47 mRT). This was obtained from the extrapolation of the final pressures of the final build-up. It is in agreement with the pressure from the initial build-up (2716.3 psia psi) and suggests that no depletion has occurred. This is consistent with the subsequent pressure analysis of the final build-up.

Extrapolation of the RFT pressures to the gauge depth gave a pressure of 2720.0 psia psi. This is 3.6 psi higher than that from the DST. This is in agreement with the build-up pressures in the DST, as the pressure difference is within the accuracy of the gauges.

---

## 5 EQUIPMENT PERFORMANCE

### 5.1 Downhole Equipment

There were no major problems with the downhole test tools.

A Halliburton LPR-N tester valve was run to provide the downhole shut-in. There was a minor problem at the end of the cleanup flow. The cleanup period was extended by 35 minutes while efforts were made to shear the 'hold open' mechanism used while running the string.

### 5.2 Surface Equipment

There was only one problem encountered with the surface equipment. One side of the choke manifold could not be isolated. To change fixed chokes, the flow had to be diverted from the fixed choke to the variable choke and back to the fixed choke once the change had been made. This was complicated by the variable choke icing up at the two low flowrates.

Other surface equipment functioned without a problem.

### 5.3 Gauge Data

#### 5.3.1 Gauge Performance

Four Halliburton HMR gauges, serial numbers 10883, 10882, 10065 and 011, were run for this DST. The gauges were pressure tested in their bundle carriers prior to testing to check for consistency. No inconsistencies were found.

Gauges were started on 9 April 1993 at 11:57. They were placed in a single gauge carrier above the permanent DB packer. Each gauge had a fixed 4 minute sampling rate for the first 17 hours to minimise data acquisition while running in the hole. This would use up 255 of the available 31000 data points.

A different sampling programme was used for each gauge. Gauges 10883 and 10882 were given fixed sampling rates of 10 and 20 seconds respectively. This gave the gauges a recording time of 3.5 and 7 days, respectively.

The other two gauges, 10065 and 011, used a variable sampling algorithm with a pressure window control. The essence of this approach is that,

- pressure is sampled (at a rate less than or equal to the minimum record duration)
- if the minimum record duration has lapsed, and, the pressure difference, between the current pressure and that projected from the previous measurement, is greater than the pressure window, it is recorded
- if not, the time since the last recorded pressure is calculated
- if it exceeds the maximum record time, the pressure is recorded
- if not, sampling continues.

There are enhancements to this procedure in the actual implementation in the gauge, but, essentially pressure is sampled in this way.

The gauges were programmed as follows :

**Table 5 : Sampling Programmes for Gauges 10065 and 011**

	Gauge 10065	Gauge 011
sample rate (secs)	4	4
minimum record (secs)	8	4
maximum record (secs)	60	60
pressure window (psi)	0.25	0.10

This gave gauge 10065 a minimum recording time of 1.4 days and, gauge 011, 2.8 days.

There were no gauge failures. However, both fixed sampling gauges, 10883 and 10882, were eliminated from the analysis due to gauge "sticking". In gauge 10883, there were small pressure humps during the final buildup from 0.2 hours onwards (see APPENDIX 5 - GAUGE SELECTION Figure 13). The effect was even more pronounced in the pressures recorded by gauge 10882. This also began around 0.2 hours (see APPENDIX 5 - GAUGE SELECTION Figure 14). The "sticking" became less obvious as pressure change decreased with time. There is as yet no explanation for the gauge "sticking". The data gathered from these gauges has been sent to Halliburton, USA for an explanation:

### 5.3.2 Gauge Comparison

Two gauges, 011 and 10065, were considered for use in the pressure analysis (see APPENDIX 5 - GAUGE SELECTION Figure 15 and Figure 16). The choice of gauge was based on the pressures recorded during the final buildup as this was the period analysed.

Upon plotting the derivative response for gauge 10065 (see APPENDIX 5 - GAUGE SELECTION Figure 17) it was clear that gauge 011 was the gauge required for analysis. It had a faster minimum record rate and, consequently, recorded more of the early time data. This in turn gave the derivative more character at early time.

A pressure profile of the difference between the two gauges ( $dp = p_{011} - p_{10065}$ ) was calculated for the final buildup (see APPENDIX 5 - GAUGE SELECTION Figure 18). It shows a pressure shift in the data. Gauge 10065 reads 0.5 to 0.6 psi higher for most of the buildup (after 0.1 hours). The shift is consistent over this period, where pressure change with time was small. However, over the crucial early period, before 0.1 hours, where pressure change was more rapid, the difference was increasing to the final value.

The sensitivity of interpretation to this variation is discussed in section 7.1.5.

---

## 6 INTERPRETATION

### 6.1 Interpretation

The well test analysis software package PANSYSTEM was used for the pressure transient analysis reported here.

#### 6.1.1 Model Selection

Given that the flowing periods could not be used for detailed interpretation, attention was focused on the final build-up. Inspection of the diagnostic and Horner plots (see APPENDIX 7 - WELL TEST PLOTS) suggests either a dual porosity or dual permeability model (see REFERENCE 3). This is based on a pronounced dip in the derivative response over the interval 0.1 to 1 equivalent time hours, and the parallel trends on the Horner plot.

It should be noted that the derivative response shown has been moderately smoothed. The default smoothing factor (in PANSYSTEM) is 0.07. This was increased to various values before settling on 0.15. This value minimised the smoothing, yet yielded sufficient character for interpretation.

Both models, dual porosity and dual permeability, were considered. The difference between the two cases is that the dual porosity case assumes that the entire flow capacity is associated with the more highly permeable conduit (either a layer or fracture network). Consequently, the low permeability conduit, layer or matrix system, is not in communication with the wellbore. This enables the model to be applied to layered systems where the low permeability layer(s) are not perforated. (see REFERENCE 3)

The dual porosity model is a limiting case of the dual permeability model, which makes no assumptions about the distribution of the flow capacity between the two systems. However, in practical terms the model is most useful where there is a high contrast in flow capacity.

For both models, there are three flow regimes, (in order of occurrence), following wellbore storage,

1. fracture / high permeability radial flow
2. a transition period
3. total system radial flow.

In addition, there is a fourth flow regime associated with boundary effects. From the derivative response, the structure map and the flow rate pressure response, it was likely that boundaries were encountered during the test. The map shows two main faults that were potentially in the area of influence of the test. Furthermore, given the mobility difference between gas and water, the gas water contact could also appear as a no-flow boundary. The faults are parallel and the gas water contact closes the system at each end. The structure is shown in APPENDIX 6 - STRUCTURE MAP Figure 19, with these boundaries indicated.

## 6.1.2 Model Analysis

Given the formation and the perforation configuration, there were three possible models for analysis,

1. a dual porosity model over the entire interval (ie. from top of the structure to the gas water contact), which assumes communication across the shale at the base of the perforations
2. a dual porosity model over the perforated interval
3. a dual permeability model over the perforated interval.

Even though downhole shut-in was used, significantly reducing wellbore storage effects, the derivative response shows no conclusive initial radial flow regime. This is due to the rapid onset of the transition flow regime. The total system regime was difficult to pick due to noise in the derivative response and the effect of boundaries. As a result, the dual porosity model was investigated first as it assumes that the slope of the lines through the two radial flow periods are parallel. This allowed a line to be fitted through the chosen total system points and a parallel line positioned, by eye, through the early time data.

### Dual Porosity - Entire Interval

The entire interval of 128.5 metres was considered first. The 'straight line' analysis gave a permeability of less than 400 md. This is contrary to the permeabilities measured in the core (which were typically greater than 1 Darcy). Furthermore, a storativity ratio of 0.10 was calculated. Storativity ratio is defined as the ratio of the volume of the fracture (high conductivity) system to the total volume ie.,

$$\omega = \frac{(\phi c_t h)_f}{(\phi c_t h)_f + (\phi c_t h)_m} \quad \dots(1)$$

where,  $\phi$  is porosity  
 $c_t$  is total system compressibility  
 $h$  is total thickness

and,  $f$  and  $m$  denote fracture (high permeability conduit) and matrix (low permeability conduit), respectively.

Assuming that porosity and compressibility are the same for both layers, storativity ratio can often be approximated by the ratio of thickness. The perforated layer is 22 metres thick and the unperforated layer thickness is 101.5 metres, which gives a minimum storativity ratio of 0.18. The straight line analysis yielded a value significantly less than this (0.10).

At this point there are two negative results for this model. Both the permeability and storativity ratio are too low. However, as the flow regime periods are difficult to pick, an optimisation routine was used to further investigate and refine the solution. Initial runs allowed storativity to vary. The optimised solution



continually sought a value lower than 0.18 and permeability remained invariant. The optimiser was run with storativity ratio set at 0.18.

The storativity ratio determines the duration and depth of the derivative curve during the transition. With the ratio set at 0.18, the match never appeared satisfactory (see APPENDIX 7 - WELL TEST PLOTS Figure 20 and Figure 21). The lack of depth in the derivative match translated to a curve that was not as flat as that measured during the actual test.

The timing of the transition period is governed by the interporosity flow parameter,  $\lambda$ . This was varied to position the matched response during the transition, but, did not improve the overall transition match. On the Horner plot, the match continued to cut across the actual pressures. Variation of  $\lambda$  changed the point of intersection only slightly.

The final results were as follows,

**Table 6 : Dual Porosity, Entire Interval Results**

<b>thickness</b>	<b>128.50 metres</b>
<b>permeability</b>	<b>391.00 md</b>
<b>total skin</b>	<b>68.80</b>
<b>Cs</b>	<b>0.00 bbl/psi</b>
$\omega$	0.18
$\lambda$	7.1E-8

The low permeability and poor quality match eliminate the dual porosity model over the entire interval.

Consequently, a model which assumes that the shale at the base of the perforations was sealing was investigated.

#### **Dual Porosity - Perforated Interval**

By considering the perforated interval only, the restriction on the storativity ratio is removed; it would be determined by the permeability contrast between the layers. With the total thickness reduced to 22 metres the permeability increases to approximate the level measured in routine core analysis.

The optimiser was allowed to reduce the storativity ratio. This gave an excellent match over the transition period (see APPENDIX 7 - WELL TEST PLOTS Figure 22 and Figure 23). It is worth considering that after early time the match is within 0.03 psi of the observed data. Even for the early time data the match is no more than 0.4 psi different than the observed pressures. Even so, the total system match looks out of character with the actual pressure response. The results of this match are as follows,

**Table 7 : Dual Porosity, Perforated Interval Results**

<b>thickness</b>	22.00 metres
<b>permeability</b>	2135.00 md
<b>total skin</b>	65.70
<b>Cs</b>	0.00 bbl/psi
$\omega$	0.05
$\lambda$	8.0E-8

A storativity ratio of 0.05 implies that only 1.1 metres of the interval is connected to the wellbore. That is, 20.9 metres of the interval is not communicating with the wellbore. The interval 1821-1825 mRT is not perforated, which accounts for 4 metres.

As discussed previously, there were two perforation runs (see section 4.3.1). Testing began on 10 April 1993 at 1545 hours. Hence, the first set of perforations sat for over two days prior to testing and the second set of perforations one day. Furthermore, the first set of perforations were bull headed with HEC. This was required after the well began to flow due to the swabbing effect of pulling the perforating guns to surface.

It is possible there was some plugging. For example, the flow rates were still cleaning up prior to the final build-up. Regardless, it is difficult to imagine that only 1.1 metres of the perforations flowed, in a formation with core permeabilities averaging over 1 Darcy.

While this model was possible for the perforated interval (given the perforating history), it appeared highly unlikely as the geology and core data do not support the permeability assumptions required by the dual porosity model. Furthermore, the post transition match, despite its absolute accuracy, did not seem correct.

### **Dual Permeability - Perforated Interval**

The dual permeability model has a parameter,  $\kappa$ , that is the ratio of permeability thickness of one layer to the permeability thickness of the total system. This can be written as,

$$\kappa = \frac{(kh)_1}{(kh)_1 + (kh)_2} \quad \dots(2)$$

where, 1 and 2 refer to the two layers. Layers 1 and 2 replace the high and low permeability conduit labels, respectively, of the dual porosity model.

No straight line analysis was attempted for the dual permeability model. The optimiser was used from the outset because :

- Experience with the dual porosity model had shown that the initial radial flow regime was not identifiable. A 'straight line' analysis of the



dual permeability model is dependent on this flow regime for the definition of the permeability thickness ratio.

- The dual porosity model is a limiting case of the dual permeability model for  $\kappa = 1$ . Hence, with a high value of the permeability thickness ratio and the good double porosity match an excellent starting position was available for the dual permeability model.

The permeability thickness ratio was set to 0.99. The optimiser quickly lowered this value. Although, the storativity was free to vary, it varied little. The total system permeability dropped 20 md, but, little else changed. Several attempts were made to improve the match by varying parameters manually, holding some parameters constant and trying different starting points for some parameters. This was tried to determine whether the final value of the permeability thickness ratio was dependent on the starting value of the storativity ratio. Also, there was a high degree of correlation between some variables, eg. permeability and skin. By optimising with one variable constant the sensitivity of the solution to that parameter was gained.

There is a high correlation between permeability and skin. In addition, the wellbore storage value is small due to downhole shutin. Skin and wellbore storage were kept constant and the optimiser was run, concentrating on early and transition time data. No attempt was made to address the boundary affects. This placed the emphasis on the storativity ratio ( $\omega$ ), the permeability thickness ratio ( $\kappa$ ) and the interporosity flow parameter ( $\lambda$ ), as they effect the early time response. Experimentation showed that the results were not sensitive to changes in  $\lambda$ . Variation of  $\omega$  showed that the match, of the transition period suffered (the match was not flat enough) as the value increased from 0.05. These were fixed and attention turned to the latter time data, including the transition. In fact, this accounted for the majority of the points.

Optimisation on permeability, distance to a fault and permeability thickness ratio revealed a high degree of correlation between the three parameters (see section 7.1.4 for details). It was decided to hold  $\kappa$  constant and optimise on the other two parameters. This revealed the non-uniqueness of the solution. Matches were obtained over a range of permeability thickness ratios. There was no difference, visually, in the match (see APPENDIX 7 - WELL TEST PLOTS, Figures 24 to 31).

**Table 8 : Optimisation Results - Permeability Thickness Ratio  
Non Uniqueness**

$\kappa =$	0.20	0.30	0.40	0.50
<b>permeability (md)</b>	2112.00	2118.00	2122.00	2126.00
<b>distance to fault (m)</b>	340.00	355.00	370.00	385.00
<b>correlation</b>	-0.74	-0.73	-0.73	-0.72
<b>optimisation error (psi)</b>	0.02	0.01	0.01	0.01

During this process, it was noticed that while permeability thickness ratio changed significantly, permeability, distance to the fault and the errors associated with the parameters (see section 7.1.4) did not. As the permeability thickness ratio increased, the permeability thickness attributed to the high permeability layer

increased. The thickness of the layer was constant (because the storativity ratio was constant), hence, the permeability of the high permeability layer value increased. These results mean that the pressure response cannot uniquely describe the high permeability layer.

The permeability thickness ratio is poorly defined because the early data is not definitive. The total permeability response and the distance to the fault vary little regardless of the considerable variation in the permeability thickness ratio. Despite the fact that both parameters are causing the derivative to increase around the same time in the buildup, the optimiser consistently arrives at the same values.

The dual porosity match ( $\kappa = 1$ ) was excellent in absolute terms, but, did not match the character of the values presented above. It would appear that as permeability thickness ratio increases to 1, at some point, the match will begin to deteriorate.

The results of the optimisation were,

**Table 9 : Dual Permeability, Perforated Interval Results**

<b>thickness</b>	<b>22.00 metres</b>
<b>total skin</b>	<b>65.70</b>
<b>Cs</b>	<b>0.00 bbl/psi</b>
$\omega$	0.05
$\lambda$	8E-8

Using the definitions of the two ratios the layer properties can be calculated for each permeability thickness ratio value. Thickness of the layers are,

<b>Layer 1</b>	<b>1.1 metres</b>
<b>Layer 2</b>	<b>20.9 metres</b>

**Table 10 : Dual Permeability, Layer Permeabilities**

$\kappa =$	<b>0.20</b>	<b>0.30</b>	<b>0.40</b>	<b>0.50</b>
<b><math>k_{1+2}</math></b>	2112.00	2118.00	2122.00	2126.00
<b><math>(kh)_{1+2}</math></b>	46472.00	46601.00	46692.00	46763.00
<b><math>(kh)_1</math></b>	9294.00	13980.00	18677.00	23381.00
<b><math>(kh)_2</math></b>	37177.00	32621.00	28015.00	23381.00
<b><math>k_1</math></b>	8449.00	12709.00	16979.00	21256.00
<b><math>k_2</math></b>	1779.00	1561.00	1340.00	1119.00

Consideration of other data (see section 7.1.3) implies that the most likely value of permeability thickness ratio lies between 0.2 and 0.3. For the purpose of other calculations  $\kappa = 0.2$  has been used as the most likely case.

### 6.1.3 Validation Of The Dual Permeability Model

There is qualitative support for the dual permeability solution proposed above.

In the core analysis (see APPENDIX 3 - CORE DATA) there is a permeability value of 10142 md at 1844.40 mRT (adjusted depth). So the core supports a permeability of the order of 10 Darcies. There are no 10 Darcy plugs in the core taken over the perforated interval, although there are permeabilities in the 3-5 Darcy range.

The 10 Darcy value occurs immediately below the shale at the base of the perforations. Inspection of the logs at 1844.40 mRT shows a distinctive deep resistivity response. It is reading almost 2000 Ohm-metres, the maximum scale value. This is consistent with a high permeability response.

The top of the perforations, 1816 to 1822 mRT, was not cored or tested by the RFT. Within that interval there is a deep resistivity response similar to that noted for the 10 Darcy core plug. The peak occurs over the interval 1819 to 1820 mRT. Thus, there is an interval of the same magnitude and permeability as that proposed by the dual permeability analysis. This is the most likely location of the high permeability layer proposed by the analysis.

This would suggest that the permeability thickness ratio lies between 0.2 and 0.3. Values higher than that yield permeabilities for the high permeability layer significantly higher than that measured over the cored interval.

Depositional evidence, from inspection of the core, suggests sands of good lateral extent with a low probability of lateral barriers. If this can be applied to the sand not cored, it would mean the high permeability sand is likely to be laterally extensive. Furthermore, there would be access for the sands above and below it. This means that the high permeability sand could be fed by the lower permeability sands surrounding it. Given the surface area available to the lower permeability sands (compared to their access to the wellbore) there could be significant flow into the high permeability sand, supporting the dual permeability concept.

#### **6.1.4 Parameter Optimisation**

##### **Definitions**

The interpretation of this test was done on PANSYSTEM. The optimiser calculates the 95% confidence intervals for each parameter and the correlation coefficients between parameters.

The confidence interval for a parameter is calculated such that there is a 95% chance that the true parameter value will be within these limits. The larger the interval the larger the standard error of the estimate of the true parameter value.

The correlation coefficient is a measure of the correlation between the two parameters. A value greater than 0.95 implies a high degree of correlation. A high correlation coefficient indicates a high level of non-uniqueness in the solution.

##### **Procedure**

Initially, the boundary model was not considered. Attention concentrated on the formation parameters. Optimisation was performed on the early time data, ie. data

prior to approximately 1 hour (equivalent time) on the diagnostic plot. For a first pass, all parameters were allowed to vary (note that only the total skin was considered and the Non-Darcy skin factor, D, was not used).

The correlation coefficients were as follows,

<b>k</b>	1.00					
<b>S</b>	1.00	1.00				
<b>Cs</b>	0.52	0.52	1.00			
$\omega$	0.94	0.95	0.31	1.00		
$\lambda$	-0.22	-0.22	-0.59	0.01	1.00	
$\kappa$	-0.29	-0.32	-0.06	-0.43	0.05	1.00
	<b>k</b>	<b>S</b>	<b>Cs</b>	$\omega$	$\lambda$	$\kappa$

There is a high degree of correlation between permeability, total skin and the storativity ratio. Skin and storativity ratio are defined, primarily, by early time data. In fact, the storativity ratio does not impact the solution by the late transition time (see REFERENCE 3). This means that the data defining this parameter occurs before approximately 0.5 hours equivalent time. There is not enough information in the early time data to uniquely determine each of these parameters.

It was decided to investigate the effect on the parameters by holding total skin constant. Furthermore, the wellbore storage coefficient was held constant. It was known to be very small due to downhole shut-in. The correlation coefficients were,

<b>k</b>	1.00			
$\omega$	-0.58	1.00		
$\lambda$	-0.21	-0.66	1.00	
$\kappa$	-0.99	-0.47	-0.07	1.00
	<b>k</b>	$\omega$	$\lambda$	$\kappa$

There is now a strong correlation between permeability and the permeability thickness ratio.

It should be noted that as parameters were fixed and the optimiser re-run, the absolute magnitude of the variable parameters changed very little. However, the fit of the generated curve improved in terms of the calculated "Goodness of match" quantity and to the eye. The parameters defining the model have a high degree of interaction by definition, eg. permeability and permeability thickness ratio. Consequently, while the decision to fix parameters was guided by the statistics of the optimiser, there was considerable experimentation done by manually varying the parameters to visually determine sensitivity.

At this point a single boundary was introduced (after experimenting with various more complicated models, see section 7.2). Only permeability, permeability thickness ratio and distance to the fault were allowed to vary, yielding the following correlation coefficients,

k	1.00		
$\kappa$	0.99		
L	0.98	0.99	1.00
	k	$\kappa$	L

The correlation between the three parameters is very high. The permeability thickness ratio was held constant and a match obtained. This was repeated for a number of values of permeability thickness ratio. While the ratio varied significantly, the quality of the match was the same to the eye and the change in the variables was small. The match was excellent, but, not unique. The correlation was

k	1.00	
L	-0.73	1.00
	k	L

### Confidence Intervals

To obtain a qualitative feeling of the uncertainty in the interpreted distance to the noflow boundary, the distance to the boundary was fixed at 20% less and 20% greater than this interpreted distance of 340m. The well test analysis program was used to find the best match by varying the other parameters.

The permeability varied by only a few millidarcies in each case, but, the pressure match was poor (see APPENDIX 7 - WELL TEST PLOTS Figures 32 to 35) indicating that the uncertainty in the distance to the fault is better than  $\pm 20\%$ .

### 6.1.5 Gauge 10065

The derivative plot of the 10065 (APPENDIX 5 - GAUGE SELECTION Figure 17) data does not have the character of the 011 data before 1 hour equivalent time. Information has been lost due to the slower sampling rate of 10065. In particular, the transition from the high permeability response to the total system response is poorly defined. Instead of the "V" shaped transition period, the data forms a hump before the 1 hour equivalent time mark. The interpretation based on the 011 gauge response would not have been possible with the 10065 response.

On the cartesian plot of the gauge difference between 011 and 10065 (APPENDIX 5 - GAUGE COMPARISON Figure 18) the 1 hour equivalent time period corresponds to the data before 0.9 hours. This is the data where the difference in gauge response is variable, prior to stabilising at around -0.55 to -0.60 psi difference.

## 6.2 Reservoir Description

### 6.2.1 Reservoir Geometry

Boundary effects coincide with the late transition period associated with the dual porosity and permeability models. Both effects cause the the derivative to increase. This explains the high degree of correlation between the permeability thickness ratio and the distance to a single fault seen in the optimisation. It is clear that a boundary has been seen from the plots where the boundary has not been simulated (see APPENDIX 8 - BOUNDARIES Figures 36-37, dual permeability, and, Figures 38-39, dual porosity). For the dual porosity model ( $\kappa = 1$ ), a significant part of the increase in the derivative is due to the dual porosity assumption. For the dual permeability model with a low permeability thickness ratio, the increase in the late transition period is due more to the presence of a boundary.

For the purposes of this discussion assumptions have been made regarding the relationship of time and depth for the draft structure map. From the logs the top of the structure at Minerva-1 is 1816 mRT. This corresponds to a time of 1375 msec, which yields a conversion factor of 1.3207 m/msec. From the RFT data, the gas water contact is at 1944.5 mRT, which in turn corresponds to 1473 msec. Hence, the 1475 msec contour was used to determine the limits of the structure.

The draft structure map presents a number of possible boundary conditions. There are two parallel faults. The well is 400 metres and 800 metres from the faults. Closing the system off at each end is the gas water contact. At the near end, the contact angles across the faults and is an average distance of about 800 metres. At the far end of the system the contact also cuts across the faults. In this case, the angle of intersection with the faults is more acute. The nearest part of the far gas water contact is 1500 metres along the far fault and the farthest part of the gas water contact is 4375 metres along the near fault.

Initially, an approximation was made for the distance to each GWC to form a closed rectangle (see APPENDIX 8 - BOUNDARIES Figure 40). However, inspection of the derivative response for the final build-up shows that the system has seen a boundary, but, is in a transient state at the end of the build-up (see APPENDIX 8 - BOUNDARIES Figure 41). That is, the derivative response is horizontal.

With the optimisation, for dual porosity and permeability, a single fault was used. For the dual permeability model the distance to the fault was 340 metres ( $\kappa = 0.2$ ). The matched value compares favourably with the 400 metres on the draft map.

Other boundary conditions were tried, eg. parallel and perpendicular faults (see APPENDIX 8 - BOUNDARIES Figures 42 to 47). PANSYSTEM has a limited number of options for the ratio of distance to the boundaries. However, even though a suitable match was not possible, it is unlikely that changes to the boundary distances would affect much improvement. It is clear that not all the boundaries were seen by the test, in particular, the far gas water contact.

### 6.2.2 Radius Of Investigation

A radius of investigation has been calculated using an equivalent Horner time of 15.56 hours.

**Table 6 : Radius of Investigation**

	$\kappa = 0.2$		$\kappa = 0.3$	
	k (md)	Radius (metres)	k (md)	Radius (metres)
Layer 1	8449.00	3796.00	12709.00	4655.00
Layer 2	1779.00	1742.00	1561.00	1631.00

The formula used to calculate the radius of investigation assumes that the drainage shape is circular (see REFERENCE 4). While one boundary has been established, the actual drainage shape is not known. In addition, the two layers defined by the analysis are not mutually exclusive and the radius calculation does not account for this. Consequently, the radii calculated here are an approximation.

If the permeability thickness ratio was 0.2, these results suggest that even the high permeability Layer 1 would not have seen the entire reservoir. Certainly, Layer 2 did not see all of the far gas water contact. This is consistent with the fact that the pressure response was in a transient state at the conclusion of the final build-up.

However, the calculated radii suggest that the pressure transient passed through the far fault and the near gas water contact were seen during the test. Given that the two boundaries are mapped at similar distances to the well, it would be expected that they would make a detectable impact on the pressure response. Attempts to fit relevant boundaries to the data were not successful (see section 7.2.1).

It would appear that, either,

1. the boundaries were seen, but, there is not enough information in the pressure response to delineate them, or
2. the boundaries are not as mapped
3. the boundaries do not act as no flow boundaries.

Inspection of the map shows that the far fault does not have a large throw in the vicinity of the well. In fact, it ceases to exist North-West of the well. A closer fault to the north of the well has been ignored due to its minor throw. It is possible that the far fault, even if in the position mapped, has not acted as an effective barrier.

### 6.3 Skin Calculations

#### 6.3.1 Discussion

There are two components to the skin determined from the dual permeability analysis, Darcy and Non-darcy. The Darcy skin is referred to as mechanical or formation damage skin, and, is independent of rate. The Non-darcy skin is rate dependent. It is assumed that there are no partial penetration effects.

It has been established that the well continued to cleanup throughout the flow period. Consequently, the flow periods do not lend themselves to conventional analysis.

The flow periods have been analysed to factorise the total skin.

#### 6.3.2 Transient Analysis

For the purposes of this analysis the  $\kappa = 0.2$  results have been used. To get a rate dependent skin for each flow period, a line of slope corresponding to the total system permeability ( $k_{1+2}=2112$  md) was fitted (by eye) to the pressures at the end of each flow period pressures (see APPENDIX 9 - SKIN FACTOR Figure 48). Extrapolation back to the y-axis enables the calculation of rate dependent skin.

By plotting the total skin against flow rate and fitting a straight line through the points the Darcy (intercept) and Non-Darcy (slope) components can be determined (see APPENDIX 9 - SKIN FACTOR Figure 49).

**Table 7 : Transient Skin Calculations**

Darcy, S	15.90
Non-Darcy, D	0.00 1/(Mscf/d)

The AOF from the PANSYSTEM transient analysis is 211.0 MMscf/d.



### 6.3.3 Partial Penetration

The Darcy skin is very high. It is unlikely to be the result of mechanical damage. If perforations were not contributing to the flow, part of the Darcy skin could be due to partial penetration effects. Plugged perforations are a definite possibility given the circumstances for the perforation of the well.

The following formula enables the calculation of the skin due to partial penetration (see REFERENCE 9),

$$S_p = \frac{(1-b)}{b} \left[ \ln \left[ \left( \frac{h}{r_w} \right) \sqrt{\frac{k_h}{k_v}} \right] - 2.73 - b(4.95 - 5.07b) \right] \quad \dots(3)$$

$$b = \frac{h_{perfs}}{h} \quad \dots(4)$$

By assuming values for horizontal to vertical permeability ratio, the value of b that yields the value for skin calculated above can be determined. From b, the contributing thickness of the perforations can be calculated.

**Table 8 : Perforation Thickness from Partial Penetration Analysis**

		Transient	
		b	$h_{perfs}$ (metres)
S=0	$\frac{k_h}{k_v}$	0.17	3.76
		0.22	4.93
		0.27	5.92
S=5	$\frac{k_h}{k_v}$	0.24	5.33
		0.30	6.69
		0.36	7.81

The calculations show that, assuming that skin is due to partial penetration only (S=0), it is feasible that the bottom set of perforations did not contribute to the flow. The contributing thicknesses calculated represent a minimum thickness as any Darcy skin would decrease the skin due to partial penetration and increase the contributing thickness. Even so, if the producing perforations were badly damaged (a Darcy skin of 5, say) it does not increase the contributing thickness significantly.

The plugging of the perforations has been considered (see section 7.1.2). This analysis supports the proposition that bottom set of perforations were affected by the delay from perforation to testing and the application of HEC.

## 6.4 Gas-In-Place Investigated

### 6.4.1 Area

The DST has not seen all the boundaries as it remains in transient flow at the conclusion of the final build-up. The dual permeability model makes the use of the radius of investigation to calculate area confusing. Furthermore, the radius of investigation calculation assumes a circular drainage shape and there is a boundary within the radii calculated.

An estimate of the area can be calculated using the radius of investigation. Using the low permeability layer (for a conservative estimate) gives an area of 9528072 m<sup>2</sup>, which is more than twice that calculated from the mapped boundaries (see APPENDIX 8 - BOUNDARIES).

## 6.5 Reservoir Pressure

### 6.5.1 Pressure Comparison

There are three measures of the initial reservoir pressure,

1. from the RFT survey
2. from the initial build-up (after the clean-up flow), and
3. from the final build-up.

**Table 9 : Reservoir Pressure at Gauge Depth**

	Measured (psia)	Extrapolated (psia)	Error (±psi)
RFT Survey		2720.00	0.38
initial build-up	2716.26	2716.32	0.00
final build-up	2716.11	2716.40	0.00

The error quoted in the table is the mean residual error of the points used in the respective regressions. It reflects the resolution of the gauge, rather than the absolute accuracy, over the range of pressures used in the regression.

### 6.5.2 Depletion

There is a 4 psi difference between the RFT initial pressure and that determined from the test. This is within the absolute accuracy of the gauges used for the measurement of the pressures.

Furthermore, there is agreement between the build-up pressures measured during the test. In fact, the final build-up reservoir pressure is higher than the initial build-up pressure by 0.1 psi.

Hence, there is no depletion within the accuracy of the gauges

## **6.6 Pseudo-Pressure**

For all pressure analysis conducted on this test, pseudo pressure has been used instead of pressure as this is conventional for gas well test analysis.

Pseudo-pressure accounts for the pressure dependency of gas viscosity and the Z-factor. While it is recognised that for small variations in pressure conventional pressure can be used in gas well analysis, pseudo pressure was used in this report for completeness.

## **6.6 Pseudo-Pressure**

For all pressure analysis conducted on this test, pseudo pressure has been used instead of pressure as this is conventional for gas well test analysis.

Pseudo-pressure accounts for the pressure dependency of gas viscosity and the Z-factor. While it is recognised that for small variations in pressure conventional pressure can be used in gas well analysis, pseudo pressure was used in this report for completeness.

## 7 SAMPLES

### 7.1 Separator Samples

Gas and condensate samples were taken during the first (low flow rate) and last (high flow rate) flow periods. There were three sets of samples taken, by the BHPP Lab representative, in each of the periods. The samples are summarised in the following table,

**Table 16 : Separator Samples**

Sample Type	Date	Time	Sample No.	Separator		Fixed Choke (inch)	Gas Rate (MMscf/d)
				Pressure (psig)	Temp. °C		
Gas (Whitey)	11/4/93	08:01	027	215.00	-1.50	20/64	5.50
	11/4/93	08:13	028	215.00	-1.50	20/64	5.50
	11/4/93	08:20	023	215.00	-1.50	20/64	5.50
	11/4/93	11:29	020	699.00	27.00	64/64	28.70
	11/4/93	11:32	005	699.00	27.00	64/64	28.70
	11/4/93	11:45	021	699.00	27.00	64/64	28.70
Condensate (Welker)	11/4/93	08:37	11813.00	215.00	-1.50	20/64	5.50
	11/4/93	08:46	5197.00	215.00	-1.50	20/64	5.50
	11/4/93	08:55	11812.00	215.00	-1.50	20/64	5.50
	12/4/93	00:08	11808.00	699.00	27.00	64/64	28.70
	12/4/93	00:25	11809.00	699.00	27.00	64/64	28.70
	12/4/93	02:01	11810.00	699.00	27.00	64/64	28.70

Three sets of samples were also taken by Halliburton Reservoir Services (HRS) while the well was producing at the maximum rate (final flow period). These samples were sent to Petrolab in Adelaide.

No analysis was available at the time of writing the report.

### 7.2 Bottomhole Samples

Two RFT samples were obtained in the gas column. Neither of these samples were taken in the perforated interval. Both were below the perforated interval at depths 1931 mRT and 1942.5 mRT.

Details of the analysis of these samples can be found in the RFT report (see REFERENCE 5).

---

## REFERENCES

1. **Minerva-1 Cores: Drilling Depth Versus Logging Depth;**  
Memorandum Ref: dp:1004:jn:Minerva-1Post Drilling,  
TO: Darwin Office, FROM: Exploration Geologist 1
2. **WELL TEST PROGRAMME**  
WELL; MINERVA-1  
LICENCE: VIC/P31  
DATE: MARCH 1993
3. **Pressure Behaviour Of Layered Reservoirs With Crossflow**  
D. Bourdet, SPE 13628.
4. **ADVANCES IN WELL TEST ANALYSIS**  
Monograph Volume 5, R.C. Earlougher, Jr.  
SPE Monograph Series
5. **ADVANCED WELL TEST ANALYSIS Vol.2**  
Gas Well Testing  
EPS Well Testing Course  
Prof. Goerge Stewart
6. **Minerva-1 RFT Report**  
C. Taylor  
BHP Petroleum (Melbourne), 9<sup>th</sup> February 1993
7. **WELL TEST DATA REPORT - Gauge Pressures**  
Minerva #1, 10-13 April 1993  
Halliburton Reservoir Services
8. **WELL TEST DATA REPORT - Surface Flow Data (not finalised)**  
Minerva #1, 10-13 April 1993  
Halliburton Reservoir Services
9. **The Effect of Restricted Fluid Entry on Well Productivity**  
F. Brons and V.E. Marting  
JPT, Feb. 1961

---

## NOMENCLATURE

A	reservoir drainage area (ft <sup>2</sup> , m <sup>2</sup> )
C <sub>A</sub>	shape factor
c <sub>t</sub>	total compressibility (v/v/psi, v/v/kPa)
D	Non-Darcy skin (1/(Mscf/d), 1/(sm <sup>3</sup> /d))
h	thickness (feet, metres)
k	permeability (mD)
k <sub>h</sub>	horizontal permeability (mD)
k <sub>v</sub>	vertical permeability (mD)
m(p)	pseudo pressure (psia <sup>2</sup> /cpx10 <sup>-6</sup> )
p	pressure (psia)
Q	gas flow rate (Mscf/d, sm <sup>3</sup> /d)
r <sub>w</sub>	wellbore radius (ft, m)
S	Darcy skin
T	temperature (°R)
φ	porosity (fraction)
ω	storativity ratio
κ	permeability thickness ratio
γ	Eulers constant (0.5772)

**DATA SHEET 1 : Summary of DST Survey**

**PHYSICAL**

<b>Well Name</b>	Minerva 1
<b>Test Type</b>	Multi-rate DST
<b>Designation</b>	Exploration
<b>Well Location</b>	Lat. 38° 42' 31.6" S Long. 142° 56' 55.2" E Northing : 5 713 724 m Easting : 669 435 m AMG Zone : 54
<b>Permit</b>	VIC/P31
<b>Rig Used</b>	Byford Dolphin
<b>KB Elevation of the rig</b>	25.00 metres
<b>Tritium Used</b>	No
<b>Datum Depth</b>	1944.50 metres (GWC)
<b>Well Total Depth</b>	2425 mRT
<b>Plug Back Total Depth</b>	2074 mRT
<b>Well Deviation</b>	vertical
<b>Well Radius</b>	0.354 ft.
<b>Perforated Interval</b>	1816 to 1821 mRT 1825 to 1838 mRT
<b>Casing Size</b>	7.000 inches
<b>Casing Weight</b>	29.00 lbs/ft
<b>Tubing OD</b>	3.50 inches
<b>Tubing ID</b>	2.75 inches

**TIMING**

<b>Well perforated</b>	07:35 8 April 1993 (1827.5-1838 mRT) 04:00 9 April 1993 (1825-1827.5 mRT 1816-1821 mRT)
<b>Well opened to flow</b>	15:45 11 April 1993 for cleanup
<b>Duration of Survey</b>	03:20 11 April 1993 start test 03:20 13 April 1993 end test 48 hours



## DATA SHEET 2 : Summary of DST Interpretation

### PRESSURE

<b>Datum Pressure</b>	2742.13 psia 1944.50 mRT (GWC)
<b>Pressure at Top Perforations</b>	2724.38 psia 1816.00 mRT
<b>Gradient to drill floor (KB)</b>	0.1693 psi/m

### INTERPRETATION

<b>Absolute Open Flow (AOF)</b>	211.29 MMscf/d
<b>kh</b>	46517 mD-m
<b>k</b>	9726 md - Layer 1 1714 md - Layer 2
<b>h</b>	1.1 metres - Layer 1 20.9 metres - Layer 2
<b>S Total</b>	65.69
<b>S Damage</b>	17.04
<b>S Non-Darcy</b>	0.0017 1/(Mscf/d)
<b>Distance to Boundary</b>	347 metres
<b>Investigated Volume</b>	77.29 Bcf (based on mapped boundaries)

### MAIN FLOW PERIOD

<b>Final Flow Rate</b>	5.76 Mmscf/d - Flow 1 16.96 Mmscf/d - Flow 2 23.14 Mmscf/d - Flow 3 28.80 Mmscf/d - Flow 4
<b>Final Well Head Pressure</b>	2319 psig - Flow 1 2013 psig - Flow 2 1726 psig - Flow 3 1243 psig - Flow 4
<b>Final Flowing Pressure</b>	2713 psia - Flow 1 2698 psia - Flow 2 2688 psia - Flow 3 2676 psia - Flow 4

### DATA SHEET 3 : Summary of reservoir and Fluid Parameters

#### PETROPHYSICAL

Hydrocarbon Column	128.50 metres
Average Porosity	0.18
Average Gas Saturation	0.81
Reservoir Temperature	216 °F

#### PVT

Bgi	0.00644 v/v
viscosity	0.0176 cp
gas gravity	0.61 (air = 1)

#### COMPRESSIBILITY

Water	3.2187E-6 1/psi
Gas	3.4874E-4 1/psi
Total	2.2125E-4 1/psi

#### FLUID GRADIENTS

Gas	0.1693 psi/m
Completion Brine	1.62 psi/m

## APPENDIX 1 - TIDAL DATA

Figure 1 : Tidal Data - Chart and Measured

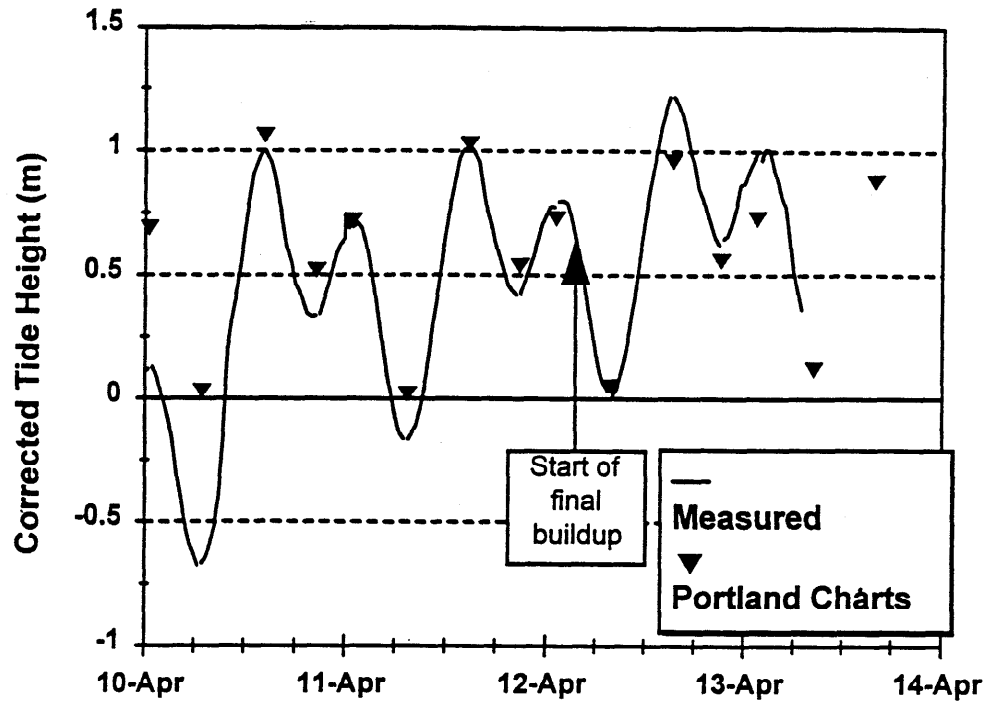


**Table 19 : Portland Chart Data**

Date	Time	Tide Height
		Corrected (metres)
10-Apr-93	00:31	0.69
10-Apr-93	06:56	0.03
10-Apr-93	14:17	1.06
10-Apr-93	20:31	0.52
11-Apr-93	00:50	0.72
11-Apr-93	07:25	0.02
11-Apr-93	14:48	1.03
11-Apr-93	20:51	0.54
12-Apr-93	01:11	0.73
12-Apr-93	07:57	0.05
12-Apr-93	15:22	0.96
12-Apr-93	21:12	0.56
13-Apr-93	01:32	0.73
13-Apr-93	08:30	0.12
13-Apr-93	15:58	0.88

**Table 20 : Measured Tidal Data**

Date	Time	Tide Height	
		Uncorrected (metres)	Corrected (metres)
09-Apr-93	17:05	3.892	0.392
09-Apr-93	17:30	3.915	0.415
09-Apr-93	18:00	3.653	0.153
09-Apr-93	18:30	3.453	-0.047
09-Apr-93	19:00	3.341	-0.159
09-Apr-93	19:30	3.319	-0.181
09-Apr-93	20:00	3.345	-0.155
09-Apr-93	20:30	3.375	-0.125
09-Apr-93	21:00	3.410	-0.090
09-Apr-93	21:30	3.430	-0.070
09-Apr-93	22:00	3.443	-0.057
09-Apr-93	22:30	3.476	-0.024
09-Apr-93	23:00	3.530	0.030
09-Apr-93	23:30	3.565	0.065
10-Apr-93	00:00	3.610	0.110
10-Apr-93	00:30	3.618	0.118
10-Apr-93	01:00	3.629	0.129
10-Apr-93	01:30	3.590	0.090
10-Apr-93	02:00	3.525	0.025
10-Apr-93	02:30	3.468	-0.032
10-Apr-93	03:00	3.402	-0.098
10-Apr-93	03:30	3.300	-0.200
10-Apr-93	04:00	3.176	-0.324
10-Apr-93	04:30	3.090	-0.410
10-Apr-93	05:00	2.981	-0.519
10-Apr-93	05:30	2.913	-0.587
10-Apr-93	06:00	2.871	-0.629
10-Apr-93	06:30	2.827	-0.673
10-Apr-93	07:00	2.835	-0.665
10-Apr-93	07:30	2.861	-0.639
10-Apr-93	08:00	2.915	-0.585
10-Apr-93	08:30	2.984	-0.516
10-Apr-93	09:00	3.100	-0.400
10-Apr-93	09:30	3.337	-0.163
10-Apr-93	10:00	3.699	0.199
10-Apr-93	10:30	3.827	0.327
10-Apr-93	11:00	3.917	0.417
10-Apr-93	11:30	4.033	0.533
10-Apr-93	12:00	4.164	0.664
10-Apr-93	12:30	4.298	0.798
10-Apr-93	13:00	4.410	0.910
10-Apr-93	13:30	4.456	0.956
10-Apr-93	14:00	4.490	0.990
10-Apr-93	14:30	4.493	0.993
10-Apr-93	15:00	4.460	0.960
10-Apr-93	15:30	4.403	0.903
10-Apr-93	16:00	4.319	0.819

10-Apr-93 16:30 4.201 0.701

Date	Time	Tide Height	
		Uncorrected (metres)	Corrected (metres)
10-Apr-93	17:00	4.111	0.611
10-Apr-93	17:30	4.051	0.551
10-Apr-93	18:00	3.966	0.466
10-Apr-93	18:30	3.935	0.435
10-Apr-93	19:00	3.884	0.384
10-Apr-93	19:30	3.845	0.345
10-Apr-93	20:00	3.834	0.334
10-Apr-93	20:30	3.837	0.337
10-Apr-93	21:00	3.843	0.343
10-Apr-93	21:30	3.902	0.402
10-Apr-93	22:00	3.959	0.459
10-Apr-93	22:30	4.023	0.523
10-Apr-93	23:00	4.089	0.589
10-Apr-93	23:30	4.125	0.625
11-Apr-93	00:00	4.148	0.648
11-Apr-93	00:30	4.186	0.686
11-Apr-93	01:00	4.194	0.694
11-Apr-93	01:30	4.211	0.711
11-Apr-93	02:00	4.189	0.689
11-Apr-93	02:30	4.133	0.633
11-Apr-93	03:00	4.049	0.549
11-Apr-93	03:30	3.941	0.441
11-Apr-93	04:00	3.832	0.332
11-Apr-93	04:30	3.717	0.217
11-Apr-93	05:00	3.605	0.105
11-Apr-93	05:30	3.514	0.014
11-Apr-93	06:00	3.430	-0.070
11-Apr-93	06:30	3.364	-0.136
11-Apr-93	07:00	3.340	-0.160
11-Apr-93	07:30	3.336	-0.164
11-Apr-93	08:00	3.369	-0.131
11-Apr-93	08:30	3.397	-0.103
11-Apr-93	09:00	3.466	-0.034
11-Apr-93	09:30	3.548	0.048
11-Apr-93	10:00	3.669	0.169
11-Apr-93	10:30	3.798	0.298
11-Apr-93	11:00	3.914	0.414
11-Apr-93	11:30	4.047	0.547
11-Apr-93	12:00	4.172	0.672
11-Apr-93	12:30	4.275	0.775
11-Apr-93	13:00	4.359	0.859
11-Apr-93	13:30	4.461	0.961
11-Apr-93	14:00	4.496	0.996
11-Apr-93	14:30	4.512	1.012
11-Apr-93	15:00	4.519	1.019
11-Apr-93	15:30	4.495	0.995
11-Apr-93	16:00	4.457	0.957
11-Apr-93	16:30	4.353	0.853

11-Apr-93	17:00	4.259	0.759
11-Apr-93	17:30	4.201	0.701
11-Apr-93	18:00	4.124	0.624
11-Apr-93	18:30	4.073	0.573

**Tide Height**

<b>Date</b>	<b>Time</b>	<b>Uncorrected (metres)</b>	<b>Corrected (metres)</b>
11-Apr-93	19:00	4.018	0.518
11-Apr-93	19:30	3.962	0.462
11-Apr-93	20:00	3.940	0.440
11-Apr-93	20:30	3.924	0.424
11-Apr-93	21:00	3.927	0.427
11-Apr-93	21:30	3.976	0.476
11-Apr-93	22:00	4.025	0.525
11-Apr-93	22:30	4.078	0.578
11-Apr-93	23:00	4.137	0.637
11-Apr-93	23:30	4.204	0.704
11-Apr-93	00:00	4.245	0.745
12-Apr-93	00:30	4.279	0.779
12-Apr-93	01:00	4.277	0.777
12-Apr-93	01:30	4.297	0.797
12-Apr-93	02:00	4.301	0.801
12-Apr-93	02:30	4.290	0.790
12-Apr-93	03:00	4.239	0.739
12-Apr-93	03:30	4.167	0.667
12-Apr-93	04:00	4.088	0.588
12-Apr-93	04:30	3.998	0.498
12-Apr-93	05:00	3.880	0.380
12-Apr-93	05:30	3.792	0.292
12-Apr-93	06:00	3.686	0.186
12-Apr-93	06:30	3.607	0.107
12-Apr-93	07:00	3.560	0.060
12-Apr-93	07:30	3.530	0.030
12-Apr-93	08:00	3.510	0.010
12-Apr-93	08:30	3.539	0.039
12-Apr-93	09:00	3.594	0.094
12-Apr-93	09:30	3.660	0.160
12-Apr-93	10:00	3.737	0.237
12-Apr-93	10:30	3.849	0.349
12-Apr-93	11:00	3.952	0.452
12-Apr-93	11:30	4.092	0.592
12-Apr-93	12:00	4.211	0.711
12-Apr-93	12:30	4.326	0.826
12-Apr-93	13:00	4.417	0.917
12-Apr-93	13:30	4.502	1.002
12-Apr-93	14:00	4.598	1.098
12-Apr-93	14:30	4.661	1.161
12-Apr-93	15:00	4.718	1.218
12-Apr-93	15:30	4.720	1.220
12-Apr-93	16:00	4.689	1.189
12-Apr-93	16:30	4.645	1.145
12-Apr-93	17:00	4.586	1.086
12-Apr-93	17:30	4.506	1.006

12-Apr-93	18:00	4.442	0.942
12-Apr-93	18:30	4.347	0.847
12-Apr-93	19:00	4.310	0.810
12-Apr-93	19:30	4.255	0.755
12-Apr-93	20:00	4.202	0.702
12-Apr-93	20:30	4.154	0.654

Date	Time	Tide Height	
		Uncorrected (metres)	Corrected (metres)
12-Apr-93	21:00	4.125	0.625
12-Apr-93	21:30	4.149	0.649
12-Apr-93	22:00	4.160	0.660
12-Apr-93	22:30	4.213	0.713
12-Apr-93	23:00	4.278	0.778
12-Apr-93	23:30	4.365	0.865
13-Apr-93	00:00	4.370	0.870
13-Apr-93	00:30	4.420	0.920
13-Apr-93	01:00	4.456	0.956
13-Apr-93	01:30	4.492	0.992
13-Apr-93	02:00	4.465	0.965
13-Apr-93	02:30	4.508	1.008
13-Apr-93	03:00	4.506	1.006
13-Apr-93	03:30	4.431	0.931
13-Apr-93	04:00	4.383	0.883
13-Apr-93	04:30	4.318	0.818
13-Apr-93	05:00	4.276	0.776
13-Apr-93	05:30	4.159	0.659
13-Apr-93	06:00	4.016	0.516
13-Apr-93	06:30	3.942	0.442
13-Apr-93	07:00	3.862	0.362

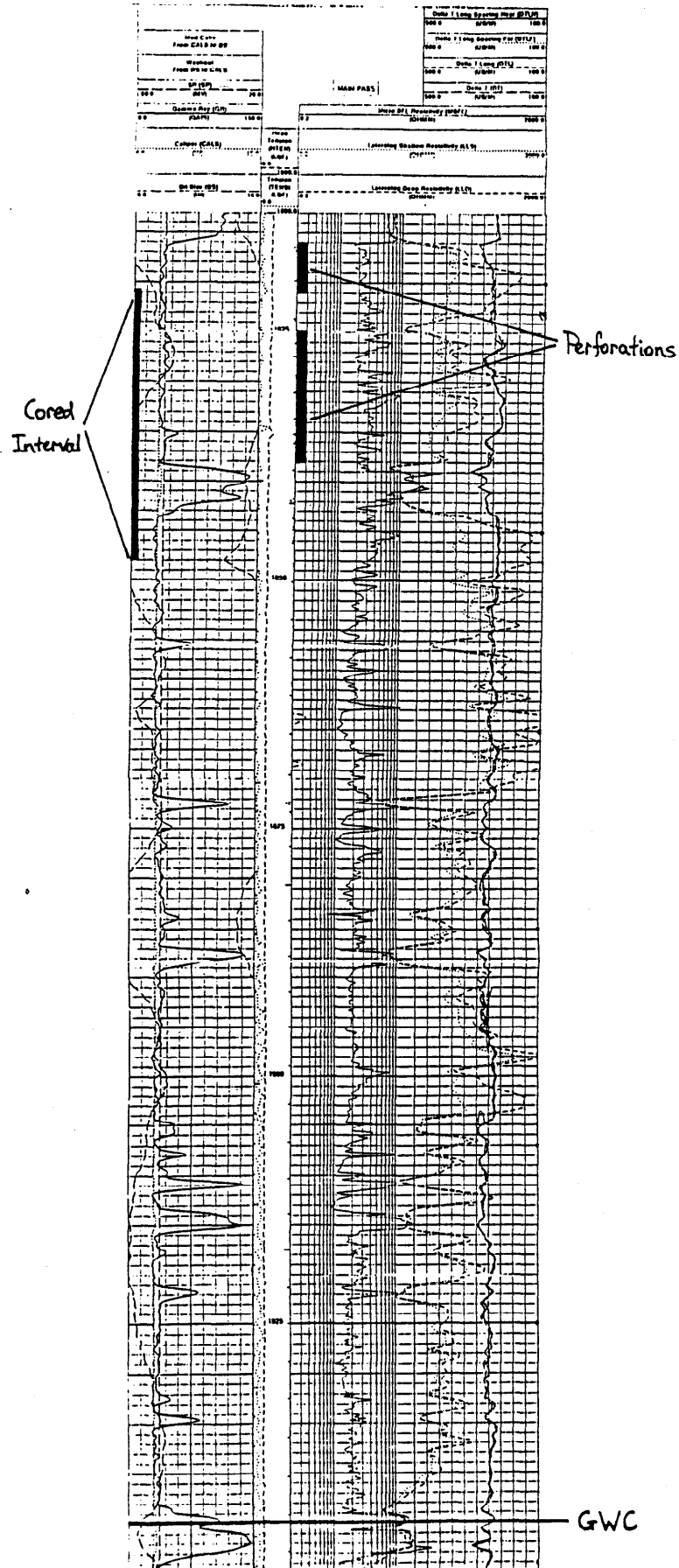
Note : tide correction = 3.5 metres

---

**APPENDIX 2 - LOG SECTION**



Figure 2 : Minerva-1 DDL-MSFL-AS-GR-AMS-DP Log



## APPENDIX 3 - CORE DATA

**Table 21 : Routine Core Analysis Data**

Depth (mRT)	Adjusted Depth (mRT)	k (md)	porosity	Sw
1821.15	1822.15	3769	0.23	0.05
1821.37	1822.37	3175	0.26	0.51
1821.67	1822.67	2061	0.18	0.43
1821.97	1822.97	332	0.15	0.36
1822.27	1823.27	1171	0.15	0.44
1822.57	1823.57	4605	0.21	0.44
1822.87	1823.87	116	0.13	0.37
1823.17	1824.17	3414	0.16	0.34
1823.47	1824.47	1945	0.17	0.31
1823.77	1824.77	646	0.21	0.39
1824.00	1825.00	229	0.24	0.34
1828.15	1829.15	1985	0.25	0.45
1828.37	1829.37	3021	0.22	0.39
1828.67	1829.67	1190	0.20	0.38
1828.97	1829.97	2267	0.19	0.33
1829.27	1830.27	3302	0.17	0.34
1829.57	1830.57	2066	0.11	0.40
1829.87	1830.87	708	0.14	0.36
1830.17	1831.17	2853	0.13	0.37
1830.47	1831.47	754	0.12	0.34
1830.77	1831.77	2391	0.17	0.40
1831.10	1832.10	709	0.18	0.36
1831.40	1832.40	644	0.18	0.34
1831.70	1832.70	503	0.15	0.32
1832.00	1833.00	694	0.14	0.35
1832.30	1833.30	426	0.16	0.33
1832.60	1833.60	432	0.13	0.35
1832.90	1833.90	9.8	0.14	0.35
1833.20	1834.20	126	0.15	0.43
1833.50	1834.50	0.62	0.11	0.44
1833.80	1834.80	23	0.21	0.47
1834.10	1835.10	138	0.20	0.47
1834.40	1835.40	303	0.22	0.43
1834.70	1835.70	188	0.20	0.44
1835.00	1836.00	2605	0.19	0.38
1835.30	1836.30	134	0.21	0.40
1835.60	1836.60	306	0.20	0.45
1835.90	1836.90	696	0.22	0.39
1836.20	1837.20	774	0.25	0.43
1836.50	1837.50	1063	0.23	0.38
1836.80	1837.80	700	0.13	0.40
1838.10	1839.10	0.04	0.05	0.47
1839.10	1840.10	0.02	0.08	0.70
1839.40	1840.40	0.02	0.08	0.72
1839.70	1840.70	0.52	0.09	0.71
1840.00	1841.00	0.32	0.08	0.76
1840.30	1841.30	66.6	0.17	0.24
1840.60	1841.60	16.8	0.20	0.45
1840.90	1841.90	311	0.19	0.58
1841.20	1842.20	155	0.18	0.39
1842.80	1843.80	719	0.16	0.24
1843.10	1844.10	2916	0.21	0.36
1843.40	1844.40	10142	0.18	0.33
1843.70	1844.70	1621	0.16	0.27
1844.05	1845.05	411	0.20	0.36
1844.30	1845.30	38.7	0.17	0.31
1844.60	1845.60	645	0.17	0.28
1844.90	1845.90	1538	0.19	0.30
1845.22	1846.22	1276	0.18	0.36
1845.52	1846.52	5009	0.17	0.39
1845.82	1846.82	3091	0.17	0.39
1846.12	1847.12	1927	0.19	0.37
1846.42	1847.42	3022	0.21	0.38
1846.72	1847.72	1429	0.17	0.36

Averages :	perforated	1280	0.18	0.38
	entire core	1356	0.17	0.40

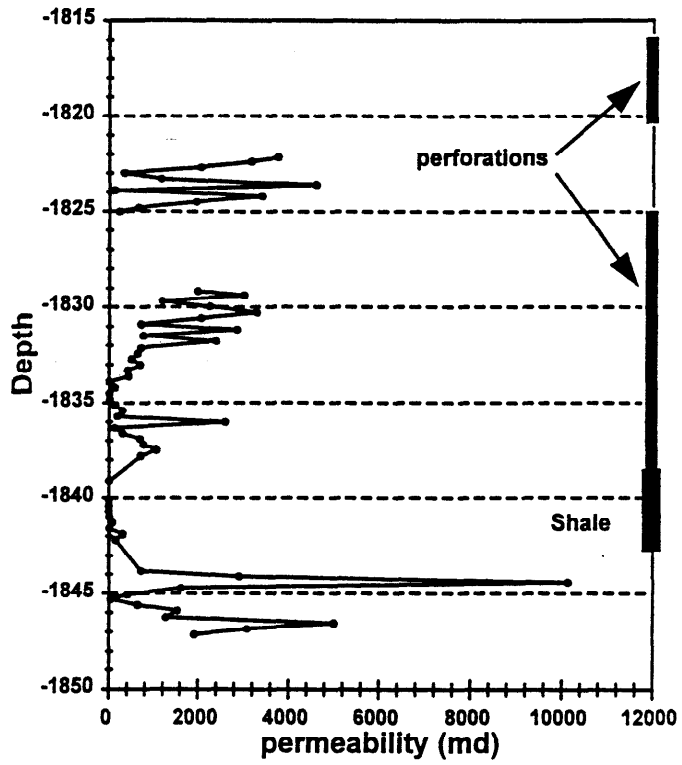


Figure 3 : Core Permeability Profile

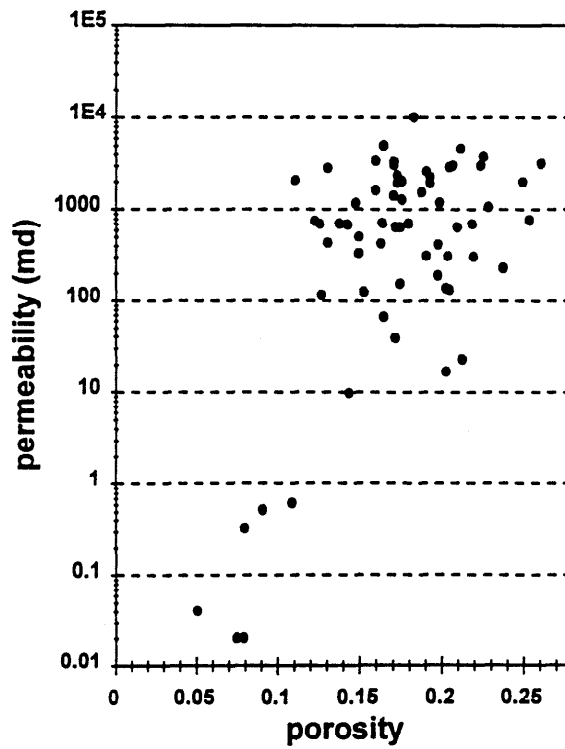


Figure 4 : Porosity - Permeability Relationship

---

**APPENDIX 4 - FLOW PERIODS**

Figure 5 : Test Sequence Cartesian Plot

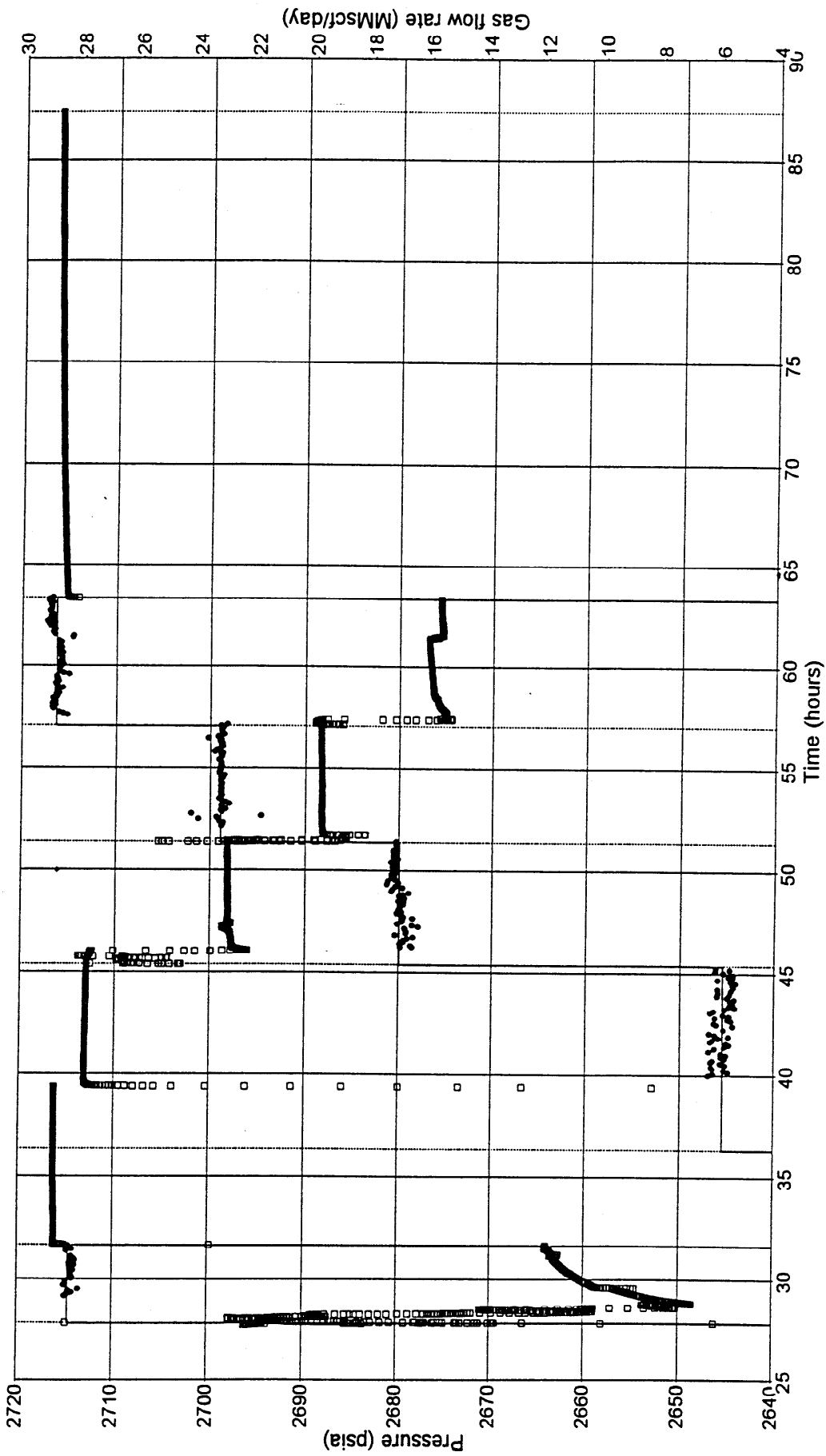


Figure 6 : Clean-up Flow Cartesian Plot

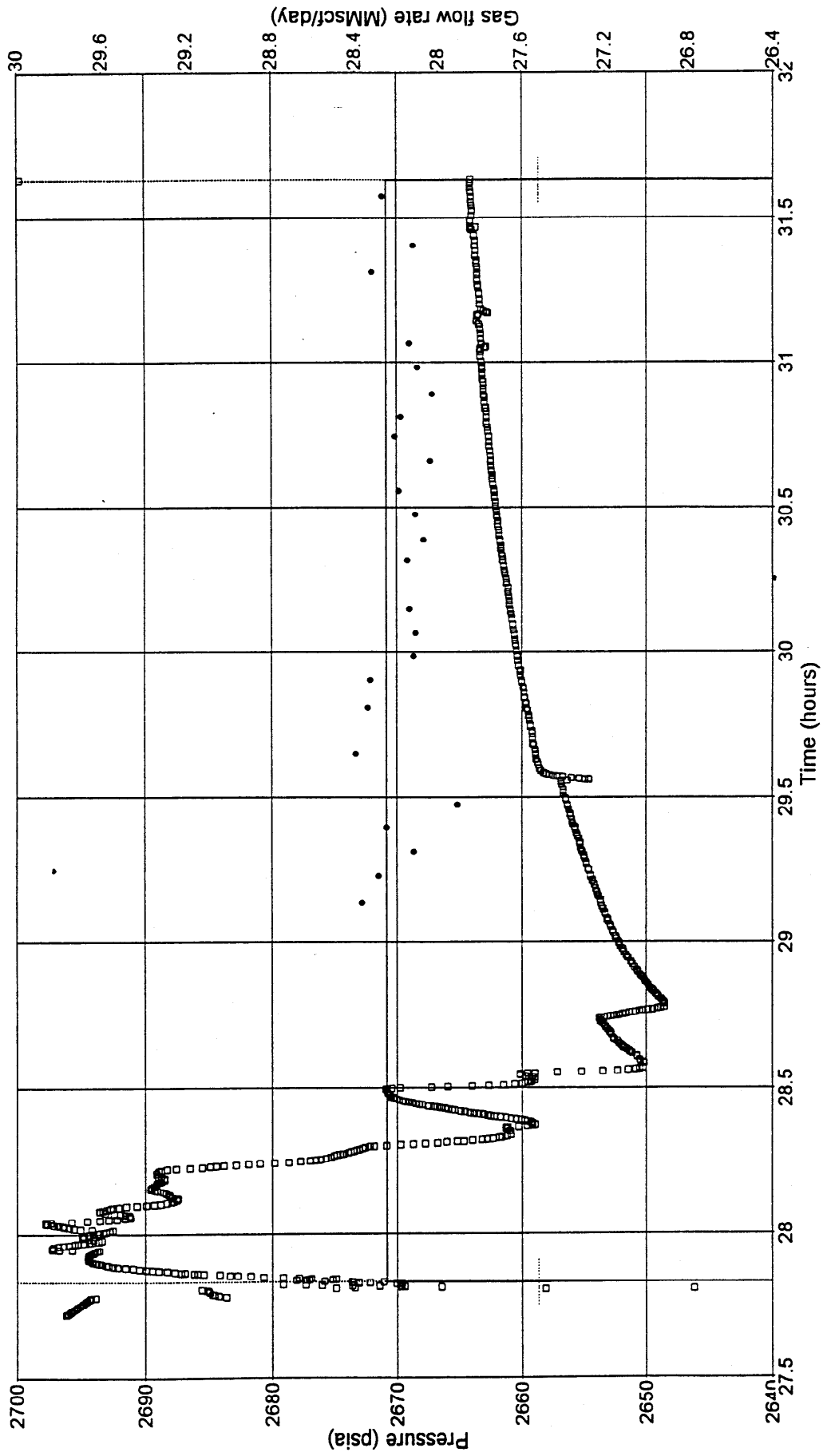


Figure 7 : Flow Period 1 Cartesian Plot

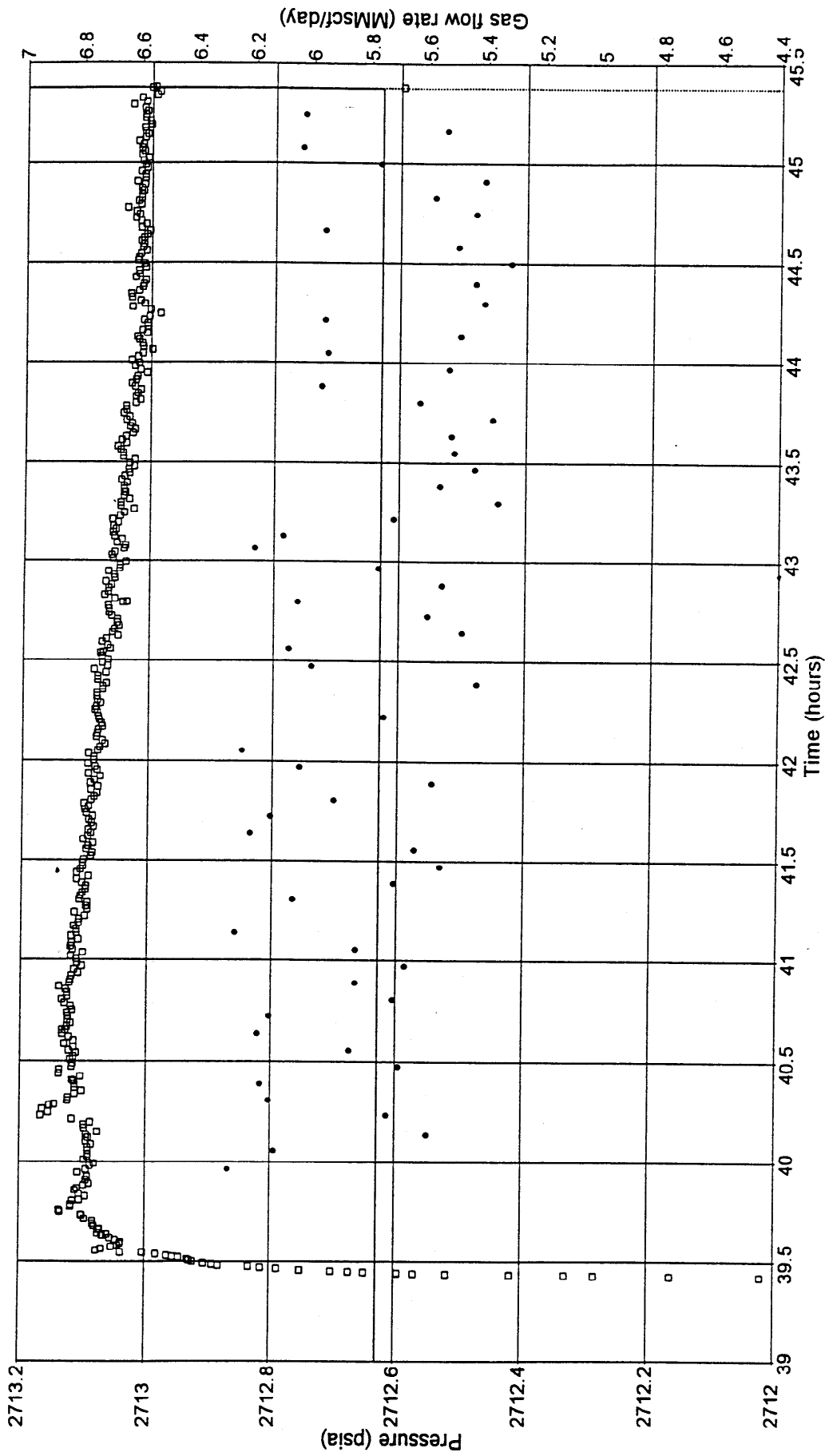
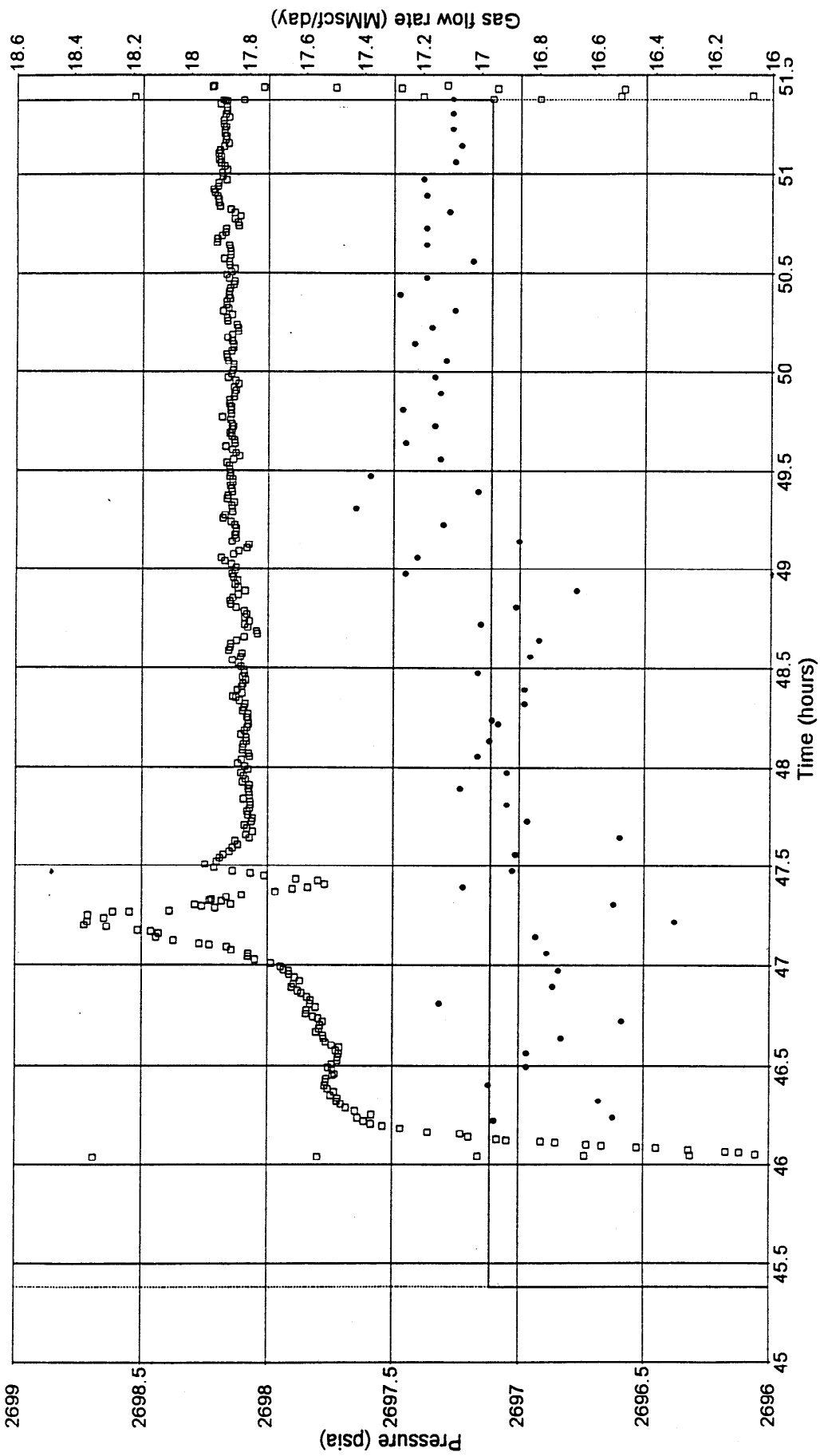


Figure 8 : Flow Period 2 Cartesian Plot





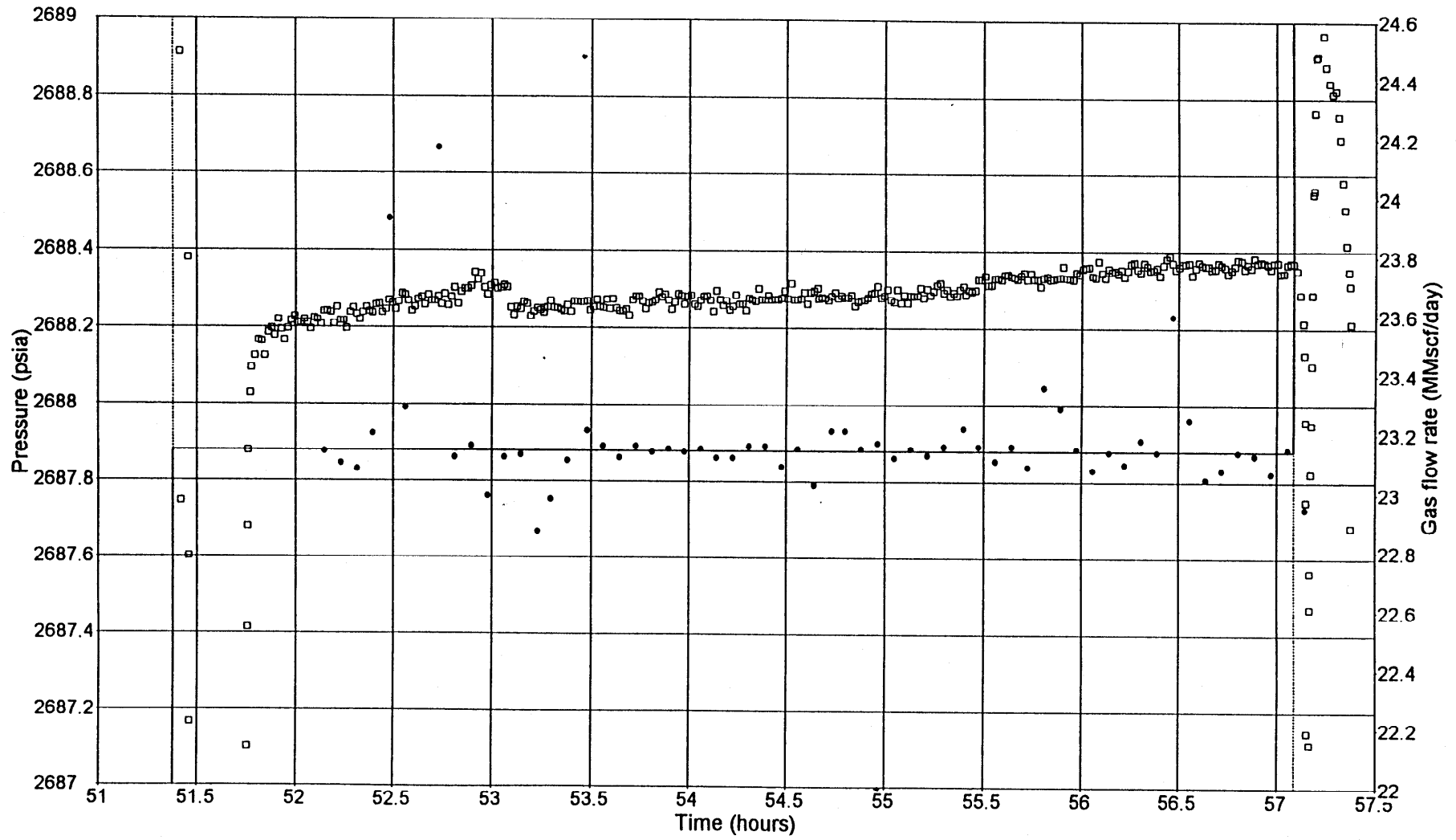
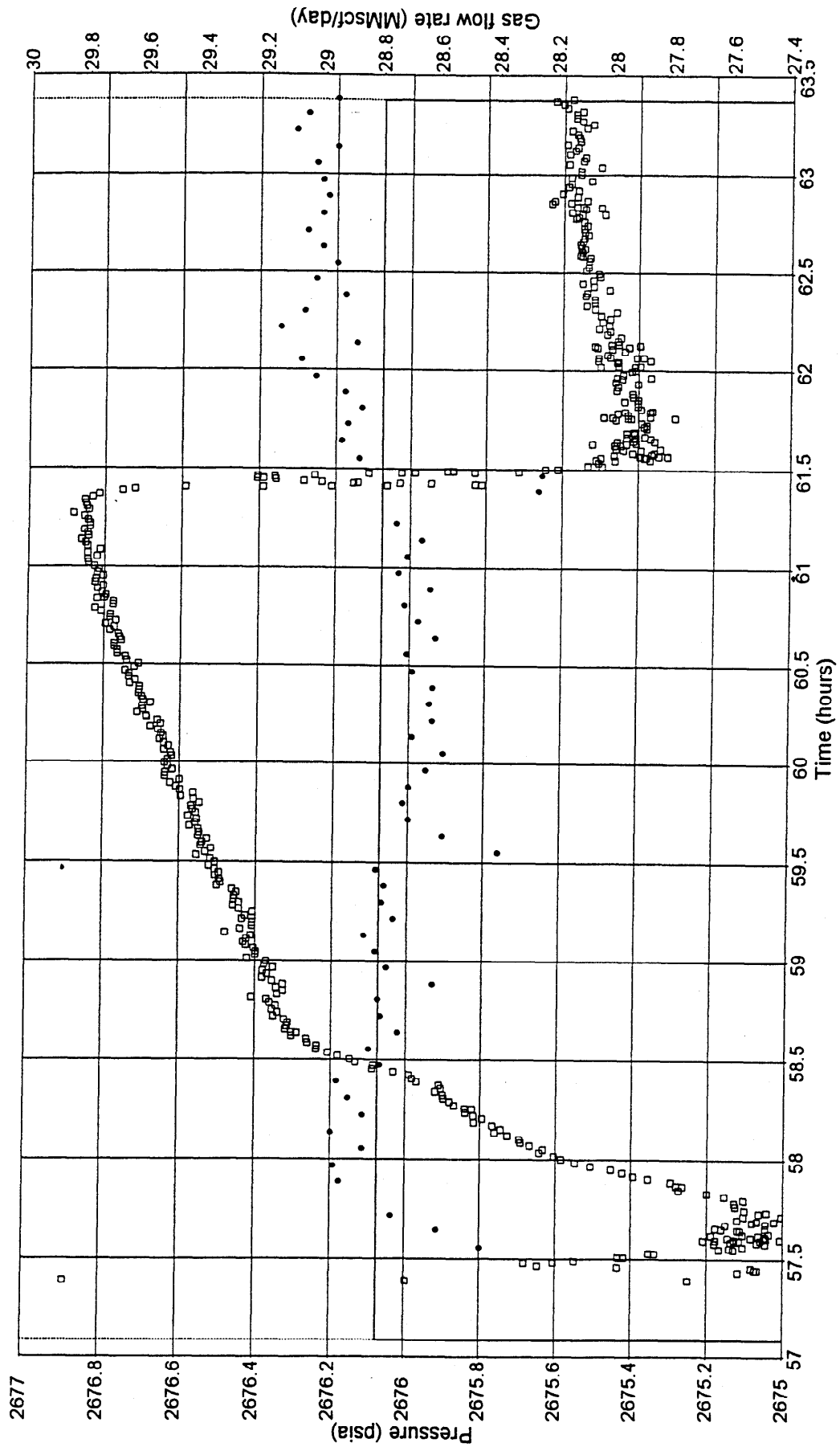


Figure 9 : Flow Period 3 Cartesian Plot

Figure 10 : Flow Period 4 Cartesian Plot



**Table 22 : Flow Period 4 - Surface Data**

<b>Time</b>	<b>WHP (psia)</b>	<b>Rate (MMscf/d)</b>	<b>Elapsed Time (hours)</b>
00:00	1229.13	28.58	2.67
00:05	1229.38	28.69	2.75
00:10	1228.50	28.62	2.83
00:15	1228.25	28.63	2.92
00:20	1227.75	28.62	3.00
00:25	1227.25	28.69	3.08
00:30	1227.63	28.71	3.17
00:40	1226.75	28.61	3.33
00:45	1226.75	28.67	3.42
00:50	1226.38	28.72	3.50
00:55	1226.13	28.63	3.58
01:00	1225.75	28.74	3.67
01:05	1225.75	28.71	3.75
01:10	1225.63	28.66	3.83
01:15	1225.25	28.75	3.92
01:20	1225.13	28.26	4.00
01:25	1209.00	28.25	4.08
01:30	1236.13	28.88	4.17
01:35	1238.50	28.94	4.25
01:40	1239.88	28.92	4.33
01:45	1240.00	28.87	4.42
01:50	1239.88	28.93	4.50
01:55	1240.38	29.03	4.58
02:00	1239.50	29.08	4.67
02:05	1240.13	28.89	4.75
02:10	1240.63	29.15	4.83
02:15	1240.88	29.07	4.92
02:20	1241.50	28.93	5.00
02:25	1241.38	29.03	5.08
02:30	1241.13	28.96	5.17
02:35	1241.50	29.01	5.25
02:40	1242.13	29.06	5.33
02:45	1241.50	29.01	5.42
02:50	1240.88	28.99	5.50
02:55	1242.13	29.01	5.58
03:00	1241.50	29.03	5.67
03:05	1241.38	28.96	5.75
03:10	1241.88	29.10	5.83
03:15	1242.63	29.06	5.92
03:20	1243.38	28.96	6.00

Figure 11 : Flow Period 4 - Surface Data

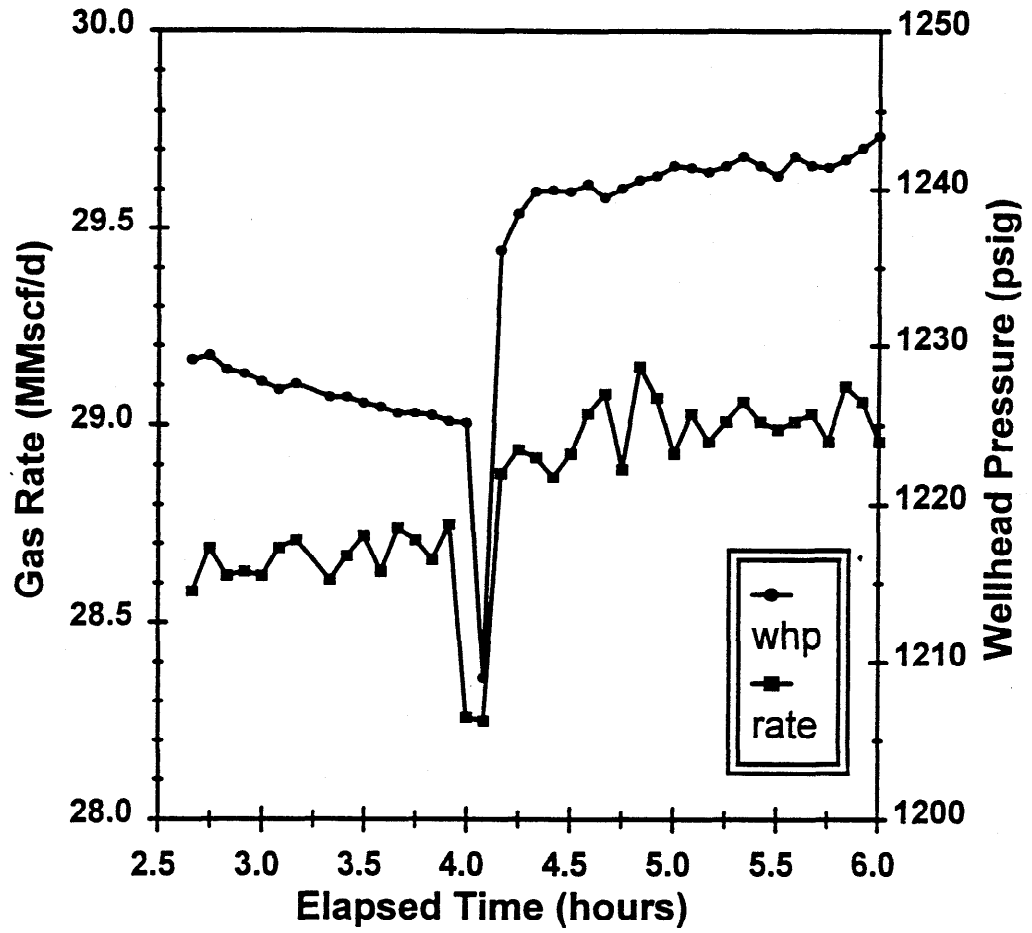
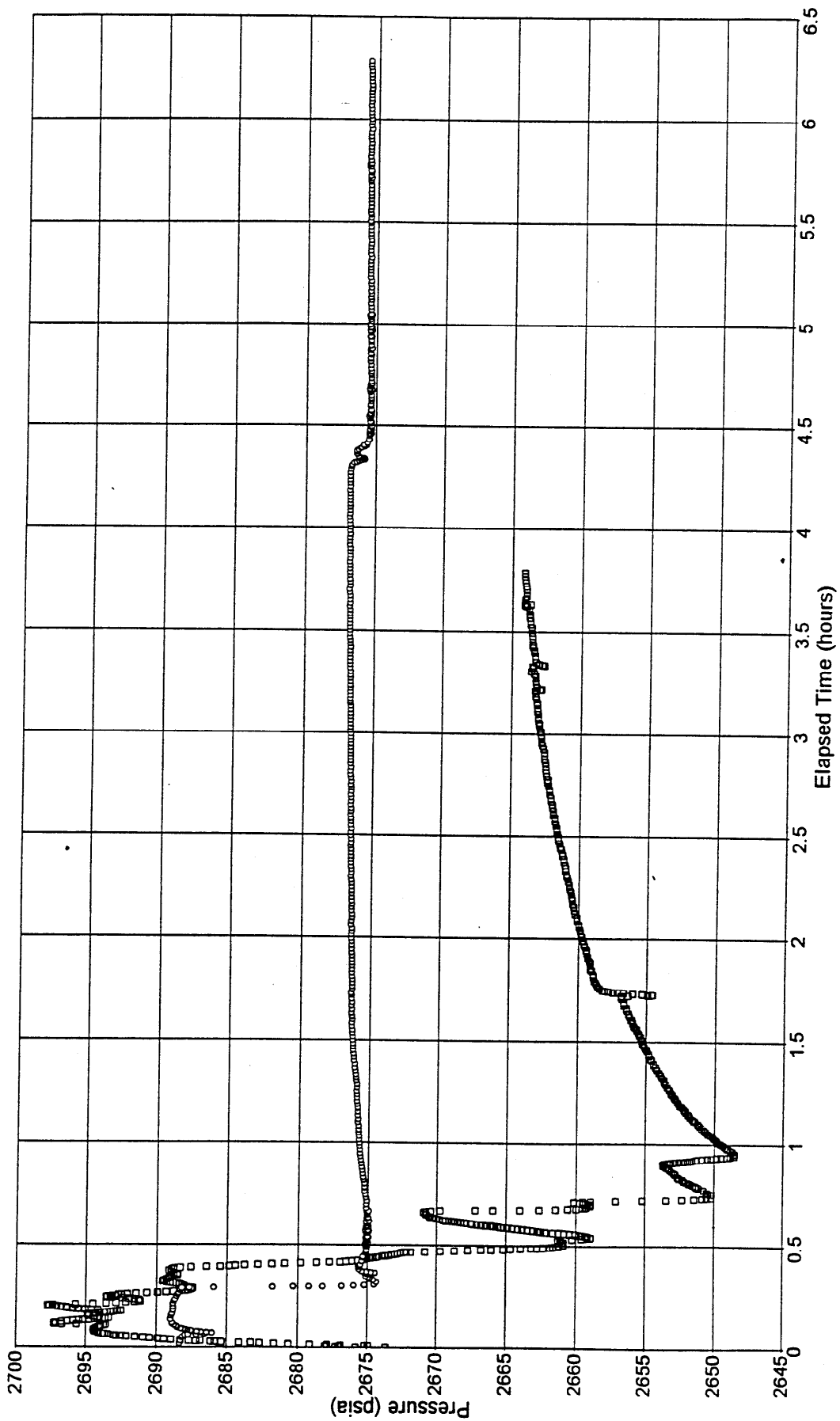


Figure 12 : Clean-up Flow and Flow Period 4 Comparison



---

**APPENDIX 5 - GAUGE SELECTION**

Figure 13 : Gauge 10883 Pressure Response

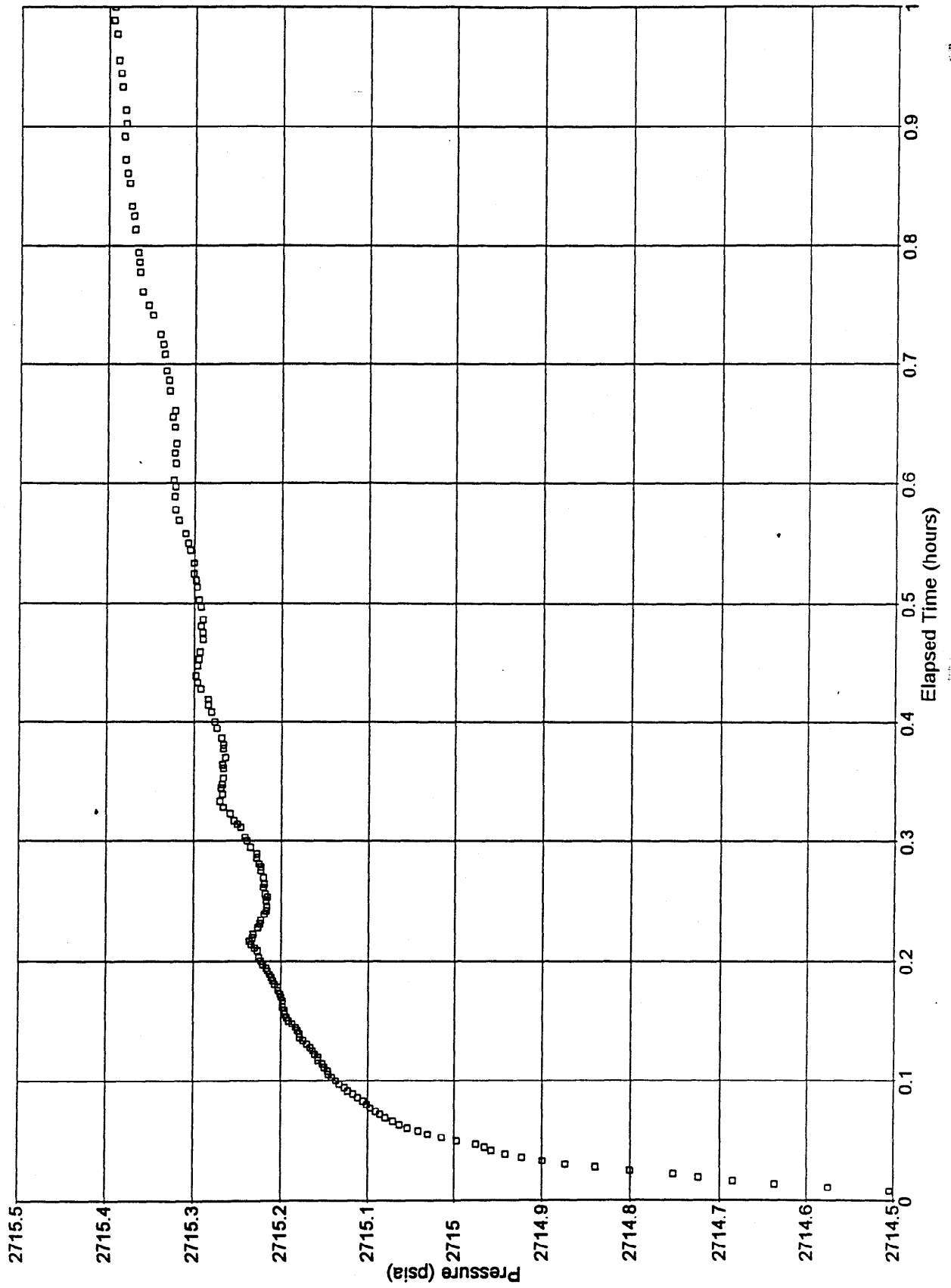


Figure 14 : Gauge 10882 Pressure Response

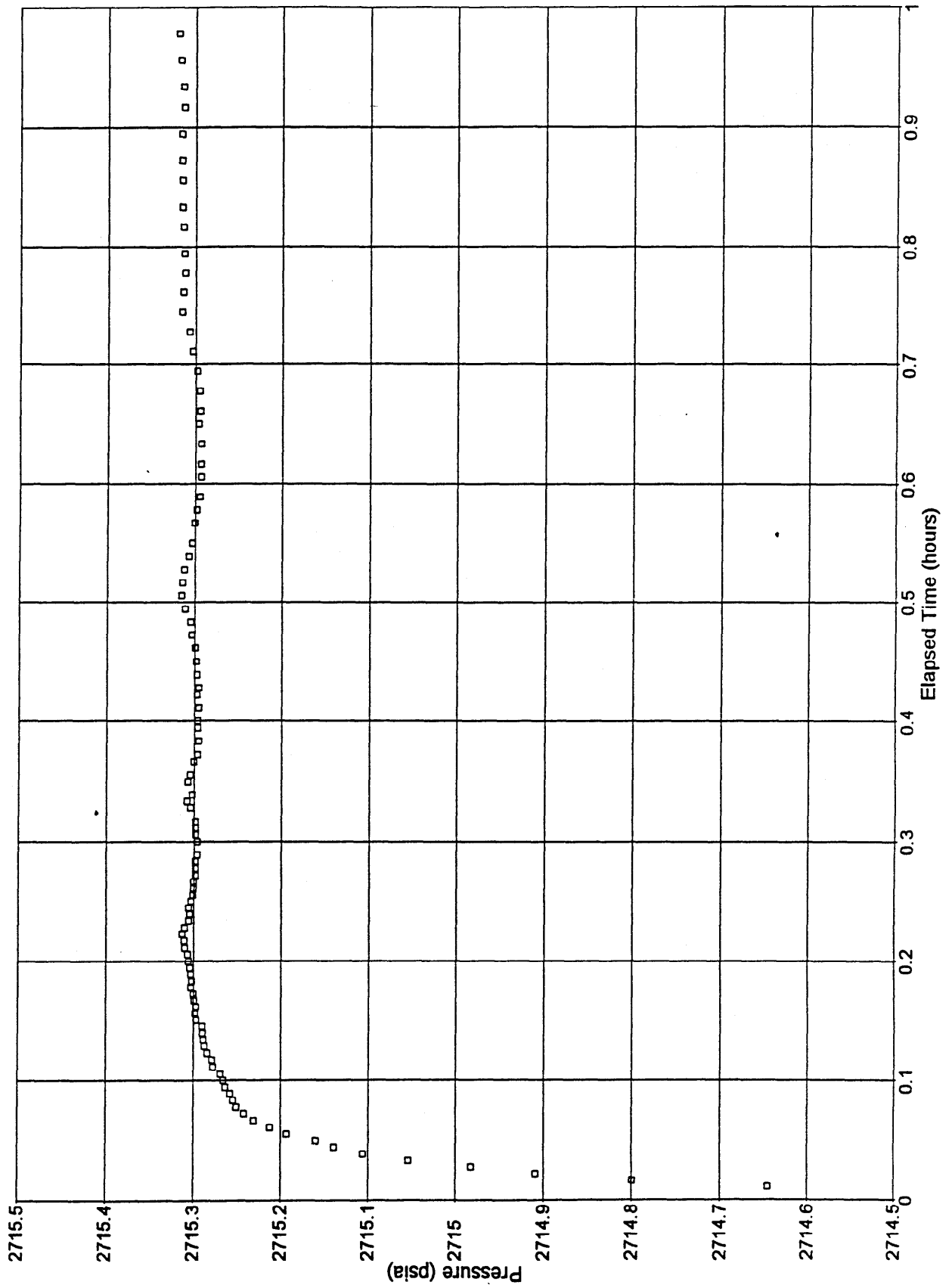




Figure 15 : Gauge 011 Pressure Response

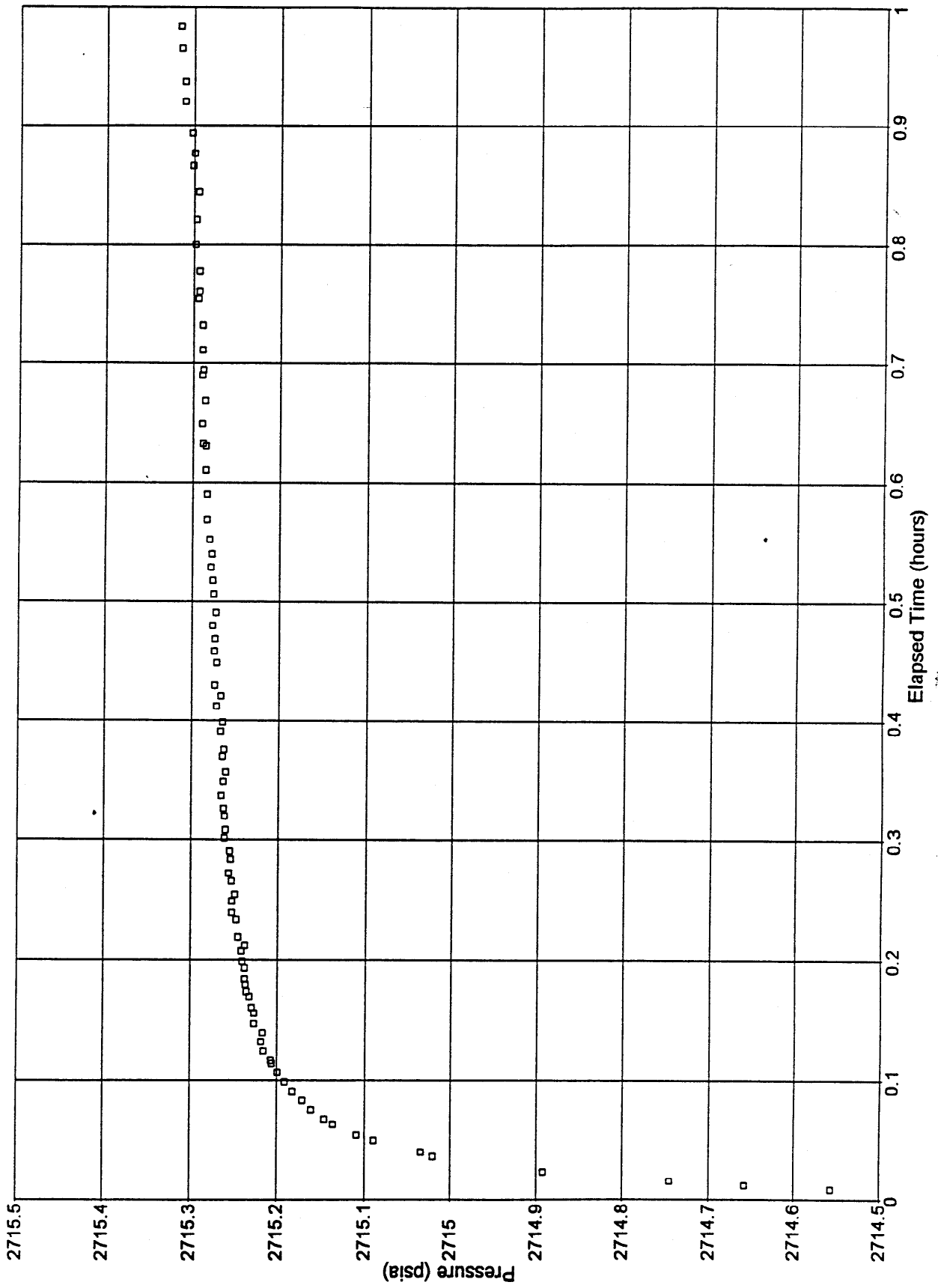


Figure 16 : Gauge 10065 Pressure Response

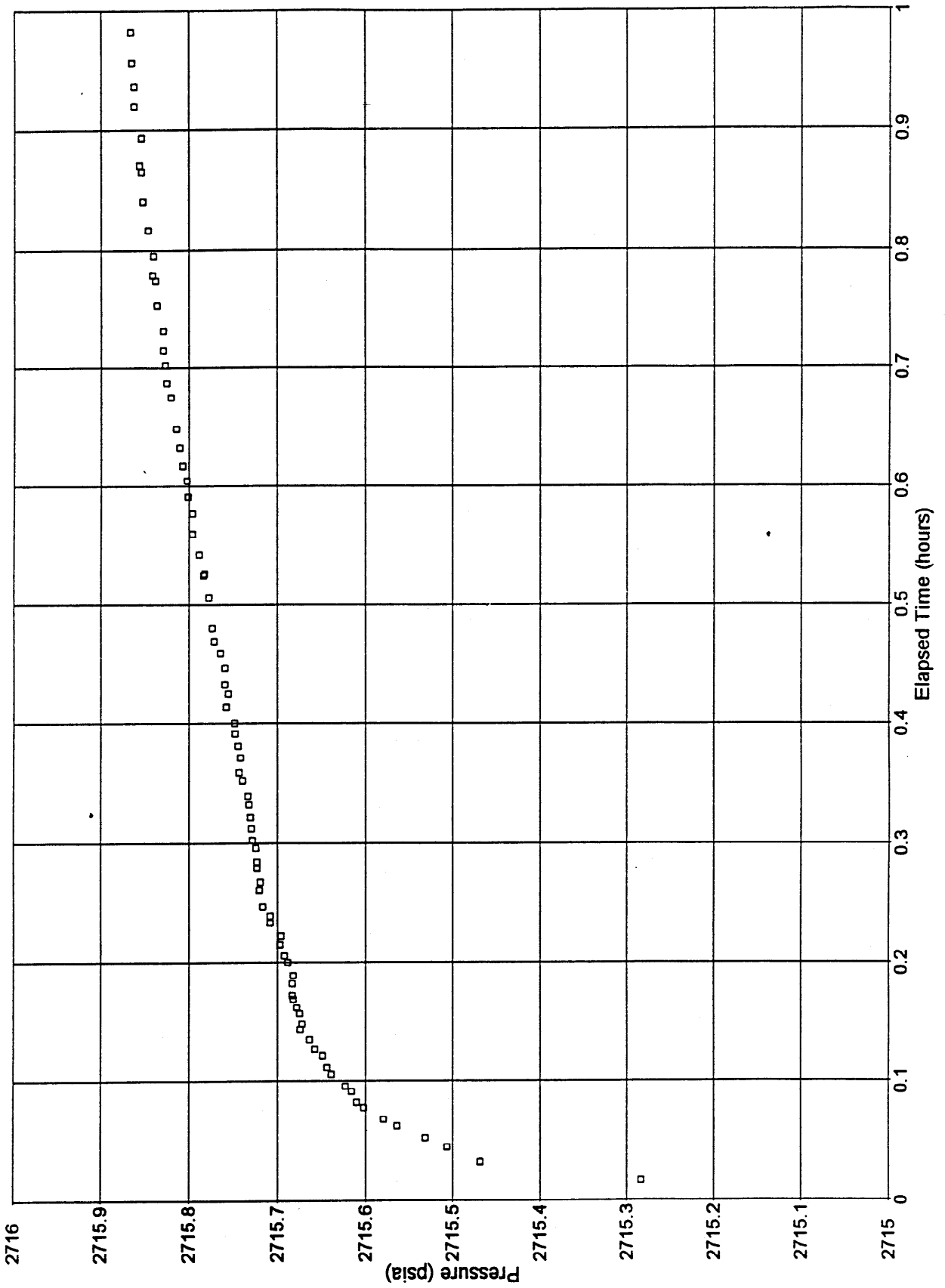


Figure 17 : Gauge 10065 Log-Log Plot

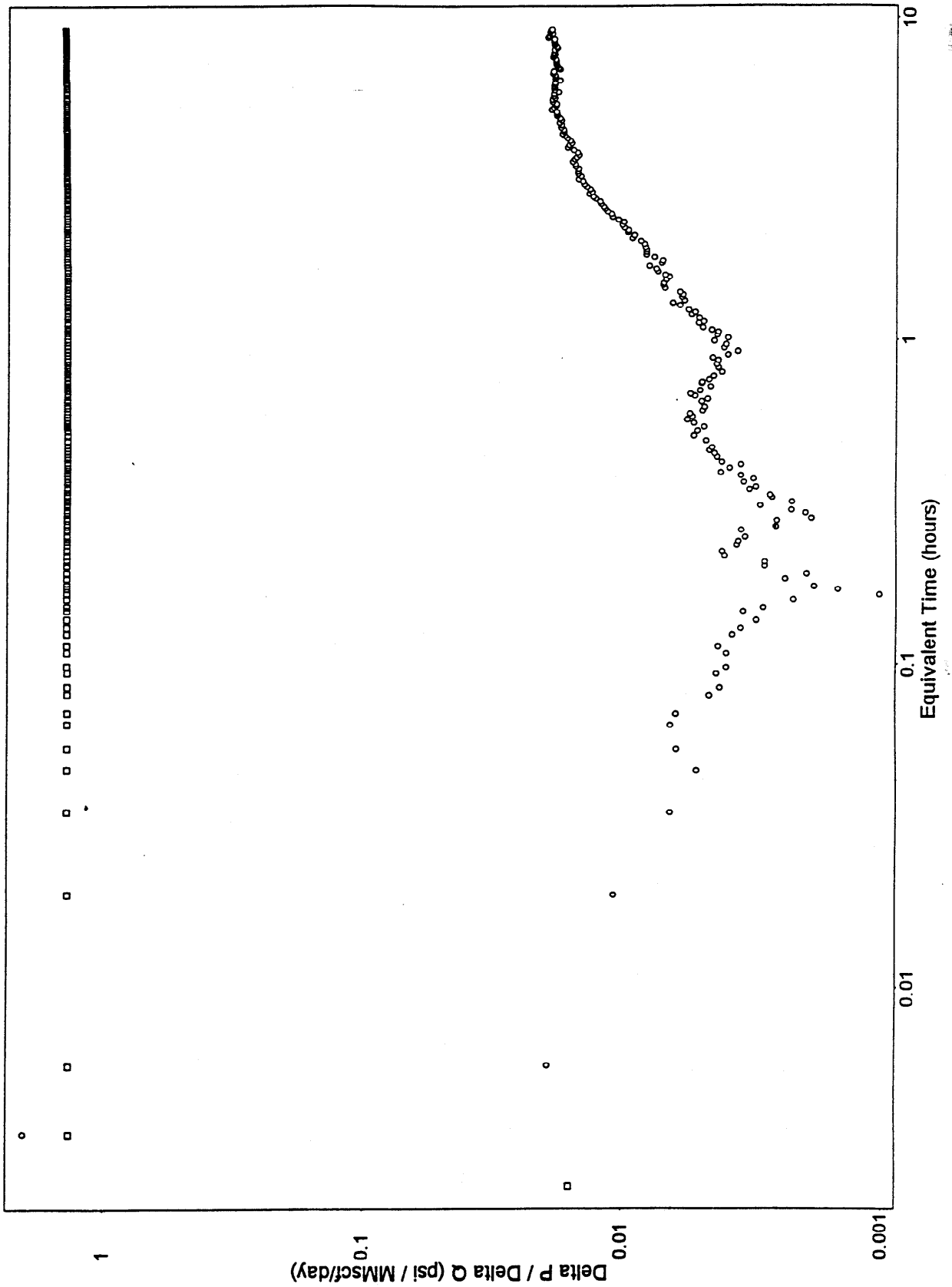
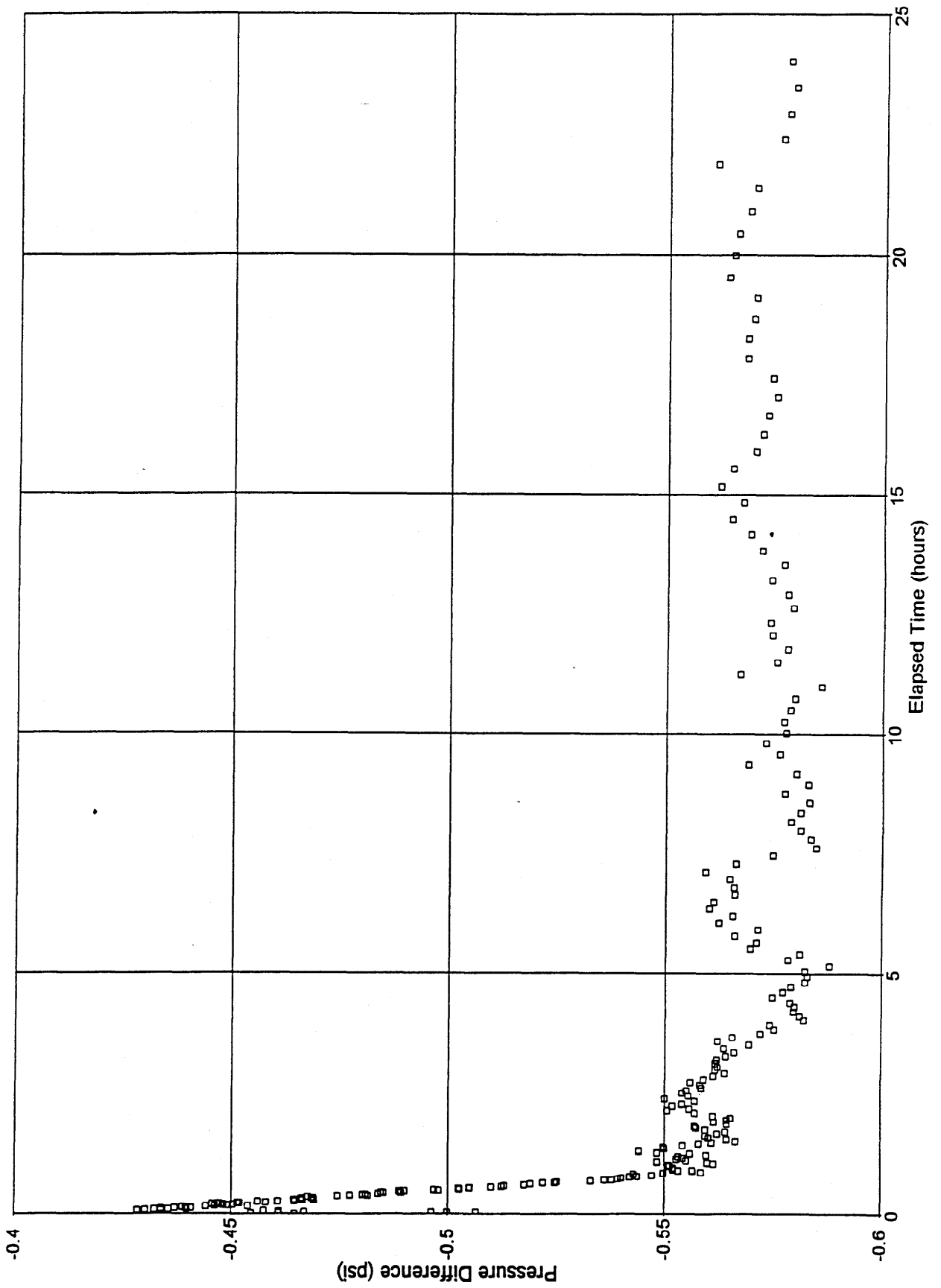
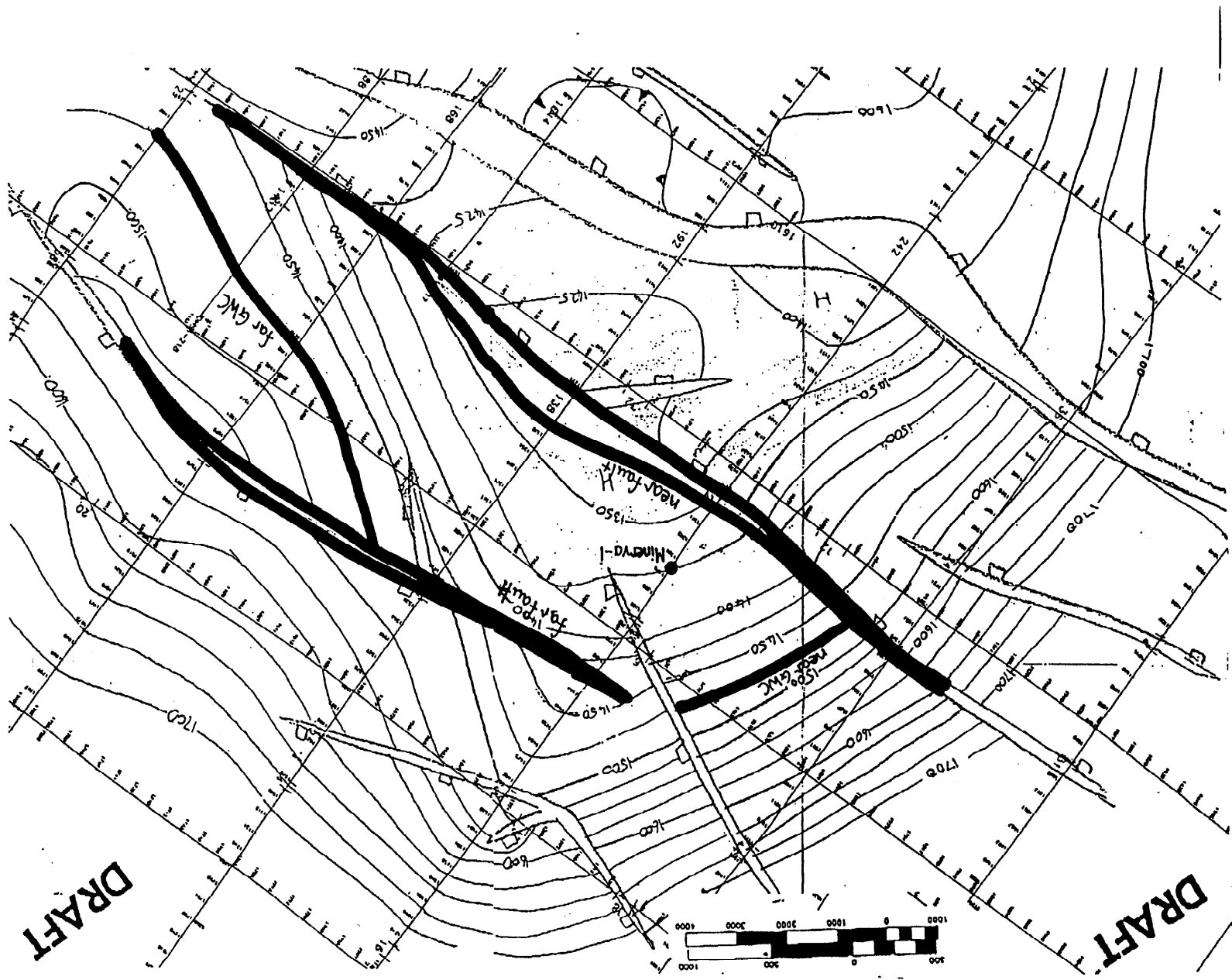


Figure 18 : Gauge 011 and 10065 Comparison



**APPENDIX 6 - STRUCTURE MAP**

**Figure 19 : Top Structure - Top Lower Shipwreck**



---

**APPENDIX 7 - WELL TEST PLOTS**

Figure 20 : Dual Porosity - Entire Interval Diagnostic Plot

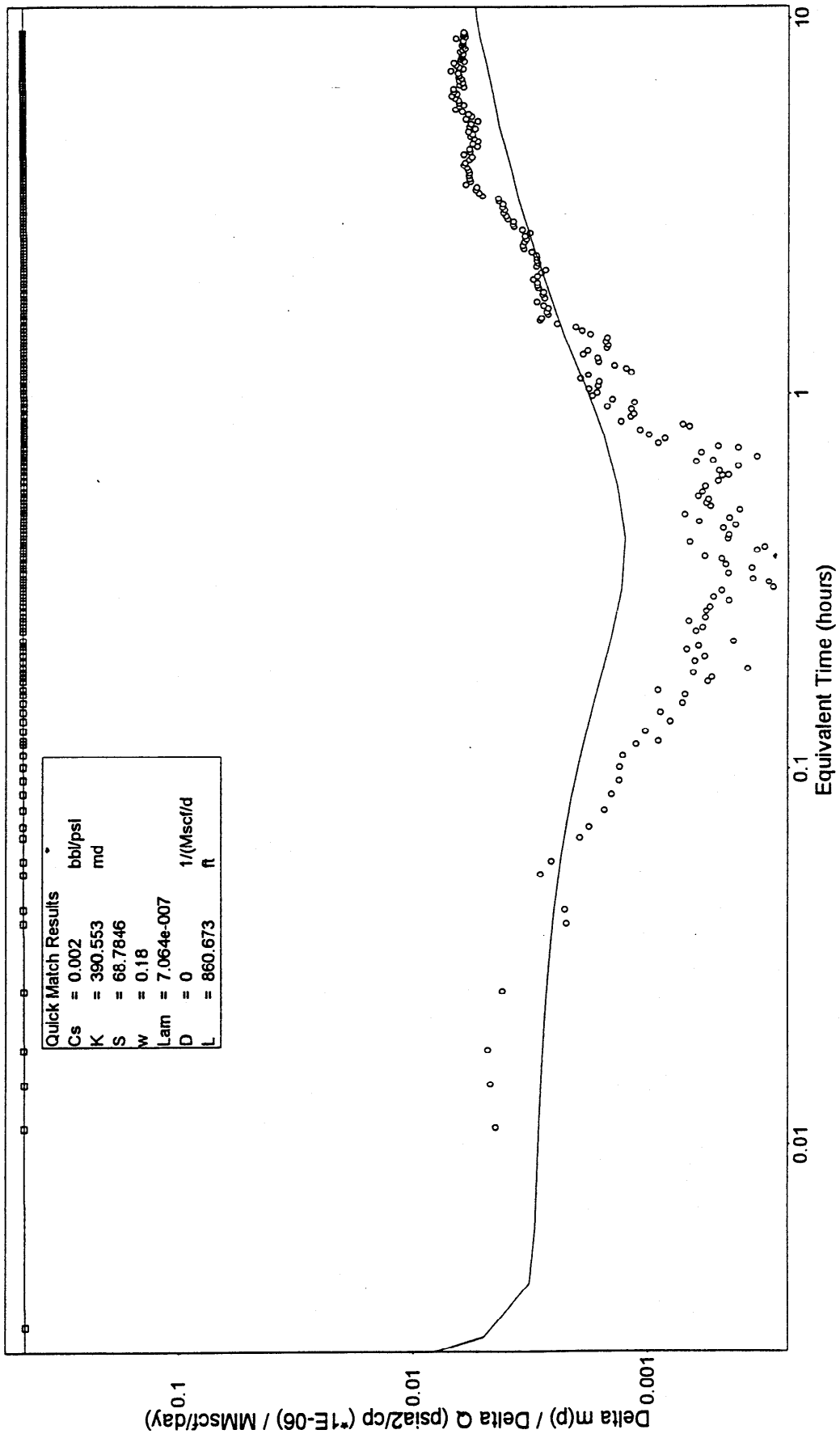


Figure 21 : Dual Porosity - Entire Interval Horner Plot

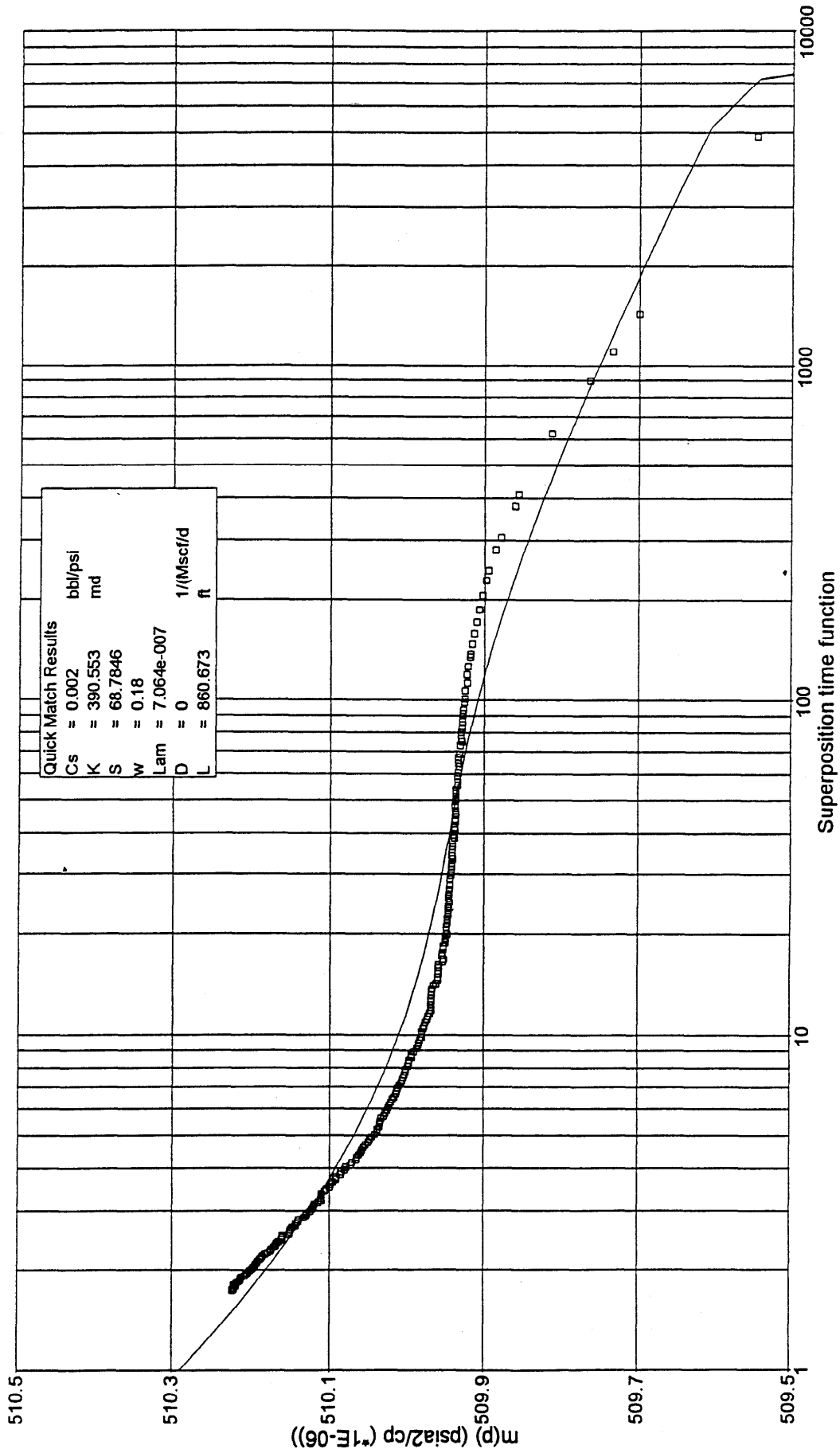




Figure 22 : Dual Porosity - Perforated Interval Diagnostic Plot

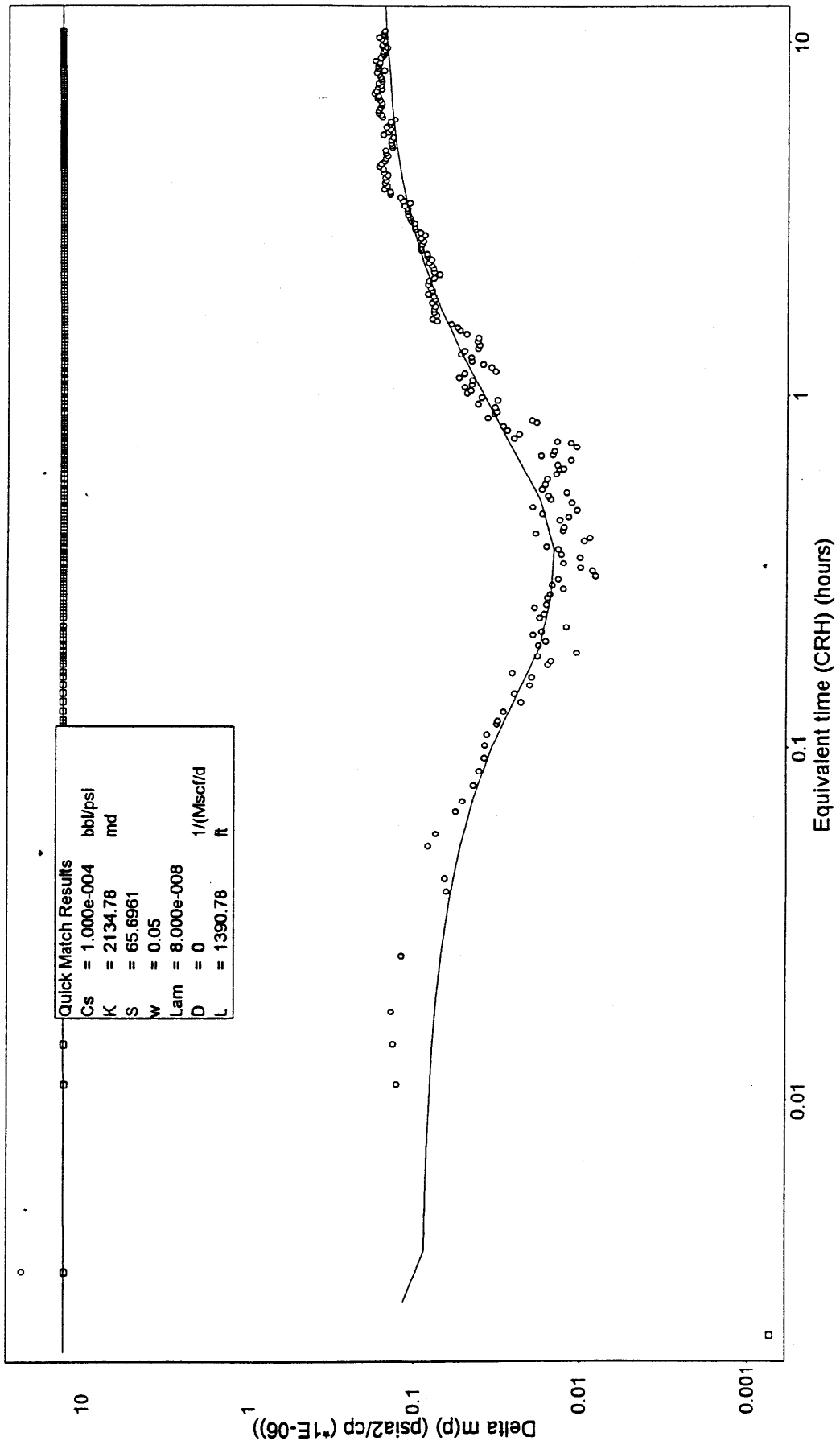


Figure 23 : Dual Porosity - Perforated Interval Horner Plot

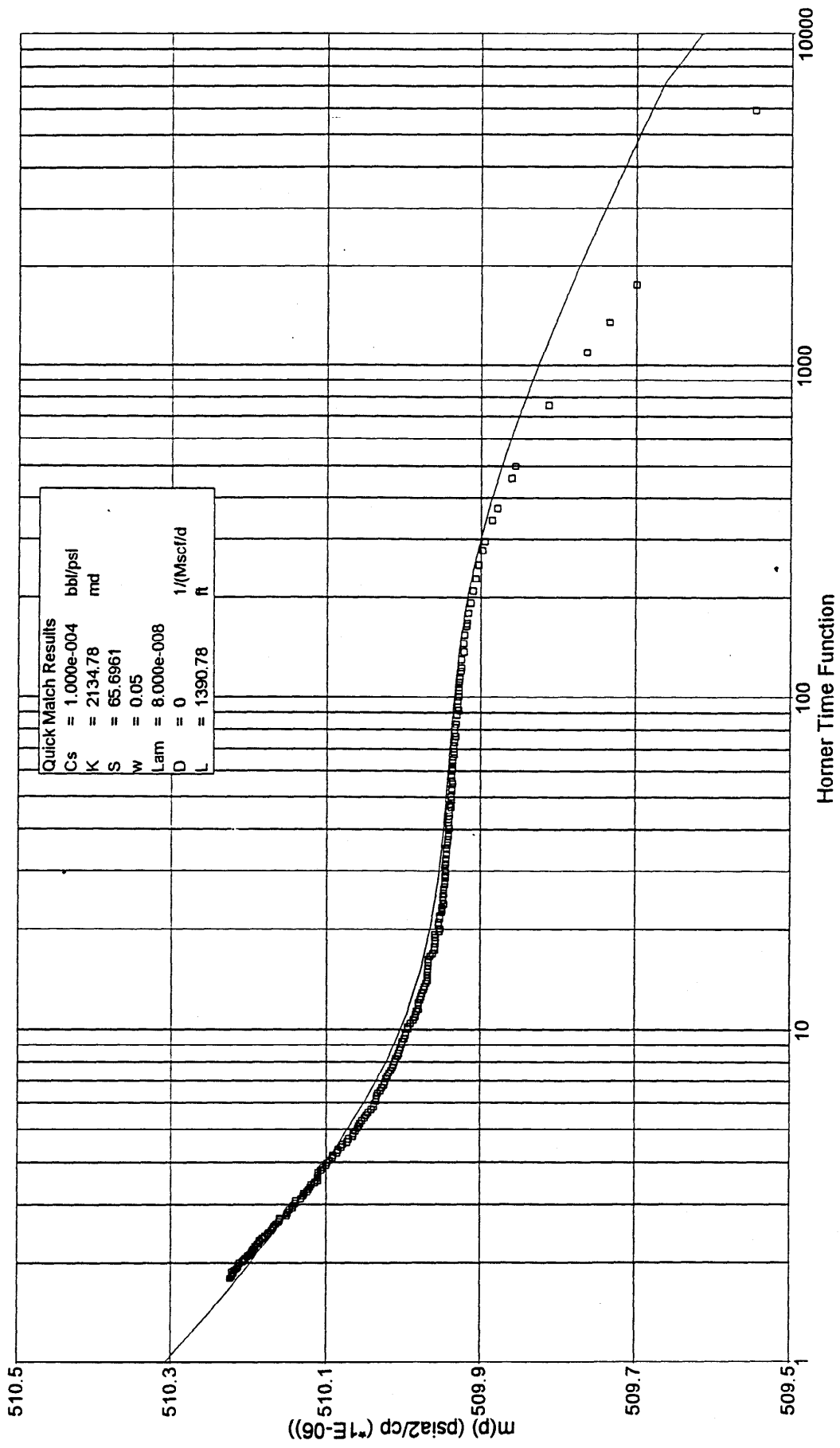


Figure 24 : Dual Permeability  $\kappa = 0.2$  - Perforated Interval Diagnostic Plot

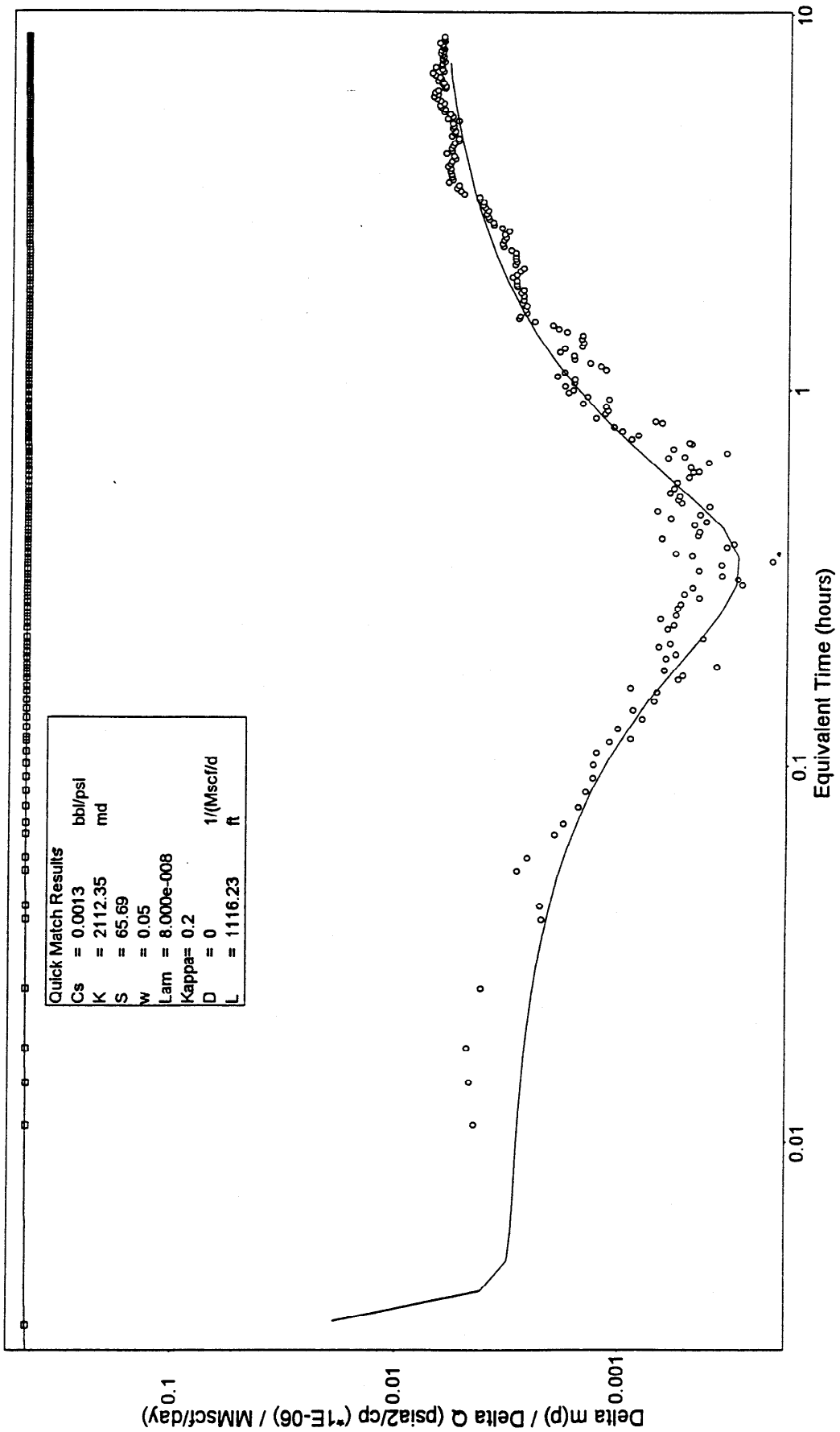


Figure 25 : Dual Permeability  $\kappa = 0.2$ - Perforated Interval Horner Plot

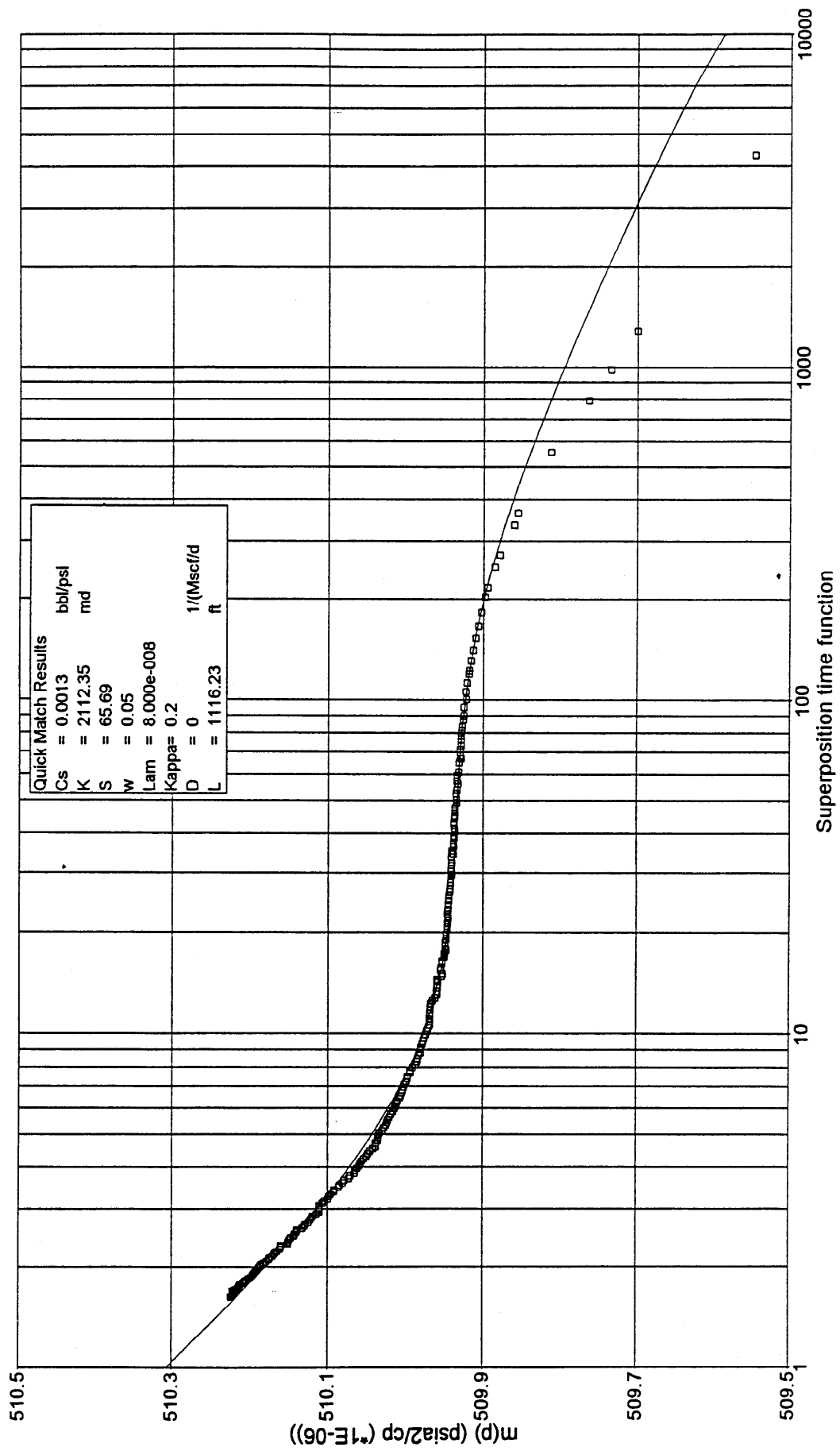


Figure 26 : Dual Permeability  $\kappa = 0.3$  - Perforated Interval Diagnostic Plot

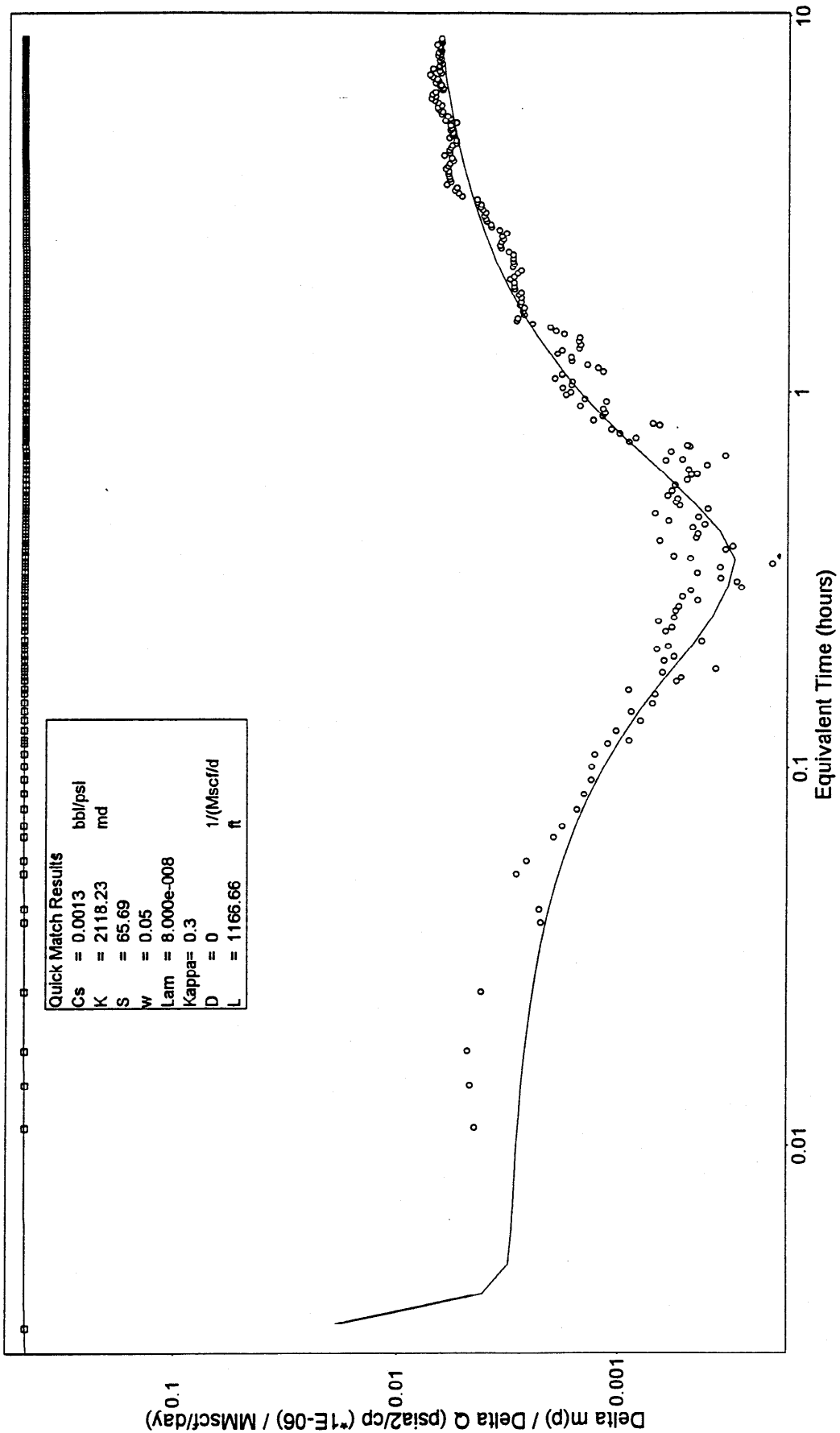


Figure 27 : Dual Permeability  $\kappa = 0.3$  - Perforated Interval Horner Plot

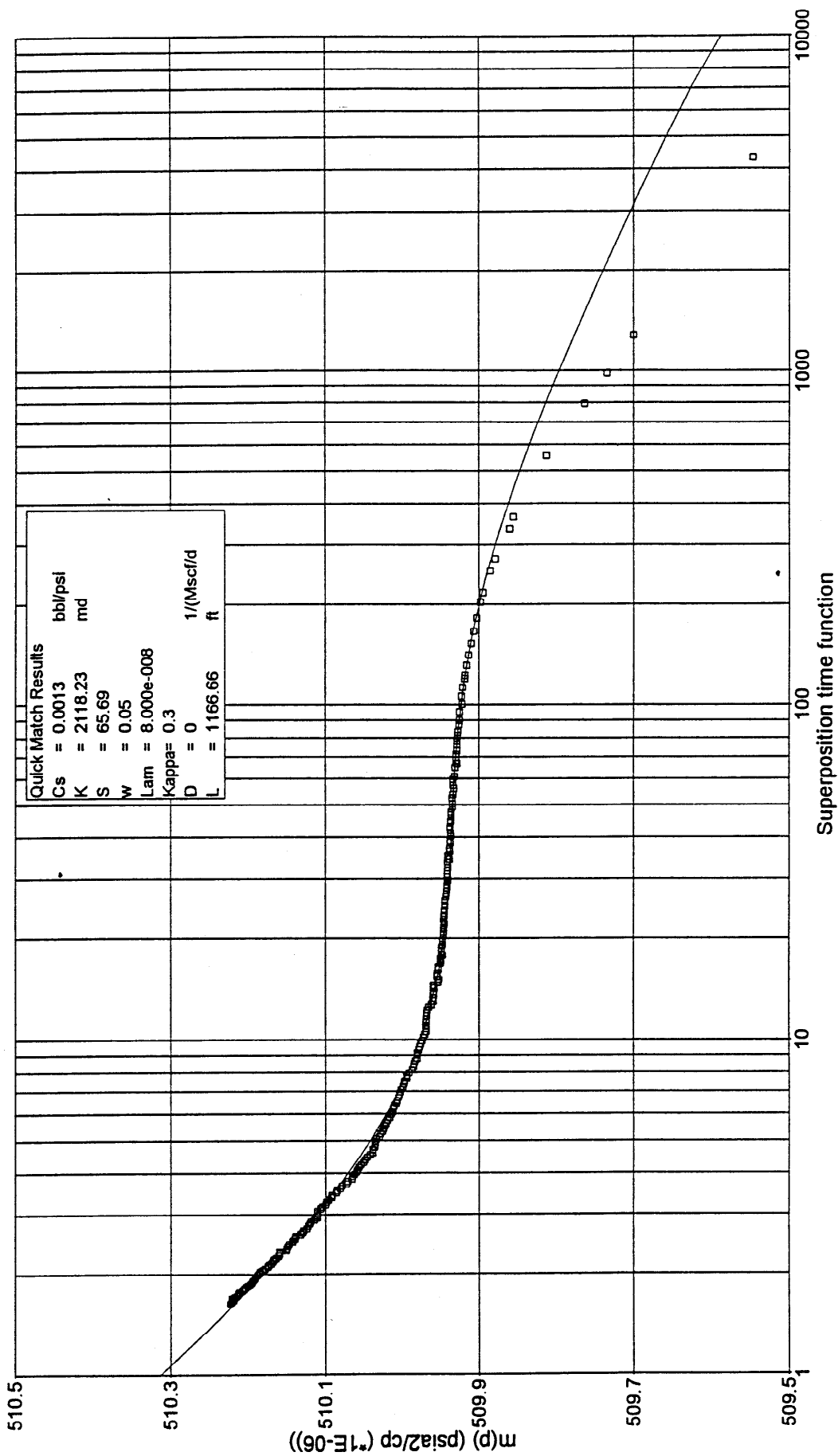


Figure 28 : Dual Permeability  $\kappa = 0.4$  - Perforated Interval Diagnostic Plot

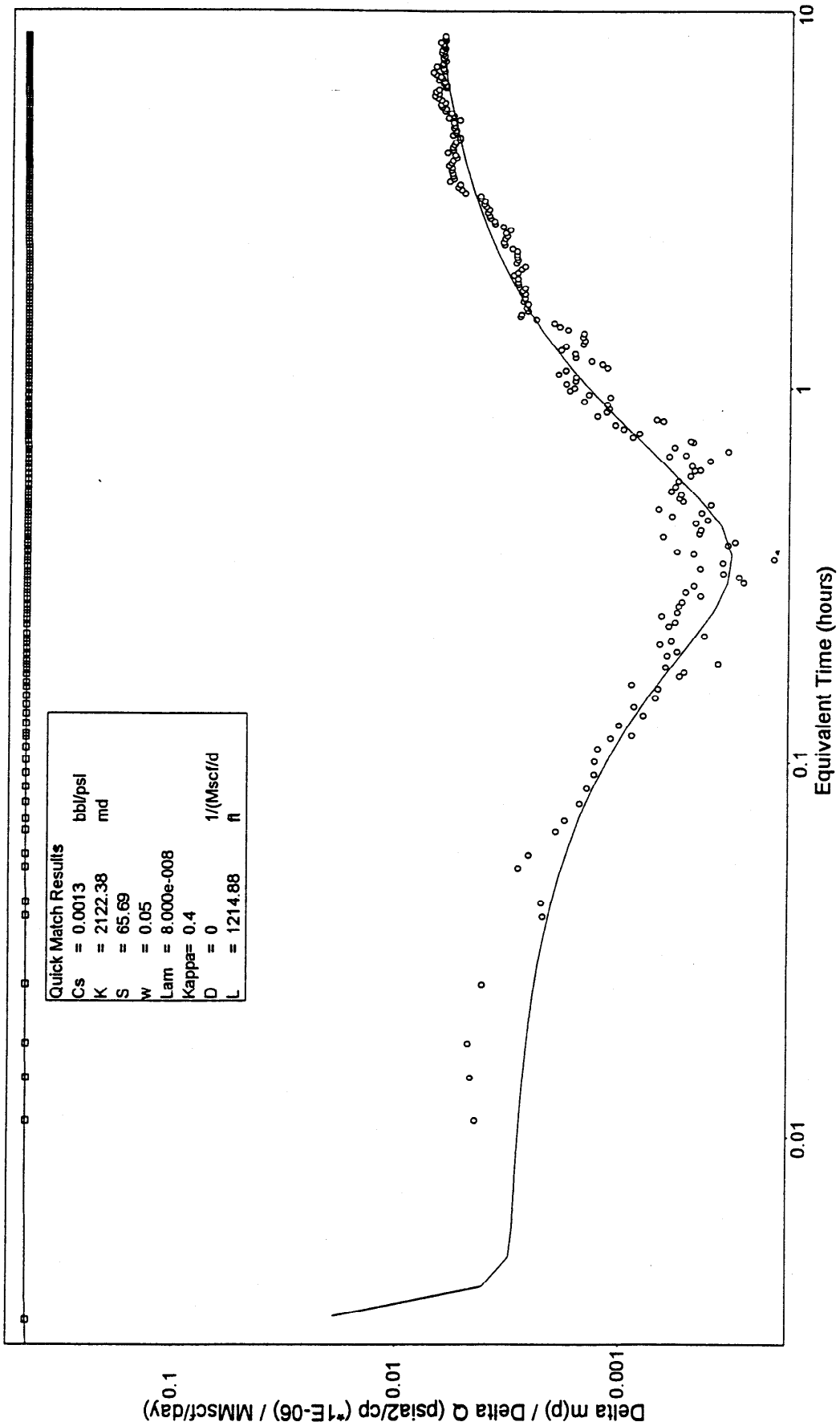


Figure 29 : Dual Permeability  $\kappa = 0.4$  - Perforated Interval Horner Plot

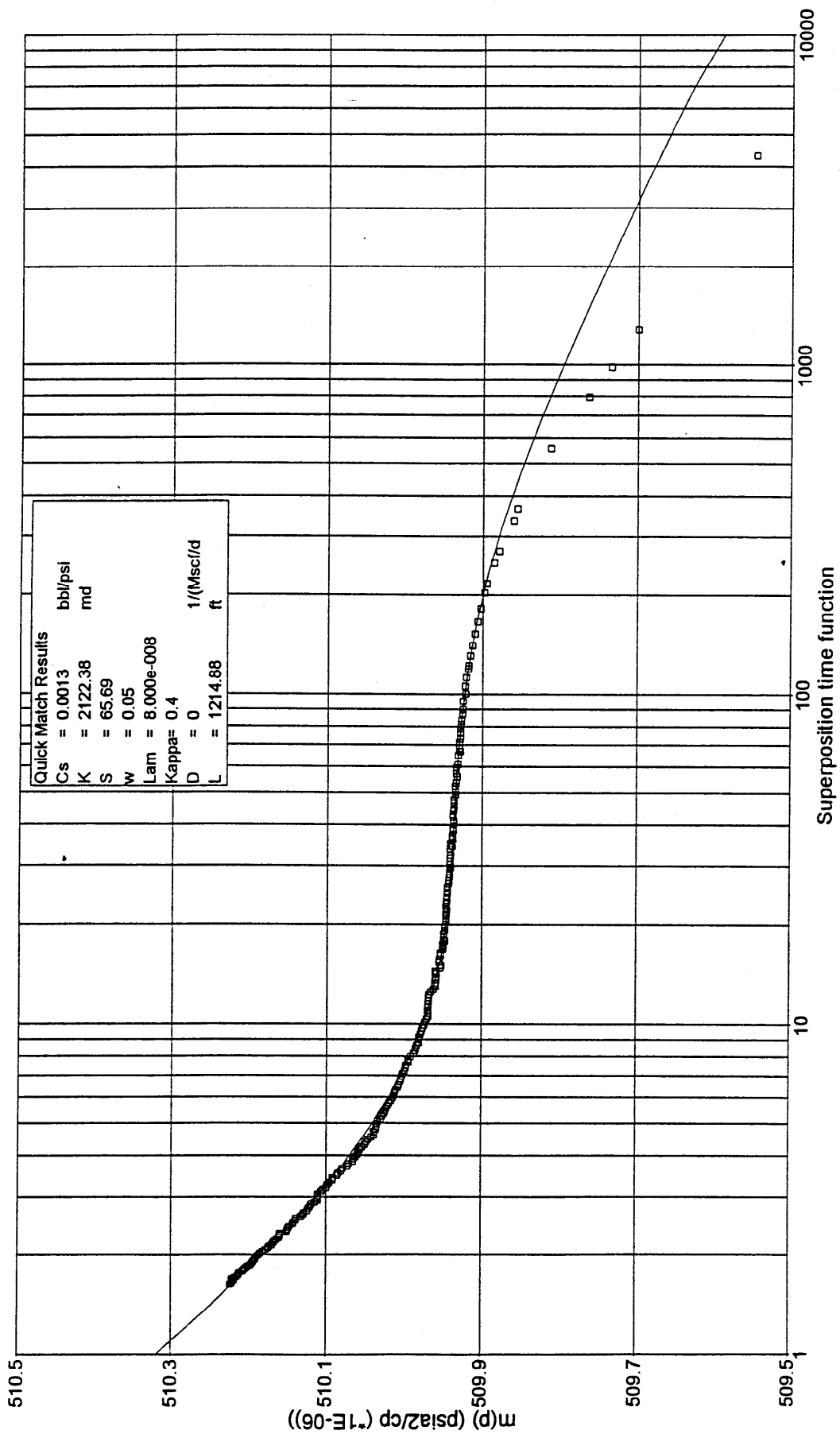




Figure 30 : Dual Permeability  $\kappa = 0.5$  - Perforated Interval Diagnostic Plot

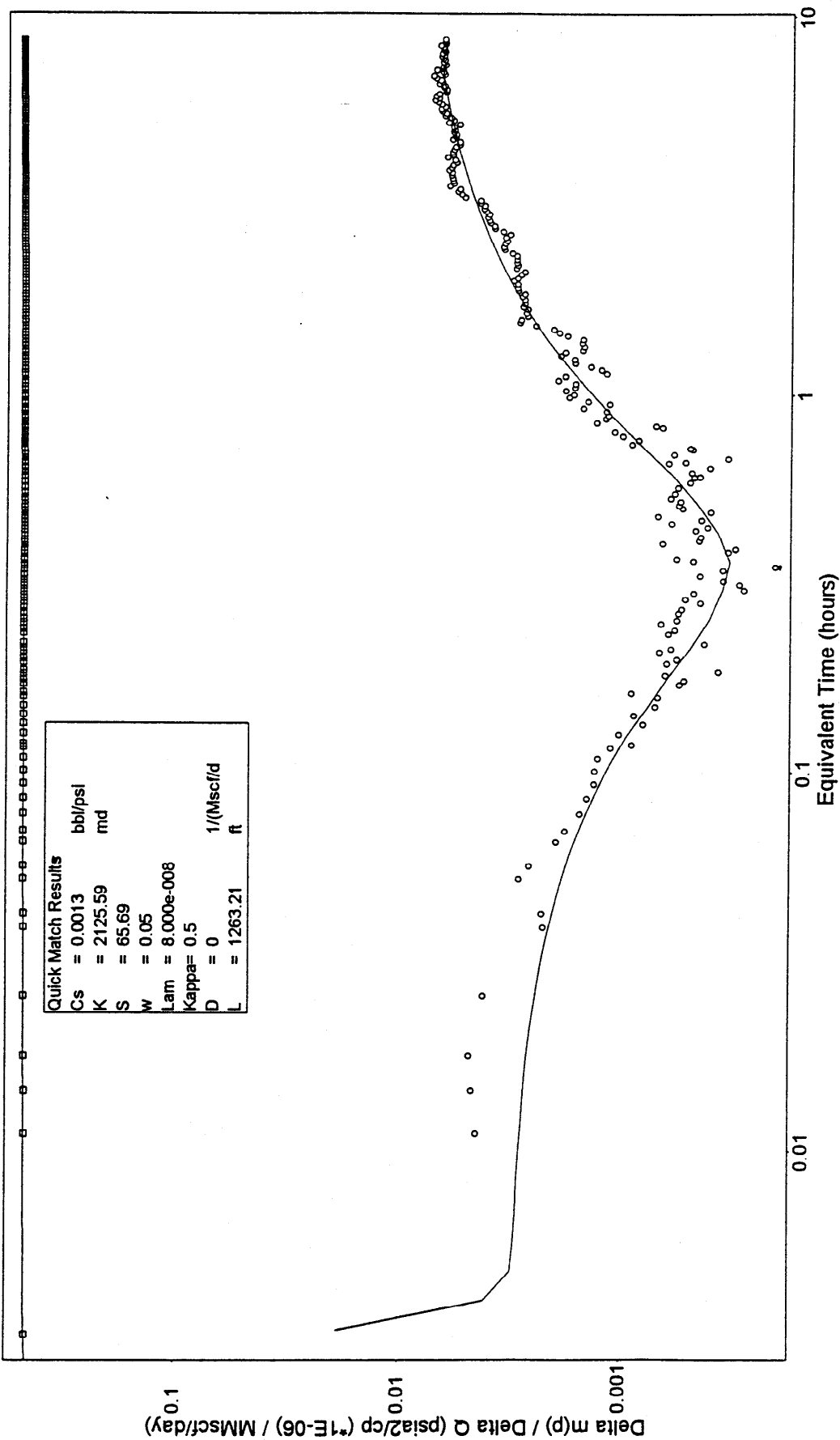


Figure 31 : Dual Permeability  $\kappa = 0.5$  - Perforated Interval Horner Plot

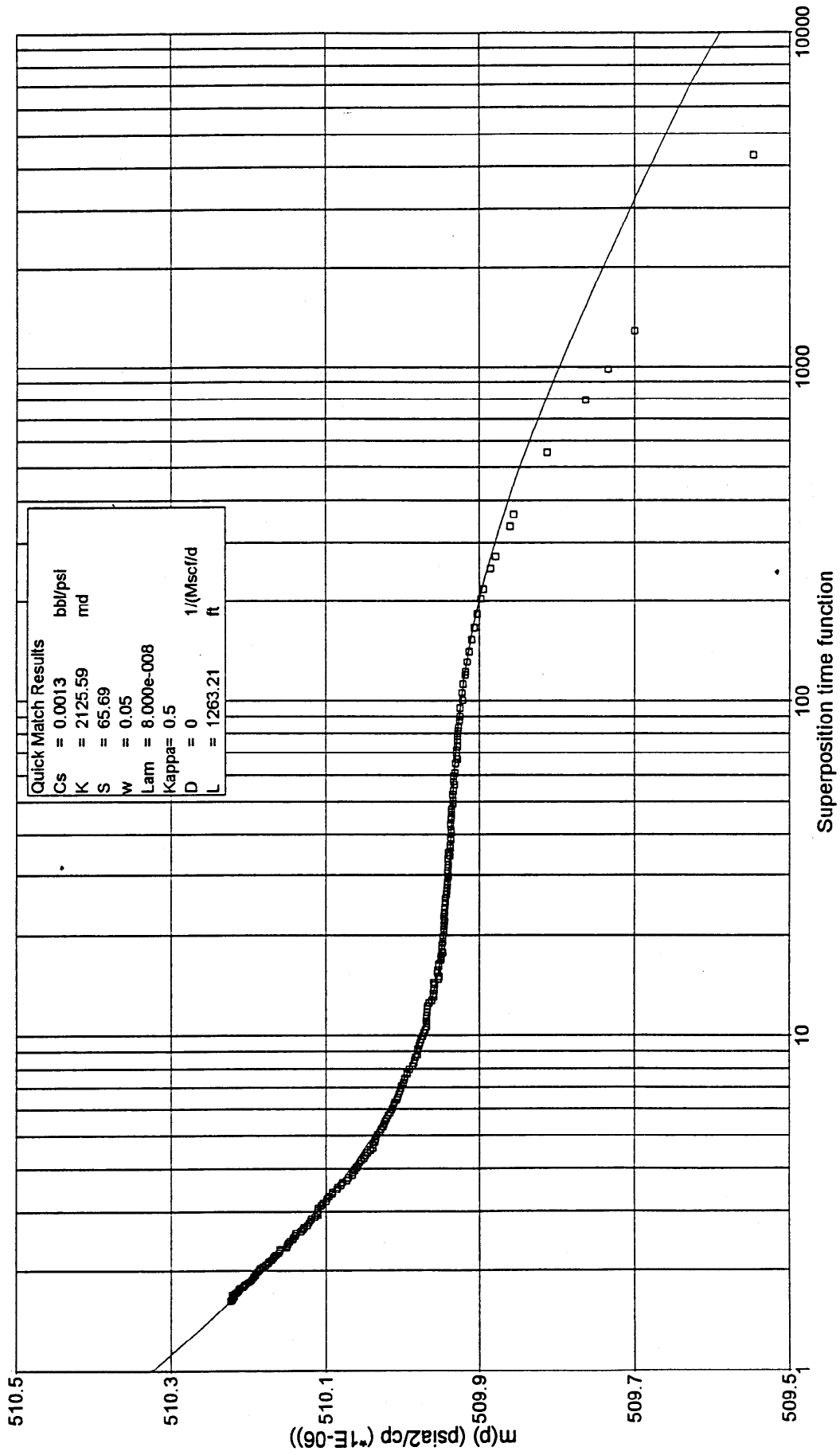


Figure 32 : Dual Permeability - 80% L Diagnostic Plot

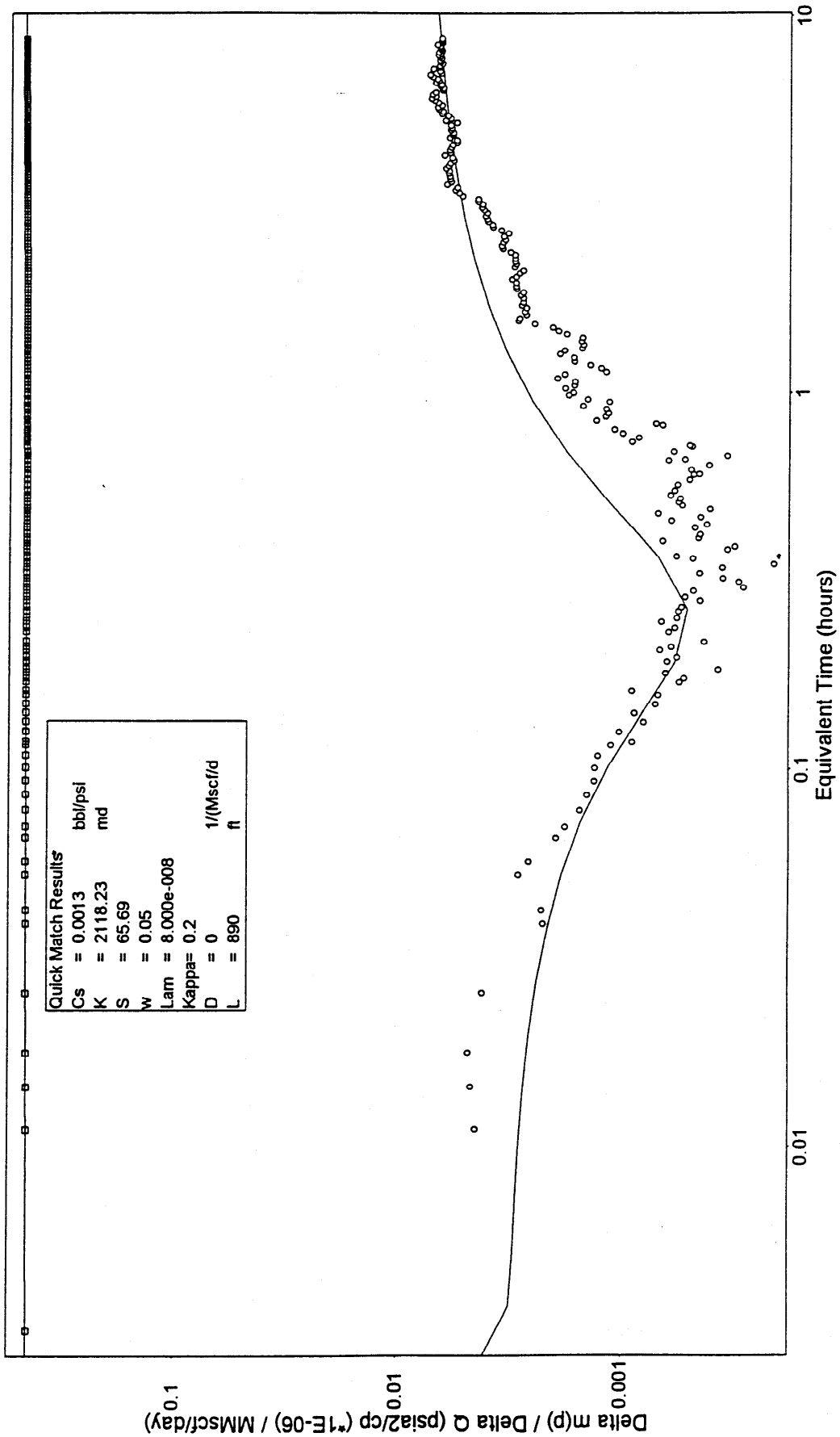


Figure 33 : Dual Permeability - 80% L Horner Plot

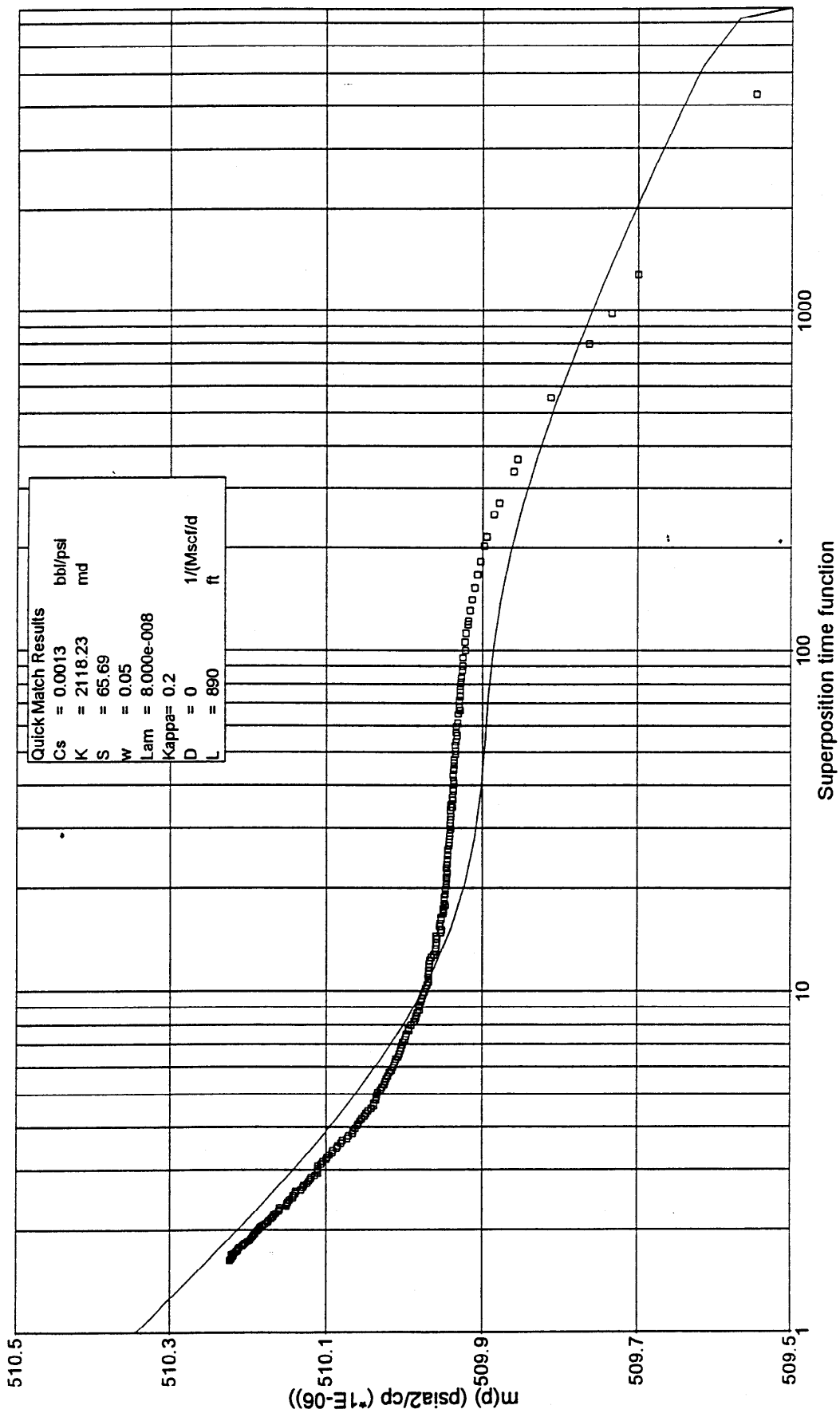


Figure 34 : Dual Permeability - 120% L Diagnostic Plot

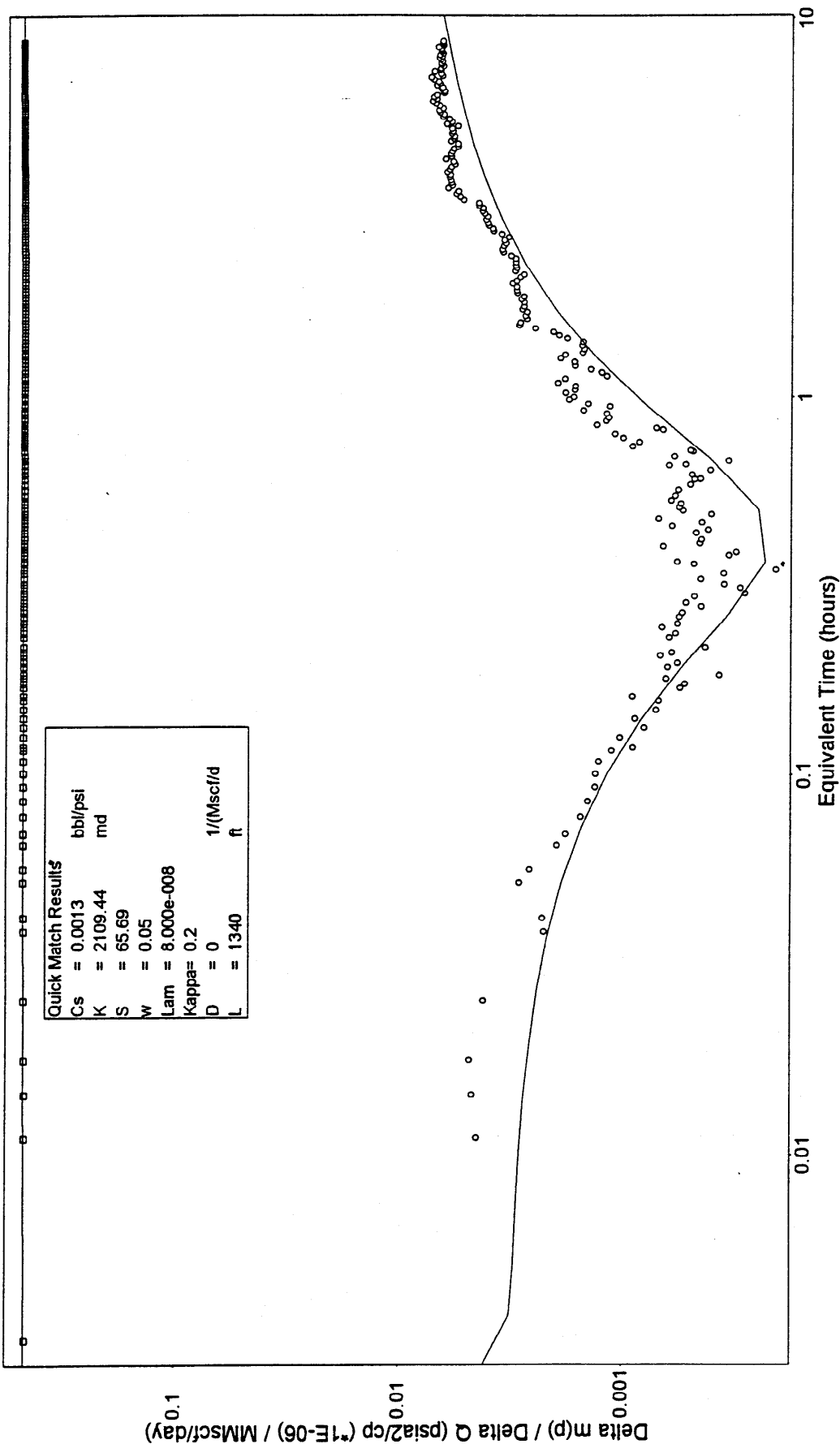
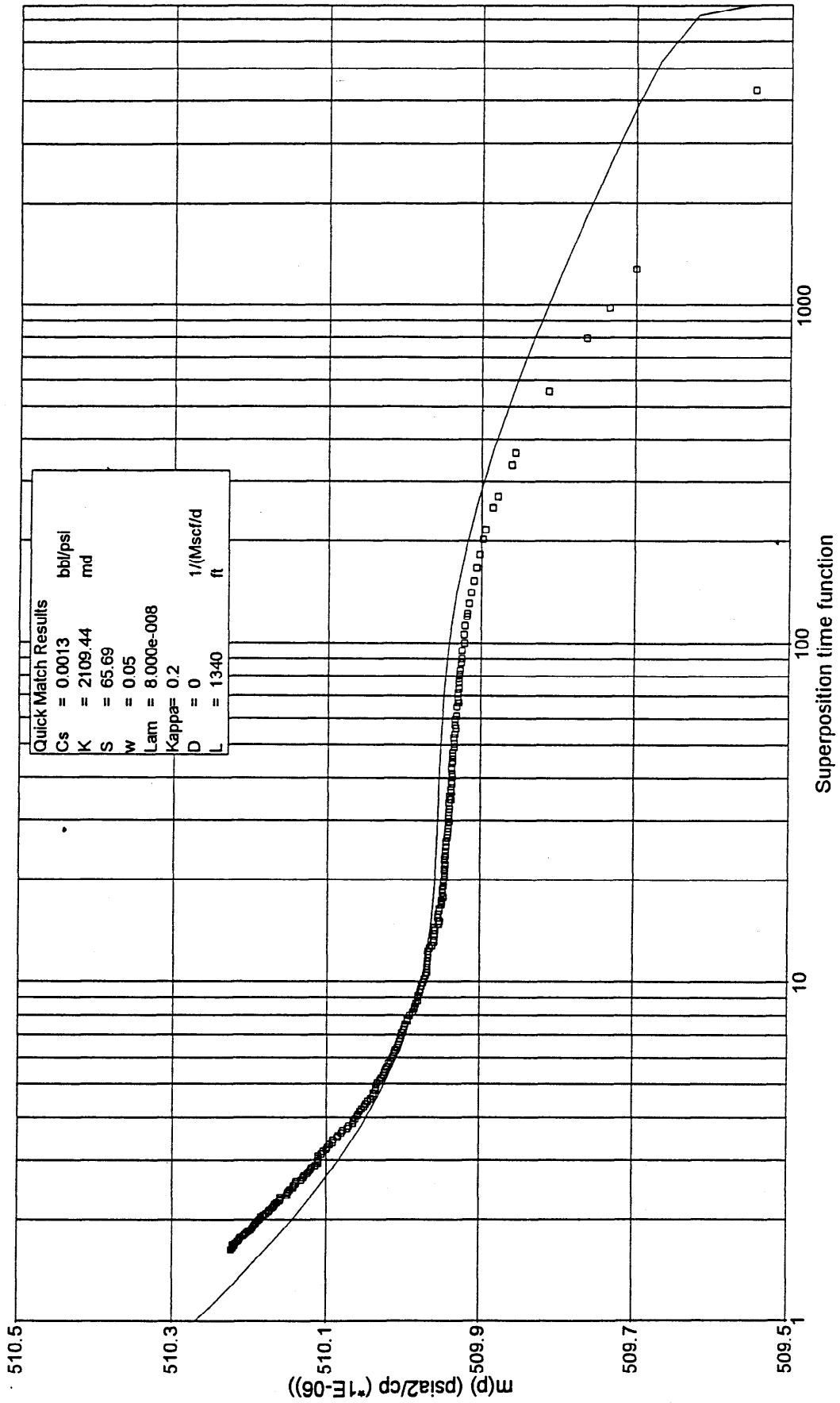


Figure 35 : Dual Permeability - 120% L Horner Plot



---

## APPENDIX 8 - BOUNDARIES

Figure 36 : Dual Permeability - No Boundary Diagnostic Plot

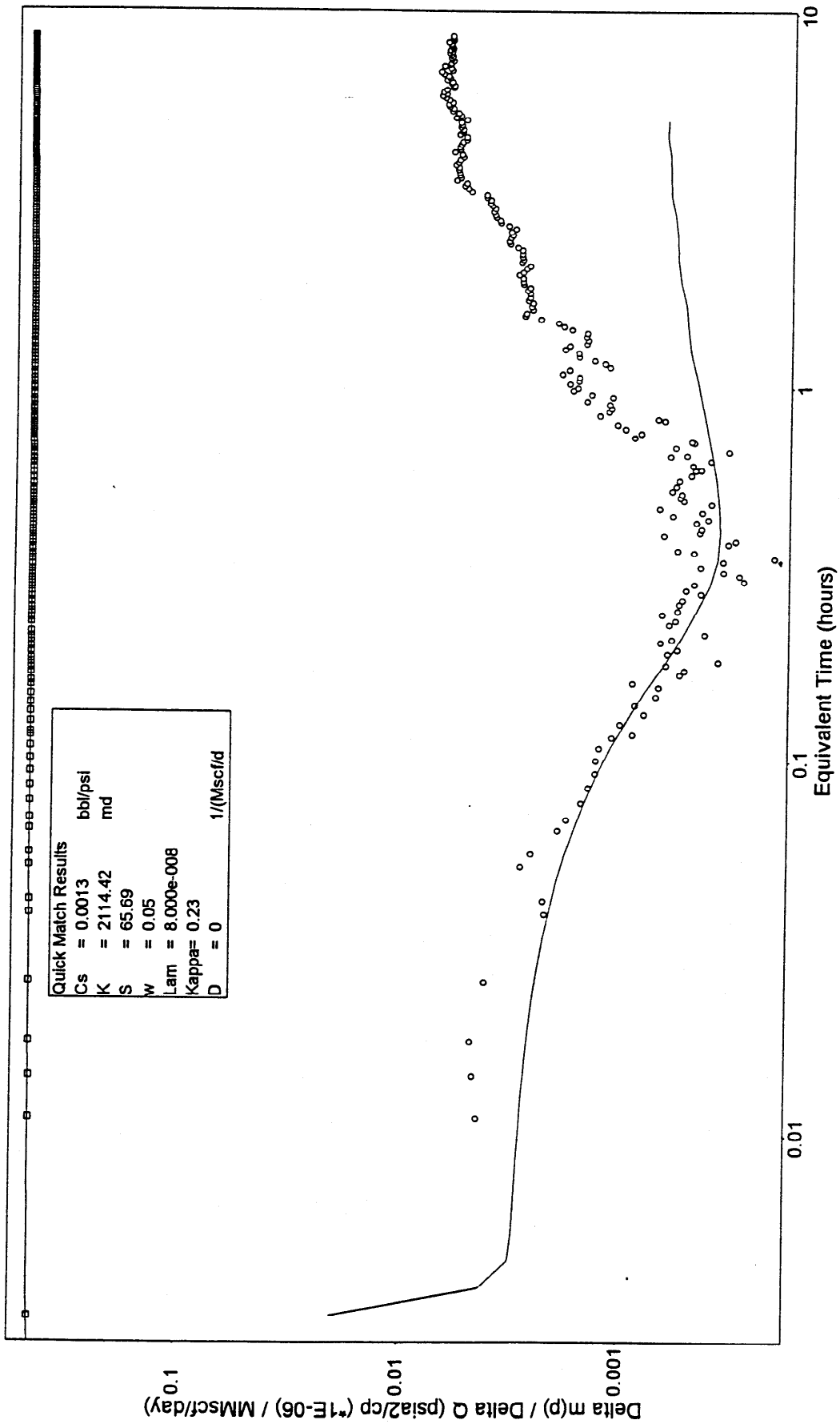




Figure 37 : Dual Permeability - No Boundary Semi-log Plot

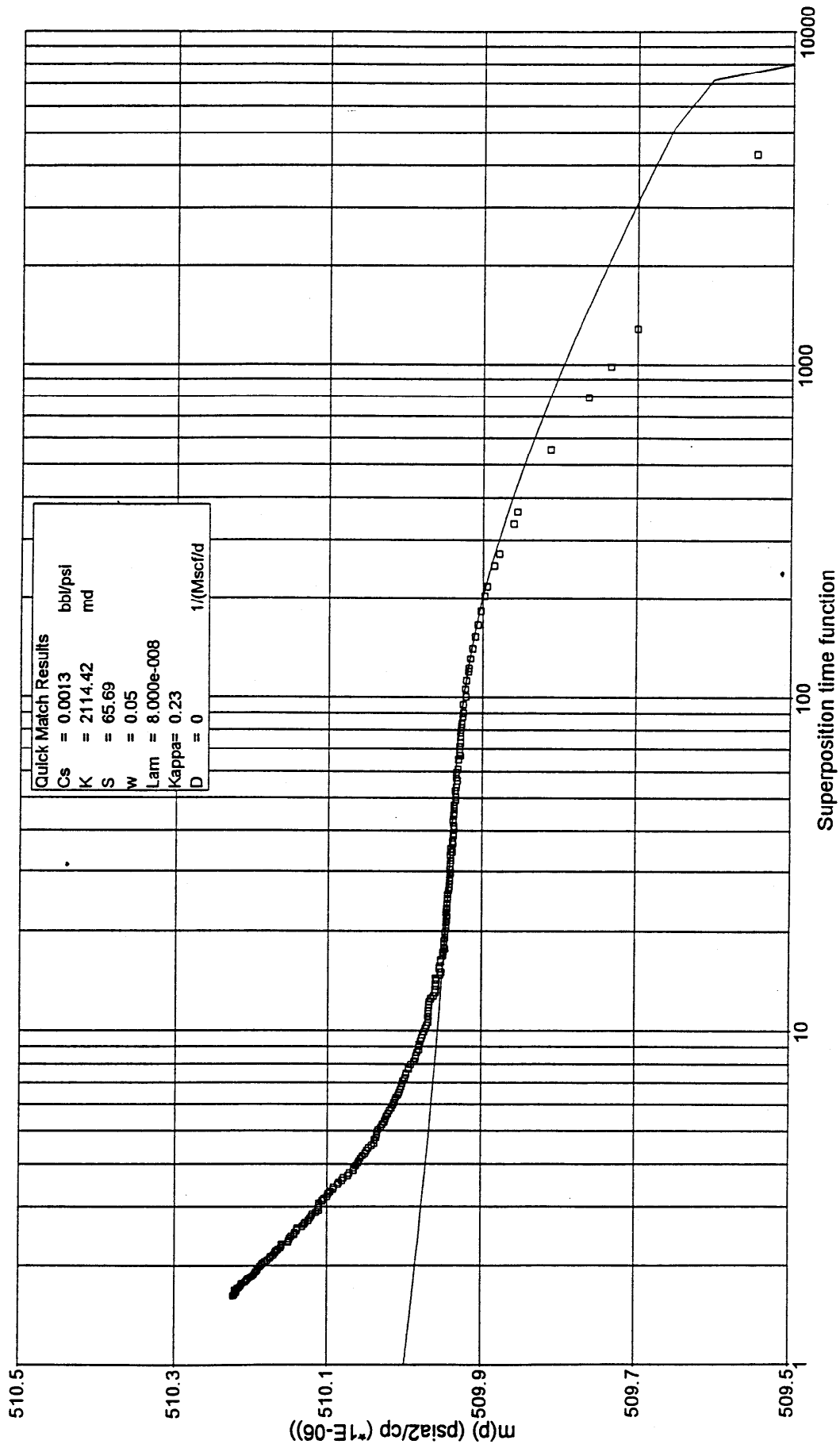


Figure 38 : Dual Porosity - No Boundary Diagnostic Plot

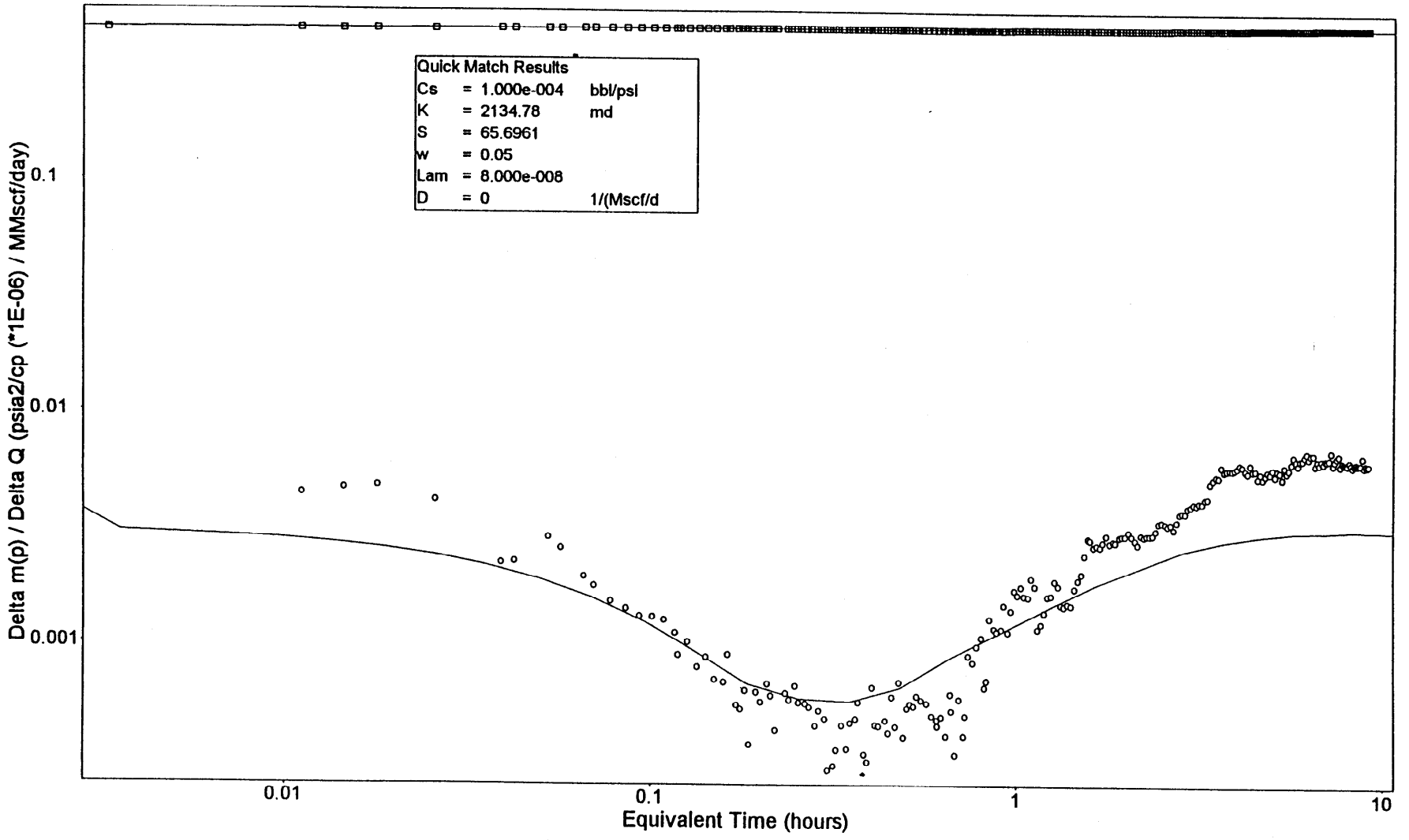


Figure 39 : Dual Porosity - No Boundary Semi-log Plot

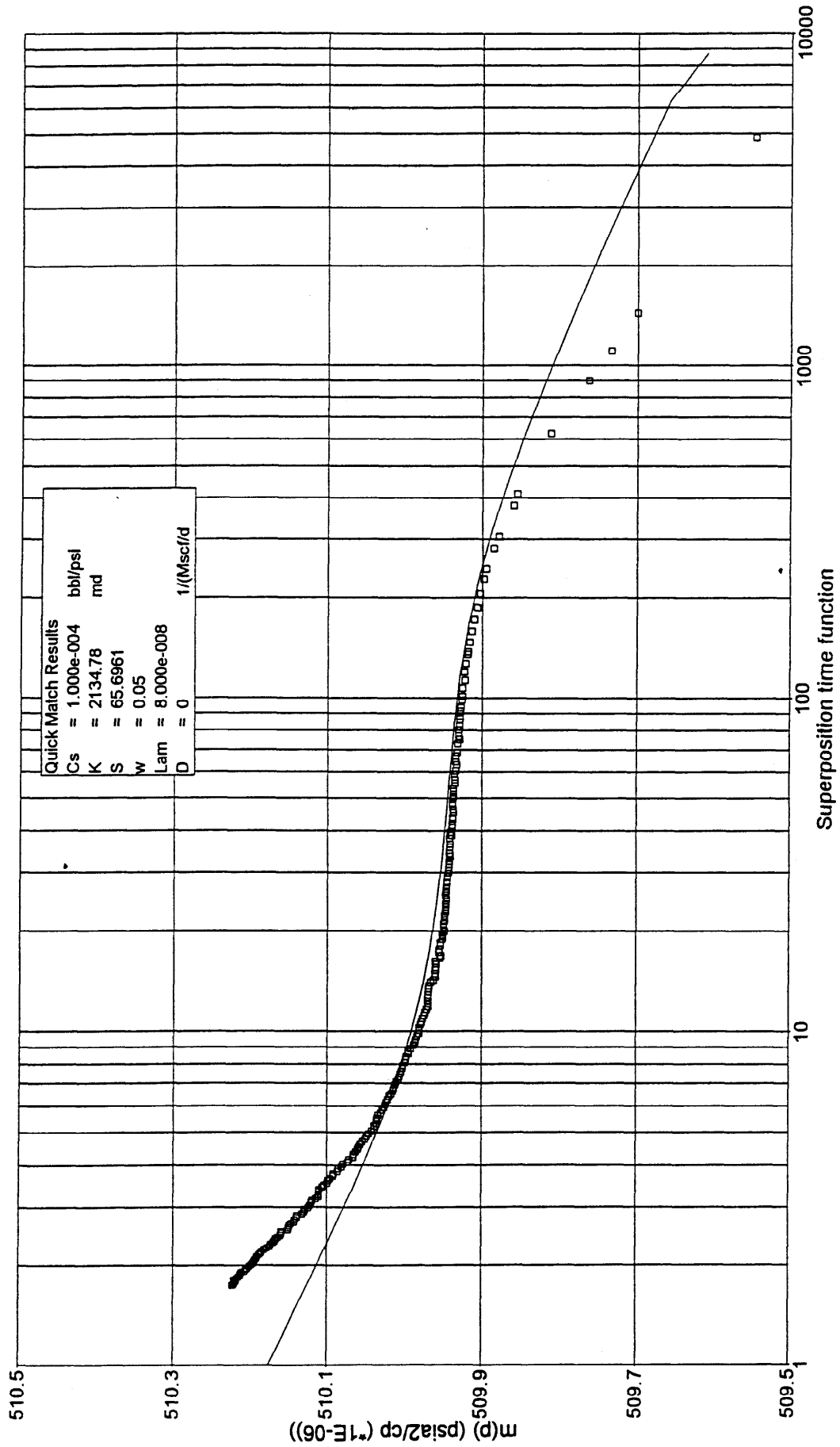
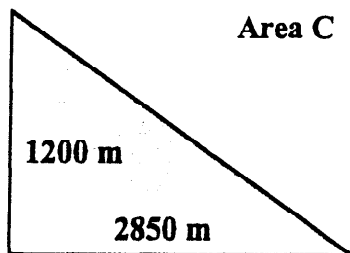
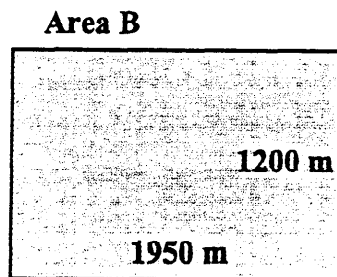
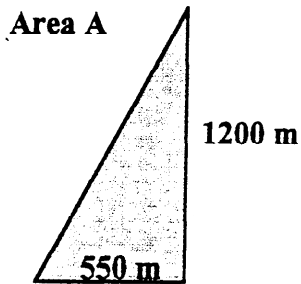
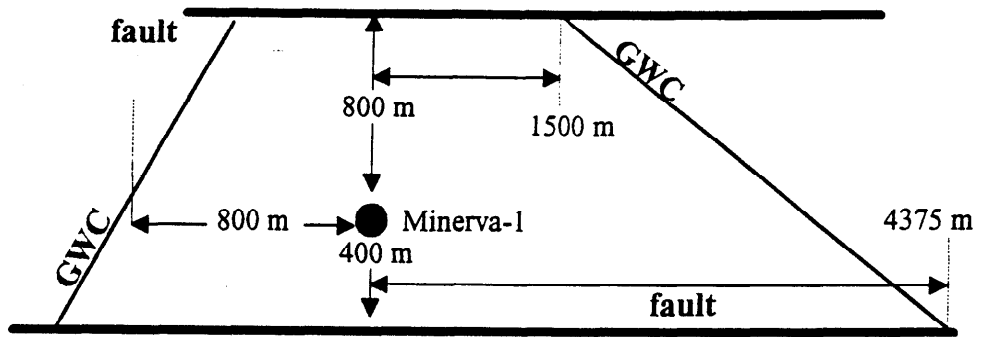


Figure 40 : Boundaries Schematic

Area Calculation

The area was divided into 3 sub-areas to calculate the mapped area :



Area A	330000 m <sup>2</sup>
Area B	2340000 m <sup>2</sup>
Area C	1725000 m <sup>2</sup>
<b>Total Mapped Area</b>	<b>4395000 m<sup>2</sup></b>

Figure 41 : Final Transient Flow Regime

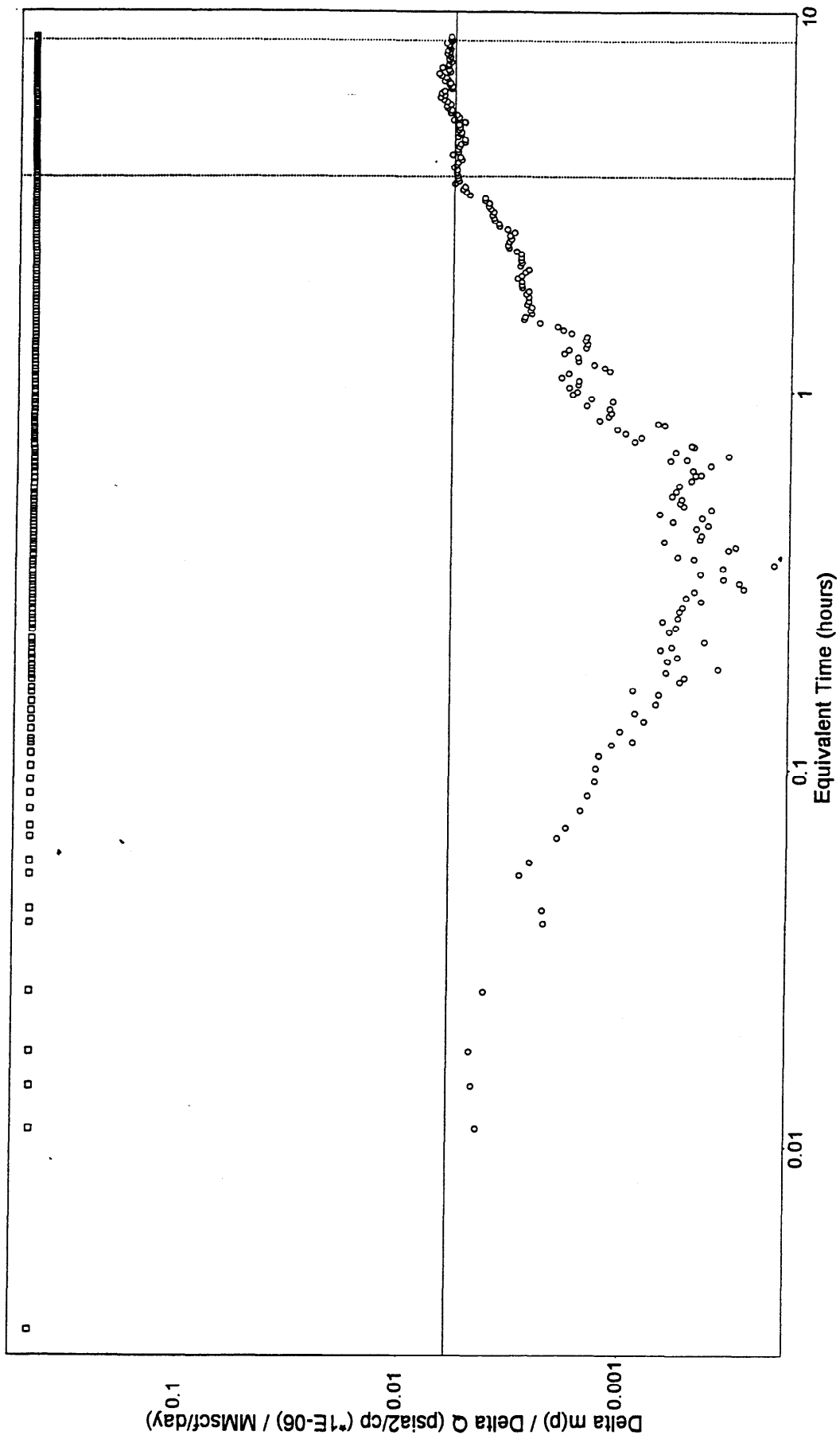


Figure 42 : Dual Permeability - Parallel Faults L:L Diagnostic Plot

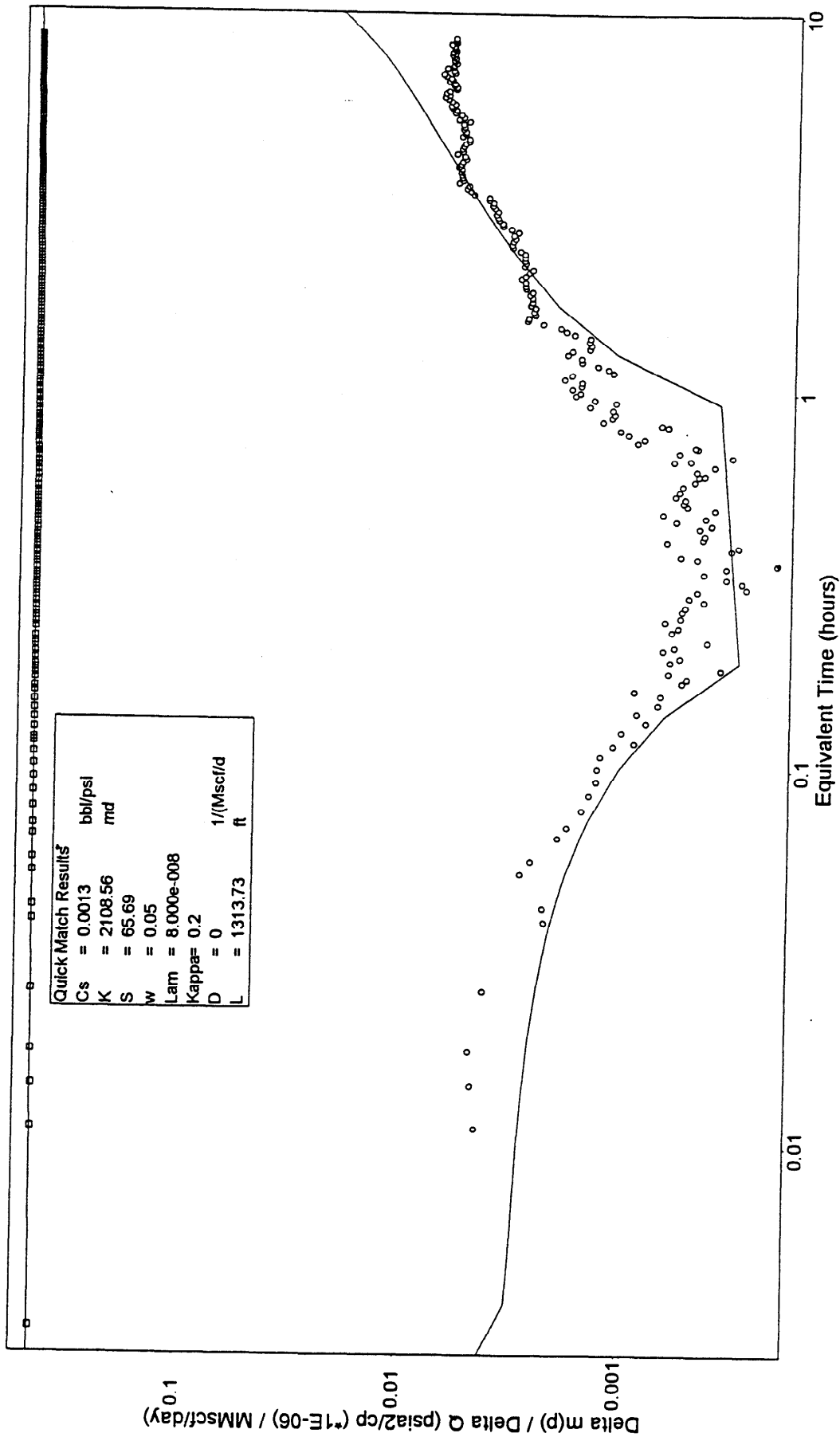


Figure 43 : Dual Permeability - Parallel Faults L:L Horner Plot

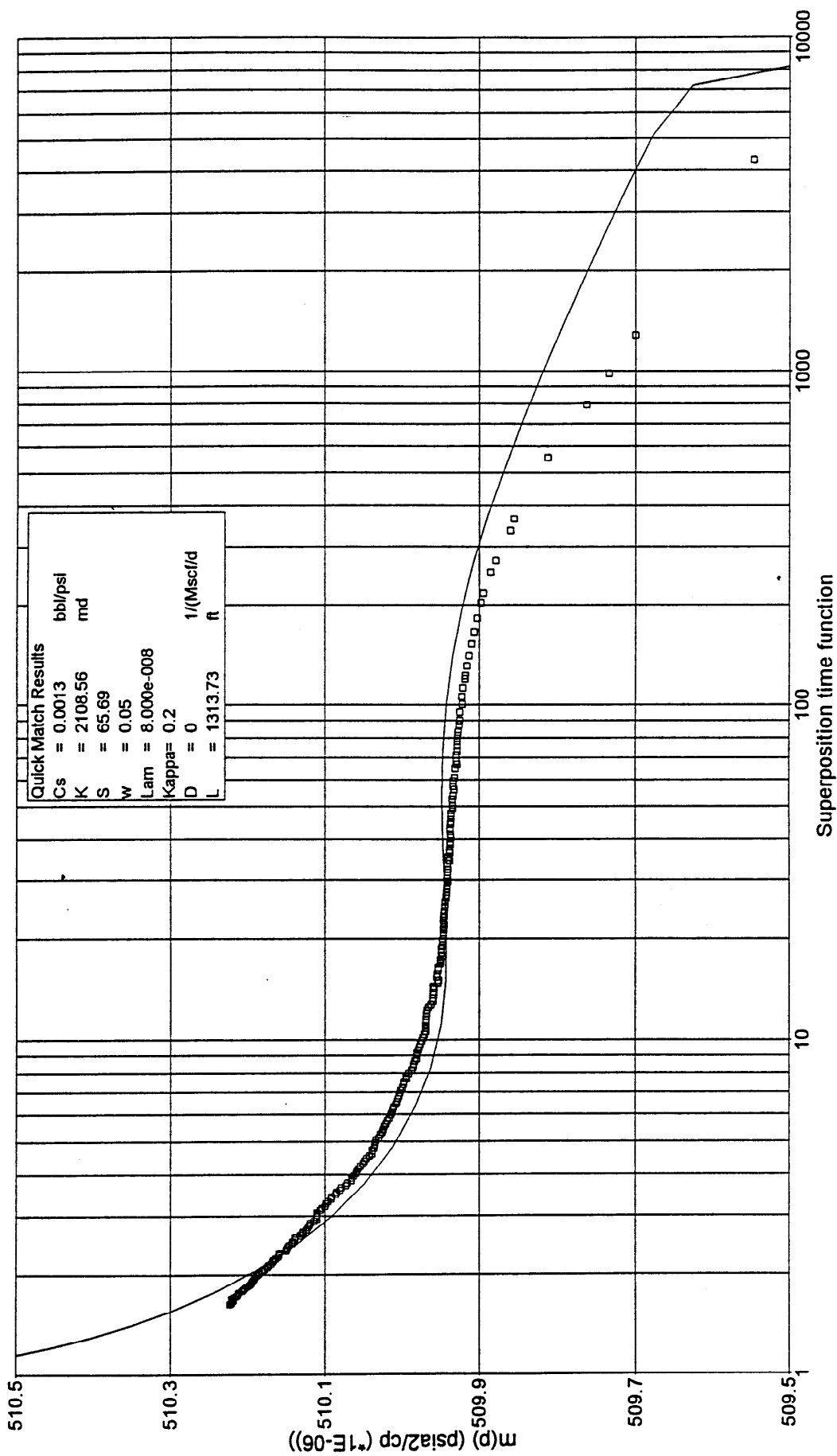


Figure 44 : Dual Permeability - Parallel Faults L:3L Diagnostic Plot

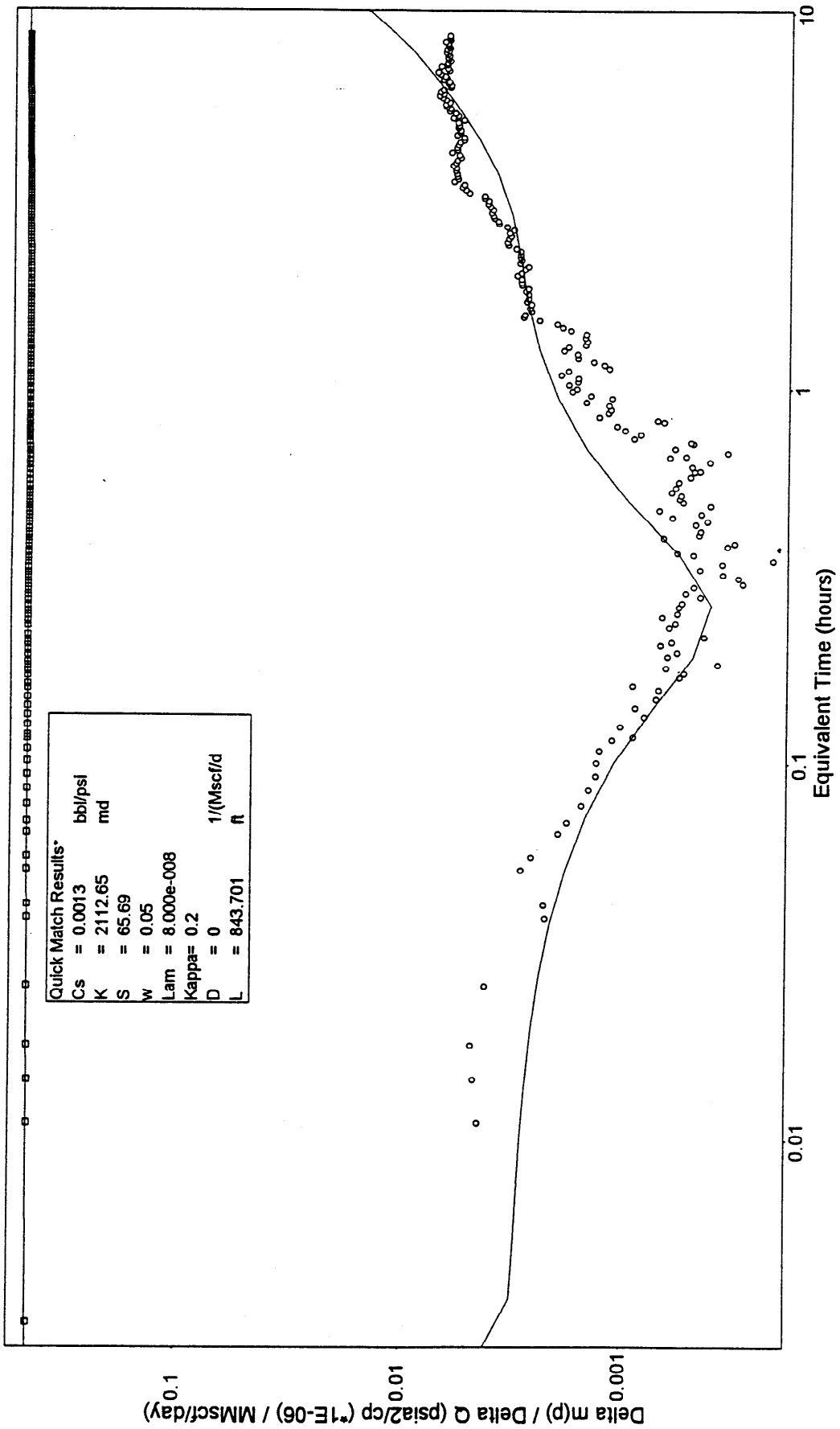




Figure 45 : Dual Permeability - Parallel Faults L:3L Horner Plot

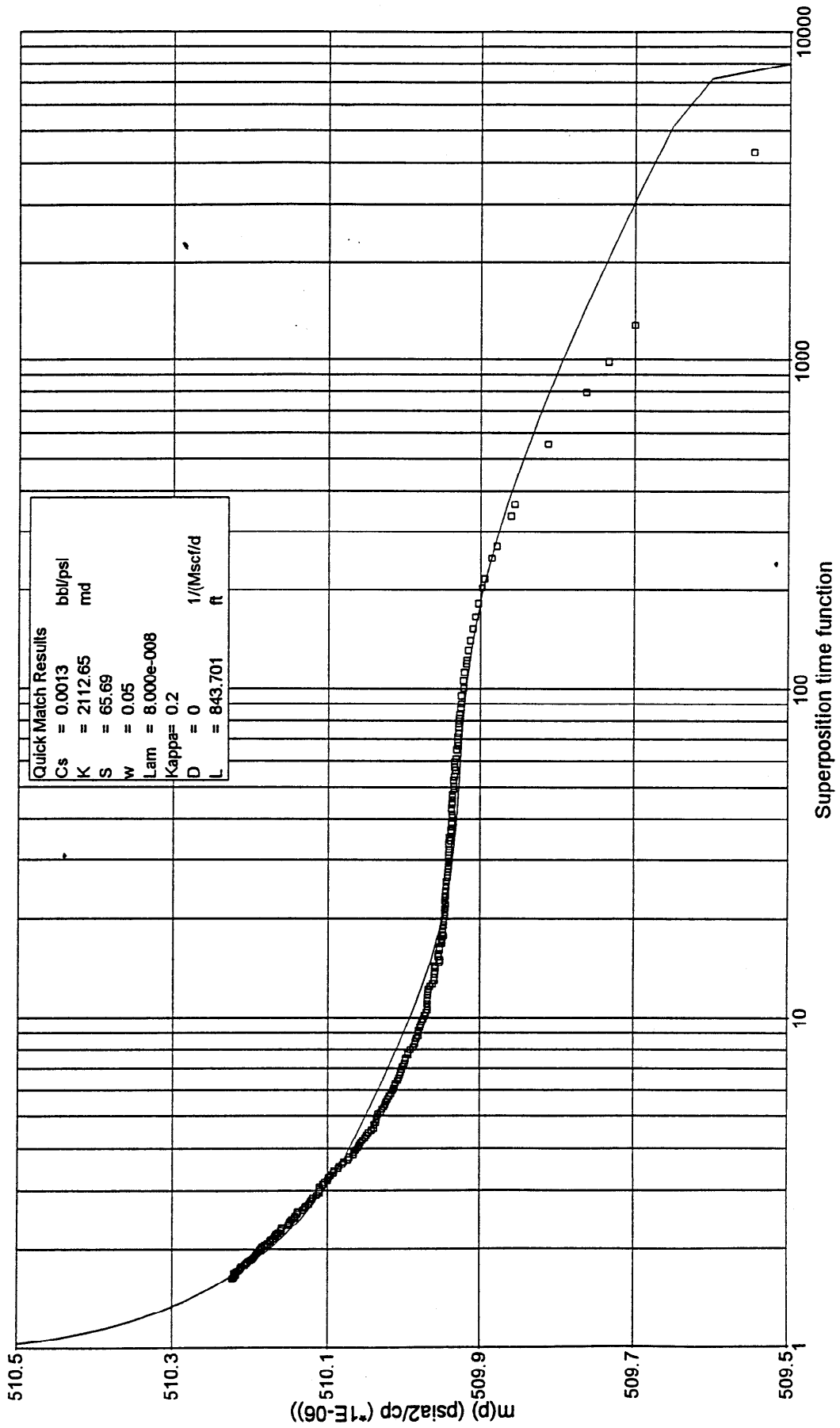


Figure 46 : Dual Permeability - 90° Faults L:2L Diagnostic Plot

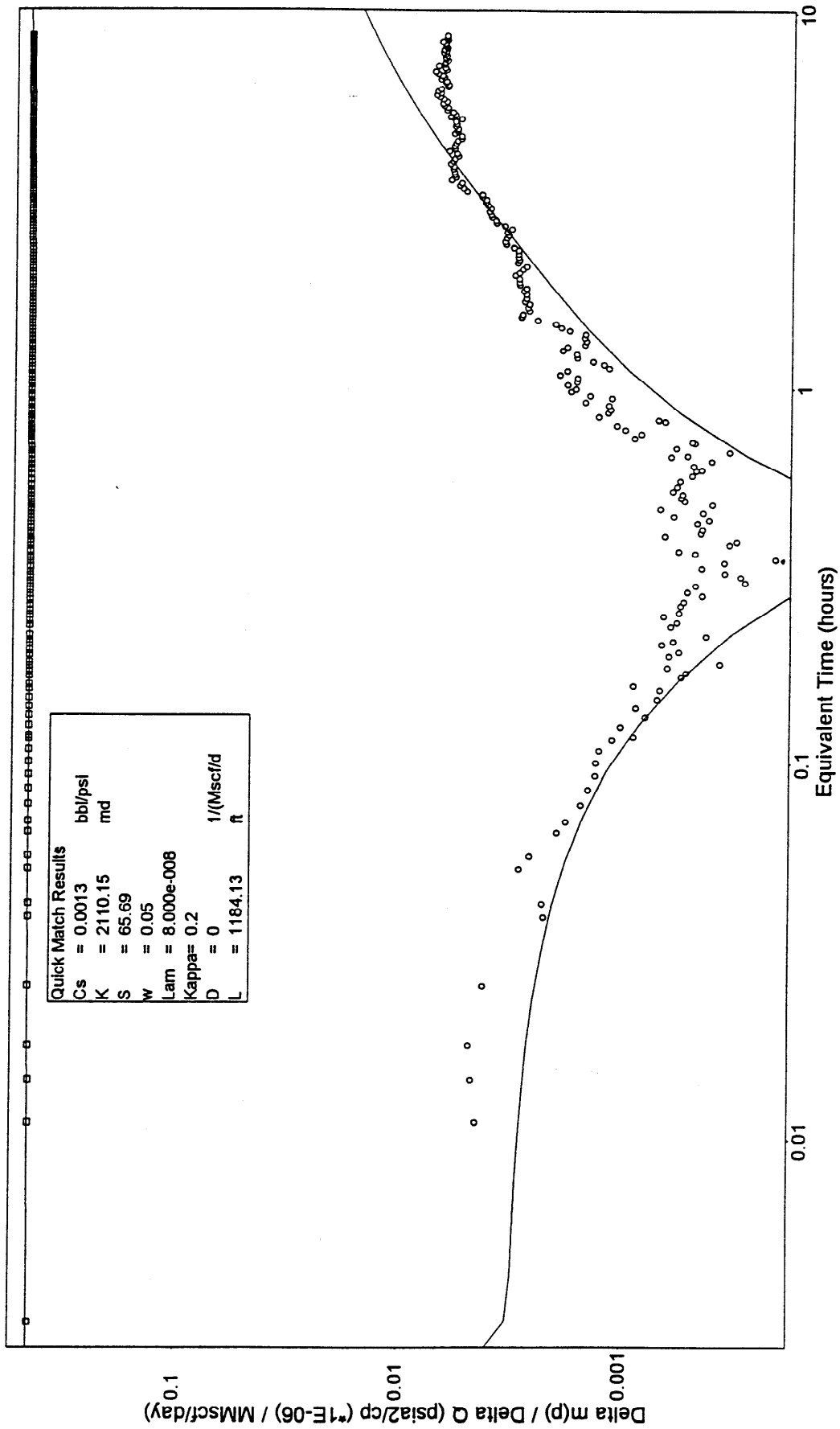
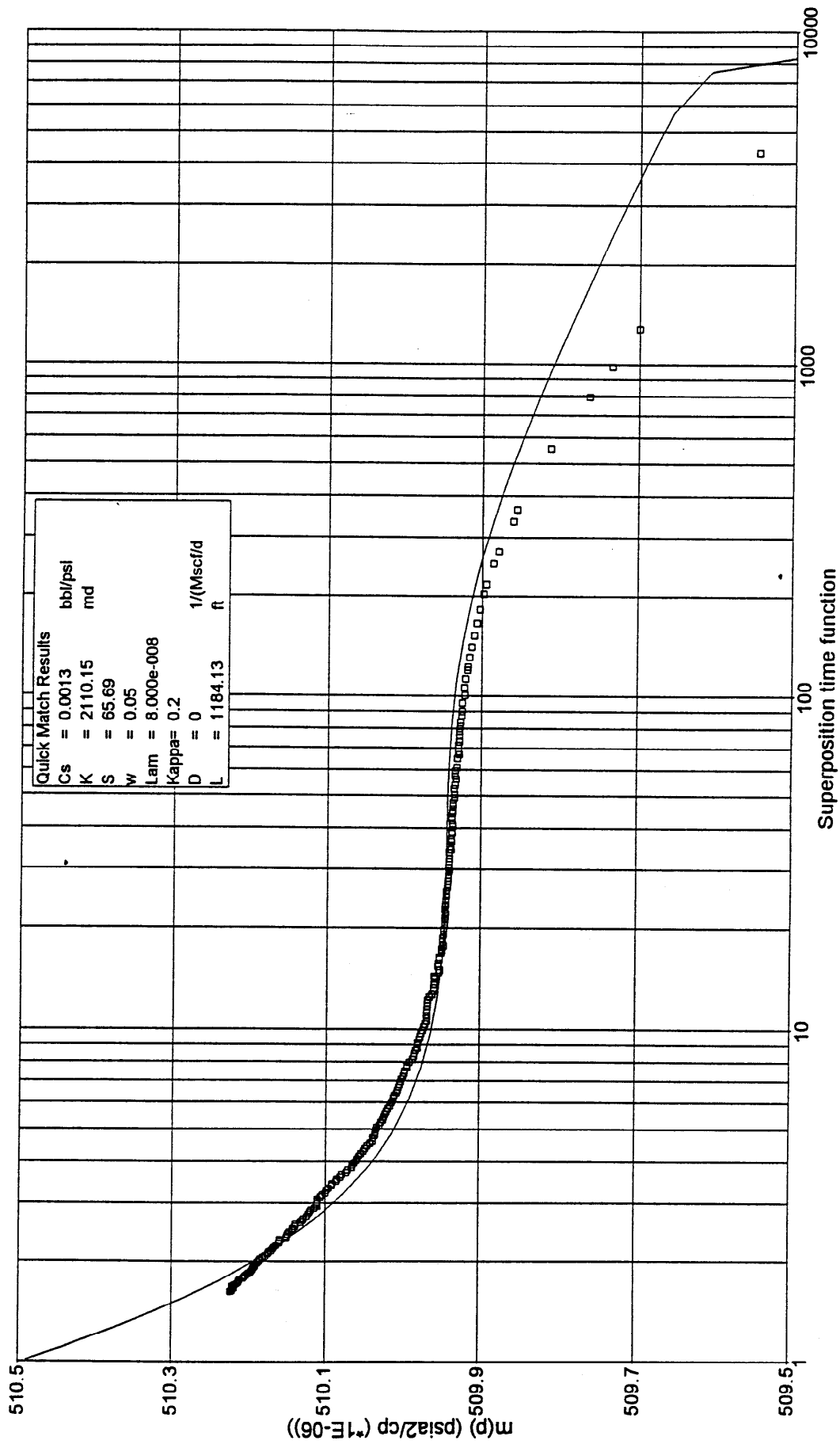


Figure 47 : Dual Permeability - 90° Faults L:2L Horner Plot



---

**APPENDIX 9 - SKIN FACTOR**

Figure 48 : Transient Flow Assumption - Semi-log Plot

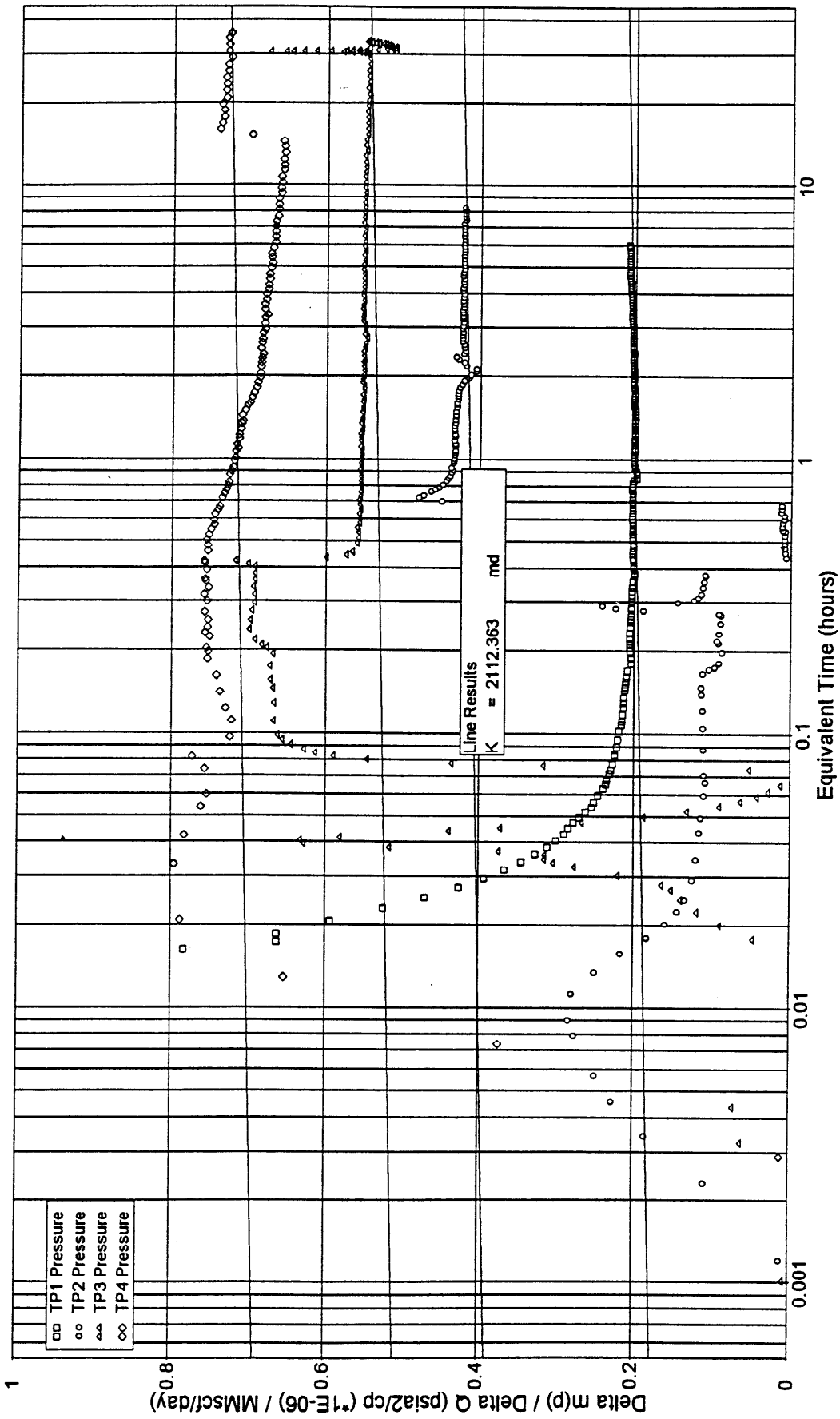
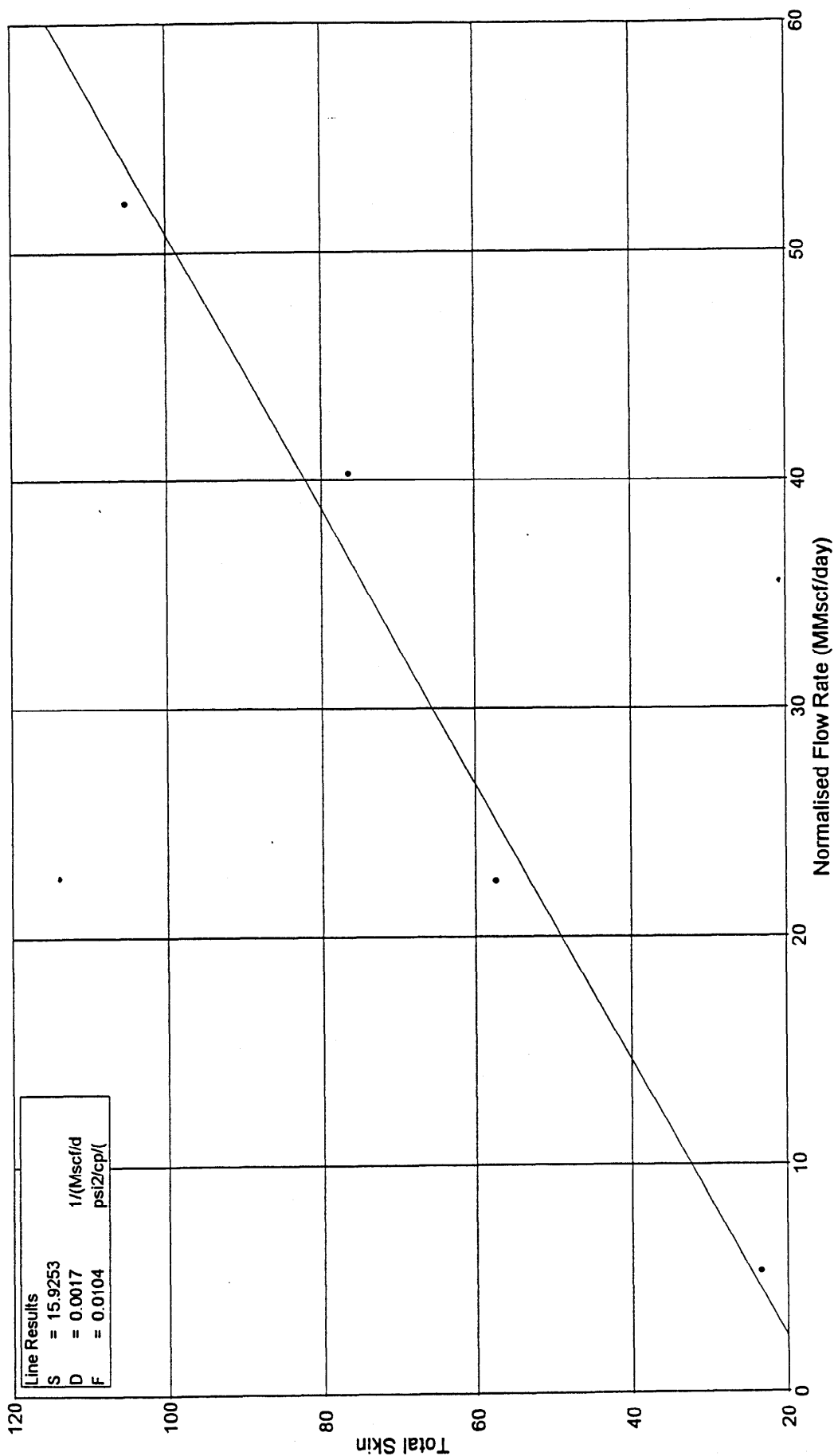


Figure 49 : Transient Flow Assumption - Skin Plot



---

## APPENDIX 10 - PRESSURE DATA

The following pages list the reduced pressure data set from gauge 011. Reduction of the data was performed on each test period (flow and build-up). The data was reduced using the criterion of 100 data points per log time cycle.

These pressures were used for the interpretation presented in this report.

Elapsed Time (hours)	pressure (psia)	Elapsed Time (hours)	pressure (psia)	Elapsed Time (hours)	pressure (psia)
39.2317	2716.261	39.5617	2713.069	40.4572	2713.137
39.3739	2576.322	39.5739	2713.053	40.4739	2713.118
39.3750	2596.297	39.5806	2713.043	40.5072	2713.120
39.3761	2609.509	39.5872	2713.039	40.5406	2713.111
39.3772	2621.014	39.5961	2713.038	40.5517	2713.122
39.3783	2630.381	39.6061	2713.046	40.5850	2713.130
39.3794	2638.450	39.6172	2713.055	40.6183	2713.122
39.3817	2652.885	39.6294	2713.067	40.6517	2713.128
39.3839	2666.680	39.6350	2713.060	40.6694	2713.126
39.3850	2673.466	39.6406	2713.075	40.7028	2713.125
39.3861	2679.970	39.6572	2713.073	40.7361	2713.126
39.3872	2685.988	39.6606	2713.071	40.7694	2713.120
39.3883	2691.359	39.6772	2713.080	40.8028	2713.134
39.3894	2696.157	39.6861	2713.083	40.8361	2713.126
39.3906	2700.341	39.7028	2713.083	40.8694	2713.139
39.3917	2703.885	39.7139	2713.096	40.9028	2713.121
39.3928	2705.799	39.7306	2713.100	40.9361	2713.109
39.3939	2705.800	39.7328	2713.101	40.9694	2713.103
39.3961	2706.894	39.7494	2713.135	41.0028	2713.112
39.3983	2707.989	39.7572	2713.136	41.0361	2713.101
39.4006	2708.852	39.7739	2713.118	41.0861	2713.119
39.4028	2709.548	39.7839	2713.118	41.1194	2713.120
39.4050	2710.074	39.8006	2713.115	41.1694	2713.116
39.4072	2710.498	39.8072	2713.104	41.2028	2713.108
39.4094	2710.841	39.8239	2713.095	41.2528	2713.095
39.4117	2711.126	39.8383	2713.105	41.2861	2713.095
39.4139	2711.370	39.8550	2713.111	41.3361	2713.103
39.4161	2711.556	39.8817	2713.097	41.3861	2713.104
39.4183	2711.726	39.8906	2713.089	41.4194	2713.093
39.4206	2711.805	39.9072	2713.094	41.4694	2713.102
39.4228	2711.910	39.9239	2713.092	41.5194	2713.090
39.4250	2712.021	39.9294	2713.092	41.5694	2713.094
39.4272	2712.163	39.9461	2713.107	41.6194	2713.095
39.4294	2712.283	39.9628	2713.094	41.6694	2713.086
39.4317	2712.329	39.9794	2713.088	41.7361	2713.097
39.4350	2712.416	39.9939	2713.081	41.7861	2713.101
39.4383	2712.516	40.0106	2713.097	41.8361	2713.081
39.4406	2712.568	40.0272	2713.092	41.9028	2713.085
39.4428	2712.594	40.0383	2713.091	41.9528	2713.081
39.4472	2712.648	40.0550	2713.092	42.0194	2713.086
39.4494	2712.672	40.0717	2713.092	42.0694	2713.077
39.4528	2712.701	40.0861	2713.086	42.1361	2713.081
39.4583	2712.751	40.1028	2713.094	42.2028	2713.078
39.4594	2712.750	40.1194	2713.091	42.2694	2713.083
39.4650	2712.787	40.1494	2713.076	42.3361	2713.082
39.4706	2712.813	40.1661	2713.097	42.4028	2713.081
39.4772	2712.833	40.1828	2713.098	42.4694	2713.066
39.4828	2712.881	40.1950	2713.088	42.5417	2713.073
39.4861	2712.891	40.2117	2713.117	42.6250	2713.049
39.4928	2712.905	40.2283	2713.166	42.6917	2713.051
39.5006	2712.923	40.2617	2713.164	42.7750	2713.066
39.5050	2712.928	40.2783	2713.152	42.8450	2713.066
39.5106	2712.931	40.3017	2713.124	42.9283	2713.057
39.5194	2712.945	40.3183	2713.123	43.0117	2713.058
39.5239	2712.955	40.3350	2713.113	43.0950	2713.053
39.5294	2712.964	40.3683	2713.113	43.1783	2713.058
39.5350	2712.982	40.3850	2713.113	43.2783	2713.047
39.5439	2713.003	40.4017	2713.114	43.3617	2713.042
39.5550	2713.077	40.4239	2713.104	43.4617	2713.035



Elapsed Time (hours)	pressure (psia)	Elapsed Time (hours)	pressure (psia)	Elapsed Time (hours)	pressure (psia)
43.5450	2713.044	45.6706	2707.910	46.7350	2697.796
43.6450	2713.028	45.6772	2708.620	46.7761	2697.843
43.7450	2713.044	45.6828	2708.806	46.8094	2697.829
43.8450	2713.021	45.6928	2708.944	46.8261	2697.827
43.9617	2713.017	45.7094	2709.012	46.8717	2697.877
44.0617	2712.998	45.7261	2709.053	46.9050	2697.893
44.1783	2713.006	45.7428	2709.130	46.9383	2697.890
44.2783	2713.031	45.7461	2709.107	46.9717	2697.913
44.3928	2713.013	45.7528	2713.033	47.0083	2697.984
44.5094	2713.023	45.7617	2713.713	47.0417	2698.079
44.6261	2713.013	45.7739	2713.852	47.0917	2698.162
44.7594	2713.025	45.7794	2713.144	47.1228	2698.375
44.8761	2713.017	45.8017	2712.766	47.1672	2698.463
45.0094	2713.015	45.8183	2712.731	47.2150	2698.713
45.1428	2713.007	45.8350	2712.699	47.2483	2698.711
45.2761	2713.012	45.8517	2712.708	47.2917	2698.260
45.3594	2712.988	45.8683	2712.704	47.3394	2698.164
45.3761	2713.001	45.8850	2712.708	47.3817	2697.899
45.3806	2712.995	45.9017	2712.723	47.4228	2697.799
45.3817	2712.596	45.9061	2712.621	47.4717	2698.139
45.3828	2709.161	45.9228	2712.585	47.5217	2698.201
45.3839	2706.513	45.9394	2712.607	47.5717	2698.152
45.3850	2705.018	45.9561	2712.681	47.6217	2698.128
45.3861	2704.255	45.9728	2712.673	47.6717	2698.060
45.3883	2703.304	45.9917	2712.547	47.7383	2698.059
45.3894	2703.041	46.0083	2712.562	47.7883	2698.072
45.3917	2703.191	46.0250	2712.558	47.8383	2698.096
45.3939	2704.224	46.0272	2712.568	47.9050	2698.072
45.3961	2705.388	46.0428	2697.159	47.9550	2698.096
45.3983	2706.582	46.0639	2696.119	48.0217	2698.119
45.4006	2707.397	46.0739	2696.321	48.0883	2698.100
45.4028	2707.912	46.0972	2696.666	48.1350	2698.085
45.4050	2708.250	46.1106	2696.851	48.2017	2698.083
45.4094	2708.578	46.1228	2697.046	48.2683	2698.079
45.4150	2708.746	46.1394	2697.196	48.3350	2698.112
45.4239	2708.872	46.1650	2697.359	48.4061	2698.104
45.4294	2708.936	46.1817	2697.467	48.4728	2698.092
45.4394	2709.076	46.1950	2697.539	48.5561	2698.108
45.4461	2709.153	46.2183	2697.613	48.6228	2698.148
45.4506	2709.094	46.2350	2697.638	48.7061	2698.080
45.4672	2709.052	46.2517	2697.583	48.7728	2698.084
45.4839	2709.048	46.2850	2697.684	48.8561	2698.139
45.5006	2709.004	46.3017	2697.705	48.9394	2698.121
45.5172	2708.962	46.3150	2697.721	49.0228	2698.145
45.5261	2708.949	46.3483	2697.746	49.1061	2698.085
45.5428	2709.014	46.3650	2697.731	49.1894	2698.126
45.5483	2709.283	46.3817	2697.757	49.2728	2698.171
45.5517	2709.544	46.4150	2697.765	49.3728	2698.159
45.5572	2709.734	46.4317	2697.764	49.4561	2698.141
45.5739	2709.866	46.4583	2697.729	49.5561	2698.138
45.5894	2709.705	46.4917	2697.756	49.6561	2698.134
45.5928	2709.651	46.5083	2697.742	49.7561	2698.152
45.6061	2709.724	46.5417	2697.718	49.8561	2698.155
45.6261	2709.810	46.5583	2697.713	49.9561	2698.130
45.6428	2709.826	46.5917	2697.712	50.0728	2698.165
45.6450	2709.742	46.6183	2697.766	50.1728	2698.163
45.6517	2706.371	46.6517	2697.776	50.2894	2698.144
45.6561	2705.116	46.6850	2697.792	50.4061	2698.157
45.6628	2704.508	46.7017	2697.787	50.5228	2698.134

Elapsed Time (hours)	pressure (psia)	Elapsed Time (hours)	pressure (psia)	Elapsed Time (hours)	pressure (psia)
50.6394	2698.157	51.5150	2686.186	52.5094	2688.247
50.7561	2698.122	51.5239	2686.135	52.5428	2688.289
50.8894	2698.204	51.5406	2686.123	52.5594	2688.286
51.0061	2698.186	51.5572	2686.190	52.5928	2688.244
51.1394	2698.178	51.5661	2686.053	52.6094	2688.254
51.2728	2698.180	51.5694	2685.929	52.6428	2688.280
51.3761	2698.165	51.5772	2685.769	52.6761	2688.286
51.3772	2698.182	51.5939	2685.649	52.7094	2688.271
51.3783	2698.098	51.6106	2685.663	52.7428	2688.261
51.3806	2697.108	51.6272	2685.697	52.7594	2688.288
51.3817	2696.921	51.6439	2685.761	52.7928	2688.280
51.3828	2699.116	51.6606	2685.757	52.8261	2688.263
51.3839	2702.313	51.6772	2685.738	52.8594	2688.301
51.3850	2705.114	51.6939	2685.769	52.8928	2688.308
51.3861	2705.452	51.7106	2685.769	52.9428	2688.341
51.3872	2704.346	51.7272	2685.773	52.9761	2688.287
51.3894	2701.435	51.7339	2685.621	53.0094	2688.315
51.3906	2700.269	51.7417	2685.305	53.0428	2688.304
51.3928	2698.533	51.7517	2687.415	53.0928	2688.253
51.3950	2697.385	51.7594	2687.878	53.1261	2688.254
51.3972	2696.601	51.7683	2688.029	53.1594	2688.268
51.3994	2696.079	51.7928	2688.126	53.2094	2688.242
51.4017	2695.711	51.8094	2688.167	53.2428	2688.246
51.4039	2695.485	51.8261	2688.164	53.2939	2688.270
51.4050	2695.272	51.8428	2688.126	53.3439	2688.248
51.4072	2694.260	51.8594	2688.187	53.3772	2688.260
51.4094	2693.249	51.8761	2688.197	53.4272	2688.269
51.4106	2692.760	51.8928	2688.179	53.4750	2688.270
51.4117	2692.554	51.9094	2688.220	53.5250	2688.275
51.4128	2692.560	51.9261	2688.194	53.5750	2688.274
51.4139	2691.495	51.9428	2688.166	53.6250	2688.252
51.4150	2688.913	51.9594	2688.198	53.6750	2688.249
51.4161	2686.901	51.9761	2688.218	53.7250	2688.282
51.4172	2686.828	51.9928	2688.229	53.7917	2688.265
51.4183	2687.747	52.0094	2688.210	53.8417	2688.293
51.4206	2690.311	52.0261	2688.213	53.8917	2688.273
51.4217	2691.522	52.0428	2688.221	53.9583	2688.284
51.4239	2693.427	52.0594	2688.212	54.0250	2688.262
51.4261	2694.863	52.0761	2688.196	54.0728	2688.283
51.4283	2695.849	52.0928	2688.224	54.1394	2688.298
51.4306	2696.588	52.1094	2688.220	54.2061	2688.248
51.4328	2697.090	52.1261	2688.208	54.2728	2688.264
51.4350	2697.471	52.1428	2688.242	54.3394	2688.270
51.4372	2697.731	52.1594	2688.243	54.4061	2688.286
51.4406	2698.020	52.1761	2688.239	54.4728	2688.278
51.4450	2698.225	52.1928	2688.209	54.5561	2688.274
51.4483	2698.218	52.2261	2688.218	54.6228	2688.293
51.4494	2697.290	52.2428	2688.218	54.6950	2688.278
51.4517	2692.528	52.2594	2688.198	54.7783	2688.285
51.4528	2690.366	52.2761	2688.239	54.8617	2688.269
51.4550	2688.380	52.2928	2688.252	54.9283	2688.291
51.4572	2687.601	52.3261	2688.220	55.0117	2688.301
51.4594	2687.167	52.3428	2688.240	55.0950	2688.287
51.4617	2686.905	52.3594	2688.253	55.1950	2688.280
51.4650	2686.605	52.3928	2688.238	55.2783	2688.318
51.4683	2686.411	52.4094	2688.260	55.3617	2688.285
51.4717	2686.293	52.4261	2688.263	55.4550	2688.300
51.4828	2686.198	52.4594	2688.247	55.5550	2688.330
51.4994	2686.215	52.4761	2688.272	55.6550	2688.332

Elapsed Time (hours)	pressure (psia)	Elapsed Time (hours)	pressure (psia)	Elapsed Time (hours)	pressure (psia)
55.7550	2688.329	57.4650	2675.647	58.7039	2676.323
55.8550	2688.329	57.4783	2675.684	58.7372	2676.341
55.9550	2688.328	57.4894	2675.549	58.7706	2676.346
56.0717	2688.332	57.5061	2675.418	58.8039	2676.371
56.1717	2688.350	57.5239	2675.337	58.8472	2676.327
56.2883	2688.354	57.5450	2675.129	58.8972	2676.356
56.4050	2688.338	57.5550	2675.140	58.9306	2676.369
56.5194	2688.368	57.5606	2675.105	58.9806	2676.376
56.6361	2688.362	57.5772	2675.179	59.0139	2676.422
56.7528	2688.344	57.5839	2675.067	59.0639	2676.404
56.8861	2688.383	57.5928	2675.126	59.1139	2676.423
57.0028	2688.372	57.6050	2675.144	59.1472	2676.479
57.0694	2688.371	57.6194	2675.063	59.1972	2676.408
57.0861	2688.369	57.6417	2675.111	59.2472	2676.408
57.1028	2688.351	57.6561	2675.045	59.2972	2676.443
57.1194	2688.290	57.6706	2675.151	59.3472	2676.450
57.1339	2688.215	57.6861	2675.080	59.3972	2676.491
57.1394	2688.133	57.6917	2675.068	59.4472	2676.496
57.1450	2687.957	57.7150	2675.103	59.5139	2676.518
57.1472	2687.750	57.7328	2675.063	59.5639	2676.516
57.1494	2687.146	57.7383	2675.042	59.6306	2676.551
57.1517	2686.581	57.7650	2675.125	59.6806	2676.574
57.1561	2686.074	57.7817	2675.128	59.7472	2676.557
57.1583	2686.423	57.7983	2675.103	59.7972	2676.547
57.1606	2686.830	57.8150	2675.154	59.8639	2676.599
57.1628	2687.116	57.8317	2675.199	59.9306	2676.640
57.1661	2687.470	57.8483	2675.274	59.9972	2676.640
57.1706	2687.823	57.8650	2675.265	60.0639	2676.641
57.1739	2687.949	57.8861	2675.295	60.1306	2676.644
57.1761	2688.104	57.9028	2675.355	60.1972	2676.650
57.1783	2688.290	57.9161	2675.394	60.2694	2676.697
57.1839	2688.551	57.9494	2675.453	60.3528	2676.709
57.1906	2688.560	57.9661	2675.506	60.4194	2676.718
57.1961	2688.764	57.9828	2675.548	60.5028	2676.708
57.2028	2688.908	57.9994	2675.585	60.5861	2676.774
57.2083	2688.911	58.0161	2675.604	60.6528	2676.763
57.2239	2689.001	58.0494	2675.633	60.7361	2676.785
57.2406	2688.966	58.0661	2675.669	60.8194	2676.776
57.2506	2688.884	58.0828	2675.693	60.9206	2676.825
57.2672	2688.843	58.1161	2675.728	61.0039	2676.828
57.2839	2688.814	58.1328	2675.762	61.0872	2676.813
57.3006	2688.822	58.1661	2675.768	61.1872	2676.854
57.3139	2688.755	58.1828	2675.816	61.2872	2676.843
57.3194	2688.695	58.1994	2675.795	61.3706	2676.815
57.3350	2688.582	58.2328	2675.839	61.4761	2676.112
57.3450	2688.511	58.2528	2675.841	61.5739	2675.365
57.3517	2688.417	58.2861	2675.881	61.6794	2675.409
57.3650	2688.349	58.3194	2675.900	61.7806	2675.454
57.3694	2688.312	58.3361	2675.920	61.8972	2675.458
57.3750	2688.213	58.3694	2675.911	62.0017	2675.408
57.3794	2681.821	58.4028	2675.982	62.1183	2675.509
57.3850	2676.891	58.4361	2676.033	62.2461	2675.495
57.3928	2674.504	58.4528	2676.089	62.3628	2675.517
57.4050	2674.364	58.4861	2676.134	62.4794	2675.502
57.4139	2674.607	58.5194	2676.181	62.6072	2675.551
57.4250	2674.986	58.5528	2676.240	62.7283	2675.547
57.4306	2675.117	58.5861	2676.262	62.8672	2675.625
57.4439	2675.074	58.6194	2676.304	63.0039	2675.556
57.4517	2674.782	58.6539	2676.321	63.1372	2675.565

Elapsed Time (hours)	pressure (psia)	Elapsed Time (hours)	pressure (psia)	Elapsed Time (hours)	pressure (psia)
63.2706	2675.554	63.8261	2715.271	65.1583	2715.392
63.3539	2675.603	63.8361	2715.274	65.2061	2715.392
63.3706	2675.622	63.8461	2715.273	65.2461	2715.399
63.3772	2675.578	63.8572	2715.276	65.2917	2715.403
63.3783	2714.100	63.8683	2715.272	65.3272	2715.406
63.3861	2714.557	63.8839	2715.275	65.3761	2715.411
63.3894	2714.658	63.8950	2715.276	65.4294	2715.422
63.3928	2714.745	63.9061	2715.278	65.4817	2715.433
63.4006	2714.892	63.9172	2715.277	65.5161	2715.432
63.4139	2715.020	63.9294	2715.280	65.5761	2715.440
63.4172	2715.034	63.9461	2715.283	65.6172	2715.443
63.4272	2715.089	63.9672	2715.283	65.6739	2715.447
63.4317	2715.109	63.9872	2715.285	65.7306	2715.455
63.4406	2715.136	64.0072	2715.285	65.7839	2715.456
63.4450	2715.146	64.0094	2715.288	65.8461	2715.461
63.4528	2715.161	64.0261	2715.289	65.8939	2715.464
63.4606	2715.171	64.0461	2715.286	65.9617	2715.468
63.4683	2715.182	64.0672	2715.289	66.0217	2715.473
63.4761	2715.191	64.0717	2715.288	66.0728	2715.479
63.4839	2715.199	64.0883	2715.289	66.1350	2715.483
63.4917	2715.206	64.1083	2715.289	66.2039	2715.488
63.4939	2715.207	64.1317	2715.294	66.2650	2715.491
63.5017	2715.215	64.1383	2715.293	66.3372	2715.498
63.5094	2715.218	64.1550	2715.293	66.3972	2715.505
63.5172	2715.216	64.1772	2715.298	66.4794	2715.512
63.5250	2715.226	64.1983	2715.297	66.5472	2715.517
63.5339	2715.226	64.2217	2715.294	66.6194	2715.522
63.5383	2715.229	64.2439	2715.301	66.7017	2715.526
63.5472	2715.232	64.2539	2715.299	66.7739	2715.533
63.5517	2715.235	64.2706	2715.302	66.8583	2715.538
63.5572	2715.236	64.2972	2715.310	66.9317	2715.548
63.5617	2715.237	64.3139	2715.310	67.0150	2715.553
63.5706	2715.237	64.3417	2715.314	67.0939	2715.554
63.5761	2715.240	64.3606	2715.315	67.1817	2715.557
63.5850	2715.241	64.3883	2715.307	67.2750	2715.565
63.5894	2715.237	64.4072	2715.312	67.3717	2715.565
63.5961	2715.245	64.4339	2715.328	67.4528	2715.575
63.6106	2715.247	64.4539	2715.324	67.5583	2715.586
63.6161	2715.252	64.4817	2715.328	67.6550	2715.593
63.6261	2715.252	64.5039	2715.327	67.7428	2715.599
63.6317	2715.249	64.5350	2715.331	67.8506	2715.610
63.6428	2715.253	64.5583	2715.329	67.9617	2715.617
63.6494	2715.256	64.5906	2715.336	68.0683	2715.624
63.6606	2715.254	64.6117	2715.347	68.1650	2715.627
63.6672	2715.255	64.6428	2715.352	68.2828	2715.634
63.6783	2715.261	64.6683	2715.355	68.3928	2715.643
63.6850	2715.260	64.6994	2715.355	68.5072	2715.645
63.6961	2715.261	64.7350	2715.356	68.6361	2715.661
63.7028	2715.262	64.7683	2715.356	68.7628	2715.666
63.7139	2715.265	64.8006	2715.358	68.8761	2715.684
63.7261	2715.263	64.8250	2715.357	69.0061	2715.691
63.7339	2715.260	64.8583	2715.356	69.1339	2715.702
63.7472	2715.264	64.8939	2715.362	69.2672	2715.706
63.7528	2715.262	64.9317	2715.368	69.4128	2715.721
63.7683	2715.266	64.9706	2715.372	69.5472	2715.724
63.7761	2715.264	65.0106	2715.377	69.6972	2715.735
63.7894	2715.271	65.0517	2715.381	69.8417	2715.742
63.7983	2715.266	65.0917	2715.386	69.9928	2715.747
63.8072	2715.273	65.1317	2715.391	70.1383	2715.759

Elapsed Time (hours)	pressure (psia)	Elapsed Time (hours)	pressure (psia)	Elapsed Time (hours)	pressure (psia)
70.3050	2715.767				
70.4650	2715.778				
70.6317	2715.779				
70.8039	2715.780				
70.9706	2715.779				
71.1494	2715.790				
71.3283	2715.803				
71.5117	2715.808				
71.7028	2715.813				
71.9028	2715.820				
72.0983	2715.832				
72.2972	2715.835				
72.5139	2715.844				
72.7172	2715.863				
72.9339	2715.864				
73.1606	2715.873				
73.3772	2715.874				
73.6106	2715.887				
73.8606	2715.892				
74.0939	2715.897				
74.3439	2715.899				
74.6106	2715.923				
74.8606	2715.924				
75.1328	2715.928				
75.4161	2715.937				
75.6828	2715.946				
75.9828	2715.949				
76.2661	2715.954				
76.5661	2715.965				
76.8817	2715.969				
77.1817	2715.979				
77.5150	2715.989				
77.8317	2715.999				
78.1817	2716.002				
78.5150	2716.008				
78.8817	2716.016				
79.2317	2716.017				
79.5983	2716.023				
79.9817	2716.027				
80.3650	2716.032				
80.7650	2716.037				
81.1650	2716.045				
81.5817	2716.053				
81.9994	2716.058				
82.4483	2716.064				
82.8817	2716.076				
83.3406	2716.080				
83.8072	2716.083				
84.2739	2716.089				
84.7672	2716.096				
85.2650	2716.107				
85.7694	2716.098				
86.2861	2716.104				
86.8272	2716.107				
87.3783	2716.112				
87.3950	2716.112				

7

**SPECIAL CORE ANALYSIS  
STUDY FOR  
MINERVA 1**

---



17 February 1994

---

BHP Petroleum Pty Ltd  
BHP Petroleum Plaza  
120 Collins Street  
MELBOURNE VIC 3000

Attention: Mr Lee Yong

REPORT: 008/225

CLIENT REFERENCE: ke:ly:1342:ec

MATERIAL: Core Plugs

LOCALITY: Minerva 1

WORK REQUIRED: Special Core Analysis

Please direct technical enquiries regarding this work to the signatory below under whose supervision the work was carried out.

A handwritten signature in black ink, appearing to read 'R D East', written over a horizontal line.

**ROBERT D EAST**  
Technical Services Manager

ACS Laboratories Pty Ltd shall not be liable or responsible for any loss, cost, damages or expenses incurred by the client, or any other person or company, resulting from any information or interpretation given in this report. In no case shall ACS Laboratories Pty Ltd be responsible for consequential damages including, but not limited to, lost profits, damages for failure to meet deadlines and lost production arising from this report.



# CONTENTS

PAGE

1.	INTRODUCTION . . . . .	1
2.	SAMPLE PREPARATION . . . . .	2
2.1	Sample Selection and Plug Photography . . . . .	2
2.2	Permeability to Air - Ambient . . . . .	2
2.3	Helium Injection Porosity - Ambient . . . . .	2
2.4	Porosity and Permeability - Overburden . . . . .	2
3.	FORMATION FACTOR (FF) . . . . .	3
4.	RESISTIVITY INDEX (RI) . . . . .	3
5.	CAPILLARY PRESSURE - Porous Plate . . . . .	4
6.	CAPILLARY PRESSURE - Centrifuge . . . . .	4
7.	BASIC WATERFLOOD . . . . .	5

# LIST OF TABLES

	<u>PAGE</u>
Table I	POROSITY AND AIR PERMEABILITY - Ambient . . . . . 6
Table II	POROSITY AND AIR PERMEABILITY - Overburden . . . . . 8
Table III	CONNATE WATER SATURATION - Phase 1a . . . . . 10
Table IV	CAPILLARY PRESSURE - Phase 1b (Sample 21) . . . . . 12
Table V	CAPILLARY PRESSURE - Phase 1b (Sample 31) . . . . . 14
Table VI	CAPILLARY PRESSURE - Phase 1b (Sample 56) . . . . . 16
Table VII	CAPILLARY PRESSURE - Phase 1b (Sample 65) . . . . . 18
Table VIII	FORMATION FACTOR - Phase 1c/d . . . . . 20
Table IX	RESISTIVITY INDEX - Phase 1c/d . . . . . 22-24
Table X	CAPILLARY PRESSURE - Phase 1c/d . . . . . 33
Table XI	EFFECTIVE PERMEABILITY - Phase 2a . . . . . 42
Table XII	RESIDUAL GAS SATURATION - Phase 2b(i) . . . . . 44
Table XIII	EFFECTIVE PERMEABILITY - Phase 2b(i) . . . . . 46
Table XIV	RESIDUAL GAS SATURATION - Phase 2b(ii) . . . . . 48
Table XV	EFFECTIVE PERMEABILITY - Phase 2b(ii) . . . . . 50
Table XVI	RESIDUAL GAS SATURATION - Phase 2b(iii) . . . . . 52
Table XVII	EFFECTIVE PERMEABILITY - Phase 2b(iii) . . . . . 57
Table XVIII	BASIC WATERFLOOD - Phase 2c . . . . . 59

# LIST OF FIGURES

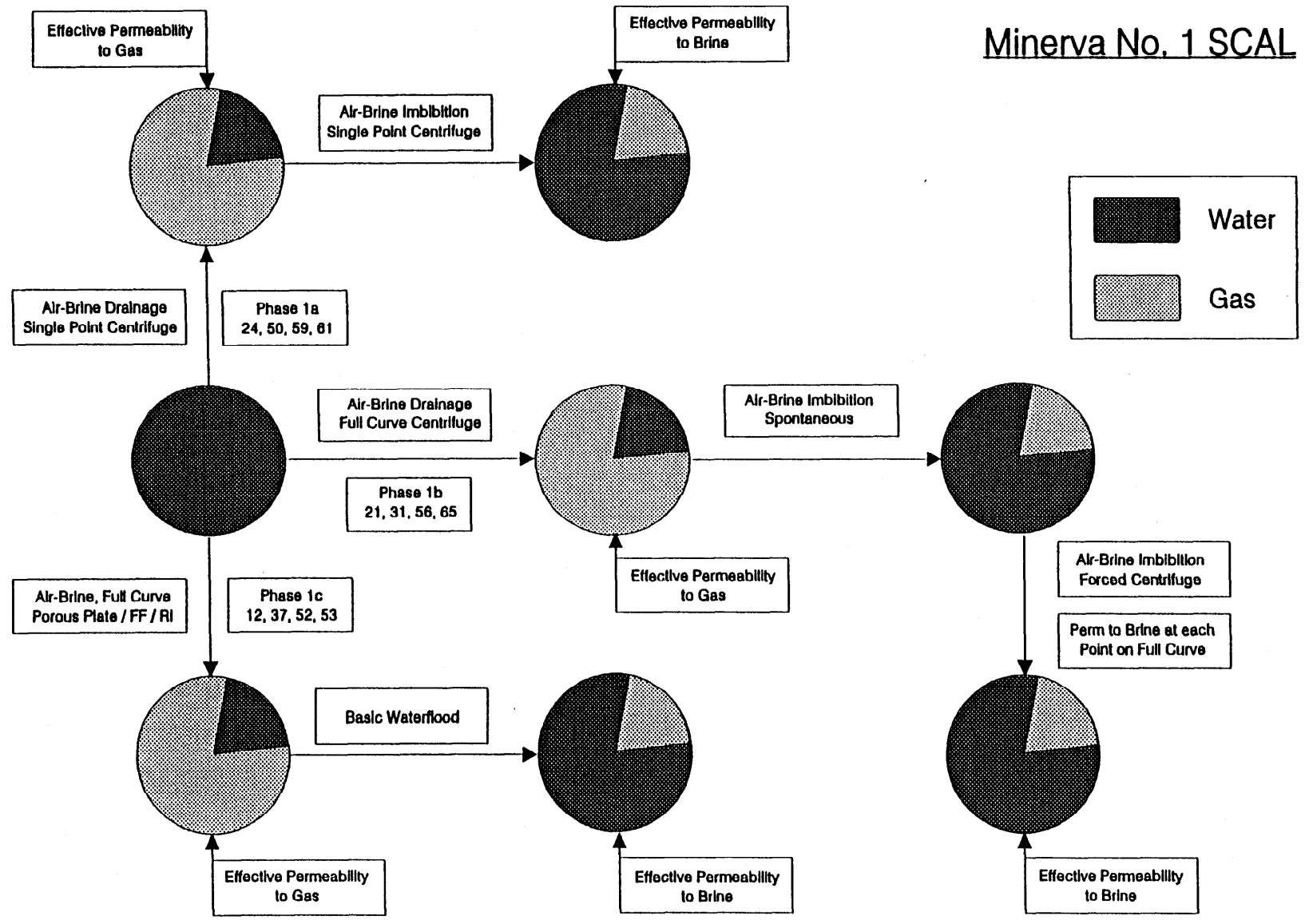
	<u>PAGE</u>
POROSITY VS PERMEABILITY - Ambient . . . . .	7
POROSITY VS PERMEABILITY - Overburden . . . . .	9
CONNATE WATER SATURATION - Phase 1a . . . . .	11
CAPILLARY PRESSURE - Phase 1b (Sample 21) . . . . .	13
CAPILLARY PRESSURE - Phase 1b (Sample 31) . . . . .	15
CAPILLARY PRESSURE - Phase 1b (Sample 56) . . . . .	17
CAPILLARY PRESSURE - Phase 1b (Sample 65) . . . . .	19
FORMATION FACTOR - Phase 1c/d . . . . .	21
RESISTIVITY INDEX - Phase 1c/d (Sample 9) . . . . .	25
RESISTIVITY INDEX - Phase 1c/d (Sample 12) . . . . .	26
RESISTIVITY INDEX - Phase 1c/d (Sample 17) . . . . .	27
RESISTIVITY INDEX - Phase 1c/d (Sample 34) . . . . .	28
RESISTIVITY INDEX - Phase 1c/d (Sample 37) . . . . .	29
RESISTIVITY INDEX - Phase 1c/d (Sample 49) . . . . .	30
RESISTIVITY INDEX - Phase 1c/d (Sample 52) . . . . .	31
RESISTIVITY INDEX - Phase 1c/d (Sample 53) . . . . .	32
CAPILLARY PRESSURE - Phase 1c/d (Sample 9) . . . . .	34
CAPILLARY PRESSURE - Phase 1c/d (Sample 12) . . . . .	35
CAPILLARY PRESSURE - Phase 1c/d (Sample 17) . . . . .	36
CAPILLARY PRESSURE - Phase 1c/d (Sample 34) . . . . .	37
CAPILLARY PRESSURE - Phase 1c/d (Sample 37) . . . . .	38
CAPILLARY PRESSURE - Phase 1c/d (Sample 49) . . . . .	39
CAPILLARY PRESSURE - Phase 1c/d (Sample 52) . . . . .	40
CAPILLARY PRESSURE - Phase 1c/d (Sample 53) . . . . .	41

# LIST OF FIGURES CONT

## PAGE

EFFECTIVE PERMEABILITY TO GAS VS WATER SATURATION - Phase 2a . . . . .	43
PERMEABILITY TO AIR VS RESIDUAL GAS SATURATION - Phase 2b . . . . .	45
EFFECTIVE PERMEABILITY TO BRINE VS GAS SATURATION - Phase 2b(i) . . . . .	47
PERMEABILITY TO AIR VS GAS SATURATION - Phase 2b(ii) . . . . .	49
EFFECTIVE PERMEABILITY TO BRINE VS GAS SATURATION - Phase 2b(ii) . . . . .	51
CAPILLARY PRESSURE - Phase (2b(iii)) (Sample 21) . . . . .	53
CAPILLARY PRESSURE - Phase (2b(iii)) (Sample 31) . . . . .	54
CAPILLARY PRESSURE - Phase (2b(iii)) (Sample 56) . . . . .	55
CAPILLARY PRESSURE - Phase (2b(iii)) (Sample 65) . . . . .	56
EFFECTIVE PERMEABILITY TO BRINE VS GAS SATURATION - Phase 2b(iii) . . . . .	58
EFFECTIVE PERMEABILITY TO GAS VS WATER SATURATION - Phase (2c(iii)) . . . . .	60
EFFECTIVE PERMEABILITY TO BRINE VS GAS SATURATION . . . . .	61

# Minerva No. 1 SCAL



## 1. INTRODUCTION

A facsimile dated 15th June 1993 was received from Keith Edwards of BHP Petroleum Pty Ltd outlining a proposed special core analysis program for Minerva 1. Further discussions between ACS Laboratories personnel and Lee Yong of BHPP refined a final SCAL program as outlined below

The SCAL program consisted of a preparatory stage and Phases 1 and 2.

STAGE	ANALYSIS	TABLES	SAMPLES SELECTED
Preliminary	Sample preparation	I, II	All
Phase 1a	Air-brine capillary pressure drainage, single point, centrifuge method	III	24, 50, 59, 61
Phase 1b	Air-brine capillary pressure drainage, full curve, centrifuge method	IV - VII	21, 31, 56, 65
Phase 1c	Air-brine capillary pressure drainage, full curve, porous plate method, with formation factor/resistivity index	VIII - X	53, 52, 12, 37
Phase 1d	as above	as above	17, 5, 34, 49
Phase 2a	Effective permeability to gas at irreducible water saturation	XI	21, 31, 56, 65, 61, 59, 24, 50
Phase 2b (i)	Air-brine capillary pressure imbibition, end point, centrifuge method, effective permeability to brine at residual gas saturation	XII - XIII	61, 24, 59, 50
Phase 2b (ii)	Air-brine spontaneous imbibition, effective permeability to gas at residual gas saturation	XIV - XV	21, 65, 56, 31
Phase 2b (iii)	Air-brine forced imbibition, centrifuge method, effective permeability to brine at residual gas saturation for each point on a full curve	XVI - XVII	21, 65, 56, 31
Phase 2c	Basic water flood, includes effective permeability to gas at irreducible water saturation and effective permeability to brine at residual gas saturation	XVIII	12, 37, 52, 53

Procedures for the analyses requested are outlined in the following text.

## 2. SAMPLE PREPARATION

Preparation of samples for the special core analysis program consisted of: plug selection and plug photography; facing all selected plug samples square; re-analysing samples for ambient and overburden pore volume (porosity) and permeability.

### 2.1 Sample Selection and Plug Photography

One-and-a-half inch diameter plug samples were initially selected by BHPP from routine core analysis data (ACS Report HG/205). These samples were photographed and copies delivered to BHPP Melbourne. Due to the initial unsuitability of some of the selected plugs, replacements were chosen. These were then photographed and delivered to BHPP to comprise a complete set of final SCAL plugs.

Samples were then faced square using a diamond impregnated wheel.

Since facing of samples slightly alters their dimensions permeability to air and porosity were redetermined.

### 2.2 Permeability to Air - Ambient

Air permeability was determined on the plug samples. The samples were firstly placed in a Hassler cell with a confining pressure of 250 psi. The confining pressure was used to prevent bypassing of air around the samples when the measurement was made. To determine permeability a known air pressure was applied to the upstream face of the sample, creating a flow of air through the core plug. Permeability for the samples was calculated using Darcy's Law through knowledge of the upstream pressure, flow rate, viscosity of air and the samples' dimensions.

### 2.3 Helium Injection Porosity - Ambient

The porosity of the clean dry core plugs was determined as follows. The plugs were first placed in a sealed matrix cup. Helium held at 100 psi reference pressure was then introduced to the cup. From the resultant pressure change the unknown grain volume was calculated using Boyle's Law.

The bulk volume was determined by mercury immersion. The difference between the grain volume and the bulk volume is the pore volume and from this the 'effective' porosity was calculated as the volume percentage of pores with respect to the bulk volume.

### 2.4 Porosity and Permeability - Overburden

To determine the porosity and air permeability of the core plugs at overburden pressure the samples were first placed in a thick walled rubber sleeve. This assembly was loaded into a hydrostatic cell and the pore volume determined at 'ambient' pressure. An overburden pressure of 2100 psi was then applied to the samples and the pore volume reduction caused by this increase in pressure determined. By this means the actual overburden pore volume and bulk volume was determined. These data are used to derive porosity at the applied overburden

pressure. Air permeability at overburden pressure was then measured in the hydrostatic cell as described previously.

### 3. FORMATION FACTOR (FF)

On completion of porosity and air permeability determinations, samples were evacuated and pressure saturated with a 36,000 ppm NaCl brine. Resistivity of the brine was measured as 0.18 ohm.m at 25°C. Samples were removed from the pressure saturator and weighed to ensure that 100% brine saturation had been achieved. A quality control check was made on measurements of ambient porosity by determining the porosity of the fully saturated plug by Archimedes' principle.

Samples were then placed on the cell electrodes with a thin silver leaf between the plug endface and electrode to ensure contact. A strongly hydrophilic filter was placed at one end of the sample. This assembly was then loaded into a rubber sleeve and placed into the hydrostatic cell. The cell was pressured to the desired overburden pressure of 2100 psi using a mineral oil.

Brine was slowly flowed through the sample and electrical resistivity readings recorded until stable. The samples were left to stand for a further 24 hours and readings repeated to ensure that ionic equilibrium had been attained.

### 4. RESISTIVITY INDEX (RI)

After formation factor measurements were completed, humidified air was introduced to the samples as a means of establishing the required water saturation<sup>1</sup>. Air pressure was continually applied to the samples.

Volumes of displaced brine were monitored as a function of time. Resistivity values and temperatures were recorded.

All electrical properties readings were recorded at room temperature and converted to a standard temperature of 25°C using the following equation derived by Hilchie<sup>2</sup>.

---

de Waal et al, J.A., Measurement and Evaluation of Resistivity Index Curves, Koninklijke/Shell Exploratie en Produktie Laboratorium, SPWLA 13th Annual Logging Symposium, June 11-14 1989.

<sup>2</sup> Hilchie, D.W., A New Water Resistivity versus Temperature Equation, The Log Analyst, Jul-Aug 1984, pp. 20-22.



$$R_T = R_1[(T_1+X)/(T+X)]$$

and  $X = 10^{(-0.340396 \log R_1 + 0.641427)}$

where:  $R_T$  = resistivity at temperature T (ohm.m)  
 $T$  = temperature (°C) i.e. 25°C  
 $R_1$  = resistivity at temperature  $T_1$  (ohm.m)  
 $T_1$  = temperature at room conditions (°C)

#### 5. CAPILLARY PRESSURE - Porous Plate

All samples selected to undergo these analyses were firstly pressure saturated with the 36,000 ppm NaCl brine. 100% brine saturation was determined gravimetrically and as an additional quality control check, porosity was determined by Archimedes' principle. Samples were then placed into individual cells with a strongly hydrophilic porous plate at one end.

A humidified air was then introduced to the samples at the first pressure of 0.5 psi. Effluent water displaced by the gas was collected in a pipette. Displacement was monitored as a function of time. When the volume of brine displaced had stabilised, the pressure on the gas phase was increased to obtain the next point on the capillary pressure versus fluid saturation profile.

#### 6. CAPILLARY PRESSURE - Centrifuge

The samples selected for these analyses (after saturation with the brine using the procedures described above) were placed into individual cups and loaded into the centrifuge. At each rotor speed, the water displaced by centrifugal forces was monitored as a function of time. As standard practices require<sup>3</sup>, samples were left at each rotational speed for a minimum of 24 hours, or until there was no change in consecutive readings of produced water. The induced capillary pressures were then calculated from the following equation<sup>4</sup>:-

<sup>3</sup> Omeregie, Zuwa, Factors Affecting the Equivalency of Different Capillary Pressure Measurement Techniques, S. Chevron Oilfield Research Co., SPE Formation Evaluation, March 1988, pp. 157-155.

<sup>4</sup> Hassler, Brunner, Measurement of Capillary Pressures in Small Core Samples, AIME, Vol. 160, 1945, pp. 114-123.

$$P_c = \frac{1}{2} \Delta \rho \omega^2 (r_2^2 - r_1^2) \times (1.013 \times 14.696 \times 10^{-6})$$

- where:
- $P_c$  = capillary pressure at the inlet face of the core (psi).
  - $\Delta \rho$  = density difference of the two fluids, ie. air and water (gms/cm<sup>3</sup>).
  - $\omega$  = angular velocity (rad/sec)  
=  $2\pi(\text{RPM})/60$
  - $r_2$  = radius from the centre of the centrifuge to the bottom of the core plug (cm).
  - $r_1$  = radius from the centre of the centrifuge to the top of the core plug (cm).

The centrifuge method of determining the relation between saturation and capillary pressure provides values of average saturation. These average saturation values must then be converted to obtain the endface saturation which is equivalent to the induced capillary pressure, thereby obtaining the true profile of capillary pressure versus saturation. The true endface saturation has been calculated by applying a series of data regressions to the average saturation values.

## 7. BASIC WATERFLOOD

Connate (irreducible) water saturation was obtained through one of the above capillary pressure procedures. Each sample in turn was placed into a hydrostatic core holder under a confining pressure of 2100 psi. At this stage effective permeability to gas was measured.

The gas was displaced using a 36,000 ppm brine, and effluent volumes of gas and water recorded. Finally, effective permeability to brine was determined at residual gas saturation.

The flow rate used for Basic Waterflood measurement was approximately 4 ccs/min. Brine permeability readings were taken once gas flow from the sample had ceased. Consecutive constant brine permeability readings were taken to indicate stable residual gas saturation values. The differential pressure across the sample is a function of flow rate and permeability. Pore volume throughput to achieve stable residual gas saturations was approximately 2 pore volumes for samples 37 and 52 and 5 pore volumes for 12 and 53.

## POROSITY AND AIR PERMEABILITY

Company BHP Petroleum Pty Ltd  
Well Minerva 1

Ambient

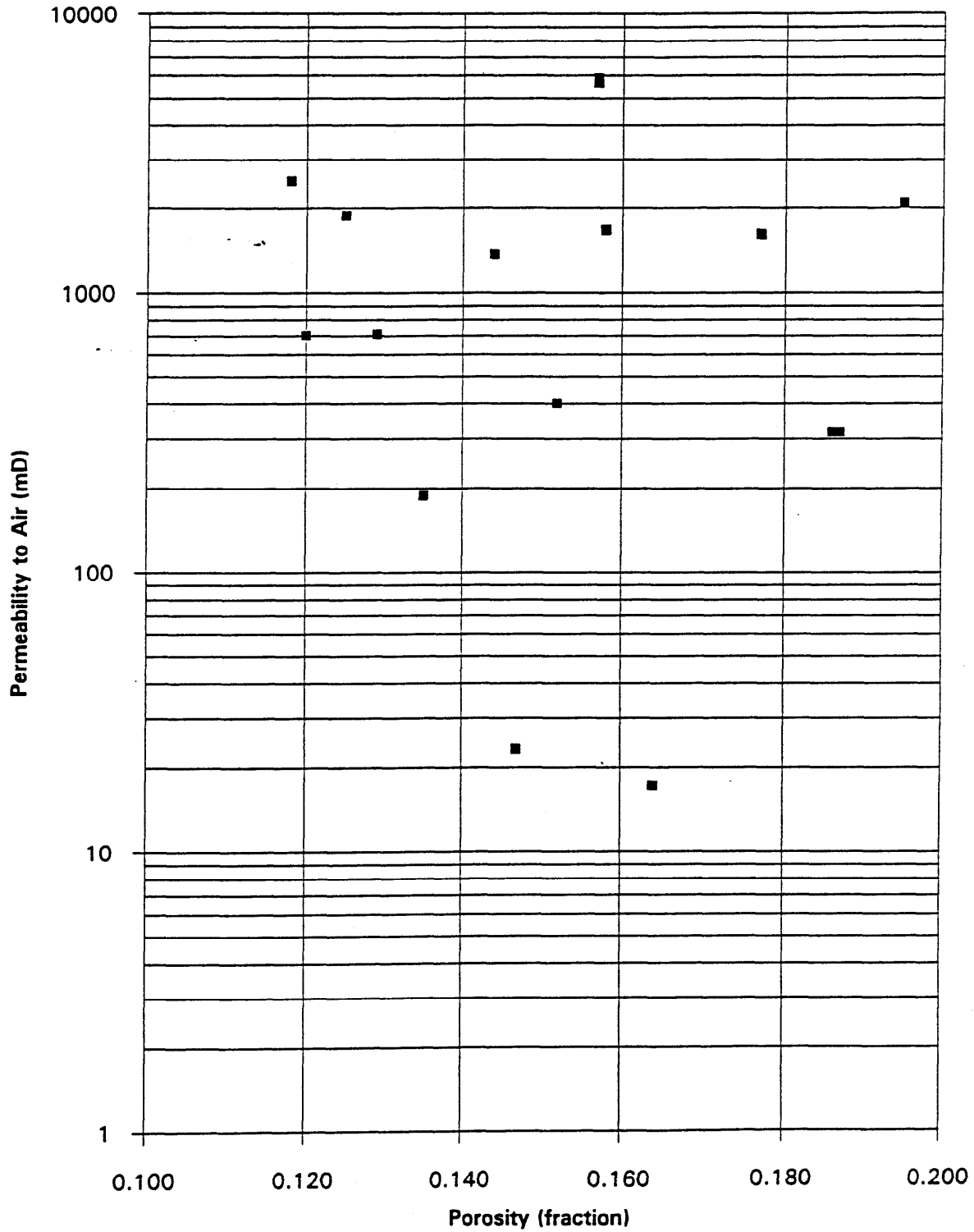
Table I

Sample Number	Depth, metres	Permeability to Air, millidarcies	Porosity, fraction	Grain Density (gms/cm <sup>3</sup> )
9	1823.47	1660	0.158	
12	1828.15	2076	0.195	
17	1829.57	1874	0.125	
21	1830.77	2502	0.118	
24	1831.70	701	0.120	
31	1833.80	23.3	0.147	
34	1834.70	188	0.135	
37	1835.60	318	0.186	
49	1840.60	17.2	0.164	
50	1840.90	318	0.187	
52	1842.80	709	0.129	
53	1843.10	5854	0.157	
56	1844.05	402	0.152	
59	1844.90	1601	0.177	
61	1845.52	5641	0.157	
65	1846.72	1371	0.144	

# Porosity vs Permeability

Company: BHP Petroleum Pty Ltd  
Well: Minerva 1

Ambient



## POROSITY AND AIR PERMEABILITY

Company                    BHP Petroleum Pty Ltd  
Well                        Minerva 1

Overburden Pressure    2100 psi

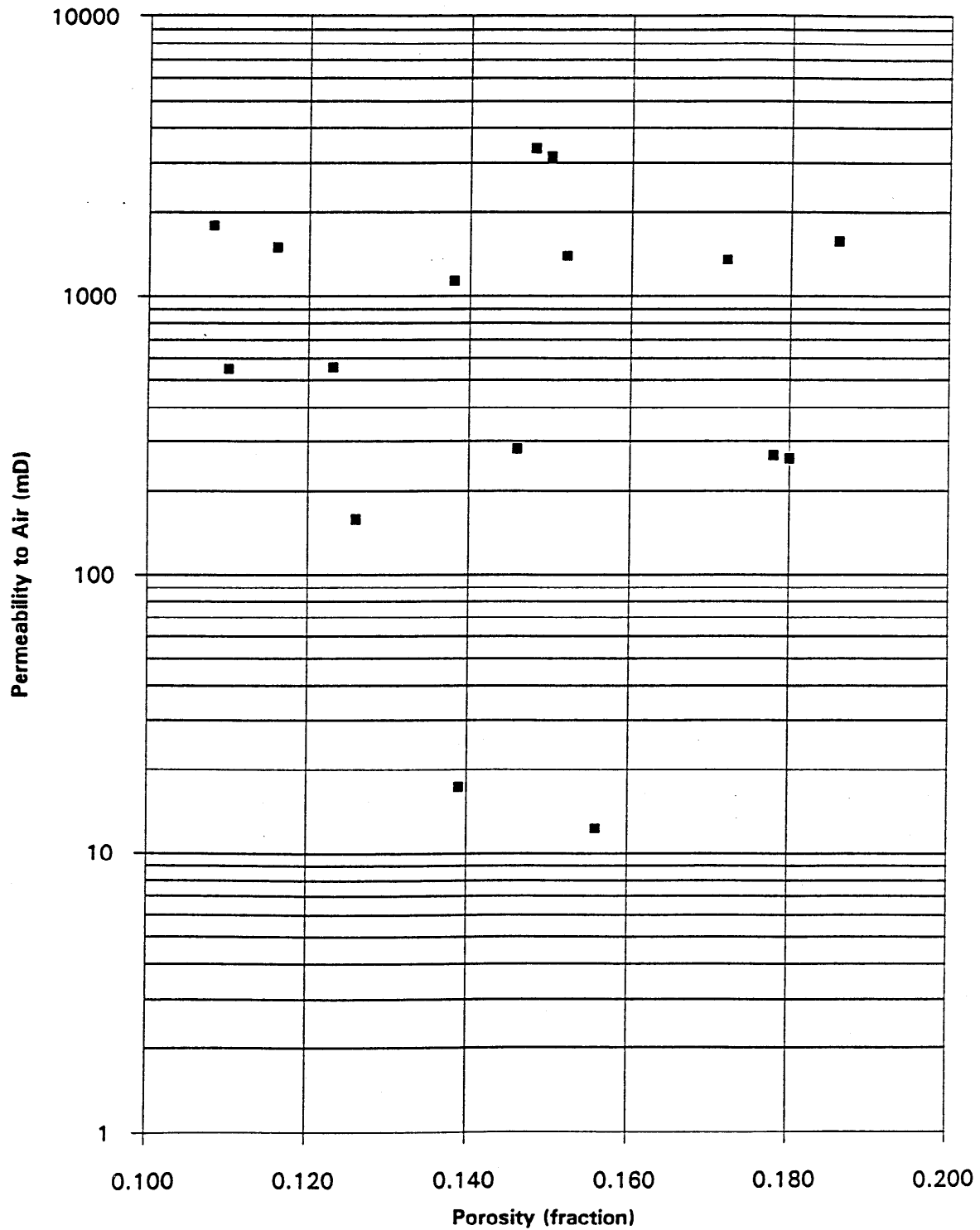
Table II

Sample Number	Depth, metres	Overburden Permeability to Air, millidarcies	Overburden Porosity, fraction	Grain Density (gms/cm <sup>3</sup> )
9	1823.47	1389	0.152	
12	1828.15	1571	0.186	
17	1829.57	1494	0.116	
21	1830.77	1793	0.108	
24	1831.70	551	0.110	
31	1833.80	17.3	0.139	
34	1834.70	158	0.126	
37	1835.60	268	0.178	
49	1840.60	12.3	0.156	
50	1840.90	261	0.180	
52	1842.80	558	0.123	
53	1843.10	3366	0.148	
56	1844.05	283	0.146	
59	1844.90	1348	0.172	
61	1845.52	3145	0.150	
65	1846.72	1133	0.138	

# Porosity vs Permeability

Company: BHP Petroleum Pty Ltd  
Well: Minerva 1

Overburden Pressure 2100 psi



## CONNATE WATER SATURATION

**Company** BHP Petroleum  
**Well** Minerva 1  
**Test Method** Centrifuge Air/Brine Drainage  
**Ambient**  
**Phase 1a**

Table III

Sample Number	Capillary Pressure, psi	Permeability to Air, millidarcies	Porosity, fraction	Average Saturation, fraction	End-Face* Saturation
24	77.8	701	0.1200	.075	0.065
50	93.5	318	0.1870	.178	0.158
59	93.6	1601	0.1770	.100	0.088
61	93.7	5641	0.1570	.081	0.071

\* End-Face saturation (extrapolated)

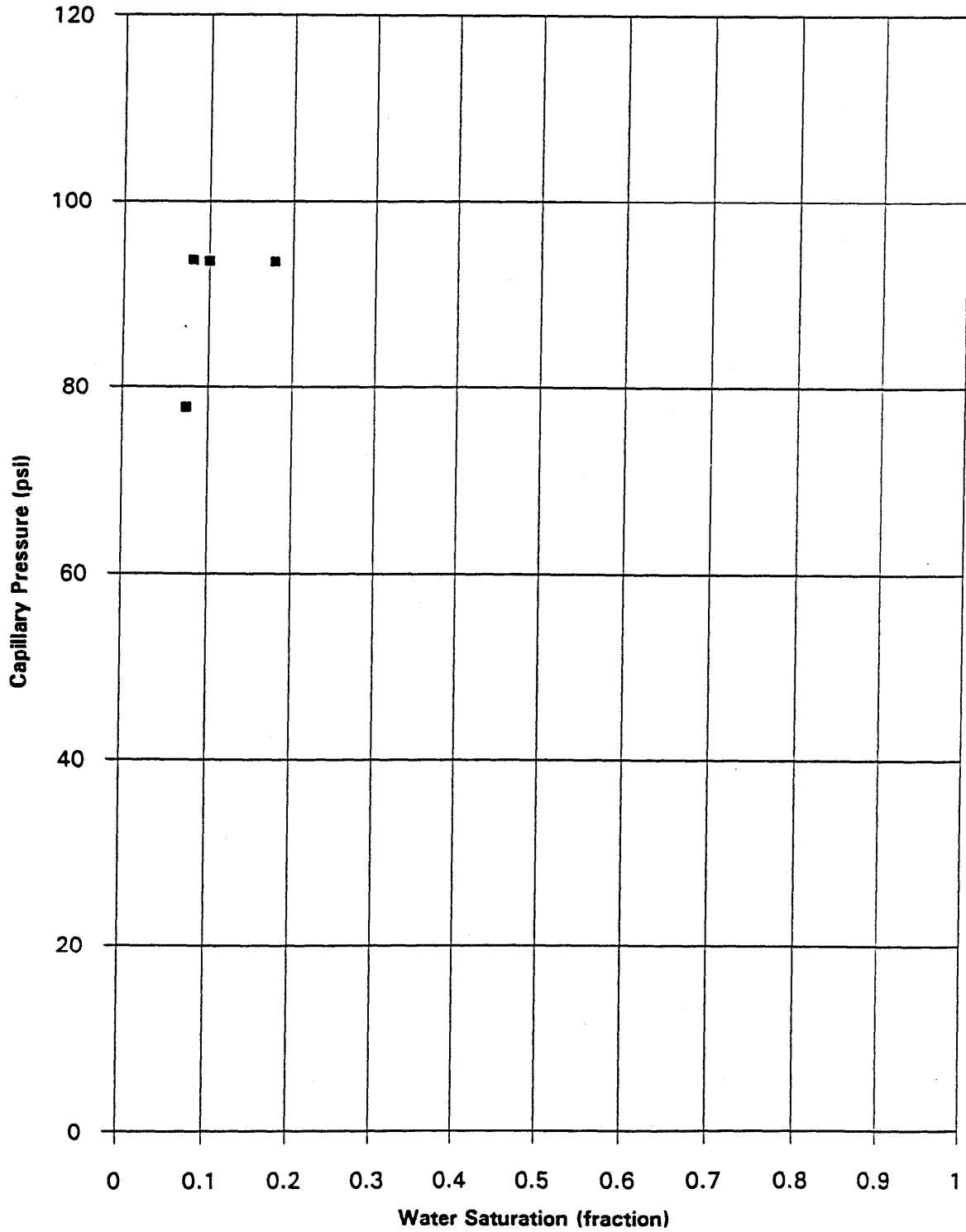
# Connate Water Saturation

Company: BHP Petroleum Pty Ltd

Well: Minerva 1

Ambient

Phase 1a





## CAPILLARY PRESSURE

Company	BHP Petroleum
Well	Minerva 1
Test Method	Centrifuge: Air/Brine Drainage
Sample Number	21
Depth	1830.77 metres
Permeability to Air	2502 millidarcies
Porosity	0.118 fraction
Ambient	

Phase 1b

Table IV

Capillary Pressure (psi)	Average Saturation, fraction	End-Face Saturation, fraction
0.4	0.722	0.216
1.9	0.243	0.113
3.8	0.165	0.088
6.9	0.134	0.075
10.8	0.119	0.068
16.2	0.104	0.063
22.0	0.088	0.060
28.3	0.077	0.058
36.6	0.070	0.056
43.8	0.068	0.055
63.6	0.068	0.053
69.1	0.067	0.053
74.7	0.067	0.053
86.6	0.067	0.052

# Capillary Pressure

Company: BHP Petroleum Pty Ltd

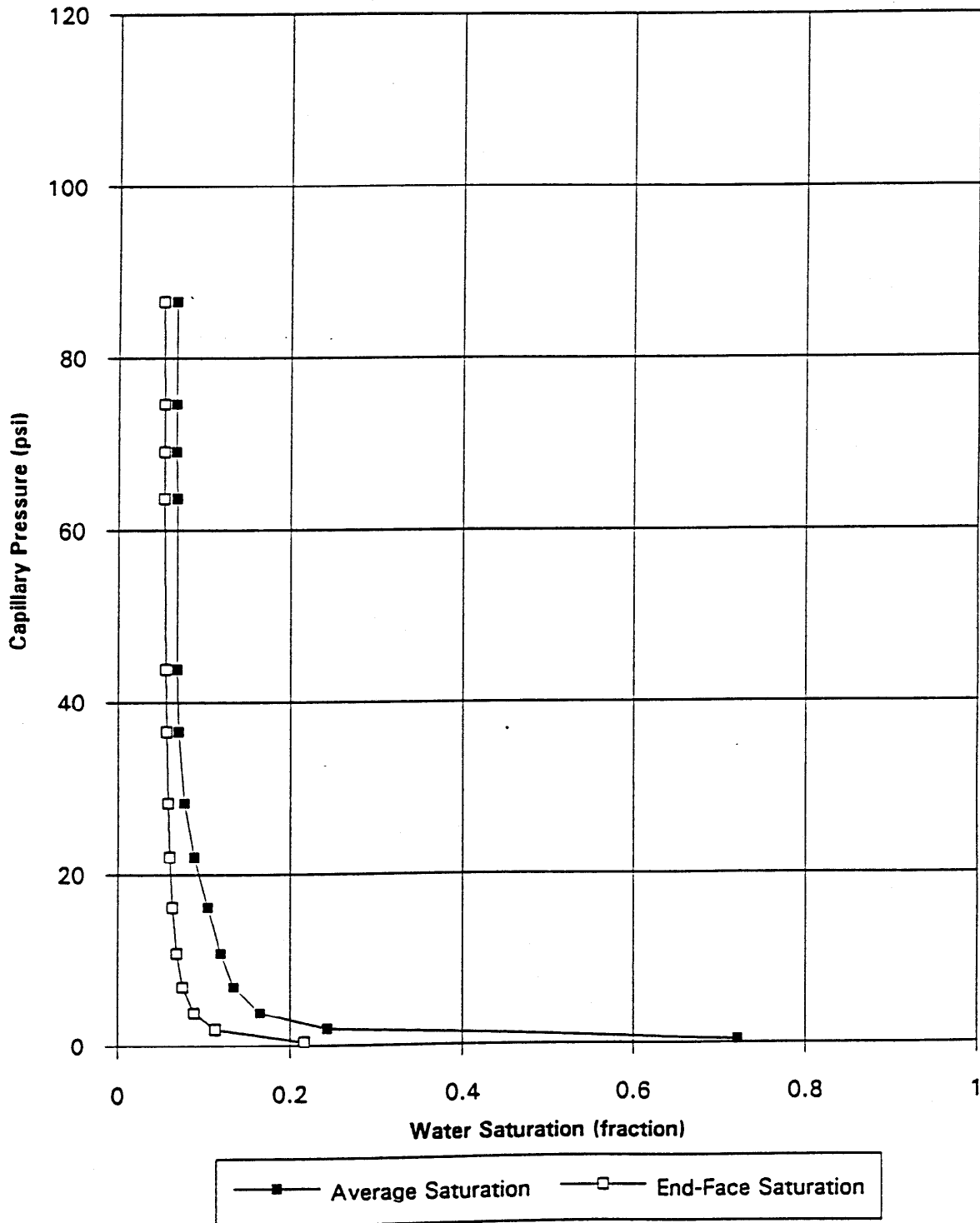
Well: Minerva 1

Sample: 21

Test Method: Centrifuge Air/Brine Drainage

Ambient

Phase 1b



## CAPILLARY PRESSURE

Company	BHP Petroleum
Well	Minerva 1
Test Method	Centrifuge: Air/Brine Drainage
Sample Number	31
Depth	1833.80 metres
Permeability to Air	23.3 millidarcies
Porosity	0.147 fraction
Ambient	

Phase 1b

Table V

Capillary Pressure (psi)	Average Saturation, fraction	End-Face Saturation, fraction
0.5	0.853	0.794
2.2	0.818	0.553
4.7	0.689	0.445
8.3	0.583	0.385
13.1	0.501	0.350
19.6	0.436	0.325
26.6	0.407	0.309
34.2	0.377	0.299
44.3	0.346	0.289
53.0	0.330	0.283
77.0	0.324	0.272
83.6	0.321	0.270
90.4	0.320	0.268
104.8	0.318	0.265

# Capillary Pressure

Company: BHP Petroleum Pty Ltd

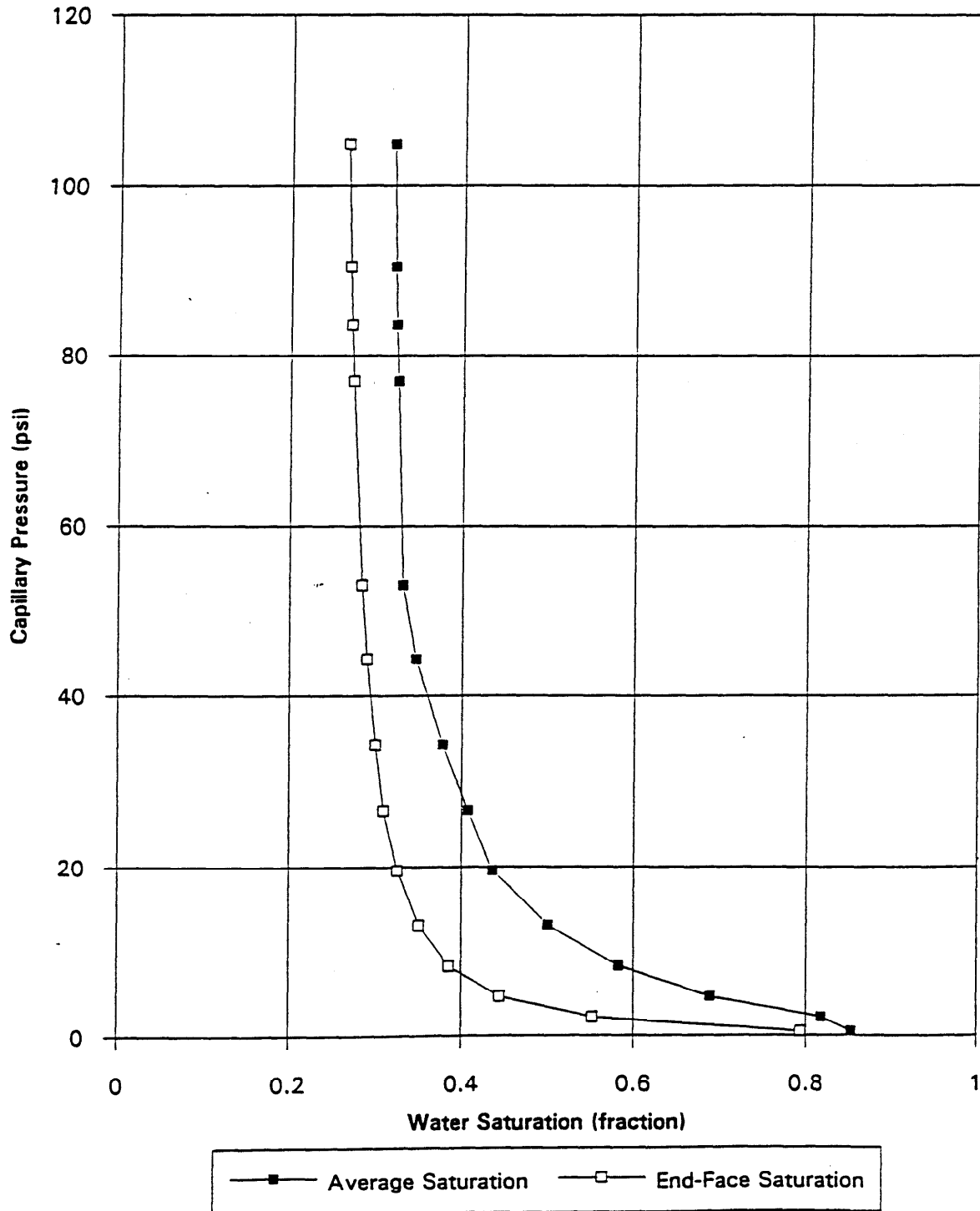
Well: Minerva 1

Sample: 31

Test Method: Centrifuge Air/Brine Drainage

Ambient

Phase 1b



## CAPILLARY PRESSURE

Company	BHP Petroleum
Well	Minerva 1
Test Method	Centrifuge: Air/Brine Drainage
Sample Number	56
Depth	1844.05 metres
Permeability to Air	402 millidarcies
Porosity	0.152 fraction
Ambient	

Phase 1b

Table VI

Capillary Pressure (psi)	Average Saturation, fraction	End-Face Saturation, fraction
0.5	0.707	0.506
2.2	0.448	0.282
4.6	0.307	0.216
8.3	0.254	0.179
13.1	0.200	0.157
19.6	0.166	0.140
26.6	0.149	0.130
34.2	0.132	0.123
44.2	0.121	0.115
52.9	0.119	0.112
76.9	0.114	0.104
83.5	0.113	0.103
90.3	0.113	0.100
104.7	0.113	0.099

# Capillary Pressure

Company: BHP Petroleum Pty Ltd

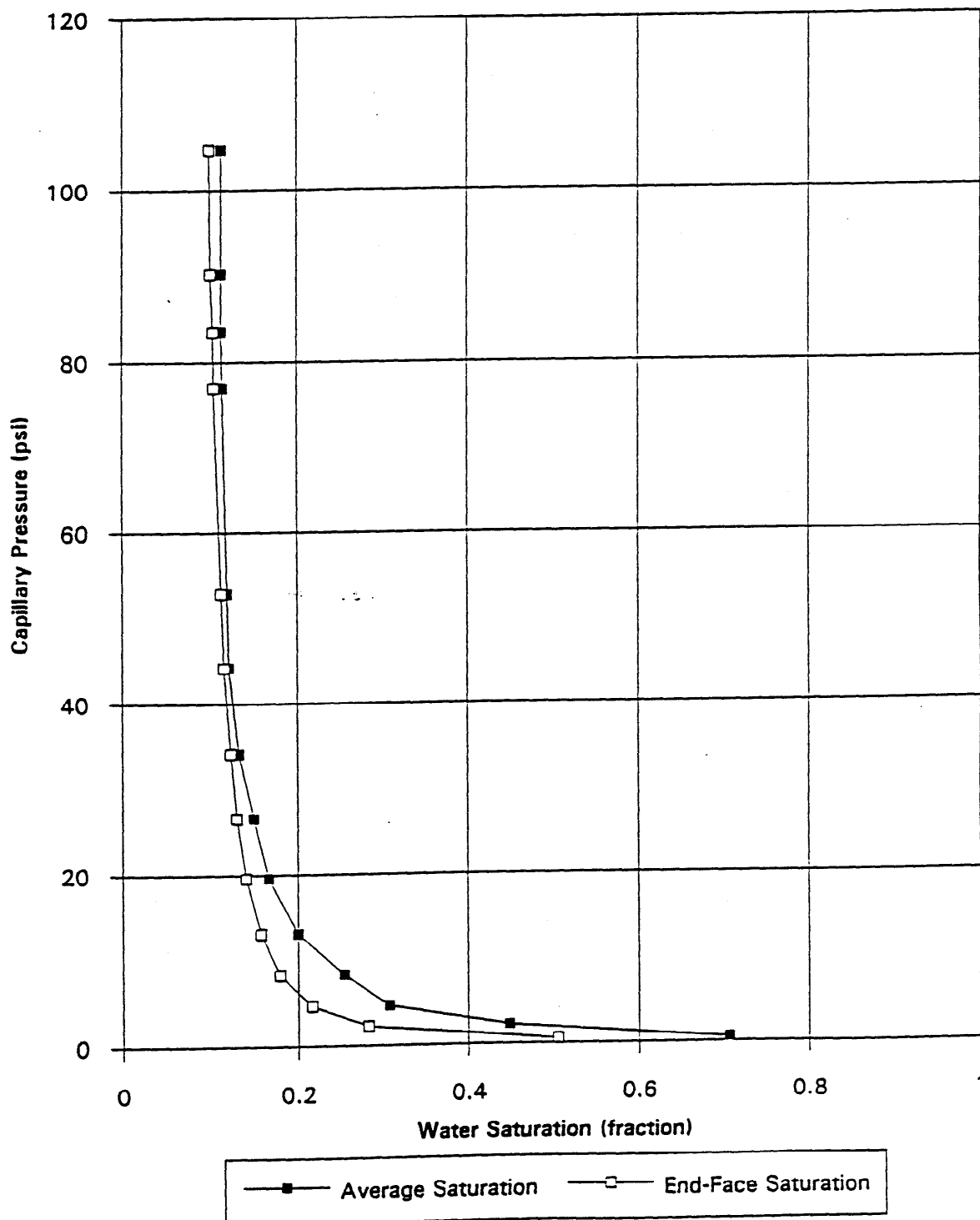
Well: Minerva 1

Sample: 56

Test Method: Centrifuge Air/Brine Drainage

Ambient

Phase 1b



## CAPILLARY PRESSURE

Company BHP Petroleum  
 Well Minerva 1

Test Method Centrifuge: Air/Brine Drainage  
 Sample Number 65  
 Depth 1846.77 metres  
 Permeability to Air 1371 millidarcies  
 Porosity 0.144 fraction  
 Ambient

Phase 1b

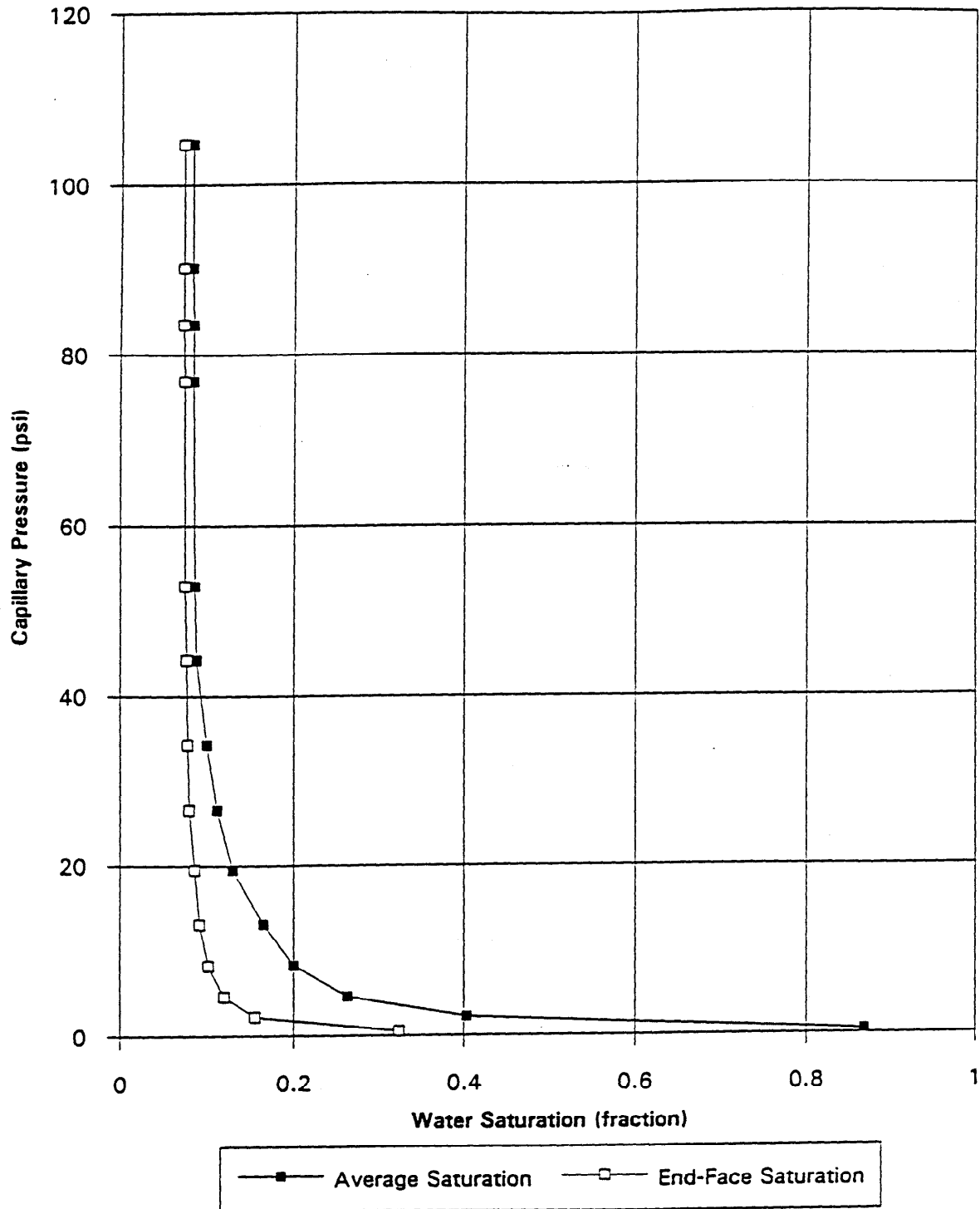
Table VII

Capillary Pressure (psi)	Average Saturation, fraction	End-Face Saturation, fraction
0.5	0.869	0.324
2.2	0.403	0.155
4.6	0.263	0.119
8.3	0.200	0.101
13.1	0.165	0.091
19.5	0.129	0.085
26.5	0.111	0.079
34.2	0.099	0.077
44.2	0.087	0.076
52.9	0.085	0.074
76.9	0.083	0.073
83.5	0.083	0.072
90.3	0.082	0.072
104.7	0.082	0.072

# Capillary Pressure

Company: BHP Petroleum Pty Ltd  
Well: Minerva 1  
Sample: 65

Test Method: Centrifuge Air/Brine Drainage  
Ambient  
Phase 1b





## FORMATION FACTOR

Company                    BHP Petroleum Pty Ltd  
Well                        Minerva 1

Saturant                    35,000 ppm brine  
Rw of Saturant            0.18 ohm-m @ 25°C  
Overburden Pressure    2100 psi

Phase 1c/d

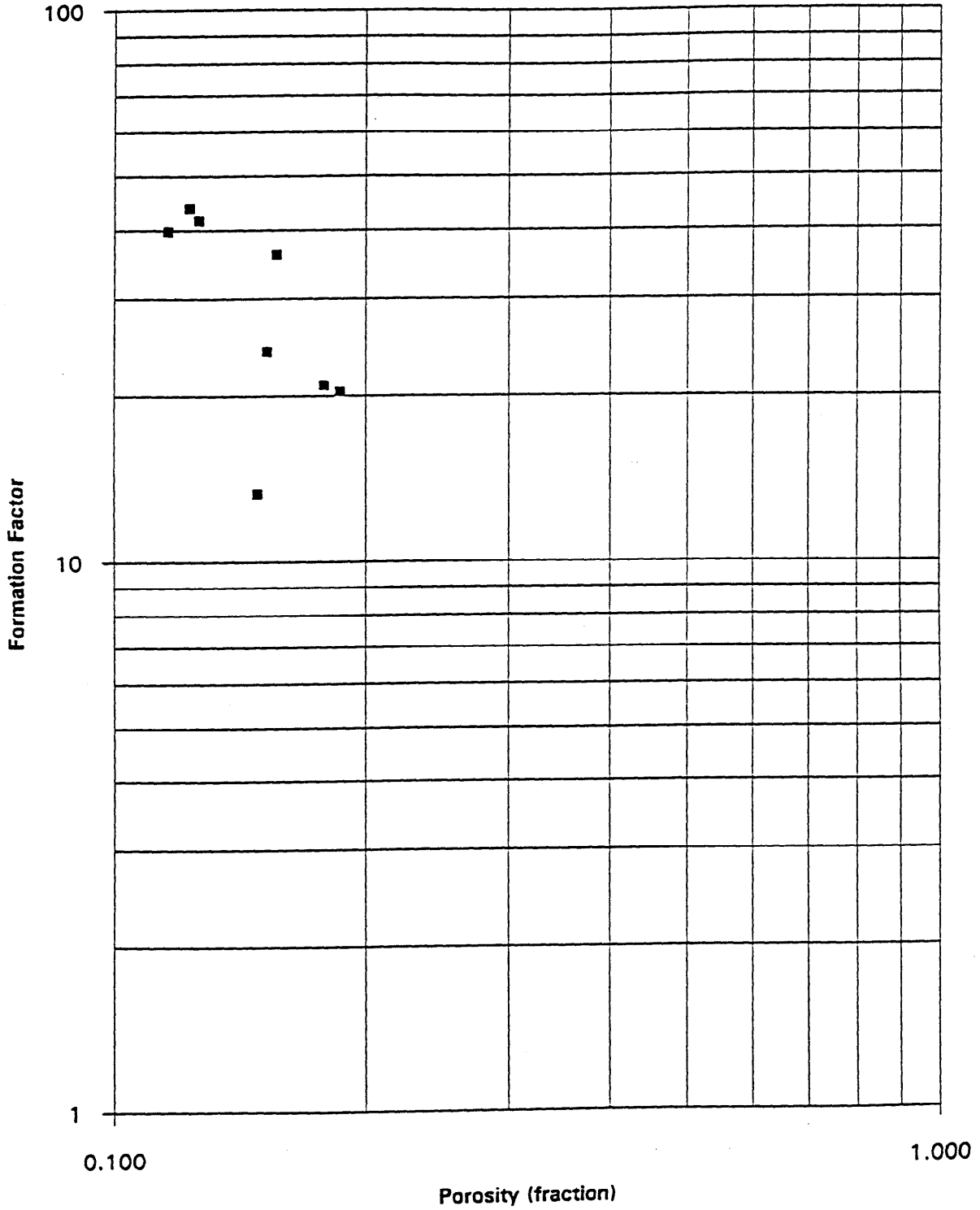
Table VIII

Sample Number	Depth, metres	Overburden Permeability to Air, millidarcies	Overburden Porosity, fraction	Formation Factor (FF)	Cementation Exponent, 'm'
9	1823.47	1389	0.152	24.1	1.69
12	1828.15	1571	0.186	20.4	1.79
17	1829.57	1494	0.116	39.8	1.71
34	1834.70	158	0.126	41.6	1.80
37	1835.60	268	0.178	20.9	1.76
49	1840.60	12.3	0.156	36.0	1.93
52	1842.80	558	0.123	43.8	1.80
53	1843.10	3366	0.148	13.3	1.36

# Formation Factor

Company: BHP Petroleum Pty Ltd  
Well: Minerva 1

Overburden Pressure 2100 psi  
Phase 1c/d



## RESISTIVITY INDEX

Company BHP Petroleum Pty Ltd  
Well Minerva 1

Saturant 35,000 ppm brine  
Rw of Saturant 0.18 ohm-m @ 25°C  
Overburden Pressure 2,100 psi

Phase 1c/d Table IX

Sample Number	Depth, metres	Overburden Permeability to Air, millidarcies	Overburden Porosity, fraction	Formation Factor (FF)	Brine Saturation, fraction	Resistivity Index (RI)	Saturation Exponent, 'n'
9	1823.47	1389	0.152	24.0	1.000	1.00	-
					0.751	1.65	1.73
					0.475	3.54	1.78
					0.374	5.86	1.80
					0.314	8.85	1.88
					0.279	11.1	1.89
					0.258	13.7	1.93
					0.223	19.5	1.98
					0.199	26.6	2.01
					0.118	72.3	2.00
				0.074	195	2.01	
					mean 'n'	1.90	
12		1571	0.186	20.3	1.000	1.00	-
					0.743	1.69	1.77
					0.422	4.49	1.74
					0.372	5.60	1.74
					0.327	6.53	1.68
					0.283	7.96	1.64
					0.240	10.3	1.63
					0.224	10.9	1.60
					0.220	11.8	1.63
17		1494	0.116	39.8	1.000	1.00	-
					0.476	3.66	1.75
					0.383	5.52	1.78
					0.338	7.12	1.81
					0.294	8.92	1.77
					0.194	18.7	1.79
					0.168	23.3	1.77
					0.148	33.0	1.83
					mean 'n'	1.87	

Sample Number	Depth, metres	Overburden Permeability to Air, millidarcies	Overburden Porosity, fraction	Formation Factor (FF)	Brine Saturation, fraction	Resistivity Index (RI)	Saturation Exponent, 'n'
34	1834.70	158	0.126	41.6	1.000	-	-
					0.753	1.73	1.93
					0.725	1.85	1.91
					0.674	2.12	1.90
					0.546	3.18	1.91
					0.490	3.98	1.93
					0.455	4.73	1.97
					0.393	6.18	1.95
					0.374	6.68	1.93
						mean 'n'	1.93
37	1835.60	268	0.178	20.9	1.000	1.00	-
					0.681	2.13	1.97
					0.567	3.23	2.06
					0.473	4.61	2.04
					0.330	9.71	2.05
					0.294	12.5	2.06
					0.264	17.1	2.13
					0.248	18.6	2.10
	mean 'n'	2.06					
49	1840.60	12.3	0.156	37.2	1.000	1.00	-
					0.791	1.49	1.69
					0.653	2.35	1.88
					0.593	2.68	1.89
					0.543	3.24	1.92
					0.458	4.44	1.91
					0.401	5.79	1.92
	mean 'n'	1.87					
52	1842.80	558	0.123	43.8	1.000	1.00	-
					0.822	1.47	1.97
					0.464	4.55	1.97
					0.368	7.46	2.01
					0.344	8.71	2.03
					0.250	15.1	1.96
					0.224	17.6	1.91
					0.197	26.4	2.01
					0.184	27.9	1.96
					0.177	30.0	1.96
	mean 'n'	1.98					

Sample Number	Depth, metres	Overburden Permeability to Air, millidarcies	Overburden Porosity, fraction	Formation Factor (FF)	Brine Saturation, fraction	Resistivity Index (RI)	Saturation Exponent, 'n'
53	1843.10	3366	0.148	13.3	1.000	1.00	-
					0.323	10.0	2.04
					0.255	14.6	1.96
					0.193	21.8	1.88
					0.179	27.4	1.93
					0.158	34.9	1.93
					0.137	45.1	1.92
					0.111	68.8	1.92
						mean 'n'	1.94

# Resistivity Index

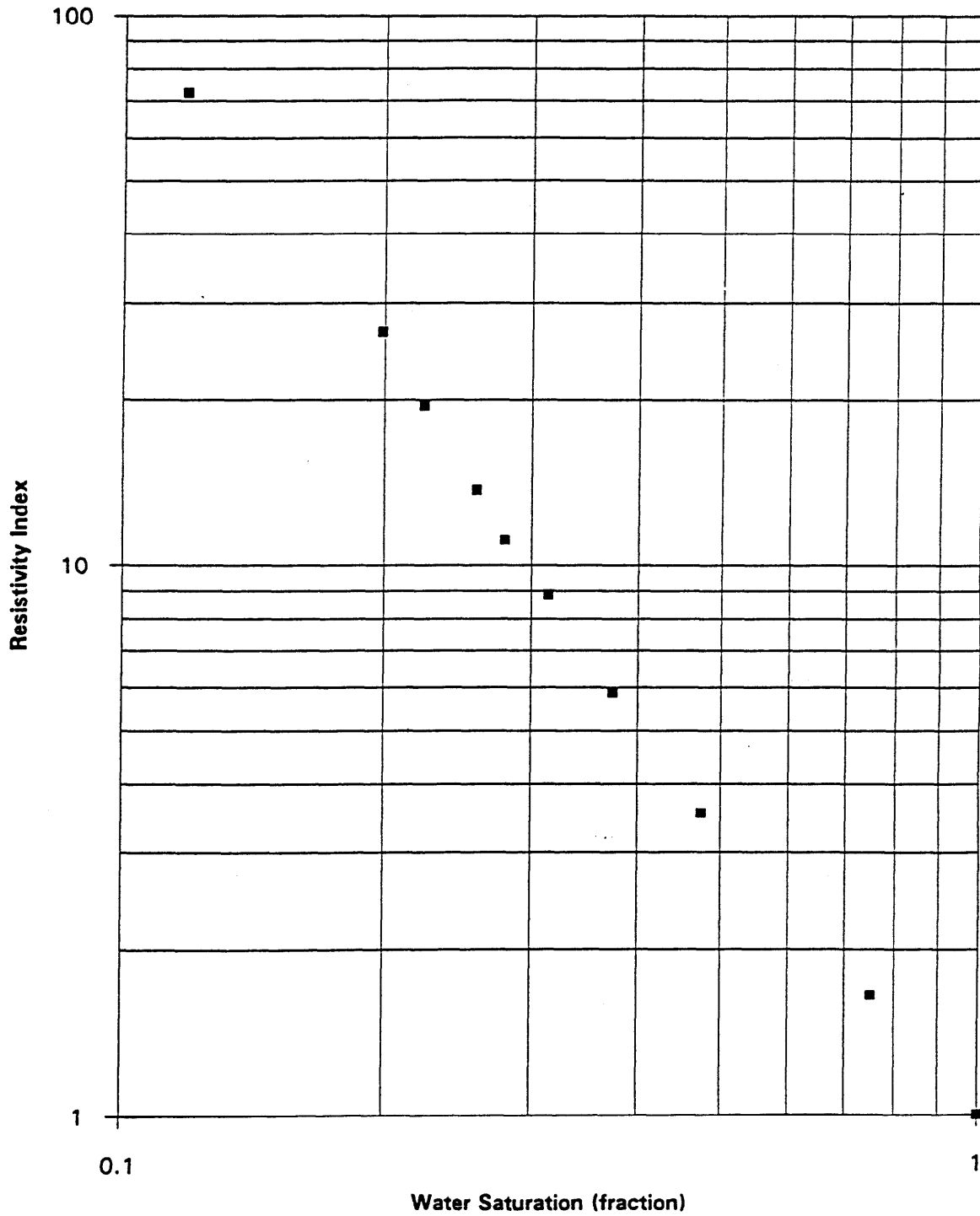
Company: BHP Petroleum Pty Ltd

Well: Minerva 1

Sample: 9

Overburden Pressure 2100 psi

Phase 1c/d



# Resistivity Index

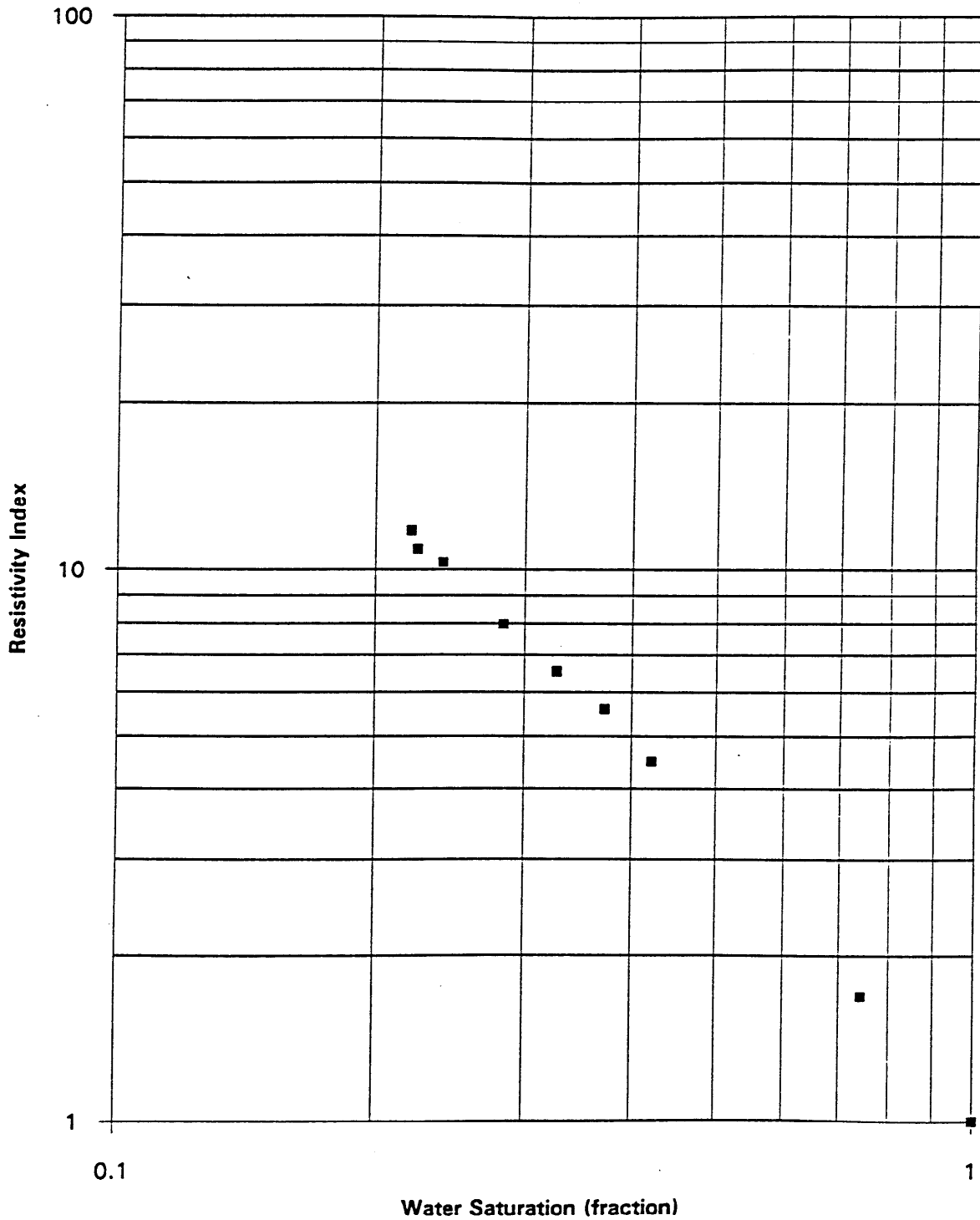
Company: BHP Petroleum Pty Ltd

Well: Minerva 1

Sample: 12

Overburden Pressure 2100 psi

Phase 1c/d



# Resistivity Index

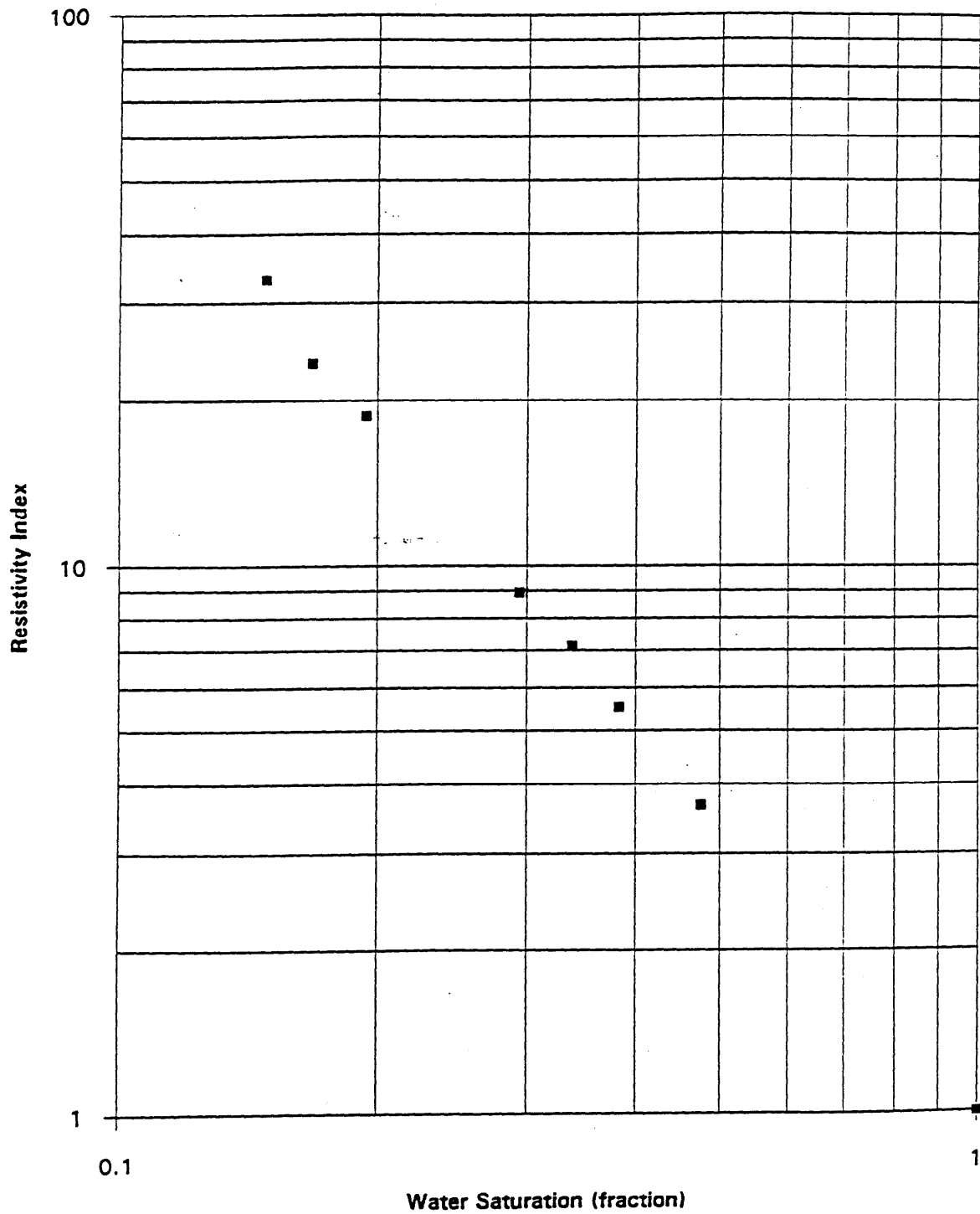
Company: BHP Petroleum Pty Ltd

Well: Minerva 1

Sample: 17

Overburden Pressure 2100 psi

Phase Ic/d

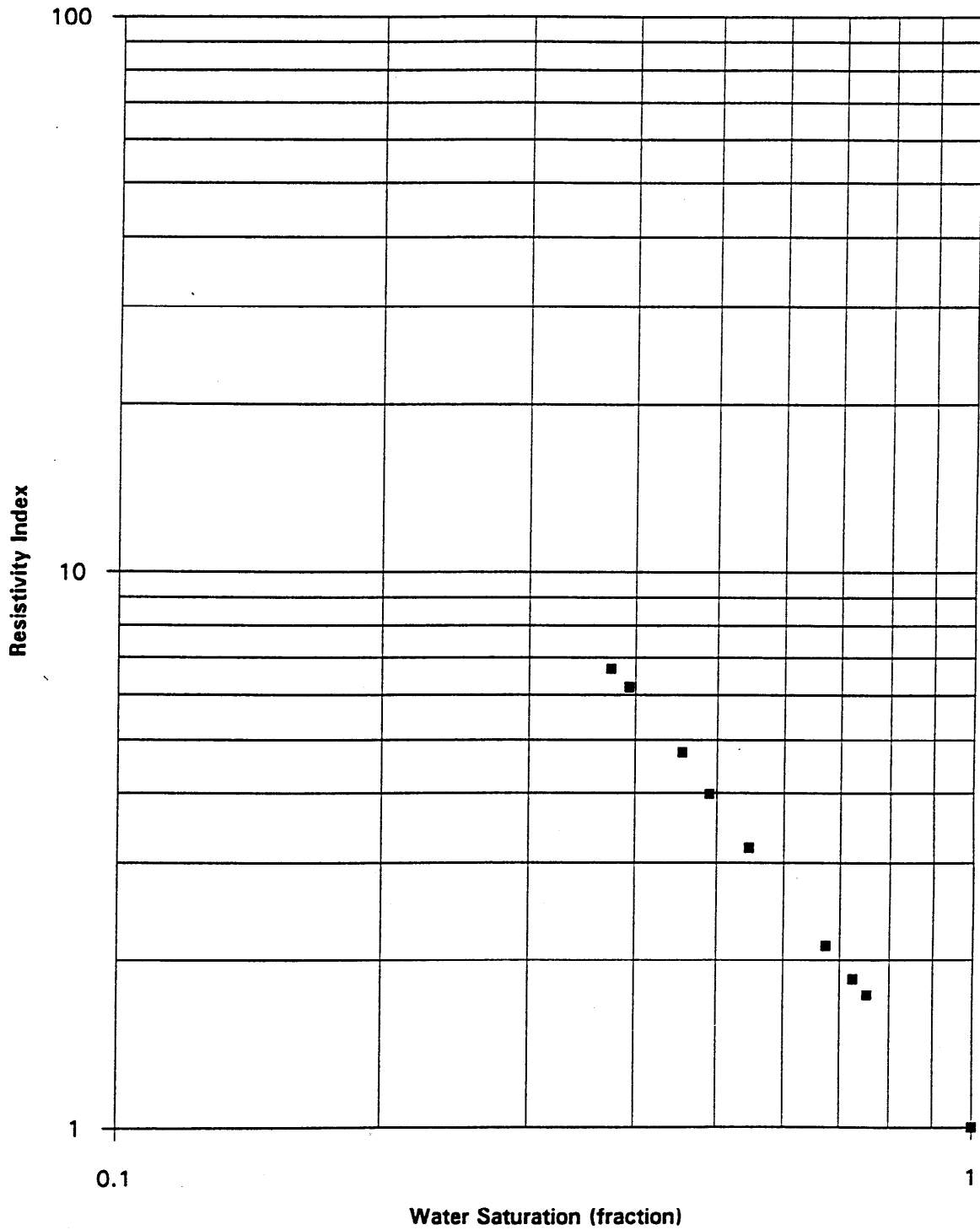




# Resistivity Index

Company: BHP Petroleum Pty Ltd  
Well: Minerva 1  
Sample: 34

Overburden Pressure 2100 psi  
Phase 1c/d



# Resistivity Index

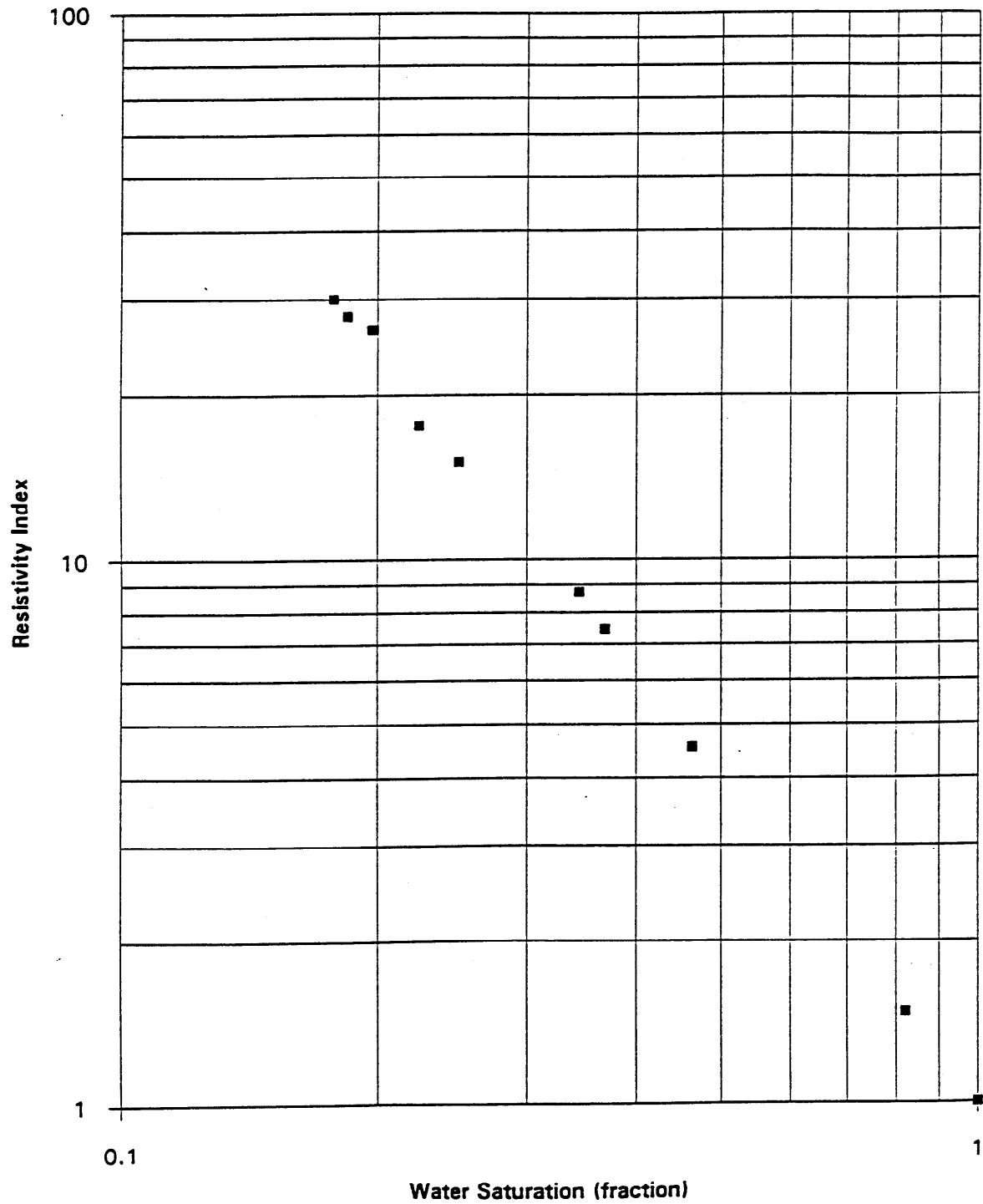
Company: BHP Petroleum Pty Ltd

Well: Minerva 1

Sample: 52

Overburden Pressure 2100 psi

Phase 1c/d



# Resistivity Index

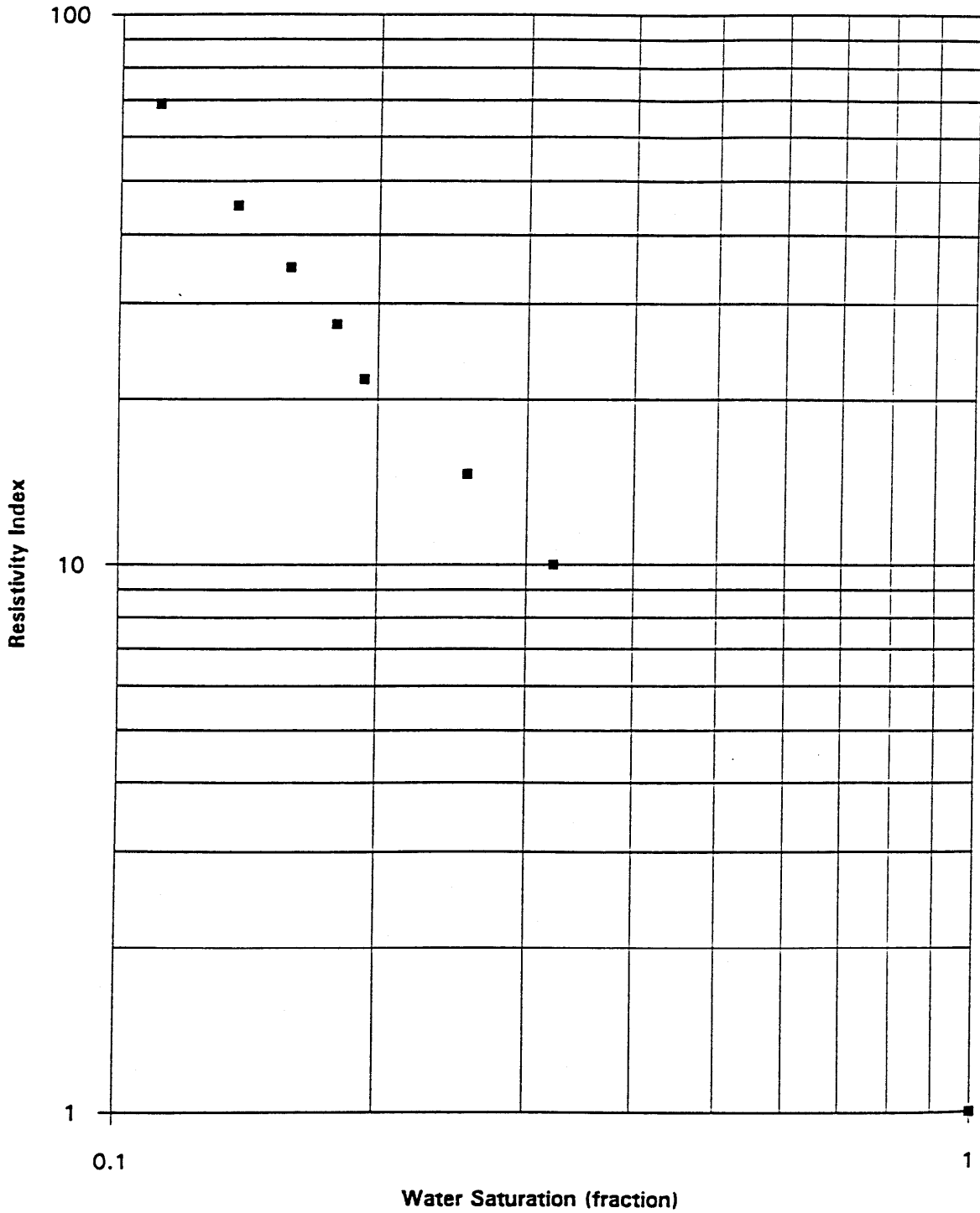
Company: BHP Petroleum Pty Ltd

Well: Minerva 1

Sample: 53

Overburden Pressure 2100 psi

Phase 1c/d



CAPILLARY PRESSURE - ATTACHEMNT 1

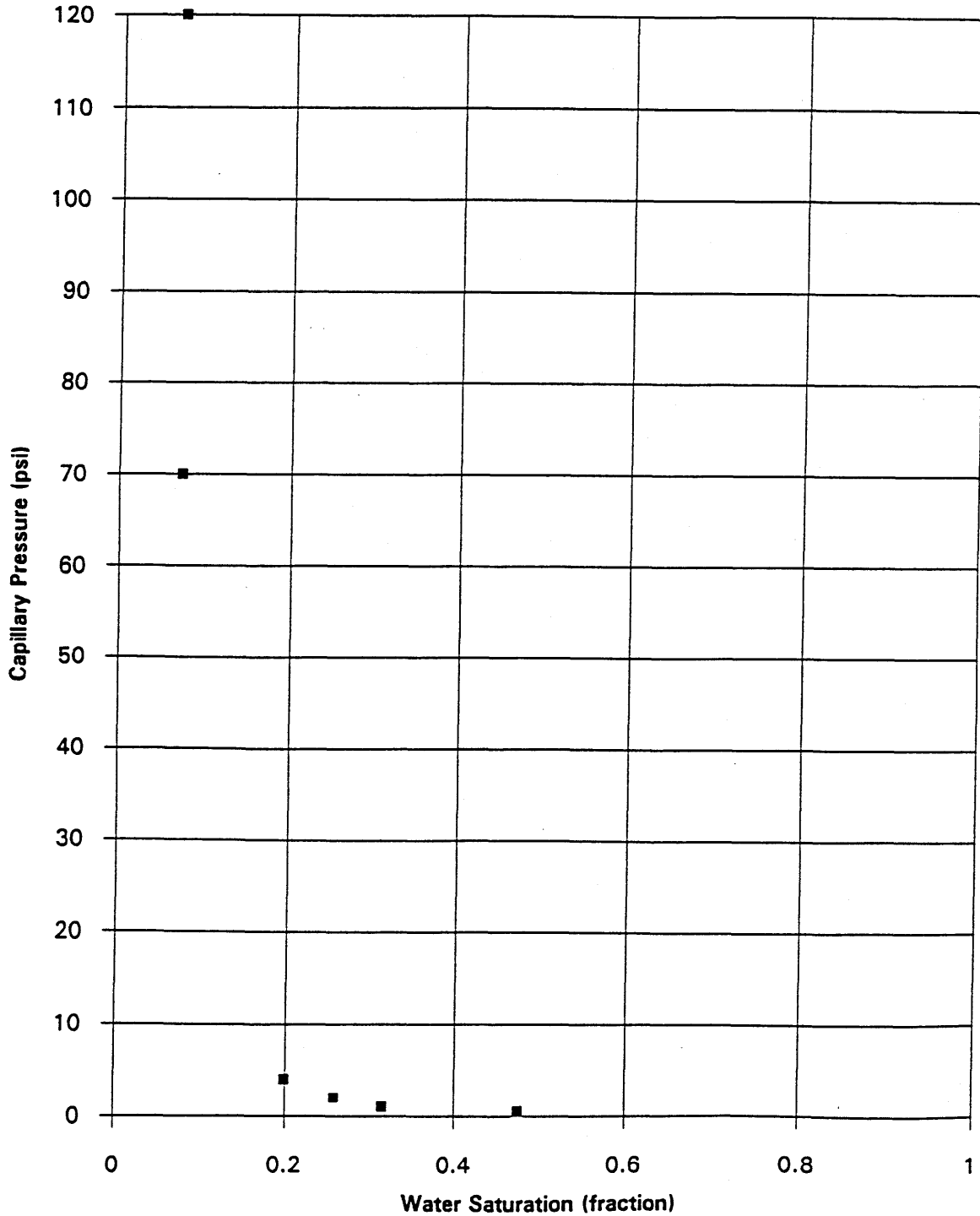
Company BHP Petroleum Pty Ltd  
 Well Minerva 1  
 Test Method Air/Brine Porous Plate Drainage  
 Overburden Pressure 2100 psi

Phase 1c/d Table X

Sample Number	Depth, metres	Permeability to air, millidarcies	Porosity, fraction	Pressure (psi)									
				0.5	1.0	2.0	4.0	10 15 30 Saturation, fraction			70 120 200 (interpolated)		
9	1823.47	1389	0.152	0.475	0.314	0.258	0.199	-	-	-	0.074	0.071	0.065
12	1828.15	1571	0.186	0.743	0.422	0.372	0.327	-	-	-	0.224	0.222	0.220
17	1829.57	1494	0.116	0.476	0.383	0.338	0.294	-	-	-	0.150	0.149	0.148
34	1834.70	158	0.126	0.858	0.753	0.725	0.674	-	-	-	0.393	0.386	0.374
37	1835.60	268	0.178	-	0.681	0.567	0.473	-	0.294	-	0.248	0.240	0.227
49	1840.60	12.3	0.156	-	-	-	0.791	0.635	0.593	0.543	0.458	0.436	0.401
52	1842.80	558	0.123	0.822	0.464	0.368	-	-	0.224	0.197	-	0.187	0.177
53	1843.10	3366	0.148	0.255	0.193	-	0.158	-	0.111	-	0.099	0.098	0.098

# Capillary Pressure

Company: BHP Petroleum Pty Ltd  
Well: Minerva 1  
Sample: 9  
Test Method: Porous Plate Air/Brine Drainage  
Overburden Pressure 2100 psi  
Phase 1c/d



# Capillary Pressure

Company: BHP Petroleum Pty Ltd

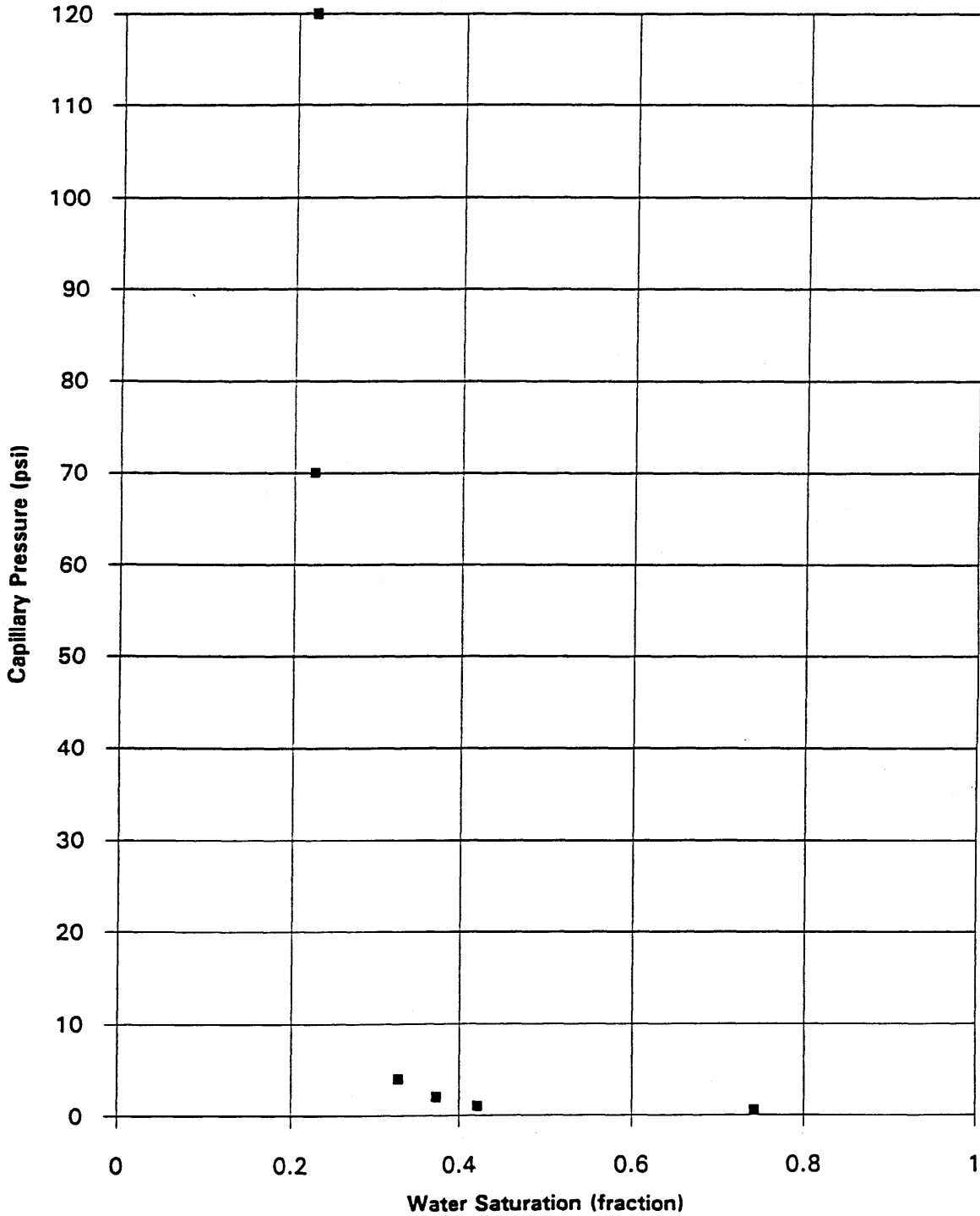
Well: Minerva 1

Sample: 12

Test Method: Porous Plate Air/Brine Drainage

Overburden Pressure 2100 psi

Phase 1c/d



# Capillary Pressure

Company: BHP Petroleum Pty Ltd

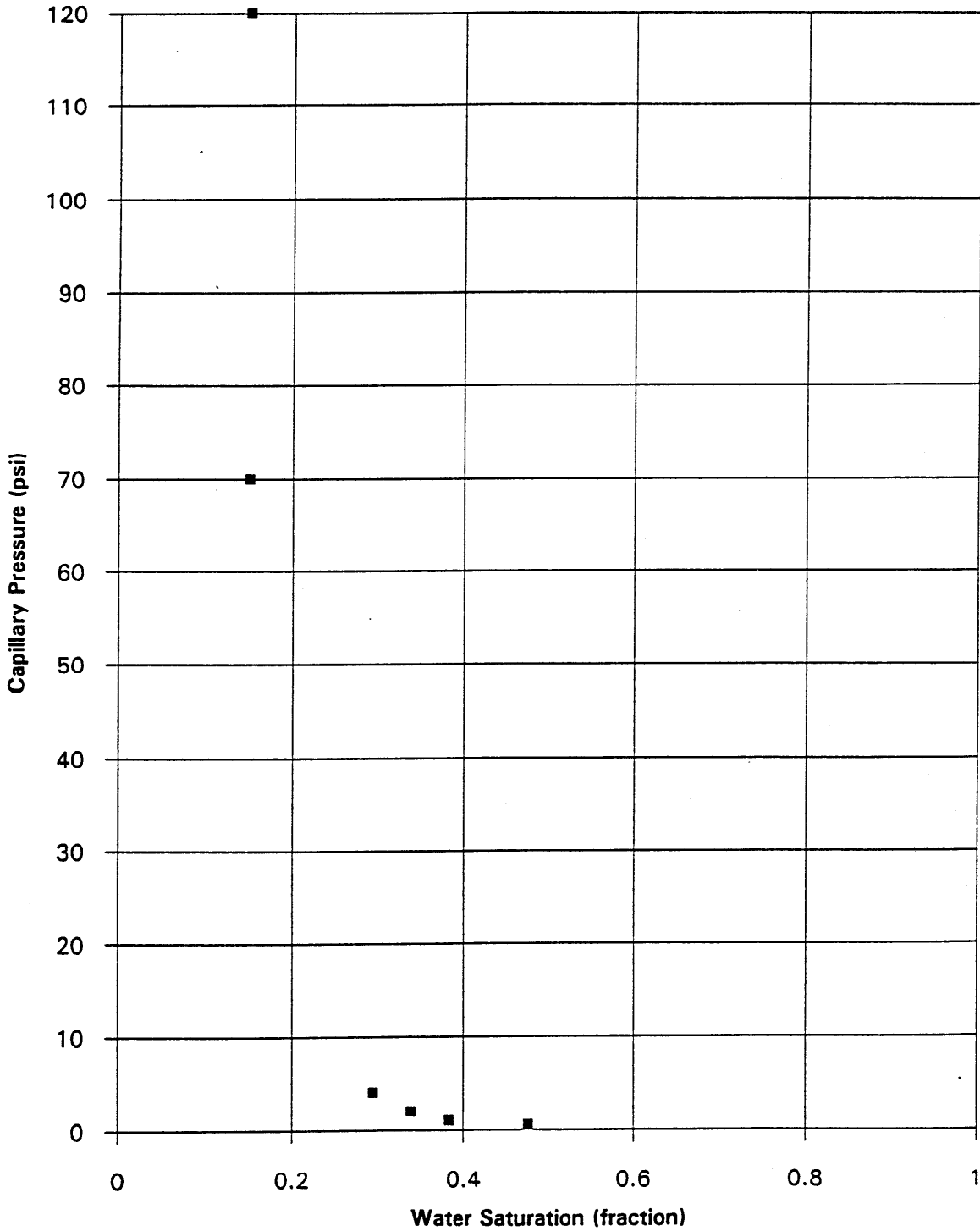
Well: Minerva 1

Sample: 17

Test Method: Porous Plate Air/Brine Drainage

Overburden Pressure 2100 psi

Phase 1c/d



# Capillary Pressure

Company: BHP Petroleum Pty Ltd

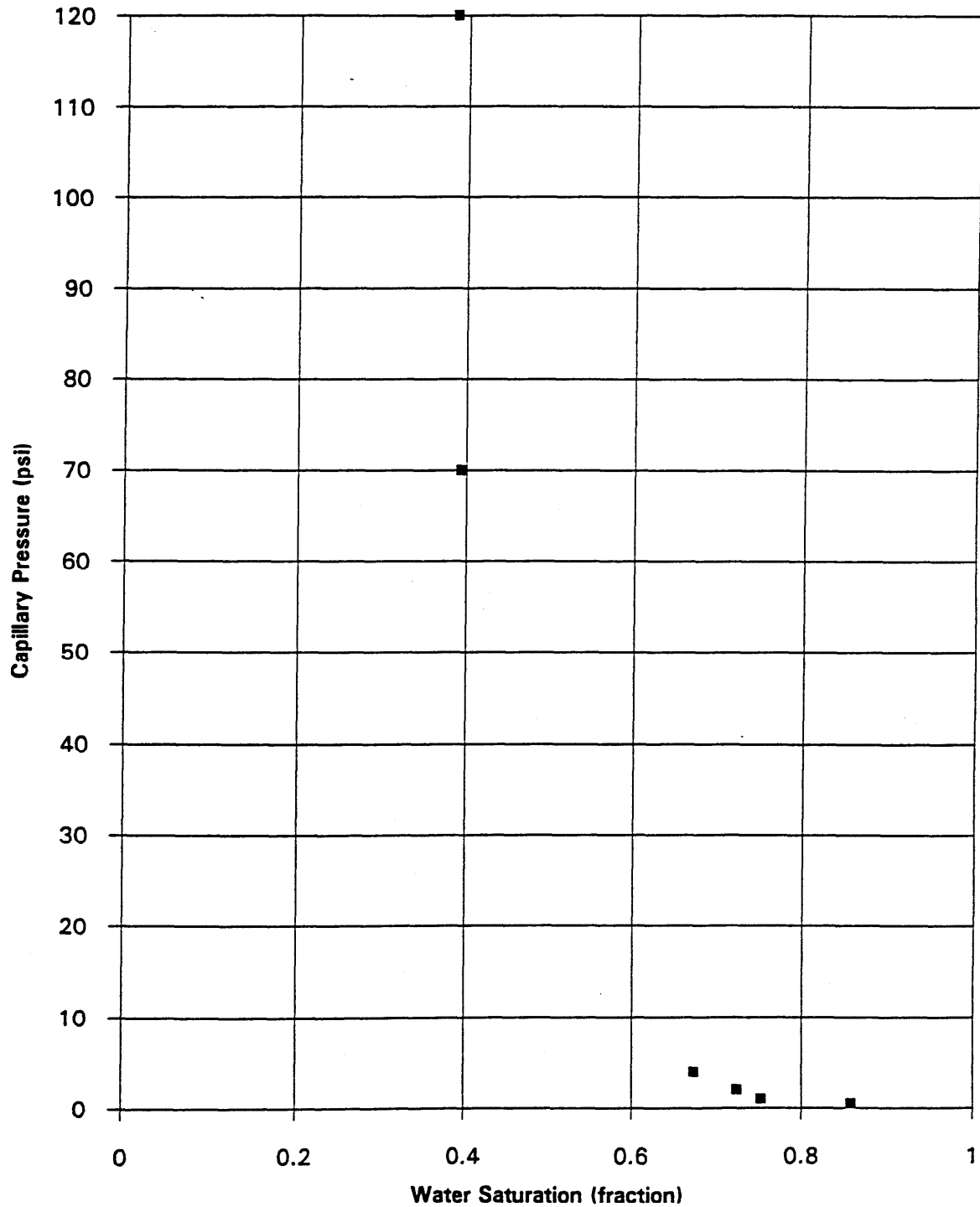
Well: Minerva 1

Sample: 34

Test Method: Porous Plate Air/Brine Drainage

Overburden Pressure 2100 psi

Phase 1c/d





# Capillary Pressure

Company: BHP Petroleum Pty Ltd

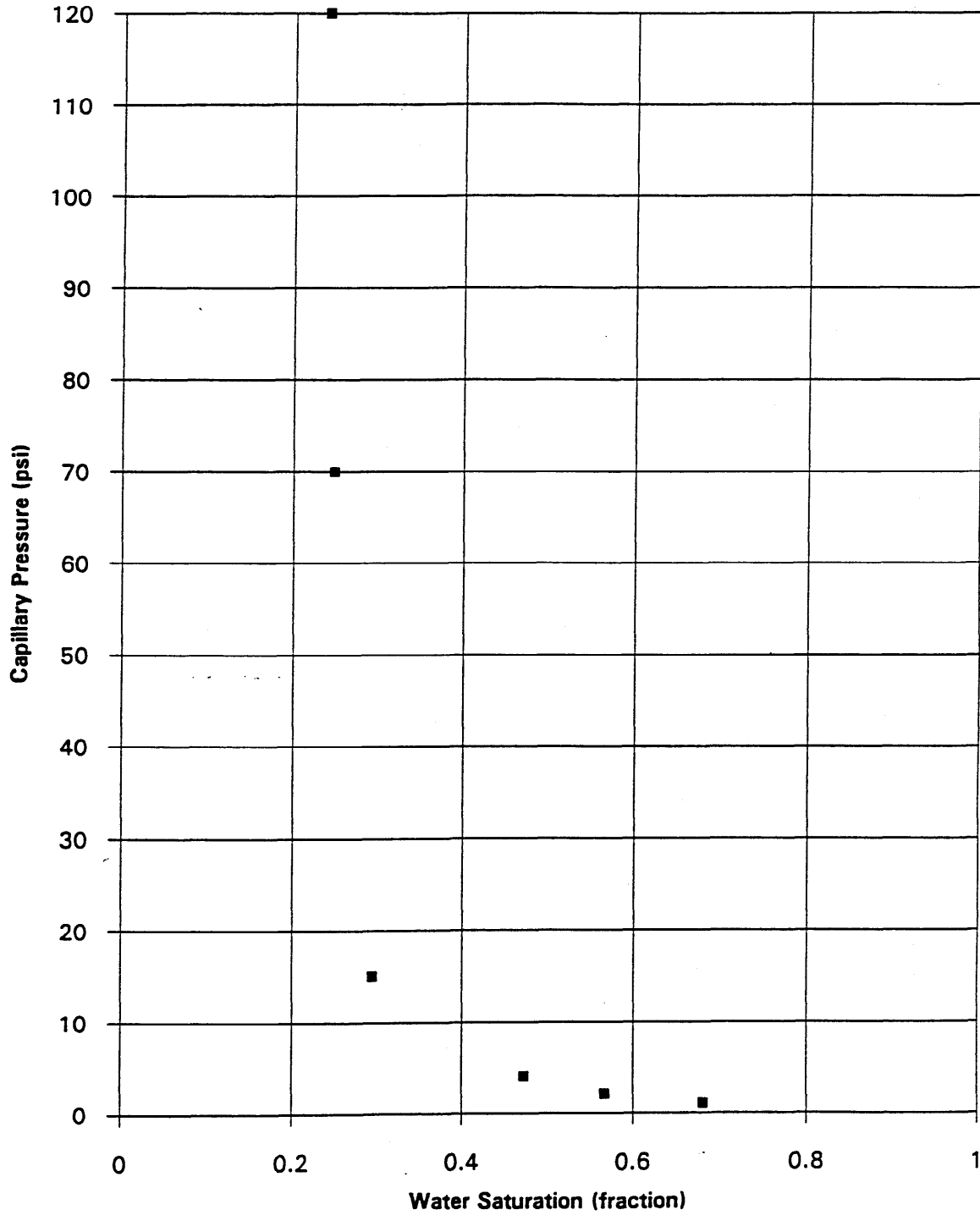
Well: Minerva 1

Sample: 37

Test Method: Porous Plate Air/Brine Drainage

Overburden Pressure 2100 psi

Phase 1c/d



# Capillary Pressure

Company: BHP Petroleum Pty Ltd

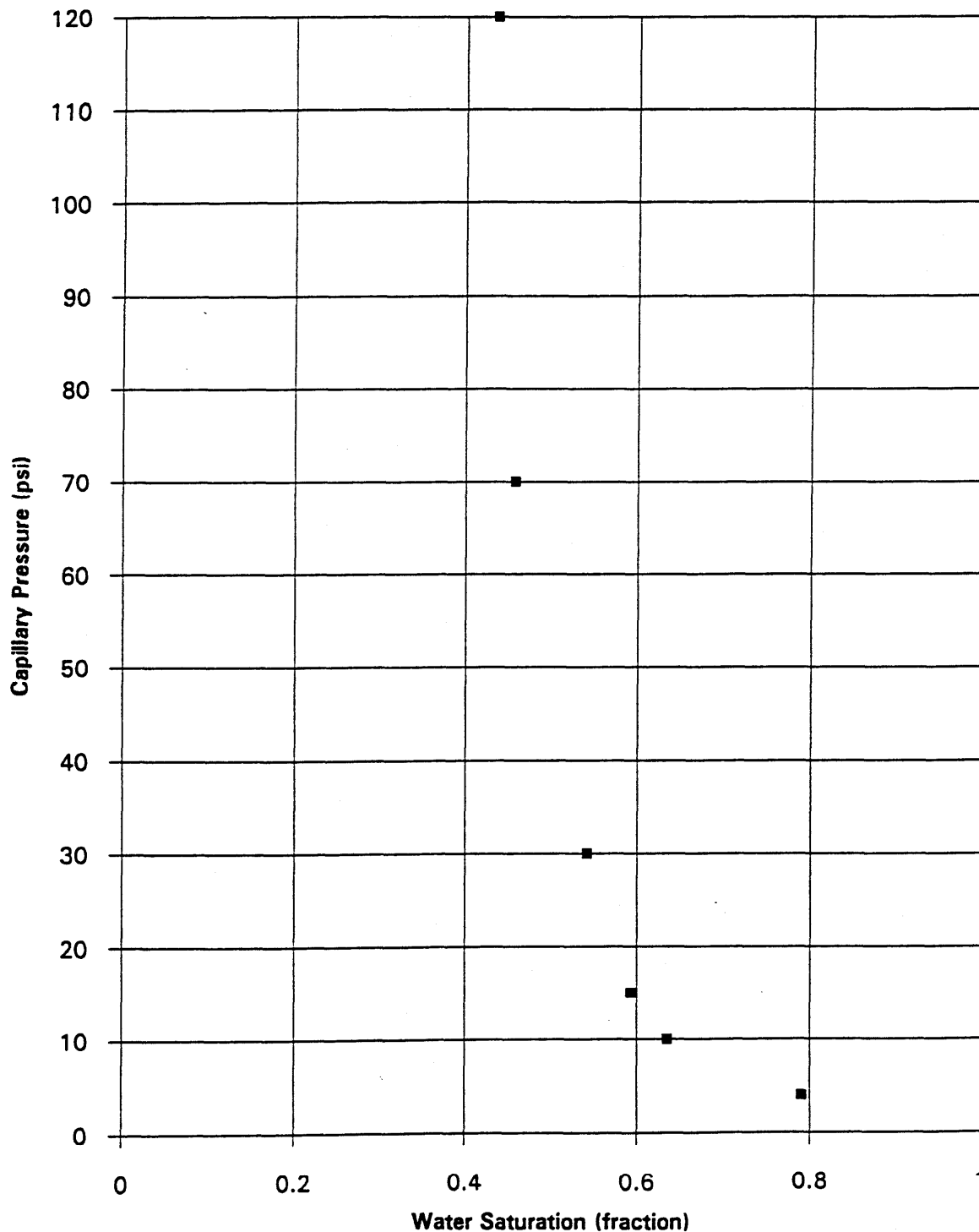
Well: Minerva 1

Sample: 49

Test Method: Porous Plate Air/Brine Drainage

Overburden Pressure 2100 psi

Phase 1c/d



# Capillary Pressure

Company: BHP Petroleum Pty Ltd

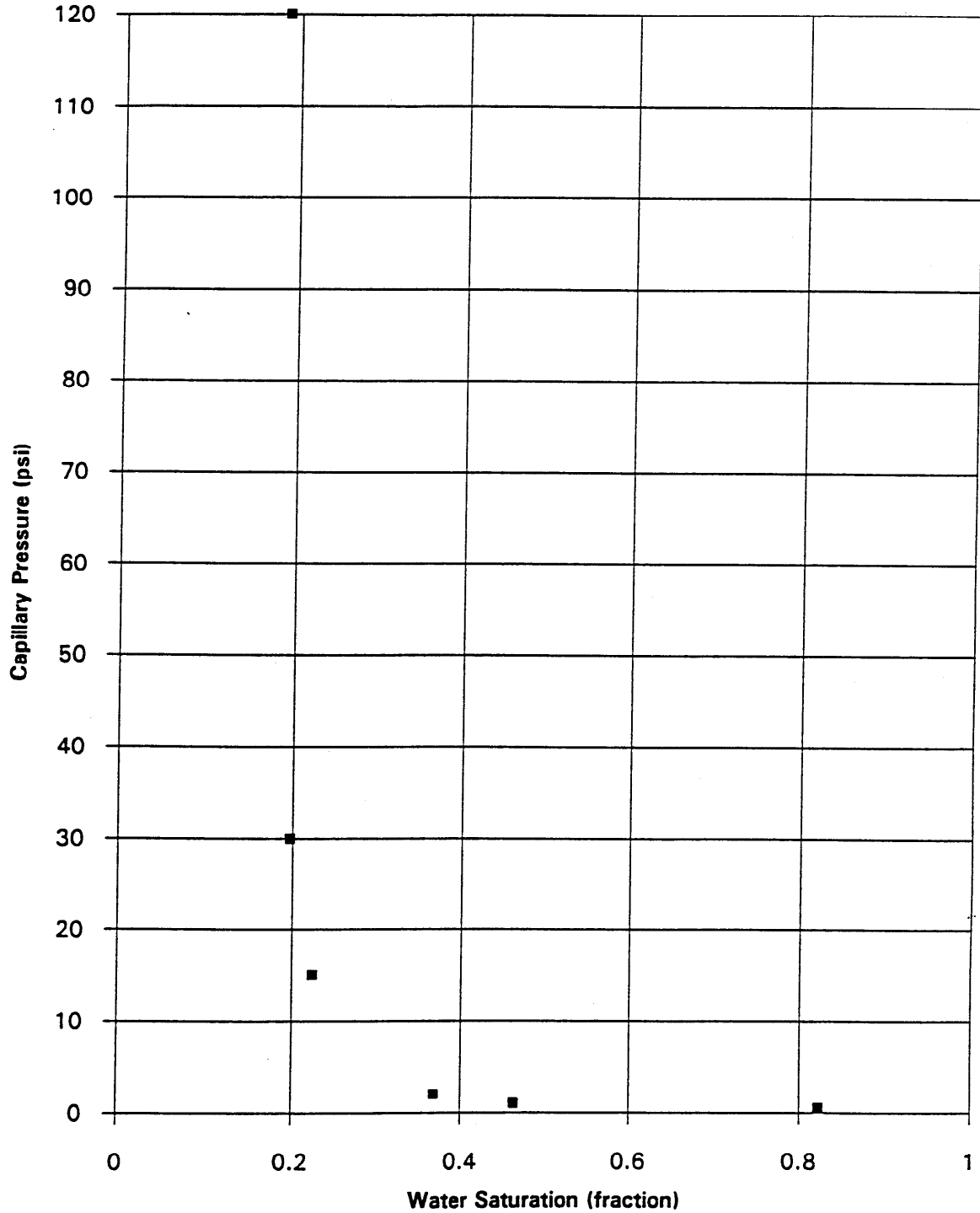
Well: Minerva 1

Sample: 52

Test Method: Porous Plate Air/Brine Drainage

Overburden Pressure 2100 psi

Phase 1c/d



# Capillary Pressure

Company: BHP Petroleum Pty Ltd

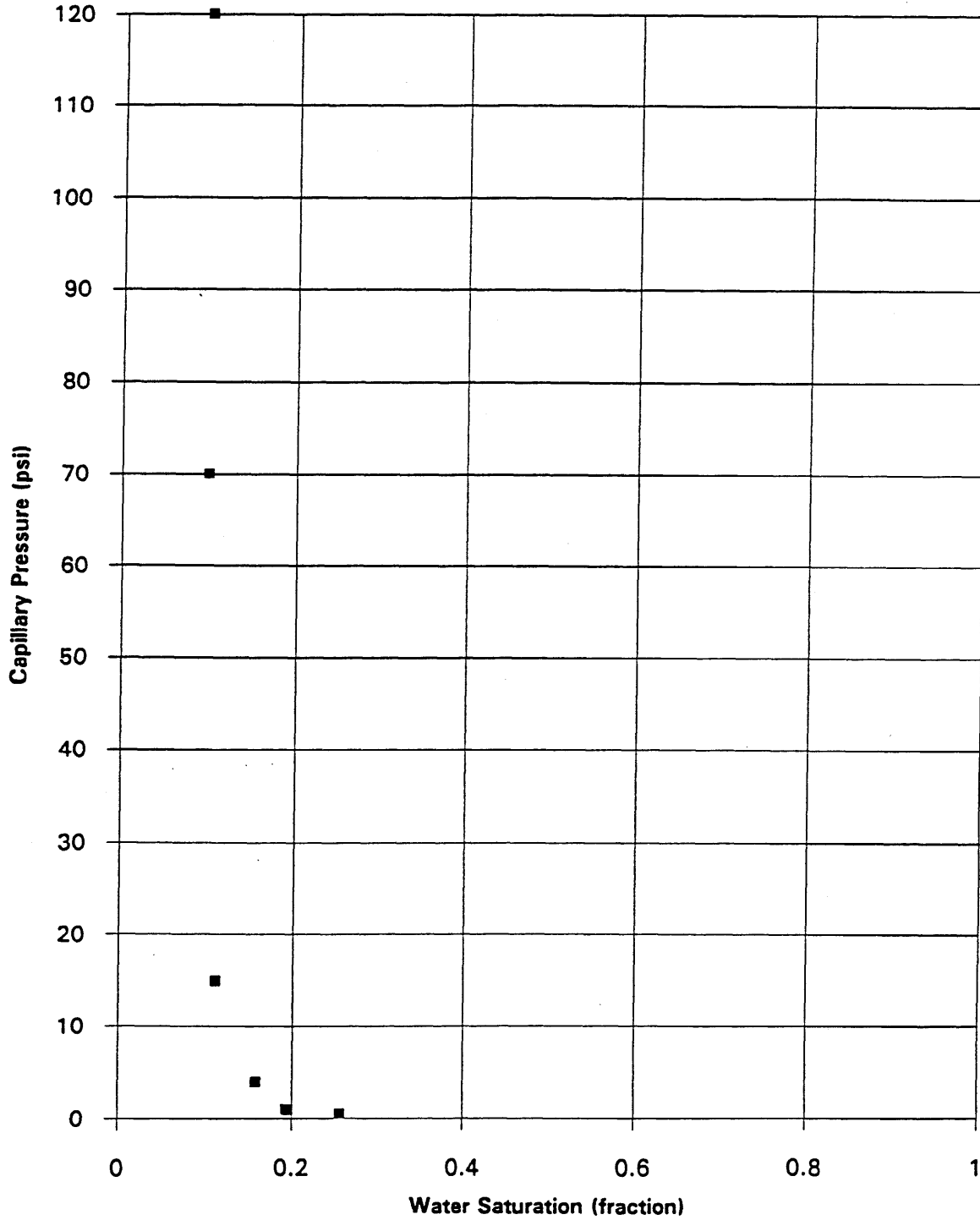
Well: Minerva 1

Sample: 53

Test Method: Porous Plate Air/Brine Drainage

Overburden Pressure 2100 psi

Phase 1c/d



## EFFECTIVE PERMEABILITY TO GAS

Company BHP Petroleum  
Well Minerva 1

Overburden Pressure 2100 psi

Phase 2a

Table XI

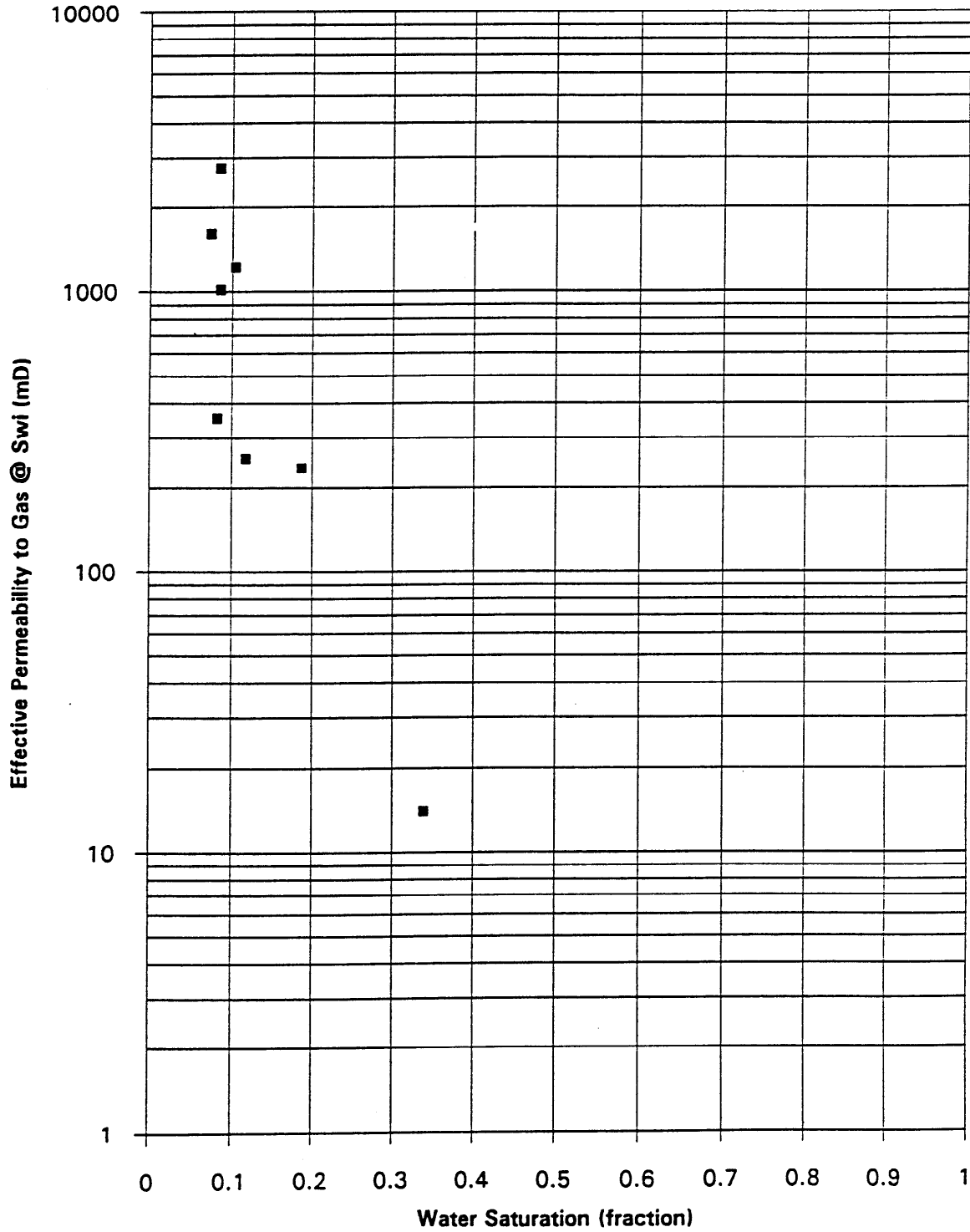
Sample Number	Depth, metres	Permeability to Air, millidarcies	Porosity, fraction	Water Saturation, fraction	Effective Permeability to Gas, millidarcys
21	1830.77	1793	0.108	0.074	1598
24	1831.70	551	0.110	0.083	352
31	1833.80	17.3	0.139	0.339	14.0
50	1840.90	261	0.180	0.187	234
56	1844.05	283	0.146	0.118	253
59	1844.90	1348	0.172	0.104	1214
61	1845.52	3145	0.150	0.085	2740
65	1846.72	1133	0.130	0.086	1014

# Effective Permeability to Gas vs Water Saturation

Company: BHP Petroleum Pty Ltd  
Well: Minerva 1

Overburden Pressure 2100 psi

Phase 2a



# RESIDUAL GAS SATURATION

Company BHP Petroleum  
Well Minerva 1  
Test Method Centrifuge Brine Imbibition  
Ambient  
Phase 2b(i) Table XII

Sample Number	Capillary Pressure, psi	Permeability to Air, millidarcys	Porosity, fraction	Gas Saturation, fraction
24	-77.8	701	0.120	0.131
50	-93.5	318	0.187	0.180
59	-93.6	1601	0.177	0.218
61	-93.7	5641	0.157	0.133

# Permeability to Air vs Water Saturation or (1-Sg)

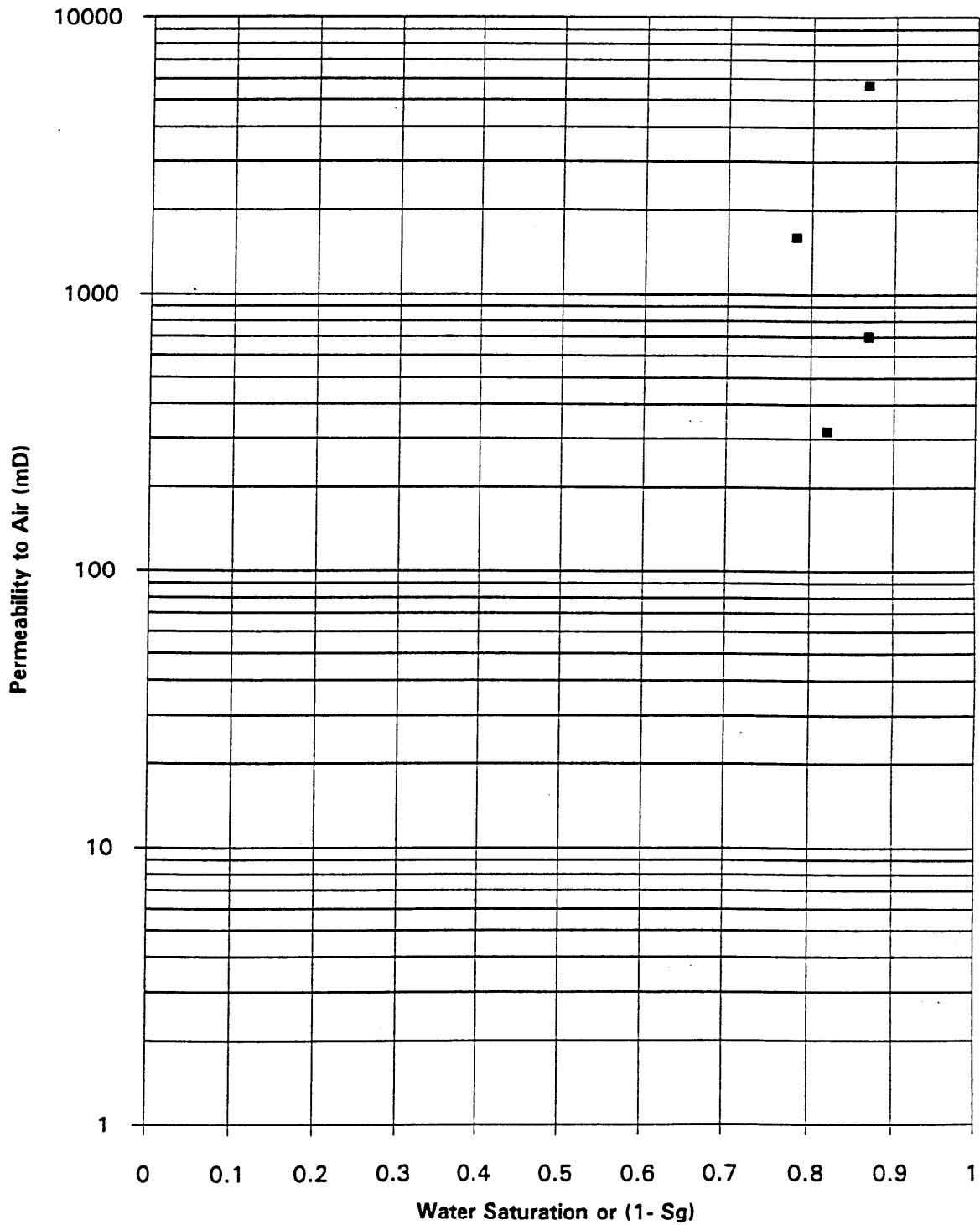
Company: BHP Petroleum Pty Ltd

Well: Minerva 1

Test Method: Air/Brine Imbibition Centrifuge

Ambient

Phase 2b(i)





## EFFECTIVE PERMEABILITY

Company BHP Petroleum  
Well Minerva 1

Overburden Pressure 2100 psi

Phase 2b(i) Table XIII

Sample Number	Depth, metres	Permeability to Air, millidarcys	Porosity, fraction	Gas Saturation, fraction	Effective Permeability to Brine, millidarcys
24	1831.70	551	0.110	0.131	20.0
50	1840.90	261	0.180	0.180	49.6
59	1844.90	1348	0.172	0.218	235
61	1845.52	3145	0.150	0.133	881

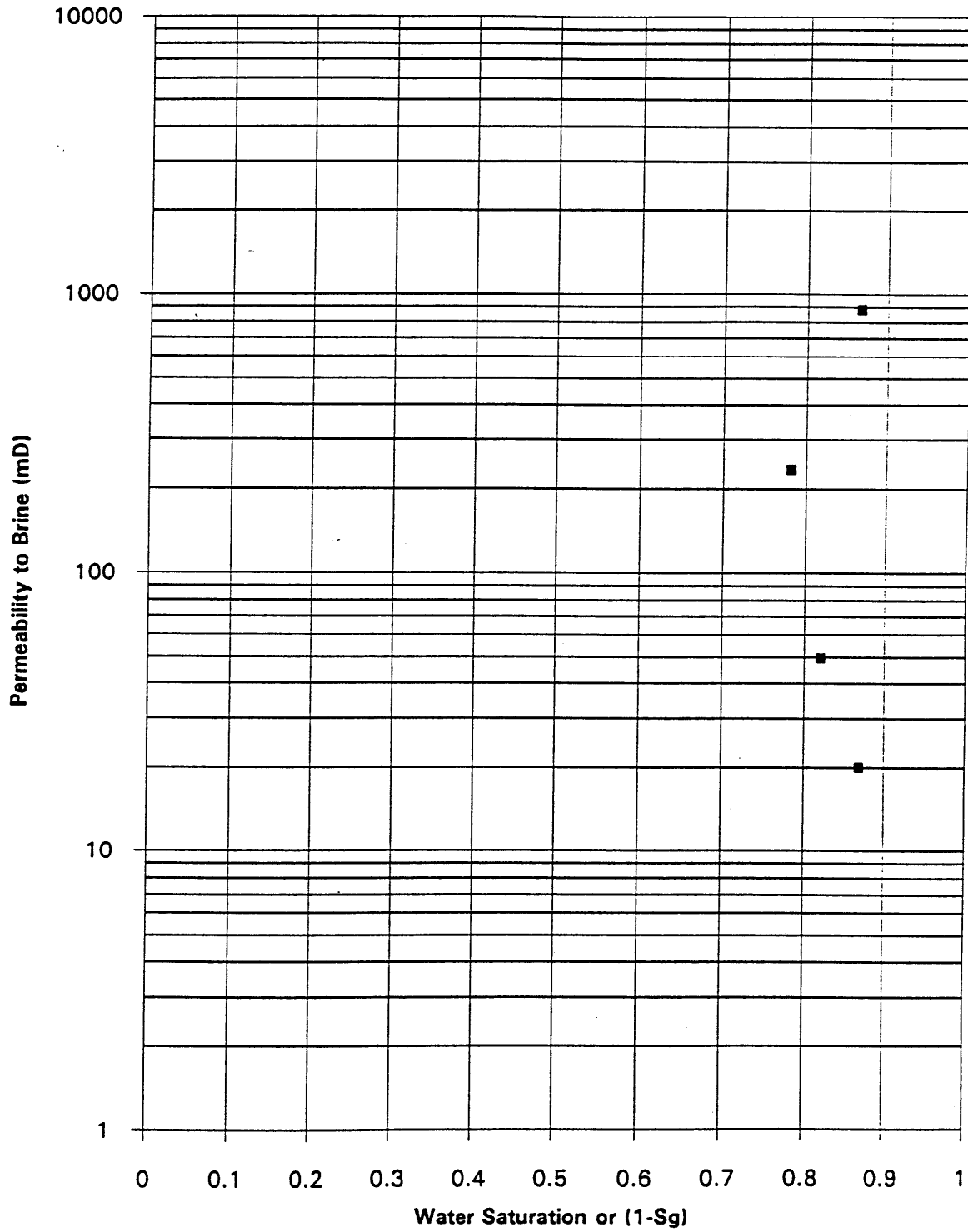
# Effective Permeability to Brine vs Water Saturation or (1-Sg)

Company: BHP Petroleum Pty Ltd

Well: Minerva 1

Overburden Pressure 2100 psi

Phase 2b(i)



## RESIDUAL GAS SATURATION

Company BHP Petroleum  
 Well Minerva 1  
 Test Method Spontaneous Brine Imbibition

Ambient

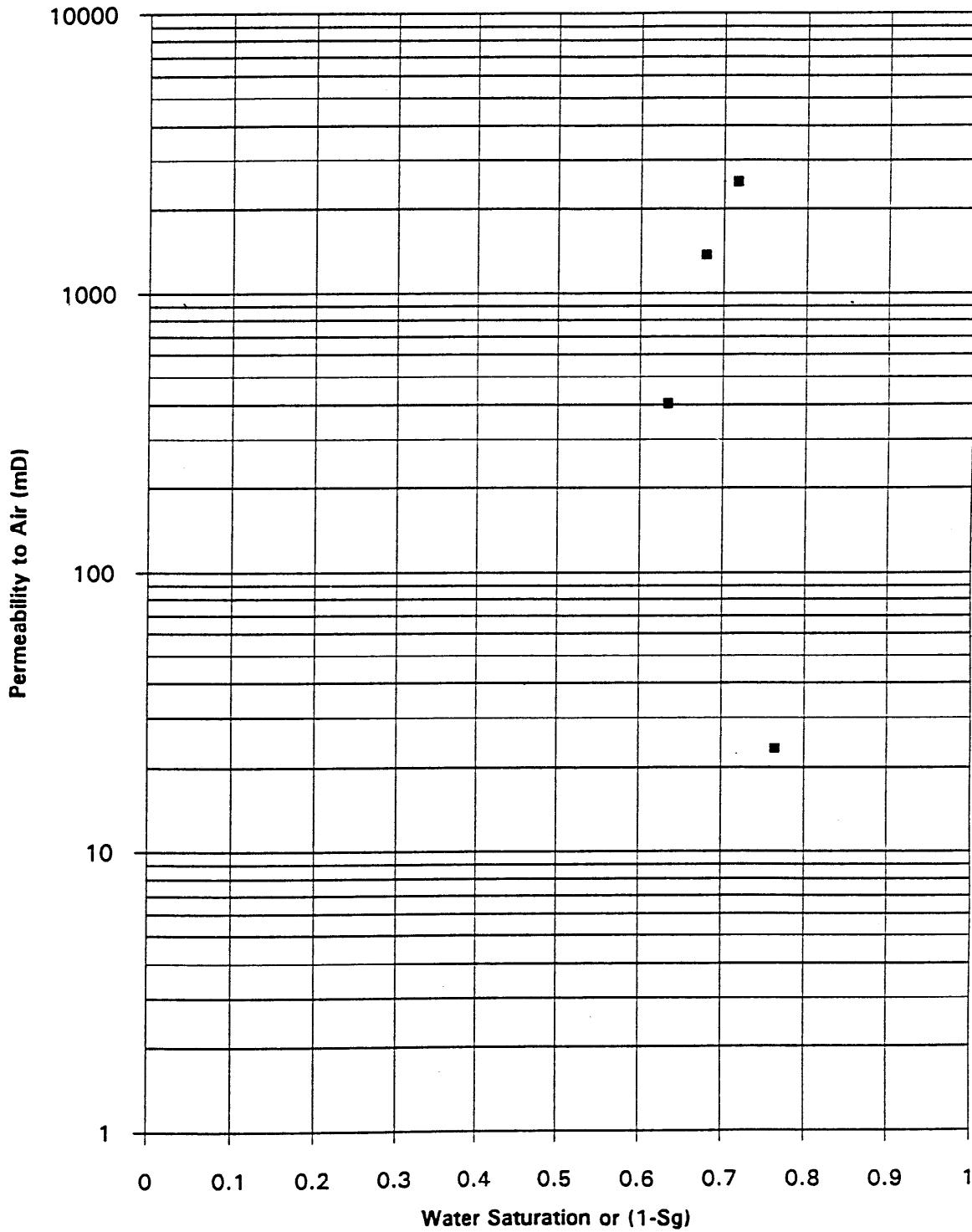
Phase 2b(ii) Table XIV

Sample Number	Depth, metres	Permeability to Air, millidarcys	Porosity, fraction	Gas Saturation, fraction
21	1830.77	2502	0.118	0.283
31	1833.80	23.3	0.147	0.235
56	1844.05	402	0.152	0.366
65	1846.72	1371	0.144	0.321

# Permeability to Air vs Water Saturation or (1-Sg)

Company: BHP Petroleum Pty Ltd  
Well: Minerva 1  
Test Method: Spontaneous Imbibition of Brine  
Ambient

Phase 2b(ii)



17 February 1994

## EFFECTIVE PERMEABILITY

Company BHP Petroleum  
Well Minerva 1

Overburden Pressure 2100 psi

Phase 2b(ii)

Table XV

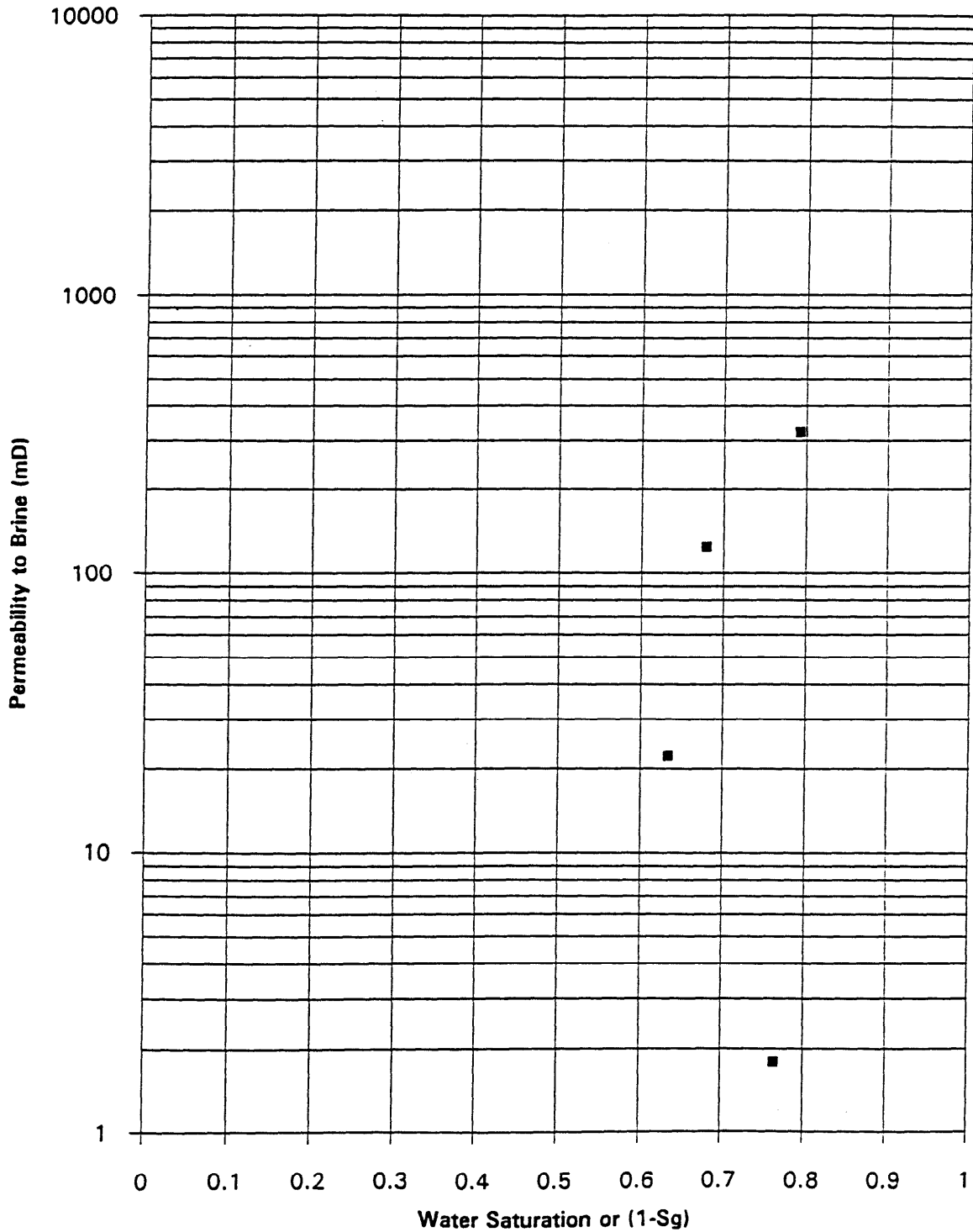
Sample Number	Depth, metres	Permeability to Air, millidarcys	Porosity, fraction	Gas Saturation, fraction	Effective Permeability to Brine, millidarcies
21	1830.77	1793	0.108	0.283	321
31	1833.80	17.3	0.139	0.235	1.78
56	1844.05	283	0.146	0.366	22.2
65	1846.72	1133	0.138	0.321	124

# Effective Permeability to Brine vs Water Saturation or (1-Sg)

Company: BHP Petroleum Pty Ltd  
Well: Minerva 1

Overburden Pressure 2100 psi

Phase 2b(ii)



## RESIDUAL GAS SATURATION

Company BHP Petroleum  
 Well Minerva 1  
 Test Method Centrifuge Brine/Air Imbibition  
 Ambient  
 Phase 2b(iii) Table XVI

Sample Number	Capillary Pressure, psi	Permeability to Air, millidarcies	Porosity, fraction	Saturation, fraction
21	-0.4	2502	0.118	0.224
	-1.8			0.207
	-5.4			0.176
	-11.0			0.146
	-24.9			0.129
	-44.2			0.117
31	-0.5	23.3	0.147	0.210
	-2.1			0.197
	-6.6			0.183
	-13.4			0.171
	-30.1			0.157
	-53.5			0.152
56	-0.5	402	0.152	0.338
	-2.1			0.319
	-6.5			0.308
	-13.4			0.298
	-30.1			0.284
	-53.4			0.276
65	-0.5	1371	0.144	0.296
	-2.1			0.289
	-6.5			0.260
	-13.4			0.246
	-30.0			0.230
	-53.4			0.222

# Capillary Pressure

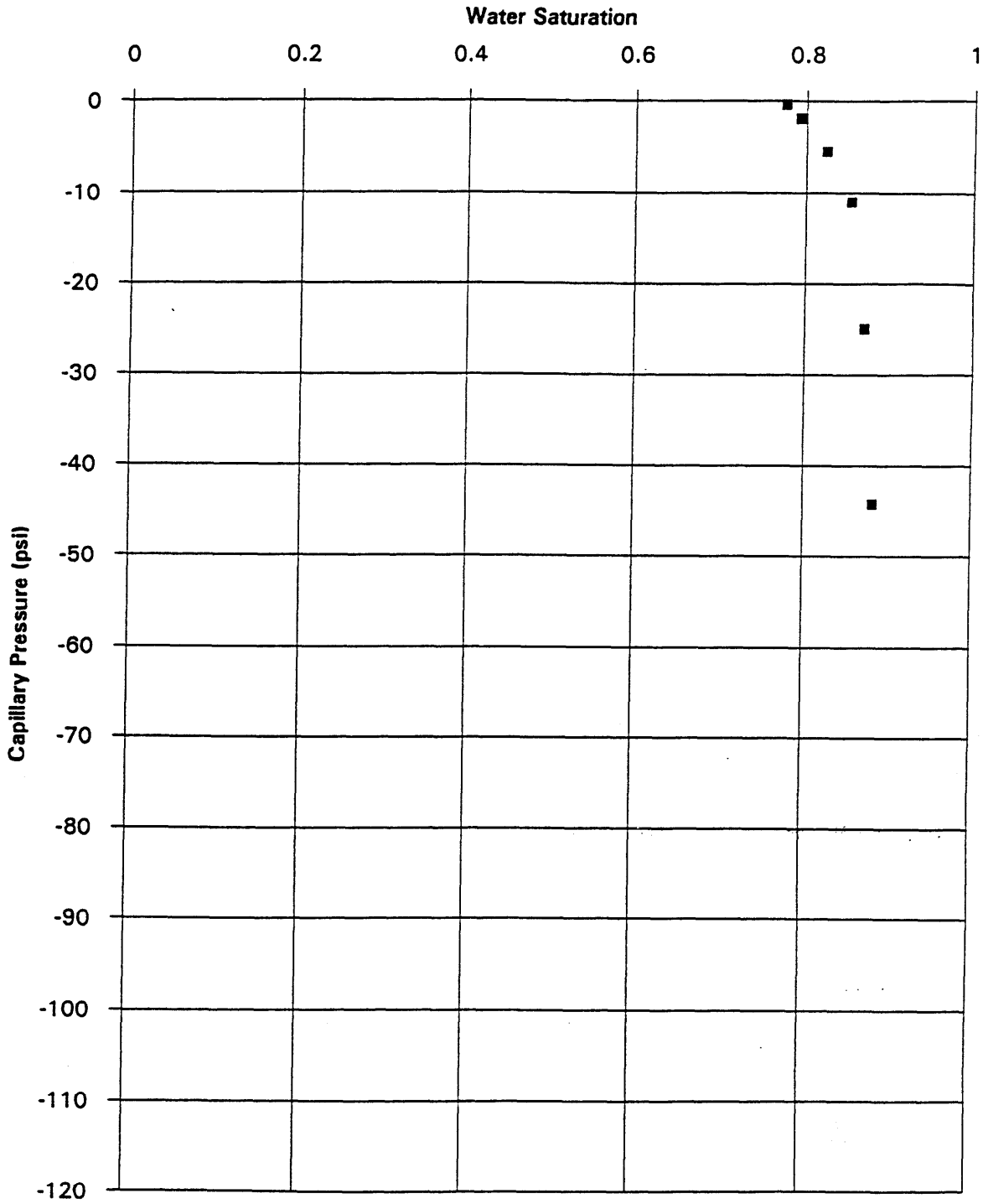
Company: BHP Petroleum Pty Ltd

Well: Minerva 1

Sample: 21

Test Method: Centrifuge Air/Brine Imbibition

Phase 2b(iii)







|

**8**

PE600590

This is an enclosure indicator page.  
The enclosure PE600590 is enclosed within the  
container PE900058 at this location in this  
document.

The enclosure PE600590 has the following characteristics:

ITEM-BARCODE = PE600590  
CONTAINER\_BARCODE = PE900058  
    NAME = MINERVA 1 WELL SUMMARY LOG, VOL 2,  
          ENCLOSURE 1  
    BASIN = OTWAY  
    PERMIT = VIC/P31  
    TYPE = WELL  
    SUBTYPE = COMPOSITE\_LOG  
    DESCRIPTION = MINERVA 1 WELL SUMMARY LOG, VOL 2,  
                  ENCLOSURE 1  
    REMARKS =  
    DATE-CREATED = \*  
    DATE-RECEIVED = \*  
    W\_NO = W1079  
    WELL-NAME = MINERVA-1  
    CONTRACTOR = BHP PETROLEUM PTY LTD  
    CLIENT\_OP\_CO =

(Inserted by DNRE - Vic Govt Mines Dept)

PE904323

This is an enclosure indicator page.  
The enclosure PE904323 is enclosed within the  
container PE900058 at this location in this  
document.

The enclosure PE904323 has the following characteristics:

ITEM\_BARCODE = PE904323  
CONTAINER\_BARCODE = PE900058  
    NAME = Minerva 1 Enclosure 2 Top Main Gas Zone  
        Depth Structure Map  
    BASIN = Otway  
    PERMIT = VIC/P31  
    TYPE = SEISMIC  
    SUBTYPE = HRZN\_CONTR\_MAP  
    DESCRIPTION = Minerva 1 Enclosure 2 Top Main Gas Zone  
        Depth Structure Map  
    REMARKS =  
    DATE\_CREATED = \*  
    DATE\_RECEIVED = \*  
    W\_NO = W1079  
    WELL\_NAME = Minerva 1  
    CONTRACTOR = BHP  
    CLIENT\_OP\_CO = BHP Petroleum

(Inserted by DNRE - Vic Govt Mines Dept)